Università degli Studi di Napoli “Federico II”

Dipartimento di Strutture per l’Ingegneria e l’Architettura

Ph. D. Thesis

SOME NEW THERMO-ELASTIC SOLUTIONS FOR CYLINDRICAL AND SPHERICAL COMPOSITES

Dottorando: Ing. Federico Carannante

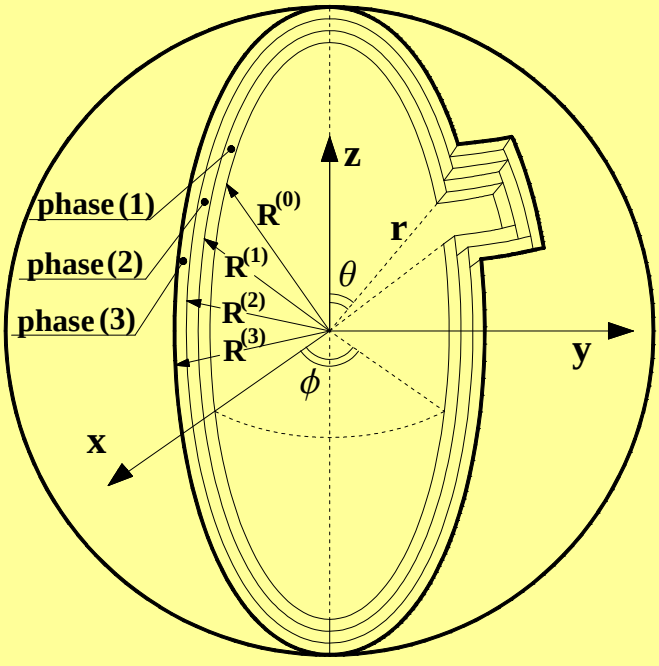

Dottorato di Ricerca in Ingegneria delle Costruzioni
- XXV CICLO - Febbraio 2013

Tutor: Prof. Ing. Luciano Nunziante
Coordinatore: Prof. Ing. Luciano Rosati

Università degli Studi di Napoli “Federico II”

Dipartimento di Strutture per l’Ingegneria e l’Architettura

Tesi di Dottorato
XXV ciclo

SOME NEW THERMO-ELASTIC SOLUTIONS FOR CYLINDRICAL AND SPHERICAL COMPOSITES

Dottorando: Federico CARANNANTE

Il Tutor: Prof. Ing. Luciano NUNZIANTE

Il Coordinatore: Prof. Ing. Luciano ROSATI

- **Dottorato di Ricerca in Ingegneria delle Costruzioni** -

INDEX

CHAPTER X – MULTILAYERD CYLINDER UNDER SAINT-VENANT'S LOADS AND HOMOGENIZATION: POISSON EFFECT ON STIFFNESS

RINGRAZIAMENTI

Desidero ringraziare per il presente lavoro di tesi tutti coloro che, direttamente o indirettamente, hanno contribuito alla mia formazione scientifica ed umana in questi anni di dottorato.
In particolare, uno speciale ringraziamento è doveroso nei confronti del prof. Luciano Nunziante, che con affetto e pazienza mi ha saputo indirizzare verso le tematiche di ricerca sviluppate all'interno della presente dissertazione, fornendomi – con la sua grande capacità ed esperienza – indicazioni e contributi essenziali per risolvere numerosi problemi di elasticità. Inoltre, desidero ringraziare il prof. Massimiliano Fraldi, che mi ha seguito in questo appassionante percorso scientifico, spesso fianco a fianco, cercando di districarci tra innumerevoli files di Mathematica!
Infine, oltre a ringraziare il prof. Antonio Gesualdo, il dott. Luca Esposito e il Coordinatore del Dottorato, prof. Luciano Rosati, un pensiero particolare lo rivolgo alla mia famiglia, che mi ha sempre dato il supporto affettivo (ed economico) senza il quale non avrei potuto raggiungere gli obiettivi sin qui ottenuti.

INTRODUCTION

In modern engineering applications, multilayered structures are extensively used due to the added advantage of combining physical, mechanical, and thermal properties of different materials. Many of these applications require a detailed knowledge of transient temperature and heat-flux distribution within the component layers. Both analytical and numerical techniques may be used to solve such problems. Nonetheless, numerical solutions are preferred and prevalent in practice, due to either unavailability or higher mathematical complexity of the corresponding exact solutions.

Rather limited use of analytical solutions should not diminish their merit over numerical ones; since exact solutions, if available, provide an insight into the governing physics of the problem, which is typically missing in any numerical solution. Moreover, analyzing closed-form solutions to obtain optimal design options for any particular application of interest is relatively simpler. In addition, exact solutions find their applications in validating and comparing various numerical algorithms to help improve computational efficiency of computer codes that currently rely on numerical techniques. Although multilayer heat conduction problems have been studied in great detail and various solution methods including *orthogonal and quasi-orthogonal expansion technique, Laplace transform method, Green's function approach, finite integral transform technique* are readily available; there is a continued need to develop and explore novel methods to solve problems for which exact solutions still do not exist. One such problem is to determine exact unsteady temperature distribution in polar coordinates with multiple layers in the radial direction.

Numerous applications involving multilayer cylindrical geometry require evaluation of temperature distribution in complete disk-type. One typical example is a nuclear fuel rod, which consists of concentric layers of different materials and often subjected to asymmetric boundary conditions.

Moreover, several other applications including multilayer insulation materials, double heat-flux conductimeter, typical laser absorption calorimetry experiments, cryogenic systems, and other cylindrical building structures would benefit from such analytical solutions.

Then, object of the present thesis is to derive new thermo-elastic solutions for composite materials constituted by multilayered spheres and cylinders under time-dependent boundary conditions. These solutions are utilized for several engineering applications and we report some applications in last analyze chapters of present thesis. In follows, we will described the contents of thesis.

In first chapters are reported the thermo-mechanical foundations and a summary of the formulation of thermo-elastic problems for isotropic material.

In chapter X it is developed an analytical approach to find exact elastic solutions for multilayered cylinder composed of isotropic constituents and determining the analytical response in terms of displacements and stresses for all the De Saint Venant (DSV) load conditions, that is axial force, torque, pure bending and combined bending moment and shear actions. Successively, on the basis of the found analytical solutions, a homogenization procedure is adopted in order to obtain the overall constitutive elastic laws for multilayered cylinder, in this way deriving the *exact* one-dimensional model characterized by the axial stiffness, flexural rigidity, shear deformability and torsional stiffness relating beam's generalized stresses and strains. By playing with the Poisson ratios of adjacent phases, some counterintuitive and engineering relevant results are shown with reference to unexpected increasing of overall stiffness of multilayered cylinder.

In chapter XI it is presented an analytical elastic solution for multilayered cylinder constituted by transversally-isotropic n-phases, under radial pressure, axial force and torque. Then, by utilizing the homogenization theory, it is obtained the overall elastic stiffness of the equivalent homogeneous transversally-isotropic solid, establishing the constitutive elastic laws relating stresses and strains.

In chapter XII it is developed an analytical approach to find exact elastic solutions for multilayered cylinder subjected to axial force, constituted by *n* orthotropic cylindrical hollow phases and a central core, each of them modelled as homogeneous and cylindrically anisotropic material.

In chapter XIII it is reported an analytical solution for multilayered cylinder composed by hollow cylindrical monoclinic phases under axial force and torsion. In this chapter, we consider the *chiral* structure for each cylindrical layer. In particular the composite material is constituted by two hollow cylindrical monoclinic phases. The cylindrical monoclinic elastic property of multilayered cylinder

is obtained by the particular chiral structure. In fact, we consider the two hollow phases constructed by right-handed and left-handed spiral helices whose long axes are all parallel. These helical spirals may be either touching or separated by a matrix material and are composed by elastic orthotropic material.

In chapters XIV, XV, XVI are reported some thermo-elastic solution, for hollow cylinders, hollow spheres and plates, respectively.

In chapter XVII we consider a steady-state thermo-elastic problem of multilayered cylinder with finite length. The thermal and mechanical loads applied on the cylinder are axisymmetric in the hoop direction and are constant in the axial direction. In order to obtain analytical solutions for temperature, displacements, and stresses for the two-dimensional thermo-elastic problem, the cylinder is assumed to be composed of n fictitious layers in the radial direction. The material properties of each layer are assumed as homogeneous.

In chapter XVIII are determined the displacements, strains, and stresses from the general analytical solution of multilayered sphere composed by an arbitrary number of layers constituted by materials with generic modulus of elasticity, thermal expansion coefficient and thermal conductivity. Material properties are assumed to be temperature-independent and homogeneous in each layer. The multilayered sphere is considered as a classical composite material whose properties abruptly vary from one hollow sphere to the other.

In chapter XIX are presented the most important standard fire curves: ISO 834, External fire curve, hydrocarbon fire curve, ASM119 and parametric fire curves (European Parametric fire curves, Swedish Fire Curves, BFD curves, CE 534 curve). Moreover in this chapter are reported the mechanical and thermal properties of steel and concrete at elevate temperature.

In chapters XX and XXI, the one-dimensional quasi-static uncoupled thermo-elastic problem of a multilayered sphere and multilayered cylinder, with time-dependent boundary conditions are considered, respectively. The body forces and heat generation vanish. In both cases, the analytical solution is obtained by applying the method of separation of variables.

In chapter XXII it is studied a spherical tank methane gas-filled exposed to fire characterized by hydrocarbon fire curve. The interaction between spherical tank and internal gas is studied. By applying a suitable simplified hypothesis on the mechanics of problem, we determine the analytical thermo-elastic solution for spherical tank. By applying the solution obtained, the increasing graded temperature of gas methane in spherical tank is determined. Finally, a numerical example is reported for a spherical tank exposed to hydrocarbon fire, showing the collapse temperature.

In chapter XXIII, an industrial insulated pipeline is modelled as multilayered cylinder, subjected to mechanical and thermal loads. By using a multi-layered approach based on the theory of laminated composites, the solutions for temperature, heat flux, displacements, and thermal/mechanical stresses are presented. By applying the analytical thermo-elastic solution reported in Chapter XVII, a parametric analysis is conducted in order to analyze the mechanical behaviour of an industrial insulated pipeline composed by three phases: steel, insulate coating, and outer layer made of polyethylene to protect the insulation. In this model, parametric analyses are conducted by varying the Young's modulus, Poisson's ratio, thermal conductivity and linear thermal expansion coefficient of insulate coating. The analysis shows the maximum Hencky von Mises's equivalent stress in steel phase and in insulate coating. Finally, it is presented a numerical example by considering three types of materials for insulate coating: (1) Expanded Polyurethane; (2) Laminate glass; (3) Syntatic foam.

In chapter XXIV it is analyzed a cylindrical concrete specimen under axial force within Fibre Polymeric Reinforcing sheets. The elastic solutions found in Chapter XII are here extended to the post-elastic range. The evolution of the stress field when the core phase is characterized by an Intrinsic Curve or Schleicher-like elastic-plastic response with associate flow rule and the cylindrically orthotropic hollow phase obeys to is shown the elastic-brittle Tsai-Hill anisotropic yield criterion. The choice of these post-elastic behaviours is suggested by experimental evidences reported in literature for these materials, as well as the cylindrical orthotropy of the hollow phase intrinsically yields to consider several perfectly bonded FRP layers as an equivalent one,

interpreting their overall mechanical response by invoking the theory of homogenization and the mechanics of composites.

At the end, a numerical example application to cylindrical concrete specimens reinforced with Carbon FRP is presented, by furnishing a predictive formula – derived from the previously obtained analytical solutions - for estimating the overall collapse mechanism, the concrete ultimate compressive strength and the confining pressure effect. The results are finally compared with several experimental literature data, highlighting the very good agreement between the theoretical predictions and the laboratory measurements.

In chapter XXV it is reported an analytical thermo-elastic solution in closed form for bi-layer hollow cylinder subjected to time-dependent boundary conditions. It is assumed that each hollow cylinder is composed by a homogeneous and thermo-isotropic material, characterized by different mechanical and thermal parameters, i.e. modulus of elasticity, thermal expansion coefficient and thermal conductivity. Moreover, these material properties in each hollow cylinder are assumed to be temperature-independent. In other words, the bi-layer hollow cylinder is considered as a classical composite material whose properties abruptly vary from one hollow cylinder to the other. In particular, it is obtained a new analytical solution for a bi-layer hollow cylinder, constituted by two phases: Ceramic (Si_3N_4) and Metal ($Ti-6Al-4V$) subjected to heat flux on inner surface.

Napoli, 25/02/2013

Dott. Ing. Federico Carannante

CHAPTER I
KINEMATICAL FOUNDATIONS

1.1. Deformations in $\mathbf{R}^3$

We assume once and for all that an origin O and an orthonormal basis $\{\mathbf{e}_1, \mathbf{e}_2, \mathbf{e}_3\}$ have been chosen in three-dimensional Euclidean space, which will therefore be identified with the space $\mathbf{R}^3$: From the notational viewpoint, we identify the point $\mathbf{x}$ with the vector $\mathbf{ox}$. Whenever we consider components of vectors in $\mathbf{R}^3$, or elements of matrices in $\mathbf{M}^3$, we make the convention that Latin indices (I,j,p,….) always take their values in the set {1,2,3}, and we combine this rule with the standard summation convention.

Let there be given a bounded, open, connected, subset Ω of $\mathbf{R}^3$ with a sufficiently smooth boundary (specific smoothness assumptions will be made subsequently). We shall think of the closure $\overline{\Omega}$ of the set Ω as representing the volume occupied by a body "before it is deformed"; for this reason, the set $\overline{\Omega}$ is called the reference configuration . A deformation of the reference configuration $\overline{\Omega}$ is a vector field:

$$\varphi : \overline{\Omega} \to \mathbf{R}^3 \tag{1.1}$$

That is smooth enough, injective possibly on the boundary of the set Ω, and orientation–preserving

Remarks

(1) The reason a deformation may loose its injectivity on the boundary of Ω is that "self-contact" must be allowed

(2) The expression "smooth enough" is simply a convenient way of saying that in a given definition, theorem, proof, etc. the smoothness of deformations involved is such that all arguments make sense. As a consequence, the underlying degree of smoothness varies from place to place. For instance, the existence of the deformation gradient (to be next introduced) implies that a deformation is differentiable at all points of the reference configuration; Theorem 1.1 relies on the Piola identify, which makes sense , at least in a classical setting, only for twice differentiable deformations; the characterization of rigid deformations (Theorem 1.2) is established for deformations that are continuously differentiable, etc.

(3) Deformations are synonymously called configurations, or placements, by some authors.

We denote by $\mathbf{x}$ a generic point in the set $\overline{\Omega}$, by x_i its components with respect to the basis $\{\mathbf{e}_i\}$, and by $\partial_i = \partial/\partial x_i$ the partial derivative with respect to variable x_i. Given a deformation $\boldsymbol{\varphi} = \varphi_i \mathbf{e}_i$. We define at each point of the set Ω the matrix

$$\nabla\boldsymbol{\varphi} := \begin{pmatrix} \partial_1\varphi_1 & \partial_2\varphi_1 & \partial_3\varphi_1 \\ \partial_1\varphi_2 & \partial_2\varphi_2 & \partial_3\varphi_2 \\ \partial_1\varphi_3 & \partial_2\varphi_3 & \partial_3\varphi_3 \end{pmatrix} \tag{1.2}$$

The matrix $\nabla\boldsymbol{\varphi}$ is called the **deformation gradient**. Since a deformation is orientation-preserving by definition, the determinant of the deformation gradient satisfies the **orientation-preserving condition**:

$$\det \nabla\boldsymbol{\varphi}(\mathbf{x}) > 0 \quad \text{for all} \quad x \in \overline{\Omega}$$

In particular, the matrix $\nabla\boldsymbol{\varphi}(\mathbf{x})$ is invertible at all points $\mathbf{x}$ of the reference configuration $\overline{\Omega}$.

Remarks:

(1) The notations $\mathbf{F} = \nabla\boldsymbol{\varphi}$ and $J = \det \nabla\boldsymbol{\varphi}$ are commonly used in the literature.

(2) The notation $\nabla\boldsymbol{\varphi}$ is confusing, since the gradient of a real-valued function f is the column vector formed by the first partial derivative $\partial_i f$, while $(\nabla\boldsymbol{\varphi})_{ij} = \partial_j \varphi_i$ (this explains why we

used the notation **grad** f , and not ∇f . Indeed, the deformation gradient is simply the matrix representing the Frechet derivative of the mapping φ, which fro real-valued functions, it is identified with the transpose of the gradient.

Together with a deformation φ , it is often convenient to introduce the displacement $\mathbf{u}$, which is the vector field:

$$\mathbf{u} : \bar{\Omega} \to \mathbf{R}^3 \tag{1.3}$$

defined by the relation :

$$\boldsymbol{\varphi} = \mathbf{id} + \mathbf{u} \tag{1.4}$$

where **id** denotes the (restriction to $\bar{\Omega}$ of the) identity map from $\mathbf{R}^3$ onto $\mathbf{R}^3$. Notice that the displacement gradient is:

$$\nabla \mathbf{u} := \begin{pmatrix} \partial_1 u_1 & \partial_2 u_1 & \partial_3 u_1 \\ \partial_1 u_2 & \partial_2 u_2 & \partial_3 u_2 \\ \partial_1 u_3 & \partial_2 u_3 & \partial_3 u_3 \end{pmatrix} \tag{1.5}$$

and the deformation gradient are related by the equation

$$\nabla \boldsymbol{\varphi} = \mathbf{I} + \nabla \mathbf{u} \tag{1.6}$$

Given a reference configuration $\bar{\Omega}$ and a deformation $\boldsymbol{\varphi} : \bar{\Omega} \to \mathbf{R}^3$, the set $\boldsymbol{\varphi}(\bar{\Omega})$ is called a **deformed configuration.** At each point

$$\mathbf{x}^{\varphi} := \boldsymbol{\varphi}(\mathbf{x}) \tag{1.7}$$

of a deformed configuration, we define the three vectors (Fig.1.1)

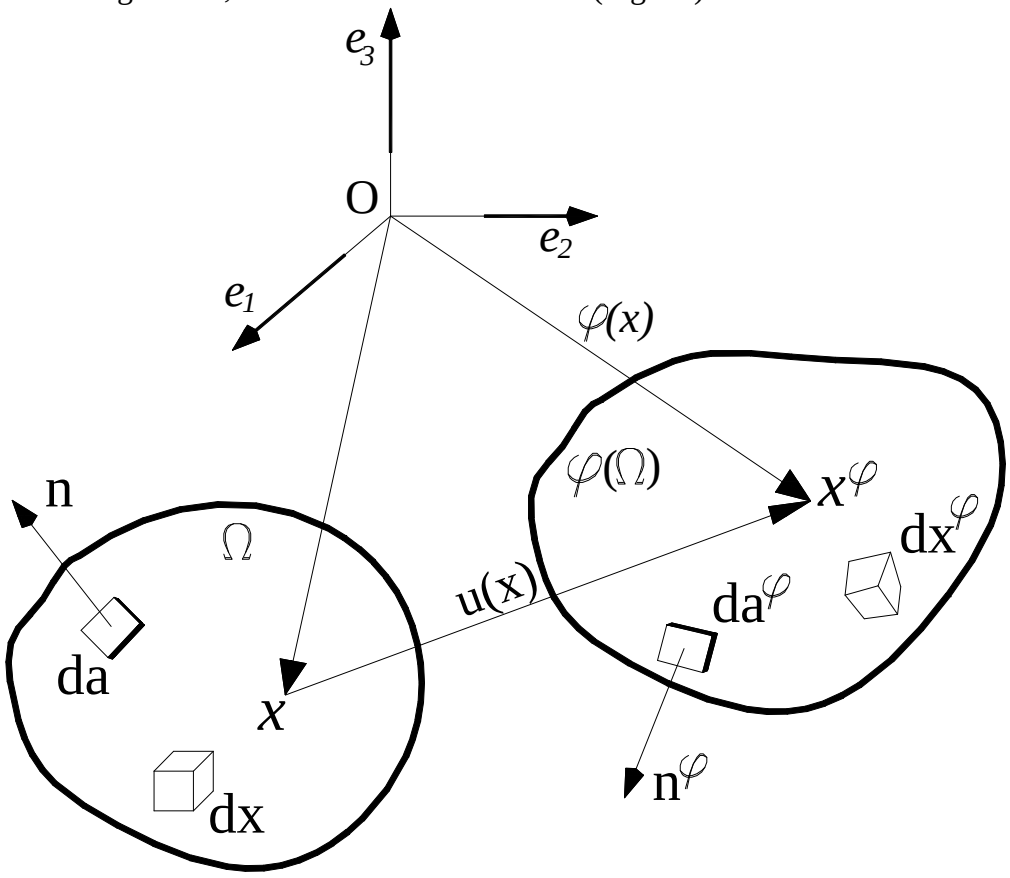

Fig. 1.1 - *Geometry of a deformation: The volume element, the area element, the unit outer normal, are denoted* $dx, da, \mathbf{n}$ *in the reference configuration* $\bar{\Omega}$, *and* $dx^{\varphi}, da^{\varphi}, \mathbf{n}^{\varphi}$ *in the deformed configuration* $\boldsymbol{\varphi}(\bar{\Omega})$. *The vectors* $\partial_j \boldsymbol{\varphi}(\mathbf{x})$ *define the deformation at a point* $x \in \bar{\Omega}$ *to within the first order.*

$$\partial_j \boldsymbol{\varphi}(\mathbf{x}) = \partial_j \varphi_i(\mathbf{x}) \mathbf{e}_i \tag{1.8}$$

Each vector $\partial_j \boldsymbol{\varphi}(\mathbf{x})$ measures the "local deformation in the direction of the vector $\mathbf{e}_j$" in the sense that, to within the first order with respect to dt, the vector $\mathbf{e}_j dt$ is transformed into the vector $\partial_j \boldsymbol{\varphi}(\mathbf{x}) dt$. Equivalently, the vector $\partial_j \boldsymbol{\varphi}(\mathbf{x})$ is the tangent vector to the jth coordinate line passing through the point $\mathbf{x}^{\varphi}$. (i.e. the image by the deformation $\boldsymbol{\varphi}$ of a segment parallel to the vector $\mathbf{e}_j$ containing the point $\mathbf{x}$ in its interior, and parametrized by t). Since the vector $\partial_j \boldsymbol{\varphi}(\mathbf{x})$ is precisely the j-th column of the matrix $\nabla \boldsymbol{\varphi}(\mathbf{x})$, the knowledge of the deformation gradient completely define the local deformation to within the first order.

Remarks:

(1) While the deformation gradient $\nabla \boldsymbol{\varphi}(\mathbf{x})$ clearly depends upon the basis $\mathbf{e}_i$, it is possible to exhibit the intrinsic geometrical character of the deformation at the point $\mathbf{x}$, by means of the polar factorization of the matrix $\nabla \boldsymbol{\varphi}(\mathbf{x})$, which then appears as the product of a "rotation tensor" by a "stretch tensor". For details about this classical results, see for instance Germain [1972, p. 97], Gurtin [1981b, p. 46], Truesdell&Noll [1965, p.52].

(2) If the point $\mathbf{x}^{\varphi} = \boldsymbol{\varphi}(\mathbf{x})$ belongs to the interior of the deformed configuration $\boldsymbol{\varphi}(\bar{\Omega})$, the three vector $\partial_j \boldsymbol{\varphi}$ define in the terminology of differential geometry the tangent vector space at the point $\mathbf{x}$ of the manifold $\operatorname{int} \boldsymbol{\varphi}(\bar{\Omega})$. This space is of dimension three since the matrix $\nabla \boldsymbol{\varphi}(\mathbf{x})$ is invertible (by definition of a deformation).

(3) The points $x \in \Omega$ and the corresponding points $\mathbf{x}^{\varphi} \in \boldsymbol{\varphi}(\Omega)$ are often called material points and spatial points respectively, and they are often denoted X and x respectively, in the continuum mechanics literature.

We next compute the volume, area, and length elements in the deformed configuration: In each case, the objective is, for a given deformation, to express quantities (volumes, surfaces, lengths) defined over the deformed configuration in terms of the same quantities, but defined over the reference configuration. To emphasize the crucial distinction between both types of quantities, we adopt the following notational device: The superscript "$\boldsymbol{\varphi}$"; this rule has already been applied, for denoting a generic point $\mathbf{x} \in \bar{\Omega}$ and the corresponding point $\mathbf{x}^{\varphi} \in \boldsymbol{\varphi}(\mathbf{x}) \in \boldsymbol{\varphi}(\bar{\Omega})$.

This correspondence between a quantity defined as a function of the Lagrange variable $\mathbf{x}$, and a similar quantity defined as a function of the Euler variable $\mathbf{x}^{\varphi} = \boldsymbol{\varphi}(\mathbf{x})$, can be extended to other quantities than volume, surfaces, and lengths: As we shall see, it applies equally well to divergences of tensor fields and applied forces

Remark. This idea can be systematized through the notions of "pullback" and "push-forward", familiar in differential geometry. In this respect, see for instance Choquet-Bruhat, Dewitt-Morette & Dillard-Bleick [1977], or Marsden 6 Hughes [1983].

1.2. Volume element in the deformed configuration

Let φ be a deformation. If dx denotes the volume element at the point $\mathbf{x}$ of the reference configuration, the volume element dx^{φ} at the point $\mathbf{x}^{\varphi} = \boldsymbol{\varphi}(\mathbf{x})$ of the deformed configuration (Fig. 1.1) is given by

$$dx^{\varphi} = \det \nabla \boldsymbol{\varphi}(x) dx \tag{1.9}$$

Since $\left|\det \nabla \boldsymbol{\varphi}(x)\right| = \det \nabla \boldsymbol{\varphi}(x) > 0$ by assumption.

The volume element dx^{φ} is used for computing volumes in the deformed configuration : If A denotes a measurable subset of the reference configuration $\bar{\Omega}$, the volume of the set A and the volume of the deformed set $A^{\varphi} := \varphi(A)$ are respectively given by:

$$vol\, A := \int_A dx, \quad vol\, A^{\varphi} := \int_{A^{\varphi}} dx^{\varphi} = \int_A \det \nabla \boldsymbol{\varphi}(x)\, dx, \tag{1.10}$$

Notice that the last equality is nothing but a special case of the formula for changes of variables in multiple integrals: Let $\boldsymbol{\varphi} : A \to \boldsymbol{\varphi}(A) = A^{\varphi}$ be an injective, continuously differentiable mapping with a continuous inverse $\boldsymbol{\varphi}^{-1} : A^{\varphi} \to A$. Then a function $u : x^{\varphi} \in A^{\varphi} \to \mathbf{R}$ is dx^{φ}- integrable over the set A^{φ} if and only if the function

$$x \in A \to (u \circ \boldsymbol{\varphi})(x) \left| \det \nabla \boldsymbol{\varphi}(x) \right| \tag{1.11}$$

is dx – integrable over the set A and if this is the case,

$$\int_{A^{\varphi} = \varphi(A)} u\left(x^{\varphi}\right) dx^{\varphi} = \int_A (u \circ \boldsymbol{\varphi})(x) \left| \det \nabla \boldsymbol{\varphi}(x) \right| dx \tag{1.12}$$

It should be remembered that the validity of this formula hinges critically on the assumption that the mapping $\boldsymbol{\varphi}$ is injective. Otherwise, it must be replaced by the more general relation:

$$\int_{\varphi(A)} u(x')\, card\, \boldsymbol{\varphi}^{-1}(x')\, dx' = \int_A (u \circ \boldsymbol{\varphi})(x) \left| \det \nabla \boldsymbol{\varphi}(x) \right| dx \tag{1.13}$$

Where card B denote in general the number of elements in a set B. For details, see Schwartz [1967, Corollaire 2, p 675], Rado & Reichelderfer [1955, p.438], Federer [1969, p.241 ff.], Smith [1983, Ch. 16], and also Bojarski & Iwaniec [1983, Sect.8], Marcus & Mizel [1973], Vodopyanov, Goldshtein & Reshetnyak [1979] for its extension to Sobolev space-valued mappings.

These properties hold in $\mathbf{R}^n$, for arbitrary n. The volume $\int_A dx$ of a dx-measurable subset of $\mathbf{R}^n$ is denoted dx-means A.

1.3. The Piola transform; Area element in the deformed configuration

As a preparation for computing the area element in the deformed configuration in terms of the area element in the reference configuration, it is convenient to introduce a particular transformation between tensors defined over the reference configuration $\bar{\Omega}$ and tensors defined over the deformed configuration $\bar{\Omega}^{\varphi}$. Besides, this transform plays a crucial role in the definition of the first Piola-Kirchhoff tensor.

Let us first review some definitions and results pertaining to tensor fields defined over either sets $\bar{\Omega}$ or $\bar{\Omega}^{\varphi}$. By a tensor, we mean here a second-order tensor

$$\mathbf{T} = \left(T_{ij}\right), \text{ i: row index, j: column index}$$

Since we ignore the distinction between covariant and controvariant components, the set of all such tensors will be identified with the set $\mathbf{M}^3$ of all square matrices of order three.

Given a smooth enough tensor field $\mathbf{T} : \bar{\Omega} \to \mathbf{M}^3$ defined over the reference configuration $\bar{\Omega}$, we define at each point of $\bar{\Omega}$ its divergence $\mathbf{div}\,\mathbf{T}$ as the vector whose components are the divergences of the transposes of the row vectors of the matrix $\mathbf{T}$. More explicitly,

$$\mathbf{T} = T_{ij} = \begin{pmatrix} T_{11} & T_{12} & T_{13} \\ T_{21} & T_{22} & T_{23} \\ T_{31} & T_{32} & T_{33} \end{pmatrix} \quad \Rightarrow \quad \mathbf{div}\,\mathbf{T} := \begin{pmatrix} \partial_1 T_{11} + \partial_2 T_{12} + \partial_3 T_{13} \\ \partial_1 T_{21} + \partial_2 T_{22} + \partial_3 T_{23} \\ \partial_1 T_{31} + \partial_2 T_{32} + \partial_3 T_{33} \end{pmatrix} = \partial_j T_{ij} \mathbf{e}_i \tag{1.14}$$

Of course, a similar definition holds for the divergence $\mathbf{div}^{\varphi}\,\mathbf{T}^{\varphi}$ of tensor fields $\mathbf{T}^{\varphi} : \mathbf{B}^{\varphi} \to \mathbf{M}^3$ defined over the deformed configuration :

$$\mathbf{T}^{\varphi} = \left(T_{ij}^{\varphi}\right) \quad \Rightarrow \quad div^{\varphi}\, T^{\varphi} := \partial_j^{\varphi} T_{ij}^{\varphi} \mathbf{e}_i \tag{1.15}$$

where $\partial_j^\varphi := \dfrac{\partial}{\partial x_j^\varphi}$ denote the partial derivatives with respect to the variables x_j^φ.

A Simple application of the fundamental Green's formula over the set $\bar{\Omega}$ shows that the divergence of a tensor field satisfies:

$$\int_\Omega \mathbf{div}\,\mathbf{T}dX = \left(\int_\Omega \partial_j T_{ij} dx\right)\mathbf{e}_i = \left(\int_{\partial\Omega} T_{ij} n_j da\right)\mathbf{e}_i \tag{1.16}$$

Or equivalently in matrix form:

$$\int_\Omega \mathbf{div}\,\mathbf{T}dx = \int_{\partial\Omega} \mathbf{T}\mathbf{n}\,da \tag{1.17}$$

Recall that a vector is always understood as a column vector when viewed as a matrix; thus the notation $\mathbf{T}\mathbf{n}$ in the previous formula represents the column vector obtained by applying the matrix $\mathbf{T}$ to the column vector $\mathbf{n}$. This Green formula is called the divergence theorem for tensor fields . A tensor field $\mathbf{T}^\varphi = \bar{\Omega}^\varphi \to \mathbf{M}^3$ likewise satisfies:

$$\int_{\Omega^\varphi} \mathbf{div}^\varphi\,\mathbf{T}^\varphi dx^\varphi = \int_{\partial\Omega^\varphi} \mathbf{T}^\varphi\,\mathbf{n}^\varphi\,da^\varphi \tag{1.18}$$

where $\mathbf{n}^\varphi$ denotes the unit outer normal vector along the boundary of the deformed configuration.

We now come to an important definition. Let $\boldsymbol{\varphi}$ be a deformation that is injective on $\bar{\Omega}$, so that the matrix $\nabla\boldsymbol{\varphi}$ is invertible at all points of the reference configuration. Then if $\mathbf{T}^\varphi\left(\mathbf{x}^\varphi\right)$ a tensor defined at the point $\mathbf{x}^\varphi = \boldsymbol{\varphi}(\mathbf{x})$ of the deformed configuration, we associate with $\mathbf{T}^\varphi\left(\mathbf{x}^\varphi\right)$ a tensor $\mathbf{T}(\mathbf{x})$ defined at the point **x** of the reference configuration by:

$$\mathbf{T}(\mathbf{x}) := \left(\det\nabla\boldsymbol{\varphi}(x)\right)\mathbf{T}^\varphi\left(\mathbf{x}^\varphi\right)\nabla\boldsymbol{\varphi}(x)^{-T} = \mathbf{T}^\varphi\left(\mathbf{x}^\varphi\right)\mathbf{Cof}\left(\nabla\boldsymbol{\varphi}(x)\right), \quad \mathbf{x}^\varphi = \boldsymbol{\varphi}(\mathbf{x}), \tag{1.19}$$

In this fashion, a correspondence, called the Piola transform, is established between tensor fields defined over the deformed and reference configurations, respectively.

Remark. It would be equally conceivable, and somehow more natural, to start with a tensor field $\mathbf{T}:\bar{\Omega}\to\mathbf{M}^3$ and to associate with it its "inverse Piola transform $\mathbf{T}^\varphi:\bar{\Omega}^\varphi\to\mathbf{M}^3$ defined by

$$\mathbf{T}^\varphi\left(\mathbf{x}^\varphi\right) := \left(\det\nabla\boldsymbol{\varphi}(x)\right)^{-1}\mathbf{T}(\mathbf{x})\nabla\boldsymbol{\varphi}(x)^T, \quad \mathbf{x}\in\bar{\Omega}, \tag{1.20}$$

As we shall see in , the reason we proceed the other way is that the starting point in elasticity is a tensor field defined over the deformed configuration (the Cauchy stress tensor field), and it is its Piola transform over three reference configuration (the first Piola –Kirchhoff stress tensor field) that subsequently plays a key role.

As shown in the next theorem , the main interest of the Piola transform is that it yields a simple relation between the divergences of the tensors $\mathbf{T}^\varphi$ and $\mathbf{T}$ and (as a corollari) the desires relation between corresponding area elements da^φ and da.

<u>Theorem (1.1)</u> (properties of the Piola transform) : Let $\mathbf{T}:\bar{\Omega}\to\mathbf{M}^3$ denote the Piola transform of $\mathbf{T}^\varphi:\bar{\Omega}\to\mathbf{M}^3$. Then

$$\mathbf{div}\,\mathbf{T}(\mathbf{x}) = \left(\det\nabla\boldsymbol{\varphi}(x)\right) div^\varphi\mathbf{T}^\varphi\left(\mathbf{x}^\varphi\right) \quad \text{for all} \quad \mathbf{x}^\varphi = \boldsymbol{\varphi}(\mathbf{x}), \quad x\in\bar{\Omega}, \tag{1.21}$$

$$\mathbf{T}(\mathbf{x})\mathbf{n}da = \mathbf{T}^\varphi\left(\mathbf{x}^\varphi\right)\mathbf{n}^\varphi da^\varphi \quad \text{for all} \quad \mathbf{x}^\varphi = \boldsymbol{\varphi}(\mathbf{x}), \quad x\in\bar{\Omega}, \tag{1.22}$$

The area elements da and da^φ at the points $x\in\partial\Omega$ and $x^\varphi = \boldsymbol{\varphi}(x)\in\partial\Omega^\varphi$, with unit outer normal vectors **n** and $\mathbf{n}^\varphi$ respectively, are related by

$$\det\nabla\boldsymbol{\varphi}(x)\left|\nabla\boldsymbol{\varphi}(x)^{-T}\,\mathbf{n}\right|da = \left|\mathbf{Cof}\,\nabla\boldsymbol{\varphi}(x)\mathbf{n}\right|da = da^\varphi \tag{1.23}$$

Proof. The key to the proof is the Piola identity

$$\mathbf{div}\left[\left(\det\nabla\boldsymbol{\varphi}\right)\nabla\boldsymbol{\varphi}^{-T}\right] = \mathbf{div}\left(\mathbf{Cof}\,\nabla\boldsymbol{\varphi}\right) = 0 \tag{1.24}$$

Which we first prove: Showing the indices modulo 3, the elements of the matrix $\mathbf{Cof}\,\nabla\boldsymbol{\varphi}$ are given by:

$$\left(\mathbf{Cof}\,\nabla\boldsymbol{\varphi}\right)_{ij} = \partial_{j+1}\varphi_{i+1}\,\partial_{j+2}\varphi_{i+2} - \partial_{j+2}\varphi_{i+1}\,\partial_{j+1}\varphi_{i+2} \quad \text{(no summation)} \tag{1.25}$$

And a direct computation shows that

$$\partial_j\left(\left(\det\nabla\boldsymbol{\varphi}\right)\nabla\boldsymbol{\varphi}^{-T}\right)_{ij} = \partial_j\left(\mathbf{Cof}\,\nabla\boldsymbol{\varphi}\right)_{ij} = 0 \tag{1.26}$$

Then the relations

$$T_{ij}(x) = \left(\det\nabla\boldsymbol{\varphi}(x)\right)T^{\varphi}_{ik}\left(x^{\varphi}\right)\left(\nabla\boldsymbol{\varphi}(x)^{-T}\right)_{kj} \tag{1.27}$$

Imply that

$$\partial_j T_{ij}(x) = \left(\det\nabla\boldsymbol{\varphi}(x)\right)\partial_j T^{\varphi}_{ik}\left(\boldsymbol{\varphi}(x)\right)\left(\nabla\boldsymbol{\varphi}(x)^{-T}\right)_{kj}, \tag{1.28}$$

Since the other term vanishes as a consequence of the Piola identity.
Next, by the chain rule,

$$\partial_j T^{\varphi}_{ik}\left(x^{\varphi}\right) = \partial^{\varphi}_l T^{\varphi}_{ik}\left(\boldsymbol{\varphi}(x)\right)\partial_j\varphi_l(x) = \partial^{\varphi}_l T^{\varphi}_{ik}\left(x^{\varphi}\right)\left(\nabla\boldsymbol{\varphi}(x)\right)_{lj}, \tag{1.29}$$

And the relation between $\mathbf{div}\,\mathbf{T}(x)$ and $\mathbf{div}^{\varphi}\,\mathbf{T}^{\varphi}\left(x^{\varphi}\right)$ follows by noting that

$$\left(\nabla\boldsymbol{\varphi}(x)\right)_{li}\left(\nabla\boldsymbol{\varphi}(x)^{-T}\right)_{ki} = \delta_{lk} \tag{1.30}$$

Combining with the relation $dx^{\varphi} = \det\nabla\boldsymbol{\varphi}\,dx$, the divergence theorem for tensor fields expressed over arbitrary sub-domains A of $\bar{\Omega}$, and the formula for changes of variables in multiple integrals, we obtain

$$\begin{aligned}&\int_{\partial A}\mathbf{T}(\mathbf{x})\mathbf{n}\,da = \int_{A}\mathbf{div}\,\mathbf{T}(\mathbf{x})\,dx = \int_{A}\mathbf{div}^{\varphi}\,\mathbf{T}^{\varphi}(\mathbf{x})\det\nabla\boldsymbol{\varphi}\,dx = \\ &= \int_{\varphi(A)}\mathbf{div}^{\varphi}\,\mathbf{T}^{\varphi}\left(\mathbf{x}^{\varphi}\right)dx^{\varphi} = \int_{\partial\varphi(A)}\mathbf{T}^{\varphi}\left(\mathbf{x}^{\varphi}\right)\mathbf{n}^{\varphi}da^{\varphi}\end{aligned} \tag{1.31}$$

Which proves the relation $\mathbf{T}(\mathbf{x})\mathbf{n}\,da = \mathbf{T}^{\varphi}\left(\mathbf{x}^{\varphi}\right)\mathbf{n}^{\varphi}da^{\varphi}$ since the domains A are arbitrary. As a special case, we obtain the relation $\left(\det\nabla\boldsymbol{\varphi}\right)\nabla\boldsymbol{\varphi}^{-T}\mathbf{n}\,da = \mathbf{n}^{\varphi}da^{\varphi}$ between the area elements da and da^{φ} by taking the Piola transform $\left(\det\nabla\boldsymbol{\varphi}\right)\nabla\boldsymbol{\varphi}^{-T}$ of the unit tensor **I**. The relation $\left(\det\nabla\boldsymbol{\varphi}\right)\nabla\boldsymbol{\varphi}^{-T}\mathbf{n}\,da = \mathbf{n}^{\varphi}da^{\varphi}$ then follows by expressing that, since $\left|\mathbf{n}^{\varphi}\right| = 1$, da^{φ} is also the Euclidean norm of the vector that appears in the left-hand side of the relation $\left(\det\nabla\boldsymbol{\varphi}\right)\nabla\boldsymbol{\varphi}^{-T}\mathbf{n}\,da = \mathbf{n}^{\varphi}da^{\varphi}$.

Remarks.

(1) Of course, the conclusions of Theorem (1.1) still hold if we replace the set Ω by any sub-domain A of Ω, in which case the corresponding area elements and outer normal vectors are to be under-stood as being defined along the corresponding boundaries ∂A and $\partial A^{\varphi} = \boldsymbol{\varphi}(\partial A)$.

(2) While the relation between the vectors $\mathbf{div}\,\mathbf{T}$ and $\mathbf{div}^{\varphi}\,\mathbf{T}^{\varphi}$ has been established here for deformations $\boldsymbol{\varphi}$ that are twice differentiable , the relations between the area elements established in Theorem (1.1) still hold under weaker regularity assumptions on the deformation.

(3) The last equation in Theorem (1.1) shows that the unit outer normal vectors at the points $x^{\varphi} = \boldsymbol{\varphi}(x)$ and x are related by $\mathbf{n}^{\varphi} = \dfrac{\mathbf{Cof}\,\nabla\boldsymbol{\varphi}(x)\mathbf{n}}{\left|\mathbf{Cof}\,\nabla\boldsymbol{\varphi}(x)\mathbf{n}\right|}$. We now have everything at our

disposal to specify how areas are transformed: If Δ is a measurable subset of the boundary ∂A of a sub-domain A, the area of the deformed set $\Delta^{\varphi} = \varphi(\Delta)$ is given by

$$\text{Area } \Delta^{\varphi} := \int_{\Delta^{\varphi}} da^{\varphi} = \int_{\Delta} \left(\det \nabla \boldsymbol{\varphi}\right) \left| \nabla \boldsymbol{\varphi}^{-\boldsymbol{T}} \mathbf{n} \right| da \tag{1.32}$$

1.4. Length element in the deformed configuration; strain tensor

If a deformation $\boldsymbol{\varphi}$ is differentiable at a point $x \in \bar{\Omega}$, then (by definition of differentiability) we can write, for all points $x + \boldsymbol{\delta}\mathbf{x} \in \bar{\Omega}$:

$$\boldsymbol{\varphi}(x + \boldsymbol{\delta}\mathbf{x}) - \boldsymbol{\varphi}(x) = \nabla \boldsymbol{\varphi}(x)\, \boldsymbol{\delta}\mathbf{x} + o\left(\left|\boldsymbol{\delta}\mathbf{x}\right|\right), \tag{1.33}$$

and whence

$$\left|\boldsymbol{\varphi}(x + \boldsymbol{\delta}\mathbf{x}) - \boldsymbol{\varphi}(x)\right|^2 = \boldsymbol{\delta}\mathbf{x}^T \nabla \boldsymbol{\varphi}^{\boldsymbol{T}}(x) \nabla \boldsymbol{\varphi}(x)\, \boldsymbol{\delta}\mathbf{x} + o\left(\left|\boldsymbol{\delta}\mathbf{x}\right|^2\right) \tag{1.34}$$

The symmetric tensor

$$C := \nabla \boldsymbol{\varphi}^{\boldsymbol{T}} \nabla \boldsymbol{\varphi} \tag{1.35}$$

found in the above expression is called in elasticity the right Cauchy-Green strain tensor. Notice that the associated quadratic form:

$$(\boldsymbol{\xi}, \boldsymbol{\xi}) \in \mathbf{R}^3 \times \mathbf{R}^3 \to \xi^T \mathbf{C}(x) \xi = \left| \nabla \boldsymbol{\varphi}(x) \xi^2 \right| \tag{1.36}$$

is positive definite at all points $x \in \bar{\Omega}$, since the deformation gradient $\nabla \boldsymbol{\varphi}$ is every where invertible by assumption . As expected, this quadratic form is used for computing lengths: Let

$$\gamma = f(I), \quad f : I \to \bar{\Omega}, \text{ I: compact interval of } \mathbf{R} \tag{1.37}$$

be a curve in the reference configuration (Fig. 1.2) . Denoting by f_i the components of the mapping $\mathbf{f}$, the length of the curve γ is given by $(f' = df/dt)$:

$$\text{length } \gamma := \int_L \left| f'(t) \right| dt = \int_L \left\{ f'(t)\, f'(t) \right\}^{1/2} dt, \tag{1.38}$$

while the length of the deformed curve $\gamma^{\varphi} : \boldsymbol{\varphi}(\gamma)$ is given by

$$\text{length } \gamma^{\varphi} := \int_L \left| \boldsymbol{\varphi} \circ f'(t) \right| dt = \int_L \left\{ C_{ij}\left(f(t)\right) f'(t)\, f'(t) \right\}^{1/2} dt. \tag{1.39}$$

Consequently, the length elements dl and dl^{φ} in the reference and deformed configurations may be symbolically written as:

$$dl = \left\{ \mathbf{dx}^T \mathbf{dx} \right\}^{1/2}, \quad dl^{\varphi} = \left\{ \mathbf{dx}^T \mathbf{C}\, \mathbf{dx} \right\}^{1/2} \tag{1.40}$$

If in particular $\mathbf{dx} = dt\, \mathbf{e}_j$, the corresponding length element in the deformed configuration is $\left\{ \mathbf{C}_{jj} \right\}^{1/2} dt = \left| \partial_j \boldsymbol{\varphi} \right| dt$.

Remark. In the language of differential geometry, the manifold $\bar{\Omega}$ is equipped with a Riemannian structure through the data of the metric tensor $\mathbf{C} = \left(C_{ij}\right)$, often denoted $\mathbf{g} = g_{ij}$ in differential geometry , whose associated form, often denoted ds^2 ,is called the first fundamental form of the manifold. For details, see e.g. Lelong Ferrand[1963], Malliavin [1972].
Although is has no immediate geometric interpretation, the left Cauchy-green strain tensor

$$B : \nabla \boldsymbol{\varphi}\, \nabla \boldsymbol{\varphi}^{\boldsymbol{T}} \tag{1.41}$$

Which is also symmetric, is equally important; in particular, it plays an essential role in the representation theorem for the response function of the Cauchy stress tensor . For the time being, we simply notice that the two matrices $\mathbf{C} = \mathbf{F}^T \mathbf{F}$ *and* $\mathbf{B} = \mathbf{F}\, \mathbf{F}^T$ have the same characteristic polynomial, since this is true in general of the products $\mathbf{F}\,\mathbf{G}$ and $\mathbf{G}\,\mathbf{F}$ of two arbitrary matrices $\mathbf{F}$

and $\mathbf{G}$ of the same order. When $\mathbf{G} = \mathbf{F}^T$, this result is a direct consequence of the polar factorization theorem.

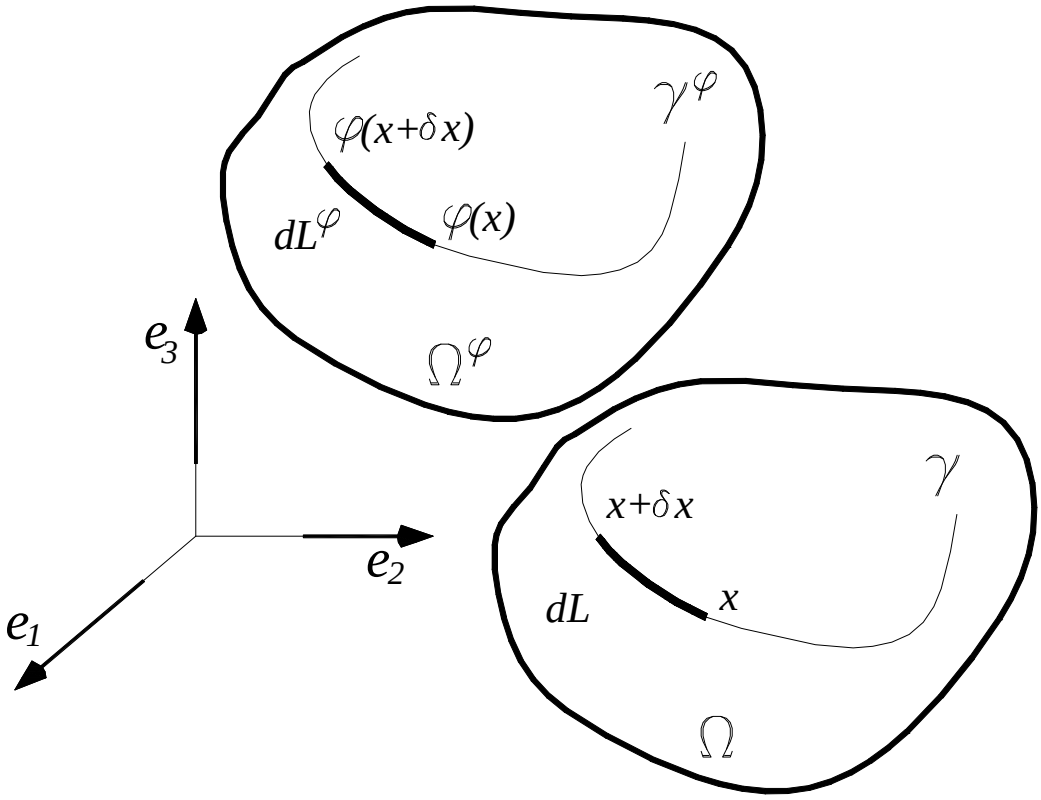

Fig. 1.2 - *The length elements* $dl = \{\mathbf{dx}^T \mathbf{dx}\}^{1/2}$ *and* $dl^{\varphi} = \{\mathbf{dx}^T \mathbf{C}\, \mathbf{dx}\}^{1/2}$ *in the reference and deformed configurations. The tensor* $\mathbf{C} = \nabla \boldsymbol{\varphi}^T \nabla \boldsymbol{\varphi}$ *is the right Cauchy-Green tensor.*

In view of showing that the tensor $\mathbf{C}$ is indeed a good measure of "strain" understood here in its intuitive sense of "change in form or size", let us first consider a class of deformations that induce no "strain":

A deformation is called a rigid deformation if it is of the form

$$\boldsymbol{\varphi}(x) = \mathbf{a} + \mathbf{Q}\, o\, \mathbf{x}, \quad \mathbf{a} \in \mathbf{R}, \quad \mathbf{Q} \in \mathbf{O}^3_+, \text{ for all } \mathbf{x} \in \bar{\Omega} \tag{1.42}$$

where $\mathbf{O}^3_+$ denotes the set of rotations in $\mathbf{R}^3$, i.e,. the set of orthogonal matrices of order 3 whose determinant is +1. In other words, the corresponding deformed configuration is obtained by rotating the reference configuration around the origin by the rotation $\mathbf{Q}$ and by translating it by the vector $\mathbf{a}$: this indeed corresponds to the idea of a "rigid" deformation, where the reference configuration is "moved", but without any "strain" (Fig. 1.3). Observe that the rotation $\mathbf{Q}$ may be performed around any point $\tilde{\mathbf{x}} \in \mathbf{R}^3$ (Fig. 1.3), since we can also write:

$$\boldsymbol{\varphi}(x) = \boldsymbol{\varphi}(\tilde{x}) + \mathbf{Q}\, \tilde{\mathbf{x}}\, \mathbf{x} \tag{1.43}$$

If $\boldsymbol{\varphi}$ is a rigid deformation , then $\nabla \boldsymbol{\varphi}(x) = \mathbf{Q} \in \mathbf{O}^3_+$ at all points $\mathbf{x} \in \bar{\Omega}$, and therefore

$$\mathbf{C} = \mathbf{I} \text{ in } \bar{\Omega}, \text{ i.e. , } \nabla \boldsymbol{\varphi}(x)^T \nabla \boldsymbol{\varphi}(x) = I \quad \text{for all } \mathbf{x} \in \bar{\Omega} \tag{1.44}$$

It is remarkable that conversely, if $\mathbf{C} = \mathbf{I}$ in $\bar{\Omega}$ and $\det \nabla \boldsymbol{\varphi} > 0$, the corresponding deformation is necessarily rigid, as we now prove under mild assumptions . We let $\mathbf{O}^n$ denote the set of all orthogonal matrices of order n.

Theorem (1.2) (characterization of rigid deformations): Let Ω be an open connected subset of $\mathbf{R}^n$, and let there be given a mapping

$$\varphi \in \mathbb{S}\left(\Omega, \mathbf{R}^n\right) \tag{1.45}$$

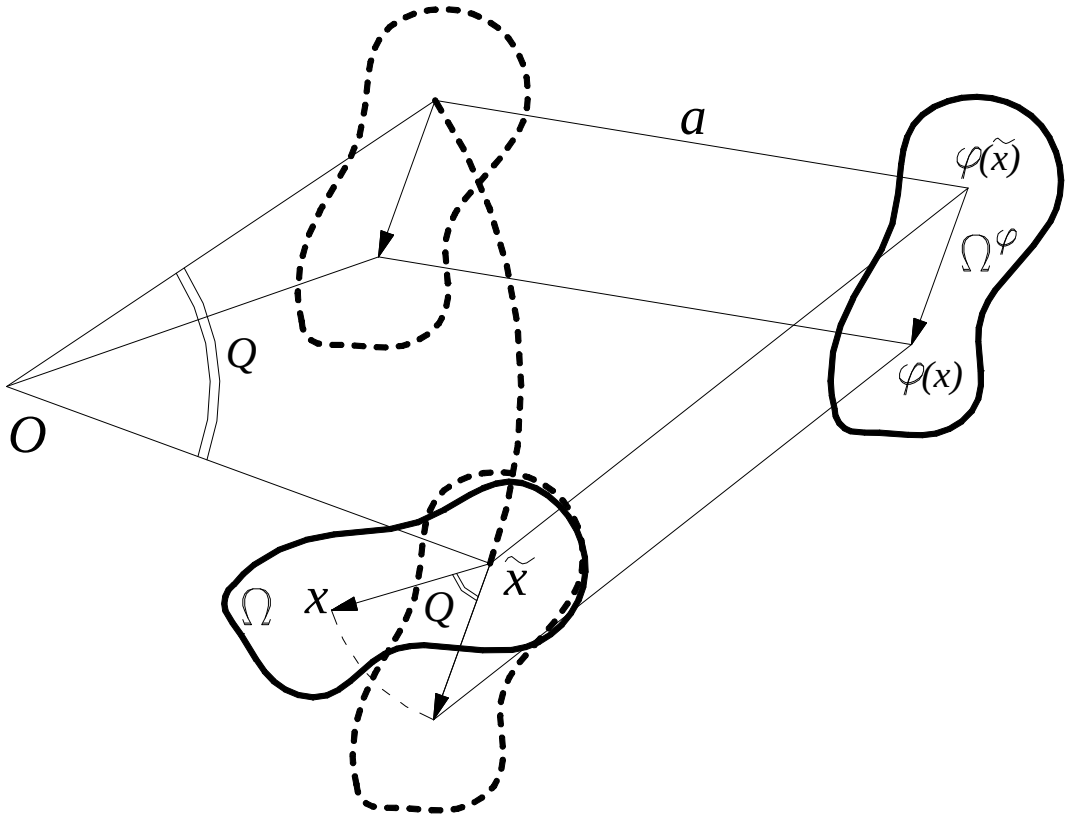

Fig. 1.3 - *A rigid deformation is a translation, followed by a rotation (or viceversa), of the reference configuration*

That satisfies

$$\nabla \boldsymbol{\varphi}(x)^{\mathbf{T}} \nabla \boldsymbol{\varphi}(x) = \mathbf{I} \text{ for all } \mathbf{x} \in \Omega \tag{1.46}$$

Then there exists a vector $\mathbf{a} \in \mathbf{R}^n$ and an orthogonal matrix $\mathbf{Q} \in \mathbf{O}^n$ such that

$$\boldsymbol{\varphi}(x) = \boldsymbol{a} + \boldsymbol{Q}\, o\, \boldsymbol{x} \quad \text{for all } \mathbf{x} \in \Omega \tag{1.47}$$

Proof . (i) Let us first establish that locally , the mapping $\boldsymbol{\varphi}$ is an isometry, i.e. given any point $x_0 \in \Omega$, there exists an open subset V such that

$$x_0 \in V \subset \Omega \text{, and } \left|\varphi(y) - \varphi(x)\right| = \left|y - x\right| \text{ fo all } x, y \in V \tag{1.48}$$

Since Ω is open, there exists $\rho > 0$, such that the open ball

$$B_\rho(x_0) := \left\{x \in \mathbf{R}^n; \left|x - x_0\right| < \rho\right\} \tag{1.49}$$

is contained in Ω. The spectral norm of an orthogonal matrix is equal to 1, since it is defined for an arbitrary square matrix A by

$$\left|A\right| := \frac{\left|\mathbf{Av}\right|}{\left|\mathbf{v}\right|} = \max_i \left\{\lambda_i\left(\mathbf{A}^T\mathbf{A}\right)\right\}^{1/2} \tag{1.50}$$

Thus we deduce from the mean value theorem (the ball $B_\rho(x_0)$ is a convex subset of Ω) that

$$\left|\boldsymbol{\varphi}(y) - \boldsymbol{\varphi}(x)\right| \le \sup_{z \in]x,y[} \left|\nabla \boldsymbol{\varphi}(x)\right| \left|y - x\right| = \left|y - x\right| \text{ for all } x, y \in B_\rho(x_0) \tag{1.51}$$

In view of proving the opposite inequality, we observe that, by the local inversion theorem, the mapping $\boldsymbol{\varphi}$ is locally invertible in Ω since the matrix $\nabla\boldsymbol{\varphi}(x)$ is invertible for all $\mathbf{x}\in\Omega$. In particular then, there exist open sets V and V^{φ} containing the points $\mathbf{x}_0$ and $\mathbf{x}_0^{\varphi}=\boldsymbol{\varphi}(x_0)$ respectively, such that the restriction of the mapping $\boldsymbol{\varphi}$ to the set V is a **S** - diffeomorphism from V onto V^{φ}, i.e., the mapping $\boldsymbol{\varphi}:V\to V^{\varphi}$ is bijective, and its inverse mapping $\boldsymbol{\psi}:V^{\varphi}\to V$ is also continuously differentiable.

Without loss of generality, we may assume that the set V is contained in the ball $B_{\rho}(x_0)$ and that the set V^{φ} is convex (otherwise we replace the set V by the inverse image by $\boldsymbol{\varphi}$ of an open ball container in $V^{\varphi}\cap\boldsymbol{\varphi}\left(B_{\rho}(x_0)\right)$ and centred at the point x_0^{φ}). Since

$$\boldsymbol{\psi}\left(\boldsymbol{\varphi}(x)\right)=x \text{ for all } x\in V \tag{1.52}$$

We deduce that the mapping $\boldsymbol{\psi}$ satisfies

$$\nabla\boldsymbol{\psi}\left(x^{\varphi}\right)=\nabla\boldsymbol{\varphi}(x)^{-1} \text{ for all } x^{\varphi}=\boldsymbol{\varphi}(x),\ x\in V \tag{1.53}$$

As a consequence, the matrix $\nabla\boldsymbol{\psi}\left(x^{\varphi}\right)$ is also orthogonal for all points $x^{\varphi}\in V^{\varphi}$. Since the set V^{φ} is convex, another application of the mean value theorem shows that

$$\left|\boldsymbol{\psi}\left(y^{\varphi}\right)-\boldsymbol{\psi}\left(x^{\varphi}\right)\right|\le\left|y^{\varphi}-x^{\varphi}\right| \text{ for all } x^{\varphi},y^{\varphi}\in V \tag{1.54}$$

This inequality can be equivalently written as

$$|y-x|\le\left|\boldsymbol{\varphi}(y)-\boldsymbol{\varphi}(x)\right| \text{ for all } x,y\in V \tag{1.55}$$

(ii) Let us next show that locally, the matrix $\nabla\boldsymbol{\varphi}$ is a constant, in the sense that the matrix $\nabla\boldsymbol{\varphi}(x)$ is independent of x for all $x\in V$. To do this, we write the property established in step (i) in the equivalent form

$$F(x,y):=\left(\varphi_k(y)-\varphi_k(x)\right)\left(\varphi_k(y)-\varphi_k(x)\right)-(y_k-x_k)(y_k-x_k)=0 \tag{1.56}$$

for all $x,y\in V$. For each $x\in V$, the function $y\in V\to G_i(x,y)$ is differentiable, with

$$G_i(x,y):=\frac{1}{2}\frac{\partial F}{\partial y_i}(x,y)=\frac{\partial\varphi_k}{\partial y_i}(y)\left(\varphi_k(y)-\varphi_k(x)\right)-\delta_{ik}(y_k-x_k)=0 \tag{1.57}$$

For all, $x,y\in V$. For each $y\in V$, each function $x\in V\to G_i(x,y)$ is differentiable , with

$$\frac{\partial G_i}{\partial x_j}(x,y)=-\frac{\partial\varphi_k}{\partial y_i}(y)\frac{\partial\varphi_k}{\partial x_i}(x)+\delta_{ij}=0, \tag{1.58}$$

i.e.,

$$\nabla\boldsymbol{\varphi}(x)^{\mathbf{T}}\nabla\boldsymbol{\varphi}(x)=\mathbf{I} \quad \text{for all } x,y\in V. \tag{1.59}$$

Letting $y=x_0$, we obtain

$$\nabla\boldsymbol{\varphi}(x)=\nabla\boldsymbol{\varphi}(x_0) \text{ for all } x\in V. \tag{1.60}$$

(iii) It follows from step (ii) that the mapping $\nabla\boldsymbol{\varphi}:\Omega\to M^3$ is differentiable and that its derivative vanishes in Ω; equivalently, the mapping $\boldsymbol{\varphi}$ is twice differentiable and its second Frechet derivative vanishes. Because the set Ω is connected(this assumption has not been used so far), a classical result from differential calculus (see e.g. Schwartz [1967, p.266]) shows that the mapping $\boldsymbol{\varphi}$ is necessarily of the form

$$\boldsymbol{\varphi}(x)=\boldsymbol{a}+\boldsymbol{Q}\,o\,\boldsymbol{x} \quad \mathbf{a}\in\mathbf{R}^n,\mathbf{Q}\in\mathbf{M}^n \text{ for all } \mathbf{x}\in\Omega \tag{1.61}$$

So that its gradient $\mathbf{Q}$ is the same constant $\nabla\boldsymbol{\varphi}(x_0)$ in all the set Ω. Thus the matrix $\mathbf{Q}=\nabla\boldsymbol{\varphi}(x_0)$ is orthogonal since $\nabla\boldsymbol{\varphi}(x_0)^{\mathbf{T}}\nabla\boldsymbol{\varphi}(x_0)=\mathrm{I}$ by assumption.

Remark. If we are provided with the additional assumption that $\det \nabla \boldsymbol{\varphi}(x) > 0$ for at least one point $\mathbf{x} \in \Omega$ (and consequently for all points in the connected set Ω), we can conclude that the orthogonal matrix $\mathbf{Q}$ obtained in the theorem is a rotation (i.e., $\det \mathbf{Q} = 1$). Notice also that if the mapping $\boldsymbol{\varphi}$ is continuous up to the boundary, the relation $\boldsymbol{\varphi}(x) = \boldsymbol{a} + \boldsymbol{Q}\, o\, \boldsymbol{x}$ holds for all points $\mathbf{x} \in \bar{\Omega}$.

The result of theorem (1.2) can be viewed as a special case (let $\boldsymbol{\psi}$ be any rigid deformation in Theorem (1.3) of the following result, which shows that two deformations corresponding to the same tensor **C** can be obtained from one another by composition with a rigid deformation.

Theorem (1.3) : Let Ω be an open connected subset of $\mathbf{R}^n$, and let here be given two mappings

$$\boldsymbol{\varphi}, \boldsymbol{\psi} \in \mathbf{S}\left(\Omega; \mathbf{R}^n\right) \tag{1.62}$$

Such that

$$\nabla \boldsymbol{\varphi}(\boldsymbol{x})^T \cdot \nabla \boldsymbol{\varphi}(\boldsymbol{x}) = \nabla \boldsymbol{\psi}(\boldsymbol{x})^T \cdot \nabla \boldsymbol{\psi}(\boldsymbol{x}) \text{ for all } x \in \Omega, \tag{1.63}$$

$$\psi : \Omega \to \mathbf{R}^n \text{ is injective, and let } \nabla \boldsymbol{\psi}(\boldsymbol{x}) \neq 0 \quad \text{for all } x \in \Omega.$$

Then here exist a vector $a \in \mathbf{R}^n$ *and an orthogonal matrix* $\mathbf{Q} \in O^n$ *such that :*

$$\boldsymbol{\varphi}(x) = \boldsymbol{a} + \boldsymbol{Q}\boldsymbol{\psi}(\mathbf{x}) \quad \text{for all } x \in \Omega. \tag{1.64}$$

Proof. Since the mapping $\boldsymbol{\psi}$ is injective and let $\nabla \boldsymbol{\psi}(\boldsymbol{x}) \neq 0$ for all $x \in \Omega$, the inverse mapping

$$\boldsymbol{\psi^{-1}} : \boldsymbol{\psi}(\Omega) \to \Omega \tag{1.65}$$

Is also continuously differentiable and it satisfies

$$\nabla \boldsymbol{\psi^{-1}}(\boldsymbol{\xi}) \nabla \boldsymbol{\psi} = \boldsymbol{I} \text{ for all } \boldsymbol{\xi} = \boldsymbol{\psi}(\mathbf{x}), \quad x \in \Omega \tag{1.66}$$

Besides, the set $\boldsymbol{\psi}(\Omega)$ is open by the invariance of domain theorem , and connected since it is the image of a connected set by a continuous mapping. The composite mapping

$$\theta := \varphi \circ \psi^{-1} : \psi(\Omega) \to \mathbf{R}^n \tag{1.67}$$

Is such that

$$\nabla \boldsymbol{\theta}(\xi) := \nabla \varphi(\mathbf{x}) \cdot \nabla \psi(\xi)^{-1} = \nabla \varphi(\mathbf{x}) \cdot \nabla \psi(x)^{-1} \text{ for all } \boldsymbol{\xi} = \boldsymbol{\psi}(\mathbf{x}), \quad x \in \Omega, \tag{1.68}$$

and consequently , by assumption,

$$\nabla \boldsymbol{\theta}(\boldsymbol{\xi})^T \nabla \boldsymbol{\theta}(\boldsymbol{\xi}) = \nabla \boldsymbol{\psi}(\mathbf{x})^{-T} \nabla \varphi(\mathbf{x})^T \nabla \varphi(\mathbf{x}) \nabla \boldsymbol{\psi}(\mathbf{x})^{-1} = \mathbf{I} \text{ for all } \boldsymbol{\xi} = \boldsymbol{\psi}(\mathbf{x}), \quad x \in \Omega, \tag{1.69}$$

We may therefore apply Theorem 1 to the mapping $\boldsymbol{\theta}$: There exists a vector $a \in \mathbf{R}^n$ and an orthogonal matrix $\mathbf{Q} \in O^n$ such that

$$\boldsymbol{\theta}(\boldsymbol{\xi}) = \mathbf{a} + \mathbf{Q} \circ \boldsymbol{\xi} \text{ for all } \boldsymbol{\xi} = \boldsymbol{\psi}(\mathbf{x}), \quad x \in \Omega \tag{1.70}$$

But this is just another equivalent statement of the conclusion of the theorem.

The previous two theorems are useful for understanding the role played by the tensor C. First, theorem 1.1 shows that the difference:

$$2\mathbf{E} := \mathbf{C} - \mathbf{I} \tag{1.71}$$

Is a measure of the "deviation" between a given deformation and a rigid deformation, since $\mathbf{C} = \mathbf{I}$ if and only if the deformation is rigid. Secondly, theorem 1.3 shows that the knowledge of the tensor field $\mathbf{C} : \Omega \to \mathbf{S}^3_>$ completely determines the deformation, up to composition with rigid deformations (the question of proving the existence of deformations for which the associated tensor field $\mathbf{C} : \Omega \to \mathbf{S}^3_>$ is equal to a given tensor field is quite another matter. These considerations are illustrated in figure 1.4. The tensor $\mathbf{E}$ is called the Green-St Venant strain tensor. Expressed in terms of the displacement gradient $\nabla \mathbf{u}$, in lieu of the deformation gradient $\nabla \boldsymbol{\varphi} = \mathbf{I} + \nabla \mathbf{u}$ (recall that $\boldsymbol{\varphi} = \mathbf{id} + \mathbf{u}$), the strain tensor $\mathbf{C}$ becomes

$$\mathbf{C} = \nabla \boldsymbol{\varphi}^T \nabla \boldsymbol{\varphi} = \mathbf{I} + \nabla \mathbf{u}^T + \nabla \mathbf{u} + \nabla \mathbf{u}^T \nabla \mathbf{u} = \mathbf{I} + 2\mathbf{E} \tag{1.72}$$

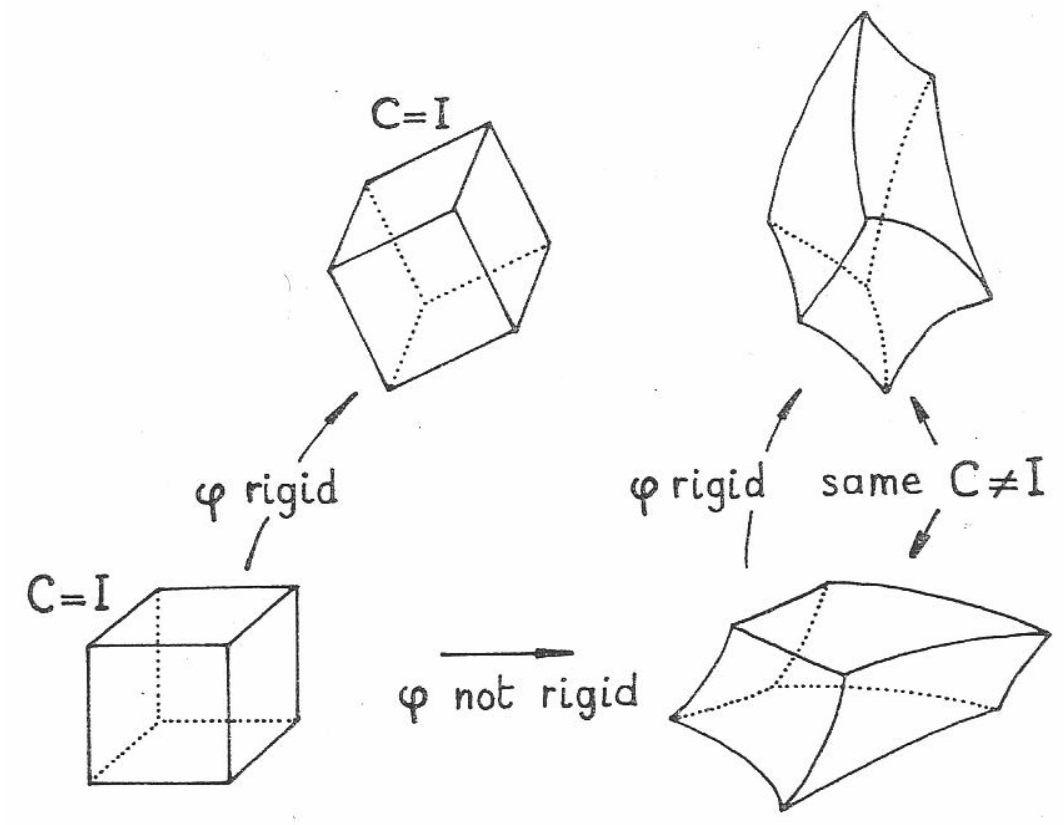

Fig. 1.4 - *The right Cauchy-Green tensor* $\mathbf{C}$ *is equal to* $\mathbf{I}$ *if and only if the deformation is rigid. Two deformations corresponding to the same tensor C differ by a rigid deformation.*

With

$$\mathbf{E}(\mathbf{u}) := \mathbf{E} = \frac{1}{2}\left(\nabla\mathbf{u}^T + \nabla\mathbf{u} + \nabla\mathbf{u}^T\nabla\mathbf{u}\right) \tag{1.73}$$

For future use, we record the formulas:

$$C_{ij} = \partial_i\varphi_k\partial\varphi_k, \quad E_{ij} = \frac{1}{2}\left(\partial_i u_j + \partial_j u_i + \partial_i u_k \partial_j u_k\right) \tag{1.74}$$

where $\boldsymbol{\varphi} = \varphi_i\mathbf{e}_i$, $\mathbf{u} = u_i\mathbf{e}_i$

Remarks.

(1) Both theorems 1.2 and 1.3 can be rephrased in terms of the Green-St Venant strain tensor, using the equivalences

$$\nabla\boldsymbol{\varphi}^T\nabla\boldsymbol{\varphi} = \mathbf{I} \text{ in } \Omega \Leftrightarrow \mathbf{E}(\mathbf{u}) = \mathbf{0} \text{ in } \Omega,\ \boldsymbol{\varphi} = \mathbf{id} + \mathbf{u}, \quad \boldsymbol{\psi} = \mathbf{id} + \mathbf{v}, \tag{1.75}$$

$$\nabla\boldsymbol{\varphi}^T\nabla\boldsymbol{\varphi} = \nabla\boldsymbol{\psi}^T\nabla\boldsymbol{\psi} \text{ in } \Omega \Leftrightarrow \mathbf{E}(\mathbf{u}) = \mathbf{E}(\mathbf{v}) \text{ in } \Omega,\ \boldsymbol{\varphi} = \mathbf{id} + \mathbf{u}, \quad \boldsymbol{\psi} = \mathbf{id} + \mathbf{v}, \tag{1.76}$$

(2) The introduction of the factor ½ in the definition of the tensor $\mathbf{E}$ is motivated by the requirement that its "first order" part $\frac{1}{2}\left(\nabla\mathbf{u}^T + \nabla\mathbf{u}\right)$ coincide with the linearized strain tensor , which played a key role in the earlier linearized theories that prevailed in elasticity. Besides, the tensor $\left(\mathbf{C}^{1/2} - \mathbf{I}\right)$ was sometimes advocated a san alternative measure of strain and the factor ½ had the effect that the first order parts of both tensor $\mathbf{E}$ and $\left(\mathbf{C}^{1/2} - \mathbf{I}\right)$ coincide.

(3) The tensor $\mathbf{E}$ is also known in the literature as the Green-Lagrange strain tensor, or the Almansi strain tensor . Let us finally identify the subset of $\mathbf{S}^3$ spanned by the Green-St Venant strain tensor $\mathbf{E} = \frac{1}{2}\left(\mathbf{F}^T\mathbf{F} + \mathbf{I}\right)$ when the matrix $\mathbf{F}$ varies in the set $\mathbf{M}^3_+$:

Theorem 1.4 The set

$$\mathbf{V}(\mathbf{0}) := \left\{ \frac{1}{2}\left(\mathbf{F}^T\mathbf{F} - \mathbf{I}\right) \in \mathbf{S}^3; \quad \mathbf{F} \in \mathbf{M}^3_+ \right\} \tag{1.77}$$

Is a neighbourhood of the origin in $\mathbf{S}^3$.

Proof . Since any matrix $\mathbf{C} \in \mathbf{S}^3_>$ can be written as $\mathbf{C} = \mathbf{C}^{1/2}\mathbf{C}^{1/2}$, the set $\mathbf{V}(\mathbf{0})$ can be also written as

$$\mathbf{V}(\mathbf{0}) := \left\{ \frac{1}{2}(\mathbf{C} - \mathbf{I}) \in \mathbf{S}^3; \quad \mathbf{C} \in \mathbf{S}^3_> \right\} = f^{-1}\left(\mathbf{S}^3_>\right), \tag{1.78}$$

where f is the continuous mapping $f : \mathbf{E} \in \mathbf{S}^3 \to (\mathbf{I} + 2\mathbf{E}) \in \mathbf{S}^3$. Since the set $\mathbf{S}^3_>$ is open $\mathbf{S}^3$ and since $\mathbf{0} \in V(\mathbf{0})$, the conclusion follows.

1.5. References

[1] Boley, B.A.,Weiner, J.H., *Theory of thermal stresses*, Dover publications, inc. Mineola, New York

[2] Ciarlet, Philiphe G., *Mathematical Elasticity, Volume I.: Three dimensional elasticity*, Elsevier Science Publishers B.V.

[3] Gurtin, M. E., *The Linear Theory of Elasticity, Handbbuch der Physik*, Springer, Berlin, 1972.

[4] Lekhnitskii, S. G., *Theory of Elasticity of an Anisotropic Body*, Mir, Moscow, 1981.

[5] Love, A. E. H., *A Treatise on the Mathematical Theory of Elasticity*, Dover Publications, Inc, New York, 1944

[6] Nunziante, L., Gambarotta, L., Tralli, A., *Scienza delle Costruzioni*, 3° Edizione, McGraw-Hill, 2011, ISBN: 9788838666971

[7] Ting TCT. *Anisotropic elasticity - Theory and applications*. Oxford University Press; 1996.

[8] Wolfram, S., *Mathematica, version 8*, Wolfram Research, Inc., Champaign, IL, 1998–2005.

CHAPTER II
STATIC FOUNDATIONS

2.1. The equations of equilibrium

A body occupying a deformed configuration $\bar{\Omega}^{\varphi}$, and subjected to applied body forces in its interior Ω^{φ} and to applied surfaces forces on a portion $\Gamma_1^{\varphi} = \varphi(\Gamma_1)$ of its boundary , is in static equilibrium if the fundamental stress principle of Euler and Cauchy is satisfied. This axiom, which is the basis of continuum mechanics, implies the celebrated Cauchy theorem , according to which there exists a symmetric tensor field $\mathbf{T}^{\varphi} : \bar{\Omega}^{\varphi} \to \mathbf{S}^3$ such that

$$\begin{cases} -div^{\varphi}\mathbf{T}^{\varphi} = \mathbf{f}^{\varphi} & in \quad \Omega^{\varphi} \\ \mathbf{T}^{\varphi}\mathbf{n}^{\varphi} = \mathbf{g}^{\varphi} & in \quad \Gamma_1^{\varphi} \end{cases} \tag{2.1}$$

where $\mathbf{f}^{\varphi}$ and $\mathbf{g}^{\varphi}$ are the densities of the applied body and surface forces respectively, and $\mathbf{n}^{\varphi}$ is the unit outer normal vector along Γ_1^{φ}. These equation are called the equilibrium over the deformed configuration , and the tensor $\mathbf{T}^{\varphi}$ is called the Cauchy stress tensor.

A remarkable feature of these equations is their "divergence structure", which makes them amenable to a variational formulation ; a disadvantage is that they are expressed in terms of the unknown $\mathbf{x}^{\varphi} = \varphi(\mathbf{x})$. In order to obviate this difficulty while retaining the divergence structure of the equations, we use the Piola transform $\mathbf{T} : \bar{\Omega} \to \mathbf{M}^3$ of the Cauchy stress tensor field, which is defined by $\mathbf{T}(\mathbf{x}) = \mathbf{T}^{\varphi}(\mathbf{x}^{\varphi}) Cof \nabla\boldsymbol{\varphi}(\mathbf{x})$. In this fashion, it is found that the equilibrium equations over $\bar{\Omega}^{\varphi}$ are equivalent to the equilibrium equations over the reference configuration $\bar{\Omega}$,

$$\begin{cases} -div\,\mathbf{T} = \mathbf{f} & in \quad \Omega \\ \mathbf{T}\mathbf{n} = \mathbf{g} & in \quad \Gamma_1 \end{cases} \tag{2.2}$$

Where $\mathbf{n}$ denotes the unit outer normal vector along Γ_1, and the fields $\mathbf{f} : \Omega \to \mathbf{R}^3$ and $\mathbf{g} : \Gamma_1 \to \mathbf{R}^3$ are related to the fields $\mathbf{f}^{\varphi} : \Omega^{\varphi} \to \mathbf{R}^3$ and $\mathbf{g}^{\varphi} : \Gamma_1^{\varphi} \to \mathbf{R}^3$ by the simple formulas $\mathbf{f}\,dx = \mathbf{f}^{\varphi}dx^{\varphi}$ and $\mathbf{g}\,dx = \mathbf{g}^{\varphi}dx^{\varphi}$. Because they are still in divergence form, these equations can be given a variational formulation, known as the principle of virtual work. This principle plays a key role as the starting point of the theory of hyperelastic materials , as well in the asymptotic theory of two-dimensional plate models.

The tensor $\mathbf{T}$ is called the first Piola-Kirchhoff stress tensor. We also introduce the symmetric second Piola-Kirchhoff stress tensor $\boldsymbol{\Sigma} = \nabla\boldsymbol{\varphi}^{-1}\mathbf{T}$, which naturally arises in the expression of the constitutive equations of elastic materials.

We conclude this chapter by describing various realistic examples of applied forces, corresponding to densities $\mathbf{f}$ and $\mathbf{g}$ of the form

$$\mathbf{f}(\mathbf{x}) = \hat{\mathbf{f}}(\mathbf{x}, \boldsymbol{\varphi}(\mathbf{x})), \quad x \in \Omega, \quad \text{and} \quad \mathbf{g}(\mathbf{x}) = \hat{\mathbf{g}}(\mathbf{x}, \boldsymbol{\varphi}(\mathbf{x})), \quad x \in \Gamma_1 \tag{2.3}$$

For given mapping $\hat{\mathbf{f}}$ and $\hat{\mathbf{g}}$.

We assume that in the deformed configuration $\bar{\Omega}^{\varphi}$ associated with an arbitrary deformation φ, the body is subjected to applied forces of two types:

(i) applied body forces , defined by a vector field

$$\boldsymbol{f}^{\varphi} := \Omega^{\varphi} \to \mathbf{R}^3, \tag{2.4}$$

Called the density of the applied body forces per unit volume in the deformed configuration ;

(ii) applied surface forces, defined by a vector field

$$\boldsymbol{g}^{\varphi} := \Omega^{\varphi} \to R^3, \tag{2.5}$$

on a da^{φ}-measurable subset Γ_1^{φ} of the boundary

$$\Gamma^{\varphi} := \partial\Omega^{\varphi}, \tag{2.6}$$

called the density of the applied surface force per unit area in the deformed configuration.
Let $\rho^\varphi : \Omega^\varphi \to \mathbf{R}$ denote the mass density in the deformed configuration , so that the mass of every dx^φ - measurable subset A^φ of $\bar{\Omega}^\varphi$ is given by the integral $\int_{A^\varphi} \rho^\varphi\left(x^\varphi\right) dx^\varphi$. We assume that

$$\rho^\varphi\left(x^\varphi\right) > 0 \text{ for all } x^\varphi \in \Omega^\varphi \tag{2.7}$$

The applied body forces can be equivalently defined by their density $\mathbf{b}^\varphi : \Omega^\varphi \to \mathbf{R}^3$ per unit mass in the deformed configuration, which is related to the density $\mathbf{f}^\varphi$ by the equation

$$f^\varphi = \rho^\varphi \mathbf{b}^\varphi \tag{2.8}$$

The applied forces describe the action of the outside world on the body: An elementary force $\mathbf{f}^\varphi\left(x\right) dx^\varphi$ is exerted on the elementary volume dx^φ at each point x^φ of the deformed configuration. For example, this is the case of the gravity field, for which $\mathbf{f}^\varphi\left(x^\varphi\right) = -g\rho^\varphi\left(x^\varphi\right)\mathbf{e}_3$ for all $x^\varphi \in \Omega^\varphi$ (assuming that the vector $\mathbf{e}_3$ is vertical and oriented "upward"), where g is the gravitational constant. Another example is given by the action of electrostatic forces
Likewise, an elementary force $\boldsymbol{g}^\varphi\left(x^\varphi\right) da^\varphi$ is exerted on the elementary area da^φ at each point x^φ of the subset Γ_1^φ of the boundary of the deformed configuration (Fig 2.1). Such forces generally represent the action of another body (whatever its nature its may be) along the portion Γ_1^φ of the boundary.

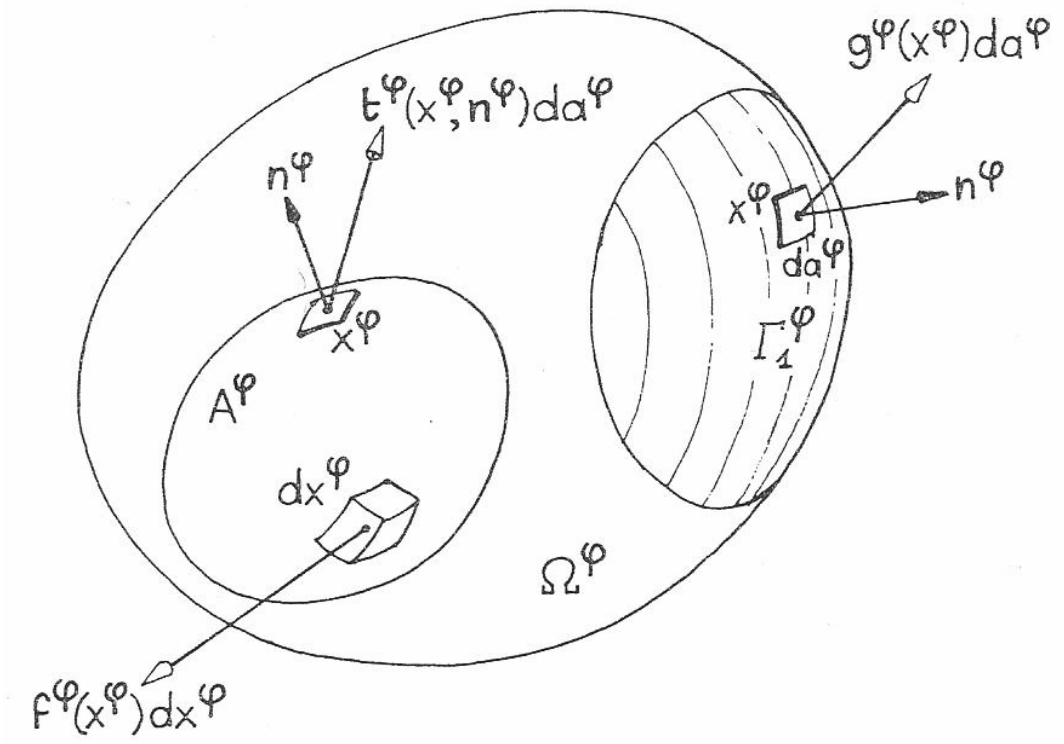

Fig. 2.1 – *Applied forces comprise applied body forces* $\mathbf{f}^\varphi\left(x\right) dx^\varphi$, $x^\varphi \in \Omega^\varphi$ *and applied surface forces* $\mathbf{g}^\varphi\left(x\right) dx^\varphi$, $x^\varphi \in \Gamma_1^\varphi$. *The stress principle of Euler and Cauchy asserts in addition the existence of elementary surface forces* $\mathbf{t}^\varphi\left(\mathbf{x}^\varphi, \mathbf{n}^\varphi\right) da^\varphi$, $x^\varphi \in \partial A^\varphi$, *along the boundary* ∂A^φ, *with unit outer normal vector* $\mathbf{n}^\varphi$, *of any sub-domain* A^φ *of the deformed configuration* $\bar{\Omega}^\varphi$.

Remark. In order to avoid introducing too many notations, we use the same symbol to denote distinct quantities in the same figure. For instance in Fig. 2.1 the symbol x^φ stands for three

different points, and the symbols da^φ and $\mathbf{n}^\varphi$ stand for two different area elements and normal vectors. Applied surface forces that are only "partially" specified (for instance, only the normal component $\mathbf{g}^\varphi(x)\cdot\mathbf{n}^\varphi$ could be prescribed along Γ_1^φ) are not excluded from our analysis, and indeed, examples of such "intermediate" cases are considered; but in order to simplify the exposition , we solely considered at this stage the "extreme" cases where either the density $\mathbf{g}^\varphi$ is fully known on Γ_1^φ, or is left completely unspecified, as on the remaining portion

$$\Gamma_0^\varphi := \Gamma^\varphi - \Gamma_1^\varphi \tag{2.9}$$

Of the boundary of the deformed configuration. This being the case, we shall see that it is the deformation itself that should be specified on the corresponding portion $\Gamma_0 := \varphi^{-1}\left(\Gamma_0^\varphi\right)$ of the boundary of the reference configuration, in order that the problem be well posed.

2.2. The stress principle of Euler and Cauchy

Continuum mechanics for static problems is founded on the following axiom, named after the fundamental contributions of Euler [1757,1771] and Cauchy [1823,1827]; for a brief story, see footnote (1) in Truesdell & Toupin [1960, sect. 200]. The exterior product in $\mathbf{R}^3$ is denoted $\wedge$.

Axiom 1 (stress principle of Euler and Cauchy) Consider a body occupying a deformed configuration $\bar{\Omega}^\varphi$, and subjected to applied forces represented by densities $\boldsymbol{f}^\varphi := \Omega^\varphi \to R^3$, and $\boldsymbol{g}^\varphi := \Omega^\varphi \to \mathbf{R}^3$. Then there exists a vector field

$$\mathbf{t}^\varphi : \Omega^\varphi \times S_1 \to R^3, \text{ where } S_1 = \left\{v \in \mathbb{R}^3; |\mathbf{v}| = 1\right\} \tag{2.10}$$

Such that:

(a) For any sub-domain A^φ of $\bar{\Omega}^\varphi$, and at any point $\mathbf{x}^\varphi \in \Gamma_1^\varphi \cap \partial A^\varphi$ where the unit outer normal vector $\mathbf{n}^\varphi$ to $\Gamma_1^\varphi \cap \partial A^\varphi$ exists : $\mathbf{t}^\varphi\left(\mathbf{x}^\varphi, \mathbf{n}^\varphi\right) = \mathbf{g}^\varphi\left(\mathbf{x}^\varphi\right)$

(b) Axiom of force balance: For any sub-domain A^φ of $\bar{\Omega}^\varphi$:

$$\int_{A^\varphi} \mathbf{f}^\varphi\left(\mathbf{x}^\varphi\right) dx^\varphi + \int_{\partial A^\varphi} \mathbf{t}^\varphi\left(\mathbf{x}^\varphi, \mathbf{n}^\varphi\right) dx^\varphi = \mathbf{0}, \tag{2.11}$$

where $\mathbf{n}^\varphi$ denotes the unit outer normal vector along ∂A^φ

(c) Axiom of moment balance : For any sub-domain A^φ of $\bar{\Omega}^\varphi$:

$$\int_{A^\varphi} \mathbf{ox}^\varphi \wedge \mathbf{f}^\varphi\left(\mathbf{x}^\varphi\right) dx^\varphi + \int_{\partial A^\varphi} \mathbf{ox}^\varphi \wedge \mathbf{t}^\varphi\left(\mathbf{x}^\varphi, \mathbf{n}^\varphi\right) dx^\varphi = \mathbf{0} \tag{2.12}$$

The stress principle thus first asserts the existence of elementary surface forces $\mathbf{t}^\varphi\left(\mathbf{x}^\varphi, \mathbf{n}^\varphi\right) da^\varphi$ along the boundaries of all domains of the reference configuration (Fig.2.1).

Secondly, the stress principle asserts that at a point $\mathbf{x}^\varphi$ of the boundary ∂A^φ of a sub-domain A^φ, the elementary surface force depends on the sub-domain A^φ, only via the normal vector $\mathbf{n}^\varphi$ to ∂A^φ at $\mathbf{x}^\varphi$. While it would be equally conceivable a priori that the elementary surface force at $\mathbf{x}^\varphi$ be also dependent on other geometrical properties of the sub-domain A^φ, for instance the curvature of ∂A^φ at $\mathbf{x}^\varphi$, etc. , it is possible to rigorously rule out such further geometrical dependences by constructing a general theory of surfaces forces, as shown by Noll [1959] (see also Gurtin & Williams [1967], Ziemer [1983])

Thirdly, the stress principle asserts that any sub-domain A^φ of the deformed configuration $\bar{\Omega}^\varphi$, including $\bar{\Omega}^\varphi$ itself, is in static equilibrium, in the sense that the torsor formed by the elementary forces $\mathbf{t}^\varphi\left(\mathbf{x}^\varphi, \mathbf{n}^\varphi\right) da^\varphi$, $x^\varphi \in \partial A^\varphi$, $\mathbf{n}^\varphi$ normal to ∂A^φ at $\mathbf{x}^\varphi$, and the body forces $\mathbf{f}^\varphi\left(\mathbf{x}^\varphi\right) d\mathbf{x}^\varphi$, $\mathbf{x}^\varphi \in A^\varphi$, is equivalent to zero. This means that its resultant vector vanishes (axiom of force balance) and that its resulting moment with respect to the origin (and thus with respect to any other point, by a classical property of torsos) vanishes (axiom of moment balance).

Hence the stress principle mathematically express, in the form of an axiom, the intuitive idea that the static equilibrium of any sub-domain A^φ of $\bar{\Omega}^\varphi$, already subjected to given applied body forces $\mathbf{f}^\varphi\left(\mathbf{x}^\varphi\right)d\mathbf{x}^\varphi, \mathbf{x}^\varphi \in A^\varphi$, and (possibly) to given applied surface forces $\mathbf{g}^\varphi\left(\mathbf{x}^\varphi\right)da^\varphi$ at those points $\mathbf{x}^\varphi \in \Gamma_1^\varphi \cap \partial A^\varphi$ where the outer normal vector to $\Gamma_1^\varphi \cap \partial A^\varphi$ exists, is made possible by the added effect of elementary surfaces forces of the specific form indicated, acting on the remaining part of the boundary ∂A^φ.

Remark. Gurtin [1981a, 1981b] calls system of forces the set formed by the applied bodu forces, corresponding to the vector field $\boldsymbol{f}^\varphi := \Omega^\varphi \to \mathbf{R}^3$, and by the surface forces, corresponding to the vector field $\boldsymbol{t}^\varphi := \Omega^\varphi \times S_1 \to \mathbf{R}^3$.

Let $\mathbf{x}^\varphi$ be a point of the deformed configuration. The vector $\mathbf{t}^\varphi\left(\mathbf{x}^\varphi, \mathbf{n}^\varphi\right)$ is called the Cauchy stress vector across an oriented surface element with normal $\mathbf{n}^\varphi$, or the density of the surface force per unit area in the deformed configuration.

2.3. Cauchy's theorem; The Cauchy stress tensor

We now derive consequences of paramount importance from the stress principle. The first one, due to Cauchy [1823,1827a] , is one of the most important results in continuum mechanics. It asserts that the dependence of the Cauchy stress vector $\mathbf{t}^\varphi\left(\mathbf{x}^\varphi, \mathbf{n}^\varphi\right)$ with respect to its second argument $\mathbf{n} \in S_1$ is linear, i.e., at each point $\mathbf{x}^\varphi \in \Omega^\varphi$, there exists a tensor $\mathbf{T}^\varphi\left(\mathbf{x}^\varphi\right) \in \mathbf{M}^3$ such that $\mathbf{t}^\varphi\left(\mathbf{x}^\varphi, \mathbf{n}^\varphi\right) = \mathbf{T}^\varphi\left(\mathbf{x}^\varphi\right)\mathbf{n}$ for all $\mathbf{n} \in S_1$; the second one asserts that at each point $\mathbf{x}^\varphi \in \Omega^\varphi$, the tensor $\mathbf{T}^\varphi\left(\mathbf{x}^\varphi\right)$ is symmetric; the third one, again due to Cauchy [1827b, 1828], is that the tensor field $\mathbf{T}^\varphi : \Omega^\varphi \to \mathbf{M}^3$ and the vector fields $\boldsymbol{f}^\varphi := \Omega^\varphi \to R^3$, and $\boldsymbol{g}^\varphi := \Gamma_1^\varphi \to \mathbf{R}^3$ are related by a partial differential equation in Ω^φ, and by a boundary condition on Γ_1^φ, respectively.

Theorem 2.1 (Cauchy's theorem): Assume that the applied body force density $\boldsymbol{f}^\varphi := \Omega^\varphi \to \mathbf{R}^3$, is continuous, and that the Cauchy stress vector field

$$\mathbf{t}^\varphi : \left(\mathbf{x}^\varphi, \mathbf{n}^\varphi\right) \in \bar{\Omega}^\varphi \times S_1 \to \mathbf{t}^\varphi\left(\mathbf{x}^\varphi, \mathbf{n}\right) \in \mathbf{R}^3 \tag{2.13}$$

Is continuously differentiable with respect to the variable $\mathbf{x}^\varphi \in \bar{\Omega}^\varphi$ for each $\mathbf{n} \in S_1$ and continuous with respect to the variable $\mathbf{n} \in S_1$ for each $\mathbf{x}^\varphi \in \bar{\Omega}^\varphi$. Then the axioms of force and moment balance imply that there exists a continuously differentiable tensor field

$$\mathbf{T}^\varphi : \mathbf{x}^\varphi \in \bar{\Omega}^\varphi \to \mathbf{T}^\varphi\left(\mathbf{x}^\varphi\right) \in \mathbf{M}^3, \tag{2.14}$$

such that the Cauchy stress vector satisfies

$$\mathbf{t}^\varphi\left(\mathbf{x}^\varphi, \mathbf{n}\right) = \mathbf{T}^\varphi\left(\mathbf{x}^\varphi\right)\mathbf{n} \quad \text{for all } \mathbf{x}^\varphi \in \bar{\Omega}^\varphi \text{ and all } \mathbf{n} \in S_1 \tag{2.15}$$

and such that

$$-div^\varphi \mathbf{T}^\varphi\left(\mathbf{x}^\varphi\right) = \mathbf{f}^\varphi\left(\mathbf{x}^\varphi\right) \text{ for all } \mathbf{x}^\varphi \in \Omega^\varphi, \tag{2.16}$$

$$\mathbf{T}^\varphi\left(\mathbf{x}^\varphi\right) = \mathbf{T}^\varphi\left(\mathbf{x}^\varphi\right)^T \text{ for all } \mathbf{x}^\varphi \in \bar{\Omega}^\varphi, \tag{2.17}$$

$$\mathbf{T}^\varphi\left(\mathbf{x}^\varphi\right)\mathbf{n}^\varphi = \mathbf{g}^\varphi\left(\mathbf{x}^\varphi\right) \text{ for all } \mathbf{x}^\varphi \in \Gamma_1^\varphi \tag{2.18}$$

where $\mathbf{n}^\varphi$ is the unit outer normal vector along Γ_1^φ.

Proof. Let $\mathbf{x}^\varphi$ be a fixed point in Ω^φ. Because the set Ω^φ is open, we can find, as a particular sub-domain of $\bar{\Omega}^\varphi$, a tetrahedron T with vertex $\mathbf{x}^\varphi$, with three faces parallel to the coordinate planes, and with a face F whose normal vector $\mathbf{n} = n_i\mathbf{e}_i$ has all its components $n_i > 0$. Let v_i denote the

vertices other than $\mathbf{x}^\varphi$, as indicated in the figure, and let F_i denote the face opposite to the vertex v_i, so that area $F_i = n_i \, area\, F$. The axiom of force balance over the tetrahedron $\mathbf{T}$ reads

$$\int_T \mathbf{f}^\varphi\left(y^\varphi\right)dy^\varphi + \int_{\partial T} \mathbf{t}^\varphi\left(y^\varphi, \mathbf{n}^\varphi\right)da^\varphi = \mathbf{0} \tag{2.19}$$

Writing this relation component wise, with

$$\mathbf{f}^\varphi\left(y^\varphi\right) = f_i^\varphi\left(y^\varphi\right)\mathbf{e}_i, \quad \mathbf{t}^\varphi\left(y^\varphi, \mathbf{n}^\varphi\right) = t_i^\varphi\left(y^\varphi, \mathbf{n}^\varphi\right)\mathbf{e}_i, \tag{2.20}$$

And using the mean value theorem for integrals (which can be applied to the integral on ∂T since the four functions $y^\varphi \in \partial T \to t^\varphi\left(y^\varphi, \mathbf{n}^\varphi\right)$ and $y^\varphi \in \partial T \to t^\varphi\left(y^\varphi, \mathbf{e}_j\right)$ are continuous by assumption) , we obtain for each index I,

$$\left|\mathbf{t}_i^\varphi\left(y_i, \mathbf{n}\right) + \mathbf{t}_i^\varphi\left(y_{ij} - \mathbf{e}_j\right)n_j\right| area\, F \le \sup_{y\in T}\left|f_i^\varphi\left(y\right)\right| vol\, \mathbf{T}, \tag{2.21}$$

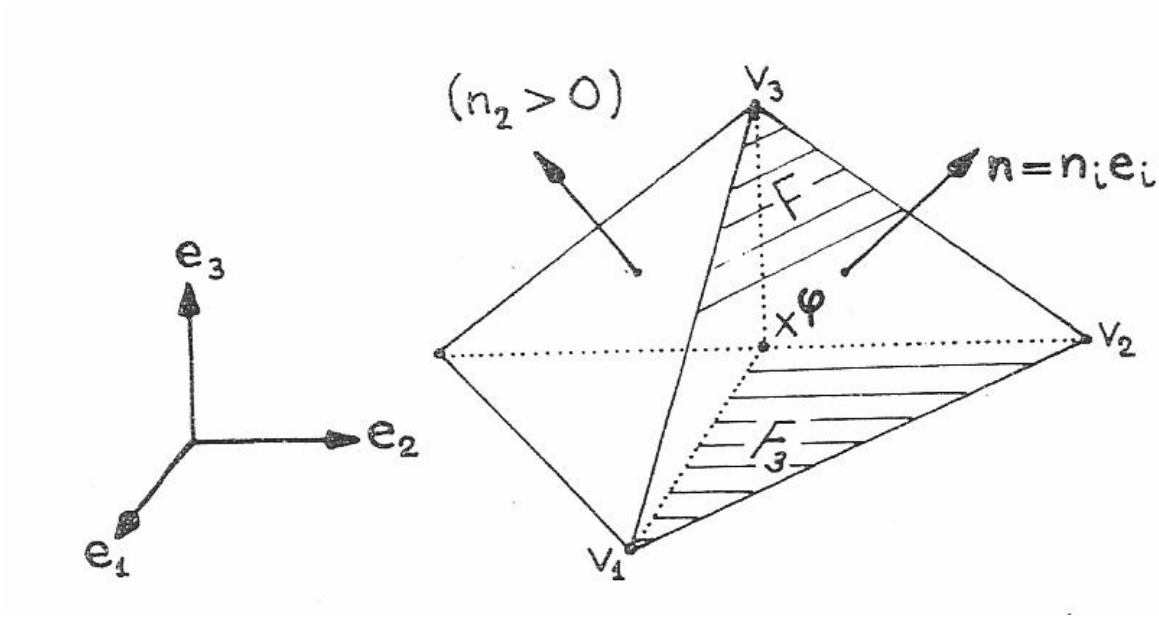

Fig. 2.2 - *Cauchy's celebrated proof of Cauchy's theorem*

for appropriate points $y_i \in F$, $y_{ij} \in F_j$. Keeping the vector $\mathbf{n}$ fixed, let the vertices v_i coalesce into the vertex x^φ. Using again the continuity of the vector field $\mathbf{t}^\varphi\left(x^\varphi, \mathbf{n}\right)$ with respect to the first variable x^φ, and using the relation $vol\, T = c\left(\mathbf{n}\right)\left(area\, F\right)^{3/2}$ coupled with the bound of the applied body forces density, we obtain :

$$\mathbf{t}^\varphi\left(x^\varphi, \mathbf{n}\right) = -n_j t^\varphi\left(x^\varphi, -\mathbf{e}_j\right) \tag{2.22}$$

Using next the continuity with respect to the second variable, let $\mathbf{n}$ approach a particular basis vector $\mathbf{e}_j$ in the above relation; we obtain in this fashion:

$$\mathbf{t}^\varphi\left(x^\varphi, \mathbf{e}_j\right) = -\mathbf{t}^\varphi\left(x^\varphi, -\mathbf{e}_j\right) \tag{2.23}$$

It follows that the relation

$$\mathbf{t}^\varphi\left(x^\varphi, \mathbf{n}\right) = -n_j \mathbf{t}^\varphi\left(x^\varphi, \mathbf{e}_j\right) \tag{2.24}$$

Also holds if some, or all, components n_i are <0 (the case $n_2 < 0$ is shown in fig. 2.1; hence it holds for all points $x^\varphi \in \bar{\Omega}^\varphi$ and all unit vectors $\mathbf{n} \in S_1$. We now define functions $\mathbf{T}_{ij}^\varphi : \bar{\Omega}^\varphi \to \mathbf{R}$ by letting

$$\mathbf{t}^\varphi\left(x^\varphi, \mathbf{e}_j\right) = T_{ij}^\varphi \mathbf{e}_i \text{ for all } x^\varphi \in \bar{\Omega}^\varphi, \tag{2.25}$$

so that $\mathbf{t}^{\varphi}\left(x^{\varphi},\mathbf{n}\right)=T_{ij}^{\varphi}\left(x^{\varphi}\right)n_j\mathbf{e}_i$, and thus

$$\mathbf{t}_i^{\varphi}\left(x^{\varphi},\mathbf{n}\right)=T_{ij}^{\varphi}\left(x^{\varphi}\right)n_j \text{ for all } x^{\varphi}\in\bar{\Omega}^{\varphi},\ \mathbf{n}\in S_1 \tag{2.26}$$

Therefore if we define a tensor $\mathbf{T}^{\varphi}\left(\mathbf{x}^{\varphi}\right)$ by

$$\mathbf{T}^{\varphi}\left(\mathbf{x}^{\varphi}\right):=T_{ij}^{\varphi}\left(\mathbf{x}^{\varphi}\right), \tag{2.27}$$

The equations $\mathbf{t}_i^{\varphi}\left(x^{\varphi},\mathbf{n}\right)=T_{ij}^{\varphi}\left(x^{\varphi}\right)n_j$ are equivalent to the vector equation

$$\mathbf{t}^{\varphi}\left(x^{\varphi},\mathbf{n}\right)=\mathbf{T}^{\varphi}\left(\mathbf{x}^{\varphi}\right)\cdot\mathbf{n} \tag{2.28}$$

The continuity assumptions with respect to both variables $\mathbf{x}^{\varphi}$ and $\mathbf{n}$ then show that this relation, which has been so far established for points $\mathbf{x}^{\varphi}$ in open set Ω^{φ} and for vectors $\mathbf{n}=n_i\mathbf{e}_i\in S_1$ with $|n_i|\neq 0$, holds in fact for all $x^{\varphi}\in\bar{\Omega}^{\varphi}$ and all $\mathbf{n}\in S_1$. The relations $\mathbf{t}_i^{\varphi}\left(x^{\varphi},\mathbf{n}\right)=T_{ij}^{\varphi}\left(x^{\varphi}\right)\mathbf{e}_i$ also show that the smoothness of the field $\mathbf{T}^{\varphi}:\bar{\Omega}^{\varphi}\to\mathbf{M}^3$ is exactly that of the Cauchy stress vector with respect to the first variable $\mathbf{x}^{\varphi}\in\bar{\Omega}^{\varphi}$.

The divergence theorem for tensor fields applied to the tensor $\mathbf{T}^{\varphi}$ implies that the surface integrals appearing in the axiom of force balance can be transformed into volume integrals: Given an arbitrary sub-domain $A^{\varphi}\subset\Omega^{\varphi}$, we can write:

$$\int_{\partial A^{\varphi}}\mathbf{t}^{\varphi}\left(x^{\varphi},\mathbf{n}^{\varphi}\right)da^{\varphi}=\int_{\partial A^{\varphi}}\mathbf{T}^{\varphi}\left(x^{\varphi}\right)\mathbf{n}^{\varphi}da^{\varphi}=\int_{A^{\varphi}}\mathbf{div}^{\varphi}\mathbf{T}^{\varphi}\left(x^{\varphi}\right)dx^{\varphi} \tag{2.29}$$

So that the axiom of force balance implies that

$$\int_{A^{\varphi}}\left\{\mathbf{div}^{\varphi}\mathbf{T}^{\varphi}\left(x^{\varphi}\right)+\mathbf{f}^{\varphi}\left(x^{\varphi}\right)\right\}dx^{\varphi}=0 \tag{2.30}$$

For all sub-domains $A^{\varphi}\subset\Omega^{\varphi}$; therefore,

$$\mathbf{div}^{\varphi}\mathbf{T}^{\varphi}\left(x^{\varphi}\right)+\mathbf{f}^{\varphi}\left(x^{\varphi}\right)=\mathbf{0} \text{ for all } \mathbf{x}^{\varphi}\in\Omega^{\varphi} \tag{2.31}$$

The surface integrals appearing in the axiom of moment balance can be likewise transformed into volume integrals by using Green's formula : For $i\neq j$, we have :

$$\begin{aligned}
&\int_{\partial A^{\varphi}}\left\{x_j^{\varphi}t_i^{\varphi}\left(x^{\varphi},\mathbf{n}^{\varphi}\right)-x_i^{\varphi}t_j^{\varphi}\left(x^{\varphi},\mathbf{n}^{\varphi}\right)\right\}da^{\varphi}=\int_{\partial A^{\varphi}}\left\{x_j^{\varphi}T_{ik}^{\varphi}\left(x^{\varphi}\right)-x_i^{\varphi}T_{jk}^{\varphi}\left(x^{\varphi}\right)\right\}n_k^{\varphi}da^{\varphi}=\\
&\int_{A^{\varphi}}\partial_k^{\varphi}\left\{x_j^{\varphi}T_{ik}^{\varphi}\left(x^{\varphi}\right)-x_i^{\varphi}T_{jk}^{\varphi}\left(x^{\varphi}\right)\right\}dx^{\varphi}=\\
&\int_{A^{\varphi}}\left\{\delta_{jk}T_{ik}^{\varphi}\left(x^{\varphi}\right)-\delta_{ik}T_{jk}^{\varphi}\left(x^{\varphi}\right)\right\}dx^{\varphi}+\int_{A^{\varphi}}\left\{x_j^{\varphi}\partial_k^{\varphi}T_{ik}^{\varphi}\left(x^{\varphi}\right)-x_i^{\varphi}\partial_k^{\varphi}T_{jk}^{\varphi}\left(x^{\varphi}\right)\right\}dx^{\varphi}=\\
&\int_{A^{\varphi}}\left\{T_{ik}^{\varphi}\left(x^{\varphi}\right)-T_{jk}^{\varphi}\left(x^{\varphi}\right)\right\}dx^{\varphi}-\int_{A^{\varphi}}\left\{x_j^{\varphi}f_i^{\varphi}\left(x^{\varphi}\right)-x_i^{\varphi}f_j^{\varphi}\left(x^{\varphi}\right)\right\}dx^{\varphi}
\end{aligned} \tag{2.32}$$

Where in the last equality we have taken into account the equation $\mathbf{div}^{\varphi}\mathbf{T}^{\varphi}\left(x^{\varphi}\right)+\mathbf{f}^{\varphi}\left(x^{\varphi}\right)=\mathbf{0}$, that was just obtained. Thus the axiom of moment balance implies that

$$\int_{A^{\varphi}}\left\{T_{ik}^{\varphi}\left(x^{\varphi}\right)-T_{jk}^{\varphi}\left(x^{\varphi}\right)\right\}dx^{\varphi}=0 \tag{2.33}$$

For all sub-domains A^{φ} of $\bar{\Omega}^{\varphi}$, and consequently $\mathbf{T}^{\varphi}\left(x^{\varphi}\right)=\mathbf{T}^{\varphi}\left(x^{\varphi}\right)^T$ for all $\mathbf{x}^{\varphi}\in\bar{\Omega}^{\varphi}$.

The boundary condition $\mathbf{T}^{\varphi}\left(x^{\varphi}\right)\cdot\mathbf{n}^{\varphi}=\mathbf{g}^{\varphi}\left(x^{\varphi}\right)$ for all $x^{\varphi}\in\Gamma_1^{\varphi}$ is an immediate consequence of the definition of the Cauchy stress vector and of its relation with the tensor $\mathbf{T}^{\varphi}$.

Remarks.

(1) The arguments showing the existence of the tensor field $\mathbf{T}^{\varphi}:\bar{\Omega}^{\varphi}\to\mathbf{M}^3$ and the validity of the relation $\mathbf{t}^{\varphi}\left(x^{\varphi},\mathbf{n}\right)=\mathbf{T}^{\varphi}\left(\mathbf{x}^{\varphi}\right)\cdot\mathbf{n}$ still hold if the Cauchy stress vector $\mathbf{t}^{\varphi}\left(x^{\varphi},\mathbf{n}\right)$ is only assumed to be separately continuous with respect to each variable x^{φ} and $\mathbf{n}$ (in which case

the mapping $\mathbf{T}^{\varphi}:\bar{\Omega}^{\varphi}\to\mathbf{M}^3$ in only continuous). Besides, these results, as well as the equation $\mathbf{div}^{\varphi}\mathbf{T}^{\varphi}\left(x^{\varphi}\right)+\mathbf{f}^{\varphi}\left(x^{\varphi}\right)=\mathbf{0}$, are consequences of the axiom of force balance only.

(2) On the other hand, the proof given here of the symmetry of the tensor $\mathbf{T}^{\varphi}\left(\mathbf{x}^{\varphi}\right)$ (a property that a priori has noting to do with a smoothness assumption) requires that the vector $\mathbf{t}^{\varphi}\left(x^{\varphi},\mathbf{n}\right)$ be continuously differentiable with respect to the variable x^{φ}. The reader interested in these aspects is referred to a basic paper of Gurtin & Martins [1976] about Cauchy's theorem, where it is shown how the smoothess assumption made in theorem 1 (Cauchy's theorem) can be considerably weakened. See also Gurtin, Misel & Williams [1968], Martins [1976].

The symmetry tensor $\mathbf{T}^{\varphi}$ is called the Cauchy stress tensor at the point $\mathbf{x}^{\varphi}\in\bar{\Omega}^{\varphi}$. It is helpful to keep in mind the interpretation of its elements $\mathbf{T}_{ij}^{\varphi}\left(\mathbf{x}^{\varphi}\right)$: Since $\mathbf{t}^{\varphi}\left(x^{\varphi},\mathbf{e}_j\right)=\mathbf{T}_{ij}^{\varphi}\left(\mathbf{x}^{\varphi}\right)\cdot\mathbf{e}_i$, the elements of the j-th row of the tensor $\mathbf{T}^{\varphi}\left(x^{\varphi}\right)$ represent the components of the Cauchy stress vector $\mathbf{t}^{\varphi}\left(x^{\varphi},\mathbf{n}\right)$ at the point $\mathbf{x}^{\varphi}$ corresponding to the particular choice $\mathbf{n}=\mathbf{e}_j$ (cf. fig. 2.2 where the case j=1 is considered). The knowledge of the three vectors $\mathbf{t}^{\varphi}\left(x^{\varphi},\mathbf{e}_j\right)$ in turn completely determines the Cauchy stress vector $\mathbf{t}^{\varphi}\left(x^{\varphi},\mathbf{n}\right)$ for an arbitrary vector $\mathbf{n}=n_i\mathbf{e}_i\in S_1$, since

$$\mathbf{t}^{\varphi}\left(x^{\varphi},\mathbf{n}\right)=n_j\mathbf{t}^{\varphi}\left(x^{\varphi},\mathbf{e}_j\right) \tag{2.37}$$

This observation is used in the drawing of figures (as in fig. 2.3), where

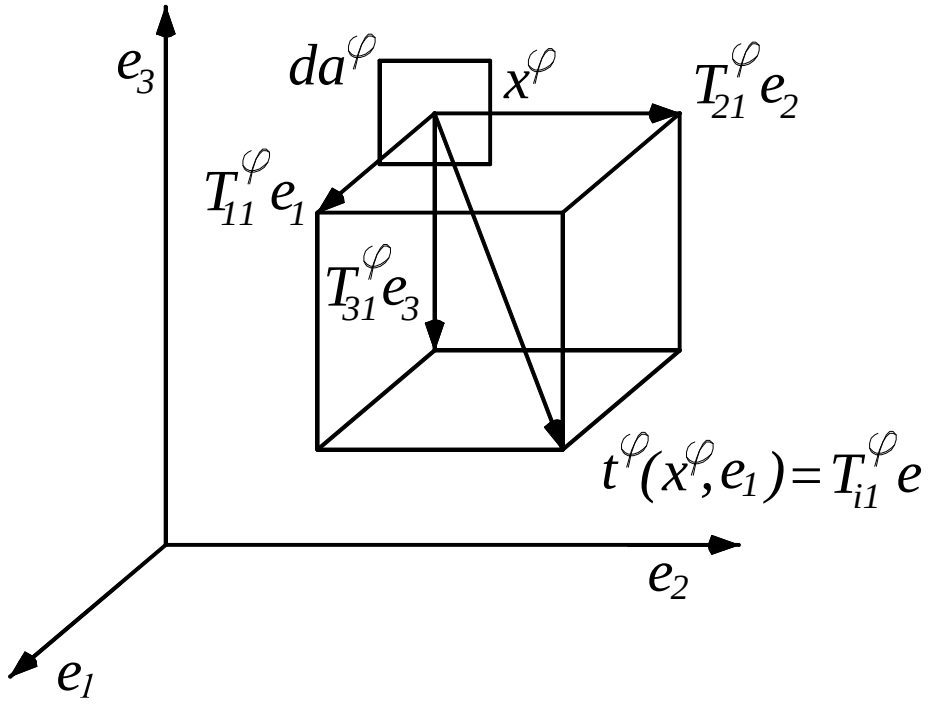

Fig. 2.3 - *Interpretation of the elements* $\mathbf{T}_{i1}^{\varphi}$ *of the Cauchy stress tensor* $\mathbf{T}^{\varphi}=\left(T_{ij}^{\varphi}\right)$

The Cauchy stress vector is often represented on three mutually perpendicular faces of a rectangular parallelepiped. The following three special cases of Cauchy stress tensors are particularly worthy of interest (cf. fig, 2.3, where in each case it is assumed that the Cauchy stress tensor is constant in the particular region considered). First, if

$$\mathbf{T}^{\varphi}\left(x^{\varphi}\right)=-\pi\mathbf{I},\quad \pi\in\mathbb{R}, \tag{2.38}$$

The Cauchy stress tensor as pressure, and the real number π is also called a pressure . In this case, the Cauchy stress vector:

$$\mathbf{t}^{\varphi}\left(x^{\varphi},\mathbf{n}\right)=-\pi\mathbf{n} \tag{2.39}$$

Is always normal to the elementary surface element, its length is constant,

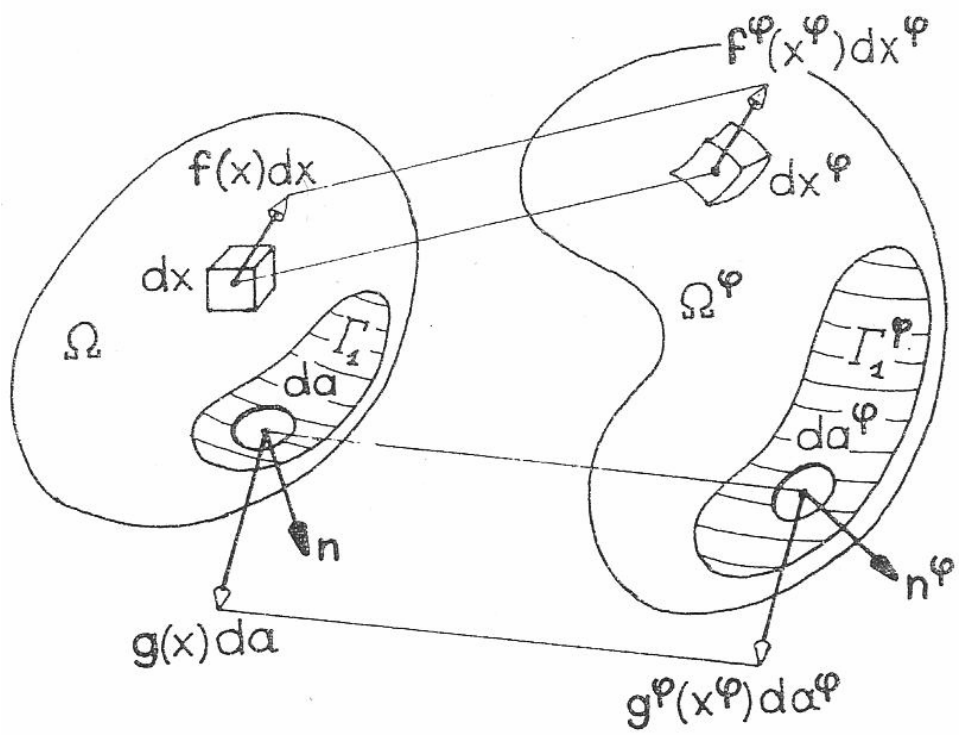

Fig. 2.4 - *Three important special case of Cauchy stress tensor: (a) Pressure* $\mathbf{T}^{\varphi}=-\pi\mathbf{I}$; *(b) Pure tension in the direction* $\mathbf{e}:\mathbf{T}^{\varphi}=\tau\mathbf{e}\otimes\mathbf{e}$; *(c) Pure shear relative to the directions* $\mathbf{e}$ *and* $\mathbf{f}:\mathbf{T}^{\varphi}=\sigma\left(\mathbf{e}\otimes\mathbf{f}+\mathbf{f}\otimes\mathbf{e}\right)$

And it is directed inward if π is <0 (Fig. 2.3 a). Secondly, if

$$\mathbf{T}^{\varphi}\left(x^{\varphi}\right)=\tau\mathbf{e}\otimes\mathbf{e},\quad \tau\in\mathbf{R},\quad \mathbf{e}\in\mathbf{R}^{3},\quad \left|\mathbf{e}\right|=1, \tag{2.40}$$

The Cauchy stress tensor is a pure tension if τ is >0, or a pure compression if τ is <0, in the direction $\mathbf{e}$, with tensile stress τ. In this case, the Cauchy stress vector

$$\mathbf{t}^{\varphi}\left(x^{\varphi},\mathbf{n}\right)=-\tau\left(\mathbf{e}\cdot\mathbf{n}\right)\mathbf{e}, \tag{2.41}$$

which is always parallel to the vector $\mathbf{e}$, is directed outward if $\tau>0$, or inward if $\tau<0$, on the faces with normal $\mathbf{n}=\mathbf{e}$ or $\mathbf{n}=-\mathbf{e}$, and it vanishes on the faces whose normal is orthogonal to the vector $\mathbf{e}$ (Fig. 2.3) . Thirdly (Fig. 2.3), if

$$\mathbf{T}^{\varphi}\left(x^{\varphi}\right)=\sigma\left(\mathbf{e}\otimes\mathbf{f}+\mathbf{f}\otimes\mathbf{e}\right),\quad \sigma\in\mathbf{R},\quad \mathbf{e},\mathbf{f}\in\mathbf{R}^{3},\quad \left|\mathbf{e}\right|=\left|\mathbf{f}\right|=1,\quad \mathbf{e}\cdot\mathbf{f}=0, \tag{2.41}$$

The Cauchy stress tensor is a pure shear , with shear stress τ, relative to the directions $\mathbf{e}$ and $\mathbf{f}$. In this case, the Cauchy stress vectors given by

$$\mathbf{t}^{\varphi}\left(x^{\varphi},\mathbf{n}\right)=\sigma\left\{\left(\mathbf{f}\cdot\mathbf{n}\right)\mathbf{e}+\left(\mathbf{e}\cdot\mathbf{n}\right)\mathbf{f}\right\} \tag{2.42}$$

The Cauchy stress tensors corresponding to these three special cases are respectively given by (for definiteness, we assume that $\mathbf{e}=\mathbf{e}_1$ and $\mathbf{f}=\mathbf{e}_2$:

$$\begin{pmatrix} -\pi & 0 & 0 \\ 0 & -\pi & 0 \\ 0 & 0 & -\pi \end{pmatrix}, \quad \begin{pmatrix} \tau & 0 & 0 \\ 0 & 0 & 0 \\ 0 & 0 & 0 \end{pmatrix}, \quad \begin{pmatrix} 0 & \sigma & 0 \\ \sigma & 0 & 0 \\ 0 & 0 & 0 \end{pmatrix}, \tag{2.43}$$

2.4. The equations of equilibrium and the principle of virtual work in the deformed configuration

As shown in Theorem 1, the axioms of force and moment balance imply that the Cauchy stress tensor field $\mathbf{T}^{\varphi} : \bar{\Omega}^{\varphi} \to \mathbf{S}^3$ satisfies a boundary value problem expressed in terms of the Euler variable x^{φ} over the deformed configuration , comprising the partial differential equation $-div^{\varphi}\mathbf{T}^{\varphi} = \mathbf{f}^{\varphi} \quad in \quad \Omega^{\varphi}$ and the boundary condition $\mathbf{T}^{\varphi}\mathbf{n}^{\varphi} = \mathbf{g}^{\varphi} \quad on \quad \Gamma_1^{\varphi}$. A remarkable property of this boundary value problem, due to its " divergence form", is that it can be given a variational formulation, as we now show . In what follows, $\mathbf{u} \cdot \mathbf{v} = u_i v_i$ denotes the Euclidean vector inner product, $\mathbf{A} : \mathbf{B} = A_{ij} B_{ji} = tr\, \mathbf{A}^T \mathbf{B}$ denotes the matrix inner product, and $\boldsymbol{\nabla}^{\varphi}\boldsymbol{\theta}^{\varphi}$ denotes the matrix $\left(\partial_j^{\varphi} \theta_i^{\varphi}\right)$.

Theorem 2.2 : The boundary value problem:

$$\begin{aligned} -div^{\varphi}\mathbf{T}^{\varphi} &= \mathbf{f}^{\varphi} \quad in \quad \Omega^{\varphi} \\ \mathbf{T}^{\varphi}\mathbf{n}^{\varphi} &= \mathbf{g}^{\varphi} \quad on \quad \Gamma_1^{\varphi} \end{aligned} \tag{2.44}$$

Is formally equivalent to the variational equations :

$$\int_{\Omega^{\varphi}} \mathbf{T}^{\varphi} : \nabla^{\varphi}\theta^{\varphi} dx^{\varphi} = \int_{\Omega^{\varphi}} \mathbf{f}^{\varphi} \cdot \boldsymbol{\theta}^{\varphi} dx^{\varphi} + \int_{\Gamma_1^{\varphi}} \mathbf{g}^{\varphi} \cdot \boldsymbol{\theta}^{\varphi} dx^{\varphi}, \tag{2.45}$$

valid for all smooth enough vector fields: $\boldsymbol{\theta}^{\varphi} : \Omega^{\varphi} \to R^3$ cthat satisfy

$$\boldsymbol{\theta}^{\varphi} = \mathbf{0} \quad on \quad \Gamma_o^{\varphi} := \Gamma^{\varphi} - \Gamma_1^{\varphi} \tag{2.46}$$

Proof. The equivalence with the variational equations rests on another Green's formula (whose proof is again a direct application of the fundamental Green formula;). For any smooth enough tensor filed $\mathbf{T}^{\varphi} : \bar{\Omega}^{\varphi} \to \mathbf{M}^3$ and vector field $\boldsymbol{\theta}^{\varphi} : \Omega^{\varphi} \to \mathbf{R}^3$

$$\int_{\Omega^{\varphi}} div^{\varphi}\mathbf{T}^{\varphi} \cdot \boldsymbol{\theta}^{\varphi} dx^{\varphi} = -\int_{\Omega^{\varphi}} \mathbf{T}^{\varphi} : \boldsymbol{\nabla}\boldsymbol{\theta}^{\varphi} dx^{\varphi} + \int_{\Gamma^{\varphi}} \mathbf{T}^{\varphi}\mathbf{n}^{\varphi} \cdot \boldsymbol{\theta}^{\varphi} da^{\varphi} \tag{2.47}$$

Thus, if we integrate over the set Ω^{φ} the inner product of the equation $div^{\varphi}\mathbf{T}^{\varphi} + \mathbf{f}^{\varphi} = \mathbf{0}$ with a vector field $\boldsymbol{\theta}^{\varphi}$ that vanishes on Γ_0^{φ}, we obtain:

$$\begin{aligned} \mathbf{0} &= \int_{\Omega^{\varphi}} \left(div^{\varphi}\mathbf{T}^{\varphi} + \mathbf{f}^{\varphi}\right) \cdot \boldsymbol{\theta}^{\varphi} dx^{\varphi} = \\ &\int_{\Omega^{\varphi}} \left\{-\mathbf{T}^{\varphi} : \nabla^{\varphi}\boldsymbol{\theta}^{\varphi} + \mathbf{f}^{\varphi} \cdot \boldsymbol{\theta}^{\varphi}\right\} dx^{\varphi} + \int_{\Gamma_1^{\varphi}} \mathbf{T}^{\varphi}\mathbf{n}^{\varphi} \cdot \boldsymbol{\theta}^{\varphi} da^{\varphi} \end{aligned} \tag{2.48}$$

And the variational equations follow, since $\mathbf{T}^{\varphi}\mathbf{n}^{\varphi} = \mathbf{g}^{\varphi} \quad on \quad \Gamma_1^{\varphi}$. Conversely, assume that the variational equations are satisfied . They reduce to

$$\int_{\Omega^{\varphi}} \mathbf{T}^{\varphi} : \nabla^{\varphi}\theta^{\varphi} dx^{\varphi} = \int_{\Omega^{\varphi}} \mathbf{f}^{\varphi} \cdot \boldsymbol{\theta}^{\varphi} dx^{\varphi} \quad \text{if } \boldsymbol{\theta}^{\varphi} = \mathbf{0} \quad on \quad \Gamma^{\varphi}, \tag{2.49}$$

And since, by the above Green formula,

$$\int_{\Omega^{\varphi}} \mathbf{T}^{\varphi} : \nabla^{\varphi}\theta^{\varphi} dx^{\varphi} = -\int_{\Omega^{\varphi}} div^{\varphi}\mathbf{T}^{\varphi} dx^{\varphi} \quad \text{if } \boldsymbol{\theta}^{\varphi} = \mathbf{0} \quad on \quad \Gamma^{\varphi}, \tag{2.50}$$

We deduce that $div^{\varphi}\mathbf{T}^{\varphi} + \mathbf{f}^{\varphi} = \mathbf{0}$ in Ω^{φ}. Taking this equation into account and using the same Green formula, we find that the variational equations reduce to the equations

$$\int_{\Gamma_1^{\varphi}} \mathbf{T}^{\varphi}\mathbf{n}^{\varphi} \cdot \boldsymbol{\theta}^{\varphi} da^{\varphi} = \int_{\Gamma_1^{\varphi}} \mathbf{g}^{\varphi} \cdot \boldsymbol{\theta}^{\varphi} da^{\varphi}, \tag{2.51}$$

which imply that the boundary condition $\mathbf{T}^{\varphi}\mathbf{n}^{\varphi} = \mathbf{g}^{\varphi}$ holds on Γ_1^{φ}.

The equations

$$\begin{aligned} -div^{\varphi}\mathbf{T}^{\varphi} &= \mathbf{f}^{\varphi} \quad in \quad \Omega^{\varphi}, \\ \mathbf{T}^{\varphi} &= \left(\mathbf{T}^{\varphi}\right)^{T} \quad in \quad \Omega^{\varphi}, \\ \mathbf{T}^{\varphi}\mathbf{n}^{\varphi} &= \mathbf{g}^{\varphi} \quad on \quad \Gamma_1^{\varphi}, \end{aligned} \tag{2.52}$$

are called the equations of equilibrium in the deformed configuration, while the associated variational equations of Theorem 2.2 constitute the principle of virtual work in the deformed configuration .

Remark: In both the axiom of force balance and the principle of virtual work , the required smoothness on the field $\mathbf{T}^{\varphi} : \bar{\Omega}^{\varphi} \to \mathbf{S}^3$ is very mild (it suffices that all integrals make sense) By contrast , a significant additional smoothness is required for writing the equations of equilibrium (in order that $div^{\varphi}\mathbf{T}^{\varphi}$ makes sense), which are only used a san intermediary between the axiom and the principle. Hence the question naturally arises as to whether the equations of equilibrium can be by-passed in this process, Antam & Osborn [1979] have shown that the principle of virtual work can be indeed directly deduced from the axiom of force balance. Their basic idea is to put on an equivalent basis the fact that the axiom is valid for all sub-domains A^{φ} while the principle holds for all mappings $\boldsymbol{\theta}^{\varphi}$, by associting special classes of sub-domains (cubes and their bi-Lipschitz continuous images) with special families of variations (basically piecewise linear functions). The methods of proff are reminiscent of those used for proving green's formulas in the theory of integration.

2.5. The Piola-Kirchkoff stress tensors

Our final objective is to determine the deformation field and the Cauchy stress tensor field that arise in a body subjected to a given system of applied forces . In this respect, the equations of equilibrium in the deformed configuration are of not much avail, since they are expressed in terms of the Euler variable $\mathbf{x}^{\varphi} = \varphi(x)$, which is precisely on of the unknows . To obviate this difficulty, we shall rewrite these equations in terms of the Lagrange variable x that is attached to the reference configuration, which is considered as being given once and for all. More specifically, we shall transform the left-hand sides $div^{\varphi}\mathbf{T}^{\varphi}$ and $\mathbf{T}^{\varphi}\mathbf{n}^{\varphi}$ and the right-hand sides $\mathbf{f}^{\varphi}$ and $\mathbf{g}^{\varphi}$ appearing in the equations of equilibrium over $\bar{\Omega}^{\varphi}$ into similar expressions over $\bar{\Omega}$.

We defined the Piola transform: $\mathbf{T} : \bar{\Omega} \to \mathbf{M}^3$ of a tensor field $\mathbf{T}^{\varphi} : \bar{\Omega}^{\varphi} = \varphi\left(\bar{\Omega}\right) \to M^3$ by letting

$$\mathbf{T}(x) = \left(\det \nabla \varphi(x)\right) T^{\varphi}\left(x^{\varphi}\right) \nabla \varphi(x)^{-T}, \quad x^{\varphi} = \varphi(x) \tag{2.53}$$

We shall therefore apply this transform to the Cauchy stress tensor $\mathbf{T}^{\varphi}$, in which case its Piola transform $\mathbf{T}$ is called the first Piola-Kirchhoff stress tensor. As shown in theorem 1 (chapter 1a), the main advantage of this transform is to induce a particularly simple between the divergences of both tensors:

$$div\mathbf{T}(x) = \left(\det \nabla \boldsymbol{\varphi}(x)\right) div^{\varphi}\mathbf{T}^{\varphi}\left(\mathbf{x}^{\varphi}\right), \quad x^{\varphi} = \varphi(x) \tag{2.54}$$

As a consequence, the equations of equilibrium over the deformed configuration will be transformed (Theorem 2.2) into equations over the reference configuration that have a similar divergence structure. This property in turn makes it possible to write these partial differential equations in variational form, as shown in Theorem 2.2 for the equations of equilibrium over the reference configuration.

On can likewise transform the Cauchy stress vector $\mathbf{t}^{\varphi}\left(x^{\varphi}, \mathbf{n}\right) = \mathbf{T}^{\varphi}\left(x^{\varphi}\right)\mathbf{n}^{\varphi}$ into a vector $\mathbf{t}(x, \mathbf{n})$ in such a way that the relation

$$\mathbf{t}(x, \mathbf{n}) = \mathbf{T}(x)\mathbf{n} \tag{2.55}$$

Holds, where $\mathbf{T}(x)$ is the first Piola-Kirchhoff stress tensor and where $\mathbf{n}$ and $\mathbf{n}^{\varphi}$ are the corresponding normal vectors at the points x and $\mathbf{x}^{\varphi}=\varphi(x)$ of the boundaries of corresponding sub-domains A and $A^{\varphi}=\varphi(A)$. Notice that there is no ambiguity in this process since the normal vector $\mathbf{n}^{\varphi}$ at the point $\mathbf{x}^{\varphi}=\varphi(x)$ is the same for all sub-domains whose boundary passes through the point x with $\mathbf{n}$ as the normal vector there. In view of the relation $\mathbf{T}(x)\mathbf{n}da=\mathbf{T}^{\varphi}\left(x^{\varphi}\right)\mathbf{n}^{\varphi}da^{\varphi}$ established in Theorem 1 (chapter 1a) , it suffices to define the vector $\mathbf{t}(x,\mathbf{n})$ by the relation:

$$\mathbf{t}(x,\mathbf{n})\,da=t^{\varphi}\left(x^{\varphi},\mathbf{n}^{\varphi}\right)da^{\varphi} \tag{2.56}$$

Since $\mathbf{t}^{\varphi}\left(x^{\varphi},\mathbf{n}\right)=\mathbf{T}^{\varphi}\left(x^{\varphi}\right)\mathbf{n}^{\varphi}$ by Cauchy' theorem, the desired relation $\mathbf{t}(x,\mathbf{n})=\mathbf{T}(x)\mathbf{n}$ holds.

The vector $\mathbf{t}(x,\mathbf{n})$ is called the first Piola-Kirchhoff stress vector at the point x of the reference configuration, across the oriented surface element with normal $\mathbf{n}$. The vector field $\mathbf{t}:\bar{\Omega}\times S_1\to\mathbf{R}^3$ defined in this fashion thus measures the density of the surface force per unit area in the reference configuration.

While the Cauchy stress tensor $\mathbf{T}^{\varphi}\left(x^{\varphi}\right)$ is symmetric (Theorem 2.1) the first Piola-Kirchhoff stress tensor $\mathbf{T}(x)$ is not symmetric in general; instead one has:

$$\mathbf{T}(x)^{T}=\nabla\boldsymbol{\varphi}(x)^{-1}\mathbf{T}(x)\nabla\boldsymbol{\varphi}(x)^{-T} \tag{2.57}$$

It is nevertheless desirable to define a symmetric stress tensor in the reference configuration, essentially because the constitutive equation in the reference configuration then takes a simpler form. More specifically, we define the second Piola-Kirchhoff stress tensor $\boldsymbol{\Sigma}(x)$ by letting

$$\boldsymbol{\Sigma}(x)=\nabla\boldsymbol{\varphi}(x)^{-1}\boldsymbol{T}(x)=\left(\det\nabla\boldsymbol{\varphi}(x)\right)\nabla\boldsymbol{\varphi}(x)^{-1}\boldsymbol{T}^{\varphi}\left(x^{\varphi}\right)\nabla\boldsymbol{\varphi}(x)^{-T},\quad x^{\varphi}=\varphi(x) \tag{2.58}$$

Remarks. (1) In fact, the question of whether or not the matrix $\boldsymbol{T}(\mathbf{x})$ is symmetric does not make sense for , as a tensor, it has one index attached to the reference configuration and one index attached to the deformed configuration. A complete discussion of these aspects can be found in Marsden & Hughes [1983].

(3) Historical reference on the Piola-Kirchhoff stress tensors are given in Truesdell & Toupin [1960, Sect. 210].

The Piola-Kirchhoff stress tensor $\boldsymbol{T}(\mathbf{x})$ and $\boldsymbol{\Sigma}(\mathbf{x})$ both depend on the deformation $\boldsymbol{\varphi}$, first through the Piola transform itself, secondly because the Cauchy stress tensor also dependent on $\boldsymbol{\varphi}$.

2.6. The equations of equilibrium and principle of virtual work in the reference configuration

It remains to transform the applied forces densities that appear in the equilibrium equations over the deformed configuration: First, with the density $\boldsymbol{f}^{\varphi}:\Omega^{\varphi}\to\mathbf{R}^3$ of the applied force per unit volume in the deformed configuration, we associate a vector field $\boldsymbol{f}:\Omega\to\mathbf{R}^3$ in such a way that

$$\boldsymbol{f}(x)\,dx=\boldsymbol{f}^{\varphi}\left(x^{\varphi}\right)dx^{\varphi}\ \text{ for all }\ x^{\varphi}=\varphi(x)\in\Omega^{\varphi} \tag{2.59}$$

Where dx and dx^{φ} denote the corresponding volume elements. Since

$$dx^{\varphi}=\left(\det\nabla\boldsymbol{\varphi}(x)\right)\boldsymbol{f}^{\varphi}\left(x^{\varphi}\right),\quad x^{\varphi}=\varphi(x), \tag{2.60}$$

So that the vector $\boldsymbol{f}(x)$ depends on the deformation $\boldsymbol{\varphi}$, via the factor $\det\nabla\boldsymbol{\varphi}(x)$ on the one hand, and via the possible dependence of the density $\boldsymbol{f}^{\varphi}$ on the deformation $\boldsymbol{\varphi}$ on the other hand. Notice that this relation displays the same factor $\det\nabla\boldsymbol{\varphi}(x)$ as the relation between the vectors $\mathbf{div}\,\mathbf{T}(x)$ and $\mathbf{div}^{\varphi}\mathbf{T}^{\varphi}\left(x^{\varphi}\right)$ (this observation will be used in the proof of Theorem 1.1)

The vector field $\boldsymbol{f}:\Omega\to\mathbf{R}^3$ measures the density of the applied body force per unit volume in the reference configuration; the vector $\boldsymbol{f}(x)$ is defined in such a way that the elementary vector $\boldsymbol{f}(x)dx$ is equal to the elementary body force $\boldsymbol{f}\left(x^\varphi\right)dx^\varphi$ acting on the corresponding volume element dx^φ at the point $x^\varphi=\boldsymbol{\varphi}(x)$ (Fig. 2.4)

Let: $\rho:\Omega\to\mathbf{R}$ denote the mass density in the reference configuration. Expressing that the mass of the elementary volumes dx and $dx^\varphi=\det\boldsymbol{\nabla\varphi}(x)dx$ is the same , we find the mass densities $\rho:\Omega\to\mathbf{R}$ and $\rho^\varphi:\Omega^\varphi\to\mathbf{R}$ are related by the equation

$$\rho(x)=\det\boldsymbol{\nabla\varphi}(x)\rho^\varphi\left(x^\varphi\right),\quad x^\varphi=\boldsymbol{\varphi}(x) \tag{2.61}$$

Incidentally, this relation also shows that, regardless of any consideration concerning the preservation of orientation, the Jacobian $\det\boldsymbol{\nabla\varphi}(x)$ should not vanish in an actual deformation, since mass density is always >0, at least macroscopically.

Then if we define the density $\mathbf{b}:\Omega\to\mathbf{R}^3$ of the applied body forces per unit mass in the reference configuration by letting

$$\boldsymbol{f}(x)=\rho(x)\mathbf{b}(x)\ \text{ for all }\ x\in\Omega, \tag{2.62}$$

it follows that the densities of the applied force per unit mass are related by

$$\mathbf{b}(x)=\mathbf{b}^\varphi\left(x^\varphi\right),\quad x^\varphi=\boldsymbol{\varphi}(x) \tag{2.63}$$

Secondly, in order to transform the boundary condition $\mathbf{T}^\varphi\mathbf{n}^\varphi=\mathbf{g}^\varphi$ over $\Gamma_1^\varphi=\boldsymbol{\varphi}(\Gamma_1)$ into a similar condition over Γ_1, it suffices to use the first Piola-Kirchhoff stress vector, which was precisely defined for this purpose : With the density $\mathbf{g}^\varphi:\Gamma_1^\varphi\to\mathbf{R}^3$ of the applied surface force per unit area in the deformed configuration, we associate the vector field $\mathbf{g}:\Gamma_1\to\mathbf{R}^3$ defined by

$$\mathbf{g}(x)da=\mathbf{g}^\varphi\left(x^\varphi\right)da^\varphi\ \text{ for all }\ x^\varphi=\boldsymbol{\varphi}(x)\in\Gamma_1^\varphi \tag{2.64}$$

where da and da^φ are the corresponding area elements. Hence by Theorem 1.1 (Properties of the Piola transform), the vector $\mathbf{g}(x)$ is given by

$$\mathbf{g}(x)=\det\boldsymbol{\nabla\varphi}(x)\left|\boldsymbol{\nabla\varphi}(x)^{-T}\mathbf{n}\right|\mathbf{g}^\varphi\left(\mathbf{x}^\varphi\right). \tag{2.65}$$

Notice that the vector $\mathbf{g}(x)$ depends on the deformation $\boldsymbol{\varphi}$, via the formula relating the corresponding area elements on the one hand and via the possible dependence of the density, $\mathbf{g}^\varphi$ on the deformation $\boldsymbol{\varphi}$ on the other hand. The vector field $\mathbf{g}:\Gamma_1\to\mathbf{R}^3$ measures the density of the applied surface force per unit area in the reference configuration; it is defined in such a way that the elementary vector $\mathbf{g}(x)da$ is equal to the elementary surface force $\mathbf{g}^\varphi\left(x^\varphi\right)da^\varphi$ acting on the corresponding area element da^φ at the point $x^\varphi=\boldsymbol{\varphi}(x)$ (Fig. 2.4)

We can now establish the analogous of Theorem 2.2 over the reference configuration:

Theorem 2.3. The first Piola-Kirchhoff stress tensor

$$\mathbf{T}(x)=\left(\det\boldsymbol{\nabla\varphi}(x)\right)\mathbf{T}^\varphi\left(\mathbf{x}^\varphi\right)\boldsymbol{\nabla\varphi}(x)^{-T} \tag{2.66}$$

satisfies the following equations in the reference configuration $\bar{\Omega}$:

$$\begin{aligned}
&-\mathbf{div}\,\mathbf{T}(x)=\boldsymbol{f}(x),\quad x\in\Omega,\\
&\boldsymbol{\nabla\varphi}(x)\mathbf{T}(x)^T=\mathbf{T}(x)\boldsymbol{\nabla\varphi}(x)^T,\quad x\in\Omega,\\
&\mathbf{T}(x)\mathbf{n}=\mathbf{g}(x),\quad x\in\Gamma_1
\end{aligned} \tag{2.67}$$

where $\mathbf{f}\,dx = \mathbf{f}^{\varphi}dx^{\varphi}$, $\mathbf{g}\,da = \mathbf{g}^{\varphi}da^{\varphi}$. The first and third equations are together equivalent to the variational equations :

$$\int_{\Omega} \mathbf{T} : \nabla\boldsymbol{\theta}\, dx = \int_{\Omega} \boldsymbol{f}\cdot\boldsymbol{\theta}\, dx + \int_{\Gamma_1} \boldsymbol{g}\cdot\boldsymbol{\theta}\, da \tag{1.144}$$

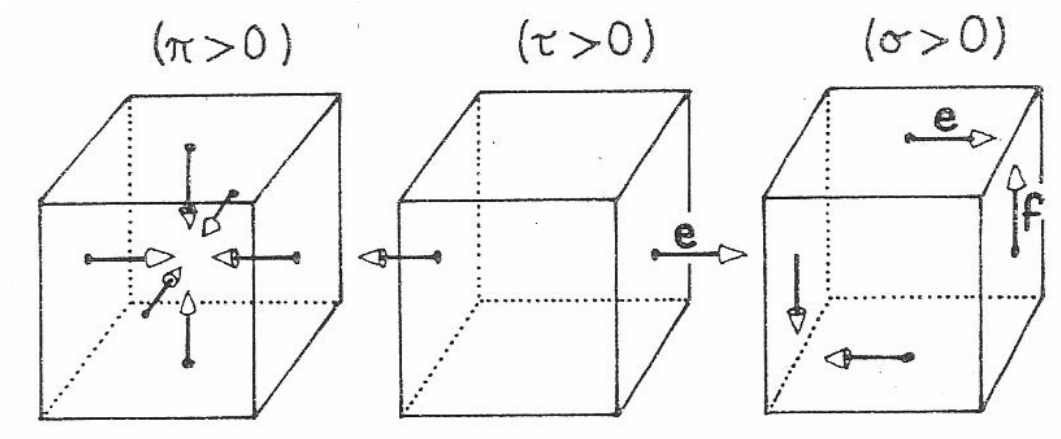

Fig. 2.5 - *The applied body force and surface force densities in the deformed configuration and in the reference configuration*

Valid for all smooth enough vector fields $\boldsymbol{\theta} : \bar{\Omega} \to R^3$ that satisfy

$$\boldsymbol{\theta} = \mathbf{0} \quad on \quad \Gamma_0 = \Gamma - \Gamma_1 \tag{2.68}$$

Proof. The first equations follows from the equations $-\mathbf{div}^{\varphi}\mathbf{T}^{\varphi} = \boldsymbol{f}^{\varphi}$ in Ω^{φ}, $\mathbf{div}^{\varphi}\mathbf{T}^{\varphi} = (\det\nabla\boldsymbol{\varphi})\,\mathbf{div}\,\mathbf{T}$, and $\boldsymbol{f} = (\det\nabla\boldsymbol{\varphi})\,\boldsymbol{f}^{\varphi}$; the second follows from the definition of the tensor $\mathbf{T}$ and the symmetry of the tensor $\mathbf{T}^{\varphi}$; the third one follows from the equations $\mathbf{T}^{\varphi}\mathbf{n}^{\varphi} = \mathbf{g}^{\varphi}$, $\mathbf{T}^{\varphi}\mathbf{n}^{\varphi}da^{\varphi} = \mathbf{T}\,\mathbf{n}\,da$, and $\mathbf{g}^{\varphi}da^{\varphi} = \mathbf{g}\,da$. The equivalence with the variational equations is then established as in Theorem 2.1.
In terms of the second Piola-Kirchhoff stress tensor, the above result becomes:

Theorem 1.8. The second Piola-Kirchhoff stress tensor

$$\boldsymbol{\Sigma}(x) = (\det\nabla\boldsymbol{\varphi}(x))\,\nabla\boldsymbol{\varphi}(x)^{-1}\boldsymbol{T}^{\varphi}(x^{\varphi})\,\nabla\boldsymbol{\varphi}(x)^{-T} \tag{2.69}$$

satisfies the following equations in the reference configuration $\bar{\Omega}$:

$$\begin{aligned} &-\mathbf{div}\big(\nabla\boldsymbol{\varphi}(x)\boldsymbol{\Sigma}(x)\big) = \boldsymbol{f}(x), \quad x\in\bar{\Omega},\\ &\boldsymbol{\Sigma}(x) = \boldsymbol{\Sigma}(x)^{T}, \quad x\in\Omega,\\ &\nabla\boldsymbol{\varphi}(x)\boldsymbol{\Sigma}(x)\mathbf{n} = \mathbf{g}(x), \quad x\in\Gamma_1 \end{aligned} \tag{2.70}$$

The first and third equations are together equivalent to the variational equations

$$\int_{\Omega} \nabla\varphi\Sigma : \nabla\boldsymbol{\theta}\, dx = \int_{\Omega} \boldsymbol{f}\cdot\boldsymbol{\theta}\, dx + \int_{\Gamma_1} \boldsymbol{g}\cdot\boldsymbol{\theta}\, da \tag{2.71}$$

Valid for all smooth enough maps $\boldsymbol{\theta} : \bar{\Omega} \to \mathbf{R}^3$ that satisfy

$$\boldsymbol{\theta} = \mathbf{0} \quad on \quad \Gamma_0 = \Gamma - \Gamma_1 \tag{2.72}$$

The equations satisfied over Ω and Γ_1 by either stress tensor are called the equations of equilibrium in the reference configuration, and their associated variational equations constitute the principal of virtual work in the reference configuration . The equation on Γ_1 is called a boundary condition of traction .
As we already mentioned, a boundary condition of place the form

$$\varphi = \varphi_0 \text{ on } \Gamma_0, \tag{2.73}$$

where $\varphi_0 : \Gamma_0 \to \mathbf{R}^3$ is a given mapping , will be later adjoined to the equations of equilibrium in the reference configuration. This being the case, we may think of each vector field $\boldsymbol{\theta} : \bar{\Omega} \to \mathbf{R}^3$ occurring in the principle of virtual work as a virtual variation of a deformation consistent with the boundary condition of place. More specifically, if we define the set

$$\boldsymbol{\Phi} := \left\{ \boldsymbol{\psi} : \bar{\Omega} \to \mathbf{R}^3; \quad \det \nabla \psi > 0 \quad in \quad \bar{\Omega}; \quad \psi = \varphi_0 \quad on \quad \Gamma_0 \right\} \tag{2.74}$$

(at this stage, we do not require that the vector fields $\boldsymbol{\psi} : \Omega \to \mathbf{R}^3$ be injective on Ω, a condition that is part of the definition of a deformation) , we remark that the tangent space at a point φ of the manifold $\boldsymbol{\Phi}$ is precisely

$$\mathbf{T}_{\varphi}\boldsymbol{\Phi} := \left\{ \boldsymbol{\theta} : \bar{\Omega} \to R^3; \quad \boldsymbol{\theta} = \boldsymbol{0} \quad on \quad \Gamma_0 \right\} \tag{2.75}$$

It si thus as elements of this tangent space that the vector fields occurring in the principle of virtual work are to be correctly understood as variations; this observation is also the basis for attaching the label variational to the equations themselves. The adjective virtual, derived from classical continuum mechanics, reflects the fact that the vector fields $\boldsymbol{\theta} \in \mathbf{T}_{\varphi}\boldsymbol{\Phi}$ appearing in the principle are essentially mathematical quantities, which need not be given a physical interpretation.

2.7. Remarks

(1) A more transparent interpretation of these variations , where the principle of virtual work will be understood as a requirement for a certain functional to be stationary.

(2) (The introduction of a tangent space can prove quite useful in more complex situations where the set o admissible deformations include other geometrical constrains, such as incompressibility (Narsden & Hughes [1983, p.279]).

(3) The regularity assumptions on the applied force densities, on the boundary of the body, etc., can be relaxed in various ways that still guarantee that the axioms of force and moment balance and the principle of virtual work make sense. In this direction, see notably Noll [1959, 1966, 1978], Gurtin & Willims [1967], Truesdell [1977] , Antman & Osborn [1979]

2.8. References

[1] Boley, B.A.,Weiner, J.H., *Theory of thermal stresses*, Dover publications, inc. Mineola, New York

[2] Ciarlet, Philiphe G., *Mathematical Elasticity, Volume I.: Three dimensional elasticity*, Elsevier Science Publishers B.V.

[3] Gurtin, M. E., *The Linear Theory of Elasticity, Handbbuch der Physik*, Springer, Berlin, 1972.

[4] Lekhnitskii, S. G., *Theory of Elasticity of an Anisotropic Body*, Mir, Moscow, 1981.

[5] Love, A. E. H., *A Treatise on the Mathematical Theory of Elasticity*, Dover Publications, Inc, New York, 1944

[6] Nunziante, L., Gambarotta, L., Tralli, A., *Scienza delle Costruzioni*, 3° Edizione, McGraw-Hill, 2011, ISBN**:** 9788838666971

[7] Ting TCT. *Anisotropic elasticity - Theory and applications*. Oxford University Press; 1996.

[8] Wolfram, S., *Mathematica, version 8*, Wolfram Research, Inc., Champaign, IL, 1998–2005.

CHAPTER III
CONSTITUTIVE ASSUMPTION

3.1. Introduction to the behaviour of materials

3.1.1. Tensile strength and tensile stress

This module outlines the basic mechanics of elastic response a physical phenomenon that materials often (but do not always) exhibit. An elastic material is one that deforms immediately upon loading, maintains a constant deformation as long as the load is held constant, and returns immediately to its original undeformed shape when the load is removed. This module will also introduce two essential concepts in Mechanics of Materials: stress and strain.

Perhaps the most natural test of a material's mechanical properties is the tension test, in which a strip or cylinder of the material, having length L and cross-sectional area A, is anchored at one end and subjected to an axial load P - a load acting along the specimen's long axis - at the other. (See Fig. 3.1.1). As the load is increased gradually, the axial deflection δ of the loaded end will increase also. Eventually the test specimen breaks or does something else catastrophic, often fracturing suddenly into two or more pieces. (Materials can fail mechanically in many different ways; for instance, recall how blackboard chalk, a piece of fresh wood, and Silly Putty break.) As engineers, we naturally want to understand such matters as how δ is related to P, and what ultimate fracture load we might expect in a specimen of different size than the original one. As materials technologists, we wish to understand how these relationships are influenced by the constitution and microstructure of the material

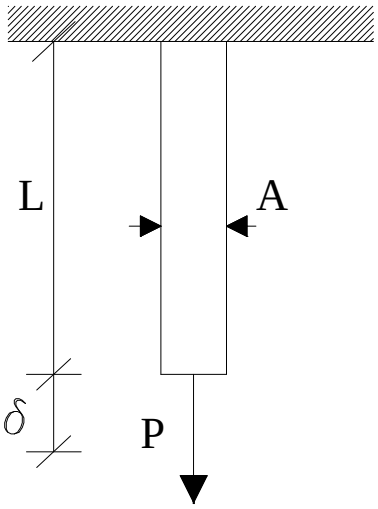

Fig. 3.1.1 - *The tension test.*

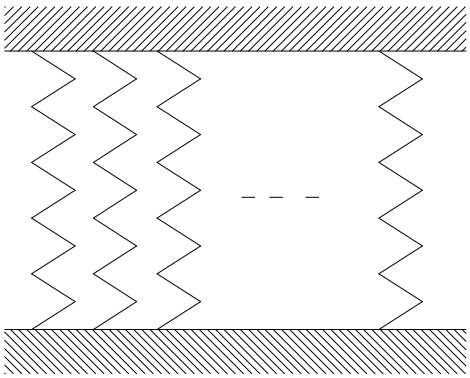

Fig. 3.1.2 - *Interplanar bonds*

One of the pivotal historical developments in our understanding of material mechanical properties was the realization that the strength of a uniaxially loaded specimen is related to the magnitude of its cross-sectional area. This notion is reasonable when one considers the strength to arise from the number of chemical bonds connecting one cross section with the one adjacent to it as depicted in Fig. 3.1.2, where each bond is visualized as a spring with a certain stiffness and strength. Obviously, the number of such bonds will increase proportionally with the section's area. The axial strength of a piece of blackboard chalk will therefore increase as the square of its diameter. In contrast, increasing the length of the chalk will not make it stronger (in fact it will likely become weaker, since the longer specimen will be statistically more likely to contain a strength-reducing flaw). Galileo (1564-1642) is said to have used this observation to note that giants, should they exist, would be very fragile creatures. Their strength would be greater than ours, since the cross-sectional areas of their skeletal and muscular systems would be larger by a factor related to the

square of their height. But their weight, and thus the loads they must sustain, would increase as their volume, that is by the cube of their height. A simple fall would probably do them great damage. Conversely, the "proportionate" strength of the famous arachnid mentioned weekly in the SpiderMan comic strip is mostly just this same size effect. There's nothing magical about the muscular strength of insects, but the ratio of L^2 to L^3 works in their behaviour when strength per body weight is reckoned. This cautions us that simple scaling of a previously proven design is not a safe design procedure. A jumbo jet is not just a small plane scaled up; if this were done the load-bearing components would be too small in cross-sectional area to support the much greater loads they would be called upon to resist.

When reporting the strength of materials loaded in tension, it is customary to account for this effect of area by dividing the breaking load by the cross-sectional area:

$$\sigma_f = \frac{P_f}{A_0} \tag{3.1.1}$$

where σ_f is the ultimate tensile stress, often abbreviated as UTS, Pf is the load at fracture, and A_0 is the original cross-sectional area. (Some materials exhibit substantial reductions in cross-sectional area as they are stretched, and using the original rather than final area gives the so-call engineering strength.) The units of stress are obviously load per unit area, N/m^2 (also called Pascals, or Pa) in the SI system and lb/in^2 (or psi) in units still used commonly in the United States.

If the specimen is loaded by an axial force P less than the breaking load Pf, the tensile stress is developed by analogy with Eqn. 1 as:

$$\sigma = \frac{P}{A_0} \tag{3.1.2}$$

The tensile stress, the force per unit area acting on a plane transverse to the applied load, is a fundamental measure of the internal forces within the material. Much of Mechanics of Materials is concerned with elaborating this concept to include higher orders of dimensionality, working out methods of determining the stress for various geometries and loading conditions, and predicting what the material's response to the stress will be.

3.1.2. Stiffness

It is important to distinguish stiffness, which is a measure of the load needed to induce a given deformation in the material, from the strength, which usually refers to the material's resistance to failure by fracture or excessive deformation. The stiffness is usually measured by applying relatively small loads, well short of fracture, and measuring the resulting deformation. Since the deformations in most materials are very small for these loading conditions, the experimental problem is largely one of measuring small changes in length accurately. Hooke made a number of such measurements on long wires under various loads, and observed that to a good approximation the load P and its resulting deformation δ were related linearly as long as the loads were sufficiently small. This relation, generally known as Hooke's Law, can be written algebraically as

$$P = k\delta \tag{3.1.3}$$

where k is a constant of proportionality called the stiffness and having units of lb/in or N/m.

The stiffness as defined by k is not a function of the material alone, but is also influenced by the specimen shape. A wire gives much more deflection for a given load if coiled up like a watch spring, for instance. A useful way to adjust the stiffness so as to be a purely materials property is to normalize the load by the cross-sectional area; i.e. to use the tensile stress rather than the load. Further, the deformation δ can be normalized by noting that an applied load stretches all parts of the wire uniformly, so that a reasonable measure of "stretching" is the deformation per unit length:

$$\varepsilon = \frac{\delta}{L_0} \tag{3.1.4}$$

Here L_0 is the original length and ε is a dimensionless measure of stretching called the strain.

Using these more general measures of load per unit area and displacement per unit length (It was apparently the Swiss mathematician Jakob Bernoulli (1655-1705) who first realized the correctness of this form, published in the final paper of his life),
Hooke's Law becomes:

$$\frac{P}{A_0} = E\frac{\delta}{L_0} \tag{3.1.5}$$

or

$$\sigma = E\varepsilon \tag{3.1.6}$$

The constant of proportionality E, called Young's modulus (After the English physicist Thomas Young (1773-1829), who also made notable contributions to the understanding of the interference of light as well as being a noted physician and Egyptologist) or the modulus of elasticity, is one of the most important mechanical descriptors of a material. It has the same units as stress, Pa or psi. As shown in Fig. 3.1.3, Hooke's law can refer to either of Eqns. 3.1.3 or 3.1.6.

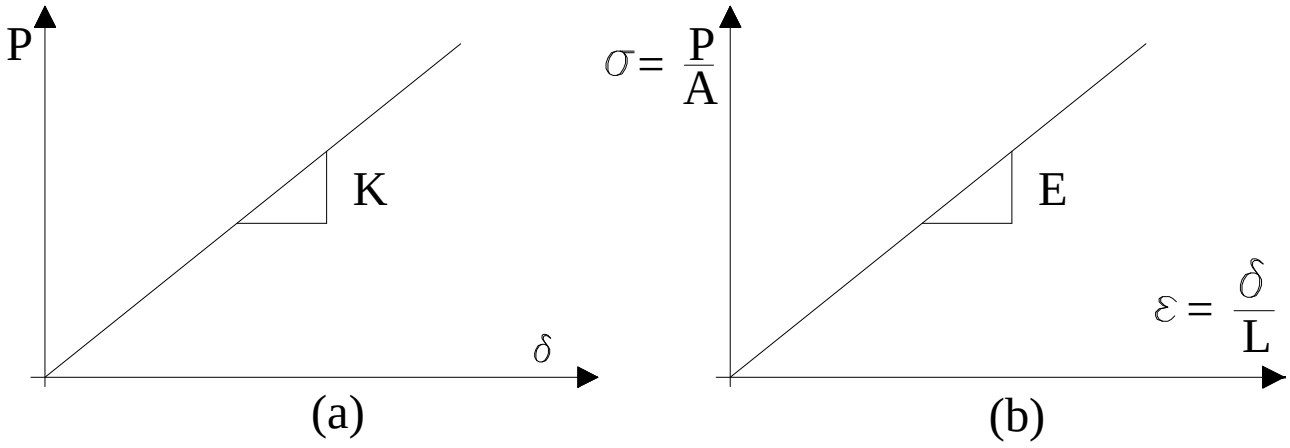

Fig. 3.1.3 - *Hooke's law in terms of (a) load-displacement and (b) stress-strain.*

The Hookean stiffness k is now recognizable as being related to the Young's modulus E and the specimen geometry as

$$k = \frac{EA}{L} \tag{3.1.7}$$

where here the 0 subscript is dropped from the area A; it will be assumed from here on (unless stated otherwise) that the change in area during loading can be neglected. Another useful relation is obtained by solving Eqn. 3.1.5 for the deflection in terms of the applied load as

$$\delta = \frac{PL}{EA} \tag{3.1.8}$$

Note that the stress $\sigma = P/A$ developed in a tensile specimen subjected to a fixed load is independent of the material properties, while the deflection depends on the material property E. Hence the stress σ in a tensile specimen at a given load is the same whether it's made of steel or polyethylene, but the strain ε would be different: the polyethylene will exhibit much larger strain and deformation, since its modulus is two orders of magnitude less than steel's. A material that obeys Hooke's Law (Eqn. 3.1.6) is called Hookean. Such a material is elastic according to the description of elasticity given in the introduction (immediate response, full recovery), and it is also linear in its relation between stress and strain (or equivalently, force and deformation). Therefore a Hookean material is linear elastic, and materials engineers use these descriptors interchangeably. It is important to keep in mind that not all elastic materials are linear (rubber is elastic but nonlinear), and not all linear materials are elastic (viscoelastic materials can be linear in the mathematical

sense, but do not respond immediately and are thus not elastic). The linear proportionality between stress and strain given by Hooke's law is not nearly as general as, say, Einstein's general theory of relativity, or even Newton's law of gravitation. It's really just an approximation that is observed to be reasonably valid for many materials as long the applied stresses are not too large. As the stresses are increased, eventually more complicated material response will be observed. Some of these effects will be outlined in the Module on Stress{Strain Curves, which introduces the experimental measurement of the strain response of materials over a range of stresses up to and including fracture. If we were to push on the specimen rather than pulling on it, the loading would be described as compressive rather than tensile. In the range of relatively low loads, Hooke's law holds for this case as well. By convention, compressive stresses and strains are negative, so the expression $\sigma = E\varepsilon$ holds for both tension and compression.

3.2. Elasticity, groups of symmetry, anisotropic solids with fourth rank tensors

3.2.1. Linear Costitutive law for Hyperelastic solids

The heterogeneous materials can be characterized by both inhomogeneity and anisotropy, since the first aspect is due to the multi-phase composition of the medium, while the second one is due to the geometrical arrangement of the different constituents within the examined heterogeneous volume.
In this section, the constitutive relations for anisotropic materials, in linear elasticity, are presented.
A linear anisotropic elastic material, as known, can have as many as 21 elastic constants. However, this number can be opportunely reduced when the examined material possesses certain material symmetry. Moreover, it is also reduced, in most cases, when a two-dimensional deformation is considered. It is worth to remember that the matrices of the elastic constants must be positive definite, because the strain energy must be positive. Hence, referring to a fixed rectangular coordinate system $\mathbf{e}_x, \mathbf{e}_y, \mathbf{e}_z$, let $\mathbf{T}$ and $\mathbf{E}$ be the stress and the strain fields, respectively, in an anisotropic hyperelastic material. The stress-strain relation can be written in the following form:

$$\mathbf{T} = \mathbf{C} : \mathbf{E} \tag{3.2.1}$$

or, in components:

$$\sigma_{ij} = C_{ijhk}\varepsilon_{hk} \tag{3.2.2}$$

where: $\mathbb{C}$ = fourth rank elastic stiffness tensor and where, for the hypothesis of iper-elasticity, the components C_{ijhk} satisfy the following conditions of full symmetry:

$$C_{ijhk} = C_{jihk} = C_{hkij} \tag{3.2.3}$$

The above written equation (3.2.3) groups in it the following equalities:

$$C_{ijhk} = C_{jihk} = C_{ijkh} = C_{jikh} \tag{3.2.4}$$

and

$$C_{ijhk} = C_{hkij} \tag{3.2.5}$$

where the (3.2.4) follows directly from the symmetry of the stress and the strain tensors, while the (3.2.5) is due to the assuming hypothesis of existence of the elastic potential ϕ. In other word, the strain energy ϕ per unit volume of the material, given by:

$$\phi = \int_0^{\varepsilon} \sigma_{ij} d\varepsilon_{ij} \tag{3.2.6}$$

is independent of the loading path, i.e. the path that ε_{ij} takes from 0 to ε while it depends on the final value of ε, only. In linear elasticity, the (3.2.6) may be written as:

$$\phi = \frac{1}{2}\sigma_{ij}\varepsilon_{ij} = \frac{1}{2}C_{ijhk}\varepsilon_{ij}\varepsilon_{hk} \tag{3.2.7}$$

and since the strain energy must be positive, it has to be:

$$C_{ijhk}\varepsilon_{ij}\varepsilon_{hk} > 0 \tag{3.2.8}$$

for any real, non zero, symmetric tensor ε_{ij}. Hence, as said before, the stiffness tensor $\mathbb{C}$ is defined positive. Analogously, the stress-strain relation can be written in the following form, inverse of (3.2.1):

$$\mathbf{E} = \mathbf{S} : \mathbf{T} \tag{3.2.9}$$

or, in components:

$$\varepsilon_{ij} = S_{ijhk}\sigma_{hk} \tag{3.2.10}$$

where: $\mathbb{S}$ = fourth rank elastic compliance tensor, and where for the hypothesis of iper-elasticity, the components S_{ijhk} satisfy the following conditions of full symmetry:

$$S_{ijhk} = S_{jihk} = S_{hkij} \tag{3.2.11}$$

The above written equation (3.2.11) groups in it the following equalities:

$$S_{ijhk} = S_{jihk} = S_{ijkh} = S_{jikh} \tag{3.2.12}$$

and

$$S_{ijhk} = S_{hkij} \tag{3.2.13}$$

where the (3.2.12) follows directly from the symmetry of the stress and the strain tensors, while the (3.2.13) is due to the assuming hypothesis of existence of the elastic complementary potential ψ, [64]. In other word, the stress energy ψ per unit volume of the material, given by:

$$\psi = \int_0^{\sigma} \varepsilon_{ij} d\sigma_{ij} \tag{3.2.14}$$

It is independent of the loading path, i.e. the path that σ_{ij} takes from 0 to σ while it depends on the final value of σ , only. In linear elasticity, the (2.2.14) may be written as:

$$\psi = \frac{1}{2}\sigma_{ij}\varepsilon_{ij} = \frac{1}{2}S_{ijhk}\sigma_{ij}\sigma_{hk} \tag{3.2.15}$$

and since the stress energy must be positive, it has to be:

$$S_{ijhk}\sigma_{ij}\sigma_{hk} > 0 \tag{3.2.16}$$

for any real, non zero, symmetric tensor σ_{ij}. Hence, as said before, the compliance tensor $\mathbb{S}$ is defined positive. Introducing, now, the contract notation, [36], such that:

$$\begin{aligned} &\sigma_{xx} = \sigma_1, \quad \sigma_{yy} = \sigma_2, \quad \sigma_{zz} = \sigma_3, \\ &\tau_{yz} = \sigma_4, \quad \tau_{xz} = \sigma_5, \quad \tau_{xy} = \sigma_6, \end{aligned} \tag{3.2.17}$$

$$\begin{aligned} &\varepsilon_{xx} = \varepsilon_1, \quad \varepsilon_{yy} = \varepsilon_2, \quad \varepsilon_{zz} = \varepsilon_3, \\ &2\varepsilon_{yz} = \varepsilon_4, \quad 2\varepsilon_{xz} = \varepsilon_5, \quad 2\varepsilon_{xy} = \varepsilon_6, \end{aligned}$$

the stress-strain laws (3.2.2) and (3.2.10) may be written, respectively, as:

$$\sigma_\alpha = C_{\alpha\beta}\varepsilon_\beta, \quad C_{\alpha\beta} = C_{\beta\alpha} \tag{3.2.18}$$

and

$$\varepsilon_\alpha = S_{\alpha\beta}\varepsilon_\beta, \quad S_{\alpha\beta} = S_{\beta\alpha} \tag{3.2.19}$$

With reference, in particular, to the equation (2.18), it may be expressed in a matrix form, as it follows:

$$\mathbf{T} = \mathbf{C} : \mathbf{E}, \quad \mathbf{C} = \mathbf{C}^T \tag{3.2.20}$$

The stress and the strain tensors, ***T*** and ***E*** , are expressed in form of 6x1 column matrices, while the stiffness tensor $\mathbb{C}$ is expressed in form of 6x6 symmetric matrix, as given in the following equation:

$$\mathbf{C}=\begin{bmatrix} C_{11} & C_{12} & C_{13} & C_{14} & C_{15} & C_{16} \\ C_{12} & C_{22} & C_{23} & C_{24} & C_{25} & C_{26} \\ C_{13} & C_{23} & C_{33} & C_{34} & C_{35} & C_{36} \\ C_{14} & C_{24} & C_{34} & C_{44} & C_{45} & C_{46} \\ C_{15} & C_{25} & C_{35} & C_{45} & C_{55} & C_{56} \\ C_{16} & C_{26} & C_{36} & C_{46} & C_{56} & C_{66} \end{bmatrix} \tag{3.2.21}$$

where the transformation between C_{ijhk} and $C_{\alpha\beta}$ is accomplished by replacing the subscripts *ij* (or *hk*) by α or β , by using the following rules:

$$\begin{aligned} &ij(or\ hk) \leftrightarrow \alpha(or\ \beta) \\ &xx \leftrightarrow 1 \\ &yy \leftrightarrow 2 \\ &zz \leftrightarrow 3 \\ &zy \ \ or \ \ yz \leftrightarrow 4 \\ &zx \ \ or \ \ xz \leftrightarrow 5 \\ &xy \ \ or \ \ yz \leftrightarrow 6 \end{aligned} \tag{3.2.22}$$

We may write the transformation (3.2.22) as:

$$\begin{aligned} \alpha &= \begin{cases} i & if \quad i=j \\ 9-i-j & if \quad i\neq j \end{cases} \\ \beta &= \begin{cases} h & if \quad h=k \\ 9-h-k & if \quad h\neq k \end{cases} \end{aligned} \tag{3.2.23}$$

Analogously, with reference to the equation (3.2.17), the stress-strain law (3.2.19) may be expressed in a matrix form, as it follows:

$$\mathbf{E}=\mathbf{S}:\mathbf{T}, \quad \mathbf{S}=\mathbf{S}^T \tag{3.2.24}$$

where also the compliance tensor $\mathbb{S}$ is expressed in form of 6x6 symmetric matrix, as given by:

$$S=\begin{bmatrix} S_{11} & S_{12} & S_{13} & S_{14} & S_{15} & S_{16} \\ S_{12} & S_{22} & S_{23} & S_{24} & S_{25} & S_{26} \\ S_{13} & S_{23} & S_{33} & S_{34} & S_{35} & S_{36} \\ S_{14} & S_{24} & S_{34} & S_{44} & S_{45} & S_{46} \\ S_{15} & S_{25} & S_{35} & S_{45} & S_{55} & S_{56} \\ S_{16} & S_{26} & S_{36} & S_{46} & S_{56} & S_{66} \end{bmatrix} \tag{3.2.25}$$

Here, the transformation between S_{ijhk} and $S_{\alpha\beta}$ is similar to that one between C_{ijhk} and $S_{\alpha\beta}$ except the following:

$$\begin{aligned} &S_{ijhk}=S_{\alpha\beta} \quad if \ \ both \quad \alpha,\beta\leq 3 \\ &2S_{ijhk}=S_{\alpha\beta} \quad if \ \ either \quad \alpha \ or \ \beta\leq 3 \\ &4S_{ijhk}=S_{\alpha\beta} \quad if \ \ both \quad \alpha,\beta>3 \end{aligned} \tag{3.2.26}$$

From (3.2.20) and (3.2.24), it is obtained the expression of the strain energy, as:

$$\phi=\frac{1}{2}\mathbf{E}^T\mathbf{C}\,\mathbf{E}=\frac{1}{2}\mathbf{T}^T\,\mathbf{E}=\frac{1}{2}\mathbf{T}^T\,\mathbf{S}\,\mathbf{T} \tag{3.2.27}$$

and, by considering that ϕ has to be positive, it must be:

$$\begin{aligned}\mathbf{E}^T\mathbf{C}\mathbf{E} &> 0\\ \mathbf{T}^T\mathbf{S}\mathbf{T} &> 0\end{aligned} \tag{3.2.28}$$

This implies that the matrices $\mathbb{C}$ and $\mathbb{S}$ are both positive definite. Moreover, by substituting of the (3.2.24) in the (3.2.20) yields:

$$\mathbf{C}\cdot\mathbf{S} = \mathbf{I} = \mathbf{S}\cdot\mathbf{C} \tag{3.2.29}$$

where the second equality follows from the first one which says that $\mathbb{C}$ and $\mathbb{S}$ are the inverses of each other and, hence, their product commute. For a linear anisotropic elastic material, like it has been anticipated before, the matrices $\mathbb{C}$ and $\mathbb{S}$ have 21 elastic independent constants. However, this number can be reduced when a two-dimensional deformation is considered. Assume, therefore, the deformation of the examined anisotropic elastic bodies to be a two-dimensional one for which $\mathbf{e}_z = 0$. When $\mathbf{e}_z = 0$, the stress-strain law given by the first equation of (3.2.18) becomes:

$$\sigma_\alpha = \sum\nolimits_{\beta\neq 3} C_{\alpha\beta}\varepsilon_\beta \quad \alpha = 1,2,3,...,6 \quad \beta = 1,2,...,6 \tag{3.2.30}$$

Ignoring the equation for σ_3 , the (3.2.30) may be written as:

$$\hat{\mathbf{T}} = \hat{\mathbf{C}} : \hat{\mathbf{E}}, \quad \hat{\mathbf{C}} = \hat{\mathbf{C}}^T \tag{3.2.31}$$

where

$$\hat{\mathbf{T}}^T = \left[\sigma_1, \sigma_2, \sigma_4, \sigma_5, \sigma_6\right] \tag{3.2.32}$$

$$\hat{\mathbf{E}}^T = \left[\varepsilon_1, \varepsilon_2, \varepsilon_4, \varepsilon_5, \varepsilon_6\right] \tag{3.2.33}$$

and

$$\hat{\mathbf{C}} = \begin{bmatrix} C_{11} & C_{12} & C_{14} & C_{15} & C_{16} \\ C_{12} & C_{22} & C_{24} & C_{25} & C_{26} \\ C_{14} & C_{24} & C_{44} & C_{45} & C_{46} \\ C_{15} & C_{25} & C_{45} & C_{55} & C_{56} \\ C_{16} & C_{26} & C_{46} & C_{56} & C_{66} \end{bmatrix} \tag{3.2.34}$$

Since $\hat{\mathbf{C}}$ is obtained from $\mathbf{C}$ by deleting the third row and the third column of it, $\hat{\mathbf{C}}$ is a principal sub-matrix of $\mathbf{C}$ and it also is positive definite. It contains 15 independent elastic constants. The stress-strain law (3.2.19) for $\mathbf{e}_z = 0$ is:

$$\mathbf{e}_z = 0 = S_{3\beta}\sigma_\beta \tag{3.2.35}$$

Solving for σ_3 , it is:

$$\sigma_3 = -\frac{1}{S_{33}}\sum\nolimits_{\beta\neq 3} S_{3\beta}\sigma_\beta \tag{3.2.36}$$

and by substituting the (3.2.36) within the first equation of the (3.2.19), it is obtained:

$$\varepsilon_\alpha = \sum\nolimits_{\beta\neq 3} S'_{\alpha\beta}\sigma_\beta \tag{2.2.37}$$

with

$$S'_{\alpha\beta} = S_{\alpha\beta} - \frac{S_{\alpha 3}S_{3\beta}}{S_{33}} = S'_{\beta\alpha} \tag{3.2.38}$$

$$S'_{\beta\alpha} = reduced \quad elastic \quad compliances$$

It is clear, moreover, that:

$$S'_{\alpha 3}=0,\quad S'_{3\beta}=0,\quad \alpha,\beta=1,2,...,6 \tag{3.2.39}$$

For this reason, there is no need to exclude $\beta=3$ in the (3.2.37). By using the notation of the (3.3.32) and (3.2.33), the (3.2.37) can be written in the following form:

$$\hat{\mathbf{E}}=\mathbf{S}'\mathbf{:}\hat{\mathbf{T}},\quad \mathbf{S}'=\mathbf{S}'^{T} \tag{3.2.40}$$

where $\mathbb{S}'$ can be defined as *reduced elastic compliance tensor* and it has a symmetric matrix form, given by:

$$\mathbf{S}'=\begin{bmatrix} S'_{11} & S'_{12} & S'_{14} & S'_{15} & S'_{16} \\ S'_{12} & S'_{22} & S'_{24} & S'_{25} & S'_{26} \\ S'_{14} & S'_{24} & S'_{44} & S'_{45} & S'_{46} \\ S'_{15} & S'_{25} & S'_{45} & S'_{55} & S'_{56} \\ S'_{16} & S'_{26} & S'_{46} & S'_{56} & S'_{66} \end{bmatrix} \tag{3.2.41}$$

Like $\hat{\mathbf{C}}$, $\mathbf{S}'$ contains 15 independent elastic constants. Moreover, the substitution of the (3.2.40) in the (3.2.31) yields:

$$\hat{\mathbf{C}}\cdot\mathbf{S}'=\mathbf{I}=\mathbf{S}'\cdot\hat{\mathbf{C}} \tag{3.2.42}$$

where the second equality follows from the first one which says that $\hat{\mathbf{C}}$ and $\mathbf{S}'$ are the inverses of each other and, hence, their product commute. This result is independent of whether $\mathbf{e}_z=0$ or not, because it represents a property of elastic constants, [64]. It has to be underlined that the positive definite of $\hat{\mathbf{C}}$ implies that $\mathbf{S}'$ is also positive definite. An alternate proof that $\hat{\mathbf{C}}$ and $\mathbf{S}'$ are positive definite is to write the strain energy as:

$$\phi=\frac{1}{2}\hat{\mathbf{E}}^{T}\hat{\mathbf{C}}\hat{\mathbf{E}}=\frac{1}{2}\hat{\mathbf{T}}^{T}\hat{\mathbf{E}}=\frac{1}{2}\hat{\mathbf{T}}^{T}\hat{\mathbf{S}}\hat{\mathbf{T}} \tag{3.2.43}$$

and to consider that ϕ has to be positive for any nonzero $\hat{\mathbf{T}}$ and $\hat{\mathbf{E}}$, so it must be:

$$\begin{aligned}\hat{\mathbf{E}}^{T}\hat{\mathbf{C}}\hat{\mathbf{E}}>0\\ \hat{\mathbf{T}}^{T}\mathbf{S}'\hat{\mathbf{T}}>0\end{aligned} \tag{3.2.44}$$

As anticipated at the beginning of this section, the number of the independent elastic constants of the 6x6 matrices $\mathbb{C}$ and $\mathbb{S}$ can be opportunely reduced, yet, when the examined anisotropic material possesses certain material symmetry. Hence, with reference to a new rectangular coordinate system $\left\{\mathbf{e}_x^*,\mathbf{e}_y^*,\mathbf{e}_z^*\right\}$, obtained from the initial fixed one $\left\{\mathbf{e}_x,\mathbf{e}_y,\mathbf{e}_z\right\}$ under an orthogonal transformation:

$$\mathbf{e}^{*}=\mathbf{Q}\cdot\mathbf{e} \tag{3.2.45}$$

or, in components:

$$e_i^{*}=Q_{ij}e_j \tag{3.2.46}$$

in which $\mathbf{Q}$ is an orthogonal matrix that satisfies the following relations:

$$\mathbf{Q}\cdot\mathbf{Q}^{T}=\mathrm{I}=\mathbf{Q}^{T}\mathbf{Q} \tag{3.2.47}$$

or:

$$Q_{ij}Q_{kj}=\delta_{ik}=Q_{ji}Q_{jk} \tag{3.2.48}$$

a material is said to possess a *symmetry* with respect to $\mathbf{Q}$ if the elastic fourth rank stiffness tensor $\mathbf{C}^{*}$ referred to the $\mathbf{e}_i$ coordinate system is equal to that one $\mathbf{C}$ referred to the coordinate system $\mathbf{e}_i$, i.e.:

$$\mathbf{C}^{*}=\mathbf{C} \tag{3.2.49}$$

or in components:

$$\mathbf{C}^{*}_{ijhk}=\mathbf{C}_{ijhk} \tag{3.2.50}$$

where:

$$\mathbf{C}^{*}_{ijhk} = Q_{ip}Q_{jq}Q_{hr}Q_{ks}\mathbf{C}_{pqrs} \tag{3.2.51}$$

An identical equation can be written for $\mathbf{S}_{ijhk}$.

In other words, when:

$$C_{ijhk} = Q_{ip}Q_{jq}Q_{hr}Q_{ks}C_{pqrs} \tag{3.2.52}$$

the material possesses a symmetry with respect to $\mathbf{Q}$.

The transformation law (3.2.51) is referred for the C_{ijhk}, but, for simplicity of the calculations, some authors adopt the transformation law for $C_{\alpha\beta}$:

$$C^{*}_{\alpha\beta} = K_{\alpha r}K_{\beta t}C_{rt} \tag{3.2.53}$$

where: **K** is a 6x6 matrix, whose elements are obtained by means of suitable assembly of the components Q_{ij}, according to proposals by Mehrabadi, Cowin et al (1995), and Mehrabadi and Cowin (1990). Then, an anisotropic material possesses the symmetry of *central inversion* (*C*) if the (3.2.52) is satisfied for:

$$\mathbf{Q} = \begin{bmatrix} -1 & 0 & 0 \\ 0 & -1 & 0 \\ 0 & 0 & -1 \end{bmatrix} = -\mathbf{I} \tag{3.2.54}$$

It is obvious that the (3.2.52) is satisfied by the $\mathbf{Q}$ given in the (3.2.54) for any C_{ijhk}. Therefore, all the anisotropic materials have the symmetry of central inversion.

If $\mathbf{Q}$ is a proper orthogonal matrix, the transformation (3.2.45) represents a rigid body rotation about an axis. So, an anisotropic material is said to possess a *rotational symmetry* if the (3.2.52) is satisfied for:

$$\mathbf{Q}^{r}(\theta) = \begin{bmatrix} \cos\theta & \sin\theta & 0 \\ -\sin\theta & \cos\theta & 0 \\ 0 & 0 & 1 \end{bmatrix} \tag{3.2.55}$$

which represents, for example, a rotation about the $\mathbf{e}_z$-axis an angle θ, as shown in the following figure.

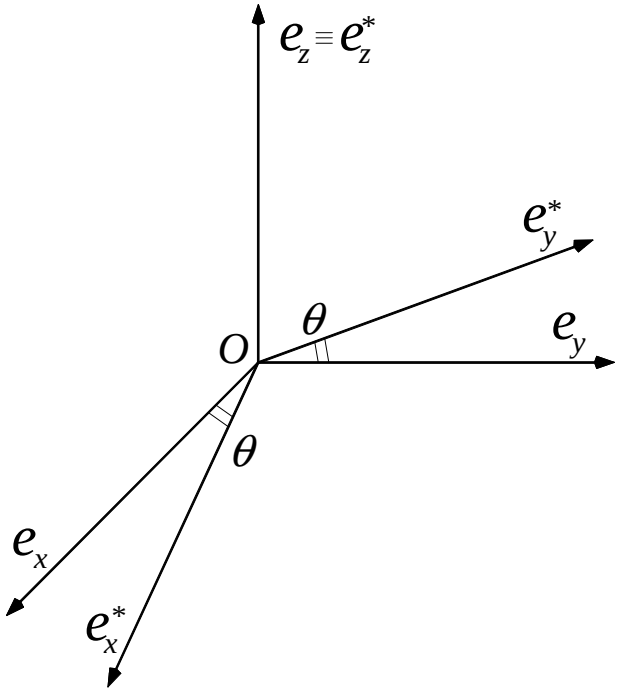

Fig. 2.2.1 - *Rigid rotation about the* $\mathbf{e}_z$ *-axis.*

By extending this property, i.e. if the (3.2.52) is satisfied by the $\mathbf{Q}$ as given through the (3.2.55) for any θ, then the material possesses a rotational symmetry with respect at any rotation in the $\mathbf{e}_z = 0$ plane. In this case, it is said that the $\mathbf{e}_z = 0$ is the *plane of transverse isotropy* or that $\mathbf{e}_z$ is *axis of elastic symmetry* with order $p = \infty$ ($L\infty$). More in general, instead, by indicating with:

$$\theta = \frac{2\pi}{p} \tag{3.2.56}$$

the rotation angle about an axis, this latter is defined as *axis of elastic symmetry* with order *p*. Since *p* may assume values equal to 2,3, 4,6 and ∞, the axis of elastic symmetry has indicated, respectively, with $L2$, $L3$, $L4$, $L6$ and $L\infty$. If $\mathbf{Q}$ is, instead, an orthogonal matrix as defined below:

$$\mathbf{Q} = \mathbf{I} - 2\,\mathbf{n} \otimes \mathbf{n}^T \tag{3.2.57}$$

where: ***n*** *is* a unit vector. Then, the transformation (3.2.45) represents a reflection about a plane whose normal is ***n***, defined as *reflection plane or symmetry plane* (*P*). In particular, if ***m*** is any vector on the plane, the following relation is satisfied:

$$\mathbf{Q}\,\mathbf{n} = -\mathbf{n}, \quad \mathbf{Q}\,\mathbf{m} = -\mathbf{m} \tag{3.2.58}$$

According to a such orthogonal matrix, therefore, a vector normal to the reflection plane reverses its direction after the transformation while a vector belonging to the reflection plane remains unchanged.

So, an anisotropic material is said to possess a *symmetry plane* if the (3.2.52) is satisfied by the $\mathbf{Q}$ as given by (3.2.57). For example, consider:

$$\mathbf{n}^T = \left[\cos\theta, \sin\theta, 0\right] \tag{3.2.59}$$

i.e. the symmetry plane contains the $\mathbf{e}_z$ -axis and its normal vector makes an angle of θ with the $\mathbf{e}_x$ -axis, as shown in the following figure.

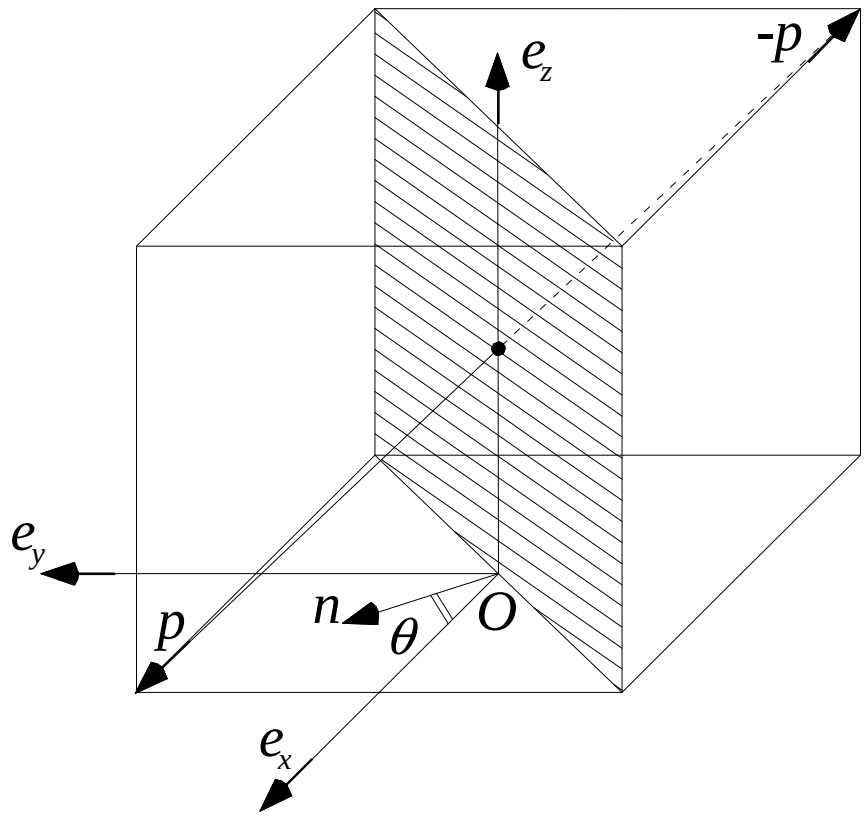

Fig. 3.2.2 - *Reflection about a plane containing the* $\mathbf{e}_z$ *-axis.*

The orthogonal matrix $\mathbf{Q}$ of the (3.2.57), so, has the following expression:

$$\mathbf{Q}(\theta)=\begin{bmatrix} 2+\cos 2\theta & \sin 2\theta & 0 \\ \sin 2\theta & 2-\cos 2\theta & 0 \\ 0 & 0 & 1 \end{bmatrix}, \quad -\frac{\pi}{2}<\theta\leq\frac{\pi}{2} \tag{3.2.60}$$

which is an improper orthogonal matrix and represents a reflection with respect to a plane whose normal is on the $(\mathbf{e}_x,\mathbf{e}_y)$ plane. Since θ and $\theta+\pi$ represent the same plane, θ is limited to the range shown in (3.2.60). In the particular case that $\theta=0$, $\mathbf{Q}$ becomes:

$$\mathbf{Q}(\theta)=\begin{bmatrix} -1 & 0 & 0 \\ 0 & 1 & 0 \\ 0 & 0 & 1 \end{bmatrix} \tag{3.2.61}$$

which represents a reflection about the plane $\mathbf{e}_x=0$. Hence, an anisotropic material for which the (3.2.52) is satisfied by the $\mathbf{Q}$ as given through the (3.2.61) is said to possess a *symmetry plane at* $\mathbf{e}_x=0$. By extending this property, i.e. if the (3.2.52) is satisfied by the $\mathbf{Q}$ as given through the (3.2.60) for any θ , then the material possesses a symmetry plane with respect at any plane that contains the $\mathbf{e}_z$ -axis. In this case, it is said that the $\mathbf{e}_z$ -axis is the *axis of symmetry* (*L*).

In analogous manner, it is considered, in the following equation, the expression of an orthogonal matrix which represents a reflection with respect to a plane whose normal is on the $(\mathbf{e}_y,\mathbf{e}_z)$ plane, making an angle φ with the $\mathbf{e}_y$ -axis:

$$\mathbf{Q}(\varphi)=\begin{bmatrix} 1 & 0 & 0 \\ 0 & -\cos 2\varphi & -\sin 2\varphi \\ 0 & -\sin 2\varphi & \cos 2\varphi \end{bmatrix}, \quad -\frac{\pi}{2}<\theta\leq\frac{\pi}{2} \tag{3.2.62}$$

In particular, the symmetry plane $\mathbf{e}_y=0$ can be represented by either $\theta=\pi/2$ or $\varphi=0$, while the symmetry plane $\mathbf{e}_z$ can be represented by $\varphi=\pi/2$, as shown in the following figure:

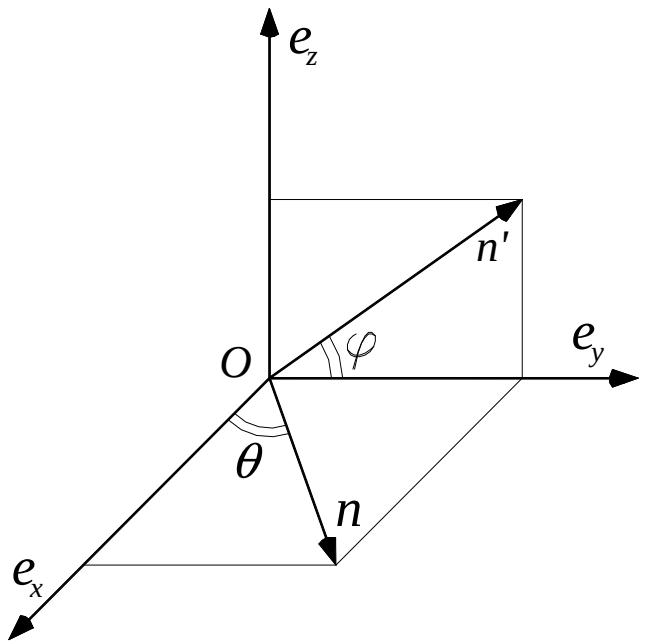

Fig. 3.2.3 - *The vectors n and n' are, respectively, the normal vectors to planes of reflection symmetry defined by the (3.2.60) and (3.2.62)*

3.2.2. Anisotropy and material symmetries

The existence of various combinations of the different symmetry forms implies a corresponding classification of the anisotropy classes of the materials. In particular, two extreme cases of anisotropic elastic materials are the *triclinic* materials and the *isotropic* ones. The first material possesses no rotational symmetry or a plane of reflection symmetry, while the second material possesses infinitely many rotational symmetries and planes of reflection symmetry. For such materials, it can be shown that:

$$C_{ijhk} = \lambda\delta_{ij}\delta_{hk} + G\left(\delta_{ih}\delta_{jk} + \delta_{ik}\delta_{jh}\right) \tag{3.2.63}$$

where λ and G are the Lamè constants, satisfies the (2.2.52) for any orthogonal $\mathbf{Q}$. It is possible to demonstrate that if an anisotropic elastic material possesses a material symmetry with the orthogonal matrix $\mathbf{Q}$, then it also possesses the material symmetry with $\mathbf{Q}^T = \mathbf{Q}^{-1}$. This means, for example, that if the material has rotational symmetry with rotation about the z -axis an angle θ, it also has the symmetry about the z -axis an angle $-\theta$. Moreover, it is possible to demonstrate, yet, that if an anisotropic elastic material possesses a symmetry with $\mathbf{Q}'$ and $\mathbf{Q}''$, then it also possesses a symmetry with $\mathbf{Q} = \mathbf{Q}'\mathbf{Q}''$. These statements, valid either for linear or nonlinear material, are useful in determining the structure of the stiffness tensor when the material possesses symmetries. Depending on the number of rotations and/or reflection symmetry a crystal possesses, Voigt (1910) in fact classified crystals into 32 classes. However, in terms of the 6x6 matrix $\mathbf{C}$, there are only 8 basic groups, since different combinations of symmetry forms may lead to the same structure of the stiffness tensor. This classification maid for crystals can be extended for non-crystalline materials, so that for them the structure of $\mathbf{C}$ can also be represented by one of the 8 basic groups.

Without loss in generality, in the follows, the list of such groups of materials are presented by choosing the symmetry plane (or planes) to coincide with the coordinate planes whenever possible. If the matrix $\mathbf{C}^*$ referred to a different coordinate system is desired, the (3.2.51) is used to obtain it.

- **Triclinic materials**

They represent the most general case, in which no symmetry form exists. The number of independent constants is, therefore, 21 and the matrix $\mathbf{C}$ assumes the following form:

$$\mathbf{C} = \begin{bmatrix} C_{11} & C_{12} & C_{13} & C_{14} & C_{15} & C_{16} \\ C_{12} & C_{22} & C_{23} & C_{24} & C_{25} & C_{26} \\ C_{13} & C_{23} & C_{33} & C_{34} & C_{35} & C_{36} \\ C_{14} & C_{24} & C_{34} & C_{44} & C_{45} & C_{46} \\ C_{15} & C_{25} & C_{35} & C_{45} & C_{55} & C_{56} \\ C_{16} & C_{26} & C_{36} & C_{46} & C_{56} & C_{66} \end{bmatrix} \quad n° = 21 \tag{3.2.64}$$

which is equal to that one of the equation (3.2.21).

- **Monoclinic materials**

The symmetry forms are: L^2, P, L^2PC; The number of the independent elastic constants is 13 and the matrix $\mathbf{C}$ assumes the following expressions:

a) Symmetry plane coinciding with $\mathbf{e}_x = 0$, i.e., $\theta = 0$

$$\mathbf{C}=\begin{bmatrix} C_{11} & C_{12} & C_{13} & C_{14} & 0 & 0 \\ C_{12} & C_{22} & C_{23} & C_{24} & 0 & 0 \\ C_{13} & C_{23} & C_{33} & C_{34} & 0 & 0 \\ C_{14} & C_{24} & C_{34} & C_{44} & 0 & 0 \\ 0 & 0 & 0 & 0 & C_{55} & C_{56} \\ 0 & 0 & 0 & 0 & C_{56} & C_{66} \end{bmatrix} \quad n^{\circ}=13 \tag{3.2.65}$$

b) Symmetry plane coinciding with $\mathbf{e}_y=0$, i.e., $\theta=\frac{\pi}{2}$ or $\varphi=0$:

$$\mathbf{C}=\begin{bmatrix} C_{11} & C_{12} & C_{13} & 0 & C_{15} & 0 \\ C_{12} & C_{22} & C_{23} & 0 & C_{25} & 0 \\ C_{13} & C_{23} & C_{33} & 0 & C_{35} & 0 \\ 0 & 0 & 0 & C_{44} & 0 & C_{46} \\ C_{15} & C_{25} & C_{35} & 0 & C_{55} & 0 \\ 0 & 0 & 0 & C_{46} & 0 & C_{66} \end{bmatrix} \quad n^{\circ}=13 \tag{3.2.66}$$

c) Symmetry plane coinciding with $\mathbf{e}_z=0$, i.e., $\varphi=\frac{\pi}{2}$:

$$\mathbf{C}=\begin{bmatrix} C_{11} & C_{12} & C_{13} & 0 & 0 & C_{16} \\ C_{12} & C_{22} & C_{23} & 0 & 0 & C_{26} \\ C_{13} & C_{23} & C_{33} & 0 & 0 & C_{36} \\ 0 & 0 & 0 & C_{44} & C_{45} & 0 \\ 0 & 0 & 0 & C_{45} & C_{55} & 0 \\ C_{16} & C_{26} & C_{36} & 0 & 0 & C_{66} \end{bmatrix} \quad n^{\circ}=13 \tag{3.2.67}$$

• **Orthotropic (or Rhombic) materials**

The symmetry forms are: $3P, 3L^2, L^2 2P, 3L^2 3PC$; with reference to the symmetry form $3P$, it means that the three coordinate planes, $\theta=0$, $\theta=\frac{\pi}{2}$ and $\varphi=\frac{\pi}{2}$ are the symmetry planes. The number of the independent elastic constants is 9 and the matrix $\mathbf{C}$ assumes the following form:

$$\mathbf{C}=\begin{bmatrix} C_{11} & C_{12} & C_{13} & 0 & 0 & 0 \\ C_{12} & C_{22} & C_{23} & 0 & 0 & 0 \\ C_{13} & C_{23} & C_{33} & 0 & 0 & 0 \\ 0 & 0 & 0 & C_{44} & 0 & 0 \\ 0 & 0 & 0 & 0 & C_{55} & 0 \\ 0 & 0 & 0 & 0 & 0 & C_{66} \end{bmatrix} \quad n^{\circ}=9 \tag{3.2.68}$$

• **Trigonal materials**

The symmetry forms are $L^3 3L^2, L^3 3P, L_6^3 3L^2 3PC$; with reference to the symmetry form $3P$, it is verified that the three coordinate planes, $\theta=0$, $\theta=+\frac{\pi}{3}$ and $\theta=-\frac{\pi}{3}$ are the symmetry planes. The number of the independent elastic constants is 6 and the matrix $\mathbf{C}$ assumes the following form:

$$\mathbf{C}=\begin{bmatrix} C_{11} & C_{12} & C_{13} & C_{14} & 0 & 0 \\ C_{12} & C_{11} & C_{13} & -C_{14} & 0 & 0 \\ C_{13} & C_{13} & C_{33} & 0 & 0 & 0 \\ C_{14} & -C_{14} & 0 & C_{44} & 0 & 0 \\ 0 & 0 & 0 & 0 & C_{44} & C_{14} \\ 0 & 0 & 0 & 0 & C_{14} & \dfrac{(C_{11}-C_{12})}{2} \end{bmatrix} \quad n^{\circ}=6 \tag{3.2.69}$$

• **Tetragonal materials**

The symmetry forms are: L^4, L^4PC, L_4^2; It is verified that the tetragonal materials show five symmetry planes at $\theta=0$, $\theta=+\dfrac{\pi}{4}$, $\theta=-\dfrac{\pi}{4}, \theta=+\dfrac{\pi}{2}$ and $\varphi=+\dfrac{\pi}{2}$. The number of the independent elastic constants is 6 and the matrix $\mathbf{C}$ assumes the following form:

$$\mathbf{C}=\begin{bmatrix} C_{11} & C_{12} & C_{13} & 0 & 0 & 0 \\ C_{12} & C_{11} & C_{13} & 0 & 0 & 0 \\ C_{13} & C_{13} & C_{33} & 0 & 0 & 0 \\ 0 & 0 & 0 & C_{44} & 0 & 0 \\ 0 & 0 & 0 & 0 & C_{44} & 0 \\ 0 & 0 & 0 & 0 & 0 & C_{66} \end{bmatrix} \quad n^{\circ}=6 \tag{3.2.70}$$

• **Transversely isotropic (or exagonal) materials**

The symmetry forms are: $L^3P, L^3 3L^2P, L^6, L^6 6L^2, L^6PC, L^6 6P, L^6 6L^2 7PC$; For the transversely isotropic materials the symmetry planes are $\varphi=+\dfrac{\pi}{2}$, i.e. $(\mathbf{e}_z=0)$, and any plane that contains the $\mathbf{e}_z$-axis. So, the $\mathbf{e}_z$-axis is the axis of symmetry. The number of the independent elastic constants is 5 and the matrix $\mathbf{C}$ assumes the following form:

$$\mathbf{C}=\begin{bmatrix} C_{11} & C_{12} & C_{13} & 0 & 0 & 0 \\ C_{12} & C_{11} & C_{13} & 0 & 0 & 0 \\ C_{13} & C_{13} & C_{33} & 0 & 0 & 0 \\ 0 & 0 & 0 & C_{44} & 0 & 0 \\ 0 & 0 & 0 & 0 & C_{44} & 0 \\ 0 & 0 & 0 & 0 & 0 & \dfrac{(C_{11}-C_{12})}{2} \end{bmatrix} \quad n^{\circ}=5 \tag{3.2.71}$$

• **Cubic materials**

The symmetry forms are $3L^2 4L^3, 3L^2 4L_6^3 3PC, 3L_4^2 4L^3 6P, 3L^4 4L^3 6L^2, 3L^4 4L_6^3 6L^2 9PC$; For the cubic materials there are nine symmetry planes, whose normal vectors are on the three coordinate axes and on the coordinate planes making an angle $\dfrac{\pi}{4}$ with coordinate axes. The number of the independent elastic constants is 3 and the matrix $\mathbf{C}$ assumes the following form:

$$\mathbf{C}=\begin{bmatrix} C_{11} & C_{12} & C_{12} & 0 & 0 & 0 \\ C_{12} & C_{11} & C_{12} & 0 & 0 & 0 \\ C_{12} & C_{12} & C_{11} & 0 & 0 & 0 \\ 0 & 0 & 0 & C_{44} & 0 & 0 \\ 0 & 0 & 0 & 0 & C_{44} & 0 \\ 0 & 0 & 0 & 0 & 0 & C_{44} \end{bmatrix} \quad n^{\circ}=3 \tag{3.2.72}$$

• Isotropic materials

For the isotropic materials any plane is a symmetry plane. The number of the independent elastic constants is 2 and the matrix $\mathbf{C}$ assumes the following form:

$$\mathbf{C}=\begin{bmatrix} C_{11} & C_{12} & C_{12} & 0 & 0 & 0 \\ C_{12} & C_{11} & C_{12} & 0 & 0 & 0 \\ C_{12} & C_{12} & C_{11} & 0 & 0 & 0 \\ 0 & 0 & 0 & \frac{C_{11}-C_{12}}{2} & 0 & 0 \\ 0 & 0 & 0 & 0 & \frac{C_{11}-C_{12}}{2} & 0 \\ 0 & 0 & 0 & 0 & 0 & \frac{C_{11}-C_{12}}{2} \end{bmatrix} \quad n^{\circ}=2 \tag{3.2.73}$$

If λ and μ are the Lamè constants, the (3.2.73) assumes the expression given by:

$$\mathbf{C}=\begin{bmatrix} 2\mu+\lambda & \lambda & \lambda & 0 & 0 & 0 \\ \lambda & 2\mu+\lambda & \lambda & 0 & 0 & 0 \\ \lambda & \lambda & 2\mu+\lambda & 0 & 0 & 0 \\ 0 & 0 & 0 & 2\mu & 0 & 0 \\ 0 & 0 & 0 & 0 & 2\mu & 0 \\ 0 & 0 & 0 & 0 & 0 & 2\mu \end{bmatrix} \quad n^{\circ}=2 \tag{3.2.74}$$

It is remarkable that, for isotropic materials, it needs only three planes of symmetry to reduce the number of elastic constants from 21 to 2. The following figure shows the hierarchical organization of the eight material symmetries of linear elasticity. It is organized so that the lower symmetries are at the upper left and, as one moves down and across the table to the right, one encounters crystal systems with greater and greater symmetry.

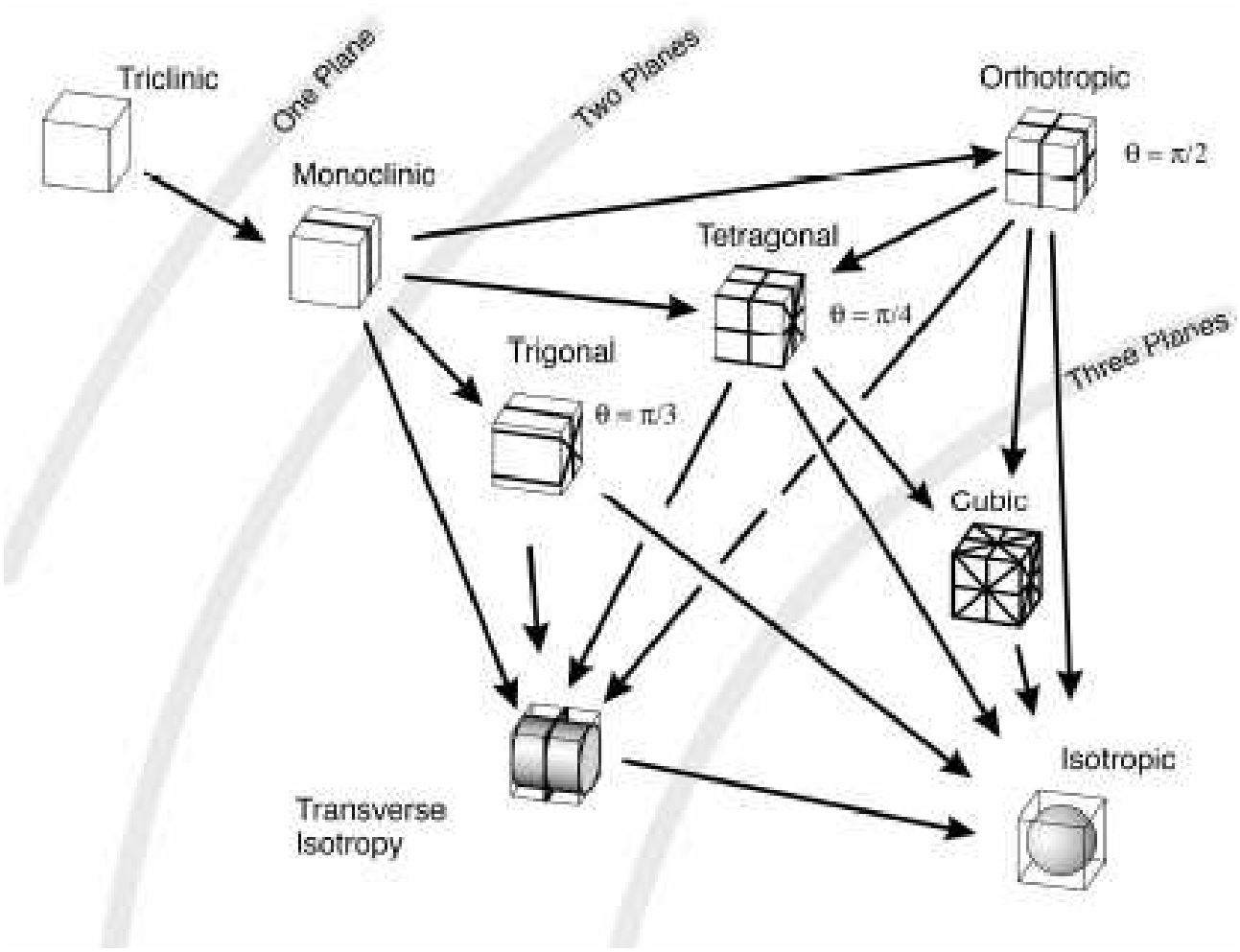

Fig. 3.2.4 - *Hierarchical organization of the eight material symmetries of linear elasticity*

It is worth to underline that the structure of the matrix $\mathbf{C}$ above obtained for each class of materials is referred to the specified coordinate system. When different coordinate systems are employed, the transformation law (3.2.51) has to be used for obtaining the structure of the new matrix $\mathbf{C}$, in which, while the number of nonzero elements may increase, the number of independent elastic constants remains constant since it does not depend on the choice of the coordinate systems. In the applications, the choice of the coordinate system is very often dictated by the boundary conditions of the problem and hence it may not coincide with the symmetry planes of the material. In these cases, the transformation of the matrix $\mathbf{C}$ to a different coordinates system becomes necessary.

The analysis until here presented for obtaining the structure of the stiffness tensor $\mathbf{C}$ may be applied analogously for obtaining the structure of the compliance tensor $\mathbf{S}$. Like $\mathbf{C}$, the elastic compliance tensor $\mathbf{S}$ is a fourth rank tensor and, under the orthogonal transformation (3.2.45), its components, S_{ijhk}, referred to a new coordinate system are related to those ones, S_{ijhk}, referred to the initial coordinate system by:

$$\mathbf{S}^{*}_{ijhk} = Q_{ip} Q_{jq} Q_{hr} Q_{ks} \mathbf{S}_{pqrs} \tag{3.2.75}$$

which is identical to (3.2.52).

Hence, the structure of the matrix $\mathbf{C}$ appearing in (3.2.64)-(3.2.73) remains valid for the matrix $\mathbf{S}$ with the following modifications required by (3.2.26).

The relation:

$$C_{56} = -C_{24} = C_{14} \tag{3.2.76}$$

in the (3.2.69) is replaced by:

$$\frac{1}{2}S_{56} = -S_{24} = S_{14} \tag{3.2.77}$$

and the elastic coefficient C_{66} in (3.2.69), (3.2.71) and (3.2.73) is replaced by:

$$C_{66} = 2\left(S_{11} - S_{12}\right) \tag{3.2.78}$$

In engineering applications the matrix $\mathbf{S}$ for isotropic materials is written as:

$$\mathbf{S} = \frac{1}{E}\begin{bmatrix} 1 & -\nu & -\nu & 0 & 0 & 0 \\ -\nu & 1 & -\nu & 0 & 0 & 0 \\ -\nu & -\nu & 1 & 0 & 0 & 0 \\ 0 & 0 & 0 & 1+\nu & 0 & 0 \\ 0 & 0 & 0 & 0 & 1+\nu & 0 \\ 0 & 0 & 0 & 0 & 0 & 1+\nu \end{bmatrix} \tag{3.2.79}$$

where:

$$E = \frac{\mu\left(3\lambda + 2\mu\right)}{\mu + \lambda}, \quad \nu = \frac{\lambda}{2\left(\lambda + \mu\right)} \tag{3.2.80}$$

are, respectively, the Young's modulus and the Poisson ratio. It can be shown that:

$$\lambda = \frac{\nu E}{\left(1+\nu\right)\left(1-2\nu\right)}, \quad \mu = \frac{E}{2\left(1+\nu\right)}, \tag{3.2.81}$$

For obtaining the structure of the elastic reduced compliance tensor $\mathbf{S}'$, the same considerations are valid with some modifications required by the (3.2.38). Hence, for example, the expression of $\mathbf{S}'$ for isotropic materials is the following one:

$$\mathbf{S}' = \frac{1}{2G}\begin{bmatrix} 1-\nu & -\nu & 0 & 0 & 0 \\ -\nu & 1-\nu & 0 & 0 & 0 \\ 0 & 0 & 1 & 0 & 0 \\ 0 & 0 & 0 & 1 & 0 \\ 0 & 0 & 0 & 0 & 1 \end{bmatrix} \quad n°2 \tag{3.2.82}$$

Like stated previously, the strong convexity condition which is equivalent to the positive definiteness of the strain energy, (3.2.8), yields that the stiffness tensor $\mathbf{C}$ is defined positive, as well as, the positive definiteness of the stress energy, (3.2.16), yields that the compliance tensor $\mathbf{S}$ is defined positive. In particular, in the contracted notation, the (3.2.8) implies that the 6x6 matrix $\mathbf{C}$ is also positive definite and, so, all its principal minors are positive, i.e.:

$$C_{ii} > 0 \quad \left(i \textit{ not summed}\right) \tag{3.2.83}$$

$$\det\begin{bmatrix} C_{ii} & C_{ij} \\ C_{ij} & C_{jj} \end{bmatrix} > 0 \quad \left(i, j \textit{ not summed}\right) \tag{3.2.84}$$

$$\det\begin{bmatrix} C_{ii} & C_{ij} & C_{ih} \\ C_{ij} & C_{jj} & C_{jh} \\ C_{ih} & C_{jh} & C_{hh} \end{bmatrix} > 0 \quad \left(i, j, k \textit{ not summed}\right) \tag{3.2.85}$$

$$\det\begin{bmatrix} C_{ii} & C_{ij} & C_{ik} & C_{ih} \\ C_{ij} & C_{jj} & C_{jk} & C_{jh} \\ C_{ik} & C_{jk} & C_{kk} & C_{kh} \\ C_{ih} & C_{jh} & C_{kh} & C_{hh} \end{bmatrix} > 0 \quad (i, j, k, h \text{ not summed}) \tag{3.2.86}$$

$$\det\begin{bmatrix} C_{ii} & C_{ij} & C_{ik} & C_{ih} & C_{im} \\ C_{ij} & C_{jj} & C_{jk} & C_{jh} & C_{jm} \\ C_{ik} & C_{jk} & C_{kk} & C_{kh} & C_{km} \\ C_{ih} & C_{jh} & C_{kh} & C_{hh} & C_{hm} \\ C_{im} & C_{jm} & C_{km} & C_{hm} & C_{mm} \end{bmatrix} > 0 \quad (i, j, k, h, m \quad \text{not summed}) \tag{3.2.87}$$

$$\det[\mathbf{C}] > 0 \tag{3.2.88}$$

where *i, j,h* are distinct integers which can have any value from 1 to 6.
In particular, according to the theorem which states that a real symmetric matrix is positive definite if and only if its leading principal minors are positive, the necessary and sufficient conditions for the 6x6 matrix $\mathbf{C}$ to be positive definite are the positivity of its 6 leading principal minors, i.e..
Analogously, the (3.2.16) implies that the 6x6 matrix $\mathbf{S}$ is also positive definite and, so, also its 6 leading principal minors are positive. The same consideration can be applied for the matrices $\hat{\mathbf{C}}$ and $\mathbf{S}'$. By imposing these conditions of positivity on the minors of the matrices, the restrictions on the elastic coefficients can be found. The above done anisotropic classification of the materials according to the number of symmetry planes is based on the assumption that, for each material, the number and the locations of the symmetry planes are known. However, this is not the case when considering an unknown material. So, often, the elastic stiffness and the elastic compliances of the material have to be determined to an arbitrarily chosen coordinate system. The result is that, if there exists a symmetry plane, it may not be one of the coordinate planes. Consequently, all elements of the matrices $\mathbf{C}$ and $\mathbf{S}$ can be nonzero. The problem is to locate the symmetry planes if they exist when $\mathbf{C}$ (or $\mathbf{S}$) is given. When a plane of symmetry exists, as already seen, the (3.2.52) is satisfied by the $\mathbf{Q}$ given in (3.2.57), which has the properties given in (3.2.58) where n is a unit vector normal to the plane symmetry and m is any vector perpendicular to n. Cowin and Mehrabadi (1987) have demonstrated that a set of necessary and sufficient conditions for $\boldsymbol{n}$ to be a unit normal vector to a plane of symmetry is:

$$C_{ijhh}n_j = \left(C_{pqss}n_p n_q\right)n_i \tag{3.2.89}$$

$$C_{ikhk}n_h = \left(C_{pqpq}n_p n_q\right)n_i \tag{3.2.90}$$

$$C_{ijhk}n_j n_k n_h = \left(C_{pqrs}n_p n_q n_r n_s\right)n_i \tag{3.2.91}$$

$$C_{ijhk}m_j m_k m_h = \left(C_{pqrs}n_p m_q n_r m_s\right)n_i \tag{3.2.92}$$

For example, if the plane $\mathbf{e}_x = 0$ is considered as plane of symmetry, by substituting in the (3.2.89)-(3.2.92) the vectors $\boldsymbol{n}$ and $\boldsymbol{m}$, defined as:

$$n_i = \delta_{i1}, \quad m_i = \delta_{i1}\cos\theta + \delta_{i3}\sin\theta \qquad \left(n_x = n_1,\ n_y = n_2,\ n_z = n_3\right) \tag{3.2.93}$$

where θ is an arbitrary constant, the independent elastic constants are obtained, according to the (3.2.65) if using the contracted notation.
More in general, the equations (3.2.89)-(3.2.92) tell that $\boldsymbol{n}$ is an eigenvector of the 3x3 symmetric matrices U , V , $R(\boldsymbol{n})$ and $R(\boldsymbol{m})$ whose elements are:

$$U_{ij} = C_{ijhh}, \quad V_{ih} = C_{ikhk}, \quad R_{ih}\left(\mathbf{n}\right) = C_{ijhk}n_j n_k \tag{3.2.94}$$

and it is stated, here, a modified Cowin-Mehrabadi theorem, as it follows:

An anisotropic elastic material with given elastic stiffness C_{ijhk} has a plane of symmetry if and only if $\boldsymbol{n}$ is an eigenvector of $R(\boldsymbol{n})$ and $R(\boldsymbol{m})$, or of U and $R(\boldsymbol{m})$ or of V and $R(\boldsymbol{m})$. The vector $\boldsymbol{n}$ is normal to the plane of symmetry, while $\boldsymbol{m}$ is any vector on the plane of symmetry.
Since this theorem is not suitable for determining $\boldsymbol{n}$ because the matrix $R(\boldsymbol{m})$ depends on $\boldsymbol{m}$ which, in turns, depends on $\boldsymbol{n}$, another theorem is used for computing $\boldsymbol{n}$:
An anisotropic elastic material with given elastic stiffness C_{ijhk} has a plane of symmetry if and only if $\boldsymbol{n}$ (normal vector to the plane of symmetry) is a common eigenvector of U and V and satisfies:

$$C_{ijhk} m_i n_j n_h n_k = 0 \tag{3.2.95}$$

$$C_{ijhk} m_i m_j m_h n_k = 0 \tag{3.2.96}$$

for any two independent vectors $\mathbf{m}^{\alpha}\ (\alpha = 1,2)$ on the plane of symmetry that do not form an angle a multiple of $\pi/3$.

3.3. References

[1] Boley, B.A.,Weiner, J.H., *Theory of thermal stresses*, Dover publications, inc. Mineola, New York
[2] Ciarlet, Philiphe G., *Mathematical Elasticity, Volume I.: Three dimensional elasticity*, Elsevier Science Publishers B.V.
[3] Gurtin, M. E., *The Linear Theory of Elasticity, Handbbuch der Physik*, Springer, Berlin, 1972.
[4] Lekhnitskii, S. G., *Theory of Elasticity of an Anisotropic Body*, Mir, Moscow, 1981.
[5] Love, A. E. H., *A Treatise on the Mathematical Theory of Elasticity*, Dover Publications, Inc, New York, 1944
[6] Nunziante, L., Gambarotta, L., Tralli, A., *Scienza delle Costruzioni*, 3° Edizione, McGraw-Hill, 2011, ISBN: 9788838666971
[7] Ting TCT. *Anisotropic elasticity - Theory and applications*. Oxford University Press; 1996.
[8] Wolfram, S., *Mathematica, version 8*, Wolfram Research, Inc., Champaign, IL, 1998–2005.
[9] Ogden, R.W. (1972). Large deformation isotropic elasticity: on the correlation of theory and experiment for incompressible rubberlike solids. *Proc. R. Soc. Lond. A* 326:565–584.
[10] Ogden, R.W. (1982). Elastic deformations of rubberlike solids. In Hopkins, H.G. and Sewell, M.J., eds., *Mechanics of Solids*, the Rodney Hill 60th Anniversary Volume. Oxford: Pergamon Press. 499–537.
[11] Ogden, R.W. (2001). Elements of the theory of finite elasticity. In Fu, Y.B. and Ogden, R.W., eds., *Nonlinear Elasticity: Theory and Applications*. Cambridge University Press. 1–57.
[12] Beatty, M.F. (1987). Topics in finite elasticity: hyperelasticity of rubber, elastomers and biological tissues— with examples. *Appl. Mech. Rev.* 40:1699–1734.
[13] Fu, Y.B. and Ogden, R.W. (2001). *Nonlinear Elasticity: Theory and Applications*. Cambridge University Press.
[14] N. Trabelsi, Z. Yosibash, C. Milgromb ,*Validation of subject-specific automated p-FE analysis of the proximal femur*, Journal of Biomechanics, 42 (2009) 234-241
[15] Benedikt Helgason, Fulvia Taddei, et al. , *A modified method for assigning material properties to FE models of bones*, Medical Engineering & Physics 30 (2008) 444-453
[16] M.J. Ciarelli, S.A. Goldstein, J.L. Kuhn, et al., *Evaluation of orthogonal mechanical properties and density of human trabecular bone from the major metaphyseal regions with materials testing and computed tomography*, J. Orthop. Res. 9 (1991) 674-682 (4)
[17] W.C. Van Buskirk, S.C. Cowin, R.N. Ward, *Ultrasonic measurement of orthotropic elastic constants of bovine femoral bone*, J. Biomech. Engrg. 103 (2) (1981) 67-72 (5)
[18] J.Y. Rho, M.C. Hobatho, R.B. Ashman, *Relations of mechanical properties to density and CT numbers in human bone*, Med. Engrg. Phys. 17 (1995) 347-355

[19] R. Schneider, G. Faust, U. Hindenlang, P. Helwig, *Inhomogeneous, orthotropic material model for the cortical structure of long bones modelled on the basis of clinical CT or density data*, Comput. Methods Appl. Mech. Engrg. 198 (2009) 2167-2174
[20] P. Helwig, G. Faust, U. Hindenlang, B. Kröplin, C. Eingartner, *Finite element analysis of a bone-implant system with the proximal femur nail* , Technol. Health Care 14 (2006) 411-419.
[21] S. Eberle, P. Augat, *A standardized finite elemente model of the human femur for biomechanical simulations of proximal fractures*, in: 14th Finite Element Workshop, University of Ulm, July 2007, ISBN:978-3-9806183-9-7, pp. 98-102
[22] S. Snyder, E. Schneider, *Estimation of mechanical properties of cortical bone by computed tomography*, J. Orthop. Res. 9 (1990) 422-431
[23] R.B. Ashman, J.Y. Rho, *Elastic modulus of trabecular bone material*, J. Biomech. 21 (3) (1988) 177-181
[24] R. Hill, *Elastic properties of reinforced solids: Some theoretical principles*. J. Mech. Phys. Solids 11 (1963) 357-372
[25] S.J. Hollister, N. Kikuchi, *A comparison of homogenization and standard mechanics analysis for periodic porous composites*, Computational Mechanics 10 (1992) 73-95
[26] B. van Rietbergen et al., *Direct mechanics assessment of elastic symmetries and properties of trabecular bone architecture*, J. Biomechanics 29 (12) (1996) 1653-1657

CHAPTER IV
THERMO-DYNAMICAL FOUNDATIONS

4.0. Thermodynamics : Basic definitions

In the development of the theory requires the introduction of a connection between the variables describing deformations and the stress. This connection depends on the existence of quantities such as energy and entropy and therefore is a part of the subject of thermodynamics.

The outline of thermodynamics which follows will emphasize the concepts most useful in the study of continuous media, including the effects of non-uniformity and dissipation.

The literature on thermodynamics, of course, quite extensive and it is difficult to give a complete listing of works which may usefully be consulted on the subject. As general references the reader may take the texts of Zemansky, Keenan or Pippard for classical thermodynamics, and the works of Progogine, DeGroot,or Biot for the thermodynamics of irreversible process.

The particular collection of matter which is being studied will be referred to as a system. Only closed systems will be considered here, that is, systems which do not exchange mass with their surroundings .

Occasionally, the further restriction is made that no interaction between the system and its surroundings occur; the system is then said to be isolated. It is assumed that the system occupies a closed region of space. It will be furthermore assumed that the material is chemically inert.

Consider now a system all of whose particles are at rest. When all the information required for the complete characterization of the system for the purposes at hand is available, it will be said that its state is known.

This information takes the form of the numerical values of several quantities, called state variables, each of which describes a different property of the system. Some of these properties will be extensive or additive, for example, volume, whereas others will be intensive, fro example, pressure. If for such a system the values of the state variables are independent of time, the system is said to be in thermodynamics equilibrium. A system is said to be uniform if the values of the intensive state variables do not vary space.

The state variables may be measured for systems not in thermodynamic equilibrium and will then generally vary with time; the system is then said to undergo a process. During a process it may be that the system is not completely characterized by the state variables alone, but may require the specification of some additional quantities.

4.1. Equations of state

The question of whether all the state variables are independent has, thus far, been left open. It is found from experimental observation, however, that are at thermodynamics equilibrium, once the values of a certain number of the state variables have been determined, the values of the others are fixed; in other words, a number of functional relationships exist between the state variables. If for a system with (m+n) state variables $X_\alpha \ \left(\alpha = 1,2,....,m+n\right)$ there exist m independent functional relations, they any n of the state variables $\left(X_1, X_2,...., X_2\right)$ may be taken as the independent ones, their selection being a matter of convenience; the others may be expressed in terms of them as follows: $X_\alpha = f_\alpha\left(X_1, X_2,..., X_n\right) \quad \alpha = n+1, n+2,..., n+m$, and will be referred to as state functions.

Equations of this type are known as equations of state. The number and form of these equations depend on the particular system under consideration. Only in the simplest systems (characterized, that is, by few state variables, as for example a gas) is it possible to establish them directly by an analysis of experimental data. It is often possible, however, to derive a considerable amount of information regarding their form from thermodynamics principles, provided only that the choice of independent variables is made.

4.2. Thermal equilibrium and the zero'th law of thermodynamics

Bring two system that are originally in thermodynamics equilibrium into perfect contact with each other (suitable precautions being taken so that both systems remain closed). If each system remains in thermodynamic equilibrium the two systems will be said to be in thermal equilibrium with each other. Two systems not in contact will be said to be in thermal equilibrium if they would be when brought into contact.

Experiments indicate that two systems, each of which is in thermal equilibrium with a third, are also in thermal equilibrium with each other. This statement express the zero, th law of thermodynamics.

Empirical temperature**:** Consider systems $A^{(1)}$ and $A^{(2)}$ with state variables $X_i^{(1)}\ \forall i \in \{1,2,...,n_1\}$ and $X_j^{(2)}\ \forall j \in \{1,2,...,n_2\}$ respectively. Experiments indicate that if these systems are in thermal equilibrium, a functional relation of the form:

$$f\left(X_i^{(1)}, X_j^{(2)}\right) = 0 \tag{4.1}$$

is satisfied. Similarly, if $A^{(1)}$ and $A^{(3)}$ with state variables $X_k^{(3)}\ \forall k \in \{1,2,...,n_3\}$ are in thermal equilibrium, then a functional relationship of the form:

$$g\left(X_i^{(1)}, X_k^{(3)}\right) = 0 \tag{4.2}$$

is found and if $A^{(2)}$ and $A^{(3)}$ are in equilibrium, then :

$$h\left(X_j^{(2)}, X_k^{(3)}\right) = 0 \tag{4.3}$$

The zero'th law of thermodynamics requires that if any two of the equations reported above (4.2)-(4.3) are satisfied, then the first also is satisfied (4.1). This is only possible if these equations can be brought into form;

$$\begin{aligned} f\left(X_i^{(1)}, X_j^{(2)}\right) &= f_1 - f_2 = 0, \\ g\left(X_i^{(1)}, X_k^{(3)}\right) &= f_1 - f_3 = 0, \\ h\left(X_j^{(2)}, X_k^{(3)}\right) &= f_2 - f_3 = 0, \end{aligned} \tag{4.4}$$

where $f_i = f_i\left(X_1^{(i)}, X_2^{(i)}, ..., X_{n_i}^{(i)}\right)$. Clearly then, there exist functions f_1, f_2, f_3 such that $f_1 = f_2 = f_3$, or, in the other words, these functions have the same value when the systems are in thermal equilibrium . This value is called the empirical temperature of these systems and will be denoted by θ. Of course, the numerical value of θ used to describe any particular state of thermal equilibrium may be chosen arbitrarily , so that the scale of the empirical temperature may be chosen at will. θ is clearly a state function and the equation:

$$\theta = f_1\left(X_1^{(1)}, X_2^{(1)}, ..., X_{n_1}^{(1)}\right) \tag{4.5}$$

Is an additional equation of state for system $A^{(1)}$. One may , of course, choose θ as a state variable, in which case on the $X_\alpha^{(1)}$ becomes a state function for system $A^{(1)}$.

External Work: Consider a system occupying a region D+B acted upon during a certain process by surface tractions $S_i^n\left(P_B, t\right)$, where P_B denotes a point on the surface, and by body forces per unit mass $F_i\left(P, t\right)$, where P is any point in the system. Let the displacement of any particle be denoted by $u_i\left(P, t\right)$. Then the rate $\dot{W}$ at which work is being done on the system is:

$$\dot{W}\left(t\right) = \int_D \rho\left[F_i\left(P,t\right)\dot{u}_i\left(P,t\right)\right]dV + \int_B \left[S_i\left(P_B,t\right)\dot{u}_i\left(P_B,t\right)\right]dA \tag{4.6}$$

In differential notation this take the form:

$$dW(t) = \int_D \rho\left[F_i(P,t)\,du_i(P,t)\right]dV + \int_B \left[S_i(P_B,t)\,du_i(P_B,t)\right]dA \tag{4.7}$$

As an example, consider the special case of zero body forces and external uniform hydrostatic pressure, that is $S_i(P_B,t) = -p\,n_i$, where n_i is the outwardly drawn unit normal to the surface B at the point P_B; then the equation (4.6) becomes:

$$\dot{W}(t) = -p\int_B n_i\,\dot{u}_i(P_B,t)\,dA = -p\dot{V} \tag{4.8}$$

Where V is the volume of the system. In the differential notation:

$$dW = -p\,dV \tag{4.9}$$

Internal energy function: It will be necessary for the following discussion to introduce the concept of an adiabatic wall. Two systems, each in thermodynamic equilibrium, but not in thermal equilibrium with each other, are brought into contact through an intermediate layer or wall; the wall is said to be adiabatic if the system remain in thermodynamic equilibrium. A process(during which the system remains uniform) is said to be adiabatic if throughout the process the system under consideration is entirely separated from its surroundings by an adiabatic wall.

Consider a system which is brought from a initial (at time $t = t_0$) thermodynamic equilibrium state characterized by state variable values $X_\alpha = X_\alpha(t_0)$ to a final (at time $t = t_1$) thermodynamics equilibrium state characterized by $X_\alpha = X_\alpha(t_1)$ by means of an adiabatic process. It is then an experimental fact that the total work done on the system , that is $\int_{t_0}^{t_1}\dot{W}(t)\,dt$, is independent of the adiabatic process used; it is, in other words, independent of the functions $X_\alpha(t)$ in the open range $t_0 < t < t_1$, but depends only on the values of these functions at the end points, that is, only on $X_\alpha(t_0)$ and $X_\alpha(t_1)$. Furthermore it is found experimentally that an adiabatic process exists which connects any two states, al least in one directions. The internal energy U of the system is then defined as the adiabatic work, namely the work done on (by) the system in an adiabatic process which takes the system from (to) an arbitrary reference state to (from) the state in question. According to the previous discussion it is clear that, once the reference state is fixed, U is a state function, that is, the additional equation of state :

$$U = U(X_1, X_2, ..., X_n) \tag{4.10}$$

applies.

It is observed experimentally that the internal energy is an extensive or additive quantity, that is, that the internal energy of a system consisting of two or more subsystems (in contact or not) is equal to the sum of the internal energies of all the subsystems. The two experimental facts concerning adiabatic work and the extensive character of internal energy form the basis for the first law of thermodynamics for uniform systems. The latter is most conveniently considered, however, after the introduction of the concept of heat.

4.3. Heat and first law of thermodynamics

Consider an arbitrary process connecting two end points characterized by $X_\alpha(t_0)$ and $X_\alpha(t_1)$ respectively . Let $U\left[X_1(t_0),...,X_n(t_0)\right] = U(t_0)$ and $U\left[X_1(t_1),...,X_n(t_1)\right] = U(t_1)$. The total work done during this process is :

$$W = \int_{t_0}^{t_1}\dot{W}(t)\,dt \tag{4.11}$$

where $\dot{W}(t)$ is calculated from eq. (4.6). If the process is adiabatic,

$$\left[U(t_1) - U(t_0)\right] - W = 0 \tag{4.12}$$

By the definition of the internal energy function. In any other process, the difference between the change in U and the work done on the system will not be zero. This difference will be called the total heat supplied to the system during the process and will be denoted by Q; thus,

$$\left[U\left(t_1\right)-U\left(t_0\right)\right]-W=Q \tag{4.13}$$

The values of W and Q will be different for different processes connecting the same two endpoints, with Q = 0 representing the particular case of an adiabatic process; the value of the sum W + Q is, however, independent of the particular process employed because of its relation to the change in the state function U. The equation (4.13) may be expressed in the more convenient derivative or differential forms respectively as follows:

$$\begin{aligned} \dot{U} &= \dot{W} + \dot{Q} \\ dU &= dW + dQ \end{aligned} \tag{4.14}$$

Consider now two system, 1 and 2, in perfect contact with each other, but separated from their surroundings by an adiabatic wall. For systems 1 and 2 respectively :

$$\begin{cases} \dot{U}_1 = \dot{W}_1 + \dot{Q}_1 \\ \dot{U}_2 = \dot{W}_2 + \dot{Q}_2 \end{cases} \tag{4.15}$$

Where the work done by system 2 on system 1 is included in W_1, and similarly for W_2 . For the entire system, eq. (4.14) takes the form :

$$\dot{U} = \dot{W}_1 + \dot{W}_2 \tag{4.16}$$

Because of the adiabatic envelope and because, according to the laws of mechanics, the rate of work done by system 1 on system 2 through the common contact surface is exactly the negative of the rate of work done by system 2 on system 1. The extensive character of U, however, requires that:

$$\dot{U} = \dot{U}_1 + \dot{U}_2 \tag{4.17}$$

and therefore comparison of the last three equations shows that :

$$\dot{Q}_1 = -\dot{Q}_2 \tag{4.18}$$

It is therefore reasonable to speak of heat as energy being transferred from one system to another. With this interpretation eq. (4.13) may be taken s the mathematical formulation of the law of conservation of energy, usually referred to as the first law of thermodynamics.

The discussion of thermodynamic principles could now be continued on the basis of an analysis of uniform system, leaving the generalization to non-uniform systems until a later point. It appeared more convenient, however, to introduce the transition to non-uniform systems at this stage of the development, and then to discuss the second law of thermodynamics immediately in the desired final form.

4.4. Transition to Non-uniform systems

In the foregoing review of the thermodynamics of uniform systems, it has been possible to introduce thermodynamics concepts (such as empirical temperature and internal energy) and thermodynamic principles (such as the law of conservation of energy) as generalization base directly upon experimental evidence. The experiments involved could be described purely in mechanical terms and although the prescribed experimental conditions could not be reproduced exactly in reality, they could be approached within any desired degree of precision.

It would at first seem possible to proceed directly from the theory of uniform systems to that of non-uniform systems, that is systems in which conditions depend on spatial position , by means of a suitable limiting process in which one subdivides the system into many small elements, each of which approximates a uniform system more and more closely as its dimensions are made smaller and smaller. However, it is difficult to perform such a limiting process rigorously since, at each stage of it, the elements represent in fact non-uniform systems, to which the previous theory does not apply. It therefore appears to be necessary to consider the thermodynamics of non-uniform systems as the more fundamental subject, introducing its concepts and principles as new postulates. The theory of uniform systems serves as a guide in this process and also provides a

"correspondence principle " that is , the theory of non-uniform systems must yield the same results as the uniform system provides the concept of the empirical temperature of an arbitrarily small uniform system (for example, a thermocouple) in perfect contact with the point in question.
Consider now a non-uniform system composed of a single homogeneous continuous substance. Quantities which are intensive state variable or state functions for this substance in a uniform state serve immediately as state variables when it is in a non-uniform state, although they will be now space-dependent. It is sometimes attempted to give an operational definition of these quantities by indicating how they may be measured in the interior of substance, but it will here be considered sufficient that a theory based on such concepts leads to the prediction of surface phenomena which agree with experiment. Quantities which are extensive state variables or state functions for uniform systems are first converted to intensive state variables for such systems by dividing the quantity in question by the mass of the system; the resulting "densities" then serve for non-uniform systems as well.
The state variables and state functions fro non-uniform systems will be denoted in general by $X_\alpha = X_\alpha(P,t)$ where P denotes a point in space. It is assumed that the number and choice of independent state variables for a non-uniform system may be taken as the same as those fro a uniform system of the same substance, and furthermore that the remaining state functions satisfy, at thermodynamic equilibrium (that is, when all particles are at rest and $(\partial X_\alpha/\partial t) = 0$ throughout the system), the same equations of state as in the uniform system.

4.5. Conservation of energy in non-uniform system

In the previous section, such state functions as the internal energy density ε have been introduced for non-uniform systems by a postulate. Similarly, le law of conservation of energy is here introduced as a postulate and expressed in terms of the postulated state functions and state variables, with no reference made to direct experimental verification as was done in the case of uniform systems.
In order to formulate this postulate, consider a portion C, which occupies a region D + B, of a homogeneous, continuous substance. Let P be a point in D + B and let ρ and $u(P,t)$ be the mass density and internal energy density , respectively, of the element of material located at P at time t. As is customary in a linear treatment of the subject, the mass density is taken as constant in what follows since consideration of its dependence on deformation leads to second-order terms. Let $v_i(P,t)$ be the velocity components of the particle at (P,t) and assume that the body is acted upon by body force components $F_i(P,t)$ per unit mass. Then the kinetic energy K of C at time is defined as :

$$K = \frac{1}{2}\int_D \rho v_i v_i dV \tag{4.19}$$

The internal energy of C at time t is defined as :

$$U = \int_D \rho u dV \tag{4.20}$$

Let $\sigma_{ij}(P,t)$ be the components of the stress tensor. The resulting surface tractions then do work on C at the rate:

$$\int_B \sigma_{ij} n_j v_i dA \tag{4.21}$$

Where $n_j(P_B)$ are the components of the unit normal to the surface B at P_B. Similarly, the body force components F_i do work on C at the rate :

$$\int_D \rho F_i v_i dV \tag{4.22}$$

It is further assumed that energy is transferred into C across B by heat transfer at the rate $-q(P_B,t)$ for unit area so that the total rate of energy transfer into D by this means is :

$$-\int_B q\,dA \tag{4.23}$$

Attention is restricted her to processes in which energy is added to a body portion there of by one of the three agencies just listed (for example, electromagnetic energy transfer is excluded). The postulated law of conservation of energy for such process then states that the rate at which the surface tractions and body forces do work on a body or portion there of plus the rate of energy transfer into it by heat transfer is equal to the rate of increase of the sum of its kinetic and internal energies; that is :

$$\int_B \sigma_{ij} n_j v_i dA + \int_D \rho F_i v_i dV - \int_B q\,dA = \frac{d}{dt}\left(\frac{1}{2}\int_D \rho v_i v_i dV + \int_D \rho u dV\right) \tag{4.24}$$

The first surface integral of this equation may be transformed by means of the divergence theorem as follows:

$$\int_B \sigma_{ij} n_j v_i dA = \int_D \left(\sigma_{ij} v_i\right)_{,j} dV \tag{4.25}$$

The differentiation of the right hand side of equation (4.24) may be brought under the integral sign as follows:

$$\frac{d}{dt}\left(\frac{1}{2}\int_D \rho v_i v_i dV + \int_D \rho u dV\right) = \int_D \rho \dot{v}_i v_i dV + \int_D \rho \dot{u} dV \tag{4.26}$$

Since, by the assumption of small displacements, the change with the time of the range of integration is neglected. This interchange of the order of differentiation and integration may also be justified without the assumption of small displacements by use of the equation of continuity which expresses the law of conservation of mass; The presence, now, of only a single surface integral in equation (4.24) and the fact that this equation applies to any portion of the body leads to the existence of a heat flux vector q_i which yields the heat flux q across any surface element with normal n_i by means of the equation:

$$q = q_i n_i \tag{4.27}$$

where, by convention, q is the heat flux form the side of the surface with negative normal to the side with positive normal. With the use of the heat flux vector, the integral:

$$\int_B q\,dA = \int_B q_i n_i\,dA = \int_D q_{i,i} dV \tag{4.28}$$

with these results eq. (4.24) may be rewritten in the form:

$$\int_D \left[\sigma_{ij,j} + \rho F_i - \rho \dot{v}_i\right] v_i dV + \int_D \left[\sigma_{ij} v_{i,j} - q_{i,i} - \rho \dot{u}\right] dV = 0 \tag{4.29}$$

Where the first integral is zero by virtue of the equation of motion. Since, by assumption, eq. (4.29) applies for any arbitrarily small portion of the body, it follows that the integrand of the second integral is identically zero at every point in the body where it is continuous , that is ,

$$\sigma_{ij} v_{i,j} - q_{i,i} = \rho \dot{u} \tag{4.30}$$

We may write $v_{i,j}$ in terms of its symmetric and anti-symmetric portions as follows:

$$v_{i,j} = \frac{1}{2}\left(v_{i,j} + v_{j,i}\right) + \frac{1}{2}\left(v_{i,j} - v_{j,i}\right) = \dot{\varepsilon}_{ij} + \dot{\omega}_{ij} \tag{4.31}$$

where $\dot{\varepsilon}_{ij} = \frac{1}{2}\left(v_{i,j} + v_{j,i}\right)$; $\quad \dot{\omega}_{ij} = \frac{1}{2}\left(v_{i,j} - v_{j,i}\right)$;

The equation (4.30) may then be rewritten in the form:

$$\sigma_{ij}\dot{\varepsilon}_{ij} - q_{i,i} = \rho \dot{u} \tag{4.32}$$

Where use has been made of the fact that the contraction $\sigma_{ij}\dot{\omega}_{ij}$ is zero since σ_{ij} is a symmetric and $\dot{\omega}_{ij}$ an anti-symmetric tensor. **Equations (4.32)-(4.30) express the law of conservation of energy for non-uniform systems.**

4.6. Preliminaries to the second law of thermodynamics for continua

To prepare the way for a suitable formulation of the second law of thermodynamics for deformable continua, it is necessary first to examine more closely some concepts , such as those of state variable and process. This will be done here by introducing a sequence of definitions as follows.

Reference state**:** The state of the substance under consideration in some arbitrary , but fixed uniform condition of thermodynamic equilibrium will be referred to as the reference state.

State deformation variables: As part of the definition of the particular kind of continua being studied, it is assumed that, at thermodynamic equilibrium, the internal energy density at an arbitrary point of the system depends upon the empirical temperature, θ, at that point and upon some (not necessarily all) aspects of the deformation from the reference state of the material element presently occupying that position. The appropriate numerical measure of these deformation characteristics, called state deformation variables, will be denoted here by $\xi_\alpha, \alpha = 1,2,...,n$ where the range of the subscript α depends upon the material under consideration. Thus, for example, for a viscous fluid, there is only a single state deformation variable, the specific volume V , whereas for an elastic solid there are six state deformation variables, which (if attention is restricted to sufficiently small displacements and displacement gradients) may be taken as the six components of the small strain tensor ε_{ij}. Thus in this case : $\xi_\alpha = \varepsilon_{ij}$; $\alpha = 1,2,..,6$; $i, j = 1,2,3$; $\varepsilon_{ij} = \varepsilon_{ji}$;

4.7. Separation of state and dissipative deformation variables in the energy equation

For the development of the second law of thermodynamics given in following article, it is necessary to rewrite the energy equation in a form which keeps separate account of the contribution of the variation of the state deformation variables since, in the case of viscous fluids or viscous elastic-solids, other contributions to the energy equation due to deformation are present giving is to what will be termed dissipative deformation variables. In the case of the elastic solid, no other contributions exist and there are consequently no dissipative deformation variables.
For these three cases, the energy equation (4.32) may be put in a common form namely:

$$s_\mu \dot{d}_\mu + \sigma_\alpha \dot{\xi}_\alpha - q_{i,i} = \rho \dot{u}; \quad \alpha = 1,...,n; \quad \mu = 1,...,m; \tag{4.33}$$

Where d_μ are the dissipative deformation variables and s_μ and σ_α are the conjugate of d_μ and ξ_α, that is, the multipliers of $\dot{d}_\mu$ and $\dot{\xi}_\alpha$ respectively in energy equation.

The description of a process for a given element of material implies the specification the functions $s_\mu(t), d_\mu(t), \sigma_\alpha(t), \xi_\alpha(t), \theta(t),\ t_0 \le t \le t_1$. This specification is here purely mathematical; no consideration has yet been given to whether a given process is physically realizable or not. Three special kinds of processes, not mutually exclusive, will now be defined:

- Restricted process: A process in which $d_\mu(t)$=0 is said to be a restricted process.

- Locally reversible process: During a process the system is not, in general, in thermodynamic equilibrium. The internal energy density u, cannot therefore be computed, according to the general theory outlined previously, from the equation which gives its value at thermodynamic equilibrium. If the additional assumption is made that the internal energy density can be computed from the instantaneous values of the state variables by use of the equation of state, then the process is said to be locally reversible. Therefore, for a locally reversible process:

$$u(t) = u\left[\xi_\alpha(t), \theta(t)\right] \tag{4.34}$$

and

$$\dot{u}(t) = \frac{\partial u}{\partial \xi_\alpha}\dot{\xi}_\alpha + \frac{\partial u}{\partial \theta}\dot{\theta} \tag{4.35}$$

Where the function $u\left[\xi_\alpha(t), \theta(t)\right]$ is the same as that applicable at thermodynamic equilibrium.

- Locally adiabatic process: A process will be called locally adiabatic if the quantity $q_{i,i}$ appearing in equation (4.33) is identically zero. With these definitions, the next step in the development may be carried out as follows. It will now be shown that the quantities σ_α are themselves state functions, that is,

$$\sigma_\alpha = \sigma_\alpha(\xi_1, ..., \xi_n, \theta) \tag{4.36}$$

And therefore σ_α depend only on the quantities which determine the internal energy. This proof will first be shown that, if a restricted process starting from an arbitrary state ξ_α^0, θ^0 is to be locally reversible and locally adiabatic, it is not possible to specify $\sigma_\alpha(t), \xi_\alpha(t), \theta(t)$ arbitrarily; therefore , in such a case a functional relationship exists between these quantities.
To prove this, assume first that it is possible to specify all these functions arbitrarily; then (since by hypothesis the process is restricted, locally reversible and adiabatic) equation (4.33) takes the form:

$$\sigma_\alpha \dot{\xi}_\alpha = \rho \dot{u} = \rho\left[\frac{\partial u}{\partial \xi_\alpha}\dot{\xi}_\alpha + \frac{\partial u}{\partial \theta}\dot{\theta}\right] \Rightarrow \left[\sigma_\alpha - \rho\frac{\partial u}{\partial \xi_\alpha}\right]\dot{\xi}_\alpha - \rho\frac{\partial u}{\partial \theta}\dot{\theta} = 0 \tag{4.37}$$

Therefore it is possible in this case to specify $\xi_\alpha(t)$ and $\theta(t)$ completely independently of each only if the material is such that $\partial u/\partial\theta = 0$ and

$$\sigma_\alpha = \rho\frac{\partial u}{\partial \xi_\alpha} = \sigma_\alpha\left(\xi_1^0, ..., \xi_n^0\right) \tag{4.38}$$

If the material is such that $\partial u/\partial\theta \neq 0$, as is generally the case, then it is seen that $\xi_\alpha(t)$ and $\theta(t)$ cannot be specified independently of each other to obtain a restricted locally adiabatic process starting from an arbitrary state ξ_α^0, θ^0. It will be assumed that it is possible however to leave this state with this type of process along arbitrary $\xi_\alpha(t)$, but that for all these processes the temperature is then determined by a relation of the type : $\theta = \theta(\xi_1, ..., \xi_n)$. Then, equation (4.33) takes the form:

$$\left[\sigma_\alpha - \rho\frac{\partial u}{\partial \xi_\alpha} - \rho\frac{\partial u}{\partial \theta}\frac{\partial \theta}{\partial \xi_\alpha}\right]\dot{\xi}_\alpha = 0 \tag{4.39}$$

And it therefore follows that : $\sigma_\alpha = \sigma_\alpha\left(\xi_1^0, ..., \xi_1^0, \theta^0\right)$. Since ξ_α^0, θ^0 represents an arbitrary state, the establishment of equation (4.36) under stated assumptions is completed.

4.8. Caratheodory's statement of the second law of thermodynamics and its consequences

The treatment of the second law of thermodynamics presented by caratheodory is characherized by a clear-up separation between the postulates regarding physical reality and the purely mathematical consequences derived from these postulates. Although limited in its original form to uniform systems, Caratheodory's postulate (that is , his statement of the second law of thermodynamics) may be rephrased, with the concepts and results of the preceding section, for non-uniform systems; the mathematical reasoning leading to the existence of an entropy-density function and a universal absolute temperature scale remains substantially unaltered .
Caratheodory's statement of the second law of thermodynamics in a form applicable to continuous non-uniform systems characterized by state variables denoted by ξ_α, θ is then as follows:

Consider a particular initial state, J_0 of the system, characterized by state-variable values of ξ_α^0, θ^0 at the generic point P. Then there exist states J characterized by state-variable values of ξ_α, θ at P which are arbitrarily close to ξ_α^0, θ^0 and which are not accessible from J_0 by means of processes which are locally reversible and locally adiabatic at P.

The purely mathematical theorem proven by Caratheodory and useful for drawing consequences from the above postulate may be stated as follows:

If in the neighbourhood of an arbitrary point G_0 there are points G which are inaccessible along solution curves of the differential equation,

$$P_\alpha\left(x_1,...,x_n\right)\frac{d\,x_\alpha}{dt}=0;\quad \alpha=1,2,...,n \tag{4.40}$$

Then this equation is integrable. Definitions of the various terms used in the above follow:

Point: A set for the variables $\left(x_1,...,x_n\right)$; *Solution curve*: A set of n functions , x_α, which yield an identity when substituted in eq. (4.40) ; *Integrable*: An equation of the form of eq. (4.40) is said to be integrable if there exist two functions, $\lambda\left(x_1,...,x_n\right)$ and $F\left(x_1,...,x_n\right)$, such that:

$$\frac{1}{\lambda}P_\alpha\frac{d\,x_\alpha}{dt}=\frac{d\,F}{dt}=\frac{\partial\,F}{\partial x_\alpha}\frac{d\,x_\alpha}{dt};\quad \alpha=1,2,...,n \tag{4.41}$$

It is now possible to apply Caratheodory's mathematical theorem to his statement of the second law thermodynamics are just rephrased. If there are neighboring states of J_0 which are not accessible, in particular, by means of any restricted locally reversible and adiabatic process. But then, eq. (4.37) is satisfied and since σ_α is a state function, it is of the same form as eq. (4.40). It follows, therefore, that the hypotheses of Caratheodory's mathematical theorem apply to eq. (4.37) and therefore that equation is integrable. That is, there exist functions $\lambda\left(\xi_1,...,\xi_n,\theta\right)$, $F\left(\xi_1,...,\xi_n,\theta\right)$ such that the equation:

$$\frac{1}{\lambda\left(\xi_\alpha,\theta\right)}\left[\left(\rho\frac{\partial u}{\partial\xi_\alpha}-\sigma_\alpha\right)\dot{\xi}_\alpha+\rho\frac{\partial u}{\partial\theta}\dot{\theta}\right]=\dot{F}\left(\xi_\alpha,\theta\right) \tag{4.42}$$

Is an identity for any set of functions $\xi_\alpha\left(t\right)$ and $\theta\left(t\right)$. It follows that eq. (4.33) may be rewritten in terms of the newly defined state functions λ and F for any locally reversible process in the following forms:

$$\rho\dot{u}-\sigma_\alpha\dot{\xi}_\alpha=\lambda\left(\xi_1,...,\xi_n,\theta\right)\,\dot{F}\left(\xi_1,...,\xi_n,\theta\right) \tag{4.43}$$

$$s_\mu d_\mu-q_{i,i}=\lambda\left(\xi_1,...,\xi_n,\theta\right)\,\dot{F}\left(\xi_1,...,\xi_n,\theta\right) \tag{4.44}$$

The work thus far has not characterized uniquely the functions λ and F. To do so, it is necessary to proceed as follows. We first specialize the foregoing discussion to a system undergoing a restricted process, so that eq. (4.44) becomes:

$$-q_{i,i}=\lambda\left(\xi_1,...,\xi_n,\theta\right)\,\dot{F}\left(\xi_1,...,\xi_n,\theta\right) \tag{4.45}$$

Integration of this equation over the volume of the system, use of the divergence theorem, and of eq. (4.28) then yields:

$$\dot{Q}=\int_D\lambda\left(\xi_1,...,\xi_n,\theta\right)\,\dot{F}\left(\xi_1,...,\xi_n,\theta\right)dV \tag{4.46}$$

Where $\dot{Q}$ is the rate of energy transfer into the system in the form of heat. We now specialize the discussion further, assuming that the system is uniform and that the system is uniform and that the heat transfer into it occurs reversibly in the sense of classical thermodynamics, that is, at a vanishingly slow rate. Since the functions λ and F are now independent of the spatial coordinates, we may rewrite the last equation as

$$\dot{Q}=\lambda\dot{F}V \tag{4.47}$$

where V is the total volume of the system, or

$$\dot{Q} = \lambda^* \dot{F} M \tag{4.48}$$

where M is the total mass of the system, and $\lambda^*(\xi_\alpha, \theta) = \lambda(\xi_\alpha, \theta) / \rho(\xi_\alpha, \theta)$.

By consideration of a second uniform system in perfect thermal contact with the one before, it is now possible to show that, for a given scale of empirical temperature, there is an unique (except for an arbitrary multiplicative constant) function λ^* which depends only upon θ and furthermore that it is the same for all systems. The derivation also indicates that this function cannot change sign; by convention it is taken as positive. The function as then chosen is known as the absolute temperature and is denoted by $T(\theta)$. Since the empirical temperature has been defined for a non-uniform system also, this function, (a universal state function) defines the absolute temperature for non-uniform system as well. The function $F(\xi_\alpha, \theta)$ corresponding to $T(\theta)$ is then a uniquely characterized (excepted for an arbitrary additive constant omitted below) state function for each system. By convention, the function $S(\xi_\alpha, \theta)$ is introduced where : $S(\xi_\alpha, \theta) = M\ F(\xi_\alpha, \theta)$ is called the entropy of the uniform system. It is clear that S is an extensive state function ; the corresponding intensive function, known as the entropy density, is obtained by division by the mass of the system and is denoted by $\eta(\xi_\alpha, \theta)$, that is $\eta(\xi_\alpha, \theta) = F(\xi_\alpha, \theta)$.

It is now possible to rewrite eqs. (4.43)-(4.44) using as a matter of convenience , T rather than θ as a state variable , as follows:

$$\sigma_\alpha \dot{\xi}_\alpha + \rho T \dot{\eta} = \rho \dot{u} \tag{4.49}$$

$$s_\mu \dot{d}_\mu - q_{i,i} = \rho T \dot{\eta} \tag{4.50}$$

These equations are valid for any locally reversible process.

4.9. Irreversible thermodynamics ; Entropy production

The foregoing has been concerned with the extension of classical thermodynamics to non-uniform. In this article some of the concepts from more recent developments in thermodynamics dealing with grossly irreversible (through still locally reversible) phenomena are introduced.

It is first noted from equation (4.50) that, depending upon the magnitude of $q_{i,i}$, the entropy density η could either increase or decrease ; however, it is known from the classical theory of uniform systems that if a system is separated by means of an adiabatic wall from its surroundings, its total entropy can never decrease. It is therefore desirable to find a density with similar properties, as may be done in the following manner. Consider a portion of a continuous system occupying the region D+B. From equation (4.50) the rate of change of the entropy of this portion of the body is

$$\int_D \rho \dot{\eta} dV = -\int_D \frac{q_{i,i}}{T} dV + \int_D \frac{s_\mu \dot{d}_\mu}{T} dV = -\int_D \left(\frac{q_i}{T} \right)_{,i} dV - \int_D \frac{q_i T_{,i}}{T^2} dV + \int_D \frac{s_\mu \dot{d}_\mu}{T} dV \tag{4.51}$$

or finally, by application of the divergence theorem to the first integral on the right-hand side,

$$\int_D \rho \dot{\eta} dV = -\int_B \frac{q_i n_i}{T} dV - \int_D \frac{q_i T_{,i}}{T^2} dV + \int_D \frac{s_\mu \dot{d}_\mu}{T} dV \tag{4.52}$$

The first term on the right-hand side of this equation represents the entropy change of the system due to the heat flow across the boundary B, and the last two terms represent the entropy change due to processes (heat conduction and variation of dissipative variables) occurring within the volume. It is therefore reasonable to call the sum of the last two terms the rate of entropy-density production denoted by $\dot{\eta}_I$, namely ,

$$\rho \dot{\eta}_I = \frac{s_\mu \dot{d}_\mu}{T} - \frac{q_i T_{,i}}{T^2} \tag{4.53}$$

It should be noted that η_I is not a state function.

One of the important postulates of irreversible thermodynamics is now introduced; it states that the entropy-density production at any point in a system is always positive, that is,

$$\dot{\eta}_I \geq 0 \tag{4.54}$$

As a consequence of this postulate and of equation (4.53) it follows that the quantities q_i, s_μ and $\left(T_{,i}/T^2\right)$, $\dot{d}_\mu$ cannot all take on arbitrary values , but that a functional relationship must exist between the first set of quantities q_i, s_μ (sometimes referred to as fluxes or effects) and the second set of quantities (referred to as forces or causes). For the purpose of simplifying the following discussion, let the following notation be adopted: $q_i = s_\mu$, $\left(T_{,i}/T^2\right) = \dot{d}_\mu$, $i = 1,2,3$, and $\mu = m+1, m+2, m+3$, respectively. As first approximation, the functional relationships between effects and causes are assumed to be linear, that is,

$$s_\mu = L_{\mu\nu}\dot{d}_\nu; \quad \mu,\nu = 1,....,m+3; \tag{4.55}$$

where the quantities $L_{\mu\nu}$ are independent of $\dot{d}_\nu$

We way now state the second important postulate of irreversible .This postulate, due to Onsager, who arrived at it through statistical mechanical considerations, states that these coupling coefficients must be symmetric, that is,

$$L_{\mu\nu} = L_{\nu\mu}; \quad \mu,\nu = 1,...,m+3 \tag{4.56}$$

Equation (4.56) states what are known as the Osanger reciprocal relations.

4.10. Stress-strain relations and energy equation for an isotropic elastic solid

On the basis of the foregoing results, it is now possible to consider detailed applications to specific types of continuous media . We will, in other words, develop here the form of the stress-strain relations for an isotropic, elastic solid subjected to deformations which obey the restrictions of linear elasticity theory and subjected to small temperature changes. It will then be possible to put the energy equation for this case in a convenient form .

The starting points is eq. (4.49) written in the form it assumes for an elastic solid, namely,

$$\sigma_{ij}\dot{\varepsilon}_{ij} + \rho T\dot{\eta} = \rho\dot{u} \tag{4.57}$$

The free-energy function , $\varphi\left(\varepsilon_{ij}, T\right)$, is introduced and defined as follows:

$$\varphi\left(\varepsilon_{ij}, T\right) = u\left(\varepsilon_{ij}, T\right) - T\eta\left(\varepsilon_{ij}, T\right) \tag{4.58}$$

Although φ depends only upon the six independent components of the symmetric tensor ε_{ij}, it is convenient to write $\varepsilon_{ij} = \frac{1}{2}\left(\varepsilon_{ij} + \varepsilon_{ji}\right)$ and to regard φ as a mathematical function of all nine components of the ε_{ij} tensor. It is clear that this method of definition of leads to the identity :

$$\frac{\partial\varphi}{\partial\varepsilon_{ij}} = \frac{\partial\varphi}{\partial\varepsilon_{ji}} \tag{4.59}$$

Substitution of eq. (4.58) into eq. (4.57) then lead to the result

$$\left(\sigma_{ij} - \rho\frac{\partial\varphi}{\partial\varepsilon_{ij}}\right)\dot{\varepsilon}_{ij} - \rho\left(\eta + \frac{\partial\varphi}{\partial T}\right)\dot{T} = 0 \tag{4.60}$$

By assumption, the coefficients of the seven independent quantities , $\dot{\varepsilon}_{ij}$ and $\dot{T}$, do not depend on these quantities; they must therefore be identically zero. Then, by use of equation (4.59) and of the symmetry of the stress tensor σ_{ij}, we obtain:

$$\sigma_{ij} = \rho\frac{\partial\varphi}{\partial\varepsilon_{ij}} \tag{4.61}$$

$$\eta = -\frac{\partial \varphi}{\partial T} \tag{4.62}$$

Note that by virtue of the adopted convention the partial differentiation of φ in equation (4.61) is with respect to the ε_{ij} regarded as nine independent variables.

The six independent components of any symmetric second-rank tensor in three-dimensional space are determined by its three principal values and by the three angles, $\theta_1, \theta_2, \theta_3$, which determine the orientation of the three (mutually orthogonal) principal directions. Furthermore, the three principal value of such a tensor are determined by its three invariants. It follows that the free energy function, $\varphi\left(\varepsilon_{ij}, T\right)$, may be alternatively expressed, using as arguments the three principal invariants of the strain tensor , $I_\varepsilon, II_\varepsilon, III_\varepsilon$, the three orientation angles, $\theta_1, \theta_2, \theta_3$, and T ; then

$$\varphi\left(\varepsilon_{ij}, T\right) = \varphi\left(I_\varepsilon, II_\varepsilon, III_\varepsilon, \theta_1, \theta_2, \theta_3, T\right) \tag{4.63}$$

If attention is restricted to an isotropic elastic solid, as is the case in this discussion, then the free energy function must be independent of the three orientation angles, $\theta_1, \theta_2, \theta_3$. Therefore, for such a solid,

$$\varphi\left(\varepsilon_{ij}, T\right) = \varphi\left(I_\varepsilon, II_\varepsilon, III_\varepsilon, T\right) \tag{4.64}$$

It follows from equation (4.61) that

$$\sigma_{ij} = \rho\left(\frac{\partial \varphi}{\partial I_\varepsilon}\frac{\partial I_\varepsilon}{\partial \varepsilon_{ij}} + \frac{\partial \varphi}{\partial II_\varepsilon}\frac{\partial II_\varepsilon}{\partial \varepsilon_{ij}} + \frac{\partial \varphi}{\partial III_\varepsilon}\frac{\partial III_\varepsilon}{\partial \varepsilon_{ij}}\right) \tag{4.65}$$

The three invariants of the strain tensor are defined as follows:

$$I_\varepsilon = \varepsilon_{ii}, \quad II_\varepsilon = \frac{1}{2!}\delta^{ij}_{lm}\varepsilon_{il}\varepsilon_{jm}, \quad III_\varepsilon = \frac{1}{3!}\delta^{ijk}_{lmn}\varepsilon_{il}\varepsilon_{jm}\varepsilon_{kn} \tag{4.66}$$

Where δ^{ij}_{lm} and δ^{ijk}_{lmn} are generalized Kronecker deltas defined as follows:

$$\delta^{ij}_{lm}\begin{cases} = +1 \text{if l and m are distinct integers (from 1 to 3)} \\ \text{and i,j are an even permutation of the same integers} \\ = \text{-1 if l and m are distinct integers and i,j are an odd} \\ \text{permutation of the same integers} \\ = \text{ 0 in all other cases} \end{cases} \tag{4.67}$$

With an analogous definition for δ^{ijk}_{lmn}. Thus note that

$$\delta^{ij}_{lm} = \gamma_{ijk}\gamma_{lmk}, \qquad \delta^{ijk}_{lmn} = \gamma_{ijk}\gamma_{lmn}, \tag{4.68}$$

In terms of the alternating tensor defined in eq. (4.58). Differentiation of eqs. (4.66) gives:

$$\frac{\partial I_\varepsilon}{\partial \varepsilon_{ij}} = \delta_{ij}, \quad \frac{\partial II_\varepsilon}{\partial \varepsilon_{ij}} = \delta_{ij} I_\varepsilon - \varepsilon_{ij}, \quad \frac{\partial III_\varepsilon}{\partial \varepsilon_{ij}} = \varepsilon_{ik}\varepsilon_{jk} - \varepsilon_{ij} I_\varepsilon + \delta_{ij} II_\varepsilon, \tag{4.69}$$

It is assumed next that there exists a reference state o the substance, at a temperature $T = T_0$, for which the material is stress-free, and that the free energy function φ may be expanded in a power series in the arguments $I_\varepsilon, II_\varepsilon, III_\varepsilon, T'$ where:

$$T' = \frac{T - T_0}{T_0} \tag{4.70}$$

Then

$$\varphi\left(I_\varepsilon, II_\varepsilon, III_\varepsilon, T'\right) = \frac{1}{\rho}\begin{pmatrix} a_0 + a_1 I_\varepsilon + a_2 II_\varepsilon + a_3 III_\varepsilon + a_4 T' + a_5 I_\varepsilon^2 \\ + a_6 II_\varepsilon^2 + a_7 III_\varepsilon^2 + a_8 T' I_\varepsilon + ... \end{pmatrix} \tag{4.71}$$

Where the quantities $a_0, a_1, ...$ are constants. The stress-strain relation may now be obtained by use of equations (4.71) and (4.61). Since a linear theory is desired, attention is restricted to the cases in which ε_{ij} and T' are sufficiently small so that their products may be neglected in the stress-strain relations and in the energy equation. Thus, the stress-strain relations resulting from this procedure are as follows:

$$\begin{aligned} &\sigma_{ij} = a_1\delta_{ij} + a_2\left(\delta_{ij}\varepsilon_{kk} - \varepsilon_{ij}\right) + 2\,a_5\,\delta_{ij}\varepsilon_{kk} + a_8\delta_{ij}T' \\ &or \quad \sigma_{ij} = \left(2a_5 + a_2\right)\delta_{ij}\varepsilon_{kk} - a_2\varepsilon_{ij} + a_8\delta_{ij}T' \end{aligned} \tag{4.72}$$

Where $a_1 = 0$ since the material is stress free in the reference state.

The constants $a_2, a_5,$ and a_8 may be renamed in terms of Lame's constants λ and μ and the coefficient of linear thermal expansion α as follows:

$$\begin{aligned} a_2 &= -2\mu \\ a_5 &= \left(\lambda + 2\mu\right)/2 \\ a_8 &= -\left(3\lambda + 2\mu\right)\alpha T_0 \end{aligned} \tag{4.73}$$

Equation (4.73) then assumes the familiar form of the linear thermoelastic stress-strain relation, namely:

$$\sigma_{ij} = \lambda\delta_{ij}\varepsilon_{kk} + 2\mu\,\varepsilon_{ij} - \left(3\lambda + 2\mu\right)\delta_{ij}\alpha\left(T - T_0\right) \tag{4.74}$$

The principle of positive rate of entropy production, equation (4.54), is employed next to determine the relation governing heat conduction in an isotropic elastic solid.

Since there are no dissipative deformation variables , equation (4.54) merely implies a relation (taken here as linear between q_i and $T_{,i}$ (the denominator T may be included in the coefficients of this relation). The most general, tensorially valid, linear relation which can exist between the quantities q_i and $T_{,i}$ is of the following form (Fourier's law of heat conduction) :

$$q_i = aT_{,i} + b_{ij}T_{,j} \tag{4.75}$$

Where the quantities a and b_{ij} are material properties of the indicated tensorial rank. Because of the assumed isotropy of the solid, the quantities b_{ij} must be components of an isotropic tensor, that is, a tensor whose components have the same numerical value in any Cartesian coordinate system. It may be shown that the most general isotropic tensor of rank two has components of the form $b_{ij} = b\delta_{ij}$; the equation (4.75) then becomes simply:

$$q_i = -k\,T_{,i} \tag{4.76}$$

Where the scalar k, known as the thermal conductivity of the solid, must be positive to insure a positive rate of entropy production, that is, to satisfy inequality (4.54). The equation (4.76) express the well-known Fourier's law of heat conduction.

The general energy equation may now be input in a more convenient form for the elastic solid and linear theory here considered. Since there are no dissipative deformation variables for an elastic solid, eq. (4.50) becomes:

$$-q_{i,i} = \rho T\dot{\eta} = \rho T\left(\frac{\partial\eta}{\partial\varepsilon_{ij}}\dot{\varepsilon}_{ij} + \frac{\partial\eta}{\partial T}\dot{T}\right) \tag{4.77}$$

Or, by use of equation (4.62), we obtain:

$$-q_{i,i} = \rho T\dot{\eta} = -\rho T\left(\frac{\partial^2\varphi}{\partial\varepsilon_{ij}\partial T}\dot{\varepsilon}_{ij} + \frac{\partial^2\varphi}{\partial T^2}\dot{T}\right) \tag{4.78}$$

It is customary to introduce a quantity, denoted by c_E, such that for a process in which $\dot{\varepsilon}_{ij} = 0,\ \forall i, j \in \{1,2,3\}$:

$$-q_{i,i} = \rho c_E \dot{T} \tag{4.79}$$

where c_E is known as the specific heat at constant deformation of the elastic solid in question. Comparison of the last two equations then yields:

$$c_E = -\frac{\partial^2 \varphi}{\partial T^2} T \tag{4.80}$$

Also from eq. (4.61), it is seen that

$$\frac{\partial^2 \varphi}{\partial \varepsilon_{ij} \partial T} = \frac{1}{\rho} \frac{\partial \sigma_{ij}}{\partial T} \tag{4.81}$$

Equation (4.78) therefore takes the form:

$$-q_{i,i} = \rho c_E \dot{T} - T \frac{\partial \sigma_{ij}}{\partial T} \dot{\varepsilon}_{ij} \tag{4.82}$$

For the linear theory under consideration here, $\partial \sigma_{ij} / \partial T$ may be evaluated by use of the linear thermo-elastic stress-strain relations, equation (4.74), $q_{i,i}$ may be evaluated by means of the Fourier law of heat conduction equation (4.76) , and $T = T_0 + T'T$ may here be replaced by T_0. The result is then the desired energy equation for the linear thermo-elastic theory, namely,

$$k T_{,ii} = \rho c_E \dot{T} + (3\lambda + 2\mu) \alpha T_0 \dot{\varepsilon}_{kk} \tag{4.83}$$

In what follows this equation will be referred to as the corrected or coupled heat conduction, since the last term is not present if the inter-convertibility of thermal and mechanical energy is ignored. Similarly, the thermo-elastic theory which employs this equation and which therefore requires the simultaneous determination of temperature and deformation will be referred to as the *coupled* thermo-elastic theory.

4.11. References

[1] Boley, B.A.,Weiner, J.H., *Theory of thermal stresses*, Dover publications, inc. Mineola, New York

[2] Ciarlet, Philiphe G., *Mathematical Elasticity, Volume I.: Three dimensional elasticity*, Elsevier Science Publishers B.V.

[3] Gurtin, M. E., *The Linear Theory of Elasticity, Handbbuch der Physik*, Springer, Berlin, 1972.

[4] Lekhnitskii, S. G., *Theory of Elasticity of an Anisotropic Body*, Mir, Moscow, 1981.

[5] Love, A. E. H., *A Treatise on the Mathematical Theory of Elasticity*, Dover Publications, Inc, New York, 1944

[6] Nunziante, L., Gambarotta, L., Tralli, A., *Scienza delle Costruzioni*, 3° Edizione, McGraw-Hill, 2011, ISBN: 9788838666971

[7] Ting TCT. *Anisotropic elasticity - Theory and applications*. Oxford University Press; 1996.

[8] Wolfram, S., *Mathematica, version 8*, Wolfram Research, Inc., Champaign, IL, 1998–2005.

CHAPTER V
UNCOUPLED QUASI-STATIC THERMO-ELASTIC THEORY

5.0 Introduction

The basic theory describing the behaviour of continuous media developed in the last chapter led to the mathematical formulation. This boundary value problem is of considerable mathematical difficulty, as it combines the theories of elasticity and of heat conduction under transient conditions. Fortunately, in most of the usual engineering applications it is possible to introduce certain simplifications without significant error. The principal such simplifications are the omission of the mechanical coupling term in the energy equation and of the inertia terms in the equations of motion. It will be necessary in this chapter to refer to a theory based on none of these approximations, or to the first only , or to both of them; the terms coupled theory, uncoupled theory, and uncoupled quasi-static theory will respectively be employed here for this purpose. In the remaining chapters however, only the last on of these theories is used and is divided into two distinct subjects; these will be referred to simply as the theories of heat conduction and thermo-elasticity. The relation between these various theories, as well as a discussion of their accuracy, forms the subject matter of the next four articles of this chapter.

5.1 General remarks on the effects of coupling and inertia

Consider first the mechanical coupling term in the heat conduction equation . If an external mechanical agency produces variations of strain within a body , this equation shows that these variations of strain are in general accompanied by variations in temperature and consequently by a flow of heat; the whole process thus gives rise to an increase of entropy and therefore to an increase in the energy stored in a mechanically irrecoverable manner. This phenomenon, known as thermo-elastic dissipation requires for its study the use of the coupled heat equation; clearly the mechanical term in the heat equation is essential to the description of this dissipative process, and its omission would here be meaningless. However, the deformation due to the external loads are accompanied only by small changes in temperature, and it would therefore appear reasonable to calculate these deformations without taking account of the thermal expansion. Similarly, if strains are produced in a body by a non-uniform temperature distribution, it would seem intuitively clear that the influence of these strains on the temperature itself should not be too large. On may therefore anticipate the conclusion that the coupling term appearing in the heat equation can be disregarded for all problems except those in which the thermo-elastic dissipation is of primary interest. This matter may be made plausible by the following reasoning. The coupled heat equation, may be rewritten as :

$$k\,T_{,ii} = \rho c_v \dot{T}\left[1+\delta\left(\frac{2\mu+\lambda}{2\mu+3\lambda}\right)\frac{\dot{\varepsilon}_{kk}}{\alpha\dot{T}}\right] \tag{5.1}$$

We note that the notations c_v, specific heat at constant volume, and c_E , specific heat at constant deformation , may be employed interchangeably in the linear theory. The non-dimensional parameter δ is defined by:

$$\delta = \frac{\left(3\lambda+2\mu\right)^2\alpha^2 T_0}{\rho^2 c_v v_e^2} \tag{5.2}$$

With the velocity of propagation of dilatation waves in an elastic medium being denoted by :

$$v_e = \sqrt{\frac{2\mu+\lambda}{\rho}} \tag{5.3}$$

The term proportional to parameter δ in eq. (5.1) is the coupling term, and it is negligible compared to unit if :

$$\delta\left(\frac{2\mu+\lambda}{2\mu+3\lambda}\right)\frac{\dot{\varepsilon}_{kk}}{\alpha\dot{T}} << 1 \;\Rightarrow\; \frac{\dot{\varepsilon}_{kk}}{3\alpha\dot{T}} << \left(\frac{\lambda+2\mu/3}{\lambda+2\mu}\right)\frac{1}{\delta} \tag{5.4}$$

For temperature distributions with no sharp variations or discontinuities in their time histories, it intuitively expected that the time rate of change of the dilation is of the same order of magnitude as that of the temperature; Thus the disregard of coupling as described previously appears to be reasonable. The preceding discussion makes it clear that the possibility of omitting the coupling terms depends not only on the fact that the inequality

$$\delta << 1 \tag{5.5}$$

must hold (as it does for most metals), but also on the fact that strain rates must be of the same order of magnitude as temperature rates. The latter condition implies that the time history of the displacements closely follows that of the temperature; in other words no pronounced lag or vibrations in the motion of the body must arise. It is therefore to be expected that the magnitude of inertia effects will also enter this question, so that a close relationship can be anticipated to exist between the two previously mentioned simplifications of the general theory.
A complete and rigorous delimitation of the class of problems for which these simplifications can be made is not available. However, it is possible to investigate the relation between the exact and the approximate theories by some specific examples.

5.2 Solution of a mono-dimensional coupled thermo-elastic problem

The problem chosen is that of an infinite medium, initially at rest and a uniform temperature, subjected to a prescribed rate of internal heat generation $Q(x,t)$ per unit volume, given by:

$$Q(x,t) = Q_1(t)\cos\left(\frac{x}{L}\right) \tag{5.6}$$

Where L is a constant. Suitable constraints are imposed so that the displacements components u, v, w in the x, y, z directions may be taken as :

$$u = u(x,t); \qquad v = w = 0 \tag{5.7}$$

The equations to be solved are then as follows:

$$k\frac{\partial^2 T}{\partial x^2} + Q(x,t) = \rho c_v \frac{\partial T}{\partial t} + (2\mu + 3\lambda)\alpha T_0 \frac{\partial^2 u}{\partial x \partial t} \tag{5.8}$$

$$\frac{\partial \sigma_{xx}}{\partial x} = \rho \frac{\partial^2 u}{\partial t^2} \tag{5.9}$$

$$\sigma_{xx} = (2\mu + \lambda)\varepsilon_{xx} - (3\lambda + 2\mu)\alpha T \tag{5.10}$$

$$\sigma_{yy} = \sigma_{zz} = \lambda \varepsilon_{xx} - (3\lambda + 2\mu)\alpha T \tag{5.11}$$

$$\tau_{xy} = \tau_{yz} = \tau_{xz} = \gamma_{xy} = \gamma_{yz} = \gamma_{xz} = 0 \tag{5.12}$$

$$\varepsilon_{xx} = \frac{\partial u}{\partial x} \tag{5.13}$$

Under suitable initial conditions to be specified shortly. As is clear from an examination of eq. (5.10) and (5.11), T here denotes the change in temperature from initial, stress-free state. It is convenient to restate first the problem in terms of two dependent variables alone, namely u and T ; this is done by eliminating ε_{xx} between eq. (5.10)-(5.13) and then substituting the resulting expression for σ_{xx} into eq. (5.9). The final result is:

$$(2\mu + \lambda)\frac{\partial^2 u}{\partial x^2} - (3\lambda + 2\mu)\alpha \frac{\partial T}{\partial x} = \rho \frac{\partial^2 u}{\partial t^2} \tag{5.14}$$

Equations (5.8) and (5.14) are to solved fro u and T, then the strain and stress components are readily found eq. (5.10)-(5.11)-(5.12)-(5.13).
In many types of problems it may be possible to neglect the coupling term in the heat equation (that is, the last term of equation (5.8)), although still retaining the temperature term in the stress-strain

relations, eq. (5.10)-(5.11) by the second term on the left-hand side. It will therefore be found convenient to rewrite these equations in the following form:

$$\begin{cases} k\dfrac{\partial^2 T}{\partial x^2}-\rho c_v\dfrac{\partial T}{\partial t}-(3\lambda+2\mu)\alpha_1 T_0\dfrac{\partial^2 u}{\partial x\,\partial t}+Q(x,t)=0 \\ (2\mu+\lambda)\dfrac{\partial^2 u}{\partial x^2}-(3\lambda+2\mu)\alpha_2\dfrac{\partial T}{\partial x}=\rho\dfrac{\partial^2 u}{\partial t^2} \end{cases} \tag{5.15}$$

Then in the *coupled theory*:

$$\alpha_1=\alpha_2=\alpha \tag{5.16}$$

and in the *uncoupled theory* :

$$\alpha_1=0;\quad \alpha_2=\alpha; \tag{5.17}$$

For the present problem, in which the internal heat generation is given by eq. (5.6), the solution will be taken in the following convenient non-dimensional form:

$$\begin{cases} u(x,t)=\dfrac{\rho c_v L}{\alpha(3\lambda+2\mu)}F(\tau)\sin\left(\dfrac{x}{L}\right) \\ T(x,t)=T_0\,G(\tau)\cos\left(\dfrac{x}{L}\right) \end{cases} \tag{5.18}$$

where time appears in the dimensionless variable:

$$\tau=\frac{k\,t}{\rho c_v L^2}=\kappa\frac{t}{L^2} \tag{5.19}$$

with κ the thermal diffusivity. Equations (5.15) then may be rewritten as follows:

$$\begin{cases} G+\dfrac{dG}{d\tau}+\dfrac{dF}{d\tau}-\dfrac{Q_1(\tau)L^2}{T_o k}=0 \\ F+K^2\dfrac{d^2F}{d\tau^2}-\delta G=0 \end{cases} \tag{5.20}$$

where

$$\delta=\frac{(3\lambda+2\mu)^2\alpha_1\alpha_2 T_0}{(2\mu+\lambda)\rho c_v};\qquad K=\frac{k}{\rho L c_v v_e}; \tag{5.21}$$

The parameter δ is identical with that of equation (5.2) for the coupled theory and is zero for the uncoupled theory.

Equations (5.20) must be solved under initial conditions:

$$F(0)=\frac{dF}{dt}(0)=G(0)=0 \tag{5.22}$$

Before discussing the particular solution of equation (5.20) (for which a special form of $Q_1(\tau)$ will be chosen), it is desirable to study the complementary solution, that is, the solution of these equation with Q_1 set equal to zero. The complementary solution (denoted by a subscript c) is :

$$\begin{aligned} F_c(\tau)&=C_1e^{m_1\tau}+C_2e^{m_2\tau}+C_3e^{m_3\tau} \\ G_c(\tau)&=C_1^*e^{m_1\tau}+C_2^*e^{m_2\tau}+C_3^*e^{m_3\tau} \end{aligned} \tag{5.23}$$

where the constants C_j and C_j^* $(j=1,2,3)$ are the nontrivial roots of

$$\begin{cases} m_jC_j+(1+m_j)C_j^*=0 \\ (1+m_j^2K^2)C_j-\delta C_j^*=0 \end{cases} \tag{5.24}$$

The summation convention is of course not employed here. Thus m_j are the three roots of the determinant equation:

$$\left(1+m_j\right)\left(1+m_j^2K^2\right)+\delta m_j=0 \tag{5.25}$$

And the constants C_j and C_j^* $\left(j=1,2,3\right)$ are related as follows:

$$\frac{C_j^*}{C_j}=\frac{1+m_j^2K^2}{\delta}=r_j \tag{5.26}$$

The discriminant of the cubic equation (5.25) is :

$$\left(1+\delta-\frac{K^2}{3}\right)^3\frac{K^6}{27}+\left(\frac{\delta}{2}-1-\frac{K^2}{9}\right)^2\frac{K^8}{9} \tag{5.27}$$

And is therefore positive; hence eq. (5.25) has one real and two conjugate complex roots. Furthermore, it is clear (by use Descartes'rule of signs) that the real root must be negative. It may now be proved that the real part of the complex roots is also negative. Hence we way write the roots of eq. (5.25) in the form:

$$m_{1,2}=-p\pm i\,q;\qquad m_3=-n; \tag{5.28}$$

Where p and n are positive. The ratios r_j then become

$$r_{1,2}=\frac{1}{\delta}\left[1+\left(p^2-q^2\right)K^2\mp 2i\,p\,q\,K^2\right],\ r_3=\frac{1+n^2K^2}{\delta} \tag{5.29}$$

The constants C_j will have the form:

$$C_{1,2}=\frac{1}{2}\left(A\pm i\,B\right);\ \ C_3=C; \tag{5.30}$$

Where A,B and C are real , because the function F_c is real ; it is then easily verified that, with expressions (5.29), the function G_c is also real. The complementary solution may finally be written as follows:

$$\begin{aligned}
&F_c=e^{-p\tau}\left[A\cos\left(q\tau\right)-B\sin\left(q\tau\right)\right]+Ce^{-\eta\tau}\\
&G_c=\frac{1}{\delta}e^{-p\tau}\begin{Bmatrix}\left[\left(1+K^2p^2-K^2q^2\right)A+2pqK^2B\right]\cos\left(q\tau\right)\\ -\left[\left(1+K^2p^2-K^2q^2\right)B-2pqK^2A\right]\sin\left(q\tau\right)\end{Bmatrix}+\frac{1+n^2K^2}{\delta}Ce^{-\eta\tau}
\end{aligned} \tag{5.31}$$

The particular solution will now be found, and the problem completed, for the following particular function Q_1:

$$Q_1=Q_0\left(1-e^{-t/t_0}\right)=Q_0\left(1-e^{-\tau/\tau_0}\right) \tag{5.32}$$

Where Q_0 and t_0 are constants and where:

$$\tau_0=\frac{\kappa t_0}{L^2} \tag{5.33}$$

A particular solution is then

$$\begin{aligned}
&F_P\left(\tau\right)=\frac{Q_0L^2\delta}{T_0k}\left(1+\frac{\tau_0^3}{D}e^{-\tau/\tau_0}\right)\\
&G_P\left(\tau\right)=\frac{Q_0L^2}{T_0k}\left(1+\frac{\tau_0\left(K^2+\tau_0\right)}{D}e^{-\tau/\tau_0}\right)
\end{aligned} \tag{5.34}$$

where $D=(K^2+\tau_0^2)(1-\tau_0)+\delta\tau_0^2$. The constants A,B and C may now be calculated so as to satisfy the initial conditions eq. (5.22). The final solution of the present problem can then be written ; it is:

$$\begin{cases} u(\tau)=\left[\dfrac{U_1 e^{-\tau/\tau_0}+U_2 e^{-\eta\tau}+U_3 e^{-p\tau}\cos(q\tau)+U_4 e^{-p\tau}\sin(q\tau)+U_5}{U_0}\right]\sin\left(\dfrac{x}{L}\right) \\ T(\tau)=\left[\dfrac{V_1 e^{-\tau/\tau_0}+V_2 e^{-\eta\tau}+V_3 e^{-p\tau}\cos(q\tau)+V_4 e^{-p\tau}\sin(q\tau)+V_5}{V_0}\right]\cos\left(\dfrac{x}{L}\right) \end{cases} \tag{5.35}$$

where the constants U_j, V_j are given by:

$$U_0=\frac{(\lambda+2\mu)k\,D\left[q^2+(p-n)^2\right]}{(3\lambda+2\mu)Q_0L^3\alpha_2},\quad U_1=\tau_0^3\left[q^2+(p-n)^2\right],$$

$$U_2=-D\left[q^2+(p-n)^2\right]-\left[K^2(1-\tau_0)+\tau_0^2(1+\delta)\right]n(2p-n)-\tau_0(1-2p\tau_0)-\tau_0^3\left[q^2+(p-n)^2\right],$$

$$U_3=\left[K^2(1-\tau_0)+\tau_0^2(1+\delta)\right]n(2p-n)+\tau_0(1-2p\tau_0),$$

$$U_4=\left\{\left[K^2(1-\tau_0)+\tau_0^2(1+\delta)\right]n\left(p^2-q^2-n\,p\right)+\tau_0(p-n)-\tau_0^2\left(p^2-q^2-n^2\right)\right\}\Big/q,$$

$$U_5=V_5=D\left[q^2+(p-n)^2\right],\ V_0=\left\{k\,D\left[q^2+(p-n)^2\right]\right\}\Big/\left(Q_0L^2\right),\ V_1=\tau_0\left(\tau_0^2+K^2\right),$$

$$V_2=-\left(1+n^2K^2\right)\begin{Bmatrix} D\left[q^2+(p-n)^2\right]+\left[K^2(1-\tau_0)+\tau_0^2(1+\delta)\right]n(2p-n)+ \\ +\tau_0(1-2p\tau_0)+\tau_0^3\left[q^2+(p-n)^2\right] \end{Bmatrix},$$

$$V_3=\left[K^2(1-\tau_0)+\tau_0^2(1+\delta)\right]n(2p-n+1)+2K^2n\,p\,\tau_0(1-n\,\tau_0)+\tau_0\left(1-2\tau_0p-n^{-1}\right),$$

$$V_4=\left[K^2(1-\tau_0)+\tau_0^2(1+\delta)\right]\left[\frac{1}{n^2K^2}+n\left(p^2-q^2-p-n\,p\right)\right]+2nq^2K^2\tau_0(1-n\,\tau_0)+$$

:

$$+\tau_0(p-n)\left(1+n^{-1}\right)-\tau_0^2\left(p^2-q^2-n^2-n+\frac{1}{n^2K^2}\right),$$

In the derivation of this solution use has been made of the following relations among the roots of the cubic equation (5.25):

$$\begin{cases} 2p+n=1 \\ K^2\left(p^2+q^2+2n\,p\right)=1+\delta \\ K^2n\left(p^2+q^2\right)=1 \end{cases} \tag{5.36}$$

The previous solution of a simple coupled thermo-elastic problem, an analysis solution follows. In first place, it may be noticed that the solutions for the displacements u and for the temperature T, consist of three types of terms, namely the damped oscillatory terms proportional to the exponential $e^{-p\tau}$, the terms proportional to the exponential $e^{-\eta\tau}$ and the remaining terms, free both these exponential functions. The first of these will be the principal object of this discussion; the other two types remain essentially unchanged even if the uncoupled quasi-static theory employed. The exponential $e^{-p\tau}$ represents the effect of the coupling term8 that is, of thermo-elastic damping), and is in fact equal to unity if the parameter δ is set equal to zero, this is easily seen from the fact that the roots of eq. (5.25)give in this case:

$$p=0,\quad q=(1/K),\quad n=1, \tag{5.37}$$

It has already been proved that all others values of δ the quantity p is positive; hence this factor truly represents a damped response. The magnitude of the damping may be estimated by noting that inequality (5.5) is satisfied by the parameter δ and that therefore we may write the roots of eq. (5.25) approximately by considering the first few terms of a power expansion in δ. Then :

$$p=\frac{\delta}{2\left(1+K^2\right)}+O\left(\delta^2\right),\ q=\frac{1}{K}+\frac{\delta}{2K\left(1+K^2\right)}+O\left(\delta^2\right),\quad n=1-\frac{\delta}{1+K^2}+O\left(\delta^2\right), \tag{5.38}$$

Which shows that thermo-elastic damping is usually small. Of course, no matter how small the coefficient p. for sufficiently large times the quantity $e^{-p\tau}$ will begin to differ appreciably from unity. We may thus conclude that for short times damping is negligible, and the response can be accurately predicted by means of an uncoupled theory in which inertia terms are retained. Such a justification for the use of this theory is, however, not satisfactory in practice, since process of long duration are also of interest. It will now be shown that it is more useful to consider the importance of the coupling terms as a function of the rapidity of heat application , and will then be seen that if the heat application is not too rapid, it is not only permissible to use the uncoupled theory , but also under the same circumstances the effect of inertia may be disregarded. There will the remain the task of determining if actual rates of temperature change are in effect sufficiently slow to make the entire argument valid. The rapidity of heat generation increase is represented in equation (5.32), by the time t_0; we may refer to this as the input time. This time must be compared with two characteristic times of the system, namely, the *characteristic mechanical time* t_M and the *characteristic thermal time* t_T defined as:

$$t_M=\frac{L}{v_e}=L\sqrt{\frac{\rho}{2\mu+\lambda}};\qquad t_T=\frac{L^2}{\kappa}=\frac{\rho c_v L^2}{k}; \tag{5.39}$$

In the present problem it is possible to select at will the relative orders of magnitude of the three times t_0, t_M, t_T, since t_0 and L are arbitrary, and latter appears raised to a different power in t_M and t_T. Three similar time arise in all coupled problems, although their mode of definition is different; their relative orders of magnitude are dictated by physical consideration. As exemplified, it will be found generally that:

$$t_T >> t_M \tag{5.40}$$

And that (for problems of this type in which the forcing disturbance is thermal in character) physical considerations limit the time t_0 to the range:

$$t_0 >> t_M \tag{5.41}$$

Where t_0 may be either larger or smaller than t_T.

It is now desired to show that, under conditions (5.40) and (5.41) , not only are the effects of inertia small, but that coupling effects are also small. The solution reported (5.35) gives the displacement and the temperature at any time in dimensionless form in terms of three dimensionless parameters, namely τ_0, K, δ. Inequalities (5.40) and (5.41) may be expressed in terms of the first two of these by their definitions as follows:

$$t_M/t_T = K << 1;\qquad t_M/t_0 = K/\tau_0 << 1; \tag{5.42}$$

Since both these inequalities are in effect restrictions on quantities proportional to K, the desired result is most readily obtained by expanding the solutions of eq. (5.35) in a series in powers of K, and then noting the character of this expansion in the range defined by equations. (5.42).

For small values of K , we may expand the quantities p, q and n in a series of ascending of K, as follows:

$$\begin{aligned} p&=\frac{\delta}{2(1+\delta)}\left[1-\frac{K^2}{(1+\delta)^3}+o\left(K^4\right)\right],\quad q=\frac{\sqrt{1+\delta}}{K}\left[1-K^2\frac{\delta(4+\delta)}{8(1+\delta)^3}+o\left(K^4\right)\right]\\ n&=\frac{\delta}{1+\delta}\left[1-K^2\frac{\delta}{(1+\delta)^3}+o\left(K^4\right)\right] \end{aligned} \tag{5.43}$$

The entire of equation (5.35) may now be expanded in a similar power series K, with the following result:

$$\frac{u(\tau)}{\sin(x/L)}\left[\frac{(\lambda+2\mu)k}{(3\lambda+2\mu)Q_0L^3\alpha_2}\right]=\frac{\left(1-e^{-\tau/\tau_0}\right)\tau_0-(1+\delta)\left(1-e^{-\eta\tau}\right)}{\tau_0-1-\delta}+$$

$$+\frac{K^2}{\tau_0}\left[\left(e^{-\eta\tau}-e^{-\tau/\tau_0}\right)\frac{\tau_0-1}{\tau_0-1+\delta}+\frac{e^{-\eta\tau}-e^{-p\tau}\cos(q\tau)}{(1+\delta)^2}\right]+.....$$

$$\frac{T(\tau)}{\cos(x/L)}\left(\frac{k}{Q_0L^2}\right)=\frac{\left(1-e^{-\tau/\tau_0}\right)\tau_0-(1+\delta)\left(1-e^{-\eta\tau}\right)}{\tau_0-1-\delta}+$$

$$+\frac{K^2\delta}{\tau_0(1+\delta)(\tau_0-1-\delta)}\left[e^{-\tau/\tau_0}\left(\frac{1+\delta}{\tau_0-1-\delta}\right)-\tau_0e^{-\eta\tau}\left(\frac{1}{\tau_0-1-\delta}-\frac{1}{1+\delta}\right)+e^{-p\tau}\cos(q\tau)\left(1-\frac{\tau_0}{1+\delta}\right)\right]+....$$

(5.44)

It may be noted that the first terms of these expansions are identical . Use of conditions (5.42) now show that it is sufficient to retain only the first term on the right-hand sides of eq. (5.44); this term is free of the oscillatory inertia terms appearing in the complete solution (and in the second term) and therefore leads to the conclusion that neglect of inertia is here permissible. The term in question may be further simplified, however, since the coupling coefficient δ appears in it only in the combination $(1+\delta)$, and this quantity may e approximated by unity in view of inequality (5.5). The solution then becomes simply:

$$\frac{u(\tau)}{\sin(x/L)}\left[\frac{(\lambda+2\mu)k}{(3\lambda+2\mu)Q_0L^3\alpha_2}\right]=\frac{T(\tau)}{\cos(x/L)}\frac{k}{Q_0L^2}=1+\frac{e^{-\tau}-\tau_0e^{-\tau/\tau_0}}{\tau_0-1} \tag{5.45}$$

Equations (5.45) are the solutions of the uncoupled quasi-static theory, that is, they satisfy the following equations (compare with equation (5.15)):

$$\begin{cases} k\dfrac{\partial^2T}{\partial x^2}-\rho c_v\dfrac{\partial T}{\partial t}+Q=0 \\ (\lambda+2\mu)\dfrac{\partial^2u}{\partial x^2}-\alpha(3\lambda+2\mu)\dfrac{\partial T}{\partial x}=0 \end{cases} \tag{5.46}$$

The latter theory may thus be considered valid whenever the appropriate input, thermal, and mechanical time satisfy inequalities (5.40)-(5.41). The preceding discussion indicates that to answer this question it is adequate to consider the effect of inertia(that is, validity of inequalities (5.40)-(5.41) and not that of coupling ; if the former is found to be negligible, the latter should be also. It is also interesting to examine what would happen in the previous illustrative problem if the input time were chosen to be large not only with respect to the characteristic mechanical time, as in eq. (5.41), but also with respect to the characteristic thermal time . In other words, it is desired to impose on the solution the restriction(in addition to those of inequalities (5.42) that:

$$t_0/t_T=\tau_0>>1 \tag{5.47}$$

Equations (5.45) then reduce to :

$$\frac{u(\tau)}{\sin(x/L)}\left[\frac{(\lambda+2\mu)k}{(3\lambda+2\mu)Q_0L^3\alpha_2}\right]=\frac{T(\tau)}{\cos(x/L)}\frac{k}{Q_0L^2}=1-e^{-\tau/\tau_0} \tag{5.48}$$

The time variation of both the displacement and the temperature becomes then proportional to the heat input, eq. (5.32) ; such a solution would be obtained if, in addition to the coupling and inertia terms, the term containing $\partial T/\partial t$ were omitted in eq. (5.8).

5.3 Uncoupled quasi-static formulation

According to the conclusions of the preceding articles, it is permissible in most thermal-stress problem to disregard the effects of both coupling and inertia. With the neglect of coupling, the

general thermal-stress problem separates into two distinct problems to be solved consecutively. The first is a problem in what is generally termed the theory of heat conduction and requires the solution of a boundary-value problem whose field equation (that is, the equation to be satisfied at every point of the body) is, for constant properties and in the absence of internal heat generation:

$$k T_{,ii} = \rho c_v \dot{T} \tag{5.49}$$

Further discussion of the problem of heat conduction, including the mathematical formulation of the boundary conditions corresponding to different physical situations, the uniqueness theorem, and methods for the solution of the resulting boundary-value problem, will be deferred. When the temperature distribution has been found , the determination of the resulting stress distribution with the neglect of inertia terms is a problem in what is termed the linear uncoupled quasi- static theory of thermo-elasticity (or, more simply, thermo-elasticity), for which the field equations are as follows:

Equilibrium equations:

$$\sigma_{ij,j} + f_i = 0 \tag{5.50}$$

Stress-strain relations:

$$\sigma_{ij} = \delta_{ij}\lambda\varepsilon_{kk} + 2\mu\varepsilon_{ij} - \delta_{ij}(3\lambda + 2\mu)\alpha T \tag{5.51}$$

Strain-displacement relations:

$$\varepsilon_{ij} = \frac{1}{2}\left(u_{i,j} + u_{j,i}\right) \tag{5.52}$$

It should be noted here that, with the neglect of the inertia terms, no derivatives with respect to time appear in any of the thermo-elastic field equations. If the boundary conditions also not involve any derivatives with to respect to time (as is usually the case), then the time t simply plays the role of a parameter in the solution of the thermo-elastic problem. In other words, there is a complete mathematical analogy between the solutions corresponding to a family of steady-state temperature distributions depending upon a parameter c, $T(P,c)$, and to transient temperature distribution, $T(P,t)$. The resulting stress distributions will depend, of course, upon c and t respectively, that is, in the latter case, the stress distribution will be time dependent. These comments hold for any functions $T(P,c)$ or $T(P,t)$ arbitrarily prescribed. If, in addition, it is known that the temperature distribution is the of a heat conduction problem, then use may be made of fact that $T(P,t)$ satisfies equation (5.49) or, in the steady case, that it is harmonic; in this manner special techniques may be developed for the determination of thermal stresses.

References

[1] Boley, B.A.,Weiner, J.H., *Theory of thermal stresses*, Dover publications, inc. Mineola, New York

[2] Ciarlet, Philiphe G., *Mathematical Elasticity, Volume I.: Three dimensional elasticity*, Elsevier Science Publishers B.V.

[3] Gurtin, M. E., *The Linear Theory of Elasticity, Handbbuch der Physik*, Springer, Berlin, 1972.

[4] Lekhnitskii, S. G., *Theory of Elasticity of an Anisotropic Body*, Mir, Moscow, 1981.

[5] Love, A. E. H., *A Treatise on the Mathematical Theory of Elasticity*, Dover Publications, Inc, New York, 1944

[6] Nunziante, L., Gambarotta, L., Tralli, A., *Scienza delle Costruzioni*, 3° Edizione, McGraw-Hill, 2011, ISBN: 9788838666971

[7] Ting TCT. *Anisotropic elasticity - Theory and applications*. Oxford University Press; 1996.

[8] Wolfram, S., *Mathematica, version 8*, Wolfram Research, Inc., Champaign, IL, 1998–2005.

CHAPTER VI
THE FORMULATION OF HEAT TRANSFER PROBLEMS

6.0. Introduction

The fundamental equations governing the temperature stresses, and deformation in a solid were derived in Chapter IV : it was noted there that from a strict viewpoint these quantities were all interrelated and had to be determined simultaneously. However, for most practical problems the effects of the stresses and deformations upon the temperature distribution is quite small and can be neglected. This procedure allows the determination of the temperature distribution in the solid resulting from prescribed thermal conditions to become the first , and independent, step of a thermal-stress analysis; the second step of such an analysis is then the determination of the stresses and deformations of the body due to this temperature distribution. In this chapter, the formulation of the mathematical boundary-value problem for the determination of the temperature distribution is discussed. Since solid, opaque bodies are of primary interest here, heat is transferred from point to point within the body solely by conduction; the field equation of the boundary-value problem will, therefore, always be some form of the Fourier heat conduction equation . However, heat may be transferred to the surface of the body by other modes of heat transfer and which mode is operative will dictate the proper choice of boundary condition. To render the problem mathematically tractable , it is necessary to idealize matters considerably in the formulation of the boundary corresponding to various thermal situations. The seriousness of the deviations from reality introduced by these simplifications depends, of course, on the nature of the purposes at hand. In particular, a formulation which is adequate only if temperatures are of interest may be inadequate for a thermal-stress investigation. For this reason, a brief outline of the elements of heat transfer is presented in this chapter, from which it is hoped that the thermal-stress specialist may acquire a feeling for the nature of the abstractions involved in the commonly employed thermal boundary conditions. The various modes of heat transfer are discussed first in paragraph 6.1. For a fuller treatment of this topic, the reader is referred to the treatises devoted solely to the subject of heat transfer.The energy balance equation was derived from fundamental thermo-dynamical concepts for various types of continuous media. These derivations were based upon the general conservation of energy law, and the resulting equations contain both thermal and mechanical terms. If the latter are neglected, the energy balance equation reduces to the heat conduction.

6.1. Modes of heat transfer

Energy in the form of heat is transferred between any two particles of matter which are at different temperatures. These two particles may be, for example, part of the same solid body, or of two different solids, or of a mass of fluid , depending on the system under consideration. Theoretically, of course, this system comprises all surrounding matter, but no difficulty is encountered in any practical problem in delimiting a closed system on which all exterior matter has negligible influence. The mechanism or mode of heat transfer will depend on the nature of the system thus defined and, more particularly, on the character of the matter between and surrounding the two particles. There are three modes of heat transfer, namely, conduction, radiation and convention:

a) Conduction: Between two particles of a solid body which are at different temperature, heat is transferred only by conduction, a process which take place at the molecular and atomic levels. He law of heat conduction for isotropic bodies may be stated as follows:

$$q = -k\frac{\partial T}{\partial n} \tag{6.1}$$

where k, with typical units of $W/m^{\circ}K$, is termed the thermal conductivity of the solid and where the heat flux q, associated with direction n at a point P, is defined in the following way: consider a finite surface of area A containing the point P, at which the surface normal is n. Let the total rate of heat flow through this area towards the side with positive normal be Q. Then:

$$q(P) = \lim_{A \to 0} \left(\frac{Q}{A} \right) \tag{6.2}$$

Where in the limiting process, the area A is shrunk so that the point P is always either contained in it or on its boundary. This law of heat conduction was stated first by Fourier, who based it on experimental observation; it may also be derived from the principles of irreversible thermodynamics.

b) Radiation : If two particles at different temperature are separated by a vacuum, then clearly heat cannot be transferred between them by conduction ; however, heat transfer will still take place by electromagnetic radiation. If the two particles are separated by a material medium, radiation also occurs, but when this medium is solid or liquid, the amount of heat transferred through it by radiation is usually negligible. In the case of gases, however, radiant heat transfer may be important. The rate Q of heat transfer by radiation between two surfaces separated by a vacuum at absolute temperature T_1 and T_2 is expressed by the Stefan-Boltzmann law in the following form:

$$Q = C_2 T_2^4 - C_1 T_1^4 \tag{6.3}$$

where the constants C_1 and C_2 depend upon the relative orientation of two surfaces, the distance between them, and the absorption and reflection properties of the surface. These constants are numerically quite small, and radiation may generally therefore be neglected unless at least one of the surfaces is at relatively high temperatures (say about 400°F) . For a through treatment of the complex subject of radiation, the reader is referred to the textbook by Jakob .

c) Convenction **:** Heat transfer in a fluid , as in any substance , takes place by the mechanisms of conduction and radiation, with the former mechanism generally predominant. If the fluid is in motion, however, increased rates of heat transfer will result since portions of the fluid at the different temperatures can be brought in closer proximity. When the motion of the fluid is due entirely to variations in density caused by a non-uniform temperature distribution, the process is called free or natural convention. If the motion is due to any other cause, the convention is said to be forced.

6.2. The Fourier heat conduction equation

The Fourier heat conduction equation is derived in an elementary manner, based on an energy balance which neglects any conversion of mechanical energy into heat, and on the Fourier law of heat conduction, equation (6.1).

Consider an isotropic solid body with thermal conductivity k subjected to arbitrary thermal conditions on its surface and with internal heat generation at the rate Q per unit time per unit volume. Both k (if the body is non-homogeneous or if the thermal conductivity is temperature dependent) and Q may vary throughout the body and with time. Consider now the elemental portion of this body shown in figure n.1 . The rate at which heat flows into the element of volume through face ABCD is:

$$-k \frac{\partial T}{\partial x} dydz \tag{6.4}$$

Whereas the rate at which it flows out through face EFGH is :

$$-\left[k \frac{\partial T}{\partial x} + \frac{\partial}{\partial x} \left(k \frac{\partial T}{\partial x} \right) dx \right] dydz \tag{6.5}$$

The net rate of heat flow into the element through these faces it then

$$\frac{\partial}{\partial x} \left(k \frac{\partial T}{\partial x} \right) dxdydz \tag{6.6}$$

And similar expressions hold for the other four faces. The rate of change on internal energy is:

$$\rho c \frac{\partial T}{\partial t} \tag{6.7}$$

Per unit volume, where t is time, ρ is the density , and c the specific heat of the material. No distinction is made here between c_p and c_v , the specific heats at constant pressure and constant volume, since all mechanical effects are being neglected. Under this assumption, an energy balance leads to the Fourier heat equation as follows:

$$\frac{\partial}{\partial x}\left(k\frac{\partial T}{\partial x}\right)+\frac{\partial}{\partial y}\left(k\frac{\partial T}{\partial y}\right)+\frac{\partial}{\partial z}\left(k\frac{\partial T}{\partial z}\right)+Q=\rho c\frac{\partial T}{\partial t} \tag{6.8}$$

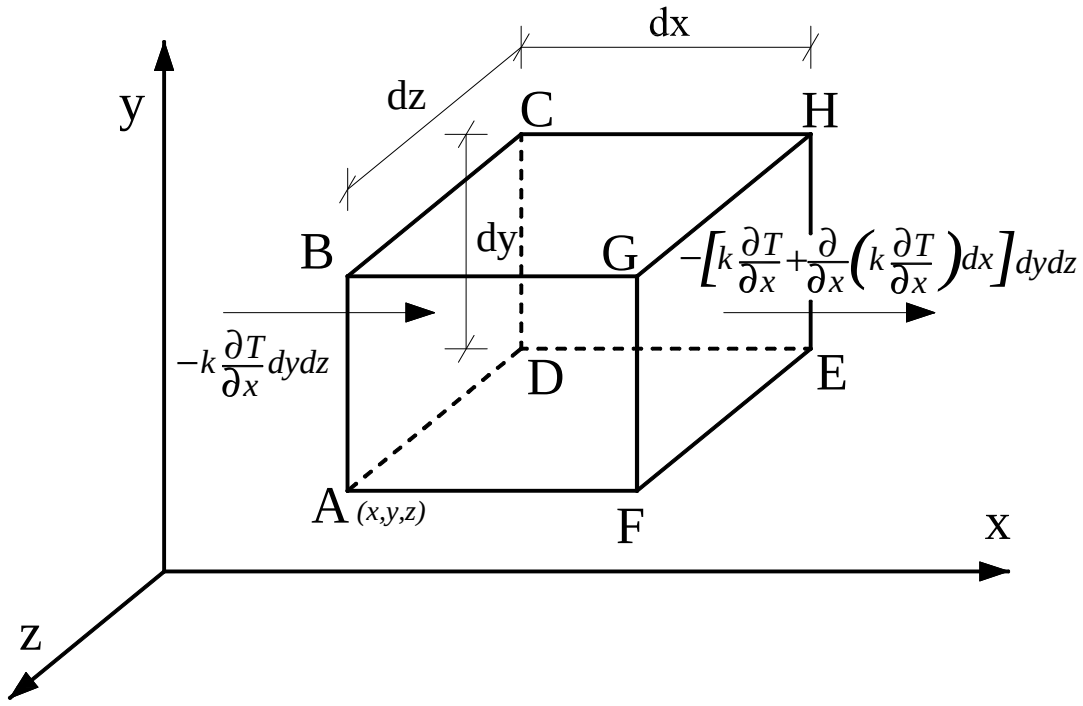

Fig. 6.1 – *Infinitesimal volume subjected to heat flux in x-direction*

The solution of this equation is, in general , difficult to obtain; it is frequently reasonable, however, to assume that the conductivity k is constant throughout the body. Equation (6.8) reduce to:

$$\kappa\nabla^2 T+\frac{Q}{\rho c}=\frac{\partial T}{\partial t} \tag{6.9}$$

where the quantity :

$$\kappa=\frac{k}{\rho c} \tag{6.10}$$

Is known as the thermal diffusivity and has dimensions, in typical units, of $m^2/\sec°K$. The quantity $\nabla^2 T$ is a follows in various coordinate systems. In Cartesian coordinate x, y, z:

$$\nabla^2 T=\frac{\partial^2 T}{\partial x^2}+\frac{\partial^2 T}{\partial y^2}+\frac{\partial^2 T}{\partial z^2} \tag{6.11}$$

Cylindrical coordinate r, θ, z:

$$\nabla^2 T=\frac{\partial^2 T}{\partial r^2}+\frac{1}{r}\frac{\partial T}{\partial r}+\frac{1}{r^2}\frac{\partial^2 T}{\partial \theta^2}+\frac{\partial^2 T}{\partial z^2} \tag{6.12}$$

Spherical coordinate r, θ, ϕ:

$$\nabla^2 T = \frac{\partial^2 T}{\partial r^2} + \frac{1}{r}\frac{\partial T}{\partial r} + \frac{1}{r^2 \sin\theta}\frac{\partial}{\partial \theta}\left(\sin\theta \frac{\partial T}{\partial \theta}\right) + \frac{1}{r^2 \sin^2\theta}\frac{\partial^2 T}{\partial \phi^2} \tag{6.13}$$

If, as is usually the case, no heat is generated within the body, then Q=0, and eq. (6.9) becomes:

$$\kappa \nabla^2 T = \frac{\partial T}{\partial t} \tag{6.14}$$

The further particular case in which the temperature distribution is independent of time and Q=0, is often of interest; when this is so $\partial T/\partial t = 0$ and the temperature distribution satisfies the equation:

$$\nabla^2 T = 0 \tag{6.15}$$

Equation (6.15) is known as Laplace's equation; any solution of this equation is called a harmonic function. We note that if the body is homogeneous but with temperature-dependent properties it is possible to put equation (6.8) in the form of equation (6.9), although κ will now be a function of T. This is accomplished by a change in temperature scale through the equation:

$$T'(t) = \frac{1}{k_0}\int_{T_0}^{T} k(T)\, dT \tag{6.16}$$

Where the constant k_0 represents the thermal conductivity at some convenient reference temperature T_0 and ha been introduced so as to give T', for convenience, the dimensions of temperature. Since

$$\begin{cases} \dfrac{\partial T'}{\partial x} = \dfrac{1}{k_0} k(T) \dfrac{\partial T}{\partial x} \\ \dfrac{\partial T'}{\partial t} = \dfrac{1}{k_0} k(T) \dfrac{\partial T}{\partial t} \end{cases} \tag{6.17}$$

We see that (6.8) assume the form:

$$\kappa(T)\nabla^2 T' + \frac{\kappa(T)}{k_0} Q = \frac{\partial T'}{\partial t} \tag{6.18}$$

The functions of T in these equations may be expressed as function of T' by use of the function $T(T')$ defined explicit by (6.16). Although equation (6.18) is still non linear , it is more convenient for numerical or electrical analogy procedures than equation (6.8).

The equation for temperature dependent properties may be linearized approximately by inverting the function $k(T)$ to obtain $T(k)$ and by then using k as the independent variable. Then:

$$\begin{cases} \dfrac{\partial T}{\partial x} = \dfrac{dT}{dk}\dfrac{\partial k}{\partial x} \\ \dfrac{\partial T}{\partial t} = \dfrac{dT}{dk}\dfrac{\partial k}{\partial t} \end{cases} \tag{6.19}$$

So that eq. (6.8)becomes :

$$\frac{\partial}{\partial x}\left(k\frac{dT}{dk}\frac{\partial k}{\partial x}\right) + \frac{\partial}{\partial y}\left(k\frac{dT}{dk}\frac{\partial k}{\partial y}\right) + \frac{\partial}{\partial z}\left(k\frac{dT}{dk}\frac{\partial k}{\partial z}\right) + Q = \rho c \frac{dT}{dk}\frac{\partial k}{\partial t} \tag{6.20}$$

Therefore , eq. (6.8) (with temperature-independent heat generation will be linearized if we find compatible solutions to the equations:

$$k\frac{dT}{dk} = \alpha, \quad \rho c \frac{dT}{dk} = \beta \tag{6.21}$$

With α, β are arbitrary constant and with the temperature-dependent product ρc expressed as a function of k by means of the function $T(k)$. In general of course, such compatible solutions will not exist, but it way still be possible to obtain a linearized equation which will give good approximations to the actual solutions of equations (6.8) over a limited range of temperature

variation by adjusting the constants α, β so that the two solutions to (6.21) agree well over the range of interest.

In the steady-state case with space-dependent conductivity, equation (6.8) may be put in a more convenient form by means to the transformation:

$$T' = \sqrt{k}T \tag{6.22}$$

The equation to be satisfied by the function T' is then:

$$\nabla^2 T' - f(x,y,z)T' + \frac{Q(x,y,z)}{\sqrt{k}} = 0 \tag{6.23}$$

Where the function f is :

$$f = \frac{1}{\sqrt{k}}\nabla^2\left(\sqrt{k}\right) \tag{6.24}$$

And may be taken as known if $k(x,y,z)$ is known.

6.3. Initial and boundary conditions

In addition to the appropriate partial differential equation (6.8) it is necessary to specify initial and boundary conditions in order to describe fully the problem. Of course, no need arises for initial conditions in the case of the steady-state problem of equation (6.15). A listing of the idealized thermal boundary conditions commonly employed follows.

The initial conditions specify the initial temperature distribution throughout the body. In most problems, the initial temperature is constant. There are five principal boundary conditions which are used in the mathematical theory o heat conduction as idealizations of actual physical processes.

Over any portion of the bounding surface of the body, one of the following conditions is usually used.

1) Prescribed surface temperature:

$$T(P,t) = f(P,t) \tag{6.25}$$

Where the point P is on the surface and $f(P,t)$ is a prescribed function.

2) Prescribed heat input:

By eq. (1.1), thi boundary condition takes the form,

$$k\frac{\partial T}{\partial n}(P,t) = q(P,t) \tag{6.26}$$

Where n is the outward normal to the surface at the point P.

3) Perfectly insulated surface:

By definition, a perfectly insulated surface is one across which there is no heat flux . Eq. (6.26) then becomes:

$$\frac{\partial T}{\partial n}(P,t) = 0 \tag{6.27}$$

4) Convection boundary condition:

In many problems, the heat flux across a bounding surface may be taken as proportional to the difference between the surface temperature $T(P,t)$ and the known temperature T_0 of the surrounding medium equation (6.26) then takes the form,

$$k\frac{\partial T}{\partial n} = h\left[T_0 - T(P,t)\right] \tag{6.28}$$

where h is termed the boundary or film conductance and may very with space and time in a prescribed manner. Other names given to h include film (or surface) heat transfer coefficient.

5) Two solid bodies in contact:

If the surface bodies are in perfect thermal contact , their temperatures at the surface must be the same. In addition, the heat flux leaving one body through the contact surface must be equal to that ending the other body. Thus for a point P on the contact surface:

$$\begin{cases} T_1(P,t) = T_2(P,t) \\ k_1 \dfrac{\partial T_1}{\partial n}(P,t) = k_2 \dfrac{\partial T_2}{\partial n}(P,t) \end{cases} \tag{6.29}$$

Where subscripts 1 and 2 refer to the two bodies and n is the common normal to the contact surface at P. If there is an imperfect thermal contact between the two bodies, the concept of a contact resistance R (or contact conductance h = 1/R) is frequently used. The equality of heat fluxes must still be enforced, but a difference between the two surface temperatures, proportional to the heat flux, will now exist. The appropriate boundary conditions are therefore:

$$k_1 \frac{\partial T_1}{\partial n_1}(P,t) = \frac{1}{R}\left[T_2(P,t) - T_1(P,t)\right] \tag{6.30}$$

$$k_1 \frac{\partial T_1}{\partial n_1}(P,t) = k_2 \frac{\partial T_2}{\partial n_1}(P,t) \tag{6.31}$$

where n_1 is the outward normal, referred to the body 1, to the contact surface at point P.

6.4. Dimensionless parameters

It is convenient at this point to note the dimensionless parameters that may be used to put the Fourier heat equation (6.14) and the boundary conditions of the preceding paragraph in dimensionless form. Attention is restricted here to geometries with some characteristic length L, while geometries with no such length are discussed in next paragraph.

We may then define the following dimensionless quantities:

$$\begin{cases} T^* = \dfrac{T}{T_R}, \\ x^* = \dfrac{x}{L},\ y^* = \dfrac{y}{L},\ z^* = \dfrac{z}{L},\ n^* = \dfrac{n}{L}, \\ t^* = \dfrac{\kappa}{L^2} t, \end{cases} \tag{6.32}$$

where T_R is a suitable chosen reference temperature.

With these quantities, equation (6.14) assumes the form:

$$\nabla^2 T^* = \frac{\partial^2 T^*}{\partial x^{*2}} + \frac{\partial^2 T^*}{\partial y^{*2}} + \frac{\partial^2 T^*}{\partial z^{*2}} = \frac{\partial T^*}{\partial t^*} \tag{6.33}$$

Equations (6.32), together with other dimensionless parameters, may be used to recast the boundary conditions of the preceding article in dimensionless form as follows

1) Prescribed surface temperature:

$$T^*(P,t) = f^*(P,t) \tag{6.34}$$

where

$$f^*(P,t) = \frac{1}{T_R} f(P,t) \tag{6.35}$$

2) Prescribed heat input:

$$\frac{\partial T^*}{\partial n^*} = \frac{q_R L}{T_R k} q^*(P,t) \tag{6.36}$$

where

$$q^*(P,t)=\frac{1}{q_R}q(P,t) \tag{6.37}$$

and q_R is a reference heat flux which may be chosen in any convenient fashion. If no other conditions dictate the choice of T_R we may set

$$T_R=\frac{q_R L}{k} \tag{6.38}$$

to make the coefficient of $q^*(P,t)$ in (6.36) unity . The reference temperature T_R then corresponds to the steady-state temperature difference across a bar of length L and conductivity k through which flows the flux q_R.

3) Perfectly insulated surface:

$$\frac{\partial T^*}{\partial n^*}(P,t)=0 \tag{6.39}$$

4) Convention boundary condition

$$\frac{\partial T^*}{\partial n^*}(P,t)=m\left[T_0^*-T^*(P,t)\right] \tag{6.40}$$

where the dimensionless parameter:

$$m=\frac{h\,L}{k} \tag{6.41}$$

Is known as the Biot Number and

$$T_0^*=\frac{T_0}{T_R} \tag{6.42}$$

If T_0 is a constant and the initial temperature, T_I , of the body is uniform, it is usually convenient to take $T_R=T_0$ with the temperature scale chosen so that $T_I=0$, or to set $T_R=T_I$ with the scale chosen so that $T_0=0$

5) Two solid bodies in contact:

Perfect contact:

$$\begin{cases} T_1^*(P,t)=T_2^*(P,t) \\ k_1\dfrac{\partial T_1^*}{\partial n^*}(P,t)=k_2\dfrac{\partial T_2^*}{\partial n^*}(P,t) \end{cases} \tag{6.43}$$

Imperfect contact

$$\begin{cases} \dfrac{\partial T_1^*}{\partial n_1^*}(P,t)=m_1\left[T_2^*(P,t)-T_1^*(P,t)\right] \\ k_1\dfrac{\partial T_1^*}{\partial n_1^*}(P,t)=k_2\dfrac{\partial T_2^*}{\partial n_1^*}(P,t) \end{cases} \tag{6.44}$$

where:

$$m_1=\frac{L}{k_1 R}=\frac{hL}{k_1} \tag{6.45}$$

6.5. Discussion of the boundary conditions

The boundary conditions listed here are idealizations of actual physical conditions. An understanding of the nature of these idealizations is necessary for a proper choice of the most suitable mathematical formulation of a given physical problem.

The surface of a body (or a portion of its surface) may receive heat either through contact with another solid or by radiation, or through contact a fluid.

a) Contact with a solid **:** When two solid surface touch each other, because of the natural roughness of any real material, actual physical contact takes place only at some projecting segments of the surface. Conduction takes place at these points contact, while heat is transferred across the gaps by radiation and by conduction through the fluid, usually air, filling them.
It has been found as a result of an experimental investigation that none of these modes of heat transfer has only predominance over the others. It therefore appears that heat transfer across a contact surface is a complex process; It may be rendered amenable to analysis by the following considerations which are illustrated in follows figure:

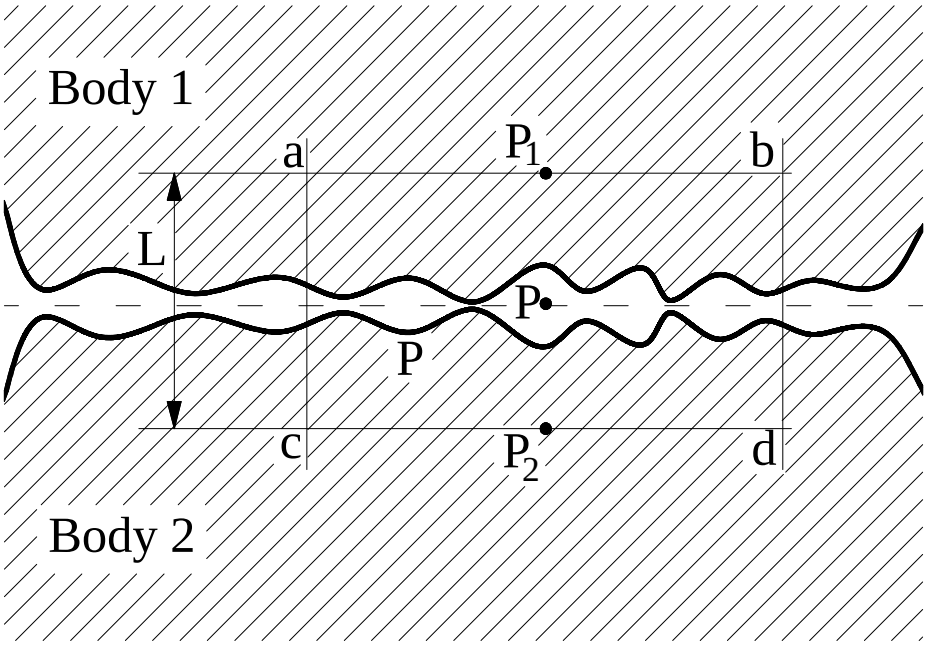

Fig. 6.2 – *Solid-to-solid contact*

Consider the small volume *abcd* of that figure enclosed by two planes (*ab* and *cd*) parallel to the common mathematical boundary, and by the planes *ac* and *bd* perpendicular to that boundary. The planes *ab* and *cd* are taken at a sufficient distance from the boundary (about two or three times the maximum dimensions of the irregularities) so that the distribution of heat flow on them is not appreciably affected by the local aberrations of the contact surfaces. Let the distance *ab = cd* be chosen large compared with *ac = bd = L* and consider the heat balance o the volume question . Because of the relative dimensions of the sides of this volume, the heat leakage through ac and bd may be neglected; the heat balance equation is then:

$$-\int_{\substack{Area\\ab}} k_1 \frac{\partial T_1}{\partial n_1} dA + \int_{\substack{Area\\cd}} k_2 \frac{\partial T_1}{\partial n_1} dA = \overline{\rho c} \frac{\partial T}{\partial t} A L \tag{6.46}$$

where A is the area of the surface ab and where a bar indicates the average value of a quantity within the volume. If the distance *ab* is small enough so that the heat flux does not vary appreciably along it, then we may write:

$$\int_{\substack{Area\\ab}} k_1 \frac{\partial T_1}{\partial n_1} dA = \left(k_1 \frac{\partial T_1}{\partial n_1} \right)_{P_1} A \tag{6.47}$$

And similarly for the second term of the left-hand side of (6.46). Since the distance L is small and since the temperature T varies slowly with time (except for very short periods, as for example,

immediately following the initial contact between two bodies at different temperatures), the term on the right-hand of (6.46) may be neglected . The resulting boundary condition namely,

$$k_1 \frac{\partial T_1}{\partial n_1}(P_1,t) = k_2 \frac{\partial T_2}{\partial n_1}(P_2,t) \tag{6.48}$$

May then be replaced by equation (6.31) because the distance L is small.

Equation (6.30) is based on the experimental observation that the heat flux across the joint is roughly proportional to the temperature difference across it. The proportionality factor 1/R must then account for all the complexities indicated earlier and can therefore be expected to depend not only on the type of joint and materials but also on the mean temperature of the joint, the roughness of both surfaces, the pressure between them, and so forth. It has been shown experimentally, however, that the contact resistance is reasonably constant for any given point if its mean temperature does not vary too widely. Experimentally determined values of the contact resistance are given in the literature for various types of joints.

It may be noted that if the contact resistance s very large (m_1 in (6.44) approaching zero), the boundary condition (6.44) may be replaced by that of equation (6.39). If , on the other hand , R is very small (m_1 in (6.44) approaching infinity), perfect contact is approached.

b) Radiation **:** If the surface of a body is exposed to high-temperature source, it will receive heat by radiation in accordance with a law of the form (6.3), namely,

$$k \frac{\partial T}{\partial n}(P,t) = C\left[\theta_0^4(t) - \theta^4(P,t)\right] \tag{6.49}$$

where $\theta_0(t)$ and $\theta(P,t)$ are the absolute temperatures of the source and surface respectively. Empirical generalizations of this equation using other values for the exponents to account for different surface and other conditions have been proposed. These boundary conditions, being nonlinear, render analytical solution of the resulting boundary –value problem extremely difficult. Two simplifications are often permissible, however: they arise either when the source temperature varies over too wide a range.

In the first case, neglect of θ^4 relative to θ_0^4 is permissible; rewriting equation (6.49) in the form:

$$k \frac{\partial T}{\partial n} = C\,\theta_0^4 \left[1 - \left(\frac{\theta}{\theta_0}\right)^4\right] \tag{6.50}$$

In fact shows that if $\theta/\theta_0 = 1/2$, for example, the resulting error in the heat flow is approximately only 6.7 percent of the actual heat flow. With this approximation , boundary condition (6.49) can therefore be replaced by the linear condition for a prescribed heat input given by equation (6.26).

For the second case the following approach may be used. The right-hand side of (6.49) may be factored to give:

$$k \frac{\partial T}{\partial n} = C\left(\theta_0^3 + \theta_0^2\theta + \theta_0\theta^2 + \theta^3\right)(\theta_0 - \theta) \tag{6.51}$$

I neither the temperature of the source nor that of the surface varies a great deal, the coefficient of $\theta_0 - \theta$ may be taken as a constant h_r, sometimes called the radiation boundary conductance. Numerical values for h_r as a function of θ and θ_0 are found in the next-books of McAdams, and Eckert and Drake. Also, since the absolute and relative temperature θ and T are related by the equation:

$$\begin{aligned} \theta(^\circ R) &= T(^\circ F) + 460 \\ \theta(^\circ K) &= T(^\circ C) + 273 \end{aligned} \tag{6.52}$$

We can replace $(\theta_0 - \theta)$ by $(T_0 - T)$ in equation (6.51). The boundary condition then becomes:

$$k\frac{\partial T}{\partial n} = h_r\left(T_0 - T\right) \tag{6.53}$$

Which is of the same form as the convent boundary condition (6.51) . For this reason, the latter is sometimes also referred to as the radiation boundary condition, particularly in English publications, as for example, in Carslaw and Jaeger.
If neither of these simplifications is permissible, the boundary condition (6.49) must used and numerical methods are then usually necessary.

c) Contact with a fluid : The determination of the temperature distribution in a solid body in contact with a fluid presents a complex problem. Strictly speaking, the entire problem must be considered as a unit; that is, it is necessary to solve the heat conduction equation in the solid and the fluid flow equations, with thermal terms included in the fluid under coupling boundary conditions at the interface analogous to those for solid–to-solid contact equations (6.29). When only the temperature distribution in the solid is of interest, it is desirable to uncouple the two problems; the heat conduction problem in the solid is then formulated with the convention boundary condition, eq. (6.28), imposed over that portion of the solid surface in contact with the fluid. The boundary conductance h must then include all the effects of the fluid ; from a strict viewpoint it will depend, in addition to any other conditions imposed upon the fluid, upon the spatial distribution of the surface temperature and its past history, that is, upon surface and time integrals of the (unknown) surface temperature; the form of these integrals is determined by a solution of the fluid problem with the surface subjected to an arbitrary temperature distribution. If it were necessary to include all these effects, the uncoupling of the fluid and solid problems would be of little value, since the partial differential equation boundary-value problem would have been thus converted to an exceedingly complex integro-differential equation problem. We therefore list first several idealizations of the actual situation which lead to successively simpler problems. We will then give some indication of the situations in which these idealizations may be employed with reasonable accuracy.
1) We may assume that :

$$h = h\left[T\left(P,t\right),P,t\right] \tag{6.54}$$

where P is a generic point on the surface of the solid in contact with the fluid. In other words, we assume that h depends only on time, position and the local present surface temperature. In this case, the formulation is now one of a partial differential equation boundary-value problem, but it involves a non-linear boundary condition.
2) The boundary condition is linearized if it can be further assumed that h is independent of the surface temperature , that is,

$$h = h\left(P,t\right) \tag{6.55}$$

3) the boundary conductance may be assumed constant
4) when the boundary conductance (not necessarily constant), is either very small or very large, the convection boundary conditions, equation (6.28) may be replaced by simpler conditions. If the dimensionless Biot number (m) is very small, equation (6.28) may be replace by (6.27), the boundary condition for a perfectly insulated surface. If m is very large, writing (6.40) as :

$$\frac{1}{m}\frac{\partial T^*}{\partial n^*} = T_0^* - T^*\left(P,t\right) \tag{6.56}$$

Shows that it becomes identical in the limiting case with (6.34), the boundary condition for a prescribed surface temperature . It should be particularly noted that this latter boundary condition seldom represents an actual physical situation but arises almost always as a limiting form of the convection boundary condition. This limiting process should be used with care since, it may give rise to large errors in transient thermal-stress analysis.
Of the idealizations described, the first two lead to problem formulations which require numerical or other approximate technique. If exact analytical solution are desired, it is necessary to resort to

one of the last two more extreme idealizations. It is not possible to give here a detailed discussion of the error thus incurred in a particular situation and we therefore refer the reader to the textbook of Eckert and Drake for a description of the presents status of this complex and active field. We will, however, outline here a simple, approximate calculation of the boundary conductance for one set of conditions since it offers considerable insight into the relevant factors.

Consider the case of a viscous fluid in laminar flow over a flat plate under steady conditions , figure n.3. The free stream velocity (that is, the velocity at a distance from the plate) is v_0 and will betaken as parallel lo the place surface, with the fluid temperature there T_0. The plate temperature surface is maintained constant at T_w. Then, as may be shown by use of the fluid flow theory , there exists a boundary layer of thickness $\delta(x)$, outside of which the fluid velocity is substantially v_0. An approximate formula for $\delta(x)$ under these conditions is (Eckert and Drake):

$$\delta(x) = 4.64\sqrt{\frac{\nu}{v_0}x} \tag{6.57}$$

where ν is the kinematic viscosity of the fluid. Similarly, there exists a thermal boundary layer whose thickness, as yet unknown, will be denoted by $\delta_T(x)$, outside of which the fluid temperature is substantially T_0. At a particular value of x, the velocity and temperature distributions then appears as in figure n.3 . We consider next a volume element fixed in space (as shown in figure n.3) where $L > \delta$. By an energy balance for this element it is found that :

$$\frac{d}{dx}\int_0^L \left[T_0 - T_f(x,y)\right] v(x,y)\,dy = \kappa_f \frac{\partial T_f}{\partial y}(x,0) \tag{6.58}$$

Where $T_f(x,y)$ is he temperature in the fluid and where $\kappa_f = \dfrac{k_f}{\rho_f (c_P)_f}$ is thermal diffusivity of the fluid. In this energy balance (see Eckert and Drake) heat transfer by conduction is neglected at a point (x,y) of the surface *abcd* in comparison with that transported at the rate $\rho_f (c_P)_f T_f(x,y) v(x,y)$ for unit area by the fluid motion; however, heat transferred into the fluid by conduction at the rate $-k_f \dfrac{\partial T_f}{\partial y}(x,0)$ is taken account of at a point $(x,0)$ of the surface ad since there is no flow across that surface. We next insert reasonable approximate expressions for $T_f(x,y)$ and $v(x,y)$ in the integral of equation (6.58) . Suitable expressions under the stated conditions are:

$$T_f(x,y) = T_w + (T_0 - T_w)\left[\frac{3}{2}\frac{y}{\delta_T(x)} - \frac{1}{2}\left(\frac{y}{\delta_T(x)}\right)^3\right] \tag{6.59}$$

$$v(x,y) = v_0\left[\frac{3}{2}\frac{y}{\delta(x)} - \frac{1}{2}\left(\frac{y}{\delta(x)}\right)^3\right] \tag{6.60}$$

where $\delta(x)$ is given by (6.57); substitution of these expressions into (6.58) leads to a differential equation for the only unknown function, $\delta_T(x)$, with the following approximate solution:

$$\delta_T(x) = 0.975\,\sigma^{-\frac{1}{3}}\delta(x) = 4.52\,\sigma^{-\frac{1}{3}}\sqrt{\frac{\nu}{v_0}x} \tag{6.61}$$

where σ is called the (dimensionless) Prandtl number of the fluid and is defined as:

$$\sigma = \frac{\nu}{\kappa_f} \tag{6.62}$$

Substitution of this expression into (6.59) then yield the following as heat flow into the fluid:

$$q = -k_f \frac{\partial T_f}{\partial y}(x,0) = -0.332\, k_f \sigma^{1/3} \sqrt{\frac{v_0}{\nu x}} \left(T_0 - T_w\right) = -k_s \frac{\partial T_s}{\partial y}(x,0) \tag{6.63}$$

Where, in the last term, k_s is the thermal conductivity of the plate, T_s is the temperature in the plate, and the last equality follows since the heat flow into the fluid is equal to the heat flow out of the solid.
Comparison with (6.28) then shows that for this case

$$h = 0.332\, k_f \sigma^{1/3} \sqrt{\frac{v_0}{\nu x}} \tag{6.64}$$

This result is well verified by more accurate calculations and experiment.
It sheds some light on the idealizations previously listed (number 1 to 3) as follows:

1) Boundary conductance dependent only upon local instantaneous conditions : Since the surface temperature is constant with respect to both time and space in this problem, it yields no direct information on the permissibility of assuming that h depends upon the present local surface temperature, rather than on integrals of it with respect to time (past history effect) and space. However, we again some in insight into the unimportance of the past history effect from the model employed in the previous calculations. In this model all the temperature change in the fluid occurs in the thermal boundary layer , and since this layer is generally very thin (equation (6.61)), it is intuitively clear that the temperature distribution in it will be, at any instant very nearly the steady-state temperature distribution corresponding to the surface (and fluid) temperature at that instant, or in other words, the past history effect will be negligible unless very rapid transients are involved.
For the effect of spatial variation of the surface temperature we may refer parenthetically to the recent work of Imai. He considers the case in which the wall temperature variation is of the form:

$$T_w = a + b x^n \tag{6.65}$$

where n is a positive integer; he also includes the possibility of variation of the free-stream velocity of the form:

$$v_0 = c\, x^m \tag{6.66}$$

Where m is a positive integer. He then finds that the boundary conductance h can be approximately given by the equation :

$$h = \frac{k_f}{(2-\beta)^{1/2}} \left[\frac{\Gamma(2/3)}{3^{2/3}\Gamma(4/3)} \left\{ \frac{1}{2} + n(2-\beta) \right\}^{1/3} (\alpha\sigma)^{1/3} - \frac{\beta}{10\alpha} \right] \sqrt{\frac{v_0}{\nu x}} \tag{6.67}$$

where, in addition to the notation previously defined,

$$\beta = \frac{2m}{m+1} \tag{6.68}$$

and

$$\alpha = \frac{1}{v_0} \left[\frac{2x\nu}{v_0(1+m)} \right]^{1/2} \frac{\partial v}{\partial y}(x,0) \tag{6.69}$$

Equation (6.67) indicates that the effect of variation of wall temperature is considerable (as seen from the role played by n in that equation) and it may be expected therefore that, for an accurate treatment of a heat conduction problem in which considerable variation of surface temperature is expected, a boundary condition involving integrals of the surface temperature is necessary.

2) Boundary conductance independent of local temperature: Returning now to the treatment of a constant wall temperature, which led to equation (6.64), we see from that equation that h, for this case, does not depend directly upon the surface temperature; this factor does enter directly however, in its effect upon the fluid properties, an effect which is large for some liquids but relatively minor for gases. However as is evident from equation (6.64), h is space dependent, particularly near the

leading edge where flow conditions are changing rapidly. It will also be time dependent if the flow conditions are.

3) Boundary conductance assumed constant: For a portion of the plate at some distance from the leading edge, h varies only slightly and a constant, average value may be employed.
The preceding discussion dealt with one of the simplest situations. We now discuss briefly some other possibilities.

Turbulent flow. The analysis just described was predicated on laminar flow conditions . Turbulent flow presents a more complex problem towards which much research is being directed . We may see qualitatively that the effect of turbulence is to increase greatly the heat transfer and therefore the boundary conductance, since there are random velocity components perpendicular to the surface in question which result in heat transfer by fluid transport as well as by conduction . There will, generally be zones of transition from laminar to turbulent flow for a given surface and flow conditions, therefore resulting in severe spatial variation of the boundary conductance. Since surface roughness plays a role in determining the laminar or turbulent nature of the flow, this surface condition will likewise affect the boundary conductance.
High speed flow-aerodynamic heating . In the simple analysis just outlined, no account was taken of the dissipation of mechanical (kinetic) energy by the action of viscosity in the boundary layer. Although such neglect is permissible at low speeds, this dissipation becomes greatly important at high speeds and leads to the phenomenon of an unheated body in a high speed gas stream attaining temperatures substantially in excess of the free-stream temperature (aerodynamic heating). This process is clarified by the introduction of the concept of the stagnant or total temperature of a fluid steam with velocity v_0 and free-steam temperature T_0. The stagnant temperature T_{ST} of this gas stream is then defined as the temperature it would attain if it were brought to rest without addition of heat or external work. It then follows from the first law of thermodynamics that

$$T_{ST} - T_0 = v_0^2 \big/ (2c_P) \tag{6.70}$$

where c_P, the specific heat at constant pressure of the gas, is to be expressed in mechanical units. If a perfect thermally insulating plate is inserted in the gas stream with its surface parallel to the flow direction, the gas layer immediately on its surface is brought to rest. However, this completely arrested layer does not attain the temperature T_{ST} because of the heat conduction from it to adjacent layers which are still in motion. Rather, it is found that it and the insulator's surface acquire a temperature, T_{AD}, known as the adiabatic wall temperature, which is given by the equation:

$$T_{AD} - T_0 = \left(r\, v_0^2\right) \big/ (2\, c_P) \tag{6.71}$$

Where r is known as the recovery factor. For laminar flow parallel to a flat place, it has been shown analytically and verified experimentally that

$$r = \sqrt{\sigma} \tag{6.72}$$

If now a conducting plate is inserted in this gate stream in place of the insulating plate, it is clear that if its wall temperature T_w happens to be equal to T_{AD}, then no heat transfer into the fluid will occur; if $T_w > T_{AD}$ heat transfer from the plate into the gas stream will occur. It is therefore reasonable to replace T_0 in the convection boundary, equation (6.28) , by T_{AD} so that it becomes:

$$k \frac{\partial T}{\partial n} = h\left(T_{AD} - T\right) \tag{6.73}$$

Since, as seen from equation (6.71), $T_{AD} \approx T_0$ for low velocity flows, it is clear that this condition reduces to the previous case for sufficiently small velocity. Furthermore it is found that the value of the boundary conductance fro small velocities , equation (6.64), may be used in equation (6.73) for the analogous case with high velocities.

Natural convection: Since for this process the fluid motion is solely because of the heat transferred into it, it is reasonable to expect that the boundary conductance for natural convection depends more strongly upon the surface temperature. An analysis, similar to that just outlined, shows that this is the case. For a vertical flat plate at constant temperature T_w losing heat by natural convention to a fluid at temperature T_0, it is found (Eckert and Drake) that the boundary layer thickness (the same velocity and temperature) is

$$\delta = 3.93\left(\frac{\nu}{\kappa_f}\right)^{-1/2}\left(0.952+\frac{\nu}{\kappa_f}\right)^{1/4}\left[\frac{g\beta(T_w-T_0)}{\nu^2}\right]^{-1/4}x^{1/4} \tag{6.74}$$

Where g is the acceleration of gravity , β is the volumetric coefficient of expansion of the fluid , and x is the vertical distance along the plate measured from the bottom edge. Since the boundary conductance is found here to be

$$h = 2k_f/\delta \tag{6.75}$$

we see that h is proportional $(T_w-T_0)^{1/4}$ and leads, therefore, to a nonlinear convection boundary condition even if the temperature dependence of fluid properties is neglected. It may be linearized, however, if for a given problem the variation in T_w is not too great. Furthermore, since the boundary conductance for natural convection for such surfaces may be sometimes replaced by that corresponding to a perfectly insulated surface.

6.6. References

[1] Boley, B.A.,Weiner, J.H., *Theory of thermal stresses*, Dover publications, inc. Mineola, New York

[2] Ciarlet, Philiphe G., *Mathematical Elasticity, Volume I.: Three dimensional elasticity*, Elsevier Science Publishers B.V.

[3] Gurtin, M. E., *The Linear Theory of Elasticity, Handbbuch der Physik*, Springer, Berlin, 1972.

[4] Lekhnitskii, S. G., *Theory of Elasticity of an Anisotropic Body*, Mir, Moscow, 1981.

[5] Love, A. E. H., *A Treatise on the Mathematical Theory of Elasticity*, Dover Publications, Inc, New York, 1944

[6] Nunziante, L., Gambarotta, L., Tralli, A., *Scienza delle Costruzioni*, 3° Edizione, McGraw-Hill, 2011, ISBN: 9788838666971

[7] Ting TCT. *Anisotropic elasticity - Theory and applications*. Oxford University Press; 1996.

[8] Wolfram, S., *Mathematica, version 8*, Wolfram Research, Inc., Champaign, IL, 1998–2005.

CHAPTER VII
METHODS OF SOLUTION OF HEAT CONDUCTION PROBLEMS

7.0. Introduction

The problem of determination of the temperature distribution in a solid heated by various types of physical processes has been formulated mathematically in chapter 6, where the choice of the appropriate partial differential equation and initial and boundary conditions was discussed. The results of such a formulation is a typical partial differential equation boundary-value problem, some solutions of which were obtained in the preceding chapter. The literature on such boundary-value problems is quite extensive, and it is the purpose of this chapter to present a survey of the principal methods of solution which are applicable to wide classes problems. No effort will thus be made to present a complete development of all the available methods solution, or to describe the general theory of partial differential equations of the parabolic type, to which the heat equation belongs. Rather, we will endeavour to present a brief development of the fundamentals of each method , together with some remarks concerning its advantages, the types of problems for which it is most likely to be suitable , and some examples. The methods treated are those of separation of variables, Laplace transformation and conformal mapping.

7.1. Separation of variables (Method of characteristic functions)

7.1.1. Homogeneous differential equation and boundary conditions

It is convenient to consider first a special case, namely one for which a typical boundary problem fro a body occupying the bounded region $V+\partial V$ takes the form:

$$\kappa\nabla^2 T=\frac{\partial T}{\partial t}\quad \forall P\in V,\ \forall t>0 \tag{7.1}$$

$$M(P)\frac{\partial T}{\partial n}+N(P)T=0\qquad \forall P\in \partial V,\ \forall t>0 \tag{7.2}$$

$$T=F(P)\qquad \forall P\in V,\ t=0 \tag{7.3}$$

where $M(P)$ and $N(P)$ are prescribed non-negative functions independent of time. Clearly eq. (7.2) includes the case in which a portion ∂V_T of the surface is kept at zero temperature $(M=0,N\neq 0)$, a portion ∂V_H is perfectly insulated $(M\neq 0,N=0)$ and a portion ∂V_C is exposed to an ambient at zero through a boundary conductance $\left[M=k,N=h(P)\right]$, where $\partial V_T+\partial V_H+\partial V_C=\partial V$. Let $T_1(P,t)$ and $T_2(P,t)$ be two functions which satisfy the differential equation (7.1) and the boundary condition (7.2) but not necessarily the initial condition . Then , because of the linearly combination $a_1T_1+a_2T_2$ (a_1,a_2 are constants) will also satisfy them. Furthermore, if an infinite number of such functions $T_n(P,t)$ are available, then a suitably convergent infinite series:

$$\sum_{n=1}^{\infty}a_nT_n(P,t) \tag{7.4}$$

Will also satisfy these equations. In this case, the coefficients a_n may then be determined so that the initial condition is satisfied , namely, so that :

$$F(P)=\sum_{n=1}^{\infty}a_nT_n(P,0) \tag{7.5}$$

Thus completing the solution of the stated boundary-value problem.

The set of functions $T_n(P,t)$ may be found as follows: assume $T(P,t)$ of the following form:

$$T(P,t)=\varphi(P)\psi(t) \tag{7.6}$$

Substitution of this into the differential equation (7.1), then yields:

$$\frac{\nabla^2\varphi(P)}{\varphi(P)}=\frac{1}{\kappa\psi(t)}\frac{d\psi(t)}{dt}=\lambda=\text{constant} \tag{7.7}$$

Since the left-hand side of the preceding equation depends only upon position and the right-hand side only upon time, it follows that both must be equal to a common constant, say λ, which is sometimes referred to as the separation constant. Equation (7.7) therefore leads to the following two separate equations for $\varphi(P)$ and $\psi(t)$ respectively:

$$\nabla^2\varphi(P)-\lambda\varphi(P)=0 \quad \forall P\in V \tag{7.8}$$

$$\frac{d\psi(t)}{dt}-\kappa\lambda\psi(t)=0 \quad \forall t>0 \tag{7.9}$$

If the function $T(P,t)$ is to satisfy the boundary condition, then it is seen that $\varphi(P)$ must satisfy

$$M(P)\frac{\partial\varphi}{\partial n}+N(P)\varphi=0 \quad \forall P\in\partial V \tag{7.10}$$

The boundary-value problem for $\varphi(P)$, defined by (7.8) and (7.10) will have a nontrivial solution (that is, $\varphi\neq 0$) only for certain particular discrete values of λ, denoted here by λ_n, $n=1,2,....,n$ which are called the eigen-values or characteristic values of the boundary- value problem on φ. The solutions for φ corresponding to each λ_n are denoted by φ_n and are termed eigen-functions or characteristic functions . The solutions of equation (7.9) corresponding to λ_n will be denoted by ψ_n. It will next be shown that all the characteristic values are non-positive. For this purpose the following identity (readily derived from the divergence theorem) is employed:

$$\begin{gathered}\nabla\cdot[f\,\nabla g]=f\,\nabla\cdot(\nabla g)+(\nabla f)\cdot(\nabla g)=f\,\nabla^2 g+(\nabla f)\cdot(\nabla g)\\ \Downarrow\\ \int_V f\nabla^2 g\,dV=\int_{\partial V} f\frac{\partial g}{\partial n}dS-\int_V(\nabla f)\cdot(\nabla g)\,dV\end{gathered} \tag{7.11}$$

where ∇f indicates the gradient of f; in extended notation this identity is :

$$\int_V f\left[\frac{\partial^2 g}{\partial x^2}+\frac{\partial^2 g}{\partial y^2}+\frac{\partial^2 g}{\partial z^2}\right]dV=\int_{\partial V} f\frac{\partial g}{\partial n}dS-\int_V\left(\frac{\partial g}{\partial x}\frac{\partial f}{\partial x}+\frac{\partial g}{\partial y}\frac{\partial f}{\partial y}+\frac{\partial g}{\partial z}\frac{\partial f}{\partial z}\right)dV \tag{7.12}$$

Equation (7.11) applies for any functions $f(P)$ and $g(P)$ defined in $V+\partial V$ which satisfy the hypotheses of the divergence theorem. If now both $f(P)$ and $g(P)$ are set equal to $\varphi_n(P)$ namely, the characteristic function corresponding to λ_n and equations. (7.8) and (7.9) employed, it is found that :

$$\begin{cases}\nabla^2\varphi_n=\lambda_n\varphi_n & \forall P\in V\\ \dfrac{\partial\varphi_n}{\partial n}=-\dfrac{h}{k}\varphi_n & \forall P\in\partial V\end{cases} \quad\Rightarrow\quad \lambda_n=-\frac{\left[\dfrac{1}{k}\displaystyle\int_{\partial V_C} h\varphi_n^2 ds+\int_V(\nabla\varphi_n)\cdot(\nabla\varphi_n)\,dV\right]}{\displaystyle\int_V\varphi_n^2\,dV} \tag{7.13}$$

Since, by its physical nature, $h(P)>0$, it is seen that $\lambda_n\le 0$. The equality sign is possible only if ∂V_C is absent and if $\nabla\varphi\equiv 0$, that is, if φ is constant; however, if it is specified that $\varphi=0$ one some part of the boundary, then only the trivial solution $\varphi\equiv 0$ is possible. A nonzero constant solution and a zero characteristic value are possible , and exist, only if the problem is one involving a perfectly insulated body , that is if $\dfrac{\partial\varphi}{\partial n}=0$ over the entire surface B .

The characteristic values therefore may be written as:

$$\lambda_n = -\alpha_n^2, \quad n = 1, 2, ... \tag{7.14}$$

The corresponding solutions for $\psi_n(t)$ are then:

$$\psi_n(t) = e^{-\kappa\alpha_n^2 t}, \ n = 1, 2, ... \tag{7.15}$$

And therefore

$$T_n(P,t) = \varphi_n(P) e^{-\kappa\alpha_n^2 t} \tag{7.16}$$

The solution of the problem may then be written in the form:

$$T(P,t) = \sum_{n=1}^{\infty} a_n \varphi_n(P) e^{-\kappa\alpha_n^2 t} \tag{7.17}$$

There now remains to determine the coefficients a_n from the initial condition, namely,

$$F(P) = \sum_{n=1}^{\infty} a_n \varphi_n(P) \tag{7.18}$$

This calculation is greatly facilitated by the fact that the functions $\varphi_n(P)$ are orthogonal, that is,

$$\int_V \varphi_n \varphi_m dV = 0, \quad n \neq m \tag{7.19}$$

If now both sides of (7.18) are multiplied by $\varphi_m(P)$, and the resulting expressions integrated over V , because of property (7.19) the following explicit formula for the coefficient a_m is found :

$$a_m = \frac{1}{b_m} \int_D F(P) \varphi_m(P) dV \tag{7.20}$$

where

$$b_m = \int_D \varphi_m^2(P) dV \tag{7.21}$$

This completes the formal procedure for the solution of a problem in which both the differential equation and boundary condition are homogeneous.

7.1.2. Non-homogeneous differential equation or boundary conditions

In most practical problems either the boundary conditions or the differential equation is not homogeneous. However, when the non-homogeneous terms are functions of position only, the problem may be reduced to the previous case, as will now be shown. We consider here the class of problems leading to the following boundary-value problem.

$$\kappa\nabla^2 T + \frac{1}{\rho c} Q(P) = \frac{\partial T}{\partial t} \quad \forall P \in V, \ \forall t > 0 \tag{7.22}$$

$$M(P)\frac{\partial T}{\partial n} + N(P)T = G(P) \quad \forall P \in \partial V, \ \forall t > 0 \tag{7.23}$$

$$T = F(P) \qquad \forall P \in V, \ t = 0 \tag{7.24}$$

Because of the linearity of the problem, it is readily verified that the solution to this problem may be written in the form,

$$T(P,t) = T_S(P) + T_C(P,t) \tag{7.25}$$

where $T_S(P)$ satisfies the following equations :

$$\kappa\nabla^2 T_S + \frac{1}{\rho c} Q(P) = 0 \quad \forall P \in V, \ \forall t > 0 \tag{7.26}$$

$$M(P)\frac{\partial T_S}{\partial n} + N(P)T_S = G(P) \quad \forall P \in \partial V, \ \forall t > 0 \tag{7.27}$$

and $T_C(P,t)$ satisfies the following equations:

$$\kappa \nabla^2 T_C = \frac{\partial T_C}{\partial t} \quad \forall P \in V,\ \forall t > 0 \tag{7.28}$$

$$M(P)\frac{\partial T_C}{\partial n} + N(P)T_C = 0 \quad \forall P \in \partial V,\ \forall t > 0 \tag{7.29}$$

$$T_C = F(P) - T_S(P), \quad \forall P \in V,\ \forall t > 0 \tag{7.30}$$

The problem for $T_S(P)$ is therefore one of a steady-state temperature distribution; once this problem is solved, the problem for $T_C(P,t)$ is completely defined and is one with homogeneous differential equation and boundary condition, that is, the type treated in a)

A solution of the preceding form will not be possible in general if $B_H = B$, that is, if the heat input, is specified at every point of the body's boundary ; in fact, application of the divergence theorem to (7.26) yields the result:

$$k\int_B \frac{\partial T}{\partial n} dS = -\int_D Q(P)\, dV \tag{7.31}$$

Whereas the heat input specified by equation (7.27) (where , for this case, $M(P) \equiv k$, $N(P) \equiv 0$) might not satisfy this equation. In physical terms, if the total specified heat input is not supplied to the body at the rate at which heat is being absorbed within the body , a steady-state solution is not possible. In this case the above procedure requires only slight modification. A solution to the problem may then be written as :

$$T(P,t) = \beta t + T_S(P) + T_C(P,t) \tag{7.32}$$

where $T_C(P,t)$ satisfies eqs. (7.28)-(7.29)-(7.30) as before and where now $T_S(P)$ satisfies the following equations :

$$\kappa \nabla^2 T_S + \frac{1}{\rho c} Q(P) = \beta \quad \forall P \in V,\ \forall t > 0 \tag{7.33}$$

$$k\frac{\partial T_S}{\partial n} = G(P); \quad \forall P \in \partial V \tag{7.34}$$

It is readily verified that

$$\beta = \frac{1}{\rho c V}\left[\int_{\partial V} G(P)\, ds + \int_V Q(P)\, dV\right] \tag{7.35}$$

where V is the volume of the body. Equation (7.35) has an interesting physical interpretation . Since $T_C(P,t)$ is the solution of a problem of the type discussed in (a) , it is of the form (7.17) and, since $\alpha_1 = 0$ in this case , approaches a constant as $t \to \infty$. From eq. (7.32) it therefore follows that the temperature distribution for a problem of this approaches on in which the spatial distribution of temperature, $T_S(P)$, remains unchanged , but the temperature level increases at a constant rate β. This is known as a quasi – steady state of heat conduction.

7.1.3. Remarks and typical problems for the method of separation of variables

This method is conveniently applicable only when the thermal properties are constant; in addition , the solid should be bounded by coordinate surfaces of a convenient coordinate system: the most usual systems are Cartesian, cylindrical and spherical. The solid must be of finite extent in any direction in which temperature variation is present. When it is applicable, this is often the simplest method . The infinite series obtained for the solution converges very rapidly for long ties, but very slowly for short times. The long-time solution may, however, be sometimes converted into one suitable for short times by means of the Poisson summation formula .

Typical problems to which this method is applicable are the following: a slab (that is, a solid bounded by two parallel planes), initially at a uniform temperature, with the surface suddenly

elevated to a prescribed uniform temperature , with the cylindrical surfaces exposed to an ambient at elevated temperature through a boundary conductance, with its end faces at a prescribed temperature.

7.1.4. Example n.1

A slab is bounded by the planes x = 0 and x = L and is infinite in extent in the y and z directions. The surface x = 0 is kept perfectly insulated while the surface x = L is exposed, for t >0, to an ambient at zero temperature through a uniform boundary conductance h. The initial temperature of the slab is $T_R f(x)$ where T_R is a constant.

The problem is of the type just discussed; with the use of dimensionless variables defined in Chapter 6, the corresponding boundary problem is as follows:

$$\frac{\partial^2 T^*}{\partial x^{*2}} = \frac{\partial T^*}{\partial t^*}; \quad 0 < x^* < 1, \quad t^* > 0 \tag{7.36}$$

$$\frac{\partial T^*}{\partial x^*} = 0, \quad x^* = 0, \; t^* > 0, \tag{7.37}$$

$$\frac{\partial T^*}{\partial x^*} + mT^* = 0; \quad x^* = 1, \; t^* > 0, \tag{7.38}$$

$$T^* = f(x); \quad 0 < x^* < 1, \quad t^* = 0, \tag{7.39}$$

We may then define the following dimensionless quantities:

$$\begin{cases} T^* = \dfrac{T}{T_R}, \\ x^* = \dfrac{x}{L}, \; y^* = \dfrac{y}{L}, \; z^* = \dfrac{z}{L}, \; n^* = \dfrac{n}{L}, \\ t^* = \dfrac{\kappa}{L^2} t, \end{cases} \tag{7.40}$$

where T_R is a suitable chosen reference temperature.

The problem is therefore on with homogeneous differential equation and boundary conditions and may be treated by the method in section 7.1.1. Since only dimensionless quantities are involved in what follows, the asterisk is henceforth omitted. As in eq. (7.6), a particular solution of the differential equation and boundary conditions of the form:

$$T(x,t) = \varphi(x)\psi(t) \tag{7.41}$$

Is sought. This then leads as in (7.8) and (7.9), to the following equations for $\varphi(x)$:

$$\frac{d^2\varphi}{dx^2} + \alpha^2 \varphi = 0; \tag{7.42}$$

$$\frac{d\varphi}{dx} = 0; \quad x = 0, \tag{7.43}$$

$$\frac{d\varphi}{dx} + m\varphi = 0; \quad x = 1, \tag{7.44}$$

And to the following equation for $\psi(t)$:

$$\frac{d\psi}{dt} + \alpha^2 \psi = 0 \tag{7.45}$$

The general solution of (7.42) is:

$$\varphi(x) = A\sin(\alpha x) + B\cos(\alpha x) \tag{7.46}$$

From (7.43) it is deduced that A = 0. From (7.44) it is seen that if $B \neq 0$ (B= 0 leads to the trivial solution $\varphi \equiv 0$), then α must satisfy the following transcendental equation

$$\alpha \tan \alpha = m \tag{7.47}$$

The roots of this equation correspond to the points of intersection of the curves $y = \tan \alpha$ and the hyperbola $y = m / \alpha$; there is an infinite number such roots , denoted here by α_n, $n = 1, 2, ...$ leading to characteristic values $\lambda_n = -\alpha_n^2$. The corresponding characteristic functions $\varphi_n(x)$ are, as calculated above,

$$\varphi_n(x) = \cos(\alpha_n x) \tag{7.48}$$

The solution to the problem may therefore be written in the form:

$$T(x,t) = \sum_{n=1}^{\infty} a_n e^{-\alpha_n^2 t} \cos(\alpha_n x) \tag{7.49}$$

Where the coefficients a_n are determined by use if eqs. (7.20) and (7.21) specialized to this case. In other words,

$$a_n = \frac{1}{b_n} \int_0^1 f(x) \cos(\alpha_n x)\, dx \tag{7.50}$$

Where

$$b_n = \int_0^1 \cos^2(\alpha_n x)\, dx = \frac{1}{2\alpha_n} \left[\sin(\alpha_n x) \cos(\alpha_n x) + \alpha_n \right]; \quad \alpha_n \neq 0 \tag{7.51}$$

or

$$b_n = \frac{1}{2} \left[\frac{\sin^2 \alpha_n}{m} + 1 \right]; \quad \alpha_n \neq 0 \tag{7.52}$$

The latter form of b_n, which is more convenient for some purposes, has been obtained by use of (7.47). It is clear from eq. (7.47) that the first root $\alpha_1 = 0$ if and only if m = 0, that is , in keeping with the general result obtained previously, if the slab is perfectly insulated over all its bounding surfaces. In this special case, the succeeding roots are:

$$\alpha_n = (n-1)\pi, \quad n = 2, 3, ... \tag{7.53}$$

And

$$b_1 = 1; \quad b_n = \frac{1}{2} \quad for \quad n = 2, 3, ... \tag{7.54}$$

The zero characteristic value which occurs in this case (and all cases of a perfectly insulated body) has an interesting physical significance. Since all terms but the first of the infinite series (7.49) are multiplied by negative exponential in time, the temperature distribution ultimately becomes:

$$\lim_{t \to \infty} T(x,t) = a_1 = \int_0^1 f(x)\, dx \tag{7.55}$$

Namely the average initial temperature.

If , on the other hand, $m \to \infty$, it seen for eq. (7.47) that

$$\lim_{m \to \infty} \alpha_n = \frac{(2n-1)}{2} \pi, \quad n = 1, 2, ... \tag{7.56}$$

and

$$\lim_{m \to \infty} b_n = \frac{1}{2}, \quad n = 1, 2, ... \tag{7.57}$$

The form assumed by eq. (7.49) for these limiting values of α_n and b_n is identical to the solution to the stated problem with the face x = 1 maintained at zero temperature , as may be verified by direct solution of the latter problem. This is therefore a particular example, in which it was pointed out that the boundary condition of imposed surface temperature is the limiting case for increasing

boundary conductance. A heuristic estimate of the type of error incurred by using the imposed surface temperature condition in place of that corresponding to a large, but finite, value of m may be obtained with eq. (7.47) . For such values of m, the first few characteristic values will differ more fro their limiting values. Because the characteristic values appear (multiplied by t) in eq. (7.49) as negative exponents, it follows that at later times the terms with large characteristic values will contribute little to the temperature and an error in the will be of very little importance. However, at early times this error may be considerable and the imposed surface-temperature idealization may be inadequate.

An important case is that of uniform initial temperature T_0. Equation (7.49) then assumes the form:

$$T^*\left(x^*,t^*\right)=2m\sum_{n=1}^{\infty}\frac{\sin\left(\alpha_n\right)\cos\left(\alpha_n x^*\right)}{\alpha_n\left[\sin^2\left(\alpha_n\right)+m\right]}e^{-\alpha_n^2 t^*} \tag{7.58}$$

or , in dimensional terms,

$$T\left(x,t\right)=2mT_0\sum_{n=1}^{\infty}\frac{\sin\left(\alpha_n\right)\cos\left(\alpha_n x/L\right)}{\alpha_n\left[\sin^2\left(\alpha_n\right)+m\right]}e^{-\kappa\alpha_n^2 t/L^2} \tag{7.59}$$

If the initial temperature of the plate is zero, and the ambient temperature is T_0, then clearly the solution is:

$$T\left(x,t\right)=T_0\left\{1-2m\sum_{n=1}^{\infty}\frac{\sin\left(\alpha_n\right)\cos\left(\alpha_n x/L\right)}{\alpha_n\left[\sin^2\left(\alpha_n\right)+m\right]}e^{-\kappa\alpha_n^2 t/L^2}\right\} \tag{7.60}$$

Various charts have been prepared based on this equation and may be found in Carslaw and Jeager, and the textbook of McAdams and Jakob .

It should be noted that all of the foregoing discussion applies equally well to a slab bounded by the planes $x=\pm L$ if all conditions depend only upon x and are symmetrical about x = 0 for then, by symmetry, $\partial T/\partial x=0$ at x = 0, as had been originally stipulated.

7.1.5. Example n.2

A slab is bounded by the planes x = 0 and x = L and is infinite in extent in the y and z directions. The surface x = 0 is kept perfectly insulated while the surface x = L is exposed , for t >0, to a constant , uniform heat input q . The initial temperature of the slab is zero. With the use of the dimensionless quantities defined in chapter 6 and with $q_R=q$, the corresponding boundary-value problem is:

$$\frac{\partial^2 T^*}{\partial x^{*2}}=\frac{\partial T^*}{\partial t^*};\quad 0<x^*<1,\quad t^*>0 \tag{7.61}$$

$$\frac{\partial T^*}{\partial x^*}=0,\quad x^*=0,\ t^*>0, \tag{7.62}$$

$$\frac{\partial T^*}{\partial x^*}=1;\quad x^*=1,\ t^*>0, \tag{7.63}$$

$$T^*=0;\quad 0<x^*<1,\quad t^*=0, \tag{7.64}$$

The asterisks will again be omitted in what follows. This is an example of a problem involving a non-homogeneous boundary condition and, in particular, with the heat input specified over the entire boundary surface. It is necessary therefore to proceed as in section 7.1.2, writing the solution in the form (7.32), that is :

$$T\left(x,t\right)=\beta t+T_S\left(x\right)+T_C\left(x,t\right) \tag{7.65}$$

where T_S satisfies the equations:

$$\frac{d^2T_S}{dx^2}=\beta;\quad 0<x<1, \tag{7.66}$$

$$\frac{dT_S}{dx}=0;\quad x=0, \tag{7.67}$$

$$\frac{dT_S}{dx}=1;\quad x=1, \tag{7.68}$$

where β may be determined either from (7.35) or, more simplicity, from the boundary conditions (7.67)-(7.68) . T_C satisfies equations:

$$\frac{\partial^2T_C}{\partial x^2}=\frac{\partial T_C}{\partial t};\quad 0<x<1,\ \ t>0 \tag{7.69}$$

$$\frac{\partial T_C}{\partial x}=0;\quad x=0,\ \ t>0, \tag{7.70}$$

$$\frac{\partial T_C}{\partial x}=0;\quad x=1,\ \ t>0, \tag{7.71}$$

$$T_C=-T_S;\quad 0<x<1,\ \ t=0, \tag{7.72}$$

The solutions to eqs. (7.66) to (7.68) for β and T_S are:

$$\beta=1,\quad T_S=\frac{x^2}{2}, \tag{7.73}$$

The solution to the problem for T_C is found in much the same says way as was followed for example n.1. In fact, the discussion there for m = 0 (eqs. (7.53) and (7.54) applies directly here, so that the solution for the problem for T_C is :

$$T_C(x,t)=\sum_{n=1}^{\infty}a_n\left[\cos(n-1)\pi x\right]e^{-(n-1)^2\pi^2 t} \tag{7.74}$$

where

$$\begin{aligned} a_1&=\int_0^1-\left(\frac{x^2}{2}\right)dx=-\frac{1}{6}\\ a_n&=2\int_0^1-\left(\frac{x^2}{2}\right)\cos\left[(n-1)\pi x\right]dx=-\frac{2(-1)^{n-1}}{(n-1)^2\pi^2};\quad n=2,3,.... \end{aligned} \tag{7.75}$$

With a change of summation index, the solution may be rewritten as:

$$T^*(x^*,t^*)=t^*+\frac{3x^{*2}-1}{6}-\frac{2}{\pi^2}\sum_{n=2}^{\infty}\frac{(-1)^n}{n^2}\cos(n\pi x^*)e^{-n^2\pi^2t^*} \tag{7.76}$$

or , in dimensional terms,

$$T(x,t)=\frac{qL}{k}\left[\frac{\kappa t}{L^2}+\frac{3x^2-L^2}{6L^2}-\frac{2}{\pi^2}\sum_{n=2}^{\infty}\frac{(-1)^n}{n^2}\cos\left(\frac{n\pi x}{L}\right)e^{-\left(\frac{n^2\pi^2\kappa}{L^2}\right)t}\right] \tag{7.77}$$

7.2. Laplace transform

7.2.1. Description of method

Consider a transient heat conduction problems which corresponds to the boundary-value problem given by equations. (7.1) to (7.3). If both sides of the first two equations are multiplied by e^{-st}, s > 0 and all terms are integrated with respect to t from 0 to ∞, they appear as follows:

$$\kappa\int_0^\infty e^{-st}\nabla^2 T(P,t)\,dt=\int_0^\infty e^{-st}\frac{\partial T(P,t)}{\partial t}dt \quad \forall P\in V \tag{7.78}$$

$$M(P)\int_0^\infty e^{-st}\frac{\partial T(P,t)}{\partial n}dt+N(P)\int_0^\infty e^{-st}T(P,t)\,dt=0 \quad \forall P\in \partial V \tag{7.79}$$

It is assumed that the solution $T(P,t)$ of the original boundary-value problem is such that the above integrals converge for sufficiently large s. Because of the integration with respect to time, these integrals do not depend upon time but they do depend upon the value of the parameter s; the notation:

$$\bar{T}(P,s)=\int_0^\infty e^{-st}T(P,t)\,dt \tag{7.80}$$

is introduced and $\bar{T}(P,s)$ is referred to as the Laplace transform of $T(P,t)$ with respect to t. The next objective is to express the other integrals in equations (7.78) and (7.79) in terms of $\bar{T}(P,s)$ and its derivatives will respect to spatial variables. This is readily accomplished if it is further assumed that the function $T(P,t)$, is such as to make permissible the interchange of differentiation with respect to spatial variables and integration with respect to time in the above integrals and the use of integration by parts. Under these circumstances:

$$\int_0^\infty e^{-st}\nabla^2 T(P,t)\,dt=\nabla^2\int_0^\infty e^{-st}T(P,t)\,dt=\nabla^2\bar{T}(P,s) \tag{7.81}$$

$$\int_0^\infty e^{-st}\frac{\partial T(P,t)}{\partial n}dt=\frac{\partial}{\partial n}\int_0^\infty e^{-st}T(P,t)\,dt=\frac{\partial\bar{T}(P,s)}{\partial n} \tag{7.82}$$

$$\begin{aligned}\int_0^\infty e^{-st}\frac{\partial T(P,t)}{\partial t}dt&=\left[e^{-st}T(P,t)\right]_0^\infty+s\int_0^\infty e^{-st}T(P,t)\,dt=\\&=-T(P,0)+s\bar{T}(P,s)=s\bar{T}(P,s)-F(P)\end{aligned} \tag{7.83}$$

Where, in last equation, the initial conditions (7.3) of the original boundary-value problem has been employed. With the use of these results, it is seen that the transformed boundary-value problem for $\bar{T}(P,s)$ is as follows:

$$\kappa\nabla^2\bar{T}=s\bar{T}-F(P); \qquad \forall P\in V \tag{7.84}$$

$$M(P)\frac{\partial\bar{T}}{\partial n}+N(P)\bar{T}=0; \quad \forall P\in\partial V \tag{7.85}$$

The important advantage which has been secured by this transformation of the original problem is that no differentiation with respect to s appears in the transformed boundary-value problem and this quantity may therefore be regarded as a fixed, but arbitrary, parameter. The number of independent variables in the original boundary-value problem has thus been reduced by one, and the solution of the transformed boundary-value problem will consequently be simpler than that of the original one. In particular , if the problem involves only on spatial dimension, eq. (7.84) of the transformed boundary-value problem will be an ordinary differential equation.

The solution $\bar{T}(P,s)$ of the transformed problem having been obtained, it is next necessary to find the function $T(P,t)$ which corresponds to it, that is, it is necessary to solve the integral equation:

$$\bar{T}(P,s)=\int_0^\infty e^{-st}T(P,t)\,dt \tag{7.86}$$

where $\bar{T}(P,s)$ is the known function and $T(P,t)$ the unknown function. $T(P,t)$ is called the inverse transform of $\bar{T}(P,s)$. Extensive table of inverse transforms are available and the use of

these tables greatly facilitates the solution of problems by the Laplace transform technique. If a particular function, $\overline{T}(P,s)$, cannot be found in the tables, it is necessary to resort to the evaluation of a general solution to the integral equation , the most useful of which is stated in terms of a complex integral as follows:

$$T(P,t)=\frac{1}{2\pi i}\lim_{\beta\to\infty}\int_{\gamma-i\beta}^{\gamma+i\beta}e^{zt}\overline{T}(P,z)\,dt \tag{7.87}$$

where $\overline{T}(P,z)$ is the function obtained by extending $\overline{T}(P,s)$ into the complex plane (by replacing the real variable s by the complex variable $z=x+i\,y$); the integration is carried out over the line $x=y$ where γ is taken sufficiently large so that all the singularities of $\overline{T}(P,z)$ lie to the left of the line of integration. Equation (7.87), which applies to a class of functions sufficiently broad to include all those to be encountered in practice, is referred to as the complex inversion formula for the Laplace transform. The evaluation of the complex integral is usually accomplished by the use of the residue theorem of functions of a complex variable. This description has been framed to give a general picture of the nature of the Laplace transform technique. In actual computations, it is not necessary to multiply explicitly all equations by e^{-st}, to integrate and carry through each time the operations of eqs. (7.81) to (7.83) may be employed immediately as the operational properties of the Laplace transform.

The follows operational property is known as the convolution (or Faltung) theorem:

$$\overline{T}_1(P,s)\overline{T}_2(P,s)=\int_0^t T_1(P,\tau)T_2(P,t-\tau)\,d\tau \tag{7.88}$$

By definition, the Laplace transform of the convolution integral:

$$\int_0^t T_1(P,\tau)T_2(P,t-\tau)\,d\tau=\int_0^\infty e^{-st}\left[\int_0^t T_1(P,t)T_2(P,t-\tau)\,d\tau\right]dt \tag{7.89}$$

Under broad conditions , we may interchange the order of integration to obtain,

$$\int_0^\infty e^{-st}\left[\int_0^t T_1(P,t)T_2(P,t-\tau)\,d\tau\right]dt=\int_0^\infty T_1(P,\tau)\int_\tau^\infty e^{-st}T_2(P,t-\tau)\,dt\,d\tau \tag{7.90}$$

Where the change in limits is readily understood by consideration of the iterated integral as a double integral in the (τ,t) plane. With $r=t-\tau$ as a new variable of integration in the inner integral, we find:

$$\begin{aligned}&\int_0^\infty T_1(P,\tau)\int_\tau^\infty e^{-st}T_2(P,t-\tau)\,dt\,d\tau=\int_0^\infty T_1(P,\tau)\int_0^\infty e^{-s(r+\tau)}T_2(P,r)\,dr\,d\tau=\\&=\int_0^\infty e^{-s\tau}T_1(P,\tau)\,d\tau\int_0^\infty e^{-sr}T_2(P,r)\,dr=\overline{T}_1(P,s)\overline{T}_2(P,s)\end{aligned} \tag{7.91}$$

As required.

7.2.2. Remarks on the method

The Laplace transform procedure is applicable to any heat conduction problem which leads to a linear boundary-value problem as long as the coefficients of the unknown temperature function are at most space-dependent. The non-homogeneous terms may be both space and time dependent.

Advantages: In many cases, some even with rather complex boundary conditions, the solution by this method is obtained by a routine (through possibly lengthy) procedure. For some geometries involving bodies of infinite extent, the solution is obtained in closed forming terms of tabulated functions. When the solution is in series form, both long and short time expressions can be found, thus insuring good convergence at all times.

Disadvantages: The inversion of the transformed solution is sometimes quite difficult; at times it can only be performed so as to leave the answer in terms of definite integrals which must be evaluated numerically.

7.2.3. Example n.3

A slab initially at zero temperature is bounded by the planes x = 0 and x = L and is infinite in extent in the y and z directions. The surface x = L is kept perfectly insulated while the surface x = 0 is maintained, for t > 0, at temperature T_0.

This problem is a special case of example n.1 (with a shift in the temperature scale and in the x coordinate). With the use of the dimensionless parameters and with $T_R = T_0$, the corresponding boundary-value problem may be written as follows:

$$\frac{\partial^2 T^*}{\partial x^{*2}} = \frac{\partial T^*}{\partial t}; \quad 0 < x^* < 1, \quad t^* > 0, \tag{7.92}$$

$$T^* = 1, \quad x^* = 0, \quad t^* > 0, \tag{7.93}$$

$$\frac{\partial T^*}{\partial x^*} = 0; \quad x^* = 1, \quad t^* > 0, \tag{7.94}$$

$$T^* = 0; \quad 0 < x^* < 1, \quad t^* = 0, \tag{7.95}$$

The asterisks are again omitted in subsequent calculations.

By use of the table of operational properties the transformed boundary-value problem for $\bar{T}(x,s)$ may be written down immediately as follows:

$$\frac{d^2 \bar{T}}{d x^2} = s\bar{T}; \quad 0 < x < 1 \tag{7.96}$$

$$\bar{T} = \frac{1}{s}; \quad x = 0 \tag{7.97}$$

$$\frac{d \bar{T}}{d x} = 0; \quad x = 1, \tag{7.98}$$

Where eq. (7.97) follows from (7.95) by a simple calculation from the definition of the Laplace transform, that is,

$$\int_0^\infty e^{-st} ds = \frac{1}{s} \tag{7.99}$$

And where (since s may be regarded as a parameter) the derivatives with respect to x are written as ordinary rather than partial derivatives.

$$\bar{T}(x,s) = \frac{\cosh\left[\sqrt{s}(x-1)\right]}{s \cosh\left(\sqrt{s}\right)} \tag{7.100}$$

The inverse transform may be found by use of the complex inversion formula (7.87), with the integral evaluated by use of the residue theorem . This procedure gives the solution in the same form as the separation of variables , namely equation (7.49). The characteristic values of that procedure, $-\alpha_n^2$, appear here as the zeroes of the denominator of the right-hand side of (7.100), which give rise to simple poles with residues.

As noted previously, the solution in the form (7.49) is a long-time solution in that the infinite series converges rapidly only for large values of time. If this is all that is desired, the separation of variables technique is probably simpler in application. On the other hand, it is possible, as will now be shown, to rewrite equation (7.100) in a form that leads to a short-time solution. To do this, the hyperbolic functions are expressed in terms of exponentials, and the function $\bar{T}(x,s)$ is then expanded in a power series in negative exponentials as follows:

$$\bar{T}(x,s)=\frac{e^{\sqrt{s}x(1-x)}+e^{-\sqrt{s}(1-x)}}{s\left(e^{\sqrt{s}x}+e^{-\sqrt{s}}\right)}=\frac{1}{s}\left[\frac{e^{-\sqrt{s}x}+e^{\sqrt{s}(x-2)}}{1+e^{-2\sqrt{s}}}\right]= \tag{7.101}$$

$$=\frac{1}{s}\left[e^{-\sqrt{s}x}+e^{\sqrt{s}(x-2)}\right]\sum_{n=0}^{\infty}(-1)^n e^{-2n\sqrt{s}}=\frac{1}{s}\sum_{n=0}^{\infty}(-1)^n e^{-\sqrt{s}(2n+x)}+\frac{1}{s}\sum_{n=0}^{\infty}(-1)^n e^{-\sqrt{s}\left[2(n+1)-x\right]}$$

Each term of the series is of the same form and may found in tables of inverse Laplace transforms (for example, Carslaw and Jaeger) . The results is, in dimensionless form,

$$T^*\left(x^*,t^*\right)=\sum_{n=0}^{\infty}(-1)^n erfc\left(\frac{2n+x^*}{2\sqrt{t^*}}\right)+\sum_{n=0}^{\infty}(-1)^n erfc\left(\frac{2(n+1)-x^*}{2\sqrt{t^*}}\right) \tag{7.102}$$

or, in dimensional terms,

$$T(x,t)=T_0\left[\sum_{n=0}^{\infty}(-1)^n erfc\left(\frac{2nL+x}{2\sqrt{\kappa t}}\right)+\sum_{n=0}^{\infty}(-1)^n erfc\left(\frac{2(n+1)L-x}{2\sqrt{\kappa t}}\right)\right] \tag{7.103}$$

where the error function complement $efrc(x)$ is defined as reported below:

$$efrc(x)=1-efr(x)=\frac{2}{\sqrt{\pi}}\int_x^{\infty}e^{-\xi^2}d\xi \tag{7.104}$$

Since this function decays rapidly with increasing argument, the series in eqs. (7.102) converge very rapidly for small t^*; for very small values of time only the first term of the first series is significant , that is,

$$T(x,t)\cong T_0\,erfc\left(\frac{x}{2\sqrt{\kappa t}}\right)\quad for\ \ t^*<<1 \tag{7.105}$$

This illustrates the intuitively clear fact that for short times a finite slab behaves like a semi-infinite solid, a fact which gives the latter idealization practical importance.

7.3. Conformal mapping

7.3.1. Description of method

The method of conformal mapping is applicable only for the solution of two-dimensional, steady-state problems with constant thermal conductivity. Solutions obtained by this method fro wedgs, angles, etc. may be found in Carslaw and Jearger; for problems of this type, the method of conformal mapping is frequently the most powerful.

Consider the problem of the determination of the steady two-dimensional temperature distribution in a cylinder whose cross section occupies the simply connected region $V_z+\partial V_z$ with boundary ∂V_z, caused by specified temperature distribution on ∂V_z (figure 7.1) . If the thermal conductivity is constant, the temperature distribution $T(x,y)$ must then satisfy the boundary-value problem,

$$\nabla^2 T=\frac{\partial^2 T}{\partial x^2}+\frac{\partial^2 T}{\partial y^2}=0\quad\forall(x,y)\in V_z \tag{7.106}$$

$$T=G(x,y)\quad\forall(x,y)\in\partial V_z \tag{7.107}$$

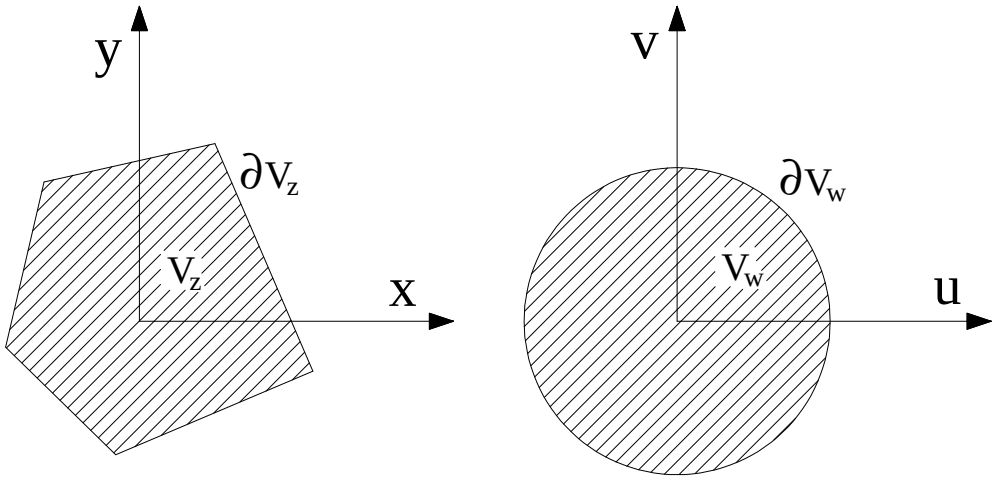

Figure 7.1 – *Example for conformal mapping technique*

The difficulty with this boundary-value problem lies not in the nature of the differential equation nor in the form of the boundary conditions but in the shape of the boundary upon which conditions are imposed. It is therefore desirable to make a change in the independents variables:

$$\begin{cases} u = u(x,y) \\ v = v(x,y) \end{cases} \tag{7.108}$$

with the inverse functions denoted by:

$$\begin{cases} x = x(u,v) \\ y = y(u,v) \end{cases} \tag{7.109}$$

In such a manner as to map the region $V_z + \partial V_z$ into one (say $V_w + \partial V_w$) in the u,v plane with a simpler boundary (figure 7.1) without increasing the complexity of the differential equation or the form of the boundary conditions. The technique of conformal mapping provides a means for accomplishing this.

Let z and w be complex variables defined as:

$$\begin{cases} z = x + i\,y \\ w = u + i\,v \end{cases} \tag{7.110}$$

So that we may speak of the x,y plane as the z plane and of the u,v as the w plane. Assume that a function:

$$w = w(z) \tag{7.111}$$

Can be found which is analytic and univalent (single-valued with a single-valuated inverse) in V_z which maps V_z onto the simpler region V_w in the w plane. If $w = w(z)$, then the point z in the z-plane is said to be mapped, thought w(z), onto w in the plane w. V_w is then the set of all values of w corresponding to all z in V_z. The mapping produced by an analytic function $w = w(z)$ may be shown to be conformal, that is it preserves both magnitude and sense of angles at any point at which $w'(z) \neq 0$. The requirement $w'(z) \neq 0$ in V_z may be shown to be necessary to the univalence of w(z) in V_z. We use here and in what follows the notation $T(x,y) = T\left[x(u,v), y(u,v)\right] = T(u,v)$ so that $T(x,y)$ and $T(u,v)$ do not represent the same mathematical functions of their arguments but are equal at corresponding values of (x,y) and (u,v).

The this function and its inverse $z = z(w)$ define functions $u = u(x, y)$, etc. as in eqs. (7.108) which represent the desired change in independent variable, since $T(u,v)$ (as will be seen) satisfies the following boundary-value problem in the w-plane:

$$\nabla^2 T = \frac{\partial^2 T}{\partial u^2} + \frac{\partial^2 T}{\partial v^2} = 0 \quad \forall (u,v) \in V_w \tag{7.112}$$

$$T = G(u,v) \quad \forall (u,v) \in \partial V_w \tag{7.113}$$

The point $P_w = P_w(u,v)$ corresponds to $P_z = P_z(x,y)$, that is, we simply require the temperature to be the same at corresponding points of ∂V_z and ∂V_w.

These statements rest on some important results of the theory of functions of a complex variable; the reasoning is outlined as follows:

1) $T(x,y)$ is a harmonic function in V_z by definition since it satisfies eq. (7.106) and will require it to be in class $C^{(2)}$ there.

2) There exists a function $S(x,y)$ such that

$$H(z) = T(x,y) + i\,S(x,y) \tag{7.114}$$

is a single-valuated analytic function in V_z.

3) If $w = w(z)$ is analytic and univalent in V_z, then its inverse function $z = z(w)$ is analytic and univalent V_w.

4) Therefore ,

$$\begin{aligned} H(z) = H\left[z(w)\right] &= T\left[x(u,v), y(u,v)\right] + i\,S\left[x(u,v), y(u,v)\right] = \\ &= T(u,v) + i\,S(u,v) \end{aligned} \tag{7.115}$$

Is analytic and single-valuated in V_w since an analytic function of an analytic function is also analytic .

5) Since the real and imaginary parts of an analytic function are harmonic, $T(u,v)$ is harmonic and single-valued in V_w, that is, it satisfies eq. (7.112). The satisfaction of boundary conditions (7.113) follows simply from the definition of $T(u,v)$.

The conformal mapping procedure for the solution of boundary-value problems of this type is then as follows:

(I) Find a univalent , analytic function $w = w(z)$ which maps the original boundary ∂V_z into a simpler boundary ∂V_w.

(II) Transform the boundary conditions on $T(x,y)$ into boundary conditions $T(u,v)$

(III) Solve problem for $T(u,v)$ in the w-plane.

(IV) Convert $T(u,v)$ to $T(x,y)$ by use of eqs. (7.108) corresponding to the mapping function $w = w(z)$

Step (I) is frequently the most difficult and usually requires an intimate knowledge of functions of a complex variables. Tables of mapping function exist and are of considerable assistance. Also, methods have been developed for constructing a function which maps a region $V_z' + \partial V_z'$ onto a simpler one, where $V_z' + \partial V_z'$ is a close approximation to the given region $V_z + \partial V_z$.

Step (II) presents no difficulty, as has been seen, for the case of imposed surface temperature. If it required that a portion of V_z be perfectly insulated $\left(\frac{\partial T(x,y)}{\partial n_z}=0\right)$ then it is simply necessary to impose the condition $\frac{\partial T(u,v)}{\partial n_w}=0$ on the corresponding portion of ∂V_w, where n_z and n_w are the normals to ∂V_z and ∂V_w, respectively. The treatment of other boundary conditions by the conformal mapping technique is also possible. Step (III) becomes routine for the case of imposed surface temperature over all of ∂V_z if the original region is mapped onto a region (for example, the unit circle or the half-plane) for which the general solution is known in a simple form. We now give an outline showing the development of this general solution for the case in which V_w is the upper half-plane since this development leads to some useful intermediate formulas. Consider first the determination of $T(u,v)$ in V_w corresponding to the boundary conditions shown in figure 7.2. The solution is :

$$T(u,v)=\arctan\left(\frac{v}{u}\right);\qquad 0\le\arctan\left(\frac{v}{u}\right)\le\pi \tag{7.116}$$

Clearly the function $T(u,v)$ so defined satisfies the boundary conditions and is bounded (as required by physical considerations and for uniqueness). Also, $T(u,v)$ is harmonic in V_w since it is the imaginary part of a function analytic in V_w, namely ,

$$T(u,v)=\mathrm{Im}\left[\log(u+iv)\right],\quad -\frac{\pi}{2}\le\arctan\left(\frac{v}{u}\right)\le-\frac{3\pi}{2} \tag{7.117}$$

This solution is now generalized to other boundary conditions as follows:

$$T(u,v)=T_1\left[1-\frac{1}{\pi}\arctan\left(\frac{v}{u}\right)\right],\quad 0\le\arctan\left(\frac{v}{u}\right)\le\pi \tag{7.118}$$

$$T(u,v)=T_1\left[1-\frac{1}{\pi}\arctan\left(\frac{v}{u-\xi_1}\right)\right],\quad 0\le\arctan\left(\frac{v}{u-\xi_1}\right)\le\pi \tag{7.119}$$

By the superposition of two solutions of the form of eq. (7.119), we obtain the solution to the next case as follows:

$$\begin{aligned}T(u,v)&=T_1\left[1-\frac{1}{\pi}\arctan\left(\frac{v}{u-\xi_1}\right)\right]-T_1\left[1-\frac{1}{\pi}\arctan\left(\frac{v}{u-\xi_2}\right)\right]=\\&=\frac{T_1}{\pi}\left[\arctan\left(\frac{v}{u-\xi_2}\right)-\arctan\left(\frac{v}{u-\xi_1}\right)\right]=\frac{T_1}{\pi}\arctan\left(\frac{u-\xi_2}{u-\xi_1}\right)\end{aligned} \tag{7.120}$$

$$0\le\arctan\left(\frac{v}{u-\xi_1}\right)\le\pi,\quad 0\le\arctan\left(\frac{v}{u-\xi_2}\right)\le\pi$$

$$T(u,v)=\frac{1}{\pi}\sum_{j=1}^{n}T_j\arctan\left(\frac{u-\xi_{j+1}}{u-\xi_j}\right);\quad 0\le\arctan\left(\frac{v}{u-\xi_j}\right)\le\pi \tag{7.121}$$

It is now possible to consider the limiting form assumed by eq. (7.121) as $n\to\infty$. The result is :

$$T(u,v)=\frac{1}{\pi}\int_{\alpha}^{\beta}\frac{f(\xi)v\,d\xi}{(u-\xi)^2+v^2} \tag{7.122}$$

For a temperature distribution corresponding to $T(u,0)=f(u)$, $\alpha \le u \le \beta$ and zero on the remainder of the boundary. For suitably bounded $f(u)$, α and β may become infinite, yielding the following general result, namely Poisson's integral formula for the half-plane:

$$T(u,v)=\frac{1}{\pi}\int_{-\infty}^{+\infty}\frac{f(\xi)v\,d\xi}{(u-\xi)^2+v^2} \tag{7.123}$$

The last step, that is, step (IV), is quite difficult if the mapping function has been determined in the form $z=z(w)$ (as is the case for example , if the Schwarz-Christoffel theorem for the mapping of polygons is used) and if this function is not readily inverted.

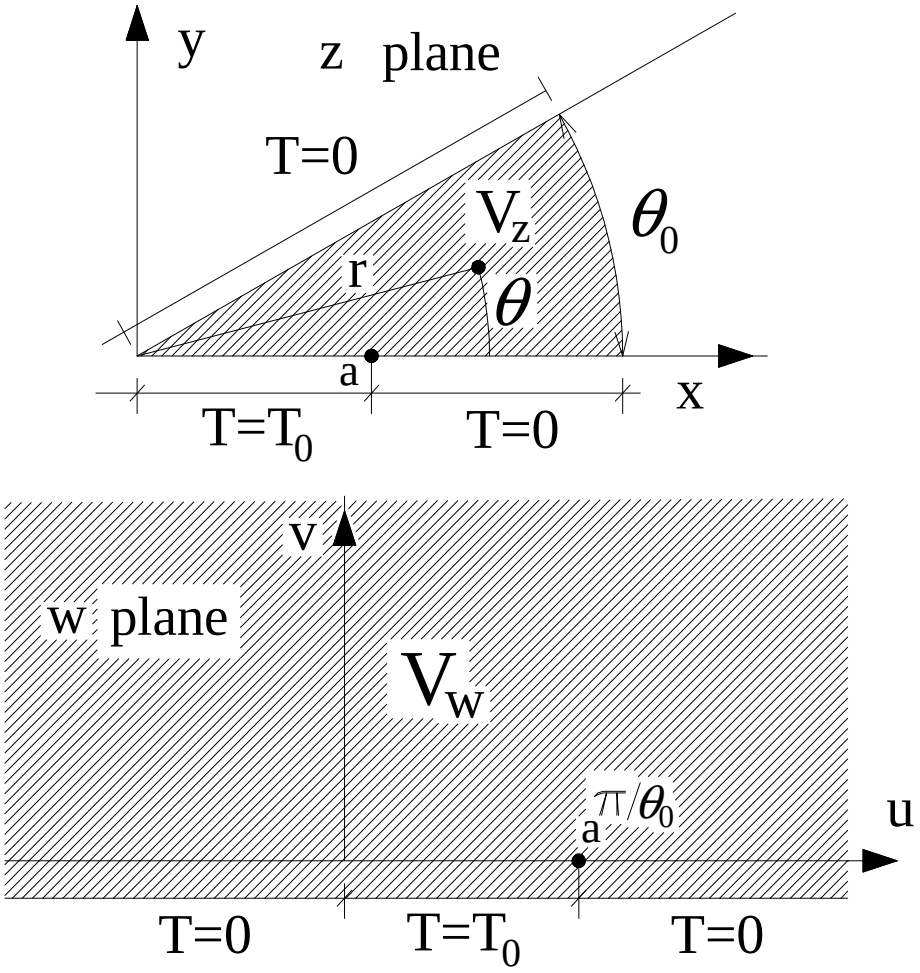

Fig. 7.2 - *Example for conformal mapping technique*

7.3.2. Example n. 4

It is required to find the steady-state temperature in the wedge of figure n.2 , subject to the boundary conditions shown.

The function:

$$w=z^c,\quad 0<\arctan\left(\frac{y}{x}\right)<\theta_0, \tag{7.124}$$

where

$$c=\frac{\pi}{\theta_0} \tag{7.125}$$

Clearly maps the region V_z onto the upper half of the w plane. The transformed boundary condition are as shown in figure n.2. The solution of the transformed problem is obtained directly from eq. (7.120) as:

$$\begin{aligned} T(u,v) &= \frac{T_1}{\pi}\arg\left(\frac{w-a^c}{w}\right) = \frac{T_1}{\pi}\arg\left(\frac{u^2+v^2-a^c u+i\,a^c v}{u^2+v^2}\right) = \\ T(u,v) &= \frac{T_1}{\pi}\arctan\left(\frac{a^c v}{u^2+v^2-a^c u}\right) \end{aligned} \tag{7.126}$$

Where the value of the arctan between 0 and π is used. The function $T(u,v)$ may be converted to $T(x,y)$ or, more conveniently, to $T(r,\theta)$ by the substitutions

$$\begin{cases} u = r^c\cos(c\,\theta_0) \\ v = r^c\sin(c\,\theta_0) \end{cases} \tag{7.127}$$

Which yield the result:

$$T(r,\theta) = \frac{T_1}{\pi}\arctan\left[\frac{a^c\sin(c\,\theta_0)}{r^c - a^c\cos(c\,\theta_0)}\right] \tag{7.128}$$

7.4 References

[1] Boley, B.A.,Weiner, J.H., *Theory of thermal stresses*, Dover publications, inc. Mineola, New York

[2] Ciarlet, Philiphe G., *Mathematical Elasticity, Volume I.: Three dimensional elasticity*, Elsevier Science Publishers B.V.

[3] Gurtin, M. E., *The Linear Theory of Elasticity, Handbbuch der Physik*, Springer, Berlin, 1972.

[4] Lekhnitskii, S. G., *Theory of Elasticity of an Anisotropic Body*, Mir, Moscow, 1981.

[5] Love, A. E. H., *A Treatise on the Mathematical Theory of Elasticity*, Dover Publications, Inc, New York, 1944

[6] Nunziante, L., Gambarotta, L., Tralli, A., *Scienza delle Costruzioni*, 3° Edizione, McGraw-Hill, 2011, ISBN: 9788838666971

[7] Ting TCT. *Anisotropic elasticity - Theory and applications*. Oxford University Press; 1996.

[8] Wolfram, S., *Mathematica, version 8*, Wolfram Research, Inc., Champaign, IL, 1998–2005.

CHAPTER VIII
SUMMARY OF THE FORMULATION OF THERMOELASTIC PROBLEMS FOR ISOTROPIC MATERIAL

8.0. Introduction

The problem considered in this chapter consists of the determination of elastic stresses and deformations in solid bodies under prescribed temperature distributions. The basic mathematical description of the behaviour of solids under the action of heat and external loads has been established in chapters I to IV. The principal results of that formulation are repeated in this chapter for purposes of reference, occasionally supplemented by discussion of their basis on physical and intuitive grounds. The reader may thus omit the earlier more precise developments and still obtain a working knowledge of the concepts involved.

The formulation employed here rest on four principal assumption:

1) *The temperature can be determined independently of the deformations of the body ;*
2) *The deformations are small;*
3) *The material behaves elastically at all times*;
4) *Stress-strain relationships related to linear isothermal and homogeneous material*;

The first of these assumptions requires the omission of mechanical coupling terms in the heat conduction equations. The second implies that the displacements are sufficiently small so that no distinction is needed between the coordinates of a particle before and after deformation and that the displacement gradients are sufficiently small so that their products may be neglected. The most common problems in which this assumption does not hold are those of buckling; Finally the third assumption implies that neither the temperature changes nor the stresses are too large; Many of the concepts and equations required for the formulation which follow are identical with those of the isothermal theory of elasticity; for these, only a brief outline will be given, the reader being referred to the one of the treatises on elasticity for more through analyses.

8.1. Thermo-elastic stress-strain relations

Broadly speaking, thermal stress may arise in a heated body either because of a non-uniform temperature distribution, or external constraints, or a combination of these causes. Since the effect of external constraints is readily understood, we confine our attention to that of non-uniform temperature. Imagine a body as made up of a number of small cubical elements of equal size which fit together to form the given continuous body. If the temperature of the body is raised uniformly, and if its bounding surfaces are unrestrained , then each element will expand an equal amount (proportional to the temperature rise) uniformly in all directions. The elements are thus still equal-sized cubes; they still fit together to form a continuous body, and no stresses arise. If, however, the temperature rise is not uniform , each element will tend to expand by a different amount, that is one proportional to its own temperature rise. The resulting different-sized cubes cannot , in general , fit together ; since, however, the body must remain continuous, each element must restrain the distortions of its neighbors, or, in other words, stresses must arise. The total strains at each point of a heated body are thus made up of two parts. The first part is a uniform expansion proportional to the temperature rise $T-T_R$, where T_R is the reference temperature. Since this expansion is the same in all directions for an isotropic body, only normal strains and no shearing strains arise in this manner. If the coefficient of linear thermal expansion is denoted by α, this normal strain in any direction is equal to $\alpha(T-T_R)$. The second part comprises the strains required to maintain the continuity of the body as well as those arising because of external load. These strain are related to the stresses by means of the usual Hooke's law of linear isothermal elasticity . The total strains are the sum of the components and are therefore related as follows to the stresses and temperature in any orthogonal coordinate system x,y,z:

$$\begin{aligned}
&\varepsilon_{xx}=\frac{1}{E}\Big[\sigma_{xx}-\nu\left(\sigma_{yy}+\sigma_{zz}\right)\Big]+\alpha\left(T-T_R\right),\ \ \varepsilon_{yy}=\frac{1}{E}\Big[\sigma_{yy}-\nu\left(\sigma_{xx}+\sigma_{zz}\right)\Big]+\alpha\left(T-T_R\right)\\
&\varepsilon_{zz}=\frac{1}{E}\Big[\sigma_{zz}-\nu\left(\sigma_{xx}+\sigma_{yy}\right)\Big]+\alpha\left(T-T_R\right),\ \gamma_{yz}=\frac{1}{G}\tau_{yz},\quad \gamma_{xz}=\frac{1}{G}\tau_{xz},\quad \gamma_{xy}=\frac{1}{G}\tau_{xy},
\end{aligned}\tag{8.1}$$

The shear modulus G is related to Young's modulus E and Poisson's ratio ν by the equation:

$$G=\frac{E}{2\left(1+\nu\right)}\tag{8.2}$$

The relation between the dilatation e and the sum of the normal stresses *I* is obtained from (8.1) as :

$$\varepsilon_V=\left(1/3\right)\left(I/E_V\right)+3\alpha\left(T-T_R\right)\tag{8.3}$$

where the bulk modulus k is

$$E_V=\frac{E}{3\left(1-2\nu\right)}\tag{8.4}$$

and where:

$$\varepsilon_V=\varepsilon_{xx}+\varepsilon_{yy}+\varepsilon_{zz},\qquad I=\sigma_{xx}+\sigma_{yy}+\sigma_{zz}\tag{8.5}$$

It is sometimes to express the stresses explicitly in terms of the strains; the relations in question are:

$$\begin{aligned}
\sigma_{xx}&=\lambda e+2\mu\varepsilon_{xx}-\left(3\lambda+2\mu\right)\alpha\left(T-T_R\right)\\
\sigma_{yy}&=\lambda e+2\mu\varepsilon_{yy}-\left(3\lambda+2\mu\right)\alpha\left(T-T_R\right)\\
\sigma_{zz}&=\lambda e+2\mu\varepsilon_{zz}-\left(3\lambda+2\mu\right)\alpha\left(T-T_R\right)\\
\tau_{yz}&=G\gamma_{yz};\quad \tau_{xy}=G\gamma_{xz};\quad \tau_{xz}=G\gamma_{xy};
\end{aligned}\tag{8.6}$$

The Lamè elastic constants λ and μ are related to E and ν as follows:

$$\lambda=\frac{\nu E}{\left(1+\nu\right)\left(1-2\nu\right)};\quad \mu=\frac{E}{2\left(1+\nu\right)}=G\tag{8.7}$$

Note that the following relations hold:

$$E_V=\frac{2}{3}\mu+\lambda;\quad E=\mu\left(\frac{3\lambda+2\mu}{\mu+\lambda}\right);\quad \nu=\frac{\lambda}{2\left(\mu+\lambda\right)};\tag{8.8}$$

The stress-strain relations supply the mathematical description of the material under consideration; it is now necessary to enforce the requirements of mechanics and of geometry: The laws of mechanics are introduced by the equations of equilibrium (or of motion); geometrical consistency is stipulated through the strain-displacements relations.

8.2. Equations of equilibrium

The equations of equilibrium are the same as those of isothermal elasticity since they are based on purely mechanical considerations. In rectangular Cartesian coordinate x, y and z these equations take the form:

$$\nabla\cdot\mathbf{T}+\mathbf{b}=\mathbf{0};\quad or\quad \begin{cases}
\dfrac{\partial\sigma_{xx}}{\partial x}+\dfrac{\partial\tau_{xy}}{\partial y}+\dfrac{\partial\tau_{xz}}{\partial z}+X=0\\
\dfrac{\partial\tau_{xy}}{\partial x}+\dfrac{\partial\sigma_{yy}}{\partial y}+\dfrac{\partial\tau_{yz}}{\partial z}+Y=0\\
\dfrac{\partial\tau_{xz}}{\partial x}+\dfrac{\partial\tau_{yz}}{\partial y}+\dfrac{\partial\sigma_{zz}}{\partial z}+Z=0
\end{cases}\tag{8.9}$$

where $\mathbf{b}=\left\{X,Y,Z\right\}$ is the vector of the body forces. It will usually be possible to omit the body forces; occasionally, however, the effect of inertia will have to be considered, in which case the body forces are equal to the negative of the inertia forces. For small displacements one may then write:

$$X = -\rho \frac{\partial^2 u}{\partial t^2}; \quad Y = -\rho \frac{\partial^2 v}{\partial t^2}; \quad Z = -\rho \frac{\partial^2 w}{\partial t^2}; \tag{8.10}$$

where ρ is the mass density, u,v and w are the components of the displacement vector in the x,y and z directions respectively, and t is time. These equations of equilibrium have been derived in Chapter II. An alternative derivation is obtained by considering the equilibrium of an infinitesimal parallelepiped such as the shown in figure 8.1. The equilibrium of all the forces acting, for example, in the x direction, readily gives the first equations. (8.9).

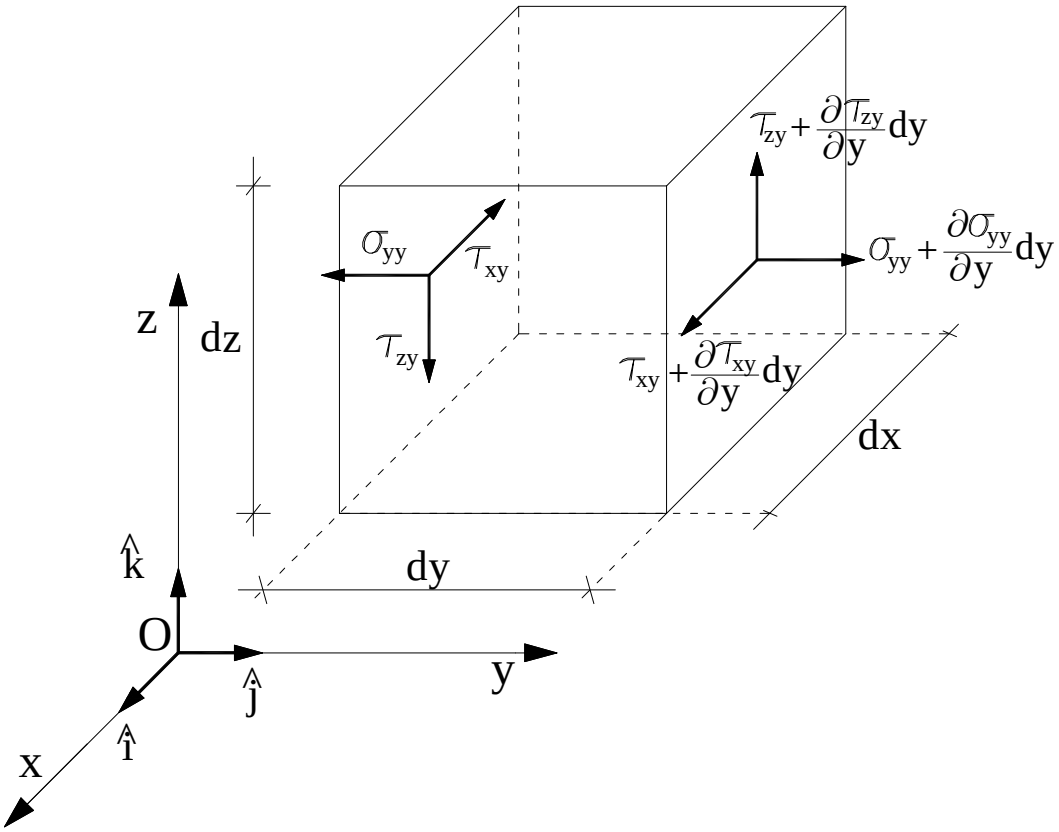

Fig. 8.1 – *Equilibrium of infinitesimal volume dxdydz*

The complementary components of the shear stress are equal, that is,

$$\tau_{xy} = \tau_{yx}; \quad \tau_{xz} = \tau_{zx}; \quad \tau_{yz} = \tau_{zy}; \tag{8.11}$$

Because of the requirement of moment equilibrium for any element such as that of figure n. 8.1. When eqs. (8.9) and (8.11) are satisfied at all points of the body, the required conditions of equilibrium of the body as a whole are automatically fulfilled, with the resultant of the surface tractions balancing the resultant of the body forces (if any). In cylindrical coordinate r, θ, z, the equilibrium equations (8.9) are (see appendix) :

$$\begin{cases} \dfrac{\partial \sigma_{rr}}{\partial r} + \dfrac{1}{r}\dfrac{\partial \tau_{r\theta}}{\partial \theta} + \dfrac{\partial \tau_{rz}}{\partial z} + \dfrac{\sigma_{rr} - \sigma_{\theta\theta}}{r} + R = 0 \\ \dfrac{\partial \tau_{\theta r}}{\partial r} + \dfrac{1}{r}\dfrac{\partial \sigma_{\theta\theta}}{\partial \theta} + \dfrac{\partial \tau_{\theta z}}{\partial z} + \dfrac{2\tau_{r\theta}}{r} + \Theta = 0 \\ \dfrac{\partial \tau_{rz}}{\partial r} + \dfrac{1}{r}\dfrac{\partial \tau_{\theta z}}{\partial \theta} + \dfrac{\partial \sigma_{zz}}{\partial x_z} + \dfrac{\tau_{rz}}{r} + Z = 0 \end{cases} \tag{8.12}$$

where the body force in the r, θ, z directions are denoted by R, Θ, Z. In spherical coordinate r, θ, ϕ (see appendix) the equilibrium equations take the form:

$$\begin{cases} \dfrac{\partial \sigma_{rr}}{\partial r}+\dfrac{1}{r}\dfrac{\partial \tau_{r\theta}}{\partial \theta}+\dfrac{1}{r\sin\theta}\dfrac{\partial \tau_{r\phi}}{\partial \phi}+\dfrac{2\sigma_{rr}-\sigma_{\theta\theta}-\sigma_{\phi\phi}}{r}+\dfrac{\tau_{r\theta}}{r\tan\theta}+R=0 \\ \dfrac{\partial \tau_{r\theta}}{\partial r}+\dfrac{1}{r}\dfrac{\partial \sigma_{\theta\theta}}{\partial \theta}+\dfrac{1}{r\sin\theta}\dfrac{\partial \tau_{\theta\phi}}{\partial \phi}+\dfrac{3\tau_{r\theta}}{r}+\dfrac{\sigma_{\theta\theta}-\sigma_{\phi\phi}}{r\tan\theta}+\Theta=0 \\ \dfrac{\partial \tau_{r\phi}}{\partial r}+\dfrac{1}{r}\dfrac{\partial \tau_{\theta\phi}}{\partial \theta}+\dfrac{1}{r\sin\theta}\dfrac{\partial \sigma_{\phi\phi}}{\partial \phi}+\dfrac{3\tau_{r\phi}}{r}+\dfrac{2\tau_{\theta\phi}}{r\tan\theta}+\Phi=0 \end{cases} \tag{8.13}$$

where the body-force components in the r,θ,ϕ directions are denoted by R,Θ,Φ.

8.3. Strain-Displacement relations

The strains are related to the displacements in the same manner as in isothermal elasticity since purely geometrical considerations are involved; in a rectangular Cartesian coordinate system the pertinent equations are as follows:

$$\begin{aligned} &\varepsilon_{xx}=\frac{\partial u}{\partial x};\ \varepsilon_{yy}=\frac{\partial v}{\partial y};\ \ \varepsilon_{zz}=\frac{\partial w}{\partial z};\ \ \varepsilon_{xy}=\frac{1}{2}\gamma_{xy}=\frac{1}{2}\left(\frac{\partial u}{\partial y}+\frac{\partial v}{\partial x}\right); \\ &\varepsilon_{yz}=\frac{1}{2}\gamma_{yz}=\frac{1}{2}\left(\frac{\partial v}{\partial z}+\frac{\partial w}{\partial y}\right);\ \ \varepsilon_{xz}=\frac{1}{2}\gamma_{xz}=\frac{1}{2}\left(\frac{\partial w}{\partial x}+\frac{\partial u}{\partial z}\right); \end{aligned} \tag{8.14}$$

where u, v and w are the components of the displacements vector in the x, y and z directions respectively.

In cylindrical coordinate (see appendix) these relations take the form:

$$\begin{aligned} &\varepsilon_{rr}=\frac{\partial u_r}{\partial r},\ \ \varepsilon_{\theta\theta}=\left(\frac{u_r}{r}+\frac{1}{r}\frac{\partial u_\theta}{\partial \theta}\right),\ \ \varepsilon_{zz}=\frac{\partial u_z}{\partial z}, \\ &\varepsilon_{r\theta}=\frac{1}{2}\left(\frac{1}{r}\frac{\partial u_r}{\partial \theta}-\frac{u_\theta}{r}+\frac{\partial u_\theta}{\partial r}\right),\ \ \varepsilon_{rz}=\frac{1}{2}\left(\frac{\partial u_r}{\partial z}+\frac{\partial u_z}{\partial r}\right),\ \ \varepsilon_{\theta z}=\frac{1}{2}\left(\frac{\partial u_\theta}{\partial z}+\frac{1}{r}\frac{\partial u_z}{\partial \theta}\right), \end{aligned} \tag{8.15}$$

where u_r,u_θ,u_z represent here the components of the displacement vector in r,θ,z directions respectively. In spherical coordinates (see appendix) these relations take the form:

$$\begin{aligned} &\varepsilon_{rr}=\frac{\partial u_r}{\partial r},\ \ \varepsilon_{\theta\theta}=\left(\frac{u_r}{r}+\frac{1}{r}\frac{\partial u_\theta}{\partial \theta}\right),\ \ \varepsilon_{\phi\phi}=\frac{u_r}{r}+\frac{u_\theta}{r\tan\theta}+\frac{1}{r\sin\theta}\frac{\partial u_\phi}{\partial \phi},\ \ \varepsilon_{r\theta}=\frac{1}{2}\left(\frac{1}{r}\frac{\partial u_r}{\partial \theta}-\frac{u_\theta}{r}+\frac{\partial u_\theta}{\partial r}\right), \\ &\varepsilon_{r\phi}=\frac{1}{2}\left(\frac{1}{r\sin\theta}\frac{\partial u_r}{\partial \phi}+\frac{\partial u_\phi}{\partial r}-\frac{u_\phi}{r}\right),\ \ \varepsilon_{\theta\phi}=\frac{1}{2}\left(\frac{1}{r}\frac{\partial u_\phi}{\partial \theta}+\frac{1}{r\sin\theta}\frac{\partial u_\theta}{\partial \phi}-\frac{u_\phi}{r\tan\theta}\right), \end{aligned} \tag{8.16}$$

where u_r,u_θ,u_ϕ represent here the components of the displacement vector in r,θ,ϕ directions respectively.

8.4. Boundary Conditions

In most problems, the boundary conditions which can be considered in connection with thermo-elastic problems, it will be possible to restrict to one of the following two special cases:

a) *Traction boundary conditions*;
b) *Displacement boundary conditions*;

In the first case, the boundary conditions for this case are expressed in terms of the stress components through the following equations, to be satisfied at every point P of the boundary surface ∂V of the solid with volume V:

$$\begin{cases} \sigma_{xx}n_x+\tau_{xy}n_y+\tau_{xz}n_z=t_x \\ \tau_{xy}n_x+\sigma_{yy}n_y+\tau_{yz}n_z=t_y \\ \tau_{xz}n_x+\tau_{yz}n_y+\sigma_{zz}n_z=t_z \end{cases} \quad \forall P\in\partial V \tag{8.17}$$

where t_x, t_y, t_z are the components of the prescribed surface traction in the x,y,z directions respectively , and n_x, n_y, n_z are the direction cosines of the outward-drawn surface normal. These formulas also give the tractions across any interior surface.
In the second case, the boundary conditions for this case are expressed through the following equations to be satisfied at every point P of the bounding surface:

$$\begin{cases} u = f(P) \\ v = g(P) \\ w = h(P) \end{cases} \qquad \forall P \in \partial V \tag{8.18}$$

where f, g, and h are prescribed functions.
Occasionally, more complicated boundary conditions may be encountered; for example, the boundary condition of equation (8.17) may be specified over a portion of the bounding surface and that of equations (8.18) over the remainder of the surface. Thus at each point either three traction components or three displacement components are prescribed; these are known as "mixed" boundary conditions. As another example, we may specify at each point of the bounding surface three quantities, some of which are traction components and the remainder displacement components. These must be chosen, however, so that not more than one quantity is associated with a particular coordinate direction; it is thus permissible to prescribe, say , t_x, t_y and w at a particular point, but not t_x, t_y and v.
Another possibility is represented by the condition of elastic support, in which a functional relation exists between some of the displacement and some of the traction components, as in the case of two bodies in contact. The difficulties arising in such problems are not peculiar to thermo-elasticity but are found in isothermal elasticity as well.

8.5. Mathematical formulation of the problem of thermo-elasticity

The problem of thermo-elasticity consists in the determination of the following "*fifteen functions*" (here in rectangular Cartesian coordinates), the temperature distribution being assumed known:

6 stress components: $\sigma_{xx}, \sigma_{yy}, \sigma_{zz}, \tau_{xy}, \tau_{yz}, \tau_{zx}$,

6 strain components: $\varepsilon_{xx}, \varepsilon_{yy}, \varepsilon_{zz}, \varepsilon_{xy}, \varepsilon_{yz}, \varepsilon_{zx}$,

3 displacement components: u, v, w

So as to satisfy the following " *fifteen equations*" throughout the body :

3 equilibrium equations: equations (8.9)
6 stress-strain relations: equations (8.1)
6 strain-displacement : equations (8.14)

And the boundary conditions reported in section 8.4.
It is possible to prove that when the problem is thus formulated, and appropriate continuity restriction are placed on the functions, the solution is unique, that is, there exist at most one set of twelve stress and strain components, and one set of three displacement components (except possibly for rigid-body motions), which satisfies the above equations and boundary conditions. This formulation holds both for simply and multiply connected bodies. The rigid-body motions are of the form:

$$\begin{cases} u = u^0 - \omega_z^0 y + \omega_y^0 z \\ v = v^0 - \omega_x^0 z + \omega_z^0 x \\ w = w^0 - \omega_y^0 x + \omega_x^0 y \end{cases} \tag{8.19}$$

where the constants u^0, v^0, w^0 represent rigid-body translations and the constants $\omega_x^0, \omega_y^0, \omega_z^0$, represent infinitesimal rigid-body rotations about the axes indicates in the subscript. In vector form the rigid-body motions are given by:

$$\mathbf{u} = \mathbf{u}^0 + \boldsymbol{\omega}^0 \wedge \mathbf{P} = \mathbf{u}^0 + \det \begin{bmatrix} \hat{\mathbf{i}} & \hat{\mathbf{j}} & \hat{\mathbf{k}} \\ \omega_x^0 & \omega_y^0 & \omega_z^0 \\ x & y & z \end{bmatrix} \tag{8.20}$$

The last statement follows by the substitution of the displacement of eqs. (8.19) in the general formulas for the infinitesimal rotation vector components, namely:

$$\omega_x^0 = \frac{1}{2}\left(\frac{\partial w}{\partial y} - \frac{\partial v}{\partial z}\right); \quad \omega_y^0 = \frac{1}{2}\left(\frac{\partial u}{\partial z} - \frac{\partial w}{\partial x}\right); \quad \omega_z^0 = \frac{1}{2}\left(\frac{\partial v}{\partial x} - \frac{\partial u}{\partial y}\right); \tag{8.21}$$

The infinitesimal rotation vector is given by the curl of the displacement vector:

$$\nabla \wedge \mathbf{u} = \det \begin{bmatrix} \hat{\mathbf{i}} & \hat{\mathbf{j}} & \hat{\mathbf{k}} \\ \partial/\partial x & \partial/\partial y & \partial/\partial z \\ u & v & w \end{bmatrix} = 2\left(\omega_x^0 \hat{\mathbf{i}} + \omega_y^0 \hat{\mathbf{j}} + \omega_z^0 \hat{\mathbf{k}}\right) \tag{8.22}$$

8.6. Principal stresses and strains

The solution of the boundary-value outlined in the previous article gives the stress, strain, and displacement components in a particular coordinate system (rectangular Cartesian). From this information, one may refer the stresses, strains, and displacements at any one point of the body to any other coordinate system by means of well-known transformation formulas. The transformations related to displacements are accomplished directly by the laws of vector transformation and present no difficulty; those pertaining to stresses and strains are a little more complicated. Of particular interest is the calculation of the maximum principal stress at any point, and a few formulas that may be useful in this connection follow.

In any stress system, three mutually perpendicular planes (called principal), on which no shear stresses act, exist at each point. The normal stresses on these planes are called principal; one of them is the maximum stress and another is the minimum stress (considered algebraically, that is, either the least positive or the greatest negative stress) at that point. Let n_x, n_y, n_z be the direction cosines of the normal to a principal plane in a rectangular coordinate system x,y,z and let λ be the corresponding principal stress; These quantities can be found from simultaneous solution of the following four equations :

$$\begin{cases} (\sigma_{xx} - \lambda) n_x + \tau_{xy} n_y + \tau_{xz} n_z = 0 \\ \tau_{xy} n_x + (\sigma_{yy} - \lambda) n_y + \tau_{yz} n_z = 0 \\ \tau_{xz} n_x + \tau_{yz} n_y + (\sigma_{zz} - \lambda) n_z = 0 \end{cases} \tag{8.23}$$

$$n_x^2 + n_y^2 + n_z^2 = 1 \tag{8.24}$$

Equation (8.23) lead to a nontrivial solution for the direction cosines only if the determinant of the coefficients is zero; the principal stresses are then the three roots (always real) of the cubic

$$\lambda^3 - I\,\lambda^2 + II\,\lambda - III = 0 \tag{8.25}$$

where the three invariant coefficients are :

$$\begin{cases} I = \sigma_{xx} + \sigma_{yy} + \sigma_{zz} \\ II = \sigma_{xx}\sigma_{yy} + \sigma_{xx}\sigma_{zz} + \sigma_{yy}\sigma_{zz} - \tau_{xy}^2 - \tau_{xz}^2 - \tau_{yz}^2 \\ III = \det \mathbf{T} \end{cases} \tag{8.26}$$

The corresponding formulas for strains are very similar to these just shown. They may in fact be obtained directly from them by substituting in equations (8.23) and (8.26) the quantities $\varepsilon_{xx}, \varepsilon_{yy}, \varepsilon_{zz}, \varepsilon_{yz}, \varepsilon_{xz}, \varepsilon_{xy}$ for the quantities $\sigma_{xx}, \sigma_{yy}, \sigma_{zz}, \tau_{yz}, \tau_{xz}, \tau_{xy}$ respectively .

In two-dimensional stress systems, the analogous results are easily obtained from these formula, since then eq. (8.25) reduces to :

$$\lambda^2 - \left(\sigma_{xx} + \sigma_{yy}\right)\lambda + \left(\sigma_{xx}\sigma_{yy} - \tau_{xy}^2\right) = 0 \tag{8.27}$$

The two principal stresses in the plane may then be written explicitly as:

$$\lambda = \frac{\sigma_{xx} + \sigma_{yy}}{2} \pm \sqrt{\left(\frac{\sigma_{xx} - \sigma_{yy}}{2}\right)^2 + \tau_{xy}^2} \tag{8.28}$$

The principal directions make an angle φ with the x-axis which is given by:

$$\tan\varphi = \frac{n_y}{n_x} = \frac{\tau_{xy}}{\sigma_{xx} - \lambda} \tag{8.29}$$

with the aid of the identity

$$\tan 2\varphi = \frac{2\tan\varphi}{1 - \tan^2\varphi} \tag{8.30}$$

The formulas for the stress components in directions x_1, y_1 , where the x_1 axis makes and angle α with the x axis, are:

$$\begin{cases} \sigma_{x_1x_1} = \sigma_{xx}\cos^2\alpha + \sigma_{yy}\sin^2\alpha + 2\tau_{xy}\sin\alpha\cos\alpha \\ \sigma_{y_1y_1} = \sigma_{xx}\sin^2\alpha + \sigma_{yy}\cos^2\alpha - 2\tau_{xy}\sin\alpha\cos\alpha \\ \sigma_{x_1y_1} = \left(\sigma_{yy} - \sigma_{xx}\right)\sin\alpha\cos\alpha + \tau_{xy}\left(\cos^2\alpha - \sin^2\alpha\right) \end{cases} \tag{8.31}$$

For future reference, note at this point the analogy between the variation, under rotation of coordinates, of the moments of inertia of an area and of the stress components in a two-dimensional system. If the moments of inertia about the x and y axes are dented by I_x and I_y, and the product of inertia about these axes by I_{xy}, the principal moments of inertia by I , and angle of the principal directions with x axis by φ, then the following formulas :

$$I = \frac{I_x + I_y}{2} \pm \sqrt{\left(\frac{I_x - I_y}{2}\right)^2 + I_{xy}^2} \tag{8.32}$$

$$\tan 2\varphi = \frac{2I_{xy}}{I_y - I_x} \tag{8.33}$$

$$\begin{cases} I_{x_1} = I_x\cos^2\alpha + I_y\sin^2\alpha + 2I_{xy}\sin\alpha\cos\alpha \\ I_{y_1} = I_x\sin^2\alpha + I_y\cos^2\alpha - 2I_{xy}\sin\alpha\cos\alpha \\ I_{x_1y_1} = \left(I_y - I_x\right)\sin\alpha\cos\alpha + I_{xy}\left(\cos^2\alpha - \sin^2\alpha\right) \end{cases} \tag{8.34}$$

The quantity

$$I_P = I_x + I_y = I_{x_1} + I_{y_1} \tag{8.35}$$

Is called the polar moment of inertia.

The reader will recognize that eqs. (8.31)-(8.34) are the formulas for the transformation of the components of a symmetric second rank tensor under rotation of a rectangular Cartesian coordinate system. Note that equations (8.34) are written in the engineering notation for moments of inertia rather than in terms of the tensor components I_x, I_y, I_{xy} of the moment of inertia; the relation between the two notations is:

$$I_{xx} = I_x; \quad I_{yy} = I_y; \quad I_{xy} = I_{xy}; \tag{8.36}$$

8.7. Separation of stresses due to temperature and to external loads

The formulation in section 8.5 accounts both for the effect of external loads and for that of non-uniform temperature distributions, and is therefore more general than often need be considered. *All the equations and boundary conditions to be satisfied are, however, linear*; it follows that it is possible to divide the problem in two separate parts and thus to calculate the stresses as the sum of (1) those due to temperature alone and (2) those due to the external loads in the absence of temperature.

(1)_ The stresses, strains and displacements due to temperature alone are obtained by the solution of equilibrium equations (8.9), stress-strain relations (8.1), and strain-displacement relations (8.14) as in the previous section but subject to the boundary conditions :

$$\begin{cases} \sigma_{xx} n_x + \tau_{xy} n_y + \tau_{xz} n_z = 0 \\ \tau_{xy} n_x + \sigma_{yy} n_y + \tau_{yz} n_z = 0 \quad \forall P \in \partial V \\ \tau_{xz} n_x + \tau_{yz} n_y + \sigma_{zz} n_z = 0 \end{cases} \tag{8.37}$$

In place of those previously stated. A body free of external tractions, for which then eqs. (8.37) hold, will be referred to as a free body.

(2)_The solution corresponding to the external loads in the absence of temperature must satisfy equilibrium equations (8.9), stress-strain relations (8.1), and strain-displacement relations (8.14), with T set equal to zero in Hooke's law. The boundary conditions depend on whether tractions, displacements, or a combination of these quantities is prescribed at the surface . If tractions are specified throughout, the appropriate boundary conditions are those of equations (8.17).

If displacements are prescribed at every point of the surface, the boundary conditions are:

$$\begin{cases} u = f(P) - u_a(P) \\ v = g(P) - v_a(P) \quad \forall P \in \partial V \\ w = h(P) - w_a(P) \end{cases} \tag{8.38}$$

In place of equation (8.18). The function $u_a(P), v_a(P), w_a(P)$ are the displacements of the boundary point P as calculated in part (1). It readily verified by direct substitution in the equations and boundary conditions listed in previous section that the sum of solutions (1) and (2) satisfies all the requirements of that formulation ; since the uniqueness theorem insures that only one solution exists, this is the desired solution of the problem.

8.8. Alternative formulation of the problem of thermo-elasticity

The formulation in section 8.5 is complete and perhaps the most natural one from a physical viewpoint. However, the equations to be solved involve fifteen dependent variables, whereas the boundary conditions usually contain either only the three displacement components or only the six stress components. Therefore it is usually convenient to simplify the formulation by expressing the boundary value problem only in terms of those variables which appear in the particular boundary conditions under consideration. In this section , this procedure is carried out in a purely formal manner and the governing equations listed; for most practical applications, this treatment will surface. A more rigorous treatment of this equation requires the utilization of the uniqueness theorem, and a discussion of the alternative formulations.

a) Displacement formulation

The equilibrium equation (8.9) may be expressed in terms of strains by means of the stress-strain relations; the strain in turn can be written in terms of displacements. The final result of these substitutions is the following equilibrium equations in terms of displacements (for rectangular Cartesian coordinates) is given by Duhamel -Neumann thermal equations :

$$\begin{cases} (\mu+\lambda)\dfrac{\partial}{\partial x}\nabla\cdot\mathbf{u}+\mu\nabla^2 u-(3\lambda+2\mu)\alpha\dfrac{\partial T}{\partial x}+X=0 \\ (\mu+\lambda)\dfrac{\partial}{\partial y}\nabla\cdot\mathbf{u}+\mu\nabla^2 v-(3\lambda+2\mu)\alpha\dfrac{\partial T}{\partial y}+Y=0 \\ (\mu+\lambda)\dfrac{\partial}{\partial z}\nabla\cdot\mathbf{u}+\mu\nabla^2 w-(3\lambda+2\mu)\alpha\dfrac{\partial T}{\partial z}+Z=0 \end{cases} \tag{8.39}$$

In vector form, we can write:

$$(\mu+\lambda)\nabla(\nabla\cdot\mathbf{u})+\mu\nabla\cdot(\nabla\otimes\mathbf{u})-(3\lambda+2\mu)\alpha\nabla T+\mathbf{b}=\mathbf{0} \tag{8.40}$$

These equations, when solved with the displacement boundary conditions (8.18), yield the functions u, v, and w fro all points in the body. The stress-strain relation and strain-displacement relation may be used in that order to determine the strains and stresses, respectively, by direct substation. The stated formulation of thermo-elasticity problems in terms of displacements holds, just as the one of section 8.5 , for both simply and multiply connected bodies.

Equations (8.39) assume the following form when written in terms of the components of rotation defined in (8.21):

$$\begin{cases} (2\mu+\lambda)\dfrac{\partial}{\partial x}\nabla\cdot\mathbf{u}-2\mu\left(\dfrac{\partial\omega_z^0}{\partial y}-\dfrac{\partial\omega_y^0}{\partial z}\right)-(3\lambda+2\mu)\alpha\dfrac{\partial T}{\partial x}+X=0 \\ (2\mu+\lambda)\dfrac{\partial}{\partial y}\nabla\cdot\mathbf{u}-2\mu\left(\dfrac{\partial\omega_x^0}{\partial z}-\dfrac{\partial\omega_z^0}{\partial x}\right)-(3\lambda+2\mu)\alpha\dfrac{\partial T}{\partial y}+Y=0 \\ (2\mu+\lambda)\dfrac{\partial}{\partial z}\nabla\cdot\mathbf{u}-2\mu\left(\dfrac{\partial\omega_y^0}{\partial x}-\dfrac{\partial\omega_x^0}{\partial y}\right)-(3\lambda+2\mu)\alpha\dfrac{\partial T}{\partial z}+Z=0 \end{cases} \tag{8.41}$$

In vector form, we can write:

$$(2\mu+\lambda)\nabla(\nabla\cdot\mathbf{u})-\mu\nabla\wedge(\nabla\wedge\mathbf{u})-(3\lambda+2\mu)\alpha\nabla T+\mathbf{b}=\mathbf{0} \tag{8.42}$$

The application to the above equation of the operators div and curl respectively leads to the following results:

$$\begin{cases} (2\mu+\lambda)\nabla^2(\nabla\cdot\mathbf{u})-(3\lambda+2\mu)\alpha\nabla^2 T+\nabla\cdot\mathbf{b}=0 \\ -\mu\nabla\wedge\left[\nabla\wedge(\nabla\wedge\mathbf{u})\right]+\nabla\wedge\mathbf{b}=\mathbf{0} \end{cases} \tag{8.43}$$

By remembering the relation:

$$\nabla^2\mathbf{u}=\nabla(\nabla\cdot\mathbf{u})-\nabla\wedge(\nabla\wedge\mathbf{u}) \tag{8.44}$$

We can rewriting the equations (8.43) as follows:

$$\begin{cases} (2\mu+\lambda)\nabla\cdot\left(\nabla^2\mathbf{u}\right)=(3\lambda+2\mu)\alpha\nabla^2 T-\nabla\cdot\mathbf{b} \\ \mu\nabla\wedge\left(\nabla^2\mathbf{u}\right)=-\nabla\wedge\mathbf{b} \end{cases} \tag{8.45}$$

In the stationary thermal-elasticity problem, if the body force field is such that div **b** and curl **b** both vanish, then both div **u** and curl **u** are harmonic fields:

$$\nabla\cdot\left(\nabla^2\mathbf{u}\right)=0;\qquad \nabla\wedge\left(\nabla^2\mathbf{u}\right)=\mathbf{0} \tag{8.46}$$

Hence, by equation (8.44) , $\nabla^2\mathbf{u}$ is a vector field that is harmonic; that is,

$$\nabla^2\left(\nabla^2\mathbf{u}\right)=0 \tag{8.47}$$

Thus, if the body force field **b** is divergence-free and curl-free, then the displacement field is bi-harmonic.

The equilibrium equations may be expressed in a similar way in other coordinate system. In cylindrical coordinate they are:

$$\begin{cases} (2\mu+\lambda)\dfrac{\partial e}{\partial r}-2\mu\left(\dfrac{1}{r}\dfrac{\partial \omega_z^0}{\partial \theta}-\dfrac{\partial \omega_\theta^0}{\partial z}\right)-(3\lambda+2\mu)\alpha\dfrac{\partial T}{\partial r}+R=0 \\ (2\mu+\lambda)\dfrac{1}{r}\dfrac{\partial e}{\partial \theta}-2\mu\left(\dfrac{\partial \omega_r^0}{\partial z}-\dfrac{\partial \omega_z^0}{\partial r}\right)-(3\lambda+2\mu)\dfrac{\alpha}{r}\dfrac{\partial T}{\partial \theta}+\Theta=0 \\ (2\mu+\lambda)\dfrac{\partial e}{\partial z}-\dfrac{2\mu}{r}\left(\dfrac{\partial\left(r\omega_\theta^0\right)}{\partial r}-\dfrac{\partial \omega_r^0}{\partial \theta}\right)-(3\lambda+2\mu)\alpha\dfrac{\partial T}{\partial z}+Z=0 \end{cases} \tag{8.48}$$

where the dilatation e and the components of rotation, in this coordinate system, are:

$$\begin{aligned} &e=\frac{\partial u_r}{\partial r}+\frac{u_r}{r}+\frac{1}{r}\frac{\partial u_\theta}{\partial \theta}+\frac{\partial u_z}{\partial z}; \\ &\omega_r^0=\frac{1}{2}\left(\frac{1}{r}\frac{\partial u_z}{\partial \theta}-\frac{\partial u_\theta}{\partial z}\right);\ \ \omega_\theta^0=\frac{1}{2}\left(\frac{1}{r}\frac{\partial u_z}{\partial \theta}-\frac{\partial u_\theta}{\partial z}\right);\ \ \omega_z^0=\frac{1}{2}\left(\frac{1}{r}\frac{\partial u_z}{\partial \theta}-\frac{\partial u_\theta}{\partial z}\right); \end{aligned} \tag{8.49}$$

In spherical coordinate the corresponding equations are:

$$\begin{cases} (2\mu+\lambda)\dfrac{\partial e}{\partial r}-\dfrac{2\mu}{r\sin\theta}\left(\dfrac{\partial\left(\omega_\phi^0\sin\theta\right)}{\partial \theta}-\dfrac{\partial \omega_\theta^0}{\partial \phi}\right)-(3\lambda+2\mu)\alpha\dfrac{\partial T}{\partial r}+R=0 \\ (2\mu+\lambda)\dfrac{1}{r}\dfrac{\partial e}{\partial \theta}-\dfrac{2\mu}{r\sin\theta}\left(\dfrac{\partial \omega_r^0}{\partial \phi}-\sin\theta\dfrac{\partial\left(r\,\omega_\phi^0\right)}{\partial r}\right)-(3\lambda+2\mu)\dfrac{\alpha}{r}\dfrac{\partial T}{\partial \theta}+\Theta=0 \\ (2\mu+\lambda)\dfrac{1}{r\sin\theta}\dfrac{\partial e}{\partial \phi}-\dfrac{2\mu}{r}\left(\dfrac{\partial\left(r\omega_\theta^0\right)}{\partial r}-\dfrac{\partial \omega_r^0}{\partial \theta}\right)-(3\lambda+2\mu)\dfrac{\alpha}{r\sin\theta}\dfrac{\partial T}{\partial \phi}+\Phi=0 \end{cases} \tag{8.50}$$

where

$$\begin{aligned} &e=\frac{1}{r^2\sin\theta}\left[\sin\theta\frac{\partial\left(r^2u_r\right)}{\partial r}r\frac{\partial\left(u_\theta\sin\theta\right)}{\partial \theta}+r\frac{\partial u_\phi}{\partial \phi}\right];\ \ \omega_r^0=\frac{1}{2r\sin\theta}\left[\frac{\partial\left(u_\phi\sin\theta\right)}{\partial \theta}-\frac{\partial u_\theta}{\partial \phi}\right]; \\ &\omega_\theta^0=\frac{1}{2r\sin\theta}\left[\frac{1}{r}\frac{\partial u_r}{\partial \phi}-\sin\theta\frac{\partial\left(r\,u_\phi\right)}{\partial r}\right];\ \ \omega_\phi^0=\frac{1}{2r}\left[\frac{\partial\left(r\,u_\theta\right)}{\partial r}-\frac{\partial u_r}{\partial \theta}\right]; \end{aligned} \tag{8.51}$$

Finally, the surface conditions (8.17) expressed in terms of the components of the displacement vector **u** are of the form:

$$\begin{cases} \left(\lambda\nabla\cdot\mathbf{u}+2\mu\dfrac{\partial u}{\partial x}\right)n_x+\mu\left(\dfrac{\partial v}{\partial x}+\dfrac{\partial u}{\partial y}\right)n_y+\mu\left(\dfrac{\partial w}{\partial x}+\dfrac{\partial u}{\partial z}\right)n_z=t_x \\ \mu\left(\dfrac{\partial v}{\partial x}+\dfrac{\partial u}{\partial y}\right)n_x+\left(\lambda\nabla\cdot\mathbf{u}+2\mu\dfrac{\partial v}{\partial y}\right)n_y+\mu\left(\dfrac{\partial w}{\partial y}+\dfrac{\partial v}{\partial z}\right)n_z=t_y \quad \forall P\in\partial V \\ \mu\left(\dfrac{\partial w}{\partial x}+\dfrac{\partial u}{\partial z}\right)n_x+\mu\left(\dfrac{\partial w}{\partial y}+\dfrac{\partial v}{\partial z}\right)n_y+\left(\lambda\nabla\cdot\mathbf{u}+2\mu\dfrac{\partial w}{\partial z}\right)n_z=t_z \end{cases} \tag{8.52}$$

In vector form, we can write:

$$\lambda(\nabla\cdot\mathbf{u})\mathbf{n}+\mu\left[\nabla\otimes\mathbf{u}+(\nabla\otimes\mathbf{u})^T\right]=\mathbf{t}=\left[t_x,t_y,t_z\right]\quad\forall P\in\partial V \tag{8.53}$$

From equations (8.40)-(8.53) it follows that the thermal problem reduces to the usual elastic problem involving body forces:

$$[X,Y,Z]=-(3\lambda+2\mu)\alpha\nabla\cdot T \tag{8.54}$$

and an external normal surface pressure:

$$p = -(3\lambda + 2\mu)\alpha T \tag{8.55}$$

(b) Stress formulation

The equilibrium equations (8.9) are already expressed in terms of the stress components. It is easy to prove that for a simply connected body, the remaining field equations contained in the formulation of section 8.5 are equivalent to the following six equations containing stress component alone:

$$\begin{cases} (1+\nu)\nabla^2\sigma_{xx} + \dfrac{\partial^2 I}{\partial x^2} + \alpha E\left(\dfrac{1+\nu}{1-\nu}\nabla^2 T + \dfrac{\partial^2 T}{\partial x^2}\right) = 0 \\ (1+\nu)\nabla^2\sigma_{yy} + \dfrac{\partial^2 I}{\partial y^2} + \alpha E\left(\dfrac{1+\nu}{1-\nu}\nabla^2 T + \dfrac{\partial^2 T}{\partial y^2}\right) = 0 \\ (1+\nu)\nabla^2\sigma_{zz} + \dfrac{\partial^2 I}{\partial z^2} + \alpha E\left(\dfrac{1+\nu}{1-\nu}\nabla^2 T + \dfrac{\partial^2 T}{\partial z^2}\right) = 0 \\ (1+\nu)\nabla^2\sigma_{xz} + \dfrac{\partial^2 I}{\partial x\,\partial z} + \alpha E\dfrac{\partial^2 T}{\partial x\,\partial z} = 0 \\ (1+\nu)\nabla^2\sigma_{xy} + \dfrac{\partial^2 I}{\partial x\,\partial y} + \alpha E\dfrac{\partial^2 T}{\partial x\,\partial y} = 0 \\ (1+\nu)\nabla^2\sigma_{yz} + \dfrac{\partial^2 I}{\partial y\,\partial z} + \alpha E\dfrac{\partial^2 T}{\partial y\,\partial z} = 0 \end{cases} \tag{8.56}$$

where $I = \sigma_{xx} + \sigma_{yy} + \sigma_{zz}$. These equations are known as the compatibility equations expressed in terms of stress components. The present formulation requires the solution of equations (8.9) and (8.56) under the boundary conditions (8.37) for traction free boundaries (or with equations (8.17) for the case of prescribed surface tractions). For multiply connected bodies the preceding compatibility equations must be supplemented by certain integral conditions.

8.9. Solution of the Lamè equations

The solution of equations (8.39) is taken in the form:

$$u = u^{(h)} + u^{(p)},\ v = v^{(h)} + v^{(p)},\ w = w^{(h)} + w^{(p)}, \tag{8.57}$$

where $u^{(h)}$ is the general solution, $u^{(p)}$ is a particular solution. By assuming, a particular solution as follows:

$$\left[u^{(p)}, v^{(p)}, w^{(p)}\right]^T = \nabla G \tag{8.58}$$

where G is a scalar function. By substituting the equation (8.58) in equation (8.42), and remembering that $\nabla \wedge \nabla G = \mathbf{0}$, we obtain the Poisson's equation for the function G:

$$\nabla^2 G = \alpha\left(\frac{3\lambda + 2\mu}{\lambda + 2\mu}\right)T \tag{8.59}$$

From which:

$$G(x,y,z) = -\frac{\alpha}{4\pi}\left(\frac{3\lambda + 2\mu}{\lambda + 2\mu}\right)\int_V \frac{T(\xi,\eta,\zeta)\,dV}{\sqrt{(x-\xi)^2 + (y-\eta)^2 + (z-\zeta)^2}} \tag{8.60}$$

where ξ, η, ζ are the coordinates of an element of volume dV, V is the volume of the whole body.

The general solution can to be assumed in form proposed by other authors as Galerkin, Papkovich's and Grodskii's, Neuber, Trefftz, Lamè. We reported the solution of these authors as follows.

It is well known that the solution in terms of displacement field **u** for an isotropic and homogeneous linear elastic material, in absence of body forces, can be written by means of the *Boussinesq-Somigliana-Galerkin* vector **F**. The **Galerkin's solution** in vector form is given by :

$$\mathbf{u} = \frac{1}{2\mu}\left[\frac{2\mu+\lambda}{(\mu+\lambda)}\nabla\cdot(\nabla\otimes\mathbf{F}) - \nabla(\nabla\cdot\mathbf{F})\right] \tag{8.61}$$

In Cartesian coordinate system, we can write:

$$\mathbf{F} = \mathbf{i}F_x + \mathbf{j}F_y + \mathbf{k}F_z \tag{8.62}$$

The Galerkin's vector **F** must be to satisfy the bi-harmonic condition $\nabla^4\mathbf{F} = 0$. In explicit the displacement solution in terms of Galerkin's vector is given by:

$$\begin{cases} u = \dfrac{1}{2\mu}\left[\dfrac{2\mu+\lambda}{(\mu+\lambda)}\left(\dfrac{\partial^2 F_x}{\partial x^2}+\dfrac{\partial^2 F_x}{\partial y^2}+\dfrac{\partial^2 F_x}{\partial z^2}\right) - \dfrac{\partial}{\partial x}\left(\dfrac{\partial F_x}{\partial x}+\dfrac{\partial F_y}{\partial y}+\dfrac{\partial F_z}{\partial z}\right)\right] \\ v = \dfrac{1}{2\mu}\left[\dfrac{2\mu+\lambda}{(\mu+\lambda)}\left(\dfrac{\partial^2 F_y}{\partial x^2}+\dfrac{\partial^2 F_y}{\partial y^2}+\dfrac{\partial^2 F_y}{\partial z^2}\right) - \dfrac{\partial}{\partial y}\left(\dfrac{\partial F_x}{\partial x}+\dfrac{\partial F_y}{\partial y}+\dfrac{\partial F_z}{\partial z}\right)\right] \\ w = \dfrac{1}{2\mu}\left[\dfrac{2\mu+\lambda}{(\mu+\lambda)}\left(\dfrac{\partial^2 F_z}{\partial x^2}+\dfrac{\partial^2 F_z}{\partial y^2}+\dfrac{\partial^2 F_z}{\partial z^2}\right) - \dfrac{\partial}{\partial z}\left(\dfrac{\partial F_x}{\partial x}+\dfrac{\partial F_y}{\partial y}+\dfrac{\partial F_z}{\partial z}\right)\right] \end{cases} \tag{8.63}$$

A more detailed are given by Westergaard, who gives expressions for the stress components in terms of **F** and uses this representation to solve a number of classical three-dimensional problems – namely those involving concentrated forces in the infinite or semi-infinite body.

8.10. References

[1] Boley, B.A.,Weiner, J.H., *Theory of thermal stresses*, Dover publications, inc. Mineola, New York

[2] Ciarlet, Philiphe G., *Mathematical Elasticity, Volume I.: Three dimensional elasticity*, Elsevier Science Publishers B.V.

[3] Gurtin, M. E., *The Linear Theory of Elasticity, Handbbuch der Physik*, Springer, Berlin, 1972.

[4] Lekhnitskii, S. G., *Theory of Elasticity of an Anisotropic Body*, Mir, Moscow, 1981.

[5] Love, A. E. H., *A Treatise on the Mathematical Theory of Elasticity*, Dover Publications, Inc, New York, 1944

[6] Nunziante, L., Gambarotta, L., Tralli, A., *Scienza delle Costruzioni*, 3° Edizione, McGraw-Hill, 2011, ISBN: 9788838666971

[7] Ting TCT. *Anisotropic elasticity - Theory and applications*. Oxford University Press; 1996.

[8] Wolfram, S., *Mathematica, version 8*, Wolfram Research, Inc., Champaign, IL, 1998–2005.

8.11. Appendix: Differential operator in cylindrical and spherical coordinates system

The treatment of a special problem may often be simplified by use of a suitable coordinate system that reflects the particular symmetry of the problem. For problems with cylindrical or spherical symmetry, it is appropriate to employ cylindrical or spherical coordinates.

8.11.1. Transformation: Cartesian-cylindrical coordinate systems

Let us consider the Cartesian and Cylindrical coordinate systems as showed in figure 8.2. At generic point P, consider a right-handed triad defined by unit base vectors $\mathbf{e}_r, \mathbf{e}_\theta, \mathbf{e}_z$, which, respectively , are in the radial, circumferential, and axial directions.

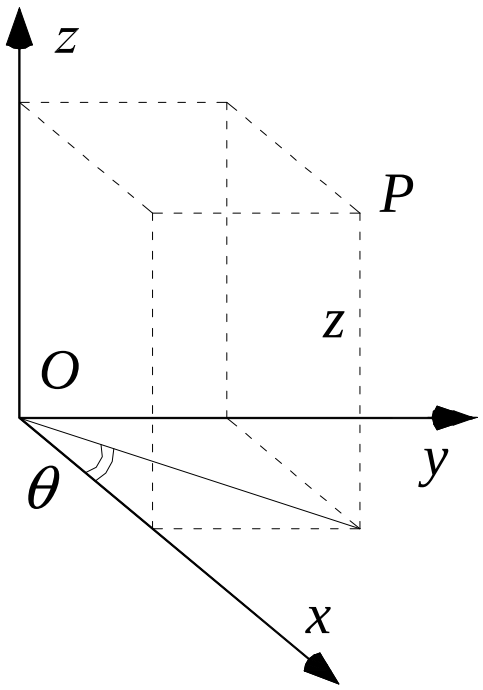

Fig. 8.2 – *Cartesian and cylindrical coordinate systems*

With reference to an rectangular coordinates $\{x, y, z\}$, the cylindrical coordinate $\{r, \theta, z\}$ are related tot the rectangular coordinates x, y, z according to the transformation:

$$\begin{cases} x = r\cos\theta \\ y = r\sin\theta \\ z = z \end{cases} \tag{A.1}$$

An vector $\mathbf{u}$ in Cartesian coordinate has component $\left(\mathbf{u}^{cart}\right)^T = \{u_x, u_y, u_z\}$, but in cylindrical coordinates has component: $\left(\mathbf{u}^{cyl}\right)^T = \{u_r, u_\theta, u_z\}$. The transformation of vector $\mathbf{u}$ in Cartesian coordinate system in to cylindrical coordinates is given by:

$$\begin{cases} u_x = u_r\cos\theta - u_\theta\sin\theta \\ u_y = u_r\sin\theta + u_\theta\cos\theta \\ u_z = u_z \end{cases} \tag{A.2}$$

The previous relationship can be rewritten in follows compact form:

$$\begin{bmatrix} u_x \\ u_y \\ u_z \end{bmatrix} = \begin{bmatrix} \cos\theta & -\sin\theta & 0 \\ \sin\theta & \cos\theta & 0 \\ 0 & 0 & 1 \end{bmatrix} \cdot \begin{bmatrix} u_r \\ u_\theta \\ u_z \end{bmatrix} = [\mathbf{Q}] \cdot \begin{bmatrix} u_r \\ u_\theta \\ u_z \end{bmatrix} \tag{A.3}$$

where **Q** is matrix rotation . The derivate partial of the generic function $f(x,y,z)$ are:

$$\begin{cases} \dfrac{\partial f}{\partial r}=\dfrac{\partial f}{\partial x}\dfrac{\partial x}{\partial r}+\dfrac{\partial f}{\partial y}\dfrac{\partial y}{\partial r}+\dfrac{\partial f}{\partial z}\dfrac{\partial z}{\partial r}=\dfrac{\partial f}{\partial x}\cos\theta+\dfrac{\partial f}{\partial y}\sin\theta \\ \dfrac{\partial f}{\partial \theta}=\dfrac{\partial f}{\partial x}\dfrac{\partial x}{\partial \theta}+\dfrac{\partial f}{\partial y}\dfrac{\partial y}{\partial \theta}+\dfrac{\partial f}{\partial z}\dfrac{\partial z}{\partial \theta}=-\dfrac{\partial f}{\partial x}r\sin\theta+\dfrac{\partial f}{\partial y}r\cos\theta \\ \dfrac{\partial f}{\partial z}=\dfrac{\partial f}{\partial x}\dfrac{\partial x}{\partial z}+\dfrac{\partial f}{\partial y}\dfrac{\partial y}{\partial z}+\dfrac{\partial f}{\partial z}\dfrac{\partial z}{\partial z}=\dfrac{\partial f}{\partial z} \end{cases} \tag{A.4}$$

To inverted the system (A.4) we can write:

$$\begin{cases} \dfrac{\partial f}{\partial x}=\dfrac{\partial f}{\partial r}\cos\theta-\dfrac{\partial f}{\partial \theta}\dfrac{\sin\theta}{r} \\ \dfrac{\partial f}{\partial y}=\dfrac{\partial f}{\partial r}\sin\theta+\dfrac{\partial f}{\partial \theta}\dfrac{\cos\theta}{r} \\ \dfrac{\partial f}{\partial z}=\dfrac{\partial f}{\partial z} \end{cases} \tag{A.5}$$

8.11.2. Differential operator in cylindrical coordinate system

a) Gradient of a scalar function

The vector gradient of the scalar function $f(x,y,z)$ in to Cartesian coordinate system is:

$$\left(\nabla^{cart} f\right)^T=\left\{\frac{\partial f}{\partial x},\frac{\partial f}{\partial y},\frac{\partial f}{\partial z}\right\} \tag{A.6}$$

The vector gradient of scalar function $f(x,y,z)$ in to cylindrical coordinate system is:

$$\nabla^{cyl} f=\mathbf{Q}^T\cdot\nabla^{cart} f \tag{A.7}$$

In explicit the equation of (A.7) is equal to:

$$\nabla^{cyl} f=\begin{bmatrix}\cos\theta & \sin\theta & 0\\ -\sin\theta & \cos\theta & 0\\ 0 & 0 & 1\end{bmatrix}\cdot\begin{bmatrix}\dfrac{\partial f}{\partial r}\cos\theta-\dfrac{\sin\theta}{r}\dfrac{\partial f}{\partial\theta}\\ \dfrac{\partial f}{\partial r}\sin\theta+\dfrac{\cos\theta}{r}\dfrac{\partial f}{\partial\theta}\\ \dfrac{\partial f}{\partial z}\end{bmatrix}=\begin{bmatrix}\dfrac{\partial f}{\partial r}\\ \dfrac{1}{r}\dfrac{\partial f}{\partial\theta}\\ \dfrac{\partial f}{\partial z}\end{bmatrix} \tag{A.8}$$

We can write the transformation for the nabla operator as follows:

$$\nabla^{cart}=\mathbf{Q}\cdot\nabla^{cyl}\quad\Rightarrow\quad\begin{bmatrix}\dfrac{\partial}{\partial x}\\ \dfrac{\partial}{\partial y}\\ \dfrac{\partial}{\partial z}\end{bmatrix}=\begin{bmatrix}\cos\theta & -\sin\theta & 0\\ \sin\theta & \cos\theta & 0\\ 0 & 0 & 1\end{bmatrix}\begin{bmatrix}\dfrac{\partial}{\partial r}\\ \dfrac{1}{r}\dfrac{\partial}{\partial\theta}\\ \dfrac{\partial}{\partial z}\end{bmatrix} \tag{A.9}$$

b) Divergence of a vector function

The divergence of the generic vector function $\left(\mathbf{u}^{cart}\right)^T=\left\{u_x,u_y,u_z\right\}$ in to Cartesian coordinate system is:

$$\left(div\,\mathbf{u}\right)^{cart}=\nabla^{cart}\cdot\mathbf{u}^{cart}=\frac{\partial u_x}{\partial x}+\frac{\partial u_y}{\partial y}+\frac{\partial u_z}{\partial z} \tag{A.10}$$

The divergence of the generic vector function $\left(\mathbf{u}^{cyl}\right)^T=\{u_r,u_\theta,u_z\}$ in to cylindrical coordinate system is:

$$\nabla^{cart}\cdot\mathbf{u}^{cart}=\left(\mathbf{Q}\cdot\nabla^{cyl}\right)\cdot\left(\mathbf{Q}\cdot\mathbf{u}^{cyl}\right)=\left(div\,\mathbf{u}\right)^{cyl} \tag{A.11}$$

In explicit the equation (A.11) is equal to:

$$\left(div\,\mathbf{u}\right)^{cyl}=\frac{\partial u_r}{\partial r}+\frac{u_r}{r}+\frac{1}{r}\frac{\partial u_\theta}{\partial\theta}+\frac{\partial u_z}{\partial z} \tag{A.12}$$

c) Curl of a vector function

The curl of a vector function $\left(\mathbf{u}^{cart}\right)^T=\left\{u_x,u_y,u_z\right\}$ is the product of the nabla operator with the vector function $\mathbf{u}^{cart}$:

$$\left(curl\,\mathbf{u}\right)^{cart}=\nabla^{cart}\times\mathbf{u}^{cart}=\left(\frac{\partial u_z}{\partial y}-\frac{\partial u_y}{\partial z}\right)\mathbf{e}_x+\left(\frac{\partial u_x}{\partial z}-\frac{\partial u_z}{\partial x}\right)\mathbf{e}_y+\left(\frac{\partial u_y}{\partial x}-\frac{\partial u_x}{\partial y}\right)\mathbf{e}_z \tag{A.13}$$

where $\left\{\mathbf{e}_x,\mathbf{e}_y,\mathbf{e}_z\right\}$ are unit vectors in the x,y,z directions. It can also be expressed in determinant form:

$$\nabla^{cart}\times\mathbf{u}^{cart}=\det\begin{vmatrix}\mathbf{e}_x & \mathbf{e}_y & \mathbf{e}_z\\ \dfrac{\partial}{\partial x} & \dfrac{\partial}{\partial y} & \dfrac{\partial}{\partial z}\\ u_x & u_y & u_z\end{vmatrix} \tag{A.14}$$

The curl of a vector function $\left(\mathbf{u}^{cyl}\right)^T=\{u_r,u_\theta,u_3\}$ in to cylindrical coordinate system is:

$$\left(curl\,\mathbf{u}\right)^{cyl}=\mathbf{Q}^T\cdot\left(\nabla^{cart}\times\mathbf{u}^{cart}\right)=\mathbf{Q}^T\cdot\left[\left(\mathbf{Q}\cdot\nabla^{cyl}\right)\times\left(\mathbf{Q}\cdot\mathbf{u}^{cyl}\right)\right] \tag{A.15}$$

In explicit the equation (A.15) becomes:

$$\left(curl\,\mathbf{u}\right)^{cyl}=\left(\frac{1}{r}\frac{\partial u_z}{\partial\theta}-\frac{\partial u_\theta}{\partial z}\right)\mathbf{e}_r+\left(\frac{\partial u_r}{\partial z}-\frac{\partial u_z}{\partial r}\right)\mathbf{e}_\theta+\left(\frac{u_\theta}{r}-\frac{1}{r}\frac{\partial u_r}{\partial\theta}+\frac{\partial u_\theta}{\partial r}\right)\mathbf{e}_z \tag{A.16}$$

where $\mathbf{e}_r,\mathbf{e}_\theta,\mathbf{e}_z$ are unit vectors in the r,θ,z directions. It can also be expressed in determinant form:

$$\left(curl\,\mathbf{u}\right)^{cyl}=\det\begin{vmatrix}\mathbf{e}_r/r & \mathbf{e}_\theta & \mathbf{e}_z/r\\ \dfrac{\partial}{\partial r} & \dfrac{\partial}{\partial\theta} & \dfrac{\partial}{\partial z}\\ u_r & r\,u_\theta & u_z\end{vmatrix} \tag{A.17}$$

d) Gradient of a vector function

The gradient of a vector function $\left(\mathbf{u}^{cart}\right)^T=\left\{u_x,u_y,u_z\right\}$ is the tensorial product of the nabla operator with the vector function $\mathbf{u}^{cart}$:

$$\left(grad\,\mathbf{u}\right)^{cart}=\nabla^{cart}\otimes\mathbf{u}^{art}=\begin{bmatrix}\dfrac{\partial u_x}{\partial x} & \dfrac{\partial u_x}{\partial y} & \dfrac{\partial u_x}{\partial z}\\ \dfrac{\partial u_y}{\partial x} & \dfrac{\partial u_y}{\partial y} & \dfrac{\partial u_y}{\partial z}\\ \dfrac{\partial u_z}{\partial x} & \dfrac{\partial u_z}{\partial y} & \dfrac{\partial u_z}{\partial z}\end{bmatrix} \tag{A.18}$$

The gradient of a vector function $\left(\mathbf{u}^{cyl}\right)^T=\{u_r,u_\theta,u_z\}$ in to cylindrical coordinate system is:

$$\left(grad\,\mathbf{u}\right)^{cyl} = \mathbf{Q}^T \cdot \left(\nabla^{cart} \otimes \mathbf{u}^{cart}\right) \cdot \mathbf{Q} = \mathbf{Q}^T \cdot \left[\left(\mathbf{Q} \cdot \nabla^{cyl}\right) \otimes \left(\mathbf{Q} \cdot \mathbf{u}^{cyl}\right)\right] \cdot \mathbf{Q} \tag{A.19}$$

In explicit the equation (A.19) becomes:

$$\left(grad\,\mathbf{u}\right)^{cyl} = \begin{bmatrix} \dfrac{\partial u_r}{\partial r} & \left(\dfrac{1}{r}\dfrac{\partial u_r}{\partial \theta} - \dfrac{u_\theta}{r}\right) & \dfrac{\partial u_r}{\partial z} \\ \dfrac{\partial u_\theta}{\partial r} & \left(\dfrac{u_r}{r} + \dfrac{1}{r}\dfrac{\partial u_\theta}{\partial \theta}\right) & \dfrac{\partial u_\theta}{\partial z} \\ \dfrac{\partial u_z}{\partial r} & \dfrac{1}{r}\dfrac{\partial u_z}{\partial \theta} & \dfrac{\partial u_z}{\partial z} \end{bmatrix} \tag{A.20}$$

If the vector function $\mathbf{u}$ is a displacement field, then the strain tensor $\mathbf{E}^{cyl}$ is defined by the symmetric part of the displacement gradient, the component of this tensor may be written from (A.20):

$$\mathbf{E}^{cyl} = \frac{1}{2}\left[\left(grad\,\mathbf{u}\right)^{cyl} + \left(\left(grad\,\mathbf{u}\right)^{cyl}\right)^T\right] \tag{A.21}$$

The component of the tensor $\mathbf{E}^{cyl}$ are:

$$\begin{aligned} &\varepsilon_{rr} = \frac{\partial u_r}{\partial r}, \quad \varepsilon_{\theta\theta} = \left(\frac{u_r}{r} + \frac{1}{r}\frac{\partial u_\theta}{\partial \theta}\right), \quad \varepsilon_{zz} = \frac{\partial u_z}{\partial z}, \\ &\varepsilon_{r\theta} = \frac{1}{2}\left(\frac{1}{r}\frac{\partial u_r}{\partial \theta} - \frac{u_\theta}{r} + \frac{\partial u_\theta}{\partial r}\right), \quad \varepsilon_{rz} = \frac{1}{2}\left(\frac{\partial u_r}{\partial z} + \frac{\partial u_z}{\partial r}\right), \quad \varepsilon_{\theta z} = \frac{1}{2}\left(\frac{\partial u_\theta}{\partial z} + \frac{1}{r}\frac{\partial u_z}{\partial \theta}\right), \end{aligned} \tag{A.22}$$

e) Divergence of a tensor function

Let us consider the follows symmetry tensor $\mathbf{T}^{cart}$:

$$\mathbf{T}^{cart} = \begin{bmatrix} \sigma_{xx} & \tau_{xy} & \tau_{xz} \\ \tau_{yx} & \sigma_{yy} & \tau_{yz} \\ \tau_{zx} & \tau_{zy} & \sigma_{zz} \end{bmatrix} \tag{A.23}$$

The divergence of a tensor function $\mathbf{T}^{cart}$ in to Cartesian coordinate system is:

$$div\,\mathbf{T}^{cart} = \nabla^{cart} \cdot \mathbf{T}^{cart} = \begin{bmatrix} \dfrac{\partial \sigma_{xx}}{\partial x} + \dfrac{\partial \tau_{xy}}{\partial y} + \dfrac{\partial \tau_{xz}}{\partial z} \\ \dfrac{\partial \tau_{yx}}{\partial x} + \dfrac{\partial \sigma_{yy}}{\partial y} + \dfrac{\partial \tau_{yz}}{\partial z} \\ \dfrac{\partial \tau_{zx}}{\partial x} + \dfrac{\partial \tau_{zy}}{\partial y} + \dfrac{\partial \sigma_{zz}}{\partial z} \end{bmatrix} \tag{A.24}$$

The divergence of a tensor function $\mathbf{T}^{cyl}$ in to cylindrical coordinate system is:

$$\left(div\,\mathbf{T}\right)^{cyl} = \mathbf{Q}^T \cdot \left(\nabla^{cart} \cdot \mathbf{T}^{cart}\right) = \mathbf{Q}^T \cdot \left[\left(\mathbf{Q} \cdot \nabla^{cyl}\right) \cdot \left(\mathbf{Q} \cdot \mathbf{T}^{cyl} \cdot \mathbf{Q}^T\right)\right] \tag{A.25}$$

where $\mathbf{T}^{cyl}$ is equal to:

$$\mathbf{T}^{cyl} = \begin{bmatrix} \sigma_{rr} & \tau_{r\theta} & \tau_{rz} \\ \tau_{\theta r} & \sigma_{\theta\theta} & \tau_{\theta z} \\ \tau_{zr} & \tau_{z\theta} & \sigma_{zz} \end{bmatrix} \tag{A.26}$$

In explicit the equation (A.25) becomes:

$$\left(div\mathbf{T}\right)^{cyl}=\begin{bmatrix}\dfrac{\partial\sigma_{rr}}{\partial r}+\dfrac{1}{r}\dfrac{\partial\tau_{r\theta}}{\partial\theta}+\dfrac{\partial\tau_{rz}}{\partial z}+\dfrac{\sigma_{rr}-\sigma_{\theta\theta}}{r}\\ \dfrac{\partial\tau_{\theta r}}{\partial r}+\dfrac{1}{r}\dfrac{\partial\sigma_{\theta\theta}}{\partial\theta}+\dfrac{\partial\tau_{\theta z}}{\partial z}+\dfrac{\tau_{r\theta}}{r}+\dfrac{\tau_{\theta r}}{r}\\ \dfrac{\partial\tau_{zr}}{\partial r}+\dfrac{1}{r}\dfrac{\partial\tau_{z\theta}}{\partial\theta}+\dfrac{\partial\sigma_{zz}}{\partial z}+\dfrac{\tau_{zr}}{r}\end{bmatrix} \tag{A.27}$$

8.11.3. Transformation: Cartesian-spherical coordinate systems

Let us consider the spherical polar coordinates r,θ,ϕ shown in fig. 8.3. The unit base vectors, in this case, are $\mathbf{e}_r,\mathbf{e}_\theta,\mathbf{e}_\phi$, which respectively, define the radial, the meridional, and circumferential directions.

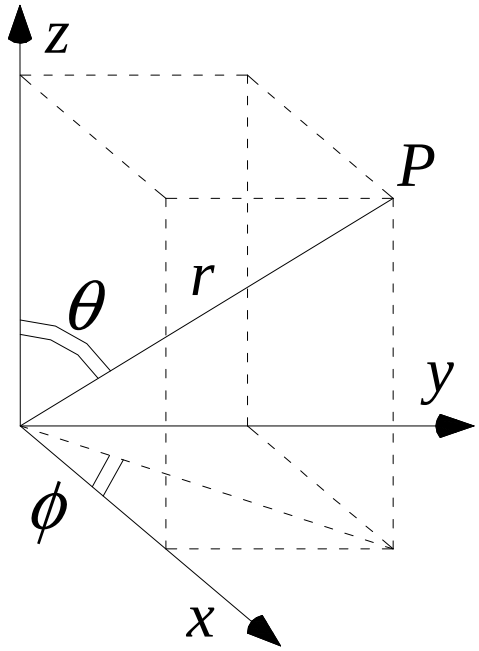

Fig. 8.3 - *Spherical polar coordinates* r,θ,ϕ

With reference to an rectangular coordinates x,y,z, the spherical polar coordinate r,θ,ϕ are related to the rectangular coordinates x,y,z according to the transformation:

$$\begin{cases}x=r\cos\phi\sin\theta\\ y=r\sin\phi\sin\theta\\ z=r\cos\theta\end{cases} \tag{A.28}$$

As is immediately evident from fig. 8.3 It should be noted that $r\geq 0$, $0\leq\theta\leq\pi$, $0\leq\phi\leq 2\pi$. An vector $\mathbf{u}$ in Cartesian coordinate has component $\left(\mathbf{u}^{cart}\right)^T=\left\{u_x,u_y,u_z\right\}$, but in spherical polar coordinates has component: $\left(\mathbf{u}^{sph}\right)^T=\left\{u_r,u_\theta,u_\phi\right\}$.

The transformation the displacement vector in Cartesian coordinate system in to spherical polar coordinates is:

$$\begin{cases}u_r=\left(u_x\cos\phi+u_y\sin\phi\right)\sin\theta+u_z\cos\theta\\ u_\theta=\left(u_x\cos\phi+u_y\sin\phi\right)\cos\theta-u_z\sin\theta\\ u_\phi=-u_x\sin\phi+u_y\cos\phi\end{cases} \tag{A.29}$$

The previous relationship can be rewritten in follows compact form:

$$\begin{bmatrix} u_r \\ u_\theta \\ u_\phi \end{bmatrix} = \begin{bmatrix} \cos\phi\sin\theta & \sin\phi\sin\theta & \cos\theta \\ \cos\phi\cos\theta & \sin\phi\cos\theta & -\sin\theta \\ -\sin\phi & \cos\phi & 0 \end{bmatrix} \cdot \begin{bmatrix} u_x \\ u_y \\ u_z \end{bmatrix} \tag{A.29}$$

The inverse relationship of the (A.29) is equal to:

$$\begin{bmatrix} u_1 \\ u_2 \\ u_3 \end{bmatrix} = \begin{bmatrix} \cos\phi\sin\theta & \cos\phi\cos\theta & -\sin\phi \\ \sin\phi\sin\theta & \sin\phi\cos\theta & \cos\phi \\ \cos\theta & -\sin\theta & 0 \end{bmatrix} \cdot \begin{bmatrix} u_r \\ u_\theta \\ u_\phi \end{bmatrix} = [\mathbf{Q}] \cdot \begin{bmatrix} u_r \\ u_\theta \\ u_\phi \end{bmatrix} \tag{A.30}$$

where $\mathbf{Q}$ is matrix rotation. The derivate partial of the generic function $f(x,y,z)$ are:

$$\begin{cases} \dfrac{\partial f}{\partial r} = \dfrac{\partial f}{\partial x}\dfrac{\partial x}{\partial r} + \dfrac{\partial f}{\partial y}\dfrac{\partial y}{\partial r} + \dfrac{\partial f}{\partial z}\dfrac{\partial z}{\partial r} = \left(\dfrac{\partial f}{\partial x}\cos\phi + \dfrac{\partial f}{\partial y}\sin\phi\right)\sin\theta + \dfrac{\partial f}{\partial z}\cos\theta \\ \dfrac{\partial f}{\partial \theta} = \dfrac{\partial f}{\partial x}\dfrac{\partial x}{\partial \theta} + \dfrac{\partial f}{\partial y}\dfrac{\partial y}{\partial \theta} + \dfrac{\partial f}{\partial z}\dfrac{\partial z}{\partial \theta} = \left(\dfrac{\partial f}{\partial x}\cos\phi + \dfrac{\partial f}{\partial y}\sin\phi\right) r\cos\theta - \dfrac{\partial f}{\partial z} r\sin\theta \\ \dfrac{\partial f}{\partial \phi} = \dfrac{\partial f}{\partial x}\dfrac{\partial x}{\partial \phi} + \dfrac{\partial f}{\partial y}\dfrac{\partial y}{\partial \phi} + \dfrac{\partial f}{\partial z}\dfrac{\partial z}{\partial \phi} = \left(-\dfrac{\partial f}{\partial x}\sin\phi + \dfrac{\partial f}{\partial y}\cos\phi\right) r\sin\theta \end{cases} \tag{A.31}$$

To inverted the system (A.31)we can write:

$$\begin{aligned} \frac{\partial f}{\partial x} &= \left(\frac{\partial f}{\partial r}\sin\theta + \frac{\partial f}{\partial \theta}\frac{\cos\theta}{r}\right)\cos\phi - \frac{\partial f}{\partial \phi}\frac{\sin\phi}{r\sin\theta} \\ \frac{\partial f}{\partial y} &= \left(\frac{\partial f}{\partial r}\sin\theta + \frac{\partial f}{\partial \theta}\frac{\cos\theta}{r}\right)\sin\phi + \frac{\partial f}{\partial \phi}\frac{\cos\phi}{r\sin\theta} \\ \frac{\partial f}{\partial z} &= \frac{\partial f}{\partial r}\cos\theta - \frac{\partial f}{\partial \theta}\frac{\sin\theta}{r} \end{aligned} \tag{A.32}$$

8.11.4. Differential operator in spherical coordinate system

a) Gradient of a scalar function

The vector gradient of scalar function $f(x,y,z)$ in to cylindrical coordinate system is:

$$\nabla^{sph} f = \mathbf{Q}^T \cdot \nabla^{cart} f \tag{A.33}$$

In explicit the equation of (A.33) is equal to:

$$\nabla^{sph} f = \begin{bmatrix} \dfrac{\partial f}{\partial r} \\ \dfrac{1}{r}\dfrac{\partial f}{\partial \theta} \\ \dfrac{1}{r\sin\theta}\dfrac{\partial f}{\partial \phi} \end{bmatrix} \tag{A.34}$$

We can write the transformation for the nabla operator as follows:

$$\nabla^{cart} = \mathbf{Q} \cdot \nabla^{sph} \quad \Rightarrow \quad \begin{bmatrix} \dfrac{\partial}{\partial x} \\ \dfrac{\partial}{\partial y} \\ \dfrac{\partial}{\partial z} \end{bmatrix} = \begin{bmatrix} \cos\phi\sin\theta & \cos\phi\cos\theta & -\sin\phi \\ \sin\phi\sin\theta & \sin\phi\cos\theta & \cos\phi \\ \cos\theta & -\sin\theta & 0 \end{bmatrix} \cdot \begin{bmatrix} \dfrac{\partial}{\partial r} \\ \dfrac{1}{r}\dfrac{\partial}{\partial \theta} \\ \dfrac{1}{r\sin\theta}\dfrac{\partial}{\partial \phi} \end{bmatrix} \tag{A.35}$$

b) Divergence of a vector function

The divergence of the generic vector function $\left(\mathbf{u}^{sph}\right)^T=\left\{u_r,u_\theta,u_\phi\right\}$ in to spherical polar coordinate system is:

$$\nabla^{cart}\cdot\mathbf{u}^{cart}=\left(\mathbf{Q}\cdot\nabla^{sph}\right)\cdot\left(\mathbf{Q}\cdot\mathbf{u}^{sph}\right)=\left(div\,\mathbf{u}\right)^{sph} \tag{A.36}$$

In explicit the equation (A.36) is equal to:

$$\left(div\,\mathbf{u}\right)^{sph}=\frac{\partial u_r}{\partial r}+\frac{2u_r}{r}+\frac{1}{r}\left(\frac{u_\theta}{\tan\theta}+\frac{\partial u_\theta}{\partial\theta}\right)+\frac{\partial u_\phi}{\partial\phi}\frac{1}{r\sin\theta} \tag{A.37}$$

c) Curl of a vector function

The curl of a vector function $\left(\mathbf{u}^{sph}\right)^T=\left\{u_r,u_\phi,u_\theta\right\}$ in to spherical polar coordinate system is:

$$\left(curl\,\mathbf{u}\right)^{sph}=\mathbf{Q}^T\cdot\left(\nabla^{cart}\times\mathbf{u}^{cart}\right)=\mathbf{Q}^T\cdot\left[\left(\mathbf{Q}\cdot\nabla^{sph}\right)\times\left(\mathbf{Q}\cdot\mathbf{u}^{sph}\right)\right] \tag{A.38}$$

In explicit the equation (A.38) becomes:

$$\left(curl\,\mathbf{u}\right)^{sph}=\begin{bmatrix}\dfrac{u_\phi}{r\tan\theta}+\dfrac{1}{r}\left(\dfrac{\partial u_\phi}{\partial\theta}-\dfrac{1}{\sin\theta}\dfrac{\partial u_\theta}{\partial\phi}\right)\\ \dfrac{1}{r}\left(\dfrac{1}{\sin\theta}\dfrac{\partial u_r}{\partial\phi}-u_\phi\right)-\dfrac{\partial u_\phi}{\partial r}\\ \dfrac{\partial u_\theta}{\partial r}+\dfrac{1}{r}\left(u_\theta-\dfrac{\partial u_r}{\partial\theta}\right)\end{bmatrix} \tag{A.39}$$

where $\mathbf{e}_r,\mathbf{e}_\theta,\mathbf{e}_\phi$ are unit vectors in the r,θ,ϕ directions. It can also be expressed in determinant form:

$$\left(curl\,\mathbf{u}\right)^{sph}=\det\begin{vmatrix}\dfrac{\mathbf{e}_r}{r^2\sin\theta} & \dfrac{\mathbf{e}_\theta}{r\sin\theta} & \dfrac{\mathbf{e}_\phi}{r}\\ \dfrac{\partial}{\partial r} & \dfrac{\partial}{\partial\theta} & \dfrac{\partial}{\partial\phi}\\ u_r & r\,u_\theta & u_\phi\,r\sin\theta\end{vmatrix} \tag{A.40}$$

d) Gradient of a vector function

The gradient of a vector function $\left(\mathbf{u}^{sph}\right)^T=\left\{u_r,u_\theta,u_\phi\right\}$ in to cylindrical coordinate system is:

$$\left(grad\,\mathbf{u}\right)^{sph}=\mathbf{Q}^T\cdot\left(\nabla^{cart}\otimes\mathbf{u}^{cart}\right)\cdot\mathbf{Q}=\mathbf{Q}^T\cdot\left[\left(\mathbf{Q}\cdot\nabla^{sph}\right)\otimes\left(\mathbf{Q}\cdot\mathbf{u}^{sph}\right)\right]\cdot\mathbf{Q} \tag{A.41}$$

In explicit the equation (A.41) becomes:

$$\left(grad\,\mathbf{u}\right)^{sph}=\begin{bmatrix}\dfrac{\partial u_r}{\partial r} & \dfrac{1}{r}\left(\dfrac{\partial u_r}{\partial\theta}-u_\theta\right) & \dfrac{1}{r}\left(\dfrac{1}{\sin\theta}\dfrac{\partial u_r}{\partial\phi}-u_\phi\right)\\ \dfrac{\partial u_\theta}{\partial r} & \dfrac{1}{r}\left(\dfrac{\partial u_\theta}{\partial\theta}+u_r\right) & \dfrac{1}{r}\left(\dfrac{1}{\sin\theta}\dfrac{\partial u_\theta}{\partial\phi}-\dfrac{u_\phi}{\tan\theta}\right)\\ \dfrac{\partial u_\phi}{\partial r} & \dfrac{1}{r}\dfrac{\partial u_\phi}{\partial\theta} & \dfrac{1}{r}\left(u_r+\dfrac{u_\theta}{\tan\theta}+\dfrac{1}{\sin\theta}\dfrac{\partial u_\phi}{\partial\phi}\right)\end{bmatrix} \tag{A.42}$$

If the vector function $\mathbf{u}$ is a displacement field, then the strain tensor $\mathbf{E}^{sph}$ is defined by the symmetric part of the displacement gradient, the component of this tensor may be written from (A.42):

$$\mathbf{E}^{sph} = \frac{1}{2}\left[\left(grad\,\mathbf{u}\right)^{sph} + \left(\left(grad\,\mathbf{u}\right)^{sph}\right)^{T} \right] \tag{A.43}$$

The component of the tensor $\mathbf{E}^{sph}$ are:

$$\begin{aligned} &\varepsilon_{rr} = \frac{\partial u_r}{\partial r}, \quad \varepsilon_{\theta\theta} = \left(\frac{u_r}{r} + \frac{1}{r}\frac{\partial u_\theta}{\partial \theta} \right), \quad \varepsilon_{\phi\phi} = \frac{u_r}{r} + \frac{u_\theta}{r\tan\theta} + \frac{1}{r\sin\theta}\frac{\partial u_\phi}{\partial \phi}, \quad \varepsilon_{r\theta} = \frac{1}{2}\left(\frac{1}{r}\frac{\partial u_r}{\partial \theta} - \frac{u_\theta}{r} + \frac{\partial u_\theta}{\partial r} \right), \\ &\varepsilon_{r\phi} = \frac{1}{2}\left(\frac{1}{r\sin\theta}\frac{\partial u_r}{\partial \phi} + \frac{\partial u_\phi}{\partial r} - \frac{u_\phi}{r} \right), \quad \varepsilon_{\theta\phi} = \frac{1}{2}\left(\frac{1}{r}\frac{\partial u_\phi}{\partial \theta} + \frac{1}{r\sin\theta}\frac{\partial u_\theta}{\partial \phi} - \frac{u_\phi}{r\tan\theta} \right), \end{aligned} \tag{A.44}$$

e) Divergence of a tensor function

Let us consider the follows symmetry tensor $\mathbf{T}^{sph}$ in to spherical polar coordinate system:

$$\mathbf{T}^{sph} = \begin{bmatrix} \sigma_{rr} & \tau_{r\theta} & \tau_{r\phi} \\ \tau_{r\theta} & \sigma_{\theta\theta} & \tau_{\theta\phi} \\ \tau_{r\phi} & \tau_{\theta\phi} & \sigma_{\phi\phi} \end{bmatrix} \tag{A.45}$$

The divergence of a tensor function $\mathbf{T}^{cyl}$ in to cylindrical coordinate system is:

$$\left(div\,\mathbf{T}\right)^{cyl} = \mathbf{Q}^{T} \cdot \left(\nabla^{cart} \cdot \mathbf{T}^{cart} \right) = \mathbf{Q}^{T} \cdot \left[\left(\mathbf{Q} \cdot \nabla^{sph} \right) \cdot \left(\mathbf{Q} \cdot \mathbf{T}^{sph} \cdot \mathbf{Q}^{T} \right) \right] \tag{A.46}$$

In explicit the equation (A.46) becomes:

$$\left(div\,\mathbf{T}\right)^{cyl} = \begin{bmatrix} \dfrac{\partial \sigma_{rr}}{\partial r} + \dfrac{1}{r}\dfrac{\partial \tau_{r\theta}}{\partial \theta} + \dfrac{1}{r\sin\theta}\dfrac{\partial \tau_{r\phi}}{\partial \phi} + \dfrac{2\sigma_{rr} - \sigma_{\theta\theta} - \sigma_{\phi\phi}}{r} + \dfrac{\tau_{r\theta}}{r\tan\theta} \\ \dfrac{\partial \tau_{r\theta}}{\partial r} + \dfrac{1}{r}\dfrac{\partial \sigma_{\theta\theta}}{\partial \theta} + \dfrac{1}{r\sin\theta}\dfrac{\partial \tau_{\theta\phi}}{\partial \phi} + \dfrac{3\tau_{r\theta}}{r} + \dfrac{\sigma_{\theta\theta} - \sigma_{\phi\phi}}{r\tan\theta} \\ \dfrac{\partial \tau_{r\phi}}{\partial r} + \dfrac{1}{r}\dfrac{\partial \tau_{\theta\phi}}{\partial \theta} + \dfrac{1}{r\sin\theta}\dfrac{\partial \sigma_{\phi\phi}}{\partial \phi} + \dfrac{3\tau_{r\phi}}{r} + \dfrac{2\tau_{\theta\phi}}{r\tan\theta} \end{bmatrix} \tag{A.47}$$

CHAPTER IX
AXIS-SYMMETRICAL SOLUTIONS FOR MULTILAYERED CILINDER UNDER STRAIN NO-DECAYING CONDITIONS

9.1. Introduction

Cylindrical shells are often used as basic structural components in engineering applications. Much research has been conducted on isotropic or laminated composite plates and shells, also with reference to thermo-elastic problems of functionally graded infinite hollow cylinders. In particular, Liew et al [62] obtained analytical solutions of a functionally graded circular cylinder by a novel limiting process that employs the solutions of homogeneous circular hollow cylinders. Shao [63] derived analytical solutions for mechanical stresses of a functionally graded circular cylinder with finite length, finding mechanical and thermal stresses for the two-dimensional thermo-elastic problems, where the cylinder is assumed to be composed of *n* homogeneous fictitious layers in the radial direction. There, only special axis-symmetrical load conditions with simply supported boundary conditions at the two ends of the object are considered, and the solutions are found by means of specific trigonometric series. Mian & Spencer [64] determined some results for isotropic laminated FGMs with specific variation of the elastic moduli in the direction of the axis of the object. Also, recently, some new results are obtained for non-homogeneous and anisotropic materials, including FGMs, by using a *Stress-Associated Solution* theorem [65]. Moreover, Alshits and Kirkhner [71] derived some elastic solutions for radially inhomogeneous and cylindrically anisotropic circular cylinders, where no variations of the stresses along the axis of the cylinder are assumed. Other interesting results for laminated composite tubes are obtained by Chouchaoui & Ochoa [72], Chen et al, [73], Tarn, J. Q., [74] and Tarn & Wang [75]. In particular, these last two authors, by employing the so-called *state space approach*, start from some results obtained by Lekhnitskii [76] and - by means of an original rearrangement of the field equations that yields to isolate new *state variables* - construct analytical solutions for elastic problems in which the stresses do not vary along the axis of the composite tube. Although under the hypothesis of *generalized plane strain and torsion*, this strategy offers the possibility to find exact solutions for laminated composite tube under extension, torsion, shearing and pressuring, by assuming cylindrically anisotropy for each phase. Huang and Dong [77] presented a procedure for the analysis of stresses and deformations in a laminated circular cylinder of perfectly bonded materials with the most general form of cylindrically anisotropy. On the other hand, some limits of these last literature proposals inhibit their use inside the present work, as it will be discussed in the following section and highlighted in the conclusions.

The new approach proposed here gives two important advantages. The first one is related to the possibility – in the framework of isotropic elasticity – of obtaining closed-form solutions for an arbitrary number of phases of multilayered cylinder, being these solutions furnished by means of a "chain" of (6×6) known matrices (see Appendices for details). Indeed, this approach, differently from that one suggested by Tarn and other authors, that requires the study of eigensolutions, yields to invert the matrix in a symbolic way, regardless the number of phases. This makes possible to obtain qualitative and quantitative information on the mechanical response of laminated cylinders composed by many layers. The second advantage is constituted by the fact that several theorems and properties are proved for establishing the well-position, existence and uniqueness of the algebraic problem obtained transforming the original differential boundary value problem for the laminated composite with core in an algebraic one, also investigating the consistency of the problem of seeking ε_{zz}-no-decaying solutions, particularly important for some engineering applications, as those presented in a subsequent paper and related to the mechanical interaction between optical fibre and materials, when the fibres are used as continuous strain sensors.

To the author's knowledge, only a limited amount of work has been carried out on closed-form solutions for multilayered cylinder, specially for some significant combination of load conditions, as linear radial pressures, axial force and shear stresses applied on the cylindrical external surface.

In this framework, the present paper will develop an analytical approach to find exact elastic solutions for multilayered cylinder, constituted by *n* cylindrical hollow phases and a central core, each of them modelled as homogeneous and isotropic material (Figure n. 9.1).

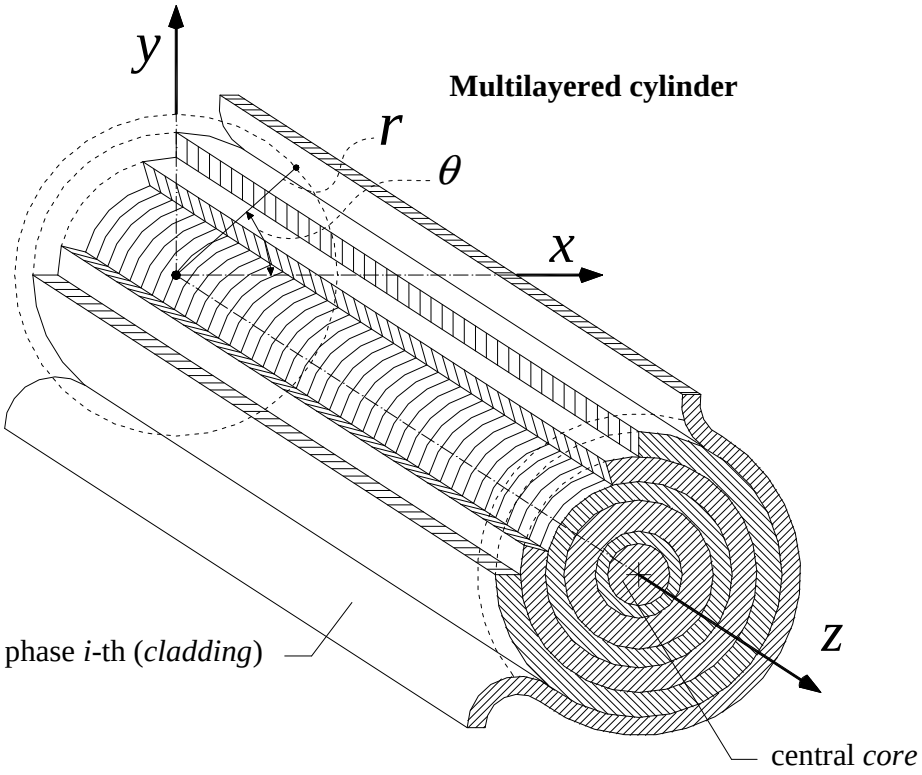

Fig. 9.1 - Typical *Multilayered cylinder*

The assumption of axis-symmetrical load conditions yields to construct a mathematical strategy based on the Love's bi-harmonic scalar function $\chi^{(i)}(r, z)$, (Love, A. E. H. [78]), for each *i*-th phase and then imposing the continuity conditions of the displacements and stresses at the interfaces. By following this way, the system of differential equations can be analytically solved in *cascade* to product a set of algebraic equations.

The specific object of the present work is to furnish a general approach to construct exact elastic solutions for multilayered cylinder, made of a central core and *n* arbitrary cylindrical hollow homogeneous and isotropic phases. Special attention is then given to problems which present *no-decaying* of selected mechanical quantities and in particular of the axial strains ε_{zz}, being z the axis of the laminated cylinder. To build a robust mathematical procedure for obtaining analytical solutions for the above mentioned axis-symmetrical multilayered cylinder, it is first given a theorem for qualifying the space of the solutions and then it is identified their mathematical form, when the object exhibits *no-decaying* of the axial strain. Thus, with reference to the generic *i*-th phase of the material, the classical *Boussinesq-Somigliana-Galerkin* vector is specialized to torsionless composite cylinders, also characterized by *no-decaying* of the axial strain: following this way, a special form of the bi-harmonic Love's function $\chi^{(i)}(r, z)$ is finally obtained. It is also demonstrated that – for these problems – is always possible to reduce the differential boundary value problem (BVP) to an equivalent linear algebraic one, first solving an *in cascade* one-dimensional Euler-like differential system (*field equations*) and then writing the *boundary conditions* through a $(6n+4)$-order square matrix $\mathbb{P}$. Moreover, further *constructive* and *existence* theorems are formulated and proved, to both show the effectiveness of the proposed method and exclude ill-posed problems. In the section 9.6 are here presented some examples in comparison with literature data.

Table of symbols

∇	delta operator	$\boldsymbol{e}_z$	unit vector of the z axis
$\cdot$	scalar product	$\boldsymbol{F}$	*Boussinesq - Somigliana - Galerkin* vector
$\times$	vector product	$\boldsymbol{x}$	position vector
$\otimes$	tensor product	$\boldsymbol{u}$	displacement vector
,	differentation	$\boldsymbol{t}$	surface tractions
∇^2, ∇^4	laplacian, double laplacian	$\Gamma^{(i)}_{j/k}, C^{(i)}_{j/k}$	scalar parameters of the i-th phase
ker, Im,	kernel, image	$f^{(i)}_k$	scalar functions of the i-th phase
det	determinant	$\boldsymbol{f}^{(i)}, \boldsymbol{h}^{(i)}, \boldsymbol{p}^{(i)}$	vectors associated to the i-th phase
$\rho[*]$	rank of a matrix $[*]$	$\mathbf{X}$	vector collecting unknowns
$i, j, ...$	indices	$\mathbf{L}$	vector collecting boundary data
n	number of material phases	χ	*Love*'s solution
$\mathbf{N}$	set of the positive integers	ν	*Poisson* ratio
$\mathbf{R}$	set of the real numbers	E	*Young* modulus
$\Omega, \bar{\Omega}$	object domain, closure of Ω	μ, λ	*Lamè* moduli
$\partial\Omega^{cyl}$	cylindrical external surface	ε_{hk}	strain components
$\{r, \theta, z\}$	cylindrical coordinates	σ_{hk}	stress components
$\mathbf{I}$	sixth-order identity matrix	$\sigma^{(i)}_{hk}, \varepsilon^{(i)}_{hk}$	stresses and strains of the i-th phase
$\mathcal{L}^E$	*Euler* differential operator	$\mathbf{P}$	$(6n+4)\times(6n+4)$ solving matrix
$\mathcal{V}, \mathcal{W}$	vector spaces	$\mathbf{P}^i_k, \mathbf{S}, \mathbf{O}$	sub-matrices of $\mathbb{P}$
$\boldsymbol{v}$	three-dimensional vector field	$P_{h/m}$	components of $\mathbb{P}$

9.2. Description of multilayered structures and composite materials

9.2.1. Multilayered structures

Multilayered structures are two-dimensional elements embedding several layers with different mechanical, thermal and electrical properties. As two-dimensional structures we consider those with a dimension, usually the thickness, negligible with respect to the other two in the in-plane directions. Typical two dimensional structures are plates, spherical and cylindrical shells. Plates do not have any curvature along the two in-plane directions, they are flat panels. Spherical and cylindrical shells are two-dimensional structures with curvature along the two in-plane directions. In the case of plates, a rectilinear Cartesian reference system is employed. In the case of cylinder and sphere, the introduction of a curvilinear Cartesian reference system is necessary. In plate, spherical and cylindrical shells cases, the third axis in the thickness direction is always rectilinear. Several materials are considered for layers embedded in multilayered structures. A first possibility are the homogeneous materials, typical homogeneous materials used in aeronautics and space field are the aluminium and titanium alloys [8], they present high strength-to-weight ratio and excellent mechanical properties. A natural development are composite materials, where two or more materials are combined on a macroscopic scale in order to obtain better engineering properties than the conventional materials (for example metals).

Composite materials are commonly formed in three different types [9]:

(1) ***fibrous composites***, which consist of s of one material in a matrix material of another;
(2) ***particulate composites***, which are composed of macro size particles of one material in a matrix of another;
(3) ***laminated composites***, which are made of layers of different materials, including composites of the first two types.

The particles and matrix in particulate composites can be either metallic or non metallic. Other typical aeronautics multilayered structures are the so-called sandwich structures. They are used to provide a stronger and stiffer structure for the same weight, or conversely a lighter structure to carry the same load as a homogenous or compact-laminate flexural member. These structures are constituted by two stiff skins (faces) and a soft core, and they are widely used to build large parts of aircraft, spacecraft, ship and automotive vehicle structures. Most of the recent applications have used skins constituted by layered structures made of anisotropic composite materials. Several important issues should be considered in the design, analysis and construction of sandwich structures and these have been fully discussed in the well-known books by Plantema [10], Allen [11], Zenkert [12], Bitzer [13] and Vinson [14] as well as in the handbook sections by Marshall [15] and Corden [16]. In the case of *smart structures*, some layers are in piezoelectric materials, they use the so-called *piezoelectric effect* which connects the electrical and mechanical fields [17]. One of the most important innovations is the possibility to consider the so-called *Functionally Graded Materials (FGMs)* embedded in multilayered structures. These materials can be used to provide the desired thermo-mechanical and piezoelectric properties, via the spatial variation in their composition. FGMs vary the elastic, electric and thermal properties in the thickness direction via a gradually changing of the volume fraction of the constituents [19], [20]. One of the advantages of a monotonous variation of the volume fraction of constituent phases is the elimination of stress discontinuity, which is often encountered in laminated composites and accordingly leads to the avoidance of delamination-related problems [21], [22].

9.2.2. Composite materials

Composite materials consist of two or more combined materials which have desirable properties that cannot be obtained with any of the constituents alone [9]. Typical examples are reinforced composite materials which have high strength and high modulus *s* in a *matrix* material. In such composites, s are the main load-carrying members and the matrix material keeps the s together, acts as a load-transfer medium between s, and protects them from being exposed to the environment. Fibres are stiffer and stronger than the same material in bulk form, matrix materials have their usual bulk-form properties. Fibres have a very high length-to-diameter ratio, paradoxically short fibres (whiskers) exhibit better structural properties than long s. Materials are studied at various levels: atomic level, nano-level, single-crystal level, a group of crystals. In this work we consider a basic unit of materials that have properties such as the modulus, strength, thermal coefficient of expansion, electrical resistance and so on, whose magnitudes depend on the direction. Fibres are materials where the desired properties are maximized in a given direction. Where materials are processed such that the basic units are randomly oriented, the resulting material tends to have the same value of the property, in an average statistical sense, in all directions. Such materials are called *isotropic* materials, a typical example is the matrix material. The fibres and matrix materials usually employed in composites can be metallic or non-metallic, the fibre materials can be common metals like aluminium, copper, iron, nickel, steel, titanium, or organic material like glass, boron and graphite [9]. In the case of structural applications, for example in aeronautics field, fibre-reinforced composite materials are often a thin layer called *lamina*. A lamina is a macro unit of material whose material properties are determined through appropriate laboratory tests. Typical structural elements, such as bars, beams, plates or shells are formed by stacking the layers to obtain desired strength and stiffness. Fibre orientation in each lamina and stacking sequence of the layers can be chosen to achieve desired strength and stiffness for a specific application. In composite materials, *fibres* are the reinforcement material, and *matrix* is the base material. Three different types of composite

materials are possible: - fibrous composites, where fibres of one material are in a matrix material of another; - particulate composites, where macro size particles of one material are in a matrix of another; - laminated composites, which are made of layers of different materials, including composites of the first two types. In composites, the particles and matrix can be metallic or nonmetallic, this permits four possible combinations: metallic in nonmetallic, non-metallic in metallic, nonmetallic in nonmetallic, and metallic in metallic. The stiffness and strength of fibrous composites come from fibres which are stiffer and stronger than the same material in bulk form. Shorter fibres (whiskers) have better strength and stiffness properties than long fibres. Whiskers are about 1 to 10 microns in diameter and 10 to 100 times as long. Fibres may be 5 microns to 0.005 inches. Some forms of graphite fibres are 5 to 10 microns in diameter [29]. A *lamina* or *ply* represents a fundamental building block. A fibre-reinforced lamina consists of many fibres embedded in a matrix material, which can be a metal like aluminium, or a nonmetal like thermoset or thermoplastic polymer. The fibres can be continuous or discontinuous, woven, unidirectional, bidirectional, or randomly distributed. Unidirectional fibre-reinforced laminae exhibit the highest strength and modulus in the fibre direction, but they have very low strength and modulus in the direction transverse to the fibres. Discontinuous fibre-reinforced composites have lower strength and modulus than continuous fibre-reinforced composites. A poor bonding between a fibre and matrix results in poor transverse properties and failures such as fibre pull out, fibre breakage and fibre buckling [30]. A collection of laminae stacked to obtain the desired stiffness and thickness is called *laminate*. The sequence of various orientations of a fibre-reinforced composite layer in a laminated is called *lamination scheme* or *stacking sequence*. The layers are usually bounded together with the same matrix material as that in a lamina. The lamination scheme and material properties of individual lamina provide an added flexibility to designers to tailor the stiffness and strength of the laminate to match the structural stiffness and strength requirements. The main disadvantages of laminates made of fibre-reinforced composite materials are the delamination and the fibre debonding. Delamination is caused by the mismatch of material properties between layers, which produces shear stresses between the layers, especially at the edges of a laminate. Fibre debonding is caused by the mismatch of material properties between matrix and fibre. Also, during manufacturing of laminates, material defects such as interlaminar voids, delamination, incorrect orientation, damaged fibres and variation in thickness may be introduced [31]. In formulating the constitutive equations of a lamina we assume that: (a) a lamina is a continuum: no gaps or empty spaces exist; (b) a lamina behaves as a linear elastic material. The assumption (a) permits to consider the macromechanical behaviour of a lamina. The assumption (b) implies that the generalized Hooke's law is valid. Composite materials are heterogeneous from the microscopic point of view. They are assumed to be homogeneous from the macroscopic point of view. In contracted notation, the generalized Hooke's law for an anisotropic material under isothermal conditions is: $\sigma_{ij} = C_{ijhk}\varepsilon_{hk}$; where σ_{ij} are the stress components, ε_{hk} are the strain components, and C_{ijhk} are the material coefficients, all referred to an orthogonal Cartesian coordinate system (x, y, z). The material coordinate system (x, y, z) is indicated in Figure 9.2. The material coordinate axis *x* is parallel to the , the *y*-axis is transverse to the s direction in the plane of the lamina, and the *z*-axis is perpendicular to the plane of the lamina. The orthotropic material properties of a lamina are obtained either by the theoretical approach or through suitable laboratory tests. In the case of theoretical approach (micromechanics approach), the assumptions to determine the engineering constants of a continuous -reinforced composite material are:

- perfect bonding exists between s and matrix;
- s are parallel and uniformly distributed throughout;
- the matrix is free of voids or microcracks and initially in a stress-free state;
- both fibres and matrix are isotropic and obey Hooke's law;
- the applied loads are either parallel or perpendicular to the fibre direction.

For a reinforced material we can define:
E_f = modulus of the ; E_m = modulus of the matrix; ν_f = Poisson's ratio of the ;
ν_m = Poisson's ratio of the matrix; V_f = volume fraction; V_m = matrix volume fraction;
in this way the lamina engineering constants are given by:

$$E_x = E_f V_f + E_m V_m, \quad E_y = \nu_f V_f + \nu_m V_m, \; E_y = \frac{E_f E_m}{E_f V_m + E_m V_f}, \;\; G_{xy} = \frac{G_f G_m}{G_f V_m + G_m V_f},$$

where E_x is the longitudinal modulus, E_y is the transverse one, ν_{xy} is the major Poisson's ratio, and G_{xy} is the shear modulus. It is important to remember that:

$$G_f = \frac{E_f}{2(1+\nu_f)}, \;\; G_m = \frac{E_m}{2(1+\nu_m)},$$

The engineering parameters $E_x, E_y, E_z, \nu_{xy}, \nu_{xz}, \nu_{yz}, G_{xy}, G_{xz}, G_{yz}$ of an orthotropic material can be determined experimentally using an appropriate test specimen made up of the material.

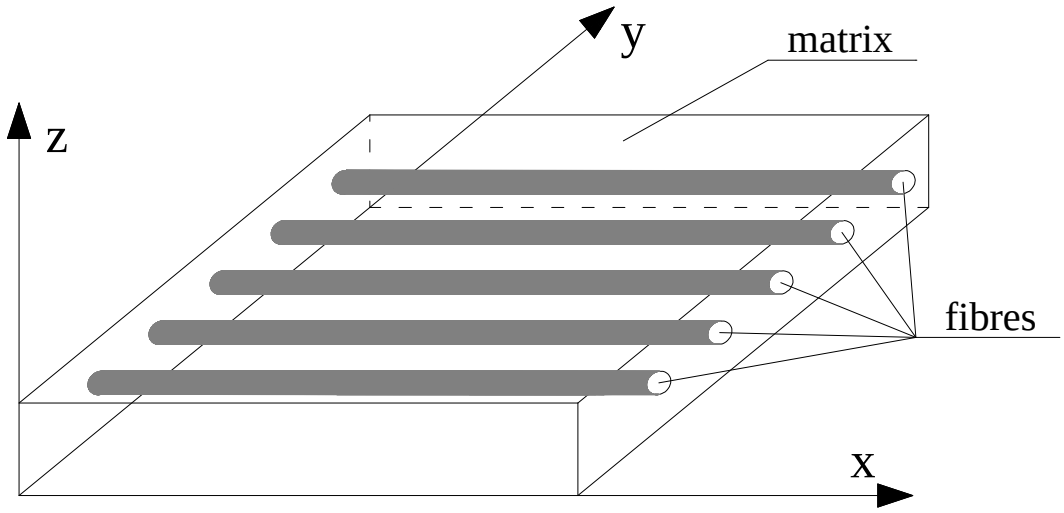

Fig. 9.2 - *Unidirectional -reinforced composite layer with the material coordinate system (x,y,z). (The x-axis is oriented along the direction).*

9.2.3. Sandwiches: foam and honeycomb cores

Sandwich structures are widely used in the aerospace, aircraft, marine, and automotive industries because they are lightweight with high bending stiffness. In general, the face sheets of sandwich panels consist of metals or laminated composites while the core is made of corrugated sheet, foam, or honeycomb. Recently, fibrous core sandwich panels have been developed by replacing the conventional core material with s aligned at small angles of inclination to the faceplates [32]. The concept of sandwich construction has been traced back to the mid 19th century, while the broad introduction of the sandwich concept in aircraft structures started at the beginning of World War II. The commonly used core materials include aluminium, alloys, titanium, stainless steel, and polymer composites. The core supports the skin, increases bending and torsional stiffness, and carries most of the shear load [33]. Structural sandwiches most often have two faces, identical in material and thickness, which primarily resist the in-plane and lateral (bending) loads. However, in special cases the faces may differ in either thickness or material or both, because one face is the primary load-carrying and low-temperature portion, while the other face must withstand an elevated temperature, corrosive environment, etc. In the case of uniform core, the sandwich with identical faces is called *symmetric sandwich*, the latter with different faces is the so-called *asymmetric sandwich* [14].

The core of a sandwich structure can be any material or architecture, but in general, there are four main types:

- foam or solid core;
- honeycomb core;
- web core;
- a corrugated or truss core.

Foam or solid cores are relatively inexpensive and can consist of balsa wood, and an almost infinite selection of foam/plastic materials with a wide variety of densities and shear moduli. The two most common types are the hexagonally-shaped cell structure (hexcell) and the square cell. Web core construction is like a group of I-beams with their flanges welded together. Truss core sandwich is a triangulated core construction. In the web core and truss core constructions, the space in the core could be used for liquid storage or as heat exchanger [14]. In the proposed construction the primary loading, both in-plane and bending, are carried by the faces, while the core resists transverse shear loads (analogous to the web of an I-beam), and keep the faces in place. In foam-core and honeycomb-core sandwiches all of the in-plane and bending loads are carried by the faces only. However, in web-core and truss-core sandwiches a portion of the in-plane and bending loads are also carried by the core elements. The most common foam cores are:

(1) Polyurethane (PUR), a thermosetting material, widely used;
(2) Polyisocyanurate (PIR), a thermosetting material;
(3) Phenolic foam (PF), a thermosetting material, not yet widely used;
(4) Polystyrene (expanded, EPS and extruded, XPS), a thermoplastic material.

Sandwich construction has been used primarily in the aircraft industry since the 1940s, with the development of the British Mosquito bomber, and later logically extended to missile and spacecraft structures. An excellent overview of the uses of core materials and applications is given by Bitzer in [34]. He lists the quantity of honeycomb sandwich being used in various Boeing aircraft . In the Boeing 747, the fuselage cylindrical shell is primarily Nomex-honeycomb sandwich, and the floors, side panels, overhead bins, and ceiling are also of sandwich construction. The Beech Starship, the first all sandwich aircraft, uses Nomex honeycomb with graphite or Kevlar faces for the entire structure. A major portion of the space shuttle is a composite-faced honeycomb-core sandwich. Europe leads the way in the use of sandwich constructions for lightweight railcars, while in the U.S. some of the rapid transit trains use honeycomb sandwich. The U.S. Navy is using honeycomb-sandwich bulkheads to reduce the ship weight above the waterline. Sailboats, racing boats, and auto racing cars are all employing sandwich construction. Sandwich construction is also used in snow skis, water skis, kayaks, canoes, pool tables, and platform tennis paddles. Honeycomb-sandwich construction is also excellent for absorbing mechanical and sound energy. It has a high-crush strength-to-weight ratio. It can also be used to transmit heat or to be an insulative barrier. In the former, a metallic honeycomb is used plus natural convection; for the latter, a non-metallic core is used with the cells filled with a foam. For a sound barrier, the honeycomb core is filled with a fibreglass batting, and a thin porous Tedlar skin can be used for the interior face. Also, honeycomb core has been used in direct fans, wind tunnel, air conditioners, heaters, grills and registers [14].

9.2.4. Functionally graded materials

The severe temperature loads involved in many engineering applications, such as thermal barrier coatings, engine components or rocket nozzles, require high temperature resistant materials. In Japan in the late 1980s the concept of Functionally Graded Materials (FGMs) has been proposed as a thermal barrier material. FGMs are advanced composite materials wherein the composition of each material constituent varies gradually with respect to spatial coordinates [20]. Therefore, in FGMs the macroscopic material properties vary continuously, distinguishing them from laminated composite materials in which the abrupt change of material properties across layer interfaces leads to large interlaminar stresses allowing for damage development. As in the case of laminated composite materials, FGMs combine the desirable properties of the constituent phases to obtain a superior performance, but avoid the problem of interfacial stresses [21], [22]. Functionally Graded

Materials (FGMs) have a large variety of applications , due their properties, not only to provide the desired thermo-mechanical properties, but also to obtain appropriate piezoelectric, and magnetic properties, via the spatial variation in their composition. So, FGMs can be applied in several fields such as tribology, electronics, biomechanics, aeronautics, and space research. The special feature of graded spatial compositions associated to FGMs provides freedom in the design and manufacturing of novel structures; on the other hand, it also poses great challenges in numerical modeling and simulation of the FGM structures [19]. Embedding a network of piezo-ceramic actuators and sensors in FGM structure creates a self-controlling and self-monitoring smart system. This newly engineered class of materials has resulted in significant improvements in the performance of integrated systems, actuation technologies, shape control, vibration and acoustic control and condition monitoring. An alternative solution could be the use of piezoelectric materials, functionally graded in the thickness direction (FGPM), in order to build smart structures which are extensively used as sensors and actuators. The development of piezoelectric materials and structures with functionally graded properties along the layer-thickness direction to improve the mechanical and electrical properties at layer interfaces, has received increasing attention in recent years [42]. Other interesting possibilities are the multilayered FGM, and the functionally graded W/Cu obtained by sintering processing. In the field of FGMs we face substantially three problems, namely:

(1) development of processing routes for functionally graded materials;
(2) determination of the spatially varying material properties (material modeling);
(3) modeling of structures comprising FGMs and FGPMs;

9.2.5. Processing routes

In a functionally graded material (FGM) the properties change gradually with position. The property gradient in the material is caused by a position-dependent chemical composition, microstructure or atomic order. The manufacturing process of a FGM can usually be divided in building the spatially inhomogeneous structure (*gradation*) and transformation of this structure into a bulk material (*consolidation*) [44]. Production of a NiTi-TiCx functionally graded material composite is possible through use of a *combustion synthesis* (CS) reaction employing the propagating mode (SHS). Distinct interfaces with good material interaction and bonding can be observed between each layer of the FGM. The TiCx particle size decreases with increasing NiTi content in the final product as a result of minimized Ostwald ripening. Microindentation performed across the length of the FGM reveals a decrease in hardness as NiTi content is increased [45]. Many fabrication methods were proposed to obtain glass-alumina FGMs, one of these is the production via *percolation* of molten glass into a sintered polycrystalline alumina substrate and via *plasma spraying*, the glass composition is designed in order to minimize the difference between the coefficients of thermal expansion of the constituent phases, which may induce thermal residual stresses in service or during fabrication [46]. The plasma spray method is very common in the case of functionally graded Al_2O_3 / ZrO_2 thermal barrier coating [47]. In order to prepare $Ni - Al_2O_3$ graded composite coatings by an electroplating preparation, a *rotating cathode* can be used. A regular octagonal cathode is employed by changing the relative position between anode and cathode. The simplicity to control, the low equipment cost, and the potential for the economic mass production of composite coatings, permit to consider this technique as a new interesting way to fabricate graded composite coatings [48]. An other interesting method is the *electrophoretic deposition* (EPD) combined with a pressureless sintering, in this way an experimental alumina/zirconia planar FGM can be prepared, this material exhibits excellent hardness in the exterior layers, comparable to that of pure alumina [49]. *Powder metallurgy* is a suitable approach for the preparation of FGMs, but its effects on the electronic properties have to be carefully checked. Powder metallurgical processing may introduce atomic defects and local strains into the material and, thereby, alter the carrier concentration. Such material may be in non-equilibrium conditions at the operating temperature with unstable thermoelectric properties. This effect can be reduced and eliminated by appropriate annealing procedures [50]. A consistent compositionally

gradient protective layer can be prepared by *chemical vapor deposition* by changing the reactant mixture composition gradually from propane to dimethyldichlorosilane. Thus an FGM with a continuous composition distribution is obtained. No thermal cracks are observed and the compositionally gradient layer remains adhesive to the base composite following repeated rapid cooling tests from 1000±C to 0±C [51]. *The centrifugal method* is applied to obtain a graded distribution in manufactured FGMs. In this case a controlling composition method is required to monitoring the movement of solid particles. The graded distribution in FGMs manufactured by the centrifugal method is significantly influenced by many processing parameters, which include the difference in density between particles and molten metal, the applied G number, the particle size, the viscosity of the molten metal, the mean volume fraction of particles, the ring thickness and the solidification time [52]. Multi-layer Mg_2Si / Al functionally graded composites can be produced by a *directional remelting and quenching process*. The structures of functionally graded materials contain three regions (unmelting, partial remelting and remelting) and form five layers (unmelting layer, transition layer, semisolid layer, partial remelting layer and remelting layer) [53]. A novel one-step method, is the *resistance sintering under ultra-high pressure*, it has been developed to fabricate W/Cu functionally graded materials without the addition of any sintering additive. A five-layered W/Cu FGM had been successfully fabricated by resistance sintering under ultra-high pressure of 8GPa and 20kW power input for 50 s. The relative density of the FGM is more than 97%. The relative density of the pure W layer is more than 96% [54]. For further information about the above processing methods, readers can refer to the cited literature and to the overview work by Kieback et alii [44].

9.2.6. Material modelling

We are concerned with graded composite materials, consisting of one or more dispersed phases of spatially variable volume fractions embedded in a matrix of another phase, that are subdivided by internal percolation thresholds or wider transition zones between the different matrix phases. A detailed description of the geometry of actual graded composite microstructures is usually not available, except perhaps for information on volume fraction distribution and approximate shape of the dispersed phase or phases. Therefore, evaluation of thermo-mechanical response and local stresses in graded materials must rely on analysis of micromechanical models with idealized geometries. While such idealizations may have much in common with those that have been developed for analysis of macroscopically homogeneous composites, there are significant differences between the analytical models for the two classes of materials. It is well known that the response of macroscopically homogeneous systems can be described in terms of certain thermo-elastic moduli that are evaluated for a selected representative volume element, subjected to uniform overall thermo-mechanical fields. However, such representative volumes are not easily defined for systems with variable phase volume fractions, subjected to non-uniform overall fields [55]. The characterization of an FGM is not easy and it changes depending the considered material. The most common methods based on micromechanical models are the rule of mixtures [55], the 3-D phases distribution micromechanical models [56], the Voronoi Cell Finite Element Method (VCFEM) [57], the stress waves methods [58], and the stochastic micromechanical models [59]. The *rule of mixtures* is an extension of the classical mixture rule for the composite materials. For example in case of a Glass-Alumina FGM, the glass, the Alumina and the residual elements are considered as three different phases with three different volume fractions V_g, V_a, V_p. The *3-D phases micromechanical models* consider a three-dimensional, arbitrary and non-linear distribution for the phases. For this aim is necessary to define an appropriate Local Representative Volume Element (LRVE) in order to define the local strains and stresses. An other method to define the elastic properties of a FGM is the definition of the *Voronoi Cell Finite Element Method* (VCFEM). In order to apply this method, the structure of the FGM must be discrete and some empty zones must be introduced to consider the porosity of the FGM. The characterization of FGMs can be done by using *elastic waves* to exciting the material. In order to apply this method a Linearly

Inhomogeneous Element (LIE) must be defined. By solving the equations of motion is possible to obtain the relation between the displacements and the mechanical properties of the functionally graded material. The elastic properties of FGM can be also obtained by using a *stochastic micromechanical model*, in this case a stochastic approach is introduced to define the volume fraction of elements and the material properties of the constituents. A Mori-Tanaka scheme [60] must be employed for the homogenization of the FGM. For further information about the above material modellings for FGMs, readers can refer to the previous cited literature.

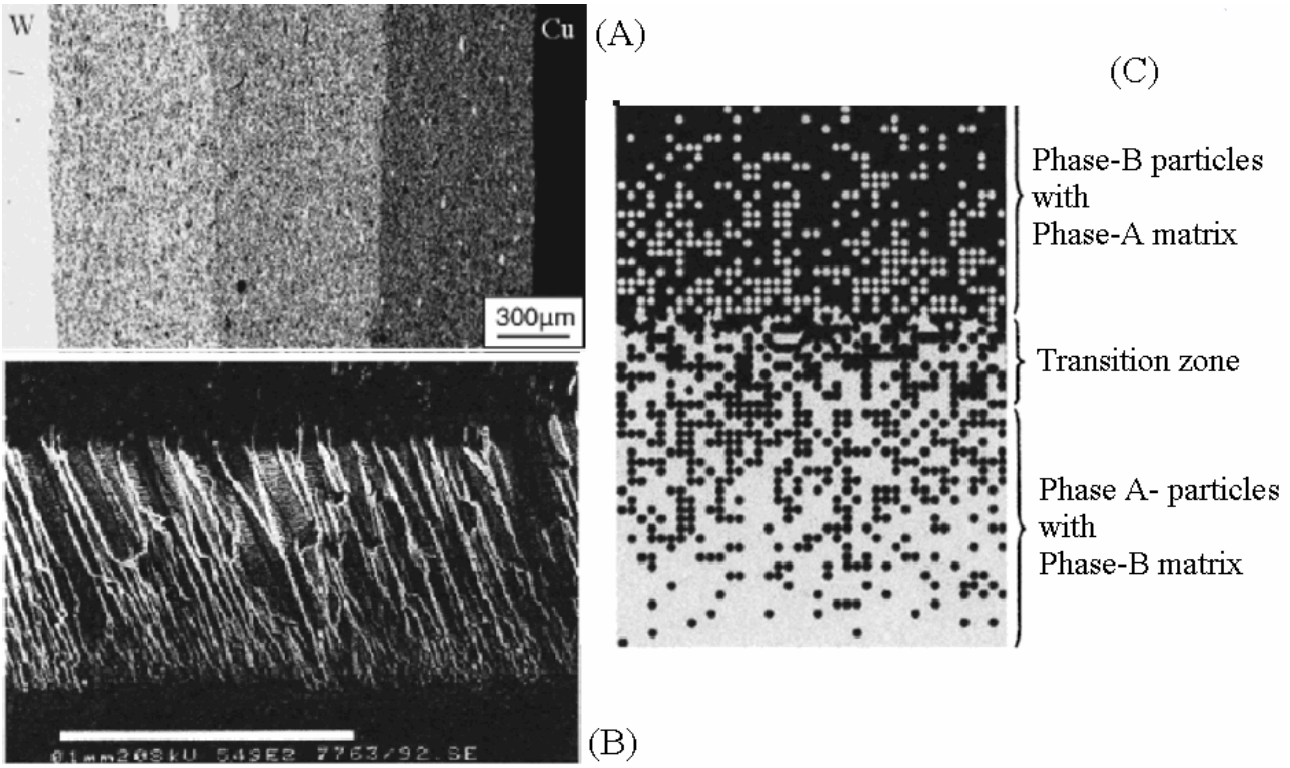

Fig. 9.3 – *(A)* Functionally graded material W/Cu *; (B) Columnar FGM: TBC processed by electron beam physical vapour deposition technique,* $ZrO_2 - Y_2O_3$ *with graded porosity ; (C) A particulate FGM with the volume fractions of constituent phases graded in one(vertical direction)*

9.3. Axis-symmetrical deformations for *multilayered cylinder*

The problem of finding exact elastic solutions for multilayered cylinder under axis-symmetrical boundary conditions is needed in many significant mechanical and structural applications related to several engineering fields. When a solid cylinder, constituted by several homogeneous linearly elastic and isotropic phases, is strained symmetrically by forces applied on both its external cylindrical surface and its ends, it is possible to express all the mechanical quantities in terms of a single function, reducing the equilibrium equations of the body to a single partial differential equation (Love, A. E. H. [75]), (Gurtin, M. E. [87]). It is well known that the solution in terms of displacement field $\boldsymbol{v}$ for an isotropic and homogeneous linear elastic material, in absence of body forces, can be written in the *Boussinesq-Somigliana-Galerkin* form as follows:

$$\boldsymbol{v} = \nabla\cdot\nabla\otimes\boldsymbol{F} - c\,\nabla\otimes\nabla\cdot\boldsymbol{F}, \quad \boldsymbol{F}\in\mathcal{C}^{(4)}(\Omega)\,\big|\,\nabla\cdot\{\nabla\otimes[\nabla\cdot(\nabla\otimes\boldsymbol{F})]\} = \boldsymbol{0}, \tag{9.1}$$

where $c = 1/[2(1-\nu)]$, $\boldsymbol{F}$ is a vector field, ν is the Poisson ratio and Ω is the solid domain occupied by the object. Here, $\nabla\cdot(*) = div\,(*)$ and $\nabla\otimes(*) = grad\,(*)$, so that $\nabla\cdot\nabla\otimes(*) = \nabla^2$ and $\nabla\cdot\nabla\otimes\{\nabla\cdot[\nabla\otimes(*)]\} = \nabla^4$ represent the Laplace and double-Laplace differential operators, respectively, while $\nabla\otimes\nabla\cdot(*) = grad\,[div(*)]$. The *completeness* of (9.1) was already proved

(Gurtin, M. E. [87]). If $\boldsymbol{e}_z$ is the unit vector of the z axis which characterizes the axis-symmetrical problems, the whole space of the so-called *torsionless and rotationally symmetric with respect to the z axis*, displacement solution $\boldsymbol{u}$ is completely described by

$$\boldsymbol{u} \equiv \{\boldsymbol{v} \in \mathcal{C}^{(4)}(\Omega) \,\big|\, \boldsymbol{e}_z \cdot \nabla \times \boldsymbol{v} = 0\}, \tag{9.2}$$

where $\nabla \times (*) = curl\,(*)$. Then, equations (9.1) and (9.2) yield

$$\boldsymbol{F} = \chi \boldsymbol{e}_z, \quad \chi \in \mathcal{C}^{(4)}(\Omega) \tag{9.3}$$

in which $\chi \in \mathcal{C}^{(4)}(\Omega)$ is a scalar function and is called the *Love*'s solution. As a consequence, (9.1) gives $\boldsymbol{u} = \boldsymbol{e}_z \nabla \cdot \nabla \otimes \chi - c \nabla \otimes [\boldsymbol{e}_z \cdot (\nabla \otimes \chi)]$ and then

$$\nabla \cdot \{\nabla \otimes [\nabla \cdot (\nabla \otimes \chi)]\} = \nabla^4 \chi = 0, \quad \chi \in \mathcal{C}^{(4)}(\Omega). \tag{9.4}$$

By referring to a cylindrical coordinate system $\{r, \theta, z\}$, where z is the axis of multilayered cylinder (Figure 9.1), the equation (9.3) gives $\chi = \chi(r, z)$ and the cylindrical components of the displacement reduce to

$$u_r = u_r(r, z), \quad u_\theta = 0, \quad u_z = u_z(r, z) \tag{9.5}$$

as well as, for homogeneous materials, the stresses are

$$\sigma_{rr} = \sigma_{rr}(r, z),\ \sigma_{\theta\theta} = \sigma_{\theta\theta}(r, z),\ \sigma_{zz} = \sigma_{zz}(r, z),\ \tau_{rz} = \tau_{rz}(r, z),\ \tau_{\theta z} = \tau_{r\theta} = 0. \tag{9.6}$$

Here, we will denote with the comma the differentiation: in particular, by taking into account axis-symmetrical problems and referring to the cylindrical coordinate system, the Laplace operator will be explicitly written as $\nabla^2(*) = (*)_{,rr} + r^{-1}(*)_{,r} + (*)_{,zz}$, being all the functions independent of θ, while

$$\nabla^4(*) = (*)_{,rrrr} + 2r^{-1}[(*)_{,rrr} + (*)_{,rzz}] - r^{-2}(*)_{,rr} + r^{-3}(*)_{,r} + 2(*)_{,rrzz} + (*)_{,zzzz}.$$

Besides, the superscript (i) will recall the *i*-th phase constituting the multilayered cylinder, therefore $\nu^{(i)}$ and $E^{(i)}$ will represent the corresponding Poisson's ratio and Young's modulus, respectively. Writing $u_r^{(i)} = U^{(i)}$ and $u_z^{(i)} = W^{(i)}$, being $u_\theta^{(i)} = V^{(i)} = 0$ due to symmetry, the compatibility equations take the form:

$$\varepsilon_{rr}^{(i)} = U_{,r}^{(i)}, \quad \varepsilon_{\theta\theta}^{(i)} = r^{-1}U^{(i)}, \quad \varepsilon_{zz}^{(i)} = W_{,z}^{(i)}, \quad \varepsilon_{rz}^{(i)} = (1/2)(U_{,z}^{(i)} + W_{,r}^{(i)}), \quad \varepsilon_{\theta z}^{(i)} = \varepsilon_{r\theta}^{(i)} = 0. \tag{9.7}$$

Finally, with reference to the generic phase "*i*-th" of multilayered cylinder and recalling equation (9.4)-(9.7), we can write

$$U^{(i)} = -\frac{1}{2\mu^{(i)}}\chi_{,rz}^{(i)}, \quad W^{(i)} = \frac{1}{2\mu^{(i)}}\left[\frac{\mu^{(i)}}{(\mu^{(i)} + \lambda^{(i)})}\nabla^2\chi^{(i)} + \chi_{,rr}^{(i)} + r^{-1}\chi_{,r}^{(i)}\right] \tag{9.8}$$

and the no vanishing stresses are

$$\begin{aligned} &\sigma_{rr}^{(i)} = (\nu^{(i)}\nabla^2\chi^{(i)} - \chi_{,rr}^{(i)})_{,z}, \quad \sigma_{\theta\theta}^{(i)} = (\nu^{(i)}\nabla^2\chi^{(i)} - r^{-1}\chi_{,r}^{(i)})_{,z}, \\ &\sigma_{zz}^{(i)} = [(2 - \nu^{(i)})\nabla^2\chi^{(i)} - \chi_{,zz}^{(i)})]_{,z}, \quad \tau_{rz}^{(i)} = [(1 - \nu^{(i)})\nabla^2\chi^{(i)} - \chi_{,zz}^{(i)})]_{,r}, \end{aligned} \tag{9.9}$$

where, for our convenience, we use the elastic moduli $E^{(i)}$ and $\nu^{(i)}$ as functions of the Lamé coefficients, by invoking the well-known following relations:

$$E^{(i)} = \frac{\mu^{(i)}(2\mu^{(i)} + 3\lambda^{(i)})}{(\mu^{(i)} + \lambda^{(i)})}, \quad \nu^{(i)} = \frac{\lambda^{(i)}}{2(\mu^{(i)} + \lambda^{(i)})}. \tag{9.10}$$

9.4. Mechanical characterization under strain no-decaying conditions

9.4.1. Preliminary remarks

In this section we will prove that the hypothesis of no decaying of the ε_{zz} passing from one phase to another (no variation in the radius direction) yields to choose the bi-harmonic Love's function $\chi^{(i)}$ with a selected mathematical form. In particular, we will show that, in order to be authorized of

imaging axis-symmetrical elastic solutions for cylindrical piece-wise homogeneous multilayered cylinder characterized by no decaying of the axial strain ε_{zz} along the radius direction, only combination of *axial forces* at the object's ends, *radial pressures* that vary linearly along the z axis and uniform *shear tractions*, are admissible. As preliminary remarks, we write down some definitions and properties which will turn useful later.
We begin by furnishing the following definition to identify the specific object taken as main actor of the present work:

DEFINITION 1: *Let us consider a proper subset* Ω *of the three-dimensional Euclidean space and let* $\Omega^{(i)} \subseteq \Omega \{i = 1,...,n\} \Big| \overline{\Omega} \equiv \bigcup_{i=1}^{n \in \mathbb{N}} \overline{\Omega}^{(i)}$ *be a partition of* Ω. *Let us consider multilayered cylinder characterized by a linearly elastic piece-wise homogeneous multi-phase material constituted by a solid circular cylinder made of a central core and* $n \in \mathbf{N}$ *isotropic hollow phases, each of them occupying a sub-domain* $\Omega^{(i)}$.
As already said, one of the goals of the paper is to establish the character of the solution for multilayered cylinder under some conditions related to the no-decaying of the mechanical strain inside the laminated material. In this context, we give the following definition:

DEFINITION 2: *Consider a* multilayered cylinder and l*et* $\varepsilon \in \mathcal{C}^{(m)}(\Omega)$ *be a generic strain component function related to the Elastostatic Boundary Value Problem* (BVP), *" m " depending by the choice. Then, the multi-phase object is said "* ε*-no-decaying" if the corresponding* BVP *admits a solution satisfying the following mathematical condition, everywhere in* Ω:

$$\varepsilon^{(i)} = \varepsilon, \quad \forall i \in \{1,2,...,n\} \subset \mathbb{N}. \tag{9.11}$$

It is worth noticing that, in general, for establishing (9.11) one could risk to incur in an *ill-posed problem*, being (9.11) a field equation that could go against to the Cauchy equations. This means that for ε-no-decaying problems the *existence* of the solution has to be demonstrated, also in the framework of linear elasticity. To make this we will have to prove that the intersection between the space of the solutions spanned by a selected class of BVPs and the space constituted by elements satisfying (9.11) is not empty.
Moreover, it must be highlighted that, with reference to multilayered cylinder with axis coincident with z, ε-no-decaying condition (9.11) implies that at most $\varepsilon^{(i)} = \varepsilon^{(i)}(z)$, that is $\varepsilon^{(i)}$ can be a function only of z, and doesn't vary along the radius directions. Then, the condition $\varepsilon^{(i)} = \varepsilon^{(i)}(z) = \varepsilon, \forall i \in \{1,2,...n\}$ represents a necessary condition for obtaining ε-no-decaying. In particular, a close examination of this condition for multilayered cylinder yields to discover the following:

PROPERTY 1: *Let us consider a multilayered cylinder, subjected to axis-symmetrical boundary conditions and let be* $\varepsilon \equiv \varepsilon_{hk}$, *where* ε_{hk} *is an arbitrarily chosen strain component. Then, the necessary condition for obtaining* ε*-no-decaying is that this strain component has to be at most a third-order polynomial function of z. In particular, this condition separately applied to each of the strain components* ε_{hk} *gives:*

i) $\forall i \in \{0,1,2,...,n\}, \quad \varepsilon \equiv \varepsilon_{zz}(z) = \varepsilon_{zz}^{(i)} \Rightarrow \varepsilon_{zz}^{(i)} = k_0^{(i)} + k_1^{(i)} z + k_2^{(i)} z^2 + k_3^{(i)} z^3$

ii) $\forall i \in \{0,1,2,...,n\}, \quad \varepsilon \equiv \varepsilon_{rr}(z) = \varepsilon_{rr}^{(i)} \Rightarrow \varepsilon_{rr}^{(i)} = k_0^{(i)} + k_1^{(i)} z + k_2^{(i)} z^2 + k_3^{(i)} z^3$

iii) $\forall i \in \{0,1,2,...,n\}, \quad \varepsilon \equiv \varepsilon_{\theta\theta}(z) = \varepsilon_{\theta\theta}^{(i)} \Rightarrow \varepsilon_{\theta\theta}^{(i)} = k_0^{(i)} + k_1^{(i)} z + k_2^{(i)} z^2 + k_3^{(i)} z^3$

iv) $\forall i \in \{0,1,2,...,n\}, \quad \varepsilon \equiv \varepsilon_{rz}(z) = \varepsilon_{rz}^{(i)} \Rightarrow \varepsilon_{rz}^{(i)} = 0$

where $k_0^{(i)}, k_1^{(i)}, k_2^{(i)}, k_3^{(i)}$ *are real coefficients depending from the i-*th *phase.*
The details about the proof of this property are analytically reported in the Appendix A.1.

9.4.2. Characterization of the solution for multilayered cylinder under ε_{zz} no-decaying condition

In this section, we will focus the problem to find exact solutions for multilayered cylinder under axis-symmetrical boundary conditions, characterized by no-decaying of the strain ε_{zz} along the radius direction. To make this, we will use the results obtained with the property above mentioned, by following an approach based on the Love's function. In order to reach the object, we can establish the following

THEOREM 1: *Let us consider a multilayered cylinder, subjected to axis-symmetrical boundary conditions and let be* $\varepsilon \equiv \varepsilon_{zz}$. *Then, the two following statements are equivalent and each of them constitutes a necessary and sufficient condition for obtaining* ε_{zz} *-no-decaying:*

i) the cylindrical external surface $\partial\Omega^{cyl}$ of the object is loaded by tractions $\boldsymbol{t}$ collecting any arbitrary combination of radial pressures that vary linearly along the z axis and uniform shear tractions, while axial forces appear at the object ends, that is:

$$\forall i \in \{0,1,2,...,n\}, \quad \varepsilon_{zz}^{(i)} = \varepsilon_{zz}(z) \Leftrightarrow \{\forall \boldsymbol{x} \in \partial\Omega^{cyl}, \boldsymbol{t}^T \equiv [p_0 + p_1 z, 0, \tau_0]\} \tag{9.12}$$

where $\{p_0, p_1, \tau_0\} \in \mathbb{R}$ *and the tractions vector* $\boldsymbol{t}$ *is referred to the cylindrical coordinates;*

ii) the axial strain $\varepsilon_{zz}^{(i)}$ *varies at most linearly upon z, that is*

$$\varepsilon_{zz}^{(i)} = \varepsilon_{zz}(z) \Leftrightarrow \varepsilon_{zz}^{(i)} = \varepsilon_0 + \varepsilon_1 z, \quad \forall i \in \{0,1,2,...,n\} \tag{9.13}$$

where ε_0 *and* ε_1 *are real coefficients independent from the i-*th *phase.*

Proof.

Necessary condition:

$$\{\forall i \in \{0,1,2,...,n\}, \varepsilon_{zz}^{(i)} = \varepsilon_{zz}(z)\} \Rightarrow \{\forall \boldsymbol{x} \in \partial\Omega^{cyl}, \boldsymbol{t}^T \equiv [p_0 + p_1 z, 0, \tau_0]\}. \tag{9.14}$$

By referring to the results obtained in the Appendix A.1, summarized above in the Property 1, we demonstrated that a necessary condition to assume ε_{zz} no-decaying in axis-symmetrical multilayered cylinder is that – in each phase of the object – $\varepsilon_{zz}^{(i)}$ possess at most a third-order polynomial form in z, see equation (A1.11). In the follows, by introducing compatibility and equilibrium equations at the interfacial boundaries, we need to prove that $\varepsilon_{zz}^{(i)}$ has to reduce to a linear function of z which presents the same coefficients for any phase. As a consequence, it will be highlighted that the emerging tractions $\boldsymbol{t}$ on $\partial\Omega^{cyl}$ can be at most given by a combination of radial pressures linearly varying along the z axis and uniform shear tractions, with additional axial forces appearing at the end basis. Then, by virtue of the Property 1, let us assume the hypothesis for which

$$\varepsilon_{zz}^{(i)} = \varepsilon^{(i)}(z) = \varepsilon_0^{(i)} + \frac{\varepsilon_1^{(i)}}{2\mu^{(i)}} z + \frac{\varepsilon_2^{(i)}}{4\mu^{(i)}} z^2 + \frac{\varepsilon_3^{(i)}}{6\mu^{(i)}} z^3$$

[see equation (A1.12)]. With reference to the results reported in the Appendix A.1, by considering that, at the centre of multilayered cylinder (cylinder *core* in $r = 0$), diverging terms in $\chi^{(0)}$ are not admissible, the results reported below must be true:

$$\Gamma_{4/1}^{(0)} = \Gamma_{1/3}^{(0)} = \Gamma_{2/1}^{(0)} = \Gamma_{5/3}^{(0)} = 0, \ \Gamma_{3/1}^{(0)} = \frac{2\Gamma_{1/1}^{(0)}\mu^{(0)}\left(\mu^{(0)} + \lambda^{(0)}\right)}{2\mu^{(0)} + \lambda^{(0)}}, \tag{9.15}$$

where the notation used for the coefficients is referred to that already introduced in Appendix A.1. Also, by imposing the equilibrium and compatibility conditions at the interfacial boundary between the central core and the first hollow phase, some coefficients can be immediately determined, that is

$$\varepsilon_3^{(0)} = \varepsilon_2^{(0)} = \varepsilon_3^{(1)} = \varepsilon_2^{(1)} = \Gamma_{1/3}^{(1)} = \Gamma_{2/1}^{(1)} = 0, \quad \varepsilon_0^{(1)} = \varepsilon_0^{(0)}, \quad \varepsilon_1^{(1)} = \varepsilon_1^{(0)} \frac{\mu^{(1)}}{\mu^{(0)}}, \tag{9.16}$$

as well as it is possible to write similar relations as a consequence of the satisfaction of the boundary conditions at the interfaces between every couple of adjacent phases. This leads to write that $\forall i \in \{0,1,2,...,n\},\ \varepsilon_0^{(i)} = \varepsilon_0, \varepsilon_1^{(i)}/\mu^{(i)} = \varepsilon_1^{(0)}/\mu^{(0)}$, and therefore

$$\forall i \in \{0,1,2,...,n\},\ \varepsilon_{zz}^{(i)} = \varepsilon_{zz}(z) = \varepsilon_0 + \varepsilon_1 z$$

where $\forall i \in \{0,1,2,...,n\},\ \varepsilon_0 = \varepsilon_0^{(i)},\ \varepsilon_1 = \dfrac{\varepsilon_1^{(i)}}{2\mu^{(i)}}$.

The results highlight that the function $\chi^{(i)}$ finally exhibits the fourth-order polynomial function in z, i.e. $\chi^{(i)} = \sum_{k=0}^{4} z^k\ f_k^{(i)}(r)$. Moreover, regardless the number *n* of phases, we have that the emerging tractions $\boldsymbol{t}$ on $\partial\Omega^{cyl}$ have to be at most a combination of radial pressures linearly varying along the z axis and uniform shear tractions, while resultant axial forces appear at the ends (Figures 9.3 - 9.4 - 9.5 - 9.6). Hence:

$$\boldsymbol{t}^T \equiv [\,p_0 + p_1 z,\ 0,\ \tau_0\,], \quad \forall \boldsymbol{x} \in \partial\Omega^{cyl}. \tag{9.17}$$

Also note that, due the axis-symmetry, only centred axial forces at the ends can emerge.

<u>*Sufficiency condition*</u>:

$$\{\forall \boldsymbol{x} \in \partial\Omega^{cyl}, \boldsymbol{t}^T \equiv [\,p_0 + p_1 z,\ 0,\ \tau_0\,]\} \Rightarrow \{\forall i \in \{0,1,2,...,n\}, \varepsilon_{zz}^{(i)} = \varepsilon_{zz}(z)\}.$$

The sufficiency condition is obtainable by invoking the Kirchhoff uniqueness theorem for linear elastic boundary value problems, with reference to the so-called *first or traction boundary problem* [Gurtin, M. E., 1972]. Note that the Boussinesq-De Saint Venant principle also ensures that, far from the ends, the obtained solutions are able to represent the stress and strain fields coming from many different normal stress distributions on the basis, as well as other possible axis-symmetrical traction fields (i.e. emerging τ_{rz}) with zero resultants. In this context, it is worth noticing that, in the proof of the theorem, we did not explicitly mention the possible presence of axial forces applied at the ends of multilayered cylinder: obviously, due to the axis-symmetry of the problem, both zero and nonzero emerging axial forces are admissible, but they will appear automatically equilibrated and their overall values can be prescribed through weak-form boundary conditions in the elastic problem. Rigorously speaking, by relaxing the above cited boundary conditions at the object's ends, we loose the uniqueness: this means that it is possible to imagine two different load cases, characterised by the same *local* load conditions on the cylindrically surface, as well as the same *global* resultants emerging from the ends, but coming out by different *local* normal stress distributions, whose related solutions will be different. However, this mathematical evidence is of interest only for *short* multilayered cylinder, that is when the external diameter of the cylinder $D := \max\{2R^{(i)}\} \equiv 2R^{(n)}$ is about of the order of magnitude of its length L. On the contrary, in the major part of the engineering applications – where the longitudinal length of the cylinder is much more greater than its maximum diameter, i.e. $D/L << 1$ – the Boussinesq-De Saint Venant principle ensures that the deformations and stresses due to the difference between two solutions differing only for the distribution of the tractions at the extremities, are of negligible magnitude at distances from the ends which are sufficiently large compared to the diameter D. *From Theorem 1, an useful corollary related to the following necessary condition can also be easily established:*

<u>COROLLARY</u>*: With reference to an arbitrary BVP for a multilayered cylinder under axis-symmetrical boundary conditions, it is possible to prove that:*

$$\varepsilon_{zz}^{(i)} = \varepsilon_{zz}(z) \Rightarrow \chi^{(i)}(r,z) = \sum_{k=0}^{4} f_k^{(i)}(r)\, z^k, \quad \forall i \in \{0,1,2,...,n\}$$

where $\chi^{(i)}(r,z)$ *is the Love's solution and* $f_k^{(i)}(r)$ *are scalar functions to determine.* The proof emerges from both Property 1 and Theorem 1.

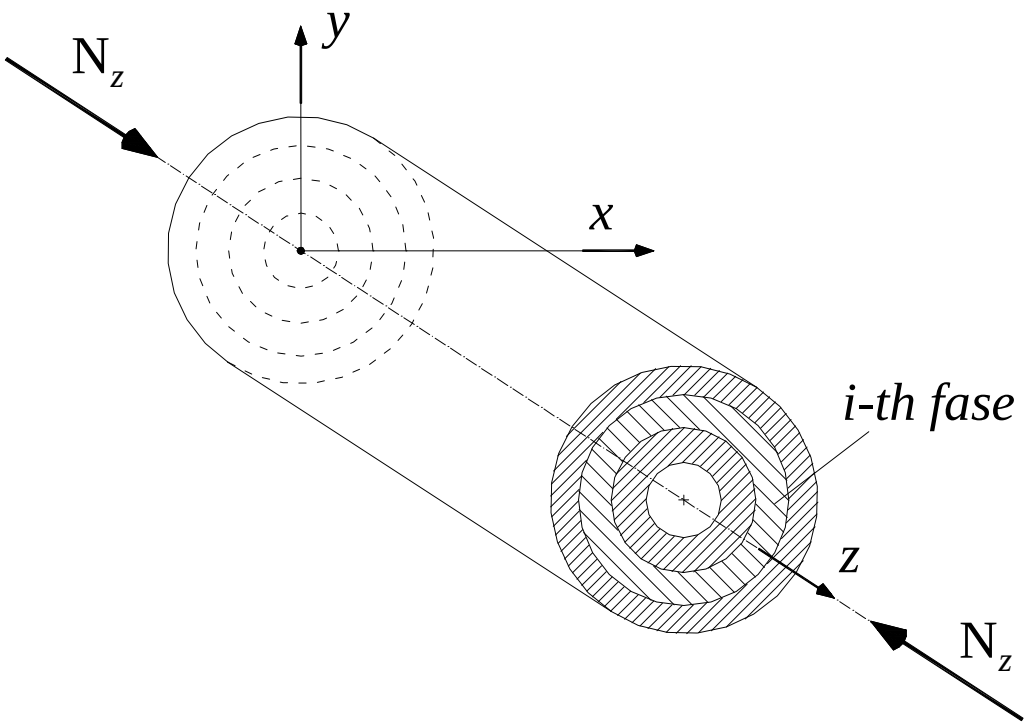

Fig. 9.4 - *Multilayered cylinder subjected by axial force* N_z *applied on the basis*

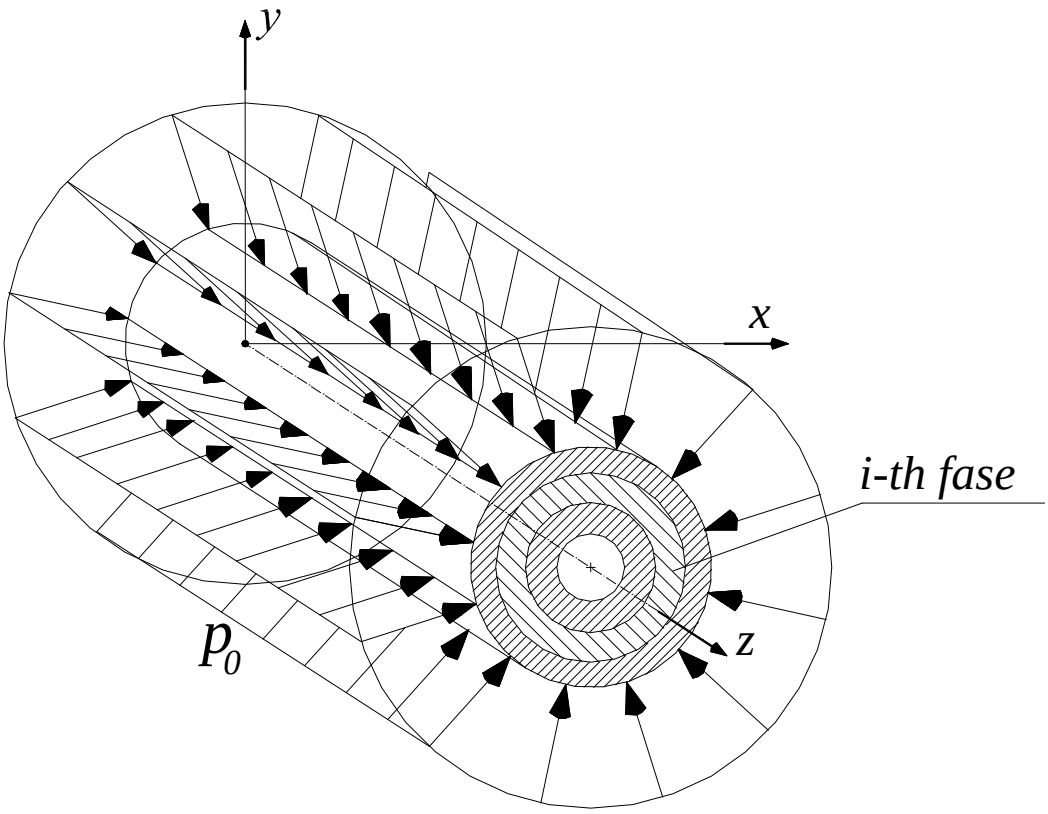

Fig. 9.5 - *Multilayered cylinder subjected by uniform radial pressures along the z axis.*

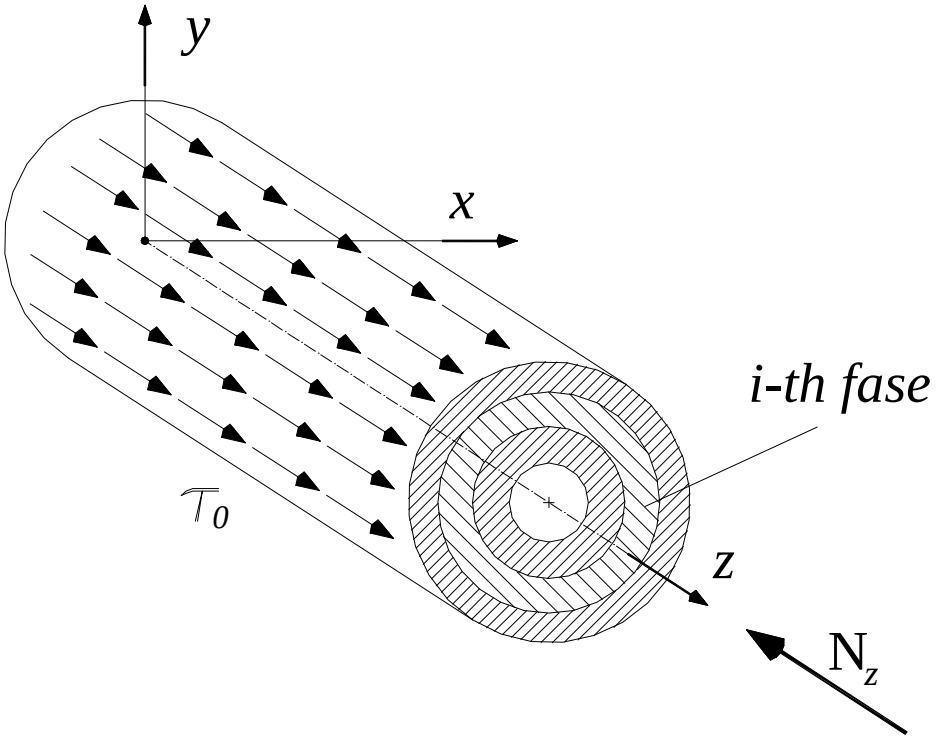

Fig. 9.6 - *Multilayered cylinder subjected by uniform shear tractions and equilibrated axial force* N_z *on the base*

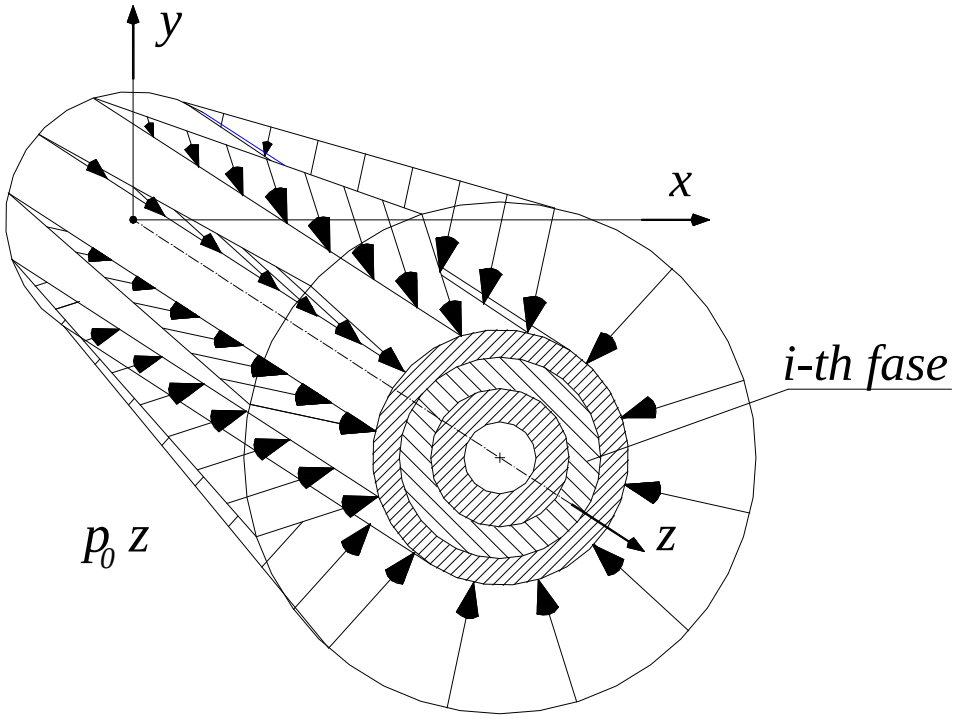

Fig. 9.7 - *Multilayered cylinder subjected by radial pressures linearly varying along the z ax*is.

9.4.3. Exact solutions for multilayered cylinder: field equations for the i-th phase

In this section we will obtain some solutions for a piece-wise homogeneous multilayered cylinder. In particular there will be presented closed-form solutions for two kinds of problems. The first one

is related to the case where the ε_{zz} in each phase of the object remains constant along the radius direction (*no-decaying case*): for this case, by invoking the proposed theorem, we will be able to construct the whole space of no-decaying solutions. The second class of problems is instead referred to elastic solutions found for two specific problems related to multilayered cylinder exhibiting variation of the ε_{zz} along the radius (*decaying case*). In order to present an unified approach, we will begin for both classes of problems starting from a more large form of the bi-harmonic function $\chi^{(i)}$. In order to solve the field equations related to the equilibrium in each phase of multilayered cylinder, we can state and prove the following

THEOREM 2: *Let us consider a* multilayered cylinder, *subjected to axis-symmetrical boundary conditions and let be* $\varepsilon \equiv \varepsilon_{zz}$. *Let also* $\chi^{(i)}(r,z)=\sum_{k=0}^{4} z^k f_k^{(i)}(r)$ *be the special representation of the Love's solution, possessing completeness for the* ε_{zz}*-no-decaying* BVPs. *Then, it is possible to prove that, for an arbitrary number of hollow phases* $n\in\mathbb{N}$, *the field equations of the differential* BVP *are always reducible to an in cascade one-dimensional Euler-like non-homogeneous differential system.*

Proof.

Due to Theorem 1, let us assume that in each *i*-th phase, $\chi^{(i)}$ possesses the form

$$\chi^{(i)}=\sum_{k=0}^{5} z^k\ f_k^{(i)}(r), \tag{9.18}$$

in which $f_k^{(i)}(r)$ are scalar functions to determine and the adding fifth order term is introduced in order to find at least one decaying solution, too. Firstly, the differential conditions required for $f_k^{(i)}(r)$ to satisfy equation (9.4) have to be established. To obtain this, we apply the fourth-order differential operator ∇^4 to the (9.18). By collecting the terms in z^k we can write explicitly:

$$\begin{aligned}\nabla^4\chi^{(i)}=0\Rightarrow\ & (f_{0,r}^{(i)}-r\,f_{0,rr}^{(i)}+2r^2 f_{0,rrr}^{(i)}+r^3 f_{0,rrrr}^{(i)}+4r^2 f_{2,r}^{(i)}+4r^3 f_{2,rr}^{(i)}+24r^3 f_4^{(i)})+\\ &+z(f_{1,r}^{(i)}-r\,f_{1,rr}^{(i)}+2r^2 f_{1,rrr}^{(i)}+r^3 f_{1,rrrr}^{(i)}+12r^2 f_{3,r}^{(i)}+12r^3 f_{3,rr}^{(i)}+120r^3 f_5^{(i)})+\\ &+z^2(f_{2,r}^{(i)}-r\,f_{2,rr}^{(i)}+2r^2 f_{2,rrr}^{(i)}+r^3 f_{2,rrrr}^{(i)}+24r^2 f_{4,r}^{(i)}+24r^3 f_{4,rr}^{(i)})+\\ &+z^3(f_{3,r}^{(i)}-r\,f_{3,rr}^{(i)}+2r^2 f_{3,rrr}^{(i)}+r^3 f_{3,rrrr}^{(i)}+40r^2 f_{5,r}^{(i)}+40r^3 f_{5,rr}^{(i)})+\\ &+z^4(f_{4,r}^{(i)}-r\,f_{4,rr}^{(i)}+2r^2 f_{4,rrr}^{(i)}+r^3 f_{4,rrrr}^{(i)})+\\ &+z^5(f_{5,r}^{(i)}-r\,f_{5,rr}^{(i)}+2r^2 f_{5,rrr}^{(i)}+r^3 f_{5,rrrr}^{(i)})=0,\end{aligned} \tag{9.19}$$

which can be written in a compact form as follows

$$\begin{aligned}\nabla^4\chi^{(i)}(r,z)=0\Rightarrow\sum_{k=0}^{5}\{z^k[&(f_{k,r}^{(i)}-r\,f_{k,rr}^{(i)}+2r^2 f_{k,rrr}^{(i)}+r^3 f_{k,rrrr}^{(i)})+\\ &+\frac{2(k+2)!}{k!}(\sum_{j=4}^{5}(1-\delta_{jk}))\,r^2(r\,f_{k+2,r}^{(i)})_{,r}+(k+4)!(\sum_{m=2}^{5}(1-\delta_{mk}))\,r^3 f_{k+4}^{(i)}]\}=0,\end{aligned} \tag{9.20}$$

where δ_{jk} and δ_{mk} are the usual Kronecker delta operators.

In order to solve (9.20) we can follow a *cascade* strategy: indeed, we see that, for the polynomial identity law, it is possible to firstly extract from equation (9.20) the following un-coupled differential system with varying coefficients, starting from the last two rows of equation (9.19):

$$f_{k,r}^{(i)}-r\,f_{k,rr}^{(i)}+2r^2 f_{k,rrr}^{(i)}+r^3 f_{k,rrrr}^{(i)}=0,\quad k=4,5. \tag{9.21}$$

The solutions of (9.21) are

$$f_k^{(i)}(r)=C_{1/k}^{(i)}\log r+C_{2/k}^{(i)}r^2+C_{3/k}^{(i)}r^2\log r+C_{4/k}^{(i)},\quad k=4,5 \tag{9.22}$$

where $\{C_{1/k}^{(i)}, C_{2/k}^{(i)}, C_{3/k}^{(i)}, C_{4/k}^{(i)}\}$ are arbitrary constant coefficients. For seek of simplicity we rename $f_k^{(i)}(r) \equiv h_k^{(i)}(r)$ to represent the specific homogeneous solution of the equations (9.21). The notation utilized here for the characterization of the coefficients $C_{n/k}^{(i)}$ must be read in this manner: the superscript (i) is referred to the material phase *i*-th, the first subscript n tells us the number of the constant, the second subscript k is related to the corresponding function $f_k^{(i)}(r)$ and therefore to the power in z^k. By utilizing the obtained solutions (9.22) and substituting them into (9.19), we can extract other two un-coupled differential equations

$$f_{k,r}^{(i)} - r\, f_{k,rr}^{(i)} + 2r^2 f_{k,rrr}^{(i)} + r^3 f_{k,rrrr}^{(i)} = -10\, r^3 (k+1)^2 \left[C_{2/k+2}^{(i)} + C_{3/k+2}^{(i)} (1+\log r) \right], \quad k = 2,3. \tag{9.23}$$

We note that the homogeneous equation associated to (9.23) is formally the same of the case (9.21) and then it is possible to write the solution of (9.23) utilizing (9.22) as follows

$$f_k^{(i)}(r) = h_k^{(i)}(r) - \left(\frac{2k-1}{4} \right) r^4 \left[2C_{2/k+2}^{(i)} + C_{3/k+2}^{(i)} (2\log r - 1) \right], \qquad k = 2,3. \tag{9.24}$$

Finally, substituting the solutions (9.24) and (9.22) into the first two lines of (9.19), the remaining two differential un-coupled equations can be extracted:

$$\begin{aligned} f_{k,r}^{(i)} - r\, f_{k,rr}^{(i)} + 2r^2 f_{k,rrr}^{(i)} + r^3 f_{k,rrrr}^{(i)} &= r^3 \{ 16(2k+1)\left(C_{2/k+2}^{(i)} + C_{3/k+2}^{(i)} \right) + \\ + (2k+3) C_{4/k+4}^{(i)} (1+\log r) + 2C_{3/k+2}^{(i)} \log r - 3(2k+3) r^2 \left(C_{2/k+4}^{(i)} + C_{3/k+4}^{(i)} \log r \right) \}, \quad k = 0,1 \end{aligned} \tag{9.25}$$

from which we obtain

$$\begin{aligned} f_k^{(i)}(r) = \frac{(2k+1) r^4}{8} \left(C_{3/k+2}^{(i)} - 2C_{2/k+2}^{(i)} \right) + \frac{(4k+1) r^4}{48} \left[27 C_{1/k+4}^{(i)} - 18 C_{4/k+4}^{(i)} + r^2 \left(6C_{2/k+4}^{(i)} - 5C_{3/k+4}^{(i)} \right) \right] + \\ - 6 \left[3(4k+1) C_{1/k+4}^{(i)} + 2(2k+1) C_{3/k+2}^{(i)} - (4k+1) C_{3/k+4}^{(i)} \log r \right] r^6 + h_k^{(i)}(r), \qquad k = 0,1. \end{aligned} \tag{9.26}$$

It is worth noticing that, since in each above mentioned group of differential equations (9.21), (9.23) and (9.25), the homogeneous solution is always furnished by $h_k^{(i)}(r)$, we can also write

$$f_k^{(i)}(r) = h_k^{(i)}(r) + p_k^{(i)}(r), \quad \forall k \in \{0,1,...,5\} \tag{9.27}$$

where $p_k^{(i)}(r)$ represents the particular solution related to the specific differential problems (9.23) – for $k = 2,3$ – and (9.25), for $k = 0,1$, being $p_k^{(i)}(r) = 0$ when $k = 4,5$. Then, the above proposed *in cascade* solving strategy leads to summarize the obtained results as follows. Let us consider the Love's function (9.18), representing the general form of the elastic solution for ε_{zz} *-no-decaying in* multilayered cylinder under axis-symmetrical boundary conditions. As already seen before, the field equation (9.19) furnishes an *in cascade* uncoupled system of Euler-like differential equations for the unknown functions $f_k^{(i)}(r)$. This result can be expressed as follows, by using some elements of Functional Analysis:

PROPERTY 2: *Let $\mathcal{V}$ and $\mathcal{W}$ be two vector spaces and $\mathbf{L} := \mathcal{L}^E \mathbf{I} \,|\, \mathcal{V} \mapsto \mathcal{W}$ a linear operator, where $\mathbf{I}$ is a sixth-order identity matrix and $\mathcal{L}^E = (*)_{,r} - r(*)_{,rr} + 2r^2 (*)_{,rrr} + r^3 (*)_{,rrrr}$ represents the Euler differential operator. Let also $\overline{\boldsymbol{f}}^{(i)} = [\overline{f}_0^{(i)}, \overline{f}_1^{(i)}, ..., \overline{f}_5^{(i)}]^T \in \mathcal{W}$ be the vector collecting the six known functions appearing to the right-hand of the equations (9.22), (9.24), (9.26) and $\boldsymbol{p}^{(i)} = [p_0^{(i)}, p_1^{(i)}, ..., p_5^{(i)}]^T \in \mathcal{V}$ a solution of the equation*

$$\mathbf{L}\, \boldsymbol{f}^{(i)} = \overline{\boldsymbol{f}}^{(i)}, \tag{9.28}$$

where $\boldsymbol{f}^{(i)} = [f_0^{(i)}, f_1^{(i)}, ..., f_5^{(i)}]^T \in \mathcal{V}$ is the unknown vector. Then, the set $\mathcal{S}$ of all the solutions of (9.28) is given by:

$$\mathcal{S} = \boldsymbol{p}^{(i)} + \ker \mathbf{L}, \tag{9.29}$$

where $\ker \mathbf{L} \equiv \{\boldsymbol{h}^{(i)} = [h_0^{(i)}, h_1^{(i)}, ..., h_5^{(i)}]^T \in \mathcal{V}\}$.

Equation (9.29) summarizes the system {(9.22), (9.24), (9.26)}, so that it gives (9.27). Therefore, Theorem 2 has to be considered a *constructive* theorem, in the sense that it suggests a procedure to find solutions to the equation (9.28) by first searching a particular solution $\boldsymbol{p}^{(i)} \in \mathcal{V}$, that exists if and only if $\overline{\boldsymbol{f}}^{(i)} \in \mathrm{Im}\,\mathbf{L}$, and hence determining $\ker \mathbf{L} \equiv \{\boldsymbol{h}^{(i)} \in \mathcal{V} \,\big|\, \mathbf{L}\,\boldsymbol{h}^{(i)} = \mathbf{0}\}$. As detailed above, the solution will be constructed by adding the two found solutions. Finally, it is worth to highlight that the functions (9.22), (9.24) and (9.26), due to both the proposed theorem and the form (9.18), constitute a class of axis-symmetrical elastic solutions of multilayered cylinder able to satisfy the field equations for all *no-decaying* BVPs, while - due to the introduction of fifth-order powers of z - only some *decaying* cases can be obtained.

9.5 Complete set of closed-form solutions for no-decaying problems

9.5.1 The engineering framework

The object of this section is to find exact elastic solutions for *multilayered cylinder* under axis-symmetrical load conditions, producing no-decaying of the strain ε_{zz} along the radius direction as already shown above. It is possible to show that these solutions result extremely useful in many engineering applications. For example, in the framework of the *distributed optical measurements*, they furnish qualitative and quantitative results which help us to better explain the mechanism of the strain transferring, as well as to set the bases for interpreting post-elastic and non-linear phenomena. Indeed, by using techniques based on the *Stimulated Brillouin Scattering Effect* (BSE), it is possible to experimentally read - in bending concrete or steel beams - the varying strain function ε_{zz} by embedding a continuous *optical fibre* in the structure. Due to both the type of link between materials and the composite nature of the optical fibre, characterized by a central glass core and one or more polymeric claddings, some dispersion phenomena appear in the transferring of the strain from the structure to the fibre itself. However, numerical simulations and laboratory tests show that possible decaying effects remain confined in limited regions around the ends of the structure, as well as in the proximity of points where changing of strain sign or significant deformation gradients appear. However, other possible decaying effects of the axial strain could also be related to the specific interactions developing at the interfaces between support material, cladding and optical fibre core. For this reason, the solution found below can be employed with the goal of highlighting qualitative and quantitative mechanical aspects in the framework of this new engineering application, as well as – more in general - in the characterization of the mechanics of laminated composites.

9.5.2 Field equations

With reference to the equation (9.8), we can write the axial strain in z-direction inside the generic *i*-th phase as follows:

$$\varepsilon_{zz}^{(i)} = W_{,z}^{(i)} = \frac{1}{2\mu^{(i)}}\left[\frac{\mu^{(i)}}{\mu^{(i)}+\lambda^{(i)}}(\nabla^2\chi^{(i)})_{,z} + \chi_{,rrz}^{(i)} + r^{-1}\chi_{,rz}^{(i)}\right]. \tag{9.30}$$

By recalling equation (9.18), the (9.30) becomes

$$\varepsilon_{zz}^{(i)} = \frac{1}{2\mu^{(i)}(\mu^{(i)}+\lambda^{(i)})}\left\{\sum_{k=0}^{5} k\left[(2\mu^{(i)}+\lambda^{(i)})z^{k-1}\left(f_{k,rr}^{(i)}(r) + r^{-1}f_{k,r}^{(i)}(r)\right) + \mu^{(i)}(k-1)(k-2)z^{k-3}f_k^{(i)}(r)\right]\right\} \tag{9.31}$$

so that, because $\varepsilon_{zz}^{(i)} = \varepsilon_0 + \varepsilon_1 z,\ \forall i \in \{0,1...n\}$ by virtue of the Theorem 1 for the *no-decaying* assumption, collecting the terms in the powers of z, we have to solve the following set of differential equations:

$$\begin{cases}(2\mu^{(i)}+\lambda^{(i)})(f^{(i)}_{1,rr}+r^{-1}f^{(i)}_{1,r})+6\mu^{(i)}f^{(i)}_{3}=2\mu^{(i)}(\mu^{(i)}+\lambda^{(i)})\varepsilon_0\\ (2\mu^{(i)}+\lambda^{(i)})(f^{(i)}_{2,rr}+r^{-1}f^{(i)}_{2,r})+12\mu^{(i)}f^{(i)}_{4}=\mu^{(i)}(\mu^{(i)}+\lambda^{(i)})\varepsilon_1\\ (2\mu^{(i)}+\lambda^{(i)})(f^{(i)}_{3,rr}+r^{-1}f^{(i)}_{3,r})+20\mu^{(i)}f^{(i)}_{5}=0\\ (f^{(i)}_{4,rr}+r^{-1}f^{(i)}_{4,r})=0\\ (f^{(i)}_{5,rr}+r^{-1}f^{(i)}_{5,r})=0.\end{cases} \tag{9.32}$$

By using the above obtained expressions (9.22), (9.24) and (9.26) for the functions $f^{(i)}(r)$, system (9.32) becomes algebraic. The solution can be written only establishing the relations between the coefficients $C^{(i)}_{j/k}$, starting from the last two equations in (9.32) and then solving the first three ones, by means of the analogous cascade technique used above. To make this, we substitute equations (9.22), (9.24) and (9.26) into (9.32), obtaining, by means of some algebraic manipulations, the following coefficients:

$$\begin{aligned}&C^{(i)}_{3/4}=C^{(i)}_{2/4}=C^{(i)}_{3/3}=C^{(i)}_{2/3}=0;\quad C^{(i)}_{1/5}=C^{(i)}_{2/5}=C^{(i)}_{3/5}=C^{(i)}_{4/5}=0;\ C^{(i)}_{1/3}=-\frac{2\mu^{(i)}+\lambda^{(i)}}{3\mu^{(i)}}C^{(i)}_{3/1};\\ &C^{(i)}_{1/4}=-\frac{2\mu^{(i)}+\lambda^{(i)}}{3\mu^{(i)}}C^{(i)}_{3/2};\quad C^{(i)}_{4/3}=-\frac{2\mu^{(i)}+\lambda^{(i)}}{3\mu^{(i)}}\left(2C^{(i)}_{3/1}+2C^{(i)}_{2/1}\right)+\frac{\varepsilon_0}{3}\left(\mu^{(i)}+\lambda^{(i)}\right);\\ &C^{(i)}_{4/4}=-\frac{2\mu^{(i)}+\lambda^{(i)}}{3\mu^{(i)}}\left(C^{(i)}_{3/2}+C^{(i)}_{2/2}\right)+\frac{\varepsilon_1}{12}\left(\mu^{(i)}+\lambda^{(i)}\right).\end{aligned} \tag{9.33}$$

It is worth to note that equation $(9.33)_2$ highlights that, for the no-decaying case, the bi-harmonic function has to be a polynomial of fourth order, being all the coefficients characterizing $f^{(i)}_5(r)$ equal to zero, as we already know. By invoking (9.8), it is possible to write the displacement field for the generic *i*-th phase as follows

$$\begin{aligned}U^{(i)}&=\frac{1}{\mu^{(i)}r}\left[-\frac{C^{(i)}_{1/1}}{2}-C^{(i)}_{1/2}z+\frac{z^2(2\mu^{(i)}+\lambda^{(i)})}{\mu^{(i)}}\left(C^{(i)}_{3/1}+\frac{2}{3}C^{(i)}_{3/2}z\right)\right]+\\ &\quad-\frac{r}{\mu^{(i)}}\left[C^{(i)}_{2/1}+C^{(i)}_{3/1}\left(\log r+\frac{1}{2}\right)+z\left(2C^{(i)}_{2/2}+C^{(i)}_{3/2}+2C^{(i)}_{3/2}\log r\right)\right],\\ W^{(i)}&=\varepsilon_0 z+\frac{\varepsilon_1 z^2}{2}+\left[\frac{C^{(i)}_{1/2}\mu^{(i)}+2C^{(i)}_{3/0}(2\mu^{(i)}+\lambda^{(i)})}{(\mu^{(i)}+\lambda^{(i)})}+\frac{C^{(i)}_{3/2}(\mu^{(i)}+\lambda^{(i)})}{2\mu^{(i)}}r^2\right]\frac{\log r}{\mu^{(i)}}+\\ &\quad+\left[\frac{4C^{(i)}_{2/2}(\mu^{(i)}+\lambda^{(i)})-\varepsilon_1\mu^{(i)}(2\mu^{(i)}+\lambda^{(i)})}{4\mu^{(i)2}}\right]r^2+w^{(i)}_0\qquad i\equiv\{1,2,...n\},\end{aligned} \tag{9.34}$$

where, due to presence of diverging terms for vanishing *r*, we assume (9.34) to hold only for the *i*-th hollow phases. On the contrary, by excluding terms affected by r^{-1} and $\log r$, for the cylindrical core phase we write down:

$$\begin{aligned}U^{(0)}&=-\frac{r}{\mu^{(0)}}\left(C^{(0)}_{2/1}+2C^{(0)}_{2/2}z\right),\\ W^{(0)}&=\varepsilon_0 z+\frac{\varepsilon_1 z^2}{2}+\left[\frac{4C^{(0)}_{2/2}(\mu^{(0)}+\lambda^{(0)})-\varepsilon_1\mu^{(0)}(2\mu^{(0)}+\lambda^{(0)})}{4\mu^{(0)2}}\right]r^2.\end{aligned} \tag{9.35}$$

where the superscript "(0)" stands for the *core*-phase. As a consequence of (9.34) and (9.35), the stresses for the hollow phases are

$$
\begin{aligned}
\sigma_{rr}^{(i)} &= +\varepsilon_0\lambda^{(i)} - \frac{C_{3/1}^{(i)}\left(3\mu^{(i)}+2\lambda^{(i)}\right)}{\mu^{(i)}} - \frac{2C_{2/1}^{(i)}\left(\lambda^{(i)}+\mu^{(i)}\right)}{\mu^{(i)}} + \frac{z}{\mu^{(i)}}\begin{bmatrix}\varepsilon_1\lambda^{(i)}\mu^{(i)} - 4C_{2/2}^{(i)}\left(\mu^{(i)}+\lambda^{(i)}\right)\\ -2C_{3/2}^{(i)}\left(3\mu^{(i)}+2\lambda^{(i)}\right)\end{bmatrix} + \\
&\quad - 2\left(C_{3/1}^{(i)}+2C_{3/2}^{(i)}z\right)\left(\frac{\lambda^{(i)}+\mu^{(i)}}{\mu^{(i)}}\right)\log r + \frac{1}{r^2}\left[C_{1/1}^{(i)} + 2C_{1/2}^{(i)}z - \frac{z^2}{\mu^{(i)}}\left(2\mu^{(i)}+\lambda^{(i)}\right)\left(C_{3/1}^{(i)}+\frac{2}{3}C_{3/2}^{(i)}z\right)\right] \\
\sigma_{\theta\theta}^{(i)} &= +\varepsilon_0\lambda^{(i)} - \frac{1}{\mu^{(i)}}\left[C_{3/1}^{(i)}\left(\mu^{(i)}+2\lambda^{(i)}\right) + 2C_{2/1}^{(i)}\left(\mu^{(i)}+\lambda^{(i)}\right)\right] - \frac{z}{\mu^{(i)}}\begin{bmatrix}-\varepsilon_1\lambda^{(i)}\mu^{(i)} + 4C_{2/2}^{(i)}\left(\mu^{(i)}+\lambda^{(i)}\right)\\ +2C_{3/2}^{(i)}\left(\mu^{(i)}+2\lambda^{(i)}\right)\end{bmatrix} + \\
&\quad - 2\left(C_{3/1}^{(i)}+2C_{3/2}^{(i)}z\right)\left(\frac{\lambda^{(i)}+\mu^{(i)}}{\mu^{(i)}}\right)\log r - \frac{1}{r^2}\left[C_{1/1}^{(i)} + 2C_{1/2}^{(i)}z - \frac{z^2}{\mu^{(i)}}\left(2\mu^{(i)}+\lambda^{(i)}\right)\left(C_{3/1}^{(i)}+\frac{2}{3}C_{3/2}^{(i)}z\right)\right] \\
\sigma_{zz}^{(i)} &= \left(2\mu^{(i)}+\lambda^{(i)}\right)\left(\varepsilon_0+\varepsilon_1 z\right) - \frac{2\lambda^{(i)}}{\mu^{(i)}}\left[\left(C_{3/1}^{(i)}+C_{2/1}^{(i)}\right) + \left(C_{3/1}^{(i)}+2C_{3/2}^{(i)}z\right)\log r + 2\left(C_{3/2}^{(i)}+C_{2/2}^{(i)}\right)z\right] \\
\tau_{\theta z}^{(i)} &= \tau_{r\theta}^{(i)} = 0 \\
\tau_{rz}^{(i)} &= \frac{2\mu^{(i)}+\lambda^{(i)}}{r\mu^{(i)}}\left[2z\left(C_{3/1}^{(i)}+C_{3/2}^{(i)}z\right) + \frac{\mu^{(i)}}{\mu^{(i)}+\lambda^{(i)}}\left(2C_{3/0}^{(i)} - \frac{C_{1/2}^{(i)}\lambda^{(i)}}{2\mu^{(i)}+\lambda^{(i)}}\right)\right] + \\
&\quad + \frac{r\lambda^{(i)}}{\mu^{(i)}}\left[2C_{2/2}^{(i)} + C_{3/2}^{(i)}\left(1+2\log r\right) - \frac{\varepsilon_1\mu^{(i)}\left(2\mu^{(i)}+\lambda^{(i)}\right)}{2\lambda^{(i)}}\right], \qquad i \equiv \{1,2,...n\}.
\end{aligned}
\tag{9.36}
$$

while those within the core are given by:

$$
\begin{aligned}
&\sigma_{rr}^{(0)} = \sigma_{\theta\theta}^{(0)} = \left(\varepsilon_0+\varepsilon_1 z\right)\lambda^{(0)} - 2\frac{\left(\mu^{(0)}+\lambda^{(0)}\right)}{\mu^{(0)}}\left(C_{2/1}^{(0)}+2C_{2/2}^{(0)}z\right), \quad \tau_{\theta z}^{(0)} = \tau_{r\theta}^{(0)} = 0, \\
&\sigma_{zz}^{(0)} = \left(\varepsilon_0+\varepsilon_1 z\right)\left(2\mu^{(0)}+\lambda^{(0)}\right) - \frac{2\lambda^{(i)}}{\mu^{(i)}}\left(C_{2/1}^{(0)}+2C_{2/2}^{(0)}z\right), \ \tau_{rz}^{(0)} = r\left(\frac{2\lambda^{(0)}}{\mu^{(0)}}C_{2/2}^{(0)} - \frac{2\mu^{(0)}+\lambda^{(0)}}{2}\varepsilon_1\right)
\end{aligned}
\tag{9.37}
$$

9.5.3. Equilibrium and compatibility conditions

The results obtained until now satisfy the equilibrium and compatibility equations inside each generic *i*-th phase of *multilayered cylinder* subjected to axis-symmetrical strains and come out from the application of Theorem 2. Under both the hypothesis of linear isotropic elastic behaviour of the homogeneous materials and the assumption of perfect bond at the cylindrical interfacial boundaries (no de-lamination or friction phenomena), we have now to establish the satisfaction of both the equilibrium and the compatibility equations at the boundary surfaces between two generic adjacent phases. To obtain this, we will make reference to the generic case, in which a functionally graded circular cylinder is constituted by a central *core* and *n* arbitrary hollow phases (Fig. 9.1). In this framework the following theorem can be established:

THEOREM 3: *Let us consider a multilayered cylinder, subjected to axis-symmetrical boundary conditions and let be* $\varepsilon \equiv \varepsilon_{zz}$. *Let also* $\chi^{(i)}(r,z) = \sum_{k=0}^{4} z^k f_k^{(i)}(r)$ *be the special representation of the Love's solution, possessing completeness for the* ε*-no-decaying* BVPs. *Then, for an arbitrary number of hollow phases* $(n \in \mathbb{N})$, *the equilibrium and compatibility conditions at the interfacial boundaries of the phases yield a linear algebraic problem in the form* $\mathbf{P}\,\mathbf{X} = \mathbf{L}$, *being* $\mathbf{X}$ *the unknown vector collecting* $C_{n/k}^{(i)}$, $\mathbf{L}$ *the vector of boundary data and* $\mathbb{P}$ *a* $(6n+4)$*-order square matrix.*

Proof.

In continuity with the way followed until now, by accounting the interfacial boundary conditions, we obtain that $C_{3/1}^{(i)} = C_{3/2}^{(i)} = 0,\ \forall i \in \{0,1,...,n\}$, therefore the total unknown parameters to determine can be summarized as follows:

$$\begin{aligned} &C_{1/2}^{(0)}, C_{2/1}^{(0)}, \\ &C_{3/0}^{(i)}, C_{1/1}^{(i)}, C_{1/2}^{(i)}, C_{2/1}^{(i)}, C_{2/2}^{(i)}, w_0^{(i)}, \quad i \in \{1,2,.....n\} \\ &\varepsilon_0, \varepsilon_1, \end{aligned} \tag{9.38}$$

where those in $(9.38)_1$ represent the unknown coefficients of the *core*, those in $(9.38)_2$ represent the unknown parameters for every hollow cylinder, while $(9.38)_3$ are the two coefficients responsible for the assigned linear form of the strain ε_{zz}, (9.13). Hence, the total number of unknowns will be $(6n+4)$, which equals the number of algebraic equations to solve. In particular, as we will show in the follows, the number of the boundary equations at the interfaces is $6n$, while 4 is the number of both strong (3) and weak (1) boundary conditions on the external cylindrical surface and on the end basis, respectively. In particular, we begin writing the 6*n* equilibrium and compatibility equations at the generic interface, that is:

$$\begin{cases} U^{(i)}(r=R^{(i)}) = U^{(i+1)}(r=R^{(i)}) \\ W^{(i)}(r=R^{(i)}) = W^{(i+1)}(r=R^{(i)}) \\ \sigma_{rr}^{(i)}(r=R^{(i)}) = \sigma_{rr}^{(i+1)}(r=R^{(i)}) \\ \tau_{rz}^{(i)}(r=R^{(i)}) = \tau_{rz}^{(i+1)}(r=R^{(i)}) \end{cases} \qquad \forall i \in \{0,1,...,n-1\} \tag{9.39}$$

where $R^{(i)}$ is the outer radius of the *i*-th phase. Recalling the previously obtained results, system (9.39) can be expressed as follows

$$\begin{cases} \dfrac{C_{1/1}^{(i+1)}}{2R^{(i)}\mu^{(i+1)}} + \dfrac{C_{2/1}^{(i+1)}R^{(i)}}{\mu^{(i+1)}} - \dfrac{C_{1/1}^{(i)}}{2R^{(i)}\mu^{(i)}} - \dfrac{C_{2/1}^{(i)}}{\mu^{(i)}} = 0 \\ \dfrac{C_{1/2}^{(i+1)}}{R^{(i)}\mu^{(i+1)}} + \dfrac{2C_{2/2}^{(i+1)}R^{(i)}}{\mu^{(i+1)}} - \dfrac{C_{1/2}^{(i)}}{R^{(i)}\mu^{(i)}} - \dfrac{2C_{2/2}^{(i)}R^{(i)}}{\mu^{(i)}} = 0 \\ w_0^{(i)} - w_0^{(i+1)} + \dfrac{C_{2/2}^{(i)}R^{(i)2}\left(\mu^{(i)}+\lambda^{(i)}\right)}{\mu^{(i)2}} - \dfrac{C_{2/2}^{(i+1)}R^{(i)2}\left(\mu^{(i+1)}+\lambda^{(i+1)}\right)}{\mu^{(i+1)2}} + \dfrac{R^{(i)2}\left(\mu^{(i)}\lambda^{(i+1)} - \lambda^{(i)}\mu^{(i+1)}\right)}{\mu^{(i+1)2}} + \\ \quad + \dfrac{C_{1/2}^{(i)}\log R^{(i)}}{\left(\mu^{(i)}+\lambda^{(i)}\right)} + \dfrac{C_{1/2}^{(i+1)}\log R^{(i)}}{\mu^{(i+1)}+\lambda^{(i+1)}} + \dfrac{2C_{3/0}^{(i)}\log R^{(i)}\left(2\mu^{(i)}+\lambda^{(i)}\right)}{\mu^{(i)}\left(\mu^{(i)}+\lambda^{(i)}\right)} - \dfrac{2C_{3/0}^{(i+1)}\log R^{(i)}\left(2\mu^{(i+1)}+\lambda^{(i+1)}\right)}{\mu^{(i+1)}\left(\mu^{(i+1)}+\lambda^{(i+1)}\right)} = 0 \\ \dfrac{C_{1/1}^{(i)}}{R^{(i)2}} - \dfrac{C_{1/1}^{(i+1)}}{R^{(i)2}} + \varepsilon_0\left(\lambda^{(i)} - \lambda^{(i+1)}\right) + 2\left[\dfrac{C_{2/1}^{(i+1)}\left(\mu^{(i+1)}+\lambda^{(i+1)}\right)}{\mu^{(i+1)}} - \dfrac{C_{2/1}^{(i)}\left(\mu^{(i)}+\lambda^{(i)}\right)}{\mu^{(i)}}\right] = 0 \\ \dfrac{2C_{1/2}^{(i)}}{R^{(i)2}} - \dfrac{2C_{1/2}^{(i+1)}}{R^{(i)2}} + \varepsilon_1\left(\lambda^{(i)} - \lambda^{(i+1)}\right) + 4\left[\dfrac{C_{2/2}^{(i+1)}\left(\mu^{(i+1)}+\lambda^{(i+1)}\right)}{\mu^{(i+1)}} - \dfrac{C_{2/2}^{(i)}\left(\mu^{(i)}+\lambda^{(i)}\right)}{\mu^{(i)}}\right] = 0 \\ \dfrac{2C_{2/2}^{(i)}R^{(i)}\lambda^{(i)}}{\mu^{(i)}} - \dfrac{C_{1/2}^{(i)}\lambda^{(i)}}{R^{(i)}\left(\mu^{(i)}+\lambda^{(i)}\right)} + \dfrac{2C_{3/0}^{(i)}\left(2\mu^{(i)}+\lambda^{(i)}\right)}{R^{(i)}\left(\mu^{(i)}+\lambda^{(i)}\right)} - \dfrac{2C_{2/2}^{(i+1)}R^{(i)}\lambda^{(i+1)}}{\mu^{(i+1)}} + \dfrac{C_{1/2}^{(i+1)}\lambda^{(i+1)}}{R^{(i)}\left(\mu^{(i+1)}+\lambda^{(i+1)}\right)} + \\ \quad + \dfrac{\varepsilon_1 R^{(i)}\left[\left(2\mu^{(i+1)}+\lambda^{(i+1)}\right) - \left(2\mu^{(i)}+\lambda^{(i)}\right)\right]}{2} - \dfrac{2C_{3/0}^{(i+1)}\left(2\mu^{(i+1)}+\lambda^{(i+1)}\right)}{R^{(i)}\left(\mu^{(i+1)}+\lambda^{(i+1)}\right)} = 0, \end{cases}$$

$$\forall i \in \{0,1,.....n-1\} \tag{9.40}$$

in which, for the *core* ($i=0$), $C_{3/0}^{(0)}=0, C_{1/1}^{(0)}=0, C_{1/2}^{(0)}=0, w_0^{(0)}=0$. It is worth to note that the initial four equations (9.39) become six in (9.40): this happens because, by invoking the polynomial identity law and then collecting the terms in the powers of z, some solutions are immediately obtained, and only six independent equations (9.40) remain to satisfy, at every interface. The equilibrium equations for the tractions on the external cylindrical boundary surface, ($i=n$), give:

$$\sigma_{rr}^{(n)}(r=R^{(n)})=p_0+p_1 z, \qquad \tau_{rz}^{(n)}(r=R^{(n)})=\tau_0 \tag{9.41}$$

from which, by applying the polynomial identity law, they transform as follows:

$$\begin{cases} \dfrac{C_{1/1}^{(n)}}{R^{(n)2}}-\dfrac{2C_{2/1}^{(n)}\left(\mu^{(n)}+\lambda^{(n)}\right)}{\mu^{(n)}}+\varepsilon_0\lambda^{(n)}=p_0 \\ \dfrac{2C_{1/2}^{(n)}}{R^{(n)2}}-\dfrac{2C_{2/2}^{(n)}\left(\mu^{(n)}+\lambda^{(n)}\right)}{\mu^{(n)}}+\varepsilon_1\lambda^{(n)}=p_1 \\ \dfrac{2C_{2/2}^{(n)}R^{(n)}\lambda^{(n)}}{\mu^{(n)}}-\dfrac{C_{1/2}^{(n)}\lambda^{(n)}}{R^{(n)}\left(\mu^{(n)}+\lambda^{(n)}\right)}-\dfrac{1}{2}R^{(n)}\varepsilon_1\left(2\mu^{(n)}+\lambda^{(n)}\right)+\dfrac{2C_{3/0}^{(n)}\left(2\mu^{(n)}+\lambda^{(n)}\right)}{R^{(n)}\left(\mu^{(n)}+\lambda^{(n)}\right)}=\tau_0 \end{cases} \tag{9.42}$$

where the set $\{p_0, p_1, \tau_0\}$ collects load parameters defining the traction field on $\partial\Omega^{cyl}$. Finally, it remains to consider the last equilibrium equation in z-direction on one of the basis, being the other end condition automatically satisfied. Therefore, without loss of generality, for $z=0$ we can write

$$\begin{aligned} &\int_0^{2\pi}\int_0^{R^{(0)}}\sigma_{zz}^{(0)}(z=0)rdrd\theta+\sum_{i=1}^{n}\int_0^{2\pi}\int_{R^{(i-1)}}^{R^{(i)}}\sigma_{zz}^{(i)}(z=0)rdrd\theta= \\ &=\pi\varepsilon_0\left[\left(2\mu^{(i)}+\lambda^{(i)}\right)R^{(n)2}+\sum_{i=0}^{n-1}R^{(i)2}\left(2\mu^{(i)}+\lambda^{(i)}-2\mu^{(i+1)}-\lambda^{(i+1)}\right)\right]+ \\ &-\frac{2\pi\lambda^{(0)}C_{2/1}^{(0)}R^{(0)2}}{\mu^{(0)}}+\sum_{i=1}^{n}\frac{2\pi\lambda^{(i)}C_{2/1}^{(i)}(R^{(i-1)2}-R^{(i)2})}{\mu^{(i)}}=N_z, \end{aligned} \tag{9.43}$$

where N_z is the total axial force applied at $z=0$. The solutions found above are then able to describe the case in which an multilayered cylinder made by n circular hollow cylinders and a central *core* is loaded by a combination of linear radial pressures, uniform shear tractions, and axial forces applied at the ends. In order to solve the algebraic system constituted by (9.40), (9.42) and (9.43), it is convenient to re-arrange the whole $(6n+4)\times(6n+4)$ algebraic system following a matrix-based procedure. Indeed, we can collect the known terms in the *load* vector $\mathbf{L}$

$$\mathbf{L}^T=\{0,...,p_0,p_1,\tau_0,N\} \tag{9.44}$$

where the only non zero terms are the last four ones, while the unknown parameters $C_{n/k}^{(i)}$, here renamed as $A_k^{(i)}$, can be collected in the vector $\mathbf{X}$ as follows

$$\mathbf{X}^T=\left\{A_4^{(0)},A_5^{(0)},A_1^{(1)},A_2^{(2)},...,A_6^{(1)},...,A_1^{(i)},A_2^{(i)},A_3^{(i)},A_4^{(i)},A_5^{(i)},A_6^{(i)},...,A_1^{(n)},A_2^{(n)},...,A_6^{(n)},\varepsilon_0,\varepsilon_1\right\} \tag{9.45}$$

so that the set of equations (9.40), (9.42) and (9.43) reads

$$\mathbf{P}\cdot\mathbf{X}=\mathbf{L} \tag{9.46}$$

where, for simplicity, we have renamed

$$A_1^{(i)}=C_{3/0}^{(i)}, A_2^{(i)}=C_{1/1}^{(i)}, A_3^{(i)}=C_{1/2}^{(i)}, A_4^{(i)}=C_{2/1}^{(i)}, A_5^{(i)}=C_{2/2}^{(i)}, A_6^{(i)}=w_0^{(i)}. \tag{9.47}$$

and $\mathbf{P}$ is a $(6n+4)\times(6n+4)$ square matrix containing the coefficients $P_{h/m}$, which are functions of both the radii and the elastic moduli of the phases. The explicit expression of the coefficients $P_{h/m}$ are reported in detail in the Appendix, section A.2. It is worth to note that, being the system (9.46) of linear and algebraic type, provided that $\det\mathbf{P}\neq 0$, it is possible to write the solution as follows

$$\mathbf{X}=\mathbf{P}^{-1}\mathbf{L}=\frac{1}{\det\mathbf{P}}\tilde{\mathbf{P}}^{T}\mathbf{L},\qquad X_m=\frac{1}{\det\mathbf{P}}\sum_{h=1}^{m=6n+4}\tilde{P}_{h/m}L_h, \tag{9.48}$$

where $\tilde{\mathbf{P}}=\mathrm{adj}[\mathbf{P}]$ is the adjoint matrix of $\mathbf{P}$ and then the *Cramer* rule has been employed. The possibility to invert the matrix $\mathbf{P}$ is ensured by invoking the uniqueness of the linear elastic solution, due to Kirchhoff's theorem, and investigating the "topological" properties of the elements of $\mathbf{P}$. This could appear not immediately evident if one directly tries to see the actual form of $\mathbb{P}$, but – on the other hand – it results essential for ensuring the existence of the solutions. For this reason, in the present paper, a rigorous proof that, for an arbitrary number of phases, $\det\mathbf{P}\neq 0$, is furnished and detailed in Section 9.7. However, as we will show in a subsequent paragraph, when the proposed strategy is applied to a three-phase composed cylinder, an analytical proof that the algebraic problem is well-posed is also given by utilizing the *Mathematica* code [Wolfram, S., 1998-2005], where the command *RowReduce* is employed. This command performs a version of Gaussian elimination, adding multiples of rows together so as to produce zero elements when possible. The final matrix is in reduced row echelon form. If this matrix is non-degenerate, as well as our case, RowReduce[$\mathbf{P}$] gives the *IdentityMatrix*[Length[$\mathbf{P}$]].
We need to remark that, by invoking the proposed theorem, the above presented procedure yields to construct the whole class of *no-decaying* solutions for multilayered cylinders, under axis-symmetrical load conditions. From the mechanical point of view, this means that this no-decaying class of solutions is constituted by any combination of z-linearly varying radial pressures, uniform shear tractions and axial forces applied at the end basis. As a trivial consequence, we can deduce that any other kind of boundary conditions shall be interpreted as producing *decaying* of the axial strain ε_{zz} along the radius direction.

9.6. Examples of closed-form solutions for "decaying" cases

9.6.1 Field equations

As previously said, in this section we need to show some possible special cases in which multilayered cylinder can exhibit decaying of the strain ε_{zz} along the radius direction. It is worth to recall that, while the proposed polynomial bi-harmonic function $\chi^{(i)}$ results able to describe the whole class of elastic solutions in the absence of decaying phenomena, the derived following solutions will furnish a particular class of problems associated with variation of the ε_{zz} along the radius direction. These solutions are here constructed in order to predict mechanical responses of multilayered cylinder in presence of *decaying* phenomena. With reference to the obtained solutions (9.22), (9.24) and (9.26) and to the above quoted elastic equilibrium equation (9.19), the number of unknown parameters of the function $\chi^{(i)}=\chi^{(i)}(r,z)$ for the generic *i*-th phase become now 24. Indeed, for each function $f_k^{(i)}(r)$ we have four coefficients to determine, that is:

$$C_{1/k}^{(i)},C_{2/k}^{(i)},C_{3/k}^{(i)},C_{4/k}^{(i)},\quad k\in\{0,1,...,5\}. \tag{9.49}$$

Actually, in order to obtain the displacement and stress field, some parameters appearing in (9.49) are unessential, so that it is possible to select as independent unknown coefficients the following 21 ones

$$\begin{aligned}&C_{2/0}^{(i)},C_{3/0}^{(i)},\qquad C_{1/1}^{(i)},C_{2/1}^{(i)},C_{3/1}^{(i)},\qquad C_{1/2}^{(i)},C_{2/2}^{(i)},C_{3/2}^{(i)},C_{4/2}^{(i)},\\&C_{1/3}^{(i)},C_{2/3}^{(i)},C_{3/3}^{(i)},C_{4/3}^{(i)},\quad C_{1/4}^{(i)},C_{2/4}^{(i)},C_{3/4}^{(i)},C_{4/4}^{(i)},\quad C_{1/5}^{(i)},C_{2/5}^{(i)},C_{3/5}^{(i)},C_{4/5}^{(i)}.\end{aligned} \tag{9.50}$$

Moreover, in analogy with the section 9.4.1, all the physical quantities referred to the central core have to be not divergent at $r=0$, so that the coefficients multiplying r^{-1} and $\log r$ must vanish. Then, the core unknown coefficients reduce to the following ten ones

$$C_{2/0}^{(0)},C_{2/1}^{(0)},C_{2/2}^{(0)},C_{4/2}^{(0)},C_{2/3}^{(0)},C_{4/3}^{(0)},C_{2/4}^{(0)},C_{4/4}^{(0)},C_{2/5}^{(0)},C_{4/5}^{(0)}. \tag{9.51}$$

9.6.2 Equilibrium and compatibility conditions

We begin by recalling the equilibrium and compatibility conditions (9.39) at the interfacial boundaries between every couple of adjacent phases, observing that:

- the $(9.39)_1$ and $(9.39)_3$ are both constituted by 5 algebraic equations, furnishing 10 overall equations;
- the $(9.39)_2$ and $(9.39)_4$ are both constituted by 6 algebraic equations, furnishing 12 overall equations;

therefore, the total number of equations becomes $22\times n$. Since the assumed mathematical structure of $\chi^{(i)}$ in (9.18) yields tractions on the external cylindrical surface characterized by radial pressures at most quadratic with z, as well as linearly varying shear, the Cauchy equilibrium equations are:

$$\sigma_{rr}^{(n)}(r=R^{(n)})=p_0+p_1z+p_2z^2,\qquad \tau_{rz}^{(n)}(r=R^{(n)})=\tau_0+\tau_1z \tag{9.52}$$

By utilizing the polynomial identity law and then collecting the terms in the powers of z, the $(9.52)_1$ is constituted by 5 equations, while the $(9.52)_2$ generates 6 equations, producing 11 overall algebraic equations to satisfy on the cylindrical boundary surface $\partial\Omega^{cyl}$. Moreover, it remains to consider the last equilibrium equation on only one of the end basis of the cylinder (for example where $z=0$), therefore

$$\int_0^{2\pi}\int_0^{R^{(0)}}\sigma_{zz}^{(0)}(z=0)rdrd\theta+\sum_{i=1}^{n}\int_0^{2\pi}\int_{R^{(i-1)}}^{R^{(i)}}\sigma_{zz}^{(i)}(z=0)\,rdrd\theta=N_z\,, \tag{9.53}$$

where N_z is the total axial force applied at $z=0$. Finally, we have $(22\times n+12)$ equations. By excluding the parameters related to rigid body motions, we reduce the unknowns to $(20\times n+8)$, that is

$$\begin{aligned}&C_{3/0}^{(i)},C_{1/1}^{(i)},C_{2/1}^{(i)},C_{3/1}^{(i)},C_{1/2}^{(i)},C_{2/2}^{(i)},C_{3/2}^{(i)},C_{1/3}^{(i)},C_{2/3}^{(i)},C_{3/3}^{(i)},C_{4/3}^{(i)},\\&C_{1/4}^{(i)},C_{2/4}^{(i)},C_{3/4}^{(i)},C_{4/4}^{(i)},\quad C_{1/5}^{(i)},C_{2/5}^{(i)},C_{3/5}^{(i)},C_{4/5}^{(i)},w^{(i)},\end{aligned} \tag{9.54}$$

for the generic hollow cylindrical phase, while for the core we have the eight parameters

$$C_{2/1}^{(0)},C_{2/2}^{(0)},C_{2/3}^{(0)},C_{4/3}^{(0)},C_{2/4}^{(0)},C_{4/4}^{(0)},C_{2/5}^{(0)},C_{4/5}^{(0)}. \tag{9.55}$$

Then, by recalling the equations (9.39) it is possible to reduce the unknowns, indeed the following parameters vanishes

$$\begin{aligned}&C_{2/4}^{(0)}=C_{2/5}^{(0)}=0,\\&C_{3/2}^{(i)}=C_{3/3}^{(i)}=C_{1/4}^{(i)}=C_{2/4}^{(i)}=C_{3/4}^{(i)}=C_{1/5}^{(i)}=C_{2/5}^{(i)}=C_{3/5}^{(i)}=0,\quad \forall i\in\{1,2,...,n\}.\end{aligned} \tag{9.56}$$

from which the number of unknown coefficients becomes $(12\times n+6)$, represented by those written down

$$\begin{aligned}&C_{2/1}^{(0)},C_{2/2}^{(0)},C_{2/3}^{(0)},C_{4/3}^{(0)},C_{4/4}^{(0)},C_{4/5}^{(0)}\\&C_{3/0}^{(i)},C_{1/1}^{(i)},C_{2/1}^{(i)},C_{3/1}^{(i)},C_{1/2}^{(i)},C_{2/2}^{(i)},C_{1/3}^{(i)},C_{2/3}^{(i)},C_{4/3}^{(i)},C_{4/4}^{(i)},C_{4/5}^{(i)},w_0^{(i)},\quad i\in\{1,2,...,n\},\end{aligned} \tag{9.57}$$

where $(9.57)_1$ represent the unknown coefficients of the *core*, while $(9.57)_2$ are the unknown parameters for the circular hollow cylinders. Finally, it was verified that the number of independent equations reduces from $(22\times n+12)$ to $(12\times n+6)$, equating the number of unknowns. It is worth to note that a peer discussion about the solvability conditions for the general case lies outside the interest of the present paper. However, in a subsequent paper, some explicit solutions for multilayered cylinder composed by three phases are found, using the results and strategies proposed above. Hence, an analogous solving strategy as that developed in section 9.4.2 will be employed for obtaining solutions for the discussed *decaying* case.

9.7. Some remarks about the present solutions: comparison with established literature data for multilayered cylinder

Object of this section is to highlight some properties characterizing the found exact elastic solutions for multilayered cylinder, in comparison with other analytical and semi-analytical results found in

literature by following different solving strategies. In the Introduction, it was already mentioned a detailed list of works where several interesting solutions have been presented in the framework of multilayered cylinder. Here, by leaving out the literature results based on numerical or semi-analytical approaches, we need to focus the attention on a set of axis-symmetrical solutions obtained for laminated composites tubes by Tarn and Wang [75], comparing them with some elements emerging from the solutions found in the present paper for isotropic phases, in both *decaying* and *no-decaying* cases.

9.7.1. Linear radial pressures and anti-plane shear stresses, with equilibrating axial force

For seek of simplicity, consider a multilayered cylinder composed by three phases ($n=2$), geometrically characterized by the radii $R^{(0)} < R^{(1)} < R^{(2)}$. With reference to the results obtained in the previous sections, the system of equilibrium and compatibility equations furnishes a set of $6n+4=16$ algebraic equations, where the unknown parameters $\mathbf{X}$ can be found by specializing the coefficients $P_{h/m}$ for the present case and then inverting the matrix $\mathbf{P}$. If we investigate the case of the sole presence of shear stresses τ_0 and linear radial pressure whose slope is p_1, with equilibrating axial force at an extremity, the corresponding load vector assumes the following form

$$\mathbf{L}^T = \{0,0,0,0,0,0,0,0,0,0,0,0,0,p_1,\tau_0,0\}.$$

By analyzing the position of the non-zero coefficients within the (16×16)-$\mathbf{P}$ matrix, it is possible to extract a (6×6) sub-matrix from it, so that the corresponding algebraic system becomes homogeneous. As a consequence, the following six unknowns vanish:

$$C_{1/1}^{(1)} = C_{1/1}^{(2)} = C_{2/1}^{(0)} = C_{2/1}^{(1)} = C_{2/1}^{(2)} = \varepsilon_0 = 0.$$

Therefore, it is worth to note that load combination constituted by anti-plane shear and linear radial pressure is associated with not uniform strain ε_{zz}, that is $\varepsilon_0 = 0$, while ten remaining non-zero unknowns have to be determined , i.e. $\{C_{2/2}^{(c)}, C_{3/0}^{(j)}, C_{1/2}^{(j)}, C_{2/2}^{(j)}, w_0^{(j)}, C_{3/0}^{(s)}, C_{1/2}^{(s)}, C_{2/2}^{(s)}, w_0^{(s)}, \varepsilon_1\}$.

By recalling the equations (9.34)-(9.37), the displacements and stresses for each hollow phase are

$$U^{(i)} = -\frac{z}{\mu^{(i)}}\left(\frac{C_{1/2}^{(i)}}{r} + 2C_{2/2}^{(i)} r\right),$$

$$W^{(i)} = \frac{\varepsilon_1 z^2}{2} + \frac{r^2\left[4C_{2/2}^{(i)}\left(\mu^{(i)}+\lambda^{(i)}\right) - \varepsilon_1\mu^{(i)}\left(2\mu^{(i)}+\lambda^{(i)}\right)\right]}{4\mu^{(i)2}} + \frac{\left[C_{1/2}^{(i)}\mu^{(i)} + 2C_{3/0}^{(i)}\left(2\mu^{(i)}+\lambda^{(i)}\right)\right]\log r}{\left(\mu^{(i)}+\lambda^{(i)}\right)\mu^{(i)}},$$

and

$$\sigma_{rr}^{(i)} = z\left[\frac{2C_{1/2}^{(i)}}{r^2} - \frac{4C_{2/2}^{(i)}\left(\mu^{(i)}+\lambda^{(i)}\right) - \varepsilon_1\mu^{(i)}\lambda^{(i)}}{\mu^{(i)}}\right], \quad \sigma_{\theta\theta}^{(i)} = z\left[\frac{\varepsilon_1\mu^{(i)}\lambda^{(i)} - 4C_{2/2}^{(i)}\left(\mu^{(i)}+\lambda^{(i)}\right)}{\mu^{(i)}} - \frac{2C_{1/2}^{(i)}}{r^2}\right],$$

$$\sigma_{zz}^{(i)} = -\frac{z}{\mu^{(i)}}\left[4C_{2/2}^{(i)}\lambda^{(i)} - \varepsilon_1\mu^{(i)}\left(2\mu^{(i)}+\lambda^{(i)}\right)\right], \quad \tau_{r\theta}^{(i)} = \tau_{\theta z}^{(i)} = 0,$$

$$\tau_{rz}^{(i)} = \frac{\left(2C_{3/0}^{(i)} - C_{1/2}^{(i)}\right)\lambda^{(i)} + 4C_{3/0}^{(i)}\mu^{(i)}}{r\left(\mu^{(i)}+\lambda^{(i)}\right)} + \frac{r\left[4C_{2/2}^{(i)}\lambda^{(i)} - \varepsilon_1\mu^{(i)}\left(2\mu^{(i)}+\lambda^{(i)}\right)\right]}{2\mu^{(i)}}.$$

For the core we have

$$U^{(0)} = -\frac{2C_{2/2}^{(0)} r\, z}{\mu^{(c)}}, \quad W^{(0)} = \frac{\varepsilon_1 z^2}{2} + \frac{r^2\left[4C_{2/2}^{(0)}\left(\mu^{(0)}+\lambda^{(0)}\right) - \varepsilon_1\mu^{(0)}\left(2\mu^{(0)}+\lambda^{(0)}\right)\right]}{4\mu^{(0)2}},$$

and

$$\sigma_{rr}^{(0)} = \varepsilon_1 \lambda^{(0)} z - \frac{4C_{2/2}^{(0)} z\left(\mu^{(0)} + \lambda^{(0)}\right)}{\mu^{(0)}},\ \sigma_{\theta\theta}^{(0)} = \varepsilon_1 \lambda^{(0)} z - \frac{4C_{2/2}^{(0)} z\left(\mu^{(0)} + \lambda^{(0)}\right)}{\mu^{(0)}},\ \tau_{r\theta}^{(0)} = \tau_{\theta z}^{(0)} = 0,$$

$$\sigma_{zz}^{(0)} = \left[\varepsilon_1\left(2\mu^{(0)} + \lambda^{(0)}\right) - \frac{4C_{2/2}^{(0)}\lambda^{(0)}}{\mu^{(0)}}\right] z,\ \tau_{rz}^{(0)} = \frac{r}{2\mu^{(0)}}\left[4C_{2/2}^{(0)}\lambda^{(0)} - \varepsilon_1\mu^{(0)}\left(2\mu^{(0)} + \lambda^{(0)}\right)\right].$$

Then, if we examine the closed-form solutions found by Tarn and Wang in [75] and specialize them to axis-symmetrical laminated tubes constituted by arbitrary isotropic phases, the comparison between their results and those proposed here shows that: 1) the general form selected in [75] for describing the displacement field doesn't involve non-linear terms in z, as well as the stresses are independent of z; on the contrary, the analytical solution obtained for the case of a multilayered cylinder constituted by three phases (it is the same for *n* arbitrary phases) yields to relax this restriction, representing load cases in which radial pressures vary linearly along the axis of the composed cylinder; 2) in the work of Tarn and Wang the anti-plane shear is characterized by the contemporary presence of shear tractions applied on both the inner and outer cylindrical surfaces of a hollow laminated tube, in which the two shear stresses must satisfy the overall equilibrium condition, $s_a\, a = s_b\, b$, where a and b represents the inner and outer radii, respectively, while s is the shear. This hypothesis excludes the possibility to have an uniform anti-plane shear prescribed only on the external cylindrical surface, that can be equilibrated by an axial force applied on one of the two bases of multilayered cylinder, as well as to reproduce the limit case of the presence of a core, that is $a \to 0$. The solution illustrated in the previous example is instead able to represent the more general case of uniform anti-plane shear on the outer cylindrical surface, with or without shear in the object hole. However, further new solutions can be found by considering the *decaying* cases, as those reported in the section 9.5.

9.8. Proof of the existence and uniqueness of the solution associated to the algebraic problem related to the matrix P for multilayered cylinder

The theorem proposed in the section 9.4.2 has to be considered as a *completeness* theorem, or - equivalently - as an *uniqueness* theorem for the "mathematical structure" of the solution. Indeed, it can be also formulated as follows:

If there exists a "ε_{zz}-no-decaying" solution for a multilayered cylinder under axis-symmetrical load conditions, this solution has to be writeable in terms of a Love's bi-harmonic function with the form $\chi^{(i)}(r,z) = \sum_{k=0}^{4} z^k f_k^{(i)}(r)$ *, where "i" is the generic phase of the object.*

Moreover, from the demonstration of the theorem, it also emerges that the hypothesis of *no-decaying* of the axial strain ε_{zz} leads to discover that it has to be linear along the axis of the multilayered cylinder, that is $\varepsilon_{zz} = \varepsilon_0 + \varepsilon_1 z$. The results of both the theorem and its above mentioned consequence are obtained by utilizing the field equations and only some boundary conditions at the interfaces between the phases of the object, not involving the whole set of equilibrium and compatibility equations at the interfacial surfaces. This authorizes the reader to suspect that the above mentioned bi-harmonic function could be too poor for representing effective elastic solutions satisfying all the boundary conditions among the phases of a generic multilayered cylinder. Therefore, in order to prove the *existence*, we establish the following:

THEOREM 4: *Let us consider a multilayered cylinder, subjected to axis-symmetrical boundary conditions and let be* $\varepsilon \equiv \varepsilon_{zz}$. *The* g*-no-decaying* BVP *can be then approached using the representation* $\chi^{(i)}(r,z) = \sum_{k=0}^{4} z^k f_k^{(i)}(r)$ *, where the functions* $f_k^{(i)}(r)$ *are formally determined by solving the in-cascade field equations as above.* **P** *is instead the* $(6n+4)$*-order square matrix*

characterizing the linear algebraic system from which depends the satisfaction of the whole set of boundary conditions (interfacial and external ones). Then, it is possible to prove that:

$$\forall n \in \mathbf{N},\ \det \mathbf{P} \neq 0,$$

which constitutes a necessary and sufficient condition for ensuring the existence.

Proof.

In order to ensure the *existence* of the proposed solutions in the form $\chi^{(i)}(r,z) = \sum_{k=0}^{4} z^k f_k^{(i)}(r)$, we utilize the results presented in the section 2, thanks to which the boundary value differential problem is transformed in the equivalent linear and algebraic problem, whose details are reported in the Appendix A.2. In this framework, to prove the *existence* it will be sufficient to demonstrate that, for any arbitrary number of phases $n \in \mathbf{N}$, the $(6n+4)\times(6n+4)$ square matrix $\mathbf{P}$ exhibits rank equal to its order, that is

$$\det \mathbf{P} \neq 0. \tag{9.58}$$

To make this, it is convenient to modify the last four rows of $\mathbf{P}$, which respectively represent the three equilibrium equations on the external cylindrical surface $\partial\Omega^{cyl}$, equations (9.42), and the *weak* equilibrium equation at one of the extremities of the object, equation (9.43). This goal is obtainable by substituting the boundary condition (9.43) with an analogous displacement condition at the base $z = L$ and at the centre of the *core*

$$W^{(i=0)}(r=0,\, z=L) = W_0 \Rightarrow \varepsilon_0 L + (1/2)\,\varepsilon_1 L^2 = W_0, \tag{9.59}$$

writeable recalling equation $(9.35)_2$, where L is the total length of the cylinder and W_0 is a prescribed displacement value, replacing now the last known term N in the vector $\mathbf{L}$, equation (9.46). This is possible because, as well-known, in linear elastostatic problems each *weak* condition, written with reference to global forces on a selected part of the boundary, can be substituted by an equivalent *average* displacement condition on the same region. By invoking the *mean value theorem*, it is possible to reduce this overall displacement condition to a *local* one, provided that it is referred to a single point belonging to the boundary. This is the case of the equation written above, where the chosen point is $(r=0,\, z=L)$. The second substitution is instead referred to the rows coming out from the three mentioned equilibrium equations (9.42). This time, we operate by starting from the observation of the specific expressions found for stresses in both the generic *i*-th phase (9.36) and the *core* (9.37). In particular, we can see that the differences between the corresponding stress components for a hollow phase and for the *core* – with specific reference to radial ones $(9.37)_1$ and shear stress $(9.37)_4$ – consist in additional terms that are present for the hollow phases, depending upon r and diverging at the origin. This leads to assume that, at the interface between core and first cladding, both the *core* radial and shear stresses have to satisfy the following equations

$$\begin{aligned}
&\sigma_{rr}^{(0)}(r=R^{(0)}) = [\varepsilon_0 \lambda^{(0)} - 2C_{2/1}^{(0)} \frac{(\lambda^{(0)}+\mu^{(0)})}{\mu^{(0)}}] + z[\varepsilon_1 \lambda^{(0)} - 4C_{2/2}^{(0)} \frac{(\lambda^{(0)}+\mu^{(0)})}{\mu^{(0)}}] = \alpha_0 p_0 + \alpha_1 p_1 z, \\
&\tau_{rz}^{(0)}(r=R^{(0)}) = \frac{R^{(0)}\lambda^{(0)}}{\mu^{(0)}}[2C_{2/2}^{(0)} - \varepsilon_1 \frac{\mu^{(0)}(2\mu^{(0)}+\lambda^{(0)})}{2\lambda^{(0)}}] = \alpha_\tau \tau_0,
\end{aligned} \tag{9.60}$$

where the real coefficients $\{\alpha_0, \alpha_1, \alpha_\tau\} \in \mathbf{R}$ represent scaling factors of the traction values $\{p_0, p_1, \tau_0\}$ prescribed on $\partial\Omega^{cyl}$. Due to the above hypotheses, the last four rows of the matrix $\mathbf{P}$ change. The problem (9.46) can be now rewritten as follows

$$
\underbrace{\left[\begin{array}{cccccccccc|cc}
\underset{(6\times2)}{\mathbf{P}_1^0} & \underset{(6\times6)}{\mathbf{P}_1^1} & \mathbb{O} & \mathbb{O} & \cdots & \mathbb{O} & \mathbb{O} & \cdots & \mathbb{O} & \mathbb{O} & \underset{(6\times1)}{p_1^{6n+3}} & \underset{(6\times1)}{p_1^{6n+4}} \\
\mathbb{O} & \underset{(6\times6)}{\mathbf{P}_2^1} & \underset{(6\times6)}{\mathbf{P}_2^2} & \mathbb{O} & \mathbb{O} & \mathbb{O} & \mathbb{O} & \mathbb{O} & \mathbb{O} & \mathbb{O} & \underset{(6\times1)}{p_2^{6n+3}} & \underset{(6\times1)}{p_2^{6n+4}} \\
\mathbb{O} & \mathbb{O} & \underset{(6\times6)}{\mathbf{P}_3^2} & \underset{(6\times6)}{\mathbf{P}_3^3} & \mathbb{O} & \mathbb{O} & \mathbb{O} & \mathbb{O} & \mathbb{O} & \mathbb{O} & \underset{(6\times1)}{p_3^{6n+3}} & \underset{(6\times1)}{p_3^{6n+4}} \\
\vdots & \mathbb{O} & \mathbb{O} & \ddots & \ddots & \mathbb{O} & \mathbb{O} & \mathbb{O} & \mathbb{O} & \mathbb{O} & \vdots & \vdots \\
\vdots & \mathbb{O} & \mathbb{O} & \mathbb{O} & \ddots & \ddots & \mathbb{O} & \mathbb{O} & \mathbb{O} & \mathbb{O} & \vdots & \vdots \\
\mathbb{O} & \mathbb{O} & \mathbb{O} & \mathbb{O} & \mathbb{O} & \underset{(6\times6)}{\mathbf{P}_k^{k-1}} & \underset{(6\times6)}{\mathbf{P}_k^{k}} & \mathbb{O} & \mathbb{O} & \mathbb{O} & \underset{(6\times1)}{p_k^{6n+3}} & \underset{(6\times1)}{p_k^{6n+4}} \\
\vdots & \mathbb{O} & \mathbb{O} & \mathbb{O} & \mathbb{O} & \mathbb{O} & \ddots & \ddots & \mathbb{O} & \mathbb{O} & \vdots & \vdots \\
\vdots & \mathbb{O} & \mathbb{O} & \mathbb{O} & \mathbb{O} & \mathbb{O} & \mathbb{O} & \ddots & \ddots & \mathbb{O} & \vdots & \vdots \\
\mathbb{O} & \mathbb{O} & \mathbb{O} & \mathbb{O} & \mathbb{O} & \mathbb{O} & \mathbb{O} & \mathbb{O} & \underset{(6\times6)}{\mathbf{P}_n^{n-1}} & \underset{(6\times6)}{\mathbf{P}_n^{n}} & \underset{(6\times1)}{p_n^{6n+3}} & \underset{(6\times1)}{p_n^{6n+4}} \\
\hline
\underset{(1\times2)}{\mathbf{P}_{n+1}^0} & \mathbb{O} & \mathbb{O} & \mathbb{O} & \mathbb{O} & \mathbb{O} & \mathbb{O} & \mathbb{O} & \mathbb{O} & \mathbb{O} & \underset{(1\times1)}{p_{n+1}^{6n+3}} & \underset{(1\times1)}{p_{n+1}^{6n+4}} \\
\underset{(1\times2)}{\mathbf{P}_{n+2}^0} & \mathbb{O} & \mathbb{O} & \mathbb{O} & \mathbb{O} & \mathbb{O} & \mathbb{O} & \mathbb{O} & \mathbb{O} & \mathbb{O} & \underset{(1\times1)}{p_{n+2}^{6n+3}} & \underset{(1\times1)}{p_{n+2}^{6n+4}} \\
\underset{(1\times2)}{\mathbf{P}_{n+3}^0} & \mathbb{O} & \mathbb{O} & \mathbb{O} & \mathbb{O} & \mathbb{O} & \mathbb{O} & \mathbb{O} & \mathbb{O} & \mathbb{O} & \underset{(1\times1)}{p_{n+3}^{6n+3}} & \underset{(1\times1)}{p_{n+3}^{6n+4}} \\
\underset{(1\times2)}{\mathbf{P}_{n+4}^0} & \mathbb{O} & \mathbb{O} & \mathbb{O} & \cdots & \mathbb{O} & \mathbb{O} & \cdots & \mathbb{O} & \mathbb{O} & \underset{(1\times1)}{p_{n+4}^{6n+3}} & \underset{(1\times1)}{p_{n+4}^{6n+4}}
\end{array}\right]}_{\begin{array}{cccc} 2 & & 6n & \end{array}\ \ \underbrace{\phantom{\begin{array}{cc}a&b\end{array}}}_{2}}
\left[\begin{array}{c}
\underset{(2\times1)}{X^0} \\ \hline \underset{(6\times1)}{X^1} \\ \underset{(6\times1)}{X^2} \\ \underset{(6\times1)}{X^3} \\ \vdots \\ \vdots \\ \underset{(6\times1)}{X^{k-1}} \\ \underset{(6\times1)}{X^k} \\ \vdots \\ \underset{(6\times1)}{X^{n-1}} \\ \underset{(6\times1)}{X^n} \\ \hline \varepsilon_0 \\ \varepsilon_1
\end{array}\right]
=
\left[\begin{array}{c}
\underset{(6\times1)}{O} \\ \underset{(6\times1)}{O} \\ \underset{(6\times1)}{O} \\ \underset{(6\times1)}{O} \\ \vdots \\ \underset{(6\times1)}{O} \\ \underset{(6\times1)}{O} \\ \vdots \\ \underset{(6\times1)}{O} \\ \underset{(6\times1)}{O} \\ \alpha_0 p_0 \\ \alpha_1 p_1 \\ \alpha_\tau \tau_0 \\ W_0
\end{array}\right]
$$

where $\underset{(m\times q)}{\mathbf{P}_k^i}$ are sub-matrices with m rows, q columns and rank $\rho[\underset{(m\times q)}{\mathbf{P}_k^i}] = m$. The superscript i denotes the phase of multilayered cylinder, to which the corresponding sub-matrix $\underset{(m\times q)}{\mathbf{P}_k^i}$ is related and the subscript k recalls the group of equations collected in the sub-matrix. From the mechanical point of view, the row-aligned couple of sub-matrices $\underset{(m\times q)}{\mathbf{P}_k^i}$ and $\underset{(m\times q)}{\mathbf{P}_k^{i+1}}$ collect the coefficients related to the set of compatibility and equilibrium conditions established between two adjacent phases. Moreover, the unknowns vector $\mathbf{X}$ and the load vector $\mathbf{L}$ can be partitioned as shown above. With reference to the specific expression of the single coefficients reported in the Appendix A.2, the generic couple of non-zero sub-matrices appears as follows

$$
\left[\underset{(6\times6)}{\mathbf{P}_k^{k-1}} \;\middle|\; \underset{(6\times6)}{\mathbf{P}_k^{k}}\right] =
\left[\begin{array}{cccccc|cccccc}
0 & * & 0 & * & 0 & 0 & 0 & * & 0 & * & 0 & 0 \\
0 & 0 & * & 0 & * & 0 & 0 & 0 & * & 0 & * & 0 \\
* & 0 & * & 0 & * & * & * & 0 & * & 0 & * & * \\
0 & * & 0 & * & 0 & 0 & 0 & * & 0 & * & 0 & 0 \\
0 & 0 & * & 0 & * & 0 & 0 & 0 & * & 0 & * & 0 \\
* & 0 & * & 0 & * & 0 & * & 0 & * & 0 & * & 0
\end{array}\right] \tag{9.61}
$$

where the symbol * is here used to distinguish the non zero coefficients from those vanishing. It is easy to verify that

$$
\forall k \,\middle|\, 2 \le k \le n, \quad \det \underset{(6\times6)}{\mathbf{P}_k^{k-1}} = -\frac{8(\lambda^{(k-1)} + 2\mu^{(k-1)})^3}{R^{(k-1)3}\mu^{(k-1)4}(\lambda^{(k-1)} + \mu^{(k-1)})} \neq 0 \;\Rightarrow \rho[\underset{(6\times6)}{\mathbf{P}_k^{k-1}}] = 6 \tag{9.62}
$$

as well as

$$\forall k \,|\, 1 \le k \le n, \quad \det \underset{(6\times6)}{\mathbf{P}_k^k} = -\frac{8(\lambda^{(k)}+2\mu^{(k)})^3}{R^{(k-1)3}\mu^{(k)4}(\lambda^{(k)}+\mu^{(k)})} \neq 0 \;\Rightarrow \rho[\underset{(6\times6)}{\mathbf{P}_k^k}] = 6\,. \tag{9.63}$$

The columns-matrices $\underset{(m\times1)}{p_k^{6n+3}}$ and $\underset{(m\times1)}{p_k^{6n+4}}$ contain the terms related to the last two unknown coefficients, i.e. $\{\varepsilon_0, \varepsilon_1\}$, and show the non-zero terms in the positions depicted below

$$\underset{(6\times1)}{p_k^{6n+3}} = \begin{bmatrix} 0 \\ 0 \\ 0 \\ * \\ 0 \\ 0 \end{bmatrix}, \quad \underset{(6\times1)}{p_k^{6n+4}} = \begin{bmatrix} 0 \\ 0 \\ * \\ 0 \\ * \\ * \end{bmatrix}, \tag{9.64}$$

while

$$\begin{aligned} &\underset{(1\times1)}{p_{n+1}^{6n+3}} = \lambda^{(0)}; \quad \underset{(1\times1)}{p_{n+1}^{6n+4}} = 0; \quad \underset{(1\times1)}{p_{n+2}^{6n+3}} = 0; \quad \underset{(1\times1)}{p_{n+2}^{6n+4}} = \lambda^{(0)}; \\ &\underset{(1\times1)}{p_{n+3}^{6n+3}} = 0; \quad \underset{(1\times1)}{p_{n+3}^{6n+4}} = -\frac{R^{(0)}}{2}(2\mu^{(0)}+\lambda^{(0)}); \quad p_{n+4}^{6n+3} = L; \quad \underset{(1\times1)}{p_{n+4}^{6n+4}} = L^2/2. \end{aligned} \tag{9.65}$$

Also, we can explicit the following sub-matrices

$$\begin{aligned} &\underset{(1\times2)}{\mathbf{P}_{n+1}^0} = \left[-2\frac{(\mu^{(0)}+\lambda^{(0)})}{\mu^{(0)}} \;\vdots\; 0 \right], \quad \underset{(1\times2)}{\mathbf{P}_{n+2}^0} = \left[0 \;\vdots\; -4\frac{(\mu^{(0)}+\lambda^{(0)})}{\mu^{(0)}} \right] \\ &\underset{(1\times2)}{\mathbf{P}_{n+3}^0} = \left[0 \;\vdots\; 2R^{(0)}\lambda^{(0)}/\mu^{(0)} \right], \quad \underset{(1\times2)}{\mathbf{P}_{n+4}^0} = [0 \;\vdots\; 0], \end{aligned} \tag{9.66}$$

noting that the square (4×4) sub-matrix, obtainable extracting from the last four rows of $\mathbb{P}$ the non-zero terms, is invertible, that is

$$\underset{(4\times4)}{\mathbf{S}} = \begin{bmatrix} \underset{(1\times2)}{\mathbf{P}_{n+1}^0} & \vdots & \underset{(1\times1)}{p_{n+1}^{6n+3}} & \underset{(1\times1)}{p_{n+1}^{6n+4}} \\ \underset{(1\times2)}{\mathbf{P}_{n+2}^0} & \vdots & \underset{(1\times1)}{p_{n+2}^{6n+3}} & \underset{(1\times1)}{p_{n+2}^{6n+4}} \\ \underset{(1\times2)}{\mathbf{P}_{n+3}^0} & \vdots & \underset{(1\times1)}{p_{n+3}^{6n+3}} & \underset{(1\times1)}{p_{n+3}^{6n+4}} \\ \underset{(1\times2)}{\mathbf{P}_{n+4}^0} & \vdots & \underset{(1\times1)}{p_{n+4}^{6n+3}} & \underset{(1\times1)}{p_{n+4}^{6n+4}} \end{bmatrix} : \quad \det \underset{(4\times4)}{\mathbf{S}} = \frac{4R^{(0)}L}{\mu^{(0)}}(\mu^{(0)}+\lambda^{(0)})(2\mu^{(0)}+3\lambda^{(0)}) \neq 0. \tag{9.67}$$

Finally, $\mathbf{O}$ are rectangular matrices containing only zero terms, with rows and columns deducible from their position inside $\mathbf{P}$, while, on the right hand, the sub-vectors $\underset{(6\times1)}{O}$ collect the vanishing known terms. Then, let us consider the partition of the matrix $\mathbf{P}$ and of the vectors $\mathbf{X}$ and $\mathbf{L}$ as above highlighted by the dashed lines. In order to prove that $\forall n \in \mathbf{N}$, $\det \mathbf{P} \neq 0$, we first prove that it is possible to solve a sub-system $(6n\times6n)$, so reducing the effective unknowns to only four, i.e. $\{A_4^{(0)}, A_5^{(0)}, \varepsilon_0, \varepsilon_1\}$, which are located at the first two places and at the last two places of the vector $\mathbf{X}$, respectively, as shown by the equation (9.45). Collecting these unknowns in (2×1) sub-vectors $\underset{(2\times1)}{X^0} = [A_4^{(0)}, A_5^{(0)}]^T$, $\underset{(2\times1)}{\varepsilon} = [\varepsilon_0, \varepsilon_1]^T$ and utilizing the above obtained results $\rho[\underset{(6\times6)}{\mathbf{P}_k^k}] = \rho[\underset{(6\times6)}{\mathbf{P}_{k-1}^k}] = 6$, it becomes possible to solve the algebraic problem (9.46), by starting from the last four equations and then solving in *cascade* the other ones. Thus, we first solve the following sub-system, obtaining

$$\underset{(4\times4)}{\mathbf{S}} \; \underset{(4\times1)}{X^{\mathbf{S}}} = \underset{(4\times1)}{t^{\mathbf{S}}} \;\Rightarrow\; X^{\mathbf{S}} = \mathbf{S}^{-1}t^{\mathbf{S}} \tag{9.68}$$

where $X^{\mathbb{S}}$ collects the unknowns vectors $\underset{(2\times1)}{X^0} = [A_4^{(0)},\ A_5^{(0)}]^T$, $\underset{(2\times1)}{\varepsilon} = [\varepsilon_0, \varepsilon_1]^T$ and $t^{\mathbb{S}}$ the corresponding non-zero terms, $t^{\mathbb{S}} = [\alpha_0 p_0, \alpha_1 p_1, \alpha_\tau \tau_0, W_0]^T$.

Finally, it remains to solve the $(6n \times 6n)$ sub-system, that can be arranged as follows

$$\begin{cases} \mathbf{P}_1^0 X^0 + \mathbf{P}_1^1 X^1 + p_1 \varepsilon = 0 \\ \mathbf{P}_2^1 X^1 + \mathbf{P}_2^2 X^2 + p_2 \varepsilon = 0 \\ \mathbf{P}_3^2 X^2 + \mathbf{P}_3^3 X^3 + p_3 \varepsilon = 0 \\ \ldots \quad \ldots \quad \ldots = 0 \\ \mathbf{P}_n^{n-1} X^{n-1} + \mathbf{P}_n^n X^n + p_n \varepsilon = 0 \end{cases} \tag{9.69}$$

from which we obtain

$$\begin{aligned} X^1 &= -(\mathbf{P}_1^1)^{-1}(\mathbf{P}_1^0 X^0 + p_1 \varepsilon) \\ X^2 &= -[\mathbf{P}_2^2]^{-1}[-\mathbf{P}_2^1(\mathbf{P}_1^1)^{-1}(\mathbf{P}_1^0 X^0 + p_1 \varepsilon) + p_2 \varepsilon] \\ X^3 &= -[\mathbf{P}_3^3]^{-1}[\mathbf{P}_3^2(\mathbf{P}_2^2)^{-1}\mathbf{P}_2^1(\mathbf{P}_1^1)^{-1}(\mathbf{P}_1^0 X^0 + p_1 \varepsilon) - \mathbf{P}_3^2(\mathbf{P}_2^2)^{-1} p_2 \varepsilon + p_3 \varepsilon] \\ &\vdots \\ X^n &= -[\mathbf{P}_n^n]^{-1}\{[p_n - \mathbf{P}_n^{n-1}(\mathbf{P}_{n-1}^{n-1})^{-1} p_{n-1} + \mathbf{P}_n^{n-1}(\mathbf{P}_{n-1}^{n-1})^{-1}\mathbf{P}_{n-1}^{n-2}(\mathbf{P}_{n-2}^{n-2})^{-1} p_{n-2} + \\ &\quad -\ldots + \mathbf{P}_n^{n-1}(\mathbf{P}_{n-1}^{n-1})^{-1}(\ldots)\mathbf{P}_2^1(\mathbf{P}_1^1)^{-1} p_1]\varepsilon + \mathbf{P}_n^{n-1}(\mathbf{P}_{n-1}^{n-1})^{-1}(\ldots)\mathbf{P}_2^1(\mathbf{P}_1^1)^{-1}\mathbf{P}_1^0 X^0\}, \end{aligned} \tag{9.70}$$

where $p_1, p_2, p_3, \ldots, p_n$ collect the first n couples of (6×1) vectors $\left[\begin{array}{c|c} \underset{(6\times1)}{p_k^{6n+3}} & \underset{(6\times1)}{p_k^{6n+4}} \end{array}\right]$, corresponding to the proposed upper-right partition of $\mathbf{P}$. It is worth to note that, to make consistent the above given solutions for the first n unknowns vectors $\underset{(6\times1)}{X^{(k)}}$, both the sub-matrices $\underset{(6\times6)}{\mathbf{P}_{k-1}^k}$ and $\underset{(6\times6)}{\mathbf{P}_k^k}$ have to be invertible. In fact, only this condition ensures that, for each $1 \le k \le n$, all the possible alternated products of those matrices and their inverse still give (6×6) invertible square matrices. The proof of the *existence* is then complete.

9.9. Conclusions

In this paragraph it is furnished a general approach to construct exact elastic solutions for multilayered cylinder, made of a central core and *n* arbitrary cylindrical hollow homogeneous and isotropic phases. The hypothesis of axis-symmetrical boundary conditions was here assumed in order to analyze a class of elastic problems which present *no-decaying* of selected mechanical quantities and in particular of the axial strains ε_{zz} in the radial direction, being z the axis of the laminated cylinder. To construct a robust mathematical procedure for obtaining exact elastic solutions for the above mentioned axis-symmetrical multilayered cylinder, it was first given a theorem for qualifying the space of the solutions and then it was identified their mathematical form, when the object exhibits *no-decaying* of the axial strain. Therefore, with reference to the generic *i*-th phase of the material, the classical *Boussinesq-Somigliana-Galerkin* vector has been specialized to torsionless composite cylinders characterized by *no-decaying* of the axial strain: following this way, a special form of the bi-harmonic Love's function $\chi^{(i)}(r, z)$ was finally obtained. A main result was that – for these problems - is always possible to reduce the differential boundary value problem (BVP) to an equivalent linear algebraic one, first solving an *in cascade* one-dimensional Euler-like differential system (*field equations*) and then writing the *boundary conditions* by means an algebraic system ruled by a $(6n+4)$-order square matrix $\mathbb{P}$. To seek of completeness, *constructive* and *existence* theorems and properties were formulated and proved, in order to show the effectiveness of the proposed method and exclude ill-posed problems.

We need to highlight that some results reported in the above cited literature are given for multilayered cylinders, introducing some specific assumptions that are instead here relaxed. In particular, these hypotheses can be summarized in the following points: (i) the stress field of the composite tube is always assumed to be independent from z- axis: when this hypothesis is removed, a semi-analytical finite element formulation is adopted; (ii) the found solutions in the works mentioned in the introduction are all related to tubes constituted by cylindrical layers without a central core: this apparently surmountable hypothesis about the geometry of the object is actually fundamental for the goal of the present paper. Indeed, the cited assumption leads to relate both the in-plane and anti-plane shears applied on the inner and outer surfaces of the tube, producing zero traction if one of those vanishes; (iii) by starting from an assumption firstly made by Lekhnitskii [Lekhnitskii, S. G., 1981], Tarn et al, for example, image that not varying traction along the z- axis authorize them to choice so the stress field. This is – in general – incorrect: an example is furnished in the present work, with reference to the case of uniform anti-plane shear and axial force; (iv) the solutions proposed by Tarn et al take a sole scalar parameter ε for representing axial strain in z-direction within the laminated object for each phase: this assumption doesn't cover all the possible axis-symmetric boundary value problems characterized by no-decaying of that strain component, because – as demonstrated by us – to find the whole class of solutions with no-decaying ε_{zz} it is necessary to include stress and strain fields depending upon z. By exceeding some of the above problems, the new approach proposed in the present work gives then two important advantages. The first one is related to the possibility of obtaining closed-form solutions for an arbitrary number of phases of multilayered cylinder, being these solutions furnished by means of a "chain" of (6×6) known matrices. Indeed, this approach, differently from that one suggested by Tarn and other authors, that requires the study of eigensolutions, yields to invert the matrix in a symbolic way, regardless the number of phases. This makes possible to obtain qualitative and quantitative information on the mechanical response of laminated cylinders composed by many layers. The second advantage is constituted by the fact that several theorems and properties was here proved for establishing the well-position, existence and uniqueness of the algebraic problem obtained transforming the original differential boundary value problem for the laminated composite with core in an algebraic one, also investigating the consistency of the problem of seeking ε_{zz}-no-decaying solutions, particularly important for many engineering applications.

9.9 References

[1] Carrera, E., Brischetto, S., Nali, P., *Variational statements and computational models for multifield problems and multilayered structures*, Mechanics of Advanced Materials and Structures, 15(3), 182-198, 2008.

[2] Chopra, I., *Review of state of art of smart structures and integrated systems*, AIAA Journal, 40(11), 2145-2187, 2002.

[3] Crawley, E., *Intelligent structures for aerospace: a technology overview and assessment*, AIAA Journal, 32(8), 1689-1699, 1994.

[4] Ikeda, T., Fundamentals of Piezoelectricity, Oxford University Press, 1990, Oxford (UK).

[5] Kapuria, S., Sengupta, S., Dumir, P.C., *Three-dimensional solution for a hybrid cylindrical shell under axisymmetric thermoelectric load*, Archive of Applied Mechanics, 67(5), 320-330, 1997.

[6] Carrera, E., Di Gifico M., Nali, P., Brischetto S., *Refined multilayered plate elements for coupled magneto-electro-elastic analysis*, Multidiscipline Modeling in Materials and Structures, 5(2), 119-138, 2009.

[7] Carrera, E., Brischetto, S., Fagiano, C., Nali, P., *Mixed multilayered plate elements for coupled magneto-electro-elastic analysis*, Multidiscipline Modeling in Materials and Structures, in press, 2009.

[8] Pantelakis, SP.G., Alexopoulos, N.D., *Assessment of the ability of conventional and advanced wrought aluminum alloys for mechanical performance in light-weight applications*, Materials & Design, 29(1), 80-91, 2008.

[9] Reddy, J.N., Mechanics of Laminated Composite Plates and Shells. Theory and Analysis, CRC Press, 2004, New York (USA).
[10] Plantema, F.J., Sandwich Construction, John Wiley & Sons, 1966, New York (USA).
[11] Allen, H.G., Analysis and Design of Structural Sandwich Panels, Pergamon Press, 1969, Oxford (UK).
[12] Zenkert, D., An Introduction to Sandwich Structures, Chamelon Press, 1995, Oxford (UK).
[13] Bitzer, T., Honeycomb Technology, Chapman & Hall, 1997, London (UK).
[14] Vinson, J.R., The Behaviour of Sandwich Structures of Isotropic and Composite Materials, Technomic Publishing Co., 1999, Lancaster, PA (USA).
[15] Marshall, A.C., Core Composite and Sandwich Structures, in Lee, S.M. editor, International Encyclopedia of Composites, 1990, vol.I, 488-607, VCH Publishers Inc., New York (USA).
[16] Corden, J., Honeycomb Structures, in Davies, J.R. editor, ASM Handbook I: Composites, 1995, 721-728, American Society of Metals, Metals Park, OH (USA).
[17] Rogacheva, N.N., The Theory of Piezoelectric Shells and Plates, CRC Press, 1994, Boca Raton, Florida (USA).
[18] Getman, I.P., Ustinov, YU.A., *On the theory of inhomogeneous electroelastic plate*, Applied Mathematics and Mechanics, 43(5), 923-932, 1979.
[19] Birman, V., Byrd, L.W., *Modeling and analysis of functionally graded materials and structures*, Applied Mechanics Reviews, 60(5), 195-216, 2007.
[20] Suresh, S., Mortensen, A., Fundamentals of Functionally Graded Materials, Processing and Thermo-mechanical Behaviour of Graded Metals and Metal- Ceramic Composites, IOM Communications Ltd, 1998, London (UK).
[21] Pindera, M.-J., Arnold, S.M., Aboudi, J., Hui, D., *Use of composites in functionally graded materials*, Composites Engineering, 4(1), 1-145, 1994.
[22] Pindera, M.-J., Aboudi, J., Arnold, S.M., Jones, W.F., *Use of composites in multi-phased and functionally graded materials*, Composites Engineering, 5(7), 743- 974, 1995.
[23] Mills, A.P., Materials of Construction: Their Manufacture and Properties, John Wiley & Sons, 1922, originally published by the University ofWisconsin, Madison (USA).
[24] Hogan, C.M., *Density of states of an insulating ferromagnetic alloy*, Physical Review, 188(2), 870-874, 1969.
[25] Woodward, R., Aluminium and Aluminium Alloys - Designations [online], Available: http://www.azom.com/Details.asp?ArticleID=310 [accessed 08/10/2008].
[26] Froes, F.H., *Titanium alloys: properties and applications*, Encyclopedia of Materials: Science and Technology, 9367-9369, 2008.
[27] Bhowmik, S., Benedictus, R., Poulis, J.A., Bonin, H.W., Bui, V.T., *Highperformance nanoadhesive bonding of titanium for aerospace and space applications*, International Journal of Adhesion and Adhesives, 29(3), 259-267, 2009.
[28] Material information service, Titanium Alloys - Physical Properties [online], Available: http://www.azom.com/Details.asp?ArticleID=1341 [accessed 08/10/2008].
[29] Jones, R.M., Mechanics of Composite Materials, Second Edition, Taylor & Francis, 1999, PA (USA).
[30] Mallick, P.K., Fiber-Reinforced Composites: Materials, Manufacturing and Design, CRC Press, 1993, New York (USA).
[31] Gibson, R.F., Principle of Composite Material Mechanics, McGraw-Hill, 1994, New York (USA).
[32] Zhou, D., Stronge, W.J., *Mechanical properties of fibrous core sandwich panels*, International Journal of Mechanical Sciences, 47(4-5), 775-798, 2005.
[33] Chen, A., Davalos, J.F., *A solution including skin effect for stiffness and stress field of sandwich honeycombe core*, International Journal of Solids and Structures, 42(9- 10), 2711-2739, 2005.

[34] Bitzer, T.N., Honeycomb Materials and Applications, in Sandwich Constructions-Proceedings of the Second International Conference on Sandwich Construction, Editors, D. Weissman-Berman and K.-A. Olsson, EMAS Publications, 1992, United Kingdom.
[35] Diab products, Divinycell - Structural Foam Cores [online], Available: http://www.diabgroup.com/europe/products/e_prods_2.html [accessed 15/10/2008].
[36] Cady, W.G., Piezoelectricity, Dover, 1964, New York (USA).
[37] Kawai, H., *The piezoelectricity of polyrinydene fluoride*, Japan Journal of Applied Physics, 8, 975-976, 1979.
[38] Tani, J., Takagi, T., Qiu, J., *Intelligent materials systems: application of functional materials*, Applied Mechanics Reviews, 51(8), 505-521, 1998.
[39] Rao, S.S., Sunar, M., *Piezoelectricity and its use in disturbance sensing and control of flexible structures: a survey*, Applied Mechanics Reviews, 47(4), 113-123, 1994.
[40] Ballhause, D., Assessment of Multilayered Theories for Piezoelectric Plates using a Unified Formulation, Master's Thesis, Universität Stuttgart, Politecnico di Torino, July 2003.
[41] Yang, J.S, Yu, J.D., *Equations for laminated piezoelectric plate,* Archives of Mechanics, 45(6), 653-664, 1993.
[42] Brischetto, S., Carrera, E., *Refined 2D models for the analysis of functionally graded piezoelectric plates*, Journal of Intelligent Material Systems and Structures, in press, 2009.
[43] Brischetto, S., Leetsch, R., Carrera, E., Wallmersperger, T., Kröplin, B., *Thermo-mechanical bending of functionally graded plates*, Journal of Thermal Stresses, 31(3), 286-308, 2008.
[44] Kieback, B., Neubrand, A., Riedel, H., *Processing techniques for functionally graded materials*, Materials Science & Engineering A, 362(1-2), 81-105, 2003.
[45] Burkes, D.E., Moore, J.J., *Microstructure and kinetics of a functionally graded NiTi- TiCx composite produced by combustion synthesis*, Journal of Alloys and Compounds, 430(1-2), 274-281, 2007.
[46] Cannillo, V., Lusvarghi, L., Manfredini, T., MOntorsi, M., Siligardi, C., Sola, A., *Glass-ceramic functionally graded materials produced with different methods*, Journal of the European Ceramic Society, 27(2-3), 1293-1298, 2007.
[47] Limarga, A.M., Widjaja, S., Yip, T.H., *Mechanical properties and oxidation resistance of plasma-sprayed multilayered Al2O3=ZrO2 thermal barrier coatings*, Surface & Coatings Technology, 197(1), 93-102, 2005.
[48] Dong, Y.S., Lin, P.H., Wang, H.X., *Electroplating preparation of* $Ni-Al_2O_3$ *graded composite coatings using a rotating cathode*, Surface & Coatings Technology, 200(11), 3633-3636, 2006.
[49] Hvizdos, P., Jonsson, D., Anglada, M., Anné, G., Van der biest, O., *Mechanical properties and thermal shock behaviour of an alumina/zirconia functionally graded material prepared by electrophoretic deposition*, Journal of the European Ceramic Society, 27(2-3), 1365-1371, 2007.
[50] Gelbstein, Y., Dashevsky, Z., Dariel, M.P., *Powder metallurgical processing of functionally graded p-Pb1¡xSnxTe materials for thermoelectric applications*, Physica B: Condensed Matter, 391(2), 256-265, 2007.
[51] Kawase, M., Tago, T., Kurosawa, M., Utsumi, H., Hashimoto, K., *Chemical vapor infiltration and deposition to produce a silicon carbide-carbon functionally gradient material*, Chemical Engineering Science, 54(15-16), 3327-3334 ,1999.
[52] Watanabe, Y., Yamanaka, N., Fukui, Y., *Control of composition gradient in a metal-ceramic functionally graded material manufactured by the centrifugal method*, Composites. Part A: Applied Science and Manufacturing, 29(5-6), 595-601, 1998.
[53] Qin, Q.D., Zhao, Y.G., Cong, P.J., Liang, Y.H., Zhou, W., *Multi-layer functionally graded Mg2Si/Al composite produced by directional remelting and quenching process*, Materials Science and Engineering: A, 418(1-2), 193-198, 2006.
[54] Zhou, Z.-J., Du, J., Song, S.-X., Zhong, Z.-H., Ge, C.-C., *Microstructural characterization of W/Cu functionally graded materials produced by a one-step resistance sintering method*, Journal of Alloys and Compounds, 428(1-2), 146-150, 2007.

[55] Reiter, T., Dvorak, G.J., Tvergaard, V., *Micromechanical models for graded composite materials*, Journal of the Mechanics and Physics and Solids, 45(8), 1281-1302, 1997.
[56] Gasik, M.M., *Micromechanical modelling of functionally graded materials*, Computational Materials Science, 13(1-3), 42-55, 1998.
[57] Grujicic, M., Zhang, Y., *Determination of effective elastic properties of functionally graded materials using Voronoi cell finite element method*, Materials Science and Engineering A, 251(1-2), 64-76, 1998.
[58] Liu, G.R., Han, X., Lam, K.Y., *Stress waves in functionally gradient materials and its use for material characterization*, Composites. Part B: Engineering, 30(4), 383-394, 1999.
[59] Rahman, S., Chakraborty, A., *A stochastic micromechanical model for elastic properties of functionally graded materials*, Mechanics of Materials, 39(6), 548-563, 2007.
[60] Mori, T., Tanaka, K., *Average stress in matrix and average elastic energy of materials with misfitting inclusions*, Acta Metallurgica, 21(5), 571-574, 1973.
[61] Brischetto. S., *Classical and mixed multilayered plate/shell models for multifield problems analysis*, Ph.D. Dissertation, April 2009
[62] Liew, K. M., Kitipornchai, S., Zhang, X. Z., and Lim, C.W., "Analysis of the thermal stress behaviour of functionally graded hollow circular cylinders," *International Journal of Solids and Structures* 40, 2355–2380 (2003).
[63] Shao, Z. S., "Mechanical and thermal stresses of a functionally graded circular hollow cylinder with finite length," *International Journal of Pressure Vessels an Piping* 82, 155–163 (2005).
[64] Mian, M., Abid, and Spencer, A. J. M., "Exact solutions for functionally graded and laminated elastic materials," *J. Mech. Phys. Solids*, 46(12), 2283–2295 (1998).
[65] Fraldi, M., and Cowin, S. C., "Inhomogeneous elastostatic problem solutions constructed from stress-associated homogeneous solutions," *Journal of the Mechanics and Physics of Solids* 52, 2207–2233 (2004).
[66] Fraldi, M., Nunziante, L., Carannante, F. (2007), *Axis-symmetrical Solutions for n-plies Functionally Graded Material Cylinders under Strain no-Decaying Conditions*, J. Mech. of Adv. Mat. and Struct. Vol. 14 (3), pp. 151-174 - DOI: 10.1080/15376490600719220
[67] M. Fraldi, L. Nunziante, F. Carannante, A. Prota, G. Manfredi, E. Cosenza (2008), *On the Prediction of the Collapse Load of Circular Concrete Columns Confined by FRP*, Journal Engineering structures, Vol. 30, Issue 11, November 2008, Pages 3247-3264 - DOI: 10.1016/j.engstruct.2008.04.036
[68] Fraldi, M., Nunziante, L., Chandrasekaran, S., Carannante, F., Pernice, MC. (2009), *Mechanics of distributed fibre optic sensors for strain measurements on rods*, Journal of Structural Engineering, 35, pp. 323-333, Dec. 2008- Gen. 2009
[69] M. Fraldi, F. Carannante, L. Nunziante (2012), *Analytical solutions for n-phase Functionally Graded Material Cylinders under de Saint Venant load conditions: Homogenization and effects of Poisson ratios on the overall stiffness*, Composites Part B: Engineering, Volume 45, Issue 1, February 2013, Pages 1310–1324
[70] Nunziante, L., Gambarotta, L., Tralli, A., *Scienza delle Costruzioni*, 3° Edizione, McGraw-Hill, 2011, ISBN: 9788838666971
[71] Alshits, V. I., and Kirchner, O. K., "Cylindrically anisotropic, radially inhomogeneous elastic materials," *Proc. Roy. Soc. Lond*. A457, 671–693 (2001).
[72] Chouchaoui, C. S., and Ochoa, O. O., "Similitude study for a laminated cylindrical tube under tensile, torsion, bending, internal and external pressure. Part I: governing equations," *Composite Structures* 44, 221–229 (1999).
[73] Chen, T., Chung, C. T., and Lin, W. L., "A revisit of a cylindrically anisotropic tube subjected to pressuring, shearing, torsion, extension and a uniform temperature change," *International Journal of Solids and Structures* 37, 5143–5159 (2000).
[74] Tarn, J. Q., "Exact solutions for functionally graded anisotropic cylinders subjected to thermal and mechanical loads," *International Journal of Solids and Structures*, 38, 8189–8206 (2001).

[75] Tarn, J. Q., and Wang, Y. M., "Laminated composite tubes under extension, torsion, bending, shearing and pressuring: a state space approach," *International Journal of Solids and Structures* 38, 9053–9075 (2001).
[76] Lekhnitskii, S. G., *Theory of Elasticity of an Anisotropic Body*, Mir, Moscow, 1981.
[77] Huang, C. H., and Dong, S. B., "Analysis of laminated circular cylinders of materials with the most general form of cylindrical anisotropy. I. Axially symmetric deformations," *International Journal of Solids and Structures* 38, 6163–6182 (2001).
[78] Love, A. E. H., *A Treatise on the Mathematical Theory of Elasticity*, Dover Publications, Inc, New York, 1944.
[79] Bernini, M., Fraldi, A., Minardo, V., Minutolo, F., Carannante, L., and Nunziante, L., Zeni, "Optical fiber-sensor measurements for safety assessment and monitoring of bridges and large structures," *Bridge Structures* 1(3), 355–363 (2005).
[80] Nobuyuki, Y., and Imai, T., "Stimulated Brillouin scattering suppression by means of applying strain distribution to fiber with cabling," *Journal of Lightwave Technology* 11, 1519–1522 (1993).
[81] Nickl`es, M., et al., "Simple distribuited fiber sensor based on Brillouin scattering gain spectrum analysis," *Optics Letters* 21, 758–761 (1996).
[82] Gusev, V., Picart, P., Mounier, D., and Breteau, J. M., "On the possibility of ultrashort shear acoustic pulse excitation due to the laser-induced electrostrictive effect," *Optics Communications*, 204, 229–234 (2002).
[83] Ye, J. Q., "Decay rate of edge effects in cross-ply-laminated hollow cylinders," *International Journal of Mechanical Sciences* 43, 455–470 (2001).
[84] Ye, J. Q., and Sheng, H. Y., "Free-edge effect in cross-ply laminated hollow cylinders subjected to axisymmetric transverse loads," *International Journal of Mechanical Sciences* 45, 1309–1326 (2003).
[85] Ye, J. Q., "Edge effects in angle-ply laminated hollowcylinders," *Composite Structures* 52, 247–253 (2001).
[86] Ansari, F., and Yuan, L., "Mechanics of bond and interface shear transfer in optical fiber sensors," *Journal of Engineering Mechanics* 124(4), 385–394 (1998).
[87] Gurtin, M. E., *The Linear Theory of Elasticity*, *Handbbuch der Physik*, Springer, Berlin, 1972.
[88] Wolfram, S., *Mathematica, version 5*, Wolfram Research, Inc., Champaign, IL, 1998–2005.

9.11. Appendix A.1 : Mathematical conditions for strain *no-decaying* in multilayered cylinder.

Object of this appendix is to prove the following property, already given in this chapter of the present thesis:

PROPERTY 1: *Let us consider a multilayered cylinder subjected to axis-symmetrical boundary conditions and let be* $\varepsilon \equiv \varepsilon_{hk}$, *where* ε_{hk} *is an arbitrarily chosen strain component. Then, the necessary condition for obtaining* ε*-no-decaying is that those strain components exhibit at most a third-order polynomial function of z. In particular, it is possible to obtain the following necessary conditions for each strain:*

i) $\forall i \in \{0,1,2,...,n\}, \quad \varepsilon \equiv \varepsilon_{zz}(z) = \varepsilon_{zz}^{(i)} \Rightarrow \varepsilon_{zz}^{(i)} = k_0^{(i)} + k_1^{(i)} z + k_2^{(i)} z^2 + k_3^{(i)} z^3$

ii) $\forall i \in \{0,1,2,...,n\}, \quad \varepsilon \equiv \varepsilon_{rr}(z) = \varepsilon_{rr}^{(i)} \Rightarrow \varepsilon_{rr}^{(i)} = k_0^{(i)} + k_1^{(i)} z + k_2^{(i)} z^2 + k_3^{(i)} z^3$

iii) $\forall i \in \{0,1,2,...,n\}, \quad \varepsilon \equiv \varepsilon_{\theta\theta}(z) = \varepsilon_{\theta\theta}^{(i)} \Rightarrow \varepsilon_{\theta\theta}^{(i)} = k_0^{(i)} + k_1^{(i)} z + k_2^{(i)} z^2 + k_3^{(i)} z^3$

iv) $\forall i \in \{0,1,2,...,n\}, \quad \varepsilon \equiv \varepsilon_{rz}(z) = \varepsilon_{rz}^{(i)} \Rightarrow \varepsilon_{rz}^{(i)} = 0$

where $k_0^{(i)}, k_1^{(i)}, k_2^{(i)}, k_3^{(i)}$ *are real coefficients depending from the i-*th *phase.*

Proof. Begin by first considering the condition *i)*. Let us assume $\varepsilon_{zz}^{(i)} = \varepsilon^{(i)}(z)$, where the superscript "*i*" is referred to the generic *i*-th phase of the object and $\varepsilon^{(i)}(z)$ is a continuous real scalar function. By virtue of (5.2.7) and $(5.2.8)_2$ it is possible to obtain $\varepsilon_{zz}^{(i)}$ as follows

$$\varepsilon_{zz}^{(i)} = \varepsilon^{(i)}(z) \Rightarrow \frac{1}{2\mu^{(i)}}\left[\frac{\mu^{(i)}}{(\mu^{(i)}+\lambda^{(i)})}\left(\nabla^2\chi^{(i)}\right)_{,z} + \chi_{,rrz}^{(i)} + r^{-1}\chi_{,rz}^{(i)}\right] = \varepsilon^{(i)}(z). \tag{A1.1}$$

Therefore, by adding and subtracting $\chi_{,zzz}^{(i)}$ inside the square parentheses at the left hand of (A1.1), we have

$$\left\{\left(2\mu^{(i)}+\lambda^{(i)}\right)\Big/\left[2\mu^{(i)}\left(\mu^{(i)}+\lambda^{(i)}\right)\right]\right\}\left(\nabla^2\chi^{(i)}\right)_{,z} = \left[1\Big/\left(2\mu^{(i)}\right)\right]\chi_{,zzz}^{(i)} + \varepsilon^{(i)}(z) \tag{A1.2}$$

and, after integrating in z, we can write

$$\left\{\left(2\mu^{(i)}+\lambda^{(i)}\right)\Big/\left[2\mu^{(i)}\left(\mu^{(i)}+\lambda^{(i)}\right)\right]\right\}\nabla^2\chi^{(i)} = \left[1\Big/\left(2\mu^{(i)}\right)\right]\chi_{,zz}^{(i)} + \tilde{\varepsilon}^{(i)}(z) + \gamma_1^{(i)}(r), \tag{A1.3}$$

where $\tilde{\varepsilon}^{(i)}(z) = \int \varepsilon^{(i)}(z)dz$, while $\gamma_1^{(i)}(r)$ represents an adding function of r. By applying the Laplace differential operator to both the sides in (A1.3) and recalling that $\nabla^4\chi^{(i)} = 0$, the right hand in (A1.3) has to vanish, that is:

$$(\nabla^2\chi^{(i)})_{,zz} + 2\mu^{(i)}[\varepsilon_{,z}^{(i)}(z) + r^{-1}\gamma_{1,r}^{(i)}(r) + \gamma_{1,rr}^{(i)}(r)] = 0. \tag{A1.4}$$

If we integrate two times the (A1.4) with reference to z, we have

$$\nabla^2\chi^{(i)} = -\mu^{(i)}\left[2\tilde{\varepsilon}^{(i)}(z) + \left(r^{-1}\gamma_{1,r}^{(i)}(r) + \gamma_{1,rr}^{(i)}(r)\right)z^2\right] + \gamma_2^{(i)}(r)\,z + \gamma_3^{(i)}(r) \tag{A1.5}$$

where two new functions $\gamma_2^{(i)}(r)$ and $\gamma_3^{(i)}(r)$ appear. Substituting (A1.5) into (A1.3) and then integrating two times again in z, we finally obtain

$$\begin{aligned}\chi^{(i)}(r,z) = &-\frac{2\mu^{(i)}\left(3\mu^{(i)}+2\lambda^{(i)}\right)}{\mu^{(i)}+\lambda^{(i)}}\tilde{\tilde{\varepsilon}}^{(i)}(z) - \frac{\left(2\mu^{(i)}+\lambda^{(i)}\right)\mu^{(i)}}{\mu^{(i)}+\lambda^{(i)}}\left[\left(r^{-1}\gamma_{1,r}^{(i)}(r) + \gamma_{1,rr}^{(i)}(r)\right)\frac{z^4}{12}\right] + \\ &+\left(\frac{2\mu^{(i)}+\lambda^{(i)}}{\mu^{(i)}+\lambda^{(i)}}\right)\left(\frac{\gamma_2^{(i)}(r)z^3}{6} + \frac{\gamma_3^{(i)}(r)z^2}{2}\right) - \mu^{(i)}\gamma_1^{(i)}(r)z^2 + \gamma_4^{(i)}(r)z + \gamma_5^{(i)}(r)\end{aligned} \tag{A1.6}$$

where two new functions $\gamma_4^{(i)}(r)$ and $\gamma_5^{(i)}(r)$ appear. The unknown functions $\gamma_j^{(i)}(r)$, $j \in \{1,...,5\}$ have to be determined, while $\tilde{\tilde{\varepsilon}}^{(i)}(z) = \int[\int \tilde{\varepsilon}^{(i)}(z)dz]dz$. Substitution of (1.VI) in the bi-harmonic condition leads

$$\begin{aligned}\nabla^4\chi^{(i)} = 0 \Rightarrow &-2\mu^{(i)}\tilde{\varepsilon}_{,z}^{(i)}(z) - \mu^{(i)}z^2[r^{-3}\gamma_{1,r}^{(i)}(r) - r^{-2}\gamma_{1,rr}^{(i)}(r) + 2r^{-1}\gamma_{1,rrr}^{(i)}(r) + \gamma_{1,rrrr}^{(i)}(r)] + \\ &+ z[r^{-1}\gamma_{2,r}^{(i)}(r) + \gamma_{2,rr}^{(i)}(r)] + r^{-1}\gamma_{3,r}^{(i)}(r) + \gamma_{3,rr}^{(i)}(r) - 2\mu[r^{-1}\gamma_{1,r}^{(i)}(r) + \gamma_{1,rr}^{(i)}(r)] = 0,\end{aligned} \tag{A1.7}$$

from which, by applying the polynomial identity law, the differential equations shown below have to be satisfied

$$\begin{cases} r^{-3}\gamma_{1,r}^{(i)}(r) - r^{-2}\gamma_{1,rr}^{(i)}(r) + 2r^{-1}\gamma_{1,rrr}^{(i)}(r) + \gamma_{1,rrrr}^{(i)}(r) = \varepsilon_3^{(i)} \\ r^{-1}\gamma_{2,r}^{(i)}(r) + \gamma_{2,rr}^{(i)}(r) = \varepsilon_2^{(i)} \\ r^{-1}\gamma_{3,r}^{(i)}(r) + \gamma_{3,rr}^{(i)}(r) - 2\mu(r^{-1}\gamma_{1,r}^{(i)}(r) + \gamma_{1,rr}^{(i)}(r)) = \varepsilon_1^{(i)} \end{cases} \tag{A1.8}$$

where $\varepsilon_k^{(i)}$, $k \in \{1,2,3\}$, are arbitrary constants. By solving the ordinary differential system (A1.8) the explicit expression of the functions $\gamma_j^{(i)}(r)$ are obtained in the following form

$$\begin{aligned}\gamma_1^{(i)}(r) &= -\frac{r^2\left[\varepsilon_3^{(i)}r^2 + 16\left(\Gamma_{1/3}^{(i)} - 2\Gamma_{1/2}^{(i)}\right)\mu^{(i)}\right]}{64\mu^{(i)}} + \left(\Gamma_{1/1}^{(i)} + \frac{\Gamma_{1/3}^{(i)}r^2}{2}\right)\log r + \Gamma_{1/4}^{(i)}, \\ \gamma_2^{(i)}(r) &= \frac{\varepsilon_2^{(i)}r^2}{4} + \Gamma_{2/1}^{(i)}\log r + \Gamma_{2/2}^{(i)}, \\ \gamma_3^{(i)}(r) &= -\frac{\varepsilon_3^{(i)}r^4}{32} + \frac{1}{4}r^2[\varepsilon_1^{(i)} + 2\mu^{(i)}(2\Gamma_{1/2}^{(i)} - \Gamma_{1/3}^{(i)})] + \Gamma_{3/1}^{(i)}\log r + \Gamma_{1/3}^{(i)}\mu^{(i)}r^2\log r + \Gamma_{3/2}^{(i)},\end{aligned} \tag{A1.9}$$

in which $\Gamma_{j/m}^{(i)}$ are other constants to determine. The notation utilized here for the characterization of the coefficients $\Gamma_{j/m}^{(i)}$ must be read in this manner: the superscript (i) is referred to the material phase *i*-th, the second subscript m tell us the order number of the integration constant, the first subscript j is related to the corresponding function $\gamma_j^{(i)}(r)$. By substituting the results (A1.9) into (A1.7) we find an ordinary linear differential equation in the unknown function $\varepsilon^{(i)}(z)$, i.e.:

$$\varepsilon_1^{(i)} + \varepsilon_2^{(i)} z + \varepsilon_3^{(i)} z^2 - 2\mu^{(i)} \varepsilon_{,z}^{(i)}(z) = 0\,. \tag{A1.10}$$

Integrating the (A1.10) we easily obtain

$$\varepsilon^{(i)}(z) = \varepsilon_0^{(i)} + \frac{\varepsilon_1^{(i)}}{2\mu^{(i)}} z + \frac{\varepsilon_2^{(i)}}{4\mu^{(i)}} z^2 + \frac{\varepsilon_3^{(i)}}{6\mu^{(i)}} z^3 \tag{A1.11}$$

where $\varepsilon_0^{(i)}$ is a constant. The equation (A1.11) represents the searched result. However, for completeness, the explicit form of the other remaining functions can be determined. Indeed, the substitution of (A1.9) and (A1.11) into (A1.6) and then into (A1.7), permits to obtain the following two uncoupled differential equations

$$r^{-3}\gamma_{4,r}^{(i)}(r) - r^{-2}\gamma_{4,rr}^{(i)}(r) + 2r^{-1}\gamma_{4,rrr}^{(i)}(r) + \gamma_{4,rrrr}^{(i)}(r) + \frac{\varepsilon_2^{(i)}\mu^{(i)}}{\mu^{(i)} + \lambda^{(i)}} = 0 \tag{A1.12}$$

$$\begin{aligned} &r^{-3}\gamma_{5,r}^{(i)}(r) - r^{-2}\gamma_{5,rr}^{(i)}(r) + 2r^{-1}\gamma_{5,rrr}^{(i)}(r) + \gamma_{5,rrrr}^{(i)}(r) + \\ &+ \frac{\varepsilon_3^{(i)}\lambda^{(i)} r^2}{2(\mu^{(i)} + \lambda^{(i)})} + \frac{\mu^{(i)}\left[\varepsilon_1^{(i)} - 2\left(2\Gamma_{1/2}^{(i)} + \Gamma_{1/3}^{(i)}\right)\lambda^{(i)}\right] - 4\Gamma_{1/3}^{(i)}\mu^{(i)}\lambda^{(i)}\log r}{\mu^{(i)} + \lambda^{(i)}} = 0. \end{aligned} \tag{A1.13}$$

from which, by invoking again the identity polynomial law, the solutions are found as follows:

$$\gamma_4^{(i)}(r) = -\frac{\varepsilon_2^{(i)}\mu^{(i)} r^4}{64(\mu^{(i)} + \lambda^{(i)})} + \Gamma_{4/1}^{(i)}\log r + \frac{r^2\left(2\Gamma_{4/2}^{(i)} - \Gamma_{4/3}^{(i)}\right)}{4} + \frac{\Gamma_{4/3}^{(i)} r^2 \log r}{2} + \Gamma_{4/4}^{(i)} \tag{A1.14}$$

$$\begin{aligned} \gamma_5^{(i)}(r) = &-\frac{\varepsilon_3^{(i)}\lambda^{(i)} r^6}{1152\left(\mu^{(i)} + \lambda^{(i)}\right)} + \frac{\mu^{(i)}\left[\varepsilon_0^{(i)} + 4\lambda^{(i)}\left(\Gamma_{1/3}^{(i)} - \Gamma_{1/2}^{(i)}\right)\right]}{64\left(\mu^{(i)} + \lambda^{(i)}\right)} - \frac{\Gamma_{1/3}^{(i)}\mu^{(i)}\lambda^{(i)}\log r}{16\left(\mu^{(i)} + \lambda^{(i)}\right)} + \\ &+ \Gamma_{5/1}^{(i)}\log r + \frac{r^2\left(2\Gamma_{5/2}^{(i)} - \Gamma_{5/3}^{(i)}\right)}{4} + \frac{\Gamma_{5/3}^{(i)} r^2 \log r}{2} + \Gamma_{5/4}^{(i)}. \end{aligned} \tag{A1.15}$$

It is worth to note that, in order to satisfy the hypothesis $\varepsilon_{zz}^{(i)} = \varepsilon^{(i)}(z)$, two last relationships have to be still ensured: they are obtainable by substituting the above obtained functions $\gamma_j^{(i)}$ into (A1.1)

$$\Gamma_{4/2}^{(i)} = \frac{\mu^{(i)}\left[\Gamma_{2/1}^{(i)} - 2\Gamma_{2/2}^{(i)} + 4\varepsilon_0^{(i)}\left(2\mu^{(i)} + \lambda^{(i)}\right)\right]}{4\left(\mu^{(i)} + \lambda^{(i)}\right)}, \quad \Gamma_{4/3}^{(i)} = -\frac{\Gamma_{2/1}^{(i)}\mu^{(i)}}{2\left(\mu^{(i)} + \lambda^{(i)}\right)}, \tag{A1.16}$$

from which $\gamma_4^{(i)}(r)$ takes the final form

$$\gamma_4^{(i)}(r) = \frac{-\varepsilon_2^{(i)}\mu^{(i)} r^4}{64(\mu^{(i)} + \lambda^{(i)})} + \Gamma_{4/1}^{(i)}\log r + \frac{\mu^{(i)} r^2\left[2\varepsilon_0^{(i)}(2\mu^{(i)} + \lambda^{(i)}) + \Gamma_{2/1}^{(i)}(1 - \log r) - \Gamma_{2/2}^{(i)}\right]}{4(\mu^{(i)} + \lambda^{(i)})} + \Gamma_{4/4}^{(i)}\,. \tag{A1.17}$$

By utilizing the above obtained results, we can see that the function $\chi^{(i)}$ exhibits a sixth-order polynomial form in z, where the corresponding coefficients are represented by functions that vary only upon r. In order to demonstrate the conditions *ii)* and *iii)*, it is possible to follow a way similar to that considered above. Indeed, with reference to the no-decaying of the radial strain, we can start from the equation

$$\varepsilon_{rr}^{(i)} = -\frac{1}{2\mu^{(i)}}\chi_{,rrz} = \varepsilon^{(i)}(z) \tag{A1.18}$$

and then integrate one time respect to z and two times along the radius r, so that

$$\chi^{(i)}(r,z) = -\mu^{(i)}\tilde{\varepsilon}^{(i)}(z)r^2 + \alpha_0^{(i)}(r) + \beta_1^{(i)}(z)r + \beta_2^{(i)}(z), \tag{A1.19}$$

where $\tilde{\varepsilon}^{(i)}(z) = \int \varepsilon^{(i)}(z)dz$, while $\beta_1^{(i)}(z)$ and $\beta_2^{(i)}(z)$ represent two adding function of z and $\alpha_0^{(i)}(r)$ is a function of r. Recalling that $\chi^{(i)}(r,z)$ has to be a bi-harmonic function and invoking the identity polynomial law, by means of some algebraic manipulation we obtain:

$$\begin{aligned}
&\varepsilon^{(i)}(z) = A_1^{(i)} + 2A_2^{(i)}z + 3A_3^{(i)}z^2 + 4A_4^{(i)}z^3, \quad \beta_1^{(i)}(z) = B_0^{(i)},\\
&\beta_2^{(i)}(z) = C_0^{(i)} + C_1^{(i)}z + C_2^{(i)}z^2 + C_3^{(i)}z^3 + C_4^{(i)}z^4 + C_5^{(i)}z^5 + \frac{2}{5}A_3^{(i)}\mu^{(i)}z^5 + \frac{4}{15}A_4^{(i)}\mu^{(i)}z^6,\\
&\alpha_0^{(i)}(r) = \frac{2D_2^{(i)} - D_3^{(i)}}{4}r^2 + D_1^{(i)}\log r + \frac{D_3^{(i)}}{2}r^2\log r + D_4^{(i)} - B_0^{(i)}r + \frac{2A_2^{(i)}\mu^{(i)} - 3C_4^{(i)}}{8}r^4 + \frac{1}{24}A_4^{(i)}\mu^{(i)}r^6,
\end{aligned} \tag{A1.20}$$

where $\{A_1^{(i)},...,A_4^{(i)},B_0^{(i)},C_0^{(i)},...,C_5^{(i)},D_1^{(i)},...,D_4^{(i)}\}$ are real coefficients to determine and the equation $(A1.20)_1$ represents the needed result. An analogous line of reasoning can be introduced to demonstrate the necessary condition for no-decaying of the hoop strain $\varepsilon_{\theta\theta}$. Indeed, by assuming that

$$\varepsilon_{\theta\theta}^{(i)} = -\frac{1}{2\mu^{(i)}r}\chi_{,rz} = \varepsilon^{(i)}(z), \tag{A1.21}$$

and integrating respect to the two field variables, we obtain

$$\chi(r,z) = -\mu^{(i)}\tilde{\varepsilon}^{(i)}(z)r^2 + \alpha_0^{(i)}(r) + \beta_0^{(i)}(z)r \tag{A1.22}$$

where $\alpha_0^{(i)}$ and $\beta_0^{(i)}$ are scalar function to determine and $\tilde{\varepsilon}^{(i)}(z) = \int \varepsilon^{(i)}(z)dz$. Imposing that the Love's function $\chi^{(i)}(r,z)$ has to be bi-harmonic, a very similar to (A1.20) set of solutions can be written

$$\begin{aligned}
&\varepsilon^{(i)}(z) = A_1^{(i)} + 2A_2^{(i)}z + 3A_3^{(i)}z^2 + 4A_4^{(i)}z^3,\\
&\beta_0^{(i)}(z) = C_0^{(i)} + C_1^{(i)}z + C_2^{(i)}z^2 + C_3^{(i)}z^3 + C_4^{(i)}z^4 + C_5^{(i)}z^5 + \frac{2}{5}A_3^{(i)}\mu^{(i)}z^5 + \frac{4}{15}A_4^{(i)}\mu^{(i)}z^6,\\
&\alpha_0^{(i)}(r) = \frac{2D_2^{(i)} - D_3^{(i)}}{4}r^2 + D_1^{(i)}\log r + \frac{D_3^{(i)}}{2}r^2\log r + D_4^{(i)} - B_0^{(i)}r + \frac{2A_2^{(i)}\mu^{(i)} - 3C_4^{(i)}}{8}r^4 + \frac{1}{24}A_4^{(i)}\mu^{(i)}r^6,
\end{aligned} \tag{A1.23}$$

where $\{A_1^{(i)},...,A_4^{(i)},B_0^{(i)},C_0^{(i)},...,C_5^{(i)},D_1^{(i)},...,D_4^{(i)}\}$ are real coefficients to determine and the equation $(A1.23)_1$ is the needed result. It is finally worth to note that, in both the cases of no-decaying of radial and hoop strains, the strain components appear to be at most characterized by a third-order polynomial function upon z and, as a consequence, the Love's function $\chi^{(i)}(r,z)$ has to possess at most a sixth-order polynomial structure in z. At the end, we investigate on the consequences of the assumption of no-decaying of the strain $\varepsilon_{rz}^{(i)}$. Begin by the Love's function giving the following relationship:

$$\varepsilon_{rz}^{(i)} = \frac{1}{2\mu^{(i)}}\left[\frac{2\mu^{(i)} + \lambda^{(i)}}{2(\mu^{(i)} + \lambda^{(i)})}\nabla^2\chi^{(i)} - \chi^{(i)}{}_{,zz}\right]_{,r} = \varepsilon^{(i)}(z) = g_{,zzzz}^{(i)}(z). \tag{A1.24}$$

Then, by integrating along the radius we obtain

$$\frac{2\mu^{(i)} + \lambda^{(i)}}{2(\mu^{(i)} + \lambda^{(i)})}\nabla^2\chi^{(i)} - \chi^{(i)}{}_{,zz} = 2\mu^{(i)}g_{,zzzz}^{(i)}(z)r + \alpha_{0,zz}^{(i)}(z) \tag{A1.25}$$

and, by applying the Laplace differential operator to both the sides in (A1.25) and recalling that $\chi^{(i)}(r,z)$ is a bi-harmonic function, we can write

$$\left(\nabla^2\chi^{(i)}\right)_{,zz} = -2\mu^{(i)}g_{,zzzzzz}^{(i)}(z)r - \alpha_{0,zzzz}^{(i)}(z) - r^{-1}g_{,zzzz}^{(i)}(z). \tag{A1.26}$$

By integrating again two times respect to z, the Laplacian of the Love's function $\chi^{(i)}(r,z)$ assumes the following form:

$$\nabla^2\chi^{(i)} = -2\mu^{(i)}g^{(i)}_{,zzzz}(z)r - \alpha^{(i)}_{0,zz}(z) - r^{-1}g^{(i)}_{,zz}(z) + \beta^{(i)}_1(r)z + \beta^{(i)}_2(r). \tag{A1.27}$$

By substituting (A1.27) into (A1.25), we have:

$$\begin{aligned}\chi^{(i)}{}_{,zz} = &-\frac{2\mu^{(i)}+\lambda^{(i)}}{2(\mu^{(i)}+\lambda^{(i)})}\left[2\mu^{(i)}g^{(i)}_{,zzzz}(z)r + \alpha^{(i)}_{0,zz}(z) + r^{-1}g^{(i)}_{,zz}(z) + \beta^{(i)}_1(r)z + \beta^{(i)}_2(r)\right] \\ &-2\mu^{(i)}g^{(i)}_{,zzzz}(z)r - \alpha^{(i)}_{0,zz}(z),\end{aligned} \tag{A1.28}$$

so that, integrating two times on z, we finally obtain

$$\begin{aligned}\chi^{(i)} = &-\frac{2\mu^{(i)}+\lambda^{(i)}}{2(\mu^{(i)}+\lambda^{(i)})}\left[2\mu^{(i)}g^{(i)}_{,zz}(z)r + \alpha^{(i)}_0(z) + r^{-1}g^{(i)}(z) + \beta^{(i)}_1(r)\frac{z^3}{6} + \beta^{(i)}_2(r)\frac{z^2}{2}\right] \\ &-2\mu^{(i)}g^{(i)}_{,zz}(z)r - \alpha^{(i)}_0(z) + \beta^{(i)}_3(r)z + \beta^{(i)}_4(r)\end{aligned} \tag{A1.29}$$

where $\alpha^{(i)}_0$ and $\beta^{(i)}_k$ are arbitrary functions to determine. At the end, by imposing again into (A1.29) that $\nabla^2\chi^{(i)}(r,z) = 0$ and invoking the identity polynomial law, we reach the following result:

$$g^{(i)}(z) = const. \Rightarrow \varepsilon^{(i)}_{rz} = \varepsilon^{(i)}(z) = 0. \tag{A1.30}$$

In conclusion, the obtained results can be interpreted from the two following points of view:
1) as *necessary conditions* to have possible strain no-decaying solutions for multilayered cylinder under axis-symmetrical boundary conditions: in other words this means that, if an arbitrary strain component is assumed to be not varying along the radius of the laminated composite cylinder, it can exhibit – in each phase of the object - at most a third-order polynomial form in z;
2) as *existence conditions* for deformations in a single layer material: this means that, with reference to a hollow homogenous and isotropic solid of revolution under prescribed axis-symmetrical boundary conditions, elastic solutions where an arbitrary strain component is assumed to be independent from r are admissible if and only if that strain component is at most a third-order polynomial function of z.

9.12. Appendix A.2 : Explicit expression of the coefficients $P_{h/m}$ of the matrix $\mathbb{P}$ for *n* arbitrary phases.

For the case of multilayered cylinder constituted by a central core and *n* hollow phases, the elastic axis-symmetrical solutions for the above described load conditions are related to the solution of the algebraic linear system reported in section 9.5, where the $(6n+4)\times(6n+4)$ matrix $\mathbf{P}$ is

$$\mathbf{P} = \begin{bmatrix}
P_{1/1} & P_{1/2} & \cdots & P_{1/6i-5} & P_{1/6i-4} & \cdots & P_{1/6i} & \cdots & P_{1/6n+1} & \cdots & P_{1/6n+4} \\
P_{2/1} & P_{2/2} & \cdots & P_{2/6i-5} & P_{2/6i-4} & \cdots & P_{2/6i} & \cdots & P_{2/6n+1} & \cdots & P_{2/6n+4} \\
\cdots & \cdots & \cdots & \cdots & \cdots & \cdots & \cdots & \cdots & \cdots & \cdots & \cdots \\
P_{6i-5/1} & P_{6i-5/2} & \cdots & P_{6i-5/6i-5} & P_{6i-5/6i-4} & \cdots & P_{6i-5/6i} & \cdots & P_{6i-5/6n+1} & \cdots & P_{6i-5/6n+4} \\
P_{6i-4/1} & P_{6i-4/2} & \cdots & P_{6i-4/6i-5} & P_{6i-4/6i-4} & \cdots & P_{6i-4/6i} & \cdots & P_{6i-4/6n+1} & \cdots & P_{6i-4/6n+4} \\
\cdots & \cdots & \cdots & \cdots & \cdots & \cdots & \cdots & \cdots & \cdots & \cdots & \cdots \\
P_{6i/1} & P_{6i/2} & \cdots & P_{6i/6i-5} & P_{6i/6i-4} & \cdots & P_{6i/6i} & \cdots & P_{6i/6n+1} & \cdots & P_{6i/6n+4} \\
\cdots & \cdots & \cdots & \cdots & \cdots & \cdots & \cdots & \cdots & \cdots & \cdots & \cdots \\
P_{6n+1/1} & P_{6n+1/2} & \cdots & P_{6n+1/6i-5} & P_{6n+1/6i-4} & \cdots & P_{6n+1/6i} & \cdots & P_{6n+1/6n+1} & \cdots & P_{6n+1/6n+4} \\
\cdots & \cdots & \cdots & \cdots & \cdots & \cdots & \cdots & \cdots & \cdots & \cdots & \cdots \\
P_{6n+4/1} & P_{6n+4/2} & \cdots & P_{6n+4/6i-5} & P_{6n+4/6i-4} & \cdots & P_{6n+4/6i} & \cdots & P_{6n+4/6n+1} & \cdots & P_{6n+4/6n+4}
\end{bmatrix}$$

and:

$$P_{1/1} = -\frac{R^{(0)}}{\mu^{(0)}},\ P_{1/4} = \frac{1}{2\mu^{(1)}R^{(0)}},\ P_{1/6} = \frac{R^{(0)}}{\mu^{(1)}},\ P_{1/2} = P_{1/3} = P_{1/5} = 0,\ \ P_{1/k} = 0\ \ \forall k \in \{7,8,...,6n+4\}$$

$$P_{2/2}=-\frac{2R^{(0)}}{\mu^{(0)}},\ P_{2/5}=\frac{1}{\mu^{(1)}R^{(0)}},\ P_{2/7}=\frac{2R^{(0)}}{\mu^{(1)}},\ P_{2/1}=P_{2/3}=P_{2/4}=P_{2/6}=0,\ P_{2/k}=0,\ \forall k\in\{8,9,...,6n+4\}$$

$$P_{3/2}=\frac{R^{(0)2}\left(\mu^{(0)}+\lambda^{(0)}\right)}{\mu^{(0)2}},\ P_{3/3}=-\frac{2\left(2\mu^{(1)}+\lambda^{(1)}\right)}{\mu^{(1)}\left(\mu^{(1)}+\lambda^{(1)}\right)}\log R^{(0)},\ P_{3/5}=-\frac{\log R^{(0)}}{\mu^{(0)}+\lambda^{(0)}},\ P_{3/1}=P_{3/4}=P_{3/6}=0,$$

$$P_{3/7}=-\frac{R^{(0)}\left(\mu^{(1)}+\lambda^{(1)}\right)}{\mu^{(1)2}},\ P_{3/8}=-1,\ P_{3/6n+4}=-\frac{R^{(0)2}\left(\mu^{(1)}\lambda^{(0)}-\mu^{(0)}\lambda^{(1)}\right)}{4\mu^{(0)}\mu^{(1)}},\ P_{3/k}=0,\quad \forall k\in\{9,10,...,6n+3\}$$

$$P_{4/1}=-\frac{2\left(\lambda^{(0)}+\mu^{(0)}\right)}{\mu^{(0)}},\ P_{4/4}=-\frac{1}{R^{(0)2}},\ P_{4/6}=\frac{2\left(\lambda^{(1)}+\mu^{(1)}\right)}{\mu^{(1)}},\ P_{4/6n+3}=\lambda^{(0)}-\lambda^{(1)},P_{4/2}=P_{4/3}=P_{4/5}=0,$$

$$P_{4/k}=0,\ \forall k\in\{7,8,...,6n+2,6n+4\}$$

$$P_{5/2}=-\frac{4\left(\lambda^{(0)}+\mu^{(0)}\right)}{\mu^{(0)}},P_{5/5}=-\frac{2}{R^{(0)2}},P_{5/7}=\frac{4\left(\lambda^{(1)}+\mu^{(1)}\right)}{\mu^{(1)}},P_{5/6n+4}=\lambda^{(0)}-\lambda^{(1)},$$

$$P_{5/1}=P_{5/3}=P_{5/4}=P_{5/6}=0,\ \ P_{5/k}=0,\ \forall k\in\{8,9,...,6n+3\}$$

$$P_{6/2}=\frac{2R^{(0)}\lambda^{(0)}}{\mu^{(0)}},\ P_{6/3}=-\frac{2\left(2\mu^{(1)}+\lambda^{(1)}\right)}{R^{(0)2}\left(\lambda^{(1)}+\mu^{(1)}\right)},\ P_{6/5}=\frac{\lambda^{(1)}}{R^{(0)}\left(\lambda^{(1)}+\mu^{(1)}\right)},\ P_{6/1}=P_{6/4}=P_{6/6}=0,$$

$$P_{6/7}=-\frac{2R^{(0)}\lambda^{(1)}}{\mu^{(1)}},\ P_{6/6n+4}=\frac{1}{2}R^{(0)}\left(2\mu^{(0)}+\lambda^{(0)}-2\mu^{(1)}-\lambda^{(1)}\right),\ P_{6/k}=0,\ \forall k\in\{8,9,...,6n+3\}$$

$$P_{6i-5/6i-8}=-\frac{1}{2R^{(i)}\mu^{(i)}},P_{6i-5/6i-6}=-\frac{R^{(i)}}{\mu^{(i)}},P_{6i-5/6i-2}=\frac{1}{2R^{(i)}\mu^{(i+1)}},P_{6i-5/6i}=\frac{R^{(i)}}{\mu^{(i+1)}},\forall i\in\{2,...,n-1\}$$

$$P_{6i-5/k}=0,\quad \forall k\in\{1,2,...,6n+4\}-\{6i-8,6i-6,6i-2,6i\}$$

$$P_{6i-4/6i-7}=-\frac{1}{R^{(i)}\mu^{(i)}},P_{6i-4/6i-5}=-\frac{2R^{(i)}}{\mu^{(i)}},P_{6i-4/6i-1}=\frac{1}{R^{(i)}\mu^{(i+1)}},P_{6i-4/6i+1}=\frac{2R^{(i)}}{\mu^{(i+1)}},\forall i\in\{2,...,n-1\}$$

$$P_{6i-4/k}=0\quad \forall k\in\{1,2,...,6n+4\}-\{6i-7,6i-5,6i-1,6i+1\}$$

$$P_{6i-1/6i-7}=\frac{2}{R^{(i)2}},P_{6i-1/6i-5}=-\frac{4\left(\mu^{(i)}+\lambda^{(i)}\right)}{\mu^{(i)}},\ P_{6i-1/6i-1}=-\frac{2}{R^{(i)2}},P_{6i-1/6i+1}=\frac{4\left(\mu^{(i+1)}+\lambda^{(i+1)}\right)}{\mu^{(i+1)}},$$

$$P_{6i-1/6n+4}=\lambda^{(i)}-\lambda^{(i+1)},\ \forall i\in\{2,...,n-1\},$$

$$P_{6i-1/k}=0,\quad \forall k\in\{1,2,...,6n+4\}-\{6i-7,6i-5,6i-1,6i+1,6n+4\}$$

$$P_{6i-3/6i-9}=\frac{2\log R^{(i)}\left(2\mu^{(i)}+\lambda^{(i)}\right)}{\mu^{(i)}\left(\mu^{(i)}+\lambda^{(i)}\right)},\ P_{6i-3/6i-7}=\frac{\log R^{(i)}}{\mu^{(i)}+\lambda^{(i)}},\ P_{6i-3/6i-5}=\frac{R^{(i)2}\left(\mu^{(i)}+\lambda^{(i)}\right)}{\mu^{(i)2}},\ P_{6i-3/6i-4}=1,$$

$$P_{6i-3/6i-3}=-\frac{2\log R^{(i)}\left(2\mu^{(i+1)}+\lambda^{(i+1)}\right)}{\mu^{(i+1)}\left(\mu^{(i+1)}+\lambda^{(i+1)}\right)},\ P_{6i-3/6i-1}=-\frac{\log R^{(i)}}{\mu^{(i+1)}+\lambda^{(i+1)}},\ P_{6i-3/6i+1}=-\frac{R^{(i)2}\left(\mu^{(i+1)}+\lambda^{(i+1)}\right)}{\mu^{(i+1)2}},$$

$$P_{6i-3/6i+2}=1,\ P_{6i-3/6n+4}=\frac{R^{(i)2}\left(\mu^{(i)}\lambda^{(i+1)}-\lambda^{(i)}\mu^{(i+1)}\right)}{4\mu^{(i)}\mu^{(i+1)}},\forall i\in\{2,...,n-1\}$$

$$P_{6i-3/k}=0\quad \forall k\in\{1,2.....,6n+3\}-\{6i-9,6i-7,6i-5,6i-4,6i-3,6i-1,6i+1,6i+2,6n+4\}$$

$$P_{6i/6i-9}=\frac{2\left(2\mu^{(i)}+\lambda^{(i)}\right)}{R^{(i)}\left(\mu^{(i)}+\lambda^{(i)}\right)},\ P_{6i/6i-7}=-\frac{\lambda^{(i)}}{R^{(i)}\left(\mu^{(i)}+\lambda^{(i)}\right)},\ P_{6i/6i-5}=\frac{2R^{(i)}\lambda^{(i)}}{\mu^{(i)}},$$

$$P_{6i/6i-3}=-\frac{2\left(2\mu^{(i+1)}+\lambda^{(i+1)}\right)}{R^{(i)}\left(\mu^{(i+1)}+\lambda^{(i+1)}\right)},\ P_{6i/6i-1}=\frac{\lambda^{(i+1)}}{R^{(i)}\left(\mu^{(i+1)}+\lambda^{(i+1)}\right)},\ P_{6i/6i+1}=-\frac{2R^{(i)}\lambda^{(i+1)}}{\mu^{(i+1)}},$$

$$P_{6i/6n+4}=\frac{R^{(i)}\left(2\mu^{(i+1)}+\lambda^{(i+1)}-2\mu^{(i)}-\lambda^{(i)}\right)}{2},\ \forall i\in\{2,...,n-1\}$$

$$P_{6i/k}=0\quad \forall k\in\{1,2,...,6n+4\}-\{6i-9,6i-7,6i-5,6i-3,6i-1,6i+1,6n+4\},$$

$$P_{6n+1/6n-2}=\frac{1}{R^{(n)2}},\ P_{6n+1/6n}=-\frac{2\left(\mu^{(n)}+\lambda^{(n)}\right)}{\mu^{(n)}},\ P_{6n+1/6n+3}=\lambda^{(n)},$$

$$P_{6n+1/k}=0,\ \forall k\in\{1,2,...,6n+4\}-\{6n-2,6n,6n+3\},$$

$$P_{6n+2/6n-1}=\frac{2}{R^{(n)2}},P_{6n+2/6n+1}=-\frac{4\left(\mu^{(n)}+\lambda^{(n)}\right)}{\mu^{(n)}},P_{6n+2/6n+4}=\lambda^{(n)},$$

$$P_{6n+2/k}=0,\ \forall k\in\{1,2,...,6n+3\}-\{6n\pm1\},$$

$$P_{6n+3/6n-3}=\frac{2\left(2\mu^{(n)}+\lambda^{(n)}\right)}{R^{(n)}\left(\mu^{(n)}+\lambda^{(n)}\right)},\ P_{6n+3/6n-1}=-\frac{\lambda^{(n)}}{R^{(n)}\left(\mu^{(n)}+\lambda^{(n)}\right)},\ P_{6n+3/6n+1}=\frac{2R^{(s)}\lambda^{(s)}}{\mu^{(s)}},$$

$$P_{6n+3/6n+4}=-\frac{R^{(n)}\left(2\mu^{(n)}+\lambda^{(n)}\right)}{2},\ P_{6n+3/k}=0,\ \forall k\in\{1,2,...,6n+3\}-\{6n-3,6n\pm1\},$$

$$P_{6n+4/1}=-\frac{2\pi\lambda^{(0)}R^{(0)2}}{\mu^{(0)}},P_{6n+4/6i}=\frac{2\pi\lambda^{(i)}\left(R^{(i-1)2}-R^{(i)2}\right)}{\mu^{(i)}},\ \forall i\in\{1,2,...,n-1\},$$

$$P_{6n+4/6n+3}=\pi\left[\sum_{i=0}^{n-1}R^{(i)2}\left(2\mu^{(i)}+\lambda^{(i)}-2\mu^{(i+1)}-\lambda^{(i+1)}\right)+R^{(n)2}\left(2\mu^{(n)}+\lambda^{(n)}\right)\right],$$

$$P_{6n+4/k}=0,\ \forall k\in\{2,...,6n+4\}-\{1,6i,6n+3\}.$$

CHAPTER X
MULTILAYERED CYLINDER UNDER SAINT-VENANT'S LOADS AND HOMOGENIZATION: *POISSON EFFECT ON STIFFNESS*

10.1. Introduction

Object of the chapter is to show exact analytical solutions for the elastic response of a long solid circular cylinder, composed by the assembly of a central core and of *n* hollow surrounding tubular phases of different homogeneous elastic materials, under De Saint Venant load conditions, and to obtain for the whole solid a one-dimensional homogenised beam description.
The solution for case of shear and bending is exact and new for this type of heterogeneous material, and is hence useful for the comparison with other simplified solutions already existing in literature.
The adopted procedure, that for this multilayered cylinder gives homogenised elastic relationships between generalised stresses and strains in cases of axial force, torque, bending and shear, is particularly useful to highlight the possible large increase of the homogenised stiffness due to composition of specific base materials having selected values of Poisson modulus. The case of negative Poisson's modulus is considered, since such type of material deriving from particular microstructures or work processes induces relevant effects on the heterogeneous material. At the end, some example applications are shown for two phase material, and carried out suitable sensitivity analyses. Multi-phase long cylinders constituted by $n \in \mathbb{N}$ hollow layers enveloping a central core have been extensively studied in recent literature works because their geometry is often met in many man-made and chemically synthesised materials and biological structures, at different scale levels (Figure 1). Cylindrical shells are indeed often used as basic structural components in engineering applications and, in order to derive macroscopic mechanical behaviours of these composites, much research has been conducted on isotropic or laminated composite plates and shells, also with reference to thermo-elastic problems involving functionally graded ideally infinite hollow cylinders. In particular, Liew et al. [1] obtained analytical solutions of a functionally graded circular cylinder by a novel limiting process that employs the solutions of homogeneous circular hollow cylinders. Shao [2] derived analytical solutions for mechanical and thermal stresses of a FGMC with finite length, and Mian, Abid and Spencer [3] determined some results for isotropic laminated FGMs with specific variation of the elastic moduli in the direction of the axis of the object. Meharabadi and Cowin [5] and Yoou et al. [6] widely discussed about the elasticity tensor of the FGM as non-homogeneous materials. Recently, some new results were obtained for non-homogeneous and anisotropic materials by using a *Stress-Associated Solution* theorem by Fraldi and Cowin [4], and Alshits and Kirkhner [7] derived some elastic solutions for radially inhomogeneous and cylindrically anisotropic circular cylinders, where no variations of the stresses along the axis of the cylinder are assumed. Other interesting results for laminated composite tubes are obtained by Chouchaoui & Ochoa [8], Chen et al, [9], Tarn [10] and Tarn & Wang [11]. In particular, these last two authors, by employing the *state space approach*, starting from results by Lekhnitskii [12], constructed analytical solutions for several elastic problems with constant stresses along the axis of the tube, also assuming cylindrically anisotropy for each phase. Moreover, Huang and Dong [13] analysed elastic response of a laminated circular cylinder with the most general form of cylindrical anisotropy. With reference to specific properties of the solution in terms of strains related to applications in the field of fiber optic sensors, Fraldi, Nunziante and Carannante derived analytical solutions for *multilayered cylinder* under axis-symmetry boundary conditions [16,17]. Starting from these just mentioned results, in the present chapter the same authors further generalize the previous work, by developing an analytical approach to find exact elastic solutions for multilayered cylinder composed of isotropic constituents and determining the analytical response in terms of displacements and stresses for all the De Saint Venant (DSV) load conditions, that is axial force, torque, pure bending and combined bending moment and shear actions [18,19]
By essentially following the line of reasoning adopted in [16], the solution strategy is unitarily constructed for all the DSV load cases separately, by first transforming the Navier-Cauchy equilibrium problem to be written on each phase of multilayered cylinder in a system of Euler

Partial Differential Equations (PDEs) and finally, through the interfacial compatibility and equilibrium equations and the weak conditions on the resultants at the object extremities, by reducing the problem to a corresponding algebraic system of equations ruled by a matrix whose coefficients are parametrically dependent on geometrical and elastic phase parameters (i.e. phases radii and Young and Poisson ratios), for each of the DSV loading obtaining an *a-priori* matrix rank ($(2n+2)$ for the axial force, $(3n+2)$ in case of pure bending, and $(5n+3)$ for combined shear forces and bending moments).
Successively, on the basis of the found analytical solutions, a homogenization procedure is adopted in order to obtain the overall constitutive elastic laws for multilayered cylinder, in this way deriving the *exact* one-dimensional model characterized by the axial stiffness, flexural rigidity, shear deformability and torsional stiffness relating beam's generalized stresses and strains. By virtue of the closed-form solutions, the *localization* procedure is also illustrated, with the aim of tracing actual stress fluctuations and peaks in each phase as functions of the geometrical and mechanical parameters of the object constituents, particularly needed to guess detachment at the material interfaces and to predict or design mechanical performance of the composite material. For this purpose, at the end, playing with the Poisson ratios of adjacent phases, some counterintuitive and engineering relevant results - already highlighted in some recent papers - are shown with reference to unexpected increasing of overall stiffness of multilayered cylinder, which apparently violate the universal Hashin-Shtrikman bounds [24,25].

10.2. Basic equations for multilayered cylinder under De Saint Venant load conditions

In this section the DSV problem is specialized to multilayered cylinder, for which elastic solutions under the action of any arbitrary combination of axial forces, bending moment and shear, torsion are obtained in closed-form, by partially using some results already found in the case of axis-symmetry [16] and starting from the Lekhnitskii formalism to determine the mathematical form of displacements and stresses in each object phases for the cases of torsion, pure bending and shear [11-12]. Then, let us consider a solid cylinder composed by a central core and by *n* cylindrical hollow phases, each of them constituted by different homogeneous and linearly isotropic materials, perfectly bonded at the interfaces (figure 2). The geometry of the object suggests cylindrical coordinates $\{r, \theta, z\}$ as natural frame, z representing the axis of the compound cylinder. Under the hypothesis of small deformation, compatibility equations relating strains and displacements are given for each phase by

$$\boldsymbol{\varepsilon}^{(i)} = \left\{ u_{r,r}^{(i)},\ r^{-1}\left(u_r^{(i)} + u_{\theta,\theta}^{(i)}\right),\ u_{z,z}^{(i)},\ u_{\theta,z}^{(i)} + r^{-1}u_{z,\theta}^{(i)},\ u_{r,z}^{(i)} + u_{z,r}^{(i)},\ r^{-1}\left(u_{r,\theta}^{(i)} - u_{\theta}^{(i)}\right) + u_{\theta,r}^{(i)} \right\} \tag{2.1}$$

where $\mathbf{u}^{(i)} \equiv \{u_r^{(i)}, u_\theta^{(i)}, u_z^{(i)}\}$ and $\boldsymbol{\varepsilon}^{(i)}$, are displacement vector and strain vector into the generic i-phase, respectively. Linearity for constitutive elastic relationships of each isotropic material phase is assumed, namely Hooke's law is satisfied:

$$\begin{bmatrix} \sigma_{rr}^{(i)} \\ \sigma_{\theta\theta}^{(i)} \\ \sigma_{zz}^{(i)} \\ \tau_{z\theta}^{(i)} \\ \tau_{rz}^{(i)} \\ \tau_{r\theta}^{(i)} \end{bmatrix} = \begin{bmatrix} 2\mu^{(i)} & \lambda^{(i)} & \lambda^{(i)} & 0 & 0 & 0 \\ \lambda^{(i)} & 2\mu^{(i)} & \lambda^{(i)} & 0 & 0 & 0 \\ \lambda^{(i)} & \lambda^{(i)} & 2\mu^{(i)} & 0 & 0 & 0 \\ 0 & 0 & 0 & 2\mu^{(i)} & 0 & 0 \\ 0 & 0 & 0 & 0 & 2\mu^{(i)} & 0 \\ 0 & 0 & 0 & 0 & 0 & 2\mu^{(i)} \end{bmatrix} \begin{bmatrix} \varepsilon_{rr}^{(i)} \\ \varepsilon_{\theta\theta}^{(i)} \\ \varepsilon_{zz}^{(i)} \\ \varepsilon_{z\theta}^{(i)} \\ \varepsilon_{rz}^{(i)} \\ \varepsilon_{r\theta}^{(i)} \end{bmatrix} \tag{2.2}$$

where $\boldsymbol{\sigma}^{(i)} = \{\sigma_{rr}^{(i)}, \sigma_{\theta\theta}^{(i)}, \sigma_{zz}^{(i)}, \tau_{\theta z}^{(i)}, \tau_{rz}^{(i)}, \tau_{r\theta}^{(i)}\}$, is the stress vector corresponding to the Cauchy stress tensor $\mathbf{T}^{(i)}$ in the generic *i*-phase, $\mu^{(i)}$, $\lambda^{(i)}$ are Lamè constants. In the cylindrical reference system, in absence of body force, equilibrium equations become:

$$\nabla\cdot\mathbf{T}^{(i)}=\begin{bmatrix}\sigma^{(i)}_{rr,r}+r^{-1}\left(\tau^{(i)}_{r\theta,\theta}+\sigma^{(i)}_{rr}-\sigma^{(i)}_{\theta\theta}\right)+\tau^{(i)}_{rz,z}\\ \tau^{(i)}_{r\theta,r}+r^{-1}\left(\sigma^{(i)}_{\theta\theta,\theta}+2\tau^{(i)}_{r\theta}\right)+\tau^{(i)}_{\theta z,z}\\ \tau^{(i)}_{rz,r}+r^{-1}\left(\tau^{(i)}_{\theta z,\theta}+\tau^{(i)}_{rz}\right)+\sigma^{(i)}_{zz,z}\end{bmatrix}=\mathbf{0} \tag{2.3}$$

By substituting equations (2.1)-(2.2) in to equilibrium equations (2.3), we obtain for each phase the Navier-Cauchy equilibrium equations in cylindrical coordinates:

$$\begin{cases}\mu^{(i)}\left(\nabla^2u^{(i)}_r-2r^{-2}u^{(i)}_{\theta,\theta}-r^{-2}u^{(i)}_r\right)+\left(\mu^{(i)}+\lambda^{(i)}\right)\left(\nabla\cdot\mathbf{u}^{(i)}\right)_{,r}=0\\ \mu^{(i)}\left(\nabla^2u^{(i)}_\theta+2r^{-2}u^{(i)}_{r,\theta}-r^{-2}u^{(i)}_\theta\right)+\left(\mu^{(i)}+\lambda^{(i)}\right)r^{-1}\left(\nabla\cdot\mathbf{u}^{(i)}\right)_{,\theta}=0\\ \mu^{(i)}\nabla^2u^{(i)}_z+\left(\mu^{(i)}+\lambda^{(i)}\right)\left(\nabla\cdot\mathbf{u}^{(i)}\right)_{,z}=0\end{cases} \tag{2.4}$$

where $\nabla\cdot\mathbf{u}^{(i)}=u^{(i)}_{r,r}+r^{-1}u^{(i)}_r+r^{-1}u^{(i)}_{\theta,\theta}+u^{(i)}_{z,z}$ is the divergence of the displacement field and $\nabla^2=\partial/\partial r^2+r^{-1}\partial/\partial r+r^{-2}\,\partial/\partial\theta^2+\partial/\partial z^2$ represents the Laplace differential operator. Then the displacement field $\mathbf{u}^{(i)}$ constituting the elastic solution of the problem, must satisfy equations (2.4) in each phase. Moreover, the strain $\boldsymbol{\varepsilon}^{(i)}$ obtained through compatibility relations from field $\mathbf{u}^{(i)}$, by means of Hooke relationships generates the stress field $\boldsymbol{\sigma}^{(i)}$. Projection of stress $\boldsymbol{\sigma}^{(i)}$ onto boundary must satisfy there equilibrium conditions of de Saint Venant type, as reported below. We will show in the following, the boundary equations at the interfaces between the two adjacent *i*-th and *(i+1)*-th phases, and boundary conditions of equilibrium on the external cylindrical surface and on the end bases. Compatibility and equilibrium equations at every interface, are:

$$\forall(r=R^{(i)}),i\in\{0,1,...,n-1\}\ :\begin{cases}u^{(i)}_r=u^{(i+1)}_r,\ u^{(i)}_\theta=u^{(i+1)}_\theta\ ,u^{(i)}_z=u^{(i+1)}_z\\ \sigma^{(i)}_{rr}=\sigma^{(i+1)}_{rr},\tau^{(i)}_{rz}=\tau^{(i+1)}_{rz},\tau^{(i)}_{r\theta}=\tau^{(i+1)}_{r\theta}\end{cases} \tag{2.5}$$

Boundary Cauchy equations on the external cylindrical surface, ($i=n$), reads:

$$r=R^{(n)}\ :\ \sigma^{(n)}_{rr}=0,\ \tau^{(n)}_{rz}=0,\ \tau^{(n)}_{r\theta}=0 \tag{2.6}$$

Finally, it remains to consider the equilibrium equations on the bases $z=0$ and $z=L$. On both bases we have, with suitable choose of sign,

$$\begin{aligned}&\sum_{i=0}^{n}\int_0^{2\pi}\int_{(1-\delta_{0i})R^{(i-1)}}^{R^{(i)}}\sigma^{(i)}_{zz}rdrd\theta=N_z, &&\sum_{i=0}^{n}\int_0^{2\pi}\int_{(1-\delta_{0i})R^{(i-1)}}^{R^{(i)}}\tau^{(i)}_{\theta z}\,r^2drd\theta=\mathcal{M}_z,\\ &\sum_{i=0}^{n}\int_0^{2\pi}\int_{(1-\delta_{0i})R^{(i-1)}}^{R^{(i)}}\tau^{(i)}_{xz}rdrd\theta=T_x, &&\sum_{i=0}^{n}\int_0^{2\pi}\int_{(1-\delta_{0i})R^{(i-1)}}^{R^{(i)}}\tau^{(i)}_{yz}rdrd\theta=T_y,\end{aligned} \tag{2.7}$$

where $T_x,T_y,N_z,\mathcal{M}_z$, are shear forces, axial force and torque couple, applied on the bases, respectively. Equilibrium equations about axes x and y for base $z=0$ give the bending couples:

$$\sum_{i=0}^{n}\int_0^{2\pi}\int_{(1-\delta_{0i})R^{(i-1)}}^{R^{(i)}}\sigma_{zz}r^2\sin\theta drd\theta=\mathcal{M}_x,\qquad\sum_{i=0}^{n}\int_0^{2\pi}\int_{(1-\delta_{0i})R^{(i-1)}}^{R^{(i)}}\sigma_{zz}r^2\cos\theta drd\theta=\mathcal{M}_y, \tag{2.8}$$

and for base $z=L$, equilibrium equations about axes x and y give:

$$\begin{aligned}\mathcal{M}_{L1}&=\sum_{i=0}^{n}\int_0^{2\pi}\int_{(1-\delta_{0i})R^{(i-1)}}^{R^{(i)}}\sigma_{zz}r^2\sin\theta drd\theta=\mathcal{M}_x+T_yL,\\ \mathcal{M}_{L2}&=\sum_{i=0}^{n}\int_0^{2\pi}\int_{(1-\delta_{0i})R^{(i-1)}}^{R^{(i)}}\sigma_{zz}r^2\cos\theta drd\theta=\mathcal{M}_y-T_xL,\end{aligned} \tag{2.9}$$

In what follows, it is proved that two distinct classes of displacement potentials are completely able to describe the whole set of solutions for multilayered cylinder under DSV load conditions, that is an *irrotational* displacement field derived by restricting the Love's function to the case of axial force, and a *solenoidal* displacement field, representing all the remaining loadings, i.e. torque and combined bending and shear forces.

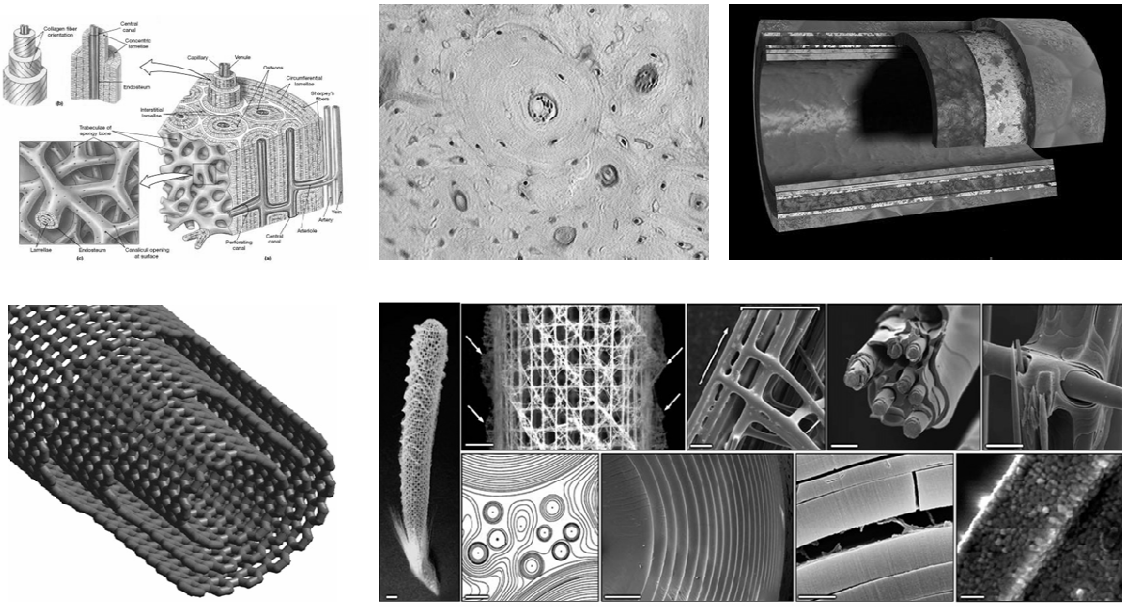

Fig. 10.1 - *Selected examples of multilayered cylinder: Osteon microstructure (top-left); Arterial walls (top-right); Multi-wall Carbon Nanotubes (bottom-left); Diatomee microstructures (bottom-right).*

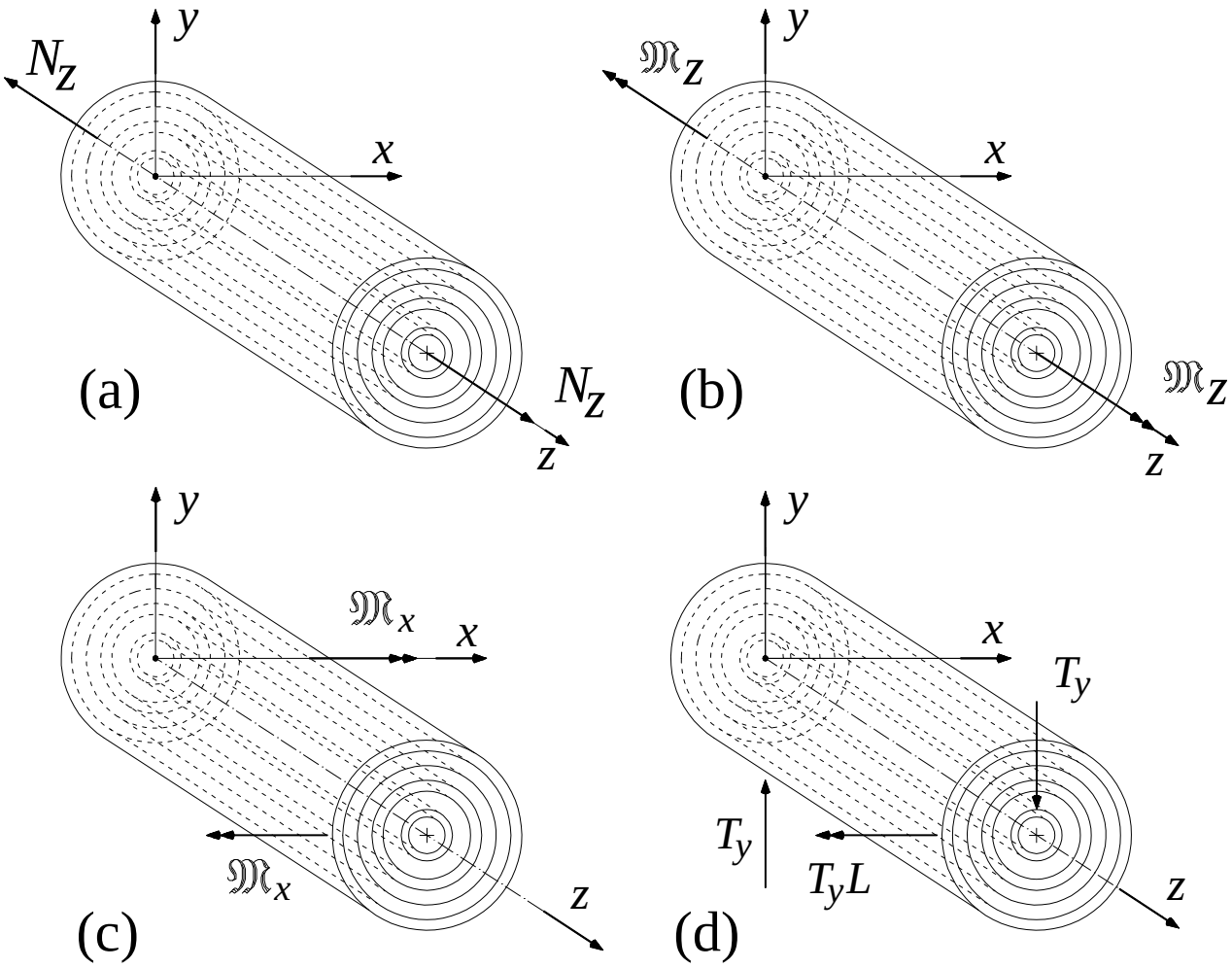

Fig. 10.2 - *de Saint Venant load conditions for multilayered cylinder: a) Axial force; b) Torque; c) Pure bending; d) Shear and bending moment.*

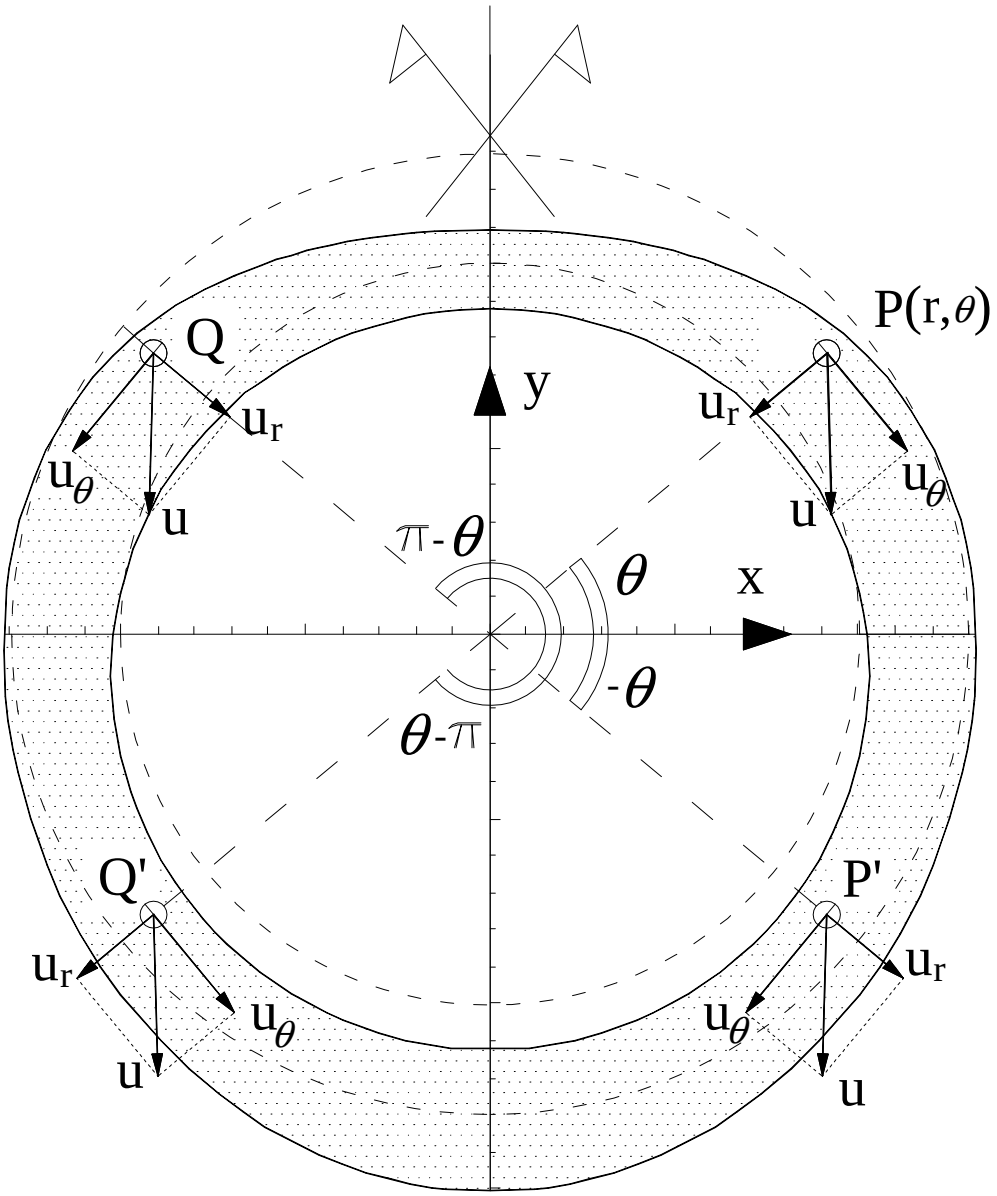

Fig. 10.3 - *Displacement of cross section in case of bending: symmetry and skew-symmetry conditions*

10.3. Irrotational displacement potentials: axial forces

In three-dimensional elasticity, the displacement solution **u** is obtained by to define a potential function representation for displacement which identically satisfies the compatibility conditions and allows to obtaining the equilibrium condition defining the governing equation.

It is well known that the solution in terms of displacement field **u** for an isotropic and homogeneous linear elastic material, in absence of body forces, can be written in the cylindrical system by means of the *Boussinesq-Somigliana-Galerkin* vector $\mathbf{F} \equiv \left[F_r, F_\theta, F_z\right]^T$, where three components of vector **F** are function of cylindrical coordinates (r, ϑ, x_3) as reported below:

$$\begin{cases} u_r = \left\{\left[(2\mu+\lambda)/(\mu+\lambda)\right]\left[\cos\theta\cdot\nabla^2 F_x + \sin\theta\cdot\nabla^2 F_y\right] - \zeta_{,r}\right\}/(2\mu) \\ u_\theta = \left\{\left[(2\mu+\lambda)/(\mu+\lambda)\right]\left[-\sin\theta\cdot\nabla^2 F_x + \cos\theta\cdot\nabla^2 F_y\right] - r^{-1}\zeta_{,\theta}\right\}/(2\mu) \\ u_z = \left\{\left[(2\mu+\lambda)/(\mu+\lambda)\right]\nabla^2 F_z - \zeta_{,z}\right\}/(2\mu) \end{cases} \tag{3.1}$$

where F_x, F_y, F_z are components of Galerkin's vector $\mathbf{F}$ in Cartesian coordinate and are given by:

$$F_x = F_r \cos\theta - F_\theta \sin\theta, \quad F_y = F_r \sin\theta + F_\theta \cos\theta, \tag{3.2}$$

and the function ζ is given by:

$$\zeta = \cos\theta \cdot F_{x,r} - \sin\theta \cdot r^{-1} F_{x,\theta} + \sin\theta \cdot F_{y,r} + \cos\theta \cdot r^{-1} F_{y,\theta} + F_{z,z} \tag{3.3}$$

The Galerkin's vector $\mathbf{F}$ must be to satisfy the bi-harmonic condition $\nabla^4 \mathbf{F} = 0$. In Cartesian coordinate system the components of Galerkin's vector $\mathbf{F}$ are bi-harmonic, but in cylindrical coordinate system the two components F_r, F_θ are not bi-harmonic. A more detailed derivation is given by Westergaard, who gives expressions for the stress components in terms of $\mathbf{F}$ and uses this representation to solve a number of classical three-dimensional problems – namely those involving concentrated forces in the infinite or semi-infinite body. The Galerkin's solution was to some extent foreshadowed by Love [15], who introduced a displacement function appropriate for an axis-symmetrical state of stress in a solid of revolution. When a solid cylinder is deformed symmetrically by forces applied on its external cylindrical surface and on its two end sections, it is possible to express all the mechanical quantities in terms of a single function, reducing the elastic equilibrium equations of the body to a single partial differential equation.

If $\mathbf{e}_z$ is the unit vector of z direction which characterizes the axis-symmetrical problem, the displacement solution is called torsion-less and rotationally symmetric with respect to the z axis. Then, displacement solution $\mathbf{u}$ satisfies the following condition:

$$\mathbf{e}_z \cdot \nabla \wedge \mathbf{u}^{(h)} = 0 \tag{3.4}$$

In order to satisfy the condition (3.4), it is assumed the Galerkin's vector as reported below:

$$\mathbf{F} \equiv \left[0, 0, \chi(r, z)\right]^T \tag{3.5}$$

in which $\chi(\mathrm{r},\mathrm{z}) \in \mathrm{C}^{(4)}(\Omega)$ is a scalar function and is called the *Love*'s solution. By substituting equation (3.5) in equation (3.1) , it is possible to determine the displacement solution in terms of *Love*'s solution as reported below:

$$u_r = -(1/2)\left(\chi_{,rz}/\mu\right), \; u_\theta = 0, \; u_z = (1/2)\left[\left(\nabla^2 \chi\right)/(\mu+\lambda) + \left(\chi_{,rr} + r^{-1}\chi_{,r}\right)/\mu\right] \tag{3.6}$$

In which $\chi(r,z)$ is the bi-harmonic function and then satisfy the follows differential equation:

$$\nabla^4 \chi = \chi_{,rrrr} + 2r^{-1}\left[\chi_{,rrr} + \chi_{,rzz}\right] - r^{-2}\chi_{,rr} + r^{-3}\chi_{,r} + 2\chi_{,rrzz} + \chi_{,zzzz} = 0, \tag{3.7}$$

The vector $\nabla \wedge \mathbf{u}$ is given by:

$$\begin{aligned} \left[\nabla \wedge \mathbf{u}\right]^T &= \left[\left(r^{-1}u_{z,\theta} - u_{\theta,z}\right) \quad \left(u_{r,z} - u_{z,r}\right) \quad \left(r^{-1}\left(u_\theta - u_{r,\theta}\right) + u_{\theta,r}\right)\right]^T = \\ &= \left[0, -\left[(2\mu+\lambda)/\left(2\mu(\mu+\lambda)\right)\right]\left(\nabla^2\chi\right)_{,r}, 0\right]^T \end{aligned} \tag{3.8}$$

Then, the curl of vector $\mathbf{u}^{(h)}$ obtained by equation (3.8) satisfies the condition (3.4). By substituting the displacement components (3.6) in (2.1), it is possible to obtain the strain components reported below:

$$\begin{aligned} &\varepsilon_{rr} = -\chi_{,rrz}/(2\mu), \; \varepsilon_{\theta\theta} = -\left(r^{-1}\chi_{,rz}\right)/(2\mu), \; \varepsilon_{zz} = \left\{\left[(2\mu+\lambda)/(\mu+\lambda)\right]\nabla^2\chi_{,z} - \chi_{,zzz}\right\}/(2\mu), \\ &\varepsilon_{rz} = \left\{(1/2)\left[(2\mu+\lambda)/(\mu+\lambda)\right]\nabla^2\chi_{,r} - \chi_{,rzz}\right\}/\mu, \; \varepsilon_{\theta z} = \varepsilon_{r\theta} = 0, \end{aligned} \tag{3.9}$$

By applying the equations (2.2) it is easy to obtain for the i-th material phase the no-vanishing stresses that depend by scalar function $\chi^{(i)}(r,z)$:

$$\begin{aligned} &\sigma_{rr} = \left\{(1/2)\left[\lambda/(\mu+\lambda)\right]\nabla^2\chi - \chi_{,rr}\right\}_{,z}, \; \sigma_{\theta\theta} = \left\{(1/2)\left[\lambda/(\mu+\lambda)\right]\nabla^2\chi - r^{-1}\chi_{,r}\right\}_{,z}, \\ &\sigma_{zz} = \left\{(1/2)\left[(4\mu+3\lambda)/(\mu+\lambda)\right]\nabla^2\chi - \chi_{,zz}\right\}_{,z}, \; \tau_{rz} = \left\{(1/2)\left[(2\mu+\lambda)/(\mu+\lambda)\right]\nabla^2\chi - \chi_{,zz}\right\}_{,r} \end{aligned} \tag{3.10}$$

In this section it is presented the closed-form elastic solution for multilayered cylinder above defined (Figure 2a), under axial forces. The multiphase solid is subjected on the two bases to equilibrating axial load distribution, whose resultants are N_z (Figure 2a). Then, the solid is subjected to axis-symmetrical boundary conditions. In follows, if it is not explicit reported the apex "i" varies in $\{0,1,....,n\}$ for any equations. If the multilayered cylinder is quite long $\left(L >> R^{(n)}\right)$ it is meaningful to assume that stresses and strains depend only on the variable r being independent from z. This condition is obtained by imposing null values to derivates of diagonal stress components respect to z:

$$\left[\sigma_{rr,z}^{(i)} \quad \sigma_{\theta\theta,z}^{(i)} \quad \sigma_{zz,z}^{(i)}\right]^T = [\mathbf{S}]\cdot\left[\chi_{,zzzz}^{(i)} \quad \chi_{,rzz}^{(i)} \quad \chi_{,rrzz}^{(i)}\right]^T = \mathbf{0} \tag{3.11}$$

where

$$\mathbf{S} = \frac{1}{2\left(\mu^{(i)}+\lambda^{(i)}\right)}\begin{bmatrix} \lambda^{(i)} & r^{-1}\lambda^{(i)} & -\left(2\mu^{(i)}+\lambda^{(i)}\right) \\ \lambda^{(i)} & -r^{-1}\left(2\mu^{(i)}+\lambda^{(i)}\right) & \lambda^{(i)} \\ 2\mu^{(i)}+\lambda^{(i)} & r^{-1}\left(4\mu^{(i)}+3\lambda^{(i)}\right) & 4\mu^{(i)}+3\lambda^{(i)} \end{bmatrix} \tag{3.12}$$

The determinant of matrix **S** in equation (3.12) is given by:

$$\det[\mathbf{S}] = -r^{-1}\left(2\mu^{(i)}+3\lambda^{(i)}\right)\Big/\left[2\left(\mu^{(i)}+\lambda^{(i)}\right)\right] = -\left(1+\nu^{(i)}\right)r^{-1} \neq 0 \tag{3.13}$$

Then, by equations (3.11)-(3.13), the following three conditions for Love's function are obtained :

$$\chi_{,zzzz}^{(i)} = 0, \quad \chi_{,rzz}^{(i)} = 0, \quad \chi_{,rrzz}^{(i)} = 0 \tag{3.14}$$

By integration of the equations (3.14), we obtain the expression of Love's function, as a polynomial of third order respect to z variable :

$$\chi^{(i)}(r,z) = \phi_0^{(i)}(r) + \phi_1^{(i)}(r)\,z + \Lambda_1^{(i)} z^2 + \Lambda_2^{(i)} z^3 \tag{3.15}$$

where $\Lambda_1^{(i)}, \Lambda_2^{(i)}$ are integration constants and $\phi_0^{(i)}(r)$, $\phi_1^{(i)}(r)$ are unknown functions of variable r. By also imposing the derivate of tangential stress $\tau_{rz}^{(i)}$ respect to variable z is equal to zero, the ordinary differential equation in the unknown function $\phi_1^{(i)}(r)$ is obtained:

$$\phi_{1,r}^{(i)}(r) - r\left(\phi_{1,rr}^{(i)}(r) + r\,\phi_{1,rrr}^{(i)}(r)\right) = 0 \tag{3.16}$$

which is an Euler-like differential equation. By solving the equation (3.16), we obtain the function $\phi_1^{(i)}(r)$ in the form:

$$\phi_1^{(i)}(r) = \Lambda_3^{(i)}\log r + \Lambda_4^{(i)} r^2 + \Lambda_5^{(i)} \tag{3.17}$$

By substituting equation (3.17) in equation (3.15), by means of equation (3.7) that express bi-harmonicity condition, the following differential equation for function $\phi_0^{(i)}(r)$ is obtained :

$$\phi_{0,r}^{(i)}(r) + r\left[-\phi_{0,rr}^{(i)}(r) + r\left(2\phi_{0,rrr}^{(i)}(r) + r\,\phi_{0,rrrr}^{(i)}(r)\right)\right] = 0 \tag{3.18}$$

Finally, by solving the equation (3.18), we obtain the function $\phi_0^{(i)}(r)$ as reported below:

$$\phi_0^{(i)}(r) = \Lambda_6^{(i)}\log r + \Lambda_7^{(i)} r^2 + \Lambda_8^{(i)} r^2\log r + \Lambda_9^{(i)} \tag{3.19}$$

By substituting the functions $\phi_1^{(i)}(r), \phi_0^{(i)}(r)$ in equation (3.15) and (3.6), the no-vanishing displacement field components are obtained:

$$u_r^{(i)} = A_1^{(i)} r^{-1}\left(1-\delta_{0i}\right) + A_2^{(i)} r, \quad u_\theta^{(i)} = 0, \quad u_z^{(i)} = \varepsilon_0\, z, \tag{3.20}$$

where $\Lambda_2^{(i)} = \left[\left(\mu^{(i)}+\lambda^{(i)}\right)A_3^{(i)} + 2A_1^{(i)}\left(2\mu^{(i)}+\lambda^{(i)}\right)\right]\Big/3$; $\Lambda_6^{(i)} = -2\mu^{(i)}A_2^{(i)}$; $\Lambda_7^{(i)} = -A_1^{(i)}\mu^{(i)}$;

The constants $\Lambda_1^{(i)}, \Lambda_4^{(i)}$ corresponding to a rigid body motion can be assumed as zero, since they do not effect the elastic solution. Moreover, by applying the boundary conditions (2.5) and (2.6) we

obtain that the constant $\Lambda_8^{(i)}$ characterizes the tangential stress component $\tau_{rz}^{(i)}$ is equal to zero in any phase of cylindrical solid, because the multilayered cylinder is not loaded on external surface. The no zero strain components become:

$$\varepsilon_{rr}^{(i)} = A_1^{(i)} - \left(1-\delta_{0i}\right) A_2^{(i)} r^{-2}, \quad \varepsilon_{\theta\theta}^{(i)} = A_1^{(i)} + \left(1-\delta_{0i}\right) A_2^{(i)} r^{-2}, \quad \varepsilon_{zz}^{(i)} = A_3^{(i)}, \tag{3.21}$$

the no zero stress components are given by:

$$\begin{aligned} \sigma_{rr}^{(i)} &= -2A_1^{(i)}\mu r^{-2}\left(1-\delta_{0i}\right) + 2A_2^{(i)}(\mu+\lambda) + A_3^{(i)}\lambda, \\ \sigma_{\theta\theta}^{(i)} &= 2A_1^{(i)}\mu r^{-2}\left(1-\delta_{0i}\right) + 2A_2^{(i)}(\mu+\lambda) + A_3^{(i)}\lambda, \\ \sigma_{zz}^{(i)} &= 2A_2^{(i)}\lambda + A_3^{(i)}(2\mu+\lambda), \end{aligned} \tag{3.22}$$

The field displacements (3.20) satisfy the equilibrium and compatibility equations inside each generic *i*-th phase composing the circular cylinder subjected to axial force. The unknown parameters to determine are $A_1^{(0)}, A_3^{(0)}$ and $A_1^{(i)}, A_2^{(i)}, A_3^{(i)}\ \forall i \in \{1,2,.....n\}$. These integration constants can to be determined, by applying the boundary conditions reported in equations from (2.5) to (2.9). It is easy to prove that the constant $A_3^{(i)}$ is same for each phases, by applying the first equation of boundary condition (2.5) and the follows relationship is obtained: $A_3^{(i)} = \varepsilon_0$, $\forall i \in \{0,1,2,...n\}$.

Then, the total number of unknown parameters is (2n+2), and are give by $\varepsilon_0, A_1^{(0)}$ and $A_1^{(i)}, A_2^{(i)}\ \forall i \in \{1,2,....,n\}$. The constant ε_0 is the axial strain of the multilayered cylinder. It is showed in the follows, that the number of boundary equations at the interfaces is 2n, while two is the number of boundary conditions to write on the external cylindrical surface and one equation of the end bases. Then, in total the number of equations is equal to number of unknown parameters to determine. In this case the tangential stress $\tau_{rz}^{(i)}$ vanishes and then by applying the equations (2.5) the equilibrium and compatibility equations at the generic interface between i-th and (i+1)-th phase are given by:

$$\begin{cases} \left[A_1^{(i)}\left(1-\delta_{0i}\right) - A_1^{(i+1)}\right] R^{(i)-1} + \left(A_2^{(i)} - A_2^{(i+1)}\right) R^{(i)} = 0 \\ \varepsilon_0\left(\lambda^{(i)} - \lambda^{i+1)}\right) + 2\left[A_2^{(i)}\left(\lambda^{(i)} + \mu^{(i)}\right) - A_2^{(i+1)}\left(\lambda^{(i+1)} + \mu^{(i+1)}\right)\right] + \\ \qquad + 2R^{(i)-2}\left[A_1^{(i+1)}\mu^{(i+1)} - A_1^{(i)}\mu^{(i)}\left(1-\delta_{0i}\right)\right] = 0 \end{cases} \tag{3.23}$$

The equilibrium equations for the tractions on the external cylindrical boundary surface given by equations (2.6) reduce to one follows equation:

$$2A_2^{(n)}\left(\mu^{(n)} + \lambda^{(n)}\right) + \varepsilon_0\lambda^{(n)} - 2A_1^{(n)}\mu^{(n)}R^{(n)-2} = 0 \tag{3.24}$$

Finally, it remains to consider the last equilibrium equation on bases given by (2.7),(2.8) and (2.9) that reduce in one equilibrium equation along z-direction on only one of the bases, being the other end condition automatically satisfied. Therefore, without loss of generality, we can write, for $z = 0$

$$\sum_{i=0}^{n} \pi\left[R^{(i)2} - R^{(i-1)2}\left(1-\delta_{0i}\right)\right]\left[2A_2^{(i)}\lambda^{(i)} + \varepsilon_0\left(2\mu^{(i)} + \lambda^{(i)}\right)\right] = N_z \tag{3.25}$$

The solutions shown above completely describes the problem of an multilayered cylinder under axial load. In order to solve the algebraic system constituted by (3.23),(3.24) and (3.25), it is convenient to re-arrange the whole $(2n+2)\times(2n+2)$ algebraic system following a matrix-based procedure, as was already shown in the paper [16]. We presented the case of an solid constituted by three phases subjected by axial force as an sample. It is reported the function's diagrams of the stress components, to select the following parameters:

$$N_z = 10^4\,Kg, \quad R^{(1)} = 4cm, \quad R^{(2)} = 10cm, \quad R^{(3)} = 10.5cm, \quad \nu^{(1)} = \nu^{(2)} = 0.16, \quad \nu^{(3)} = 0.30,$$
$$E^{(1)} = 3\cdot10^5\,kg/cm^2, \quad E^{(2)} = 3.3\cdot10^5\,kg/cm^2, \quad E^{(3)} = 10^6\,kg/cm^2,$$

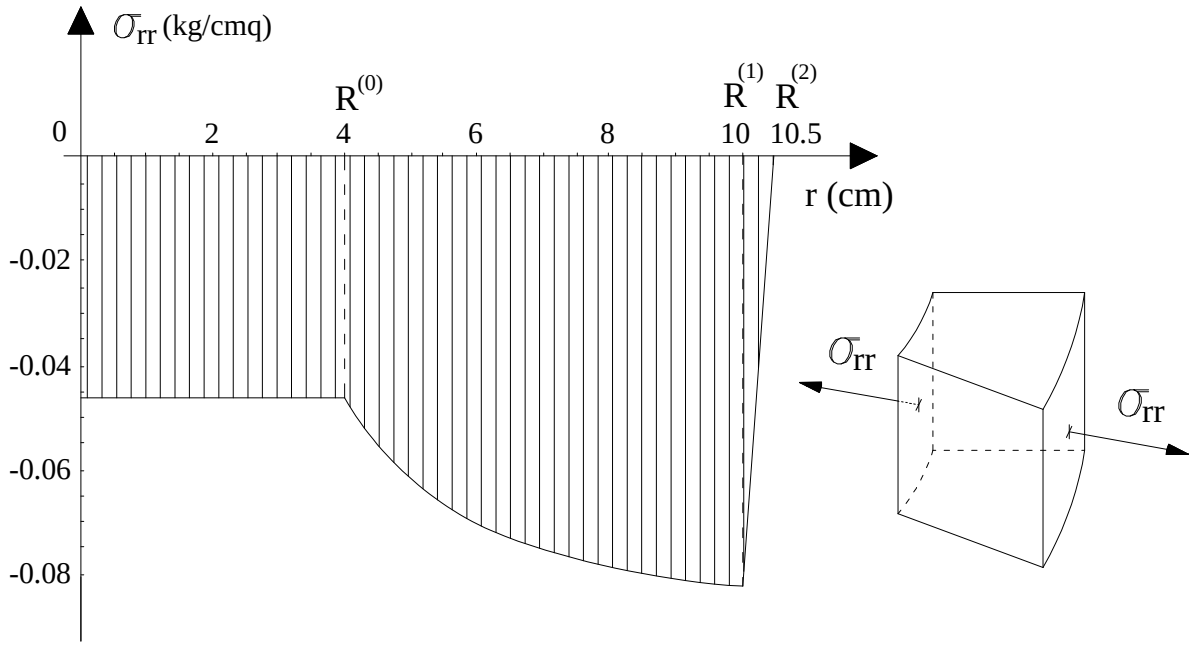

Fig. 10.4 - *The stress component* σ_{rr} *as function of the radius*

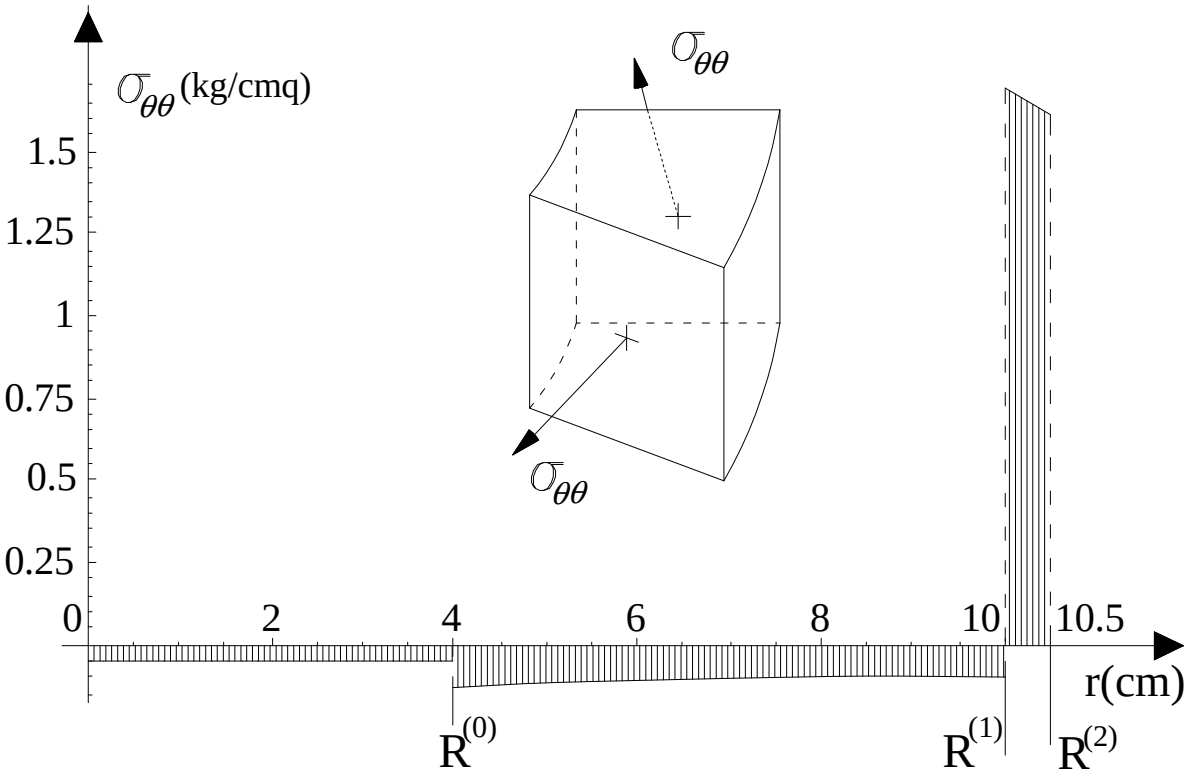

Fig. 10.5 - *The stress component* $\sigma_{\theta\theta}$ *as function of the radius*

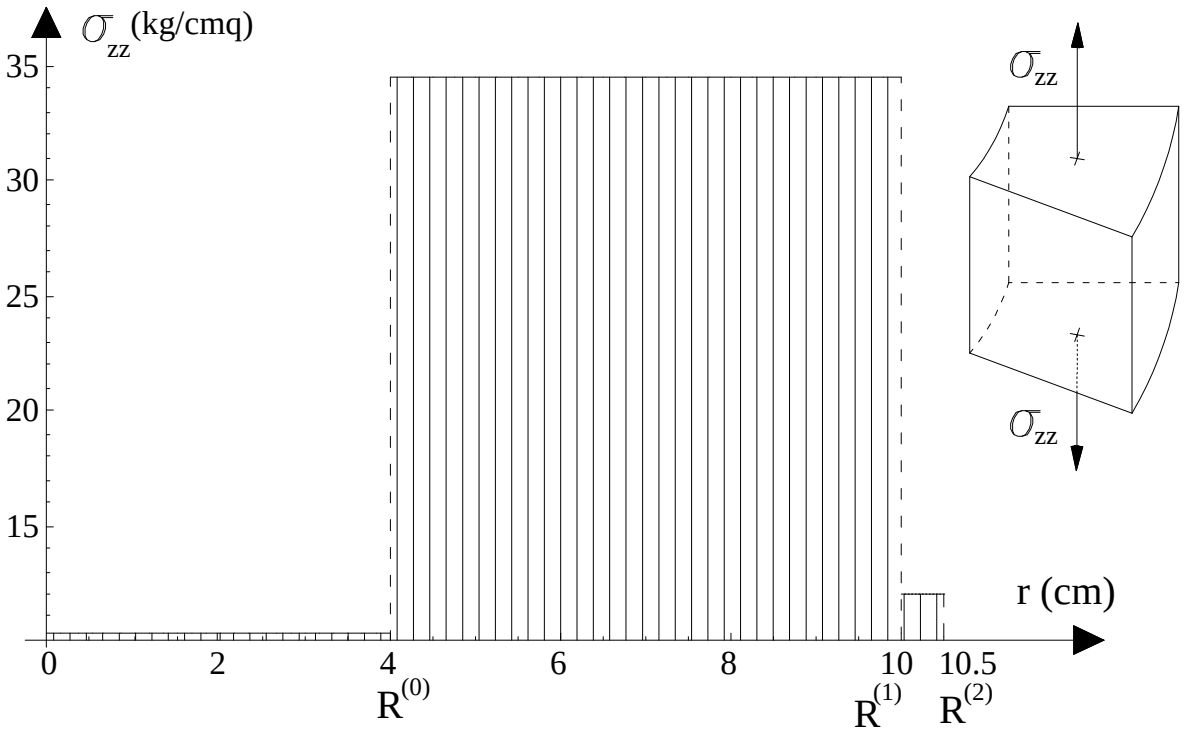

Fig. 10.6 - *The stress component* σ_{zz} *as function of the radius*

10.4. Solenoidal displacement potentials: torque, bending moment and shear

10.4.1. General treatment for bending and shear and torque

Let us consider an multilayered cylinder, constituted by (n+1) elastic isotropic homogeneous materials, as reported in figure n. 2. We will denote with apex (0) the central cylindrical core material and with apexes (1),(2),…,(n) the n-tube phases (see figure n. 2b, 2c, 2d), surrounding the core with increasing radius. In this section, for brevity we don't reported the apex (i). In the following we will consider the above mentioned load conditions for the multilayered cylinder : i) Bending and shear; ii) Pure torsion; iii) Pure bending.

In the cases of pure bending with moment M_x, or shear T_y coupled with the bending moment M_x, due to symmetry of cross-section, axis y represents a symmetry axis for displacement components u_r, u_z as shown in figure n.10.3 . But respect to displacement's component u_θ, axis y is an axis of skew-symmetry, as recognizable from figure n.10.3. On the other hand, axis x represents an axis of skew-symmetry for displacement's components u_r, u_z, u_θ. Symmetry and skew-symmetry above recognised can be expressed by following relationships:

$$\begin{cases} u_r(r,\theta,z) = u_r(r,\pi-\theta,z) = -u_r(r,-\theta,z) = -u_r(r,\theta-\pi,z), \\ u_\theta(r,\theta,z) = -u_\theta(r,\pi-\theta,z) = u_\theta(r,-\theta,z) = -u_\theta(r,\theta-\pi,z), \quad \forall\theta\in[0,\pi/2] \\ u_z(r,\theta,z) = u_z(r,\pi-\theta,z) = -u_z(r,-\theta,z) = -u_z(r,\theta-\pi,z), \end{cases} \tag{4.1}$$

For the derivates of the displacement components respect the variables r,θ,z similar relationships hold true. Above relationships allow to split in each phase displacement components in two parts: the first ones u_r, u_z symmetric , and the second one u_θ as skew-symmetric, so that the divergence takes in to account the relevant terms: $\nabla\cdot\mathbf{u} = g_1 + g_2$, where $g_1 = u_{r,r} + r^{-1}u_r + u_{z,z}$, is symmetric and $g_2 = r^{-1}u_{\theta,\theta}$, is skew-symmetric. By applying relationships (4.1), it is possible to write:

$$\begin{cases} g_1(r,\theta,z) = g_1(r,\pi-\theta,z) = -g_1(r,-\theta,z) = -g_1(r,\theta-\pi,z), \\ g_2(r,\theta,z) = -g_2(r,\pi-\theta,z) = g_2(r,-\theta,z) = -g_2(r,\theta-\pi,z), \end{cases} \quad \forall\theta\in[0,\pi/2] \tag{4.2}$$

By applying the relationship (4.2), we obtain that the integral of the divergence of displacement field over any cross section is equal to zero:

$$\int_{\omega} \nabla\cdot\mathbf{u}\, d\omega = 0 \tag{4.3}$$

where ω is the area of cross section of the generic phase. This mathematical weak condition corresponds to a vanishing volumetric change of cross-section and of whole solid, due to displacement $\mathbf{u}$. It is well known that also for pure torsion, condition (4.3) holds true. This condition holds true also in the classical De Saint Venant treatment of beam composed by a single material, where the divergence of displacement field is proportional to variable y . Moreover, let us assume this condition also to hold true in multilayered cylinder. In particular for load condition of pure torsion the divergence of displacement $\mathbf{u}$ is equal to zero in every material phase. Then, for the general De Saint Venant load condition of bending, shear and torsion, it is possible to unify the expression of divergence of displacement $\mathbf{u}$, for each material phase:

$$\nabla\cdot\mathbf{u} = \frac{1}{4}k\,\alpha^2(7-3\alpha)z^{\alpha-1}y = \begin{cases} 0 & \alpha=0 \quad pure\ \ torsion \\ k\,y & \alpha=1 \quad pure\ \ bending \\ k\,y\,z & \alpha=2 \quad shear-bending \end{cases} \tag{4.4}$$

where k is a constant of proportionality in the phase between variable y and volumetric strain, and α is a parameter that defines the load condition. By applying the formulas (4.4), it is easy to verify that the condition (4.3) is trivially satisfied, as reported below:

$$\int_{\omega^{(i)}} \nabla\cdot\mathbf{u}\, dA = \frac{1}{4}k\,\alpha^2(7-3\alpha)z^{\alpha-1}\int_{\omega^{(i)}} y\, d\omega = 0 \tag{4.5}$$

By substituting condition (4.4) in Navier-Cauchy equations (1.4), we obtain :

$$\begin{cases} \nabla^2 u_r - r^{-2}\left(u_r + 2u_{\theta,\theta}\right) = \left[(\mu+\lambda)/4\mu\right]k\,\alpha^2(3\alpha-7)z^{\alpha-1}\sin\theta \\ \nabla^2 u_\theta - r^{-2}\left(u_\theta - 2u_{r,\theta}\right) = \left[(\mu+\lambda)/4\mu\right]k\,\alpha^2(3\alpha-7)z^{\alpha-1}\cos\theta \\ \nabla^2 u_z = \left[(\mu+\lambda)/4\mu\right]k\,\alpha^2(3\alpha-7)(\alpha-1)z^{\alpha-2}r\sin\theta \end{cases} \tag{4.6}$$

By means of some algebraic manipulations, the resulting displacement field is decomposed in to the sum of two different displacements (see Appendix A1-A2):

i) The first one is characterized by divergence equal to zero (pure torsion), and corresponds to the solution of the homogeneous differential equation system, and is denoted by the symbol "*h*";

ii) The second one that is characterized by divergence equal to function reported in (4.4) with $\alpha\neq 0$, is a particular integral and will be denoted by the symbol "*p*" (bending and shear);

The two defined displacement solutions are, for every phase:

$$u_r^h = r^{-1}G_{,\theta z}, \quad u_\theta^h = \left[(1/2)r\nabla^2 G - G_{,r}\right]_{,z}, \quad u_z^h = -(1/2)\left[\nabla^2 G\right]_{,\theta} \tag{4.7}$$

$$\begin{cases} u_r^p = \left[\alpha(3\mu+\lambda)(7-3\alpha)k\,z^{\alpha+1}\sin\theta\right]/\left[4(1+\alpha)\mu\right] \\ u_\theta^p = \left\{\alpha\,k\,z^{\alpha-1}(3\alpha-7)\left[\alpha(1+\alpha)(2\mu+\lambda)r^2 - (3\mu+\lambda)z^2\right]\cos\theta\right\}/\left[4(1+\alpha)\mu\right] \\ u_z^p = \left[(\mu+\lambda)(3\alpha-7)\alpha\,k\,r\,z^{\alpha}\sin\theta\right]/(4\mu) \end{cases} \tag{4.8}$$

Then, the solving displacement is given by :

$$\mathbf{u} = \mathbf{u}^h + \mathbf{u}^p \tag{4.9}$$

where $G = G(r,\theta,z)$ is a selected function depending on the phase, that satisfies the Navier-Cauchy system. In fact, by substituting functions (4.9) in to system (4.6), we observe that the first equation is trivially satisfied, but remaining two equation yield to:

$$\left(\nabla^2\nabla^2 G\right)_{,\theta} = 0\ ;\ \left(\nabla^2\nabla^2 G\right)_{,z} = 0 \quad ,\forall\alpha\in\{0,1,2\} \tag{4.10}$$

By integrating equations (4.10), we obtain:

$$\nabla^2\nabla^2 G = f(r) \tag{4.11}$$

where $f(r)$ is a function of sole variable *r*. By substituting the displacement components of the "homogeneous" part of displacement (4.7) in to elasticity relationships, we obtain the stress components related to the part of displacement with vanishing volumetric strain , as function of the $G = G(r,\theta,z)$:

$$\begin{aligned}
&\sigma_{rr}^h = 2\mu\left(r^{-1}G^{(i)}\right)_{,r\theta z}\ ;\ \sigma_{\theta\theta}^h = \mu\left[\left(\nabla^2 G\right) - \left(2r^{-1}G\right)_{,r}\right]_{,\theta z}\ ;\ \sigma_{zz}^h = -\mu\ \left(\nabla^2 G\right)_{,\theta z}\\
&\tau_{\theta z}^h = (\mu/2)\left[r\left(\nabla^2 G\right)_{,zz} - r^{-1}\left(\nabla^2 G\right)_{,\theta\theta} - 2G_{,rzz}\right];\ \tau_{rz}^h = -\mu\left[(1/2)\left(\nabla^2 G\right)_{,r\theta} + r^{-1}G_{,\theta zz}\right]\\
&\tau_{r\theta}^h = \mu\left[\frac{r}{2}\nabla^2 G_{,r} + \nabla^2 G - G_{,zz} - 2G_{,rr}\right]_{,z}
\end{aligned} \tag{4.12}$$

By substituting the components of displacement (4.8) corresponding to the "particular" solution in to the stress-strain relationships, we obtain for each phase the stress components related to this part of displacement with volumetric strain not locally vanishing:

$$\begin{aligned}
&\sigma_{rr}^p = -\Gamma\lambda\sin\theta,\ \sigma_{\theta\theta}^p = -\Gamma(4\mu+3\lambda)\sin\theta,\ \ \sigma_{zz}^p = \Gamma(2\mu+\lambda)\sin\theta,\ \tau_{r\theta}^p = \Gamma(2\mu+\lambda)\cos\theta,\\
&\tau_{rz}^p = -\Gamma(2\mu\, z\sin\theta)/(\alpha\, r),\ \ \tau_{\theta z}^p = \Gamma\left\{\left[-2\mu z^2 + \alpha(2\mu+\lambda)(\alpha-1)r^2\right]\cos\theta\right\}/(\alpha\ r\ z),
\end{aligned} \tag{4.13}$$

where $\Gamma = \left(k\,\alpha^2(3\alpha-7)r\,z^{\alpha-1}\right)/4$;

10.4.2. Pure torsion

In the follows, by writing the problem in cylindrical coordinates, we report the essential mathematical manipulations aimed to obtaining the final analytical solution in case of pure torsion, already obtained by Lekhnitskii [12]. The divergence of displacement field is everywhere vanishing, then the condition on parameter α is: $\alpha = 0$, and the displacement solution is a function of variables r, z, since it does not depend on θ. Therefore equation (4.7) for each phase lead to:

$$\alpha = 0,\quad G^{(i)} = G^{(i)}(r,z) \ \Rightarrow\ u_r^{(i)} = 0,\ u_\theta^{(i)}(r,z) = \left[(1/2)\,r\,\nabla^2 G^{(i)} - G_{,r}^{(i)}\right]_{,z},\ u_z^{(i)} = 0 \tag{4.14}$$

In this case, the no-zero stress components (4.12) become:

$$\tau_{\theta z}^{(i)} = \mu^{(i)}\left[(1/2)\,r\,\nabla^2 G^{(i)} - G_{,r}^{(i)}\right]_{,zz},\ \tau_{r\theta}^{(i)} = \mu^{(i)}\left[(1/2)\,r\nabla^2 G_{,r}^{(i)} + r^{-1}G_{,r}^{(i)} - G_{,rr}^{(i)}\right]_{,z} \tag{4.15}$$

Moreover, the equilibrium equations (3.14) are assumed to respect condition:

$$\nabla^2\nabla^2 G^{(i)}(r,z) = 0 \tag{4.16}$$

Therefore, we begin by starting from the following form of the functions $G^{(i)}$ for each generic phase, selected as product of function $p^{(i)}(r)$ times the square of variable z:

$$G^{(i)}(r,z) = z^2\ p^{(i)}(r) \tag{4.17}$$

By substituting the function (4.17) in equilibrium equation (4.16), we obtain an ordinary Euler differential equation to solve respect to unknown function $p(r)$:

$$p_{,r}^{(i)} - r\ p_{,rr}^{(i)} + 2r^2 p_{,rrr}^{(i)} + r^3 p_{,rrrr}^{(i)} = 0 \tag{4.18}$$

By solving differential equation (4.18), we obtain the function $p^{(i)}(r)$:

$$p^{(i)}(r) = C_1^{(i)} \log r + C_2^{(i)} r^2 + C_3^{(i)} r^2 \log r + C_4^{(i)} \tag{4.19}$$

By substituting function (4.19) in (4.17) and than in (4.14), we obtain the displacement field solution, depending only by parameters $C_1^{(i)}, C_3^{(i)}$, in the form:

$$u_\theta^{(i)}(r,z) = z\,(C_3^{(i)} r - C_1^{(i)} r^{-1}) \tag{4.20}$$

As a consequence, the stress components (3.19) become:

$$\tau_{\theta z}^{(i)} = \mu\left(-C_1^{(i)} r^{-1} + C_3^{(i)} r\right), \quad \tau_{r\theta}^{(i)} = 2\mu\, C_1^{(i)} z\, r^{-2} \tag{4.21}$$

Stresses and displacement above obtained satisfy equilibrium and compatibility equations, respectively, in each phase of multilayered cylinder. Then, it remains to consider boundary conditions at the interfaces, where perfect bond is assumed. The total unknown parameters to determine can be summarized as follows: $C_3^{(0)}$ and $C_1^{(i)}, C_3^{(i)}$, $\forall i \in \{1,2,.....n\}$. Hence, the total number of unknowns is $(2n+1)$, that equals the number of algebraic equations to solve. In particular, as we will show in the follows, the number of boundary equations at the interfaces is $2n$, while the boundary conditions on the external cylindrical surface and on the two end bases are two. By means of equation (2.6) we obtain $C_1^{(i)} = 0, \forall i$ and by means of equation (2.5), we obtain $C_3^{(0)} = C_3^{(i)}$ $, \forall i$. Finally, it remains to consider the equilibrium equation around the z-axis on only one of bases of the object. At z = 0 we have

$$\sum_{i=0}^{n} \int_0^{2\pi} \int_{(1-\delta_{0i})R^{(i-1)}}^{R^{(i)}} \tau_{\theta z}^{(i)} r^2 dr d\theta = \sum_{i=0}^{n} C_3 \mu^{(i)} I_P^{(i)} = C_3 \sum_{i=0}^{n} \mu^{(i)} I_P^{(i)} = \mathcal{M}_z \quad , z = 0 \tag{4.22}$$

where $I_P^{(i)} = (\pi/2)\left[R^{(i)4} - (1-\delta_{0i})R^{(i-1)4}\right]$, $\forall i \in \{0,1,2,...,n\}$ is the polar inertia of cross-section, and $\mathcal{M}_z$ represents the total torque applied with opposite sign at $z = 0$ and $z = L$. By solving equation (4.22) we obtain :

$$C_3^{(0)} = \mathcal{M}_z \Big/ \sum_{i=0}^{n} \mu^{(i)} I_P^{(i)}, \quad \forall i \in \{0,1,...,n\} \tag{4.23}$$

Where this constant, similarly to the DSV solution, represents the specific torque angle.Substitution of the (4.23) into (4.20), allows to writing the final form of displacement, for i-th phase, as follows:

$$u_\theta^{(i)} = \left(\mathcal{M}_z\, r\, z\right) \Big/ \sum_{i=0}^{n} \mu^{(i)} I_P^{(i)}, \tag{4.24}$$

The no-vanishing strain and stresses are reduced to:

$$\gamma_{\theta z}^{(i)} = \left(\mathcal{M}_z\ r\right) \Big/ \sum_{i=0}^{n} \mu^{(i)} I_P^{(i)}, \quad \tau_{\theta z}^{(i)} = \left(\mathcal{M}_z\, \mu^{(i)}\, r\right) \Big/ \sum_{i=0}^{n} \mu^{(i)} I_P^{(i)}, \quad \forall i \in \{0,1,2,....n\} \tag{4.25}$$

It was already noted, that this solution is equal to that obtained by Lekhnitskii [12] with a different approach, and corresponds to the well known DSV solution. We presented the case of an solid constituted by three phases subjected by couple torque as an sample. It is reported the function's diagram of the stress component $\tau_{\theta z}$, to select the following parameters:

$$\mathcal{M}_z = 2 \cdot 10^3\, Kg\, cm, \quad R^{(1)} = 4cm, \quad R^{(2)} = 10cm, \quad R^{(3)} = 10.5cm, \quad \nu^{(1)} = \nu^{(2)} = 0.16,$$
$$\nu^{(3)} = 0.30, \quad E^{(1)} = 3 \cdot 10^5\, kg/cm^2, \quad E^{(2)} = 3.3 \cdot 10^5\, kg/cm^2, \quad E^{(3)} = 10^6\, kg/cm^2,$$

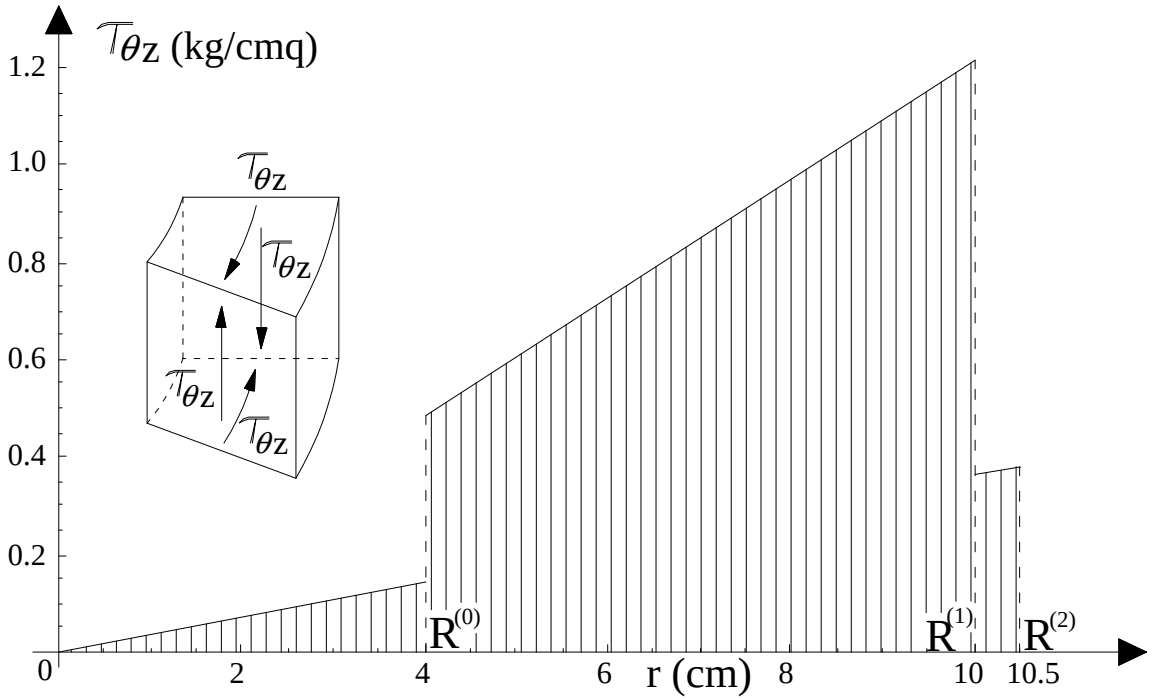

Fig. 10.7 - *The stress component $\tau_{\theta z}$ as function of the radius*

10.4.3. Pure bending

In order to solve the problem of pure bending toward axis y, it is useful to proceed from more general assumptions about the character of the state of stress by assuming that function $G^{(i)}$ in each phase is bi-harmonic , then $f(r)=0$, (4.11) . As here are absent torque and shear, we will assume that shear stresses $\tau_{\theta z}^{(i)}, \tau_{rz}^{(i)}$ acting on each section vanish. Since the bending moment is constant along z-direction, the remaining stresses must be independent on z. By applying the above hypotheses, we obtain the functions $G^{(i)}$ and parameter $k^{(i)}$ affecting the displacement field [(4.7) ,(4.8)] for each phase, as reported below (see the prove in Appendix A1):

$$G^{(i)} = -r\,z\cos\theta \begin{Bmatrix} U_5^{(i)} + \left(U_4^{(i)}/2\right) r^{-2} + \left[2U_2^{(i)}\lambda^{(i)} + U_3^{(i)}\left(\mu^{(i)} - \lambda^{(i)}\right) r^2\right] \Big/ 2\Omega^{(i)} + \\ + (2/3)\left(2U_2^{(i)} - U_3^{(i)}\right) z^2 \end{Bmatrix} \tag{4.26}$$

$$k^{(i)} = -\left[2\mu^{(i)}\left(3U_2^{(i)} - 2U_3^{(i)}\right)\right] \Big/ \Omega^{(i)} \tag{4.27}$$

where U_j, $j \in \{2,3,4,5\}$ are integration constants to determine and $\Omega^{(i)} = 3\mu^{(i)} + \lambda^{(i)}$. Finally, by substituting the function (4.26)-(4.27) into relationship (4.7), the displacement field solution becomes in each phase:

$$\begin{cases} u_r^{(i)} = \left\{U_5^{(i)} + \left(U_4^{(i)}/2\right) r^{-2} + r^2\left[U_2^{(i)}\lambda^{(i)} + \left(U_3^{(i)}/2\right)\left(\mu^{(i)} - \lambda^{(i)}\right)\right] \Big/ \Omega^{(i)} + U_2^{(i)} z^2 \right\} \sin\theta \\ u_\theta^{(i)} = \left\{U_5^{(i)} - \left(U_4^{(i)}/2\right) r^{-2} + r^2\left[U_2^{(i)}\lambda^{(i)} - \left(U_3^{(i)}/2\right)\left(5\mu^{(i)} + 3\lambda^{(i)}\right)\right] \Big/ \Omega^{(i)} + U_2^{(i)} z^2 \right\} \cos\theta \\ u_z^{(i)} = -2U_2^{(i)} z\ r\ \sin\theta \end{cases} \tag{4.28}$$

By means of the double derivative of $u_z^{(i)} = -2U_2^{(i)} z\ r\ \sin\theta = -2U_2^{(i)} y\,z$ respect to variables z and y , it is easy to show that constant $\chi = -2U_2^{(i)}$ represents the principal curvature of the solid. In core phase constant $U_4^{(i)}$ must be equal to zero. The non-zero strain components are given by:

$$\varepsilon_{rr}^{(i)} = \left\{ r\left[U_3^{(i)}\left(\mu^{(i)} - \lambda^{(i)}\right) + 2U_2^{(i)}\lambda^{(i)} \right] \Big/ \Omega^{(i)} - U_4^{(i)} r^{-3}\left(1-\delta_{0i}\right) \right\} \sin\theta,$$
$$\varepsilon_{\theta\theta}^{(i)} = \left[U_3^{(i)} r + U_4^{(i)} r^{-3}\left(1-\delta_{0i}\right) \right] \sin\theta, \;\; \varepsilon_{zz}^{(i)} = -2U_2^{(i)} r \sin\theta, \tag{4.29}$$
$$\gamma_{r\theta}^{(i)} = 2\left\{ r\left[U_2^{(i)}\lambda^{(i)} - U_3^{(i)}\left(\mu^{(i)} + \lambda^{(i)}\right) \right] \Big/ \Omega^{(i)} + U_4^{(i)} r^{-3}\left(1-\delta_{0i}\right) \right\} \cos\theta$$

and stress components are given by:

$$\sigma_{rr}^{(i)} = 2\mu^{(i)} \left\{ r\left[U_3^{(i)}\left(\mu^{(i)} + \lambda^{(i)}\right) - U_2^{(i)}\lambda^{(i)} \right] \Big/ \Omega^{(i)} - U_4^{(i)} r^{-3}\left(1-\delta_{0i}\right) \right\} \sin\theta$$
$$\sigma_{\theta\theta}^{(i)} = 2\mu^{(i)} \left\{ 3r\left[U_3^{(i)}\left(\mu^{(i)} + \lambda^{(i)}\right) - U_2^{(i)}\lambda^{(i)} \right] \Big/ \Omega^{(i)} + U_4^{(i)} r^{-3}\left(1-\delta_{0i}\right) \right\} \sin\theta,$$
$$\sigma_{zz}^{(i)} = -\left(2\mu^{(i)} / \Omega^{(i)}\right)\left[U_2^{(i)}\left(5\lambda^{(i)} + 6\mu^{(i)}\right) - 2U_3^{(i)}\lambda \right] r\sin\theta, \; \tau_{\theta z}^{(i)} = 0, \tau_{rz}^{(i)} = 0, \tag{4.30}$$
$$\tau_{r\theta}^{(i)} = 2\mu^{(i)} \left\{ r\left[U_2^{(i)}\lambda^{(i)} - U_3^{(i)}\left(\mu^{(i)} + \lambda^{(i)}\right) \right] \Big/ \Omega^{(i)} + U_4^{(i)} r^{-3}\left(1-\delta_{0i}\right) \right\} \cos\theta,$$

The displacement field satisfies the equilibrium and compatibility equations inside each generic *i*-th phase of the composite circular cylinder subjected to bending moment. Under both the hypotheses of linear and isotropic elastic behaviour of the materials and the assumption of perfect contact at the cylindrical interfacial boundaries (no de-lamination or friction phenomena), we have now to impose both equilibrium and compatibility equations at the boundary surfaces between two generic adjacent phases. Let us now observe that the expression of the displacement components (4.28), contains the following $(4n+3)$ unknown parameters: $U_2^{(0)}, U_3^{(0)}, U_5^{(0)}$ for the core, and $U_j^{(i)}$, $\forall j \in (2,3,4,5)$, and $\forall i \in \{1,2,...n\}$ for the n phases. In particular, the 5*n* equilibrium and compatibility equations at the interfaces, are:

$$r = R^{(i)}: \;\; u_r^{(i)} = u_r^{(i+1)},\; u_\theta^{(i)} = u_\theta^{(i+1)},\; u_z^{(i)} = u_z^{(i+1)}; \;\; \sigma_{rr}^{(i)} = \sigma_{rr}^{(i+1)},\; \tau_{r\theta}^{(i)} = \tau_{r\theta}^{(i+1)},\; \forall i \in \{0,1,...,n-1\} \tag{4.31}$$

where $R^{(i)}$ is the outer radius of the *i*-th phase. Cauchy equilibrium equations on the external cylindrical boundary surface, ($i = n$), give:

$$r = R^{(n)} \;:\; \sigma_{rr} = 0 \;,\; \tau_{r\theta} = 0 \tag{4.32}$$

Finally, it remains to consider the twelve equilibrium equations in z-direction on the bases (2.7)-(2.8)-(2.9), to be particularized for null values of forces and couples, except for $\mathcal{M}_x$. By invoking the polynomial identity law, by means of equations (4.31) we determine the following condition:

$$U_2^{(i)} = U_2^{(0)},\; \forall i \in \{1,2,...n\} \tag{4.33}$$

expressing that curvature on every material phase is the same, in same way as for Eulero-Bernoully's beam, under hypothesis of plane axial strain over cross-section. Moreover the integration constant vanishes $U_5^{(0)} = 0$. Then, the $(3n+2)$ unknown parameters are:

$$U_2^{(0)}, U_3^{(0)} \;;\; U_j^{(i)} \;\;\; , \forall j \in \{3,4,5\} \;\; , \forall i \in \{1,2,...n\} \tag{4.34}$$

By applying conditions (4.33), the equations (4.31) give the $3n$ linearly independent equations :

$$f_j^{(i+1)} - f_j^{(i)} = 0 \quad \forall j \in \{1,2,3\}, \quad \forall i \in \{0,1,2,....(n-1)\} \tag{4.35}$$

where functions $f_j^{(i)}$ that depend only on integration constants, are reported below:

$$f_1^{(i)} = \left(U_4^{(i)} R^{(i)-2} + 2U_5^{(i)}\right)\left(1-\delta_{0i}\right) + \left\{ R^{(i)2}\left[2U_2^{(0)}\lambda^{(i)} + U_3^{(i)}\left(\mu^{(i)} - \lambda^{(i)}\right) \right] \right\} \Big/ \Omega^{(i)};$$
$$f_2^{(i)} = \left(U_4^{(i)} R^{(i)-2} + 2U_5^{(i)}\right)\left(1-\delta_{0i}\right) + \left\{ R^{(i)2}\left[2U_2^{(0)}\lambda^{(i)} - U_3^{(i)}\left(3\lambda^{(i)} + 5\mu^{(i)}\right) \right] \right\} \Big/ \Omega^{(i)} \tag{4.36}$$
$$f_3^{(i)} = \left\{ R^{(i)4}\left[U_3^{(i)}\left(\lambda^{(i)} + \mu^{(i)}\right) - U_2^{(0)}\lambda^{(i)} \right] \right\} \Big/ \Omega^{(i)} - U_4^{(i)}\left(1-\delta_{0i}\right)$$

Only one of equations (4.32) is independent from others, and is:

$$R^{(n)4}\left[U_3^{(n)}\left(\lambda^{(n)} + \mu^{(n)}\right) - U_2^{(n)}\lambda^{(n)} \right] - \left(\lambda^{(n)} + 3\mu^{(n)}\right) U_4^{(n)} = 0 \tag{4.37}$$

As already noted, equilibrium on two bases gives the sole couple of equations:

$$\sum_{i=0}^{n}\left\{2\mu^{(i)}I^{(i)}\left[U_2^{(0)}\left(5\lambda^{(i)}+6\mu^{(i)}\right)-2U_3^{(i)}\lambda^{(i)}\right]\right\}\Big/\Omega^{(i)}=\mathcal{M}_x \tag{4.38}$$

Where $I^{(i)}=(\pi/4)\left[R^{(i)4}-(1-\delta_{0i})R^{(i-1)4}\right]$ is inertia of cross section of generic phase. By summarizing the results, we have $(3n+2)$ equations to solve in the $(3n+2)$ unknown parameters. In order to solve the algebraic system constituted by equations (4.35), (4.37) and (4.38), it is useful to re-arrange the whole system $(3n+2)\times(3n+2)$ following a matrix-based procedure. Indeed, we can collect the known terms in the *load* vector **L :**

$$\mathbf{L}^T=\left\{0,0,.....,0,\mathcal{M}_x\right\} \tag{4.39}$$

Moreover the constants $U_k^{(i)}$, can be collected in the vector $\mathbf{X}$ as follows:

$$\mathbf{X}^T=\left\{U_2^{(0)},U_3^{(0)},U_3^{(1)},U_4^{(1)},U_5^{(1)},...,U_3^{(i)},U_4^{(i)},U_5^{(i)},...,U_3^{(n)},U_4^{(n)},U_5^{(n)}\right\} \tag{4.40}$$

so that the set of equations (4.35), (4.37) and (4.38) reads :

$$\mathbf{P}\cdot\mathbf{X}=\mathbf{L} \tag{4.41}$$

where $\mathbf{P}$ is a square matrix containing the coefficients $P_{h/m}$, which are functions of both the radii and of the elastic modulus of the phases. It is worth to note that, being the system (4.41) of linear and algebraic type, provided that $\det\mathbf{P}\neq 0$, it is possible to obtain the solution as :

$$\mathbf{X}=\mathbf{P}^{-1}\mathbf{L}=\left(\tilde{\mathbf{P}}^T\mathbf{L}\right)\Big/\det\mathbf{P},\quad X_m=\left[\sum_{n=1}^{m=3n+2}\tilde{P}_{h/m}L_h\right]\Big/\det\mathbf{P}, \tag{4.42}$$

where $\tilde{P}=adj\left[\mathbf{P}\right]$ is the adjunct matrix of $\mathbf{P}$ and then the *Cramer* rule has been employed. This procedure was already followed by Authors in paper [16], to which reader is referred. It is worth to note here that the same procedure can be followed for an multilayered cylinder solid missing the core phase. In this case the system remains the same, only the interface equilibrium equations between core and phase *1* become Cauchy boundary equilibrium equations. On the contrary, compatibility equations between core and phase *1* lose their meaning. By summarizing the result for multilayered cylinder without the core, we have $(3n)$ equations to solve in $(3n)$ unknowns parameters. By invoking polynomial identity law, we determine following condition:

$$U_2^{(i)}=U_2^{(1)},\quad \forall i\in\{2,3,...n\} \tag{4.43}$$

Moreover the integration constant $U_5^{(1)}=0$. Then, the remaining unknown $(3n)$ parameters are :

$$U_2^{(1)},U_3^{(1)},U_4^{(1)};\quad U_j^{(i)}\quad ,\forall j\in\{3,4,5\}\ ,\ \forall i\in\{2,3,...n\} \tag{4.44}$$

We presented the case of an solid constituted by three phases subjected by bending moment as an sample. It is reported the function's diagrams of the stress components, to select the following parameters:

$$\mathcal{M}_x=4\cdot10^4\,Kg\,cm,\quad R^{(1)}=4cm,\quad R^{(2)}=10cm,\quad R^{(3)}=10.5cm,\quad \nu^{(1)}=\nu^{(2)}=0.16,$$
$$\nu^{(3)}=0.30,\quad E^{(1)}=3\cdot10^5\,kg/cm^2,\quad E^{(2)}=3.3\cdot10^5\,kg/cm^2,\quad E^{(3)}=10^6\,kg/cm^2,$$

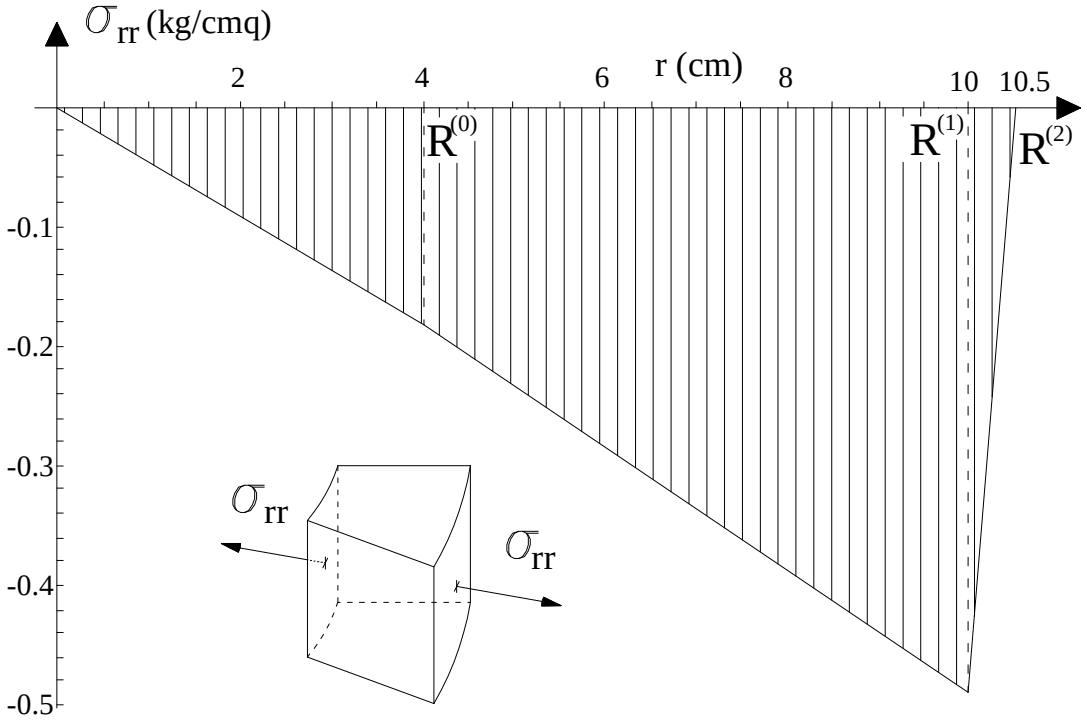

Fig. 10.8 - *The stress component* σ_{rr} *as function of the radius*

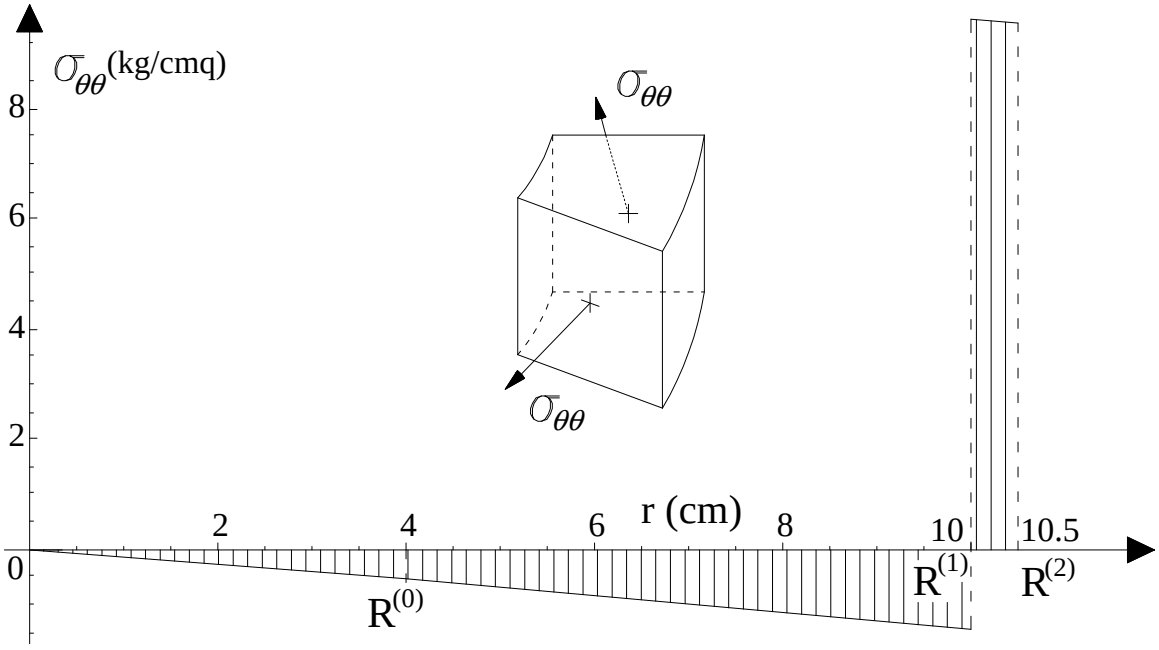

Fig. 10.9 - *The stress component* $\sigma_{\theta\theta}$ *as function of the radius*

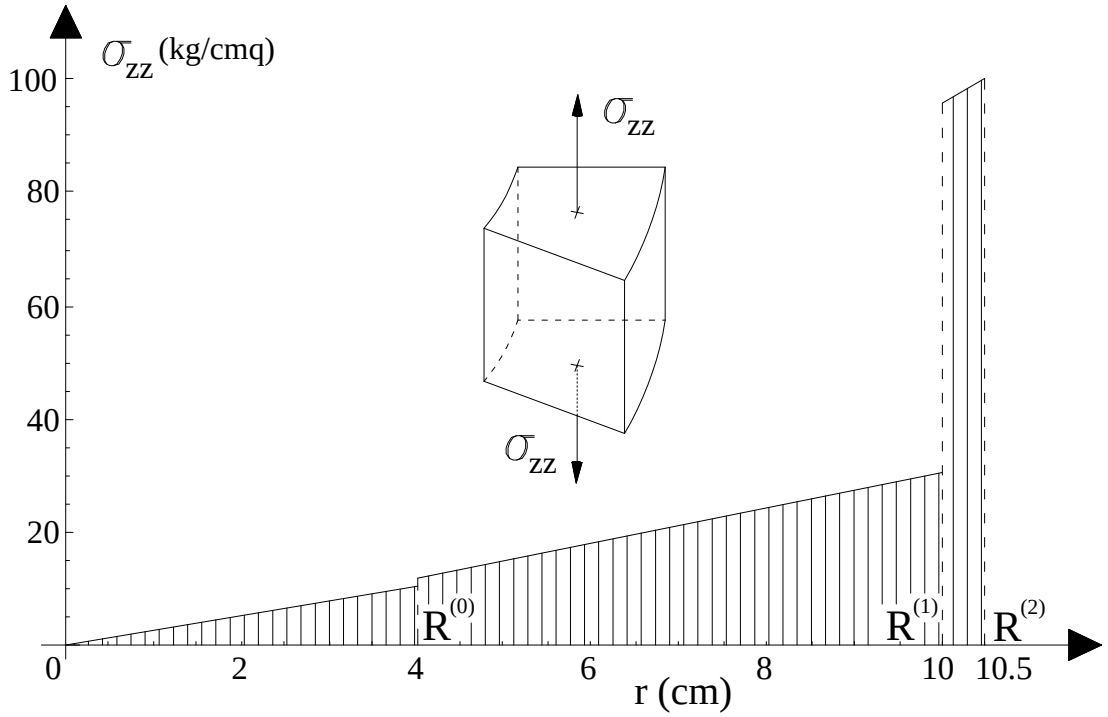

Fig. 10.10 - *The stress component* σ_{zz} *as function of the radius*

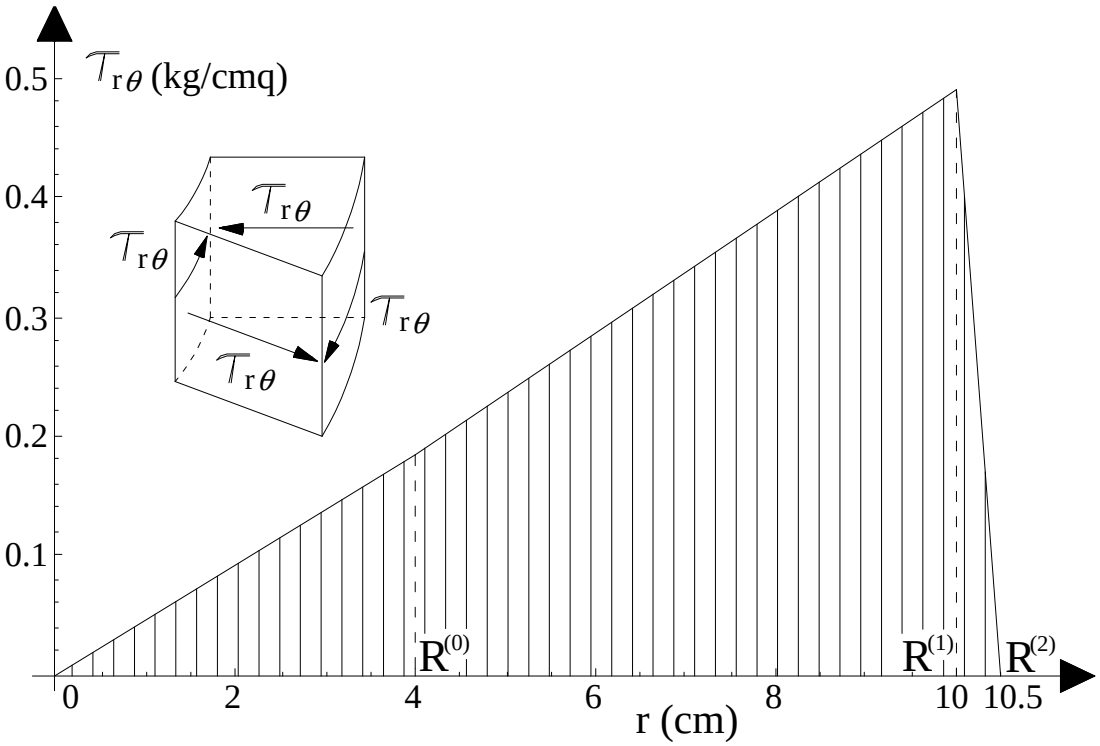

Fig. 10.11 - *The stress component* $\tau_{r\theta}$ *as function of the radius*

10.4.4. Combined bending and shear force

In order to solve the problem of bending and shear, functions $G^{(i)}$ introduced in paragraph 10.4 above are assumed as bi-harmonic in each phase, then $f(r)=0$. Also in this case the integral of divergence of solving displacement vanishes on every cross section. In presence of constant shear on the solid, we will assume shear stresses $\tau_{\theta z}^{(i)}, \tau_{rz}^{(i)}$ acting on the solid, to be independent on z. Since the bending moment is linear along z direction, the remaining stresses depend linearly upon z direction. By applying the above hypotheses, we obtain for each material phase the function $G^{(i)}$ and the parameter $k^{(i)}$ in the form (see Appendix A2):

$$G^{(i)} = \left(G_0^{(i)} + G_1^{(i)} z^2 + G_2^{(i)} z^4\right)\cos\theta, \quad k^{(i)} = 2\left[2V_3^{(i)} - 9V_2^{(i)}\right] \Big/ \Omega^{(i)}, \tag{4.45}$$

where the functions $G_0^{(i)}, G_1^{(i)}, G_2^{(i)}$ are given by:

$$\begin{aligned}
G_0^{(i)} &= \left(V_4^{(i)} + 4V_7^{(i)}\right)\left(2\log r - 1\right)\left(r/8\right) + \left(V_5^{(i)} + 2V_6^{(i)}\right)\left(r^3/8\right) + \\
&\quad + \left[18V_2^{(i)}\left(\mu^{(i)} + \lambda^{(i)}\right) - V_3^{(i)}\left(3\lambda^{(i)} + \mu^{(i)}\right)\right]\left(r^5/48\Omega^{(i)}\right), \\
G_1^{(i)} &= \left(V_4^{(i)}/4\right) r^{-1} + \left(V_5^{(i)}/2\right) r + r^3\left[\left(3/2\right)V_2^{(i)}\lambda^{(i)} + \left(V_3^{(i)}/4\right)\left(\mu^{(i)} - \lambda^{(i)}\right)\right] \Big/ \Omega^{(i)}, \\
G_2^{(i)} &= \left(V_2^{(i)} - V_3^{(i)}/6\right) r,
\end{aligned} \tag{4.46}$$

where V_j, $j \in \{2,3,4,5,6,7\}$ are integration constants to determine for each material phase. Finally, by substitution of functions (4.45) into relationship (4.7)-(4.8), the solving displacement field is obtained for each phase:

$$\begin{aligned}
u_r^{(i)} &= \left\{V_5^{(i)} + V_2^{(i)} z^2 + \left(1/2\right)V_4^{(i)} r^{-2} + \left(r^2/2\Omega^{(i)}\right)\left[V_3^{(i)}\left(\mu^{(i)} - \lambda^{(i)}\right) + 6V_2^{(i)}\lambda^{(i)}\right]\right\} z\sin\theta \\
u_\theta^{(i)} &= \left\{V_5^{(i)} + V_2^{(i)} z^2 - \left(1/2\right)V_4^{(i)} r^{-2} + \left(r^2/2\Omega^{(i)}\right)\left[6V_2^{(i)}\lambda^{(i)} - V_3^{(i)}\left(3\lambda^{(i)} + 5\mu^{(i)}\right)\right]\right\} z\cos\theta \\
u_z^{(i)} &= \left\{\begin{array}{l} V_6^{(i)} + -3V_2^{(i)} z^2 + V_7^{(i)} r^{-2}\left(1 - \delta_{0i}\right) + \\ + \left(r^2/2\Omega^{(i)}\right)\left[3\left(2\lambda^{(i)} + 3\mu^{(i)}\right)V_2^{(i)} - \left(\lambda^{(i)} + \mu^{(i)}\right)V_3^{(i)}\right] \end{array}\right\} r\sin\theta
\end{aligned} \tag{4.47}$$

In core the phase the integration constants V_4, V_7 are equal to zero. The strain components (2.1) are given for *i-th* phase by:

$$\begin{aligned}
\varepsilon_{rr}^{(i)} &= -\left\{\left[V_3^{(i)}\left(\lambda^{(i)} - \mu^{(i)}\right) - 6V_2^{(i)}\lambda^{(i)}\right]\left(r/\Omega^{(i)}\right) + V_4^{(i)} r^{-3}\left(1 - \delta_{0i}\right)\right\} z\sin\theta, \\
\varepsilon_{\theta\theta}^{(i)} &= \left[V_3^{(i)} r + V_4^{(i)} r^{-3}\left(1 - \delta_{0i}\right)\right] z\sin\theta, \qquad \varepsilon_{zz}^{(i)} = -6V_2^{(i)} r\, z\sin\theta, \\
\gamma_{\theta z}^{(i)} &= \left\{\begin{array}{l} \left[4\lambda^{(i)}\left(3V_2^{(i)} - V_3^{(i)}\right) + 3\mu^{(i)}\left(3V_2^{(i)} - 2V_3^{(i)}\right)\right]\left(r^2/2\Omega^{(i)}\right) + \\ + V_5^{(i)} + V_6^{(i)} + r^{-2}\left(V_7^{(i)} - V_4^{(i)}/2\right)\left(1 - \delta_{0i}\right) \end{array}\right\} \cos\theta \\
\gamma_{rz}^{(i)} &= \left\{\begin{array}{l} \left[4\lambda^{(i)}\left(6V_2^{(i)} - V_3^{(i)}\right) + \mu^{(i)}\left(27V_2^{(i)} - 2V_3^{(i)}\right)\right]\left(r^2/2\Omega^{(i)}\right) + \\ + V_5^{(i)} + V_6^{(i)} + r^{-2}\left(V_7^{(i)} - V_4^{(i)}/2\right)\left(1 - \delta_{0i}\right) \end{array}\right\} \sin\theta \\
\gamma_{r\theta}^{(i)} &= 2\left\{\left[3V_2^{(i)}\lambda^{(i)} - V_3^{(i)}\left(\mu^{(i)} + \lambda^{(i)}\right)\right]\left(r/\Omega^{(i)}\right) + V_4^{(i)} r^{-3}\left(1 - \delta_{0i}\right)\right\} z\cos\theta
\end{aligned} \tag{4.48}$$

By applying Hooke equations, following stress components are obtained for each *i-th* phase:

$$\sigma_{rr}^{(i)} = 2\left\{\left[V_3^{(i)}\left(\mu^{(i)}+\lambda^{(i)}\right)-3V_2^{(i)}\lambda^{(i)}\right]\left(r/\Omega^{(i)}\right)-V_4^{(i)}r^{-3}\left(1-\delta_{0i}\right)\right\}\mu^{(i)}z\sin\theta$$

$$\sigma_{\theta\theta}^{(i)} = 2\left\{\left[V_3^{(i)}\left(\mu^{(i)}+\lambda^{(i)}\right)-3V_2^{(i)}\lambda^{(i)}\right]\left(3r/\Omega^{(i)}\right)+V_4^{(i)}r^{-3}\left(1-\delta_{0i}\right)\right\}\mu^{(i)}z\sin\theta,$$

$$\sigma_{zz}^{(i)} = \left\{2\left[2V_3^{(i)}\lambda^{(i)}-3V_2^{(i)}\left(5\lambda^{(i)}+6\mu^{(i)}\right)\right]/\Omega^{(i)}\right\}\mu^{(i)}r\,z\sin\theta$$

$$\tau_{\theta z}^{(i)} = \left\{\begin{array}{l}\left[2\lambda^{(i)}\left(3V_2^{(i)}-V_3^{(i)}\right)+(3/2)\mu^{(i)}\left(3V_2^{(i)}-2V_3^{(i)}\right)\right]\left(r^2/\Omega^{(i)}\right)+\\ +V_5^{(i)}+V_6^{(i)}+r^{-2}\left(V_7^{(i)}-(1/2)V_4^{(i)}\right)\left(1-\delta_{0i}\right)\end{array}\right\}\mu^{(i)}\cos\theta \qquad (4.49)$$

$$\tau_{rz}^{(i)} = \left\{\begin{array}{l}\left[2\lambda^{(i)}\left(6V_2^{(i)}-V_3^{(i)}\right)+(1)\mu^{(i)}\left(27V_2^{(i)}-2V_3^{(i)}\right)\right]\left(r^2/\Omega^{(i)}\right)+\\ +V_5^{(i)}+V_6^{(i)}+r^{-2}\left(V_7^{(i)}-(1/2)V_4^{(i)}\right)\left(1-\delta_{0i}\right)\end{array}\right\}\mu^{(i)}\sin\theta$$

$$\tau_{r\theta}^{(i)} = 2\left\{\left[3V_2^{(i)}\lambda^{(i)}-V_3^{(i)}\left(\mu^{(i)}+\lambda^{(i)}\right)\right]\left(r/\Omega^{(i)}\right)+V_4^{(i)}r^{-3}\left(1-\delta_{0i}\right)\right\}\mu^{(i)}z\cos\theta$$

As above marked, the displacement field satisfies the equilibrium and compatibility equations inside each generic *i*-th phase of multilayered cylinder subjected to shear and bending moment. Under both the hypotheses of linear and isotropic elastic behaviour of the materials and the assumption of perfect contact at the cylindrical interfacial boundaries (no de-lamination or friction phenomena), now both equilibrium and compatibility equations at the interfaces between two generic adjacent phases must be satisfied. Moreover if we consider the displacement components (4.47), we note that the $(6n+4)$ unknown parameters are: $V_2^{(0)}, V_3^{(0)}, V_5^{(0)}, V_6^{(0)}$ for the core, and $V_j^{(i)}$, $\forall j\in(2,3,...,7)$, $\forall i\in\{1,2,...n\}$ for n phases. In particular, the boundary equations of equilibrium and compatibility at the interfaces between *i*-phase and *i+1*-phase (2.5), are

$$f_j^{(i+1)} - f_j^{(i)} = 0 \quad ,\forall j\in\{1,2,3,4,5\},\quad \forall i\in\{0,1,2,....(n-1)\} \qquad (4.50)$$

where the functions $f_j^{(i)}$ that depend only on integration constants, are reported below:

$$\begin{aligned}
f_1^{(i)} &= V_4^{(i)}\left(1-\delta_{0i}\right)R^{(i)-2}+2V_5^{i}+R^{(i)2}\left[6V_2^{(0)}\lambda^{(i)}-V_3^{(i)}\left(\lambda^{(i)}-\mu^{(i)}\right)\right]/\Omega^{(i)};\\
f_2^{(i)} &= V_4^{(i)}\left(1-\delta_{0i}\right)R^{(i)-2}+2V_5^{i}+R^{(i)2}\left[6V_2^{(0)}\lambda^{(i)}-V_3^{(i)}\left(3\lambda^{(i)}+5\mu^{(i)}\right)\right]/\Omega^{(i)}\\
f_3^{(i)} &= R^{(i)}V_6^{(i)}\left(1-\delta_{0i}\right)+V_7^{(i)}\left(1-\delta_{0i}\right)R^{(i)-1}+\left(R^{(i)3}/6\right)\left[V_3^{(i)}+\left(9V_2^{(0)}-2V_3^{(i)}\right)\left(\lambda^{(i)}/\Omega^{(i)}\right)\right]\\
f_4^{(i)} &= R^{(i)4}\left[V_3^{(i)}\left(\lambda^{(i)}+\mu^{(i)}\right)-3V_2^{(0)}\lambda^{(i)}\right]/\Omega^{(i)}-V_4^{(i)}\left(1-\delta_{0i}\right)\\
f_5^{(i)} &= \left[2R^{(i)2}\left(V_5^{(i)}+V_6^{(i)}\left(1-\delta_{0i}\right)\right)+\left(V_4^{(i)}-2V_7^{(i)}\right)\left(1-\delta_{0i}\right)\right]+\\
&\quad +R^{(i)4}\left[-2V_3^{(i)}\left(2\lambda^{(i)}+\mu^{(i)}\right)+3V_2^{(0)}\left(8\lambda^{(i)}+9\mu^{(i)}\right)\right]/\Omega^{(i)}
\end{aligned} \qquad (4.51)$$

The equilibrium equations (2.6) on external cylindrical boundary become:

$$\begin{aligned}
&R^{(n)4}\left[V_3^{(n)}\left(\lambda^{(n)}+\mu^{(n)}\right)-3V_2^{(n)}\lambda^{(n)}\right]-\left(\lambda^{(n)}+3\mu^{(n)}\right)V_4^{(n)}=0\\
&\left[2R^{(n)2}\left(V_5^{(n)}+V_6^{(n)}\right)+V_4^{(n)}-2V_7^{(n)}\right]\left(\lambda^{(n)}+3\mu^{(n)}\right)+\\
&\quad +R^{(n)4}\left[-2V_3^{(n)}\left(2\lambda^{(n)}+\mu^{(n)}\right)+3V_2^{(n)}\left(8\lambda^{(n)}+9\mu^{(n)}\right)\right]=0
\end{aligned} \qquad (4.52)$$

On the bases, only the following equilibrium equation must be written:

$$\sum_{i=0}^{n}\mu^{(i)}\omega^{(i)}\left[V_5^{(i)}+\left(1-\delta_{oi}\right)V_6^{(i)}\right]+\sum_{i=0}^{n}2\mu^{(i)}I^{(i)}\left(2V_3^{(i)}+9V_2^{(i)}\right)\frac{\left(\mu^{(i)}+\lambda^{(i)}\right)}{\left(3\mu^{(i)}+\lambda^{(i)}\right)}=T_y \qquad (4.53)$$

where $\omega^{(i)}=\pi\left[R^{(i)2}-(1-\delta_{0i})R^{(i-1)2}\right]$, $I^{(i)}=(\pi/4)\left[R^{(i)4}-(1-\delta_{0i})R^{(i-1)4}\right]$

Then, the $(5n+3)$ unknown parameters are: $V_2^{(0)}, V_3^{(0)}, V_5^{(0)}$ for the core, and $V_j^{(i)}$, $\forall j \in \{3,4,5,6,7\}$ $\forall i \in \{1,2,...n\}$ for the n phases. By summarizing the results, there are $(5n+3)$ equations to solve in the $(5n+3)$ unknown parameters. In order to solve the algebraic system (4.50)-(4.52)-(4.53), it is convenient to re-arrange the whole algebraic system $(5n+3)\times(5n+3)$ following the matrix-based procedure previously presented [16]. Also for the case of shear and bending, in absence of the core phase, the solution can be easily obtained with the procedure already shown in previous section. The result is that here are present $(5n)$ equations to solve in $(5n)$ unknown parameters. Then, the unknown $(5n)$ parameters become: $V_2^{(1)}, V_3^{(1)}, V_4^{(1)}, V_5^{(1)}, V_7^{(1)}$ for first phase and $V_j^{(i)}$ $\forall j \in \{3,4,5,6,7\}$, and $\forall i \in \{2,3,...n\}$ for other phases.

We presented the case of an solid constituted by three phases subjected by two shear forces and equilibrating bending couple as an sample. It is reported the function's diagrams of the stress components, to select the following parameters:

$T_y = 10^3 Kg$, $L = 200cm$, $R^{(1)} = 4cm$, $R^{(2)} = 10cm$, $R^{(3)} = 10.5cm$, $\nu^{(1)} = \nu^{(2)} = 0.16$, $\nu^{(3)} = 0.30$,

$E^{(1)} = 3 \cdot 10^5 kg/cm^2$, $E^{(2)} = 3.3 \cdot 10^5 kg/cm^2$, $E^{(3)} = 10^6 kg/cm^2$,

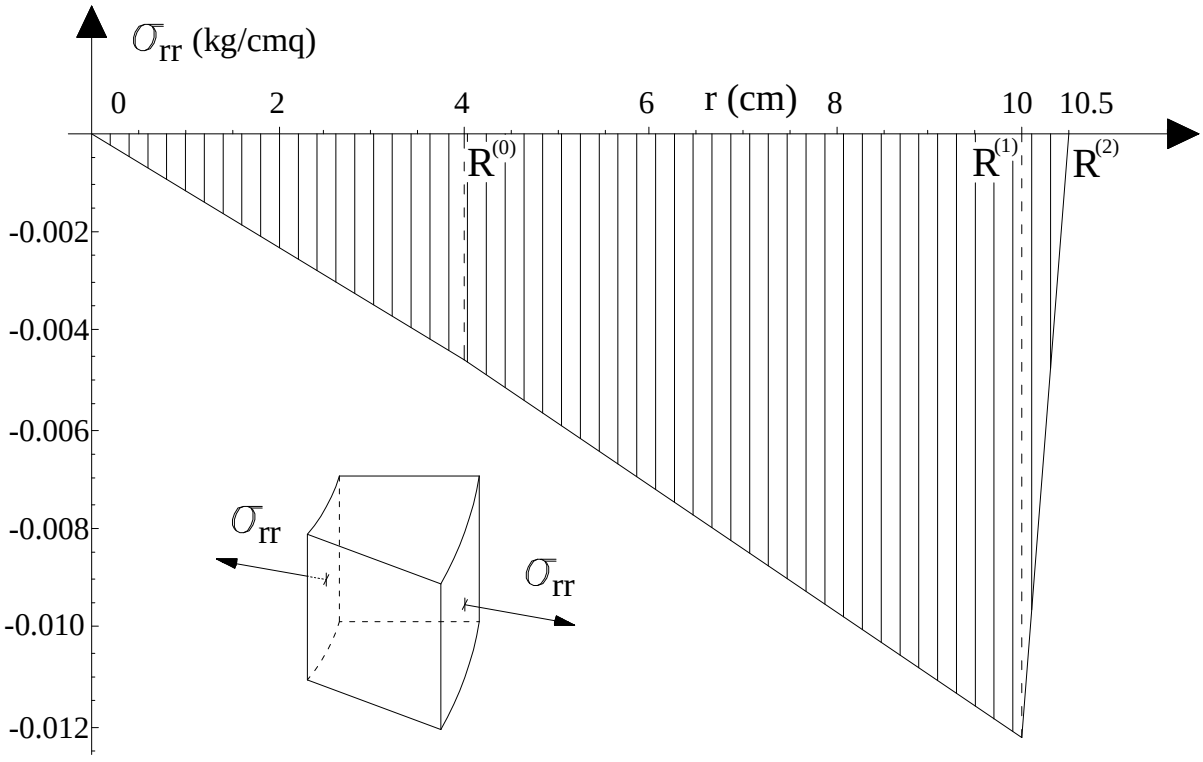

Fig. 10.12 - *The stress component σ_{rr} as function of the radius*

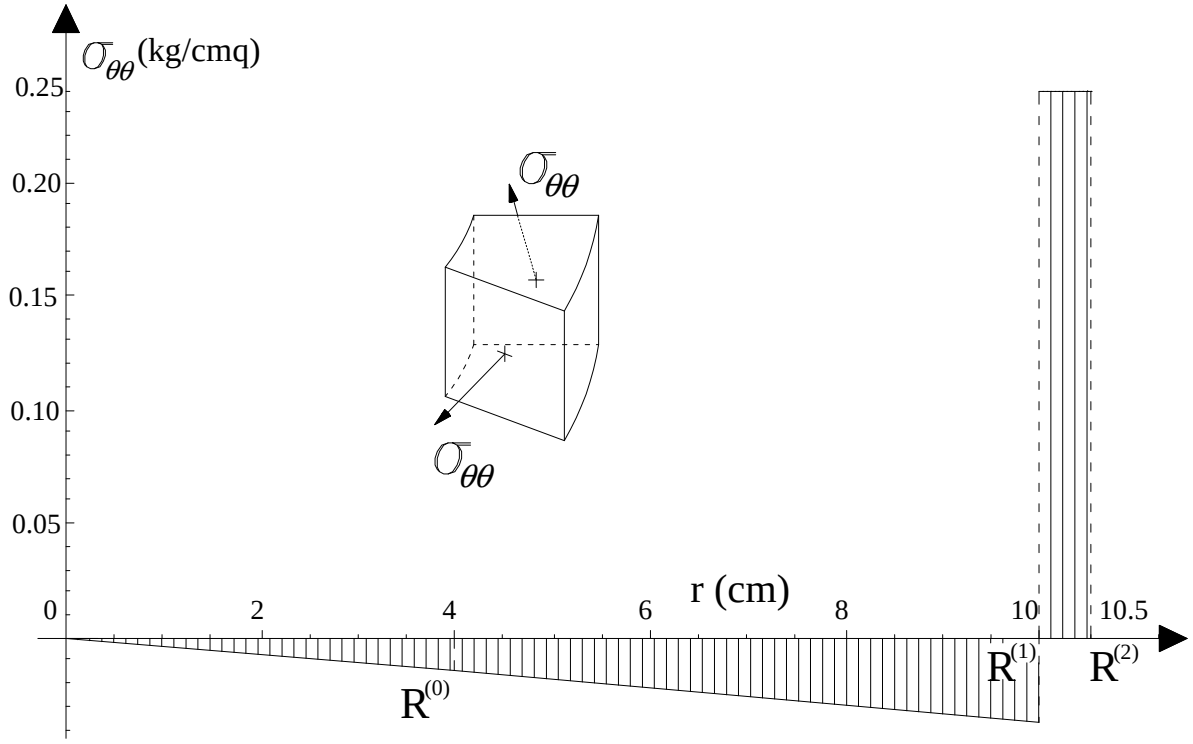

Fig. 10.13 - *The stress component* $\sigma_{\theta\theta}$ *as function of the radius*

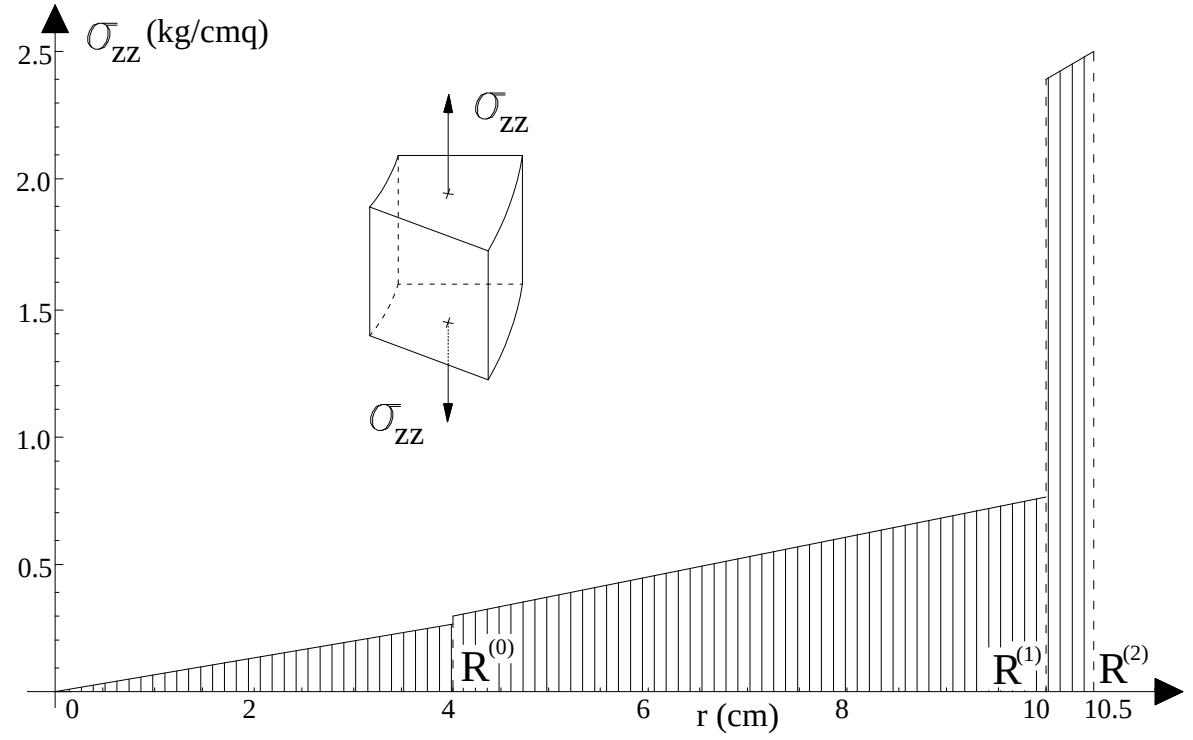

Fig. 10.14 - *The stress component* σ_{zz} *as function of the radius*

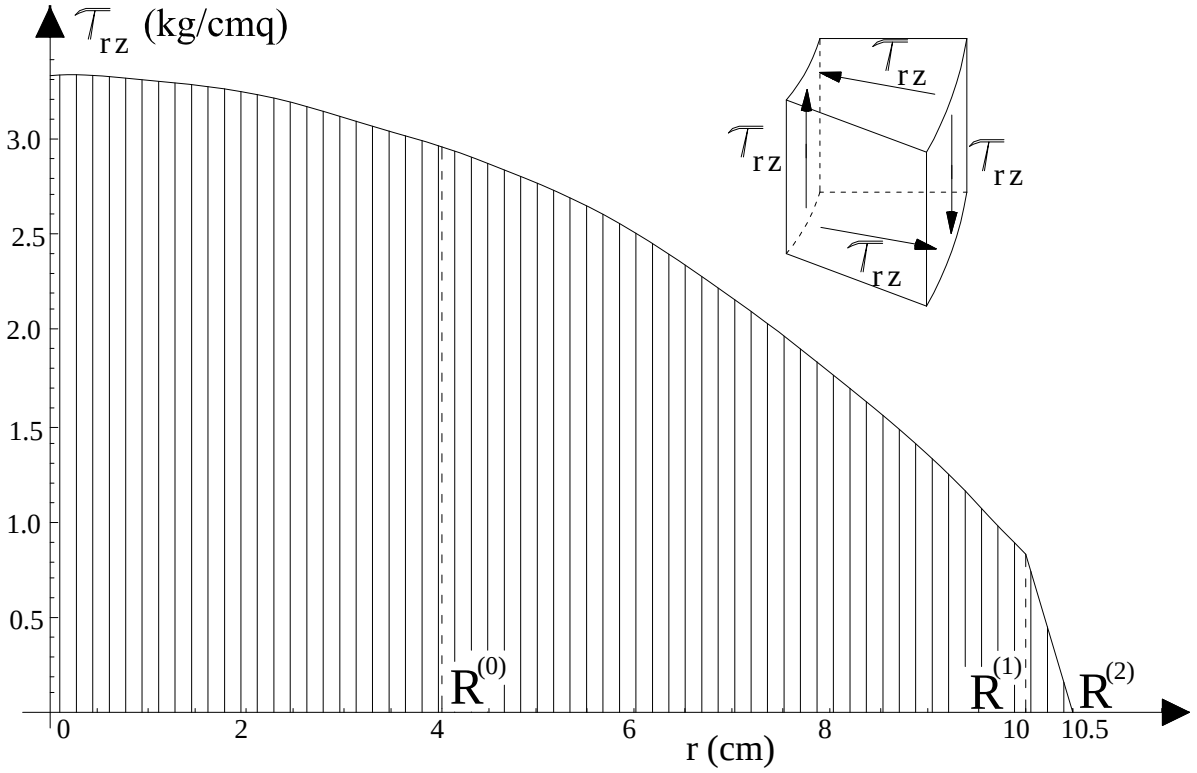

Fig. 10.15 - *The stress component τ_{rz} as function of the radius*

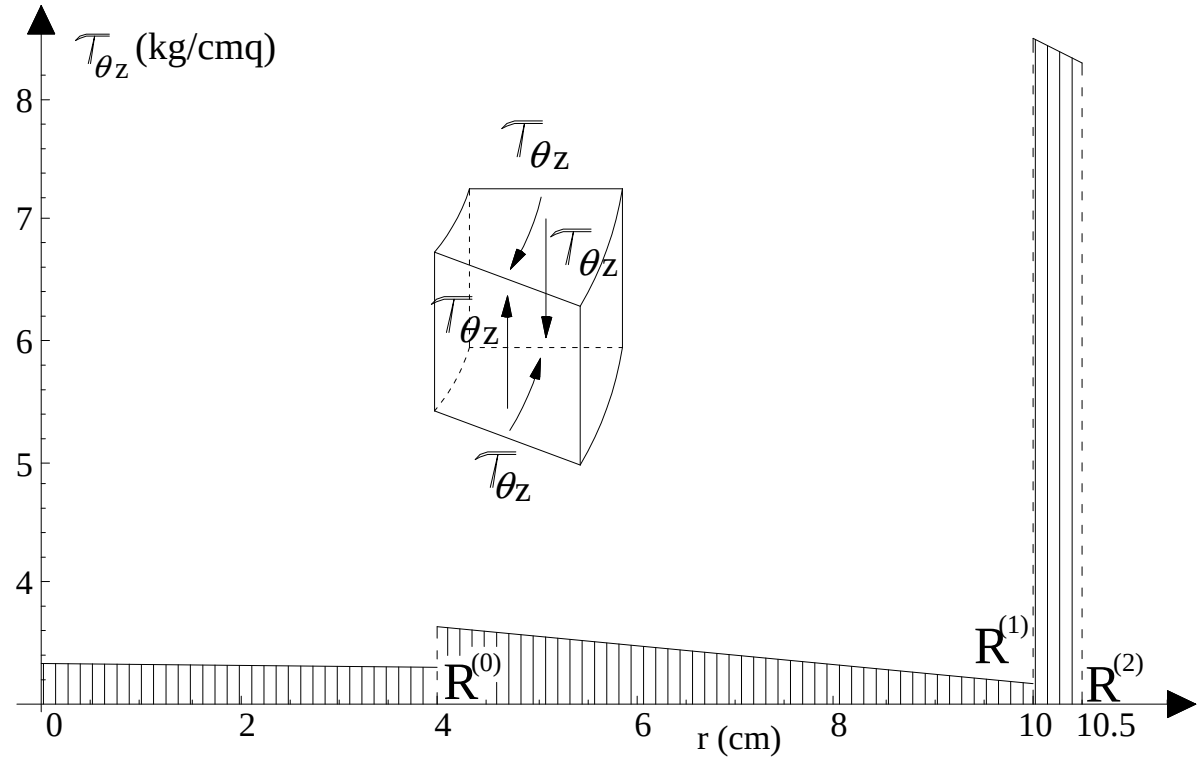

Fig. 10.16 - *The stress component $\tau_{\theta z}$ as function of the radius*

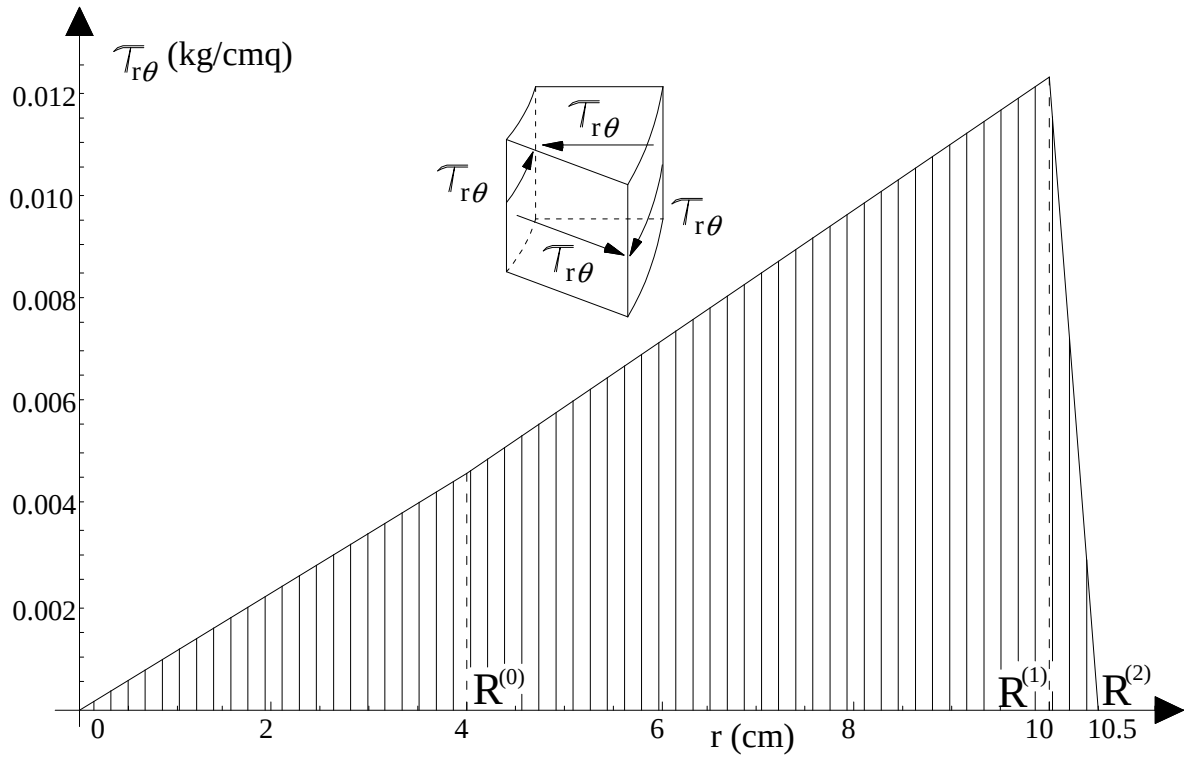

Fig. 10.17 - *The stress component* $\tau_{r\theta}$ *as function of the radius*

10.5. Homogenization of multilayered cylinder under de Saint Venant like loads: Equivalent stress-strain relationships

In the previous Sections, the exact solutions for an multilayered cylinder constituted by *n* arbitrary isotropic and linearly elastic hollow phases imprisoning a central *core* under the action of axial forces, combined shear and bending moments, and torque have been rigorously derived in the framework of linear theory of elasticity. The mathematical approach followed to find the closed–form solution for each single load case has thus furnished the possibility of reducing the partial differential equations governing the elastic problem and the related boundary conditions in to a simpler linear algebraic problem, where a prescribed number of coefficients has to be determined. As a consequence, at least in principle, the overall mechanical response to selected loads of the composite material object can be obtained fully preserving the parametric influence of the whole set of geometrical and elastic features characterizing each phase of multilayered cylinder.

Because the proposed analytical method offers the possibility of controlling the evolution of the local stress field inside each object's layer and at the material interfaces when volume fractions and elastic modulus of the constituents are prescribed, the present Section is firstly dedicated to derive – via homogenization – an equivalent one-dimensional beam-like model, representing the overall behaviour of an multilayered cylinder under the action of the above mentioned DSV load conditions, explicitly constructing the corresponding stiffness matrix governing the elastic law among generalized stresses and strains.

Successively, without loss of generality and by making reference to an multilayered cylinder constituted by two phases (a central core and a perfectly bonded hollow cylinder) a sensitivity analysis is finally conducted on the overall elasticity of the composite material, analysing in detail the influence of the phases volume fractions and of elastic modulus on the homogenized stiffness. Moreover, it is also investigated the role played by geometrical and mechanical features on the stress peaks and spurious stress regimes kindled inside the layers and at the interfaces, as effect of the coupling of different materials.

10.5.1. Axial stiffness

With reference to the solutions obtained for an multilayered cylinder under axial force, stress components obtained by means (3.22) and by utilizing the relationship between Lame's constants and Young's modulus, Poisson's ratio, we obtain

$$\sigma_{rr}^{(i)}=\frac{E^{(i)}\left(A_2^{(i)}+\varepsilon_0\nu^{(i)}\right)}{1-\nu^{(i)}-2\nu^{(i)2}}-\frac{A_1^{(i)}E^{(i)}\left(1-\delta_{0i}\right)}{\left(1+\nu^{(i)}\right)r^2},\quad \sigma_{\theta\theta}^{(i)}=\frac{E^{(i)}\left(A_2^{(i)}+\varepsilon_0\nu^{(i)}\right)}{1-\nu^{(i)}-2\nu^{(i)2}}+\frac{A_1^{(i)}E^{(i)}\left(1-\delta_{0i}\right)}{\left(1+\nu^{(i)}\right)r^2},$$
$$\sigma_{zz}^{(i)}=\frac{E^{(i)}\left[\varepsilon_0\left(1-\nu^{(i)}\right)+2A_2^{(i)}\nu^{(i)}\right]}{1-\nu^{(0)}-2\nu^{(0)2}},\quad \tau_{\theta z}^{(i)}=\tau_{r\theta}^{(i)}=\tau_{rz}^{(i)}=0,\quad \forall i\in\{1,2,...,n\} \tag{5.1}$$

where Lame's constants utilised in equation (5.1) are :

$$\mu^{(i)}=E^{(i)}\Big/\left[2\left(1+\nu^{(i)}\right)\right],\quad \lambda^{(i)}=\left(E^{(i)}\nu^{(i)}\right)\Big/\left[\left(1+\nu^{(i)}\right)\left(1-2\nu^{(i)}\right)\right], \tag{5.2}$$

and $E^{(i)}$ and $\nu^{(i)}$ represent the Young's modulus and the Poisson's ratio of the i-th phase.

By equating the internal virtual work to the external virtual work of true tractions times the solving displacement , it is possible to obtain the equivalent homogenized axial stiffness k_ε for multilayered cylinder:

$$k_\varepsilon : N_z = k_\varepsilon\,\bar{\varepsilon}_{zz} \tag{5.3}$$

where $N_z=\sum_{i=0}^{n}N_z^{(i)}$, and $N_z^{(i)}$ represents the axial resultant in the generic phase, and $\bar{\varepsilon}_{zz}$ is the averaged strain on every cross-section of the relevant phase. In particular, by starting from the external work for an infinitesimal element whose length is "dz", we have:

$$dL_E=\sum_{i=0}^{n}\int_{\omega^{(i)}}\sigma_{zz}^{(i)}(\xi)\cdot n_z(\xi)\cdot u_z^{(i)}(\xi)dS+\sum_{i=0}^{n}\int_{\omega^{(i)}}\sigma_{zz}^{(i)}(\xi_0)\cdot n_z(\xi_0)\cdot u_z^{(i)}(\xi_0)dS \tag{5.4}$$

where $\xi=z+dz,\ \xi_0=z$, and $\omega^{(i)}=\pi[R^{(i)^2}-(1-\delta_{0i})R^{(i-1)^2}]$ is the area of the beam cross-section of the phase. By applying the equations (5.1), we note that the emerging stresses $\sigma_{zz}^{(i)}$ are uniform in each material phase. Moreover, by means of equation (3.20) we note that displacement component $u_z^{(i)}$ does not depend on variables r and θ, then the infinitesimal actual external work for the choosed element is given by:

$$dL_E=\varepsilon_0\left(\xi-\xi_0\right)\sum_{i=0}^{n}\sigma_{zz}^{(i)}\omega^{(i)}=F\,\varepsilon_0\,dz \tag{5.5}$$

where $n_z\left(\xi\right)=-n_z\left(\xi_0\right)=1$, and $\sum_{i=0}^{n}\sigma_{zz}^{(i)}\omega^{(i)}=\sum_{i=0}^{n}N_z^{(i)}=N_z$ represents the axial force on the beam element. The infinitesimal internal work can be written as:

$$dL_I=dz\sum_{i=0}^{n}\int_{\omega^{(i)}}\boldsymbol{\sigma}^{(i)}:\boldsymbol{\varepsilon}^{(i)}ds=dz\sum_{i=0}^{n}\int_{0}^{2\pi}\int_{(1-\delta_{0i})R^{(i-1)}}^{R^{(i)}}\left(\sigma_{rr}^{(i)}\varepsilon_{rr}^{(i)}+\sigma_{\theta\theta}^{(i)}\varepsilon_{\theta\theta}^{(i)}+\sigma_{zz}^{(i)}\varepsilon_{zz}^{(i)}\right)r\,dr\,d\vartheta=\Psi_\varepsilon dz \tag{5.6}$$

where

$$\Psi_\varepsilon=\sum_{i=0}^{n}\int_{\omega^{(i)}}\boldsymbol{\sigma}^{(i)}:\boldsymbol{\varepsilon}^{(i)}ds=\sum_{i=0}^{n}\frac{E^{(i)}\omega^{(i)}}{1-\nu^{(i)}-2\nu^{(i)2}}\left[(1-\delta_{0i})\frac{A_1^{(i)2}\left(2-4\nu^{(i)}\right)}{R^{(i)2}R^{(i-1)2}}+2A_2^{(i)2}+\varepsilon_0^2+\left(4A_2^{(i)}-\varepsilon_0\right)\nu^{(i)}\varepsilon_0\right]$$

By invoking the virtual work principle, we obtain:

$$N_z\,\varepsilon_0\,dz=\Psi_\varepsilon dz \tag{5.7}$$

For the present case, by applying the equations (3.20) and (3.21), the averaged strain $\bar{\varepsilon}_0$ in z-direction is equal to:

$$\bar{\varepsilon}_{zz}=\varepsilon_0 \tag{5.8}$$

By recalling the equation (5.3)-(5.8), we can determine the average axial strain:

$$N_z = k_\varepsilon\, \varepsilon_0 \Rightarrow \quad \varepsilon_0 = N_z\, k_\varepsilon^{-1} \tag{5.9}$$

By substituting the average axial strain in equation (5.7), we obtain the homogenised axial stiffness k_ε of multilayered cylinder:

$$k_\varepsilon = N_z{}^2\, \Psi_\varepsilon^{-1} \tag{5.10}$$

Without loss of generality, we set $N_z = 1$, then, the overall axial stiffness k_ε of multilayered cylinder can be finally written as:

$$k_\varepsilon = \Psi_\varepsilon^{-1} = \sum_{i=0}^{n} E^{(i)} \omega^{(i)} \psi_\varepsilon^{(i)} \tag{5.11}$$

where $\psi_\varepsilon^{(i)}$ is a modulating coefficient that depends on geometrical and mechanical parameters:

$$\psi_\varepsilon^{(i)} = \eta_\varepsilon^{(i)} \Bigg/ \left[\sum_{i=0}^{n} E^{(i)} \omega^{(i)} \eta_\varepsilon^{(i)} \right]^2 = \frac{1}{E^{(i)} \omega^{(i)}} \left(\frac{dL_I^{(i)}}{dL_I^2} \right), \tag{5.12}$$

where coefficients $\eta_\varepsilon^{(i)}$ are:

$$\eta_\varepsilon^{(i)} = \frac{1}{E^{(i)} \omega^{(i)}} \int_{\omega^{(i)}} \boldsymbol{\sigma}^{(i)} : \boldsymbol{\varepsilon}^{(i)} ds = \frac{2A_2^{(i)2} + \varepsilon_0^2 + (4A_2^{(i)} - \varepsilon_0)\nu^{(i)} \varepsilon_0}{1 - \nu^{(i)} - 2\nu^{(i)2}} + \frac{2(1-\delta_{i0}) A_1^{(i)2}}{\left(1+\nu^{(i)}\right) R^{(i)2} R^{(i-1)2}}, \tag{5.13}$$

It is worth to note that, by solving the problem by setting $\nu^{(i)} = \nu,\ \forall i \in \{0,1,2,...,n\}$, $\psi_\varepsilon^{(i)} = 1$ in each phase , equation (5.11) reduces to the more simple expression:

$$k_\varepsilon = \sum\nolimits_{i=0}^{n} E^{(i)} \omega^{(i)} \tag{5.14}$$

10.5.2. Torsion stiffness

The object of the present section is the determination of the homogenised torsion stiffness of multilayered cylinder, for the case of pure torsion with couples $\pm \mathcal{M}_z$ applied at the bases of the solid. With reference to the results illustrated above, the solving displacement field reduces to (4.24) and no-vanishing strain and stresses are given by (4.25). By utilizing the same strategy followed for the axial stiffness, it is possible to obtain the homogenized overall torsion stiffness k_ϕ of multilayered cylinder by means of Virtual Work Equation equating external work to the internal one related to true strain and stresses. The torsion stiffness of cross-section is defined as follows

$$k_\phi : \mathcal{M}_z = k_\phi\, \phi \tag{5.15}$$

where ϕ is the mean value of the twist angle per unit length. The infinitesimal actual external work for an arbitrary element of multilayered cylinder, with infinitesimal length "dz" can be written as:

$$\begin{aligned} dL_E &= \sum_{i=0}^{n} \int_{\omega^{(i)}} \mathbf{t}^{(i)}(\xi) \cdot \mathbf{u}^{(i)}(\xi)\, ds + \sum_{i=0}^{n} \int_{\omega^{(i)}} \mathbf{t}^{(i)}(\xi_0) \cdot \mathbf{u}^{(i)}(\xi_0)\, ds = \\ &= \sum_{i=0}^{n} \int_{\omega^{(i)}} \tau_{\theta z}^{(i)}(\xi) \cdot n_z(\xi) \cdot u_\theta^{(i)}(\xi)\, ds + \sum_{i=0}^{n} \int_{\omega^{(i)}} \tau_{\theta z}^{(i)}(\xi_0) \cdot n_z(\xi_0) \cdot u_\theta^{(i)}(\xi_0)\, ds \end{aligned} \tag{5.16}$$

where $\xi = z + dz,\ \xi_0 = z$. The twist angle is defined as $\Theta^{(i)} = r^{-1} u_\theta^{(i)}$. By means of equation (4.24) , we note that the twist angle $\Theta^{(i)}$ is constant respect to r and θ variables:

$$\Theta^{(i)} = u_\theta^{(i)} r^{-1} = \left(\mathcal{M}_z\, z \right) \Bigg/ \sum_{i=0}^{n} \mu^{(i)} I_P^{(i)} \tag{5.17}$$

Then, we can write following relationship:

$$dL_E = \sum_{i=0}^{n} r^{-1} u_\theta^{(i)}(\xi) \int_{\omega^{(i)}} \tau_{\theta z}^{(i)}(\xi)\, r^2 dr d\theta - \sum_{i=0}^{n} r^{-1} u_\theta^{(i)}(\xi_0) \int_{\omega^{(i)}} \tau_{\theta z}^{(i)}(\xi_0)\, r^2 dr d\theta \tag{5.18}$$

where $n_z(\xi) = -n_z(\xi_0) = 1$. Moreover, the twist angle takes the same value in every phase and by means of equation (4.22), we can write:

$$dL_E = \left[\Theta(\xi) - \Theta(\xi_0)\right] \sum_{i=0}^{n} \mathcal{M}_z^{(i)} = \mathcal{M}_z \, d\Theta(z) \tag{5.19}$$

where $\mathcal{M}_z^{(i)}$ is the relevant torque. The infinitesimal internal work for infinitesimal element is :

$$dL_I = dz \sum_{i=0}^{n} \int_{\omega^{(i)}} \boldsymbol{\sigma}^{(i)} : \boldsymbol{\varepsilon}^{(i)} ds = dz \sum_{i=0}^{n} \int_{0}^{2\pi} \int_{(1-\delta_{0i})R^{(i-1)}}^{R^{(i)}} \tau_{\theta z}^{(i)} \gamma_{\theta z}^{(i)} r dr d\theta = \Psi_\phi dz \tag{5.20}$$

where $\Psi_\phi = \sum_{i=0}^{n} \int_{\omega^{(i)}} \boldsymbol{\sigma}^{(i)} : \boldsymbol{\varepsilon}^{(i)} ds = \mathcal{M}_z^2 \Big/ \left(\sum_{i=0}^{n} \mu^{(i)} I_P^{(i)} \right)$. The twist angle for unit length ϕ is defined as:

$$\phi = \Theta_{,z} = \mathcal{M}_z \Big/ \sum_{i=0}^{n} \mu^{(i)} I_P^{(i)} = const \tag{5.21}$$

Above equation (5.21), coupled with equation (5.19) determines the differential of the twist angle $\Omega(z)$:

$$\mathcal{M}_z = k_\phi \, \phi = k_\phi \Theta_{,z} \quad \Rightarrow \quad d\Theta(z) = \mathcal{M}_z \, k_\phi^{-1} dz \tag{5.22}$$

By substitution, we obtain:

$$dL_E = \mathcal{M}_z \, d\Omega(z) = \mathcal{M}_z^2 \, k_\phi^{-1} dz \tag{5.23}$$

Finally, equations (5.20) and(5.23), yield the overall torsion stiffness k_ϕ of multilayered cylinder:

$$k_\phi = \mathcal{M}_z^2 \, \Psi_\phi^{-1} = \sum_{i=0}^{n} \mu^{(i)} I_P^{(i)} \tag{5.24}$$

10.5.3. Bending stiffness

Let us now consider the case in which an multilayered cylinder is subjected to pure bending, whose value is $\mathcal{M}_x$, works in direction x. By recalling the reported displacement solutions in (4.28) and results in (4.33)-(4.34), the displacement field for the generic *i*-th phase is as follows:

$$\begin{aligned}
u_r^{(i)} &= (1/2)\left\{ \left(2U_5^{(i)} + U_4^{(i)} r^{-2}\right)(1-\delta_{oi}) + \left[\chi_0 \lambda^{(i)} + U_3^{(i)} \left(\mu^{(i)} - \lambda^{(i)}\right) \right] \left(r^2 / \Omega^{(i)} \right) + \chi_0 z^2 \right\} \sin\theta \\
u_\theta^{(i)} &= (1/2)\left\{ \left(2U_5^{(i)} - U_4^{(i)} r^{-2}\right)(1-\delta_{oi}) + \left[\chi_0 \lambda^{(i)} - U_3^{(i)} \left(5\mu^{(i)} + 3\lambda^{(i)}\right) \right] \left(r^2 / \Omega^{(i)} \right) + \chi_0 z^2 \right\} \cos\theta \\
u_z^{(i)} &= -\chi_0 \, z \, r \, \sin\theta
\end{aligned} \tag{5.25}$$

where $2U_2^{(0)} = \chi_0$ represents the curvature of the solid. In order to determine the equivalent overall bending stiffness k_χ we can follow the same homogenization procedure used above. The bending stiffness is defined as:

$$k_\chi : \mathcal{M}_x = k_\chi \, \overline{\chi} \tag{5.26}$$

The infinitesimal actual external work for an arbitrary element of multilayered cylinder:

$$dL_E = \sum_{i=0}^{n} \int_{\omega^{(i)}} \sigma_{zz}^{(i)}(\xi) \cdot n_z(\xi) \cdot u_z^{(i)}(\xi) ds + \sum_{i=0}^{n} \int_{\omega^{(i)}} \sigma_{zz}^{(i)}(\xi_0) \cdot n_z(\xi_0) \cdot u_z^{(i)}(\xi_0) ds \tag{5.27}$$

The rotation $\varphi_x(z)$ around the x-axis is given by the first component of curl of displacement field:

$$\varphi_x(z) = -(1/2)(\nabla \times \boldsymbol{u})_x = (1/2)\left(u_{y,z} - u_{z,y}\right) = \chi_0 \, z = -u_z^{(i)} / (r \sin\theta) \tag{5.28}$$

From equation (5.25) , we note that the rotation $\varphi_x(z)$ is constant respect to r and θ variables, then we can write (5.27) as:

$$dL_E = \sum_{i=0}^{n} \left[\frac{u_z^{(i)}(\xi)}{r \sin\theta} \int_{\omega^{(i)}} \sigma_{zz}^{(i)}(\xi) r^2 \sin\theta dr d\theta \right] - \sum_{i=0}^{n} \left[\frac{u_z^{(i)}(\xi_0)}{r \sin\theta} \int_{\omega^{(i)}} \sigma_{zz}^{(i)}(\xi_0) r^2 \sin\theta dr d\theta \right] \tag{5.29}$$

where $n_z(\xi) = -n_z(\xi_0) = 1$. Moreover, the rotation $\varphi_x(z)$ is uniform for the present case in every phase and by applying the equation (5.29), we can write:

$$dL_E = \varphi_x(\xi)\sum_{i=0}^{n}\mathcal{M}_x^{(i)}(\xi) - \varphi_x(\xi_0)\sum_{i=0}^{n}\mathcal{M}_x^{(i)}(\xi_0) \tag{5.30}$$

where $\mathcal{M}_x^{(i)}$ represents the bending moment of the *i*-th phase. Finally, the infinitesimal external work is given by:

$$dL_E = \mathcal{M}_x\left[\varphi_x(\xi) - \varphi_x(\xi_0)\right] = \mathcal{M}_x\, d\varphi(z) \tag{5.31}$$

where $\mathcal{M}_x(\xi) = \mathcal{M}_x(\xi_0) = \mathcal{M}_x = const$. The infinitesimal internal work for the element is given by:

$$dL_I = dz\sum_{i=0}^{n}\int_{\omega^{(i)}}\boldsymbol{\sigma}^{(i)}:\boldsymbol{\varepsilon}^{(i)}ds = dz\sum_{i=0}^{n}\int_{0}^{2\pi}\int_{(1-\delta_{0i})R^{(i-1)}}^{R^{(i)}}\left(\sigma_{rr}^{(i)}\varepsilon_{rr}^{(i)} + \sigma_{\theta\theta}^{(i)}\varepsilon_{\theta\theta}^{(i)} + \sigma_{zz}^{(i)}\varepsilon_{zz}^{(i)} + \tau_{r\theta}^{(i)}\gamma_{r\theta}^{(i)}\right) r dr d\theta = \Psi_\chi\, dz \tag{5.32}$$

where $\Psi_\chi = \sum_{i=0}^{n}\int_{\omega^{(i)}}\boldsymbol{\sigma}^{(i)}:\boldsymbol{\varepsilon}^{(i)}ds = \sum_{i=0}^{n}\frac{4E^{(i)}I^{(i)}}{\left(1+\nu^{(i)}\right)}\left[\frac{U_4^{(i)2}(1-\delta_{0i})}{R^{(i)4}R^{(i-1)4}} + \frac{4U_3^{(i)2} + \chi_0^2\left(3-\nu^{(i)}\right) - 8\chi_0 U_3^{(i)}\nu^{(i)}}{4\left(3-4\nu^{(i)}\right)}\right]$;

The curvature χ can be defined as:

$$\chi = \varphi_{x,z} = \left[u_z^{(i)}/\left(r\sin\theta\right)\right]_{,z} = \chi_0 = const \tag{5.33}$$

The curvature is same in any phase and then the cross section of the beam remains plane in agreement with Bernoulli's theory of the beam. By recalling equation (5.26), we can determine the differential of the rotation $\varphi_x(z)$:

$$\mathcal{M}_x = k_\chi\,\chi = k_\chi\,\varphi_{x,z} \;\Rightarrow\; d\varphi_x(z) = \mathcal{M}_x\, k_\chi^{-1} dz \tag{5.34}$$

By equating the equations (5.31) and (5.32), and substituting equation (5.22), we obtain the overall bending stiffness k_χ of multilayered cylinder:

$$k_\chi = \mathcal{M}_x^2\,\Psi_\chi^{-1} \tag{5.35}$$

Finally, the overall bending stiffness k_χ can be written as follows:

$$k_\chi = \Psi_\chi^{-1} = \sum\nolimits_{i=0}^{n} E^{(i)}I^{(i)}\psi_\chi^{(i)} \tag{5.36}$$

where $\psi_\chi^{(i)}$ is correction coefficient that depends on geometrical and mechanical parameters:

$$\psi_\chi^{(i)} = \eta_\chi^{(i)}\Big/\left[\sum_{i=0}^{n}E^{(i)}I^{(i)}\eta_\chi^{(i)}\right]^2 = \frac{1}{E^{(i)}I^{(i)}}\left(\frac{dL_I^{(i)}}{dL_I^2}\right), \tag{5.37}$$

where coefficient $\eta_\chi^{(i)}$ is given by following expression:

$$\eta_\chi^{(i)} = \frac{1}{E^{(i)}I^{(i)}}\int_{\omega^{(i)}}\boldsymbol{\sigma}^{(i)}:\boldsymbol{\varepsilon}^{(i)}ds = \frac{4}{\left(1+\nu^{(i)}\right)}\left[\frac{U_4^{(i)2}(1-\delta_{0i})}{R^{(i)4}R^{(i-1)4}} + \frac{4U_3^{(i)2} + \chi_0^2\left(3-\nu^{(i)}\right) - 8\chi_0 U_3^{(i)}\nu^{(i)}}{4\left(3-4\nu^{(i)}\right)}\right] \tag{5.38}$$

where, without loss of generality, $U_3^{(i)}, U_4^{(i)}, \chi_0$ are coefficients to determine by setting $\mathcal{M}_x = 1$. It is worth to note that, by solving the problem for the case where $\nu^{(i)} = \nu,\ \forall i \in \{0,1,2,...,n\}$, $\psi_\chi^{(i)} = 1$ in any phase, and bending stiffness reduces to:

$$k_\chi = \sum\nolimits_{i=0}^{n} E^{(i)}I^{(i)} \tag{5.39}$$

It is important to note here that the homogenised stiffness obtained for the bent solid in the general case (5.36) ($\nu^{(i)} \neq \nu^{(j)}$) is quite different from the one (5.39) obtained for particular case, that represent the trivial sum of phase's stiffness. This new and relevant result depends principally from the presence of stress component $\tau_{r\theta}$ and relevant strain component $\gamma_{r\theta}$, generated by Poisson effect between different adjacent phases.

10.5.4. Shear stiffness

In order to complete the set of homogenised constitutive equations for multilayered cylinder involving generalized stresses and strains, we finally consider the case in which the object is subjected to shear force $T = \pm T_y$ and to bending deriving from equilibrating couple $\mathcal{M}_x = T_y L$ on base $z = L$. With reference to above elastic solutions for the shear case in (4.47) is reported the actual displacement field. In order to determine the equivalent overall shear stiffness k_γ we will follow the same homogenization procedure used above. The shear stiffness is defined as:

$$k_\gamma : T_y = k_\gamma \gamma \tag{5.40}$$

where γ is the transverse mean shear strain on the cross-section. By reference to an internal arbitrary element of multilayered cylinder, with infinitesimal length "dz", the work made by emerging tractions is given by:

$$dL_E^{(i)} = \sum_{i=0}^{n} \int_{\partial V_L^{(i)}} \mathbf{t}^{(i)}(\xi) \cdot \mathbf{u}^{(i)}(\xi)\, dS + \sum_{i=0}^{n} \int_{\partial V_L^{(i)}} \mathbf{t}^{(i)}(\xi_0) \cdot \mathbf{u}^{(i)}(\xi_0)\, dS \tag{5.41}$$

where $\xi_0 = z$, $\xi = z + dz$, and by means of emerging stresses:

$$\begin{aligned} dL_E = &\sum_{i=0}^{n} \int_{\partial V_L^{(i)}} \tau_{rz}^{(i)}(\xi) n_z(\xi) u_r^{(i)}(\xi) + \tau_{\theta z}^{(i)}(\xi) n_z(\xi) u_\theta^{(i)}(\xi) + \sigma_{zz}^{(i)}(\xi) n_z(\xi) u_z^{(i)}(\xi)\, ds + \\ &+ \sum_{i=0}^{n} \int_{\partial V_L^{(i)}} \tau_{rz}^{(i)}(\xi_0) n_z(\xi_0) u_r^{(i)}(\xi_0) + \tau_{\theta z}^{(i)}(\xi_0) n_z(\xi_0) u_\theta^{(i)}(\xi_0) + \sigma_{zz}^{(i)}(\xi_0) n_z(\xi_0) u_z^{(i)}(\xi_0)\, ds \end{aligned} \tag{5.42}$$

For sake of simplicity, by utilising stress and displacement components in Cartesian coordinates, we obtain:

$$\begin{aligned} dL_E = &\sum_{i=0}^{n} \int_{\partial V_L^{(i)}} \tau_{xz}^{(i)}(\xi) n_z(\xi) u_x^{(i)}(\xi) + \tau_{yz}^{(i)}(\xi) n_z(\xi) u_y^{(i)}(\xi) + \sigma_{zz}^{(i)}(\xi) n_z(\xi) u_z^{(i)}(\xi)\, ds + \\ &+ \sum_{i=0}^{n} \int_{\partial V_L^{(i)}} \tau_{xz}^{(i)}(\xi_0) n_z(\xi_0) u_x^{(i)}(\xi_0) + \tau_{yz}^{(i)}(\xi_0) n_z(\xi_0) u_y^{(i)}(\xi_0) + \sigma_{zz}^{(i)}(\xi_0) n_z(\xi_0) u_z^{(i)}(\xi_0)\, ds \end{aligned} \tag{5.43}$$

The bending moment in beam is given by:

$$M_x(z) = T_y z, \quad dM_x = T_y\, dz \tag{5.44}$$

and on the selected infinitesimal element equation (5.43) gives:

$$dL_E = T_y\left(u_y + du_y\right) - T_y u_y + M_x\left(\varphi_x + d\varphi_x\right) - \left(M_x + dM_x\right)\varphi_x \tag{5.45}$$

where $d\varphi_x$ represents the rotation's differential :

$$d\varphi_x = \chi\, dz \tag{5.46}$$

where χ is the curvature of the beam. By substituting the equations (5.44)-(5.46) in to equation (5.45), we obtain the infinitesimal external work:

$$dL_E = T_y\left[\left(u_{y,z} - \varphi_x\right) + \chi z\right] dz \tag{5.47}$$

The rotation $\varphi_x(z)$ around the x-axis is given by the first component of the curl of displacement field:

$$\varphi_x(z) = -(1/2)(\nabla \times \boldsymbol{u})_1 = (1/2)\left(u_{y,z} - u_{z,y}\right) \tag{5.48}$$

The actual transverse mean shear strain on the cross-section is:

$$\gamma_{eff} = u_{y,z} - \varphi_x = (1/2)\left(u_{y,z} - u_{z,y}\right) = (1/2)\gamma_{yz} \tag{5.49}$$

Finally, the actual external work is given by:

$$dL_E = T_2\left(\gamma_{eff} + \chi z\right) dz \tag{5.50}$$

The infinitesimal internal work results:

$$dL_I = dz\sum_{i=0}^{n}\int_{\omega^{(i)}} \boldsymbol{\sigma}^{(i)}\boldsymbol{\varepsilon}^{(i)}ds = \\ = dz\sum_{i=0}^{n}\int_{0}^{2\pi}\int_{(1-\delta_{0i})R^{(i-1)}}^{R^{(i)}} \left(\sigma_{rr}^{(i)}\varepsilon_{rr}^{(i)} + \sigma_{\theta\theta}^{(i)}\varepsilon_{\theta\theta}^{(i)} + \sigma_{zz}^{(i)}\varepsilon_{zz}^{(i)} + \tau_{r\theta}^{(i)}\gamma_{r\theta}^{(i)} + \tau_{\theta z}^{(i)}\gamma_{\theta z}^{(i)} + \tau_{rz}^{(i)}\gamma_{rz}^{(i)}\right) r\,dr\,d\theta = \Psi_{\gamma}dz \tag{5.51}$$

We can rewrite the infinitesimal internal energy as follows:

$$dL_I = \left(\Psi_{\gamma}^{0} + \Psi_{\gamma}^{1}\,z^2\right)dz \tag{5.52}$$

By recalling equations (5.26)-(5.40), we can determine the curvature and shear deformation:

$$\begin{aligned} T_y\,z = k_{\chi}\,\chi \quad &\Rightarrow \quad \chi = T_y\,z\,k_{\chi}^{-1} \\ T_y = k_{\gamma}\,\gamma_{eff} \quad &\Rightarrow \quad \gamma_{eff} = T_2\,k_{\gamma}^{-1} \end{aligned} \tag{5.53}$$

By equating the equations (5.50) and (5.51) and applying the polynomial identity law, we obtain the follows relationship:

$$T_y\,\gamma_{eff} = \Psi_{\gamma}^{0}; \quad T_y\,\chi = \Psi_{\gamma}^{1}\,z; \tag{5.54}$$

By substituting the equation (5.53) in Equation (5.54), we obtain the overall shear stiffness k_{γ} and bending stiffness of multilayered cylinder:

$$k_{\gamma} = T_y^2 \big/ \Psi_{\gamma}^{0}; \quad k_{\chi} = T_y^2 \big/ \Psi_{\gamma}^{1}; \tag{5.55}$$

By setting $T_y = 1$, we can to write shear and bending stiffness as follows:

$$k_{\gamma} = \left[\Psi_{\gamma}^{0}\right]^{-1}; \quad k_{\chi} = \left[\Psi_{\gamma}^{1}\right]^{-1}; \tag{5.56}$$

It is easy to prove that the bending stiffness calculated in equation (5.56) is same of the (5.35) obtained for pure bending, since $\Psi_{\gamma}^{1} = \Psi_{\chi}$. Then, the bending stiffness does not change in presence of shear, and depends only on geometry of cross section. Finally, the overall shear stiffness k_{γ} can be written as follows:

$$k_{\gamma} = \sum\nolimits_{i=0}^{n} \mu^{(i)}\omega^{(i)}\psi_{\gamma}^{(i)} \tag{5.57}$$

where $\psi_{\gamma}^{(i)}$ is a coefficient that depends on geometrical and mechanical parameters:

$$\psi_{\gamma}^{(i)} = \eta_{\gamma}^{(i)} \Bigg/ \left[\sum_{i=0}^{n} \mu^{(i)}\omega^{(i)}\eta_{\gamma}^{(i)}\right]^2 = \frac{1}{\mu^{(i)}\omega^{(i)}}\left(\frac{dL_I^{(i)}}{dL_I^2}\right), \tag{5.58}$$

where coefficient $\eta_{\gamma}^{(i)}$ is given by follows expression:

$$\eta_{\gamma}^{(i)} = \frac{1}{\mu^{(i)}\omega^{(i)}}\int_{\omega^{(i)}} \boldsymbol{\sigma}^{(i)}\boldsymbol{\varepsilon}^{(i)}ds = \zeta_1^{(i)} + \zeta_2^{(i)} + \zeta_3^{(i)} + \zeta_4^{(i)}, \tag{5.59}$$

where $\zeta_j^{(i)}\ \forall j \in \{1,2,3,4\}$, are coefficients to determine by setting $T_y = 1$. These coefficients assume following expressions:

$$\begin{aligned} \zeta_1^{(i)} &= \left[\mu^{(i)}\pi^2\left(1-\delta_{0i}\right)\left(V_4^{(i)} - 2V_7^{(i)}\right)\right] \Big/ \left(4\,\omega^{(i)}\right); \\ \zeta_2^{(i)} &= \left[4\mu^{(i)}I^{(i)}\left(\lambda^{(i)} + \mu^{(i)}\right)\left(V_5^{(i)} + V_6^{(i)}\right)\left(9V_2^{(i)} - 2V_3^{(i)}\right)\right] \Big/ \Omega^{(i)}; \\ \zeta_3^{(i)} &= \frac{\mu^{(i)}\omega^{(i)}}{\left(2\lambda^{(i)} + 3\mu^{(i)}\right)}\left[2\left(\lambda^{(i)} + 3\mu^{(i)}\right)\left(V_5^{(i)} + V_6^{(i)}\right) + \left(V_4^{(i)} - 2V_7^{(i)}\right)\left(3V_2^{(i)}\lambda^{(i)} + \mu^{(i)}\left(9V_2^{(i)} + 2V_3^{(i)}\right)\right)\right] \\ \zeta_4^{(i)} &= \frac{\pi\,\mu^{(i)}\left[R^{(i)6} - \left(1-\delta_{0i}\right)R^{(i-1)6}\right]}{12\left(\lambda^{(i)} + 3\mu^{(i)}\right)^2}\begin{bmatrix} 4V_3^2\left(4\lambda^{(i)2} + 8\lambda^{(i)}\mu^{(i)} + 5\mu^{(i)2}\right) \\ -12V_2^{(i)}V_3^{(i)}\left(12\lambda^{(i)2} + 22\lambda^{(i)}\mu^{(i)} + 9\mu^{(i)2}\right) \\ 9V_2^{(i)2}\left(40\lambda^{(i)2} + 84\lambda^{(i)}\mu^{(i)} + 45\mu^{(i)2}\right) \end{bmatrix} \end{aligned} \tag{5.60}$$

In particular for solid composed by only one hollow phase with Poisson's modulus ν, tangential shear modulus μ, area of cross section ω, external radius R_e, and internal radius R_i, the shear stiffness is given by:

$$k_\gamma = \left\{6\mu\omega(1+\nu)^2\left[R_e^2+R_i^2\right]^2\right\}\Big/\left\{\left(7+14\nu+8\nu^2\right)\left[R_e^4+R_i^4\right]+2\left(17+34\nu+16\nu^2\right)R_e^2R_i^2\right\} \quad (5.61)$$

By means of the position $R_i = \beta R_e$, we can rewrite the equation (5.61) as follows:

$$\begin{aligned} k_\gamma &= \left[6\mu\omega\left(1+\beta^2\right)^2(1+\nu)^2\right]\Big/\left[\left(1+\beta^4\right)\left(7+14\nu+8\nu^2\right)+\beta^2\left(34+68\nu+32\nu^2\right)\right] \\ k_\gamma &\cong 0.85\mu\omega\left[\left(1+\beta^2\right)^2\Big/\left(1+4.85\beta^2+\beta^4\right)\right] = \kappa\mu\omega \quad \forall\nu\in[0,0.5] \end{aligned} \quad (5.62)$$

In particular, the shear stiffness for the beam with hollow circular section is given by $\mu\omega$ for a coefficient κ (inverse shear's factor) that vary in the range [0.5,0.85]. For small thickness $\beta\to 1 \Rightarrow k_\gamma \cong 0.5\mu\omega$, in agreement with of Jourawsky's theory of the shear, but for big thickness $\beta = 0 \Rightarrow k_\gamma \cong 0.85\mu\omega$. For solid composed by a sole phase with circular section, the shear stiffness is given by :

$$k_\gamma = 6\mu\omega\left[(1+\nu)^2\Big/\left(7+14\nu+8\nu^2\right)\right] \cong 0.85\mu\omega \quad \forall\nu\in[0,0.5] \quad (5.63)$$

For negative values of Poisson's Modulus, the shear stiffness reduces. In particular for $\nu=-1$, the shear stiffness is equal to zero. As a result of what has been obtained above, it is worth to note here that it isn't possible to assume the shear stiffness of multilayered cylinder by summing those of the single phases, as so far is made for the sake of approximation.

10.6 Sensitivity analyses: closed-form solutions for solid composed by two phases

In this section, we report an application for a solid composed by only two isotropic phases. We will determine the axial, torsion, bending and shear stiffness of the solid mentioned above. Then, we will carry out the comparison between the stiffness of multilayered cylinder beam calculated utilising the exact analytical solution with the approximate one given above by means of the homogenization procedure.

10.6.1 Axial Stiffness

Here we show the comparison between the axial stiffness k_ε calculated by applying the formula (5.11) and approximate axial stiffness $\bar{k}_\varepsilon$ estimated as usually done as sum of the single phase's stiffness. The results are reported in figures n. 4,5,6,7,8. The simplified axial stiffness $\bar{k}_\varepsilon$ is given by following formula:

$$\bar{k}_\varepsilon = \sum_{i=0}^{1} E^{(i)}\omega^{(i)} \quad (6.1)$$

In order to stress the influence of Poisson's modulus ν, comparison is developed by considering different values of ν for two phases. Let us consider the error percentage between k_ε and $\bar{k}_\varepsilon$ calculated by applying following formula : $err\% = 100\left(k_\varepsilon - \bar{k}_\varepsilon\right)\Big/\bar{k}_\varepsilon$. In explicit, for case of axial force, this formula becomes:

$$err\% = \frac{200\alpha\beta^2\left(\beta^2-1\right)\left(\nu^{(0)}-\nu^{(1)}\right)^2}{\left[(\alpha-1)\beta^2+1\right]\left\{\left(\beta^2-1\right)\left(1-\nu^{(0)}-2\nu^{(0)2}\right)-\alpha\left(1+\nu^{(1)}\right)\left[1+\beta^2\left(2\nu^{(1)}-1\right)\right]\right\}} \quad (6.2)$$

where $\alpha = E^{(0)}/E^{(1)}$, $\beta = R^{(0)}/R^{(1)}$ are ratio between Young's modulus and ratio between radii of two phases, respectively. By assuming that two phases have same area and same Young's modulus: $\alpha=1$, $\beta=1/\sqrt{2}$, we obtain that percentage error given by (6.2) is a function only of Poisson's modulus of two phases. In this case the function (6.2) becomes:

$$err\%\left(\alpha=1,\beta=\frac{1}{\sqrt{2}}\right)=\left[100\left(\nu^{(0)}-\nu^{(1)}\right)^2\right]\Big/\left[4+\nu^{(1)}\left(1-2\nu^{(1)}\right)-\nu^{(0)}\left(1+2\nu^{(0)}\right)\right] \qquad (6.3)$$

In figure 10.18 is represented the error percentage (6.3) when Poisson's modulus of internal phase varies on abscissa, and every curve refers to the selected Poisson's modulus of external phase. By applying the relationship (6.3), if the Poisson's modulus in both phases are positive, the maximum error percentage is equal to 8.33 corresponding to following value of Poisson's moduli: $\nu^{(0)}=0.5,\ \nu^{(1)}=0.0$. The function (6.3) can assume values greater than 8.33 if the Poisson's modulus assumes positive and negative values in two phases, respectively. For example, if $\nu^{(0)}=0.5,\ \nu^{(1)}=-0.5$ the percentage error assumes the value 50. It is interesting to note that for design purposes aimed to obtaining stiffness of multilayered cylinder, also in technical applications involving new materials, the actual stiffness could be increased until the 50%, respect to that usually evaluated. By assuming $\alpha=1,\ \nu^{(0)}=0.50$ (incompressible core) the function (6.2) becomes:

$$err\%\left(\alpha=1,\nu^{(0)}=0.5\right)=\left[50\beta^2\left(\beta^2-1\right)\left(1-2\nu^{(1)}\right)^2\right]\Big/\left\{\left(1+\nu^{(1)}\right)\left[\beta^2\left(2\nu^{(1)}-1\right)-1\right]\right\} \qquad (6.4)$$

In figure 10.19 is plotted the function (6.4) for the case $\alpha=1,\ \nu^{(0)}=0.50$ where on abscissa varies the radii's ratio $\beta=R^{(0)}/R^{(1)}$ and every curve refers to the selected Poisson's modulus of the external phase. By assuming $\alpha=1,\ \nu^{(1)}=0.50$ (incompressible shell) the function (6.2) becomes:

$$err\%\left(\alpha=1,\nu^{(1)}=0.5\right)=\left[200\beta^2\left(\beta^2-1\right)\left(\nu^{(0)}-1/2\right)\right]\Big/\left[\left(\beta^2-1\right)\left(-1+\nu^{(0)}+2\nu^{(0)2}\right)+3/2\right] \qquad (6.5)$$

Figure 10.20 shows the function (6.5) where on abscissa varies the radii's ratio $\beta=R^{(0)}/R^{(1)}$ and every curve refers to selected Poisson's ratio for internal phase. Finally, in figure 10.21 and 10.22 are reported the plots for cases $\nu^{(0)}=0.5,\ \nu^{(1)}=0.0$ and $\nu^{(0)}=0.0,\ \nu^{(1)}=0.5$, respectively. In these figures the free parameters are α,β.

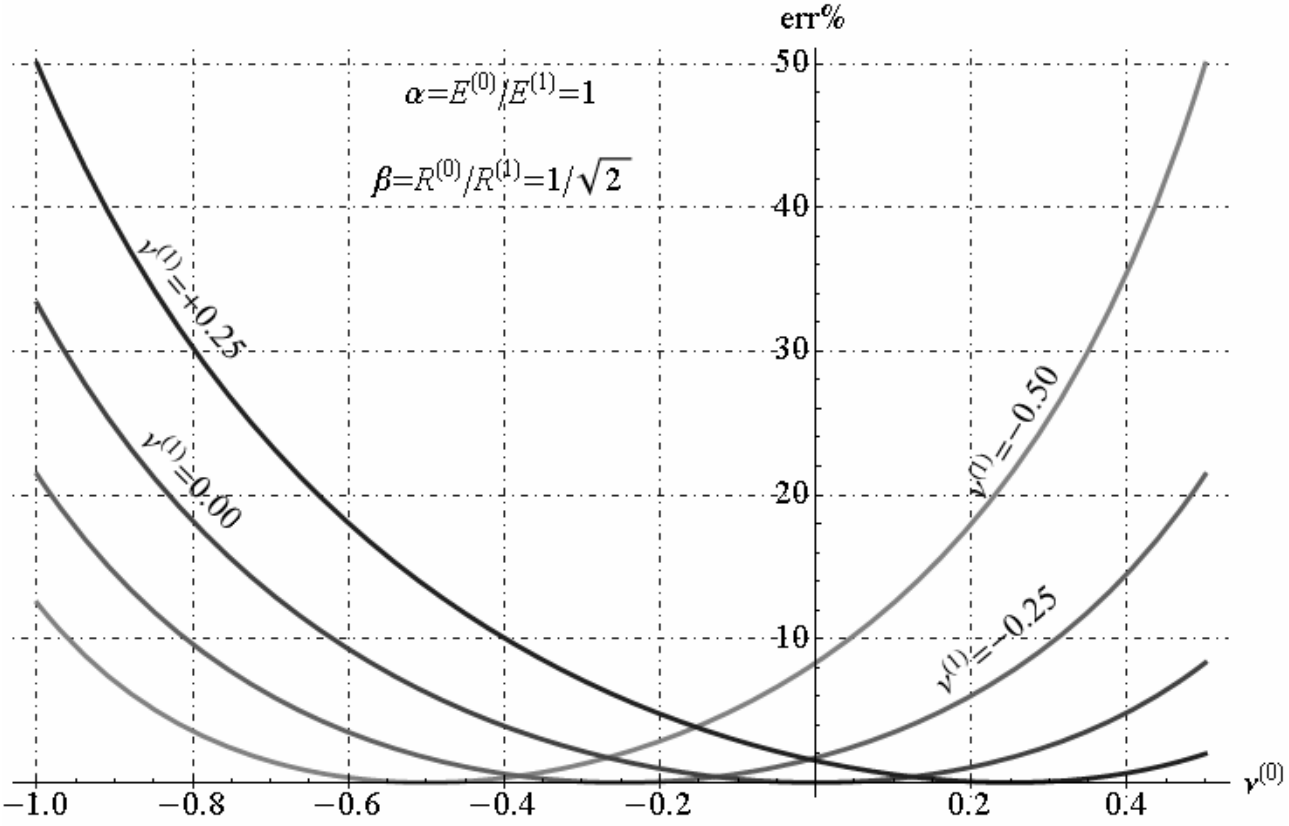

Fig. 10.18 - *Percentage error between the k_ε and $\bar{k}_\varepsilon$: Variation respect to Poisson's modulii of two phases with fixed parameters: $\alpha=E^{(0)}/E^{(1)}=1,\ \beta=R^{(0)}/R^{(1)}=\sqrt{2}/2$;*

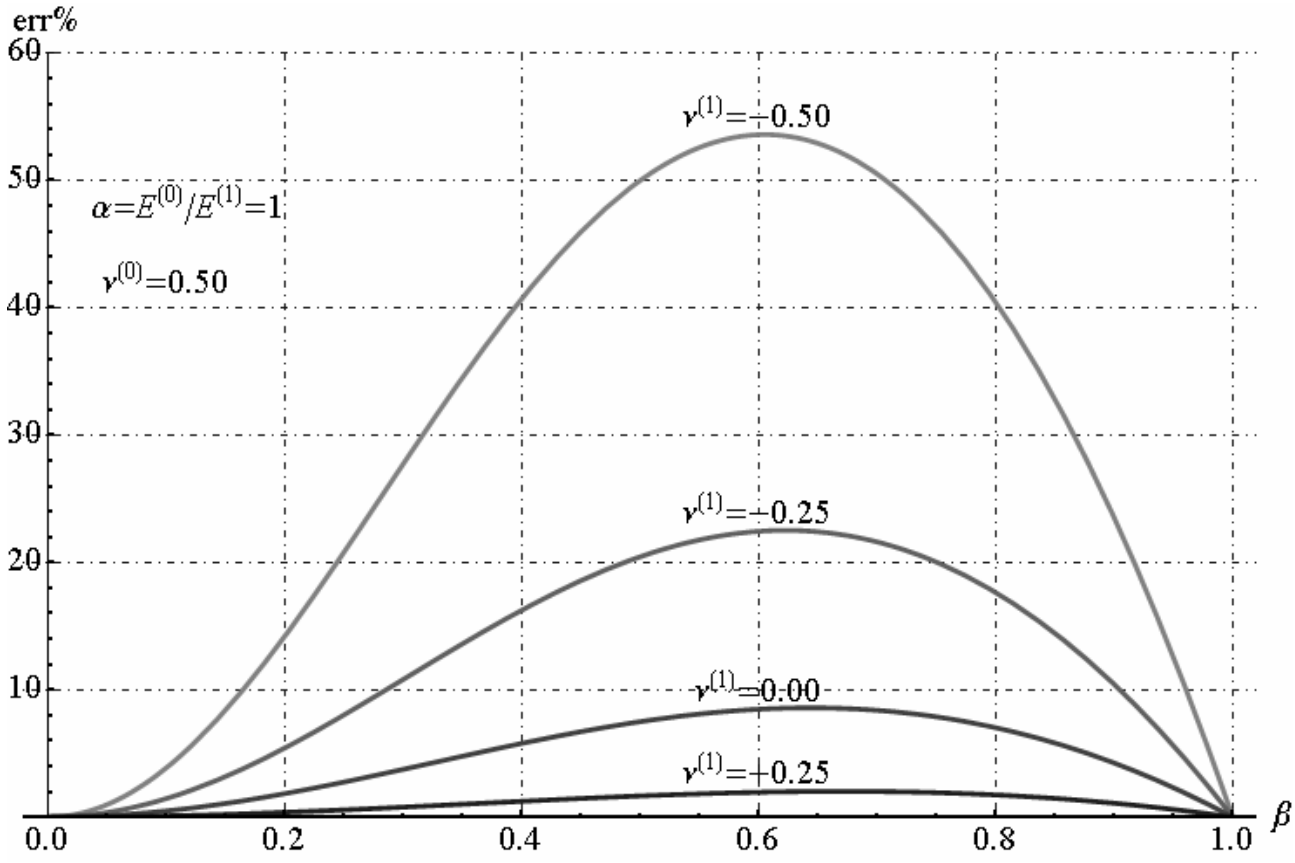

Fig. 10.19 - *Percentage error between the* k_ε *and* $\overline{k}_\varepsilon$*: Variation respect to* β *and* $\nu^{(1)}$ *with fixed parameters* $\alpha = E^{(0)}/E^{(1)} = 1,\ \nu^{(0)} = 0.5$ *(incompressible core);*

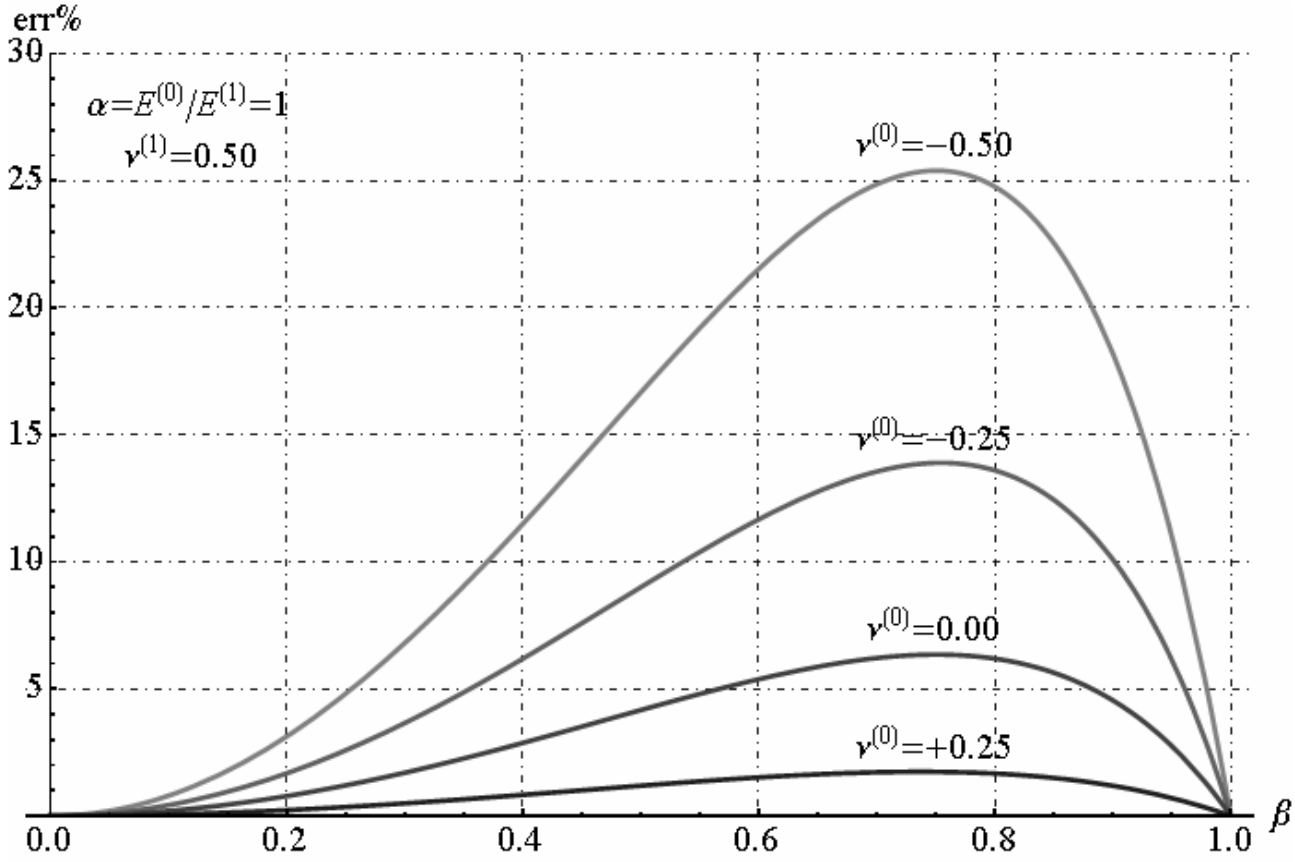

Fig. 10.20 - *Percentage error between the* k_ε *and* $\overline{k}_\varepsilon$*: Variation respect to* β *and* $\nu^{(0)}$ *with fixed parameters* $\alpha = E^{(0)}/E^{(1)} = 1,\ \nu^{(1)} = 0.5$ *(incompressible shell);*

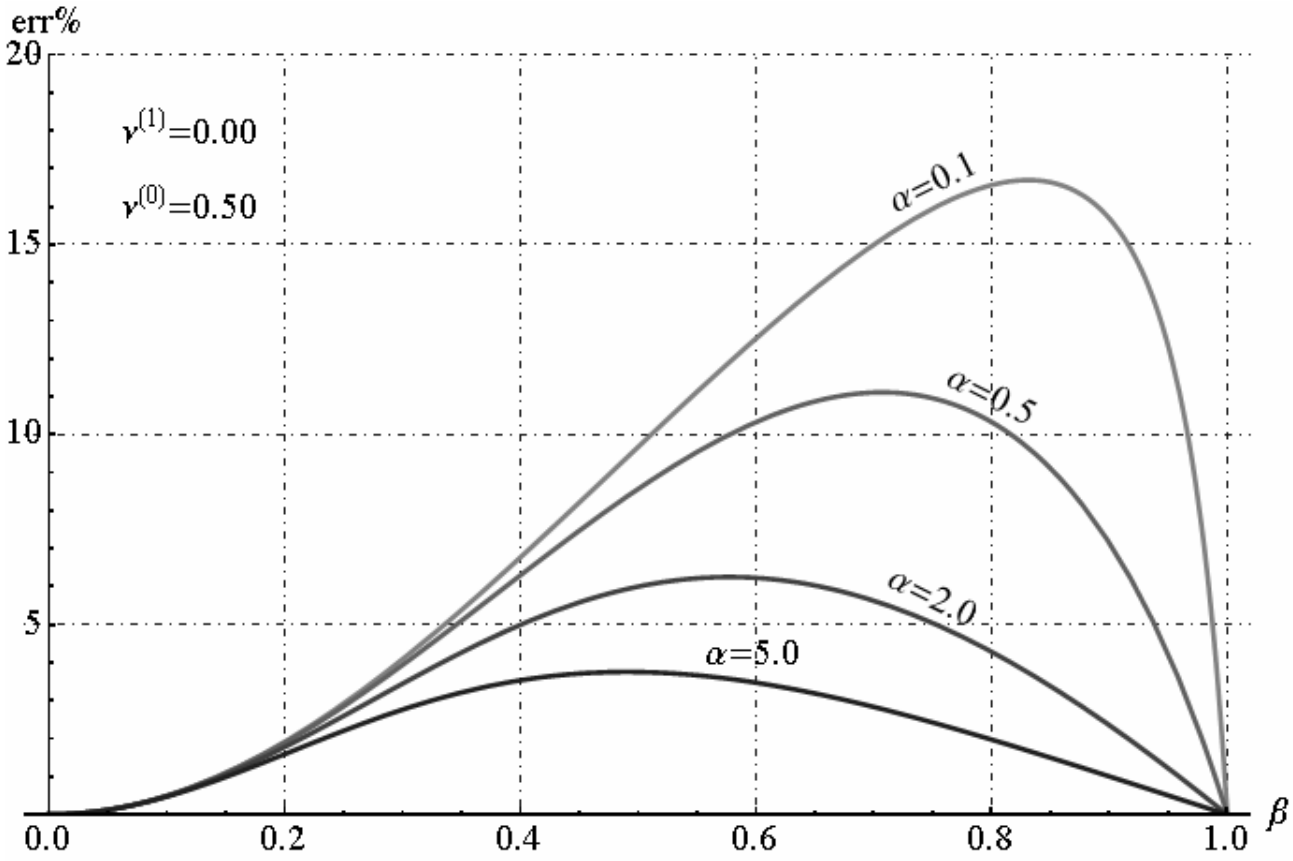

Fig. 10.21 - *Percentage error between the* k_ε *and* $\bar{k}_\varepsilon$*: Variation respect to Young's modulii of two phases and* β *with fixed parameters* $\nu^{(0)} = 0.5$, $\nu^{(1)} = 0.0$ *(incompressible core);*

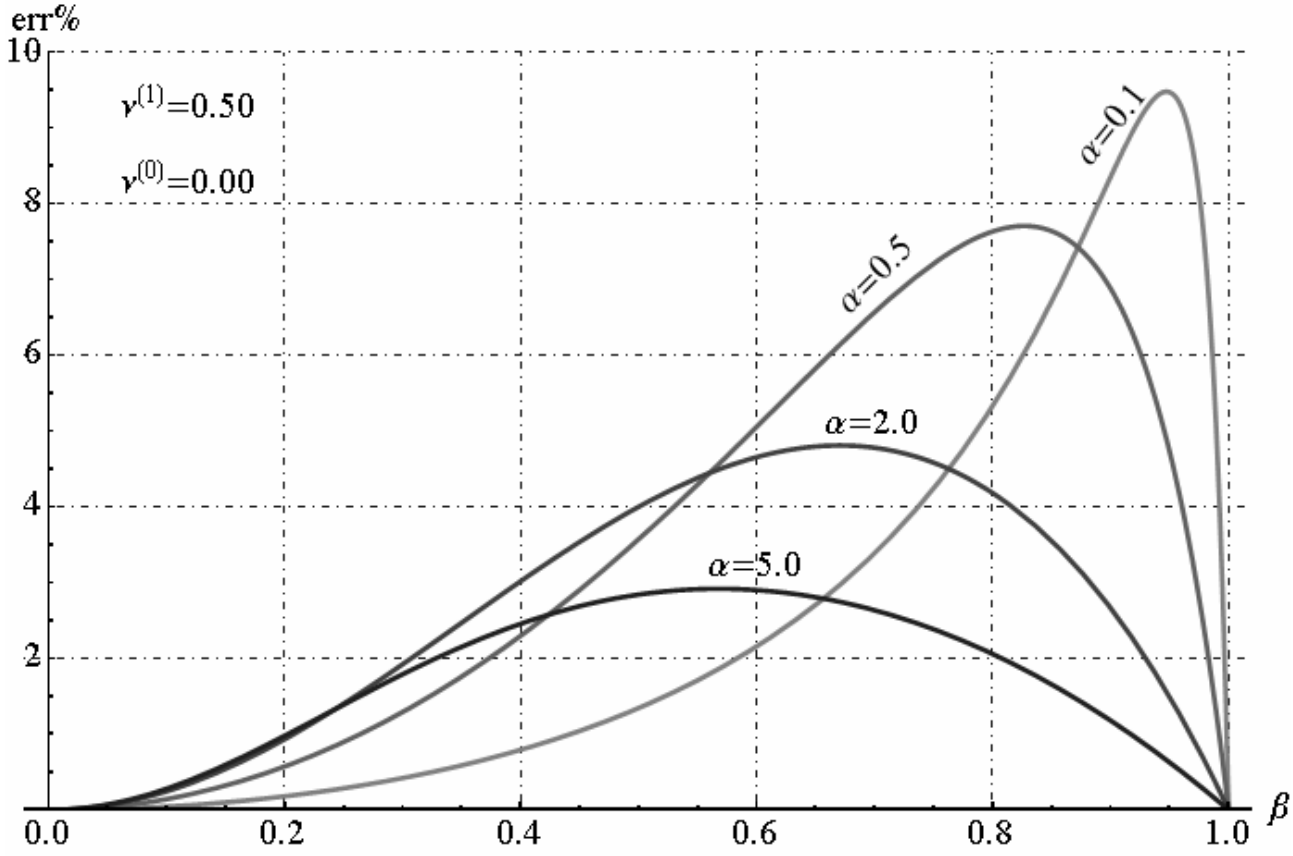

Fig. 10.22 - *Percentage error between the* k_ε *and* $\bar{k}_\varepsilon$*: Variation respect to Young's modulii of two phases and* β *with fixed parameters* $\nu^{(0)} = 0.0$, $\nu^{(1)} = 0.5$ *(incompressible shell);*

10.6.2 Bending stiffness

Figures 10.23, 10.24, 10.25, 10.26, 10.27 shows the comparison between the bending stiffness k_χ calculated by proposed model, evaluated with the formula (5.36) and bending stiffness $\bar{k}_\chi$ estimated as the sum of the single phase's stiffness. The approximate bending stiffness $\bar{k}_\chi$ is evaluated by following formula:

$$\bar{k}_\chi = \sum_{i=0}^{1} E^{(i)} I^{(i)} \tag{6.6}$$

where $I^{(i)}$ is the inertia of single phase. In order to stress the influence of Poisson's moduli, comparison is developed by considering two phases. Let us consider the error percentage between k_ε and $\bar{k}_\varepsilon$ calculated by applying following formula : $err\% = 100\left(k_\chi - \bar{k}_\chi\right)/\bar{k}_\chi$. In explicit for case of pure bending this formula becomes:

$$err\% = \frac{400\,\alpha\,\beta^4\left(1+\beta^4\right)\left(\nu^{(0)}-\nu^{(1)}\right)^2}{\left[\beta^4\left(\alpha-1\right)+1\right]\left\{\left(\beta^4-1\right)\left(3-\nu^{(0)}-4\nu^{(0)2}\right)+\alpha\left(1+\nu^{(1)}\right)\left[\beta^4\left(4\nu^{(1)}-3\right)-1\right]\right\}} \tag{6.7}$$

By assuming same area and same Young's modulus for two phases: $\alpha = 1,\ \beta = 1/\sqrt[4]{2}$, that percentage error given by (6.7) becomes a function of the Poisson's moduli of two phases. In this case the function (6.7) becomes:

$$err\%\left(\alpha = 1, \beta = \frac{1}{\sqrt[4]{2}}\right) = \frac{200\left(\nu^{(1)}-\nu^{(0)}\right)^2}{8+\nu^{(1)}\left(1-4\nu^{(1)}\right)-\nu^{(0)}\left(1+4\nu^{(0)}\right)} \tag{6.8}$$

In figure 10.23 is represented the error percentage (6.8) when Poisson's modulus of internal phase varies on abscissa, and every curve refers to the selected Poisson's modulus of external phase. By applying the relationship (6.8), if the Poisson's modulii in both phases are positive, the maximum error percentage is equal to 7.69 corresponding to following value of Poisson's moduli: $\nu^{(0)} = 0.5,\ \nu^{(1)} = 0.0$. The function (6.3) can assume values greater than 7.69 if the Poisson's modulus assumes alternate signs in two phases. As example, if $\nu^{(0)} = 0.5,\ \nu^{(1)} = -0.5$ the percentage error assumes the value 40. By assuming $\alpha = 1,\ \nu^{(0)} = 0.50$ (incompressible core) the function (6.7) becomes:

$$err\%\left(\alpha = 1, \nu^{(0)} = 0.5\right) = \frac{200\,\beta^4\left(1-\beta^4\right)\left(1-2\nu^{(1)}\right)^2}{5+2\nu^{(1)}+\beta^4\left(3-2\nu^{(1)}-8\nu^{(1)2}\right)} \tag{6.9}$$

In figure 10.24 is plotted the function (6.9) where on abscissa varies the radii's ratio $\beta = R^{(0)}/R^{(1)}$ and every curve refers to the selected Poisson's modulus of the external phase. By assuming $\alpha = 1,\ \nu^{(1)} = 0.50$ (incompressible shell) the function (6.7) becomes:

$$err\%\left(\alpha = 1, \nu^{(1)} = 0.5\right) = \frac{200\,\beta^4\left(\beta^4-1\right)\left(1-2\nu^{(0)}\right)^2}{2\nu^{(0)}\left(1+4\nu^{(0)}\right)+\beta^4\left(3-2\nu^{(0)}-8\nu^{(0)2}\right)-9} \tag{6.10}$$

The figure 10.25 shows the function (6.10) where on abscissa varies the radii's ratio $\beta = R^{(0)}/R^{(1)}$ and every curve refers to the selected Poisson's ratio for internal phase. Finally, in figure 10.26 and 10.27 are reported the results for cases $\nu^{(0)} = 0.5,\ \nu^{(1)} = 0.0$ and $\nu^{(0)} = 0.0,\ \nu^{(1)} = 0.5$, respectively. In these last figures the free parameters are α, β.

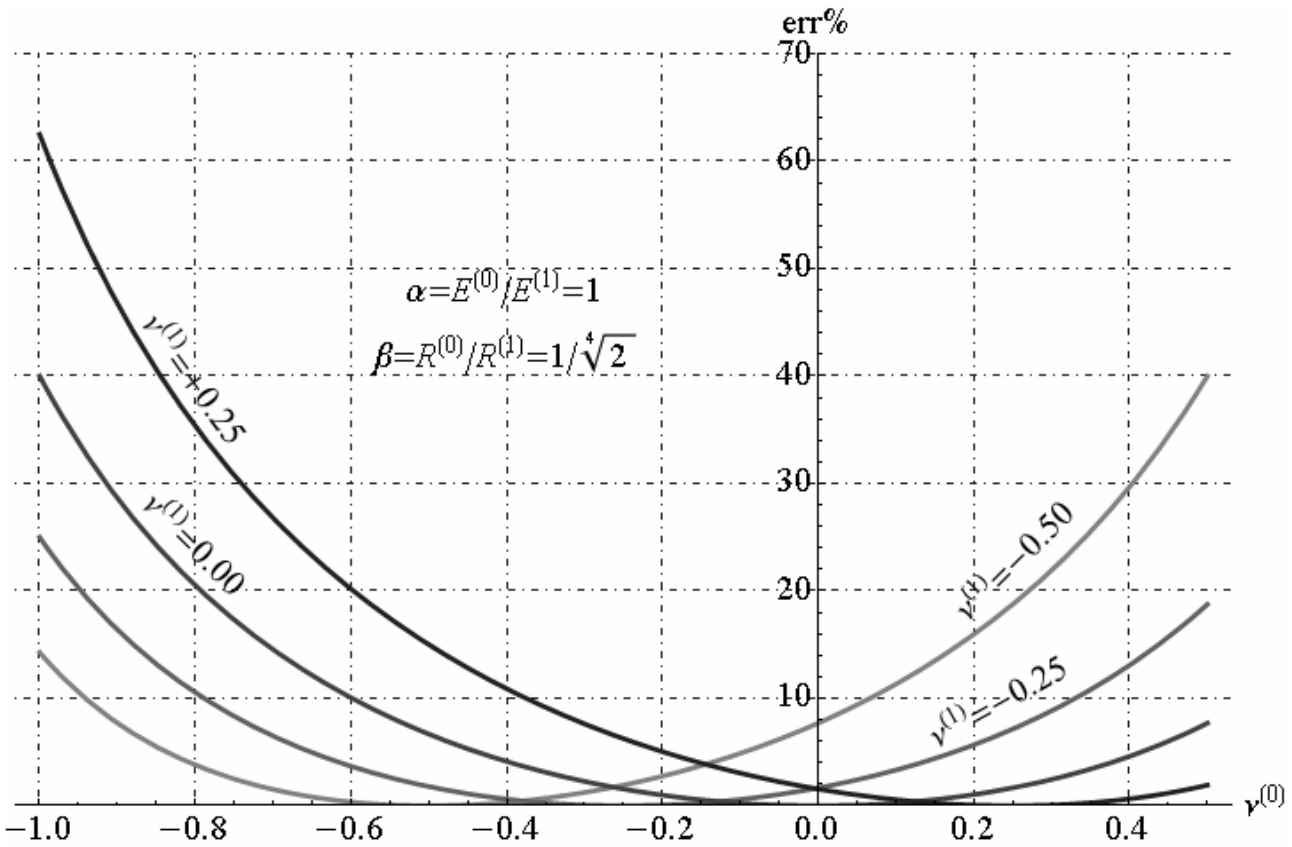

Fig. 10.23 - *Percentage error between the* k_χ *and* $\bar{k}_\chi$*: Variation respect to Poisson's modulii of two phases with fixed parameters* $\alpha = E^{(0)}/E^{(1)} = 1, \quad \beta = R^{(0)}/R^{(1)} = 1/\sqrt[4]{2}$ *;*

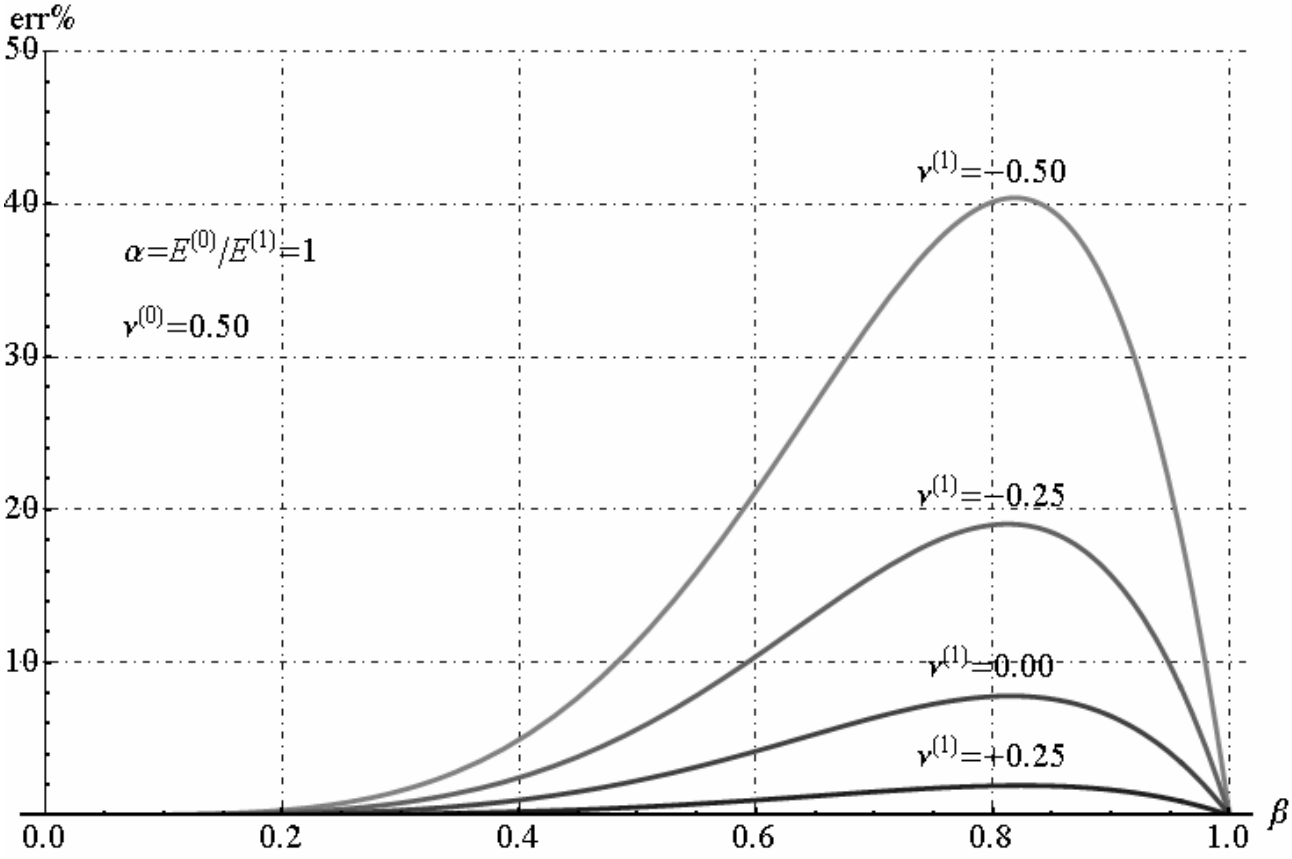

Fig. 10.24 - *Percentage error between the* k_χ *and* $\bar{k}_\chi$*: Variation respect to* β *and* $\nu^{(1)}$ *with fixed parameters:* $\alpha = E^{(0)}/E^{(1)} = 1, \quad \nu^{(0)} = 0.5$ *(incompressible core);*

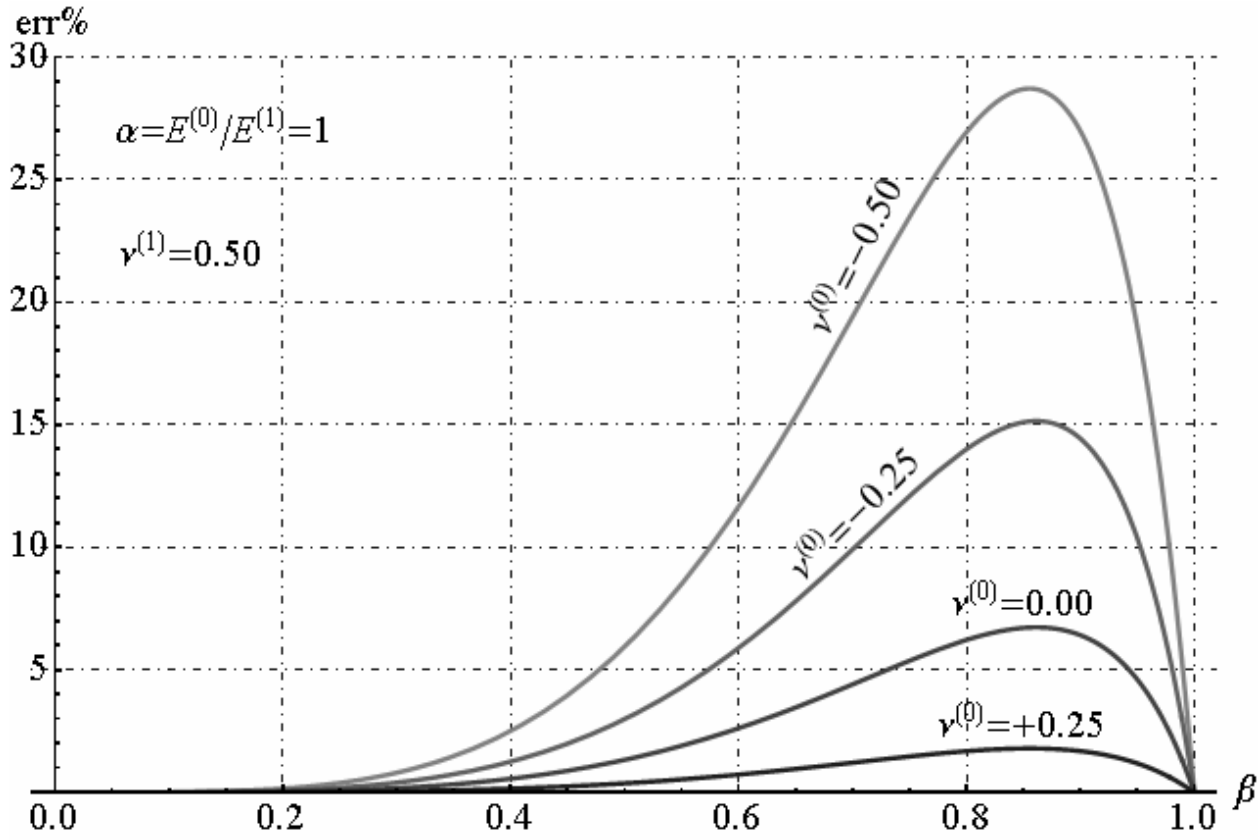

Fig. 10.25 - *Percentage error between the* k_χ *and* $\bar{k}_\chi$*: Variation respect to* β *and* $\nu^{(0)}$ *with fixed parameters* $\alpha = E^{(0)}/E^{(1)} = 1,\ \nu^{(1)} = 0.5$ *(incompressible shell);*

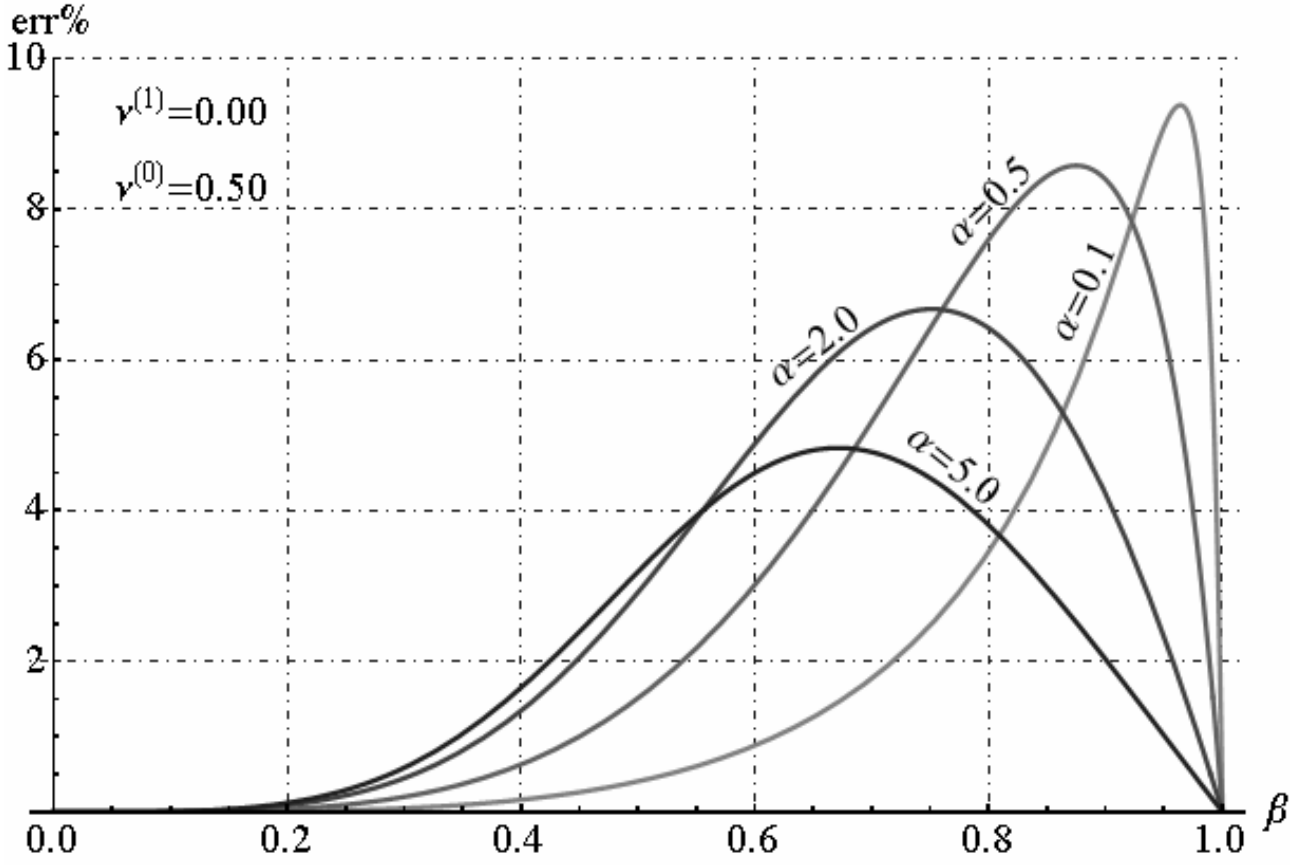

Fig. 10.26 - *Percentage error between the* k_χ *and* $\bar{k}_\chi$*: Variation respect to Young's modulii of two phases and* β *with fixed parameters* $\nu^{(0)} = 0.5,\ \nu^{(1)} = 0.0$ *(incompressible core);*

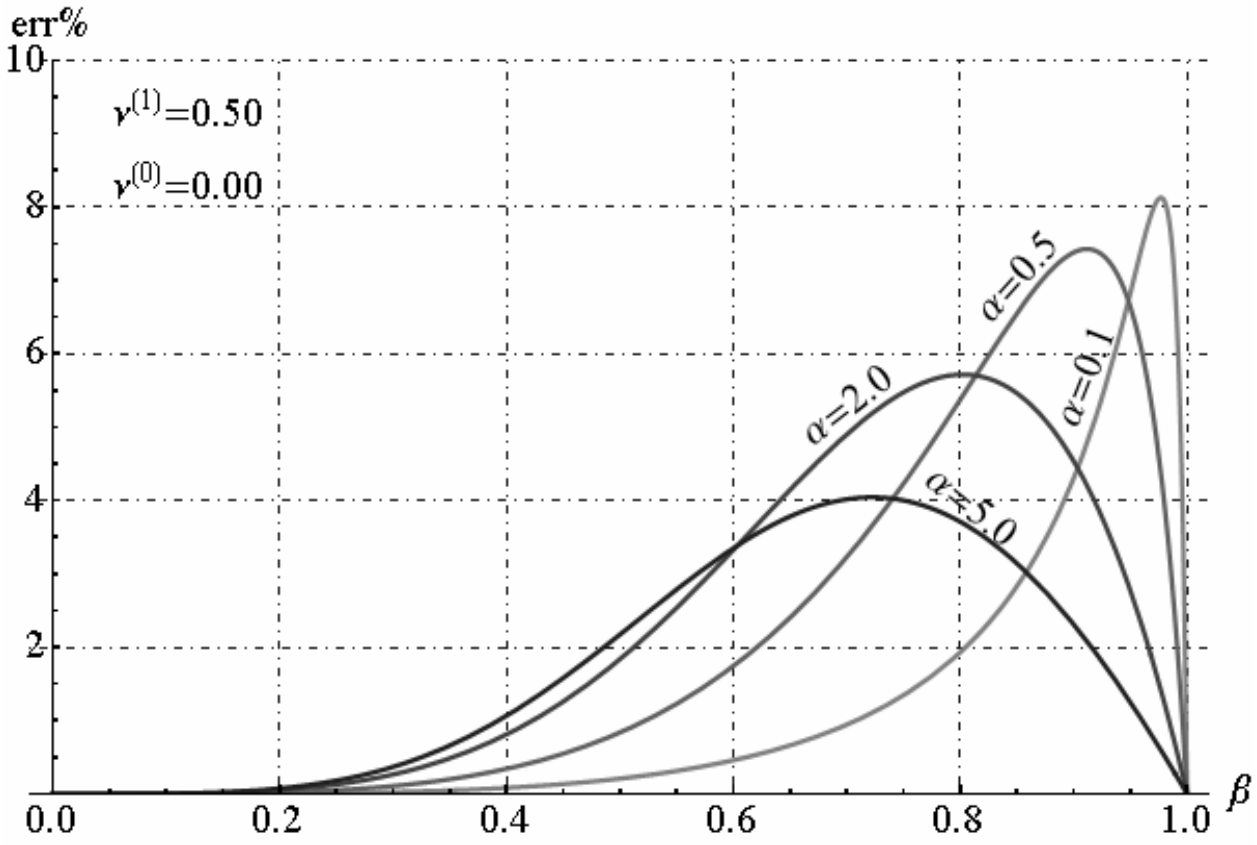

Fig. 10.27 - *Percentage error between the* k_χ *and* $\bar{k}_\chi$*: Variation respect to Young's modulii of two phases and* β *with fixed parameters* $\nu^{(0)}=0.0$, $\nu^{(1)}=0.5$ *(incompressible shell);*

10.6.3. Shear stiffness

Figures 10.28, 10.29, 10.30, 10.31, 10.32, highlights the comparison between the bending stiffness k_γ calculated by means of the new analytical solution (5.57) and the shear stiffness $\bar{k}_\gamma$ obtained by summing the single phase's stiffness, see equations (5.61) and (5.63):

$$\bar{k}_\gamma = 6\pi R^{(1)}\mu^{(1)}\left[\frac{\dfrac{\beta^2\mu^{(0)}\left(1+\nu^{(0)}\right)}{7+2\nu^{(0)}\left(7+4\nu^{(0)}\right)}+\dfrac{\left(1-\beta^2\right)\left(1+\beta^2\right)^2\left(1+\nu^{(1)}\right)}{\left[7+2\nu^{(1)}\left(7+4\nu^{(1)}\right)\right]\left(1+\beta^4\right)+\left[34+4\nu^{(1)}\left(17+8\nu^{(1)}\right)\right]\beta^2}}\right] \tag{6.11}$$

where $\gamma=\mu^{(0)}/\mu^{(1)}$ is the ratio between tangential elastic modulus in two phases. This comparison is implemented by selecting same elastic moduli for two phases. For the chosen parameters, $\bar{k}_\gamma$ and k_γ are functions of Poisson's modulus of two phases. The error percentage between k_γ and $\bar{k}_\gamma$ is evaluated by applying following formula:

$$err\% = 100\left(k_\gamma-\bar{k}_\gamma\right)/\bar{k}_\gamma \tag{6.12}$$

For sake of brevity, we don't report the explicit expression of function (6.12). Figure 10.28 shows the error percentage (6.12) when Poisson's modulus of internal phase varies on abscissa, and every curve refers to the selected Poisson's modulus of external phase. In figure 10.29 is plotted the function (6.12) for the case $\alpha=1$, $\nu^{(0)}=0.50$ (incompressible core), where on abscissa varies the radii's ratio $\beta=R^{(0)}/R^{(1)}$ and every curve refers to the selected Poisson's modulus of the external phase. The figure 10.30 shows the function (6.12) for the case $\alpha=1$, $\nu^{(1)}=0.50$ (incompressible

shell), where on abscissa varies the radii's ratio $\beta = R^{(0)}/R^{(1)}$ and every curve refers to the selected Poisson's ratio for internal phase. Finally, in figure 10.31 and 10.32 are reported the results obtained for cases $\nu^{(0)} = 0.5,\ \nu^{(1)} = 0.0$ and $\nu^{(0)} = 0.0,\ \nu^{(1)} = 0.5$, respectively. In these last figures the free parameters are α, β.

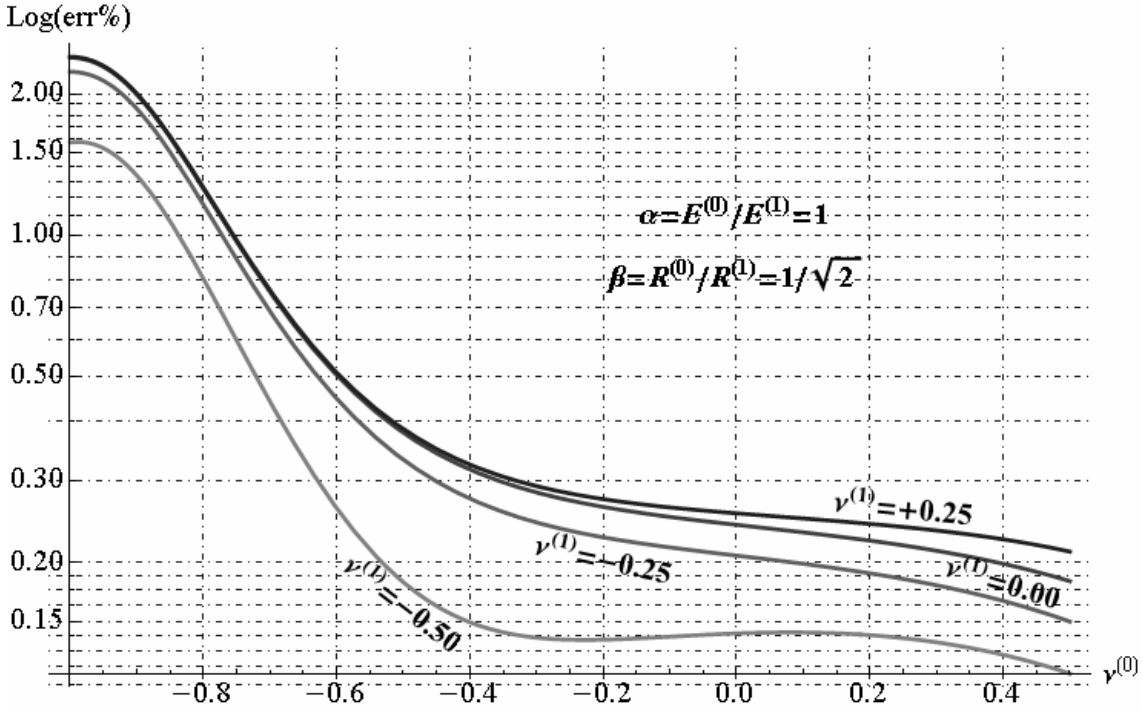

Fig. 10.28 - *Percentage error between the k_γ and $\bar{k}_\gamma$: Variation respect to Poisson's modulii of two phases with fixed parameters $\gamma = \mu^{(0)}/\mu^{(1)} = 1,\ \beta = R^{(0)}/R^{(1)} = \sqrt{2}/2$;*

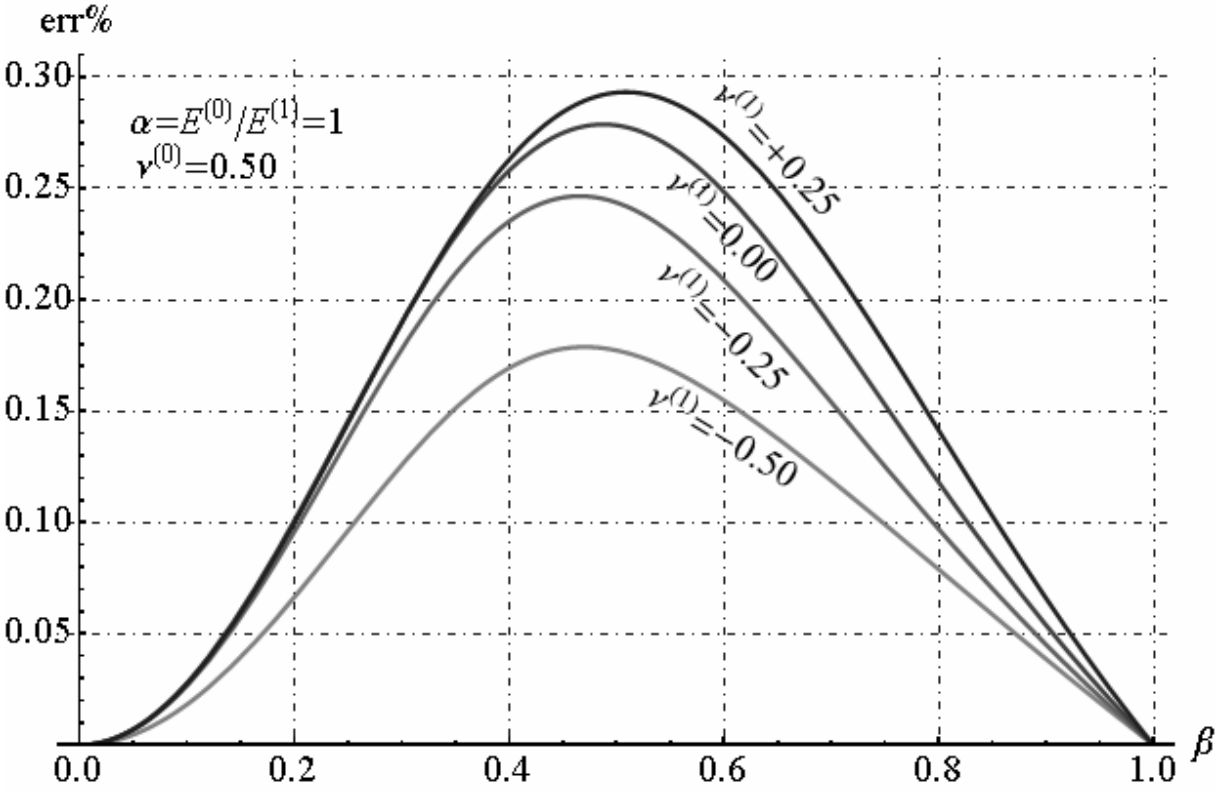

Fig. 10.29 - *Percentage error between the k_γ and $\bar{k}_\gamma$: Variation respect to β and $\nu^{(1)}$ with fixed parameters $\alpha = \mu^{(0)}/\mu^{(1)} = 1,\ \nu^{(0)} = 0.5$ (incompressible core);*

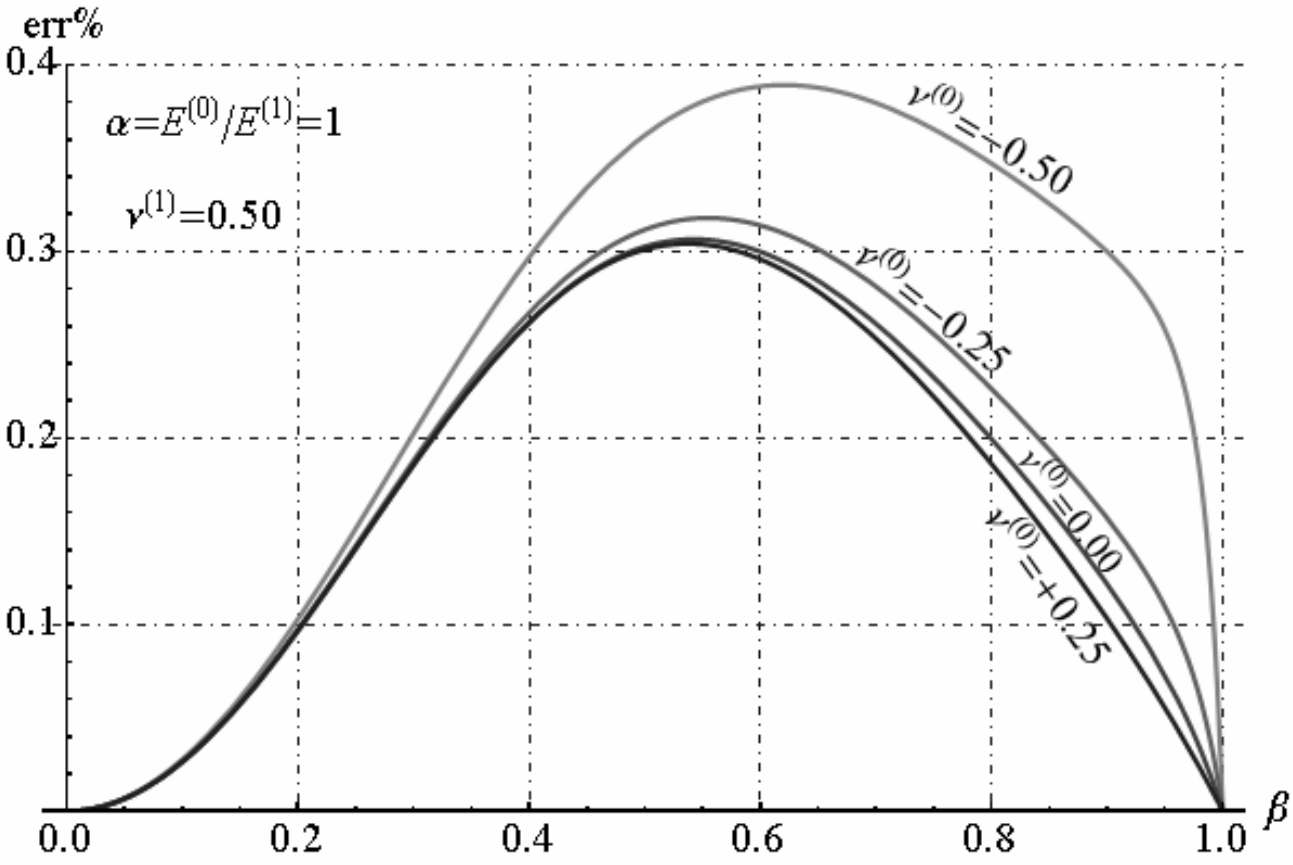

Fig. 10.30 - *Percentage error between the* k_γ *and* $\bar{k}_\gamma$*: Variation respect to* β *and* $\nu^{(0)}$ *with fixed parameters* $\alpha=\mu^{(0)}/\mu^{(1)}=1,\ \nu^{(1)}=0.5$ *(incompressible shell);*

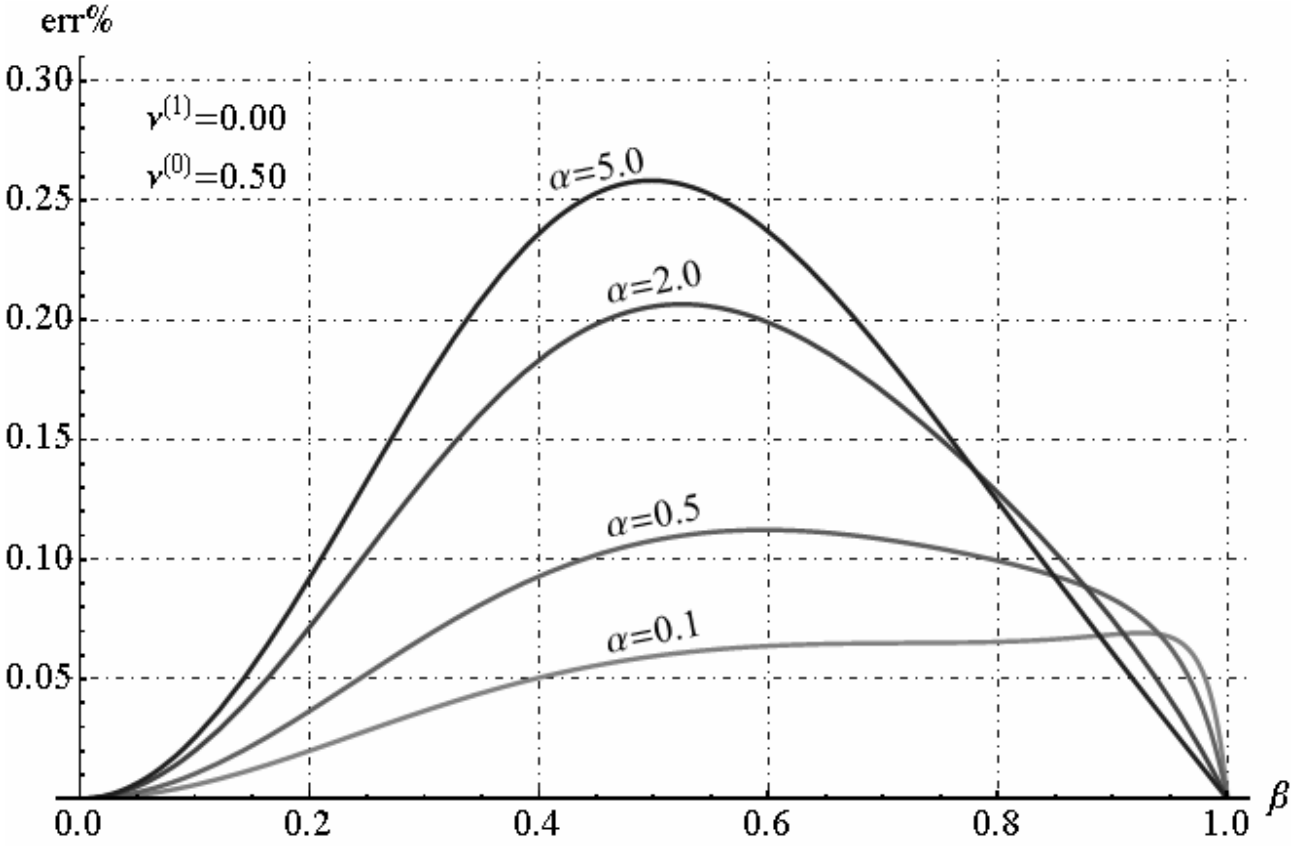

Fig. 10.31 - *Percentage error between the* k_γ *and* $\bar{k}_\gamma$*: Variation respect to shear modulii of two phases and* β *with fixed parameters* $\nu^{(0)}=0.5,\ \nu^{(1)}=0.0$ *(incompressible core);*

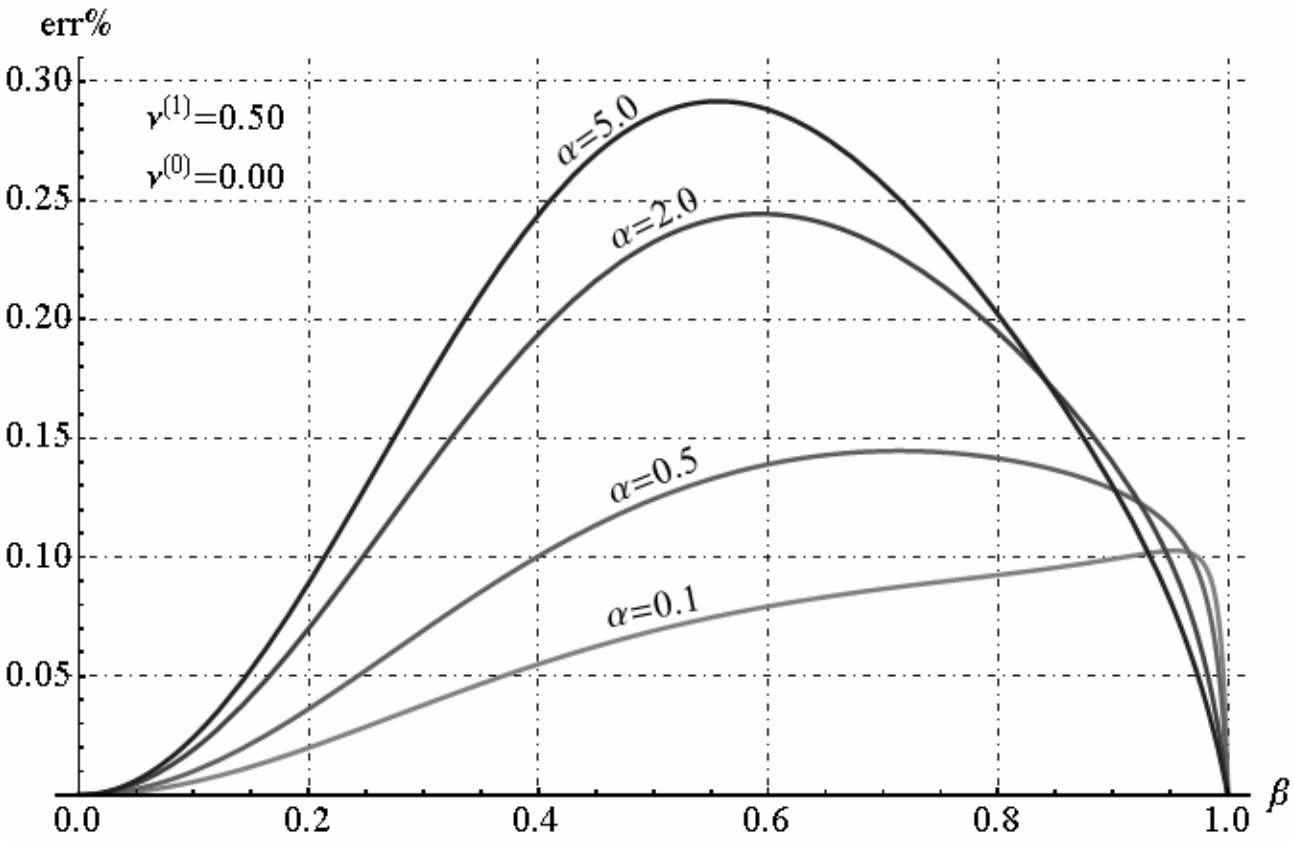

Fig. 10.32 - *Percentage error between the k_γ and $\bar{k}_\gamma$: Variation respect to shear modulii of two phases and β with fixed parameters $\nu^{(0)} = 0.0, \nu^{(1)} = 0.5$ (incompressible shell);*

10.7. Conclusions

In this work, we considered a beam constituted by multilayered cylinder composed by n+1 isotropic phases subjected to De Saint Venant's load condition: axial force, torsion, pure bending, shear and bending moment. We showed the elastic solution for these load conditions and proposed a new mathematical procedure to determine in explicit the integration constants of the solution displacement field related to cases of the axial, bending, and torsion. The above elastic solutions are already present in literature. On the other hand, the work presents a new elastic solution for cylindrical multiphase solid composed by n-isotropic phases under the shear and bending load condition: this solution is not yet known in the literature. By using the solution presented, were calculated axial, bending, torsion and shear stiffness of the solid considered. The axial stiffness k_ε, bending stiffness k_χ, shear stiffness k_γ are not equal to the sum of stiffness of single phases, as so far usually assumed in simplified procedures, but strongly dependent on values of Poisson's moduli and on geometrical parameters. It is analysed the case study of the solid composed by two isotropic phases. The comparison between the stiffness calculated by exact solution proposed in this work and the approximate corresponding stiffness estimated as sum of the single stiffness was shown, for any of De Saint Venant load conditions. The percentage error between exact and approximate stiffness depending on change of the mechanical and geometrical parameters of multilayered cylinder solid, was widely analyzed. For axial and bending stiffness, if $\nu^{(0)} = 0.5, \nu^{(1)} = 0$, the maximum value of the percentage error between exact and approximate stiffness was found, for any ratio of the Young's modulus and radius. It is easy to prove that percentage error don't can be greater than the 25% for axial stiffness, and of the 10% for bending stiffness, respectively. On the contrary, in the case of the shear and bending, if $\nu^{(0)} = 0$, $\nu^{(1)} = 0.5$ the percentage error reaches the maximum values for any value of parameters α, β. In this case, if the ratio between Young's modulus of the two phases "$\alpha << 1$" the percentage error might reach negative relevant values. In

other words, if $E^{(1)} << E^{(0)}$ the approximate shear stiffness is greater than the exact shear stiffness. In particular the percentage error can reach the 100%. Due to the wide presence of biological, chemical-based and man-made materials and structures presenting significant analogies with multilayered cylinder, it is felt that the proposed strategy can be helpfully utilized for designing composites and for a better understanding of optimality criteria to which Nature obeys.

10.8. Table of symbols

ε_0	Axial deformation	n	number of material phases
$C_{h/k}^{(i)}$	Scalar parameters of the *i*-th phase	$i, j, ...$	indices
$\mathrm{L_I}$	total internal work	$R^{(i)}$	radius of the *i*-th phases
$\mathrm{L_E}$	total external work	$\{r, \theta, z\}$	cylindrical coordinates
N_z	Axial force	ε_{hk}	strain components
$\mathcal{M}_x$	Bending moment acting in plane $y-z$	σ_{hk}	stress components
$\mathcal{M}_y$	Bending moment acting in plane $x-z$	$\sigma_{hk}^{(i)}, \varepsilon_{hk}^{(i)}$	stresses and strains of the *i*-th phase
$\mathcal{M}_z$	Torque moment	ν	*Poisson* ratio
T_x	Shear force in x direction	E	*Young* modulus
T_y	Shear force in y direction	μ, λ	*Lamè* moduli
k_ε	Axial stiffness, k_χ Bending stiffness	$\partial V_0^{(i)}$	base(z=0) surface of the *i*-th phase
k_ω	Torsion stiffness, k_γ Shear stiffness	$\partial V_L^{(i)}$	base(z=L) surface of the *i*-th phase
$\mathbf{L}$	load vector	$\partial V_{CYL}^{(i)}$	cylindrical surface of the *i*-th phase

10.9. References

[1] Liew, K.M., Kitipornchai, S., Zhang, X.Z., Lim, C.W., (2003), Analysis of the thermal stress behaviour of functionally graded hollow circular cylinders, *International Journal of Solids and Structures*, vol. 40, 2355-2380.

[2] Shao, Z. S., (2005), Mechanical and thermal stresses of a functionally graded circular hollow cylinder with finite length, *International Journal of Pressure Vessels an Piping*, vol. 82, 155-163.

[3] Mian, M., Abid, Spencer, A. J. M., (1998), Exact solutions for functionally graded and laminated elastic materials, *J. Mech. Phys. Solids*, Vol. 46, n. 12, 2283-2295.

[4] Fraldi, M, Cowin, S. C., (2004), Inhomogeneous elastostatic problem solutions constructed from stress-associated homogeneous solutions, *Journal of the Mechanics and Physics of Solids*, 52, 2207-2233.

[5] Morteza M. Mehrabadi, Stephen C. Cowin and Jovo Jaric, (1995), Six-dimensional orthogonal tensor representation of the rotation about an axis in three dimensions, *International Journal Solids Structures*, Vol. 32, N0. 3/4 , pp. 439-449.

[6] Y.J. Yoon, G. Yang, S.C. Cowin, (2002), Estimation of the effective transversally isotropic elastic constants of a material from known values of the material's orthotropic elastic constants, *Biomechan Model Mechanobiol* , Vol 1 , pag. 83-93.

[7] Alshits, V. I., Kirchner, O. K., (2001). Cylindrically anisotropic, radially inhomogeneous elastic materials. *Proc. Roy. Soc. Lond*. A457, 671-693.

[8] Chouchaoui, C. S., Ochoa, O. O. (1999), Similitude study for a laminated cylindrical tube under tensile, torsion, bending, internal and external pressure. Part I: governing equations, *Composite Structures*, 44, 221-229.

[9] Chen, T., Chung, C. T., Lin, W. L., (2000), A revisit of a cylindrically anisotropic tube subjected to pressuring, shearing, torsion, extension and a uniform temperature change, *International Journal of Solids and Structures*, 37, 5143-5159.

[10] Tarn, J. Q., (2001), Exact solutions for functionally graded anisotropic cylinders subjected to thermal and mechanical loads, *International Journal of Solids and Structures*, 38, 8189-8206.
[11] Tarn, J. Q., Wang, Y. M., (2001), Laminated composite tubes under extension, torsion, bending, shearing and pressuring: a state space approach, *International Journal of Solids and Structures*, 38, 9053-9075.
[12] Lekhnitskii, S. G., (1981), *Theory of Elasticity of an Anisotropic Body*, Mir, Moscow.
[13] Huang, C. H., Dong, S. B., (2001), Analysis of laminated circular cylinders of materials with the most general form of cylindrical anisotropy. I. Axially symmetric deformations. *International Journal of Solids and Structures*, 38, 6163-6182.
[14] Ting, T. C. T., (1999), Pressuring, shearing, torsion and extension of a circular tube or bar of cylindrically anisotropic material, *Proc. Roy. Soc. Lond*. A452, 2397-2421.
[15] Love, A. E. H., (1944), *A treatise on the mathematical theory of elasticity*, Dover Publications, Inc, New York.
[16] Fraldi, M., Nunziante, L., Carannante, F. (2007), *Axis-symmetrical Solutions for n-plies Functionally Graded Material Cylinders under Strain no-Decaying Conditions*, J. Mech. of Adv. Mat. and Struct. Vol. 14 (3), pp. 151-174 - DOI: 10.1080/15376490600719220
[17] M. Fraldi, L. Nunziante, F. Carannante, A. Prota, G. Manfredi, E. Cosenza (2008), *On the Prediction of the Collapse Load of Circular Concrete Columns Confined by FRP*, Journal Engineering structures, Vol. 30, Issue 11, November 2008, Pages 3247-3264 - DOI: 10.1016/j.engstruct.2008.04.036
[18] Fraldi, M., Nunziante, L., Chandrasekaran, S., Carannante, F., Pernice, MC. (2009), *Mechanics of distributed fibre optic sensors for strain measurements on rods*, Journal of Structural Engineering, 35, pp. 323-333, Dec. 2008- Gen. 2009
[19] M. Fraldi, F. Carannante, L. Nunziante (2012), *Analytical solutions for n-phase Functionally Graded Material Cylinders under de Saint Venant load conditions: Homogenization and effects of Poisson ratios on the overall stiffness*, Composites Part B: Engineering, Volume 45, Issue 1, February 2013, Pages 1310–1324
[20] Nunziante, L., Gambarotta, L., Tralli, A., *Scienza delle Costruzioni*, 3° Edizione, McGraw-Hill, 2011, ISBN: 9788838666971
[21] Bernini, R. , Fraldi, M., Minardo, A., Minutolo, V., Carannante, F., Nunziante, L., Zeni, L., (2006). Identification of defects and strain error estimation for bending steel beams using time domain Brillouin distributed optical fiber sensors. *Smart Materials and Structures*. Vol. n. 15, pp. 612-622- ISSN 0964-1726
[22] Christensen, R. M., (1997), Stress based Yield/Failure criteria for fiber composites, *International Journal Solid and Structures*, vol. 34, No. 5, pp. 529-543.
[23] Gurtin, M. E., (1972), *The Linear Theory of Elasticity*, Handbbuch der Physik, Springer, Berlin.
[24] H. Altenbach, G.A. Magin (2001). *Mechanics of Generalised Continuo*. Springer
[25] Z. Hashin, S. Shtrikman (1963). A variational approach to the theory of the elastic behavoiur of multiphase materials. *Journal of the Mechanics and Physics of Solids*. Vol. 11, n.2, pp. 127-140
[26] S. Nemat-Nasser, M. Hori (1993). Micromechanics: overall properties of heterogeneous materials. North-Holland.

10.10. Appendix A1: Integration of the function $G^{(i)}$ for pure bending

Let us assume that the function $G^{(i)}(r,\theta,z)$ is given by :

$$G^{(i)}(r,\theta,z) = p^{(i)}(r,z)\, q^{(i)}(\theta) \tag{A1.1}$$

As here are absent torque and shear, we will assume that shear stresses $\tau_{\theta z}^{(i)}, \tau_{rz}^{(i)}$ acting on each section vanish. Since the bending moment is constant along z direction, the remaining stresses do not depend on z variable. Then, the derivates of stress component $\sigma_{rr}^{(i)}, \sigma_{\theta\theta}^{(i)}, \sigma_{zz}^{(i)}, \tau_{r\theta}^{(i)}$ respect to z variable are equal to zero. We can write these conditions as follows:

$$\sigma_{rr,z}^{(i)} = \sigma_{\theta\theta,z}^{(i)} = \sigma_{zz,z}^{(i)} = \tau_{r\theta,z}^{(i)} = 0, \quad \tau_{\theta z}^{(i)} = \tau_{rz}^{(i)} = 0, \tag{A1.2}$$

By substituting eqs. (A1.1) in relationships (4.7)-(4.8) and (4.12)-(4.13), and remember the conditions (A1.2), we obtain:

$$\left(\sigma_{\theta\theta}^{(i)} - \sigma_{zz}^{(i)}\right)_{,z} = 0 \;\Rightarrow\; q_{,\theta\theta\theta}^{(i)} \big/ q_{,\theta}^{(i)} = -1 - r^2 \left\{ \left[p_{,zz}^{(i)} + p_{,rr}^{(i)} \right]_{,zz} \Big/ p_{,zz}^{(i)} \right\} = \alpha_0^{(i)} \tag{A1.3}$$

where $\alpha_0^{(i)}$ is a constant to determine. Moreover, by applying the conditions (A1.2), we can write :

$$\sigma_{rr,z}^{(i)} = 0 \;\Rightarrow\; r\, p_{,rzz}^{(i)} - p_{,zz}^{(i)} = 0 \tag{A1.4}$$

By deriving the relationship (A1.4) respect to variable *r* :

$$\left(\sigma_{rr,z}^{(i)}\right)_{,r} = 0 \;\Rightarrow\; p_{,rrzz}^{(i)} = 0 \tag{A1.5}$$

By substituting the eq. (A1.5) in to eq. (A1.3), we obtain:

$$q_{,\theta\theta\theta}^{(i)} \big/ q_{,\theta}^{(i)} = -1 - r^2 \left(p_{,zzzz}^{(i)} \big/ p_{,zz}^{(i)} \right) = \alpha_0^{(i)} \;\Rightarrow\; -r^2 p_{,zzzz}^{(i)} = \left(\alpha_0^{(i)} + 1\right) p_{,zz}^{(i)} \tag{A1.6}$$

By deriving the equation (A1.6) in two times respect to variable r and applying the condition (A1.4) , we obtain:

$$\left(2 p_{,zz}^{(i)} + 4r\, p_{,rzz}^{(i)} + r^2 p_{,rrzz}^{(i)}\right)_{,zz} = p_{,zzzz}^{(i)} = 0 \tag{A1.7}$$

By means the equation (A1.7) and equation (A1.5), we obtain $\alpha_0^{(i)} = -1$, and then the function $q(\theta)$ must satisfy the equation:

$$q_{,\theta\theta\theta}^{(i)}(\theta) + q_{,\theta}^{(i)}(\theta) = 0 \;\Rightarrow q^{(i)}(\theta) = \alpha_1^{(i)} \cos\theta + \alpha_2^{(i)} \sin\theta + \alpha_3^{(i)} \tag{A1.8}$$

Thanks to above discussed symmetry of displacement solution respect to y -direction, we deduce that the constants $\alpha_2^{(i)}, \alpha_3^{(i)}$ vanish, then : $G^{(i)}(r,\theta,z) = p(r,z)\cos\theta$

By recalling equations (A1.7), we determine the form of function $p^{(i)}(r,z)$:

$$p_{,zzzz}^{(i)} = 0 \;\Rightarrow\; p^{(i)}(r,z) = g_0^{(i)}(r) + z\, g_1^{(i)}(r) + z^2\, g_2^{(i)}(r) + z^3\, g_3^{(i)}(r) \tag{A1.9}$$

Then, we determine the function $G^{(i)}(r,\theta,z)$ as reported below:

$$G^{(i)}(r,\theta,z) = \left[g_0^{(i)}(r) + z\, g_1^{(i)}(r) + z^2\, g_2^{(i)}(r) + z^3\, g_3^{(i)}(r) \right] \cos\theta \tag{A1.10}$$

By substituting equation (A1.10) in to relationships (4.7) and (2.1)-(2.2), we obtain the following conditions:

$$\sigma_{rr,z}^{(i)} = 0 \;\Rightarrow\; \begin{cases} g_3^{(i)}(r) - r\, g_{3,r}^{(i)}(r) = 0 \\ g_2^{(i)}(r) - r\, g_{2,r}^{(i)}(r) = 0 \end{cases} \Rightarrow \begin{cases} g_3^{(i)}(r) = C_1^{(i)} r \\ g_2^{(i)}(r) = C_2^{(i)} r \end{cases} \tag{A1.11}$$

where $C_1^{(i)}, C_2^{(i)}$ are integration constants. By means functions in equation (A1.11) and the conditions (A1.2), we determine the equations involving functions $g_0^{(i)}(r), g_1^{(i)}(r)$:

$$\tau_{\theta z}^{(i)} = 0 \;\Rightarrow \begin{cases} -g_0^{(i)} + r\, g_{0,r}^{(i)} + r^2\, g_{0,rr}^{(i)} = 2C_2^{(i)} r^3 \\ -g_1^{(i)} + r\, g_{1,r}^{(i)} + r^2\, g_{1,rr}^{(i)} = \left(6C_1^{(i)} - 4k^{(i)}\right) r^3 \end{cases} \tag{A1.12}$$

By integrating the differential equations (A1.12), we determine the functions $g_0^{(i)}(r), g_1^{(i)}(r)$:

$$\begin{cases} g_0^{(i)}(r) = C_3^{(i)} r + C_4^{(i)} r^{-1} + \left(C_2^{(i)} \big/ 4\right) r^3 \\ g_1^{(i)}(r) = C_5^{(i)} r^{-1} + C_6^{(i)} r + C_7^{(i)} r^2 + \left(3C_1^{(i)} - 2k^{(i)}\right)\left(r^3 \big/ 4\right) \end{cases} \tag{A1.13}$$

where $C_3^{(i)}, C_4^{(i)}, C_5^{(i)}, C_6^{(i)}, C_7^{(i)}$ are integration constants.

By applying the conditions (4.11) on function $G^{(i)}(r,\theta,z)$:

$$\nabla^2\nabla^2 G^{(i)} = f^{(i)}(r) \;\Rightarrow\; C_7^{(i)} = 0, \tag{A1.14}$$

Moreover, the constants $C_2^{(i)}, C_3^{(i)}, C_4^{(i)}$ can be assumed equal to zero because they characterize rigid body motion of the solid, then the function $G^{(i)}(r,\theta,z)$ becomes:

$$G^{(i)}(r,\theta,z)=\left[C_1^{(i)}z^2+C_5^{(i)}r^{-2}+C_6^{(i)}+\left(3C_1^{(i)}-2\,k^{(i)}\right)\left(r^2/4\right)\right]r\,z\cos\theta \qquad \text{(A1.15)}$$

By renaming the integration constants with following relationships:

$$C_1^{(i)}=(2/3)\left(U_3^{(i)}-2U_2^{(i)}\right),\ C_5^{(i)}=-U_4^{(i)}/2,\ \ C_6^{(i)}=-U_5^{(i)},\ k^{(i)}=\left[2\mu^{(i)}\left(2U_3^{(i)}-3U_2^{(i)}\right)\right]\Big/\Omega^{(i)}, \qquad \text{(A1.16)}$$

and by substituting relationships (A1.16) in eq. (A1.15), we obtain the explicit expression of the function $G^{(i)}(r,\theta,z)$ reported in equation (4.26).

Appendix A2: Integration of the function $G^{(i)}$ for shear coupled with bending

Let us assume the function $G^{(i)}(r,\theta,z)$ be given by :

$$G^{(i)}(r,\theta,z)=p(r,z)\,q(\theta) \qquad \text{(A2.1)}$$

In presence of constant shear on the solid respect to z, we will assume the shear stresses $\tau_{\theta z}^{(i)}, \tau_{rz}^{(i)}$ acting on each section as constant respect to variable z. Since the bending moment is linear respect to z the remaining stresses are assumed to depend linearly upon variable z. Then, the derivates in two times of stress components $\sigma_{rr}^{(i)}, \sigma_{\theta\theta}^{(i)}, \sigma_{zz}^{(i)}, \tau_{r\theta}^{(i)}$ respect to z variable are equal to zero. We can write these conditions as follows:

$$\sigma_{rr,zz}^{(i)}=\sigma_{\theta\theta,zz}^{(i)}=\sigma_{zz,zz}^{(i)}=\tau_{r\theta,zz}^{(i)}=0,\quad \tau_{\theta z,z}^{(i)}=\tau_{rz,z}^{(i)}=0, \qquad \text{(A2.2)}$$

By substituting equation (A2.1) in relationships (4.7)-(4.8) and (4.12)-(4.13), and by remembering conditions (A2.2), we obtain:

$$\left(\sigma_{\theta\theta}^{(i)}-\sigma_{zz}^{(i)}\right)_{,zz}=0\ \Rightarrow\ q_{,\theta\theta\theta}^{(i)}/q_{,\theta}^{(i)}=-1-r^2\left[\left(p_{,zz}^{(i)}+p_{,rr}^{(i)}\right)_{,zzz}\Big/p_{,zzz}^{(i)}\right]=\alpha_0^{(i)} \qquad \text{(A2.3)}$$

with $\alpha_0^{(i)}$ a constant to determine. Moreover, by applying condition (A2.2), we can write :

$$\sigma_{rr,zz}^{(i)}=0\ \Rightarrow\ r\,p_{,rzzz}^{(i)}-p_{,zzz}^{(i)}=0 \qquad \text{(A2.4)}$$

By deriving the relationship (A2.4) respect to variable r :

$$\left(\sigma_{rr,zz}^{(i)}\right)_{,r}=0\ \Rightarrow\ p_{,rrzzz}^{(i)}=0 \qquad \text{(A2.5)}$$

By substituting the equation (A2.5) in to equation (A2.3), we obtain:

$$q_{,\theta\theta\theta}^{(i)}/q_{,\theta}^{(i)}=-1-r^2\left(p_{,zzzzz}^{(i)}/p_{,zzz}^{(i)}\right)=\alpha_0^{(i)}\ \Rightarrow\ -r^2p_{,zzzzz}^{(i)}=\left(\alpha_0^{(i)}+1\right)p_{,zzz}^{(i)} \qquad \text{(A2.6)}$$

By deriving the equation (A2.6) in two times respect to variable *r* and by applying condition (A2.4), we obtain:

$$\left(2p_{,zz}^{(i)}+4r\,p_{,rzz}^{(i)}+r^2p_{,rrzz}^{(i)}\right)_{,zzz}=p_{,zzzzz}^{(i)}=0 \qquad \text{(A2.7)}$$

By means equations. (A2.7) and (A2.5) , we obtain $\alpha_0^{(i)}=-1$, and then the function $q(\theta)$ must satisfy the equation:

$$q_{,\theta\theta\theta}^{(i)}(\theta)+q_{,\theta}^{(i)}(\theta)=0\ \Rightarrow q^{(i)}(\theta)=\alpha_1^{(i)}\cos\theta+\alpha_2^{(i)}\sin\theta+\alpha_3^{(i)} \qquad \text{(A2.8)}$$

By applying the consideration of symmetry of the displacement solution respect to y-direction, we deduce that the constants $\alpha_2^{(i)}, \alpha_3^{(i)}$ must vanish, then : $G^{(i)}(r,\theta,z)=p(r,z)\cos\theta$

By recalling equations (A2.7), we determine the form of function $p^{(i)}(r,z)$:

$$p_{,zzzzz}^{(i)}=0\ \Rightarrow\ p^{(i)}(r,z)=g_0^{(i)}(r)+z\,g_1^{(i)}(r)+z^2\,g_2^{(i)}(r)+z^3\,g_3^{(i)}(r)+z^4\,g_4^{(i)}(r) \qquad \text{(A2.9)}$$

Then, by substitution we determine the function $G^{(i)}(r,\theta,z)$ as reported below:

$$G^{(i)}(r,\theta,z)=\left[g_0^{(i)}(r)+z\,g_1^{(i)}(r)+z^2\,g_2^{(i)}(r)+z^3\,g_3^{(i)}(r)+z^4\,g_4^{(i)}(r)\right]\cos\theta \qquad \text{(A2.10)}$$

By substitution of equation (A2.10) in relationships (4.7) and (2.1)-(2.2), we obtain the following conditions:

$$\sigma_{rr,zz}^{(i)}=0 \;\Rightarrow\; \begin{cases} g_4^{(i)}(r)-r\,g_{4,r}^{(i)}(r)=0 \\ g_3^{(i)}(r)-r\,g_{3,r}^{(i)}(r)=0 \end{cases} \Rightarrow \begin{cases} g_4^{(i)}(r)=C_1^{(i)}r \\ g_3^{(i)}(r)=C_2^{(i)}r \end{cases} \tag{A2.11}$$

where $C_1^{(i)}, C_2^{(i)}$ are integration constants. By means of functions in equation (A2.11) and the conditions (A2.2), we determine the differential equations involving functions $g_0^{(i)}(r), g_1^{(i)}(r)$:

$$\tau_{\theta z,z}^{(i)}=0 \quad \Rightarrow \begin{cases} -g_1^{(i)}+r\,g_{1,r}^{(i)}+r^2\,g_{1,rr}^{(i)}=2C_2^{(i)}r^3 \\ -2g_2^{(i)}+2r\,g_{2,r}^{(i)}+2r^2\,g_{2,rr}^{(i)}=4\left(6C_1^{(i)}-k\right)r^3 \end{cases} \tag{A2.12}$$

By integrating the differential equations (A2.12), we determine the functions $g_1^{(i)}(r), g_2^{(i)}(r)$:

$$\begin{cases} g_1^{(i)}(r)=C_3^{(i)}r+C_4^{(i)}r^{-1}+\left(C_2^{(i)}/4\right)r^3 \\ g_2^{(i)}(r)=C_5^{(i)}r^{-1}+C_6^{(i)}r+\left(6C_1^{(i)}-k^{(i)}\right)\left(r^3/4\right) \end{cases} \tag{A2.13}$$

where $C_3^{(i)}, C_4^{(i)}, C_5^{(i)}, C_6^{(i)}$ are integration constants.

By applying the conditions (4.11) on function $G^{(i)}(r,\theta,z)$:

$$\begin{aligned} &\nabla^2\nabla^2 G^{(i)}=f^{(i)}(r)=0 \quad \Rightarrow \\ &-3g_0^{(i)}+r\left\{3g_{0,r}^{(i)}+r\left[-3g_{0,rr}^{(i)}+r\left(2g_{0,rrr}^{(i)}+r\left(72C_1^{(i)}-8k^{(i)}r+g_{0,rrrr}^{(i)}\right)\right)\right]\right\}=0 \end{aligned} \tag{A2.14}$$

By solving the differential equation (A2.14), we obtain :

$$g_0^{(i)}(r)=\left(-9C_1^{(i)}+k^{(i)}\right)\left(r^5/24\right)+C_7^{(i)}r^{-1}+C_8^{(i)}r+C_9^{(i)}r^3+C_{10}^{(i)}r\log r \tag{A2.15}$$

where $C_7^{(i)}, C_8^{(i)}, C_9^{(i)}, C_{10}^{(i)}$ are integration constants. The constants $C_3^{(i)}, C_7^{(i)}$ are assumed here equal to zero since they characterize rigid body motion of the solid. Moreover, the constants $C_2^{(i)}, C_4^{(i)}$ vanish because the stress components $\sigma_{rr}^{(i)}, \sigma_{\theta\theta}^{(i)}, \sigma_{zz}^{(i)}, \tau_{r\theta}^{(i)}$ vary linearly respect to variable z and do not contain constant terms respect the same variable. Then the function $G^{(i)}(r,\theta,z)$ becomes:

$$\begin{aligned} G^{(i)}(r,\theta,z)=&\left[C_8^{(i)}+C_9^{(i)}r^2+\left(k-9C_1^{(i)}\right)\left(r^4/24\right)+C_{10}^{(i)}\log r+C_1^{(i)}z^4\right]r\cos\theta+ \\ &+\left[C_5^{(i)}+C_6^{(i)}r^{-2}+\left(6C_1^{(i)}-k\right)\left(r^2/2\right)\right]r\,z^2\cos\theta; \end{aligned} \tag{A2.16}$$

The integration constants are now renamed by means of following relationships:

$$\begin{aligned} &C_1^{(i)}=\left(V_3^{(i)}-6V_2^{(i)}\right)/6,\; C_5^{(i)}=-V_5^{(i)}/2,\; C_6^{(i)}=-V_4^{(i)}/4,\; C_8^{(i)}=-\left(V_4^{(i)}+4V_7^{(i)}\right)/8, \\ &C_9^{(i)}=\left(V_5^{(i)}+2V_6^{(i)}\right)/8,\; C_{10}^{(i)}=V_4^{(i)}/4+V_7^{(i)},\; k^{(i)}=\left[2\mu^{(i)}\left(2V_3^{(i)}-9V_2^{(i)}\right)\right]/\Omega^{(i)}, \end{aligned} \tag{A2.17}$$

Finally, by substituting relationships (A2.17) in equation (A2.16), we obtain the explicit expression of the function $G^{(i)}(r,\theta,z)$ reported in equation (4.45).

CHAPTER XI
MULTILAYERED CYLINDER CONSTITUTED BY TRASVERSALLY-ISOTROPIC PHASES SUBJECTED TO AXIAL FORCE AND PURE TORSION

11.1 Introduction

Object of the present chapter is to derive an homogenized theory from the micromechanical analysis of a composite solid cylinder made by a central core and *n* hollow phases, under the assumption of linear elastic behavior and perfect bond at the interfaces.
To make this, we first obtain the analytical elastic solutions for multilayered cylinder constituted by transversally-isotropic n-phase, under some prescribed load conditions. In particular those load related to radial pressure, axial force and torque. Then, by utilizing the homogenization theory, we obtain the overall elastic stiffness of the equivalent homogeneous transversally-isotropic solid, establishing the constitutive elastic laws relating stresses and strains.

11.2. General theory for torsion strains in composite transversally-isotropic cylinders

11.2.1 Solution of the field equations for the i-th phase of multilayered cylinder

In the present section, let us first investigate the problem the torsion. We consider an elastic body constituted by transversally-isotropic n-phase, are quite unlike each other, bounded by one cylindrical surfaces. The solid is stresses by the twisting moments $\mathcal{M}_0$ and $\mathcal{M}_L$ act on the ends. In addition, stresses τ_0 directed tangent to the contours of the cross sections (that is, parallel), and not varying along there contours are distributed on the lateral surface.
Let us choose the axis of a transversally-isotropic body of revolution with planes of anisotropy perpendicular to it as the z-axis of cylindrical coordinate system; the polar x-axis is directed arbitrarily. We shall denote the components of the body forces per unit volume by R and Z, and the superscript (i) is referred to the single phase of the solid. The equations of the generalized Hooke's law are written in the same way as in Cartesian coordinates for *i*-th phase:

$$\begin{aligned}
&\varepsilon_{rr}^{(i)} = a_{11}^{(i)}\sigma_{rr}^{(i)} + a_{12}^{(i)}\sigma_{\theta\theta}^{(i)} + a_{13}^{(i)}\sigma_{zz}^{(i)}, \quad \varepsilon_{\theta\theta}^{(i)} = a_{12}^{(i)}\sigma_{rr}^{(i)} + a_{11}^{(i)}\sigma_{\theta\theta}^{(i)} + a_{13}^{(i)}\sigma_{zz}^{(i)} \\
&\varepsilon_{zz}^{(i)} = a_{13}^{(i)}\sigma_{rr}^{(i)} + a_{13}^{(i)}\sigma_{\theta\theta}^{(i)} + a_{33}^{(i)}\sigma_{zz}^{(i)}, \quad \varepsilon_{\theta z}^{(i)} = \left(a_{44}^{(i)}/2\right)\tau_{\theta z}^{(i)} \\
&\varepsilon_{rz}^{(i)} = \left(a_{44}^{(i)}/2\right)\tau_{rz}^{(i)}, \quad \varepsilon_{r\theta}^{(i)} = \left(a_{11}^{(i)} - a_{12}^{(i)}\right)\tau_{r\theta}^{(i)}
\end{aligned} \tag{11.2.1}$$

According to P. Bekhterev, the constants $a_{jk}^{(i)}$ are called the coefficients of deformation. Expressing the coefficients of deformation by means of the "technical constants", we have:

$$\begin{aligned}
&a_{11}^{(i)} = 1/E^{(i)}, \quad a_{12}^{(i)} = -\nu^{(i)}/E^{(i)}, \quad a_{33}^{(i)} = -1/E_z^{(i)}, \\
&a_{13}^{(i)} = -\nu_z^{(i)}/E_z^{(i)}, \quad a_{44}^{(i)} = 1/G_z^{(i)}, \quad a_{11}^{(i)} - a_{12}^{(i)} = \left(1+\nu^{(i)}\right)/E^{(i)} = 1/\left(2G^{(i)}\right),
\end{aligned} \tag{11.2.2}$$

where $E^{(i)}$, $E_z^{(i)}$ are Young's moduli for the tension-compression in the direction perpendicular to the plane of isotropy, $\nu^{(i)}$ is the Poisson coefficient which corresponds to tension in the plane of isotropy and which characterizes the transverse compression in this plane, $\nu_z^{(i)}$ is the Poisson coefficient which characterizes the transverse compression in the plane of isotropy for tension in direction perpendicular to it, and $G^{(i)}$, $G_z^{(i)}$ are the shear moduli for the planes of isotropy and for the perpendicular planes in the radial directions. In this case, as in the case of an isotropic body, let us assume that the cross sections are not twisted, and the displacements in the radial and axial directions are absent, that is :

$$u_r^{(i)} = 0, \quad u_\theta^{(i)} = u_\theta^{(i)}(r,z), \quad u_z^{(i)} = 0, \tag{11.2.3}$$

Then,

$$\varepsilon_{rr}^{(i)} = \varepsilon_{\theta\theta}^{(i)} = \varepsilon_{zz}^{(i)} = \varepsilon_{rz}^{(i)} = 0, \quad \varepsilon_{\theta z}^{(i)} = \frac{1}{2}u_{\theta,z}^{(i)}, \quad \varepsilon_{r\theta}^{(i)} = \frac{1}{2}\left(u_{\theta,r}^{(i)} - r^{-1}u_\theta^{(i)}\right), \tag{11.2.4}$$

And from equations (11.2.1), it follows that $\sigma_{rr}^{(i)}=\sigma_{\theta\theta}^{(i)}=\sigma_{zz}^{(i)}=\tau_{rz}^{(i)}=0$. The remaining two components of stress $\tau_{\theta z}^{(i)}$ and $\tau_{r\theta}^{(i)}$ depend only on r and z and satisfy the equation of equilibrium:

$$\tau_{r\theta,r}^{(i)}+\tau_{\theta z,z}^{(i)}+2\,r^{-1}\tau_{r\theta}^{(i)}=0 \tag{11.2.5}$$

Eliminating $u_\theta^{(i)}$ from the expression for $\varepsilon_{\theta z}^{(i)}$ and $\varepsilon_{r\theta}^{(i)}$, we obtain:

$$\left(r^{-1}\varepsilon_{\theta z}^{(i)}\right)_{,r}-\left(r^{-1}\varepsilon_{r\theta}^{(i)}\right)_{,z}=0 \tag{11.2.6}$$

Or, on the basis of the last two equations of (2.1),

$$a_{44}^{(i)}\left(r^{-1}\tau_{\theta z}^{(i)}\right)_{,r}-2\left(a_{11}^{(i)}-a_{12}^{(i)}\right)\left(r^{-1}\tau_{r\theta}^{(i)}\right)_{,z}=0 \tag{11.2.7}$$

We can satisfy the equation of equilibrium (11.2.5) by introducing the stress function $\psi^{(i)}(r,z)$; we set

$$\tau_{\theta z}^{(i)}=r^{-2}\psi_{,r}^{(i)},\quad \tau_{r\theta}^{(i)}=-r^{-2}\psi_{,z}^{(i)}, \tag{11.2.8}$$

From (11.2.7), we obtain an equation satisfied by stress function $\psi^{(i)}(r,z)$:

$$a_{44}^{(i)}\psi_{,rr}^{(i)}-3a_{44}^{(i)}r^{-1}\psi_{,r}^{(i)}-2\left(a_{11}^{(i)}-a_{12}^{(i)}\right)\psi_{,zz}^{(i)}=0 \tag{11.2.9}$$

For an isotropic rod the stress function satisfies the equation :

$$\psi_{,rr}^{(i)}-3r^{-1}\psi_{,r}^{(i)}+\psi_{,zz}^{(i)}=0 \tag{11.2.10}$$

Let us consider the particular case when the solid is stresses by the twisting moments $\mathcal{M}_0$ and $\mathcal{M}_L$ act on the ends, and the load traction τ_0 is constant along z-direction. With this admission, we can to hypothesize that the function $\tau_{r\theta}^{(i)}$ depend only of the variable r. Hence, from (11.2.8) , to follow, that :

$$\psi_{,zz}^{(i)}=0\quad\Rightarrow\quad\psi^{(i)}\left(r,z\right)=p_0^{(i)}(r)+z\,p_1^{(i)}(r) \tag{11.2.11}$$

The equation (11.2.9) becomes :

$$p_{0,rr}^{(i)}-3r^{-1}p_{0,r}^{(i)}+z\left[\,p_{1,rr}^{(i)}-3r^{-1}p_{1,r}^{(i)}\right]=0 \tag{11.2.11}$$

By applying the polynomial identity law respect to variable z, we must to solve two uncouple differential equation into unknown function $p_0^{(i)}(r),p_1^{(i)}(r)$:

$$p_{j,rr}^{(i)}-3r^{-1}p_{j,r}^{(i)}=0\quad(j=0,1) \tag{11.2.12}$$

Solving the (11.2.12), we obtained the expression of the stress function $\psi^{(i)}(r)$:

$$\psi^{(i)}(r,z)=\left(C_1^{(i)}r^4+C_2^{(i)}\right)z+C_3^{(i)}r^4+C_4^{(i)} \tag{11.2.13}$$

From (11.2.8), we can to obtain the expression of the stress components:

$$\begin{aligned}\tau_{\theta z}^{(i)}&=4r\left(C_3^{(i)}+C_1^{(i)}z\right)\\ \tau_{r\theta}^{(i)}&=-\left(C_1^{(i)}r^2+C_2^{(i)}r^{-2}\right)\end{aligned} \tag{11.2.14}$$

The strain components are:

$$\begin{aligned}\varepsilon_{\theta z}^{(i)}&=2a_{44}^{(i)}\left(C_3^{(i)}+C_1^{(i)}z\right)r\\ \varepsilon_{r\theta}^{(i)}&=-\left(a_{11}^{(i)}-a_{12}^{(i)}\right)\left(C_1^{(i)}r^2+C_2^{(i)}r^{-2}\right)\end{aligned} \tag{2.15}$$

The displacement component $u_\theta^{(i)}$ can to obtain by solving the follows differential equation system:

$$\begin{cases}\left(r^{-1}u_\theta^{(i)}\right)_{,r}=-2\left(a_{11}^{(i)}-a_{12}^{(i)}\right)\left(C_1^{(i)}r+C_2^{(i)}r^{-3}\right)\\ \left(r^{-1}u_\theta^{(i)}\right)_{,z}=4a_{44}^{(i)}\left(C_3^{(i)}+C_1^{(i)}z\right)\end{cases} \tag{11.2.16}$$

Integrating the (11.2.16), we obtain the displacement vector solution of the field equations for the i-th phase of multilayered cylinder:

$$u_\theta^{(i)}=4a_{44}^{(i)}r\left[C_3^{(i)}z+(1/2)C_1^{(i)}z^2\right]-\left(a_{11}^{(i)}-a_{12}^{(i)}\right)\left(C_1^{(i)}r^3-C_2^{(i)}r^{-1}\right)+C_5^{(i)}r \tag{11.2.17}$$

where, due to presence of diverging terms for vanishing r, $r=0$, we assume (11.2.14) and (11.2.17) to hold only for the i-th hollow phases. Instead, by excluding terms affected by r^{-1}, for the cylindrical core phase we can write down

$$u_\theta^{(0)}(r,z)=4a_{44}^{(0)}r\left[C_3^{(0)}z+(1/2)C_1^{(0)}z^2\right]-\left(a_{11}^{(0)}-a_{12}^{(0)}\right)C_1^{(0)}r^3,\ C_2^{(0)}=0,\quad C_5^{(0)}=0, \tag{11.2.18}$$

where the superscript "(0)" stands for the *core*-phase. ($C_5^{(0)}=0$). Written the elastic solution for the generic i-th phase in Cartesian coordinate, the field displacement is shown below :

$$\begin{aligned}
u_x^{(i)}&=y\left\{\left(a_{11}^{(i)}-a_{12}^{(i)}\right)\left[C_1^{(i)}\left(x^2-y^2\right)-\frac{C_2^{(i)}\left(1-\delta_{0i}\right)}{x^2+y^2}\right]-2a_{44}^{(i)}z\left(2C_3^{(i)}+C_1^{(i)}z\right)-C_5^{(i)}\left(1-\delta_{0i}\right)\right\}\\
u_y^{(i)}&=-x\left\{\left(a_{11}^{(i)}-a_{12}^{(i)}\right)\left[C_1^{(i)}\left(x^2-y^2\right)-\frac{C_2^{(i)}\left(1-\delta_{0i}\right)}{x^2+y^2}\right]-2a_{44}^{(i)}z\left(2C_3^{(i)}+C_1^{(i)}z\right)-C_5^{(i)}\left(1-\delta_{0i}\right)\right\}\\
u_z^{(i)}&=0
\end{aligned} \tag{11.2.19}$$

where δ_{0i} is the usual Kronecker delta symbol. The stress component in Cartesian coordinate are:

$$\sigma_{xx}^{(i)}=-\sigma_{yy}^{(i)}=\left(y^2-x^2\right)\left[C_1^{(i)}-\frac{C_2^{(i)}\left(1-\delta_{0i}\right)}{\left(x^2+y^2\right)^2}\right],\quad \tau_{xy}^{(i)}=\left(y^2-x^2\right)\left[C_1^{(i)}+\frac{C_2^{(i)}\left(1-\delta_{0i}\right)}{\left(x^2+y^2\right)^2}\right], \tag{11.2.20}$$

$$\tau_{yz}^{(i)}=4x\left[C_3^{(i)}\left(1-\delta_{0i}\right)+C_1^{(i)}z\right],\quad \tau_{xz}^{(i)}=-4y\left[C_3^{(i)}\left(1-\delta_{0i}\right)+C_1^{(i)}z\right],\quad \sigma_{zz}^{(i)}=0,$$

Renamed the integration constants as follows, we rewritten the displacement field:

$$T_1^{(i)}=4a_{44}^{(i)}C_3^{(i)},\quad T_2^{(i)}=2a_{44}^{(i)}C_1^{(i)},\quad T_3^{(i)}=\left(a_{11}^{(i)}-a_{12}^{(i)}\right)C_2^{(i)},\quad T_4^{(i)}=C_5^{(i)}, \tag{11.2.21}$$

The displacement vector solution for the i-th phase of multilayered cylinder becomes:

$$u_\theta^{(i)}=\left(T_1^{(i)}+T_2^{(i)}z\right)r\,z-\frac{\left(a_{11}^{(i)}-a_{12}^{(i)}\right)T_2^{(i)}r^3}{2a_{44}^{(i)}}+\left(T_3^{(i)}r^{-1}+T_4^{(i)}r\right)\left(1-\delta_{0i}\right)\quad i\in\{0,1,...,n\} \tag{11.2.22}$$

The no-zero strain components are:

$$\varepsilon_{\theta z}^{(i)}=\left(\frac{T_1^{(i)}}{2}+T_2^{(i)}z\right)r,\quad \varepsilon_{r\theta}^{(i)}=-\frac{\left(a_{11}^{(i)}-a_{12}^{(i)}\right)T_2^{(i)}r^2}{2a_{44}^{(i)}}-\left(1-\delta_{0i}\right)T_3^{(i)}r^{-2} \tag{11.2.23}$$

The no-zero stress components becomes:

$$\tau_{\theta z}^{(i)}=\frac{r}{a_{44}^{(i)}}\left(T_1^{(i)}+2T_2^{(i)}z\right),\quad \tau_{r\theta}^{(i)}=-\frac{T_2^{(i)}r^2}{2a_{44}^{(i)}}-\frac{\left(1-\delta_{0i}\right)T_3^{(i)}r^{-2}}{a_{11}^{(i)}-a_{12}^{(i)}}, \tag{11.2.24}$$

11.2.2. Equilibrium and compatibility conditions

The results obtained until now satisfy the equilibrium and compatibility equations inside each generic i-th phase of a composite circular cylinder subjected to torsion strains. Under both the hypothesis of linear and transversally-isotropic elastic behavior of the materials and the assumption of perfect contact at the cylindrical interfacial boundaries (no de-lamination or friction phenomena), we have now to establish the satisfaction of both the equilibrium and the compatibility equations at the boundary surfaces between two generic adjacent phases. To obtain this, we will make first reference to the generic case in which an assembled functionally graded circular cylinder is constituted by a central *core* and n arbitrary *cladding* phases (Fig. 11.1).

The total unknown parameters to determine can be summarized as follows:

$$\begin{aligned}
&T_1^{(0)},T_2^{(0)}\\
&T_1^{(i)},T_2^{(i)},T_3^{(i)},T_4^{(i)}\quad i\in\{1,2,.....n\}\\
&\tau_0
\end{aligned} \tag{11.2.21}$$

where those in $(11.2.21)_1$ represent the unknown coefficients of the *core*, those in $(11.2.21)_2$ represent the unknown parameters for every circular hollow cylinder, $(11.2.21)_3$ represents load

parameter defining the traction field on $\partial\Omega^{cyl}$. Hence, the total number of unknowns will be $(4n+3)$, which equals the number of algebraic equations to solve. In particular, as we will show in the follows, the boundary equations at the interfaces is $4n$, while 1 is the number of boundary conditions on the external cylindrical surface and one the end basis, respectively. In particular, we begin writing the 4*n* equilibrium and compatibility equations at the interfaces, that is:

$$\begin{cases} u_\theta^{(i)}(r=R^{(i)}) = u_\theta^{(i+1)}(r=R^{(i)}) \\ \tau_{r\theta}^{(i)}(r=R^{(i)}) = \tau_{r\theta}^{(i+1)}(r=R^{(i)}) \end{cases} \qquad i \in \{0,1,...,n-1\} \tag{11.2.22}$$

where $R^{(i)}$ is the outer radius of the *i*-th phase. Recalling the previously obtained results, the system (11.2.22) can be expressed as follows:

$$\begin{cases} \left(\dfrac{a_{11}^{(i+1)} - a_{12}^{(i+1)}}{2a_{44}^{(i+1)}} T_2^{(i+1)} - \dfrac{a_{11}^{(i)} - a_{12}^{(i)}}{2a_{44}^{(i)}} T_2^{(i)} \right) R^{(i)3} + \left[\dfrac{T_3^{(i)} - T_3^{(i+1)}}{R^{(i)}} + \left(T_4^{(i)} - T_4^{(i+1)} \right) R^{(i)} \right] (1-\delta_{0i}) = 0 \\ R^{(i)} \left(T_1^{(i)} - T_1^{(i+1)} \right) = 0 \\ R^{(i)} \left(T_2^{(i)} - T_2^{(i+1)} \right) = 0 \\ \dfrac{\left(a_{11}^{(i+1)} - a_{12}^{(i+1)} \right) T_2^{(i+1)} R^{(i+1)4} + 2a_{44}^{(i+1)} T_3^{(i+1)} (1-\delta_{0i})}{2\left(a_{11}^{(i+1)} - a_{12}^{(i+1)} \right) a_{44}^{(i+1)} R^{(i)2}} - \dfrac{\left(a_{11}^{(i)} - a_{12}^{(i)} \right) T_2^{(i)} R^{(i)4} + 2a_{44}^{(i)} T_3^{(i)} (1-\delta_{0i})}{2\left(a_{11}^{(i)} - a_{12}^{(i)} \right) a_{44}^{(i)} R^{(i)2}} = 0 \end{cases} \tag{11.2.23}$$

$$\forall i \in \{0,1,...,n-1\}$$

It is worth to note that the initial two equations (11.2.22) become four in (11.2.23): this happens because, by invoking the polynomial identity law and then collecting the terms in the powers of z, some solutions are immediately obtained, and only four independent equations (11.2.23) remain to satisfy. The Cauchy equilibrium equation on the external cylindrical boundary surface, $(i=n)$, give:

$$\tau_{rz}^{(n)}(r=R^{(n)}) = \tau_0 \tag{11.2.24}$$

This equations in explicit become:

$$\frac{\left(a_{11}^{(n)} - a_{12}^{(n)} \right) T_2^{(n)} R^{(n)4} + 2a_{44}^{(n)} T_3^{(n)}}{2\left(a_{11}^{(n)} - a_{12}^{(n)} \right) a_{44}^{(n)} R^{(n)2}} + \tau_0 = 0 \tag{11.2.25}$$

where τ_0 represents mechanical load parameter defining the traction field on $\partial\Omega^{cyl}$. Finally, it remains to consider the equilibrium equation to rotation about to x-direction on two basis for $z=0$ and for $z=L$. Therefore, this two equations are:

$$\begin{cases} \sum_{i=0}^{n} \int_0^{2\pi} \int_{\delta_{0i} R^{(i-1)}}^{R^{(i)}} \tau_{\theta z}^{(i)}(z=0)\, r^2 dr d\theta = -\mathcal{M}_z \\ \sum_{i=0}^{n} \int_0^{2\pi} \int_{\delta_{0i} R^{(i-1)}}^{R^{(i)}} \tau_{\theta z}^{(i)}(z=L)\, r^2 dr d\theta = \mathcal{M}_z \end{cases} \tag{11.2.26}$$

where $\mathcal{M}_z$ is the total couple torque applied on each base of the solid. The equations (11.2.26) in explicit becomes:

$$\begin{cases} \sum_{i=0}^{n} \dfrac{T_1^{(i)} \pi}{2a_{44}^{(i)}} \left[R^{(i)4} - (1-\delta_{0i}) R^{(i-1)4} \right] = -\mathcal{M}_z \\ \sum_{i=0}^{n} \dfrac{\left(T_1^{(i)} + 2T_2^{(i)} L \right) \pi}{2a_{44}^{(i)}} \left[R^{(i)4} - (1-\delta_{0i}) R^{(i-1)4} \right] = \mathcal{M}_z \end{cases} \tag{11.2.27}$$

However, from (11.2.23) to note that $T_1^{(0)} = T_1^{(i)}$, $T_2^{(0)} = T_2^{(i)}$, $\forall i \in \{1,2,...,n\}$, consequently we can to reduce the unknown parameters number to determine to $(2n+3)$. Them are following :

$$\begin{aligned} &T_1^{(0)}, T_2^{(0)}, \tau_0, \\ &T_3^{(i)}, T_4^{(i)} \quad i \in \{1,2,.....n\} \end{aligned} \tag{11.2.28}$$

The system (11.2.23) become :

$$\begin{cases} \left(\dfrac{a_{11}^{(i+1)} - a_{12}^{(i+1)}}{2a_{44}^{(i+1)}} - \dfrac{a_{11}^{(i)} - a_{12}^{(i)}}{2a_{44}^{(i)}} \right) T_2^{(0)} R^{(i)3} + \left[\dfrac{T_3^{(i)} - T_3^{(i+1)}}{R^{(i)}} + \left(T_4^{(i)} - T_4^{(i+1)} \right) R^{(i)} \right] \left(1 - \delta_{0i} \right) = 0 \\ \dfrac{\left(a_{11}^{(i+1)} - a_{12}^{(i+1)} \right) T_2^{(0)} R^{(i+1)4} + 2a_{44}^{(i+1)} T_3^{(i+1)} \left(1 - \delta_{0i} \right)}{2\left(a_{11}^{(i+1)} - a_{12}^{(i+1)} \right) a_{44}^{(i+1)} R^{(i)2}} - \dfrac{\left(a_{11}^{(i)} - a_{12}^{(i)} \right) T_2^{(0)} R^{(i)4} + 2a_{44}^{(i)} T_3^{(i)} \left(1 - \delta_{0i} \right)}{2\left(a_{11}^{(i)} - a_{12}^{(i)} \right) a_{44}^{(i)} R^{(i)2}} = 0 \end{cases} \tag{11.2.29}$$

$$\forall i \in \{0,1,...,n-1\}$$

We can write the (11.2.27) as follows:

$$\begin{cases} \dfrac{T_1^{(0)} \pi}{2} \displaystyle\sum_{i=0}^{n} \left[\frac{R^{(i)4} - \left(1 - \delta_{0i} \right) R^{(i-1)4}}{a_{44}^{(i)}} \right] = \mathfrak{M}_z \\ \dfrac{\left(T_1^{(0)} + 2T_2^{(0)} L \right) \pi}{2} \displaystyle\sum_{i=0}^{n} \left[\frac{R^{(i)4} - \left(1 - \delta_{0i} \right) R^{(i-1)4}}{a_{44}^{(i)}} \right] = -\mathfrak{M}_z \end{cases} \tag{11.2.30}$$

The algebraic equations (11.2.30) in the unknown parameter $C_1^{(0)}, C_2^{(0)}$, are independent of the n phases number . Therefore, the solution of algebraic system (11.2.30) furnished:

$$T_1^{(0)} = -\frac{\mathfrak{M}_z}{\displaystyle\sum_{i=0}^{n} \frac{I_P^{(i)}}{a_{44}^{(i)}}}, \quad T_2^{(0)} = \frac{\mathfrak{M}_z}{L \displaystyle\sum_{i=0}^{n} \frac{I_P^{(i)}}{a_{44}^{(i)}}}, \tag{11.2.31}$$

where $I_P^{(i)} = \dfrac{\pi}{2}\left(R^{(i)4} - R^{(i-1)4} \right)$. To replace (11.2.31) in to $(11.2.29)_2$ we find expression of the constants $T_3^{(i)}$ that shown below:

$$T_3^{(i)} = \frac{T_2^{(0)} \left(a_{11}^{(i)} - a_{12}^{(i)} \right)}{2} \sum_{j=1}^{i} R^{(j-1)4} \left(\frac{1}{a_{44}^{j-1}} - \frac{1}{a_{44}^{j}} \right) = \frac{\mathfrak{M}_z \left(a_{11}^{(i)} - a_{12}^{(i)} \right)}{2L \displaystyle\sum_{k=0}^{n} \frac{I_P^{(k)}}{a_{44}^{(k)}}} \sum_{j=1}^{i} R^{(j-1)4} \left(\frac{1}{a_{44}^{j-1}} - \frac{1}{a_{44}^{j}} \right) \tag{11.2.32}$$

$$\forall i \in \{1,2,...n\}$$

By invoking the (11.2.32) and substitute them in to (11.2.25), we obtained the constant τ_0:

$$\tau_0 = -\frac{\mathfrak{M}_z}{\pi L R^{(n)2}} \tag{11.2.33}$$

It is worth to note that (11.2.33) derive too, from condition of the global equilibrium between uniform tractions τ_0 and the torque couples on basis. Substitute (11.2.32) in to $(11.2.29)_1$ we find expression of the constants $T_4^{(i)}$ as follows:

$$T_4^{(i)} = \frac{T_2^{(0)}}{2} \sum_{j=1}^{i} \left(\frac{a_{11}^{(j-1)} - a_{12}^{(j-1)}}{a_{44}^{(j-1)}} - \frac{a_{11}^{(j)} - a_{12}^{(j)}}{a_{44}^{(j)}} \right) + \sum_{j=1}^{i} T_3^{(j)} \left[\frac{\left(1 - \delta_{ij} \right)}{R^{(j)2}} - \frac{1}{R^{(j-1)2}} \right], \quad \forall i \in \{1,2,...n\} \tag{11.2.34}$$

Substituting the (11.2.31) and (11.2.32) into (11.2.34), we obtain :

$$T_4^{(i)} = \frac{\mathfrak{M}_z}{2L \displaystyle\sum_{t=0}^{n} \frac{I_P^{(t)}}{a_{44}^{(t)}}} \left\{ \begin{aligned} &\sum_{j=1}^{i} \left(\frac{a_{11}^{(j-1)} - a_{12}^{(j-1)}}{a_{44}^{(j-1)}} - \frac{a_{11}^{(j)} - a_{12}^{(j)}}{a_{44}^{(j)}} \right) + \\ &+ \sum_{j=1}^{i} \left(\frac{1 - \delta_{ij}}{R^{(j)2}} - \frac{1}{R^{(j-1)2}} \right) \left(a_{11}^{(j)} - a_{12}^{(j)} \right) \sum_{k=1}^{j} R^{(k-1)4} \left(\frac{1}{a_{44}^{k-1}} - \frac{1}{a_{44}^{k}} \right) \end{aligned} \right\} \tag{11.2.35}$$

$$\forall i \in \{1,2,...n\}$$

11.2.3 Elastic solution for multilayered cylinder subjected to pure torsion

In this case the equation no-change are (11.2.29), but equations (11.2.25) and (11.2.30) becomes respectively:

$$\left(a_{11}^{(n)}-a_{12}^{(n)}\right)T_2^{(n)}R^{(n)4}+2a_{44}^{(n)}T_3^{(n)}=0 \tag{11.2.36}$$

$$\begin{cases}\dfrac{T_1^{(0)}\pi}{2}\displaystyle\sum_{i=0}^{n}\left[\frac{R^{(i)4}-\left(1-\delta_{0i}\right)R^{(i-1)4}}{a_{44}^{(i)}}\right]=\mathfrak{M}_z\\ \dfrac{\left(T_1^{(0)}+2T_2^{(0)}L\right)\pi}{2}\displaystyle\sum_{i=0}^{n}\left[\frac{R^{(i)4}-\left(1-\delta_{0i}\right)R^{(i-1)4}}{a_{44}^{(i)}}\right]=\mathfrak{M}_z\end{cases} \tag{11.2.37}$$

By equation (11.2.37), we obtain:

$$T_1^{(0)}=\mathfrak{M}_z\Big/\sum_{i=0}^{n}\frac{I_P^{(i)}}{a_{44}^{(i)}},\quad T_2^{(0)}=0, \tag{11.2.38}$$

From the (11.2.38), substituting $T_2^{(0)}=0$ in to equations (11.2.29), we obtain :

$$T_3^{(i)}=0,\quad T_4^{(i)}=0, \tag{11.2.39}$$

The displacement solution is :

$$u_\theta^{(i)}=\frac{\mathfrak{M}_z\, r\, z}{\displaystyle\sum_{i=0}^{n}\frac{I_P^{(i)}}{a_{44}^{(i)}}}\quad i\in\{0,1,...,n\} \tag{11.2.40}$$

The only no-zero strain component is $\varepsilon_{\theta z}^{(i)}$:

$$\varepsilon_{\theta z}^{(i)}=\frac{\mathfrak{M}_z\, r}{2\displaystyle\sum_{i=0}^{n}\frac{I_P^{(i)}}{a_{44}^{(i)}}}, \tag{11.2.41}$$

The only no-zero stress component becomes:

$$\tau_{\theta z}^{(i)}=\frac{\mathfrak{M}_z\, r}{a_{44}^{(i)}\displaystyle\sum_{i=0}^{n}\frac{I_P^{(i)}}{a_{44}^{(i)}}}, \tag{11.2.42}$$

11.3. General theory for axis-symmetrical strains in composite transversally-isotropic cylinders

11.3.1. Solution of the field equations for the i-th phase of multilayered cylinder

The problem of finding exact elastic solutions for multi-phase circular cylinders under axis-symmetrical stress states covers many significant mechanical and structural fields. When a solid cylinder constituted by several linearly elastic and transversally-isotropic phases is strained symmetrically by forces applied on both its external cylindrical surface and its ends, it is possible to express all the mechanical quantities in terms of a single function, reducing the equilibrium equations of the body to a single partial differential equation. Let us consider an elastic body constituted by transversally-isotropic n-phase bounded by one cylindrical surfaces in equilibrium under the influence of surface and body forces possessing rotational symmetry. An isotropic body, under deformation, remains a body of revolution, and its deformation will be axially-symmetric. If, however, a body is made from anisotropic material, the above situation occurs only for certain special cases. We shall study the question of symmetric deformation only case where the material is transversally- isotropic. Let us choose the axis of a transversally-isotropic body of revolution with planes of anisotropy perpendicular to it as the z-axis of cylindrical coordinate system; the polar x-axis is directed arbitrarily. We shall denote the components of the body forces per unit volume by R and Z, and the superscript (i) is referred to the single phase of the solid. The equations of the generalized Hooke's law are written in the same way as in Cartesian coordinates for *i*-th phase as

the relationship (11.2.1). In this case, it is natural to assume that the radial sections remain planar, and the body remains a body of revolution in the deformed state, that is,

$$u_r^{(i)} = u_r^{(i)}(r,z), \quad u_\theta^{(i)} = 0, \quad u_z^{(i)} = u_z^{(i)}(r,z), \tag{11.3.1}$$

Hence, it follows that $\varepsilon_{\theta z}^{(i)} = \varepsilon_{rz}^{(i)} = 0$ and $\tau_{\theta z}^{(i)} = \tau_{rz}^{(i)} = 0$. The remaining components of deformation and stresses will not depended on θ; moreover,

$$\varepsilon_{rr}^{(i)} = u_{r,r}^{(i)}, \quad \varepsilon_{\theta\theta}^{(i)} = r^{-1}u_r^{(i)}, \quad \varepsilon_{zz}^{(i)} = u_{z,z}^{(i)}, \quad \varepsilon_{rz}^{(i)} = (1/2)\left(u_{r,z}^{(i)} + u_{z,r}^{(i)}\right), \tag{11.3.2}$$

The four components of stresses which are not equal zero satisfy the equations of equilibrium:

$$\begin{cases} \sigma_{rr,r}^{(i)} + \tau_{rz,z}^{(i)} + r^{-1}\left(\sigma_{rr}^{(i)} - \sigma_{\theta\theta}^{(i)}\right) + R = 0 \\ \tau_{rz,r}^{(i)} + r^{-1}\tau_{rz}^{(i)} + \sigma_{zz,z}^{(i)} + Z = 0 \end{cases} \tag{11.3.3}$$

where the comma denotes the differentiation, the superscript (i) is referred to the single phase. Let us consider the case when body forces are absent, that is, where $R = Z = 0$. It is possible to satisfy the first equations of equilibrium (11.3.4) (for $R = 0$) by introducing a function $\varphi^{(i)}(r,z)$ in expression of the displacement components (11.3.2) for *i*-th phase. For transversally-isotropic body the displacement components will be connected with $\varphi^{(i)}(r,z)$ by the relationship:

$$\begin{cases} u_r^{(i)} = \Gamma_1^{(i)}\varphi_{,rz}^{(i)} \\ u_z^{(i)} = \Gamma_2^{(i)}\varphi_{,zz}^{(i)} + \Gamma_3^{(i)}\left(\varphi_{,rr}^{(i)} + r^{-1}\varphi_{,r}^{(i)}\right) \end{cases} \tag{11.3.5}$$

where the constants $\Gamma_1^{(i)}, \Gamma_2^{(i)}, \Gamma_3^{(i)}$ are:

$$\Gamma_1^{(i)} = \Gamma_2^{(i)} - \frac{a_{33}^{(i)}\left(a_{11}^{(i)} + a_{12}^{(i)}\right)\left(a_{11}^{(i)} - a_{12}^{(i)}\right)}{a_{11}^{(i)}a_{33}^{(i)} - a_{13}^{(i)2}}, \quad \Gamma_2^{(i)} = \frac{\left(a_{11}^{(i)} - a_{12}^{(i)}\right)\left[2a_{13}^{(i)2} - a_{33}^{(i)}\left(a_{11}^{(i)} + a_{12}^{(i)}\right)\right]}{a_{11}^{(i)}a_{33}^{(i)} - a_{13}^{(i)2}}, \quad \Gamma_3^{(i)} = a_{44}^{(i)} \tag{11.3.6}$$

The relationships between the stresses components and function $\varphi^{(i)}(r,z)$ are:

$$\begin{aligned} &\sigma_{rr}^{(i)} = -\left(\varphi_{,rr}^{(i)} + b^{(i)}\, r^{-1}\varphi_{,r}^{(i)} + a^{(i)}\,\varphi_{,zz}^{(i)}\right)_{,z}, \quad \sigma_{\theta\theta}^{(i)} = -\left(b^{(i)}\,\varphi_{,rr}^{(i)} + r^{-1}\varphi_{,r}^{(i)} + a^{(i)}\,\varphi_{,zz}^{(i)}\right)_{,z} \\ &\sigma_{zz}^{(i)} = \left(c^{(i)}\,\varphi_{,rr}^{(i)} + c^{(i)}\, r^{-1}\varphi_{,r}^{(i)} + d^{(i)}\,\varphi_{,zz}^{(i)}\right)_{,z}, \ \tau_{rz}^{(i)} = \left(\varphi_{,rr}^{(i)} + r^{-1}\varphi_{,r}^{(i)} + a^{(i)}\,\varphi_{,zz}^{(i)}\right)_{,r} \end{aligned} \tag{11.3.7}$$

where the constants $a^{(i)}, b^{(i)}, c^{(i)}, d^{(i)}$ are:

$$\begin{aligned} a^{(i)} &= \frac{a_{13}^{(i)}\left(a_{11}^{(i)} - a_{12}^{(i)}\right)}{a_{11}^{(i)}a_{13}^{(i)} - a_{13}^{(i)2}}, \quad b^{(i)} = \frac{a_{13}^{(i)}\left(a_{13}^{(i)} + a_{44}^{(i)}\right) - a_{12}^{(i)}a_{33}^{(i)}}{a_{11}^{(i)}a_{13}^{(i)} - a_{13}^{(i)2}}, \\ c^{(i)} &= \frac{a_{13}^{(i)}\left(a_{11}^{(i)} - a_{12}^{(i)}\right) + a_{11}^{(i)}a_{44}^{(i)}}{a_{11}^{(i)}a_{13}^{(i)} - a_{13}^{(i)2}}, \quad d^{(i)} = \frac{a_{11}^{(i)2} - a_{12}^{(i)2}}{a_{11}^{(i)}a_{13}^{(i)} - a_{13}^{(i)2}}, \end{aligned} \tag{11.3.8}$$

From the second equation of equilibrium (11.3.4) (for $Z = 0$), we obtain the following equation for the stress function $\varphi^{(i)}(r,z)$:

$$\varphi_{,r}^{(i)} + r\left\{-\varphi_{,rr}^{(i)} + r\left[r\, d\,\varphi_{,zzzz}^{(i)} + (a+c)\left(\varphi_{,rrz}^{(i)} + r\varphi_{,rrzz}^{(i)}\right) + 2\varphi_{,rrr}^{(i)} + r\varphi_{,rrrr}^{(i)}\right]\right\} = 0 \tag{11.3.9}$$

Introducing the following notation:

$$\lambda_1^{(i)} = a^{(i)} + c^{(i)} + \sqrt{\left(a^{(i)} + c^{(i)}\right)^2 - 4d^{(i)}}, \quad \lambda_2^{(i)} = a^{(i)} + c^{(i)} - \sqrt{\left(a^{(i)} + c^{(i)}\right)^2 - 4d^{(i)}}, \tag{11.3.10}$$

and the operators $\nabla_j^2 = \partial/\partial r^2 + r^{-1}\,\partial/\partial r + \lambda_j\,\partial/\partial z^2$, $(j = 1,2)$.

It is possible to write (11.3.9) as follows:

$$\nabla_1^2\nabla_2^2\varphi^{(i)} = 0 \tag{11.3.11}$$

Since we can easily verify that $\nabla_1^2\nabla_2^2\varphi^{(i)} = \nabla_2^2\nabla_1^2\varphi^{(i)}$, the operators can be interchanged. It is possible to prove the following theorem concerning the number $\lambda_1^{(i)}, \lambda_2^{(i)}$ which depend on the

elastic constants in following way: " The number $\lambda_1^{(i)}, \lambda_2^{(i)}$ can be only real or complex, but cannot be purely imaginary. In the case of an isotropic body:

$$a^{(i)} = b^{(i)} = -\frac{\nu^{(i)}}{1-\nu^{(i)}}, \quad c^{(i)} = \frac{2-\nu^{(i)}}{1-\nu^{(i)}}, \quad d^{(i)} = 1, \quad a^{(i)} + c^{(i)} = 2, \quad \lambda_1^{(i)} = \lambda_2^{(i)} = 1, \tag{11.3.12}$$

By introducing the new function $\chi^{(i)} = \varphi^{(i)} \Big/ \left(1-\nu^{(i)}\right)$, we obtain the following known formulas for displacement components from (11.3.5)

$$u_r^{(i)} = -\frac{1+\nu^{(i)}}{E^{(i)}} \chi_{,rz}^{(i)}, \quad u_z^{(i)} = \frac{1+\nu^{(i)}}{E^{(i)}} \left[\left(1-2\nu^{(i)}\right) \nabla^2 \chi^{(i)} + \chi_{,rr}^{(i)} + r^{-1} \chi_{,r}^{(i)} \right] \tag{11.3.13}$$

where $\nabla^2 = \partial / \partial r^2 + r^{-1} \partial / \partial r + \partial / \partial z^2$,

The stresses component become from (11.3.7):

$$\begin{aligned} &\sigma_{rr}^{(i)} = (\nu^{(i)} \nabla^2 \chi^{(i)} - \chi_{,rr}^{(i)})_{,z}, \quad \sigma_{\theta\theta}^{(i)} = (\nu^{(i)} \nabla^2 \chi^{(i)} - r^{-1} \chi_{,r}^{(i)})_{,z}, \\ &\sigma_{zz}^{(i)} = [(2-\nu^{(i)}) \nabla^2 \chi^{(i)} - \chi_{,zz}^{(i)})]_{,z}, \quad \tau_{rz}^{(i)} = [(1-\nu^{(i)}) \nabla^2 \chi^{(i)} - \chi_{,zz}^{(i)})]_{,r}, \end{aligned} \tag{11.3.14}$$

The function $\chi^{(i)}$ satisfies the equation

$$\nabla^2 \nabla^2 \chi^{(i)} = \nabla^4 \chi^{(i)} = 0 . \tag{11.3.15}$$

that is, the function is bi-harmonic.

11.3.2. Elastic solution for the i-th phase of multilayered cylinder subjected to axial force and radial pressure

In this section we will obtain elastic solutions for multilayered cylinder subjected to axial force and radial pressure. In order to present an unified approach, we will begin for both classes of problems starting from a more large form of the function $\varphi^{(i)}$. We consider the constants $c_{jk}^{(i)}$ that are called the "moduli of elasticity". The constants $c_{jk}^{(i)}$ are connected with the coefficients of deformation $a_{jk}^{(i)}$, by means follows relationship:

$$\begin{aligned} &a_{11}^{(i)} = \frac{c_{11}^{(i)} c_{33}^{(i)} - c_{13}^{(i)2}}{\left(c_{11}^{(i)} - c_{12}^{(i)}\right) \left[\left(c_{11}^{(i)} + c_{12}^{(i)}\right) c_{33}^{(i)} - 2 c_{13}^{(i)2} \right]}, \quad a_{12}^{(i)} = \frac{c_{13}^{(i)2} - c_{12}^{(i)} c_{33}^{(i)}}{\left(c_{11}^{(i)} - c_{12}^{(i)}\right) \left[\left(c_{11}^{(i)} + c_{12}^{(i)}\right) c_{33}^{(i)} - 2 c_{13}^{(i)2} \right]}, \\ &a_{13}^{(i)} = \frac{c_{13}^{(i)}}{2 c_{13}^{(i)2} - \left(c_{11}^{(i)} + c_{12}^{(i)}\right) c_{33}^{(i)}}, \quad a_{33}^{(i)} = \frac{c_{11}^{(i)} + c_{12}^{(i)}}{\left(c_{11}^{(i)} + c_{12}^{(i)}\right) c_{33}^{(i)} - 2 c_{13}^{(i)2}}, \quad a_{44}^{(i)} = \frac{1}{c_{44}^{(i)}}, \end{aligned} \tag{11.3.16}$$

Let us consider the elastic equilibrium of a transversally-isotropic body in the form of a cylinder solid or hollow circular cylinder loaded by axial force or radial pressure. We shall take the centre of any section as the origin of coordinates; the z-axis is directed along the axis of the cylinder.

By equations (11.3.7), let us that the tensor stress no-dependent by z variable. Then, we can write:

$$\begin{cases} \left(\varphi_{,rr}^{(i)} + b^{(i)} r^{-1} \varphi_{,r}^{(i)} + a^{(i)} \varphi_{,zz}^{(i)} \right)_{,zz} = 0 \\ \left(b^{(i)} \varphi_{,rr}^{(i)} + r^{-1} \varphi_{,r}^{(i)} + a^{(i)} \varphi_{,zz}^{(i)} \right)_{,zz} = 0 \\ \left(c^{(i)} \varphi_{,rr}^{(i)} + c^{(i)} r^{-1} \varphi_{,r}^{(i)} + d^{(i)} \varphi_{,zz}^{(i)} \right)_{,zz} = 0 \end{cases} \Rightarrow \quad \begin{bmatrix} 1 & b^{(i)} r^{-1} & a^{(i)} \\ b^{(i)} & r^{-1} & a^{(i)} \\ c^{(i)} & c^{(i)} r^{-1} & d^{(i)} \end{bmatrix} \cdot \begin{bmatrix} \varphi_{,rrzz}^{(i)} \\ \varphi_{,rzz}^{(i)} \\ \varphi_{,zzzz}^{(i)} \end{bmatrix} = \begin{bmatrix} 0 \\ 0 \\ 0 \end{bmatrix} \tag{11.3.17}$$

The determinant of matrix of the coefficient is:

$$\det \begin{bmatrix} 1 & b^{(i)} r^{-1} & a^{(i)} \\ b^{(i)} & r^{-1} & a^{(i)} \\ c^{(i)} & c^{(i)} r^{-1} & d^{(i)} \end{bmatrix} = \frac{\left(c_{11}^{(i)} - c_{12}^{(i)}\right) \left[c_{33}^{(i)} \left(c_{11}^{(i)} + c_{12}^{(i)}\right) - 2 c_{13}^2 \right] \left(c_{13}^{(i)} + c_{44}^{(i)}\right)^2}{c_{11}^{(i)3} c_{44}^{(i)2} r} \neq 0 \tag{11.3.18}$$

The determinant (3.18) is not negative because $c_{11}^{(i)} - c_{12}^{(i)} > 0, \quad c_{33}^{(i)} \left(c_{11}^{(i)} + c_{12}^{(i)}\right) - 2 c_{13}^2 > 0$. In fact the determinant of the elastic constant matrix $c_{jk}^{(i)}$ must to be greater to zero. It is equal to:

$$\det\left[c_{jk}^{(i)}\right]=4\left(c_{11}^{(i)}-c_{12}^{(i)}\right)^2\left[c_{33}^{(i)}\left(c_{11}^{(i)}+c_{12}^{(i)}\right)-2c_{13}^2\right]c_{44}^2>0 \quad\Rightarrow\quad c_{33}^{(i)}\left(c_{11}^{(i)}+c_{12}^{(i)}\right)-2c_{13}^2>0 \tag{11.3.19}$$

Moreover the determinant of the sub-matrix $\begin{bmatrix} c_{11}^{(i)} & c_{12}^{(i)} \\ c_{12}^{(i)} & c_{11}^{(i)} \end{bmatrix}$ must to be grater to zero:

$$\det\begin{bmatrix} c_{11}^{(i)} & c_{12}^{(i)} \\ c_{12}^{(i)} & c_{11}^{(i)} \end{bmatrix}>0 \quad\Rightarrow\quad c_{11}^{(i)2}-c_{12}^{(i)2}>0 \quad\Rightarrow\quad \begin{cases} c_{11}^{(i)}-c_{12}^{(i)}>0 \\ c_{11}^{(i)}+c_{12}^{(i)}>0 \end{cases} \tag{11.3.20}$$

From (3.18), we obtain the following differential equation system:

$$\begin{cases} \varphi_{,rrzz}^{(i)}=0 \\ \varphi_{,rzz}^{(i)}=0 \\ \varphi_{,zzzz}^{(i)}=0 \end{cases} \quad\Rightarrow\quad \varphi^{(i)}(r,z)=p^{(i)}(r)z+q^{(i)}(r)+A_0^{(i)}+A_1^{(i)}z+A_2^{(i)}z^2+A_3^{(i)}z^3 \tag{11.3.21}$$

Substituting (11.3.21) into $(11.3.7)_4$, we can obtain:

$$\tau_{rz}^{(i)}=q_{,rrr}^{(i)}+r^{-1}q_{,rr}^{(i)}-r^{-2}q_{,r}^{(i)}+\left(p_{,rrr}^{(i)}+r^{-1}p_{,rr}^{(i)}-r^{-2}p_{,r}^{(i)}\right)z \tag{11.3.22}$$

Since, the stress component $\tau_{rz}^{(i)}$ no-dependent by z variable, we can obtain the function $p^{(i)}(r)$:

$$p_{,rrr}^{(i)}+r^{-1}p_{,rr}^{(i)}-r^{-2}p_{,r}^{(i)}=0 \quad\Rightarrow\quad p^{(i)}(r)=B_1^{(i)}r^2+B_2^{(i)}\left(1-\delta_{0i}\right)\log r+B_3^{(i)} \tag{11.3.23}$$

Substituting the expression the function $\varphi^{(i)}(r,z)$ into (11.3.11), we obtain a differential equation in unknown function $q^{(i)}(r)$:

$$\nabla_1^2\nabla_2^2\varphi^{(i)}=0 \quad\Rightarrow\quad q_{,r}^{(i)}-r\,q_{,rr}^{(i)}+2r^2q_{,rrr}^{(i)}+r^3q_{,rrrr}^{(i)}=0 \tag{11.3.24}$$

To solve the (11.3.24), we obtain the function $q^{(i)}(r)$:

$$q^{(i)}(r)=C_1^{(i)}r^2+\left(1-\delta_{0i}\right)\left(C_2^{(i)}+C_3^{(i)}r^2\right)\log r \tag{11.3.25}$$

The field displacement solution becomes:

$$\begin{cases} u_r^{(i)}=-\dfrac{c_{13}^{(i)}+c_{44}^{(i)}}{c_{11}^{(i)}c_{44}^{(i)}}\left[2B_1^{(i)}r+\left(1-\delta_{0i}\right)B_2^{(i)}r^{-1}\right] \\ u_z^{(i)}=2z\left(\dfrac{3A_3^{(i)}}{c_{11}^{(i)}}+\dfrac{2B_1^{(i)}}{c_{44}^{(i)}}\right)+\dfrac{2A_2^{(i)}}{c_{11}^{(i)}}+\dfrac{4}{c_{44}^{(i)}}\left[C_1^{(i)}+C_3^{(i)}\left(1-\delta_{0i}\right)\left(1+\log r\right)\right] \end{cases} \tag{11.3.26}$$

The stress component $\tau_{rz}^{(i)}$ is:

$$\tau_{rz}^{(i)}=4C_3^{(i)}\left(1-\delta_{0i}\right)r^{-1} \tag{11.3.27}$$

On the external surface of the solid the shear tractions are zero, therefore $C_3^{(i)}=0 \quad \forall i\in\{0,1,...,n\}$. Moreover, the unknown constants $C_1^{(i)}, A_2^{(i)}$ are zero, because their represent rigid motion . Finally, the field displacement solution becomes:

$$\begin{cases} u_r^{(i)}=D_1^{(i)}r+\left(1-\delta_{0i}\right)D_2^{(i)}r^{-1} \\ u_z^{(i)}=\varepsilon_0\,z \end{cases} \tag{11.3.28}$$

where $D_1^{(i)}=-\dfrac{2\left(c_{13}^{(i)}+c_{44}^{(i)}\right)}{c_{11}^{(i)}c_{44}^{(i)}}B_1^{(i)}, \quad D_2^{(i)}=-\dfrac{\left(c_{13}^{(i)}+c_{44}^{(i)}\right)}{c_{11}^{(i)}c_{44}^{(i)}}B_2^{(i)}, \quad \varepsilon_0=2\left(\dfrac{3A_3^{(i)}}{c_{11}^{(i)}}+\dfrac{2B_1^{(i)}}{c_{44}^{(i)}}\right)$

The non-zero strains component are:

$$\varepsilon_{rr}^{(i)}=D_1^{(i)}-D_2^{(i)}\left(1-\delta_{0i}\right)r^{-2}, \ \varepsilon_{\theta\theta}^{(i)}=D_1^{(i)}+D_2^{(i)}\left(1-\delta_{0i}\right)r^{-2}, \ \varepsilon_{zz}^{(i)}=\varepsilon_0 \tag{11.3.29}$$

The non-zero stresses component are:

$$\begin{aligned} \sigma_{rr}^{(i)}&=D_1^{(i)}\left(c_{11}^{(i)}+c_{12}^{(i)}\right)-D_2^{(i)}\left(1-\delta_{0i}\right)\left(c_{11}^{(i)}+c_{12}^{(i)}\right)r^{-2}+c_{13}^{(i)}\varepsilon_0 \\ \sigma_{\theta\theta}^{(i)}&=D_1^{(i)}\left(c_{11}^{(i)}+c_{12}^{(i)}\right)+D_2^{(i)}\left(1-\delta_{0i}\right)\left(c_{11}^{(i)}+c_{12}^{(i)}\right)r^{-2}+c_{13}^{(i)}\varepsilon_0, \quad \sigma_{zz}^{(i)}=2D_1^{(i)}c_{13}^{(i)}+c_{33}^{(i)}\varepsilon_0 \end{aligned} \tag{11.3.30}$$

11.3.3. Equilibrium and compatibility conditions

The results obtained until now satisfy the equilibrium and compatibility equations inside each generic *i*-th phase of a composite circular cylinder subjected to torsion strains. Under both the hypothesis of linear and transversally-isotropic elastic behavior of the materials and the assumption of perfect contact at the cylindrical interfacial boundaries (no de-lamination or friction phenomena), we have now to establish the satisfaction of both the equilibrium and the compatibility equations at the boundary surfaces between two generic adjacent phases. To obtain this, we will make first reference to the generic case in which an multilayered cylinder is constituted by a central *core* and *n* arbitrary *cladding* phases. The total unknown parameters to determine can be summarized as follows:

$$\begin{aligned} &D_1^{(c)} \\ &D_1^{(i)}, D_2^{(i)} \quad i \in \{1,2,.....n\}, \\ &\varepsilon_0 \end{aligned} \tag{11.3.31}$$

where those in $(11.3.31)_1$ represent the unknown coefficient of the *core*, those in $(11.3.31)_2$ represent the unknown parameters for every circular hollow cylinder, while $(11.3.31)_3$ is coefficient responsible for the assigned constant form of the strain ε_{zz} . Hence, the total number of unknowns will be $(2n+2)$, which equals the number of algebraic equations to solve. In particular, as we will show in the follows, the number of the boundary equations at the interfaces $2n$, while 2 is the number boundary conditions on the external cylindrical surface and on the end basis. In particular, we begin writing the 2*n* equilibrium and compatibility equations at the generic interface, that is:

$$\begin{cases} u_r^{(i)}(r=R^{(i)}) = u_r^{(i+1)}(r=R^{(i)}) \\ \sigma_{rr}^{(i)}(r=R^{(i)}) = \sigma_{rr}^{(i+1)}(r=R^{(i)}) \end{cases} \qquad i \in \{0,1,...,n-1\} \tag{11.3.32}$$

where $R^{(i)}$ is the outer radius of the *i*-th phase. Recalling the previously obtained results, system (11.3.32) can be expressed as follows

$$\begin{cases} (1-\delta_{0i})\left(\dfrac{D_2^{(i+1)}-D_2^{(i)}}{R^{(i)}}\right)+\left(D_1^{(i+1)}-D_1^{(i)}\right)R^{(i)}=0 \\ \varepsilon_0\left(c_{13}^{(i+1)}-c_{13}^{(i)}\right)+D_1^{(i+1)}\left(c_{11}^{(i+1)}+c_{12}^{(i+1)}\right)-D_1^{(i)}\left(c_{11}^{(i)}+c_{12}^{(i)}\right)+ \\ \quad +(1-\delta_{0i})\left[\dfrac{D_2^{(i+1)}\left(c_{12}^{(i+1)}-c_{11}^{(i+1)}\right)}{R^{(i)2}}-\dfrac{D_2^{(i)}\left(c_{12}^{(i)}-c_{11}^{(i)}\right)}{R^{(i)2}}\right]=0 \end{cases} \qquad i \in \{0,1,...,n-1\} \tag{11.3.33}$$

The equilibrium equation to the tractions on the external cylindrical boundary surface, ($i=n$), give:

$$\sigma_{rr}^{(n)}(r=R^{(n)}) = p_0 \tag{11.3.34}$$

where p_0 are radial pressure on $\partial\Omega^{cyl}$. The (11.3.34) can be expressed as follows:

$$\frac{D_2^{(n)}\left(c_{12}^{(n)}-c_{11}^{(n)}\right)}{R^{(n)2}}+D_1^{(n)}\left(c_{11}^{(n)}+c_{12}^{(n)}\right)+c_{13}^{(n)}\varepsilon_0 R^{(n)2}=p_0 \tag{11.3.35}$$

Finally, it remains to consider the last equilibrium equation in z-direction on one of the basis, being the other end condition automatically satisfied. Therefore, without loss of generality, for $z=0$ we can write

$$\sum_{i=0}^{n}\int_0^{2\pi}\int_{(1-\delta_{0i})R^{(i-1)}}^{R^{(i)}}\sigma_{zz}^{(i)}(z=0)\,r\,dr\,d\theta = N_z, \tag{11.3.36}$$

where N_z is the total axial force applied at $z=0$. The equation (11.3.36) can be to rewritten as follows :

$$\sum_{i=0}^{n}\pi\left[R^{(i)}-R^{(i-1)}(1-\delta_{0i})\right]\left(2D_1^{(i)}c_{13}^{(i)}+c_{33}^{(i)}\varepsilon_0\right)=N_z \tag{11.3.37}$$

The solutions found above are then able to describe the case in which an multilayered cylinder made by n circular hollow cylinders and a central *core* is loaded by a combination of radial pressures and axial forces applied at the ends. In order to solve the algebraic system constituted by (11.3.33), (11.3.35) and (11.3.37), it could be convenient to re-arrange the whole $(2n+2)\times(2n+2)$ algebraic system following a matrix-based procedure. Indeed, we can collect the known terms in the *load* vector $\mathbf{L}$

$$\mathbf{L}^T = \{0,...,p_0,N_z\} \tag{11.3.38}$$

where the only non zero terms are the last two ones, while the unknown parameters can be collected in the vector $\mathbf{X}$ as follows:

$$\mathbf{X}^T = \left\{\varepsilon_0, D_1^{(0)}, D_1^{(1)}, D_2^{(1)}, D_1^{(2)}, D_2^{(2)}, ..., D_1^{(n)}, D_2^{(n)}\right\} \tag{11.3.39}$$

so that the set of equations (11.3.33), (11.3.35) and (11.3.37) reads

$$\mathbb{P}\cdot\mathbf{X} = \mathbf{L} \tag{11.3.40}$$

The algebraic system (11.3.40) has only solution. The equations (11.3.33) can be rewritten as follows:

$$\mathbf{P}^{(i)}\mathbf{D}^{(i)} - \mathbf{Q}^{(i)}\mathbf{D}^{(i+1)} + \mathbf{H}^{(i)}\mathbf{D}^{(0)} = 0 \qquad \forall i \in \{0,1,...,n\} \tag{11.3.41}$$

where the matrix $\mathbf{P}^{(i)}, \mathbf{Q}^{(i)}, \mathbf{H}^{(i)}$ and vector $\mathbf{D}^{(i)}, \mathbf{D}^{(0)}$ are :

$$\mathbf{P}^{(i)} = \left(1-\delta_{0i}\right)\begin{bmatrix} R^{(i)} & \dfrac{1}{R^{(i)}} \\ c_{11}^{(i)} + c_{12}^{(i)} & \dfrac{c_{12}^{(i)}}{R^{(i)2}} - \dfrac{c_{11}^{(i)}}{R^{(i)2}} \end{bmatrix} \qquad \forall i \in \{0,2,...,n-1\}, \tag{11.3.42}$$

$$\mathbf{Q}^{(i)} = \begin{bmatrix} R^{(i)} & \dfrac{1}{R^{(i)}} \\ c_{11}^{(i+1)} + c_{12}^{(i+1)} & \dfrac{c_{12}^{(i+1)}}{R^{(i)2}} - \dfrac{c_{11}^{(i+1)}}{R^{(i)2}} \end{bmatrix} \quad \forall i \in \{0,1,...,n-1\}, \tag{11.3.43}$$

$$\mathbf{H}^{(i)} = \begin{bmatrix} R^{(i)}\delta_{0i} & 0 \\ \left(c_{11}^{(i)} + c_{12}^{(i)}\right)\delta_{0i} & c_{13}^{(i)} + c_{13}^{(i+1)} \end{bmatrix} \quad \forall i \in \{0,1,...,n-1\} \tag{11.3.44}$$

$$\mathbf{D}^{(i)} \equiv \begin{bmatrix} D_1^{(i)} & D_2^{(i)} \end{bmatrix}^T \quad \forall i \in \{1,2,...,n\}, \qquad \mathbf{D}^{(0)} \equiv \begin{bmatrix} D_1^{(0)} & \varepsilon_0 \end{bmatrix}^T \tag{11.3.45}$$

Then, the matrix $\mathbf{P}^{(i)}, \mathbf{Q}^{(i)}, \mathbf{H}^{(i)}$ are dependent by geometrical and mechanical parameters:

$$\mathbf{P}^{(i)} = \mathbf{P}^{(i)}\left(c_{11}^{(i)}, c_{12}^{(i)}, R^{(i)}\right),\ \mathbf{Q}^{(i)} = \mathbf{Q}^{(i)}\left(c_{11}^{(i)}, c_{12}^{(i)}, R^{(i)}\right),\ \mathbf{H}^{(i)} = \mathbf{H}^{(i)}\left(c_{13}^{(i)}, c_{11}^{(i)}, c_{12}^{(i)}, R^{(i)}\right) \tag{11.3.46}$$

The equations (11.3.41) constituted an algebraic system (with order $2n\times 2n$) in the unknown parameters $D_1^{(i)}, D_2^{(i)}$ for $i \in \{1,2,...,n\}$. By solving the equations (11.3.41) , we obtained the constants $D_1^{(i)}, D_2^{(i)}$ as function of the unknown parameters $D_1^{(0)}, \varepsilon_0$:

$$\mathbf{D}^{(i)} = \left[\mathbf{Q}^{(i)-1}\mathbf{H}^{(i)} + \mathbf{Q}^{(i)-1}\mathbf{P}^{(i)}\mathbf{Q}^{(i-1)-1}\mathbf{H}^{(i-1)} + ... + \mathbf{Q}^{(i)-1}\mathbf{P}^{(i)}\mathbf{Q}^{(i-1)-1}\mathbf{P}^{(i-1)}\cdot....\cdot\mathbf{Q}^{(1)-1}\mathbf{P}^{(1)}\mathbf{Q}^{(0)-1}\mathbf{H}^{(0)}\right]\cdot\mathbf{D}^{(0)}$$
$$\forall i \in \{1,2,...,n\} \tag{11.3.47}$$

The equations (11.3.41) can be write as follows:

$$\begin{bmatrix} \mathbf{D}^{(1)} \\ \mathbf{D}^{(2)} \\ \mathbf{D}^{(3)} \\ \vdots \\ \mathbf{D}^{(n)} \end{bmatrix} = \begin{bmatrix} \mathbf{\Pi}^{(1)} \\ \mathbf{\Pi}^{(2)} \\ \mathbf{\Pi}^{(3)} \\ \vdots \\ \mathbf{\Pi}^{(n)} \end{bmatrix}\cdot\mathbf{D}^{(0)} = \mathbf{\Pi}\cdot\mathbf{D}^{(0)} \tag{11.3.48}$$

where $\mathbf{\Pi}^{(i)} = \left[\mathbf{Q}^{(i)-1}\mathbf{H}^{(i)} + \mathbf{Q}^{(i)-1}\mathbf{P}^{(i)}\mathbf{Q}^{(i-1)-1}\mathbf{H}^{(i-1)} + ... + \mathbf{Q}^{(i)-1}\mathbf{P}^{(i)}\mathbf{Q}^{(i-1)-1}\mathbf{P}^{(i-1)}\cdot....\cdot\mathbf{Q}^{(1)-1}\mathbf{P}^{(1)}\mathbf{Q}^{(0)-1}\mathbf{H}^{(0)}\right]$.

The matrix $\mathbf{\Pi}$ has order $2n\,x\,2$. The equations (11.3.35) and (11.3.37) become:

$$\begin{bmatrix} 0 & 0 & 0 & 0 & \cdots & D_1^{(n)}\left(c_{11}^{(n)}+c_{12}^{(n)}\right) & \dfrac{D_2^{(n)}\left(c_{12}^{(n)}-c_{11}^{(n)}\right)}{R^{(n)2}} \\ 2c_{13}^{(1)}A^{(1)} & 0 & 2c_{13}^{(2)}A^{(2)} & 0 & \cdots & 2c_{13}^{(n)}A^{(n)} & 0 \end{bmatrix}\cdot\begin{bmatrix} \mathbf{D}^{(1)} \\ \mathbf{D}^{(2)} \\ \mathbf{D}^{(3)} \\ \vdots \\ \mathbf{D}^{(n)} \end{bmatrix}+ \tag{11.3.49}$$

$$+\begin{bmatrix} 0 & c_{13}^{(n)}R^{(n)2} \\ 2c_{13}^{(0)}A^{(0)} & c_{33}^{(0)}A^{(0)} \end{bmatrix}\cdot\mathbf{D}^{(0)}=\begin{bmatrix} p_0 \\ N_z \end{bmatrix}$$

where $A^{(i)}=\sum_{i=0}^{n}\pi\left[R^{(i)2}-(1-\delta_{0i})R^{(i-1)2}\right]$. By substituting the constants $D_1^{(i)}, D_2^{(i)}$, in to equations (11.3.49), we can obtained the algebraic system in to unknown parameters $D_1^{(0)}, \varepsilon_0$:

$$\left[\mathbf{\Lambda}\right]\cdot\mathbf{D}^{(0)}=\begin{bmatrix} p_0 \\ N_z \end{bmatrix} \tag{11.3.50}$$

where the matrix $\mathbf{\Lambda}$ is:

$$\mathbf{\Lambda}=\begin{bmatrix} 0 & 0 & 0 & 0 & \cdots & D_1^{(n)}\left(c_{11}^{(n)}+c_{12}^{(n)}\right) & \dfrac{D_2^{(n)}\left(c_{12}^{(n)}-c_{11}^{(n)}\right)}{R^{(n)2}} \\ 2c_{13}^{(1)}A^{(1)} & 0 & 2c_{13}^{(2)}A^{(2)} & 0 & \cdots & 2c_{13}^{(n)}A^{(n)} & 0 \end{bmatrix}\cdot\begin{bmatrix} \mathbf{\Pi}^{(1)} \\ \mathbf{\Pi}^{(2)} \\ \mathbf{\Pi}^{(3)} \\ \vdots \\ \mathbf{\Pi}^{(n)} \end{bmatrix}+ \tag{11.3.51}$$

$$+\begin{bmatrix} 0 & c_{13}^{(n)}R^{(n)2} \\ 2c_{13}^{(0)}A^{(0)} & c_{33}^{(0)}A^{(0)} \end{bmatrix}$$

The system of the equations (11.3.50) has solution because $\det\left[\mathbf{\Lambda}\right]\neq 0$.

11.4. Application of the homogenization theory to composite transversally-isotropic cylinders

The average strain tensor is denoted by

$$\bar{\boldsymbol{\varepsilon}}^{T}\equiv\left\{\bar{\varepsilon}_{rr}\quad\bar{\varepsilon}_{\theta\theta}\quad\bar{\varepsilon}_{zz}\quad\bar{\varepsilon}_{\theta z}\quad\bar{\varepsilon}_{rz}\quad\bar{\varepsilon}_{r\theta}\right\} \tag{11.4.1}$$

and the average stress tensor is denoted by

$$\bar{\boldsymbol{\sigma}}^{T}\equiv\left\{\bar{\sigma}_{rr}\quad\bar{\sigma}_{\theta\theta}\quad\bar{\sigma}_{zz}\quad\bar{\tau}_{\theta z}\quad\bar{\tau}_{rz}\quad\bar{\tau}_{r\theta}\right\} \tag{11.4.2}$$

The average stress-strain relation for the multiphase solid can be written in the following form:

$$\bar{\boldsymbol{\varepsilon}}=\mathbf{A}^{H}\bar{\boldsymbol{\sigma}} \tag{11.4.3}$$

The average elastic compliance tensor is:

$$\mathbf{A}^{H}=\begin{bmatrix} \frac{1}{\overline{E}} & -\frac{\overline{\nu}}{\overline{E}} & -\frac{\overline{\nu}_z}{\overline{E}_z} & 0 & 0 & 0 \\ -\frac{\overline{\nu}}{\overline{E}} & \frac{1}{\overline{E}} & -\frac{\overline{\nu}_z}{\overline{E}_z} & 0 & 0 & 0 \\ -\frac{\overline{\nu}_z}{\overline{E}_z} & -\frac{\overline{\nu}_z}{\overline{E}_z} & \frac{1}{\overline{E}_z} & 0 & 0 & 0 \\ 0 & 0 & 0 & \frac{1}{2\overline{\mu}_z} & 0 & 0 \\ 0 & 0 & 0 & 0 & \frac{1}{2\overline{\mu}_z} & 0 \\ 0 & 0 & 0 & 0 & 0 & \frac{1+\overline{\nu}}{\overline{E}} \end{bmatrix} \tag{11.4.4}$$

where $\overline{E}_z, \overline{E}$ are average elastic modulus in z direction and in isotropic plane, respectively;

$\overline{\nu}_z, \overline{\nu}$ are average Poisson's modulus in z direction and in isotropic plane, respectively;

and $\overline{\mu}_z$ is shear modulus;

The strain tensor for *i*-th phase is denoted by

$$\boldsymbol{\varepsilon}^{(i)T} \equiv \left\{ \varepsilon_{rr}^{(i)} \quad \varepsilon_{\theta\theta}^{(i)} \quad \varepsilon_{zz}^{(i)} \quad \varepsilon_{\theta z}^{(i)} \quad \varepsilon_{rz}^{(i)} \quad \varepsilon_{r\theta}^{(i)} \right\} \tag{11.4.5}$$

and the stress tensor for *i*-th phase is:

$$\boldsymbol{\sigma}^{(i)T} \equiv \left\{ \sigma_{rr}^{(i)} \quad \sigma_{\theta\theta}^{(i)} \quad \sigma_{zz}^{(i)} \quad \tau_{\theta z}^{(i)} \quad \tau_{rz}^{(i)} \quad \tau_{r\theta}^{(i)} \right\} \tag{11.4.6}$$

The stress-strain relation for generic i-phase can be written in the following form:

$$\sigma^{(i)} = \mathbf{C}^{(i)} \varepsilon^{(i)} \tag{11.4.7}$$

The elastic stiffness tensor for generic i-phase is characterized by follows matrix $\mathbf{C}^{(i)}$:

$$\mathbf{C}^{(i)}=\begin{bmatrix} c_{11}^{(i)} & c_{12}^{(i)} & c_{13}^{(i)} & 0 & 0 & 0 \\ c_{12}^{(i)} & c_{11}^{(i)} & c_{13}^{(i)} & 0 & 0 & 0 \\ c_{13}^{(i)} & c_{13}^{(i)} & c_{33}^{(i)} & 0 & 0 & 0 \\ 0 & 0 & 0 & 2c_{44}^{(i)} & 0 & 0 \\ 0 & 0 & 0 & 0 & 2c_{44}^{(i)} & 0 \\ 0 & 0 & 0 & 0 & 0 & c_{11}^{(i)} - c_{12}^{(i)} \end{bmatrix} \tag{11.4.8}$$

and the elastic compliance tensor for generic i-phase is characterized by follows matrix $\mathbf{A}^{(i)}$:

$$\mathbf{A}^{(i)}=\begin{bmatrix} \frac{1}{E^{(i)}} & -\frac{\nu^{(i)}}{E^{(i)}} & -\frac{\nu_z^{(i)}}{E_z^{(i)}} & 0 & 0 & 0 \\ -\frac{\nu^{(i)}}{E^{(i)}} & \frac{1}{E^{(i)}} & -\frac{\nu_z^{(i)}}{E_z^{(i)}} & 0 & 0 & 0 \\ -\frac{\nu_z^{(i)}}{E_z^{(i)}} & -\frac{\nu_z^{(i)}}{E_z^{(i)}} & \frac{1}{E^{(i)}} & 0 & 0 & 0 \\ 0 & 0 & 0 & \frac{1}{2\mu_z^{(i)}} & 0 & 0 \\ 0 & 0 & 0 & 0 & \frac{1}{2\mu_z^{(i)}} & 0 \\ 0 & 0 & 0 & 0 & 0 & \frac{1+\nu^{(i)}}{E^{(i)}} \end{bmatrix} \tag{11.4.9}$$

The relationships between the component of the matrix $\mathbf{C}^{(i)}$ and component the matrix $\mathbf{A}^{(i)}$ of the generic i-phase are follows:

$$c_{11}^{(i)}=\frac{E^{(i)}\left(E^{(i)2}\nu_z^{(i)}-E_z^{(i)}\right)}{\left(1+\nu^{(i)}\right)\left[E_z^{(i)}\left(\nu^{(i)}-1\right)+2E^{(i)}\nu_z^{(i)2}\right]},\qquad c_{12}^{(i)}=-\frac{E^{(i)}\left(E^{(i)}\nu_z^{(i)2}+E_z^{(i)}\nu^{(i)}\right)}{\left(1+\nu^{(i)}\right)\left[E_z^{(i)}\left(\nu^{(i)}-1\right)+2E^{(i)}\nu_z^{(i)2}\right]},$$

$$c_{13}^{(i)}=\frac{E^{(i)}E_z^{(i)}\nu_z^{(i)}}{E_z^{(i)}\left(1-\nu^{(i)}\right)-2E^{(i)}\nu_z^{(i)2}},\quad c_{33}^{(i)}=\frac{E_z^{(i)2}\left(\nu^{(i)}-1\right)}{E_z^{(i)}\left(1-\nu^{(i)}\right)-2E^{(i)}\nu_z^{(i)2}},\qquad c_{44}^{(i)}=\mu_z^{(i)},\tag{11.4.10}$$

Let us consider the case which the external forces are constituted by two axial force N_z applied on the basis ∂V_0 and ∂V_L. We can obtained the mean stress tensor and mean strain tensor in the following manner:

$$\bar{\sigma}_{hk}=\frac{1}{V}\sum_{i=0}^{n}\int_{V^{(i)}}\sigma_{hk}^{(i)}dV,\qquad \bar{\varepsilon}_{hk}=\frac{1}{V}\sum_{i=0}^{n}\int_{V^{(i)}}\varepsilon_{hk}^{(i)}dV,\tag{11.4.11}$$

where $V=\sum_{i=0}^{n}V^{(i)}$. The average stresses components are:

$$\begin{cases}\bar{\sigma}_{rr}=\dfrac{1}{A}\sum_{i=0}^{n}A^{(i)}\left[D_1^{(i)}\left(c_{11}^{(i)}+c_{12}^{(i)}\right)+\varepsilon_0 c_{13}^{(i)}\right]-2\pi\delta_{0i}D_2^{(i)}\left(c_{11}^{(i)}-c_{12}^{(i)}\right)\log\dfrac{R^{(i)}}{R^{(i-1)}}\\ \bar{\sigma}_{\theta\theta}=\dfrac{1}{A}\sum_{i=0}^{n}A^{(i)}\left[D_1^{(i)}\left(c_{11}^{(i)}+c_{12}^{(i)}\right)+\varepsilon_0 c_{13}^{(i)}\right]+2\pi\delta_{0i}D_2^{(i)}\left(c_{11}^{(i)}-c_{12}^{(i)}\right)\log\dfrac{R^{(i)}}{R^{(i-1)}}\\ \bar{\sigma}_{zz}=\dfrac{1}{A}\sum_{i=0}^{n}A^{(i)}\left(2D_1^{(i)}c_{13}^{(i)}+\varepsilon_0 c_{33}^{(i)}\right)\end{cases}\tag{11.4.12}$$

where $A^{(i)}=\sum_{i=0}^{n}\pi\left[R^{(i)2}-(1-\delta_{0i})R^{(i-1)2}\right]$. The average strains components are:

$$\begin{cases}\bar{\varepsilon}_{rr}=\dfrac{1}{A}\sum_{i=0}^{n}D_1^{(i)}A^{(i)}-2\pi\delta_{0i}D_2^{(i)}\log\dfrac{R^{(i)}}{R^{(i-1)}}\\ \bar{\varepsilon}_{\theta\theta}=\dfrac{1}{A}\sum_{i=0}^{n}D_1^{(i)}A^{(i)}+2\pi\delta_{0i}D_2^{(i)}\log\dfrac{R^{(i)}}{R^{(i-1)}}\\ \bar{\varepsilon}_{zz}=\varepsilon_0\end{cases}\tag{11.4.13}$$

Moreover, for solid constituted by n-phase, it is easy to obtain the following relationship:

$$\bar{\sigma}_{rr}+\bar{\sigma}_{\theta\theta}=0,\quad \bar{\sigma}_{zz}=\frac{N_z}{A},\tag{11.4.14}$$

The mean Young's moduli $\bar{E}_z$ and the mean Poisson's moduli $\bar{\nu}_z$ are:

$$\bar{E}_z=\frac{\bar{\sigma}_{zz}}{\bar{\varepsilon}_{zz}},\quad \bar{\nu}_z=-\frac{\bar{\varepsilon}_{rr}+\bar{\varepsilon}_{\theta\theta}}{2\bar{\varepsilon}_{zz}},\quad \bar{\nu}=\frac{\left(\bar{\varepsilon}_{\theta\theta}-\bar{\varepsilon}_{rr}\right)\bar{E}}{2\bar{\sigma}_{\theta\theta}}-1\tag{11.4.15}$$

$$\begin{cases}\bar{E}_z=\dfrac{1}{A}\sum_{i=0}^{n}A^{(i)}\left(c_{33}^{(i)}+\dfrac{2D_1^{(i)}c_{13}^{(i)}}{\varepsilon_0}\right)\\ \bar{\nu}_z=-\dfrac{1}{A\varepsilon_0}\sum_{i=0}^{n}D_1^{(i)}A^{(i)}\end{cases}\tag{11.4.16}$$

where $A^{(i)}=\pi\left[R^{(i)2}-\left(1-\delta_{0i}\right)R^{(i-1)2}\right]$, $A=\sum_{i=0}^{n}A^{(i)}$, and $D_1^{(i)},D_2^{(i)},\varepsilon_0$ are integration constants valuated to put $F=1$.

$$\begin{cases} \overline{E}_z = \dfrac{1}{A\varepsilon_0}\displaystyle\sum_{i=0}^{n} A^{(i)} E_z^{(i)} \left[\dfrac{\varepsilon_0 E_z^{(i)} \left(\nu^{(i)} - 1\right) + 2D_1^{(i)} E^{(i)} \nu_z^{(i)}}{E_z^{(i)} \left(\nu^{(i)} - 1\right) + 2E^{(i)} \nu_z^{(i)2}} \right] \\ \overline{\nu}_z = -\dfrac{1}{A\varepsilon_0} \sum_{i=0}^{n} D_1^{(i)} A^{(i)} \end{cases} \tag{11.4.17}$$

Let us consider the case which the solid loaded on external cylindrical surface by uniform radial pressure. Moreover, for solid constituted by n-phase, it is easy to obtain the following relationship:

$$\overline{\sigma}_{rr} + \overline{\sigma}_{\theta\theta} = 2p_0, \quad \overline{\sigma}_{zz} = 0, \tag{11.4.18}$$

The average Young's moduli $\overline{E}$ and the average Poisson's moduli $\overline{\nu}$ are:

$$\overline{E} = \frac{\overline{\sigma}_{rr}^2 - \overline{\sigma}_{\theta\theta}^2}{\overline{\sigma}_{rr}\overline{\varepsilon}_{rr} - \overline{\sigma}_{\theta\theta}\overline{\varepsilon}_{\theta\theta}}, \quad \overline{\nu} = \frac{\overline{\sigma}_{\theta\theta}\overline{\varepsilon}_{rr} - \overline{\sigma}_{rr}\overline{\varepsilon}_{\theta\theta}}{\overline{\sigma}_{rr}\overline{\varepsilon}_{rr} - \overline{\sigma}_{\theta\theta}\overline{\varepsilon}_{\theta\theta}}, \quad \overline{\nu}_z = -\frac{\overline{E}_z\,\overline{\varepsilon}_{zz}}{\overline{\sigma}_{rr} + \overline{\sigma}_{\theta\theta}}, \tag{11.4.19}$$

$$\overline{E} = \frac{2\displaystyle\sum_{i=0}^{n} A^{(i)} \left[D_1^{(i)} \left(c_{11}^{(i)} + c_{12}^{(i)}\right) + c_{13}^{(i)} \varepsilon_0 \right] \cdot \sum_{i=1}^{n} D_2^{(i)} \left(c_{11}^{(i)} - c_{12}^{(i)}\right) \log \dfrac{R^{(i)}}{R^{(i-1)}}}{\left(\displaystyle\sum_{i=0}^{n} D_1^{(i)} A^{(i)} \right) \left(\displaystyle\sum_{i=1}^{n} D_2^{(i)} \left(c_{11}^{(i)} - c_{12}^{(i)}\right) \log \dfrac{R^{(i)}}{R^{(i-1)}} \right) + \left(\displaystyle\sum_{i=1}^{n} D_2^{(i)} \log \dfrac{R^{(i)}}{R^{(i-1)}} \right) \left[\displaystyle\sum_{i=0}^{n} A^{(i)} \left(D_1^{(i)} \left(c_{11}^{(i)} + c_{12}^{(i)}\right) + c_{13}^{(i)} \varepsilon_0 \right) \right]} \tag{11.4.20}$$

$$\frac{1}{\overline{E}} = \frac{\displaystyle\sum_{i=1}^{n} D_2^{(i)} \log \dfrac{R^{(i)}}{R^{(i-1)}}}{2\displaystyle\sum_{i=1}^{n} D_2^{(i)} \left(c_{11}^{(i)} - c_{12}^{(i)}\right) \log \dfrac{R^{(i)}}{R^{(i-1)}}} + \frac{\displaystyle\sum_{i=0}^{n} D_1^{(i)} A^{(i)}}{2\displaystyle\sum_{i=0}^{n} A^{(i)} \left[D_1^{(i)} \left(c_{11}^{(i)} + c_{12}^{(i)}\right) + c_{13}^{(i)} \varepsilon_0 \right]} \tag{11.4.21}$$

$$\overline{\nu} = \frac{\left(\displaystyle\sum_{i=1}^{n} D_2^{(i)} \log \dfrac{R^{(i)}}{R^{(i-1)}} \right) \left[\displaystyle\sum_{i=0}^{n} A^{(i)} \left(D_1^{(i)} \left(c_{11}^{(i)} + c_{12}^{(i)}\right) + c_{13}^{(i)} \hat{\varepsilon}_0 \right) \right] - \left(\displaystyle\sum_{i=0}^{n} D_1^{(i)} A^{(i)} \right) \left(\displaystyle\sum_{i=1}^{n} D_2^{(i)} \left(c_{11}^{(i)} - c_{12}^{(i)}\right) \log \dfrac{R^{(i)}}{R^{(i-1)}} \right)}{\left(\displaystyle\sum_{i=0}^{n} D_1^{(i)} A^{(i)} \right) \left(\displaystyle\sum_{i=1}^{n} D_2^{(i)} \left(c_{11}^{(i)} - c_{12}^{(i)}\right) \log \dfrac{R^{(i)}}{R^{(i-1)}} \right) + \left(\displaystyle\sum_{i=1}^{n} D_2^{(i)} \log \dfrac{R^{(i)}}{R^{(i-1)}} \right) \left[\displaystyle\sum_{i=0}^{n} A^{(i)} \left(D_1^{(i)} \left(c_{11}^{(i)} + c_{12}^{(i)}\right) + c_{13}^{(i)} \varepsilon_0 \right) \right]} \tag{11.4.22}$$

$$\frac{\overline{\nu}}{\overline{E}} = \frac{\displaystyle\sum_{i=1}^{n} D_2^{(i)} \log \dfrac{R^{(i)}}{R^{(i-1)}}}{2\displaystyle\sum_{i=1}^{n} D_2^{(i)} \left(c_{11}^{(i)} - c_{12}^{(i)}\right) \log \dfrac{R^{(i)}}{R^{(i-1)}}} - \frac{\displaystyle\sum_{i=0}^{n} D_1^{(i)} A^{(i)}}{2\displaystyle\sum_{i=0}^{n} A^{(i)} \left[D_1^{(i)} \left(c_{11}^{(i)} + c_{12}^{(i)}\right) + c_{13}^{(i)} \varepsilon_0 \right]} \tag{11.4.23}$$

In the case the external forces are constituted by two couple torque $\mathfrak{M}_z$ applied on the basis ∂V_0 and ∂V_L, the only stress component is $\overline{\tau}_{\theta z}$ and only strain component is $\overline{\varepsilon}_{\theta z}$:

$$\begin{cases} \overline{\tau}_{\theta z} = \dfrac{2}{3} \dfrac{T_1^{(0)}}{R^{(n)2}} \displaystyle\sum_{i=0}^{n} \left[\dfrac{R^{(i)3} - \left(1 - \delta_{0i}\right) R^{(i-1)3}}{a_{44}^{(i)}} \right] = \dfrac{2\mathfrak{M}_z}{3R^{(n)2} \displaystyle\sum_{i=0}^{n} \dfrac{I_P^{(i)}}{a_{44}^{(i)}}} \sum_{i=0}^{n} \left[\dfrac{R^{(i)3} - \left(1 - \delta_{0i}\right) R^{(i-1)3}}{a_{44}^{(i)}} \right] \\ \overline{\varepsilon}_{\theta z} = \dfrac{2}{3} T_1^{(0)} R^{(n)} = \dfrac{\mathfrak{M}_z R^{(n)}}{3\displaystyle\sum_{i=0}^{n} \dfrac{I_P^{(i)}}{a_{44}^{(i)}}} \end{cases} \tag{11.4.24}$$

Expressing the coefficients of deformation by means of the "moduli of elasticity", we have:

$$\begin{cases} \overline{\tau}_{\theta z} = \dfrac{2\mathfrak{M}_z}{3R^{(n)2}\displaystyle\sum_{i=0}^{n} c_{44}^{(i)} I_P^{(i)}} \sum_{i=0}^{n} c_{44}^{(i)} \left[R^{(i)3} - \left(1-\delta_{0i}\right) R^{(i-1)3} \right] \\ \overline{\varepsilon}_{\theta z} = \dfrac{\mathfrak{M}_z R^{(n)}}{3\displaystyle\sum_{i=0}^{n} c_{44}^{(i)} I_P^{(i)}} \end{cases} \tag{11.4.25}$$

$$\overline{c}_{44} = \frac{1}{\overline{a}_{44}} = \frac{\overline{\tau}_{\theta z}}{2\overline{\varepsilon}_{\theta z}} = \frac{\overline{\tau}_{\theta z}}{\overline{\gamma}_{\theta z}} = \frac{1}{R^{(n)3}} \sum_{i=0}^{n} c_{44}^{(i)} \left[R^{(i)3} - \left(1-\delta_{0i}\right) R^{(i-1)3} \right] \tag{11.4.26}$$

11.5. References

[1] Liew, K. M., Kitipornchai, S., Zhang, X. Z., and Lim, C.W., "Analysis of the thermal stress behaviour of functionally graded hollow circular cylinders," *International Journal of Solids and Structures* 40, 2355–2380 (2003).

[2] Shao, Z. S., "Mechanical and thermal stresses of a functionally graded circular hollow cylinder with finite length," *International Journal of Pressure Vessels an Piping* 82, 155–163 (2005).

[3] Mian, M., Abid, and Spencer, A. J. M., "Exact solutions for functionally graded and laminated elastic materials," *J. Mech. Phys. Solids*, 46(12), 2283–2295 (1998).

[4] Fraldi, M., and Cowin, S. C., "Inhomogeneous elastostatic problem solutions constructed from stress-associated homogeneous solutions," *Journal of the Mechanics and Physics of Solids* 52, 2207–2233 (2004).

[5] Alshits, V. I., and Kirchner, O. K., "Cylindrically anisotropic, radially inhomogeneous elastic materials," *Proc. Roy. Soc. Lond*. A457, 671–693 (2001).

[6] Chouchaoui, C. S., and Ochoa, O. O., "Similitude study for a laminated cylindrical tube under tensile, torsion, bending, internal and external pressure. Part I: governing equations," *Composite Structures* 44, 221–229 (1999).

[7] Chen, T., Chung, C. T., and Lin, W. L., "A revisit of a cylindrically anisotropic tube subjected to pressuring, shearing, torsion, extension and a uniform temperature change," *International Journal of Solids and Structures* 37, 5143–5159 (2000).

[8] Tarn, J. Q., "Exact solutions for functionally graded anisotropic cylinders subjected to thermal and mechanical loads," *International Journal of Solids and Structures*, 38, 8189–8206 (2001).

[9] Tarn, J. Q., and Wang, Y. M., "Laminated composite tubes under extension, torsion, bending, shearing and pressuring: a state space approach," *International Journal of Solids and Structures* 38, 9053–9075 (2001).

[10] Lekhnitskii, S. G., *Theory of Elasticity of an Anisotropic Body*, Mir, Moscow, 1981.

[11] Huang, C. H., and Dong, S. B., "Analysis of laminated circular cylinders of materials with the most general form of cylindrical anisotropy. I. Axially symmetric deformations," *International Journal of Solids and Structures* 38, 6163–6182 (2001).

[12] Love, A. E. H., *A Treatise on the Mathematical Theory of Elasticity*, Dover Publications, Inc, New York, 1944.

[13] Bernini, M., Fraldi, A., Minardo, V., Minutolo, F., Carannante, L., and Nunziante, L., Zeni, "Optical fiber-sensor measurements for safety assessment and monitoring of bridges and large structures," *Bridge Structures* 1(3), 355–363 (2005).

[14] Fraldi, M., Nunziante, L., Carannante, F. (2007), *Axis-symmetrical Solutions for n-plies Functionally Graded Material Cylinders under Strain no-Decaying Conditions*, J. Mech. of Adv. Mat. and Struct. Vol. 14 (3), pp. 151-174 - DOI: 10.1080/15376490600719220

[15] M. Fraldi, L. Nunziante, F. Carannante, A. Prota, G. Manfredi, E. Cosenza (2008), *On the Prediction of the Collapse Load of Circular Concrete Columns Confined by FRP*, Journal Engineering structures, Vol. 30, Issue 11, November 2008, Pages 3247-3264 - DOI: 10.1016/j.engstruct.2008.04.036

[16] Fraldi, M., Nunziante, L., Chandrasekaran, S., Carannante, F., Pernice, MC. (2009), *Mechanics of distributed fibre optic sensors for strain measurements on rods*, Journal of Structural Engineering, 35, pp. 323-333, Dec. 2008- Gen. 2009
[17] M. Fraldi, F. Carannante, L. Nunziante (2012), *Analytical solutions for n-phase Functionally Graded Material Cylinders under de Saint Venant load conditions: Homogenization and effects of Poisson ratios on the overall stiffness*, Composites Part B: Engineering, Volume 45, Issue 1, February 2013, Pages 1310–1324
[18] Nunziante, L., Gambarotta, L., Tralli, A., *Scienza delle Costruzioni*, 3° Edizione, McGraw-Hill, 2011, ISBN: 9788838666971
[19] Nobuyuki, Y., and Imai, T., "Stimulated Brillouin scattering suppression by means of applying strain distribution to fiber with cabling," *Journal of Lightwave Technology* 11, 1519–1522 (1993).
[20] Nickl`es, M., et al., "Simple distribuited fiber sensor based on Brillouin scattering gain spectrum analysis," *Optics Letters* 21, 758–761 (1996).
[21] Gusev, V., Picart, P., Mounier, D., and Breteau, J. M., "On the possibility of ultrashort shear acoustic pulse excitation due to the laser-induced electrostrictive effect," *Optics Communications*, 204, 229–234 (2002).
[22] Ye, J. Q., "Decay rate of edge effects in cross-ply-laminated hollow cylinders," *International Journal of Mechanical Sciences* 43, 455–470 (2001).
[23] Ye, J. Q., and Sheng, H. Y., "Free-edge effect in cross-ply laminated hollow cylinders subjected to axisymmetric transverse loads," *International Journal of Mechanical Sciences* 45, 1309–1326 (2003).
[24] Ye, J. Q., "Edge effects in angle-ply laminated hollowcylinders," *Composite Structures* 52, 247–253 (2001).
[25] Ansari, F., and Yuan, L., "Mechanics of bond and interface shear transfer in optical fiber sensors," *Journal of Engineering Mechanics* 124(4), 385–394 (1998).
[26] Gurtin, M. E., *The Linear Theory of Elasticity*, *Handbbuch der Physik*, Springer, Berlin, 1972.
[27] Wolfram, S., *Mathematica, version 5*, Wolfram Research, Inc., Champaign, IL, 1998–2005.

CHAPTER XII
MULTILAYERED CYLINDER CONSTITUTED BY ORTHOTROPIC PHASES UNDER AXIAL LOAD

12.1. Introduction

Today, usage of composite materials in aeronautic industries, submarines, automotive engineering, sport equipments and etc has been noticeably progressed. This remarkable usage of these kinds of materials is because of its high strength and having high module with low density.
Therefore, in many applications, use of these materials is commodious compare to isotropic materials and these materials are preferable. So far, a lot of researches have been carried out about mechanical and thermo mechanical behaviour of composite laminates while very few works are available about heat transfer of these materials [1]-[3]. Primary research in this field has been carried out on anisotropic crystals [4],[5]. Ma and Chang [6] studied analytical heat conduction in anisotropic multilayer media. They changed anisotropic problem to a simple isotropic problem by using a linear coordinate transformation. There are some accomplished researches about heat transfer in composite materials that are reviewed briefly. Kulkarani and Brady [7] presented a thermal mathematical model for heat transfer in laminated carbon composites. This model was based on volumetric percentage of matrix and fibres and using of this model also heat transfer coefficient indirection of fibres and perpendicular to fibres has been estimated. Johansson and Lesnic [8] showed applications of MFS methods for transient heat conduction in layered materials and developed this method for numerical estimation of heat flux in these materials. Sun and Wichman [9] presented a theoretical solution for transient heat transfer in a one-dimensional three layer composite slab and compared obtained resultants with finite element solution. Karageorghis and Lesnic [10] introduced a solution for heat conduction in laminated composite material that its conduction coefficient was dependence to temperature and boundary condition consisted of convection and radiation. Haji-sheikh *et al.* [11] obtained a mathematical formulation for steady-state heat conduction and temperature distribution in multi-layer bodies. They affirmed that if layers are homogenous, eigenvalues will be real numbers but for orthotropic state these values can be imaginary numbers. Guo *et al*. [12] studied temperature distribution in thick polymeric matrix laminates and compared it with results of numerical solution. They solved transient heat transfer in polymeric matrix composite laminates using finite element method. They considered the internal energy generation due to chemical reactions in the heat transfer equation. Singh *et al.* [13] obtained an analytical solution for conductive heat transfer in multilayer polar coordinate system in radial direction. Bahadur and Bar-Cohen [14] presented analytical solution for temperature distribution and heat flux in a cylindrical fin with orthotropic conductive coefficient and compared its results with obtained results from finite element solution. Onyejekwe [15] obtained an exact analytical solution for conductive heat transfer in composite media using boundary integral theory.
Tarn and Wang [16],[17] studied conductive heat transfer in cylinders that are made of functional graded material (FGM) and composite laminates. Furthermore, many studies about conductive heat transfer have been carried out in nano-composites [18],[19]. One of the applications of composite materials is in manufacturing super conductive materials. Cha *et al*. [20] investigated inverse temperature distribution and heat generation in super conductor composite materials.
In this framework, the present chapter will firstly develop an analytical approach to find exact elastic solutions for multilayered cylinder, constituted by *n* cylindrical hollow phases and a central core, each of them modelled as homogeneous and cylindrically anisotropic material. This new solutions for the *n jacket* phases cylindrically anisotropic are given, by means of a mathematical procedure that yields to reduce the differential anisotropic boundary value problem (BVP) in the equivalent linear algebraic one. The closed-form solutions are finally obtained in the realm of the Complex Potential theory, for an arbitrary number of phases *n*.

12.2. Elastic solutions for multilayered cylinder constituted by *N* cylindrically orthotropic phase

12.2.1. Field equations for the i-th phase

In this section, let us consider multilayered cylinder composed by an isotropic core, and by n orthotropic cylindrical shells: r,θ,z are the principal directions of the material cylindrical orthotropy. With reference to the cylindrical coordinate system $\{r,\theta,z\}$, the equilibrium equations, in the absence of body forces, are:

$$\begin{cases} \sigma_{rr,r} + r^{-1}\tau_{r\theta,\theta} + \tau_{rz,z} + r^{-1}\left(\sigma_{rr} - \sigma_{\theta\theta}\right) = 0 \\ \tau_{r\theta,r} + r^{-1}\sigma_{\theta\theta,\theta} + \tau_{\theta z,z} + 2r^{-1}\tau_{r\theta} = 0 \\ \tau_{rz,r} + r^{-1}\tau_{\theta z,\theta} + \sigma_{zz,z} + r^{-1}\tau_{rz} = 0 \end{cases} \tag{12.2.1}$$

In the framework of the analysis of multilayered cylinder, due to the cylindrical geometry of the phases, it results extremely useful to adopt the formalism introduced by Ting [31], which yields to rewrite the equilibrium equations (12.2.1) in vector form, introducing the "emerging" stresses (e.g. tractions on the boundary surface of a single phase) as follows:

$$\left(r\,\mathbf{t}_r\right)_{,r} + \left(\mathbf{t}_\theta\right)_{,\theta} + r\,\mathbf{t}_{z,z} + \mathbf{K}\,\mathbf{t}_\theta = 0 \tag{12.2.2}$$

where

$$\mathbf{t}_r = \begin{bmatrix} \sigma_{rr} \\ \tau_{r\theta} \\ \tau_{rz} \end{bmatrix}, \quad \mathbf{t}_\theta = \begin{bmatrix} \tau_{\theta r} \\ \sigma_{\theta\theta} \\ \tau_{\theta z} \end{bmatrix}, \quad \mathbf{t}_z = \begin{bmatrix} \tau_{zr} \\ \tau_{z\theta} \\ \sigma_{zz} \end{bmatrix}, \tag{12.2.3}$$

represent the traction vectors on the surfaces $r = const.$, $\theta = const.$, and $z = const.$, respectively, and $\mathbf{K}$ is a 3x3 constant matrix given by

$$\mathbf{K} = \begin{bmatrix} 0 & -1 & 0 \\ 1 & 0 & 0 \\ 0 & 0 & 0 \end{bmatrix} \quad . \tag{12.2.4}$$

The relations between the strain ε_{ij} and displacement u_i are:

$$\begin{aligned} &\varepsilon_{rr} = u_{r,r}, \quad \varepsilon_{\theta\theta} = r^{-1}\left(u_{\theta,\theta} + u_r\right), \quad \gamma_{r\theta} = r^{-1}\left(u_{r,\theta} + r\,u_{\theta,r} - u_\theta\right) \\ &\varepsilon_{zz} = u_{z,z}, \quad \gamma_{rz} = u_{z,r} + u_{r,z}, \quad \gamma_{\theta z} = r^{-1}\left(u_{z,\theta} + r\,u_{\theta,z}\right), \end{aligned} \tag{12.2.5}$$

Under the assumption of cylindrical anisotropy, by identifying $\left(x,y,z\right) \equiv \left(r,\theta,z\right)$ the stress-strain law becomes:

$$\sigma_{ij} = C_{ijhk}\varepsilon_{hk} \quad . \tag{12.2.6}$$

Hence

$$\left(\mathbf{t}_r\right)_j = \sigma_{rj} = C_{1jhk}\varepsilon_{hk} = C_{1j11}\varepsilon_{rr} + C_{1j22}\varepsilon_{\theta\theta} + C_{1j33}\varepsilon_{zz} + C_{1j23}\gamma_{\theta z} + C_{1j13}\gamma_{rz} + C_{1j12}\gamma_{r\theta} \tag{12.2.7}$$

Similar equations hold for $\left(\mathbf{t}_\theta\right)_j$ and for $\left(\mathbf{t}_z\right)_j$. Making use of (12.2.5) it can be shown that:

$$\begin{aligned} \mathbf{t}_r &= \mathbf{Q}\,\mathbf{u}_{,r} + r^{-1}\mathbf{R}\left(\mathbf{u}_{,\theta} + \mathbf{K}\,\mathbf{u}\right) + \mathbf{P}\,\mathbf{u}_{,z} \\ \mathbf{t}_\theta &= \mathbf{R}^T\,\mathbf{u}_{,r} + r^{-1}\mathbf{T}\left(\mathbf{u}_{,\theta} + \mathbf{K}\,\mathbf{u}\right) + \mathbf{S}\,\mathbf{u}_{,z} \\ \mathbf{t}_z &= \mathbf{P}^T\,\mathbf{u}_{,r} + r^{-1}\mathbf{S}^T\left(\mathbf{u}_{,\theta} + \mathbf{K}\,\mathbf{u}\right) + \mathbf{M}\,\mathbf{u}_{,z} \end{aligned} \tag{12.2.8}$$

where superscript "*T*" means "transposition", and

$$\mathbf{u}^T = \begin{bmatrix} u_r & u_\theta & u_z \end{bmatrix} \tag{12.2.9}$$

while $\mathbf{Q},\mathbf{R},\mathbf{P},\mathbf{M},\mathbf{T},\mathbf{S},$ are 3x3 matrices, explicitly reported below:

$$\mathbf{Q}=\begin{bmatrix} c_{11} & c_{16} & c_{15} \\ c_{16} & c_{66} & c_{56} \\ c_{15} & c_{56} & c_{55} \end{bmatrix},\mathbf{R}=\begin{bmatrix} c_{16} & c_{12} & c_{14} \\ c_{66} & c_{26} & c_{46} \\ c_{56} & c_{25} & c_{45} \end{bmatrix},\mathbf{P}=\begin{bmatrix} c_{15} & c_{14} & c_{13} \\ c_{56} & c_{46} & c_{36} \\ c_{55} & c_{45} & c_{35} \end{bmatrix}$$
$$\mathbf{M}=\begin{bmatrix} c_{55} & c_{45} & c_{35} \\ c_{45} & c_{44} & c_{34} \\ c_{35} & c_{34} & c_{33} \end{bmatrix},\mathbf{T}=\begin{bmatrix} c_{66} & c_{26} & c_{46} \\ c_{26} & c_{22} & c_{24} \\ c_{46} & c_{24} & c_{44} \end{bmatrix},\mathbf{S}=\begin{bmatrix} c_{56} & c_{46} & c_{36} \\ c_{25} & c_{24} & c_{23} \\ c_{45} & c_{44} & c_{34} \end{bmatrix}. \tag{12.2.10}$$

Substitution of (12.2.8) in (12.2.2) leads to a differential equation for $\mathbf{u}$. It should be pointed out that the elastic constants C_{ijhk} are here referred to the cylindrical coordinate system. Therefore the matrices $\mathbf{Q},\mathbf{R},\mathbf{P},\mathbf{M},\mathbf{T},\mathbf{S},$ are not constant matrices even for homogeneous materials, that is – for example – in a Cartesian reference system. In particular, for a *cylindrically anisotropic* material , the matrices $\mathbf{Q},\mathbf{R},\mathbf{P},\mathbf{M},\mathbf{T},\mathbf{S},$ are constant. By inserting (12.2.8) into (12.2.2) a single equation for the displacement $\mathbf{u}$ is obtained as follows:

$$\begin{aligned} &r^2\left(\mathbf{Q}\,\mathbf{u}_{,rr}+\mathbf{M}\,\mathbf{u}_{,zz}\right)+\mathbf{T}\,\mathbf{u}_{,\theta\theta}+r\left[\left(\mathbf{R}+\mathbf{R}^T\right)\mathbf{u}_{,r\theta}+r\left(\mathbf{P}+\mathbf{P}^T\right)\mathbf{u}_{,rz}+\left(\mathbf{S}+\mathbf{S}^T\right)\mathbf{u}_{,\theta z}\right]+ \\ &+r\left(\mathbf{R}\,\mathbf{K}+\mathbf{K}\,\mathbf{R}^T+\mathbf{Q}\right)\mathbf{u}_{,r}+\left(\mathbf{T}\,\mathbf{K}+\mathbf{K}\,\mathbf{T}\right)\mathbf{u}_{,\theta}+r\left(\mathbf{K}\,\mathbf{S}+\mathbf{S}^T\mathbf{K}+\mathbf{P}\right)\mathbf{u}_{,z}+\mathbf{K}\,\mathbf{T}\,\mathbf{K}\,\mathbf{u}=0 \end{aligned} \tag{12.2.11}$$

In the case that the material possesses cylindrically orthotropy, the linearly elastic constitutive relation of the i[th] phase, in the Voigt notation, is

$$\sigma_k=C_{kj}^{(i)}\varepsilon_j \tag{12.2.12}$$

where stress and strain vectors and the Elasticity matrix are respectively:

$$\left[\sigma_k\right]=\begin{bmatrix} \sigma_{rr} \\ \sigma_{\theta\theta} \\ \sigma_{zz} \\ \tau_{\theta z} \\ \tau_{rz} \\ \tau_{r\theta} \end{bmatrix},\ \left[\varepsilon_j\right]=\begin{bmatrix} \varepsilon_{rr} \\ \varepsilon_{\theta\theta} \\ \varepsilon_{zz} \\ \gamma_{\theta z} \\ \gamma_{rz} \\ \gamma_{r\theta} \end{bmatrix},\ \mathbb{C}^{(i)}=\begin{bmatrix} c_{11}^{(i)} & c_{12}^{(i)} & c_{13}^{(i)} & 0 & 0 & 0 \\ c_{12}^{(i)} & c_{22}^{(i)} & c_{23}^{(i)} & 0 & 0 & 0 \\ c_{13}^{(i)} & c_{23}^{(i)} & c_{33}^{(i)} & 0 & 0 & 0 \\ 0 & 0 & 0 & c_{44}^{(i)} & 0 & 0 \\ 0 & 0 & 0 & 0 & c_{55}^{(i)} & 0 \\ 0 & 0 & 0 & 0 & 0 & c_{66}^{(i)} \end{bmatrix}$$

and the superscript (i) denotes the elastic moduli of the generic *i*-th phase of multilayered cylinder. As a consequence, the matrices (12.2.10) become:

$$\mathbf{Q}=\begin{bmatrix} c_{11} & 0 & 0 \\ 0 & c_{66} & 0 \\ 0 & 0 & c_{55} \end{bmatrix},\mathbf{R}=\begin{bmatrix} 0 & c_{12} & 0 \\ c_{66} & 0 & 0 \\ 0 & 0 & 0 \end{bmatrix},\mathbf{P}=\begin{bmatrix} 0 & 0 & c_{13} \\ 0 & 0 & 0 \\ c_{55} & 0 & 0 \end{bmatrix},$$
$$\mathbf{M}=\begin{bmatrix} c_{55} & 0 & 0 \\ 0 & c_{44} & 0 \\ 0 & 0 & c_{33} \end{bmatrix},\mathbf{T}=\begin{bmatrix} c_{66} & 0 & 0 \\ 0 & c_{22} & 0 \\ 0 & 0 & c_{44} \end{bmatrix},\mathbf{S}=\begin{bmatrix} 0 & 0 & 0 \\ 0 & 0 & c_{23} \\ 0 & c_{44} & 0 \end{bmatrix}. \tag{12.2.13}$$

Let us now consider the case of axis-symmetry of both the geometry of multilayered cylinder and of the load conditions, in which the displacement field is therefore independent from the variable θ, as well as the displacement component u_θ vanishes. The equilibrium equation (12.2.11) becomes:

$$\begin{aligned} &r^2\left[\mathbf{Q}\,\mathbf{u}_{,rr}+\mathbf{M}\,\mathbf{u}_{,zz}+\left(\mathbf{P}+\mathbf{P}^T\right)\mathbf{u}_{,rz}\right]+\mathbf{K}\,\mathbf{T}\,\mathbf{K}\,\mathbf{u}+ \\ &+r\left(\mathbf{R}\,\mathbf{K}+\mathbf{K}\,\mathbf{R}^T+\mathbf{Q}\right)\mathbf{u}_{,r}+r\left(\mathbf{K}\,\mathbf{S}+\mathbf{S}^T\mathbf{K}+\mathbf{P}\right)\mathbf{u}_{,z}=0 \end{aligned} \tag{12.2.14}$$

Due to the results obtained by the Authors in a previous work [26,27,29], we now find the displacement field solution for multilayered cylinder under pure axial loads in the form:

$$\mathbf{u}^T=\left[u_r(r),\,0,\,\varepsilon_0\,z\right] \tag{12.2.15}$$

where ε_{zz} is a real scalar parameter to determine, that we will discover to be the same for all phases of the solid [26]. Moreover, the equilibrium equation (12.2.14) reduces to the following scalar one:

$$c_{11}\, r\left[r\, u_r^{''}(r)+u_r^{'}(r)\right]-c_{22}u_r(r)+\varepsilon_0\left(c_{13}-c_{23}\right)r=0 \qquad (12.2.16)$$

By recalling the classical results of the Complex Potential Theory [24] for anisotropic elastic materials, we can assume the solution of the homogeneous equation related to equation (12.2.16), with the form $u_r^H(r)=C_1\, r^{\lambda_1}+iC_2 r^{\lambda_2}$, so that the following characteristic polynomials in λ_1 and λ_2 are given:

$$\begin{cases} c_{22}-c_{11}\lambda_1^2=0 \\ c_{22}-c_{11}\lambda_2^2=0 \end{cases} \Rightarrow \quad \lambda_1=\lambda_2=\pm\sqrt{c_{22}/c_{11}} \qquad . \qquad (12.2.17)$$

The result (12.2.17) leads to construct the general form of the homogeneous solution $u_r^H\left(r\right)$ as follows:

$$u_r^H(r)=C_1\left(r^{\sqrt{c_{22}/c_{11}}}+r^{-\sqrt{c_{22}/c_{11}}}\right)+i\,C_2\left(r^{\sqrt{c_{22}/c_{11}}}+r^{-\sqrt{c_{22}/c_{11}}}\right) \qquad . \qquad (12.2.18)$$

Moreover, a particular solution u_r^P of equation (12.2.16) is trivially obtained

$$u_r^P(r)=\frac{\varepsilon_0(c_{23}-c_{13})}{(c_{11}-c_{22})}r \qquad . \qquad (12.2.19)$$

Thus, the general integral of equation(12.2.16) is writeable as:

$$u_r(r)=u_r^P(r)+u_r^H(r)=\frac{\varepsilon_0(c_{23}-c_{13})}{(c_{11}-c_{22})}r+C_1\cosh\left(\sqrt{\frac{c_{22}}{c_{11}}}\log r\right)+i\,C_2\sinh\left(\sqrt{\frac{c_{22}}{c_{11}}}\log r\right) \qquad (12.2.20)$$

where i is unit imaginary. By substituting the displacement function (12.2.20) in to compatibility equations (12.2.5), we obtain the following expression for the strain components:

$$\begin{aligned}
\varepsilon_{rr}&=\frac{\varepsilon_0\left(c_{23}-c_{13}\right)}{\left(c_{11}-c_{22}\right)}+\frac{C_1}{r}\sqrt{\frac{c_{22}}{c_{11}}}\sinh\left(\sqrt{\frac{c_{22}}{c_{11}}}\log r\right)+i\frac{C_2}{r}\sqrt{\frac{c_{22}}{c_{11}}}\cosh\left(\sqrt{\frac{c_{22}}{c_{11}}}\log r\right),\\
\varepsilon_{\theta\theta}&=\frac{\varepsilon_0\left(c_{23}-c_{13}\right)}{\left(c_{11}-c_{22}\right)}+\frac{C_1}{r}\cosh\left(\sqrt{\frac{c_{22}}{c_{11}}}\log r\right)+i\frac{C_2}{r}\sinh\left(\sqrt{\frac{c_{22}}{c_{11}}}\log r\right), \qquad (12.2.21)\\
\varepsilon_{zz}&=\varepsilon_0,\quad \gamma_{r\theta}=\gamma_{rz}=\gamma_{\theta z}=0,
\end{aligned}$$

where $\varepsilon_{ij}=\gamma_{ij}/2$, $i\neq j$. From the constitutive law for cylindrically orthotropic material (12.2.12), the no-zero stress components assume the following explicit form:

$$\begin{aligned}
\sigma_{rr}&=\frac{\varepsilon_0\left[c_{23}\left(c_{11}+c_{12}\right)-c_{13}\left(c_{22}+c_{12}\right)\right]}{c_{11}-c_{22}}+\left(C_1c_{12}+i\,C_2\sqrt{c_{11}c_{22}}\right)r^{-1}\cosh\left(\sqrt{c_{22}/c_{11}}\log r\right)+\\
&\left(C_1\sqrt{c_{11}c_{22}}+i\,C_2c_{12}\right)r^{-1}\sinh\left(\sqrt{c_{22}/c_{11}}\log r\right)\\
\sigma_{\theta\theta}&=\frac{\varepsilon_0\left[c_{23}\left(c_{11}+c_{12}\right)-c_{13}\left(c_{22}+c_{12}\right)\right]}{c_{11}-c_{22}}+r^{-1}\left(C_1c_{12}+i\,C_2\sqrt{c_{11}c_{22}}\right)\sqrt{c_{22}/c_{11}}\sinh\left(\sqrt{c_{22}/c_{11}}\log r\right)+\\
&r^{-1}\left(C_1\sqrt{c_{11}c_{22}}+i\,C_2c_{12}\right)\sqrt{c_{22}/c_{11}}\cosh\left(\sqrt{c_{22}/c_{11}}\log r\right),\\
\sigma_{zz}&=\frac{\varepsilon_0\left[c_{23}^2-c_{13}^2+c_{33}\left(c_{11}-c_{22}\right)\right]}{c_{11}-c_{22}}+r^{-1}\left(C_1\,c_{23}+i\,C_2\,c_{13}\sqrt{c_{22}/c_{11}}\right)\cosh\left(\sqrt{c_{22}/c_{11}}\log r\right)+\\
&\left(C_1\,c_{13}\sqrt{c_{22}/c_{11}}+iC_2\,c_{23}\right)\sinh\left(\sqrt{c_{22}/c_{11}}\log r\right),
\end{aligned} \qquad (12.2.22)$$

It is worth to note that the found solution results able to also represent, as particular cases, the situations where isotropy or different types of transverse isotropy occur. In order to show this property of the solution, we summarize in the following these special cases:

A) In the case in which the material possesses transverse isotropy, with plane of isotropy coincident with the (r,θ)-plane, we will have:

$$c_{22}=c_{11},\quad c_{23}=c_{13},\quad c_{55}=c_{44},\quad c_{66}=\left(c_{11}-c_{12}\right)/2,$$

and, by virtue of (19), the displacement components become:

$$u_r=C_1\,r+C_2\,r^{-1},\quad u_\theta=0,\quad u_z=\varepsilon_0\,z\ . \tag{12.2.23}$$

B) In the case in which the material possesses transverse isotropy, with plane of isotropy coincident with the (r,z)-plane, we will have:

$$c_{33}=c_{11},\quad c_{23}=c_{12},\quad c_{66}=c_{44},\quad c_{55}=\left(c_{11}-c_{13}\right)/2,$$

and the displacement components reduce to:

$$u_r=\frac{\varepsilon_0(c_{12}-c_{13})}{(c_{11}-c_{22})}r+C_1\cosh\left(\sqrt{\frac{c_{22}}{c_{11}}}\log r\right)+i\,C_2\sinh\left(\sqrt{\frac{c_{22}}{c_{11}}}\log r\right),\ u_\theta=0,\ u_z=\varepsilon_0\,z, \tag{12.2.24}$$

C) In the case in which the material possesses transverse isotropy, with plane of isotropy coincident with the (θ,z)-plane, we will have:

$$c_{22}=c_{33},\quad c_{12}=c_{13},\quad c_{66}=c_{55},\quad c_{44}=\left(c_{22}-c_{23}\right)/2,$$

and the displacement components assume the form:

$$u_r=\frac{\varepsilon_0(c_{23}-c_{12})}{(c_{11}-c_{22})}r+C_1\cosh\left(\sqrt{\frac{c_{22}}{c_{11}}}\log r\right)+i\,C_2\sinh\left(\sqrt{\frac{c_{22}}{c_{11}}}\log r\right),\ u_\theta=0,\ u_z=\varepsilon_0\,z. \tag{12.2.25}$$

The case of full isotropy is treated in [26].

12.2.2. Equilibrium and compatibility conditions at the interfaces

By making reference to an multilayered cylinder made of an central isotropic *core* and to $n\in\mathbb{N}$ arbitrary hollow phases, the displacement field for to the core is [26]:

$$u_r^{(0)}=\varepsilon_r^{(0)}r,\quad u_\theta^{(0)}=0,\quad u_z^{(0)}=\varepsilon_0^{(0)}z \tag{12.2.26}$$

while the displacement components for the *i*-th generic phase are (12.2.20):

$$u_r^{(i)}=\frac{\varepsilon_0^{(i)}(c_{23}^{(i)}-c_{13}^{(i)})}{(c_{11}^{(i)}-c_{22}^{(i)})}r+C_1^{(i)}\cosh\left(\sqrt{\frac{c_{22}^{(i)}}{c_{11}^{(i)}}}\log r\right)+i\,C_2^{(i)}\sinh\left(\sqrt{\frac{c_{22}^{(i)}}{c_{11}^{(i)}}}\log r\right) \tag{12.2.27}$$

$$u_\theta^{(i)}=0,\quad u_z^{(i)}=\varepsilon_0^{(i)}z.$$

The stress components for *i*-th generic phase are given by equation (12.2.22), but the stress components for core phase are reported below:

$$\begin{aligned}&\sigma_{rr}^{(0)}=\left(c_{11}^{(0)}+c_{12}^{(0)}\right)\varepsilon_r^{(0)}+c_{12}^{(0)}\varepsilon_0^{(0)},\quad \sigma_{\theta\theta}^{(0)}=\left(c_{11}^{(0)}+c_{12}^{(0)}\right)\varepsilon_r^{(0)}+c_{12}^{(0)}\varepsilon_0^{(0)}\\&\sigma_{zz}^{(0)}=2c_{12}^{(0)}\varepsilon_r^{(0)}+c_{11}^{(0)}\varepsilon_0^{(0)}\end{aligned} \tag{12.2.28}$$

As reported in Fraldi and Cowin [25], the displacement field (12.2.26) for the core is assumed by considering isotropy in this solid central phase, due to the inadmissibility of cylindrical anisotropy at $r=0$. The equations above obtained satisfy equilibrium and compatibility equations in the inner of each phase of multilayered cylinder. Then, it remains to consider the boundary conditions at the interfaces, where perfect bond is assumed. In particular, we will analyse a special load condition, that is the sole presence of axial forces applied at the extremities of the object. The unknown parameters to determine are here summarized by the sole:

$$\begin{aligned}&\varepsilon_r^{(0)},\varepsilon_0^{(0)},\\&\varepsilon_0^{(i)},C_1^{(i)},C_2^{(i)}\quad \forall i\in\{1,2,....,n\}\end{aligned} \tag{12.2.29}$$

The constants in equation (12.2.29)$_1$ represent the unknown coefficients of the *core*, while the other ones in (12.2.29)$_2$, whose number is $3\times n$, represent the unknown parameters corresponding to the hollow phases. Hence, the total number of unknowns will be $(2+3\times n)$, which equals the number of algebraic equations to solve. In particular, as we will show in the following, the boundary equations at the interfaces are 3, while the boundary conditions on the external cylindrical surface and on the end basis are two. We can begin by writing the equilibrium and compatibility equations at the interfaces, that is:

$$\begin{cases} u_z^{(i)}(r=R^{(i)}) = u_z^{(i+1)}(r=R^{(i)}) \\ u_r^{(i)}(r=R^{(i)}) = u_r^{(i+1)}(r=R^{(i)}) \\ \sigma_{rr}^{(i)}(r=R^{(i)}) = \sigma_{rr}^{(i+1)}(r=R^{(i)}) \end{cases} \qquad i\in\{0,1,2,...,n-1\} \tag{12.2.30}$$

where $R^{(i)}$ is the outer radius of the generic phase. The Cauchy equilibrium equation on the external cylindrical boundary surface, in the absence of applied traction, gives:

$$\sigma_{rr}^{(n)}(r=R^{(n)}) = 0 \tag{12.2.31}$$

Finally, it remains to consider the last equilibrium equations along the z-direction on one of the end bases of the object. Without loss of generality, we can consider the weak condition at $z=0$, writing:

$$\sum_{i=0}^{n}\int_0^{2\pi}\int_0^{R^{(i)}} \sigma_{zz}^{(i)} r dr d\theta = N_z \tag{12.2.32}$$

where $\mp N_z$ are the axial forces applied on the bases $z=0,\ z=L$, respectively.

Making explicit (12.2.30$_1$) and by means of the polynomial identity law, we have:

$$\varepsilon_0^{(0)} = ... = \varepsilon_0^{(i)} = \varepsilon_0^{(i+1)} = ... = \varepsilon_0^{(n)}. \tag{12.2.33}$$

Therefore, by recalling (12.2.26) and (12.2.27), the equation (12.2.30$_2$) furnishes:

$$\begin{aligned} &\delta_{0i}(\varepsilon_r^{(0)}R^{(0)}) + (1-\delta_{0i})\left[\varepsilon_0^{(0)}\alpha^{(i)}R^{(i)} + C_1^{(i)}\cosh\left(\eta^{(i)}\log R^{(i)}\right) + iC_2^{(i)}\sinh\left(\eta^{(i)}\log R^{(i)}\right)\right] = \\ &= \varepsilon_0^{(0)}\alpha^{(i+1)}R^{(i)} + C_1^{(i+1)}\cosh\left(\eta^{(i+1)}\log R^{(i)}\right) + iC_2^{(i+1)}\sinh\left(\eta^{(i+1)}\log R^{(i)}\right) \qquad \forall i\in\{0,1,...n-1\} \end{aligned} \tag{12.2.34}$$

Equation (12.2.30$_3$) can be rewriting as follows

$$\begin{aligned} &\delta_{0i}\left[\varepsilon_r^{(0)}\left(c_{11}^{(i)}+c_{12}^{(i)}\right)+c_{13}^{(i)}\varepsilon_0^{(0)}\right] + (1-\delta_{0i})\left[\varepsilon_0^{(0)}\beta^{(i)} + \left(\frac{C_1^{(i)}c_{12}^{(i)} + iC_2^{(i)}\Lambda^{(i)}}{R^{(i)}}\right)\cosh\left(\eta^{(i)}\log R^{(i)}\right)\right] + \\ &+ (1-\delta_{0i})\left[\left(\frac{C_1^{(i)}\Lambda^{(i)} + iC_2^{(i)}c_{12}^{(i)}}{R^{(i)}}\right)\sinh\left(\eta^{(i)}\log R^{(i)}\right)\right] = \\ &= \varepsilon_0^{(0)}\beta^{(i+1)} + \left(\frac{C_1^{(i+1)}c_{12}^{(i+1)} + iC_2^{(i+1)}\Lambda^{(i+1)}}{R^{(i)}}\right)\cosh\left(\eta^{(i+1)}\log R^{(i)}\right) + \\ &+ \left(\frac{C_1^{(i+1)}\Lambda^{(i+1)} + iC_2^{(i+1)}c_{12}^{(i+1)}}{R^{(i)}}\right)\sinh\left(\eta^{(i+1)}\log R^{(i)}\right) \qquad \forall i\in\{0,1,...n-1\} \end{aligned} \tag{12.2.35}$$

Finally, the boundary condition (12.2.31) becomes

$$\begin{aligned} &\varepsilon_0^{(0)}\beta^{(n)} + \left(\frac{C_1^{(n)}c_{12}^{(n)} + iC_2^{(n)}\Lambda^{(n)}}{R^{(n)}}\right)\cosh\left(\eta^{(n)}\log R^{(n)}\right) + \\ &+ \left(\frac{C_1^{(n)}\Lambda^{(n)} + iC_2^{(n)}c_{12}^{(n)}}{R^{(n)}}\right)\sinh\left(\eta^{(n)}\log R^{(n)}\right) = 0 \end{aligned} \tag{12.2.36}$$

where the following parameters were assumed:

$$\eta^{(i)}=\sqrt{\frac{c_{22}^{(i)}}{c_{11}^{(i)}}},\quad \Lambda^{(i)}=\sqrt{c_{22}^{(i)}c_{11}^{(i)}},\quad \alpha^{(i)}=\frac{(c_{23}^{(i)}-c_{13}^{(i)})}{(c_{11}^{(i)}-c_{22}^{(i)})},$$
$$\beta^{(i)}=\frac{\left[c_{23}^{(i)}\left(c_{11}^{(i)}+c_{12}^{(i)}\right)-c_{13}^{(i)}\left(c_{22}^{(i)}+c_{12}^{(i)}\right)\right]}{c_{11}^{(i)}-c_{22}^{(i)}},\quad \gamma^{(i)}=\frac{\left[c_{23}^{2}-c_{13}^{2}+c_{33}\left(c_{11}-c_{22}\right)\right]}{c_{11}-c_{22}}. \tag{12.2.37}$$

Then, the algebraic system to solve is composed by 2n+2 equations. This algebraic system is given by equations (12.2.32), (12.2.34), (12.2.35) and (12.2.36). The 2n+2 unknown parameters to determine are given by:

$$\left\{\varepsilon_r^{(0)},\varepsilon_0^{(0)}\right\},\quad \left\{C_1^{(i)},C_2^{(i)}\right\}\quad \forall i\in\{1,2,....,n\} \tag{12.2.38}$$

12.3. Closed-form elastic solutions for multilayered cylinder constituted by isotropic central core and cylindrically orthotropic hollow phases

Let us now consider the case in which the multilayered cylinder is constituted by an isotropic central core and an cylindrically orthotropic hollow phase, under axis-symmetrical boundary conditions characterized by the sole presence of axial forces applied at the extremities of composite solid. In fact this one is a particular case of great utility for many applications. In this case, the displacements field for the two phase are represented by the equations (12.2.26) and (12.2.27) respectively, while (12.2.28) furnishes the stress within the core and (12.2.22) gives the stresses inside the hollow phase. In the following, we will denote with the apices “0” and “1” the quantities related to core and hollow phase, respectively. In order to obtain the analytical solution of the problem in explicit form, we should solve the algebraic system corresponding to the boundary conditions (12.3.32),(12.2.34), (12.2.35) and (12.2.36) by setting i=1, for determining the four unknown coefficients $\{\varepsilon_r^{(0)},\varepsilon_0^{(0)},C_1^{(1)},C_2^{(1)}\}$ reported in equation (12.2.38) with i=1. After some algebraic manipulations, let us write the algebraic system to solve in the following matrix form :

$$\mathbf{P}\,\mathbf{X}=\mathbf{L} \tag{12.3.3}$$

where $\mathbf{X}=[\varepsilon_r^{(0)},\varepsilon_0^{(0)},C_1^{(1)},C_2^{(1)}]^T$ is the vector collecting the unknown to determine, and $\mathbf{L}=[0,0,0,N_z]^T$ represents the load vector. In the (12.3.3)

$$\mathbf{P}=\begin{bmatrix}P_{11} & P_{12} & P_{13} & P_{14}\\ P_{21} & P_{22} & P_{23} & P_{24}\\ P_{31} & P_{32} & P_{33} & P_{34}\\ P_{41} & P_{42} & P_{43} & P_{44}\end{bmatrix} \tag{12.3.4}$$

is a (4×4) square matrix containing all the geometrical and mechanical parameters characterizing the geometry of multilayered cylinder (i.e. the core radius $R^{(0)}$ and the external radius of the hollow phase, $R^{(1)}$, and the elastic constants $c_{11}^{(0)},c_{12}^{(0)}$ of the isotropic core phase and the elastic constants $c_{ij}^{(1)}$ of the cylindrically orthotropic phase. Explicitly, we have:

$$P_{11}=R^{(0)},\ P_{12}=\frac{\left(c_{23}^{(1)}-c_{13}^{(1)}\right)\eta^{(1)}R^{(0)}}{\left(\eta^{(1)2}-1\right)\Lambda^{(1)}},\ P_{13}=-\cosh\left(\eta^{(1)}\log R^{(0)}\right),\ P_{14}=-\imath\sinh\left(\eta^{(1)}\log R^{(0)}\right),$$
$$P_{21}=c_{11}^{(0)}+c_{12}^{(0)},\quad P_{22}=c_{12}^{(0)}+\frac{c_{12}^{(1)}\left(c_{23}^{(1)}-c_{13}^{(1)}\right)\eta^{(1)}+\Lambda^{(1)}\left(c_{23}^{(1)}-c_{13}^{(1)}\eta^{(1)2}\right)}{\Lambda^{(1)}\left(\eta^{(1)2}-1\right)},$$
$$P_{23}=-\left[R^{(0)}\right]^{-1}\left[c_{12}^{(1)}\cosh\left(\eta^{(1)}\log R^{(0)}\right)+\Lambda^{(1)}\sinh\left(\eta^{(1)}\log R^{(0)}\right)\right],$$
$$P_{24}=-\imath\left[R^{(0)}\right]^{-1}\left[\Lambda^{(1)}\cosh\left(\eta^{(1)}\log R^{(0)}\right)+c_{12}^{(1)}\sinh\left(\eta^{(1)}\log R^{(0)}\right)\right],$$

$$P_{31}=0,\quad P_{32}=\frac{c_{12}^{(1)}\left(c_{13}^{(1)}-c_{23}^{(1)}\right)\eta^{(1)}+\Lambda^{(1)}\left(c_{13}^{(1)}\eta^{(1)2}-c_{23}^{(1)}\right)}{\Lambda^{(1)}\left(\eta^{(1)2}-1\right)},$$

$$P_{33}=\left[R^{(1)}\right]^{-1}\left[c_{12}^{(1)}\cosh\left(\eta^{(1)}\log R^{(1)}\right)+\Lambda^{(1)}\sinh\left(\eta^{(1)}\log R^{(1)}\right)\right],$$

$$P_{34}=i\left[R^{(1)}\right]^{-1}\left[\Lambda^{(1)}\cosh\left(\eta^{(1)}\log R^{(1)}\right)+c_{12}^{(1)}\sinh\left(\eta^{(1)}\log R^{(1)}\right)\right],\quad P_{41}=2c_{12}^{(0)}\pi R^{(0)2},$$

$$P_{42}=c_{11}^{(0)}\pi R^{(0)2}+\pi\left[R^{(1)2}-R^{(0)2}\right]\left[\frac{\left(c_{13}^{(1)2}-c_{23}^{(1)2}\right)\eta^{(1)}}{\left(\eta^{(1)2}-1\right)\Lambda^{(1)}}+c_{33}^{(1)}\right],$$

$$P_{43}=\left(\frac{2\pi}{\eta^{(1)2}-1}\right)\left\{\begin{array}{l}R^{(0)}\left(c_{23}^{(1)}-c_{13}^{(1)}\eta^{(1)2}\right)\cosh\left(\eta^{(1)}\log R^{(0)}\right)+R^{(1)}\left(c_{13}^{(1)}\eta^{(1)2}-c_{23}^{(1)}\right)\cosh\left(\eta^{(1)}\log R^{(1)}\right)+\\+\left(c_{13}^{(1)}-c_{23}^{(1)}\right)\eta^{(1)}\left[R^{(0)}\sinh\left(\eta^{(1)}\log R^{(0)}\right)-R^{(1)}\sinh\left(\eta^{(1)}\log R^{(1)}\right)\right]\end{array}\right\},$$

$$P_{44}=\left(\frac{2\pi i}{\eta^{(1)2}-1}\right)\left\{\begin{array}{l}R^{(0)}\eta^{(1)}\left(c_{13}^{(1)}-c_{23}^{(1)}\right)\cosh\left(\eta^{(1)}\log R^{(0)}\right)+R^{(1)}\eta^{(1)}\left(c_{23}^{(1)}-c_{13}^{(1)}\right)\cosh\left(\eta^{(1)}\log R^{(1)}\right)+\\+\left(c_{23}^{(1)}-c_{13}^{(1)}\eta^{(1)}\right)\left[R^{(0)}\sinh\left(\eta^{(1)}\log R^{(0)}\right)-R^{(1)}\sinh\left(\eta^{(1)}\log R^{(1)}\right)\right]\end{array}\right\},\tag{12.3.5}$$

where the following parameters were assumed:

$$\eta^{(1)}=\sqrt{\frac{c_{22}^{(1)}}{c_{11}^{(1)}}},\quad \Lambda^{(1)}=\sqrt{c_{22}^{(1)}c_{11}^{(1)}},\tag{12.3.6}$$

Finally, the whole set of unknown coefficients can be obtained by inverting matrix $\mathbb{P}$, that is

$$\mathbf{X}=\mathbf{P}^{-1}\mathbf{L}=\frac{1}{\det\mathbf{P}}\tilde{\mathbf{P}}^{T}\mathbf{L}\tag{12.3.7}$$

where $\tilde{\mathbf{P}}=\mathrm{adj}[\mathbf{P}]$ is the adjoint matrix of $\mathbf{P}$ and then the *Cramer* rule has been employed, provided that $\det\mathbf{P}\neq 0$.

12.4. References

[1] C. K. Chao, F.M. Che, and M.H. Shen, "An exact solution for thermal stresses in a three-phase composite cylinder under uniform heat flow, " *Int. J. Solids and Structures*, vol.44, pp.926-940, 2007.

[2] V. Pradeep, and N. Ganesan, "Thermal buckling and vibration behaviour of multi-layer rectangular viscoelastic sandwich plates," *Journal of Sound and Vibration*, vol. 310, pp.169-183, 2008.

[3] J.Q. Tarn, "state space formalism for anisotropic elasticity. PartII: cylindrical anisotropy," *Int. J. Solids Struct*. Vol.39, pp.5157-5172, 2002.

[4] W.A. Wooster, *A textbook in crystal physics*. Cambridge University Press, London, 1957, pp.455

[5] J.F. Nye, *Physical properties of crystals*. Clarendon Press, London, 1957, pp.309.

[6] C.C. Ma and S.S Chang, "Analytical exact solutions of heat conduction problems for anisotropic multilayered media, " *Int. J. Heat and Mass Transfer* vol.47 pp.1643-1655, 2004.

[7] M.R. Kulkarani, and R.P. Brady, "A model of global thermal conductivity in laminated Carboncarbon composites, " *Composites science and Technology* vol.57, pp.277-285, 1997.

[8] B.T. Johansson, and D. Lesnic, " A method of fundamental solutions for transient heat conduction in layered materials, " *Engineering Analysis with Boundary Elements*, vol.33, pp.1362-1367, 2009.

[9] Y. Sun, and I.S. Wichman, "On transient heat conduction in a onedimensional composite slab, " *Int J Heat and Mass Transfer*, *vol.*47, pp.1555-1559, 2004.

[10] A. Karageorghis, and D. Lesnic, "Steady-state nonlinear heat conduction in composite materials, ", *Comput. Methods Appl .Mech. Engrg*, vol. 197, pp. 3122-3137, 2008.

[11] A. Haji-Sheikh, J.V. Beck, and D. Agonater, "Steady-state heat conduction in multi-layer bodies, " *Int J Heat and Mass Transfer* vol.46 pp.2363-2379, 2003.
[12] Z-S Guo, et al. "Temperature distribution of thick thermo set composites, " *J Model Simul Mater SciEng*, vol.12 pp.443-452, 2004.
[13] S. Singh, P.K. Jain, and Rizwan-uddin, "Analytical solution to transient heat conduction in polar coordinates with multiple layers in radial direction, " *Int. J. Thermal Sciences* vol.47 pp.261–273, 2008.
[14] R. Bahadur, A. Bar-Cohen, "Orthotropic thermal conductivity effect on cylindrical pin fin heat transfer, " *Int. J. Heat and Mass Transfer* vol.50 pp.1155-1162, 2007.
[15] O.O. Onyejekwe, "heat conduction in composite media: a boundary integral approach, " *Computers and chemical Engineering* vol.26 pp. 1621-1632, 2002.
[16] J.Q. Tarn, Y.M. Wang, "Heat conduction in a cylindrically anisotropic tube of a functionally graded material, " *Chin J. Mech.*, Vol.19 pp.365- 372, 2003.
[17] J.Q. Tarn, Y.M. Wang, "End effects of heat conduction in circular cylinders of functionally graded materials and laminated composites, " *Inter. J. Heat Mass Transfer* vol.47, pp.5741-5747, 2004.
[18] J. Zhang, M. Tanaka, and T. Matsumoto, "A simplified approach for heat conduction analysis of CNT-based nano-composites, " *Comput. Methods Appl. Mech. Engrg.*, vol.193 pp.5597-5609, 2004.
[19] N.A. Roberts, D.G. Walker, D.Y. Li, "Molecular dynamics simulation of thermal conductivity of nanocrystalline composite films, " *Int. J. Heat and Mass Transfer,* Vol.52, pp.2002- 2008, 2008.
[20] Y.S. Cha, W.J. Minkowycz, and S.Y. Seol, "Transverse temperature distribution and heat generation rate in composite superconductors subjected to constant thermal disturbance, " *Int. Comm. Heat Mass Transfer*, Vol. 22, No.4, pp. 461-474, 1995.
[21] M.H. Kayhani, M. Shariati, M. Nourozi, M., Karimi Demneh, "Exact solution of conductive heat transfer in cylindrical composite laminate, " *Int. J. Heat and Mass Transfer*, Vol 46, pp.83-94, 2009.
[22] T. Myint-U, and L. Debnath, *LinearPartial Differential Equations for Scientists and Engineers*, Birkhauser Boston, 2007.
[23] Y.S. Touloukian, C.Y. Ho, *Thermophysical properties of matter*, plenumpress, vol.2, Thermal Conductivity of Nonmetallic Solids, New York, 1972, pp.740, 1972.
[24] Lekhnitskii, S. G., *Theory of Elasticity of an Anisotropic Body*, Mir, Moscow, 1981.
[25] Fraldi M, Cowin SC. Inhomogeneous elastostatic problem solutions constructed from stress-associated homogeneous solutions. J Mech Phys Solids 2004;52:2207_33.
[26] Fraldi, M., Nunziante, L., Carannante, F. (2007), *Axis-symmetrical Solutions for n-plies Functionally Graded Material Cylinders under Strain no-Decaying Conditions*, J. Mech. of Adv. Mat. and Struct. Vol. 14 (3), pp. 151-174 - DOI: 10.1080/15376490600719220
[27] M. Fraldi, L. Nunziante, F. Carannante, A. Prota, G. Manfredi, E. Cosenza (2008), *On the Prediction of the Collapse Load of Circular Concrete Columns Confined by FRP*, Journal Engineering structures, Vol. 30, Issue 11, November 2008, Pages 3247-3264 - DOI: 10.1016/j.engstruct.2008.04.036
[28] Fraldi, M., Nunziante, L., Chandrasekaran, S., Carannante, F., Pernice, MC. (2009), *Mechanics of distributed fibre optic sensors for strain measurements on rods*, Journal of Structural Engineering, 35, pp. 323-333, Dec. 2008- Gen. 2009
[29] M. Fraldi, F. Carannante, L. Nunziante (2012), *Analytical solutions for n-phase Functionally Graded Material Cylinders under de Saint Venant load conditions: Homogenization and effects of Poisson ratios on the overall stiffness*, Composites Part B: Engineering, Volume 45, Issue 1, February 2013, Pages 1310–1324
[30] Nunziante, L., Gambarotta, L., Tralli, A., *Scienza delle Costruzioni*, 3° Edizione, McGraw-Hill, 2011, ISBN**:** 9788838666971
[31] Ting, T. C. T., (1999), Pressuring, shearing, torsion and extension of a circular tube or bar of cylindrically anisotropic material, *Proc. Roy. Soc. Lond*. A452, 2397-2421.

CHAPTER XIII
MULTILAYERED CYLINDER CONSTITUTED BY CYLINDRICAL MONOCLINIC PHASES SUBJECTED TO AXIAL FORCE AND PURE TORSION

13.1. Introduction
In this chapter, let us consider the *chiral* structure characterized by multilayered cylinder, composed by two hollow cylindrical monoclinic phases. The cylindrical monoclinic elastic property of multilayered cylinder is obtained by the particular chiral structure. In fact, we consider the two hollow phases constructed by right-handed and left-handed spiral helices whose long axes are all parallel. These helical spirals may be either touching or separated by a matrix material and are composed by elastic orthotropic material. Let us the helical angle be ψ and let us negative values of ψ correspond to otherwise similar left-handed helices; the vanishing of ψ then corresponds to a straight reinforcement fibre. We show that when the effective elastic constants for this material are calculated, the sign of the constants "*chiral constants"* is determined by the sign of ψ and vanishes when ψ is zero. It is then possible to geometrically visualize the chiral, symmetry-breaking character of the "*chiral constants"* as these constants pass from positive to negative (or negative to positive) values through zero as the vanishing of a helical angle of one handedness occurs and the initiating of a helical angle of the opposite handedness commences. At the dividing line between the two types of handedness, the reinforcing fibres are straight. In terms of the elastic symmetry, as the constants "*chiral constants"* pass from positive to negative (or negative to positive) values through zero, the elastic material is first a monoclinic material of a certain chirality, then a orthotropic material, and then a monoclinic material of an opposite chirality.

13.2. Cylindrical monoclinic material
If the internal composition of a material possesses symmetry of any kind, then symmetry can be observed in its elastic properties. This will occur because the elastic properties are identical to the directions of symmetry which are developed in the body (the equivalent directions). F. Neumann set forth a principle for crystals which establishes the connection between symmetry of construction and elastic symmetry. This principle can be formulated in the following way: a material , in regard to its physical properties, has the same kind of symmetry as its crystallographic form. This principle can be expanded to include bodies which are not crystalline, but which posses a symmetry of structure (wood, plywood). However, elastic symmetry is usually more extensive than geometric symmetry; in addition to the equivalent directions which coincide with the symmetric directions of the structure, other directions exist for which the elastic properties are identical. If an anisotropic body possesses an elastic symmetry, then the equations of the generalized Hooke's law are simplified: We find the simplifications by applying the following method: we refer the body to the first coordinate system $\{x, y, z\}$ and then to the second coordinate system $\{x', y', z'\}$; the second system is symmetric to the first in accordance with the form of its elastic symmetry . Since the directions of similar axes of both systems are equivalent with respect to elastic properties, the equations of the generalized Hooke's law and expression of elastic potential will have the same form in both the first and second systems; the corresponding elastic constants entering into their composition also will be identical. For the first coordinate system $\{x, y, z\}$:

$$V = \frac{1}{2}(\mathbf{C}:\mathbf{E})^T:\mathbf{E} = \frac{1}{2}C_{ijhk}\varepsilon_{ij}\varepsilon_{hk} \tag{13.2.1}$$

For the second coordinate system $\{x', y', z'\}$:

$$V = \frac{1}{2}(\mathbf{C}:\mathbf{E}')^T:\mathbf{E}' = \frac{1}{2}C_{ijhk}\varepsilon'_{ij}\varepsilon'_{hk} \tag{13.2.2}$$

Since one and the same quantity is being discussed, we have:

$$\frac{1}{2}\left(\mathbf{C}:\mathbf{E}\right)^{T}:\mathbf{E}=\frac{1}{2}\left(\mathbf{C}:\mathbf{E}'\right)^{T}:\mathbf{E}' \tag{13.2.3}$$

Let us consider in more detail the first coordinate system. We shall express the components $\varepsilon_{ij}^{'}$ of the strain tensor $\mathbf{E}'$ in terms of the components ε_{ij} using the transformation law of the tensors. Substituting the obtained expressions into the right side of (13.2.3) and equating the coefficients for the components ε_{ij} in the left and right sides, we conclude that certain coefficients C_{ijhk} are equal to zero, and other coefficients are connected by definite relations. As a result, it turns out that bodies possessing elastic symmetry have a smaller number of independent elastic constants than 21 (for example, 13, 9, and so forth). Considering the elastic potential expressed in terms of the components of stress, we derive the relationships between the moduli A_{ijhk} in the same way. If we consider , instead of the expression of elastic potential, the equations of the generalized Hooke's law written for two symmetric coordinate systems, we can arrive at the same results in a different way . We shall state the equations of the generalized Hooke's law and the structure of the expressions of elastic potential for the basic cases of elastic symmetry. If a material has one plane of elastic symmetry , then independent elastic constants are 13. Let us assume that through each point of a body we draw a plane possessing the property that any two directions symmetric with respect to this plane are equivalent with respect to the elastic properties. Directing the x- axis normal to the plane of elastic symmetry, we obtain, after simplifications, the following equations of the generalized Hooke's law:

$$\begin{bmatrix}\sigma_{xx}\\ \sigma_{yy}\\ \sigma_{xx}\\ \tau_{yz}\\ \tau_{xz}\\ \tau_{xy}\end{bmatrix}=\begin{bmatrix}c_{11} & c_{12} & c_{13} & c_{14} & 0 & 0\\ c_{12} & c_{22} & c_{23} & c_{24} & 0 & 0\\ c_{13} & c_{23} & c_{33} & c_{34} & 0 & 0\\ c_{14} & c_{24} & c_{34} & c_{44} & 0 & 0\\ 0 & 0 & 0 & 0 & c_{55} & c_{56}\\ 0 & 0 & 0 & 0 & c_{56} & c_{66}\end{bmatrix}\cdot\begin{bmatrix}\varepsilon_{xx}\\ \varepsilon_{yy}\\ \varepsilon_{zz}\\ 2\varepsilon_{yz}\\ 2\varepsilon_{xz}\\ 2\varepsilon_{xy}\end{bmatrix} \tag{13.2.4}$$

13.3. Transformation of elastic stiffness tensor from helicoidal into cylindrical coordinate systems

Let us consider the helicoidal coordinate system (r,t,c) characterized by unit vectors $(\mathbf{e}_r,\mathbf{e}_t,\mathbf{e}_c)$ as showed in figure 13.1. This coordinate system has unit vector $\mathbf{e}_t$ that tangent to helix; the unit vector $\mathbf{e}_r$ is perpendicular to $\mathbf{e}_t$; and unit vector $\mathbf{e}_c$ is perpendicular to plane definite by axis "r" and "t". Let us consider a new coordinate system characterized by cylindrical system (r,θ,z). The unit vectors of the cylindrical system are denote by $(\mathbf{e}_r,\mathbf{e}_\theta,\mathbf{e}_z)$, as showed in figure 13.1. If cylindrical system has the same origin of the helicoidal system, then the unit vector $\mathbf{e}_r$ is coincident into two coordinate systems. The angle between two unit vectors $\mathbf{e}_t$ and $\mathbf{e}_\theta$ is identified by ψ, that equal to angle between two vector $\mathbf{e}_c$ e $\mathbf{e}_z$. Euler's theorem on the representation of rigid body rotations (Brand, 1947; Lamb, 1929; Goldstein, 1950; Pars, 1979; Whittaker, 1937) has many forms. The theorem concerns the characterization of a three-dimensional rotation by an angle ψ about a specific axis, here indicated by the unit vector $\mathbf{p}$. This theorem is represented by the formula (Beatty, 1966, 1977; Finger, 1892; Gurtin, 1976; Truesdell and Toupin, 1960):

$$\mathbf{Q}=1+\mathbf{P}\sin\psi+\left(1-\cos\psi\right)\mathbf{P}^{2} \tag{13.3.1}$$

where the three-dimensional shew-symmetric tensor $\mathbf{P}$ with components P_{ij} is introduced to represent the unit vector $\mathbf{p}$,

$$\mathbf{P}=\begin{bmatrix} 0 & -p_z & p_y \\ p_z & 0 & -p_x \\ -p_y & p_x & 0 \end{bmatrix} \quad or \quad P_{ij}=e_{ijk}\,p_k \tag{13.3.2}$$

It is easy to show that $\mathbf{P}$ has the following properties:

$$\mathbf{P}=-\mathbf{P}^T, \quad \mathbf{P}\,\mathbf{p}=0, \quad \mathbf{P}^2=\mathbf{p}\otimes\mathbf{p}-\mathbf{I}, \quad \mathbf{P}^3=-\mathbf{P}. \tag{13.3.3}$$

The transformation law between cylindrical and helicoidal coordinate system is characterized by a rotation about the radial axis. Then, in this case the vector $\mathbf{p}=\{1,0,0\}$ and shew-symmetric tensor $\mathbf{P}$ becomes:

$$\mathbf{P}=\begin{bmatrix} 0 & 0 & 0 \\ 0 & 0 & -1 \\ 0 & 1 & 0 \end{bmatrix} \tag{13.3.4}$$

By applying the formula (13.3.1), we can obtain the rotation matrix

$$\mathbf{Q}=\begin{bmatrix} 1 & 0 & 0 \\ 0 & \cos\psi & -\sin\psi \\ 0 & \sin\psi & \cos\psi \end{bmatrix} \tag{13.3.5}$$

Then, the transformation law between two coordinate system is:

$$\begin{bmatrix} e_r \\ e_\theta \\ e_z \end{bmatrix}=\begin{bmatrix} 1 & 0 & 0 \\ 0 & \cos\psi & -\sin\psi \\ 0 & \sin\psi & \cos\psi \end{bmatrix}\cdot\begin{bmatrix} e_r \\ e_t \\ e_c \end{bmatrix}=\mathbf{Q}\cdot\begin{bmatrix} e_r \\ e_t \\ e_c \end{bmatrix} \tag{13.3.6}$$

In a space of six dimensions, the representation of a three-dimensional rotation by an angle ψ about a specific axis, characterized by the unit vector $\mathbf{p}=\left[p_x,p_y,p_z\right]^T$, is represented as a six-dimensional orthogonal tensor by the formula:

$$\hat{\mathbf{Q}}=\mathbf{I}+\hat{\mathbf{P}}\sin\psi+(1-\cos\psi)\hat{\mathbf{P}}^2+\frac{1}{3}\sin\psi(1-\cos\psi)\left(\hat{\mathbf{P}}+\hat{\mathbf{P}}^3\right)+\frac{1}{6}(1-\cos\psi)^2\left(\hat{\mathbf{P}}^2+\hat{\mathbf{P}}^4\right) \tag{13.3.7}$$

Where the six-dimensional shew-symmetric tensor $\hat{\mathbf{P}}$ with components

$$\hat{\mathbf{P}}=\begin{bmatrix} 0 & 0 & 0 & 0 & \sqrt{2}p_y & -\sqrt{2}p_z \\ 0 & 0 & 0 & -\sqrt{2}p_x & 0 & \sqrt{2}p_z \\ 0 & 0 & 0 & \sqrt{2}p_x & \sqrt{2}p_y & 0 \\ 0 & \sqrt{2}p_x & -\sqrt{2}p_x & 0 & p_z & p_y \\ -\sqrt{2}p_y & 0 & \sqrt{2}p_y & -p_z & 0 & p_x \\ \sqrt{2}p_z & -\sqrt{2}p_z & 0 & p_y & -p_x & 0 \end{bmatrix} \tag{13.3.8}$$

Satisfies the following conditions:

$$\hat{\mathbf{P}}=-\hat{\mathbf{P}}^T, \quad \hat{\mathbf{P}}^5+5\hat{\mathbf{P}}^3+4\hat{\mathbf{P}}=0, \quad \hat{\mathbf{P}}^6+5\hat{\mathbf{P}}^4+4\hat{\mathbf{P}}^2=0 \tag{13.3.9}$$

Matrices of six-dimensional tensor components are distinguished with circumflexes. Note that formulae (13.3.1) and (13.3.7) show that a change in the sense of $\mathbf{p}$ is the same as a reversal of the direction of the angle from $\mathbf{p},\psi$ to $-\mathbf{p},-\psi$. Formula (13.3.7) is of interest in anisotropic elasticity because the elastic tensor can be expressed as a second rank tensor in six dimensions Mehrabadi and Cowin [27] as well as in its more traditional representation as a fourth rank tensor in three dimensions. Formula (13.3.7) connects the geometric operation in three dimensions to the matrix algebra of six dimensions. Since the tensor transformation rules for a second rank tensor rather than a fourth rank tensor apply, transformations of the reference coordinate system for the elasticity tenor may be accomplished in a very straightforward fashion using matrix multiplication. The

anisotropic form of Hooke' law is often written in indicial notation as $\sigma_{ij} = C_{ijkm}\varepsilon_{km}$, where the C_{ijkm} are the components of the three-dimensional fourth rank elasticity tensor. There are three important symmetric restrictions on the fourth rank tensor components C_{ijkm} . These restrictions, which require that components with the subscripts *ijkm*, *jikm* and *kmij* be equal, follow from the symmetry of the stress tensor, the symmetry of the strain tensor, and the requirement that no work be produced by the elastic material in a closet loading cycle, respectively . Written as a linear transformation in six dimensions, Hooke's law has the representation $\mathbf{T} = \mathbf{c}\,\mathbf{E}$ or

$$\begin{bmatrix} \sigma_{xx} \\ \sigma_{yy} \\ \sigma_{zz} \\ \tau_{yz} \\ \tau_{xz} \\ \tau_{xy} \end{bmatrix} = \begin{bmatrix} c_{11} & c_{12} & c_{13} & c_{14} & c_{15} & c_{16} \\ c_{12} & c_{22} & c_{23} & c_{24} & c_{25} & c_{26} \\ c_{13} & c_{23} & c_{33} & c_{34} & c_{35} & c_{36} \\ c_{14} & c_{24} & c_{34} & c_{44} & c_{45} & c_{46} \\ c_{15} & c_{25} & c_{35} & c_{45} & c_{55} & c_{56} \\ c_{16} & c_{26} & c_{36} & c_{46} & c_{56} & c_{66} \end{bmatrix} . \begin{bmatrix} \varepsilon_{xx} \\ \varepsilon_{yy} \\ \varepsilon_{zz} \\ 2\varepsilon_{yz} \\ 2\varepsilon_{xz} \\ 2\varepsilon_{xy} \end{bmatrix} \tag{13.3.10}$$

In the two subscript notation of Voigt [21] for the components of C_{ijkm}. In the Voigt notation the components of $\mathbf{c}$ and C_{ijkm} are related by replacing the six-dimensional indices 1,2,3,4,5 and 6 by the pairs of the three-dimensional indices 1,2 and 3; thus 1,2,3,4,5 and 6 become 11, 22, 33, 23 or 32, 13 or 31, 12 or 21, respectively. The members of the paired indices 23 or 32, 13 or 31 , 12 or 21 are equivalent because of the symmetry of the tensors of the stress and strain. The matrix $\mathbf{c}$ in equation (13.3.10) is not a matrix of tensor components in six dimensions, although it is formed from the components of a three-dimensional fourth rank tensor. Six-dimensional vector base and notations are introduced so that stress and strain can be considered as vectors in a six-dimensional vector space as well as second rank tensors in three-dimensional Cartesian reference systems. The six-dimensional quantities will be indicated by a circumflex ; thus, the six-dimensional vectors of stress and strain will be denoted by $\hat{\mathbf{T}}$ and $\hat{\mathbf{E}}$, respectively, whereas the three-dimensional second rank tensors of stress and strain are denoted by $\mathbf{T}$ and $\mathbf{E}$, respectively. The direct relationship between the components of $\hat{\mathbf{T}}$ and $\mathbf{T}$, and $\hat{\mathbf{E}}$ and $\mathbf{E}$, are dual representations given by

$$\begin{aligned} \hat{\mathbf{T}} &= \begin{bmatrix} \hat{\sigma}_1 & \hat{\sigma}_2 & \hat{\sigma}_3 & \hat{\sigma}_4 & \hat{\sigma}_5 & \hat{\sigma}_6 \end{bmatrix}^T = \begin{bmatrix} \sigma_{xx} & \sigma_{yy} & \sigma_{zz} & \sqrt{2}\tau_{yz} & \sqrt{2}\tau_{xz} & \sqrt{2}\tau_{xy} \end{bmatrix}^T \\ \hat{\mathbf{E}} &= \begin{bmatrix} \hat{\varepsilon}_1 & \hat{\varepsilon}_2 & \hat{\varepsilon}_3 & \hat{\varepsilon}_4 & \hat{\varepsilon}_5 & \hat{\varepsilon}_6 \end{bmatrix}^T = \begin{bmatrix} \varepsilon_{xx} & \varepsilon_{yy} & \varepsilon_{zz} & \sqrt{2}\varepsilon_{yz} & \sqrt{2}\varepsilon_{xz} & \sqrt{2}\varepsilon_{xy} \end{bmatrix}^T \end{aligned} \tag{13.3.11}$$

where the shearing components of these new six-dimensional stress and strain vectors are the shearing components of these three-dimensional stress and strain tensors multiplied by $\sqrt{2}$. This $\sqrt{2}$ factor ensures that the scalar product of the two six-dimensional vectors is equal to the trace of the product of the corresponding second rank tensors, $\hat{\mathbf{T}} \cdot \hat{\mathbf{E}} = tr\,\mathbf{T} \cdot \mathbf{E}$. Introducing the new notation of equation (13.3.11) into equation (13.3.10), the equation (13.3.10) can be rewritten in the form:

$$\hat{\mathbf{T}} = \hat{\mathbf{c}}\,\hat{\mathbf{E}} \tag{13.3.12}$$

where $\hat{\mathbf{c}}$ is a new six-by-six matrix. The matrix form of equation (13.3.9) is given by:

$$\begin{bmatrix} \sigma_{xx} \\ \sigma_{yy} \\ \sigma_{zz} \\ \sqrt{2}\tau_{yz} \\ \sqrt{2}\tau_{xz} \\ \sqrt{2}\tau_{xy} \end{bmatrix} = \begin{bmatrix} c_{11} & c_{12} & c_{13} & \sqrt{2}c_{14} & \sqrt{2}c_{15} & \sqrt{2}c_{16} \\ c_{12} & c_{22} & c_{23} & \sqrt{2}c_{24} & \sqrt{2}c_{25} & \sqrt{2}c_{26} \\ c_{13} & c_{23} & c_{33} & \sqrt{2}c_{34} & \sqrt{2}c_{35} & \sqrt{2}c_{36} \\ \sqrt{2}c_{14} & \sqrt{2}c_{24} & \sqrt{2}c_{34} & 2c_{44} & 2c_{45} & 2c_{46} \\ \sqrt{2}c_{15} & \sqrt{2}c_{25} & \sqrt{2}c_{35} & 2c_{45} & 2c_{55} & 2c_{56} \\ \sqrt{2}c_{16} & \sqrt{2}c_{26} & \sqrt{2}c_{36} & 2c_{46} & 2c_{56} & 2c_{66} \end{bmatrix} . \begin{bmatrix} \varepsilon_{xx} \\ \varepsilon_{yy} \\ \varepsilon_{zz} \\ \sqrt{2}\varepsilon_{yz} \\ \sqrt{2}\varepsilon_{xz} \\ \sqrt{2}\varepsilon_{xy} \end{bmatrix} \tag{13.3.13}$$

or

$$\begin{bmatrix} \hat{\sigma}_{xx} \\ \hat{\sigma}_{yy} \\ \hat{\sigma}_{zz} \\ \hat{\tau}_{yz} \\ \hat{\tau}_{xz} \\ \hat{\tau}_{xy} \end{bmatrix} = \begin{bmatrix} \hat{c}_{11} & \hat{c}_{12} & \hat{c}_{13} & \hat{c}_{14} & \hat{c}_{15} & \hat{c}_{16} \\ \hat{c}_{12} & \hat{c}_{22} & \hat{c}_{23} & \hat{c}_{24} & \hat{c}_{25} & \hat{c}_{26} \\ \hat{c}_{13} & \hat{c}_{23} & \hat{c}_{33} & \hat{c}_{34} & \hat{c}_{35} & \hat{c}_{36} \\ \hat{c}_{14} & \hat{c}_{24} & \hat{c}_{34} & \hat{c}_{44} & \hat{c}_{45} & \hat{c}_{46} \\ \hat{c}_{15} & \hat{c}_{25} & \hat{c}_{35} & \hat{c}_{45} & \hat{c}_{55} & \hat{c}_{56} \\ \hat{c}_{16} & \hat{c}_{26} & \hat{c}_{36} & \hat{c}_{46} & \hat{c}_{56} & \hat{c}_{66} \end{bmatrix} \cdot \begin{bmatrix} \hat{\varepsilon}_{xx} \\ \hat{\varepsilon}_{yy} \\ \hat{\varepsilon}_{zz} \\ \hat{\varepsilon}_{yz} \\ \hat{\varepsilon}_{xz} \\ \hat{\varepsilon}_{xy} \end{bmatrix} \tag{13.3.14}$$

The relationship between the non-tensorial Voigt notation $\mathbf{c}$ and six-dimensional second rank tensor components $\hat{\mathbf{c}}$ is easily constructed from equation (13.3.13) ; a table of this relationship is given in Mehrabadi and Cowin [27] . The symmetric matrix $\hat{\mathbf{c}}$ can be shown Mehrabadi and Cowin [27] to represent the components of a second rank tensor in a six-dimensional space, whereas the components of the matrix $\mathbf{c}$ appearing in equation (13.3.10) do not form a tensor. It is easy to prove that if the material has rhombic syngony in the helicoidal system, then in the cylindrical coordinate system, the material has a monoclinic anisotropy. The monoclinic crystal system has exactly one pale of reflective symmetry (Cowin and Mehrabadi, 1987; Gurtin, 1972; Hearmon, 1961; Lekhnitskii, 1963; Fedorov,1968). A material is said to have a plane of reflective symmetry with respect to a plane passing through the point. In particular, we show that in the cylindrical coordinate the plane of elastic symmetry is $\theta - z$. Remember that vector $\mathbf{p}$ is equal to $\{1,0,0\}$, then, six-dimensional shew-symmetric tensor $\hat{\mathbf{P}}$, becomes:

$$\hat{\mathbf{P}} = \begin{bmatrix} 0 & 0 & 0 & 0 & 0 & 0 \\ 0 & 0 & 0 & -\sqrt{2} & 0 & 0 \\ 0 & 0 & 0 & \sqrt{2} & 0 & 0 \\ 0 & \sqrt{2} & -\sqrt{2} & 0 & 0 & 0 \\ 0 & 0 & 0 & 0 & 0 & 1 \\ 0 & 0 & 0 & 0 & -1 & 0 \end{bmatrix} \tag{13.3.15}$$

The six-dimensional orthogonal tensor $\hat{\mathbf{Q}}$ is equal to:

$$\hat{\mathbf{Q}} = \begin{bmatrix} 1 & 0 & 0 & 0 & 0 & 0 \\ 0 & \cos^2\psi & \sin^2\psi & -(\sin 2\psi)/\sqrt{2} & 0 & 0 \\ 0 & \sin^2\psi & \cos^2\psi & (\sin 2\psi)/\sqrt{2} & 0 & 0 \\ 0 & (\sin 2\psi)/\sqrt{2} & -(\sin 2\psi)/\sqrt{2} & \cos 2\psi & 0 & 0 \\ 0 & 0 & 0 & 0 & \cos\psi & \sin\psi \\ 0 & 0 & 0 & 0 & -\sin\psi & \cos\psi \end{bmatrix} \tag{13.3.16}$$

In the helicoidal coordinate system the elastic constant matrix is:

$$\mathbf{c}^{hel} = \begin{bmatrix} c_{11}^{hel} & c_{12}^{hel} & c_{13}^{hel} & 0 & 0 & 0 \\ c_{12}^{hel} & c_{22}^{hel} & c_{23}^{hel} & 0 & 0 & 0 \\ c_{13}^{hel} & c_{23}^{hel} & c_{33}^{hel} & 0 & 0 & 0 \\ 0 & 0 & 0 & 2c_{44}^{hel} & 0 & 0 \\ 0 & 0 & 0 & 0 & 2c_{55}^{hel} & 0 \\ 0 & 0 & 0 & 0 & 0 & 2c_{66}^{hel} \end{bmatrix} \tag{13.3.17}$$

where, the vector stress is obtained multiplying the matrix $\mathbf{c}^{hel}$ by the strain vector, in Voigt notation. and the moduli of elasticity c_{ij}^{hel} are linked with elastic moduli E_{rr}, E_{tt}, E_{cc}, $\nu_{rt}, \nu_{tc}, \nu_{rc}, G_{rt}, G_{tc}, G_{rc}$. By invoking the equation (13.3.7), the elastic constant matrix in the cylindrical coordinate system becomes:

$$\mathbf{c}^{cyl}=\begin{bmatrix} c_{11}^{cyl} & c_{12}^{cyl} & c_{13}^{cyl} & 2c_{14}^{cyl} & 0 & 0 \\ c_{12}^{cyl} & c_{22}^{cyl} & c_{23}^{cyl} & 2c_{24}^{cyl} & 0 & 0 \\ c_{13}^{cyl} & c_{23}^{cyl} & c_{33}^{cyl} & 2c_{34}^{cyl} & 0 & 0 \\ c_{14}^{cyl} & c_{24}^{cyl} & c_{34}^{cyl} & 2c_{44}^{cyl} & 0 & 0 \\ 0 & 0 & 0 & 0 & 2c_{55}^{cyl} & c_{56}^{cyl} \\ 0 & 0 & 0 & 0 & c_{56}^{cyl} & 2c_{66}^{cyl} \end{bmatrix} \tag{13.3.18}$$

where the constant c_{ij}^{cyl} are linked with constant c_{ij}^{hel} and angle θ of the helix.

$$\begin{gathered} c_{11}^{cyl}=c_{11}^{hel},\quad c_{12}^{cyl}=c_{12}^{hel}\cos^2\psi+c_{13}^{hel}\sin^2\psi,\quad c_{13}^{cyl}=c_{13}^{hel}\cos^2\psi+c_{12}^{hel}\sin^2\psi, \\ c_{22}^{cyl}=c_{22}^{hel}\cos^4\psi+2\left(c_{23}^{hel}+2c_{44}^{hel}\right)\cos^2\psi\sin^2\psi+c_{33}^{hel}\sin^4\psi \\ c_{23}^{cyl}=c_{23}^{hel}\cos^2 2\psi+\frac{1}{4}\left(c_{22}^{hel}+2c_{23}^{hel}+c_{33}^{hel}-4c_{44}^{hel}\right)\sin^2 2\psi \\ c_{24}^{cyl}=\frac{1}{4}\left[c_{22}^{hel}-c_{33}^{hel}+\left(c_{22}^{hel}-2c_{23}^{hel}+c_{33}^{hel}-4c_{44}^{hel}\right)\cos 2\psi\right]\sin 2\psi \\ c_{33}^{cyl}=c_{33}^{hel}\cos^4\psi+2\left(c_{23}^{hel}+2c_{44}^{hel}\right)\cos^2\psi\sin^2\psi+c_{22}^{hel}\sin^4\psi \\ c_{34}^{cyl}=\frac{1}{4}\left[c_{22}^{hel}-c_{33}^{hel}+\left(4c_{44}^{hel}-c_{33}^{hel}+2c_{23}^{hel}-c_{22}^{hel}\right)\cos 2\psi\right]\sin 2\psi \\ c_{44}^{cyl}=c_{44}^{hel}\cos^2 2\psi+\frac{1}{4}\left(c_{22}^{hel}-2c_{23}^{hel}+c_{33}^{hel}\right)\sin^2 2\psi,\quad c_{14}^{cyl}=(1/2)\left(c_{12}^{hel}-c_{13}^{hel}\right)\sin 2\psi, \\ c_{55}^{cyl}=c_{55}^{cyl}\cos^2\psi+c_{66}^{cyl}\sin^2\psi,\quad c_{56}^{cyl}=(1/2)\left(c_{66}^{cyl}-c_{55}^{cyl}\right)\sin 2\psi,\quad c_{66}^{cyl}=c_{55}^{cyl}\sin^2\psi+c_{66}^{cyl}\cos^2\psi \\ c_{55}^{cyl}=\frac{E\left(\cos^2\psi+\alpha\sin^2\psi\right)}{2(1+\nu)},\quad c_{56}^{cyl}=\frac{E(\alpha-1)\sin 2\psi}{4(1+\nu)},\quad c_{66}^{cyl}=\frac{E\left(\alpha\cos^2\psi+\sin^2\psi\right)}{2(1+\nu)}, \end{gathered} \tag{13.3.19}$$

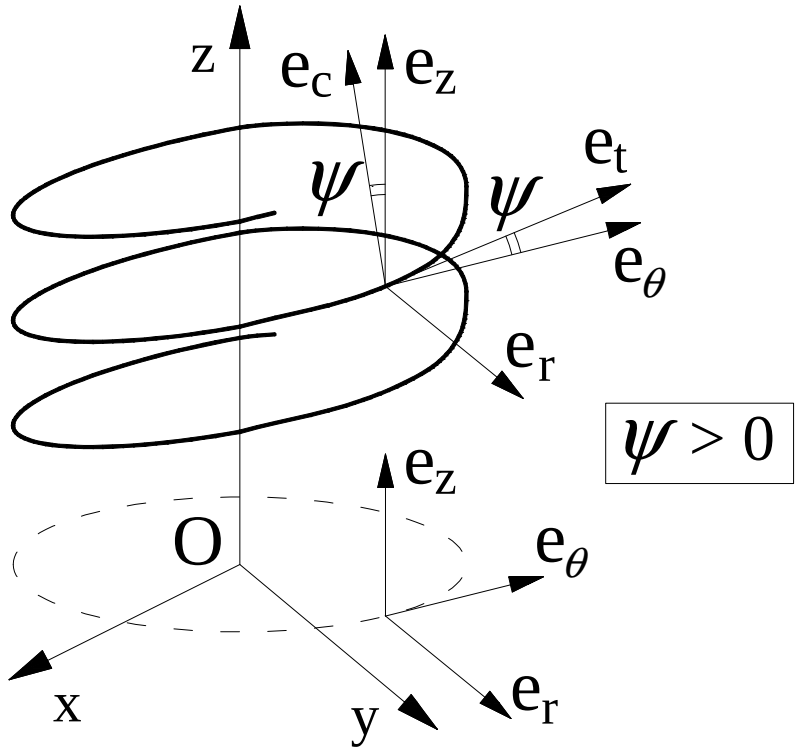

Fig. 13.1 - *Helicoidal coordinate system* (r,t,c) *characterized by unit vectors* $(\mathbf{e}_r,\mathbf{e}_t,\mathbf{e}_c)$ *and cylindrical system* (r,θ,z) *characterized by unit vectors* $(\mathbf{e}_r,\mathbf{e}_\theta,\mathbf{e}_z)$.

13.4. General theory of the linear elastostatic problems in cylindrical coordinate system

With reference to the cylindrical coordinate system $\{r,\theta,z\}$, the equilibrium equations, in the absence of body forces, are:

$$\begin{cases} \sigma_{rr,r}+r^{-1}\tau_{r\theta,\theta}+\tau_{rz,z}+r^{-1}\left(\sigma_{rr}-\sigma_{\theta\theta}\right)=0 \\ \tau_{r\theta,r}+r^{-1}\sigma_{\theta\theta,\theta}+\tau_{\theta z,z}+2r^{-1}\tau_{r\theta}=0 \\ \tau_{rz,r}+r^{-1}\tau_{\theta z,\theta}+\sigma_{zz,z}+r^{-1}\tau_{rz}=0 \end{cases} \tag{13.4.1}$$

In the framework of the analysis of *multilayered cylinder*, due to the cylindrical geometry of the phases, it results extremely useful to adopt the formalism introduced by Ting [19], which yields to rewrite the equilibrium equations (13.4.1) in vector form, introducing the "emerging" stresses (e.g. tractions on the boundary surface of a single phase) as follows:

$$\left(r\,\mathbf{t}_r\right)_{,r}+\left(\mathbf{t}_\theta\right)_{,\theta}+r\,\mathbf{t}_{z,z}+\mathbf{K}\,\mathbf{t}_\theta=0 \tag{13.4.2}$$

where

$$\mathbf{t}_r=\begin{bmatrix}\sigma_{rr}\\ \tau_{r\theta}\\ \tau_{rz}\end{bmatrix},\quad \mathbf{t}_\theta=\begin{bmatrix}\tau_{\theta r}\\ \sigma_{\theta\theta}\\ \tau_{\theta z}\end{bmatrix},\quad \mathbf{t}_z=\begin{bmatrix}\tau_{zr}\\ \tau_{z\theta}\\ \sigma_{zz}\end{bmatrix}, \tag{13.4.3}$$

represent the traction vectors on the surfaces $r=const.$, $\theta=const.$, and $z=const.$, respectively, and $\mathbf{K}$ is a 3x3 constant matrix given by

$$\mathbf{K}=\begin{bmatrix}0 & -1 & 0\\ 1 & 0 & 0\\ 0 & 0 & 0\end{bmatrix}\quad . \tag{13.4.4}$$

The relations between the strain ε_{ij} and displacement u_i are:

$$\begin{aligned} &\varepsilon_{rr}=u_{r,r},\quad \varepsilon_{\theta\theta}=r^{-1}\left(u_{\theta,\theta}+u_r\right),\quad \gamma_{r\theta}=r^{-1}(u_{r,\theta}+r\,u_{\theta,r}-u_\theta)\\ &\varepsilon_{zz}=u_{z,z},\quad \gamma_{rz}=u_{z,r}+u_{r,z},\quad \gamma_{\theta z}=r^{-1}\left(u_{z,\theta}+r\,u_{\theta,z}\right), \end{aligned} \tag{13.4.5}$$

Under the assumption of cylindrical anisotropy, by identifying $\left(x,y,z\right)\equiv\left(r,\theta,z\right)$ the stress-strain law becomes:

$$\sigma_{ij}=C_{ijhk}\varepsilon_{hk}\quad . \tag{13.4.6}$$

Hence

$$\left(\mathbf{t}_r\right)_j=\sigma_{rj}=C_{1jhk}\varepsilon_{hk}=C_{1j11}\varepsilon_{rr}+C_{1j22}\varepsilon_{\theta\theta}+C_{1j33}\varepsilon_{zz}+C_{1j23}\gamma_{\theta z}+C_{1j13}\gamma_{rz}+C_{1j12}\gamma_{r\theta} \tag{13.4.7}$$

Similar equations hold for $\left(\mathbf{t}_\theta\right)_j$ and for $\left(\mathbf{t}_z\right)_j$. Making use of (13.4.5) it can be shown that:

$$\begin{aligned} \mathbf{t}_r&=\mathbf{Q}_{rr}\,\mathbf{u},_r+r^{-1}\mathbf{Q}_{r\theta}\left(\mathbf{u},_\theta+\mathbf{K}\,\mathbf{u}\right)+\mathbf{Q}_{rz}\,\mathbf{u},_z\\ \mathbf{t}_\theta&=\mathbf{Q}_{r\theta}^T\mathbf{u},_r+r^{-1}\mathbf{Q}_{\theta\theta}\left(\mathbf{u},_\theta+\mathbf{K}\,\mathbf{u}\right)+\mathbf{Q}_{\theta z}\,\mathbf{u},_z\\ \mathbf{t}_z&=\mathbf{Q}_{rz}^T\,\mathbf{u},_r+r^{-1}\mathbf{Q}_{\theta z}^T\left(\mathbf{u},_\theta+\mathbf{K}\,\mathbf{u}\right)+\mathbf{Q}_{zz}\mathbf{u},_z \end{aligned} \tag{13.4.8}$$

where superscript "*T*" means "transposition", and

$$\mathbf{u}^T=\begin{bmatrix}u_r & u_\theta & u_z\end{bmatrix}^T \tag{13.4.9}$$

while $\mathbf{Q}_{rr},\mathbf{Q}_{r\theta},\mathbf{Q}_{rz},\mathbf{Q}_{\theta\theta},\mathbf{Q}_{\theta z},\mathbf{Q}_{zz}$ are 3x3 matrices, explicitly reported below:

$$\mathbf{Q}_{rr}=\begin{bmatrix}c_{11} & c_{16} & c_{15}\\ c_{16} & c_{66} & c_{56}\\ c_{15} & c_{56} & c_{55}\end{bmatrix},\quad \mathbf{Q}_{r\theta}=\begin{bmatrix}c_{16} & c_{12} & c_{14}\\ c_{66} & c_{26} & c_{46}\\ c_{56} & c_{25} & c_{45}\end{bmatrix},\quad \mathbf{Q}_{rz}=\begin{bmatrix}c_{15} & c_{14} & c_{13}\\ c_{56} & c_{46} & c_{36}\\ c_{55} & c_{45} & c_{35}\end{bmatrix},$$

$$\mathbf{Q}_{\theta\theta}=\begin{bmatrix} c_{66} & c_{26} & c_{46} \\ c_{26} & c_{22} & c_{24} \\ c_{46} & c_{24} & c_{44} \end{bmatrix},\quad \mathbf{Q}_{\theta z}=\begin{bmatrix} c_{56} & c_{46} & c_{36} \\ c_{25} & c_{24} & c_{23} \\ c_{45} & c_{44} & c_{34} \end{bmatrix},\quad \mathbf{Q}_{zz}=\begin{bmatrix} c_{55} & c_{45} & c_{35} \\ c_{45} & c_{44} & c_{34} \\ c_{35} & c_{34} & c_{33} \end{bmatrix}. \tag{13.4.10}$$

Substitution of (13.4.8) in (13.4.2) leads to a differential equation for $\mathbf{u}$. It should be pointed out that the elastic constants C_{ijhk} are here referred to the cylindrical coordinate system. Therefore the matrices $\mathbf{Q}_{hk}\quad h,k\in\{r,\theta,z\}$ are not constant matrices even for homogeneous materials, that is – for example – in a Cartesian reference system. In particular, for a *cylindrically anisotropic* material , the matrices $\mathbf{Q}_{hk}\quad h,k\in\{r,\theta,z\}$ are constant. By inserting (13.4.8) into (13.4.2) a single equation for the displacement $\mathbf{u}$ is obtained as follows:

$$\begin{aligned}&\mathbf{Q}_{rr}\,\mathbf{u}_{,rr}+\mathbf{Q}_{zz}\,\mathbf{u}_{,zz}+\left(\mathbf{Q}_{rz}+\mathbf{Q}_{rz}^{T}\right)\mathbf{u}_{,rz}+r^{-2}\left[\mathbf{Q}_{\theta\theta}\mathbf{u}_{,\theta\theta}+\mathbf{K}\,\mathbf{Q}_{\theta\theta}\,\mathbf{K}\,\mathbf{u}+\left(\mathbf{Q}_{\theta\theta}\,\mathbf{K}+\mathbf{K}\,\mathbf{Q}_{\theta\theta}\right)\mathbf{u}_{,\theta}\right]+\\&+r^{-1}\begin{bmatrix}\left(\mathbf{Q}_{r\theta}+\mathbf{Q}_{r\theta}^{T}\right)\mathbf{u}_{,r\theta}+\left(\mathbf{Q}_{\theta z}+\mathbf{Q}_{\theta z}^{T}\right)\mathbf{u}_{,\theta z}+\left(\mathbf{Q}_{r\theta}\,\mathbf{K}+\mathbf{K}\,\mathbf{Q}_{r\theta}^{T}+\mathbf{Q}_{rr}\right)\mathbf{u}_{,r}+\\+\left(\mathbf{K}\,\mathbf{Q}_{\theta z}+\mathbf{Q}_{\theta z}^{T}\mathbf{K}+\mathbf{Q}_{rz}\right)\mathbf{u}_{,z}\end{bmatrix}=0\end{aligned} \tag{13.4.11}$$

In the case that the material possesses cylindrically monoclinic, and the plane of elastic symmetry is $(\theta-z)$, the linearly elastic constitutive relation of the i[th] phase, in the Voigt notation, is:

$$\sigma_k=C_{kj}^{(i)}\varepsilon_j \tag{13.4.12}$$

where stress and strain vectors and the Elasticity matrix are respectively:

$$[\sigma_k]=\begin{bmatrix}\sigma_{rr}\\ \sigma_{\theta\theta}\\ \sigma_{zz}\\ \tau_{r\theta}\\ \tau_{\theta z}\\ \tau_{rz}\end{bmatrix},[\varepsilon_j]=\begin{bmatrix}\varepsilon_{rr}\\ \varepsilon_{\theta\theta}\\ \varepsilon_{zz}\\ \gamma_{r\theta}\\ \gamma_{\theta z}\\ \gamma_{rz}\end{bmatrix},\ \mathbf{C}^{(i)}=\begin{bmatrix} c_{11}^{(i)} & c_{12}^{(i)} & c_{13}^{(i)} & c_{14}^{(i)} & 0 & 0\\ c_{12}^{(i)} & c_{22}^{(i)} & c_{23}^{(i)} & c_{24}^{(i)} & 0 & 0\\ c_{13}^{(i)} & c_{23}^{(i)} & c_{33}^{(i)} & c_{34}^{(i)} & 0 & 0\\ c_{14}^{(i)} & c_{24}^{(i)} & c_{34}^{(i)} & c_{44}^{(i)} & 0 & 0\\ 0 & 0 & 0 & 0 & c_{55}^{(i)} & c_{56}^{(i)}\\ 0 & 0 & 0 & 0 & c_{56}^{(i)} & c_{66}^{(i)}\end{bmatrix} \tag{13.4.13}$$

and the superscript (i) denotes the elastic moduli of the generic *i*-th phase of multilayered cylinder. As a consequence, the matrices (13.4.10) become:

$$\begin{aligned}&\mathbf{Q}_{rr}=\begin{bmatrix} c_{11} & 0 & 0\\ 0 & c_{66} & c_{56}\\ 0 & c_{56} & c_{55}\end{bmatrix},\quad \mathbf{Q}_{r\vartheta}=\begin{bmatrix} 0 & c_{12} & c_{14}\\ c_{66} & 0 & 0\\ c_{56} & 0 & 0\end{bmatrix},\quad \mathbf{Q}_{rz}=\begin{bmatrix} 0 & c_{14} & c_{13}\\ c_{56} & 0 & 0\\ c_{55} & 0 & 0\end{bmatrix},\\&\mathbf{Q}_{\vartheta\vartheta}=\begin{bmatrix} c_{66} & 0 & 0\\ 0 & c_{22} & c_{24}\\ 0 & c_{24} & c_{44}\end{bmatrix},\quad \mathbf{Q}_{\vartheta z}=\begin{bmatrix} c_{56} & 0 & 0\\ 0 & c_{24} & c_{23}\\ 0 & c_{44} & c_{34}\end{bmatrix},\quad \mathbf{Q}_{zz}=\begin{bmatrix} c_{55} & 0 & 0\\ 0 & c_{44} & c_{34}\\ 0 & c_{34} & c_{33}\end{bmatrix}\end{aligned} \tag{13.4.14}$$

Let us now consider the case of axis-symmetry in which the displacement field is therefore independent from the variable θ. The equilibrium equation (13.4.11) becomes:

$$\begin{aligned}&\mathbf{Q}_{rr}\,\mathbf{u}_{,rr}+\mathbf{Q}_{zz}\,\mathbf{u}_{,zz}+\left(\mathbf{Q}_{rz}+\mathbf{Q}_{rz}^{T}\right)\mathbf{u}_{,rz}+r^{-2}\mathbf{K}\,\mathbf{Q}_{\theta\theta}\,\mathbf{K}\,\mathbf{u}+\\&+r^{-1}\left[\left(\mathbf{Q}_{r\theta}\,\mathbf{K}+\mathbf{K}\,\mathbf{Q}_{r\theta}^{T}+\mathbf{Q}_{rr}\right)\mathbf{u}_{,r}+\left(\mathbf{K}\,\mathbf{Q}_{\theta z}+\mathbf{Q}_{\theta z}^{T}\mathbf{K}+\mathbf{Q}_{rz}\right)\mathbf{u}_{,z}\right]=0\end{aligned} \tag{13.4.14}$$

In compact form, the equilibrium equation becomes:

$$\mathbf{A}_1\,\mathbf{u}_{,rr}+\mathbf{A}_2\,\mathbf{u}_{,zz}+\mathbf{A}_z\mathbf{u}_{,rz}+r^{-1}\left[\mathbf{A}_4\mathbf{u}_{,r}+\mathbf{A}_5\mathbf{u}_{,z}\right]+r^{-2}\mathbf{A}_6\,\mathbf{u}=0 \tag{13.4.15}$$

where

$$\begin{aligned}&\mathbf{A}_1=\mathbf{Q}_{rr},\quad \mathbf{A}_2=\mathbf{Q}_{zz},\quad \mathbf{A}_3=\mathbf{Q}_{rz}+\mathbf{Q}_{rz}^{T},\quad \mathbf{A}_4=\mathbf{Q}_{r\theta}\mathbf{K}+\mathbf{K}\,\mathbf{Q}_{r\theta}^{T}+\mathbf{Q}_{rr},\\&\mathbf{A}_5=\mathbf{K}\,\mathbf{Q}_{\theta z}+\mathbf{Q}_{\theta z}^{T}\mathbf{K}+\mathbf{Q}_{rz},\quad \mathbf{A}_6=\mathbf{K}\mathbf{Q}_{\theta\theta}\mathbf{K},\end{aligned} \tag{13.4.16}$$

13.5. Exact solution for jacket phases

The displacement solution for i-th generic phase is:

$$u_r^{(i)} = u_r^{(i)}(r,z), \quad u_\theta^{(i)} = u_\theta^{(i)}(r,z), \quad u_z^{(i)} = u_z^{(i)}(r,z) \tag{13.5.1}$$

Applying the elastic constitutive , the stress component becomes:

$$\begin{bmatrix} \sigma_{rr}^{(j)} \\ \sigma_{\theta\theta}^{(j)} \\ \sigma_{zz}^{(j)} \\ \tau_{\theta z}^{(j)} \\ \tau_{rz}^{(j)} \\ \tau_{r\theta}^{(j)} \end{bmatrix} = \begin{bmatrix} c_{11}^{(j)} & c_{12}^{(j)} & c_{13}^{(j)} & c_{14}^{(j)} & 0 & 0 \\ c_{12}^{(j)} & c_{22}^{(j)} & c_{23}^{(j)} & c_{24}^{(j)} & 0 & 0 \\ c_{13}^{(j)} & c_{23}^{(j)} & c_{33}^{(j)} & c_{34}^{(j)} & 0 & 0 \\ c_{14}^{(j)} & c_{24}^{(j)} & c_{34}^{(j)} & c_{44}^{(j)} & 0 & 0 \\ 0 & 0 & 0 & 0 & c_{55}^{(j)} & c_{56}^{(j)} \\ 0 & 0 & 0 & 0 & c_{56}^{(j)} & c_{66}^{(j)} \end{bmatrix} \begin{bmatrix} u_{r,r}^{(j)} \\ u_r^{(j)}/r \\ u_{z,z}^{(j)} \\ u_{\theta,z}^{(j)} \\ u_{r,z}^{(j)} + u_{z,r}^{(j)} \\ u_{\theta,r}^{(j)} - u_\theta^{(j)}/r \end{bmatrix} \tag{13.5.2}$$

The stress component are independent of the z variable, then we can obtained the follow differential equations:

$$u_{r,rz}^{(j)} = 0, \quad u_{r,z}^{(j)} = 0, \quad u_{z,zz}^{(j)} = 0, \quad u_{\theta,zz}^{(j)} = 0, \quad u_{r,zz}^{(j)} + u_{z,rz}^{(j)} = 0, \quad u_{\theta,rz}^{(j)} + r^{-1} u_{\theta,z}^{(j)} = 0, \tag{13.5.3}$$

By solving the equations (13.5.3), we can write:

$$\begin{aligned} u_r^{(i)} &= p_1^{(j)}(r), \\ u_\theta^{(i)} &= p_2^{(j)}(r) + \phi^{(j)} r z, \\ u_z^{(i)} &= p_3^{(j)}(r) + \varepsilon_0^{(j)} z, \end{aligned} \tag{13.5.4}$$

Substituting the displacement field (13.5.4) into Navier-Cauchy equilibrium equations, we obtain the follows ordinary differential equations system in the unknown functions $p_1^{(j)}(r), p_2^{(j)}(r), p_3^{(j)}(r)$:

$$\begin{cases} c_{11}^{(j)}\left(p_{1,r}^{(j)} + r\, p_{1,rr}^{(j)}\right) - c_{22}^{(j)} p_1^{(j)} + \left(c_{13}^{(j)} - c_{23}^{(j)}\right)\varepsilon_0^{(j)} r + \left(2c_{14}^{(j)} - c_{24}^{(j)}\right)\phi^{(j)} r^2 = 0 \\ c_{56}^{(j)}\left(2r\, p_{3,r}^{(j)} + r^2 p_{3,rr}^{(j)}\right) + c_{66}^{(j)}\left(r^2 p_{2,rr}^{(j)} + r\, p_{2,r}^{(j)} - p_2^{(j)}\right) = 0 \\ c_{55}^{(j)}\left(p_{3,r}^{(j)} + r\, p_{3,rr}^{(j)}\right) + c_{56}^{(j)} r\, p_{2,rr}^{(j)} = 0 \end{cases} \tag{13.5.5}$$

By to integrate the first equations of the (13.5.5) , we can obtained the function $p_1^{(j)}(r)$

$$p_1^{(j)}(r) = C_1^{(j)}\left(r^{\lambda^{(j)}} + r^{-\lambda^{(j)}}\right) + i\, C_2^{(j)}\left(r^{\lambda^{(j)}} - r^{-\lambda^{(j)}}\right) + h_1^{(j)}\varepsilon_0^{(j)} r + h_2^{(j)}\phi^{(j)} r^2 \tag{13.13}$$

where $h_1^{(j)} = \dfrac{c_{23}^{(j)} - c_{13}^{(j)}}{c_{11}^{(j)} - c_{22}^{(j)}}$, $h_2^{(j)} = \dfrac{c_{24}^{(j)} - 2c_{14}^{(j)}}{4c_{11}^{(j)} - c_{22}^{(j)}}$ $\lambda^{(j)} = \sqrt{\dfrac{c_{22}^{(j)}}{c_{11}^{(j)}}}$,

By to integrate the second and third equations of the (13.5.5), we can obtained the functions $p_2^{(j)}(r)$ and $p_3^{(j)}(r)$:

$$p_2^{(j)}(r) = h_4^{(j)} C_4^{(j)} - \frac{h_3^{(j)} C_3^{(j)}}{r}, \quad p_3^{(j)}(r) = \frac{h_4^{(j)} C_3^{(j)}}{r} + h_5^{(j)} C_4^{(j)} \log r \tag{13.5.7}$$

where $h_3^{(j)} = \dfrac{c_{55}^{(j)}}{2\left(c_{56}^{(j)2} - c_{55}^{(j)} c_{66}^{(j)}\right)}$, $h_4^{(j)} = \dfrac{c_{56}^{(j)}}{\left(c_{56}^{(j)2} - c_{55}^{(j)} c_{66}^{(j)}\right)}$, $h_5^{(j)} = \dfrac{c_{66}^{(j)}}{\left(c_{56}^{(j)2} - c_{55}^{(j)} c_{66}^{(j)}\right)}$

Then, the displacement solution is:

$$\begin{cases} u_r^{(j)} = C_1^{(j)}\left(r^{\lambda^{(j)}} + r^{-\lambda^{(j)}}\right) + i\, C_2^{(j)}\left(r^{\lambda^{(j)}} - r^{-\lambda^{(j)}}\right) + h_1^{(j)}\varepsilon_0^{(j)} r + h_2^{(j)}\phi^{(j)} r^2 \\ u_\theta^{(j)} = \phi^{(j)} r z + h_4^{(j)} C_4^{(j)} - \dfrac{h_3^{(j)} C_3^{(j)}}{r} \\ u_z^{(j)} = \varepsilon_0^{(j)} z + \dfrac{h_4^{(j)} C_3^{(j)}}{r} + h_5^{(j)} C_4^{(j)} \log r \end{cases} \tag{13.5.8}$$

The core phase is isotropic and vanishes the terms that diverge in r = 0, then the displacement solution and for core phase is:

$$\begin{cases} u_r^{(c)} = C_0^{(c)} r \\ u_\theta^{(c)} = \phi^{(c)}\, r\, z \\ u_z^{(c)} = \varepsilon_0^{(c)} z \end{cases} \tag{13.5.9}$$

By applying the constitutive law for isotropic material, the stress component for core phase are:

$$\begin{aligned} &\sigma_{rr}^{(c)} = \left(c_{11}^{(c)} + c_{12}^{(c)}\right) C_0^{(c)} + c_{12}^{(c)} \varepsilon_0^{(c)}, \quad \sigma_{\theta\theta}^{(c)} = \left(c_{11}^{(c)} + c_{12}^{(c)}\right) C_0^{(c)} + c_{12}^{(c)} \varepsilon_0^{(c)} \\ &\sigma_{zz}^{(c)} = 2c_{12}^{(c)} C_0^{(c)} + c_{11}^{(c)} \varepsilon_0^{(c)}, \quad \tau_{\theta z}^{(c)} = \left(c_{11}^{(c)} - c_{12}^{(c)}\right) \phi^{(c)}\, r \end{aligned} \tag{13.5.10}$$

From the constitutive law for cylindrically monoclinic material (13.5.2), the stress components assume the following explicit form:

$$\begin{bmatrix} \sigma_{rr}^{(j)} \\ \sigma_{\theta\theta}^{(j)} \\ \sigma_{zz}^{(j)} \\ \tau_{\theta z}^{(j)} \\ \tau_{rz}^{(j)} \\ \tau_{r\theta}^{(j)} \end{bmatrix} = \begin{bmatrix} \left(k_{11}^{(j)} r^{\lambda-1} + k_{12}^{(j)} r^{-(\lambda+1)}\right) & i\left(k_{13}^{(j)} r^{\lambda-1} + k_{14}^{(j)} r^{-(\lambda+1)}\right) & 0 & 0 & k_{15}^{(j)} & k_{16}^{(j)} r \\ \left(k_{21}^{(j)} r^{\lambda-1} + k_{22}^{(j)} r^{-(\lambda+1)}\right) & i\left(k_{23}^{(j)} r^{\lambda-1} + k_{24}^{(j)} r^{-(\lambda+1)}\right) & 0 & 0 & k_{25}^{(j)} & k_{26}^{(j)} r \\ \left(k_{31}^{(j)} r^{\lambda-1} + k_{32}^{(j)} r^{-(\lambda+1)}\right) & i\left(k_{33}^{(j)} r^{\lambda-1} + k_{34}^{(j)} r^{-(\lambda+1)}\right) & 0 & 0 & k_{35}^{(j)} & k_{36}^{(j)} r \\ \left(k_{41}^{(j)} r^{\lambda-1} + k_{42}^{(j)} r^{-(\lambda+1)}\right) & i\left(k_{43}^{(j)} r^{\lambda-1} + k_{44}^{(j)} r^{-(\lambda+1)}\right) & 0 & 0 & k_{45}^{(j)} & k_{46}^{(j)} r \\ 0 & 0 & 0 & -r^{-1} & 0 & 0 \\ 0 & 0 & -r^{-2} & 0 & 0 & 0 \end{bmatrix} \begin{bmatrix} C_1^{(j)} \\ C_2^{(j)} \\ C_3^{(j)} \\ C_4^{(j)} \\ \varepsilon_0^{(j)} \\ \phi^{(j)} \end{bmatrix} \tag{13.5.11}$$

where

$$\begin{aligned} &k_{11}^{(j)} = k_{13}^{(j)} = c_{12}^{(j)} + c_{11}^{(j)} \lambda^{(j)}, \quad k_{12}^{(j)} = -k_{14}^{(j)} = c_{12}^{(j)} - c_{11}^{(j)} \lambda^{(j)}, \\ &k_{15}^{(j)} = k_{25}^{(j)} = \frac{c_{23}^{(j)}\left(c_{11}^{(j)} + c_{12}^{(j)}\right) - c_{13}^{(j)}\left(c_{12}^{(j)} + c_{22}^{(j)}\right)}{c_{11}^{(j)} - c_{22}^{(j)}}, \\ &k_{26}^{(j)} = 2k_{16}^{(j)} = \frac{2c_{24}^{(j)}\left(2c_{11}^{(j)} + c_{12}^{(j)}\right) - 2c_{14}^{(j)}\left(2c_{12}^{(j)} + c_{22}^{(j)}\right)}{4c_{11}^{(j)} - c_{22}^{(j)}}, \\ &k_{21}^{(j)} = k_{23}^{(j)} = c_{22}^{(j)} + c_{12}^{(j)} \lambda^{(j)}, \quad k_{22}^{(j)} = -k_{24}^{(j)} = c_{22}^{(j)} - c_{12}^{(j)} \lambda^{(j)}, \\ &k_{31}^{(j)} = k_{33}^{(j)} = c_{23}^{(j)} + c_{13}^{(j)} \lambda^{(j)}, \quad k_{32}^{(j)} = -k_{34}^{(j)} = c_{23}^{(j)} - c_{13}^{(j)} \lambda^{(j)}, \\ &k_{35}^{(j)} = c_{33}^{(j)} - \frac{c_{13}^{(j)2} - c_{23}^{(j)2}}{c_{11}^{(j)} - c_{22}^{(j)}}, \quad k_{36}^{(j)} = c_{34}^{(j)} + \frac{\left(c_{24}^{(j)} - 2c_{14}^{(j)}\right)\left(c_{23}^{(j)} + 2c_{13}^{(j)}\right)}{4c_{11}^{(j)} - c_{22}^{(j)}}, \\ &k_{41}^{(j)} = k_{43}^{(j)} = c_{24}^{(j)} + c_{14}^{(j)} \lambda^{(j)}, \quad k_{42}^{(j)} = -k_{44}^{(j)} = c_{24}^{(j)} - c_{14}^{(j)} \lambda^{(j)}, \\ &k_{45}^{(j)} = c_{34}^{(j)} - \frac{\left(c_{14}^{(j)} + c_{24}^{(j)}\right)\left(c_{13}^{(j)} - c_{23}^{(j)}\right)}{c_{11}^{(j)} - c_{22}^{(j)}}, \quad k_{46}^{(j)} = c_{44}^{(j)} + \frac{c_{24}^{(j)2} - 4c_{14}^{(j)2}}{4c_{11}^{(j)} - c_{22}^{(j)}}, \end{aligned} \tag{13.5.12}$$

For brevity, in matrix (13.5.11) the coefficient $\lambda^{(j)}$ is written with symbol λ. The results obtained until now satisfy the equilibrium and compatibility equations inside each generic *i*-th phase of a composite circular cylinder subjected to axis-symmetrical strains. Under both the hypothesis of linear elastic behaviour of the materials and the assumption of perfect contact at the cylindrical interfacial boundaries (no de-lamination or friction phenomena), we have now to establish the satisfaction of both the equilibrium and the compatibility equations at the boundary surfaces between two generic adjacent phases. To obtain this, we will make first reference to the generic case in which an assembled functionally graded circular cylinder is constituted by a central *core* and *n* arbitrary *cladding* phases. The total unknown parameters to determine can be summarized as follows:

$$\begin{aligned} &C_0^{(c)},\phi^{(c)},\varepsilon_0^{(c)} \\ &C_1^{(j)},C_2^{(j)},C_3^{(j)},C_4^{(j)},\phi^{(j)},\varepsilon_0^{(j)} \quad j\in\{1,2,.....n\} \end{aligned} \tag{13.5.13}$$

where those in $(13.5.13)_1$ represent the unknown coefficient of the *core*, those in $(13.5.13)_2$ represent the unknown parameters for every circular hollow cylinder, while $(13.5.13)_3$ are the two coefficients that represent unit angle warping and the axial strain, respectively. Hence, the total number of unknowns will be $(6n+3)$, which equals the number of algebraic equations to solve. In particular, as we will show in the follows, the boundary equations at the interfaces is $6n$, while 3 is the number of boundary conditions on the external cylindrical surface and on the end basis. In particular, we begin writing the 6*n* equilibrium and compatibility equations at the interfaces, that is:

$$\begin{cases} u_r^{(j)}(r=R^{(j)})=u_r^{(j+1)}(r=R^{(j)}) \\ u_\theta^{(j)}(r=R^{(j)})=u_\theta^{(j+1)}(r=R^{(j)}) \\ u_z^{(j)}(r=R^{(j)})=u_z^{(j+1)}(r=R^{(j)}) \\ \sigma_{rr}^{(j)}(r=R^{(j)})=\sigma_{rr}^{(j+1)}(r=R^{(j)}) \\ \tau_{rz}^{(j)}(r=R^{(j)})=\tau_{rz}^{(j+1)}(r=R^{(j)}) \\ \tau_{r\theta}^{(j)}(r=R^{(j)})=\tau_{r\theta}^{(j+1)}(r=R^{(j)}) \end{cases} \quad \forall j\in\{0,1,...,n-1\} \tag{13.5.14}$$

where $R^{(j)}$ is the outer radius of the *j*-th phase. By writing in explicit the equations $(13.5.14)_2$-$(13.5.14)_3$-$(13.5.14)_5$-$(13.5.14)_6$, we obtained:

$$\phi^{(c)}=\phi^{(j)}=\phi,\quad \varepsilon_0^{(c)}=\varepsilon_0^{(j)}=\varepsilon_0,\quad C_3^{(j)}=C_4^{(j)}=0,\quad \forall j\in\{0,1,...,n-1\}, \tag{13.5.15}$$

Recalling the previously obtained results, the system (13.5.14) reduce to :

$$\begin{cases} u_{rr}^{(j)}(r=R^{(j)})=u_{rr}^{(j+1)}(r=R^{(j)}) \\ \sigma_{rr}^{(j)}(r=R^{(j)})=\sigma_{rr}^{(j+1)}(r=R^{(j)}) \end{cases} \quad j\in\{0,1,...,n-1\} \tag{13.5.16}$$

In explicit the system (13.5.16) can be expressed as follows:

$$\begin{cases} \left(C_1^{(j)}-C_1^{(j+1)}\right)\left(R^{(j)\lambda}+R^{(j)-\lambda}\right)+i\left(C_2^{(j)}-C_2^{(j+1)}\right)\left(R^{(j)\lambda}-R^{(j)-\lambda}\right)+\left(h_1^{(j)}-h_1^{(j+1)}\right)\varepsilon_0\,R^{(j)} \\ +\left(h_2^{(j)}-h_2^{(j+1)}\right)\phi\,R^{(j)2}+R^{(j)}C_0^{(0)}\delta_{0j}=0 \\ \left(C_1^{(i)}k_{11}^{(i)}-C_1^{(i+1)}k_{11}^{(i+1)}\right)R^{(i)\lambda-1}+\left(C_1^{(i)}k_{12}^{(i)}-C_1^{(i+1)}k_{12}^{(i+1)}\right)R^{(i)-\lambda-1}+\left(k_{15}^{(i)}-k_{15}^{(i+1)}+\frac{E\,\nu\,\delta_{0j}}{1-\nu-2\nu^2}\right)\varepsilon_0+ \\ i\left(C_2^{(i)}k_{13}^{(i)}-C_2^{(i+1)}k_{13}^{(i+1)}\right)R^{(i)\lambda-1}+i\left(C_2^{(i)}k_{14}^{(i)}-C_2^{(i+1)}k_{14}^{(i+1)}\right)R^{(i)-\lambda-1}+\left(k_{16}^{(i)}-k_{16}^{(i+1)}\right)\phi\,R^{(i)}+\frac{E\,C_0\delta_{0j}}{1-\nu-2\nu^2}=0 \end{cases} \tag{13.5.17}$$

The Cauchy equilibrium equations on the external cylindrical boundary surface, ($i=n$), give:

$$\sigma_{rr}^{(n)}(r=R^{(n)})=0 \tag{13.5.18}$$

The equations (13.5.17) in explicit becomes:

$$\begin{aligned} &C_1^{(n)}\left(k_{11}^{(n)}R^{(n)\lambda-1}+k_{12}^{(n)}R^{(n)-\lambda-1}\right)+i\,C_2^{(n)}\left(k_{13}^{(n)}R^{(n)\lambda-1}+k_{14}^{(n)}R^{(n)-\lambda-1}\right)+ \\ &+k_{15}^{(n)}\varepsilon_0+k_{16}^{(n)}\phi\,R^{(n)}=0 \end{aligned} \tag{13.5.19}$$

Finally, it remains to consider the equilibrium equation in z-direction and about z-direction on one of the basis. Therefore, without loss of generality, for $z=0$ we can write

$$\begin{aligned} &\int_0^{2\pi}\int_0^{R^{(0)}}\sigma_{zz}^{(0)}(z=0)r\,dr\,d\theta+\sum_{i=1}^{n}\int_0^{2\pi}\int_{R^{(i-1)}}^{R^{(i)}}\sigma_{zz}^{(i)}(z=0)\,r\,dr\,d\theta=N_z, \\ &\int_0^{2\pi}\int_0^{R^{(0)}}\tau_{\theta z}^{(0)}(z=0)r^2\,dr\,d\theta+\sum_{i=1}^{n}\int_0^{2\pi}\int_{R^{(i-1)}}^{R^{(i)}}\tau_{\theta z}^{(i)}(z=0)\,r^2\,dr\,d\theta=\mathfrak{M}_z, \end{aligned} \tag{13.5.20}$$

where $N_z,\mathfrak{M}_z$ are the total axial force and torque moment applied at $z=0$, respectively. In order to solve the algebraic system constituted by (13.5.17), (13.5.19) and (13.5.20), it could be convenient

to re-arrange the whole $(2n+3)\times(2n+3)$ algebraic system following a matrix-based procedure. Indeed, we can collect the known terms in the *loads* vector $\mathbf{L}$

$$\mathbf{L}^T=\{0,0,...,0,N_z,\mathfrak{M}_z\} \tag{13.5.21}$$

where the only non zero terms is the last two ones, while the unknown parameters can be collected in the vector $\mathbf{X}$ as follows

$$\mathbf{X}^T=\left\{C_0^{(0)},C_1^{(1)},C_2^{(1)},C_1^{(2)},C_2^{(2)},...,C_1^{(i)},C_2^{(i)},...,C_1^{(n)},C_2^{(n)},\varepsilon_0,\phi\right\} \tag{13.5.22}$$

so that the set of equations (5.15), (5.17) and (5.18) reads

$$\mathbb{P}\cdot\mathbf{X}=\mathbf{L} \tag{13.5.23}$$

where, $\mathbb{P}$ is a $(2n+3)\times(2n+3)$ square matrix containing the coefficients $P_{h/m}$, which are functions of both the radii and the elastic moduli of the phases. The explicit expression of the coefficients $P_{h/m}$ are reported in detail in the Appendix. Finally, being the system (13.5.23) of linear and algebraic type, provided that $\det\mathbb{P}\neq 0$, it is possible to write the solution as follows

$$\mathbf{X}=\mathbb{P}^{-1}\mathbf{L}=\frac{1}{\det\mathbb{P}}\text{adj}[\mathbb{P}]\mathbf{L}=\frac{1}{\det\mathbb{P}}\tilde{\mathbb{P}}\mathbf{L},\qquad X_m=\frac{1}{\det\mathbb{P}}\sum_{h=1}^{m=2n+3}\tilde{P}_{h/m}L_h, \tag{13.5.24}$$

where $\text{adj}[\mathbb{P}]=\tilde{\mathbb{P}}$ is the adjoint matrix of $\mathbb{P}$ and then the *Cramer* rule has been employed. The possibility to invert the matrix $\mathbb{P}$ is ensured by invoking the uniqueness of the linear elastic solution, due to Kirchhoff's theorem. This could appear not immediately evident if one directly tries to see the actual form of $\mathbb{P}$. When the proposed strategy is applied to a three-phase composed cylinder, an analytical proof that the algebraic problem is well-posed is also given by utilizing the *Mathematica* code, where the command *RowReduce* is employed. This command performs a version of Gaussian elimination, adding multiples of rows together so as to produce zero elements when possible. The final matrix is in reduced row echelon form. If is a non-degenerate square matrix, as well as our case, *RowReduce*[$\mathbb{P}$] gives the *IdentityMatrix*[Length[$\mathbb{P}$]]. In linear elastostatic problem with displacement boundary condition, the equations (13.5.20) on the basis of the solid, must be to substitute by analogous displacement condition at the base $z=L$*:*

$$\begin{cases}u_z^{(j)}(z=L)=W_0\\ u_\theta^{(j)}(z=L)=\varphi_0\, r\end{cases}\qquad \forall j\in\{0,1,...n\} \tag{13.5.25}$$

where L is the total length of the cylinder, W_0 is a prescribed displacement value, φ_0 is a prescribed angle of rotation. By solving the conditions (13.5.25), we obtain the uniform deformation in z - direction ε_0 and unit angle of rotation ϕ as function of W_0 and φ_0 :

$$\begin{cases}\varepsilon_0 L=W_0 \quad\Rightarrow\quad \varepsilon_0=W_0/L\\ \phi\, L\, r=\varphi_0 r \;\Rightarrow\quad \phi=\varphi_0/L\end{cases} \tag{13.5.26}$$

Then, in the linear problem with displacement prescribed on basis of multilayered cylinder, the equations to solve are (13.5.17) and (13.5.20), where ε_0,ϕ are note. In explicit, the equations (13.5.17) in this case become:

$$\begin{aligned}&\left(C_1^{(i)}-C_1^{(i+1)}\right)\left(R^{(i)\lambda}+R^{(i)-\lambda}\right)+i\left(C_2^{(i)}-C_2^{(i+1)}\right)\left(R^{(i)\lambda}-R^{(i)-\lambda}\right)+R^{(j)}C_0^{(0)}\delta_{0j}=\\ &\qquad=\frac{1}{L}\left[\left(h_1^{(i+1)}-h_1^{(i)}\right)W_0R^{(i)}+\left(h_2^{(i+1)}-h_2^{(i)}\right)\varphi_0R^{(i)2}\right]\end{aligned} \tag{13.5.27)a}$$

$$\begin{aligned}&\left(C_1^{(i)}k_{11}^{(i)}-C_1^{(i+1)}k_{11}^{(i+1)}\right)R^{(i)\lambda-1}+\left(C_1^{(i)}k_{12}^{(i)}-C_1^{(i+1)}k_{12}^{(i+1)}\right)R^{(i)-\lambda-1}+i\left(C_2^{(i)}k_{13}^{(i)}-C_2^{(i+1)}k_{13}^{(i+1)}\right)R^{(i)\lambda-1}+\\ &+i\left(C_2^{(i)}k_{14}^{(i)}-C_2^{(i+1)}k_{14}^{(i+1)}\right)R^{(i)-\lambda-1}+\frac{E\,C_0\delta_{0j}}{1-\nu-2\nu^2}=\\ &\qquad=\frac{1}{L}\left[\left(k_{16}^{(i+1)}-k_{16}^{(i)}+\frac{E\,\nu\,\delta_{0j}}{1-\nu-2\nu^2}\right)\varphi_0\,R^{(i)}+\left(k_{15}^{(i+1)}-k_{15}^{(i)}\right)W_0\right]\end{aligned} \tag{13.5.27)b}$$

The equation (13.5.20) becomes

$$C_1^{(n)}\left(k_{11}^{(n)}R^{(n)\lambda-1}+k_{12}^{(n)}R^{(n)-\lambda-1}\right)+iC_2^{(n)}\left(k_{13}^{(n)}R^{(n)\lambda-1}+k_{14}^{(n)}R^{(n)-\lambda-1}\right)=-\frac{1}{L}\left[k_{15}^{(n)}W_0+k_{16}^{(n)}\varphi_0\,R^{(n)}\right] \quad (13.5.28)$$

In order to solve the algebraic system constituted by (13.5.27)-(13.5.28), it could be convenient to re-arrange the whole $(2n+1)\times(2n+1)$ algebraic system following a matrix-based procedure. Indeed, we can collect the known terms in the *displacements* vector $\mathbf{D}$

$$\mathbf{D}=\frac{1}{L}\begin{bmatrix} h_1^{(1)}R^{(0)} & h_2^{(1)}R^{(0)2} \\ k_{15}^{(1)} & k_{16}^{(1)}R^{(0)}+E\nu\left(2\nu^2+\nu-1\right)^{-1} \\ \vdots & \vdots \\ \left(h_1^{(j+1)}-h_1^{(j)}\right)R^{(j)} & \left(h_2^{(j+1)}-h_2^{(j)}\right)R^{(j)2} \\ k_{15}^{(j+1)}-k_{15}^{(j)} & \left(k_{16}^{(j+1)}-k_{16}^{(j+1)}\right)R^{(j)} \\ \vdots & \vdots \\ \left(h_1^{(n)}-h_1^{(n-1)}\right)R^{(n-1)} & \left(h_2^{(n)}-h_2^{(n-1)}\right)R^{(n-1)2} \\ k_{15}^{(n)}-k_{15}^{(n-1)} & \left(k_{16}^{(n)}-k_{16}^{(n-1)}\right)R^{(n-1)} \\ -k_{15}^{(n)} & -k_{16}^{(n)}R^{(n)} \end{bmatrix}\cdot\begin{bmatrix} W_0 \\ \varphi_0 \end{bmatrix} \quad (13.5.29)$$

the unknown parameters can be collected in the vector $\mathbf{Y}$ as follows

$$\mathbf{Y}^T=\left\{C_0^{(0)},C_1^{(1)},C_2^{(1)},C_1^{(2)},C_2^{(2)},...,C_1^{(i)},C_2^{(i)},...,C_1^{(n)},C_2^{(n)}\right\} \quad (13.5.30)$$

so that the set of equations (5.15), (5.17) and (5.18) reads

$$\mathbb{Q}\cdot\mathbf{Y}=\mathbf{D} \quad (13.5.31)$$

where, $\mathbb{Q}$ is a $(2n+1)\times(2n+1)$ square matrix containing the coefficients $Q_{h/m}$, which are functions of both the radii and the elastic moduli of the phases. Finally, being the system (5.31) of linear and algebraic type, provided that $\det\mathbb{Q}\neq 0$, it is possible to write the solution as follows

$$\mathbf{Y}=\mathbb{Q}^{-1}\mathbf{D}=\frac{\mathrm{adj}[\mathbb{Q}]}{\det\mathbb{Q}}\mathbf{D}=\frac{\tilde{\mathbb{Q}}}{\det\mathbb{Q}}\mathbf{D},\qquad Y_m=\frac{1}{\det\mathbb{Q}}\sum_{h=1}^{m=2n+1}\tilde{Q}_{h/m}D_h, \quad (13.5.32)$$

where $\mathrm{adj}[\mathbb{Q}]=\tilde{\mathbb{Q}}$ is the adjoint matrix of $\mathbb{Q}$ and then the *Cramer* rule has been employed.

13.6. Example application for solid with three phases

Multilayered cylinder subjected by axial force

We consider the case of multilayered cylinder constituted by a central core and two hollow cylinder phases (1) and (2). The three phase have the same volume equal to π and the solid is loaded by axial force N_z applied on basis, as showed in figure 13.2. Let us consider that the two hollow phase are transversally isotropic in the helicoidal coordinate system and the plane of the isotropy is "r-c", but the central core is composed by isotropic material. Moreover, we consider that the following relationship between the elastic constants:

$$E_{rr}=E_{cc}=E,\quad E_{tt}=\alpha E,\quad \nu_{rt}=\nu_{tc}=\nu_{rc}=\nu,$$
$$G_{rt}=G_{tc}=\frac{\alpha E}{2\left(1+\nu\right)},\quad G_{rc}=\frac{E}{2\left(1+\nu\right)}, \quad (13.6.1)$$

Applying the relationship (13.6.1), we determine the elastic constants in helicoidal system as function of the Young's moduli E , Poisson's moduli and parameter α :

$$c_{11}^{hel}=c_{33}^{hel}=\frac{E\left(\nu^2-\alpha\right)}{\left(1+\nu\right)\left[\alpha\left(\nu-1\right)+2\nu^2\right]},\qquad c_{55}^{hel}=\frac{E}{2\left(1+\nu\right)},\quad c_{13}^{hel}=-\frac{E\nu\left(\nu+\alpha\right)}{\left(1+\nu\right)\left[\alpha\left(\nu-1\right)+2\nu^2\right]},$$

$$c_{12}^{hel}=c_{23}^{hel}=-\frac{\alpha\nu E}{\alpha(\nu-1)+2\nu^2},\quad c_{22}^{hel}=\frac{E\alpha^2(\nu-1)}{\alpha(\nu-1)+2\nu^2},\quad c_{44}^{hel}=c_{66}^{hel}=\frac{\alpha E}{2(1+\nu)},\tag{13.6.2}$$

Substituting the equations (13.6.2) in to (13.3.19), we obtained the connection between the elastic constant of helicoidal system and these in the cylindrical system:

$$c_{11}^{cyl}=\frac{E(\nu^2-\alpha)}{(1+\nu)\left[\alpha(\nu-1)+2\nu^2\right]},\quad c_{12}^{cyl}=-\frac{E\nu\left[\nu+\alpha(2+\nu)+(\alpha-1)\nu\cos 2\psi\right]}{2(1+\nu)\left[\alpha(\nu-1)+2\nu^2\right]},$$

$$c_{13}^{cyl}=-\frac{E\nu\left[(\alpha+\nu)\cos^2\psi+\alpha(1+\nu)\sin^2\psi\right]}{(1+\nu)\left[\alpha(\nu-1)+2\nu^2\right]},\quad c_{14}^{cyl}=-\frac{E\nu^2(\alpha-1)\sin^2 2\psi}{2(1+\nu)\left[\alpha(\nu-1)+2\nu^2\right]},$$

$$c_{22}^{cyl}=\frac{E\left[\alpha^2(\nu^2-1)\cos^4\psi+2\alpha(\nu-1)(\alpha+\nu)\sin^2 2\psi\cos^2 2\psi+(\nu^2-\alpha)\sin^4\psi\right]}{(1+\nu)\left[\alpha(\nu-1)+2\nu^2\right]},$$

$$c_{23}^{cyl}=\frac{E\left\{\left[\alpha(\alpha-1)-2\alpha(1+\alpha)\nu+\nu^2(1+\alpha(\alpha-6))\right]\sin^2 2\psi-4\alpha\nu(\nu)\cos^2 2\psi\right\}}{4(1+\nu)\left[\alpha(\nu-1)+2\nu^2\right]},$$

$$c_{24}^{cyl}=\frac{E(\alpha-1)\left[\nu^2+\alpha(\nu^2-1)+\left(\alpha(\nu-1)^2-\nu^2\right)\cos 2\psi\right]\sin 2\psi}{4(1+\nu)\left[\alpha(\nu-1)+2\nu^2\right]},$$

$$c_{33}^{cyl}=\frac{E\left[(\nu^2-\alpha)\cos^4\psi+2\alpha(\nu-1)(\alpha+\nu)\sin^2 2\psi\cos^2 2\psi+\alpha^2(\nu^2-1)\sin^4\psi\right]}{(1+\nu)\left[\alpha(\nu-1)+2\nu^2\right]},$$

$$c_{34}^{cyl}=-\frac{E(\alpha-1)\left[\alpha-(1+\alpha)\nu^2+\left(\alpha(\nu-1)^2-\nu^2\right)\cos 2\psi\right]\sin 2\psi}{4(1+\nu)\left[\alpha(\nu-1)+2\nu^2\right]},$$

$$c_{44}^{cyl}=\frac{E\alpha\left[2\nu^2+\alpha(\nu-1)\right](1+\cos 4\psi)+E\left\{(1+\alpha)\left[\nu^2(1+\alpha)-\alpha\right]+2\nu\alpha\right\}\sin^2 2\psi}{4(1+\nu)\left[\alpha(\nu-1)+2\nu^2\right]},\tag{13.6.3}$$

We assume that in the phase (1) helix slope is equal to ψ, but in the phase (2) is $-\psi$. Then , we obtain the following relationship between elastic constants of the two hollow phases in cylindrical coordinate system:

$$\begin{aligned}
&c_{11}^{(1)}=c_{11}^{(2)},\ \ c_{12}^{(1)}=c_{12}^{(2)},\ \ c_{13}^{(1)}=c_{13}^{(2)},\\
&c_{22}^{(1)}=c_{22}^{(2)},\ \ c_{23}^{(1)}=c_{23}^{(2)},\ \ c_{33}^{(1)}=c_{33}^{(2)},\\
&c_{44}^{(1)}=c_{44}^{(2)},\quad c_{55}^{(1)}=c_{55}^{(2)},\ \ c_{66}^{(1)}=c_{66}^{(2)},\\
&c_{14}^{(1)}=-c_{14}^{(2)},\quad c_{24}^{(1)}=-c_{24}^{(2)},\ \ c_{34}^{(1)}=-c_{34}^{(2)},\ \ c_{56}^{(1)}=-c_{56}^{(2)},
\end{aligned}\tag{13.6.4}$$

Moreover, it is easy to obtain other relationship between the constants $k_{ij}^{(1)}$ and $k_{ij}^{(2)}$:

$$\begin{aligned}
&\lambda^{(1)}=\lambda^{(2)},\quad h_1^{(1)}=h_1^{(2)},\ \ h_2^{(1)}=h_2^{(2)},\\
&k_{ij}^{(1)}=k_{ij}^{(2)}\quad \forall j\in\{1,...,5\},\ \ and\ \ \ k_{i6}^{(1)}=-k_{i6}^{(2)}\quad \forall i\in\{1,2,3\}\\
&k_{4j}^{(1)}=-k_{4j}^{(2)}\quad \forall j\in\{1,...,5\},\ \ and\ \ \ k_{46}^{(1)}=k_{46}^{(2)}
\end{aligned}\tag{13.6.5}$$

Recalling the equations (13.5.17)-(13.5.19)-(13.5.20), we obtain that the total number of unknowns will be 7, which equals the number of algebraic equations to solve. The unknowns parameter are $C_0^{(c)},\phi,\varepsilon_0,C_1^{(1)},C_2^{(1)},C_1^{(2)},C_2^{(2)}$ and coefficient of the matrix $\mathbb{P}$ becomes:

$$p_{11}=R^{(0)},\quad p_{12}=-R^{(0)-\lambda^{(1)}}\left(1+2R^{(0)2\lambda^{(1)}}\right),\quad p_{13}=-i\left(R^{(0)\lambda^{(1)}}-R^{(0)-\lambda^{(1)}}\right),\quad p_{14}=0,\quad p_{15}=0,$$

$$p_{16}=-h_1^{(1)}R^{(0)},\quad p_{17}=-h_2^{(1)}R^{(0)2},\quad p_{21}=\frac{E}{1-\nu-2\nu^2},\quad p_{22}=-R^{(0)-\left(1+\lambda^{(1)}\right)}\left(k_{12}^{(1)}+k_{11}^{(1)}R^{(0)2\lambda^{(1)}}\right),$$

$$p_{23}=-i\,R^{(0)-\left(1+\lambda^{(1)}\right)}\left(k_{14}^{(1)}+k_{13}^{(1)}R^{(0)2\lambda^{(1)}}\right),\ p_{24}=0,\ p_{25}=0,\qquad p_{26}=-k_{15}^{(1)}+\frac{E\nu}{1-\nu-2\nu^2},\quad p_{27}=-k_{16}^{(1)}R^{(0)},$$

$$p_{31}=0,\quad p_{32}=2^{-\lambda^{(1)}/2}R^{(0)-\lambda^{(1)}}\left(1+2^{\lambda^{(1)}}R^{(0)2\lambda^{(1)}}\right),\ p_{33}=-i\,2^{-\lambda^{(1)}/2}R^{(0)-\lambda^{(1)}}\left(-1+2^{\lambda^{(1)}}R^{(0)2\lambda^{(1)}}\right),$$

$$p_{34}=-2^{-\lambda^{(1)}/2}R^{(0)-\lambda^{(1)}}\left(1+2^{\lambda^{(1)}}R^{2\lambda^{(1)}}\right),\quad p_{35}=-i\,2^{-\lambda^{(1)}/2}R^{(0)-\lambda^{(1)}}\left(1+2^{\lambda^{(1)}}R^{(0)2\lambda^{(1)}}\right),\quad p_{36}=0,$$

$$p_{37}=4h_2^{(1)}R^{(0)2},\qquad p_{41}=0,\ p_{42}=2^{-\left(\lambda^{(1)}+1\right)/2}R^{(0)-\left(1+\lambda^{(1)}\right)}\left(k_{12}^{(1)}+2^{\lambda^{(1)}}k_{11}^{(1)}R^{(0)2\lambda^{(1)}}\right),$$

$$p_{43}=-i\,2^{-\left(\lambda^{(1)}+1\right)/2}R^{(0)-\left(1+\lambda^{(1)}\right)}\left(k_{14}^{(1)}+2^{\lambda^{(1)}}k_{13}^{(1)}R^{(0)2\lambda^{(1)}}\right),\ p_{44}=-2^{-\left(\lambda^{(1)}+1\right)/2}R^{(0)-\left(1+\lambda^{(1)}\right)}\left(k_{12}^{(1)}+2^{\lambda^{(1)}}k_{11}^{(1)}R^{2\lambda^{(1)}}\right),$$

$$p_{45}=-i\,2^{-\left(\lambda^{(1)}+1\right)/2}R^{(0)-\left(1+\lambda^{(1)}\right)}\left(k_{14}^{(1)}+2^{\lambda^{(1)}}k_{13}^{(1)}R^{(0)2\lambda^{(1)}}\right),\quad p_{46}=0,\quad p_{47}=2\sqrt{2}\,k_{16}^{(1)}R^{(0)},\quad p_{51}=0,$$

$$p_{52}=0,\quad p_{53}=0,\ p_{55}=i\,3^{-\left(1+\lambda^{(1)}\right)/2}R^{-\left(1+\lambda^{(1)}\right)}\left(k_{14}^{(1)}+3^{\lambda^{(1)}}k_{13}^{(1)}R^{(0)2\lambda^{(1)}}\right),$$

$$p_{54}=3^{-\left(1+\lambda^{(1)}\right)/2}R^{-\left(1+\lambda^{(1)}\right)}\left(k_{12}^{(1)}+3^{\lambda^{(1)}}k_{11}^{(1)}R^{(0)2\lambda^{(1)}}\right),\ p_{56}=k_{15}^{(1)},\quad p_{57}=-\sqrt{3}\,k_{16}^{(1)}R^{(0)},\ p_{61}=\frac{2E\pi\nu R^{(0)2}}{1-\nu-2\nu^2},$$

$$p_{62}=\frac{2^{1-\lambda^{(1)}/2}\pi R^{(0)1-\lambda^{(1)}}\left[2^{\lambda^{(1)}/2}\left(2^{\left(1+\lambda^{(1)}\right)/2}-1\right)\left(\lambda^{(1)}-1\right)k_{31}^{(1)}R^{(0)2\lambda^{(1)}}-\left(\sqrt{2}-2^{\lambda^{(1)}/2}\right)\left(1+\lambda^{(1)}\right)k_{32}^{(1)}\right]}{\lambda^{(1)2}-1},$$

$$p_{63}=\frac{i\,2^{1-\lambda^{(1)}/2}\pi R^{(0)1-\lambda^{(1)}}\left[2^{\lambda^{(1)}/2}\left(2^{\left(1+\lambda^{(1)}\right)/2}-1\right)\left(\lambda^{(1)}-1\right)k_{33}^{(1)}R^{(0)2\lambda^{(1)}}-\left(\sqrt{2}-2^{\lambda^{(1)}/2}\right)\left(1+\lambda^{(1)}\right)k_{34}^{(1)}\right]}{\lambda^{(1)2}-1},$$

$$p_{64}=\frac{\pi R^{(0)1-\lambda^{(1)}}\left[\left(2^{\left(3-\lambda^{(1)}\right)/2}-2\,3^{\left(1-\lambda^{(1)}\right)/2}\right)k_{32}^{(1)}-2\left(2^{\left(1+\lambda^{(1)}\right)/2}-3^{\left(1+\lambda^{(1)}\right)/2}\right)k_{31}^{(1)}R^{(0)2\lambda^{(1)}}\right]}{\lambda^{(1)2}-1},$$

$$p_{65}=\frac{i\,2^{1-\lambda^{(1)}/2}3^{-\lambda^{(1)}/2}\pi R^{(0)1-\lambda^{(1)}}\left[\begin{array}{l}6^{\lambda^{(1)}/2}\left(2^{\left(1+\lambda^{(1)}\right)/2}-3^{\left(1+\lambda^{(1)}\right)/2}\right)\left(\lambda^{(1)}-1\right)k_{33}^{(1)}R^{(0)2\lambda^{(1)}}+\\ \left(\sqrt{3}\,2^{\lambda^{(1)}/2}-\sqrt{2}\,3^{\lambda^{(1)}/2}\right)\left(1+\lambda^{(1)}\right)k_{34}^{(1)}\end{array}\right]}{\lambda^{(1)2}-1},$$

$$p_{66}=\frac{\pi R^{(0)2}\left[E\left(\nu-1\right)+2k_{35}^{(1)}\left(2\nu^2+\nu-1\right)\right]}{2\nu^2+\nu-1},\quad p_{67}=\frac{2}{3}\left(4\sqrt{2}-3\sqrt{3}-1\right)k_{36}^{(1)}\pi R^{(0)3},$$

$$p_{71}=0,\ p_{72}=\frac{2^{1-\lambda^{(1)}/2}\pi R^{(0)2-\lambda^{(1)}}\left[2^{\lambda^{(1)}/2}\left(2^{1+\lambda^{(1)}/2}-1\right)\left(\lambda^{(1)}-2\right)k_{41}^{(1)}R^{(0)2\lambda^{(1)}}+\left(2^{\lambda^{(1)}/2}-2\right)\left(2+\lambda^{(1)}\right)k_{42}^{(1)}\right]}{\lambda^{(1)2}-4},$$

$$p_{73}=\frac{i\,2^{1-\lambda^{(1)}/2}\pi R^{(0)2-\lambda^{(1)}}\left[2^{\lambda^{(1)}/2}\left(2^{1+\lambda^{(1)}/2}-1\right)\left(\lambda^{(1)}-2\right)k_{43}^{(1)}R^{(0)2\lambda^{(1)}}+\left(2^{\lambda^{(1)}/2}-2\right)\left(2+\lambda^{(1)}\right)k_{44}^{(1)}\right]}{\lambda^{(1)2}-1},$$

$$p_{74}=\frac{2^{1-\lambda^{(1)}/2}3^{-\lambda^{(1)}/2}\pi R^{(0)2-\lambda^{(1)}}\left[\begin{array}{l}6^{\lambda^{(1)}/2}\left(2^{1+\lambda^{(1)}/2}-3^{1+\lambda^{(1)}/2}\right)\left(\lambda^{(1)}-2\right)k_{41}^{(1)}R^{(0)2\lambda_1}\lambda^{(1)}+\\ +\left(3\,2^{\lambda^{(1)}/2}-2\,3^{\lambda^{(1)}/2}\right)\left(2+\lambda^{(1)}\right)k_{42}^{(1)}\end{array}\right]}{\lambda^{(1)2}-4},$$

$$p_{75}=\frac{i\,2^{1-\lambda^{(1)}/2}3^{-\lambda^{(1)}/2}\pi R^{(0)2-\lambda^{(1)}}\left[\begin{array}{l}6^{\lambda^{(1)}/2}\left(2^{1+\lambda^{(1)}/2}-3^{1+\lambda^{(1)}2}\right)\left(\lambda_1-2\right)k_{43}^{(1)}R^{(0)2\lambda^{(1)}}+\\ +\left(3\cdot 2^{\lambda^{(1)}/2}-2\cdot 3^{\lambda^{(1)}/2}\right)\left(2+\lambda^{(1)}\right)k_{44}^{(1)}\end{array}\right]}{\lambda^{(1)2}-4},$$

$$p_{76}=\frac{2}{3}\left(4\sqrt{2}-3\sqrt{3}-1\right)k_{45}^{(1)}\pi R^{(0)3},\quad p_{77}=\pi R^{(0)4}\left(\frac{E}{2\left(1+\nu\right)}+4k_{46}^{(1)}\right),$$

The *loads* vector $\mathbf{L}$ becomes: $\mathbf{L}^T=\{0,0,...,0,N_z,0\}$

Multilayered cylinder subjected by couple torque

Multilayered cylinder, described below, is loaded only by couple torque $\mathfrak{M}_z$, as showed in figure 13.13. The unknowns parameter are $C_0^{(c)},\phi,\varepsilon_0,\ C_1^{(1)},C_2^{(1)}\ ,C_1^{(2)},C_2^{(2)}$ and coefficient of the matrix $\mathbb{P}$ are same to coefficient of the case 6.1, but the *loads* vector $\mathbf{L}$ becomes:

$$\mathbf{L}^T=\{0,0,...,0,0,\mathfrak{M}_z\}$$

Multilayered cylinder with angle of rotation prescribed

Multilayered cylinder, described below, is loaded only by displacement condition on basis. In particular, we consider that the displacement in z direction W_0 on base for $z=L$ is equal to zero, but the angle of rotation φ_0 is equal to 0.1 rad. For this load condition the stress results are reported in figures 13.3, 13.4, 13.5, 13.6. The axial force and couple torque resultants are function of slope of helicoidal fibres, as showed in figure 13.11(A)

Multilayered cylinder with displacement in z direction prescribed

Multilayered cylinder, described below, is loaded only by displacement condition on basis. In particular, we consider that the displacement in z direction W_0 on base for $z=L$ is equal to 0.1 mm , but the angle of rotation φ_0 is equal to zero. For this load condition the stress results are reported in figures 13.7, 13.8, 13.9, 13.10. The axial force and couple torque resultants are function of slope of helicoidal fibres, as showed in figure 13.11(B)

13.7. Strategies for obtaining overall elasticity tensors: Voigt and Reuss estimating

In this section, we consider an volume V bounded by ∂V , which constituted by n elastic cylindrical hollow phases with volume $V^{(i)}$ and a elastic cylindrical central core $V^{(0)}$. Any hollow phase having elasticity tensors $\mathbf{C}^{(i)}\ (i=1,2,...,n)$ and central core having elasticity tensor $\mathbf{C}^{(0)}$. It is assumed that any phase is perfectly bonded to contact phase. All the phases of the cylindrical solid are assumed to be linearly elastic. Hence, the overall response of the solid is linearly elastic, too. Each phase is assumed to be homogeneous, and the central core is isotropic, but hollow phases are monoclinic anisotropy . In general, the overall response of the solid may be anisotropic. This depends on the geometry and arrangement of the phases. The overall elasticity tensors of the cylindrical solid, denoted by $\overline{\mathbf{C}}$. The goal is to calculate the overall elasticity tensor $\overline{\mathbf{C}}$ of the cylindrical solid. In order to do it, obtain the average value of the strain field over each phase as:

$$\overline{\mathbf{E}}^{(i)}=\left\langle\mathbf{E}^{(i)}\left(\mathbf{x}\right)\right\rangle=\frac{1}{V^{(i)}}\int_{V^{(i)}}\mathbf{E}^{(i)}\left(\mathbf{x}\right)dV \tag{13.7.1}$$

and the average value of the stress field over phase is:

$$\overline{\mathbf{T}}^{(i)}=\left\langle\mathbf{T}^{(i)}\left(\mathbf{x}\right)\right\rangle=\frac{1}{V^{(i)}}\int_{V^{(i)}}\mathbf{T}^{(i)}\left(\mathbf{x}\right)dV \tag{13.7.2}$$

For i-generic cylindrical hollow phase, we can write:

$$\overline{\mathbf{T}}^{(i)}=\mathbf{C}^{(i)}:\overline{\mathbf{E}}^{(i)} \tag{13.7.3}$$

but for cylindrical central core the relationship (7.3) becomes:

$$\overline{\mathbf{T}}^{(0)}=\mathbf{C}^{(0)}:\overline{\mathbf{E}}^{(0)} \tag{13.7.4}$$

Since:

$$\overline{\mathbf{T}}=\overline{\mathbf{C}}:\overline{\mathbf{E}}=f_0\overline{\mathbf{T}}^{(0)}+\sum_{i=1}^{n}f_i\,\overline{\mathbf{T}}^{(i)}=f_0\mathbf{C}^{(0)}\overline{\mathbf{E}}^{(0)}+\sum_{i=1}^{n}f_i\,\mathbf{C}^{(i)}\overline{\mathbf{E}}^{(i)} \tag{13.7.5}$$

where $f^{(i)}=\frac{V^{(i)}}{V}$ is the volume fraction of the $i-th$ cylindrical hollow phase, $f^{(0)}=\frac{V^{(0)}}{V}$ is the volume fraction of the cylindrical central core; $\overline{\mathbf{T}},\overline{\mathbf{E}}$ are the average stress and strain tensor of the cylindrical solid, respectively. In the case of the macrostrain prescribed, we assume that $\overline{\mathbf{E}}=\overline{\mathbf{E}}^{(0)}=\overline{\mathbf{E}}^{(i)}$, then we obtain:

$$\overline{\mathbf{C}}=f_0\mathbf{C}^{(0)}+\sum_{i=1}^{n}f_i\,\mathbf{C}^{(i)} \tag{13.7.6}$$

In the cases considered (13.6.1) and (13.6.2), if we assume that the cylindrical hollow phases (1) and (2) have same volume, then the overall elasticity tensor $\overline{\mathbf{C}}$ is not depended by sign of the helix angle θ. However, the elastic response of the cylindrical solid multiphase is dependent by sign of the helix angle ψ. If in the case (13.6.2) the torque couple is positive , and $\psi>0$ in the phase (1), then $\varepsilon_{zz}=\varepsilon_0<0$, but if $\psi<0$ in the phase (1), then $\varepsilon_{zz}=\varepsilon_0>0$.

13.8. Conclusions

In this chapter is analysed the mechanical behaviour of multilayered cylinder constituted by three phase composed by helicoidal fibres, under axial forces and torsion. The phase (0) is assumed isotropic, but the phase (1) is constituted by fibres with slope $\psi^{(1)}=\psi$ and the phase (2) is constituted by fibres with slope $\psi^{(2)}=-\psi$. In this model the orientation of the helicoidal fibre influence the global mechanical behaviour. In particular, if the axial force N_z applied on the basis is of traction and $\psi>0$ (where $\psi^{(1)}>-\psi^{(2)}=\psi$), then we obtained that the axial deformation is more than zero (elongation : $\varepsilon_{zz}=\varepsilon_0>0$), the unitary twisted angle is more than zero (anticlockwise : $\phi>0$), as showed in figure 13.12 . The integration constants assumed the follows sign: $C_0^{(0)}<0$, $C_1^{(1)}<0$, $C_1^{(2)}<0$, $C_2^{(1)}=i\,a$ $C_2^{(2)}=i\,b$ where $a>0$, $b>0$. Conversely, if the axial force N_z applied on the basis is of traction and $\psi<0$ (where $\psi^{(1)}>-\psi^{(2)}=\psi$), we obtained that the axial strain is more less zero (elongation: $\varepsilon_{zz}=\varepsilon_0>0$), but the unitary twisted angle is more less zero (clockwise : $\phi<0$), as showed in figure 13.12. The integration constants assumed the follows sign: $C_0^{(0)}<0$, $C_1^{(1)}<0$, $C_1^{(2)}<0$, $C_2^{(1)}=i\,a$ $C_2^{(2)}=i\,b$, where $a>0$, $b>0$. If twist couple $\mathfrak{M}_t$ applied on basis is anticlockwise and $\psi>0$ (where $\psi^{(1)}>-\psi^{(2)}=\psi$), then we obtained that the unitary twisted angle is more less zero (anticlockwise : $\phi>0$), but axial strain is more then zero (elongation : $\varepsilon_{zz}=\varepsilon_0>0$), as showed in figure 13.13. The integration constants assumed the follows sign: $C_0^{(0)}<0$, $C_1^{(1)}<0$, $C_1^{(2)}<0$, $C_2^{(1)}=i\,a$ $C_2^{(2)}=i\,b$, where $a>0$, $b<0$. Conversely, if twist couple $\mathfrak{M}_z$ applied on basis is anticlockwise and $\psi<0$, (where $\psi^{(1)}>-\psi^{(2)}=\psi$), then we obtained that the unitary twisted angle is more less zero (anticlockwise : $\phi>0$), but axial strain is more less zero (contraction : $\varepsilon_{zz}=\varepsilon_0<0$), as showed in figure 13.13. The integration constants assumed the follows sign: $C_0^{(0)}>0$, $C_1^{(1)}>0$, $C_1^{(2)}>0$, $C_2^{(1)}=i\,a$ $C_2^{(2)}=i\,b$ where $a<0$, $b>0$,

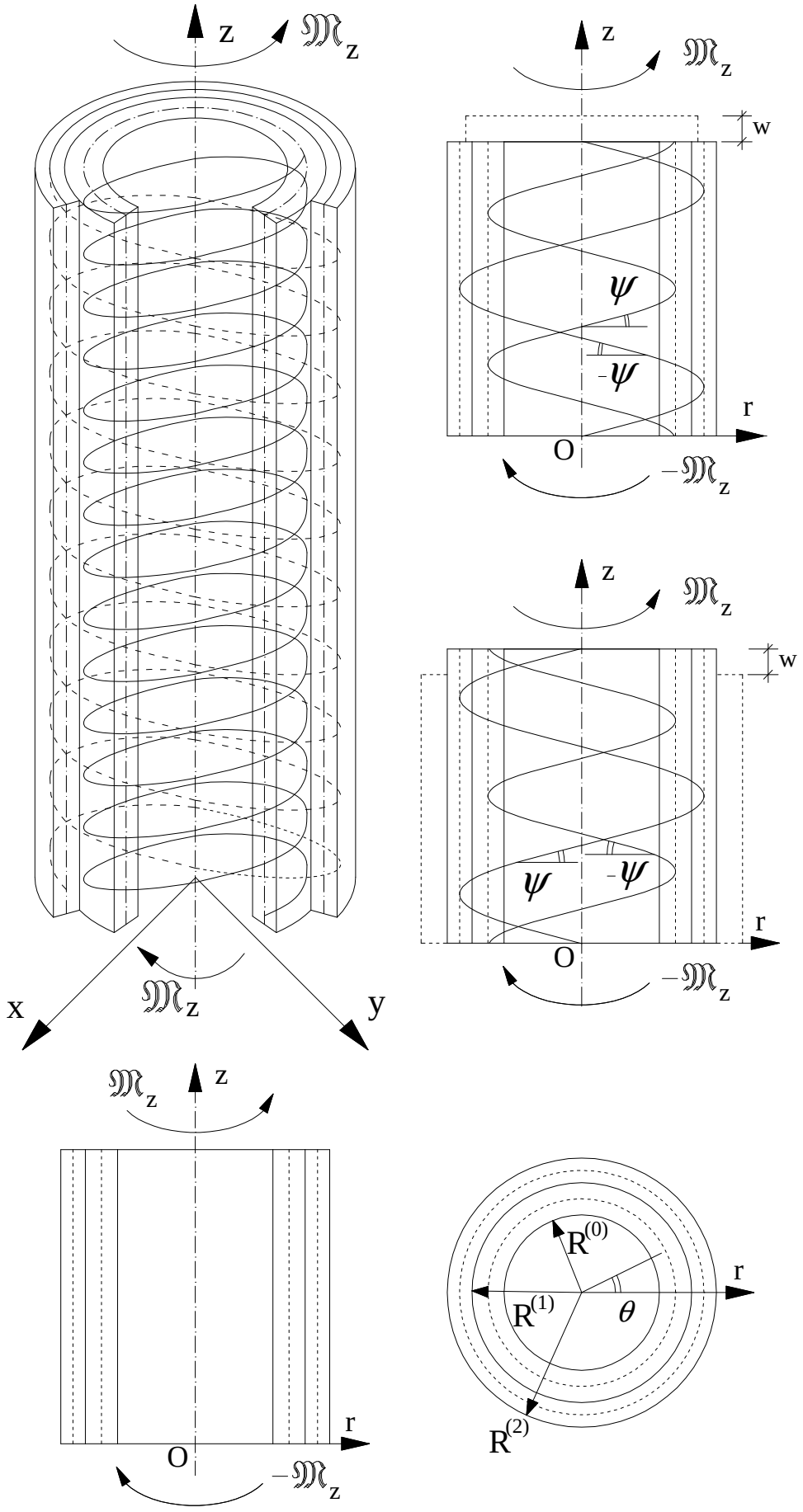

Fig. 13.2 - *Multilayered cylinder composed by three phases constituted by helicoidal fibres*

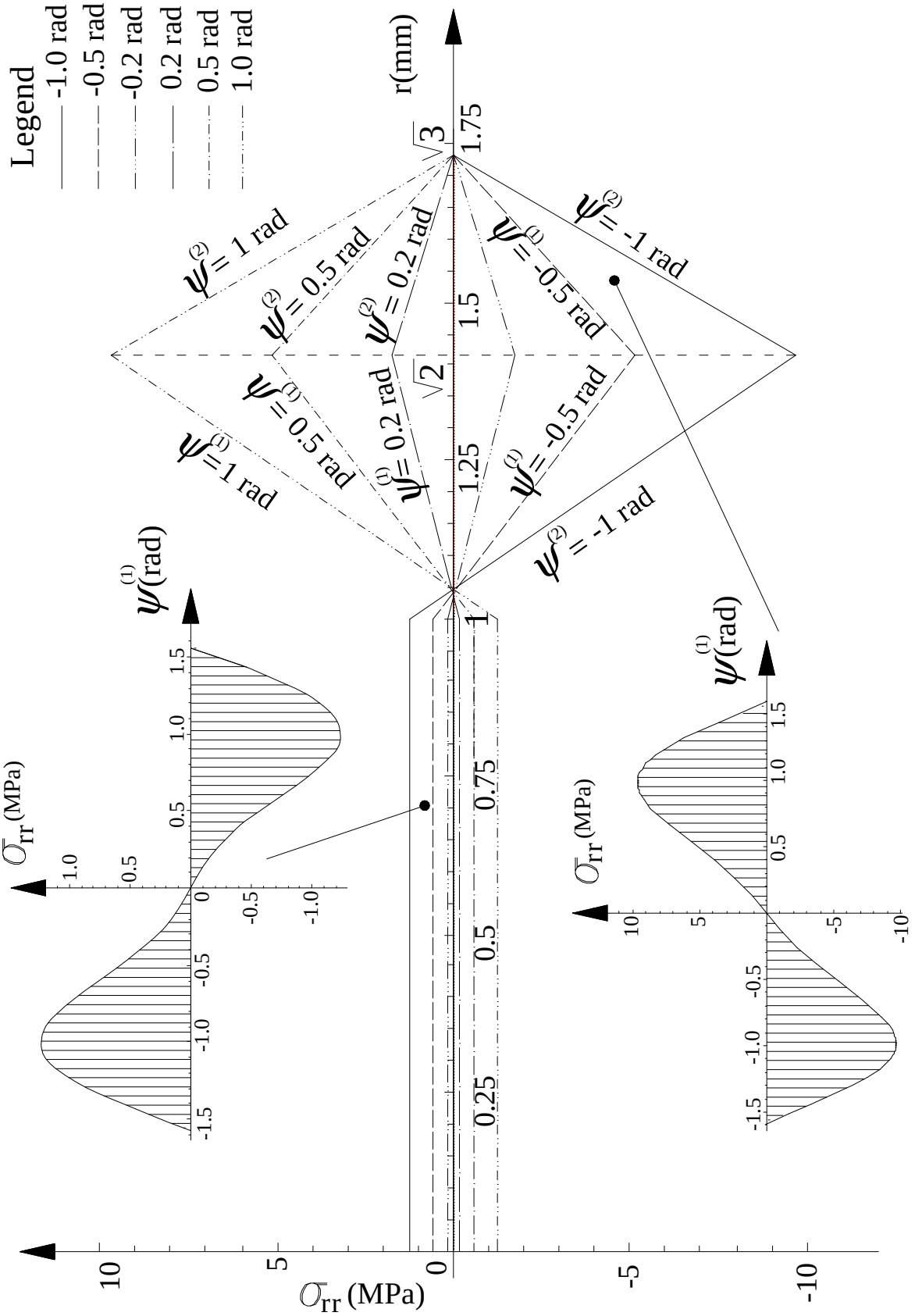

Fig. 13.3 - *The stress component* σ_{rr} *as function of the radius and slope of the fibres.*
($w_0 = 0mm,\ \varphi_0 = 0.1rad$ *)*

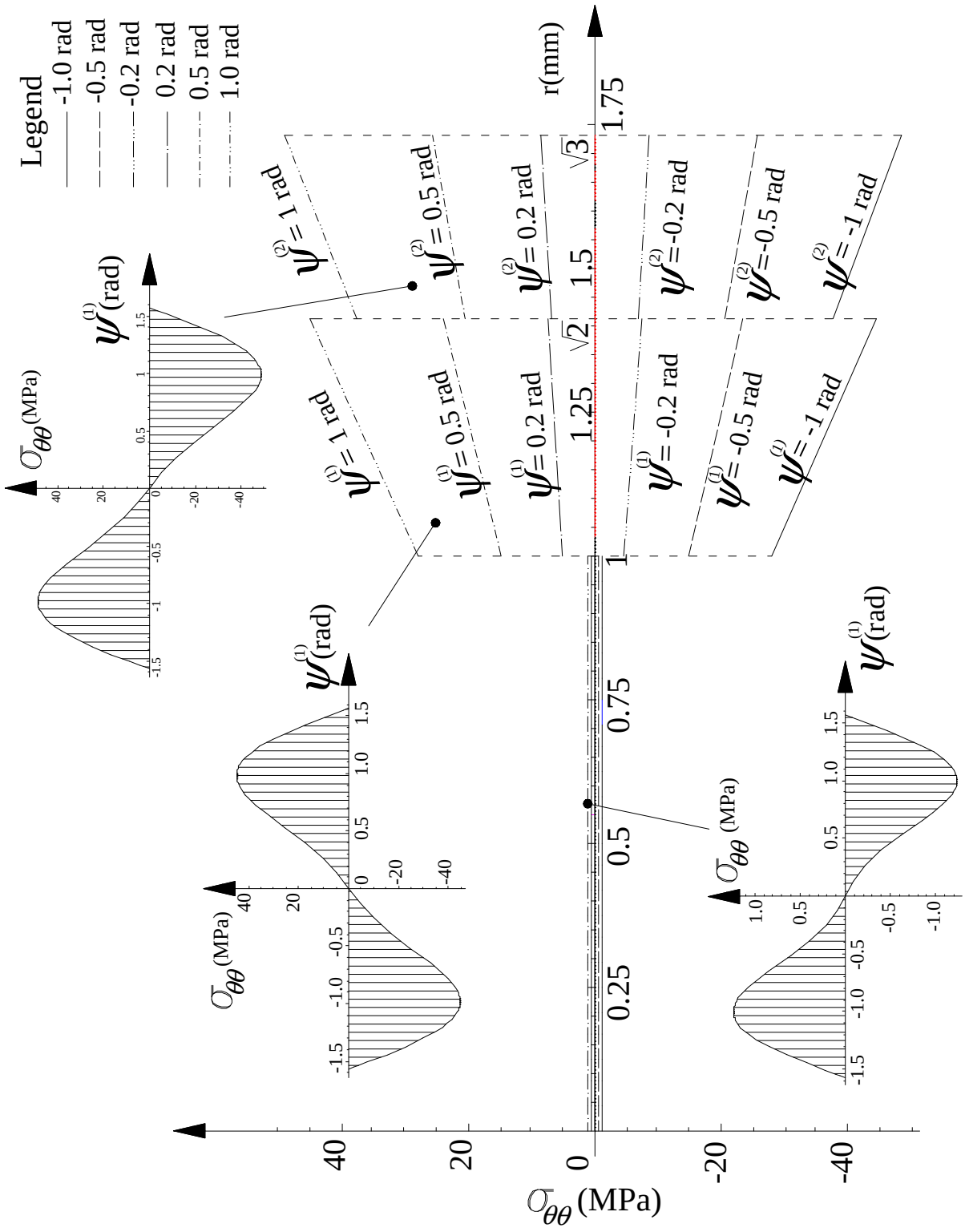

Fig. 13.4 - *The stress component* $\sigma_{\theta\theta}$ *as function of the radius and slope of the fibres* ($w_0 = 0mm,\ \varphi_0 = 0.1rad$)

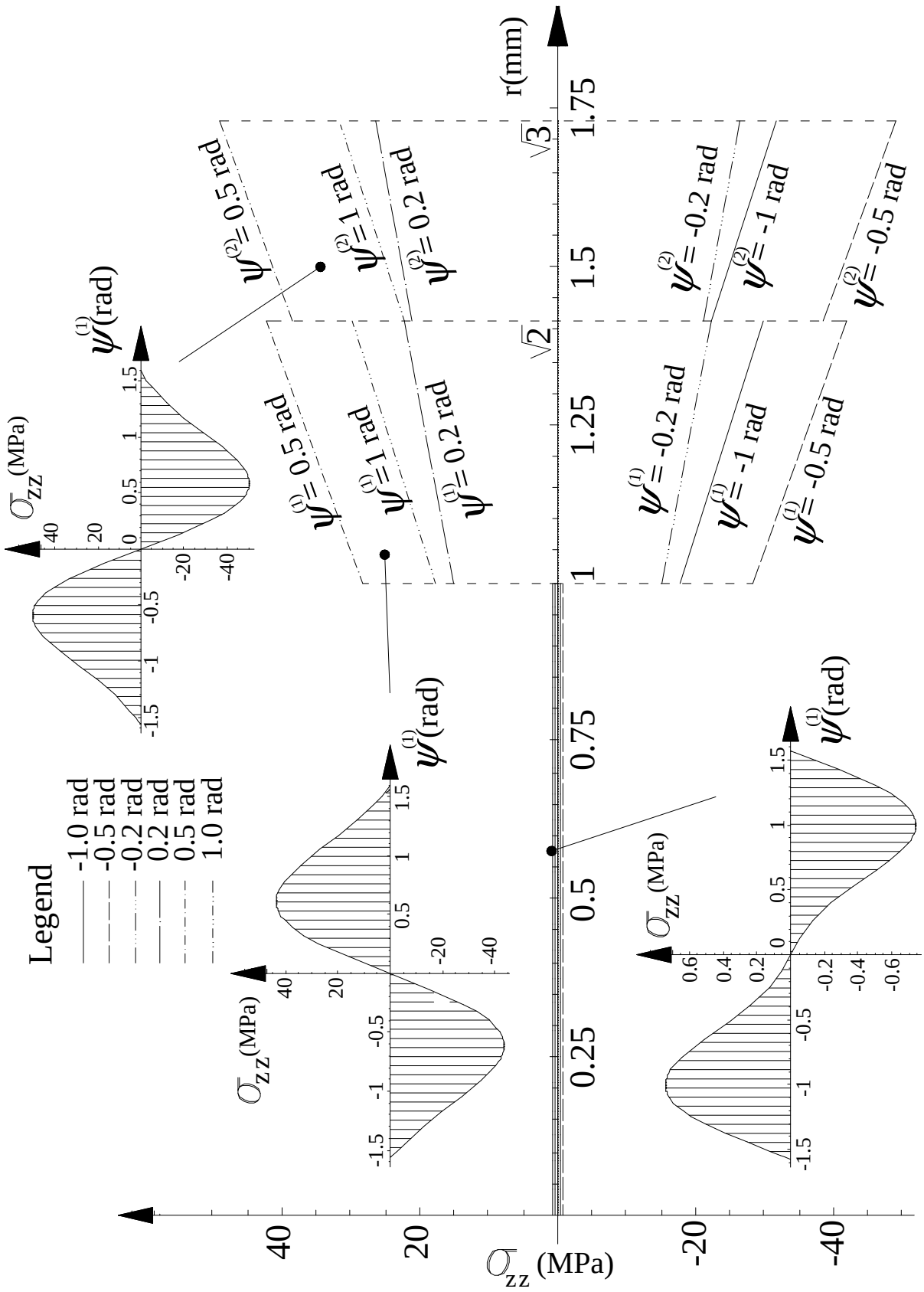

Fig. 13.5 - *The stress component* σ_{zz} *as function of the radius and slope of the fibres* ($w_0 = 0mm,\ \varphi_0 = 0.1rad$)

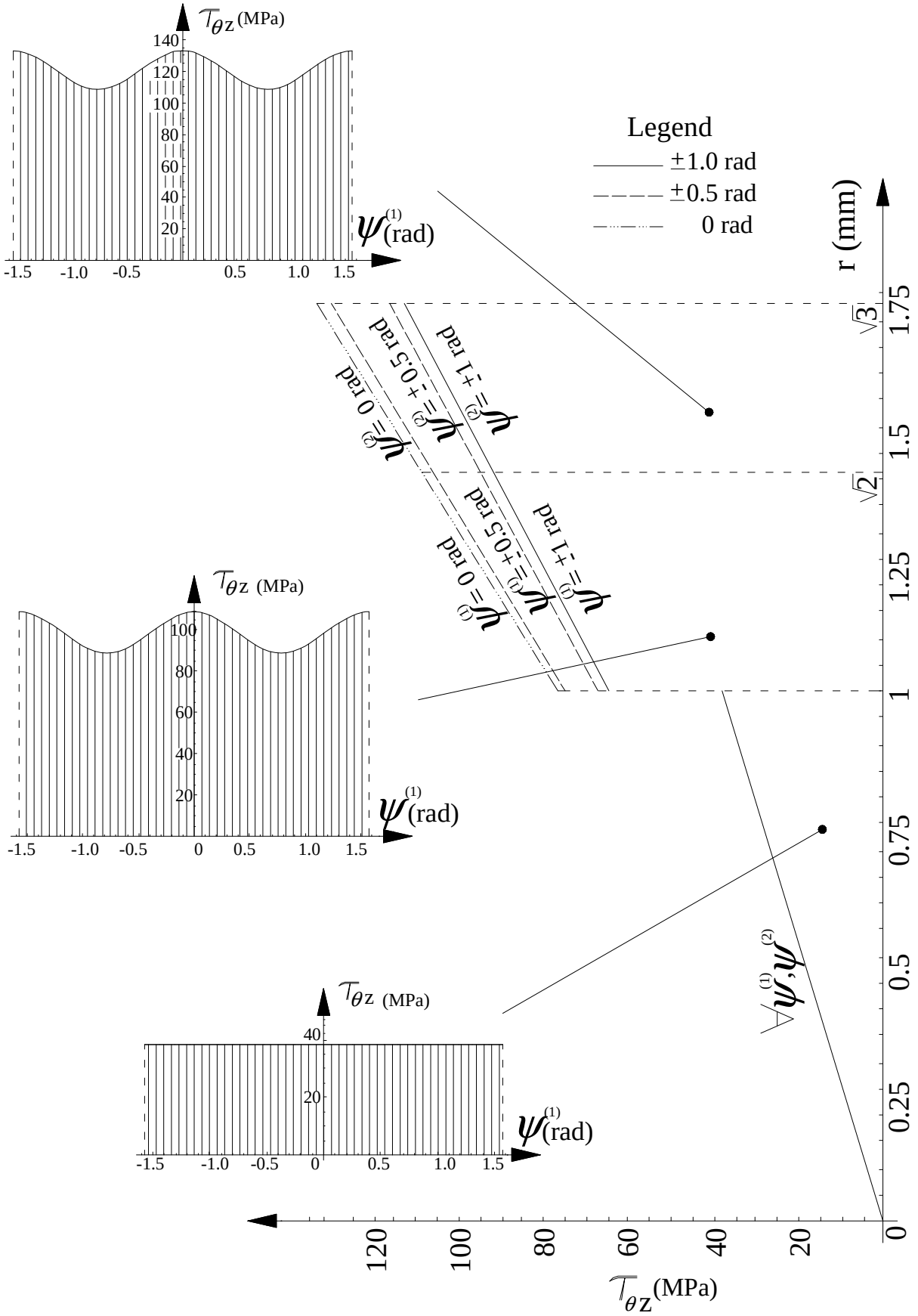

Fig. 13.6 - *The stress component* τ_{θ_z} *as function of the radius and slope of the fibres* ($w_0 = 0mm,\ \varphi_0 = 0.1rad$)

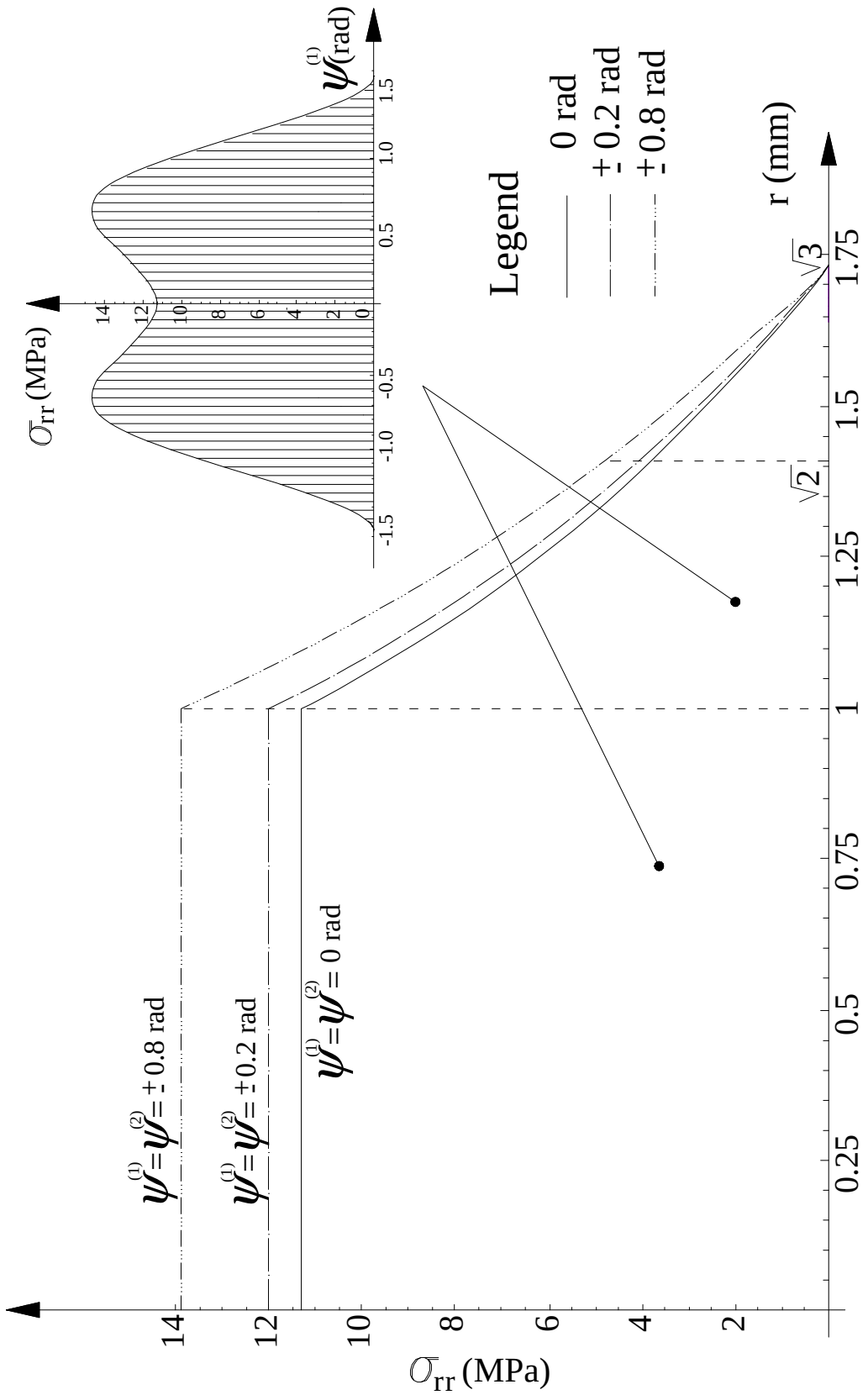

Fig. 13.7 - *The stress component* σ_{rr} *as function of the radius and slope of the fibres* ($w_0 = 0.1mm,\ \varphi_0 = 0rad$)

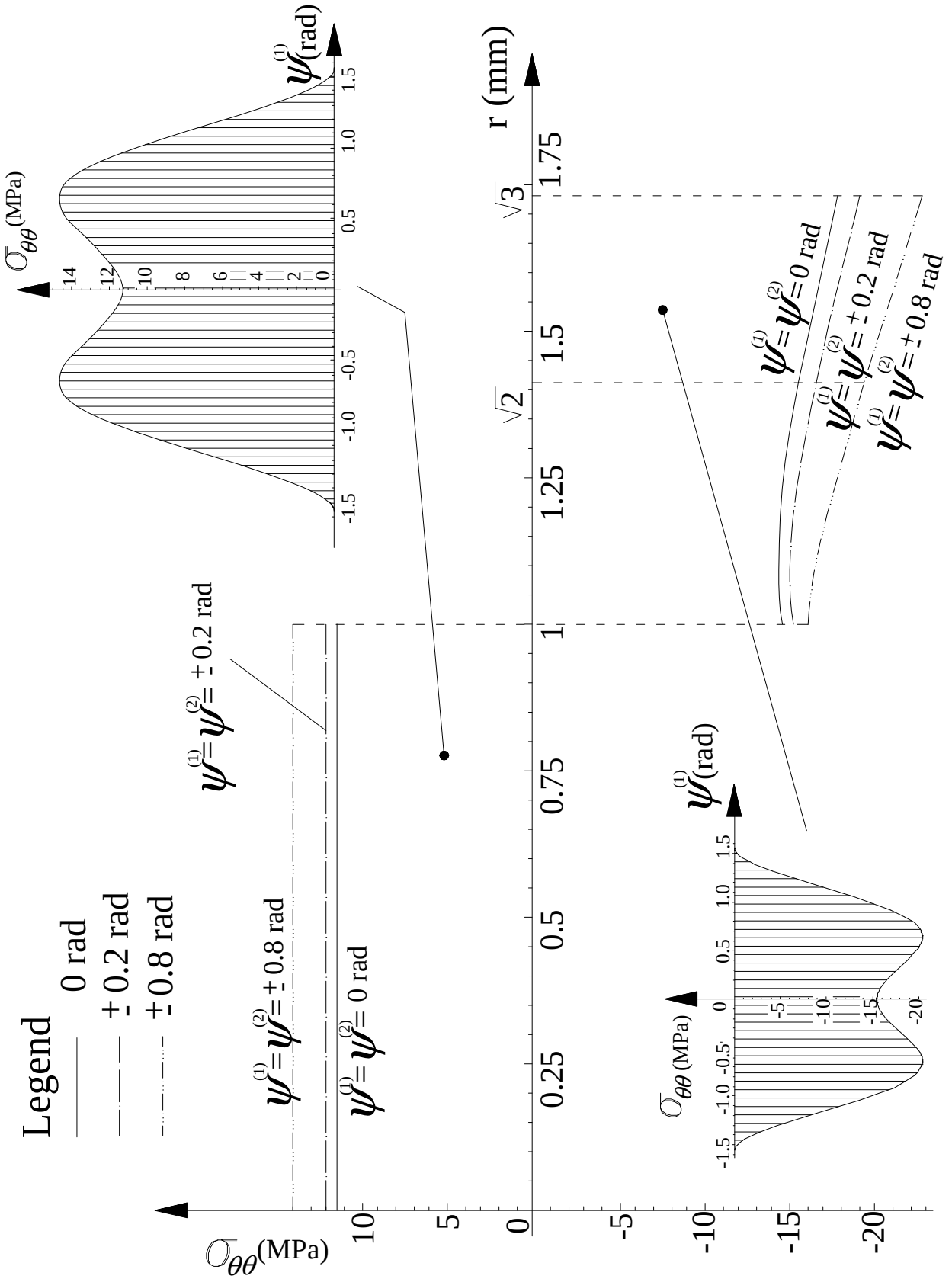

Fig. 13.8 - *The stress component* $\sigma_{\theta\theta}$ *as function of the radius and slope of the fibres* ($w_0 = 0.1mm,\ \varphi_0 = 0rad$)

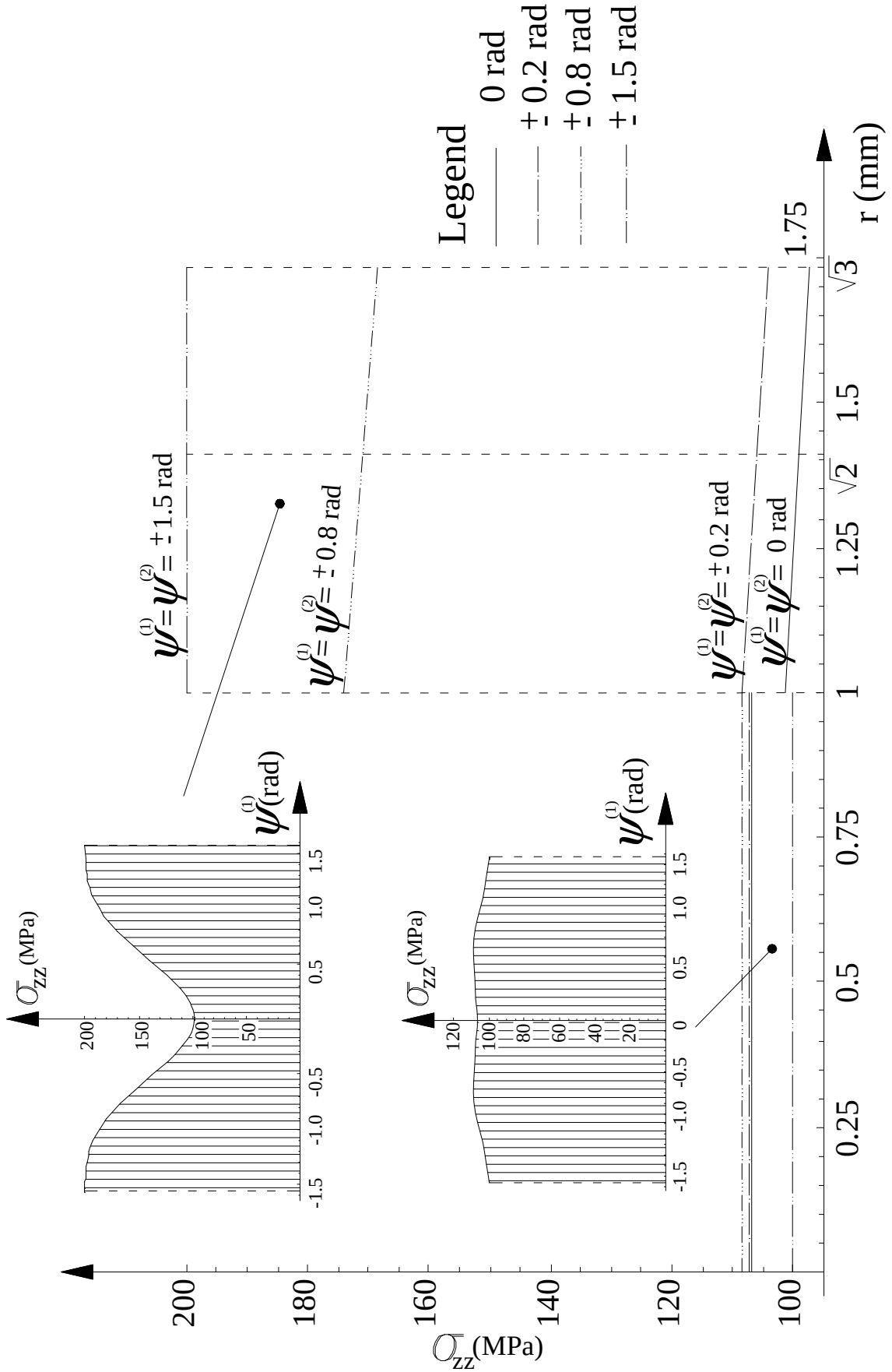

Fig. 13.9 - *The stress component* σ_{zz} *as function of the radius and slope of the fibres* ($w_0 = 0.1mm,\ \varphi_0 = 0rad$)

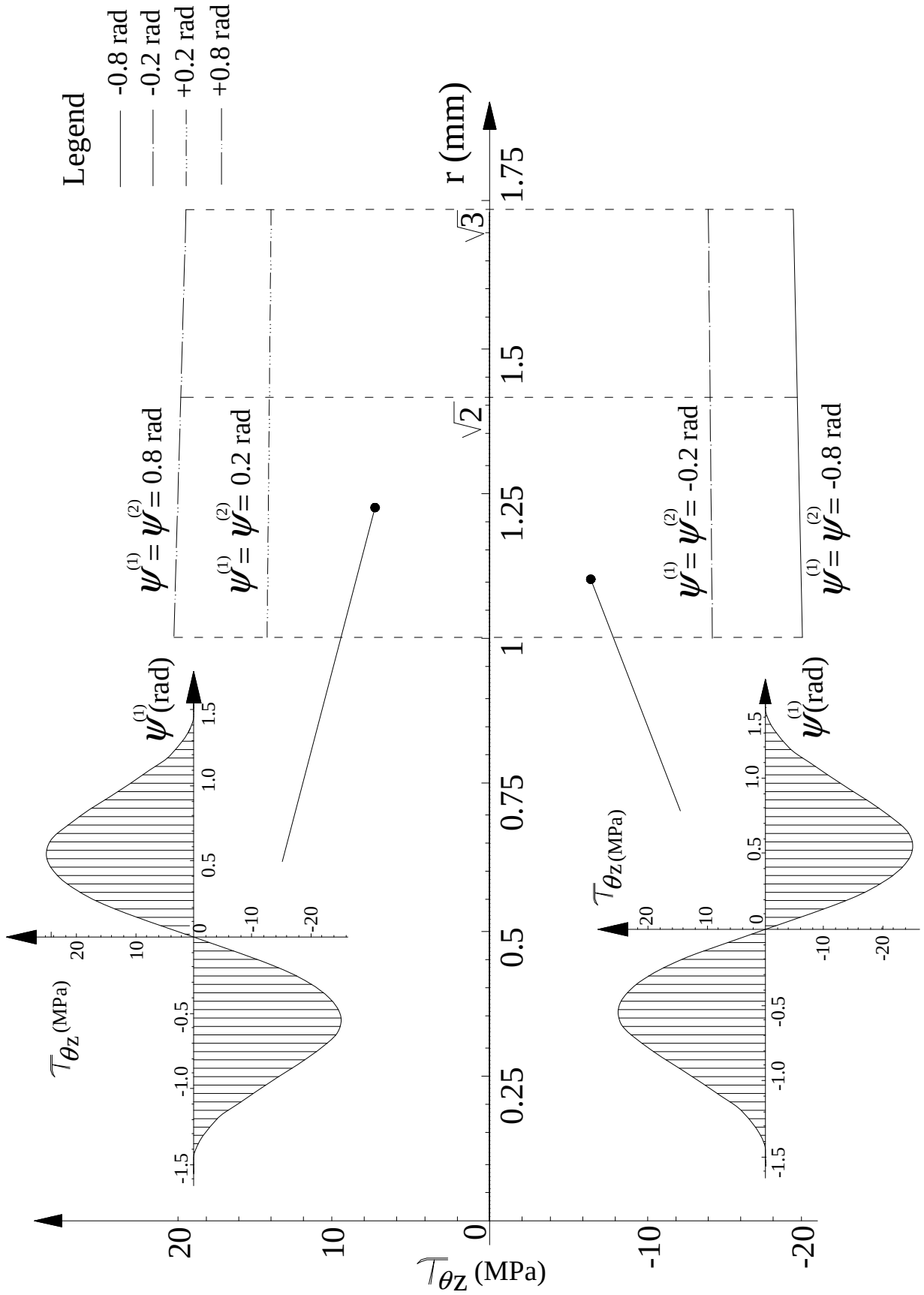

Fig. 13.10 - *The stress component* $\tau_{\theta z}$ *as function of the radius and slope of the fibres* ($w_0 = 0.1mm,\ \varphi_0 = 0rad$)

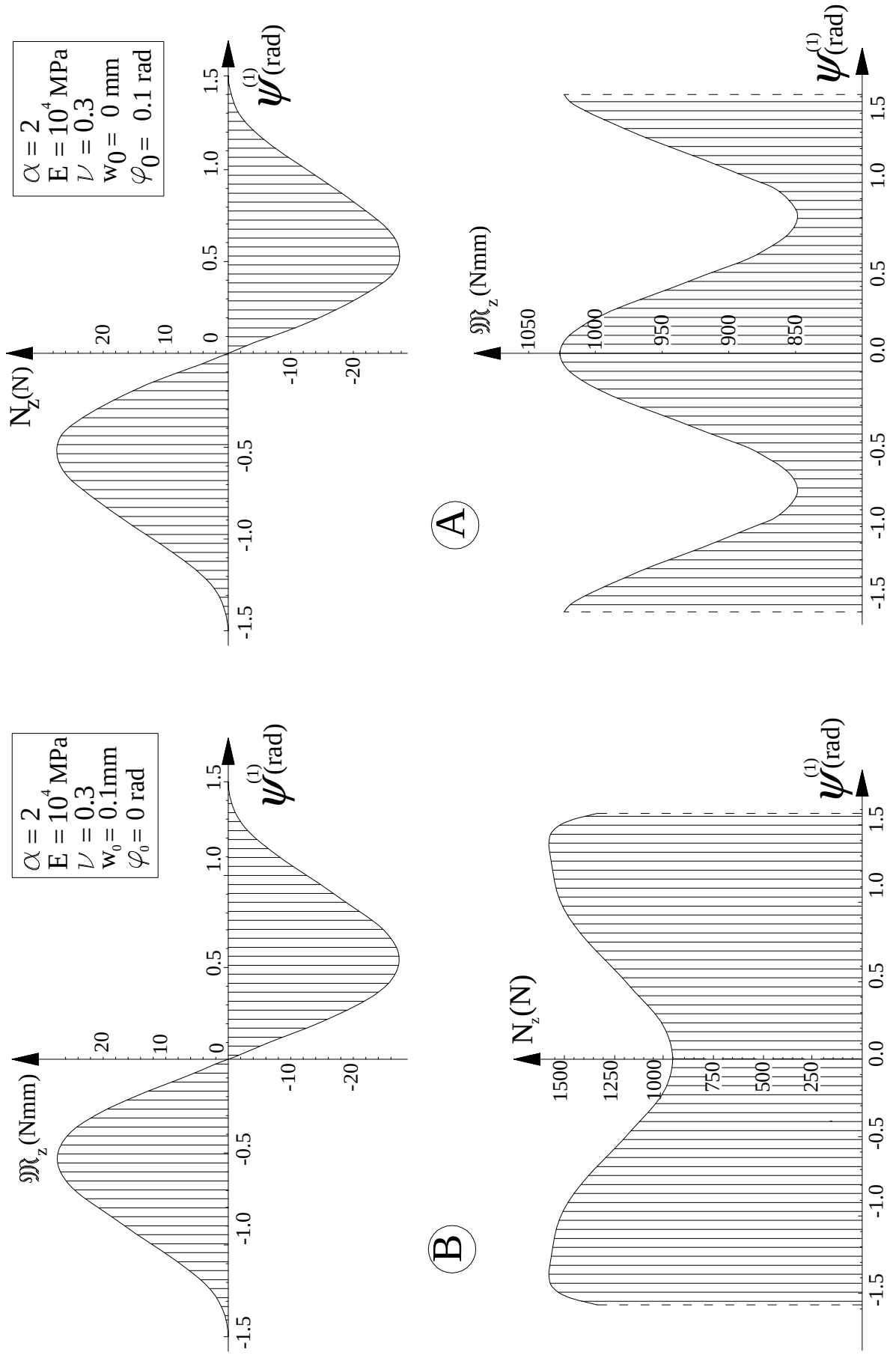

Fig. 13.11 - *The axial force and couple torque reaction on basis of the solid for displacement imposed. We reported the diagram of the* $\mathfrak{M}_z$ *and* N_z *as function of slope of the fibres*

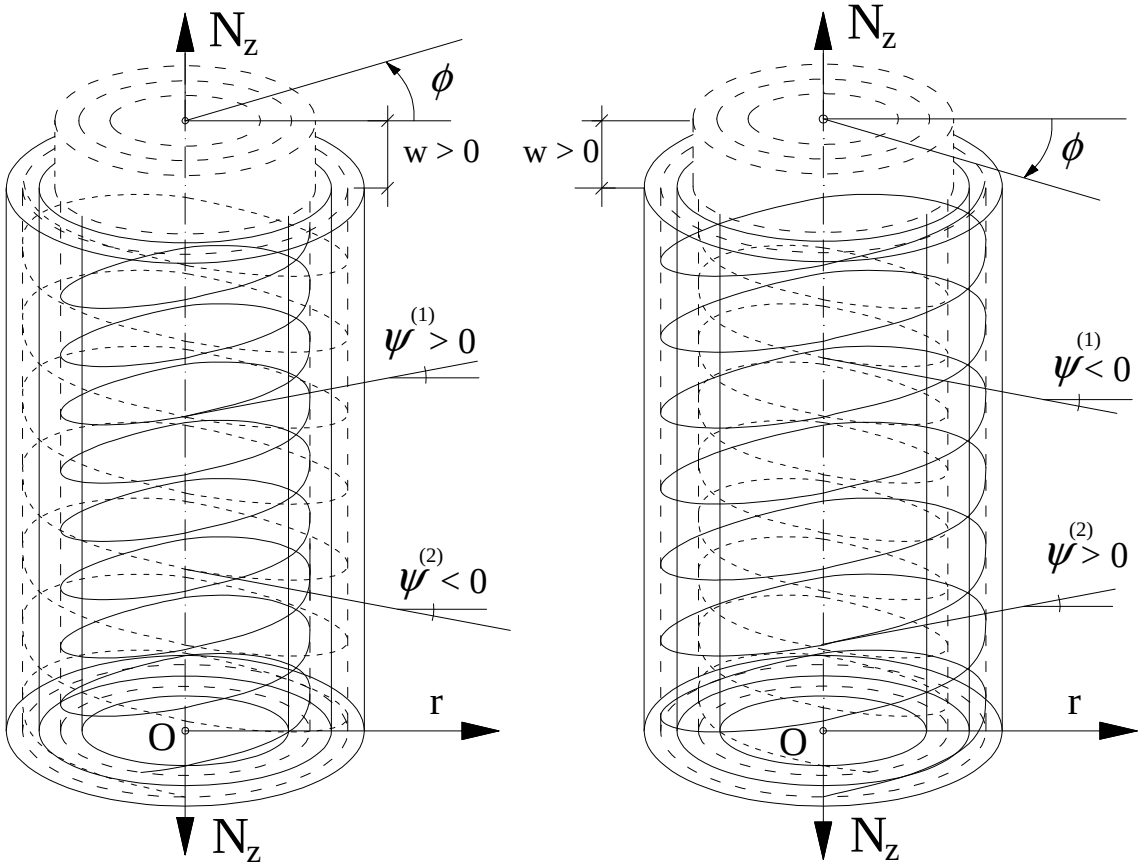

Fig. 13.12 - *The mechanical behaviour of multilayer cylinder subjected to axial tensile force*

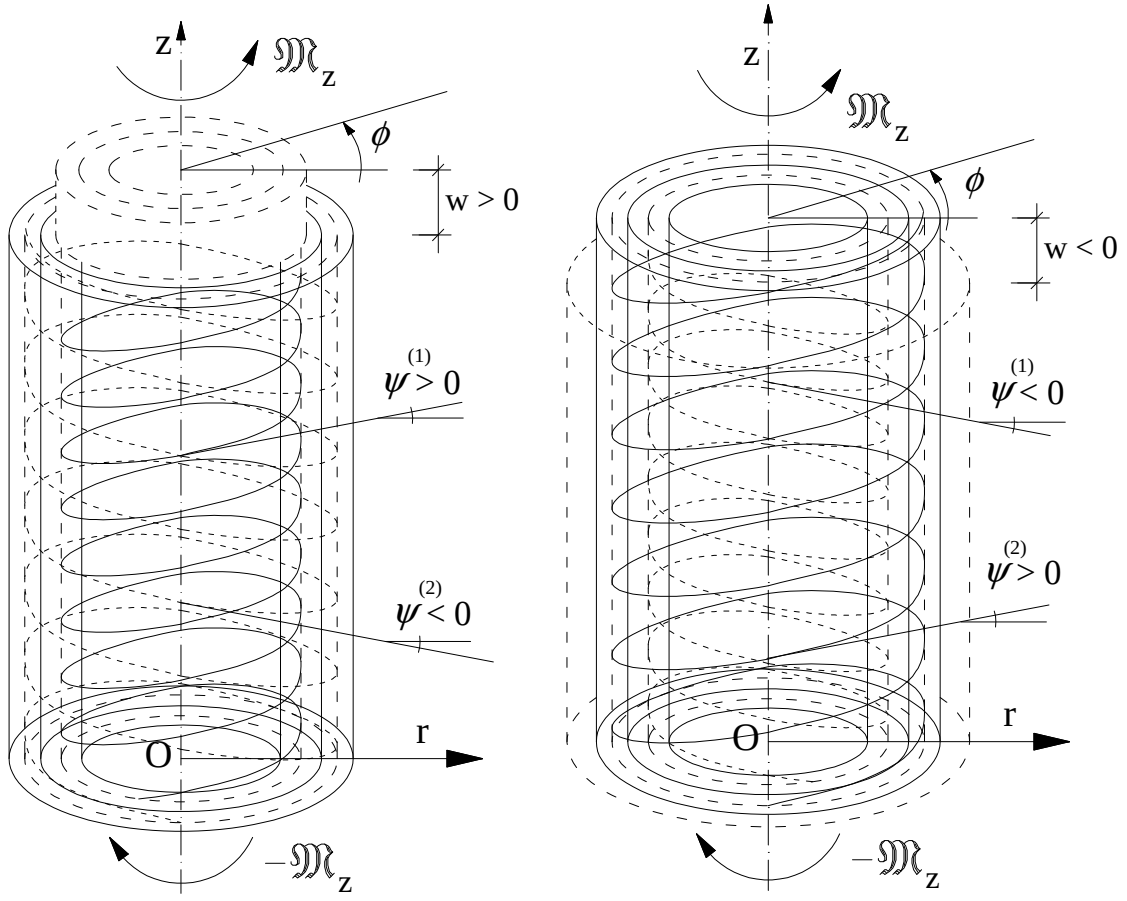

Fig. 13.13 - *The mechanical behaviour of multilayered cylinder subjected to couple torque*

13.9 References

[1] Anonymous, *Hierarchical Structures in Biology as a Guide for New Materials Technology*, Committee on Synthetic Hierarchical Structures, National Materials Advisory Board, National Research Council, NMAB - 464, National Academy Press, Washington, D.C, 1994.

[2] E. Baer, A. Hiltner and R. Morgan, Biological and synthetic hierarchical composites, *Physics Today*, October (1992) 60-67.

[3] K. Brear, J.D. Currey, C.M. Pond and M. Ramsey, The mechanical properties of the dentine and cement of the tusk of the narwhal monodon monoceros compared with those of other mineralized tissues. *Journal of Biomechanics*, 35 (1990) 615-621.

[4] K. Brear, J.D. Currey, M.C.S. Kingsley and M. Ramsey, The mechanical design of the tusk of the narwhal (Monodon monoceros: Cetecea), *Journal of Zoology*, London 230 (1993) 411-23.

[5] P. Chadwick, M. Vianello and S. C. Cowin, A new proof that the number of linear anisotropic elastic symmetries is eight, *J. Mech. Phys. Solids*, 49 (2001) 2471-2492.

[6] G. A. Costello, *Theory of Wire Rope*, 2nd ed., Springer, New York (1997).

[7] S. C. Cowin and M. M. Mehrabadi, On the Identification of Material Symmetry for Anisotropic Elastic Materials, *Quart. J. Mech. Appl. Math.*, 40 (1987) 451-476.

[8] S. C. Cowin and M. M. Mehrabadi, Anisotropic symmetries of linear elasticity, *Appl. Mech. Rev.* 48 (1995) 247-285.

[9] S. C. Cowin Elastic symmetry restrictions from structural gradients *in*, *Rational Continua, Classical and New- A collection of papers dedicated to Gianfranco Capriz on the occasion of his 75th birthday*, (P. Podio-Guidugli, M. Brocato eds.), *Springer Verlag*, ISBN 88-470-0157-9, (2002).

[10] D'arcy Thompson, W. *On Growth and Form*, Cambridge University Press, Cambridge (1942).

[11] S. J. Gould, D'Arcy Thompson and the Science of Form, *In* M. Grene and E. Mendelsohn, eds., *Topics in the Philosophy of Biology*, pp. 66-97, D. Reidel, Dordrecht (1976)

[12] M. C. S. Kingsley and M. A. Ramsay, The spiral tusk of the narwhal, *ARctic*, 41 (1988) 236-238.

[13] R. S. Lakes, Elastic and viscoelastic behaviour of chiral materials, *Int. J. of Mechanical Sciences*, 43 (2001) 1579-1589.

[14] Lekhnitskii, S. G., (1981), *Theory of Elasticity of an Anisotropic Body*, Mir, Moscow.

[15] C. McManus, *Left Hand, Right Hand-The origins of asymmetry in brains, bodies, atoms and cultures*, Harvard, Cambridge MA (2002).

[16] A. C. Neville, Molecular and mechanical aspects of helicoid development in plant cell walls, *BioEssays*, 3 (1985) 4-8.

[17] A. C. Neville, *Biology of Fibrous Composites*, Cambridge University Press, Cambridge, (1993).

[18] A. F. Noskowlak, Spiral grain in trees. A review, *Forest Products Journal*, 13 (1963), 266-275.

[19] T. C. T. Ting, *Anisotropic Elasticity –Theory and Applications*, Oxford University Press, New York & Oxford (1996).

[20] W. Thompson (Lord Kelvin), *Baltimore Lectures on Molecular Dynamics and the Wave Theory of Light*, London (1904).

[21] W. Voigt, *Lehrbuch der Kristallphysik*, Leipzig, (1928).

[22] J. Woodhead-Galloway, *Collagen: the Anatomy of a Protein* (Studies in Biology no. 117), Arnold, London (1980).

[23] Liew, K.M., Kitipornchai, S., Zhang, X.Z., Lim, C.W., (2003), Analysis of the thermal stress behaviour of functionally graded hollow circular cylinders, *International Journal of Solids and Structures*, vol. 40, 2355-2380.

[24] Shao, Z. S., (2005), Mechanical and thermal stresses of a functionally graded circular hollow cylinder with finite length, *International Journal of Pressure Vessels an Piping*, vol. 82, 155-163.

[25] Mian, M., Abid, Spencer, A. J. M., (1998), Exact solutions for functionally graded and laminated elastic materials, *J. Mech. Phys. Solids*, Vol. 46, n. 12, 2283-2295.

[26] Fraldi, M, Cowin, S. C., (2004), Inhomogeneous elastostatic problem solutions constructed from stress-associated homogeneous solutions, *Journal of the Mechanics and Physics of Solids*, 52, 2207-2233.
[27] Morteza M. Mehrabadi, Stephen C. Cowin and Jovo Jaric, (1995), Six-dimensional orthogonal tensor representation of the rotation about an axis in three dimensions, *International Journal Solids Structures*, Vol. 32, N0. 3/4 , pp. 439-449.
[28] Y.J. Yoon, G. Yang, S.C. Cowin, (2002), Estimation of the effective transeversaly isotropic elastic constants of a material from known values of the material's orthotropic elastic constants, *Biomechan Model Mechanobiol* , Vol 1 , pag. 83-93.
[29] Alshits, V. I., Kirchner, O. K., (2001). Cylindrically anisotropic, radially inhomogeneous elastic materials. *Proc. Roy. Soc. Lond*. A457, 671-693.
[30] Chouchaoui, C. S., Ochoa, O. O. (1999), Similitude study for a laminated cylindrical tube under tensile, torsion, bending, internal and external pressure. Part I: governing equations, *Composite Structures*, 44, 221-229.
[31] Chen, T., Chung, C. T., Lin, W. L., (2000), A revisit of a cylindrically anisotropic tube subjected to pressuring, shearing, torsion, extension and a uniform temperature change, *International Journal of Solids and Structures*, 37, 5143-5159.
[32] Tarn, J. Q., (2001), Exact solutions for functionally graded anisotropic cylinders subjected to thermal and mechanical loads, *International Journal of Solids and Structures*, 38, 8189-8206.
[33] Tarn, J. Q., Wang, Y. M., (2001), Laminated composite tubes under extension, torsion, bending, shearing and pressuring: a state space approach, *International Journal of Solids and Structures*, 38, 9053-9075.
[34] Huang, C. H., Dong, S. B., (2001), Analysis of laminated circular cylinders of materials with the most general form of cylindrical anisotropy. I. Axially symmetric deformations. *International Journal of Solids and Structures*, 38, 6163-6182.
[35] Ting, T. C. T., (1999), Pressuring, shearing, torsion and extension of a circular tube or bar of cylindrically anisotropic material, *Proc. Roy. Soc. Lond*. A452, 2397-2421.
[36] Love, A. E. H., (1944), *A treatise on the mathematical theory of elasticity*, Dover Publications, Inc, New York.
[37] Fraldi, M., Nunziante, L., Carannante, F. (2007), *Axis-symmetrical Solutions for n-plies Functionally Graded Material Cylinders under Strain no-Decaying Conditions*, J. Mech. of Adv. Mat. and Struct. Vol. 14 (3), pp. 151-174 - DOI: 10.1080/15376490600719220
[38] M. Fraldi, L. Nunziante, F. Carannante, A. Prota, G. Manfredi, E. Cosenza (2008), *On the Prediction of the Collapse Load of Circular Concrete Columns Confined by FRP*, Journal Engineering structures, Vol. 30, Issue 11, November 2008, Pages 3247-3264 - DOI: 10.1016/j.engstruct.2008.04.036
[39] Fraldi, M., Nunziante, L., Chandrasekaran, S., Carannante, F., Pernice, MC. (2009), *Mechanics of distributed fibre optic sensors for strain measurements on rods*, Journal of Structural Engineering, 35, pp. 323-333, Dec. 2008- Gen. 2009
[40] M. Fraldi, F. Carannante, L. Nunziante (2012), *Analytical solutions for n-phase Functionally Graded Material Cylinders under de Saint Venant load conditions: Homogenization and effects of Poisson ratios on the overall stiffness*, Composites Part B: Engineering, Volume 45, Issue 1, February 2013, Pages 1310–1324
[41] Nunziante, L., Gambarotta, L., Tralli, A., *Scienza delle Costruzioni*, 3° Edizione, McGraw-Hill, 2011, ISBN: 9788838666971
[42] Christensen, R. M., (1997), Stress based Yield/Failure criteria for fiber composites, *International Journal Solid and Structures*, vol. 34, No. 5, pp. 529-543.
[43] Gurtin, M. E., (1972), *The Linear Theory of Elasticity*, Handbbuch der Physik, Springer, Berlin.

CHAPTER XIV
THERMAL STRESS IN HOLLOW CYLINDERS

14.0. Introduction

In the preceding chapter, the basic formulation of problems of thermo-elasticity were reviewed. Before proceeding to an examination of the practical solution of thermo-elastic problems, it is useful to take up here a number of special case. The solutions presented are rigorous from the standpoint of the formulations of the previous chapter (as opposed, for example, to those based on assumptions of the type under lying strength of material analyses, considered in the next chapter); nevertheless, they are obtainable without difficulty by elementary methods.
Although these methods are sometimes difficult to generalize to more complex situations, the results obtained are of interest in themselves since they represent cases of frequent practical occurrence and, at the same time, serve to illustrate in a general way the nature of thermal stresses.

14.1. Uncoupled thermo-elastic problem in plane strain with radial temperature variation

The calculations for the stresses and deformations in a solid or hollow circular cylindrical body of outer radius b and of height h are given in this section for the case in which the temperature distributions a function of the radial distance r only and the cylindrical surface is free of tractions.
The problem is one of plane stress if the ratio h/b is very small compared to unity (that is, for a disc) and the end faces are free of tractions. On the other hand , if the ratio h/b is large compared to unity and if axial displacement are prevented, the problem is one of plane strain. It is to prove that the solutions for the two problems are mathematically analogous; therefore, only the solution for the plane-strain problem will be obtained here in detail. If the ratio h/b is of the same order of magnitude as unity, neither the plane stress nor the plane-strain components assumptions are useful and the complete three-dimensional theory must be employed. The solution for the hollow cylinder of inner radius a will be obtained first, and the solution for the solid disc then derived as a special case. Although we are considering the case of plane strain, it is convenient, in order to derive the basic equation of the problem, to write the equilibrium equations in terms of displacements in cylindrical coordinates. For the case of plane strain, the displacement components assume the form:

$$u_r = U(r,\theta,t), \quad u_\theta = V(r,\theta,t), \quad u_z = 0 \tag{14.1}$$

The equilibrium equations in this case become:

$$\begin{cases} (2\mu+\lambda)\dfrac{\partial}{\partial r}\left[\dfrac{1}{r}\dfrac{\partial(rU)}{\partial r}+\dfrac{1}{r}\dfrac{\partial V}{\partial\theta}\right]-\dfrac{\mu}{r}\dfrac{\partial}{\partial\theta}\left[\dfrac{1}{r}\dfrac{\partial(rV)}{\partial r}-\dfrac{1}{r}\dfrac{\partial U}{\partial\theta}\right]=\alpha(3\lambda+2\mu)\dfrac{\partial T}{\partial r} \\ \dfrac{(2\mu+\lambda)}{r}\dfrac{\partial}{\partial\theta}\left[\dfrac{1}{r}\dfrac{\partial(rU)}{\partial r}+\dfrac{1}{r}\dfrac{\partial V}{\partial\theta}\right]+\mu\dfrac{\partial}{\partial r}\left[\dfrac{1}{r}\dfrac{\partial(rV)}{\partial r}-\dfrac{1}{r}\dfrac{\partial U}{\partial\theta}\right]=\alpha\dfrac{(3\lambda+2\mu)}{r}\dfrac{\partial T}{\partial\theta} \end{cases} \tag{14.2}$$

If the cylinder is subjected to radial temperature variation and zero external load (axial symmetry of loads applied), let us assume that displacement components reduce to sole $u_r = U(r,t)$. In this case the equilibrium equations reduce to one equation as reported below:

$$\frac{\partial}{\partial r}\left[\frac{1}{r}\frac{\partial(rU)}{\partial r}\right]=\alpha\left(\frac{3\lambda+2\mu}{\lambda+2\mu}\right)\frac{\partial T}{\partial r}=\alpha\left(\frac{1+\nu}{1-\nu}\right)\frac{\partial T}{\partial r} \tag{14.3}$$

The Fourier heat conduction for uncoupled thermo-elastic problem, becomes:

$$\frac{\partial^2 T}{\partial r^2}+\frac{1}{r}\frac{\partial T}{\partial r}=\frac{\rho c_v}{k}\frac{\partial T}{\partial t}=\frac{1}{\kappa}\frac{\partial T}{\partial t} \tag{14.4}$$

where $\kappa=\dfrac{k}{\rho c_v}$ is thermal diffusivity in the case of uncoupled thermo-elastic problem.

The general solution of equation (14.3) is :

$$u_r = U(r,t) = \frac{\alpha(1+\nu)}{r(1-\nu)}\int_a^r \xi T(\xi,t)\,d\xi + f_1(t)\,r + \frac{f_2(t)}{r} \tag{14.5}$$

where in the integral the effective variable is radius, but ξ is the mute variable and $f_1(t)$, $f_2(t)$ are two unknown functions of the time. By solving the Fourier's equation (14.4) with one method reported in chapter 7, and substituting the function of temperature $T(r,t)$ in equation (14.5), we obtain the explicit displacement solution.

Since the boundary conditions stipulate zero tractions on the surface r = a and r = b, the function of the time $f_1(t)$, $f_2(t)$ are best obtained by first determining the stresses. By use of the strain-displacement relations, the strain components are:

$$\begin{aligned}
\varepsilon_{rr} &= f_1(t) - \frac{f_2(t)}{r^2} - \frac{\alpha}{r^2}\left(\frac{1+\nu}{1-\nu}\right)\int_a^r \xi T(\xi,t)\,d\xi + \alpha\left(\frac{1+\nu}{1-\nu}\right)T(r,t);\\
\varepsilon_{\theta\theta} &= f_1(t) + \frac{f_2(t)}{r^2} + \frac{\alpha}{r^2}\left(\frac{1+\nu}{1-\nu}\right)\int_a^r \xi T(\xi,t)\,d\xi;\\
\varepsilon_{zz} &= \varepsilon_{\theta z} = \varepsilon_{rz} = \varepsilon_{r\theta} = 0;
\end{aligned} \tag{14.6}$$

By applying the Hooke's law, we obtain the stress components as follows:

$$\begin{aligned}
\sigma_{rr} &= \frac{E}{1-\nu-2\nu^2}\left[f_1(t) - \frac{f_2(t)}{r^2}(1-2\nu)\right] + \frac{\alpha E T_R}{1-2\nu} - \left(\frac{\alpha E}{1-\nu}\right)\left[\frac{1}{r^2}\int_a^r \xi T(\xi,t)\,d\xi\right];\\
\sigma_{\theta\theta} &= \frac{E}{1-\nu-2\nu^2}\left[f_1(t) + \frac{f_2(t)}{r^2}(1-2\nu)\right] + \frac{\alpha E T_R}{1-2\nu} + \left(\frac{\alpha E}{1-\nu}\right)\left[\frac{1}{r^2}\int_a^r \xi T(\xi,t)\,d\xi - T(r,t)\right];\\
\sigma_{zz} &= \frac{2E\nu C_1(t)}{1-\nu-2\nu^2} + \frac{\alpha E T_R}{1-2\nu} - \left(\frac{\alpha E}{1-\nu}\right)T(r,t); \quad \tau_{\theta z} = 0; \quad \tau_{rz} = 0; \quad \tau_{r\theta} = 0;
\end{aligned} \tag{14.7}$$

where T_R is the reference temperature. The boundary conditions of zero tractions on the cylindrical surfaces are then

$$\sigma_{rr} = 0 \quad at \quad r = a \quad \text{and} \quad r = b \tag{14.8}$$

and thus the functions of the time $C_1(t), C_2(t)$ may now be determined:

$$\begin{cases}
f_1(t) = \alpha\left(\frac{1+\nu}{1-\nu}\right)\left[\left(\frac{1-2\nu}{b^2-a^2}\right) - T_R(1-\nu)\right]\int_a^b \xi T(\xi,t)\,d\xi\\
f_2(t) = \alpha\left(\frac{1+\nu}{1-\nu}\right)\left(\frac{a^2}{b^2-a^2}\right)\int_a^b \xi T(\xi,t)\,d\xi
\end{cases} \tag{14.9}$$

The final expression for the displacement solution is:

$$u_r = \frac{\alpha}{r}\left(\frac{1+\nu}{1-\nu}\right)\left[\int_a^r \xi T(\xi,t)\,d\xi + \frac{a^2 + (1-2\nu)r^2}{\left(b^2-a^2\right)}\int_a^b \xi T(\xi,t)\,d\xi\right] - \alpha(1+\nu)\,r\,T_R \tag{14.10}$$

Then, the expressions of the non zero strain components become:

$$\begin{aligned}
\varepsilon_{rr} &= -\frac{\alpha}{r^2}\left(\frac{1+\nu}{1-\nu}\right)\left[\left(\frac{r^2(2\nu-1)+a^2}{b^2-a^2}\right)\int_a^b \xi T(\xi,t)\,d\xi + \int_a^r \xi T(\xi,t)\,d\xi - r^2 T(r,t)\right] - \alpha(1+\nu)T_R\\
\varepsilon_{\theta\theta} &= \frac{\alpha}{r^2}\left(\frac{1+\nu}{1-\nu}\right)\left[\left(\frac{r^2(1-2\nu)+a^2}{b^2-a^2}\right)\int_a^b \xi T(\xi,t)\,d\xi + \int_a^r \xi T(\xi,t)\,d\xi\right] - \alpha(1+\nu)T_R
\end{aligned} \tag{14.11}$$

Finally, the non zero stress components are given by:

$$\sigma_{rr}=\frac{\alpha E}{(1-\nu)r^2}\left[\left(\frac{r^2-a^2}{b^2-a^2}\right)\int_a^b \xi T(\xi,t)\,d\xi+\int_a^r \xi T(\xi,t)\,d\xi\right]$$

$$\sigma_{\theta\theta}=\frac{\alpha E}{(1-\nu)r^2}\left[\left(\frac{r^2+a^2}{b^2-a^2}\right)\int_a^b \xi T(\xi,t)\,d\xi-\int_a^r \xi T(\xi,t)\,d\xi-r^2T(r,t)\right] \qquad (14.12)$$

$$\sigma_{zz}=\frac{\alpha E}{(1-\nu)}\left[\frac{2\nu}{b^2-a^2}\int_a^b \xi T(\xi,t)\,d\xi-T(r,t)\right]+\alpha E T_R$$

In the particular instance of constant temperature T_0, the radial displacement is :

$$u_r=\alpha(1+\nu)(T_0-T_R)r \qquad (14.13)$$

The strain components become:

$$\varepsilon_{rr}=\varepsilon_{\theta\theta}=\alpha(1+\nu)(T_0-T_R) \qquad (14.14)$$

and the stress components are:

$$\sigma_{rr}=\sigma_{\theta\theta}=0;\qquad \sigma_{zz}=-\alpha E(T_0-T_R); \qquad (14.15)$$

For the special case of a solid cylinder, the inner radius a may be set equal to zero and the results are as follows:

$$u_r=\alpha\left(\frac{1+\nu}{1-\nu}\right)\left[\frac{r(1-2\nu)}{b^2}\int_0^b \xi T(\xi,t)\,d\xi+\frac{1}{r}\int_0^r \xi T(\xi,t)\,d\xi\right]-\alpha(1+\nu)rT_R \qquad (14.16)$$

The corresponding strain components become:

$$\varepsilon_{rr}=\alpha\left(\frac{1+\nu}{1-\nu}\right)\left[\left(\frac{1-2\nu}{b^2}\right)\int_0^b \xi T(\xi,t)\,d\xi-\frac{1}{r^2}\int_0^r \xi T(\xi,t)\,d\xi+T(r,t)\right]-\alpha(1+\nu)T_R$$

$$\varepsilon_{\theta\theta}=\alpha\left(\frac{1+\nu}{1-\nu}\right)\left[\left(\frac{1-2\nu}{b^2}\right)\int_0^b \xi T(\xi,t)\,d\xi+\frac{1}{r^2}\int_0^r \xi T(\xi,t)\,d\xi\right]-\alpha(1+\nu)T_R \qquad (14.17)$$

and, the stress components are:

$$\sigma_{rr}=\frac{\alpha E}{(1-\nu)}\left[\frac{1}{b^2}\int_0^b \xi T(\xi,t)\,d\xi-\frac{1}{r^2}\int_0^r \xi T(\xi,t)\,d\xi\right]$$

$$\sigma_{\theta\theta}=\frac{\alpha E}{(1-\nu)}\left[\frac{1}{b^2}\int_0^b \xi T(\xi,t)\,d\xi+\frac{1}{r^2}\int_0^r \xi T(\xi,t)\,d\xi-T(r,t)\right] \qquad (14.18)$$

$$\sigma_{zz}=\frac{\alpha E}{(1-\nu)}\left[\frac{2\nu}{b^2}\int_0^b \xi T(\xi,t)\,d\xi-T(r,t)\right]+\alpha E T_R$$

These expressions become indeterminate for r = 0. However, if the temperature is finite there (as is the case, for example if concentrated heat sources are absent) then, by use of l'Hospital's rule, the following limits are found:

$$\lim_{r\to 0}\frac{1}{r^2}\int_0^r \xi T(\xi,t)\,d\xi=\frac{1}{2}T(r=0)$$

$$\lim_{r\to 0}\frac{1}{r}\int_0^r \xi T(\xi,t)\,d\xi=0 \qquad (14.19)$$

In this case the centre displacement is zero, and the stresses there are given by:

$$\sigma_{rr}(0)=\sigma_{\theta\theta}(0)=\frac{\alpha E}{(1-\nu)}\left[\frac{1}{b^2}\int_0^b \xi T(\xi,t)\,d\xi-\frac{1}{2}T(0)\right] \qquad (14.20)$$

14.2. Coupled thermo-elastic problem in plane strain with radial temperature variation

Let us consider a hollow cylinder with inner radius "a" and outer radius "b", subjected to radial temperature variation. In this case the displacement components and temperature are functions of radius and time as reported in previous section. Let us consider the hypotheses that the ratio h/b is large compared to unity and if axial displacement are prevented, the problem is one of plane strain. The equilibrium equation remaining the same in the case of uncoupled thermo-elastic problem, but change the Fourier's equation as reported below:

$$\begin{cases} \dfrac{\partial}{\partial r}\left[\dfrac{1}{r}\dfrac{\partial\left(r\,u_r\right)}{\partial r}\right]=\alpha\left(\dfrac{3\lambda+2\mu}{\lambda+2\mu}\right)\dfrac{\partial T}{\partial r}=\alpha\left(\dfrac{1+\nu}{1-\nu}\right)\dfrac{\partial T}{\partial r} \\ \dfrac{\partial^2 T}{\partial r^2}+\dfrac{1}{r}\dfrac{\partial T}{\partial r}=\dfrac{\rho c_v}{k}\dfrac{\partial T}{\partial t}+\left(\dfrac{3\lambda+2\mu}{k}\right)\alpha T_R\dfrac{\partial}{\partial t}\left[\dfrac{1}{r}\dfrac{\partial\left(r\,u_r\right)}{\partial r}\right] \end{cases} \tag{14.21}$$

where T_R is the reference temperature. By integrating the equilibrium equation (the first of eqs. (14.21)), respect to variable r , we obtain:

$$\frac{1}{r}\frac{\partial\left(r\,u_r\right)}{\partial r}=\left(\frac{3\lambda+2\mu}{2\mu+\lambda}\right)\alpha T+f_1(t) \tag{14.22}$$

where $f_1(t)$ is an function of sole variable time. By utilizing the equation (14.22), we can rewrite the Fourier's equation in follows manner:

$$\frac{\partial^2 T}{\partial r^2}+\frac{1}{r}\frac{\partial T}{\partial r}=\left[\frac{\rho c_v}{k}+\frac{\left(3\lambda+2\mu\right)^2\alpha^2 T_R}{k\left(\lambda+2\mu\right)}\right]\frac{\partial T}{\partial t}+\frac{\alpha T_R}{k}\left(3\lambda+2\mu\right)\frac{df_1}{dt} \tag{14.23}$$

By deriving the equations (14.23) respect to variable r , the follows equation is obtained:

$$\frac{\partial^3 T}{\partial r^3}+\frac{1}{r}\frac{\partial^2 T}{\partial r^2}-\frac{1}{r^2}\frac{\partial T}{\partial r}=\left[\frac{\rho c_v}{k}+\frac{\left(3\lambda+2\mu\right)^2\alpha^2 T_R}{k\left(\lambda+2\mu\right)}\right]\frac{\partial^2 T}{\partial r\,\partial t} \tag{14.24}$$

The general solution of equilibrium equation is reported in eq. (14.5). By solving the Fourier's equation (14.23) with one method reported in chapter VII (for example with method separation of variables), and substituting the function of temperature $T(r,t)$ in equation (14.5), we obtain the explicit displacement solution.

14.3. Uniform pressure with constant temperature (plain strain)

Let us consider a hollow cylinder with inner radius "a" and outer radius "b" , subjected to uniform pressure for r = b equal to p_e and subjected to uniform pressure for r = a equal to p_i . Moreover the profile of temperature is constant ($T=T_0>T_R$) along radius and in the time. In this case, let us consider the plane strain problem, then the only displacement component u_r is function of radius :

$$u_r=u_r(r);\quad u_\theta=0;\quad u_z=0;\quad T=T_0; \tag{14.25}$$

The results in this case are conveniently obtained from the displacement formulation in cylindrical coordinates. By omitting all displacement components and all derivatives in the θ and z directions, The equilibrium equations are reduced simply to:

$$\frac{\partial}{\partial r}\left[\frac{1}{r}\frac{\partial\left(r\,u_r\right)}{\partial r}\right]=0 \tag{14.26}$$

The general solution of equation (14.26) is :

$$u_r=C_1\,r+r^{-1}C_2 \tag{14.27}$$

For the hollow sphere of inner radius a and outer radius b the constants C_1 and C_2 must be determined from the condition that :

$$\sigma_{rr}(r=a)=p_i,\quad \sigma_{rr}(r=b)=p_e \tag{14.28}$$

From the strain-displacement relation and Hooke's law the non-zero stress components for this case are:

$$\begin{aligned}\sigma_{rr} &= 2C_1(\mu+\lambda)-\frac{2\mu C_2}{r^2}-\alpha(T_0-T_R)(3\lambda+2\mu);\\ \sigma_{\theta\theta} &= 2C_1(\mu+\lambda)+\frac{2\mu C_2}{r^2}-\alpha(T_0-T_R)(3\lambda+2\mu);\\ \sigma_{zz} &= 2C_1\lambda-\alpha(T_0-T_R)(3\lambda+2\mu)\end{aligned} \tag{14.29}$$

where T_R is the reference temperature. By substituting the stress functions (14.29) in boundary conditions (14.28), we determine the constants integration C_1 and C_2:

$$C_1=\alpha(T_0-T_R)\frac{(3\lambda+2\mu)}{(\lambda+\mu)}+\frac{p_e b^2-p_i a^2}{(\lambda+\mu)\left(b^2-a^2\right)};\quad C_2=\frac{a^2b^2(p_e-p_i)}{2\mu\left(b^2-a^2\right)}; \tag{14.30}$$

Finally, the displacement solution for a hollow sphere is :

$$u_r=\frac{\alpha(T_0-T_R)(3\lambda+2\mu)}{(\lambda+\mu)}r+\frac{1}{\left(b^2-a^2\right)}\left[\frac{a^2b^2(p_e-p_i)}{2\mu r}+\frac{p_e b^2-p_i a^2}{(\lambda+\mu)}r\right]; \tag{14.31}$$

The non-zero strain components are:

$$\begin{aligned}\varepsilon_{rr} &= \alpha(T_0-T_R)\frac{(3\lambda+2\mu)}{(\lambda+\mu)}+\frac{p_e b^2-p_i a^2}{(\lambda+\mu)\left(b^2-a^2\right)}-\frac{a^2b^2(p_e-p_i)}{2\mu\left(b^2-a^2\right)r^2};\\ \varepsilon_{\theta\theta} &= \alpha(T_0-T_R)\frac{(3\lambda+2\mu)}{(\lambda+\mu)}+\frac{p_e b^2-p_i a^2}{(\lambda+\mu)\left(b^2-a^2\right)}+\frac{a^2b^2(p_e-p_i)}{2\mu\left(b^2-a^2\right)r^2};\end{aligned} \tag{14.32}$$

The non-zero stress components are:

$$\begin{aligned}\sigma_{rr} &= \frac{1}{\left(b^2-a^2\right)}\left[p_e b^2\left(1-\frac{a^2}{r^2}\right)+p_i a^2\left(\frac{b^2}{r^2}-1\right)\right];\\ \sigma_{\theta\theta} &= \frac{1}{\left(b^2-a^2\right)}\left[p_e b^2\left(1+\frac{a^2}{r^2}\right)-p_i a^2\left(1+\frac{b^2}{r^2}\right)\right];\\ \sigma_{zz} &= \frac{1}{(\mu+\lambda)}\left[\frac{\lambda\left(p_e b^2-p_i a^2\right)}{\left(b^2-a^2\right)}-\alpha(T_0-T_R)\mu(3\lambda+2\mu)\right];\end{aligned} \tag{14.33}$$

If the external pressure vanishing $p_e=0$, the internal pressure $p_i=-p_0$, and thickness of hollow cylinder is very small ($\frac{s}{a}=\frac{b-a}{a}<<1$), we obtain the well known Mariotte's formula for cylinder tank subjected to internal uniform pressure:

$$\sigma_{\theta\theta}\cong\frac{p_0 a}{\delta}; \tag{14.34}$$

where $s=b-a$ is the thickness of the hollow cylinder .

The radial stress vanishes in solid ($\sigma_{rr}\cong 0$), but the stress component σ_{zz} do not vanish because in plane-strain problem the displacement component u_z is equal to zero. Then, the expression of the stress component σ_{zz} is given by:

$$\sigma_{zz}\cong\left(\frac{1}{\mu+\lambda}\right)\left[\frac{p_o a}{2s}\lambda-\alpha(T_0-T_R)(3\lambda+2\mu)\mu\right] \tag{14.35}$$

For example, let us consider a hollow cylinder characterized by following relations:

$$b=(1+\bar{s})\,a,\quad \bar{s}=s/a,\quad T_0=T_R, \tag{14.36}$$

where s is the thickness of the hollow cylinder: $b-a=s$ and $\bar{s}$ is the ratio between the thickness and the inner radius. Moreover, the cylinder is subjected to uniform pressure $p_i=-p_0,\ p_0>0$, for r = a and $p_e=0$ for r = b. Let us assume the following non-dimensional parameter for graphics of the displacement, strain and stress functions:

$$\begin{aligned}&\bar{r}=\frac{r-a}{b-a}=\frac{r-a}{a\,\bar{s}};\ \bar{\sigma}_{rr}=\frac{\sigma_{rr}}{p_0};\ \bar{\sigma}_{\theta\theta}=\frac{\sigma_{\theta\theta}}{p_0};\ \bar{\sigma}_{zz}=\frac{\sigma_{zz}}{p_0}\\&\bar{\sigma}_{eq}=\frac{\sigma_{eq}}{p_0};\quad \sigma_{eq}=\sqrt{\frac{(\sigma_{\theta\theta}-\sigma_{rr})^2+(\sigma_{\theta\theta}-\sigma_{zz})^2+(\sigma_{zz}-\sigma_{rr})^2}{2}};\end{aligned} \tag{14.37}$$

By applying the relations (14.37), we obtain that the non-dimensional stress components $\bar{\sigma}_{rr},\bar{\sigma}_{\theta\theta}$ depend only two non-dimensional parameters $\bar{s}$ and $\bar{r}$, as reported below:

$$\bar{\sigma}_{rr}=\frac{(1-\bar{r})\left[2+\bar{r}\,(1+\bar{s})\right]}{(2+\bar{s})(1+\bar{s}\,\bar{r})^2};\quad \bar{\sigma}_{\theta\theta}=-\frac{2+\bar{s}\left[2+\bar{s}+\bar{r}\,(2+\bar{s}\,\bar{r})\right]}{\bar{s}\,(2+\bar{s})(1+\bar{s}\,\bar{r})^2}; \tag{14.38}$$

The non-dimensional stress component $\bar{\sigma}_{zz}$ depends only two non-dimensional parameters ν and $\bar{s}$:

$$\bar{\sigma}_{zz}=-\frac{2\nu}{\bar{s}\,(2+\bar{s})}, \tag{14.39}$$

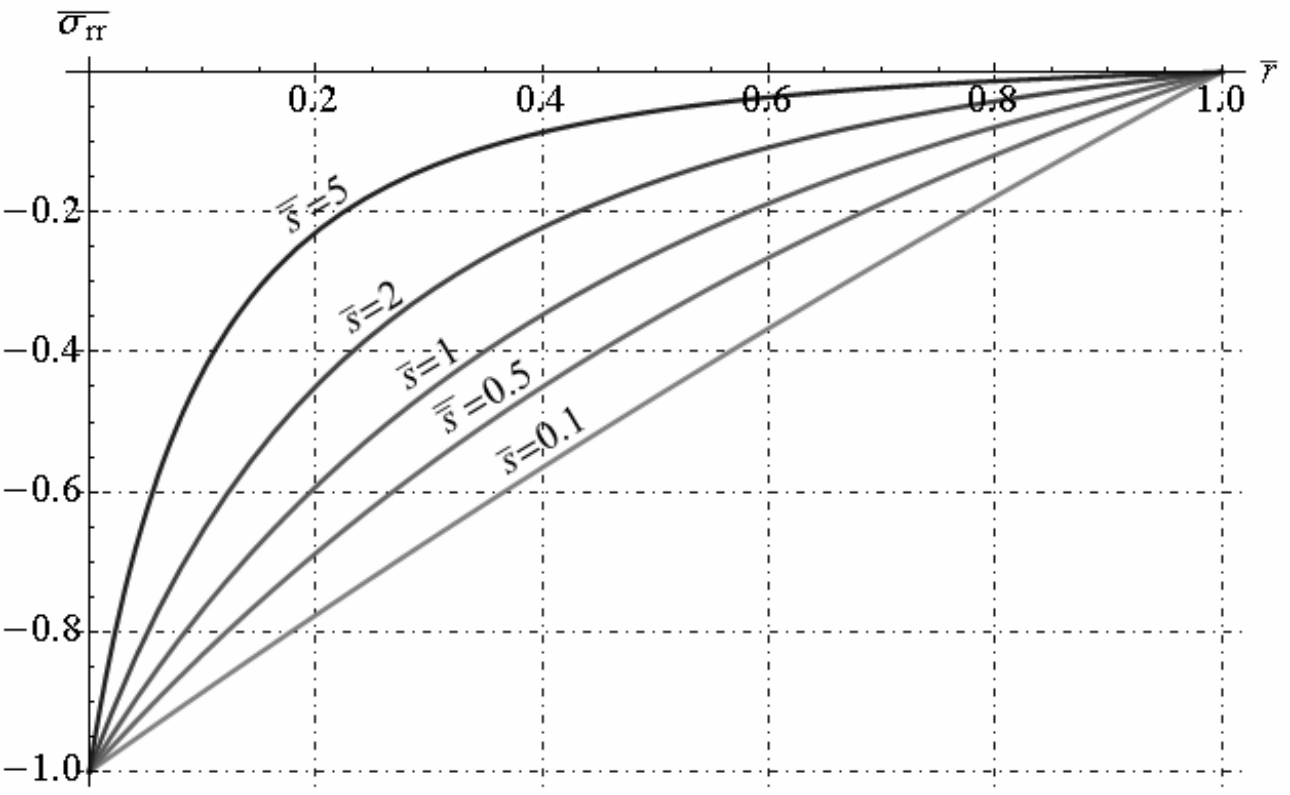

Fig. 14.1 - *Non-dimensional radial stress distribution along radial direction*

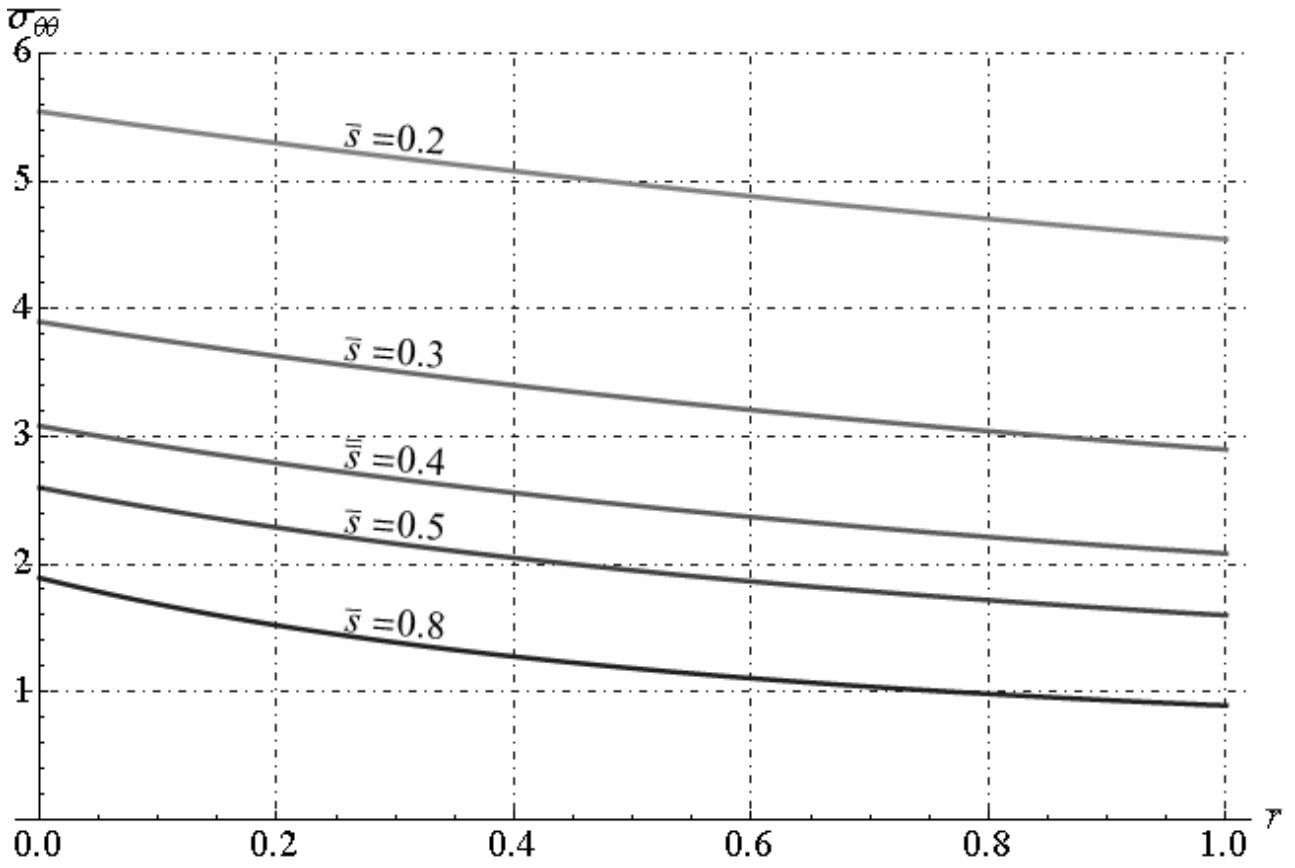

Fig. 14.2 - *Non-dimensional circumferential stress distribution along radial direction*

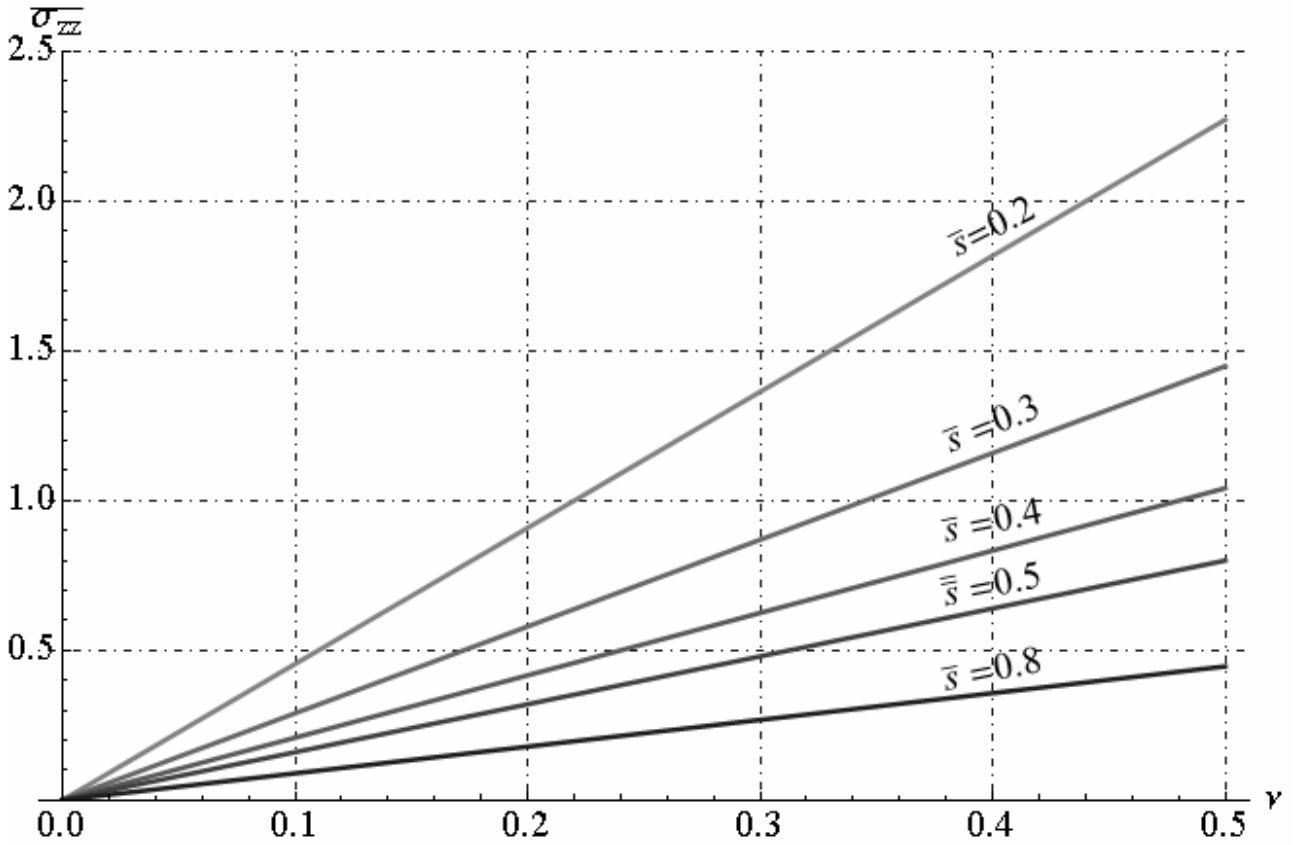

Fig. 14.3 - *Non-dimensional axial stress distribution versus Poisson's modulus*

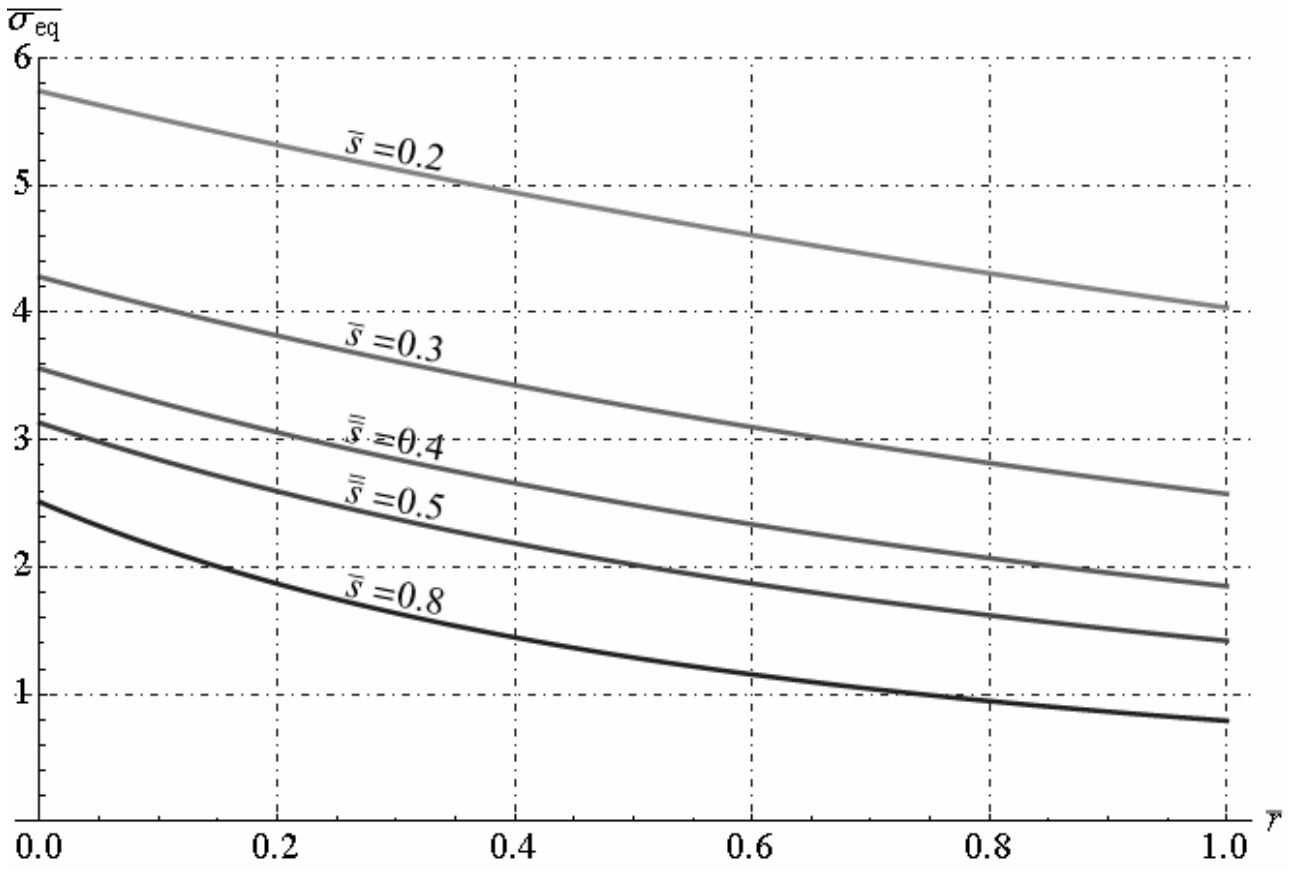

Fig. 14.4 - *Non-dimensional equivalent stress distribution along radial direction (with fixed Poisson's modulus $\nu = 0.3$)*

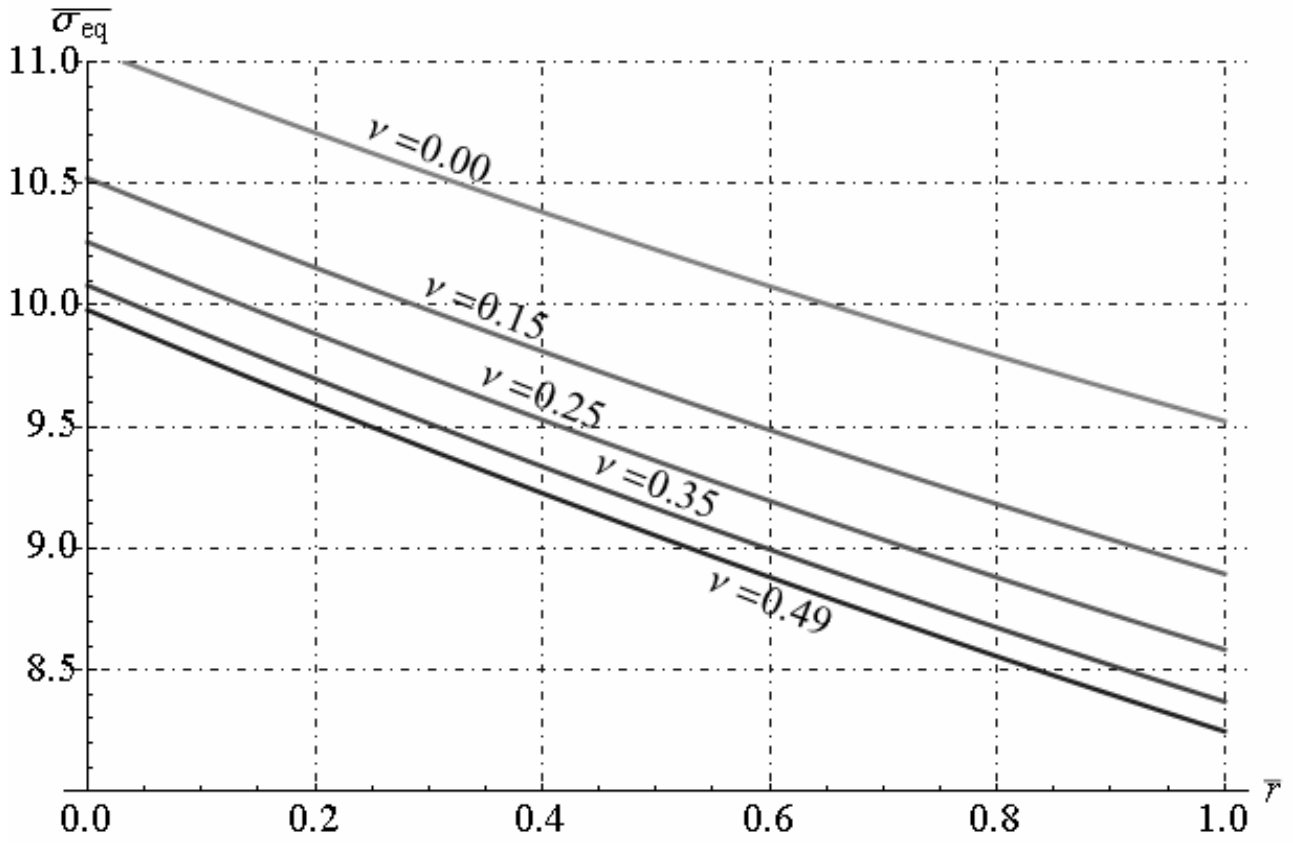

Fig. 14.5 - *Non-dimensional equivalent stress distribution along radial direction (with fixed ratio $\bar{s} = 0.1$)*

14.4 Radial temperature variation and uniform pressure (plane-strain)

Let us consider a hollow cylinder with inner radius "a" and outer radius "b" , subjected to uniform pressure for r = a equal to $p_i = -p_0$. Moreover the hollow cylinder is subjected to radial temperature variation. In this case, the equilibrium equation is reported in equation and Fourier's equation is reported in equation (14.23) for coupled thermo-elastic problem (or equivalent equation (14.4) for uncoupled thermo-elastic problem). The general solution of the equilibrium equation in terms of radial displacement function is given by equation (14.5). In this case, the boundary conditions for the hollow cylinder of inner radius a and outer radius b are:

$$\begin{cases} \sigma_{rr}(r=a) = -p_0 \\ \sigma_{rr}(r=b) = 0 \end{cases} \tag{14.40}$$

By solving the equations (14.40) we obtain the functions $C_1(t)$ and $C_2(t)$, we obtain:

$$\begin{aligned} C_1(t) &= \frac{1}{\left(b^2-a^2\right)(\lambda+\mu)}\left[\frac{p_0 a^2}{2} + \alpha\frac{\mu(3\lambda+2\mu)}{(\lambda+2\mu)}\int_a^b \xi T(\xi,t)\,d\xi\right] - \frac{\alpha T_R(3\lambda+2\mu)}{2(\lambda+\mu)}; \\ C_2(t) &= \frac{a^2}{\left(b^2-a^2\right)}\left[\frac{p_0 b^2}{2\mu} + \frac{\alpha(3\lambda+2\mu)}{(\lambda+2\mu)}\int_a^b \xi T(\xi,t)\,d\xi\right]; \end{aligned} \tag{14.41}$$

By substituting the function of the time $C_1(t)$ and $C_2(t)$ in equation (14.5), we determine the displacement solution:

$$\begin{aligned} u_r = &-\frac{\alpha T_R(3\lambda+2\mu)}{2(\lambda+\mu)}r + \frac{p_0 a^2}{2\left(b^2-a^2\right)}\left[\frac{r}{(\mu+\lambda)} + \frac{b^2}{\mu r}\right] + \\ &+\frac{\alpha}{r}\left(\frac{3\lambda+2\mu}{\lambda+2\mu}\right)\left\{\left[\frac{a^2(\mu+\lambda)+\mu r^2}{\left(b^2-a^2\right)(\mu+\lambda)}\right]\int_a^b \xi T(\xi,t)\,d\xi + \int_a^r \xi T(\xi,t)\,d\xi\right\} \end{aligned} \tag{14.42}$$

14.5 Steady-state problem with radial temperature variation (plane strain)

Let us consider a hollow cylinder with inner radius "a" and outer radius "b" , subjected to radial temperature variation. In this section we study the steady-state problem, then the temperature displacement, strain and stress components are functions only variable r. Let us consider the case in which the inner surface r = a is exposed, to an ambient at temperature T_i and external surface r = b is exposed to a temperature T_e. The differential equation related to heat conduction and the corresponding boundary conditions are reported below:

$$\frac{d^2T(r)}{dr^2} + \frac{1}{r}\frac{dT(r)}{dr} = 0; \quad a < r < b, \tag{14.43}$$

$$T(r=a) = T_i, \tag{14.44}$$

$$T(r=b) = T_e, \tag{14.45}$$

By solving the differential equation (14.43), we obtain the function of temperature:

$$T(r) = A_1 \log r + A_2 \tag{14.46}$$

where A_1, A_2 are constants integration to determine. By solving the boundary conditions (14.44)-(14.45), we determine the constants integration as reported below:

$$A_1 = (T_i - T_e)\log\left(\frac{a}{b}\right), \quad A_2 = (T_e \log a - T_i \log b)\log\left(\frac{a}{b}\right) \tag{14.47}$$

By substituting the expressions of constants integration (14.47) in equation (14.46) , we obtain the function of the temperature:

$$T(r)=\left[(T_i-T_e)\log r+T_e\log a-T_i\log b\right]\log\left(\frac{a}{b}\right) \tag{14.48}$$

If the hollow cylinder is subjected to radial temperature variation and zero external load, let us assume that the displacement components reduce to sole $u_r=u_r(r)$. In this case the equilibrium equations reduce to one ordinary differential equation as reported below:

$$\frac{d}{dr}\left[\frac{1}{r}\frac{d(r\,u_r)}{\partial r}\right]=\alpha\left(\frac{1+\nu}{1-\nu}\right)\frac{d\,T}{d\,r} \tag{14.49}$$

The general solution of equation (14.49) is :

$$u_r(r)=\frac{\alpha(1+\nu)}{r(1-\nu)}\int_a^r \xi T(\xi)\,d\xi+C_1\,r+\frac{C_2}{r} \tag{14.50}$$

where C_1, C_2 are constants integration to determine. By substituting the function (14.48) in equation (14.50) , we determine the expression of the displacement solution are reported below:

$$u_r=D_1\,r+\frac{D_2}{r}+D_3\,r\log r \tag{14.51}$$

where D_1, D_2, D_3 are following constants:

$$\begin{aligned}
&D_1=C_1+\frac{\alpha(1+\nu)\left[T_e-T_i+2\left(T_e\log a-T_i\log b\right)\right]}{4(1-\nu)\log(a/b)};\\
&D_2=C_2-\frac{\alpha(1+\nu)a^2\left[T_e-T_i+2T_i\log(a/b)\right]}{4(1-\nu)\log(a/b)};\quad D_3=-\frac{\alpha(1+\nu)(T_e-T_i)}{2(1-\nu)\log(a/b)};
\end{aligned} \tag{14.52}$$

By applying the strain-displacement relationship, we determine the non-zero strain components:

$$\varepsilon_{rr}=D_1-\frac{D_2}{r^2}+D_3(1+\log r);\quad \varepsilon_{\theta\theta}=D_1+\frac{D_2}{r^2}+D_3\log r; \tag{14.53}$$

By applying the stress-strain relationship, we obtain the non-zero stress components:

$$\begin{aligned}
\sigma_{rr}&=\left(\frac{E}{1-2\nu-\nu^2}\right)\left[D_1-\frac{D_2}{r^2}(1-2\nu)+D_3(1-\nu+\log r)\right]-\frac{\alpha E}{1-2\nu}\left(A_1\log r+A_2-T_R\right)\\
\sigma_{\theta\theta}&=\left(\frac{E}{1-2\nu-\nu^2}\right)\left[D_1+\frac{D_2}{r^2}(1-2\nu)+D_3(\nu+\log r)\right]-\frac{\alpha E}{1-2\nu}\left(A_1\log r+A_2-T_R\right)\\
\sigma_{zz}&=\left(\frac{E\,\nu}{1-2\nu-\nu^2}\right)\left[2D_1+D_3(1-2\log r)\right]-\frac{\alpha E}{1-2\nu}\left(A_1\log r+A_2-T_R\right)
\end{aligned} \tag{14.54}$$

The boundary conditions of zero tractions on the cylindrical surfaces are then

$$\sigma_{rr}=0\quad at\quad r=a\quad \text{and}\quad r=b \tag{14.55}$$

By solving the equations (14.55), respect to integration constants C_1, C_2, we obtain the explicit expressions of the coefficient D_1, D_2, D_3 as reported below:

$$\begin{aligned}
&D_1=\frac{\alpha(1+\nu)}{2\log(a/b)}\left\{\begin{aligned}&T_e-T_i+\frac{2\left(T_e b^2\log a+T_i a^2\log b\right)}{b^2-a^2}-2T_R\log(a/b)\\&+\frac{a^2\log a\left[T_e+T_i(1-2\nu)\right]+b^2\log b\left[T_i+T_e(1-2\nu)\right]}{(1-\nu)\left(b^2-a^2\right)}\end{aligned}\right\};\\
&D_2=\frac{\alpha(1+\nu)a^2b^2(T_e-T_i)}{2(1-\nu)\left(b^2-a^2\right)};\quad D_3=-\frac{\alpha(1+\nu)(T_e-T_i)}{2(1-\nu)\log(a/b)};
\end{aligned} \tag{14.56}$$

If the thickness of hollow cylinder is very small ($\frac{s}{a}=\frac{b-a}{a}<<1$), we obtain the well known approximate formula for cylindrical tank subjected to temperature gradient :

$$\begin{aligned}
&u_r \cong \frac{\alpha\left(T_e-T_i\right)(1+\nu)a}{2};\\
&\varepsilon_{rr} \cong \frac{\alpha(1+\nu)(2-\nu)\left(T_e-T_i\right)}{2(1-\nu)};\quad \varepsilon_{\theta\theta} \cong \frac{\alpha(1+\nu)\left(T_e-T_i\right)}{2};\ \varepsilon_{zz}=0;\\
&\sigma_{rr} \cong 0;\quad \sigma_{\theta\theta} \cong \frac{\alpha E\left(T_e-T_i\right)}{2(\nu-1)};\ \sigma_{zz} \cong -\frac{\alpha E\left(T_e-T_i\right)(2-\nu)}{2(1-\nu)};
\end{aligned} \tag{14.57}$$

where $s=b-a$ is the thickness of the hollow cylinder.
For example, let us consider a hollow cylinder characterized by following relations:

$$b=(1+\bar{s})a,\quad \bar{s}=s/a,\quad T_i=T_R, \tag{14.58}$$

where s is the thickness of the hollow cylinder: $b-a=s$ and $\bar{s}$ is the ratio between the thickness and the inner radius. Moreover, the cylinder is subjected to temperature gradient $\Delta T=T_e-T_i$. Let us assume the following non-dimensional parameter for graphics of the displacement, strain and stress functions:

$$\begin{aligned}
&\bar{r}=\frac{r-a}{b-a}=\frac{r-a}{\bar{s}\,a};\ \bar{\sigma}_{rr}=\frac{\sigma_{rr}}{\beta};\ \bar{\sigma}_{\theta\theta}=\frac{\sigma_{\theta\theta}}{\beta};\ \bar{\sigma}_{zz}=\frac{\sigma_{zz}}{\beta};\quad \beta=\frac{\alpha E\Delta T}{2(1-\nu)}\\
&\bar{\sigma}_{eq}=\frac{\sigma_{eq}}{\beta};\quad \sigma_{eq}=\sqrt{\frac{\left(\sigma_{\theta\theta}-\sigma_{rr}\right)^2+\left(\sigma_{\theta\theta}-\sigma_{zz}\right)^2+\left(\sigma_{zz}-\sigma_{rr}\right)^2}{2}};
\end{aligned} \tag{14.59}$$

By applying the relations (14.59) we obtain that the non-dimensional stress components $\bar{\sigma}_{rr},\bar{\sigma}_{\theta\theta},\bar{\sigma}_{zz}$ depend only two non-dimensional parameters $\bar{s}$ and $\bar{r}$, as reported below:

$$\bar{\sigma}_{rr}=-\frac{(1+\bar{s})^2\log\left[1/(1+\bar{s})\right]+(1+\bar{r}\bar{s})^2\left\{(1+\bar{s})^2\log\left[(1+\bar{s})/(1+\bar{r}\,\bar{s})\right]+\log(1+\bar{r}\,\bar{s})\right\}}{\bar{s}(2+\bar{s})(1+\bar{r}\,\bar{s})^2\log\left[1/(1+\bar{s})\right]} \tag{14.60}$$

$$\bar{\sigma}_{\theta\theta}=-\frac{(1+\bar{s})^2\left[2+\bar{r}\,\bar{s}(2+\bar{r}\,\bar{s})\right]\log(1+\bar{s})+\bar{s}(2+\bar{s})(1+\bar{r}\,\bar{s})^2\left[1+\log(1+\bar{r}\,\bar{s})\right]}{\bar{\delta}(2+\bar{s})(1+\bar{r}\,\bar{s})^2\log\left[1/(1+\bar{s})\right]} \tag{14.61}$$

The non-dimensional stress component $\bar{\sigma}_{zz}$ depends only three non-dimensional parameters $\nu,\bar{r}$ and $\bar{s}$:

$$\bar{\sigma}_{zz}=\frac{-2\nu(1+\bar{s})^2\log(1+\bar{s})+\bar{s}(2+\bar{s})\left[\nu+2\log(1+\bar{r}\,\bar{s})\right]}{\bar{\delta}(2+\bar{s})\log\left[1/(1+\bar{s})\right]} \tag{14.62}$$

The distribution of the non-dimensional stress components along radial direction are reported below:

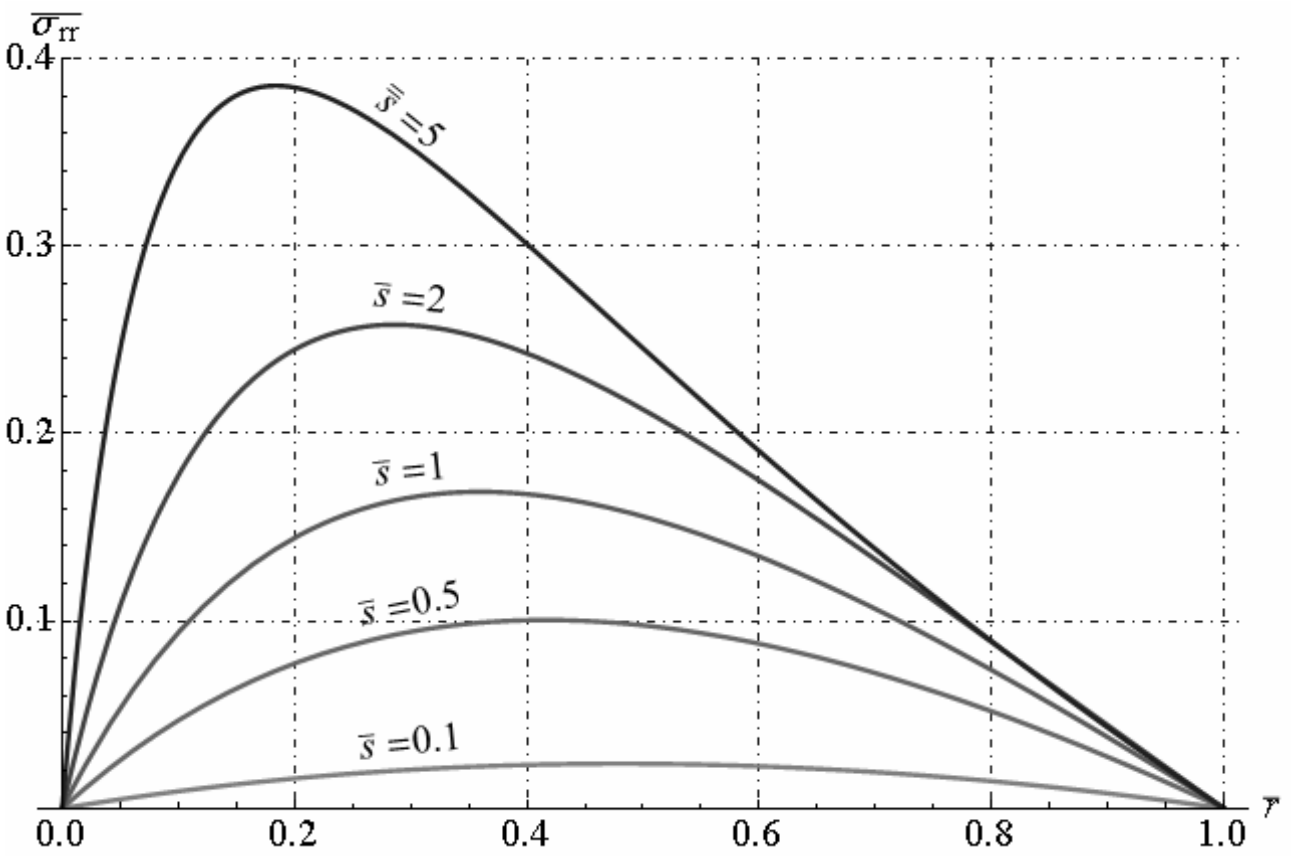

Fig. 14.6 - *Non-dimensional radial stress distribution along radial direction*

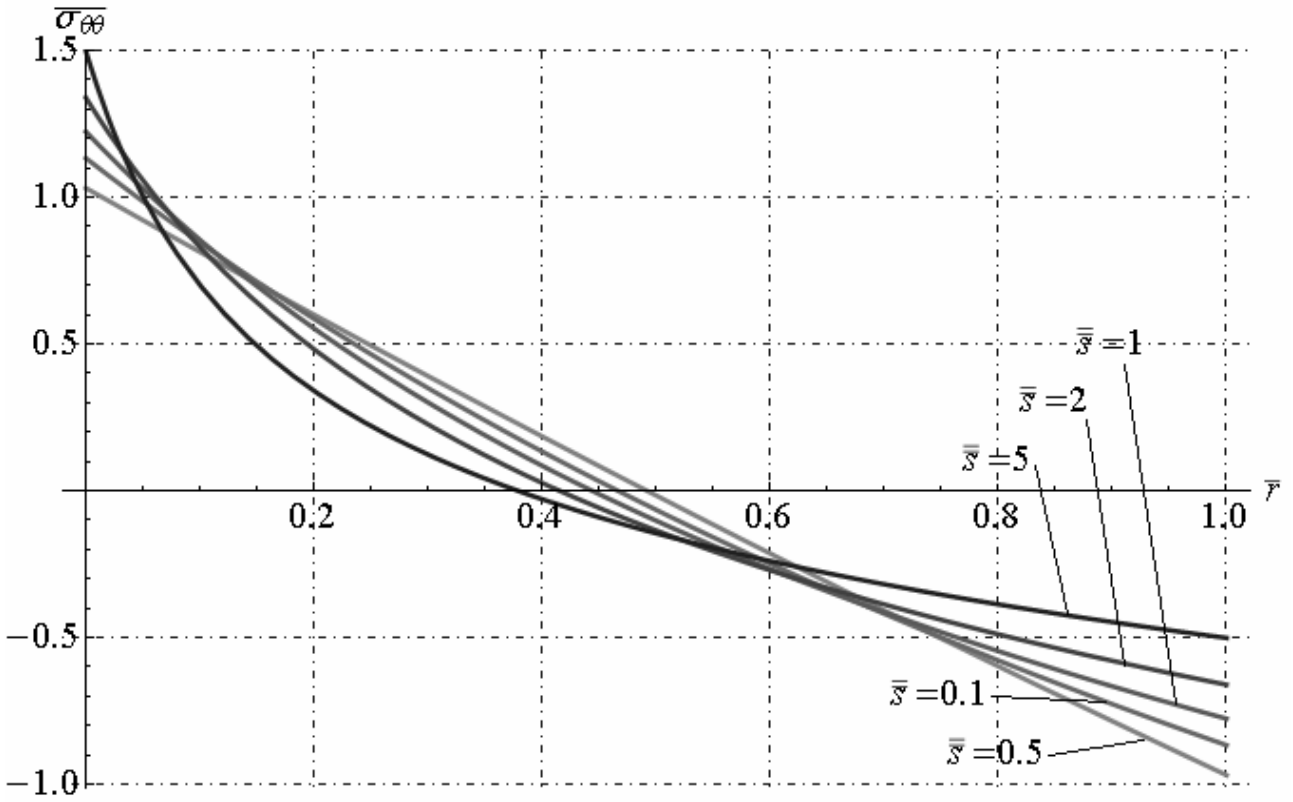

Fig. 14.7 - *Non-dimensional circumferential stress distribution along radial direction*

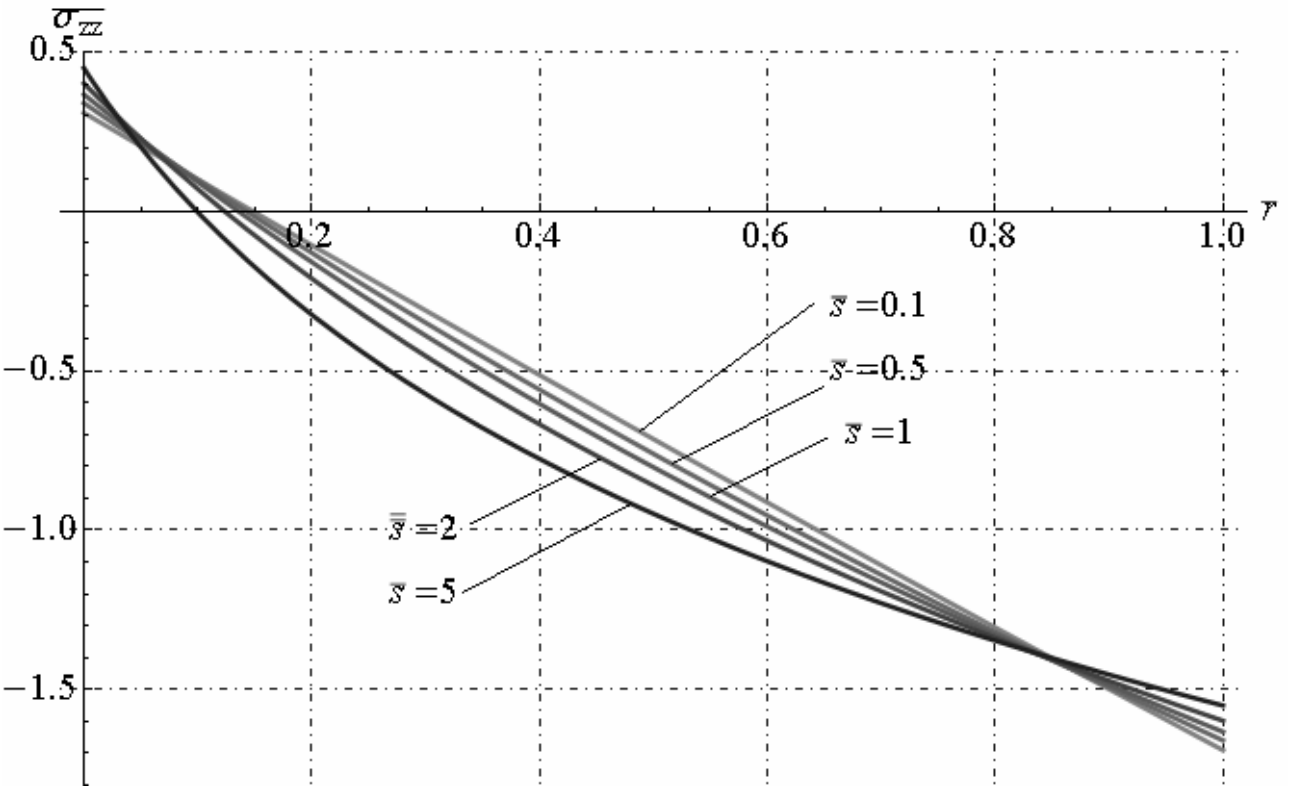

Fig. 14.8 - *Non-dimensional axial stress distribution along radial direction (with fixed Poisson's modulus* $\nu = 0.30$*)*

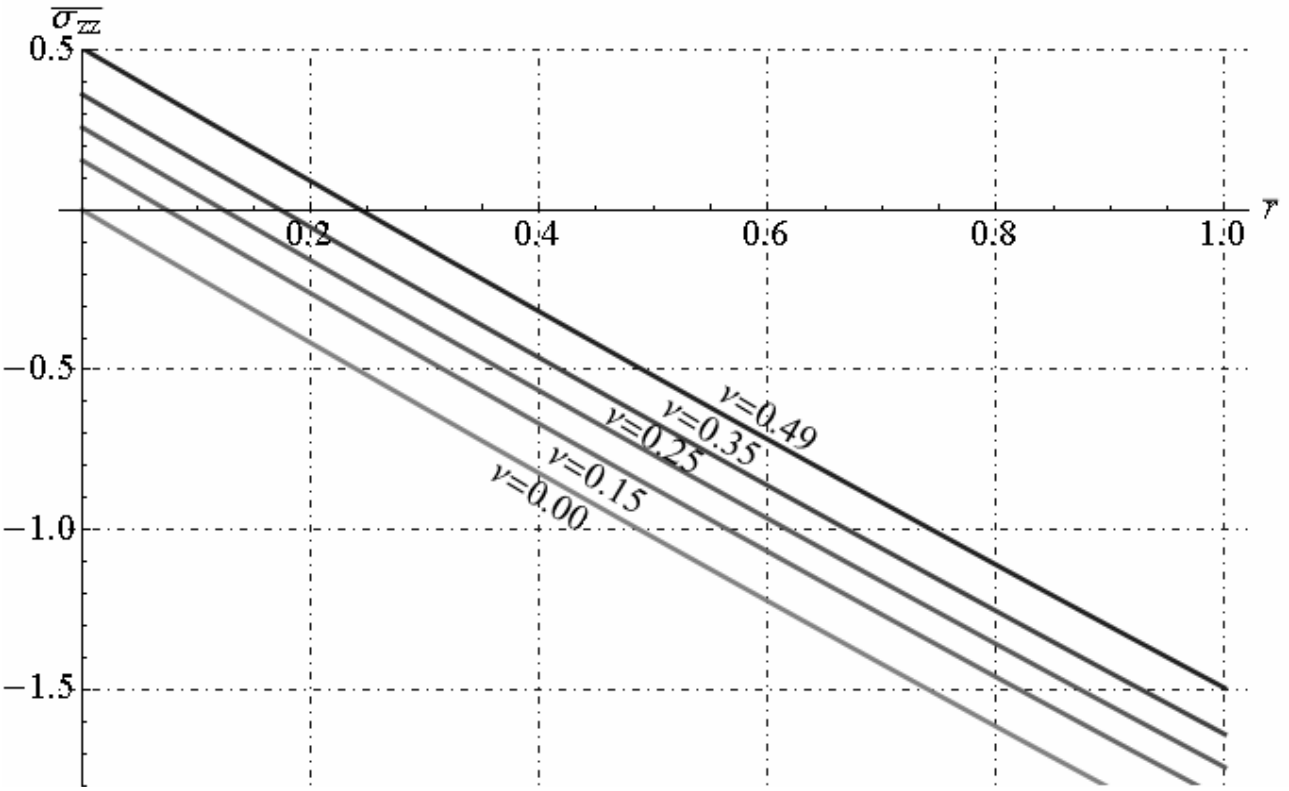

Fig. 14.9 - *Non-dimensional axial stress distribution along radial direction (with fixed ratio* $\bar{s} = 0.10$*)*

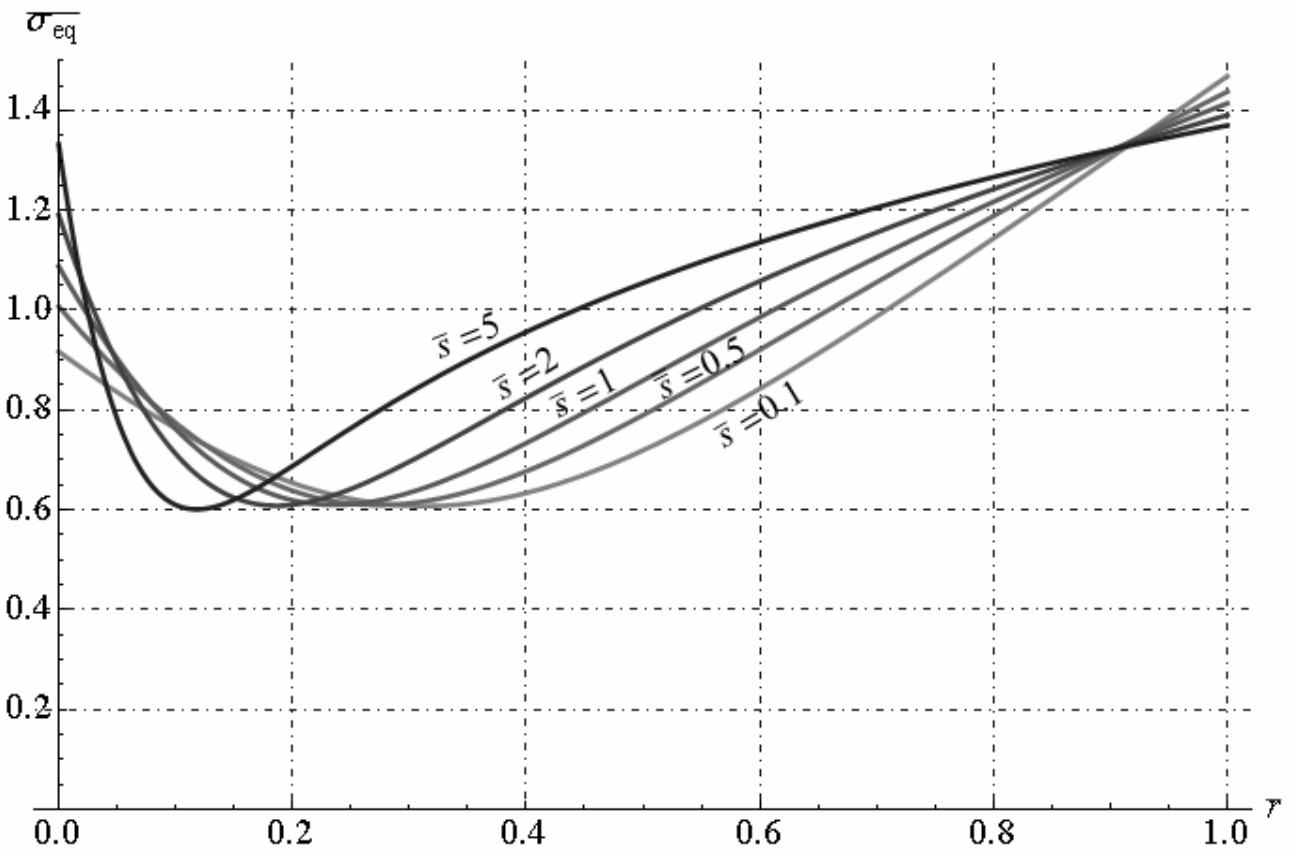

Fig. 14.10 - *Non-dimensional equivalent stress distribution along radial direction (with fixed Poisson's modulus $\nu = 0.30$)*

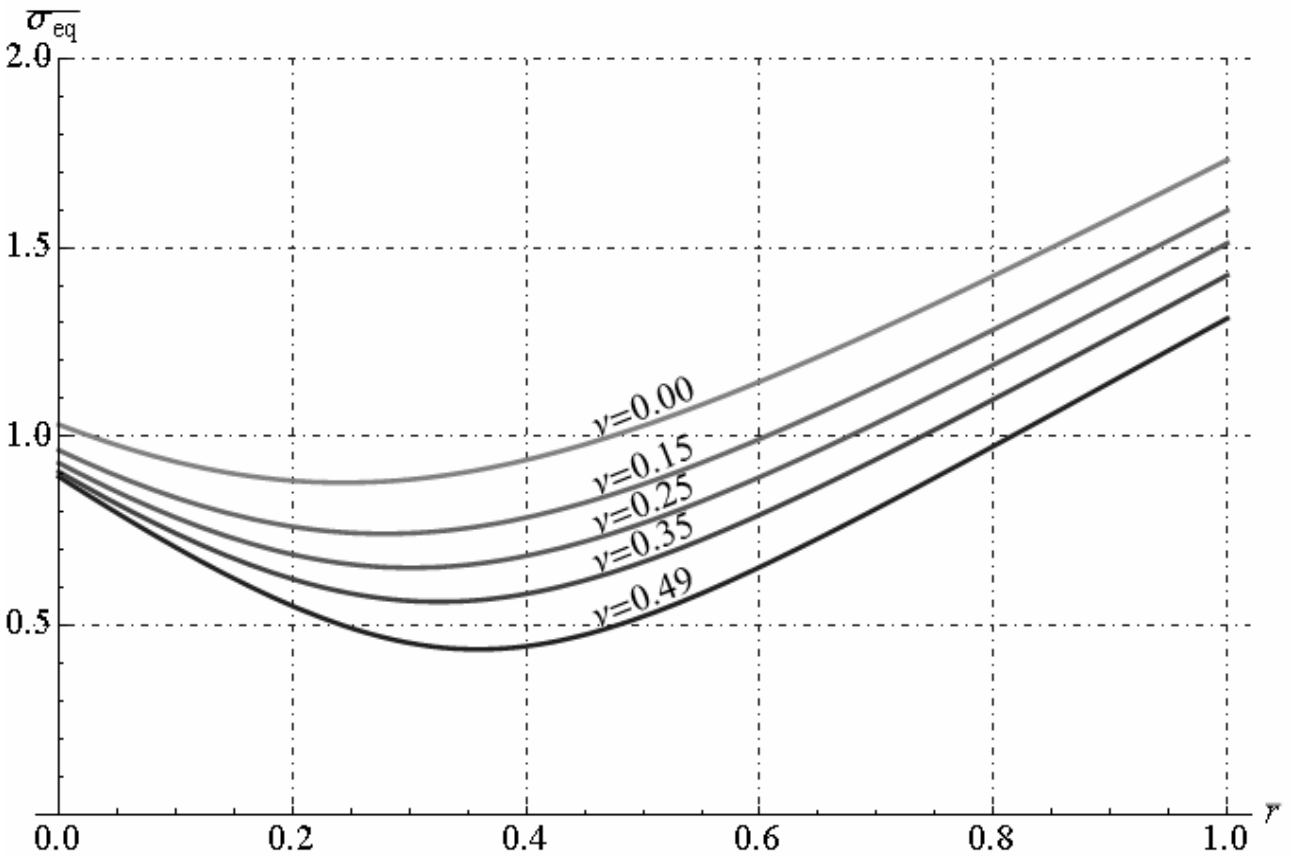

Fig. 14.11 - *Non-dimensional equivalent stress distribution along radial direction (with fixed ratio $\overline{s} = 0.10$)*

14.6 Hollow Cylinder with plane-harmonic temperature distribution (steady-state problem)

The solution of the preceding section was obtained, by means of the displacement formulation, for the case of a temperature distribution varying with r only. We will now allow the temperature to vary with the angle θ as well, but we will take it to be that corresponding to a steady state, that is:

$$\nabla^2 T(r,\theta) = \frac{1}{r^2}\frac{\partial^2 T}{\partial \theta^2} + \frac{1}{r}\frac{\partial}{\partial r}\left(r\frac{\partial T}{\partial r}\right) = 0 \tag{14.63}$$

The solution will be obtained here by means of the stress formulation; for convenience of reference, the statement of that formulation will be repeated here in extended notation. It is then required to satisfy the following equations, which for a circular cylinder in a state of plane strain, with inner radius a and outer radius b and with free cylindrical surface:

Differential equation:

$$\nabla^4 \varphi + \alpha_1 E_1 \nabla^2 T = 0; \quad a < r < b \tag{14.64}$$

Boundary conditions:

$$\varphi = \frac{\partial \varphi}{\partial r} = 0; \quad r = b \tag{14.65}$$

$$\left.\begin{aligned} \varphi &= a_1 x + a_2 y + b_0; && r = a \\ \frac{\partial \varphi}{\partial r} &= a_1 \cos\theta + a_2 \sin\theta; && r = a \end{aligned}\right\} \tag{14.66}$$

Michell conditions

$$\left.\begin{aligned} \int_0^{2\pi}\left(y\frac{\partial \nabla^2\varphi}{\partial r} - \frac{x}{r}\frac{\partial \nabla^2\varphi}{\partial \theta}\right) r d\theta &= -E_1\alpha_1 \int_0^{2\pi}\left(y\frac{\partial T}{\partial r} - \frac{x}{r}\frac{\partial T}{\partial \theta}\right) \\ \int_0^{2\pi}\left(x\frac{\partial \nabla^2\varphi}{\partial r} - \frac{y}{r}\frac{\partial \nabla^2\varphi}{\partial \theta}\right) r d\theta &= -E_1\alpha_1 \int_0^{2\pi}\left(x\frac{\partial T}{\partial r} - \frac{y}{r}\frac{\partial T}{\partial \theta}\right) \end{aligned}\right\} \; r = a \tag{14.67}$$

$$\int_0^{2\pi} \frac{\partial \nabla^2 \varphi}{\partial r} r d\theta = -E_1\alpha_1 \int_0^{2\pi} \frac{\partial T}{\partial r} r d\theta; \quad r = a \tag{14.68}$$

where

$$x = r\cos\theta; \quad y = r\sin\theta \tag{14.69}$$

and where the constants a_1, a_2, b_0 are arbitrary as far the boundary value problem of equations. (14.64) to (14.66) is concerned and are used to satisfy the Mitchell conditions.

For a solid cylinder (a = 0) equations (14.66) - (14.68) do not apply, and are replaced by the condition that the solution must be finite at r = 0. It is easily verified that in this case for a harmonic temperature distribution the solution (which is unique) is $\varphi = 0$.

For a hollow cylinder the results, as will be seen, are not quite as simple. It is convenient to express the temperature in the form of a Fourier series, that is,

$$T(r,\theta) = \sum_{n=0}^{\infty} F_n(r)\cos(n\theta) + \sum_{n=0}^{\infty} G_n(r)\sin(n\theta) \tag{14.70}$$

where, if the temperature is to be plane harmonic, the coefficients F_n and G_n must satisfy the relations

$$\left.\begin{aligned} \frac{1}{r}\frac{d}{dr}\left(r\frac{dF_n}{dr}\right) - \frac{n^2}{r^2}F_n = 0 \quad n = 0,1,2,..... \\ \frac{1}{r}\frac{d}{dr}\left(r\frac{dG_n}{dr}\right) - \frac{n^2}{r^2}G_n = 0 \quad n = 1,2,3,..... \end{aligned}\right. \tag{14.71}$$

For a temperature distribution in this form we take:

$$\varphi(r,\theta)=\sum_{n=0}^{\infty} f_n(r)\cos(n\theta)+\sum_{n=0}^{\infty} g_n(r)\sin(n\theta) \tag{14.72}$$

Substitution of eqs. (14.70)-(14.72) into the basic equations (14.64)-(14.68) to be satisfied by the solution gives (where primes indicate differentiation with respect to r):
Differential equation for f_n:

$$f_n^{IV}+\frac{2}{r}f_n^{III}-\frac{1+2n^2}{r^2}f_n^{II}+\frac{1+2n^2}{r^3}f_n^{I}+\frac{n^2\left(n^2-4\right)}{r^4}f_n=0 \quad n=0,1,2,.... \tag{14.73}$$

Boundary conditions for f_n:

$$f_n(b)=\frac{df_n(b)}{dr}=0 \qquad n=0,1,2,..... \tag{14.74}$$

$$\left.\begin{aligned} &f_0(a)=b_0; \quad f_1(a)=a_1 a; \quad f_n(a)=0 \quad for \;\; n\geq 2\\ &\frac{df_0(a)}{dr}=0; \quad \frac{df_1(a)}{dr}=a_1; \quad \frac{df_n(a)}{dr}=0 \quad for \;\; n\geq 2 \end{aligned}\right\} \tag{14.75}$$

Mitchell conditions for f_n at r = a:

$$\left(\frac{1}{r}-\frac{d}{dr}\right)\left[-\frac{f_1}{r^2}+\frac{1}{r}\frac{d}{dr}\left(r\frac{df_1}{dr}\right)\right]=-\alpha_1 E_1\left(\frac{1}{r}-\frac{d}{dr}\right)\left[F_1(r)\right] \tag{14.76}$$

$$\frac{d}{dr}\left[\frac{1}{r}\frac{d}{dr}\left(r\frac{df_0}{dr}\right)\right]=-\alpha_1 E_1\frac{dF_0}{dr} \tag{14.77}$$

and differential equation for g_n:

$$g_n^{IV}+\frac{2}{r}g_n^{III}-\frac{1+2n^2}{r^2}g_n^{II}+\frac{1+2n^2}{r^3}g_n^{I}+\frac{n^2\left(n^2-4\right)}{r^4}g_n=0 \quad n=1,2,.... \tag{14.78}$$

Boundary conditions for g_n:

$$g_n(b)=\frac{dg_n(b)}{dr}=0 \qquad n=1,2,..... \tag{14.79}$$

$$\left.\begin{aligned} &g_1(a)=a\,a_2; \quad g_n(a)=0 \quad for \;\; n\geq 2\\ &\frac{dg_1(a)}{dr}=a_2; \quad \frac{dg_n(a)}{dr}=0 \quad for \;\; n\geq 2 \end{aligned}\right\} \tag{14.80}$$

Mitchell conditions for g_n at r = a:

$$\left(\frac{1}{r}-\frac{d}{dr}\right)\left[-\frac{g_1}{r^2}+\frac{1}{r}\frac{d}{dr}\left(r\frac{dg_1}{dr}\right)\right]=-\alpha_1 E_1\left(\frac{1}{r}-\frac{d}{dr}\right)\left[G_1(r)\right] \tag{14.81}$$

In derivation of the Michell conditions in the form just given the required integrations with respect to θ have been performed with the aid of the orthogonality relations

$$\int_0^{2\pi}\sin(n\theta)\sin(m\theta)\,d\theta=\int_0^{2\pi}\cos(n\theta)\cos(m\theta)\,d\theta=\begin{cases}0 & n\neq m\\ \pi & n=m\neq 0\end{cases} \tag{14.82}$$

The reader will therefore notice that Mitchell conditions arise only for the functions f_0, f_1, g_1, whereas those for $n\geq 2$ are automatically satisfied. It is then immediately clear by inspection of the boundary-value problems for f_n, g_n that the solution is :

$$f_n=g_n=0; \quad n\geq 0 \tag{14.83}$$

We have thus obtained the important result that only the terms of a plane-harmonic temperature distribution for which n = 0 and n = 1 contribute to the stress components in the plane. It will be convenient to consider these contributions separately and to denote them by $\sigma_{rr}^{(n)}, \sigma_{\theta\theta}^{(n)}, n=0,1$. Thus $\sigma_{rr}^{(0)}, \sigma_{\theta\theta}^{(0)}$ correspond to a plane-harmonic temperature distribution of the form:

$$T^{(0)}(r,\theta) = F_0(r) \tag{14.84}$$

and $\sigma_{rr}^{(1)}, \sigma_{\theta\theta}^{(1)}$ correspond to a plane-harmonic temperature distribution of the form:

$$T^{(1)}(r,\theta) = F_1(r)\cos\theta + G_1(r)\sin\theta \tag{14.85}$$

where of course the functions F_0, F_1, G_1 must satisfy (14.71). The stress components in the plane corresponding to the general plane-harmonic temperature distribution of equation (14.70) are then simply the sum of those caused by these two contributions. The axial stress component, σ_{zz}, however, for the case of plane strain under consideration here, will depend upon the entire temperature distribution.

We first determine $\sigma_{rr}^{(0)}, \sigma_{\theta\theta}^{(0)}$. These can, of course, be found as a special case of the solution of section 14.1 , but it will be instructive to proceed with the present formulation and to compare the two derivations . With n = 0 the solution of (14.73) is:

$$f_0(r) = C_1 + C_2 \log\left(\frac{r}{a}\right) + C_3\left(\frac{r}{a}\right)^2 + C_4\left(\frac{r}{a}\right)^2 \log\left(\frac{r}{a}\right) \tag{14.86}$$

The five constants C_1, C_2, C_3, C_4, b_0 must now determined from eqs. (14.74),(14.75)-(14.77). The form of $T^{(0)}(r,\theta)$ is from (14.71):

$$T^{(0)}(r,\theta) = F_0(r) = T_0 \log\left(\frac{r}{a}\right) + T_1 \tag{14.87}$$

where T_0, T_1 are constant; thus expressions (14.10) for the stresses must reduce, for this special temperature, to those corresponding to the stress function f_0 of equation (14.86) and given by the formulas:

$$\begin{aligned}
\sigma_{rr} &= \frac{1}{r}\frac{df_0}{dr} = \frac{C_2}{r^2} + \frac{2C_3}{a^2} + \frac{C_4}{a^2}\left(1 + 2\log\frac{r}{a}\right) \\
\sigma_{\theta\theta} &= \frac{d^2 f_0}{dr^2} = -\frac{C_2}{r^2} + \frac{2C_3}{a^2} + \frac{C_4}{a^2}\left(3 + 2\log\frac{r}{a}\right) \\
\tau_{r\theta} &= 0
\end{aligned} \tag{14.88}$$

The constant temperature T_1 causes no stresses and we can omit if from the calculations. The constants appearing in equations. (14.88) are:

$$\begin{aligned}
C_2 &= \frac{\alpha_1 E_1 T_0 b^2 a^2}{2\left(b^2 - a^2\right)} \log\frac{r}{a}; \\
C_3 &= \frac{\alpha_1 E_1 T_0 a^2}{8\left(b^2 - a^2\right)}\left[\left(1 + 2\log\frac{r}{a}\right)b^2 - a^2\right]; \\
C_4 &= -\frac{\alpha_1 E_1 T_0 a^2}{4}
\end{aligned} \tag{14.89}$$

where the relation:

$$F_0'(a) = \left(\frac{T_0}{a}\right) \tag{14.90}$$

Has been used. With these constants we find

$$\sigma_{rr}=\frac{\alpha_1 E_1 T_0}{2}\left[\left(\frac{b}{r}\right)^2\left(\frac{r^2-a^2}{b^2-a^2}\right)\log\frac{b}{a}-\log\frac{r}{a}\right]$$
$$\sigma_{\theta\theta}=\frac{\alpha_1 E_1 T_0}{2}\left[\left(\frac{b}{r}\right)^2\left(\frac{r^2+a^2}{b^2-a^2}\right)\log\frac{b}{a}-\log\frac{r}{a}-1\right] \tag{14.91}$$

and it easily verified that equations. (14.10) do indeed give the same result. We now turn to the determination of $\sigma_{rr}^{(1)},\sigma_{\theta\theta}^{(1)}$. It is obvious that identical expressions will be found for F_1,G_1; we shall therefore deal in detail with only the former. For n = 1 the solution of (14.73) is:

$$f_1(r)=C_1\left(\frac{r}{a}\right)+C_2\left(\frac{a}{r}\right)+C_3\left(\frac{r}{a}\right)^3+C_4\left(\frac{r}{a}\right)\log\left(\frac{r}{a}\right) \tag{14.92}$$

and the stress components corresponding to it are

$$\sigma_{rr}^{(1)}=\frac{1}{r}\frac{\partial\varphi}{\partial r}+\frac{1}{r^2}\frac{\partial^2\varphi}{\partial\theta^2}=\left(\frac{1}{r}\frac{d\,f_1}{dr}-\frac{f_1}{r^2}\right)\cos\theta=\left(-\frac{2a\,C_2}{r^3}+\frac{2r\,C_3}{a^3}+\frac{C_4}{a\,r}\right)\cos\theta$$
$$\sigma_{\theta\theta}^{(1)}=\frac{\partial^2\varphi}{\partial r^2}=\frac{d^2 f_1}{dr^2}\cos\theta=\left(\frac{2a\,C_2}{r^3}+\frac{6r\,C_3}{a^3}+\frac{C_4}{a\,r}\right)\cos\theta \tag{14.93}$$
$$\tau_{r\theta}^{(1)}=-\frac{\partial}{\partial r}\left(\frac{1}{r}\frac{\partial\varphi}{\partial\theta}\right)=\frac{d}{dr}\left(\frac{f_1}{r}\right)\sin\theta=\left(-\frac{2a\,C_2}{r^3}+\frac{2r\,C_3}{a^3}+\frac{C_4}{a\,r}\right)\sin\theta$$

The five constants C_1,C_2,C_3,C_4,a_1 are found from equations. (14.74) to (14.76). The function $T^{(1)}$ has the form:

$$T^{(1)}(r,\theta)=\left(\frac{A_0}{r}+A_1 r\right)\cos\theta+\left(\frac{B_0}{r}+B_1 r\right)\sin\theta \tag{14.94}$$

Where the coefficient of $\cos\theta$ (that is, F_1) has been found so as to satisfy eq. (14.71) with n = 1 and similarly for the coefficient of $\sin\theta$ (namely G_1). The terms proportional to A_1 and B_1, however, cause no stress. The final expressions for the stresses are:

$$\sigma_{rr}^{(1)}=\frac{\alpha_1 E_1 r}{2\left(a^2+b^2\right)}\left(1-\frac{a^2}{r^2}\right)\left(1-\frac{b^2}{r^2}\right)\left(A_0\cos\theta+B_0\sin\theta\right)$$
$$\sigma_{\theta\theta}^{(1)}=\frac{\alpha_1 E_1 r}{2\left(a^2+b^2\right)}\left(3-\frac{a^2+b^2}{r^2}-\frac{a^2b^2}{r^4}\right)\left(A_0\cos\theta+B_0\sin\theta\right) \tag{14.95}$$
$$\tau_{r\theta}^{(1)}=\frac{\alpha_1 E_1 r}{2\left(a^2+b^2\right)}\left(1-\frac{a^2}{r^2}\right)\left(1-\frac{b^2}{r^2}\right)\left(A_0\sin\theta-B_0\cos\theta\right)$$

Since the constants C_2,C_3,C_4 are as follows (for the A_0 term):

$$C_2=-\frac{\alpha_1 E_1 A_0 b^2 a}{4\left(b^2+a^2\right)};\ C_3=\frac{\alpha_1 E_1 A_0 a^3}{4\left(b^2+a^2\right)};\ C_4=-\frac{\alpha_1 E_1 A_0 a}{2}; \tag{14.96}$$

Also, note that, the stress component $\sigma_{zz}^{(1)}$ is given by:

$$\sigma_{zz}^{(1)}=\frac{\nu\,\alpha_1 E_1 r}{a^2+b^2}\left(2-\frac{a^2+b^2}{r^2}\right)\left(A_0\cos\theta+B_0\sin\theta\right)-\frac{\alpha_1 E_1 T}{1+\nu_1} \tag{14.97}$$

for the present plane-strain problem.

14.7 Hollow cylinder under axial-symmetric mechanical and thermal loads

It is well known that the thermo-elastic equilibrium problem, for homogeneous and linearly isotropic materials, is ruled by the Duhamel-Neumann thermal equations, that in absence of body forces, in Cartesian Coordinate System (x,y,z) is given by :

$$\mu\nabla\cdot(\nabla\otimes\mathbf{u})+(\mu+\lambda)\nabla(\nabla\cdot\mathbf{u})-(3\lambda+2\mu)\alpha\nabla T=0 \tag{14.98}$$

where $\mathbf{u}^T=\left[u_x,u_y,u_z\right]$ is the displacement field, T is temperature, μ,λ are Lamè constants and α is the linear thermal expansion coefficient. The differential operators appearing in equation (14.98) are the Nabla operator ∇, the divergence $\nabla\cdot(*)=\partial/\partial x+\partial/\partial y+\partial/\partial z$, and the gradient $\nabla\otimes(*)$.

Conduction equation is written in hypothesis of steady-state problem:

$$\nabla^2T=T_{,rr}+r^{-1}T_{,r}+r^{-2}T_{,\theta\theta}+T_{,zz}=0 \tag{14.99}$$

where ∇^2 is the Laplacian differential operator. In order to study the multilayered cylinders, it is considered the cylindrical reference system (O,r,θ,z), selected with its origin O as the same of the Cartesian one. The coordinate θ is measured starting from axis x and it is positive if anti-clockwise. The axis of cylinder solid coincide with z direction of cylindrical reference system selected. It is worth to note that throughout the whole paper no external constraints acting on the multilayered cylinder will be considered. The cylindrical coordinates (r,θ,z) are related to the rectangular coordinates (x,y,z) according to the transformation:

$$x=r\cos\theta,\quad y=r\sin\theta,\quad z=z \tag{14.100}$$

where the domain Ω occupied by multilayered cylinder, is defined as $0<r\le R,\quad 0\le\vartheta\le 2\pi,\quad 0\le z\le L$. The displacement vector $\mathbf{u}$ in the rectangular system has components $\mathbf{u}^{cart}=\left[u_x,u_y,u_z\right]^T$, and in the cylindrical system has components: $\mathbf{u}^{cyl}=\left[u_r,u_\theta,u_z\right]^T$.The transformation of vector $\mathbf{u}$ between the two coordinate systems is given by:

$$u_x=u_r\cos\theta-u_\theta\sin\theta,\quad u_y=u_r\sin\theta+u_\theta\cos\theta,\quad u_z=u_z \tag{14.101}$$

The Duhamel-Neumann thermal equations (14.98) in the cylindrical coordinate system become:

$$\begin{cases}\mu\left[\nabla^2u_r-\left(2u_{\theta,\theta}+u_r\right)r^{-2}\right]+(\mu+\lambda)\left(\nabla\cdot\mathbf{u}\right)_{,r}-(3\lambda+2\mu)\alpha T_{,r}=0\\ \mu\left[\nabla^2u_\theta+\left(2u_{r,\theta}-u_\theta\right)r^{-2}\right]+(\mu+\lambda)r^{-1}\left(\nabla\cdot\mathbf{u}\right)_{,\theta}-(3\lambda+2\mu)\alpha r^{-1}T_{,\theta}=0\\ \mu\nabla^2u_z+(\mu+\lambda)\left(\nabla\cdot\mathbf{u}\right)_{,z}-(3\lambda+2\mu)\alpha T_{,z}=0\end{cases} \tag{14.102}$$

In compact form the equations (14.102) can be written as follows:

$$(2\mu+\lambda)\nabla(\nabla\cdot\mathbf{u})-\mu\nabla\wedge(\nabla\wedge\mathbf{u})-(3\lambda+2\mu)\alpha\nabla T \tag{14.103}$$

where $\nabla\wedge(*)$ is curl differential operator. The solution of equations (14.102) is taken in the form:

$$u_r=u_r^{(h)}+u_r^{(p)},\quad u_\theta=u_\theta^{(h)}+u_\theta^{(p)},\quad u_z=u_z^{(h)}+u_z^{(p)}, \tag{14.104}$$

where $\mathbf{u}^{(h)}\equiv\left[u_r^{(h)},u_\theta^{(h)},u_z^{(h)}\right]$ is the general solution, $\mathbf{u}^{(p)}\equiv\left[u_r^{(p)},u_\theta^{(p)},u_z^{(p)}\right]$ is a particular solution.

By assuming, a particular solution $\mathbf{u}^{(p)}$ as follows:

$$\left[u_r^{(p)},u_\theta^{(p)},u_z^{(p)}\right]^T=\nabla G \tag{14.105}$$

where G is a scalar function. By substituting the equation (14.105) in equation (14.103), and remembering that $\nabla\wedge\nabla G=\mathbf{0}$, we obtain the Poisson's equation for the function G:

$$\nabla^2G=\alpha\left(\frac{3\lambda+2\mu}{\lambda+2\mu}\right)T \tag{14.106}$$

By substituting the equation (14.106) in Fourier's equation (14.99), the bi-harmonic condition for the scalar function G is obtained:

$$\nabla^2\left(\nabla^2G\right)=\nabla^4G=0 \tag{14.107}$$

By considering axial-symmetry of thermal loads, in explicit the equation (14.107) becomes:

$$\nabla^4 G = G_{,rrrr} + 2r^{-1}\left[G_{,rrr} + G_{,rzz}\right] - r^{-2}G_{,rr} + r^{-3}G_{,r} + 2G_{,rrzz} + G_{,zzzz} = 0 \tag{14.108}$$

In three-dimensional elasticity, the general solution $\mathbf{u}^{(h)}$ is obtained by to define a potential function representation for displacement which identically satisfies the compatibility conditions and allows to obtaining the equilibrium condition defining the governing equation. It is well known that the solution in terms of displacement field **u** for an isotropic and homogeneous linear elastic material, in absence of body forces, can be written in the cylindrical system by means of the *Boussinesq-Somigliana-Galerkin* vector $\mathbf{F} \equiv \left[F_r, F_\theta, F_z\right]^T$, where three component of vector **F** are function of cylindrical coordinates (r,θ,z) as:

$$\begin{cases} u_r^{(h)} = \dfrac{2\mu+\lambda}{2\mu(\mu+\lambda)}\left[\cos\theta\cdot\nabla^2 F_x + \sin\theta\cdot\nabla^2 F_y\right] - \dfrac{1}{2\mu}\omega_{,r} \\ u_\theta^{(h)} = \dfrac{2\mu+\lambda}{2\mu(\mu+\lambda)}\left[-\sin\theta\cdot\nabla^2 F_x + \cos\theta\cdot\nabla^2 F_y\right] - \dfrac{1}{2\mu r}\omega_{,\theta} \\ u_z^{(h)} = \dfrac{2\mu+\lambda}{2\mu(\mu+\lambda)}\nabla^2 F_z - \dfrac{1}{2\mu}\omega_{,z} \end{cases} \tag{14.109}$$

where F_x, F_y, F_z are components of Galerkin's vector **F** in Cartesian coordinate and are given by:

$$F_x = F_r\cos\theta - F_\theta\sin\theta, \quad F_y = F_r\sin\theta + F_\theta\cos\theta, \tag{14.110}$$

and the function ω is given by:

$$\omega = \cos\theta\cdot F_{x,r} - \sin\theta\cdot r^{-1}F_{x,\theta} + \sin\theta\cdot F_{y,r} + \cos\theta\cdot r^{-1}F_{y,\theta} + F_{z,z} \tag{14.111}$$

The Galerkin's vector **F** must be to satisfy the bi-harmonic condition $\nabla^4\mathbf{F} = 0$. In Cartesian coordinate system the components of Galerkin's vector **F** are bi-harmonic, but in cylindrical coordinate system the two components F_r, F_θ are not bi-harmonic. A more detailed derivation [19] is given by Westergaard, who gives expressions for the stress components in terms of **F** and uses this representation to solve a number of classical three-dimensional problems – namely those involving concentrated forces in the infinite or semi-infinite body. The Galerkin's solution was to some extent foreshadowed by Love [15], who introduced a displacement function appropriate for an axis-symmetrical state of stress in a solid of revolution. When a solid cylinder is deformed symmetrically by forces applied on its external cylindrical surface and on its two end sections, it is possible to express all the mechanical quantities in terms of a single function, reducing the elastic equilibrium equations of the body to a single partial differential equation [18].

If $\mathbf{e}_z$ is the unit vector of z direction which characterizes the axis-symmetrical problem, the displacement solution is called torsion-less and rotationally symmetric with respect to the z axis. Then, displacement solution **u** satisfies the following condition:

$$\mathbf{e}_z \cdot \nabla \wedge \mathbf{u}^{(h)} = 0 \tag{14.112}$$

In order to satisfy the condition (14.112), it is assumed the Galerkin's vector as reported below:

$$\mathbf{F} \equiv \left[0, 0, \chi(r,z)\right]^T \tag{14.113}$$

in which $\chi(\mathrm{r},\mathrm{z}) \in \mathrm{C}^{(4)}(\Omega)$ is a scalar function and is called the *Love*'s solution. By substituting equation (14.113) in equation (14.109) , it is possible to determine the displacement solution in terms of *Love*'s solution as reported below:

$$u_r^{(h)} = -\frac{1}{2\mu}\chi_{,rz}, \quad u_\theta^{(h)} = 0, \quad u_z^{(h)} = \frac{1}{2\mu}\left[\frac{\mu}{\mu+\lambda}\nabla^2\chi + \chi_{,rr} + r^{-1}\chi_{,r}\right] \tag{14.114}$$

In which $\chi(r,z)$ is the bi-harmonic function and then satisfy the follows differential equation:

$$\nabla^4\chi = \chi_{,rrrr} + 2r^{-1}\left[\chi_{,rrr} + \chi_{,rzz}\right] - r^{-2}\chi_{,rr} + r^{-3}\chi_{,r} + 2\chi_{,rrzz} + \chi_{,zzzz} = 0, \tag{14.115}$$

The vector $\nabla \wedge \mathbf{u}^{(h)}$ is given by:

$$\nabla \wedge \mathbf{u}^{(h)} = \begin{bmatrix} r^{-1}u_{z,\theta}^{(h)} - u_{\theta,z}^{(h)} \\ u_{r,z}^{(h)} - u_{z,r}^{(h)} \\ r^{-1}\left(u_{\theta}^{(h)} - u_{r,\theta}^{(h)}\right) + u_{\theta,r}^{(h)} \end{bmatrix} = \begin{bmatrix} 0 \\ -\dfrac{2\mu+\lambda}{2\mu(\mu+\lambda)}\left(\nabla^2\chi\right)_{,r} \\ 0 \end{bmatrix} \tag{14.116}$$

Then, the curl of vector $\mathbf{u}^{(h)}$ obtained by equation (14.116) satisfies the condition (14.112).
By summarizing, the thermo-elastic steady-state problem, under axial-symmetric load conditions, is governed by two bi-harmonic scalar functions $\chi(r,z)$ and $G(r,z)$. The temperature and the vector displacement, are given by:

$$\begin{cases} T = \dfrac{2\mu+\lambda}{\alpha(3\lambda+2\mu)}\nabla^2 G \\ u_r = G_{,r} - \dfrac{1}{2\mu}\chi_{,rz}, \quad u_\theta = 0, \quad u_z = G_{,z} + \dfrac{1}{2\mu}\left[\dfrac{\mu}{\mu+\lambda}\nabla^2\chi + \chi_{,rr} + r^{-1}\chi_{,r}\right] \end{cases} \tag{14.117}$$

By differentiating displacement's components (14.117), it is possible to obtain the strain components reported below:

$$\begin{aligned} &\varepsilon_{rr} = u_{r,r} = G_{,rr} - \frac{\chi_{,rrz}}{2\mu}, \ \varepsilon_{\theta\theta} = \frac{u_r}{r} = \frac{1}{r}\left(G_{,r} - \frac{\chi_{,rz}}{2\mu}\right), \\ &\varepsilon_{zz} = u_{z,z} = G_{,zz} + \frac{(2\mu+\lambda)\nabla^2\chi_{,z}}{2\mu(\mu+\lambda)} - \frac{\chi_{,zzz}}{2\mu}, \\ &\gamma_{rz} = u_{r,z} + u_{z,r} = 2G_{,rz} + \frac{(2\mu+\lambda)\nabla^2\chi_{,r}}{2\mu(\mu+\lambda)} - \frac{\chi_{,rzz}}{\mu}, \ \gamma_{\theta z} = \gamma_{r\theta} = 0 \end{aligned} \tag{14.118}$$

The stress-strain relations are given by well known Hooke's law for thermo-isotropic material:

$$\sigma_{kh} = 2\mu\varepsilon_{hk} + \delta_{hk}\left[\lambda\left(\varepsilon_{rr}+\varepsilon_{\theta\theta}+\varepsilon_{zz}\right) - \alpha(3\lambda+2\mu)(T-T_R)\right] \qquad \forall h,k \in \{r,\theta,z\} \tag{14.119}$$

where T_R is the reference temperature and δ_{hk} is the Kronecker's delta. By applying the equations (14.119) it is easy to obtain for the i-th material phase the no-vanishing stresses that depend by two scalar functions $\chi(r,z)$ and $G(r,z)$:

$$\begin{aligned} &\sigma_{rr} = \left[\frac{\lambda\nabla^2\chi}{2(\mu+\lambda)} - \chi_{,rr}\right]_{,z} - 2\mu\left(\nabla^2 G - G_{,rr}\right) + \alpha(3\lambda+2\mu)T_R, \\ &\sigma_{\theta\theta} = \left[\frac{\lambda\nabla^2\chi}{2(\mu+\lambda)} - r^{-1}\chi_{,r}\right]_{,z} - 2\mu\left(\nabla^2 G - r^{-1}G_{,r}\right) + \alpha(3\lambda+2\mu)T_R, \\ &\sigma_{zz} = \left[\frac{(4\mu+3\lambda)\nabla^2\chi}{2(\mu+\lambda)} - \chi_{,zz}\right]_{,z} - 2\mu\left(\nabla^2 G - G_{,zz}\right) + \alpha(3\lambda+2\mu)T_R, \\ &\tau_{rz} = \left[\frac{(2\mu+\lambda)\nabla^2\chi}{2(\mu+\lambda)} - \chi_{,zz}\right]_{,r} + 2\mu G_{,rz}, \qquad \tau_{\theta z} = \tau_{r\theta} = 0 \end{aligned} \tag{14.120}$$

14.8. Uncoupled thermo-elastic analysis in hollow cylinder exposed to an ambient at zero temperature through a uniform boundary conductance (plane strain)

Let us consider a hollow cylinder with inner radius "a" and outer radius "b" , subjected to radial temperature variation. The surface r = a is kept perfectly insulated while the surface r = b is exposed, for t >0, to an ambient at zero temperature through a uniform boundary conductance h. The initial temperature (for t = 0) of the hollow cylinder is $T_0 = T_R = const$ where $T_R > 0$. In this section, we determine the heat conduction and profile of temperature in hollow cylinder under

decreasing of temperature from $T_R > 0$ until to zero. The differential equation related to heat conduction and the corresponding boundary conditions are reported below:

$$\frac{\partial^2 T}{\partial r^2}+\frac{1}{r}\frac{\partial T}{\partial r}=\frac{1}{\kappa}\frac{\partial T}{\partial t};\quad a<r<b,\quad t>0 \tag{14.121}$$

$$-k\frac{\partial T}{\partial r}=0,\quad r=a,\ t>0, \tag{14.122}$$

$$-k\frac{\partial T}{\partial r}=hT;\quad r=b,\ t>0, \tag{14.123}$$

$$T=T_R;\quad a<r<b,\quad t=0, \tag{14.124}$$

where $T_0 = T_R$ is a suitable chosen reference temperature in initial condition (for t = 0) and h is convection coefficient on surface r=b . The problem is therefore on with homogeneous differential equation and boundary conditions and may be treated by the method separation of variables. A particular solution of the differential equation (14.121) and boundary conditions (14.122)-(14.123) is given by:

$$T(r,t)=\varphi(r)\,\psi(t) \tag{14.125}$$

By substituting the function (14.125) in eqs.(14.121)-(14.123), we obtain:

$$\frac{d^2\varphi}{dr^2}+\frac{1}{r}\frac{d\varphi}{dr}+\omega^2\varphi=0; \tag{14.126}$$

$$-k\frac{d\varphi}{dr}=0;\quad r=a, \tag{14.127}$$

$$-k\frac{d\varphi}{dr}=h\varphi;\quad x=b, \tag{14.128}$$

And to the following equation for $\psi(t)$:

$$\frac{d\psi}{dt}+\omega^2\kappa\psi=0 \tag{14.129}$$

The general solution of (14.129) is:

$$\psi(t)=e^{-\omega^2\kappa t} \tag{14.130}$$

The equation (14.126) is an Bessel differential equation and the solution is given by:

$$\varphi(r)=A\,J_0(\omega r)+B\,Y_0(\omega r) \tag{14.131}$$

where $J_0(\omega r), Y_0(\omega r)$ are *Bessel function* and A, B are constants integration. From (14.127) it is deduced that the constant B is given by:

$$B=-\frac{J_1(a\,\omega)}{Y_1(a\,\omega)}A \tag{14.132}$$

The equations (14.127) and (14.128) are an homogenous algebraic system as reported below :

$$[\Lambda]\cdot\begin{bmatrix}A\\B\end{bmatrix}=\begin{bmatrix}0\\0\end{bmatrix} \tag{14.133}$$

where the matrix $[\Lambda]$ is given by:

$$[\Lambda]=\begin{bmatrix}\omega a^2 J_1(\omega a) & \omega a^2 Y_1(\omega a)\\ b^2\left[k\omega J_1(\omega b)-hJ_0(\omega b)\right] & b^2\left[k\omega Y_1(\omega b)-hY_0(\omega b)\right]\end{bmatrix} \tag{14.134}$$

The algebraic system (14.133) admit not trivial solution if the determinant of the matrix $[\Lambda]$ is equal to zero. By imposing this condition, we obtain the transcendental equation in unknown parameter ω:

$$\begin{aligned}\det[\mathbf{\Lambda}] = g(\omega) = a^2b^2\omega h\left[J_0(\omega b)Y_1(\omega a) - J_1(\omega a)Y_0(\omega b)\right] + \\ + a^2b^2\omega^2 k\left[J_1(\omega b)Y_1(\omega a) - J_1(\omega a)Y_1(\omega b)\right] = 0\end{aligned} \tag{14.135}$$

The roots of this transcendental equation (14.135) are an infinite number such, denoted here by ω_m, $m = 1,2,....N$ leading to eigenvalues or characteristic values $\lambda_m = -\omega_m^2$. The corresponding eigenfunctions or characteristic functions $\bar{\varphi}_m(r)$ are, as calculated above,

$$\bar{\varphi}_m(r) = \frac{\varphi_m(r)}{A_m} = \frac{Y_1(\omega_m a)J_0(\omega_m r) - J_1(\omega_m a)Y_0(\omega_m r)}{Y_1(\omega_m a)} \tag{14.136}$$

The solution to the problem may therefore be written in the form:

$$T(r,t) = \sum_{m=1}^{\infty} A_m \bar{\varphi}_m(r) e^{-\omega_m^2 \kappa t} \tag{14.137}$$

where the coefficients A_m are determined by applying the initial condition (14.124) that yields the following relationship:

$$A_m = \left[\int_0^{2\pi}\int_a^b T_R \bar{\varphi}_m(r)\, r\, dr d\theta\right] \Big/ \left[\int_0^{2\pi}\int_a^b \bar{\varphi}_m^2(r)\, r\, dr d\theta\right] \tag{14.138}$$

By calculating numerically the relationship (14.138) we obtain the constants A_m as function ω_m. The expression of function temperature $T(r,t)$ is given by substituting the constant A_m in equation (14.137). Although we are considering the case of plane strain and then by applying the equations reported in section 14.1, we obtain radial displacement function and stress function in hollow cylinder. The radial displacement function is given by :

$$u_r = -\frac{\alpha T_R(3\lambda+2\mu)r}{2(\lambda+\mu)} + \sum_{m=1}^{\infty}\left\{C_m r + \frac{D_m}{r} + \frac{\alpha(3\lambda+2\mu)}{\omega_m(\lambda+2\mu)}\left[A_m J_1(\omega_m r) + B_m Y_1(\omega_m r)\right]\right\} e^{-\omega_m^2\kappa t} \tag{14.139}$$

where the constants integration A_m, B_m are given by equations (14.138) and (14.132), respectively. The other displacement components are vanishing in hypothesis of plane strain and axial-symmetry. The constants C_m, D_m are determined by utilizing the boundary conditions given by equations(14.8) In explicit the expressions of constants C_m, D_m are given by:

$$\begin{aligned}C_m &= \frac{\alpha(3\lambda+2\mu)\mu b A_m}{(\lambda+2\mu)(\lambda+\mu)} \cdot \frac{\left[J_1(\omega_m b)Y_1(\omega_m a) - J_1(\omega_m a)Y_1(\omega_m b)\right]}{\omega_m(b^2-a^2)Y_1(a\omega_m)}, \\ D_m &= \frac{\alpha(3\lambda+2\mu)a^2 b A_m}{(\lambda+2\mu)} \cdot \frac{\left[J_1(\omega_m b)Y_1(\omega_m a) - J_1(\omega_m a)Y_1(\omega_m b)\right]}{\omega_m(b^2-a^2)Y_1(a\omega_m)},\end{aligned} \tag{14.140}$$

Radial, circumferential and axial stress components are given by:

$$\sigma_{rr} = 2\sum_{m=1}^{\infty}\left\{C_m(\lambda+\mu) - \frac{\mu D_m}{r^2} - \frac{\alpha\mu(3\lambda+2\mu)}{(\lambda+2\mu)\omega_m r}\left[A_m J_1(\omega_m r) + B_m Y_1(\omega_m r)\right]\right\} e^{-\omega_m^2\kappa t} \tag{14.141}$$

$$\begin{aligned}\sigma_{\theta\theta} = \sum_{m=1}^{\infty} 2\left[C_m(\lambda+\mu) + \frac{\mu D_m}{r^2}\right] e^{-\omega_m^2\kappa t} + \\ - 2\sum_{m=1}^{\infty}\frac{\alpha\mu(3\lambda+2\mu)}{(\lambda+2\mu)\omega_m r}\left\{A_m J_1(\omega_m r) + B_m Y_1(\omega_m r) - \omega_m r\left[A_m J_0(\omega_m r) + B_m Y_0(\omega_m r)\right]\right\} e^{-\omega_m^2\kappa t}\end{aligned} \tag{14.142}$$

$$\sigma_{zz} = \frac{\alpha T_R\,\mu(3\lambda+2\mu)}{\lambda+\mu} + 2\sum_{m=1}^{\infty}\left\{C_m\lambda - \frac{\alpha\mu(3\lambda+2\mu)}{(\lambda+2\mu)\omega_m r}\left[A_m J_0(\omega_m r) + B_m Y_0(\omega_m r)\right]\right\} e^{-\omega_m^2\kappa t} \tag{14.143}$$

It is important to note that component stress σ_{zz} assumes no-zero value for $t \to \infty$, but other stress components vanish. The axial force applied on bases of hollow cylinder is given by:

$$N_z = \int_0^{2\pi}\int_a^b \sigma_{zz} r dr d\theta = \pi\left(b^2 - a^2\right)\left[\frac{\alpha T_R \mu\left(3\lambda+2\mu\right)}{\mu+\lambda} + 2\lambda\sum_{m=1}^{\infty} C_m\, e^{-\omega_m^2 \kappa t}\right] +$$
$$+\frac{4\pi\alpha\mu\left(3\lambda+2\mu\right)}{\left(\lambda+2\mu\right)}\sum_{m=1}^{\infty}\left\{\frac{A_m}{\omega_m}\left[aJ_1\left(\omega_m a\right) - bJ_1\left(\omega_m b\right)\right] + \frac{B_m}{\omega_m}\left[aY_1\left(\omega_m a\right) - bY_1\left(\omega_m b\right)\right]\right\} e^{-\omega_m^2 \kappa t} \tag{14.144}$$

For example, let us consider, an hollow cylinder constituted by steel, under decreasing temperature. The geometrical, mechanical and thermal parameters considered for hollow cylinder are reported below:

$$E = 210\cdot 10^9\, N/m^2,\ \nu = 0.3,\ c_v = 440 J/kg\cdot °K,\ k = 45 W/m\cdot °K,$$
$$\rho = 7.8\cdot 10^3 kg/m^3, b = 1.05m,\ a = 1.00m,\ s = b - a = 0.05m, \tag{14.145}$$
$$h = 20 W/m^2\cdot °K,\quad \alpha = 1.2\cdot 10^{-5} °K^{-1},\ T_0 = T_R = 300°K$$

In this case the graphics function $g(\omega)$ given by equation (14.135) is reported below:

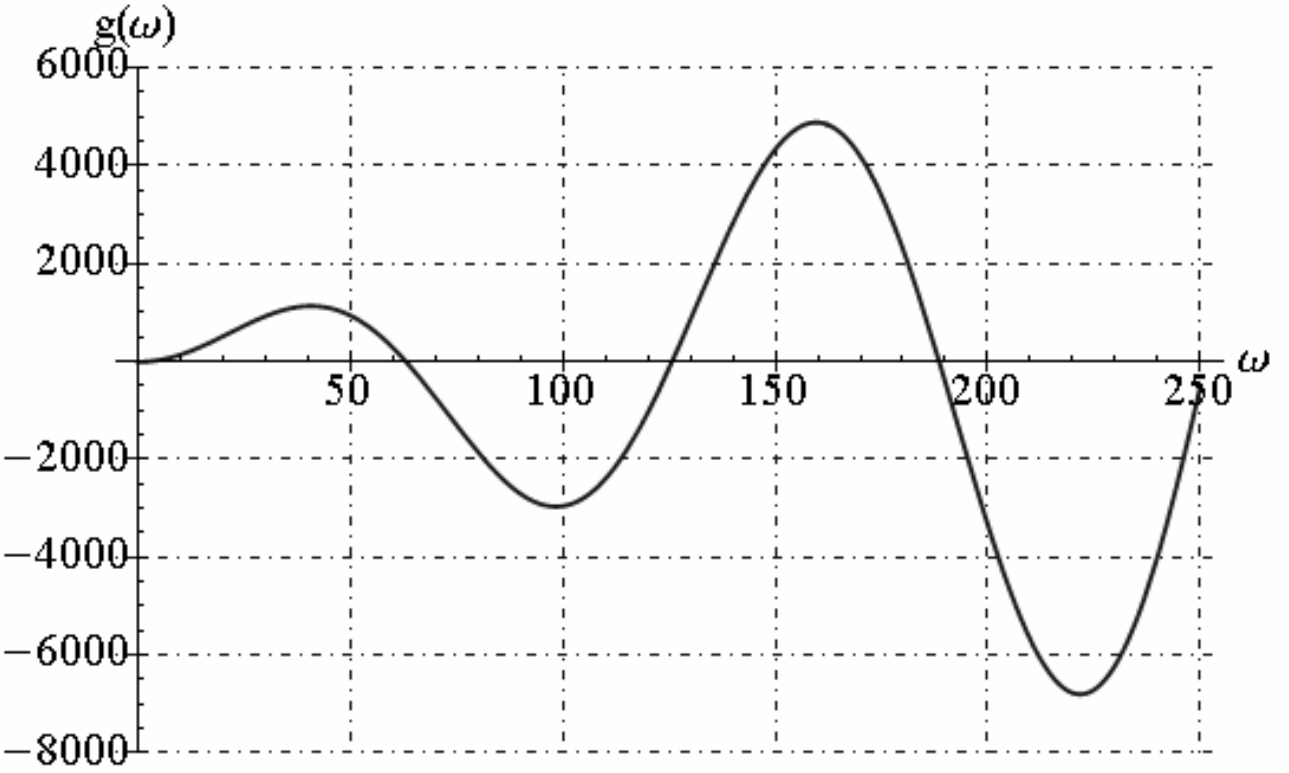

By fixed m= 20, the eigenvalues ω_m and corresponding values of constants integration A_m are reported in table 14.1:

ω_m	3.006	62.979	125.737	188.545	251.364
A_m	−464.16	−11.03	3.69	−1.96	1.26
ω_m	314.189	377.016	439.844	502.673	565.503
A_m	−0.896	0.678	−0.536	0.438	−0.366
ω_m	628.333	691.164	753.994	816.825	879.656
A_m	0.312	−0.270	0.237	−0.210	0.188
ω_m	942.488	1005.319	1068.150	1130.982	1193.813
A_m	−0.169	0.153	−0.140	0.128	−0.118

Table 14.1 – *Eigenvalues ω_m and corresponding values of constants integration A_m*

We reported the graphics of temperature function along the radial direction and in time:

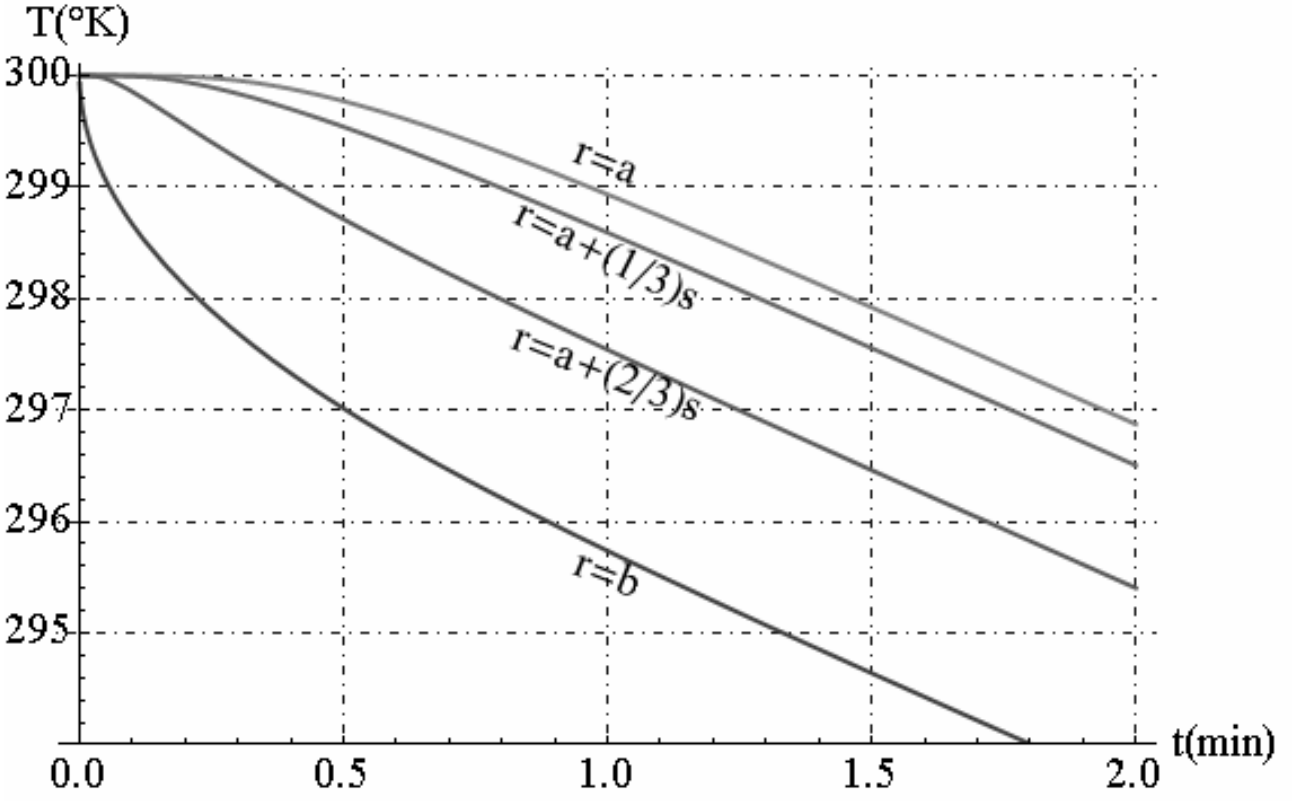

Fig. 14.12 - *Temperature function versus the time*

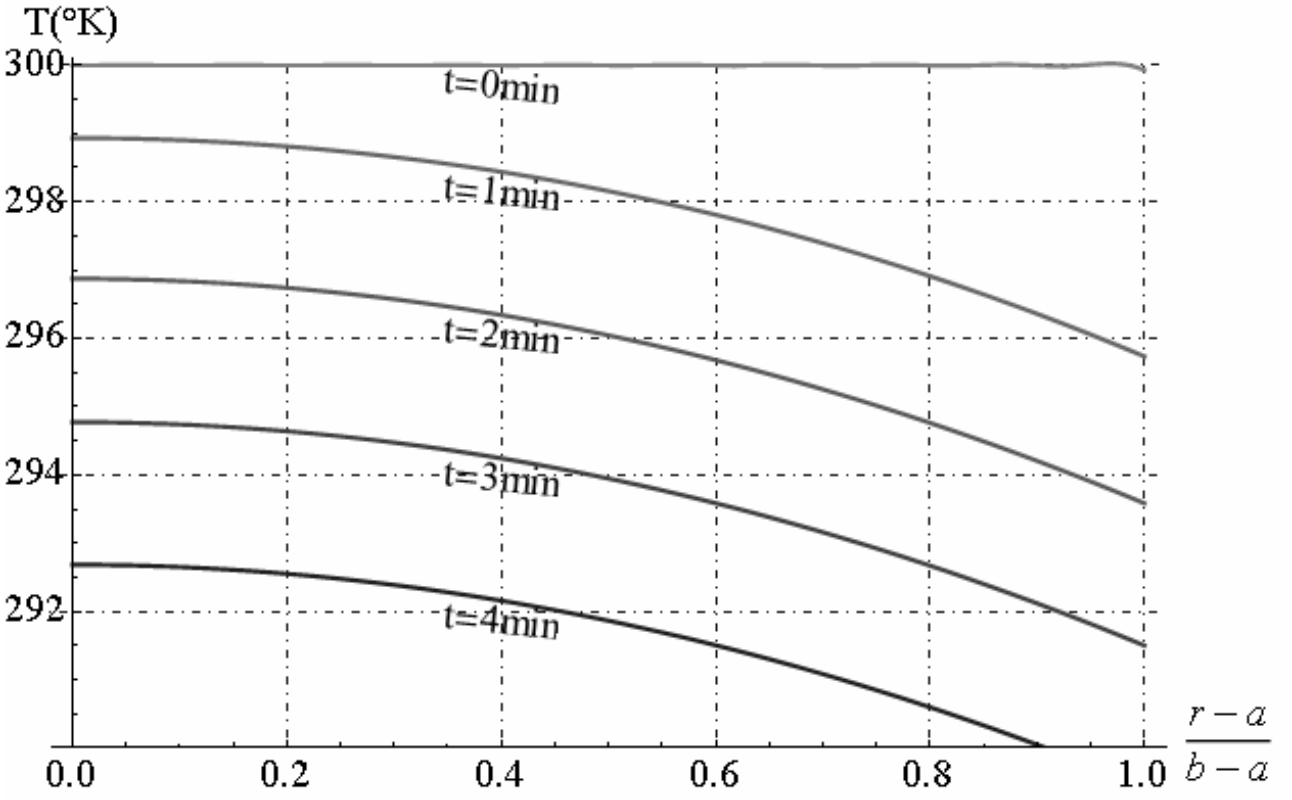

Fig. 14.13 - *Temperature function along radial direction*

We reported the graphic of radial displacement component function along the radial direction:

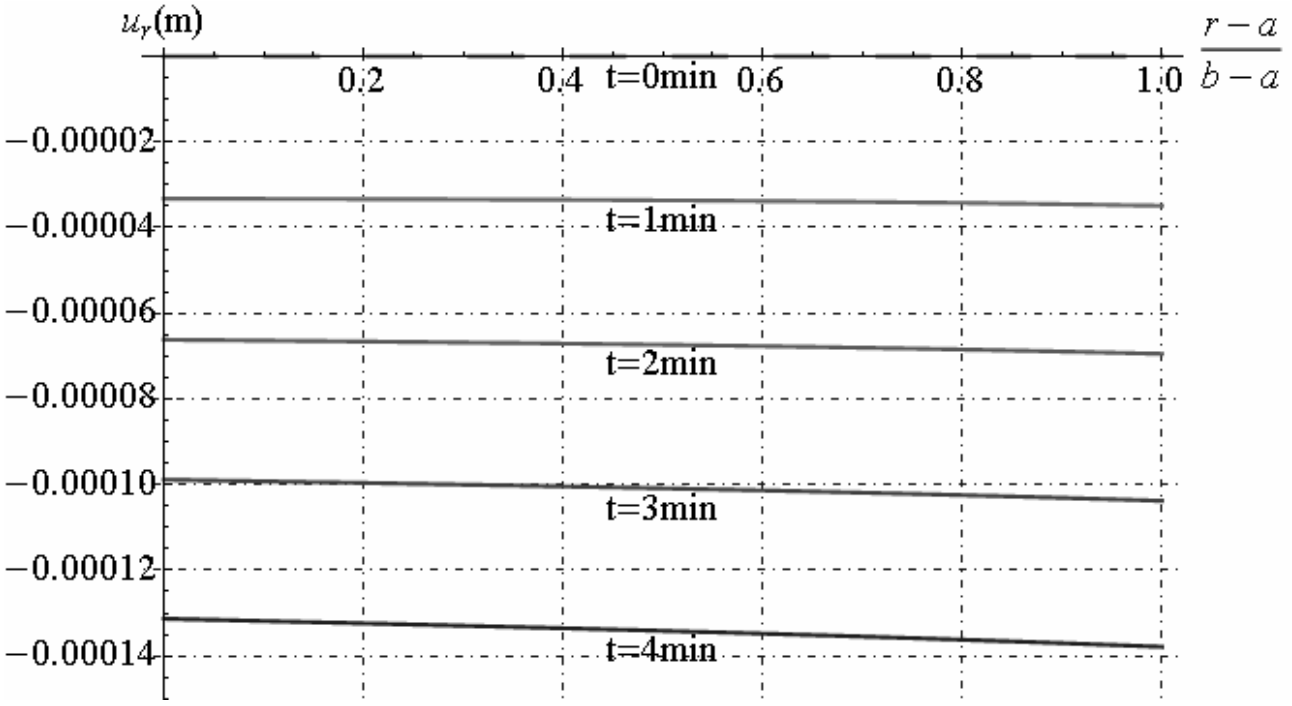

Fig. 14.14 - *Radial displacement distribution along radial direction*

We reported the graphics of stress components along the radial direction and in time:

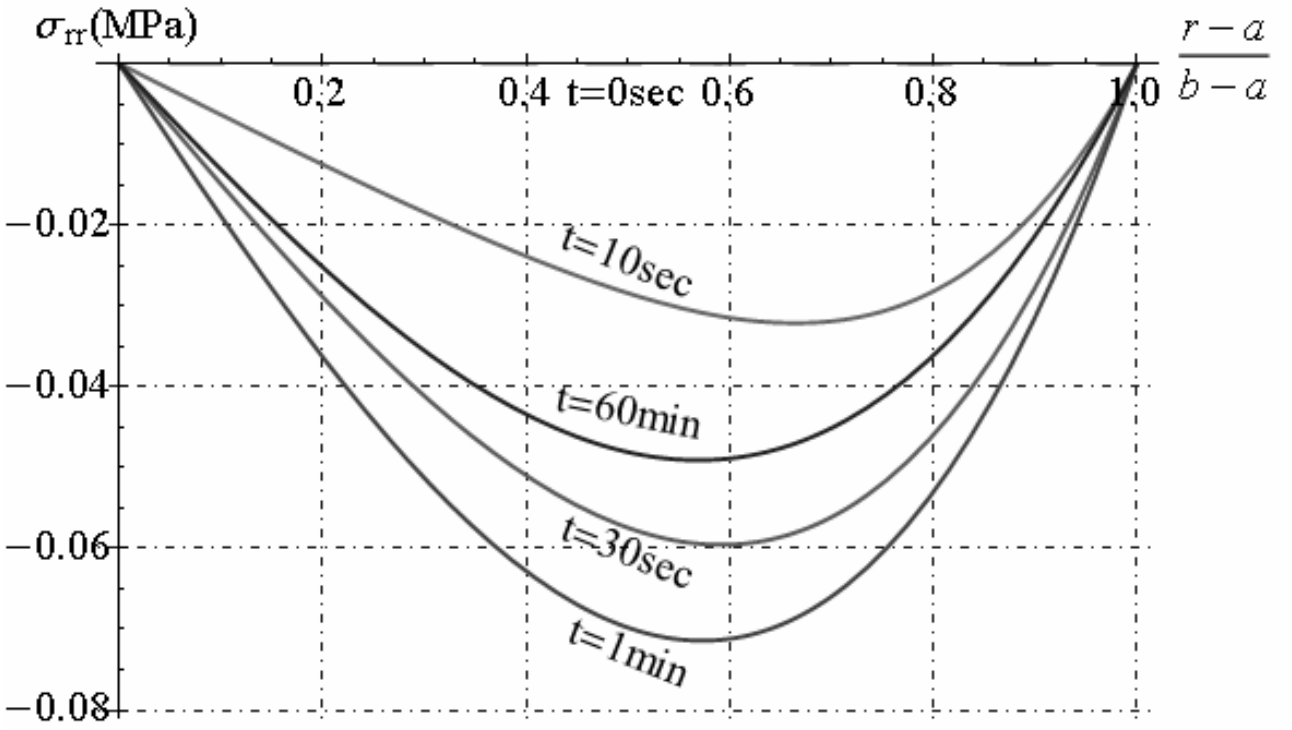

Fig. 14.15 - *Radial stress distribution along radial direction*

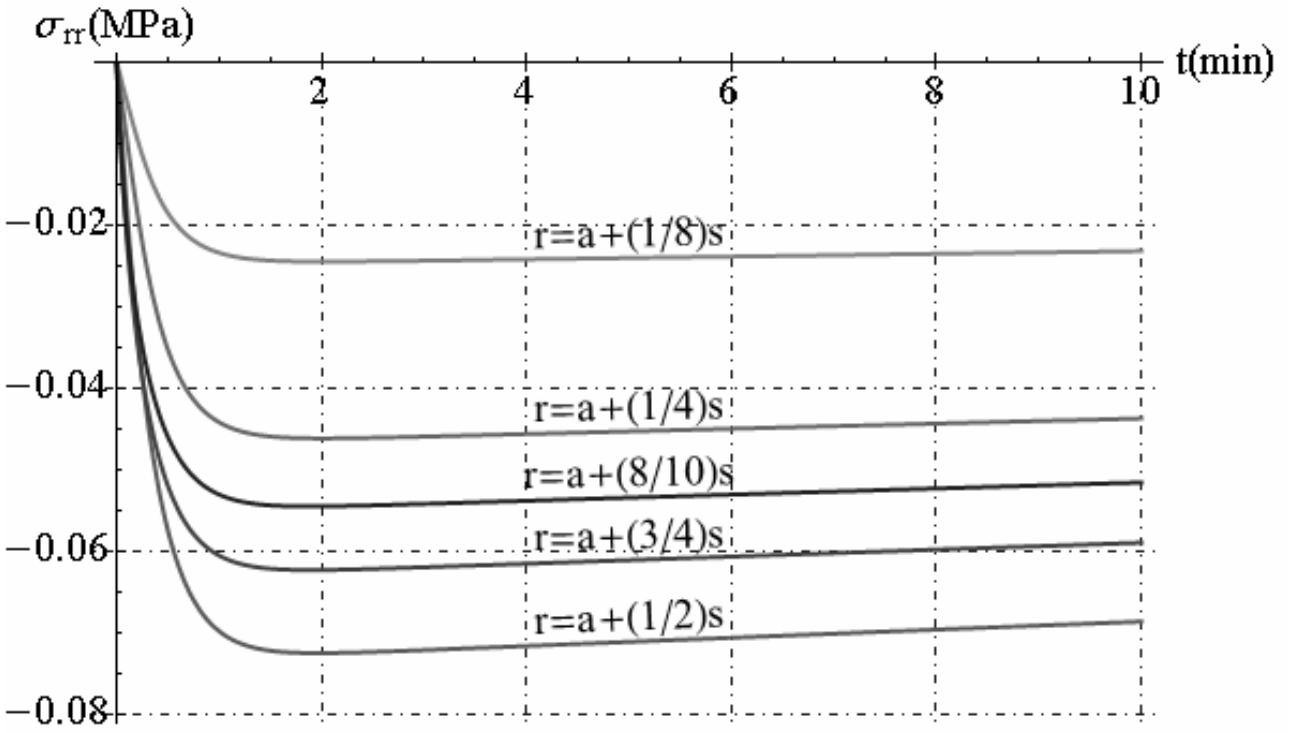

Fig. 14.16 - *Radial stress distribution in time*

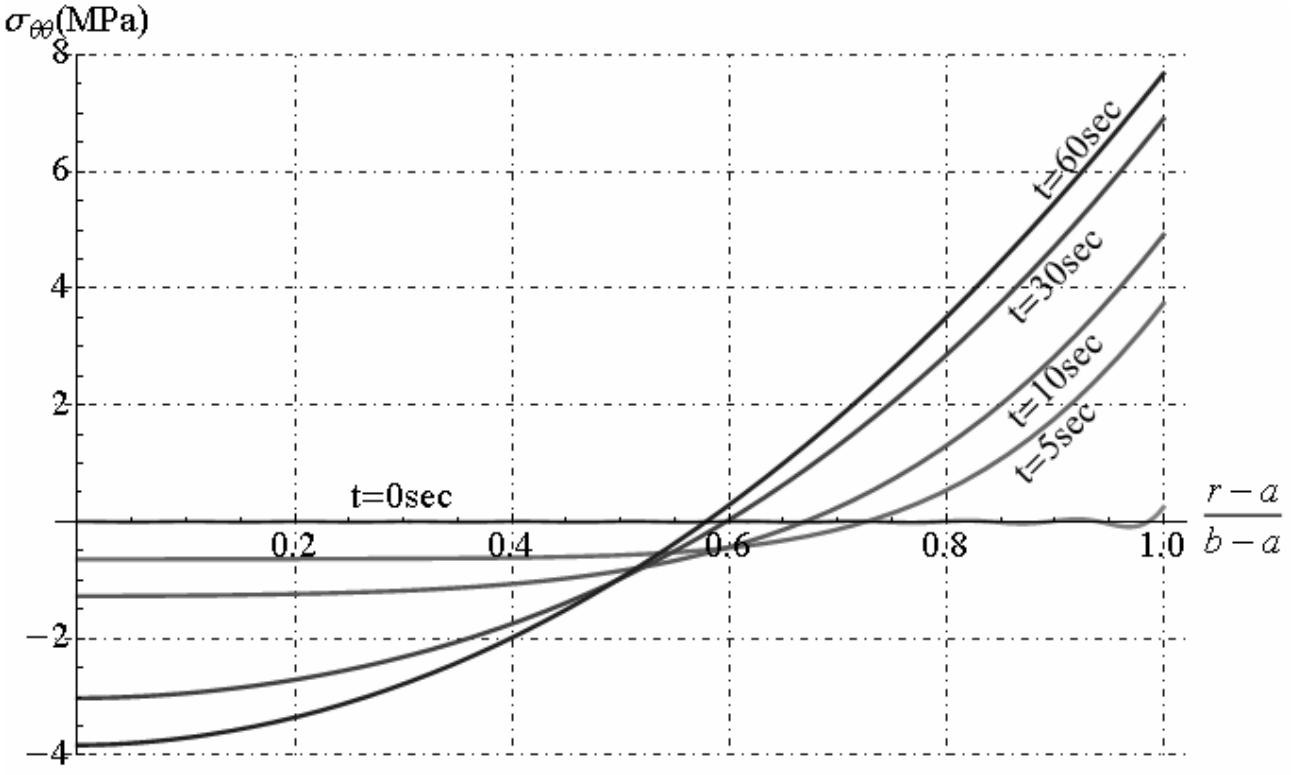

Fig. 14.17 - *Circumferential stress distribution along radial direction*

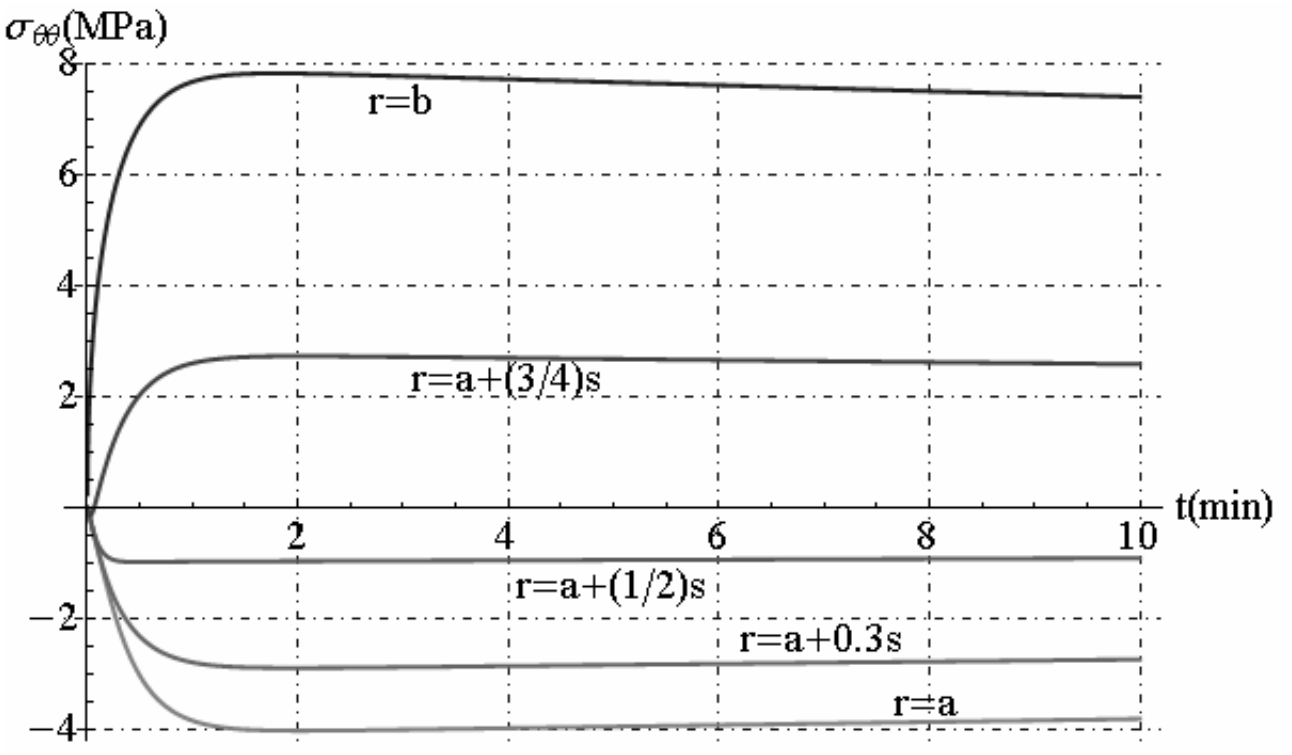

Fig. 14.18 - *Circumferential stress distribution in time*

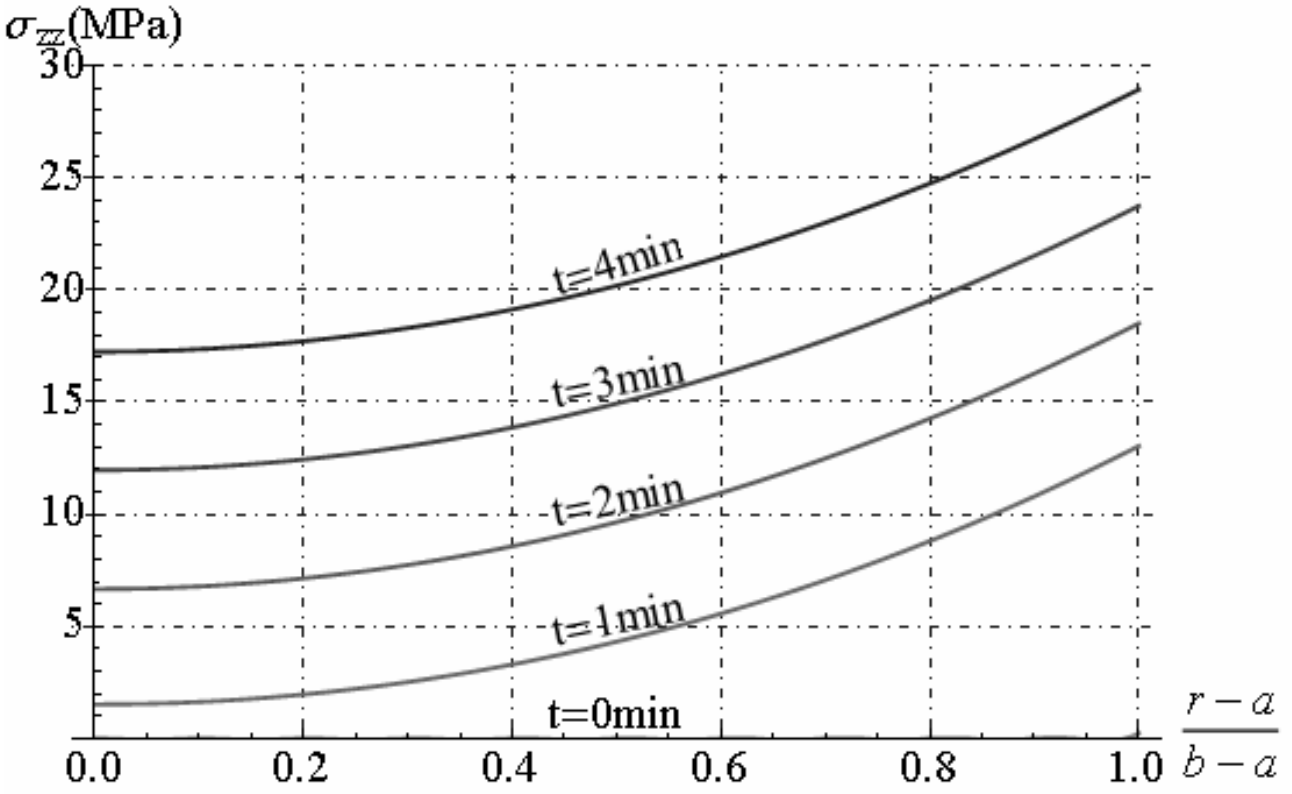

Fig. 14.19 - *Axial stress distribution along radial direction*

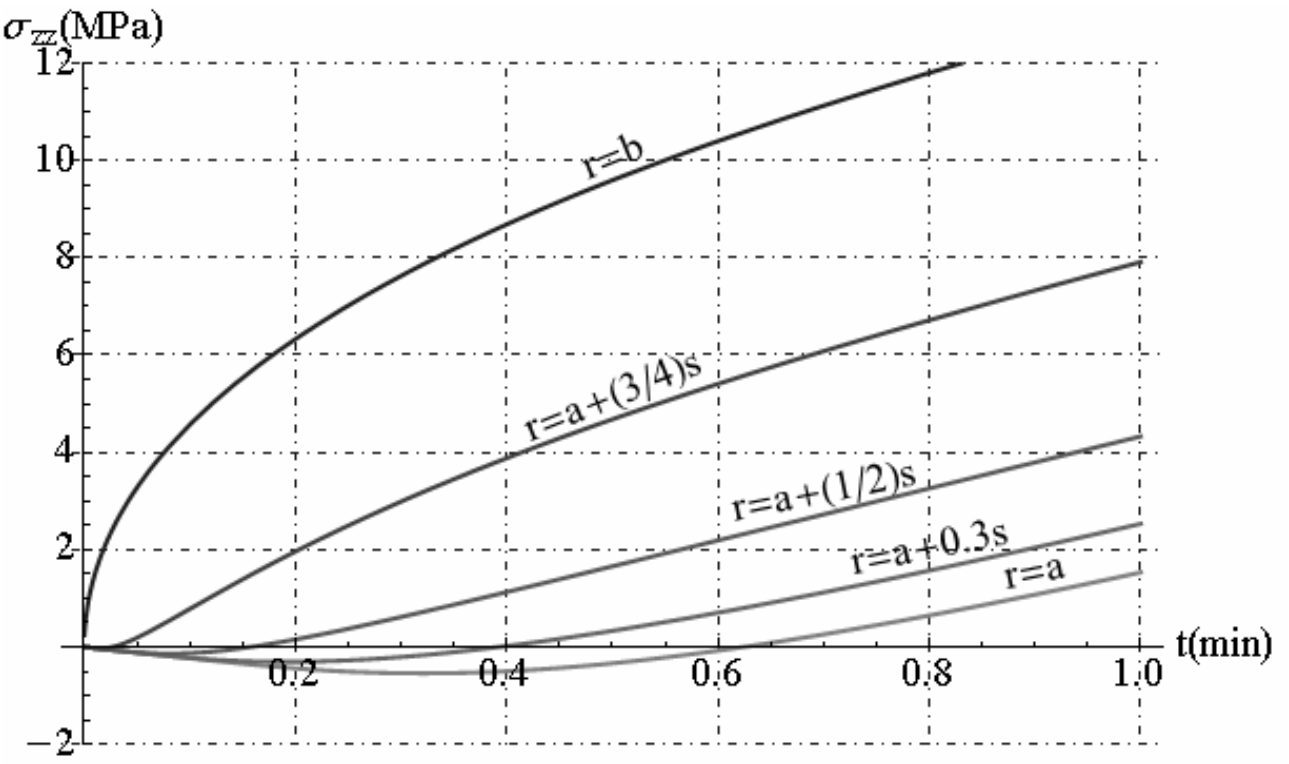

Fig. 14.20 - *Axial stress distribution in time*

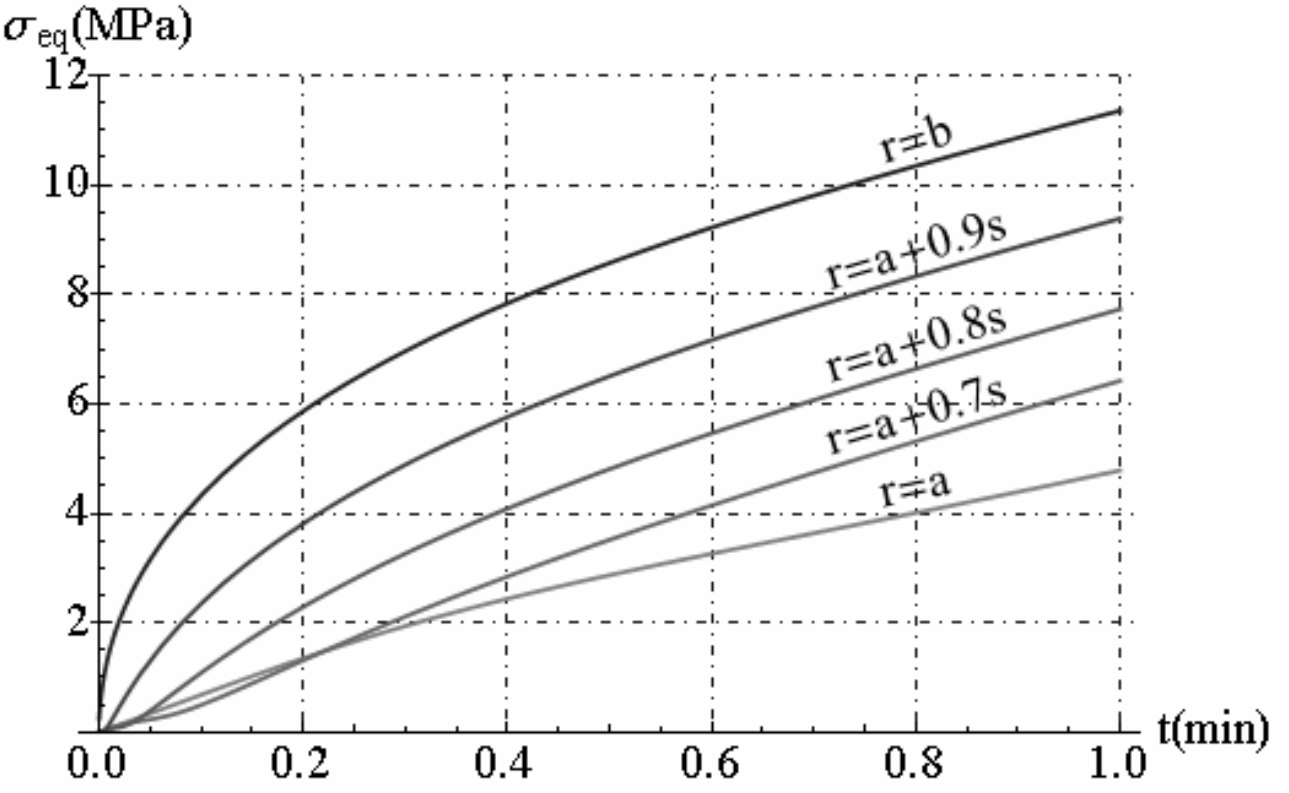

Fig. 14.21 - *Hencky von Mises's equivalent stress distribution along radial direction*

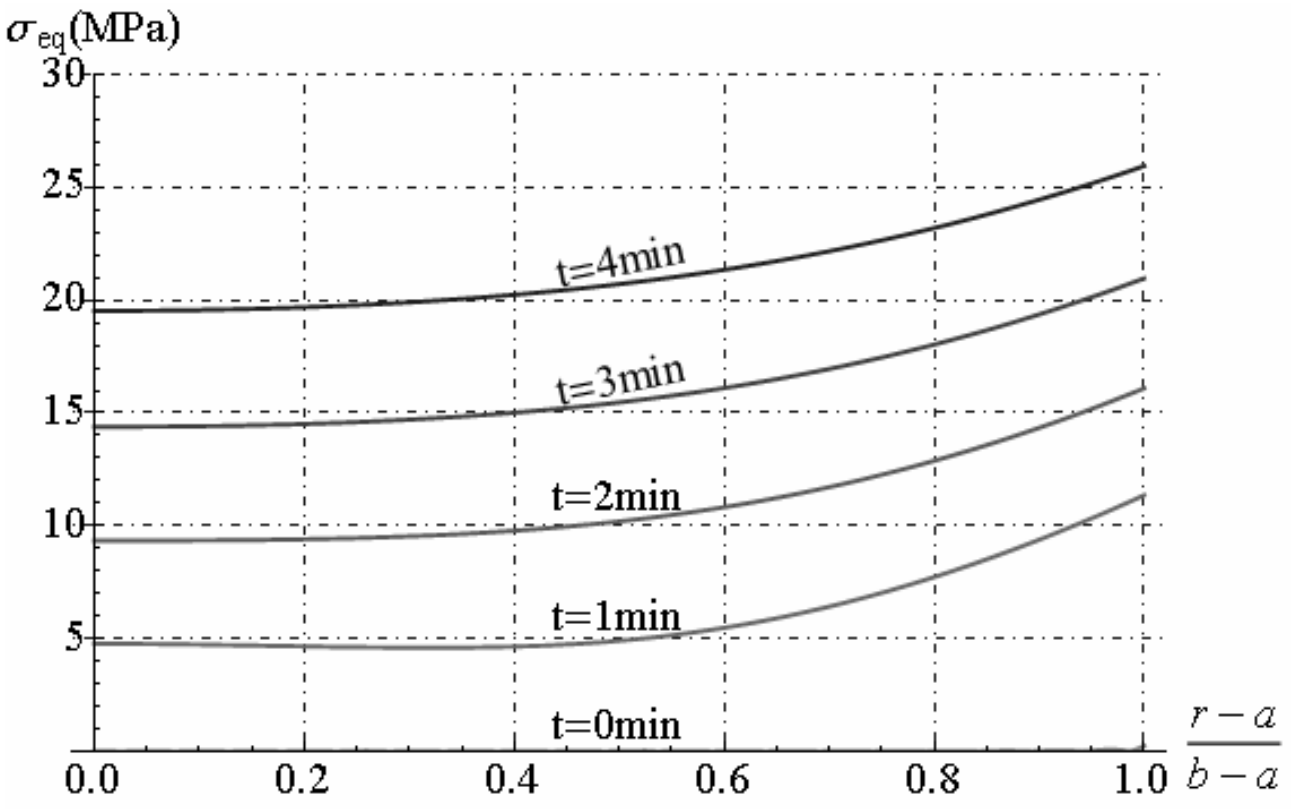

Fig. 14.22 - *Hencky von Mises's equivalent stress distribution in time*

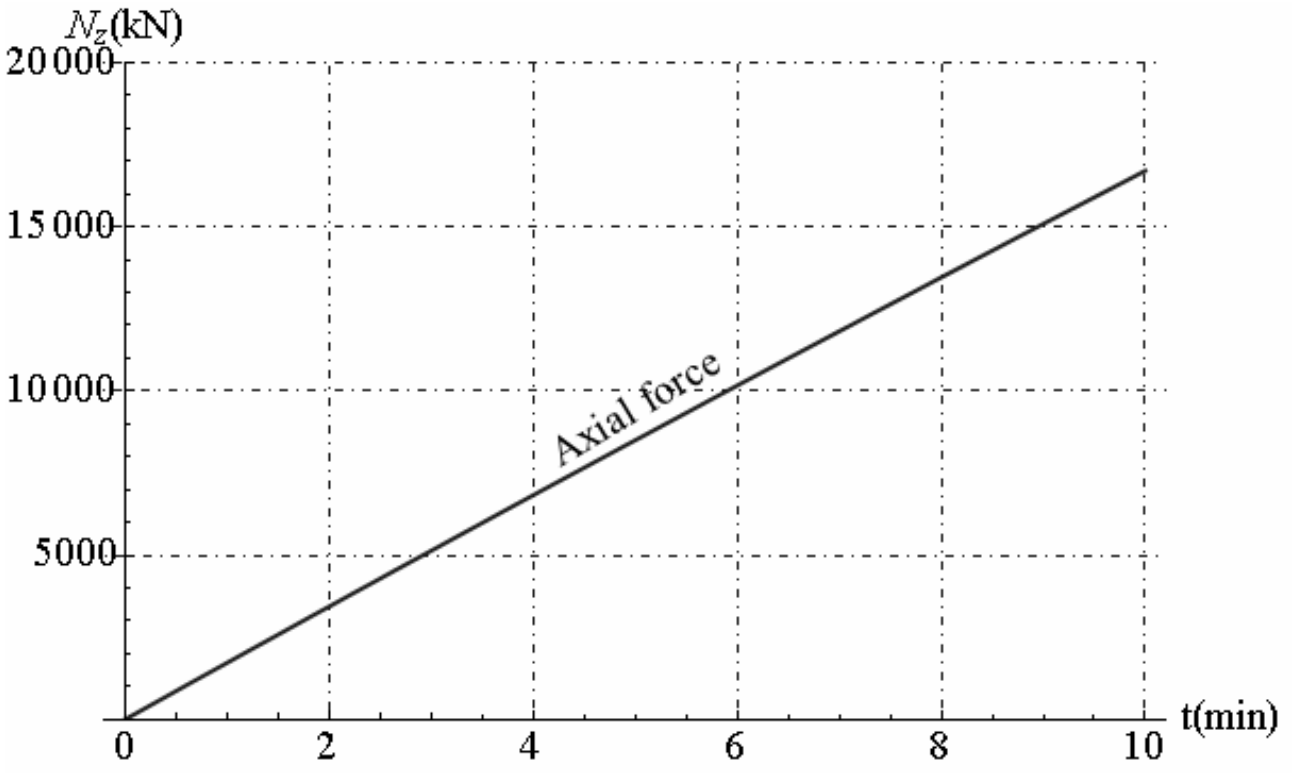

Fig. 14.23 - *Axial force applied on bases of hollow cylinder versus time*

14.9. Uncoupled thermo-elastic analysis in hollow cylinder exposed to uniform heat flux in plane strain

Let us consider a hollow cylinder with inner radius "a" and outer radius "b" , subjected to radial temperature variation. The surface r = a is kept perfectly insulated while the surface r = b is exposed, for t >0, to a constant, uniform heat input q_0. In this section, we determine the heat conduction and temperature profile in hollow cylinder subjected to uniform heat input q_0 applied on external surface, starting to initial temperature in solid equal to $T_0 = T_R = const$. The differential equation related to heat conduction and the corresponding boundary conditions are reported below:

$$\frac{\partial^2 T}{\partial r^2} + \frac{1}{r}\frac{\partial T}{\partial r} = \frac{1}{\kappa}\frac{\partial T}{\partial t}; \quad a < r < b, \quad t > 0 \tag{14.146}$$

$$-k\frac{\partial T}{\partial r} = 0, \quad r = a, \ t > 0, \tag{14.147}$$

$$-k\frac{\partial T}{\partial r} = q_0, \quad r = b, \ t > 0, \tag{14.148}$$

$$T = T_0; \quad a < r < b, \quad t = 0, \tag{14.149}$$

This is an case of a problem involving a non-homogeneous boundary condition and, in particular, with the heat input specified over the entire boundary surface. It is necessary writing the solution in the follows form (see Chapter VII) :

$$T(r,t) = T_0 + \xi t + T_S(r) + T_C(r,t) \tag{14.150}$$

where T_S satisfies the equations:

$$\frac{d^2 T_S}{d r^2} + \frac{1}{r}\frac{d T_S}{d r} = \frac{\xi}{\kappa}; \quad a < r < b, \tag{14.151}$$

$$-k\frac{d T_S}{d r} = 0; \quad r = a, \tag{14.152}$$

$$-k\frac{d T_S}{d r} = q_0; \quad r = b, \tag{14.153}$$

$$\int_V T_S(r)\,dV = \int_0^{2\pi}\int_a^b r\,T_S(r)\,dr d\theta = 0 \tag{14.154}$$

where ξ may be determined either from the boundary conditions (14.152)-(14.154). T_C satisfies equations:

$$\frac{\partial^2 T_C}{\partial r^2} + \frac{1}{r}\frac{\partial T_C}{\partial r} = \frac{1}{\kappa}\frac{\partial T_C}{\partial t}; \quad a < r < b, \quad t > 0 \tag{14.155}$$

$$-k\frac{\partial T_C}{\partial r} = 0; \quad r = a, \ t > 0, \tag{14.156}$$

$$-k\frac{\partial T_C}{\partial r} = 0; \quad r = b, \ t > 0, \tag{14.157}$$

$$T_C = -T_S; \quad a < r < b, \ t = 0, \tag{14.158}$$

The solutions to equations. (14.151) to (14.154) for ξ and T_S are:

$$T_S(r)=\frac{\rho c_v \xi}{4k}r^2+C+D\log r,\quad \xi=-\frac{2bq_0}{\rho c_v\left(b^2-a^2\right)},$$
$$C=\frac{a^2bq_0}{\left(b^2-a^2\right)k},\ D=\frac{bq_0\left[b^4+2a^2b^2-3a^4+4a^2\left(a^2\log a-b^2\log b\right)\right]}{4k\left(b^2-a^2\right)^2}, \tag{14.159}$$

The parameter ξ is equal to ratio between total external heat and internal energy of hollow cylinder with unit high:

$$\xi=-\frac{2bq_0}{\rho c_v\left(b^2-a^2\right)}=-\frac{q_0S}{\rho c_v V},\quad S=1\cdot 2\pi b^2,\ V=1\cdot\pi\left(b^2-a^2\right), \tag{14.160}$$

where S and V are area of external surface and volume of hollow cylinder with unit high, respectively. The solution to the problem for T_C is found in much the same says way as was followed in section 14.8. The problem is therefore on with homogeneous differential equation and boundary conditions and may be treated by the method separation of variables. We can select a particular solution of the differential equation and boundary conditions in the form:

$$T_C(r,t)=\varphi(r)\,\psi(t) \tag{14.161}$$

By substituting the function (14.161) in equations (14.155)-(14.157), we obtain:

$$\frac{d^2\varphi}{dr^2}+\frac{1}{r}\frac{d\varphi}{dr}+\omega^2\varphi=0; \tag{14.162}$$

$$\frac{d\varphi}{dr}=0;\quad r=a, \tag{14.163}$$

$$\frac{d\varphi}{dr}=0;\quad x=b, \tag{14.164}$$

And to the following equation for $\psi(t)$:

$$\frac{d\psi}{dt}+\omega^2\kappa\psi=0 \tag{14.165}$$

The general solution of (14.165) is:

$$\psi(t)=e^{-\kappa\omega^2 t} \tag{14.166}$$

The general solution of (14.162) is:

$$\varphi(r)=AJ_0(\omega r)+BY_0(\omega r) \tag{14.167}$$

where $J_0(\omega r), Y_0(\omega r)$ are Bessel functions and A, B are constants integration. From (14.163) it is deduced that the constant C_2 is given by:

$$B=-\frac{J_1(a\omega)}{Y_1(a\omega)}A \tag{14.168}$$

The equations (14.163) and (14.164) are an homogenous algebraic system as reported below :

$$[\Lambda]\cdot\begin{bmatrix}A\\B\end{bmatrix}=\begin{bmatrix}0\\0\end{bmatrix} \tag{14.169}$$

where the matrix $[\Lambda]$ is given by:

$$[\Lambda]=\begin{bmatrix}a^2\omega J_1(a\omega) & a^2\omega Y_1(a\omega)\\ a^2\omega J_1(b\omega) & b^2\omega Y_1(b\omega)\end{bmatrix} \tag{14.170}$$

The algebraic system (14.169) admit not trivial solution if the determinant of the matrix $[\Lambda]$ is equal to zero. By imposing this condition, we obtain the transcendental equation in unknown parameter ω:

$$\det\left[\mathbf{\Lambda}\right]=g\left(\omega\right)=a^2b^2\omega\left[J_1\left(a\omega\right)Y_1\left(b\omega\right)-J_1\left(b\omega\right)Y_1\left(a\omega\right)\right]=0 \tag{14.171}$$

The roots of this transcendental equation (14.171) are an infinite number such, denoted here by ω_m, $m=1,2,....N$ leading to eigenvalues or characteristic values $\lambda_m=-\omega_m^2$. The corresponding eigenfunctions or characteristic functions $\overline{\varphi}_m\left(r\right)$ are, as calculated above,

$$\overline{\varphi}_m\left(r\right)=\frac{\varphi_m\left(r\right)}{A_m}=\frac{Y_1\left(\omega_m a\right)J_0\left(\omega_m r\right)-J_1\left(\omega_m a\right)Y_0\left(\omega_m r\right)}{Y_1\left(\omega_m a\right)} \tag{14.172}$$

The solution to the problem may therefore be written in the form:

$$T\left(r,t\right)=T_0+\xi t+\frac{\rho c_v\xi}{4k}r^2+C+D\log r+\sum_{m=1}^{\infty}A_m\overline{\varphi}_m\left(r\right)e^{-\kappa\omega_m^2 t} \tag{14.173}$$

where the coefficients A_m are determined by applying the initial condition (14.158) that yields the following relationship:

$$A_m=\left[\int_0^{2\pi}\int_a^b -T_S\left(r\right)\overline{\varphi}_m\left(r\right)\,r\,dr\,d\theta\right]\Bigg/\left[\int_0^{2\pi}\int_a^b r\,\overline{\varphi}_m^2\left(r\right)dr\,d\theta\right] \tag{14.174}$$

By substituting the constant A_m in equation (14.173), we obtain the expression of function temperature $T\left(r,t\right)$. The radial displacement function is given by:

$$\begin{aligned}u_r=&G\,r+\frac{H}{r}+t\left(N\,r+\frac{M}{r}\right)+\frac{\alpha\left(3\lambda+2\mu\right)}{2\left(\lambda+2\mu\right)}\left[C+D\left(\log r-\frac{1}{2}\right)+\frac{2\rho c_v\xi}{k}r^2\right]+\\&+\sum_{m=1}^{\infty}\left\{P_m\,r+\frac{Q_m}{r}+\frac{\alpha\left(3\lambda+2\mu\right)}{\omega_m\left(\lambda+2\mu\right)}\left[A_mJ_1\left(\omega_m r\right)+B_mY_1\left(\omega_m r\right)\right]\right\}e^{-\omega_m^2\kappa t}\end{aligned} \tag{14.175}$$

where the constants integration A_m,B_m are given by equations (14.174) and (14.168), respectively. The constants integrations P_m,Q_m,G,H,M,N are determined by solving the boundary conditions (14.8) . In explicit these constants are given by :

$$\begin{aligned}&P_m=\frac{\left[J_1\left(\omega_m b\right)Y_1\left(\omega_m a\right)-J_1\left(\omega_m a\right)Y_1\left(\omega_m b\right)\right]A_m b\alpha\mu(3\lambda+2\mu)}{(\lambda+\mu)(\lambda+2\mu)(b^2-a^2)\omega_mY_1\left(\omega_m a\right)},\ M=0,\\&Q_m=\frac{a^2b\left[J_1\left(\omega_m b\right)Y_1\left(\omega_m a\right)-J_1\left(\omega_m a\right)Y_1\left(\omega_m b\right)\right]A_m\alpha(3\lambda+2\mu)}{(\lambda+2\mu)(b^2-a^2)\omega_mY_1\left(\omega_m a\right)},\ N=-\frac{bq_0\alpha(3\lambda+2\mu)}{\rho c_v(b^2-a^2)(\lambda+\mu)},\\&G=\frac{\alpha(T_0-T_R)(3\lambda+2\mu)}{2(\lambda+\mu)},H=-\frac{a^2b^3q_0\alpha(3\lambda+2\mu)\left[b^2-a^2+4a^2(\log a-\log b)\right]}{8k(b^2-a^2)^2(\lambda+2\mu)},\end{aligned} \tag{14.176}$$

In explicit the radial and circumferential stress components are given by:

$$\begin{aligned}\sigma_{rr}=&2\left\{G\left(\lambda+\mu\right)-\mu Hr^{-2}+t\left[N\left(\lambda+\mu\right)-\mu Mr^{-2}\right]\right\}+\\&-\alpha\left(3\lambda+2\mu\right)\left\{T_0-T_R+\xi t+\frac{\rho c_v\mu\xi r^2}{8k\left(2\mu+\lambda\right)}+\frac{\mu}{\lambda+2\mu}\left[C+D\left(\log r-\frac{1}{2}\right)\right]\right\}\\&+2\sum_{m=1}^{\infty}\left\{P_m\left(\lambda+\mu\right)-\frac{\mu Q_m}{r^2}-\frac{\alpha\mu\left(3\lambda+2\mu\right)}{\left(\lambda+2\mu\right)\omega_m r}\left[A_mJ_1\left(\omega_m r\right)+B_mY_1\left(\omega_m r\right)\right]\right\}e^{-\omega_m^2\kappa t}\end{aligned} \tag{14.177}$$

$$\sigma_{\theta\theta}=2\left\{G(\lambda+\mu)+\mu Hr^{-2}+t\left[N(\lambda+\mu)+\mu Mr^{-2}\right]\right\}+\sum_{m=1}^{\infty}2\left[P_m(\lambda+\mu)+\frac{\mu Q_m}{r^2}\right]e^{-\omega_m^2\kappa t}+$$
$$-\alpha(3\lambda+2\mu)\left\{T_0-T_R+\xi t+\frac{3\rho c_v\mu\xi r^2}{8k(2\mu+\lambda)}+\frac{\mu}{\lambda+2\mu}\left[C+D\left(\log r+\frac{1}{2}\right)\right]\right\}+ \qquad (14.178)$$
$$-2\sum_{m=1}^{\infty}\frac{\alpha\mu(3\lambda+2\mu)}{(\lambda+2\mu)\omega_m r}\left\{A_mJ_1(\omega_m r)+B_mY_1(\omega_m r)-\omega_m r\left[A_mJ_0(\omega_m r)+B_mY_0(\omega_m r)\right]\right\}e^{-\omega_m^2\kappa t}$$

$$\sigma_{zz}=2\lambda(G+tN)-\alpha(3\lambda+2\mu)\left\{T_0-T_R+\xi t+\frac{\rho c_v\mu\xi r^2}{2k(2\mu+\lambda)}+\frac{2\mu}{\lambda+2\mu}(C+D\log r)\right\}+$$
$$+2\sum_{m=1}^{\infty}\left\{P_m\lambda-\frac{\alpha\mu(3\lambda+2\mu)}{(\lambda+2\mu)\omega_m r}\left[A_mJ_0(\omega_m r)+B_mY_0(\omega_m r)\right]\right\}e^{-\omega_m^2\kappa t} \qquad (14.179)$$

The circumferential stress assumes asymptotic values in r = a and r = b for $t\to\infty$, as showed in figure 14.30. These asymptotic values are given by:

$$\sigma_{\theta\theta}(r=a,t\to\infty)=-\frac{\alpha Eb\,q_0}{k(1-\nu)}\left[\frac{b^4-a^4+4a^2b^2(\log a-\log b)}{4(b^2-a^2)^2}\right],$$
$$\sigma_{\theta\theta}(r=b,t\to\infty)=\frac{\alpha Eb\,q_0}{k(1-\nu)}\left[\frac{b^4+3a^4-4a^2b^2+4a^4(\log a-\log b)}{4(b^2-a^2)^2}\right], \qquad (14.180)$$

The axial force applied on bases of hollow cylinder is given by:

$$N_z=\int_0^{2\pi}\int_a^b\sigma_{zz}r\,dr\,d\theta=2\pi(b^2-a^2)\lambda\left[G+tN-\frac{\alpha(3\lambda+2\mu)}{2\lambda}(T_0-T_R+\xi t)+\frac{1}{\lambda}\sum_{m=1}^{\infty}P_m\,e^{-\omega_m^2\kappa t}\right]+$$
$$-\frac{\pi(b^2-a^2)\alpha\mu(3\lambda+2\mu)}{(\lambda+2\mu)}\left[\frac{\rho c_v\xi(b^2+a^2)}{4k}+2C-\left(\frac{b^2-a^2+2a^2\log a-2b^2\log b}{b^2-a^2}\right)D\right] \qquad (14.181)$$
$$+\frac{4\pi\alpha\mu(3\lambda+2\mu)}{(\lambda+2\mu)}\sum_{m=1}^{\infty}\left\{\frac{A_m}{\omega_m}\left[aJ_1(\omega_m a)-bJ_1(\omega_m b)\right]+\frac{B_m}{\omega_m}\left[aY_1(\omega_m a)-bY_1(\omega_m b)\right]\right\}e^{-\omega_m^2\kappa t}$$

For example, let us consider, a hollow cylinder constituted by steel, under uniform heat flux. The geometrical, mechanical and thermal parameters considered for hollow cylinder are reported below:

$$E=210\cdot10^9\,N/m^2,\ \nu=0.3,\ c=440\,J/kg\cdot°K,\ k=45W/m\cdot°K,$$
$$\rho=7.8\cdot10^3\,kg/m^3,\ \ b=10.5m,\ \ a=10.0m,\ s=b-a=0.5m,$$
$$q=-500W/m^2,\quad \alpha=1.2\cdot10^{-5}°K^{-1},\quad T_0=T_R=300°K$$

By fixed m= 20, the eigenvalues ω_m and corresponding values of constants integration A_m are reported in table 14.2:

ω_m	6.284	12.567	18.850	25.133	31.416
A_m	8.20	-2.88	1.57	-1.02	0.73
ω_m	37.699	43.982	50.266	56.549	62.832
A_m	-0.552	0.438	-0.359	0.301	-0.257
ω_m	69.115	75.398	81.681	87.965	94.248
A_m	0.222	-0.195	0.173	-0.155	0.140
ω_m	100.531	106.814	113.097	119.381	125.664
A_m	-0.127	0.116	-0.106	0.098	-0.091

Table 14.2 – *Eigenvalues ω_m and corresponding values of constants integration A_m*

In this case the graphics function $g(\omega)$ given by equation (14.171) is reported below:

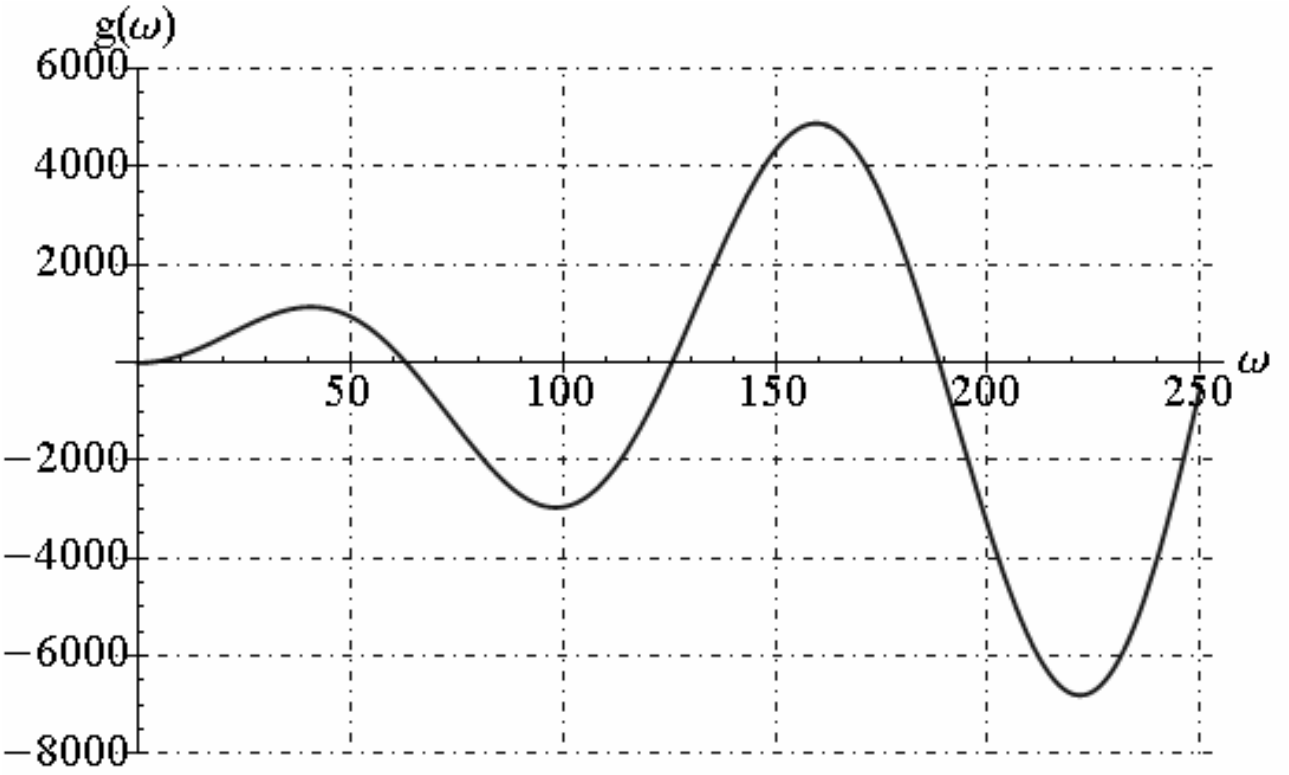

We reported the graphics of temperature function along the radial direction and in time:

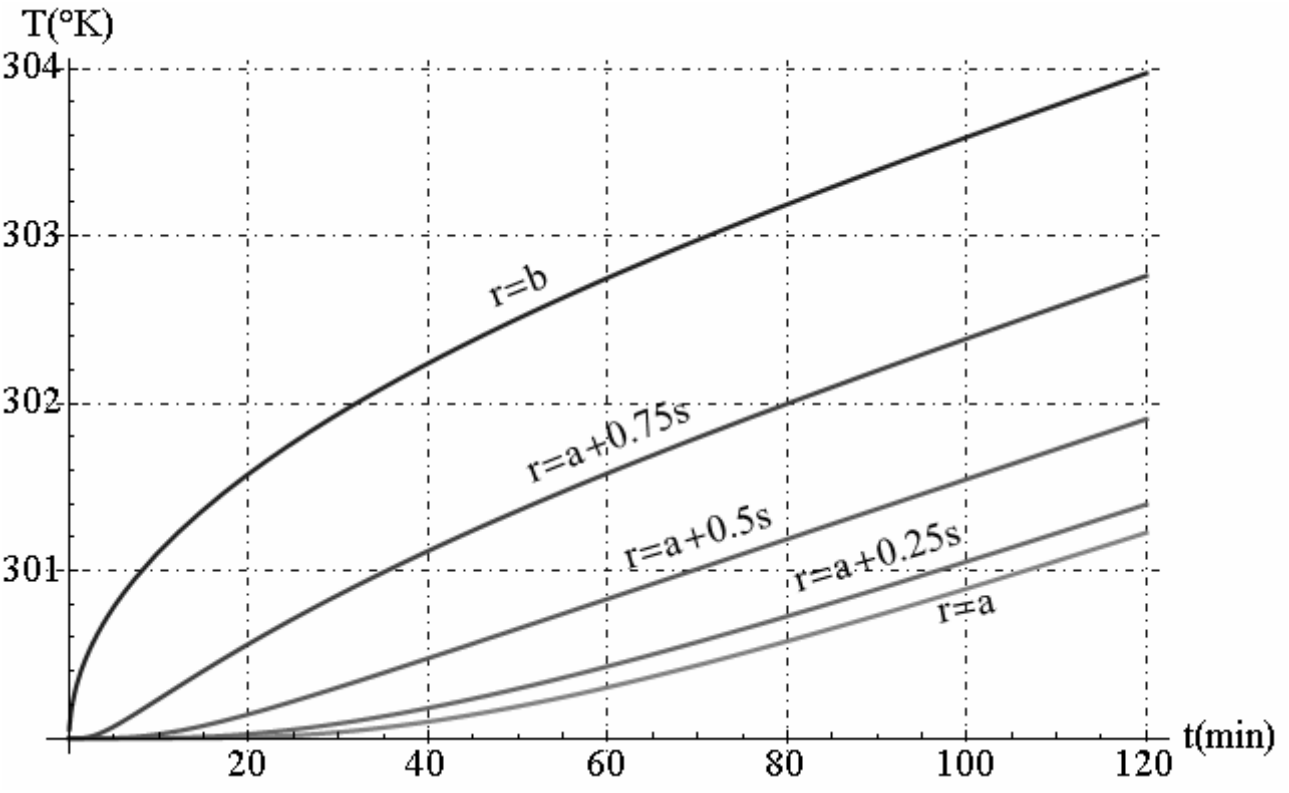

Fig. 14.24 - *Temperature function versus the time*

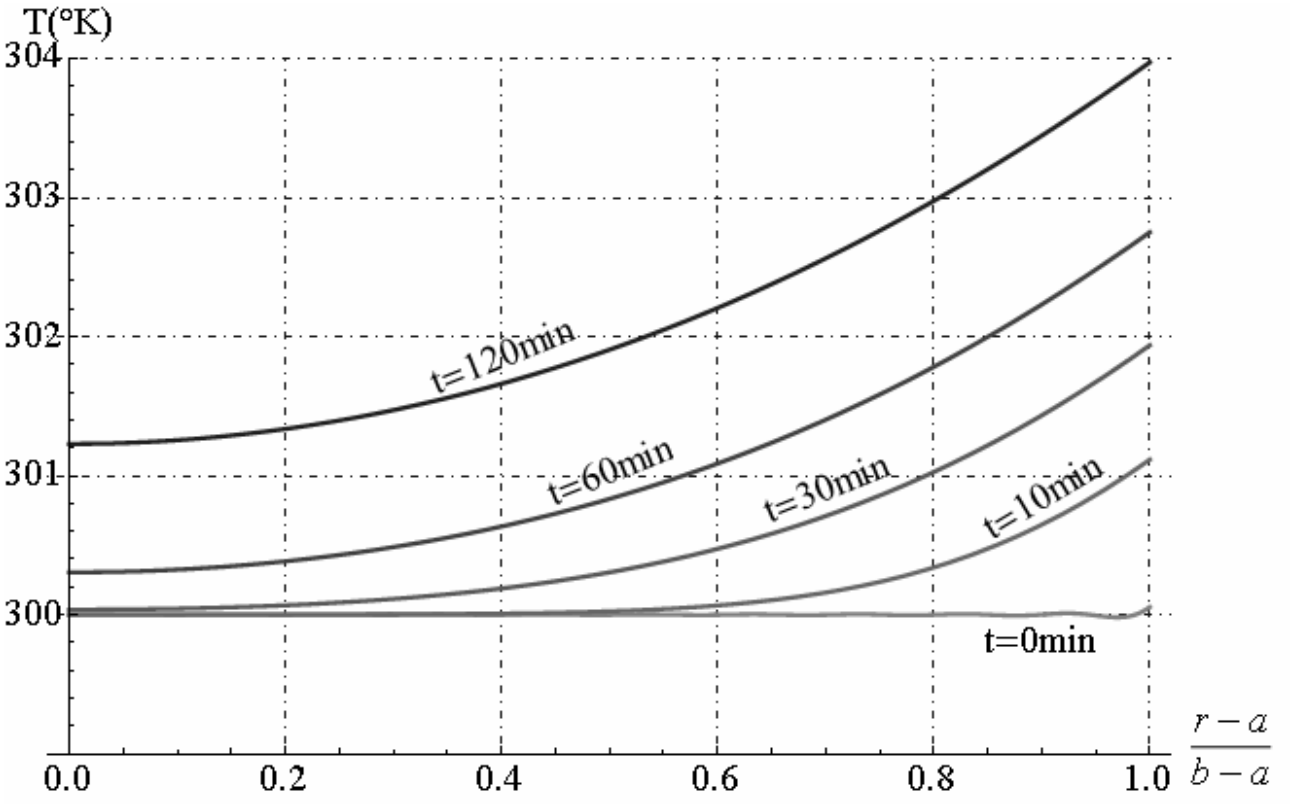

Fig. 14.25 - *Temperature function along radial direction*

We reported the graphic of radial displacement component function along the radial direction:

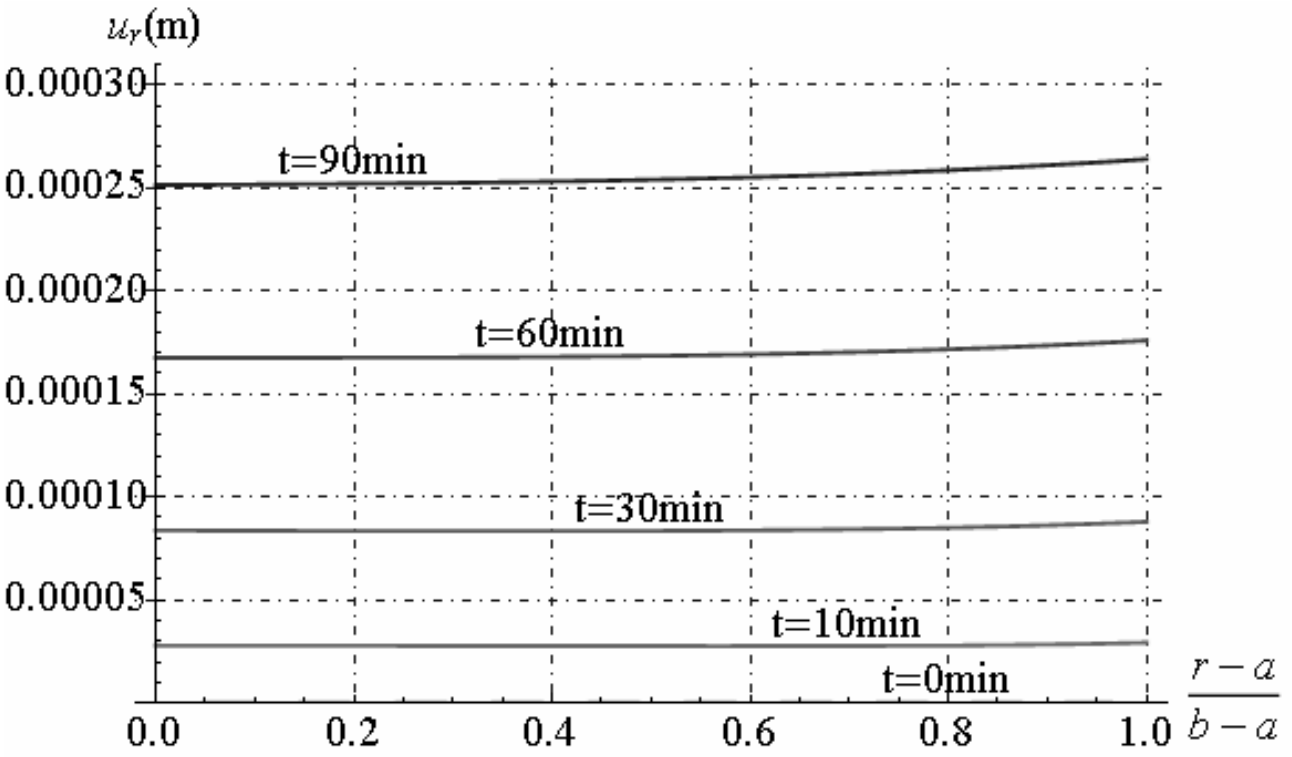

Fig. 14.26 - *Radial displacement distribution along radial direction*

We reported the graphics of stress components along the radial direction and in time:

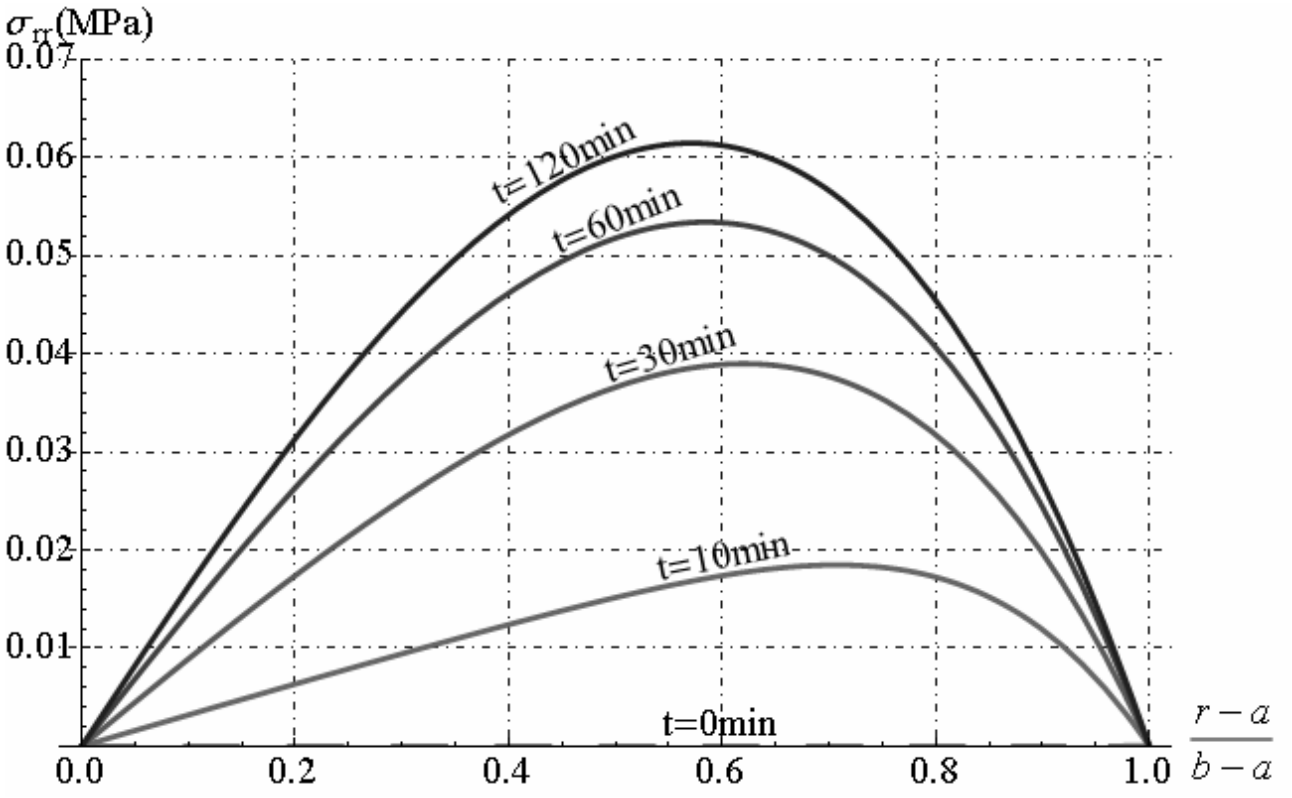

Fig. 14.27 - *Radial stress distribution along radial direction*

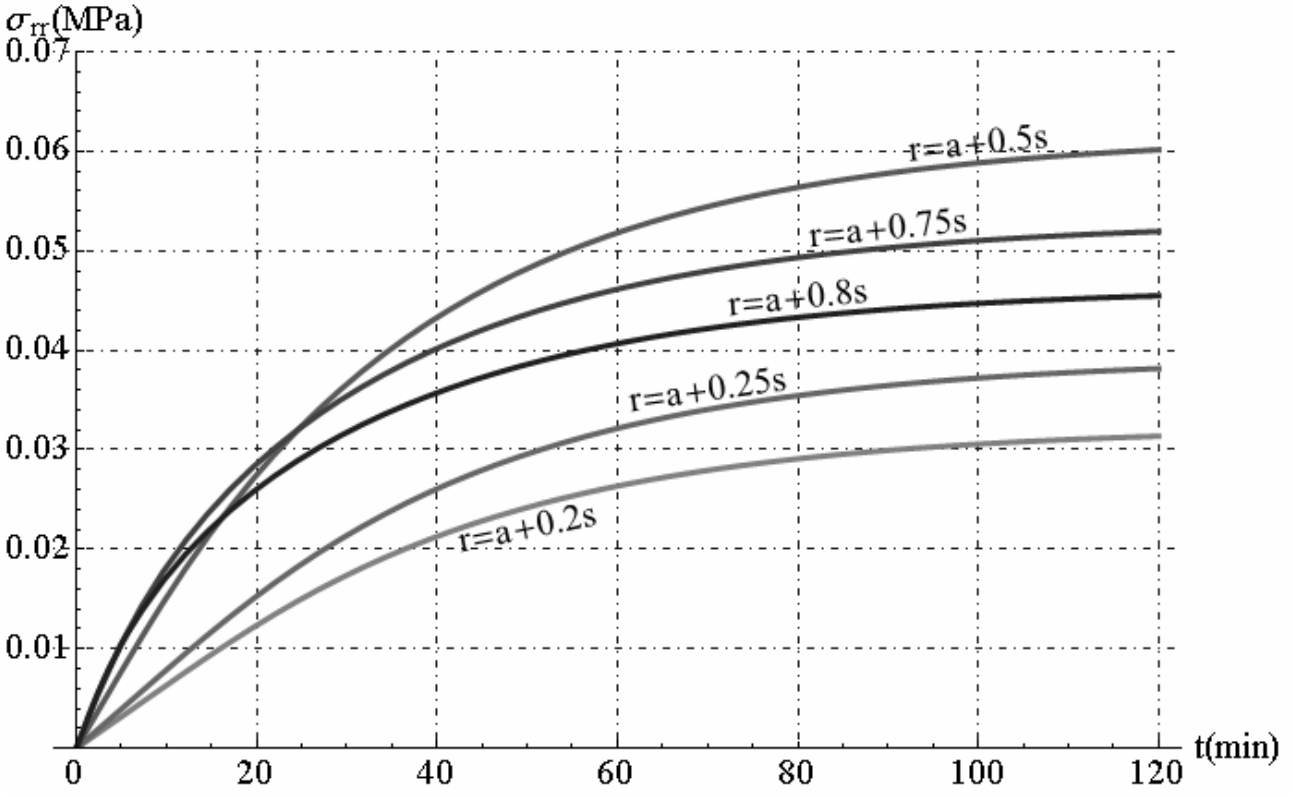

Fig. 14.28 - *Radial stress distribution in time*

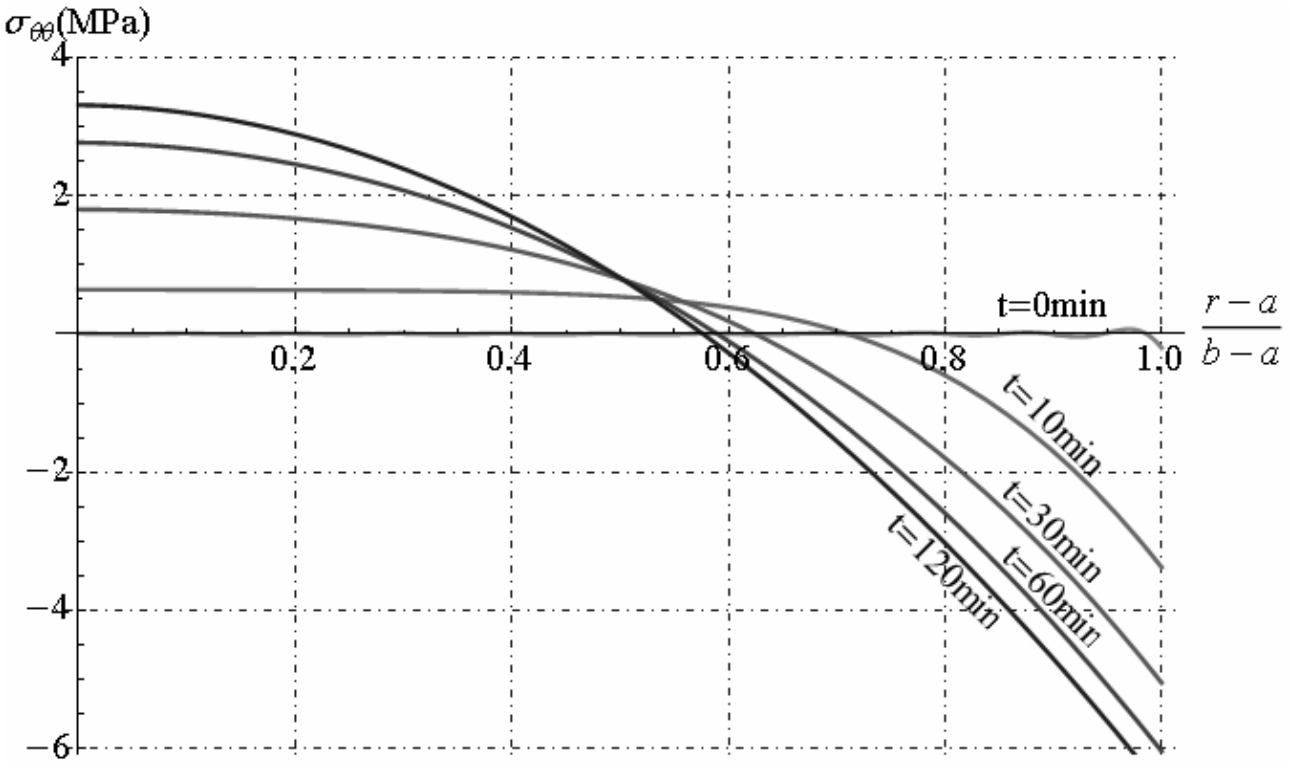

Fig. 14.29 - *Circumferential stress distribution along radial direction*

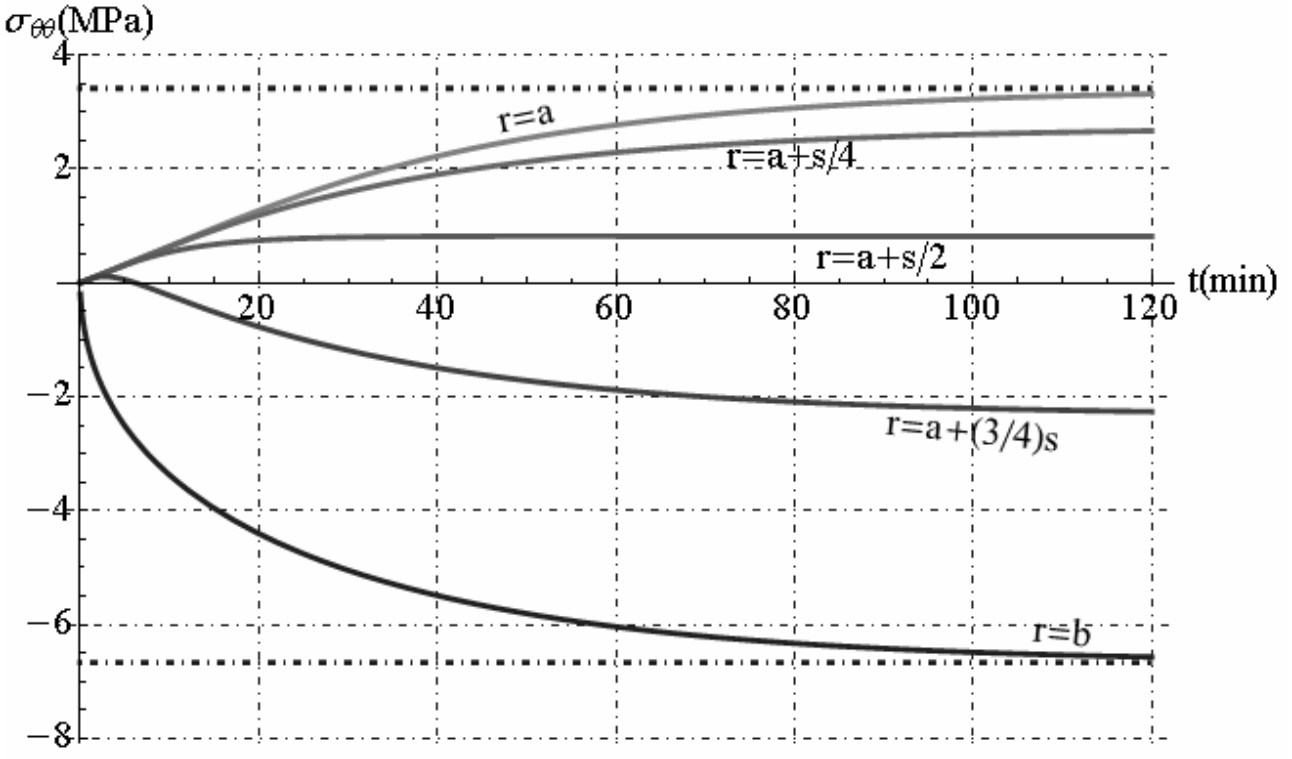

Fig. 14.30 - *Circumferential stress distribution in time*

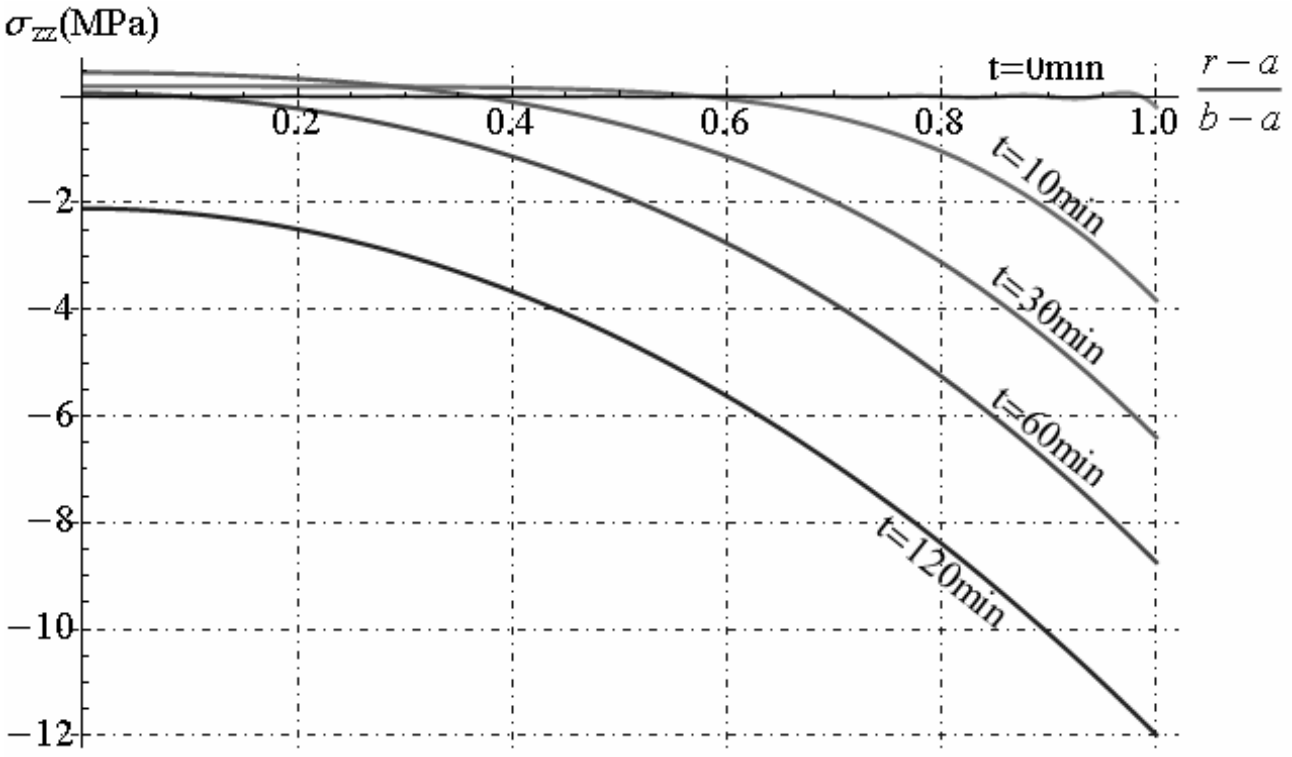

Fig. 14.31 - *Axial stress distribution along radial direction*

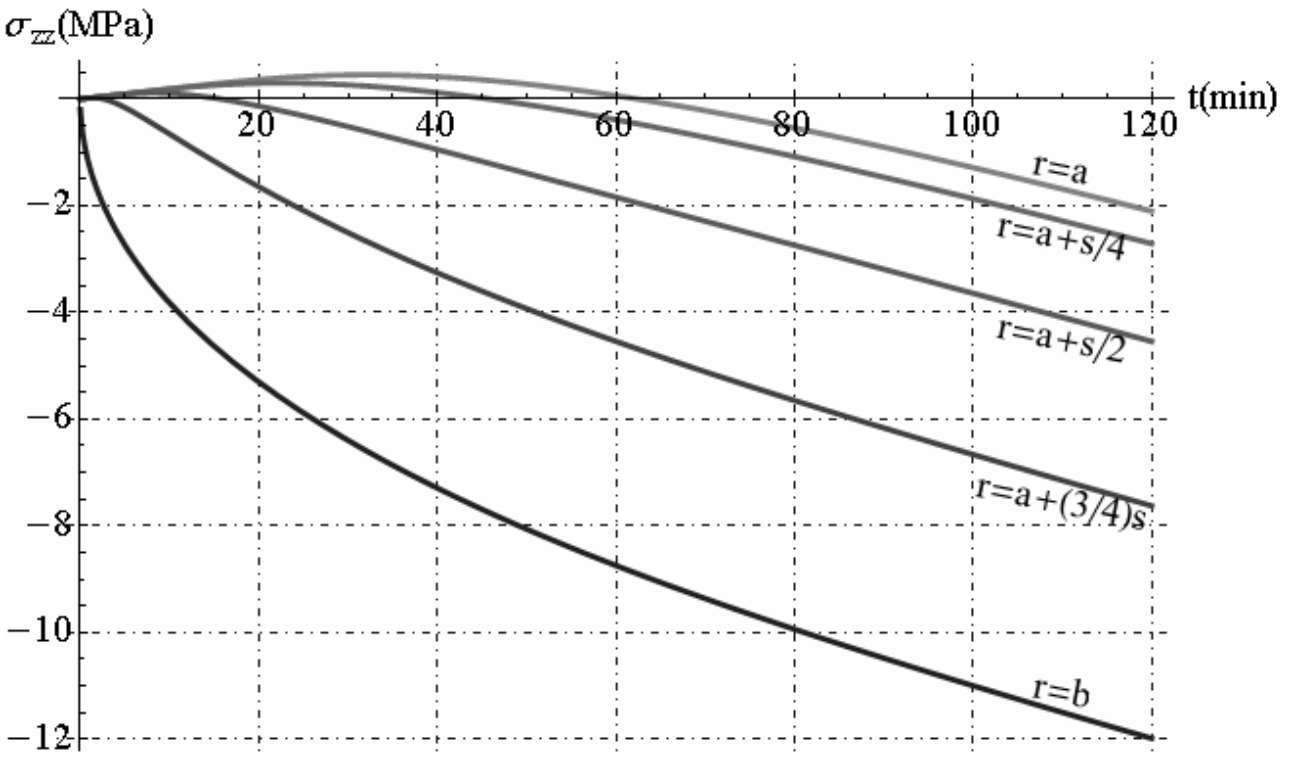

Fig. 14.32 - *Axial stress distribution in time*

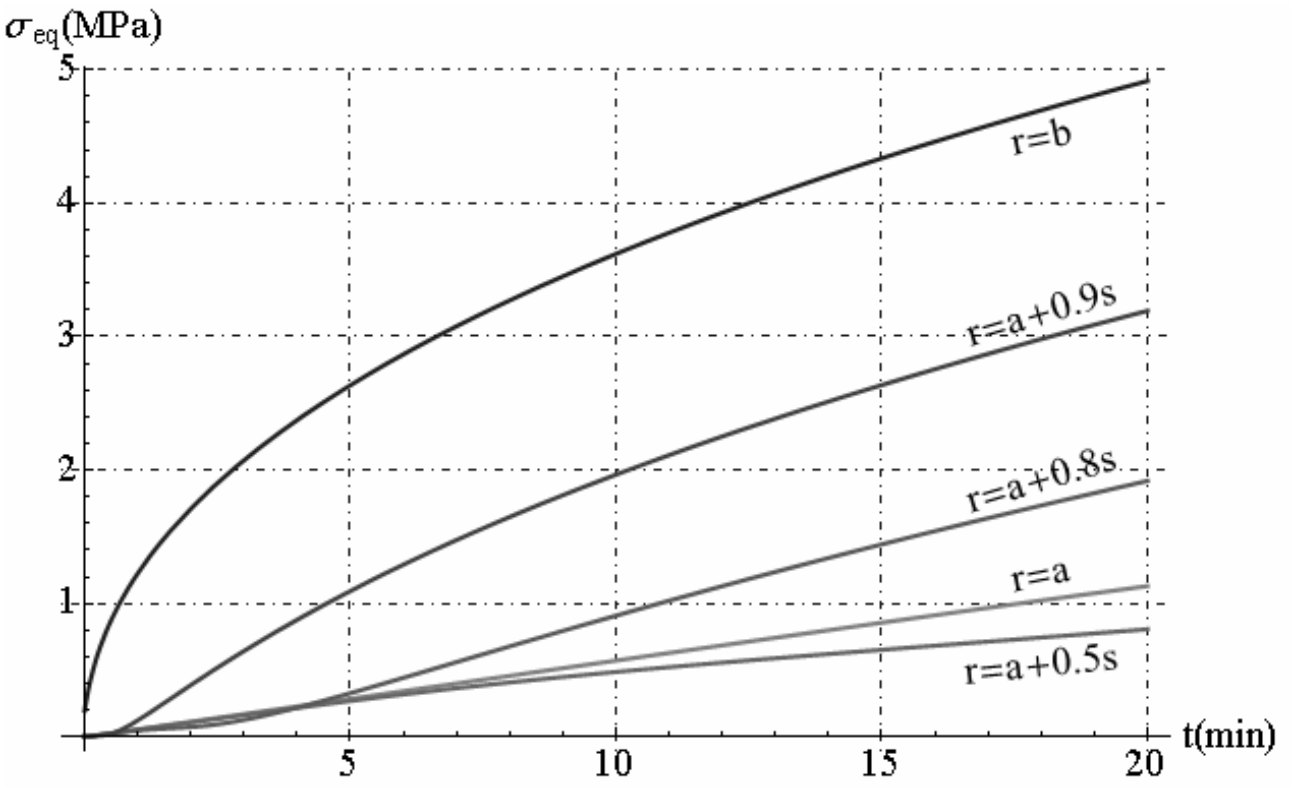

Fig. 14.33 - *Hencky von Mises's equivalent stress distribution along radial direction*

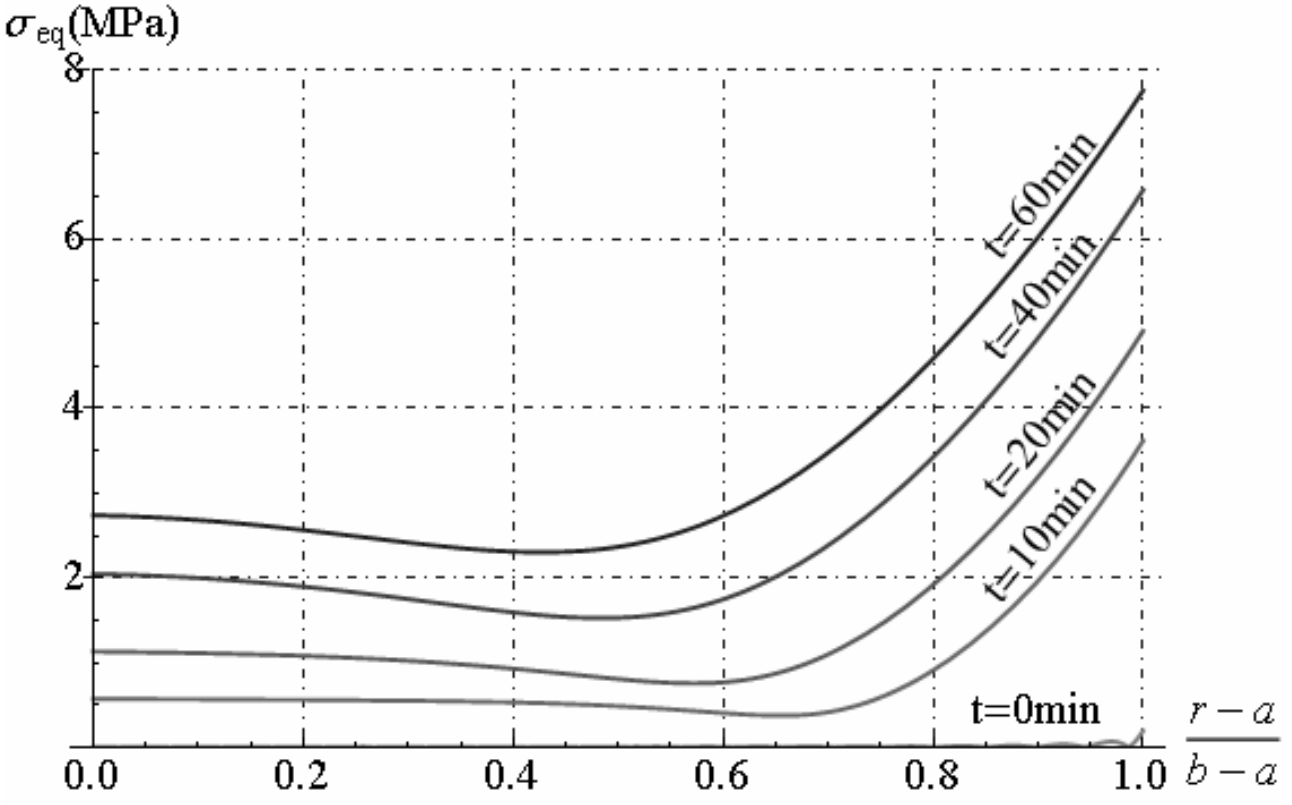

Fig. 14.34 - *Hencky von Mises's equivalent stress distribution in time*

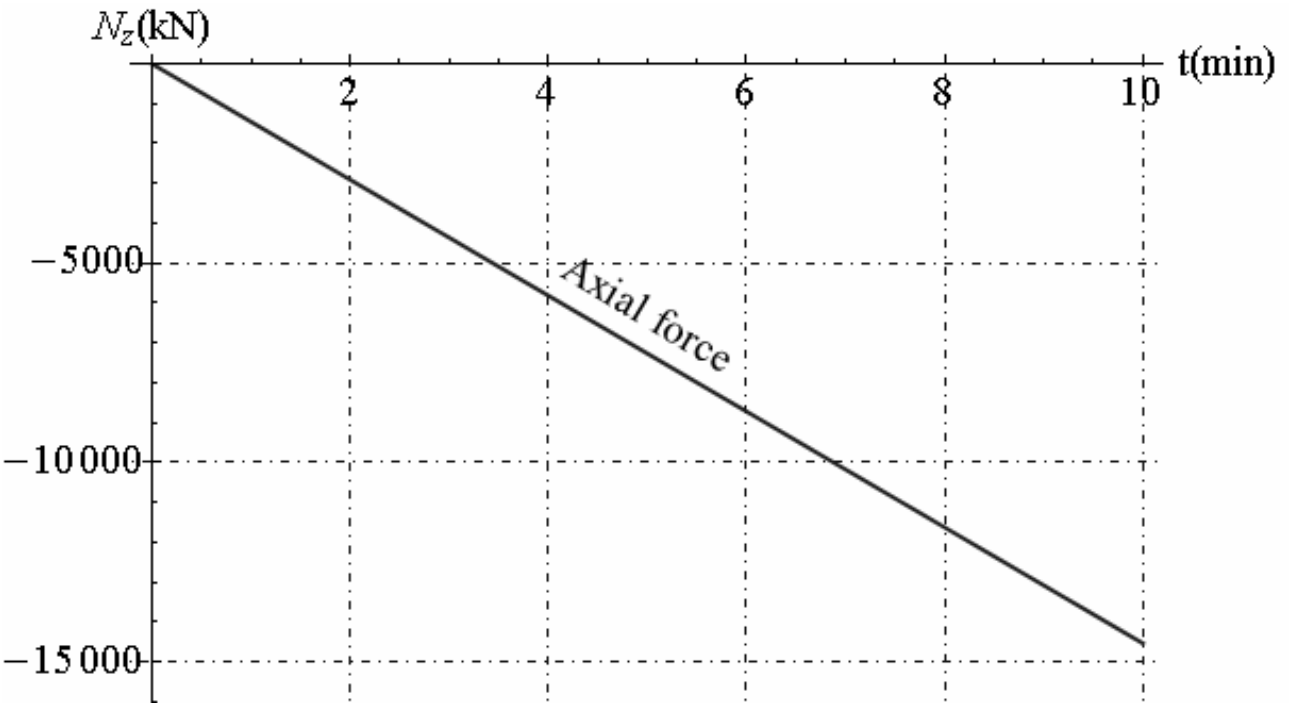

Fig. 14.35 - *Axial force applied on bases of hollow cylinder versus time*

14.10 References

[1] Boley, B.A.,Weiner, J.H., *Theory of thermal stresses*, Dover publications, inc. Mineola, New York

[2] Ciarlet, Philiphe G., *Mathematical Elasticity, Volume I.: Three dimensional elasticity*, Elsevier Science Publishers B.V.

[3] Fraldi, M., Nunziante, L., Carannante, F. (2007), *Axis-symmetrical Solutions for n-plies Functionally Graded Material Cylinders under Strain no-Decaying Conditions*, J. Mech. of Adv. Mat. and Struct. Vol. 14 (3), pp. 151-174 - DOI: 10.1080/15376490600719220

[4] M. Fraldi, L. Nunziante, F. Carannante, A. Prota, G. Manfredi, E. Cosenza (2008), *On the Prediction of the Collapse Load of Circular Concrete Columns Confined by FRP*, Journal Engineering structures, Vol. 30, Issue 11, November 2008, Pages 3247-3264 - DOI: 10.1016/j.engstruct.2008.04.036

[5] Fraldi, M., Nunziante, L., Chandrasekaran, S., Carannante, F., Pernice, MC. (2009), *Mechanics of distributed fibre optic sensors for strain measurements on rods*, Journal of Structural Engineering, 35, pp. 323-333, Dec. 2008- Gen. 2009

[6] M. Fraldi, F. Carannante, L. Nunziante (2012), *Analytical solutions for n-phase Functionally Graded Material Cylinders under de Saint Venant load conditions: Homogenization and effects of Poisson ratios on the overall stiffness*, Composites Part B: Engineering, Volume 45, Issue 1, February 2013, Pages 1310–1324

[7] Gurtin, M. E., *The Linear Theory of Elasticity, Handbbuch der Physik*, Springer, Berlin, 1972.

[8] Lekhnitskii, S. G., *Theory of Elasticity of an Anisotropic Body*, Mir, Moscow, 1981.

[9] Love, A. E. H., *A Treatise on the Mathematical Theory of Elasticity*, Dover Publications, Inc, New York, 1944

[10] Nunziante, L., Gambarotta, L., Tralli, A., *Scienza delle Costruzioni*, 3° Edizione, McGraw-Hill, 2011, ISBN: 9788838666971

[11] Ting TCT. *Anisotropic elasticity - Theory and applications*. Oxford University Press; 1996.

[12] Wolfram, S., *Mathematica, version 8*, Wolfram Research, Inc., Champaign, IL, 1998–2005.

CHAPTER XV
THERMAL STRESS IN HOLLOW SPHERES

15.1. Uncoupled thermo-elastic problem with radial temperature variation

Let us consider a hollow sphere with inner radius "a" and outer radius "b" , subjected to radial temperature variation. In this case the displacement components and temperature are functions of radius and time:

$$u_r = u_r(r,t); \quad u_\theta = 0; \quad u_\phi = 0; \quad T = T(r,t); \tag{15.1}$$

The results in this case are conveniently obtained from the displacement formulation in spherical coordinates. By omitting all displacement components and all derivatives in the θ and ϕ directions, The equilibrium equations are reduced simply to:

$$\frac{\partial}{\partial r}\left[\frac{1}{r^2}\frac{\partial\left(r^2 u_r\right)}{\partial r}\right] = \left(\frac{3\lambda+2\mu}{2\mu+\lambda}\right)\alpha\frac{\partial T}{\partial r} = \alpha\left(\frac{1+\nu}{1-\nu}\right)\frac{\partial T}{\partial r} \tag{15.2}$$

The Fourier heat conduction for uncoupled thermo-elastic problem, becomes:

$$\frac{\partial^2 T}{\partial r^2} + \frac{2}{r}\frac{\partial T}{\partial r} = \frac{\rho c_v}{k}\frac{\partial T}{\partial t} = \frac{1}{\kappa}\frac{\partial T}{\partial t} \tag{15.3}$$

where $\kappa = \dfrac{k}{\rho c_v}$ is thermal diffusivity. The general solution of equation (15.2) is :

$$u_r = \alpha\left(\frac{3\lambda+2\mu}{\lambda+2\mu}\right)\frac{1}{r^2}\int_a^r \xi^2 T(\xi,t)\,d\xi + f_1(t)\,r + \frac{f_2(t)}{r^2} \tag{15.4}$$

where in the integral the effective variable is radius, but ξ is the mute variable. By solving the Fourier's equation (15.3) with one method reported in Chapter VII, and substituting the function of temperature T(r,t) in equation (15.4), we obtain the explicit displacement solution.

For the hollow sphere of inner radius a and outer radius b the function of the time $f_1(t)$ and $f_2(t)$ must be determined from the condition that :

$$\sigma_{rr} = 0 \quad \text{at} \quad r = a, b \tag{15.5}$$

From the strain-displacement relation and Hooke's law the non-zero stress components for this case are:

$$\begin{aligned}
\sigma_{rr} &= \lambda\left(\frac{\partial u_r}{\partial r} + \frac{2u_r}{r}\right) + 2\mu\frac{\partial u_r}{\partial r} - \alpha(3\lambda+2\mu)(T-T_R) = \\
&= \left[f_1(t) + \alpha T_R\right](3\lambda+2\mu) - \frac{4\mu f_2(t)}{r^3} - \frac{4\mu\alpha}{r^3}\left(\frac{3\lambda+2\mu}{\lambda+2\mu}\right)\int_a^r \xi^2 T(\xi,t)\,d\xi; \\
\sigma_{\theta\theta} &= \sigma_{\phi\phi} = \lambda\left(\frac{\partial u_r}{\partial r} + \frac{2u_r}{r}\right) + \frac{2\mu u_r}{r} - \alpha(3\lambda+2\mu)(T-T_R) = \\
&= \left[f_1(t) + \alpha T_R\right](3\lambda+2\mu) - \frac{2\mu f_2(t)}{r^3} - 2\mu\alpha\left(\frac{3\lambda+2\mu}{\lambda+2\mu}\right)\left[T(r,t) - \frac{1}{r^3}\int_a^r \xi^2 T(\xi,t)\,d\xi\right];
\end{aligned} \tag{15.6}$$

where T_R is the reference temperature. By solving the boundary condition (15.6) , we obtain the functions $f_1(t)$ and $f_2(t)$, as reported below:

$$f_1(t) = -\alpha T_R + \frac{4\alpha\mu}{\left(b^3-a^3\right)(\lambda+2\mu)}\int_a^b \xi^2 T(\xi,t)\,d\xi; \quad f_2(t) = \frac{\alpha(3\lambda+2\mu)a^3}{\left(b^3-a^3\right)(\lambda+2\mu)}\int_a^b \xi^2 T(\xi,t)\,d\xi \tag{15.7}$$

The final result for a hollow sphere is :

$$u_r=\frac{\alpha}{b^3-a^3}\left(\frac{3\lambda+2\mu}{\lambda+2\mu}\right)\left[\frac{a^3}{r^2}\int_r^b\xi^2T(\xi,t)\,d\xi+\frac{b^3}{r^2}\int_a^r\xi^2T(\xi,t)\,d\xi+\frac{4\mu r}{3\lambda+2\mu}\int_a^b\xi^2T(\xi,t)\,d\xi\right]-\alpha T_R r$$

$$\sigma_{rr}=\frac{4\mu\alpha}{a^3-b^3}\left(\frac{3\lambda+2\mu}{\lambda+2\mu}\right)\left[\frac{a^3}{r^2}\int_r^b\xi^2T(\xi,t)\,d\xi+\frac{b^3}{r^2}\int_a^r\xi^2T(\xi,t)\,d\xi-\int_a^b\xi^2T(\xi,t)\,d\xi\right] \tag{15.8}$$

$$\sigma_{\theta\theta}=\sigma_{\phi\phi}=$$

$$=\frac{2\mu\alpha}{b^3-a^3}\left(\frac{3\lambda+2\mu}{\lambda+2\mu}\right)\left[\frac{a^3}{r^2}\int_r^b\xi^2T(\xi,t)\,d\xi+\frac{b^3}{r^2}\int_a^r\xi^2T(\xi,t)\,d\xi+2\int_a^b\xi^2T(\xi,t)\,d\xi+\left(a^3-b^3\right)T(r,t)\right]$$

In the special case in which the temperature T_0 is constant, these equations show that all stress components are zero, and that:

$$u_r=\alpha r\left(T_0-T_R\right) \tag{15.9}$$

The results for a solid sphere of radius b may be obtained by setting a = 0 ; they are:

$$u_r=\alpha\left(\frac{3\lambda+2\mu}{\lambda+2\mu}\right)\left[\frac{1}{r^2}\int_0^r\xi^2T(\xi,t)\,d\xi+\frac{4\mu}{(3\lambda+2\mu)}\frac{r}{b^3}\int_0^b\xi^2T(\xi,t)\,d\xi\right]-\alpha T_R r$$

$$\sigma_{rr}=4\mu\alpha\left(\frac{3\lambda+2\mu}{\lambda+2\mu}\right)\left[\frac{1}{b^3}\int_0^b\xi^2T(\xi,t)\,d\xi-\frac{1}{r^3}\int_0^r\xi^2T(\xi,t)\,d\xi\right] \tag{15.10}$$

$$\sigma_{\theta\theta}=\sigma_{\phi\phi}=2\mu\alpha\left(\frac{3\lambda+2\mu}{\lambda+2\mu}\right)\left[\frac{1}{r^3}\int_0^r\xi^2T(\xi,t)\,d\xi+\frac{2}{b^3}\int_0^b\xi^2T(\xi,t)\,d\xi-T(r,t)\right]$$

As in the case of the cylinder indeterminate form arise for r = 0; if however, the temperature is finite , the following limits hold::

$$\lim_{r\to0}\frac{1}{r^3}\int_0^r\xi^2T(\xi,t)\,d\xi=\frac{1}{3}T(0,t)$$

$$\lim_{r\to0}\frac{1}{r^2}\int_0^r\xi^2T(\xi,t)\,d\xi=0 \tag{15.11}$$

As may be shown by means of Hospital's rule. Then at r = 0, the radial displacement is zero and the normal stress components are :

$$\sigma_{rr}(0,t)=\sigma_{\theta\theta}(0,t)=\sigma_{\phi\phi}(0,t)=4\mu\alpha\left(\frac{3\lambda+2\mu}{\lambda+2\mu}\right)\left[\frac{1}{b^3}\int_0^b\xi^2T(\xi,t)\,d\xi-\frac{1}{3}T(0,t)\right] \tag{15.12}$$

As a special case of the solid sphere, we may obtain the solution for an infinite body under radial temperature distributions by letting $b\to\infty$ in equations (15.10). The result is (with $\int_0^\infty\xi^2T(\xi,t)\,d\xi$ assumed convergent):

$$u_r=\frac{\alpha}{r^2}\left(\frac{3\lambda+2\mu}{\lambda+2\mu}\right)\int_0^r\xi^2T(\xi,t)\,d\xi-\alpha T_R r$$

$$\sigma_{rr}=-\frac{4\mu\alpha}{r^3}\left(\frac{3\lambda+2\mu}{\lambda+2\mu}\right)\int_0^r\xi^2T(\xi,t)\,d\xi \tag{15.13}$$

$$\sigma_{\theta\theta}=\sigma_{\phi\phi}=\frac{2\mu\alpha}{r^3}\left(\frac{3\lambda+2\mu}{\lambda+2\mu}\right)\left[\int_0^r\xi^2T(\xi,t)\,d\xi-r^3T(r,t)\right]$$

15.2 Coupled thermo-elastic problem with radial temperature variation

Let us consider a hollow sphere with inner radius "a" and outer radius "b" , subjected to radial temperature variation. In this case the displacement components and temperature are functions of

radius and time as reported in previous section. The equilibrium equation remaining the same in the case of uncoupled thermo-elastic problem, but change the Fourier's equation as reported below:

$$\begin{cases} \dfrac{\partial}{\partial r}\left[\dfrac{1}{r^2}\dfrac{\partial\left(r^2 u_r\right)}{\partial r}\right]=\left(\dfrac{3\lambda+2\mu}{2\mu+\lambda}\right)\alpha\dfrac{\partial T}{\partial r}=\alpha\left(\dfrac{1+\nu}{1-\nu}\right)\dfrac{\partial T}{\partial r} \\ \dfrac{\partial^2 T}{\partial r^2}+\dfrac{2}{r}\dfrac{\partial T}{\partial r}=\dfrac{\rho c_v}{k}\dfrac{\partial T}{\partial t}+\left(\dfrac{3\lambda+2\mu}{k}\right)\alpha T_R\dfrac{\partial}{\partial t}\left[\dfrac{1}{r^2}\dfrac{\partial\left(r^2 u_r\right)}{\partial r}\right] \end{cases} \tag{15.14}$$

where T_R is the reference temperature. By integrating the equilibrium equation (the first of eqs. (15.14)), respect to variable r , we obtain:

$$\frac{1}{r^2}\frac{\partial\left(r^2 u_r\right)}{\partial r}=\left(\frac{3\lambda+2\mu}{2\mu+\lambda}\right)\alpha T+f_1(t) \tag{15.15}$$

where $f_1(t)$ is an function of sole variable time. By utilizing the equation (15.15), we can rewrite the Fourier's equation in follows manner:

$$\frac{\partial^2 T}{\partial r^2}+\frac{2}{r}\frac{\partial T}{\partial r}=\left[\frac{\rho c_v}{k}+\frac{\left(3\lambda+2\mu\right)^2\alpha^2 T_R}{k\left(\lambda+2\mu\right)}\right]\frac{\partial T}{\partial t}+\left(\frac{3\lambda+2\mu}{k}\right)\alpha T_R\frac{df_1}{dt} \tag{15.16}$$

By deriving the equations (15.16) respect to variable r , the follows equation is obtained:

$$\frac{\partial^3 T}{\partial r^3}+\frac{2}{r}\frac{\partial^2 T}{\partial r^2}-\frac{2}{r^2}\frac{\partial T}{\partial r}=\left(1+\delta\right)\frac{\rho c_v}{k}\frac{\partial^2 T}{\partial r\,\partial t}=\frac{\left(1+\delta\right)}{\kappa}\frac{\partial^2 T}{\partial r\,\partial t} \tag{15.17}$$

where $\kappa=\dfrac{k}{\rho c_v}$ is thermal diffusivity and the non-dimensional parameter δ is defined by:

$$\delta=\frac{\left(3\lambda+2\mu\right)^2\alpha^2 T_R}{\rho^2 c_v v_e^2}=\frac{\left(3\lambda+2\mu\right)^2\alpha^2 T_R}{\rho c_v\left(2\mu+\lambda\right)}=\left[\frac{1+\nu}{\left(1-\nu\right)\left(1-2\nu\right)}\right]\frac{\alpha^2 E T_R}{\rho c_v} \tag{15.18}$$

with the velocity of propagation of dilatational waves in an elastic medium being denoted by:

$$v_e=\sqrt{\frac{2\mu+\lambda}{\rho}}=\sqrt{\frac{1-\nu}{1-\nu-2\nu^2}}\cdot\sqrt{\frac{E}{\rho}} \tag{15.19}$$

The term δ characterized the coupled problem, and it is negligible compared to unity if $\delta\ll 1$.
The general solution of equilibrium equation is reported in eq.(15.4). By solving the Fourier's equation (15.17) with one method reported in chapter 7 (for example with method separation of variables), and substituting the function of temperature $T(r,t)$ in equation (15.4), we obtain the explicit displacement solution. Moreover, the function $f_1(t)$, $f_2(t)$ present in equation (15.4) can be to determine by applying the relationships (15.7). Then, we can to determine the integration constants of the function temperature by applying the boundary conditions for heat conduction problem.

15.3 Uniform pressure with constant temperature

Let us consider a hollow sphere with inner radius "a" and outer radius "b" , subjected to uniform pressure for r = b equal to p_e and subjected to uniform pressure for r = a equal to p_i . Moreover the profile of temperature is constant ($T=T_0>T_R$) along radius and in the time. In this case the only displacement component u_r is function of radius :

$$u_r=u_r\left(r\right);\quad u_\theta=0;\quad u_\phi=0;\quad T=T_0; \tag{15.20}$$

The results in this case are conveniently obtained from the displacement formulation in spherical coordinates. By omitting all displacement components and all derivatives in the θ and ϕ directions, The equilibrium equations are reduced simply to:

$$\frac{\partial}{\partial r}\left[\frac{1}{r^2}\frac{\partial\left(r^2 u_r\right)}{\partial r}\right]=0 \tag{15.21}$$

The general solution of equation (15.21) is :

$$u_r = C_1 r + \frac{C_2}{r^2} \tag{15.22}$$

For the hollow sphere of inner radius a and outer radius b the constants C_1 and C_2 must be determined from the condition that :

$$\begin{cases}\sigma_{rr}\left(r=a\right)=p_i\\ \sigma_{rr}\left(r=b\right)=p_e\end{cases} \tag{15.23}$$

From the strain-displacement relation and Hooke's law the non-zero stress components for this case are:

$$\begin{aligned}\sigma_{rr} &= \left(3\lambda+2\mu\right)\left[C_1-\alpha\left(T_0-T_R\right)\right]-\frac{4\mu C_2}{r^3};\\ \sigma_{\theta\theta}=\sigma_{\phi\phi} &= \left(3\lambda+2\mu\right)\left[C_1-\alpha\left(T_0-T_R\right)\right]+\frac{2\mu C_2}{r^3};\end{aligned} \tag{15.24}$$

By substituting the stress functions (15.24) in boundary conditions (15.23), we determine the constants integration C_1 and C_2 :

$$C_1=\alpha\left(T_0-T_R\right)+\frac{p_e b^3-p_i a^3}{\left(3\lambda+2\mu\right)\left(b^3-a^3\right)};\quad C_2=\frac{a^3b^3\left(p_e-p_i\right)}{4\mu\left(b^3-a^3\right)}; \tag{15.25}$$

Finally, the displacement solution for a hollow sphere is :

$$u_r=\alpha\left(T_0-T_R\right)r+\frac{1}{\left(b^3-a^3\right)}\left[\left(p_e-p_i\right)\frac{a^3b^3}{4\mu}r+\frac{p_e b^3-p_i a^3}{\left(3\lambda+2\mu\right)}\frac{1}{r^2}\right] \tag{15.26}$$

The strain components are:

$$\begin{aligned}\varepsilon_{rr} &= \alpha\left(T_0-T_R\right)+\frac{1}{\left(b^3-a^3\right)}\left[-\left(p_e-p_i\right)\frac{a^3b^3}{2\mu}\frac{1}{r^3}+\frac{p_e b^3-p_i a^3}{\left(3\lambda+2\mu\right)}\right];\\ \varepsilon_{\theta\theta}=\varepsilon_{\phi\phi} &= \alpha\left(T_0-T_R\right)+\frac{1}{\left(b^3-a^3\right)}\left[\left(p_e-p_i\right)\frac{a^3b^3}{4\mu}\frac{1}{r^3}+\frac{p_e b^3-p_i a^3}{\left(3\lambda+2\mu\right)}\right]\end{aligned} \tag{15.27}$$

The stress components are:

$$\begin{aligned}\sigma_{rr} &= \frac{1}{\left(b^3-a^3\right)}\left[p_e b^3\left(1-\frac{a^3}{r^3}\right)+p_i a^3\left(\frac{b^3}{r^3}-1\right)\right];\\ \sigma_{\theta\theta}=\sigma_{\phi\phi} &= \frac{1}{2\left(b^3-a^3\right)}\left[p_e b^3\left(2+\frac{a^3}{r^3}\right)-p_i a^3\left(2+\frac{b^3}{r^3}\right)\right]\end{aligned} \tag{15.28}$$

If the external pressure vanishing $p_e=0$, the internal pressure $p_i=-p_0$, and thickness of hollow sphere is very small ($\frac{s}{a}=\frac{b-a}{a}<<1$), we obtain the well known approximate formula for spherical tank subjected to internal uniform pressure:

$$\sigma_{rr} \cong 0; \quad \sigma_{\theta\theta} = \sigma_{\phi\phi} \cong \frac{p_0\, a}{2\, s}; \tag{15.29}$$

where $s = b - a$ is the thickness of the hollow sphere.
For example, let us consider a hollow sphere characterized by following relations:

$$b = (1+\bar{s})\, a, \quad \bar{s} = s/a, \quad T_0 = T_R \tag{15.30}$$

where s is the thickness of the hollow sphere: $b - a = s$ and $\bar{s}$ is the ratio between the thickness and the inner radius. Moreover, the sphere is subjected to uniform pressure $p_i = -p_0$ for r = a and $p_e = 0$ for r = b. Let us assume the following non-dimensional parameter for graphics of the displacement, strain and stress functions:

$$\bar{r} = \frac{r-a}{b-a} = \frac{r-a}{\bar{s}\, a}; \ \bar{\sigma}_{rr} = \frac{\sigma_{rr}}{p_0}; \ \bar{\sigma}_{\theta\theta} = \bar{\sigma}_{\phi\phi} = \frac{\sigma_{\theta\theta}}{p_0}; \ \bar{\sigma}_{eq} = \frac{\sigma_{eq}}{p_0}; \ \sigma_{eq} = \sqrt{(\sigma_{rr} - \sigma_{\theta\theta})^2}; \tag{15.31}$$

By applying the relations (15.31), we obtain that the non-dimensional stress components $\bar{\sigma}_{rr}, \bar{\sigma}_{\theta\theta}, \bar{\sigma}_{\phi\phi}, \bar{\sigma}_{eq}$ depend only two parameters $\bar{s}$ and $\bar{r}$, as reported below:

$$\begin{aligned}
&\bar{\sigma}_{rr} = \frac{(\bar{r}-1)\left\{3+\bar{s}\left[3+\bar{s}+(3+\bar{r})\,\bar{s}\,\bar{r}\right]\right\}}{(1+\bar{s}\,\bar{r})^3\left[3+\bar{s}\,(3+\bar{s})\right]}; \quad \bar{\sigma}_{eq} = \frac{3(1+\bar{s})^3}{2\bar{s}\,(1+\bar{s}\,\bar{r})^3\left[3+\bar{s}\,(3+\bar{s})\right]}; \\
&\bar{\sigma}_{\theta\theta} = \bar{\sigma}_{\phi\phi} = \frac{3+3\bar{s}\left[\bar{s}\left(2\bar{r}^2+1\right)+1+2\bar{r}\right]+\bar{s}^3\left(2\bar{r}^3+1\right)}{2\bar{s}\,(1+\bar{s}\,\bar{r})^3\left[3+\bar{s}\,(3+\bar{s})\right]};
\end{aligned} \tag{15.32}$$

The distribution of the non-dimensional stress components along radial direction are reported below:

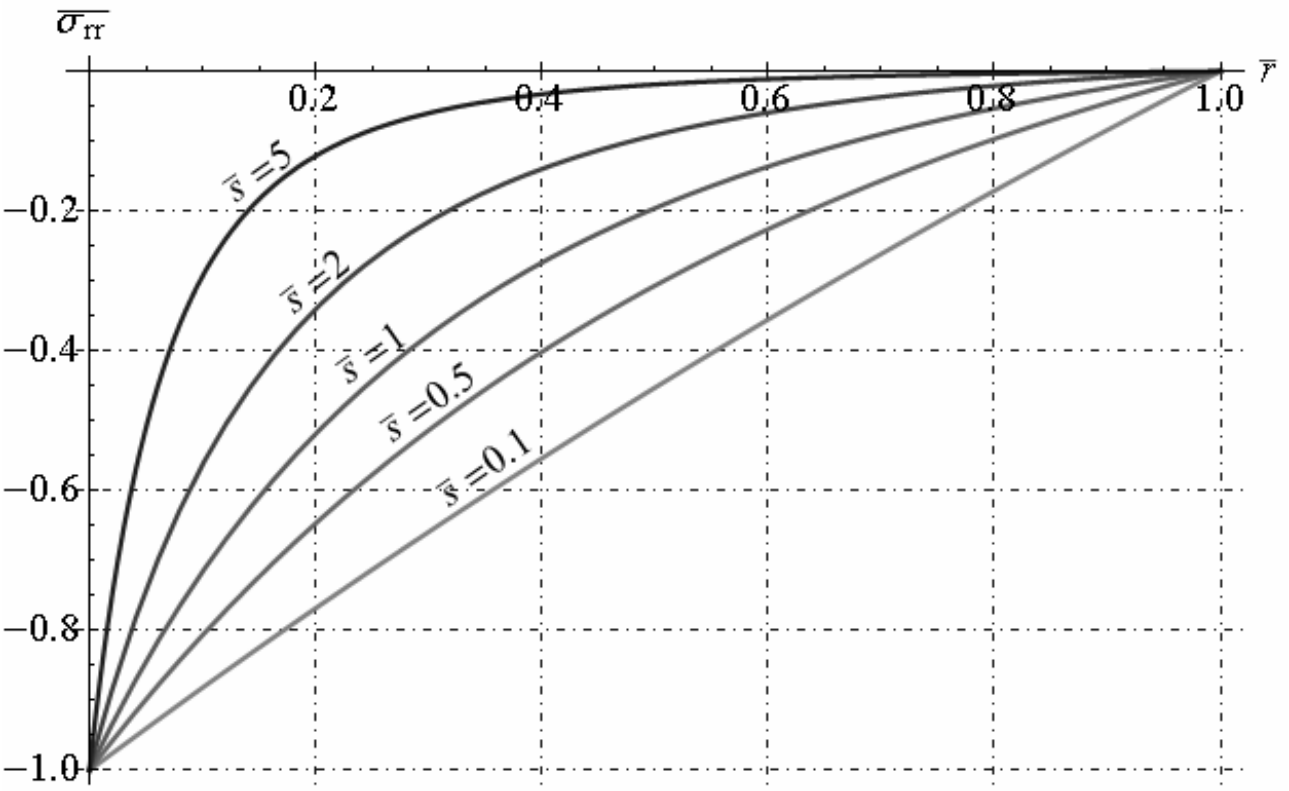

Fig. 15.1 - *Non-dimensional radial stress distribution along radial direction*

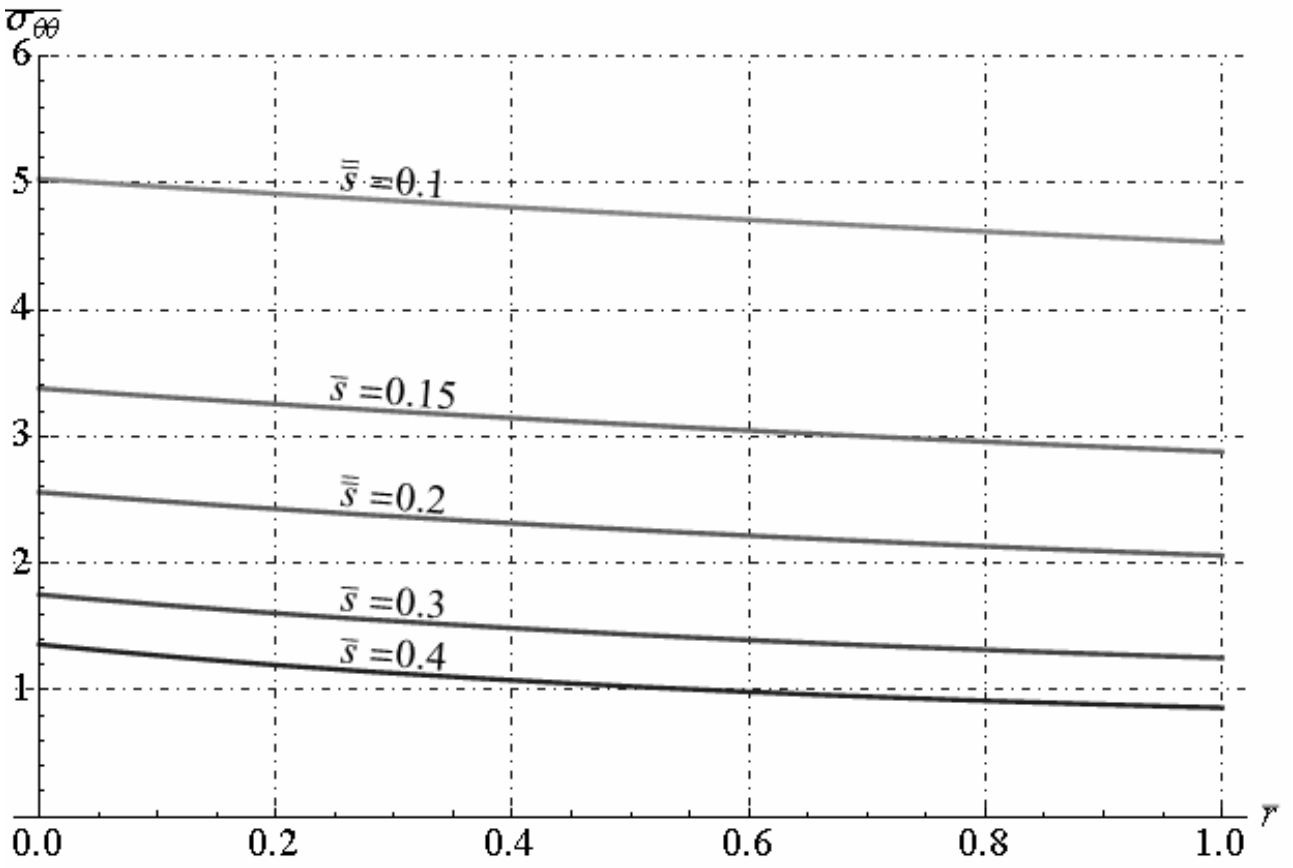

Fig. 15.2 - *Non-dimensional circumferential stress distribution along radial direction*

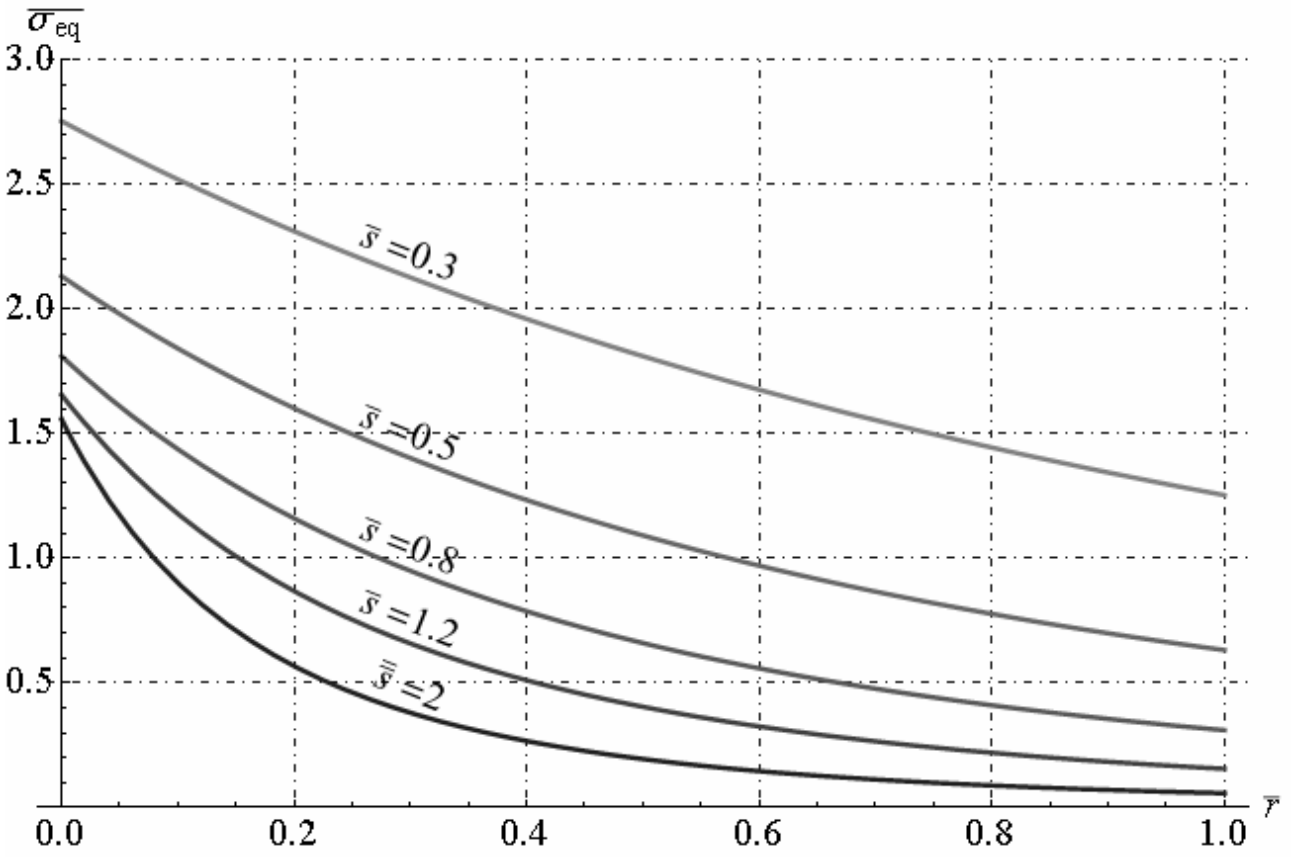

Fig. 15.3 - *Non-dimensional equivalent stress distribution along radial direction*

15.4. Radial temperature variation and uniform pressure

Let us consider a hollow sphere with inner radius "a" and outer radius "b", subjected to uniform pressure for r = a equal to $p_i = -p_0$. Moreover the hollow sphere is subjected to radial temperature variation. In this case, the equilibrium equation is reported in equation (15.2) and Fourier's equation is reported in equation (15.16) for coupled thermo-elastic problem (or equivalent equation (15.3) for uncoupled thermo-elastic problem). The general solution of the equilibrium equation in terms of radial displacement function is given by equation (15.4). In this case, the boundary conditions for the hollow sphere of inner radius a and outer radius b are:

$$\begin{cases} \sigma_{rr}(r=a) = -p_0 \\ \sigma_{rr}(r=b) = 0 \end{cases} \tag{15.33}$$

By solving the equations (15.33) we obtain the functions $f_1(t)$ and $f_2(t)$ as reported below:

$$\begin{aligned} f_1(t) &= -\alpha T_R + \frac{1}{\left(b^3-a^3\right)}\left[\frac{p_0 a^3}{(3\lambda+2\mu)} + \frac{4\alpha\mu}{(\lambda+2\mu)}\int_a^b \xi^2 T(\xi,t)\,d\xi\right]; \\ f_2(t) &= \frac{a^3}{\left(b^3-a^3\right)}\left[\frac{p_0 b^3}{4\mu} + \frac{\alpha(3\lambda+2\mu)}{(\lambda+2\mu)}\int_a^b \xi^2 T(\xi,t)\,d\xi\right] \end{aligned} \tag{15.34}$$

By substituting the function of the time $f_1(t)$ and $f_2(t)$ in equation (15.4), we determine the displacement solution:

$$\begin{aligned} u_r &= \frac{p_0 a^3}{\left(b^3-a^3\right)}\left[\frac{b^3}{4\mu}r + \frac{1}{(3\lambda+2\mu)r^2}\right] - \alpha T_R\, r + \\ &+ \frac{\alpha}{\left(b^3-a^3\right)}\left(\frac{3\lambda+2\mu}{\lambda+2\mu}\right)\left[\frac{a^3}{r^2}\int_r^b \xi^2 T(\xi,t)\,d\xi + \frac{b^3}{r^2}\int_a^r \xi^2 T(\xi,t)\,d\xi + \frac{4\mu r}{3\lambda+2\mu}\int_a^b \xi^2 T(\xi,t)\,d\xi\right] \end{aligned} \tag{15.35}$$

The stress components are:

$$\begin{aligned} \sigma_{rr} &= \frac{p_0\, a^3}{\left(b^3-a^3\right)}\left(\frac{b^3}{r^3}-1\right) + \\ &+ \frac{4\mu\alpha}{a^3-b^3}\left(\frac{3\lambda+2\mu}{\lambda+2\mu}\right)\left[\frac{a^3}{r^2}\int_r^b \xi^2 T(\xi,t)\,d\xi + \frac{b^3}{r^2}\int_a^r \xi^2 T(\xi,t)\,d\xi - \int_a^b \xi^2 T(\xi,t)\,d\xi\right]; \\ \sigma_{\theta\theta} = \sigma_{\phi\phi} &= \frac{p_0\, a^3}{2\left(b^3-a^3\right)}\left(2+\frac{b^3}{r^3}\right) + \\ &\frac{2\mu\alpha}{b^3-a^3}\left(\frac{3\lambda+2\mu}{\lambda+2\mu}\right)\left[\frac{a^3}{r^2}\int_r^b \xi^2 T(\xi,t)\,d\xi + \frac{b^3}{r^2}\int_a^r \xi^2 T(\xi,t)\,d\xi + 2\int_a^b \xi^2 T(\xi,t)\,d\xi + \left(a^3-b^3\right)T(r,t)\right] \end{aligned} \tag{15.36}$$

15.5 Steady-state problem with radial temperature variation

Let us consider a hollow sphere with inner radius "a" and outer radius "b" , subjected to radial temperature variation. In this section we study the steady-state problem, then the temperature displacement, strain and stress components are functions only variable r. Let us consider the case in which the inner surface r = a is exposed, to an ambient at temperature T_i and external surface r = b is exposed to a temperature T_e. The differential equation related to heat conduction and the corresponding boundary conditions are reported below:

$$\frac{d^2T(r)}{dr^2} + \frac{2}{r}\frac{dT(r)}{dr} = 0; \quad a < r < b, \tag{15.37}$$

$$T\left(r=a\right)=T_i, \tag{15.38}$$

$$T\left(r=b\right)=T_e, \tag{15.39}$$

By solving the differential equation (15.37), we obtain the function of temperature:

$$T\left(r\right)=A_1+\frac{A_2}{r} \tag{15.40}$$

where A_1, A_2 are constants integration to determine. By solving the boundary conditions (15.38)-(15.39), we determine the constants integration as reported below:

$$A_1=\frac{bT_e-aT_i}{b-a},\ A_2=\frac{ab\left(T_e-T_i\right)}{a-b}; \tag{15.41}$$

By substituting the expressions of constants integration (15.41) in equation (15.40) , we obtain the function of the temperature:

$$T\left(r\right)=\frac{1}{\left(a-b\right)}\left[\frac{ab\left(T_e-T_i\right)}{r}+aT_i-bT_e\right]; \tag{15.42}$$

If the hollow sphere is subjected to radial temperature variation and zero external load, let us assume that the displacement components reduce to sole $u_r=u_r(r)$. In this case the equilibrium equations reduce to one ordinary differential equation as reported below:

$$\frac{d}{dr}\left[\frac{1}{r^2}\frac{d\left(r^2u_r\right)}{\partial r}\right]=\alpha\left(\frac{1+\nu}{1-\nu}\right)\frac{dT}{dr} \tag{15.43}$$

The general solution of equation (15.43) is :

$$u_r(r)=\frac{\alpha\left(1+\nu\right)}{r^2\left(1-\nu\right)}\int_a^r\xi^2T\left(\xi\right)d\xi+C_1r+\frac{C_2}{r^2} \tag{15.44}$$

where C_1, C_2 are constants integration to determine. By substituting the function (15.42) in equation (15.44) , we determine the expression of the displacement solution are reported below:

$$u_r=D_1r+\frac{D_2}{r^2}+D_3 \tag{15.45}$$

where D_1, D_2, D_3 are following constants:

$$\begin{aligned}&D_1=C_1+\frac{\alpha\left(1+\nu\right)\left[bT_e-aT_i\right]}{3\left(1-\nu\right)\left(b-a\right)};\quad D_2=C_2+\frac{\alpha\left(1+\nu\right)a^3\left[b\left(T_e-3T_i\right)+2aT_i\right]}{6\left(1-\nu\right)\left(b-a\right)};\\&D_3=-\frac{\alpha\left(1+\nu\right)ab\left(T_e-T_i\right)}{2\left(1-\nu\right)\left(b-a\right)};\end{aligned} \tag{15.46}$$

By applying the strain-displacement relationship, we determine the non-zero strain components:

$$\varepsilon_{rr}=D_1-\frac{2D_2}{r^3};\quad \varepsilon_{\theta\theta}=\varepsilon_{\phi\phi}=D_1+\frac{D_2}{r^3}+\frac{D_3}{r}; \tag{15.47}$$

By applying the stress-strain relationship, we obtain the non-zero stress components:

$$\begin{aligned}&\sigma_{rr}=\left(\frac{2E}{1-2\nu-\nu^2}\right)\left[\frac{\left(1+\nu\right)}{2}D_1-\left(1-2\nu\right)\frac{D_2}{r^3}+\nu\frac{D_3}{r}\right]-\frac{\alpha E}{1-2\nu}\left(\frac{A_1}{r}+A_2-T_R\right)\\&\sigma_{\theta\theta}=\sigma_{\phi\phi}=\left(\frac{E}{1-2\nu-\nu^2}\right)\left[\left(1+\nu\right)D_1+\left(1-2\nu\right)\frac{D_2}{r^3}+\frac{D_3}{r}\right]-\frac{\alpha E}{1-2\nu}\left(\frac{A_1}{r}+A_2-T_R\right)\end{aligned} \tag{15.48}$$

The boundary conditions of zero tractions on the cylindrical surfaces are then

$$\sigma_{rr}=0\quad at\quad r=a\ \text{ and }\ r=b \tag{15.49}$$

By solving the equations (15.49), respect to integration constants C_1, C_2, we obtain the explicit expressions of the coefficient D_1, D_2, D_3 as reported below:

$$D_1=\alpha\left[\frac{\left(T_e b^3-T_i a^3\right)}{\left(b^3-a^3\right)}+\frac{\nu\left(T_e-T_i\right)a\,b\left(a+b\right)}{\left(1-\nu\right)\left(b^3-a^3\right)}-T_R\right];$$
$$D_2=\frac{\alpha\left(1+\nu\right)a^3b^3\left(T_e-T_i\right)}{2\left(1-\nu\right)\left(b^3-a^3\right)};\quad D_3=-\frac{\alpha\left(1+\nu\right)a\,b\left(T_e-T_i\right)}{2\left(1-\nu\right)\left(b-a\right)};\tag{15.50}$$

If the thickness of hollow sphere is very small respect to radius ($\frac{s}{a}=\frac{b-a}{a}<<1$), we obtain the well known approximate formula for spherical tank subjected to temperature gradient :

$$u_r\cong\frac{\alpha\left(T_e-T_i\right)a}{2};\ \varepsilon_{rr}\cong\frac{\alpha\left(T_e-T_i\right)}{\left(1-\nu\right)};\ \varepsilon_{\theta\theta}=\varepsilon_{\phi\phi}\cong\frac{\alpha\left(T_e-T_i\right)}{2};$$
$$\sigma_{rr}\cong 0;\quad \sigma_{\theta\theta}=\sigma_{\phi\phi}\cong\frac{\alpha E\left(T_e-T_i\right)}{2\left(\nu-1\right)};\tag{15.51}$$

For example, let us consider a hollow sphere characterized by following relations:

$$b=\left(1+\bar{s}\right)a,\quad \bar{s}=s/a,\quad T_i=T_R\tag{15.52}$$

where "s" is the thickness of the hollow sphere: $b-a=s$ and $\bar{s}$ is the ratio between the thickness and the inner radius. Moreover, the sphere is subjected to temperature gradient $\Delta T=T_e-T_i$. Let us assume the following non-dimensional parameter for graphics of the displacement, strain and stress functions:

$$\bar{r}=\frac{r-a}{b-a}=\frac{r-a}{\bar{s}\,a};\ \bar{\sigma}_{rr}=\frac{\sigma_{rr}}{\beta};\ \bar{\sigma}_{\theta\theta}=\bar{\sigma}_{\phi\phi}=\frac{\sigma_{\theta\theta}}{\beta};$$
$$\beta=\frac{\alpha E\Delta T}{2\left(1-\nu\right)};\ \bar{\sigma}_{eq}=\frac{\sigma_{eq}}{\beta};\ \sigma_{eq}=\sqrt{\left(\sigma_{rr}-\sigma_{\theta\theta}\right)^2};\tag{15.53}$$

By applying the relations (15.53), we obtain that the non-dimensional stress components $\bar{\sigma}_{rr},\bar{\sigma}_{\theta\theta},\bar{\sigma}_{\phi\phi},\bar{\sigma}_{eq}$ depend only two parameters $\bar{s}$ and $\bar{r}$, as reported below:

$$\bar{\sigma}_{rr}=\frac{2\bar{s}\,\bar{r}\left(1-\bar{r}\right)\left(1+\bar{s}\right)\left[3+\bar{s}\left(2+\bar{r}\left(2+\bar{s}\right)\right)\right]}{\left(1+\bar{s}\,\bar{r}\right)^3\left[3+\bar{s}\left(3+\bar{s}\right)\right]};$$
$$\bar{\sigma}_{\theta\theta}=\bar{\sigma}_{\phi\phi}=-\frac{\left(1+\bar{s}\right)\left[\bar{r}\left(6+\bar{s}\left(-2\bar{s}+\bar{r}\left(9+\bar{s}\left(3-\bar{s}+2\bar{r}\left(2+\bar{s}\right)\right)\right)\right)\right)-3-2\bar{s}\right]}{\left(1+\bar{s}\,\bar{r}\right)^3\left[1+\left(1+\bar{s}\right)^3\right]};\tag{15.54}$$
$$\bar{\sigma}_{eq}=\frac{\left(1+\bar{s}\right)\left[\bar{r}\left(2+\bar{s}\,\bar{r}\right)\left(3+\bar{s}\left(3+\bar{s}\right)\right)-3-2\bar{s}\right]}{\left(1+\bar{s}\,\bar{r}\right)^3\left[3+\bar{s}\left(3+\bar{s}\right)\right]};$$

The distribution of the non-dimensional stress components along radial direction are reported below:

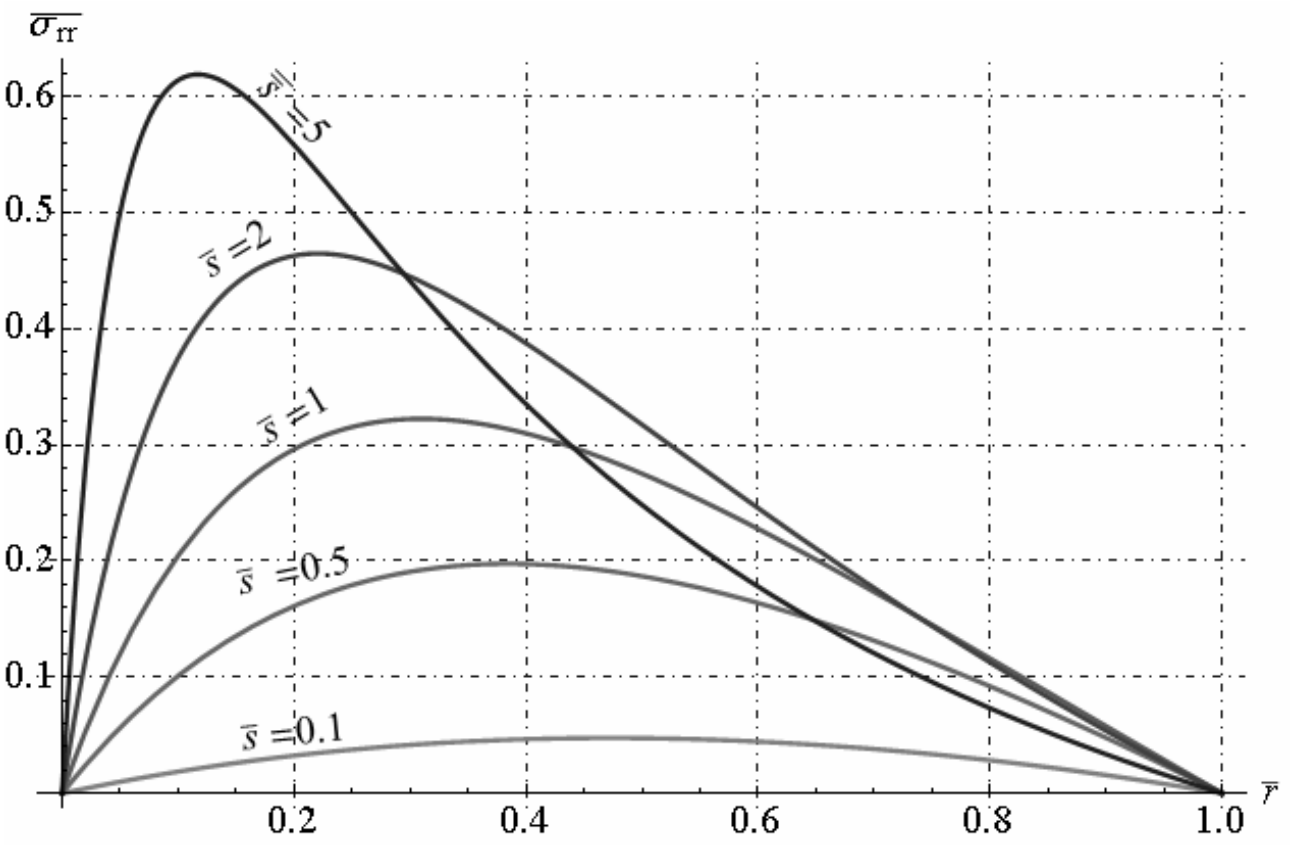

Fig. 15.4 - *Non-dimensional radial stress distribution along radial direction*

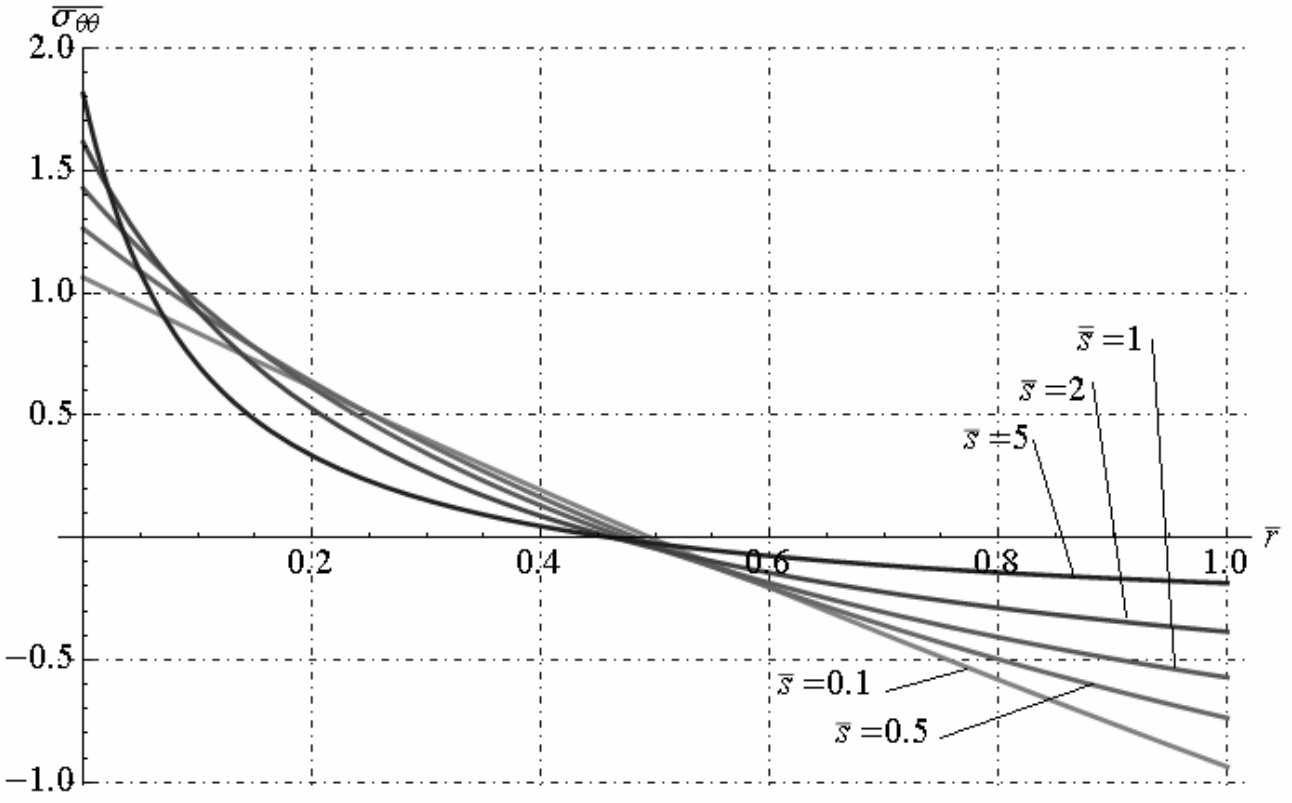

Fig. 15.5 - *Non-dimensional circumferential stress distribution along radial direction*

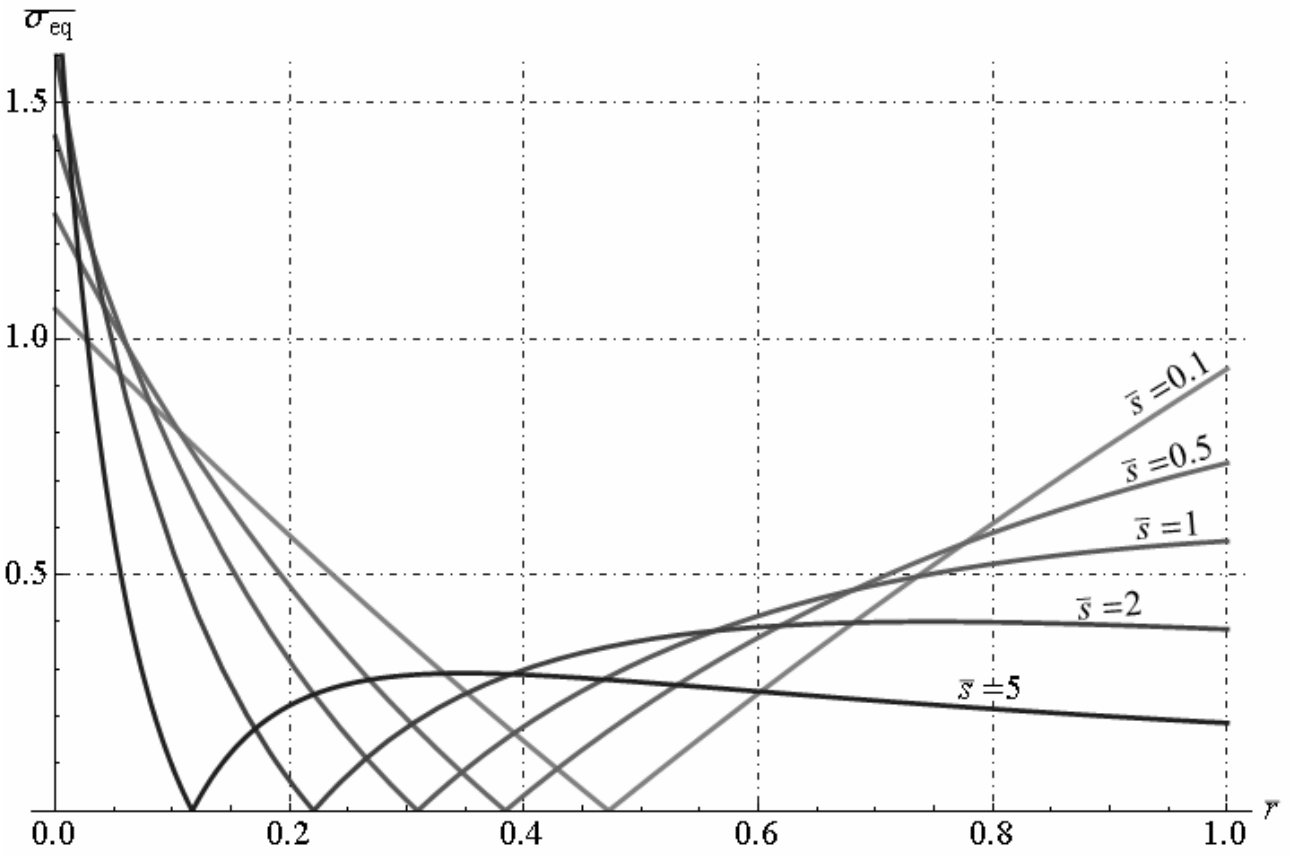

Fig. 15.6 - *Non-dimensional equivalent stress distribution along radial direction*

15.6. Uncoupled thermo-elastic analysis in hollow sphere exposed to an ambient at zero temperature through a uniform boundary conductance

Let us consider an hollow sphere with inner radius "a" and outer radius "b" , subjected to radial temperature variation. The surface r = a is kept perfectly insulated while the surface r = b is exposed, for t >0, to an ambient at zero temperature through a uniform boundary conductance h. The initial temperature (for t = 0) of the hollow sphere is $T_0 = T_R = const$ where $T_R > 0$. In this section, we determine the heat conduction, displacement and stress function in hollow sphere under decreasing of temperature from $T_R > 0$ until to zero. The differential equation related to heat conduction and the corresponding boundary conditions are reported below:

$$\frac{\partial^2 T}{\partial r^2} + \frac{2}{r}\frac{\partial T}{\partial r} = \frac{1}{\kappa}\frac{\partial T}{\partial t}; \quad a < r < b, \quad t > 0 \tag{15.55}$$

$$-k\frac{\partial T}{\partial r} = 0, \quad r = a, \ t > 0, \tag{15.56}$$

$$-k\frac{\partial T}{\partial r} = hT; \quad r = b, \ t > 0, \tag{15.57}$$

$$T = T_R; \quad a < r < b, \quad t = 0, \tag{15.58}$$

where $T_0 = T_R$ is a suitable chosen reference temperature in initial condition (for t = 0). The problem is therefore on with homogeneous differential equation and boundary conditions and may be treated by the method separation of variables. As in eq.(15.55), a particular solution of the differential equation and boundary conditions of the form:

$$T(r,t) = \varphi(r)\,\psi(t) \tag{15.59}$$

By substituting the function (15.59) in eqs. (15.55)-(15.57), we obtain:

$$\frac{d^2\varphi}{d\,r^2}+\frac{2}{r}\frac{d\varphi}{d\,r}+\omega^2\varphi=0; \tag{15.60}$$

$$-k\frac{d\,\varphi}{d\,r}=0;\quad r=a, \tag{15.61}$$

$$-k\frac{d\,\varphi}{d\,r}=h\varphi;\quad x=b, \tag{15.62}$$

And to the following equation for $\psi(t)$:

$$\frac{d\psi}{dt}+\omega^2\kappa\psi=0 \tag{15.63}$$

The general solution of (15.63) is:

$$\psi(t)=e^{-\omega^2\kappa t} \tag{15.64}$$

The general solution of (15.60) is:

$$\varphi(r)=r^{-1}\left[C_1e^{i\,\omega r}+C_2e^{-i\,\omega r}\right] \tag{15.65}$$

where C_1, C_2 are constants integration. From (15.61) it is deduced that the constant C_2 is given by:

$$C_2=\left[\frac{(i+\omega a)^2}{1+\omega^2\,a^2}\right]C_1e^{2\,i\,\omega a} \tag{15.66}$$

The equations (15.61) and (15.62) are an homogenous algebraic system as reported below :

$$[\mathbf{\Lambda}]\cdot\begin{bmatrix}C_1\\C_2\end{bmatrix}=\begin{bmatrix}0\\0\end{bmatrix} \tag{15.67}$$

where the matrix $[\mathbf{\Lambda}]$ is given by:

$$[\mathbf{\Lambda}]=\begin{bmatrix}(1-ia\omega)e^{ia\omega} & (1+ia\omega)e^{-ia\omega}\\ \left(1-ib\omega-\dfrac{bh}{k}\right)e^{ib\omega} & \left(1+ib\omega-\dfrac{bh}{k}\right)e^{-ib\omega}\end{bmatrix} \tag{15.68}$$

The algebraic system (15.67) admit not trivial solution if the determinant of the matrix $[\mathbf{\Lambda}]$ is equal to zero. By imposing this condition, we obtain the transcendental equation in unknown parameter ω:

$$\begin{aligned}\det[\mathbf{\Lambda}]=g(\omega)=\omega\cos\left[\omega(a-b)\right]\left[a\,b\,h+k(b-a)\right]+\\ +\sin\left[\omega(a-b)\right]\left[k\left(1+a\,b\,\omega^2\right)-b\,h\right]=0\end{aligned} \tag{15.69}$$

Finally, we can rewrite the equation (15.69) in follows manner:

$$\tan\left[\omega(a-b)\right]=\frac{\omega\left[a\,b\,h+k(b-a)\right]}{b\,h-k\left(1+a\,b\,\omega^2\right)} \tag{15.70}$$

The roots of this transcendental equation (15.70) are an infinite number such, denoted here by ω_m, $m=1,2,....\infty$ leading to eigenvalues or characteristic values $\lambda_m=-\omega_m^2$. The corresponding eigenfunctions or characteristic functions $\overline{\varphi}_m(r)$ are, as calculated above,

$$\begin{aligned}\overline{\varphi}_m(r)=\frac{\varphi_m(r)}{C_{1m}}=\frac{1}{r}\left[\cos(\omega_m r)+i\sin(\omega_m r)\right]+\\ +\frac{(i+\omega a)^2}{\left(1+\omega^2\,a^2\right)r}\left\{\cos\left[\omega_m(2a-r)\right]-i\sin\left[\omega_m(2a-r)\right]\right\}\end{aligned} \tag{15.71}$$

The solution to the problem may therefore be written in the form:

$$T(r,t)=\sum_{m=1}^{\infty} C_{1m}\,\bar{\varphi}_m(r)\,e^{-\omega_m^2\kappa t} \tag{15.72}$$

where the coefficients C_{1m} are determined by applying the initial condition (15.58) that yields the following relationship:

$$C_{1m}=\frac{\int_0^{2\pi}\int_0^{\pi}\int_a^b T_R\,\bar{\varphi}_m(r)\,r^2\sin\theta\,dr\,d\theta\,d\phi}{\int_0^{2\pi}\int_0^{\pi}\int_a^b \bar{\varphi}_m^{-2}(r)\,r^2\sin\theta\,dr\,d\theta\,d\phi} \tag{15.73}$$

By applying the relationship (15.73) we obtain the explicit expression of the constant C_{1m} as reported below:

$$C_{1m}=-\frac{2T_R e^{i\omega_m a}\left(a\,\omega_m-i\right)\left\{(b-a)\,\omega_m\cos\left[(a-b)\,\omega_m\right]+\left(1+a\,b\,\omega_m^2\right)\sin\left[(a-b)\,\omega_m\right]\right\}}{\omega_m\left\{2\omega_m\left(b+a^2(a-b)\,\omega_m^2-a\cos\left[2(a-b)\,\omega_m\right]\right)+\left(1-a^2\omega_m^2\right)\sin\left[2(a-b)\,\omega_m\right]\right\}} \tag{15.74}$$

By substituting the constant C_{1m} in equation (15.72), we obtain the expression of function temperature $T(r,t)$. By applying the equations in section 15.1, we obtain displacement function and stress function in hollow sphere . The displacement function is given by eq. (15.8)

$$u_r=-\alpha T_R r+\sum_{m=1}^{\infty}\frac{C_{1n}\,e^{-\omega_m^2\kappa t}}{b^3-a^3}\alpha\left(\frac{3\lambda+2\mu}{\lambda+2\mu}\right)\left[\frac{a^3}{r^2}\int_r^b\varphi_m\,r^2dr+\frac{b^3}{r^2}\int_a^r\varphi_m r^2dr+\frac{4\mu r}{3\lambda+2\mu}\int_a^b\varphi_m r^2dr\right] \tag{15.75}$$

The radial stress is given by:

$$\sigma_{rr}=\sum_{m=1}^{\infty}\frac{4\mu\alpha C_{1m}\,e^{-\omega_m^2\kappa t}}{a^3-b^3}\left(\frac{3\lambda+2\mu}{\lambda+2\mu}\right)\left[\frac{a^3}{r^2}\int_r^b\varphi_m r^2dr+\frac{b^3}{r^2}\int_a^r\varphi_m r^2dr-\int_a^b\varphi_m r^2dr\right] \tag{15.76}$$

The circumferential stress is reported below:

$$\sigma_{\theta\theta}=\sigma_{\phi\phi}=$$

$$=\sum_{m=1}^{\infty}\frac{2\mu\alpha C_{1m}\,e^{-\omega_m^2\kappa t}}{b^3-a^3}\left(\frac{3\lambda+2\mu}{\lambda+2\mu}\right)\left[\frac{a^3}{r^2}\int_r^b\varphi_m r^2dr+\frac{b^3}{r^2}\int_a^r\varphi_m r^2dr+2\int_a^b\varphi_m r^2d\xi+\left(a^3-b^3\right)\varphi_m\right] \tag{15.77}$$

In explicit the function radial displacement given by equation (15.75) is reported below:

$$u_r=-\alpha T_R r+\sum_{m=1}^{\infty}\left\{\begin{array}{l} Q_{1m}r+\frac{Q_{2m}}{r^2}+\\ +\frac{\alpha(3\lambda+2\mu)}{\omega_m^2(\lambda+2\mu)r^2}\left[C_{1m}\left(1-i\,\omega_m r\right)e^{i\omega_m r}+C_{2m}\left(1+i\,\omega_m r\right)e^{-i\omega_m r}\right]\end{array}\right\}e^{-\omega_m^2\kappa t} \tag{15.78}$$

where the constants integration C_{1m},C_{2m} are given by equations (15.74) and (15.66), respectively. The constants integrations Q_{1m},Q_{2m} are determined by solving the boundary conditions (15.5). In explicit the expressions of constants Q_{1m},Q_{2m} are given by:

$$\begin{aligned} Q_{1m}&=\frac{4\alpha\mu e^{-ib\omega_m}\left[e^{2ib\omega_m}(a\,\omega_m-i)(i+b\,\omega_m)-e^{2ia\omega_m}(i+a\,\omega_m)(b\,\omega_m-i)\right]}{(b^3-a^3)(1+i\,a\,\omega_n)(\lambda+2\mu)\omega_n^2}C_{1m},\\ Q_{2m}&=\frac{\alpha(3\lambda+2\mu)a^3e^{-ib\omega_m}\left[e^{2ib\omega_m}(a\,\omega_m-i)(i+b\,\omega_m)-e^{2ia\omega_m}(i+a\,\omega_m)(b\,\omega_m-i)\right]}{(b^3-a^3)(1+i\,a\,\omega_m)(\lambda+2\mu)\omega_m^2}C_{1m},\end{aligned} \tag{15.79}$$

In explicit the radial and circumferential stress components are given by:

$$\sigma_{rr}=\sum_{m=1}^{\infty}\left\{\begin{array}{l}Q_{1m}\left(3\lambda+2\mu\right)-4\mu\,Q_{2m}\,r^{-3}+\\+\dfrac{4\alpha\mu\,i\left(3\lambda+2\mu\right)}{\omega_m^2\left(\lambda+2\mu\right)r^3}\left[C_{1m}\left(i+\omega_m\,r\right)e^{i\,\omega_m\,r}+C_{2m}\left(i-\omega_m\,r\right)e^{-i\,\omega_m\,r}\right]\end{array}\right\}e^{-\omega_m^2\kappa t} \tag{15.80}$$

$$\sigma_{\theta\theta}=\sum_{m=1}^{\infty}\left[Q_{1m}\left(3\lambda+2\mu\right)+2\mu\,Q_{2m}r^{-3}\right]e^{-\omega_m^2\kappa t}+$$

$$+\sum_{m=1}^{\infty}\left\{\frac{2\alpha\mu\left(3\lambda+2\mu\right)}{\omega_m^2\left(\lambda+2\mu\right)r^3}\left[C_{1m}\left(1-r\omega_m\left(1+i\,\omega_m\,r\right)\right)e^{i\,\omega_m\,r}+C_{2m}\left(1-r\omega_m\left(\omega_m\,r-i\right)\right)e^{-i\,\omega_m\,r}\right]\right\}e^{-\omega_m^2\kappa t} \tag{15.81}$$

For example, let us consider, a spherical tank constituted by steel, under decreasing temperature. The geometrical, mechanical and thermal parameters considered for spherical tank are reported below:

$$\begin{aligned}&E=210\cdot10^9\,N/m^2,\ \nu=0.3,\ c_v=440J/kg\cdot°K,\ k=45W/m\cdot°K,\\&\rho=7.8\cdot10^3kg/m^3,b=1.01m,\ \ a=1.00m,\ \ s=b-a=0.01m,\\&h=200W/m^2\cdot°K,\quad \alpha=1.2\cdot10^{-5}°K^{-1},\ \ T_0=T_R=300°K\end{aligned} \tag{15.82}$$

In this case the graphics function $g(\omega)$ given by equation (15.69) is reported below:

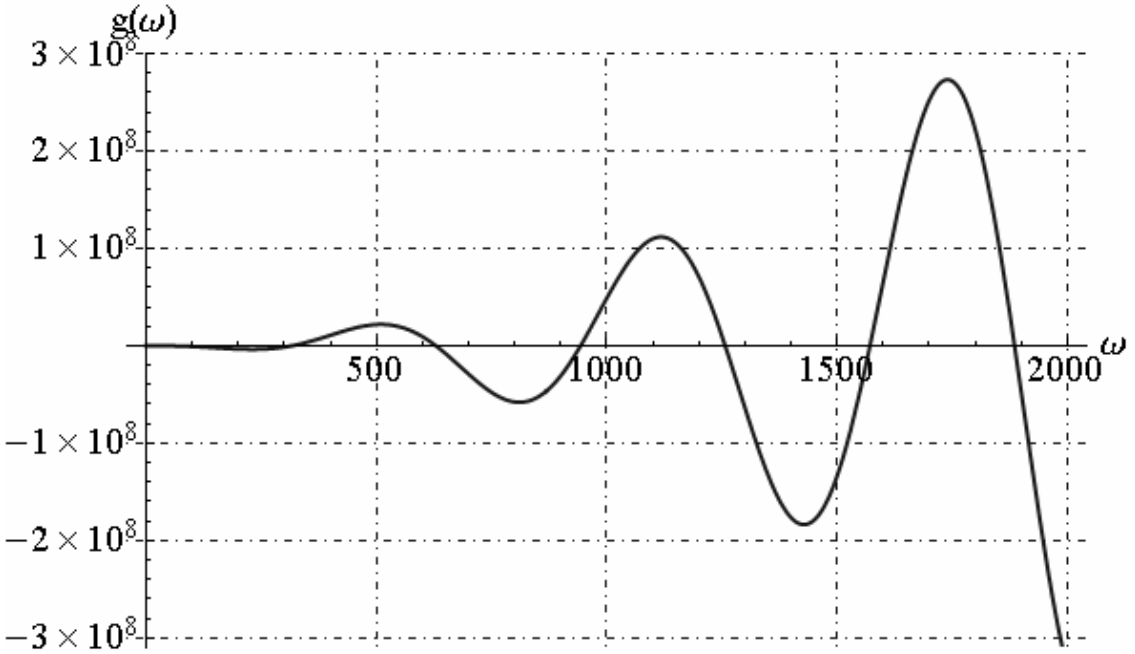

By fixed m= 20, the eigenvalues ω_m and corresponding values of constants integration A_m are reported in table 15.1:

ω_m	21.031	315.571	629.027	942.950	1256.991
A_m	-92.528 - 119.679 i	-0.209 + 1.330 i	0.258 - 0.222 i	-0.135 + 0.069 i	0.080 - 0.030 i
ω_m	1571.080	1885.192	2199.317	2513.451	2827.591
A_m	-0.0524 + 0.0153 i	0.0368 - 0.0089 i	-0.0273 + 0.0056 i	0.0210 - 0.0038 i	-0.0166 + 0.0026 i
ω_m	3141.734	3455.881	3770.029	4084.180	4398.331
A_m	0.0135 - 0.0019 i	-0.0112 + 0.0015 i	0.0094 - 0.0011 i	-0.0080 + 0.0009 i	0.0069 - 0.0007 i
ω_m	4712.484	5026.637	5340.791	5654.946	5969.101
A_m	-0.0060 + 0.0006 i	0.0053 - 0.0005 i	-0.0047 + 0.0004 i	0.0042 - 0.0003 i	-0.0038 + 0.0003 i

Table 15.1 – *Eigenvalues ω_m and corresponding values of constants integration A_m*

We reported the graphics of temperature function along the radial direction and in time:

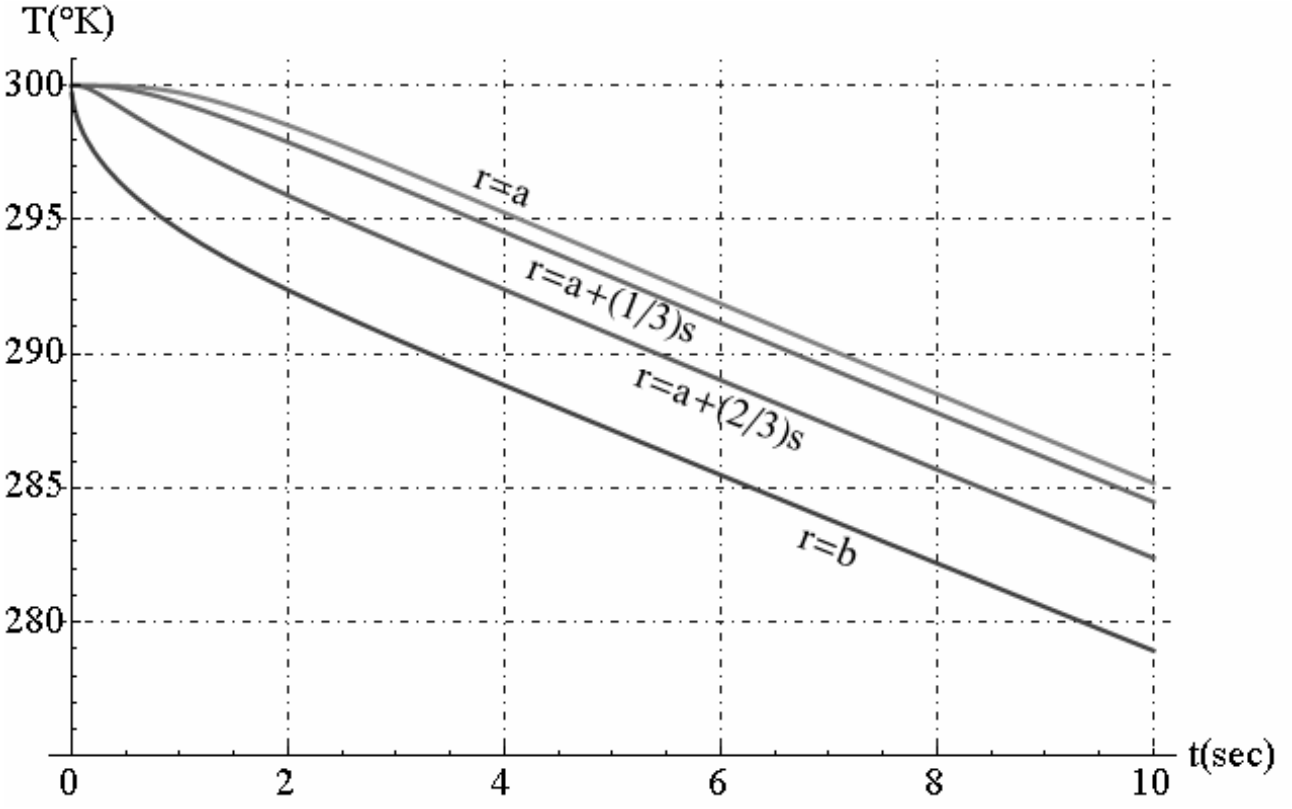

Fig. 15.7 - *Temperature function versus the time*

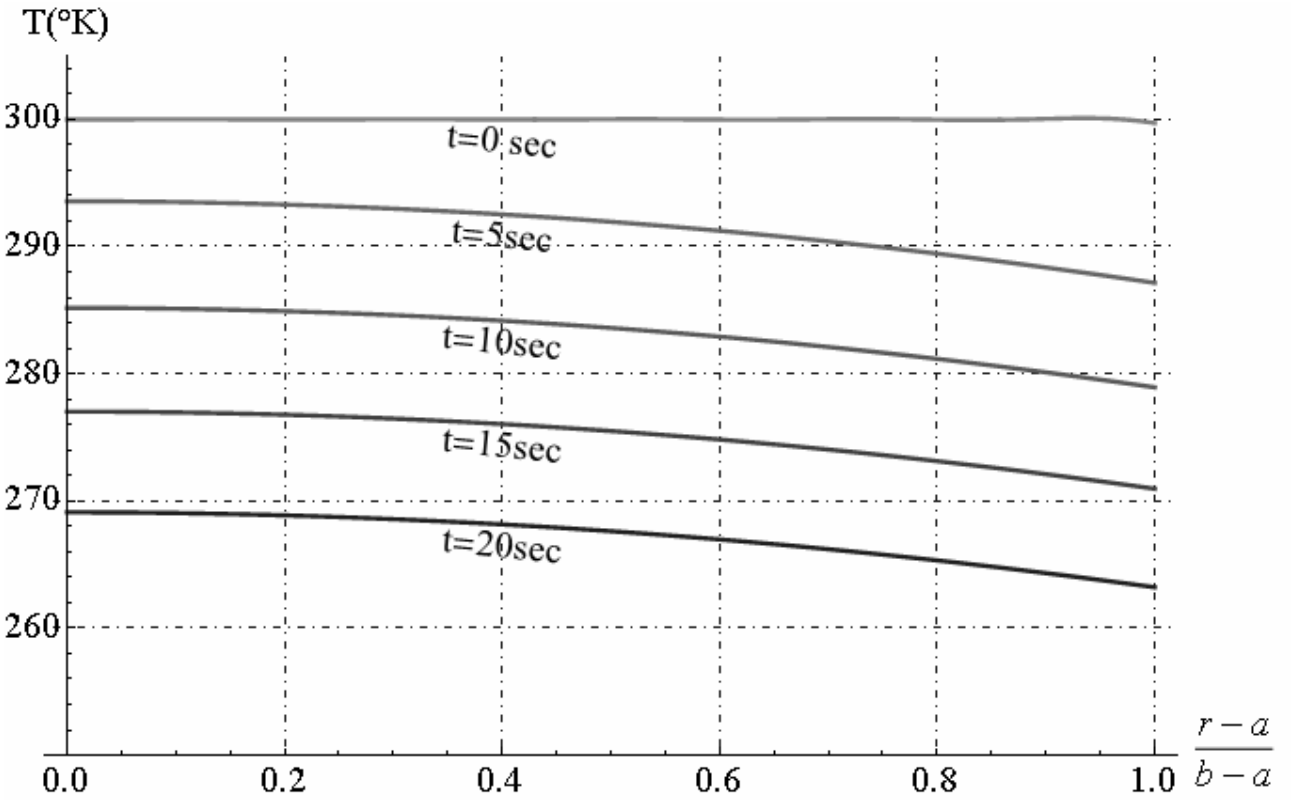

Fig. 15.8 - *Temperature function along radial direction*

We reported the graphic of radial displacement component function along the radial direction:

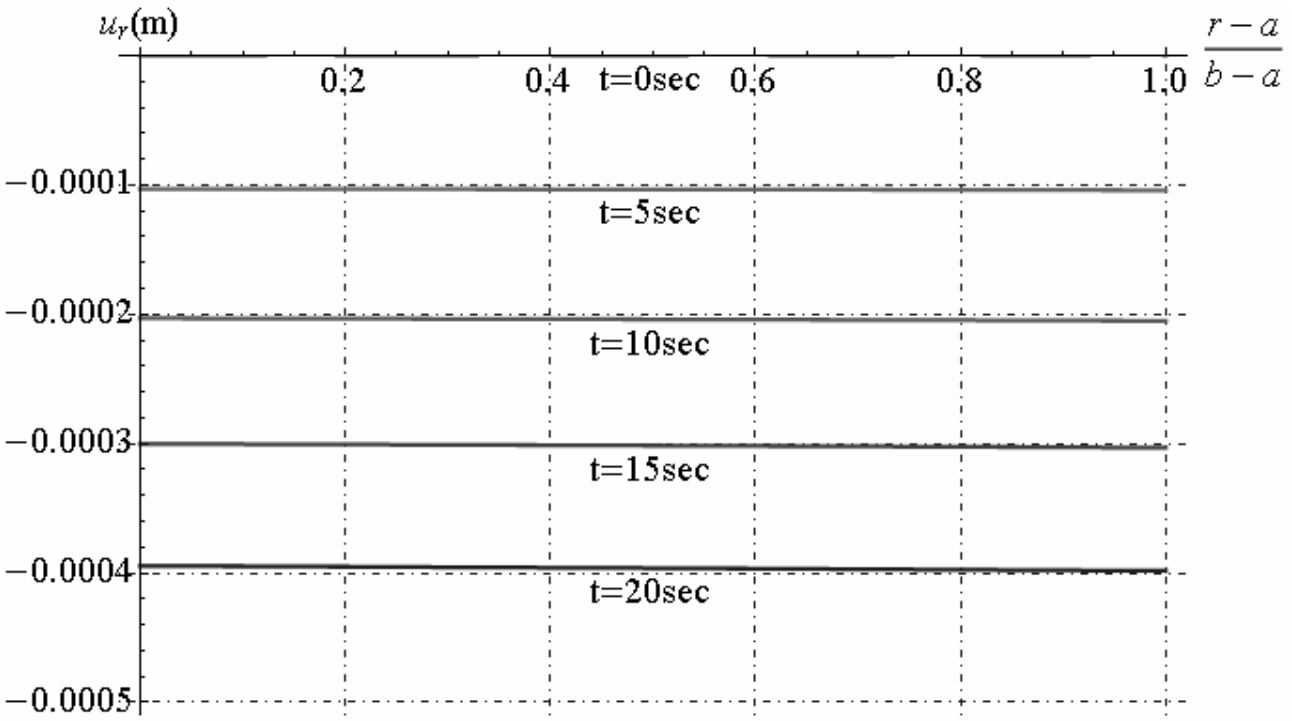

Fig. 15.9 - *Radial displacement distribution along radial direction*

We reported the graphics of stress components along the radial direction and in time:

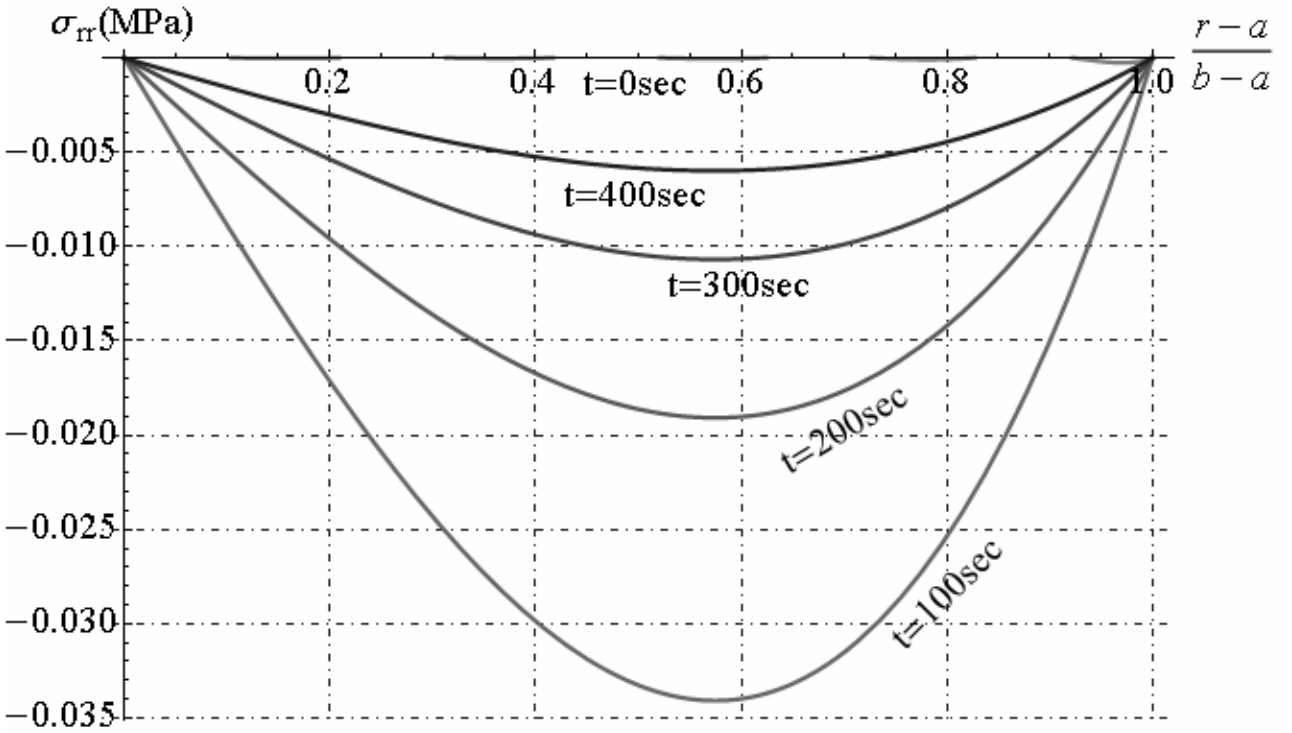

Fig. 15.10 - *Radial stress distribution along radial direction*

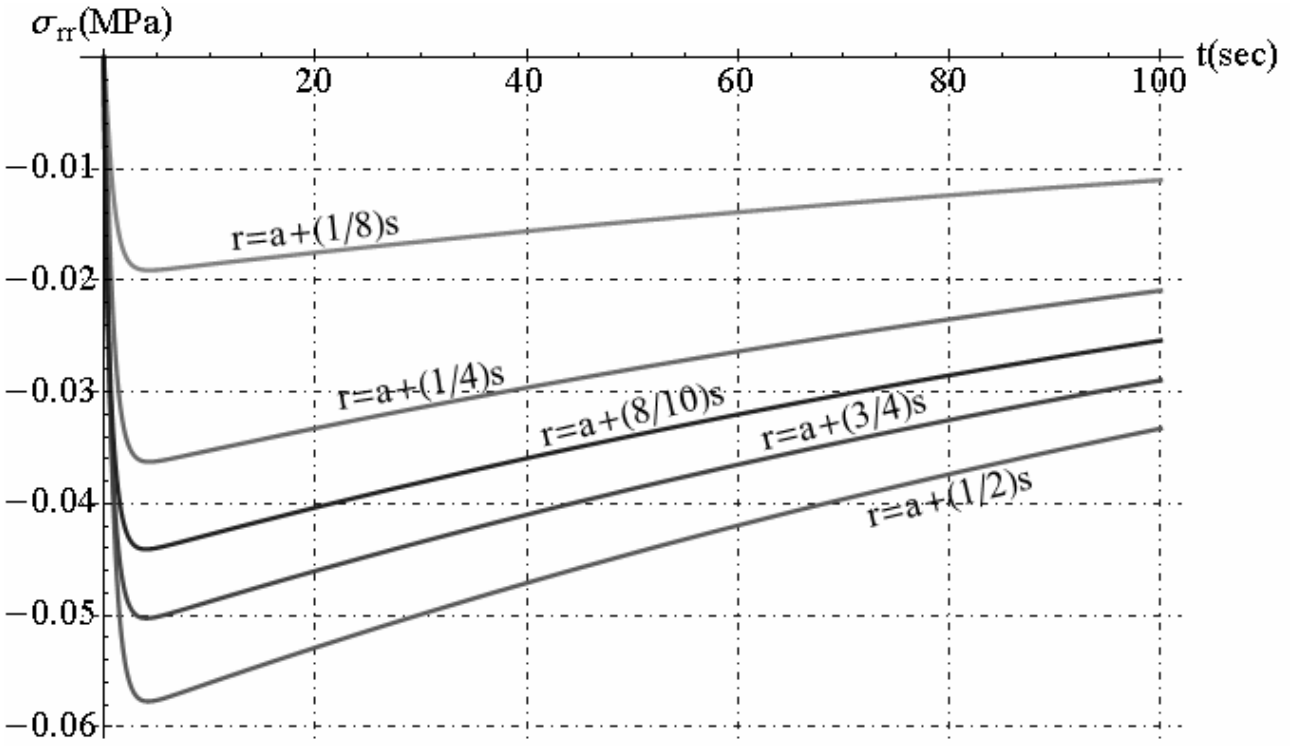

Fig. 15.11 - *Radial stress distribution in time*

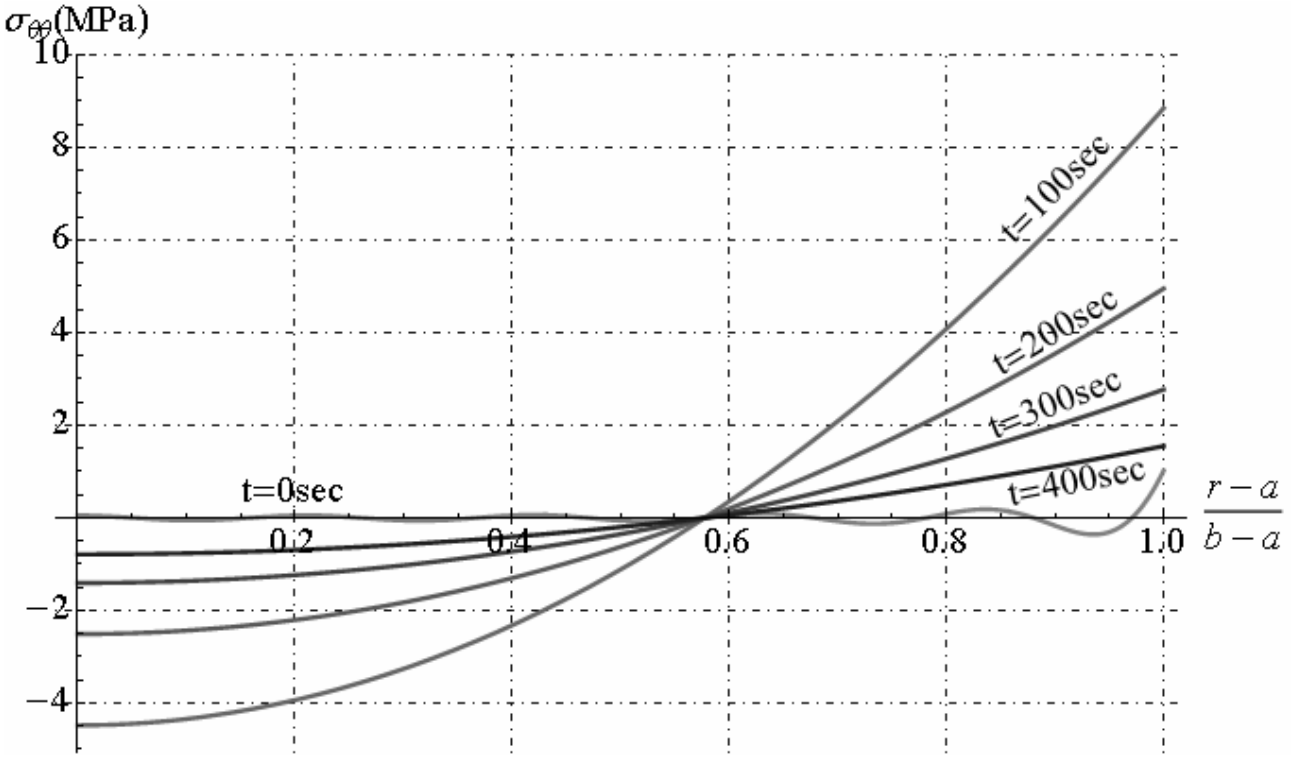

Fig. 15.12 - *Circumferential stress distribution along radial direction*

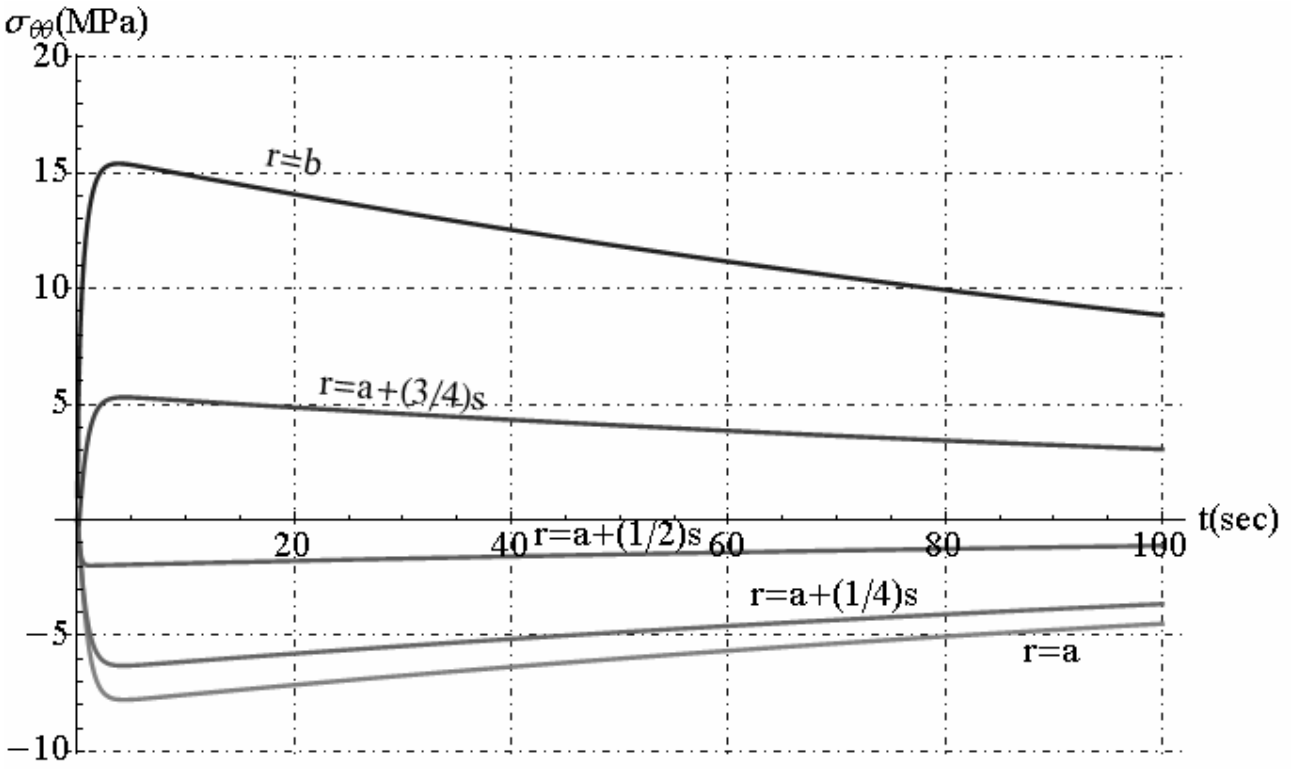

Fig. 15.13 - *Circumferential stress distribution in time*

15.7. Uncoupled thermo-elastic analysis in hollow sphere exposed to uniform heat flux

Let us consider a hollow sphere with inner radius "a" and outer radius "b" , subjected to radial temperature variation. The surface r = a is kept perfectly insulated while the surface r = b is exposed, for t >0, to a constant , uniform heat input q_0. In this section, we determine the heat conduction, displacement and stress function in hollow sphere subjected to uniform heat input q_0 applied on external surface, starting to initial temperature in solid equal to $T_0 = T_R = const$. The differential equation related to heat conduction and the corresponding boundary conditions are reported below:

$$\frac{\partial^2 T}{\partial r^2} + \frac{2}{r}\frac{\partial T}{\partial r} = \frac{1}{\kappa}\frac{\partial T}{\partial t}; \quad a < r < b, \quad t > 0 \tag{15.83}$$

$$-k\frac{\partial T}{\partial r} = 0, \quad r = a, \ t > 0, \tag{15.84}$$

$$-k\frac{\partial T}{\partial r} = q_0, \quad r = b, \ t > 0, \tag{15.85}$$

$$T = T_0; \quad a < r < b, \quad t = 0, \tag{15.86}$$

This is an case of a problem involving a non-homogeneous boundary condition and, in particular, with the heat input specified over the entire boundary surface. It is necessary writing the solution in the follows form (see Chapter VII) :

$$T(r,t) = T_0 + \xi t + T_S(r) + T_C(r,t) \tag{15.87}$$

where T_S satisfies the equations:

$$\frac{d^2 T_S}{d r^2} + \frac{2}{r}\frac{d T_S}{d r} = \frac{\xi}{\kappa}; \quad a < r < b, \tag{15.88}$$

$$-k\frac{d T_S}{d r} = 0; \quad r = a, \tag{15.89}$$

$$-k\frac{d\,T_S}{d\,r}=q_0;\quad r=b, \tag{15.90}$$

$$\int_V T_S\left(r\right)dV=\int_0^{2\pi}\int_0^{\pi}\int_a^{b}\left(T_S\left(r\right)r^2\sin\theta\right)drd\theta d\phi=0 \tag{15.91}$$

where ξ may be determined either from the boundary conditions (15.89)-(15.91). T_C satisfies equations:

$$\frac{\partial^2 T_C}{\partial r^2}+\frac{2}{r}\frac{\partial T_C}{\partial r}=\frac{1}{\kappa}\frac{\partial T_C}{\partial t};\quad a<r<b,\quad t>0 \tag{15.92}$$

$$-k\frac{\partial T_C}{\partial r}=0;\quad r=a,\ \ t>0, \tag{15.93}$$

$$-k\frac{\partial T_C}{\partial r}=0;\quad r=b,\ \ t>0, \tag{15.94}$$

$$T_C=-T_S;\quad a<r<b,\ \ t=0, \tag{15.95}$$

The solutions to equations (15.88) to (15.91) for ξ and T_S are:

$$T_S\left(r\right)=\left[\left(\rho c_v\xi\right)/\left(6k\right)\right]r^2+r^{-1}A_1+A_2,$$

$$\xi=-\frac{3b^2q_0}{\rho c_v\left(b^3-a^3\right)},\quad A_1=-\frac{a^3b^2q_0}{\left(b^3-a^3\right)k},\ A_2=\frac{3b^2q_0\left(6a^4+6a^3b+a^2b^2+ab^3+b^4\right)}{10k\left(b^3-a^3\right)\left(a^2+ab+b^2\right)}, \tag{15.96}$$

The parameter ξ is equal to ratio between total heat and internal energy of hollow sphere:

$$\xi=-\left(3b^2q_0\right)\Big/\left[\rho c_v\left(b^3-a^3\right)\right]=-\left(q_0S\right)/\left(\rho c_vV\right),\quad S=4\pi b^2,\ \ V=\left(4/3\right)\pi\left(b^3-a^3\right), \tag{15.97}$$

where S and V are area of external surface and volume of hollow sphere, respectively. The solution to the problem for T_C is found in much the same says way as was followed in section 10.5. The problem is therefore on with homogeneous differential equation and boundary conditions and may be treated by the method separation of variables. We can select a particular solution of the differential equation and boundary conditions in the form:

$$T_C\left(r,t\right)=\varphi\left(r\right)\psi\left(t\right) \tag{15.98}$$

By substituting the function (15.98) in eqs.(15.92)-(15.94), we obtain:

$$\frac{d^2\varphi}{d\,r^2}+\frac{2}{r}\frac{d\varphi}{d\,r}+\omega^2\varphi=0; \tag{15.99}$$

$$\frac{d\,\varphi}{d\,r}=0;\quad r=a, \tag{15.100}$$

$$\frac{d\,\varphi}{d\,r}=0;\quad x=b, \tag{15.101}$$

And to the following equation for $\psi\left(t\right)$:

$$\frac{d\psi}{dt}+\omega^2\kappa\psi=0 \tag{15.102}$$

The general solution of (15.102) is:

$$\psi\left(t\right)=e^{-\kappa\omega^2t} \tag{15.103}$$

The general solution of (15.99) is:

$$\varphi\left(r\right)=r^{-1}\left(C_1e^{i\,\omega r}+C_2e^{-i\,\omega r}\right) \tag{15.104}$$

where C_1,C_2 are constants integration. From (15.100) it is deduced that the constant C_2 is given by:

$$C_2 = \left[(i+\omega a)^2 \Big/ \left(1+\omega^2 a^2\right) \right] C_1 e^{2i\omega a} \tag{15.105}$$

The equations (15.100) and (15.101) are an homogenous algebraic system as reported below :

$$[\mathbf{\Lambda}] \cdot \begin{bmatrix} C_1 \\ C_2 \end{bmatrix} = \begin{bmatrix} 0 \\ 0 \end{bmatrix} \tag{15.106}$$

where the matrix $[\mathbf{\Lambda}]$ is given by:

$$[\mathbf{\Lambda}] = \begin{bmatrix} (1-ia\omega)e^{ia\omega} & (1+ia\omega)e^{-ia\omega} \\ (1-ib\omega)e^{ib\omega} & (1+ib\omega)e^{-ib\omega} \end{bmatrix} \tag{15.107}$$

The algebraic system (15.106) admit not trivial solution if the determinant of the matrix $[\mathbf{\Lambda}]$ is equal to zero. By imposing this condition, we obtain the transcendental equation in unknown parameter ω:

$$\det[\mathbf{\Lambda}] = g(\omega) = \omega(b-a)\cos\left[\omega(a-b)\right] + \left(1+ab\omega^2\right)\sin\left[\omega(a-b)\right] = 0 \tag{15.108}$$

Finally, we can rewrite the equation (15.108) in follows manner:

$$\tan\left[\omega(a-b)\right] = \left[\omega(a-b)\right] \Big/ \left(1+ab\omega^2\right) \tag{15.109}$$

The roots of this transcendental equation (15.109) are an infinite number such, denoted here by ω_m, $m = 1,2,....\infty$ leading to eigenvalues or characteristic values $\lambda_m = -\omega_m^2$. The corresponding eigenfunctions or characteristic functions $\bar{\varphi}_m(r) = \varphi_m(r)/C_{1m}$ are, as calculated above,

$$\bar{\varphi}_m(r) = \frac{1}{r}\left[\cos(\omega_m r) + i\sin(\omega_m r)\right] + \frac{(i+\omega a)^2}{\left(1+\omega^2 a^2\right) r}\left\{\cos\left[\omega_m(2a-r)\right] - i\sin\left[\omega_m(2a-r)\right]\right\} \tag{15.110}$$

The solution to the problem may therefore be written in the form:

$$T(r,t) = T_0 + \xi t + \frac{\rho c_v \xi}{6k} r^2 + \frac{A_1}{r} + A_2 + \sum_{m=1}^{\infty} C_{1m} \bar{\varphi}_m(r) e^{-\kappa\omega_m^2 t} \tag{15.111}$$

where the coefficients C_{1m} are determined by applying the initial condition (15.95) that yields the following relationship:

$$C_{1m} = -\frac{\int_0^{2\pi}\int_0^{\pi}\int_a^b T_S(r)\bar{\varphi}_m(r)\, r^2 \sin\theta\, dr\, d\theta\, d\phi}{\int_0^{2\pi}\int_0^{\pi}\int_a^b \bar{\varphi}_m^2(r)\, r^2 \sin\theta\, dr\, d\theta\, d\phi} \tag{15.112}$$

By substituting the constant C_{1m} in equation (15.111), we obtain the expression of function temperature $T(r,t)$. By applying the relationships in section 15.1 and 15.2, we obtain displacement function and stress function in hollow sphere . The displacement function is given by eq. (15.4)

$$\begin{aligned} u_r = {} & \frac{\alpha}{b^3-a^3}\left(\frac{3\lambda+2\mu}{\lambda+2\mu}\right)\left[\frac{a^3}{r^2}\int_r^b (\xi t+T_S) r^2 dr + \frac{b^3}{r^2}\int_a^r (\xi t+T_S) r^2 dr + \frac{4\mu r}{3\lambda+2\mu}\int_a^b (\xi t+T_S) r^2 dr\right] + \\ & + \sum_{m=1}^{\infty} \frac{\alpha\, C_{1n}}{b^3-a^3}\left(\frac{3\lambda+2\mu}{\lambda+2\mu}\right)\left[\frac{a^3}{r^2}\int_r^b \varphi_m r^2 dr + \frac{b^3}{r^2}\int_a^r \varphi_m r^2 dr + \frac{4\mu r}{3\lambda+2\mu}\int_a^b \varphi_m r^2 dr\right] e^{-\omega_m^2\kappa t} - \alpha T_R r \end{aligned} \tag{15.113}$$

The radial stress is given by:

$$\begin{aligned} \sigma_{rr} = {} & \frac{4\mu\alpha}{a^3-b^3}\left(\frac{3\lambda+2\mu}{\lambda+2\mu}\right)\left[\frac{a^3}{r^2}\int_r^b (\xi t+T_S) r^2 dr + \frac{b^3}{r^2}\int_a^r (\xi t+T_S) r^2 dr - \int_a^b (\xi t+T_S) r^2 dr\right] \\ & + \sum_{m=1}^{\infty} \frac{4\mu\alpha\, C_{1m}}{a^3-b^3}\left(\frac{3\lambda+2\mu}{\lambda+2\mu}\right)\left[\frac{a^3}{r^2}\int_r^b \varphi_m r^2 dr + \frac{b^3}{r^2}\int_a^r \varphi_m r^2 dr - \int_a^b \varphi_m r^2 dr\right] e^{-\omega_m^2\kappa t} \end{aligned} \tag{15.114}$$

The circumferential stress is reported below:

$$\sigma_{\theta\theta}=\sigma_{\phi\phi}=\frac{2\mu\alpha}{b^3-a^3}\left(\frac{3\lambda+2\mu}{\lambda+2\mu}\right)\left[\frac{a^3}{r^2}\int_r^b(\xi t+T_S)r^2dr+\frac{b^3}{r^2}\int_a^r(\xi t+T_S)r^2dr\right]+$$
$$+\frac{2\mu\alpha}{b^3-a^3}\left(\frac{3\lambda+2\mu}{\lambda+2\mu}\right)\left[2\int_a^b(\xi t+T_S)r^2d\xi+\left(a^3-b^3\right)(\xi t+T_S)\right]+ \tag{15.115}$$
$$+\sum_{m=1}^{\infty}\frac{2\mu\alpha C_{1m}}{b^3-a^3}\left(\frac{3\lambda+2\mu}{\lambda+2\mu}\right)\left[\frac{a^3}{r^2}\int_r^b\varphi_m r^2dr+\frac{b^3}{r^2}\int_a^r\varphi_m r^2dr+2\int_a^b\varphi_m r^2d\xi+\left(a^3-b^3\right)\varphi_m\right]e^{-\omega_m^2\kappa t}$$

In explicit the displacement function is given by:

$$u_r=N_1 r+\frac{N_2}{r^2}+t\left(P_1 r+\frac{P_2}{r^2}\right)+\frac{\alpha(3\lambda+2\mu)}{6(\lambda+2\mu)}\left(3A_1+2A_2 r+\frac{\rho c_v\xi}{5k}r^3\right)+$$
$$+\sum_{m=1}^{\infty}\left\{Q_{1m}r+\frac{Q_{2m}}{r^2}+\frac{\alpha(3\lambda+2\mu)}{\omega_m^2(\lambda+2\mu)r^2}\left[C_{1m}(1-i\omega_m r)e^{i\omega_m r}+C_{2m}(1+i\omega_m r)e^{-i\omega_m r}\right]\right\}e^{-\omega_m^2\kappa t} \tag{15.116}$$

where the constants integration C_{1m}, C_{2m} are given by equations (15.112) and (15.105), respectively. The constants integrations $Q_{1m}, Q_{2m}, P_1, P_2, N_1, N_2$ are determined by solving the boundary conditions (15.5). In explicit these constants are given by :

$$Q_{1m}=\frac{4\alpha\mu e^{-ia\omega_m}\left[e^{2ia\omega_m}(1-ia\omega_m)(b\omega_m-i)+e^{2ib\omega_m}(1+ia\omega_m)(i+b\omega_m)\right]}{\omega_m^2(a^3-b^3)(b\omega_m-i)(\lambda+2\mu)}C_{1m},$$
$$Q_{2m}=\frac{\alpha(3\lambda+2\mu)\left[e^{2ia\omega_m}(i+a\omega_m)(b\omega_m-i)-e^{2ib\omega_m}(-i+a\omega_m)(i+b\omega_m)\right]b^3e^{-ia\omega_m}}{\omega_m^2(a^3-b^3)(b\omega_m-i)(\lambda+2\mu)}C_{1m}, \tag{15.117}$$
$$P_1=\frac{3\alpha b^2q_0}{(a^3-b^3)\rho c_v}, P_2=0, N_1=\alpha(T_0-T_R), N_2=-\frac{\alpha(3\lambda+2\mu)q_0}{k(\lambda+2\mu)}\left[\frac{a^3b^4(5a^2-ab-b^2)}{10(a-b)(a^2+ab+b^2)^2}\right],$$

In explicit the radial and circumferential stress components are given by:

$$\sigma_{rr}=N_1(3\lambda+2\mu)-4\mu N_2r^{-3}-\frac{2\alpha\mu(3\lambda+2\mu)}{(\lambda+2\mu)}\left[\frac{\lambda+2\mu}{2\mu}(T_0-T_R+\xi t)\right]$$
$$-\frac{2\alpha\mu(3\lambda+2\mu)}{(\lambda+2\mu)}\left[\frac{2}{3}A_2+\frac{A_1}{r}+\frac{\rho c_v\xi}{15k}r^2\right]+\sum_{m=1}^{\infty}\left\{Q_{1m}(3\lambda+2\mu)-4\mu Q_{2m}r^{-3}\right\}e^{-\omega_m^2\kappa t} \tag{15.118}$$
$$+t\left[P_1(3\lambda+2\mu)-4\mu P_2r^{-3}\right]+\sum_{m=1}^{\infty}\left\{\frac{4\alpha\mu i(3\lambda+2\mu)}{\omega_m^2(\lambda+2\mu)r^3}\left[\begin{matrix}C_{1m}(1+i\omega_m r)e^{i\omega_m r}+\\+C_{2m}(1-i\omega_m r)e^{-i\omega_m r}\end{matrix}\right]\right\}e^{-\omega_m^2\kappa t}$$

$$\sigma_{\theta\theta}=N_1(3\lambda+2\mu)+2\mu N_2r^{-3}-\frac{2\alpha\mu(3\lambda+2\mu)}{(\lambda+2\mu)}\left[\frac{\lambda+2\mu}{2\mu}(T_0-T_R+\xi t)\right]$$
$$-\frac{2\alpha\mu(3\lambda+2\mu)}{(\lambda+2\mu)}\left[\frac{2}{3}A_2+\frac{A_1}{2r}+\frac{2\rho c_v\xi}{15k}r^2\right]+\sum_{m=1}^{\infty}\left(Q_{1m}(3\lambda+2\mu)+2\mu Q_{2m}r^{-3}\right)e^{-\omega_m^2\kappa t} \tag{15.119}$$
$$+t\left[P_1(3\lambda+2\mu)+2\mu P_2r^{-3}\right]+\sum_{m=1}^{\infty}\left\{\frac{2\alpha\mu(3\lambda+2\mu)}{\omega_m^2r^3(\lambda+2\mu)}\left[\begin{matrix}C_{1m}(1-r\omega_m(1+i\omega_m r))e^{i\omega_m r}+\\+C_{2m}(1-r\omega_m(\omega_m r-i))e^{-i\omega_m r}\end{matrix}\right]\right\}e^{-\omega_m^2\kappa t}$$

The circumferential stress assumes asymptotic values in r = a and r = b for $t\to\infty$, as showed in figure 15.20. These asymptotic values are given by:

$$\sigma_{\theta\theta}\left(r=a,t\to\infty\right)=\frac{\alpha E q_0}{k(1-\nu)}\left[\frac{3b^2(a-b)(a^2+3ab+b^2)}{10(a^2+ab+b^2)^2}\right],$$
$$\sigma_{\theta\theta}\left(r=b,t\to\infty\right)=\frac{\alpha E q_0}{k(1-\nu)}\left[\frac{b(b-a)(5a^3+6a^2b+3ab^2+b^3)}{5(a^2+ab+b^2)^2}\right], \tag{15.120}$$

For example, let us consider, a spherical tank constituted by steel, under uniform heat flux. The geometrical, mechanical and thermal parameters considered for spherical tank are reported below:

$$E=210\cdot10^9\,N/m^2,\ \nu=0.3,\ c=440J/kg\cdot°K,\ k=45W/m\cdot°K,$$
$$\rho=7.8\cdot10^3\,kg/m^3,\ \ b=10.5m,\ \ a=10.0m,\ s=b-a=0.5m,$$
$$q=-500W/m^2,\quad \alpha=1.2\cdot10^{-5}°K^{-1},\quad T_0=T_R=300°K$$

In this case the graphics function $g(\omega)$ given by equation (15.108) is reported below:

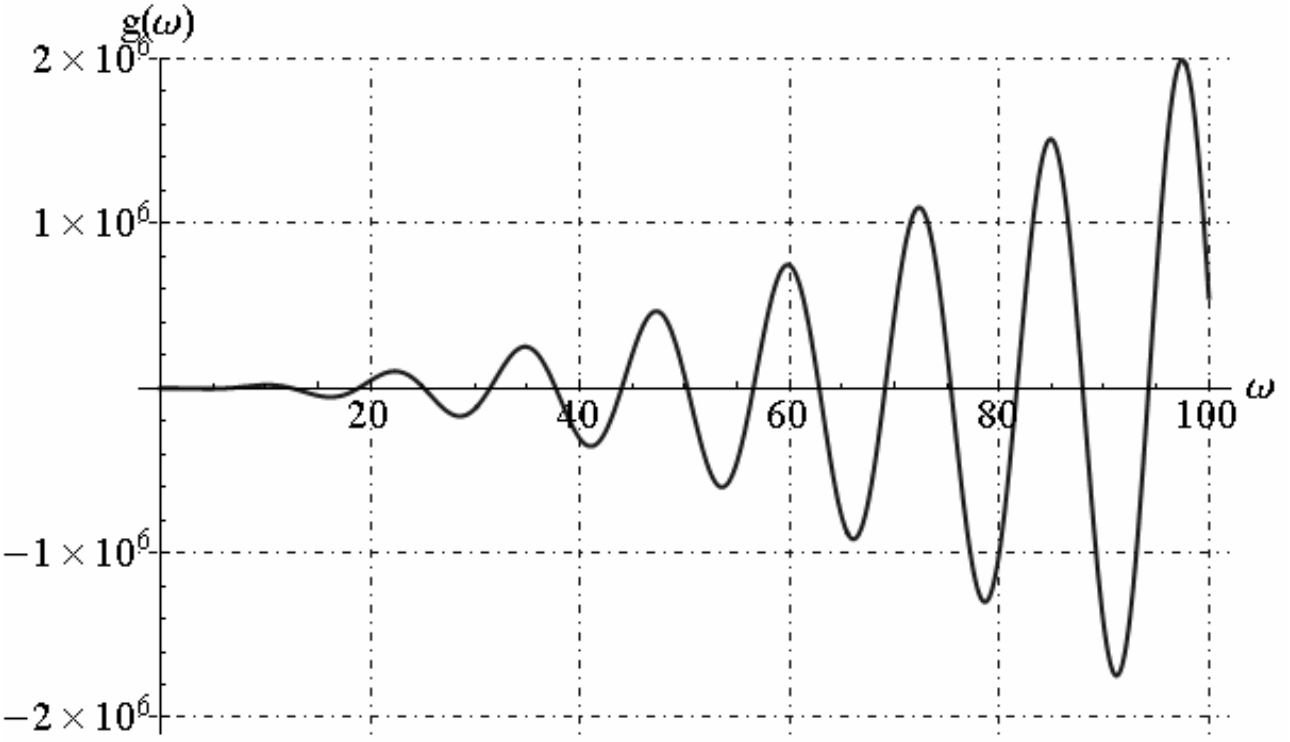

By fixed m= 20, the eigenvalues ω_m and corresponding values of constants integration A_m are reported in table 15.2:

ω_m	6.285	12.567	18.850	25.133	31.416
A_m	5.903 - 0.183 i	-1.477 + 0.023 i	0.657 - 0.007 i	-0.369 + 0.003 i	0.236 - 0.001 i
ω_m	37.699	43.983	50.266	56.549	62.832
A_m	-0.1642 + 0.0009 i	0.1206 - 0.0005 i	-0.0923 + 0.0004 i	0.0730 - 0.0003 i	-0.0591 + 0.0002 i
ω_m	69.115	75.398	81.682	87.965	94.248
A_m	0.0488 - 0.0001 i	-0.0410 + 0.0001 i	0.0350 - 0. × 10^-5 i	-0.0302 + 0. × 10^-5 i	0.0263 + 0. × 10^-5 i
ω_m	100.531	106.814	113.097	119.381	125.664
A_m	-0.0231 + 0. × 10^-5 i	0.0205 + 0. × 10^-5 i	-0.0182 + 0. × 10^-5 i	0.0164 + 0. × 10^-5 i	-0.0148 + 0. × 10^-5 i

Table 15.1 – *Eigenvalues ω_m and corresponding values of constants integration A_m*

We reported the graphics of temperature, radial displacement and stress components along the radial direction and in time:

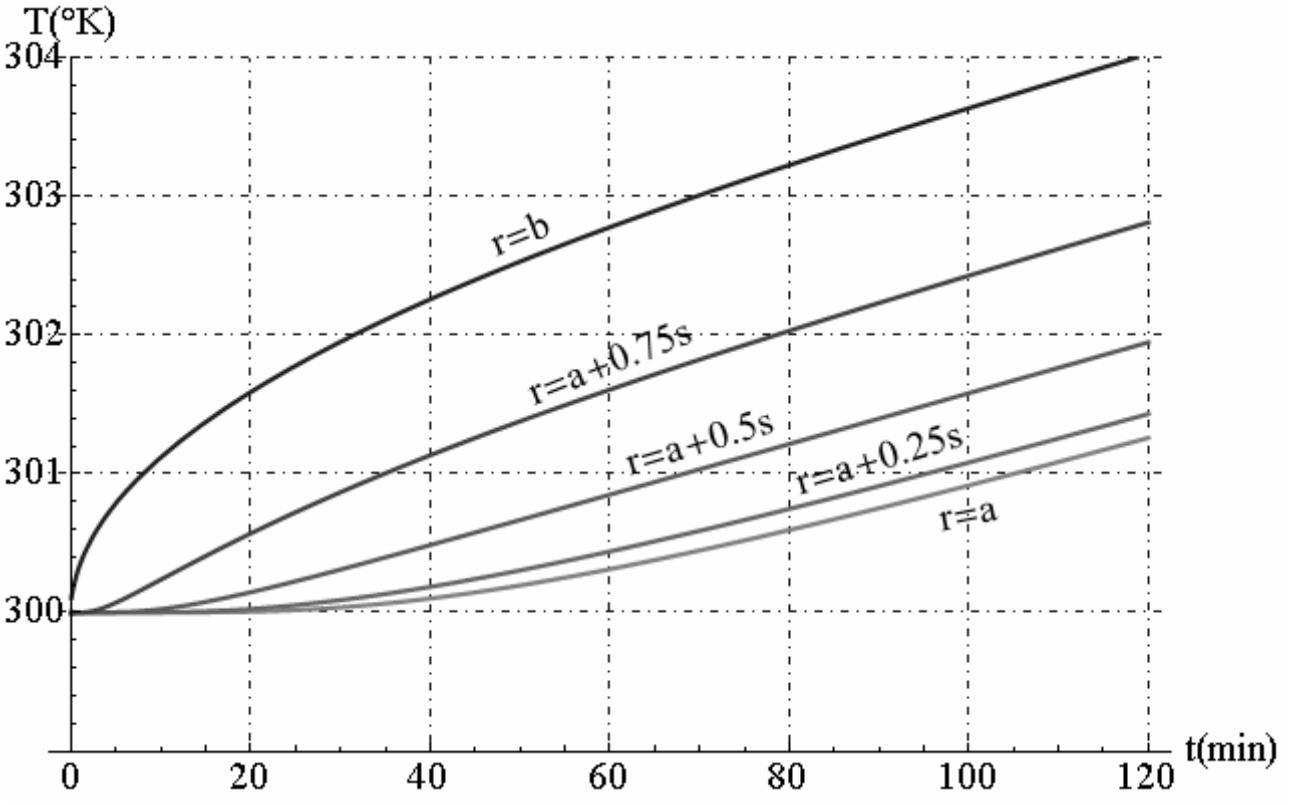

Fig. 15.14 - *Temperature function versus the time*

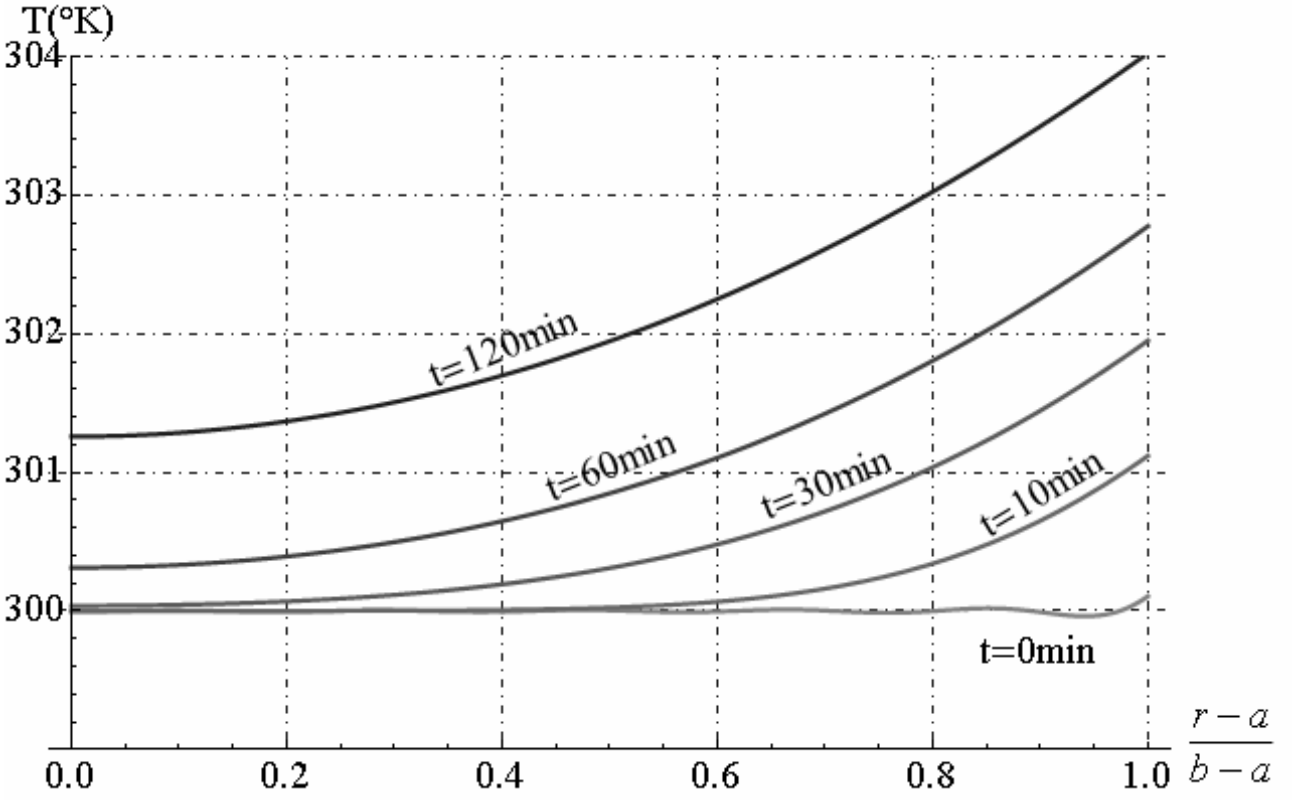

Fig. 15.15 - *Temperature function along radial direction*

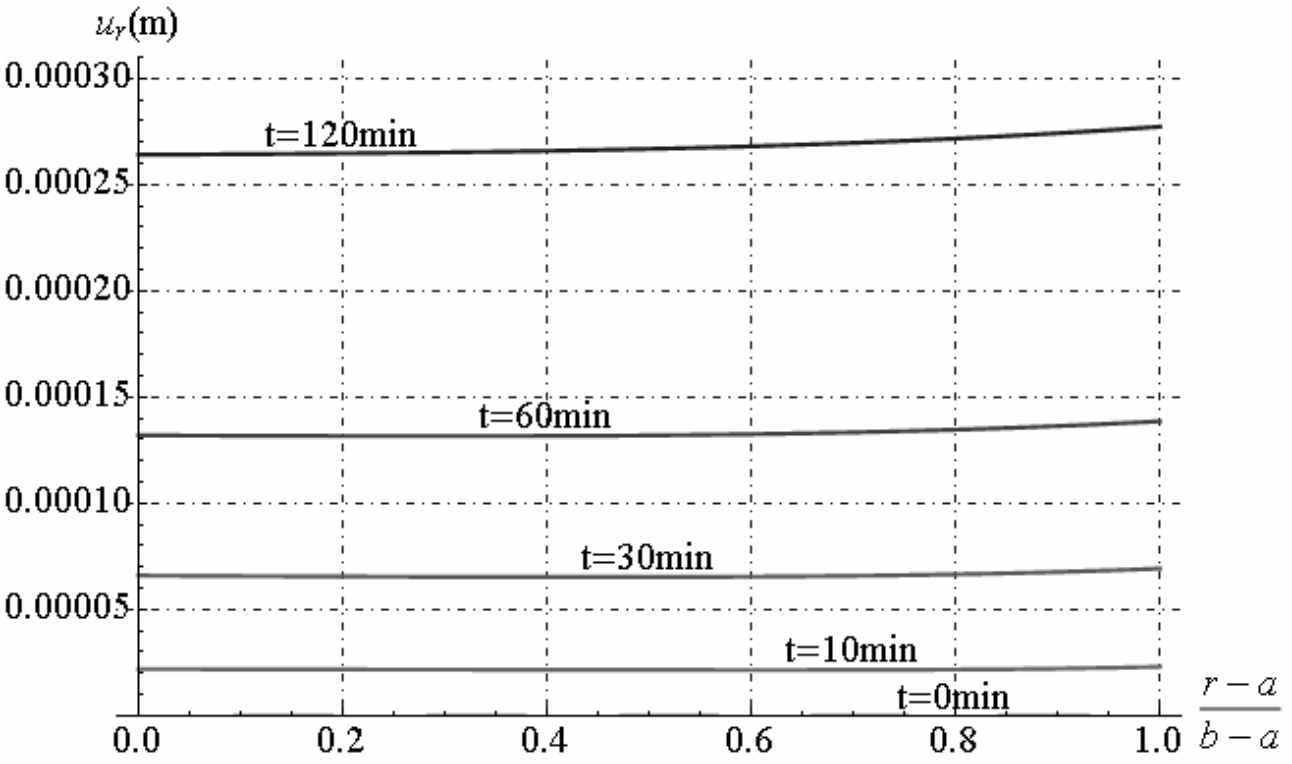

Fig. 15.16 - *Radial displacement distribution versus the time*

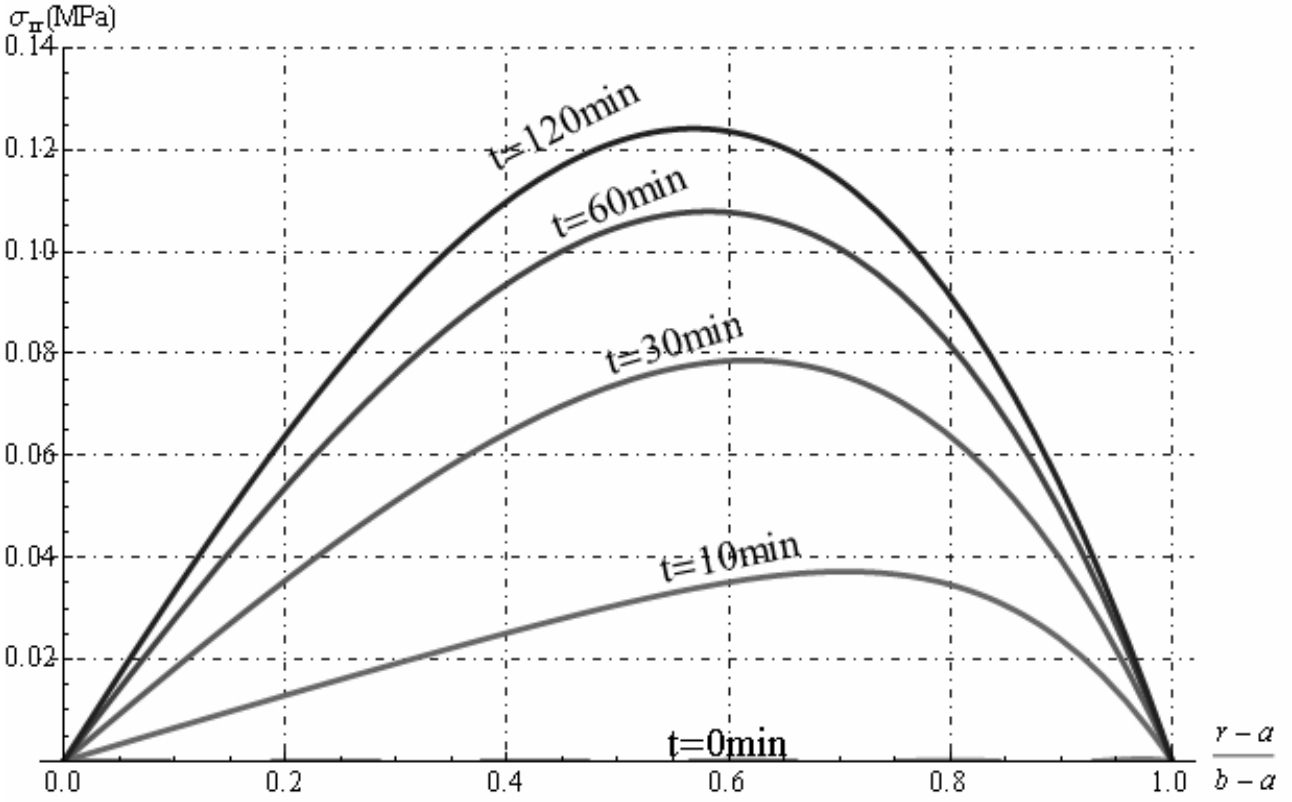

Fig. 15.17 - *Radial stress distribution along radial direction*

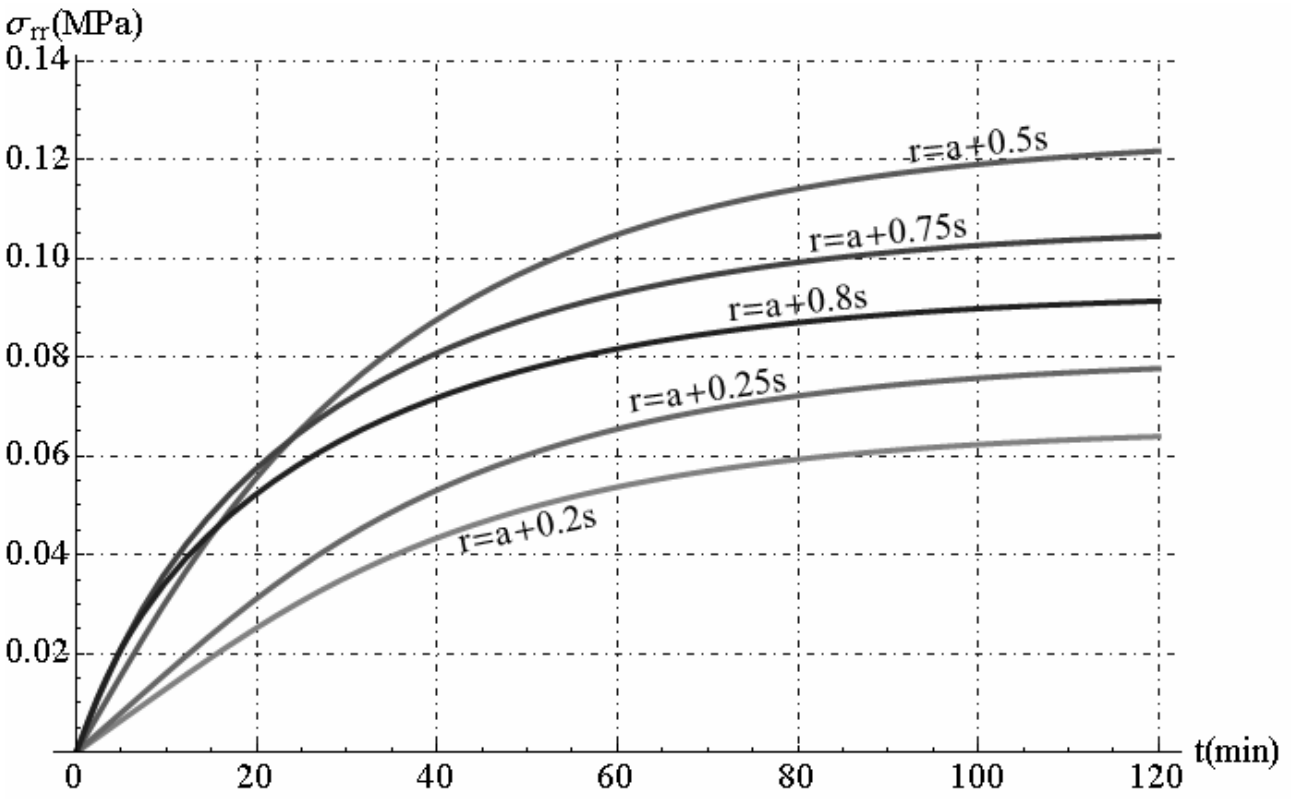

Fig. 15.18 - *Radial stress distribution in time*

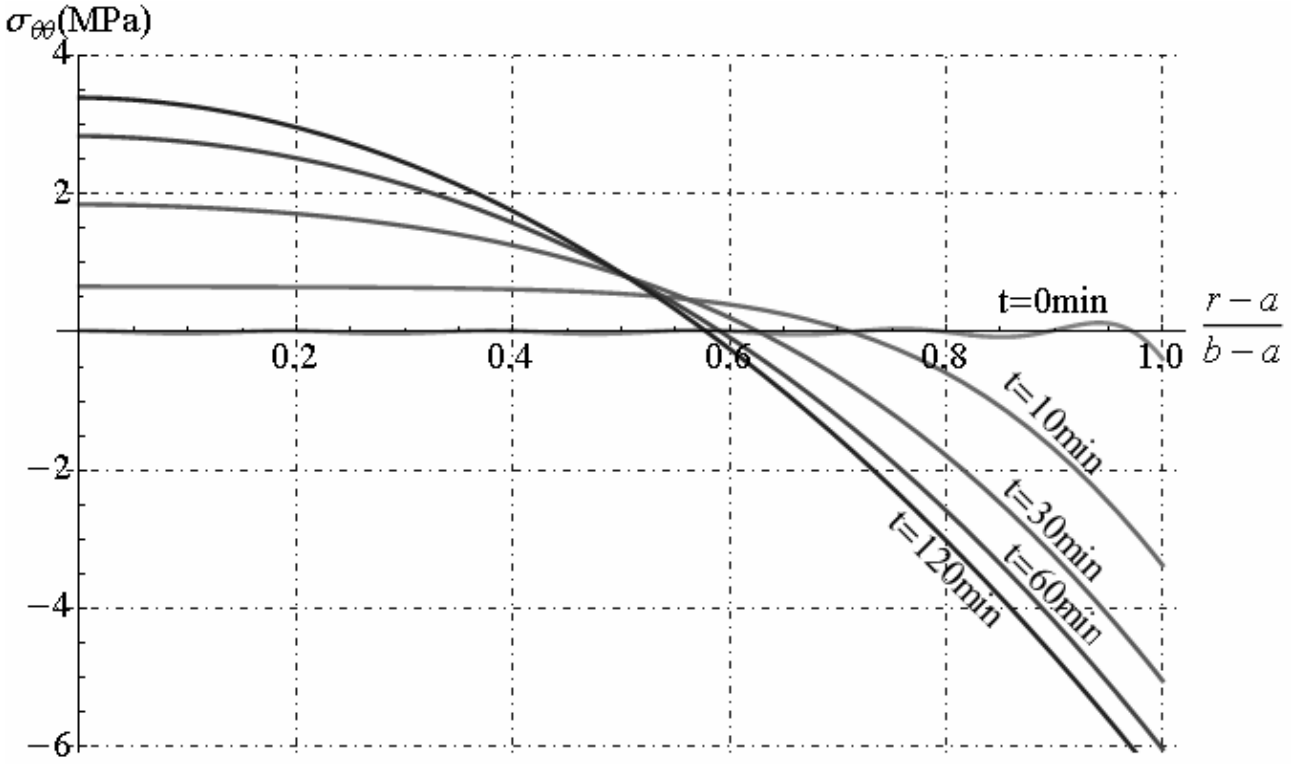

Fig. 15.19 - *Circumferential stress distribution along radial direction*

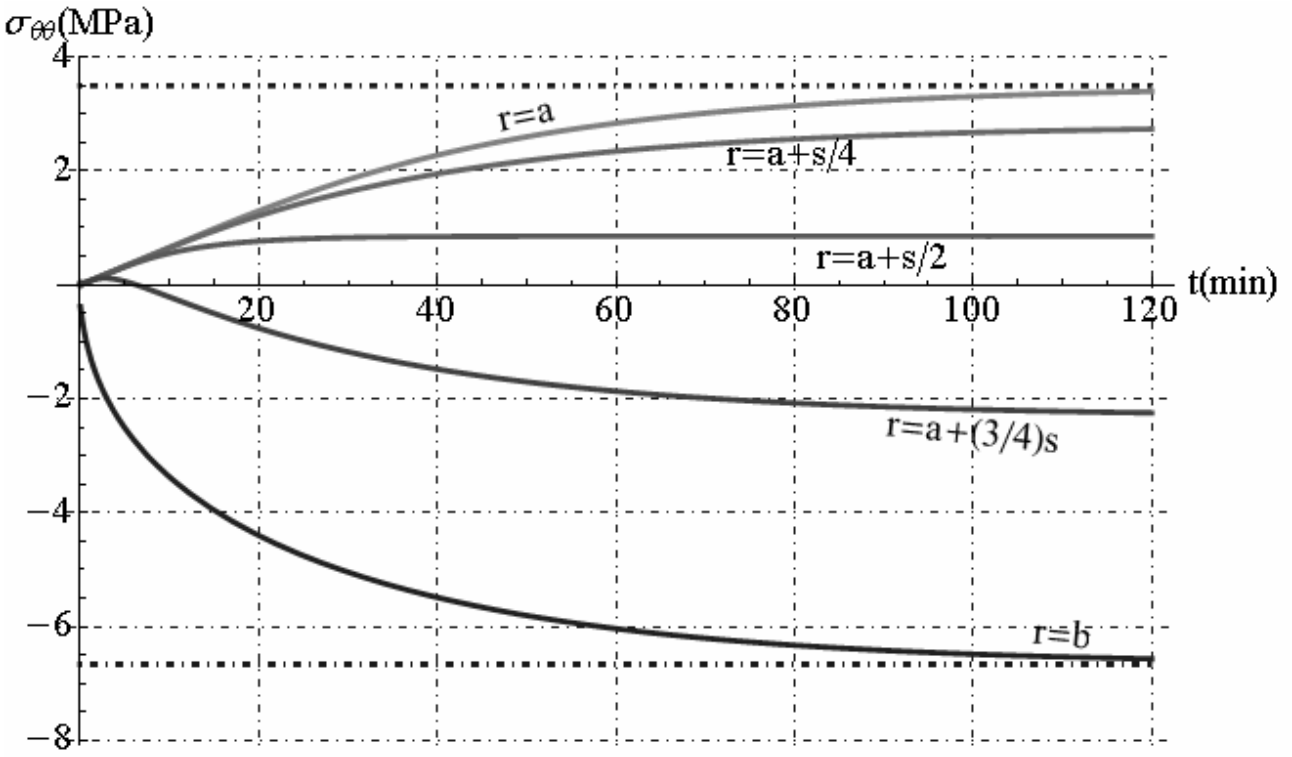

Fig. 15.20 - *Circumferential stress distribution in time*

15.8. Approximate solution for hollow sphere exposed to uniform heat flux

Let us consider a hollow sphere with inner radius "a" and outer radius "b" , subjected to uniform heat flux q_0 applied on external surface, but inner surface is kept perfectly insulated. In this section, we consider a hollow sphere with small thickness respect to radius:

$$\overline{s} = s/a = (b-a)/a, \quad \overline{s} \ll 1 \tag{15.121}$$

In this case, it is possible to determine an approximate solution by applying the hypothesis (15.121). An approximate solution of transcendental equation (15.109) is given by:

$$\omega_m \cong \pi m s^{-1} = (\pi m)/(b-a) = (\pi m)/(a\overline{s}) \quad \forall m \in \{1,2,....N\} \tag{15.122}$$

By substituting the equation (15.122) in to (15.110), we obtain the characteristic function :

$$\psi(r) = \frac{2}{r(m\pi - i\overline{s})} e^{\frac{im\pi}{\overline{s}}} \left\{ m\pi \cos\left[\frac{m\pi(a-r)}{a\overline{s}}\right] - \overline{s}\sin\left[\frac{m\pi(a-r)}{a\overline{s}}\right]\right\} \quad \forall m \in \{1,2,....N\} \tag{15.123}$$

By substituting the characteristic function $\psi(r)$ given by (15.123) in to equation (15.112), we obtain in explicit the integration constants C_{1m}, $\forall m \in \{1,2,....N\}$, as reported below:

$$C_{1m} = \frac{(-1)^m q_0 a^2 \overline{s} e^{-\frac{im\pi}{\overline{s}}} (1+\overline{s}^2)\left\{15\overline{s}^2\left[3+\overline{s}(3+\overline{s})\right] + m^2\pi^2\left[45+\overline{s}(45+15\overline{s}-\overline{s}^3)\right]\right\}}{5m^3\pi^3 k(m\pi + i\overline{s})\left[3+\overline{s}(3+\overline{s})\right]^2} \tag{15.124}$$

Now, by utilizing the equation (15.116) and (15.118), it is possible to determine symbolic expression of radial displacement, strain and stress components in hollow sphere. The approximate solution give possibility to make parametric analyses for hollow sphere. In this case the parameter considered are seven: Young's modulus, Poisson's ratio, linear thermal expansion coefficient, density, specific heat coefficient, thermal conductivity and ratio between thickness and radius of hollow sphere. In order to visualize the typical behaviour of a diffusive phenomenon, such as the non-stationary heat conduction described above, it can be useful thermal time constant τ_C (thus characterizing heat transfer rates) depend strongly on particle size and on its thermal diffusivity $k/\rho c_v$. In this case thermal time constant τ_C is given by:

$$\tau_C = \rho c_v s^2 k^{-1} = \rho c_v a^2 \bar{s}^2 k^{-1} \tag{15.125}$$

We reported variation the maximum value assumed by $\sigma_{\theta\theta}$ with parameter considered. By fixing the radius $a = 10m$, heat flux $q_0 = 1000 Wm^{-2}$ and initial temperature $T_0 = T_R = 300°K$, we obtain the following graphics:

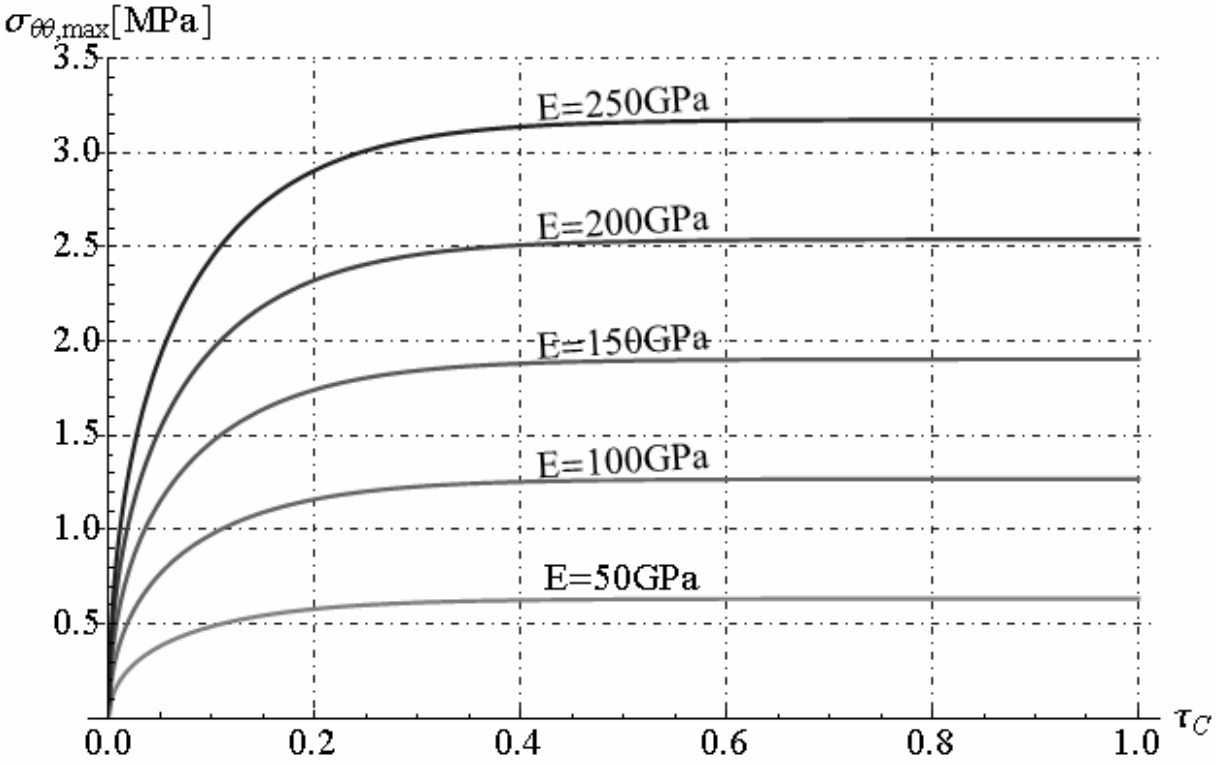

Fig. 15.21 - *Variation of Young's modulus with fixed values of other parameters:* $\nu = 0.3, \alpha = 1.2 \cdot 10^{-6} °K^{-1}$, $c_v = 440 J\, kg^{-1} °K^{-1}, k = 45 Wm^{-1} °K^{-1}, \rho = 7800 kgm^{-3}, \bar{s} = 0.01$,

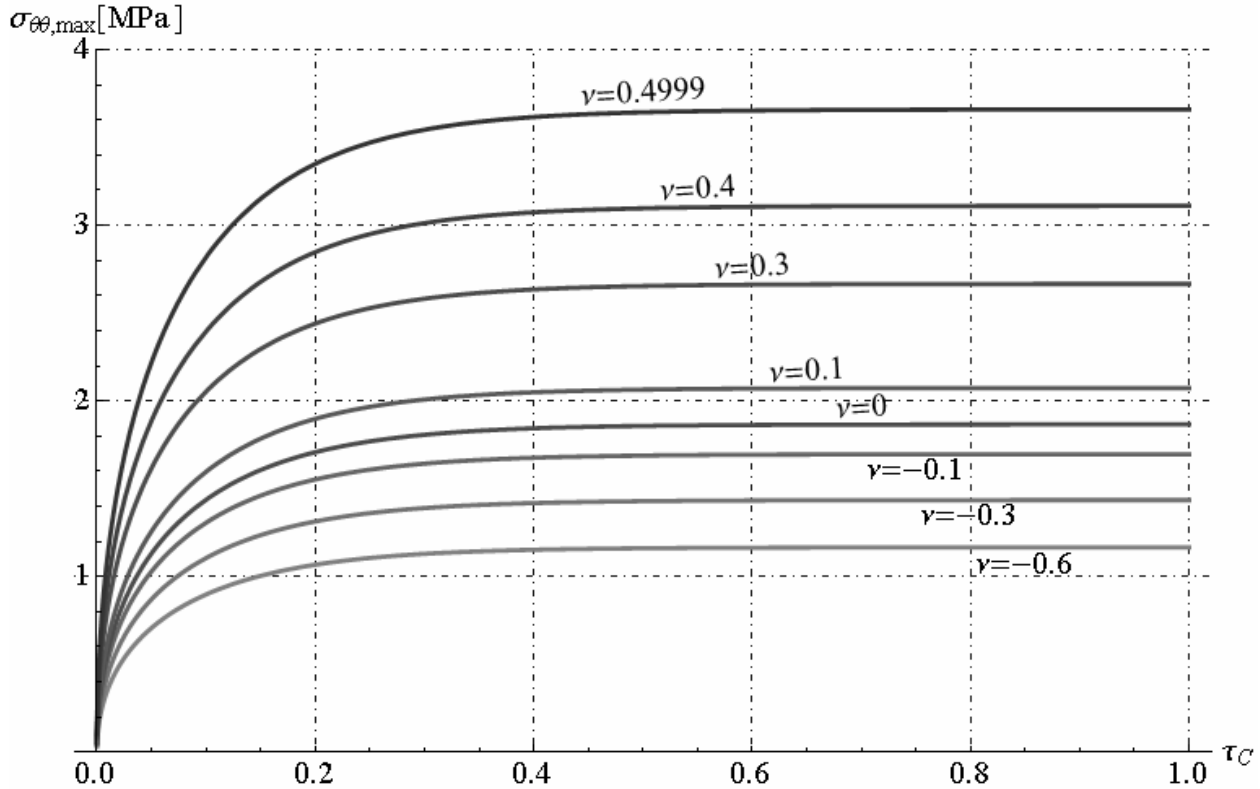

Fig. 15.22 - *Variation of Poisson's ratio with fixed values of other parameters:* $E = 210 GPa, \alpha = 1.2 \cdot 10^{-6} °K^{-1}$, $c_v = 440 J\, kg^{-1} °K^{-1}, k = 45 Wm^{-1} °K^{-1}, \rho = 7800 kgm^{-3}, \bar{s} = 0.01$,

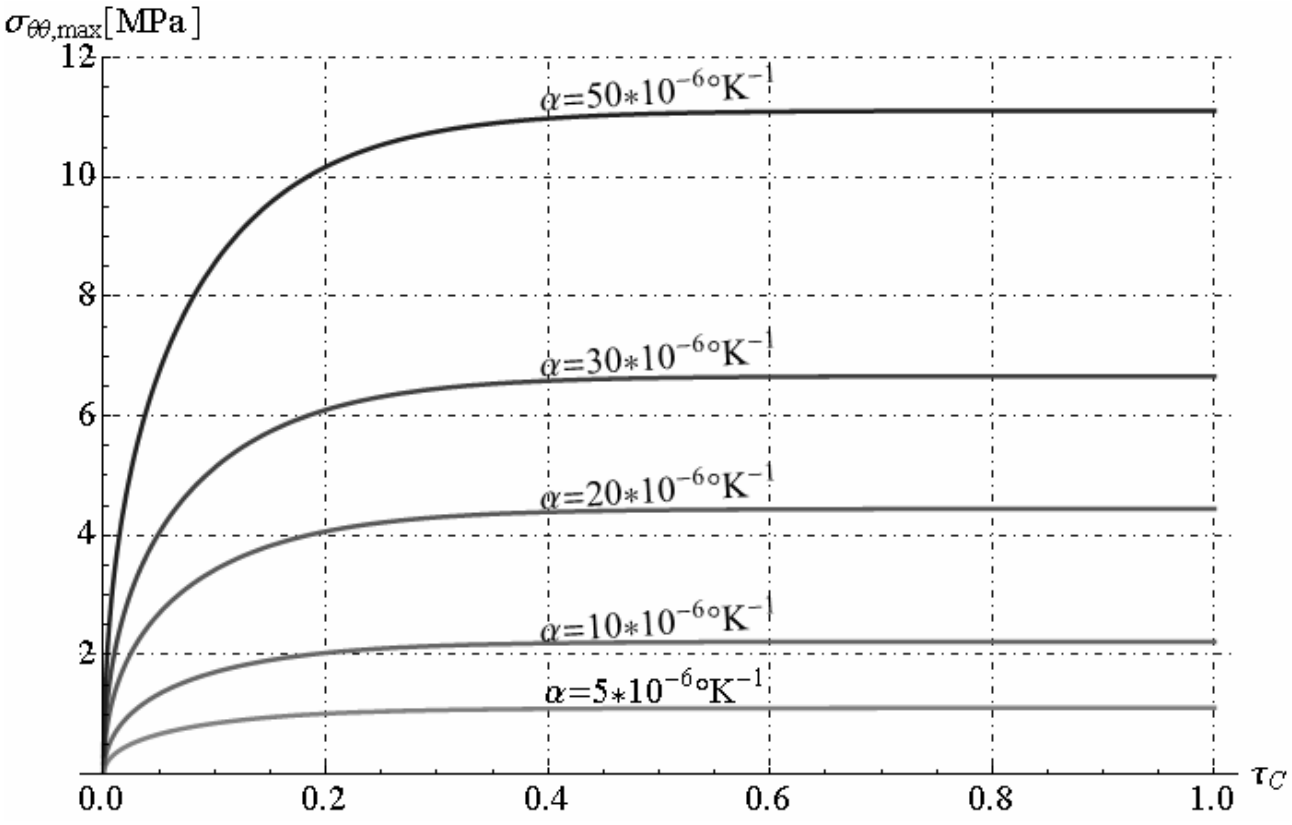

Fig. 15.23 - *Variation of linear thermal expansion coefficient with fixed values of other parameters:* $E = 210GPa, \nu = 0.3,\ c_v = 440J\ kg^{-1}{}^{\circ}K^{-1}, k = 45Wm^{-1}{}^{\circ}K^{-1}, \rho = 7800kgm^{-3}, \overline{s} = 0.01,$

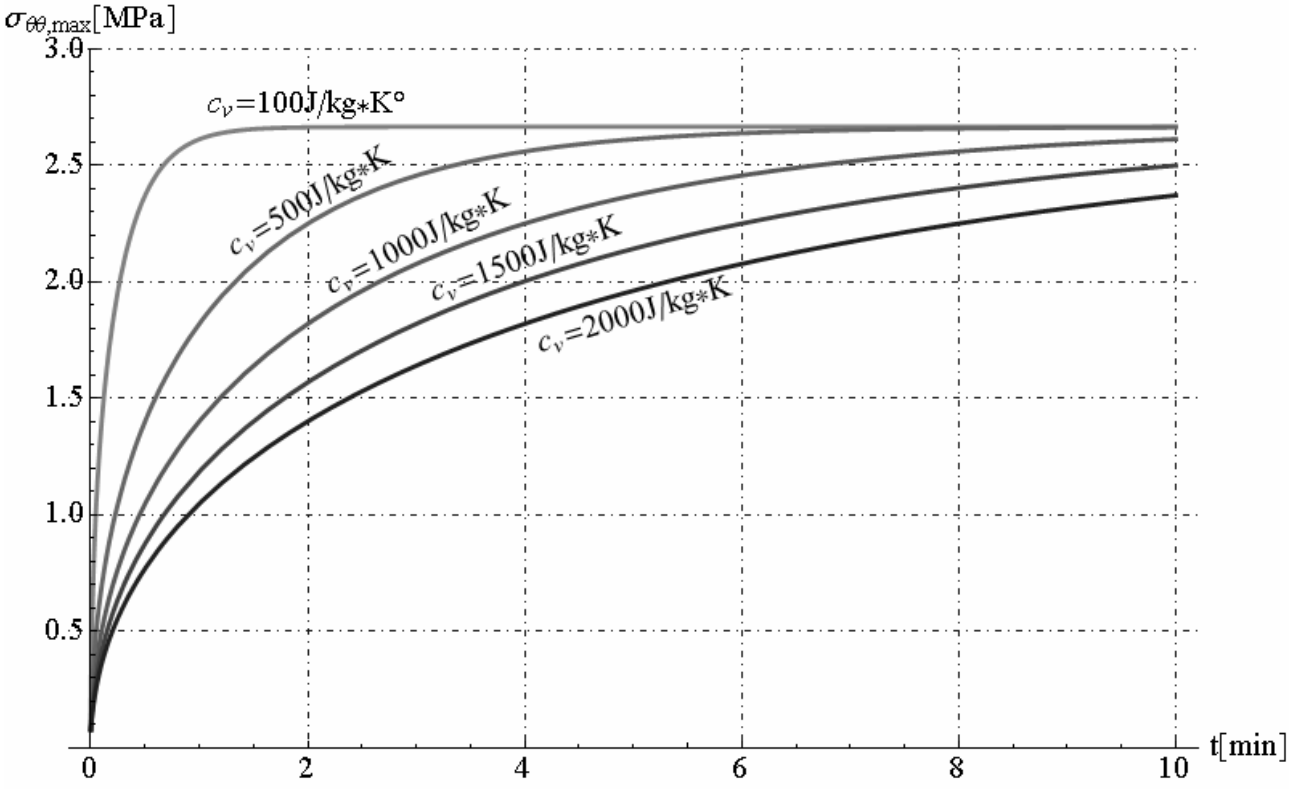

Fig. 15.24 - *Variation of specific heat coefficient with fixed values of other parameters:* $E = 210GPa, \nu = 0.3, \alpha = 1.2 \cdot 10^{-6}{}^{\circ}K^{-1},\ k = 45Wm^{-1}{}^{\circ}K^{-1}, \rho = 7800kgm^{-3}, \overline{s} = 0.01,$

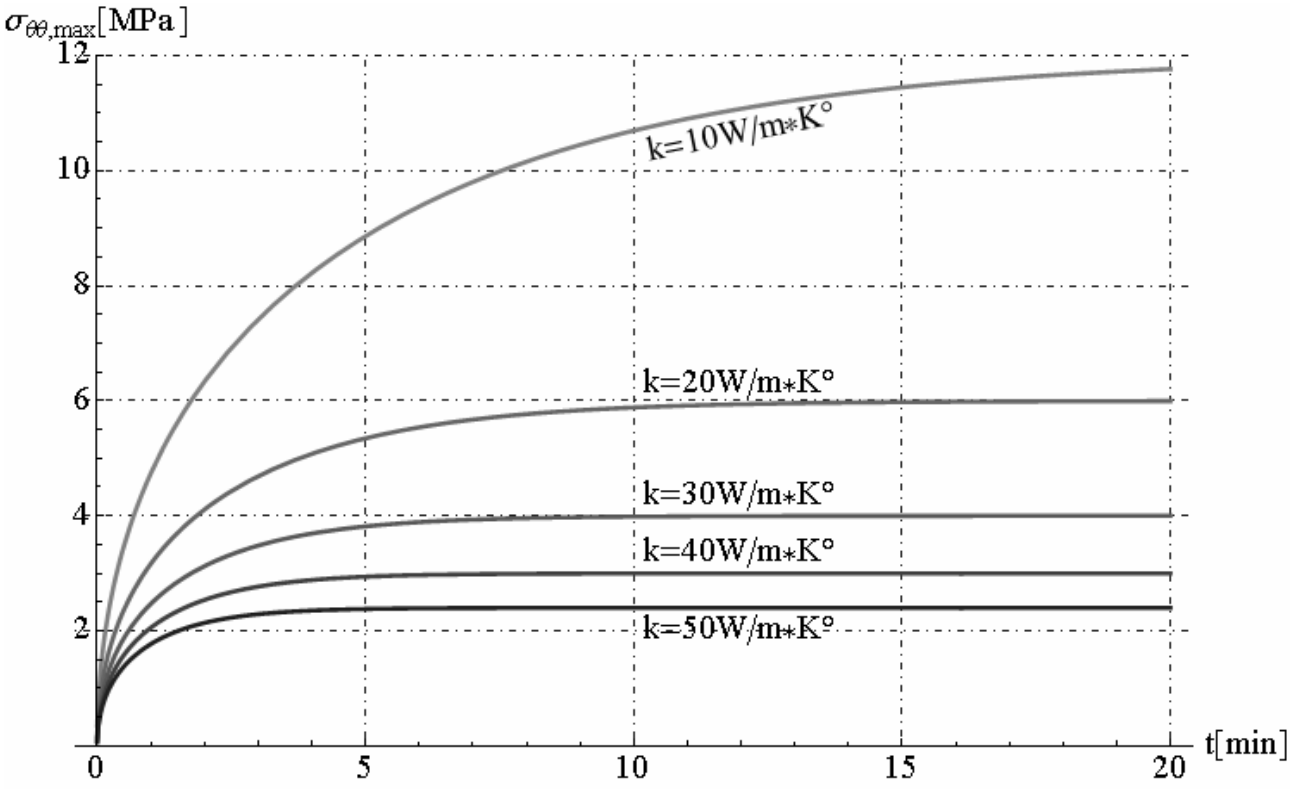

Fig. 15.25 - *Variation of thermal conductivity with fixed values of other parameters:* $E = 210GPa, \nu = 0.3, \alpha = 1.2 \cdot 10^{-6\circ} K^{-1}$, $c_v = 440 J\, kg^{-1\circ} K^{-1}$, $\rho = 7800 kgm^{-3}$, $\overline{s} = 0.01$,

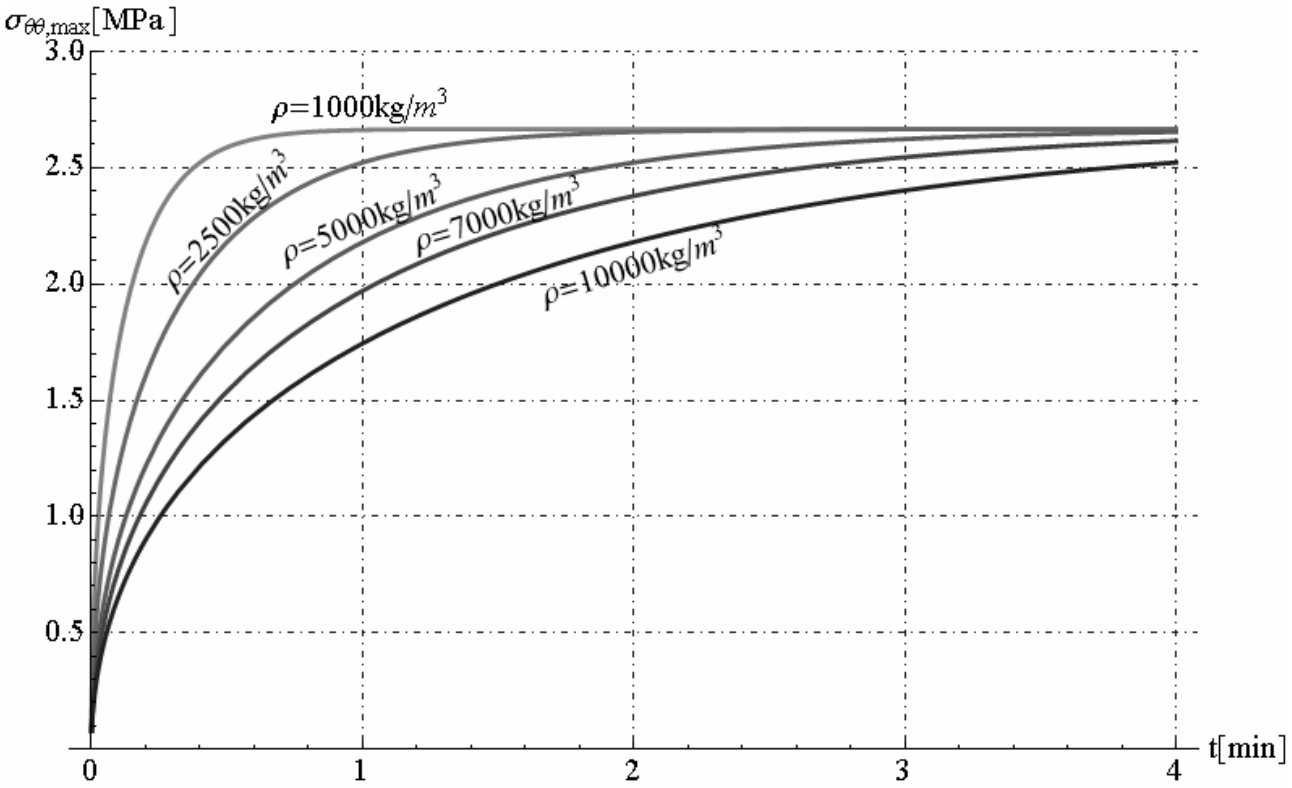

Fig. 15.26 - *Variation of density with fixed values of other parameters:* $E = 210GPa, \nu = 0.3, \alpha = 1.2 \cdot 10^{-6\circ} K^{-1}$, $c_v = 440 J\, kg^{-1\circ} K^{-1}$, $k = 45 Wm^{-1\circ} K^{-1}$, $\overline{s} = 0.01$,

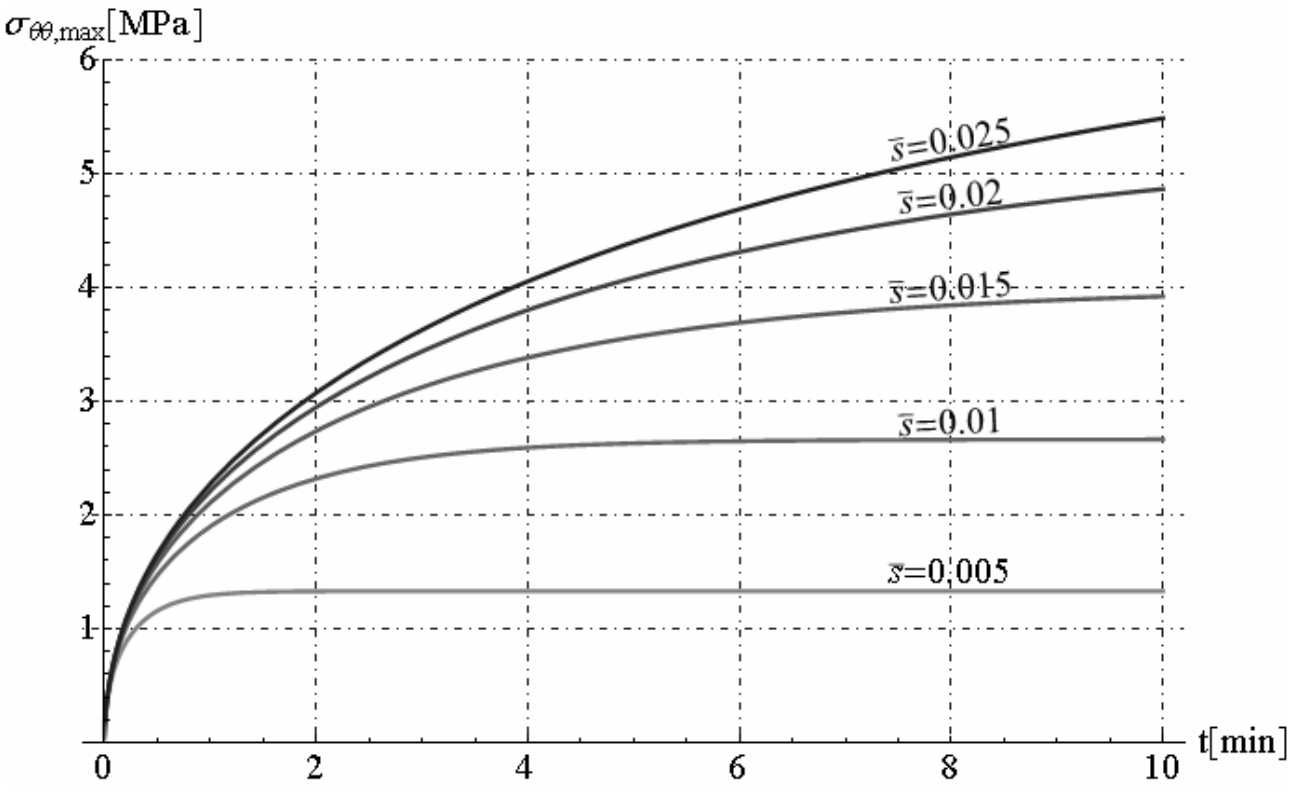

Fig. 15.27 - *Variation of ratio* $\bar{s}$ *with fixed values of other parameters:* $E = 210GPa, \nu = 0.3, \alpha = 1.2 \cdot 10^{-6} {}^{\circ} K^{-1}$, $c_v = 440 J\, kg^{-1} {}^{\circ} K^{-1}, k = 45 Wm^{-1} {}^{\circ} K^{-1}, \rho = 7800 kgm^{-3}$,

15.9. Coupled thermo-elastic analysis in hollow sphere exposed to an ambient at zero temperature through a uniform boundary conductance

Let us consider a hollow sphere with inner radius "a" and outer radius "b" , subjected to radial temperature variation as described in section 15.6. The surface r = a is kept perfectly insulated while the surface r = b is exposed, for t >0, to an ambient at zero temperature through a uniform boundary conductance h. The initial temperature (for t = 0) of the hollow sphere is $T_0 = T_R = const$ where $T_R > 0$. We determine the heat conduction, displacement and stress function in hollow sphere under decreasing of temperature from $T_R > 0$ until to zero. In this paragraph, by applying the equation of section 15.2, the coupled thermo-elastic analyses is conducted.

The differential equation related to heat conduction and the corresponding boundary conditions are reported below:

$$\frac{\partial^3 T}{\partial r^3} + \frac{2}{r}\frac{\partial^2 T}{\partial r^2} - \frac{2}{r^2}\frac{\partial T}{\partial r} = \frac{(1+\delta)}{\kappa}\frac{\partial^2 T}{\partial r \partial t}, \quad a < r < b, \quad t > 0 \tag{15.126}$$

$$-k\frac{\partial T}{\partial r} = 0, \quad r = a, \ t > 0, \tag{15.127}$$

$$-k\frac{\partial T}{\partial r} = hT; \quad r = b, \ t > 0, \tag{15.128}$$

$$T = T_R; \quad a < r < b, \quad t = 0, \tag{15.129}$$

where $T_0 = T_R$ is a suitable chosen reference temperature in initial condition (for t = 0).

The problem is therefore on with homogeneous differential equation and boundary conditions and may be treated by the method separation of variables. As in eq.(15.126), a particular solution of the differential equation and boundary conditions of the form:

$$T(r,t) = \varphi(r)\,\psi(t) \tag{15.130}$$

By substituting the function (15.130) in equations.(15.126)-(15.128), we obtain:

$$\frac{d^3\varphi(r)}{d\,r^3}+\frac{2}{r}\frac{d^2\varphi(r)}{d\,r^2}-\left(\frac{2}{r^2}-\omega^2\right)\frac{d\varphi(r)}{d\,r}=0; \tag{15.131}$$

$$-k\frac{d\,\varphi}{d\,r}=0;\quad r=a, \tag{15.132}$$

$$-k\frac{d\,\varphi}{d\,r}=h\varphi;\quad x=b, \tag{15.133}$$

And to the following equation for $\psi(t)$:

$$\frac{d\psi(t)}{dt}+\frac{\kappa\omega^2}{(1+\delta)}\psi(t)=0 \tag{15.134}$$

The general solution of (15.134) is:

$$\psi(t)=e^{-\left(\kappa\omega^2 t\right)/(1+\delta)} \tag{15.135}$$

The general solution of (15.131) is:

$$\varphi(r)=\frac{1}{r}\left(C_1e^{i\,\omega r}+C_2e^{-i\,\omega r}\right)+C_3 \tag{15.136}$$

where C_1,C_2,C_3 are constants integration to determine . Then, the temperature solution is given by:

$$T(r,t)=\left[\left(C_1e^{i\omega r}+C_2e^{-i\omega r}\right)r^{-1}+C_3\right]e^{-\left(\kappa\omega^2 t\right)/(1+\delta)} \tag{15.137}$$

By substituting the function (15.137), in equation (15.14), and by integrating in two times, respect to variable r, we obtain in explicit the displacement function in hollow sphere:

$$\begin{aligned}u_r=&-\alpha T_R\,r+\frac{C_4}{r^2}e^{-\left(\kappa\omega^2 t\right)/(1+\delta)}+\\&+\frac{\alpha(3\lambda+2\mu)}{(\lambda+2\mu)\omega^2\,r^2}\left[C_1(1-i\omega r)e^{i\omega r}+C_2(1+i\omega r)e^{-i\omega r}-\frac{C_3\,\omega^2 r^3}{3\delta}\right]e^{-\left(\kappa\omega^2 t\right)/(1+\delta)}\end{aligned} \tag{15.138}$$

where C_4 is an other constant integration to determine. By recalling the boundary conditions reported in equations (15.5), (15.132) and (15.133), we obtain the homogeneous algebraic system in four unknown parameters C_1,C_2,C_3,C_4 as reported below:

$$\begin{cases}e^{ia\omega}(1-ia\,\omega)C_1+e^{-ia\omega}(1+ia\,\omega)C_2=0\\ e^{ib\omega}\left(1-\dfrac{bh}{k_1}-ib\,\omega\right)C_1+e^{-ib\omega}\left(1-\dfrac{bh}{k_1}+ib\,\omega\right)C_2-\dfrac{b^2h}{k_1}C_3=0\\ e^{ia\omega}(1+ia\,\omega)C_1+e^{-ia\omega}(1-ia\,\omega)C_2+\\ \quad+\dfrac{ia^3\omega^2\left[3(1+\delta)\lambda+2(1+3\delta)\mu\right]C_3}{12\,\delta\,\mu}+\dfrac{i\,\omega^2(\lambda+2\mu)C_4}{\alpha(3\lambda+2\mu)}=0\\ e^{ia\omega}(1+ia\,\omega)C_1+e^{-ia\omega}(1-ia\,\omega)C_2\\ \quad+\dfrac{ib^3\omega^2\left[3(1+\delta)\lambda+2(1+3\delta)\mu\right]C_3}{12\,\delta\,\mu}+\dfrac{i\omega^2(\lambda+2\mu)C_4}{\alpha(3\lambda+2\mu)}=0\end{cases} \tag{15.139}$$

By solving the first , third and fourth equations of (15.139), respect to constants C_2,C_3,C_4, we obtain the follows solution:

$$C_2=\frac{e^{2ia\omega}(i+a\omega)}{a\omega-i}C_1,\ C_3=\frac{12e^{-ib\omega}\mu\delta\left[e^{2ib\omega}(a\omega-i)(1-ib\omega)+e^{2ia\omega}(i+a\omega)(1+ib\omega)\right]}{(a^3-b^3)\omega^2(a\omega-i)\left[3(1+\delta)\lambda+2(1+3\delta)\mu\right]}C_1,$$
$$C_4=\frac{\alpha(3\lambda+2\mu)a^3e^{-ib\omega}\left[e^{2ib\omega}(a\omega-i)(i+b\omega)-e^{2ia\omega}(i+a\omega)(b\omega-i)\right]}{(a^3-b^3)\omega^2(-1-ia\omega)(\lambda+2\mu)}C_1, \tag{15.140}$$

The algebraic system (15.139) can to be rewritten in follows manner:

$$\begin{bmatrix}\Phi_{11}&\Phi_{12}&\Phi_{13}&\Phi_{14}\\ \Phi_{21}&\Phi_{22}&\Phi_{23}&\Phi_{24}\\ \Phi_{31}&\Phi_{32}&\Phi_{33}&\Phi_{34}\\ \Phi_{41}&\Phi_{42}&\Phi_{43}&\Phi_{44}\end{bmatrix}\cdot\begin{bmatrix}C_1\\C_2\\C_3\\C_4\end{bmatrix}=\begin{bmatrix}0\\0\\0\\0\end{bmatrix}, \tag{15.141}$$

where the elements of matrix $\left[\Phi_{ij}\right]$ are given by following expressions:

$$\Phi_{11}=e^{ia\omega}(1-ia\omega),\ \Phi_{12}=e^{-ia\omega}(1+ia\omega),\ \Phi_{13}=\Phi_{14}=0,\ \Phi_{21}=e^{ib\omega}(1-\frac{hb}{k_1}-ib\omega),$$
$$\Phi_{22}=e^{-ib\omega}(1-\frac{hb}{k_1}+ib\omega),\ \Phi_{23}=-\frac{hb^2}{k_1},\ \Phi_{24}=0,\ \ \Phi_{31}=e^{ia\omega}(1+ia\omega),$$
$$\Phi_{32}=e^{-ia\omega}(1-ia\omega),\ \Phi_{33}=\frac{ia^3\omega^2\left[3(1+\delta)\lambda+2(1+3\delta)\mu\right]}{12\delta\mu},\ \Phi_{34}=\frac{i\omega^2(\lambda+2\mu)}{\alpha(3\lambda+2\mu)}, \tag{15.142}$$
$$\Phi_{41}=e^{ib\omega}(1+ib\omega),\ \Phi_{42}=e^{-ib\omega}(1-ib\omega),\ \Phi_{43}=\frac{ib^3\omega^2\left[3(1+\delta)\lambda+2(1+3\delta)\mu\right]}{12\delta\mu},$$
$$\Phi_{44}=\frac{i\omega^2(\lambda+2\mu)}{\alpha(3\lambda+2\mu)},$$

The algebraic system (15.141) admit not trivial solution if the determinant of the matrix $\left[\Phi_{ij}\right]$ is equal to zero. By imposing this condition, we obtain the transcendental equation in unknown parameter ω:

$$\det\left[\Phi_{ij}\right]=0\ \Rightarrow\ g(\omega)=0 \tag{15.143}$$

The roots of this transcendental equation (15.143) are an infinite number such, denoted here by ω_m, $m=1,2,....\infty$ leading to characteristic values $\lambda_m=-\omega_m^2$. The corresponding characteristic functions $\overline{\varphi}_m(r)$ are, as calculated above,

$$\overline{\varphi}_m(r)=\frac{\varphi_m(r)}{C_{1m}}=\frac{1}{r}\left(e^{i\omega_m r}+\frac{C_{2m}}{C_{1m}}e^{-i\omega_m r}\right)+\frac{C_{3m}}{C_{1m}} \tag{15.144}$$

The solution to the problem may therefore be written in the form:

$$T(r,t)=\sum_{m=1}^{\infty}\left[\left(C_{1m}e^{i\omega_m r}+C_{2m}e^{-i\omega_m r}\right)r^{-1}+C_{3m}\right]e^{-\left(\kappa\omega_m^2 t\right)/(1+\delta)} \tag{15.145}$$

where the coefficients C_{2m},C_{3m} depend of coefficients C_{1m} as showed equations (15.140). The coefficient C_{1m} are determined by applying the initial condition (15.129) that yields the following relationship:

$$C_{1m}=\frac{\int_0^{2\pi}\int_0^{\pi}\int_a^b T_R\,\overline{\varphi}_m(r)\,r^2\sin\theta\,dr\,d\theta\,d\phi}{\int_0^{2\pi}\int_0^{\pi}\int_a^b \overline{\varphi}_m^{-2}(r)\,r^2\sin\theta\,dr\,d\theta\,d\phi} \tag{15.146}$$

Finally, the displacement function can to be rewritten as follows:

$$u_r = -\alpha T_R\, r + \sum_{m=1}^{\infty} C_{4m}\, r^{-2} e^{-\left(\kappa\omega_m^2 t\right)/(1+\delta)} + \\ + \sum_{m=1}^{\infty} \frac{\alpha(3\lambda+2\mu)}{(\lambda+2\mu)\,\omega_m^2 r^2}\left[C_{1m}(1-i\omega_m r)e^{i\omega_m r} + C_{2m}(1+i\omega_m r)e^{-i\omega_m r} - \frac{C_{3m}\omega_m^2 r^3}{3\delta} \right] e^{-\left(\kappa\omega_m^2 t\right)/(1+\delta)} \tag{15.147}$$

It is important to note that if the parameter $\delta \to 0$ in expressions of temperature and radial displacement, by means the solution (15.140), we obtain the solution for uncoupled problem.
For example, let us consider, a spherical tank constituted by ***Rubidio***, under decreasing temperature. In this case the parameter $\delta = 0.048$ and then the solution for coupled is very closed respect to uncoupled problem. The geometrical, mechanical and thermal parameters considered for spherical tank are reported below:

$$E = 2.4\cdot 10^9\, N/m^2,\ \nu = 0.3,\ c = 363 J/kg\cdot °K,\ k = 58.2 W/m\cdot K°, \\ \rho = 1532 kg/m^3,\quad b = 1.05m,\quad a = 1.00m, s = b-a = 0.05m, \\ h = 50 W/m^2\cdot °K,\quad \alpha = 9\cdot 10^{-5} °K^{-1},\quad T_0 = T_R = 293°K, \tag{15.148}$$

In this case the graphics function $g(\omega)$ given by equation (15.143) is reported below:

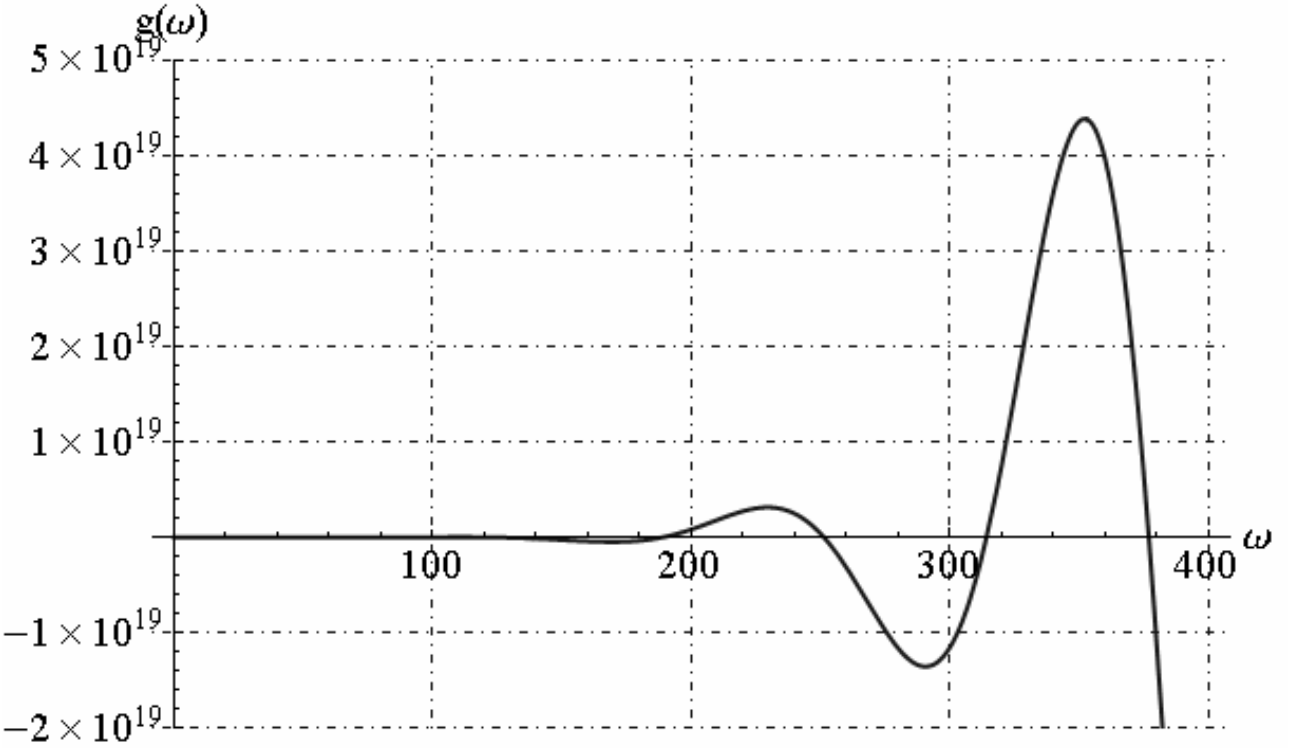

By fixed m= 20, the eigenvalues ω_m and corresponding values of constants integration A_m are reported in table 15.3:

ω_m	4.158	63.119	125.808	188.592	251.400
A_m	-48.832 + 148.161 i	-1.226 + 0.383 i	0.321 - 0.049 i	-0.144 + 0.015 i	0.081 - 0.006 i
ω_m	314.217	377.039	439.864	502.691	565.519
A_m	-0.0520 + 0.0032 i	0.0361 - 0.0018 i	-0.0266 + 0.0012 i	0.0203 - 0.0008 i	-0.0161 + 0.0005 i
ω_m	628.347	691.177	754.006	816.836	879.667
A_m	0.0130 - 0.0004 i	-0.0108 + 0.0003 i	0.0090 - 0.0002 i	-0.0077 + 0.0002 i	0.0066 - 0.0001 i
ω_m	942.497	1005.328	1068.158	1130.989	1193.820
A_m	-0.0058 + 0.0001 i	0.0051 - 0. × 10^-4 i	-0.0045 + 0. × 10^-5 i	0.0040 + 0. × 10^-5 i	-0.0036 + 0. × 10^-5 i

Table 15.3 – *Eigenvalues ω_m and corresponding values of constants integration A_m*

We reported the comparison between uncoupled and coupled solution obtained for temperature, radial displacement and stress components along the radial direction and in time:

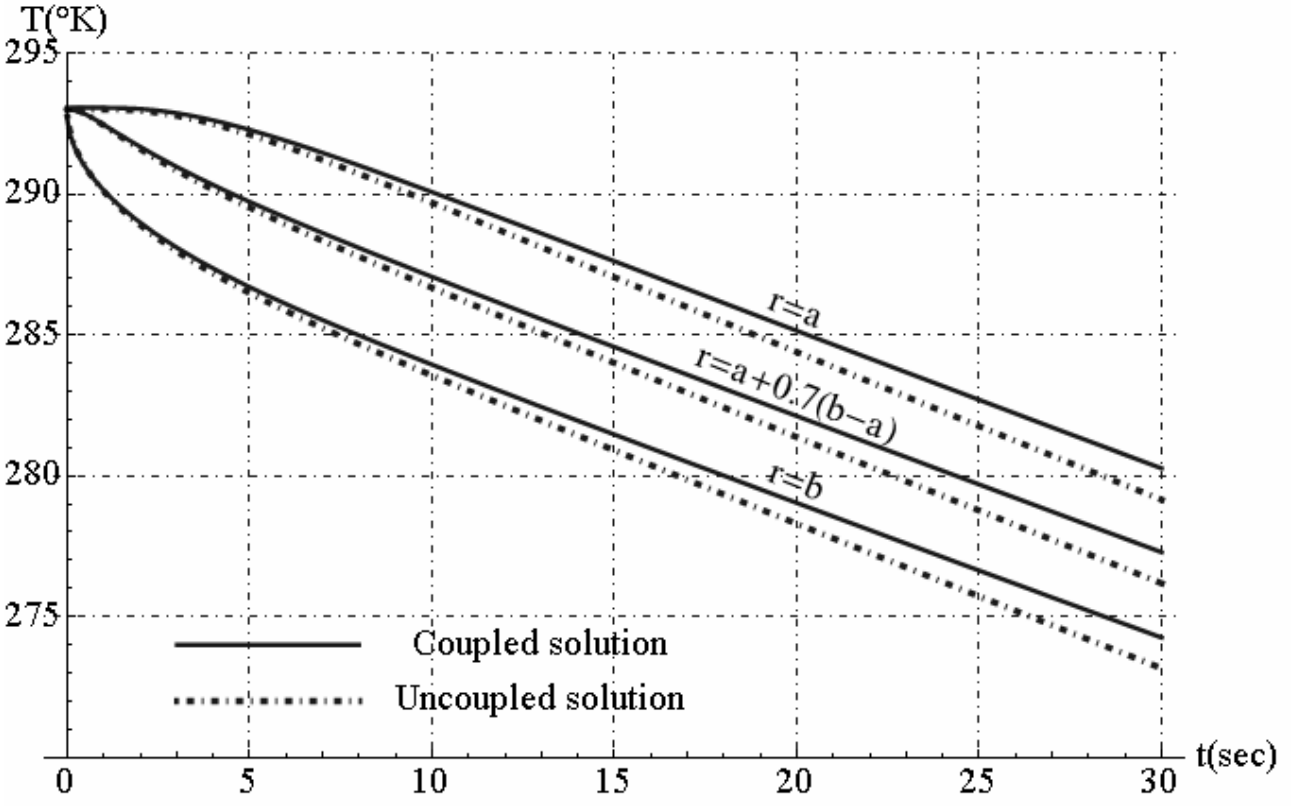

Fig. 15.28 - *Temperature function versus the time*

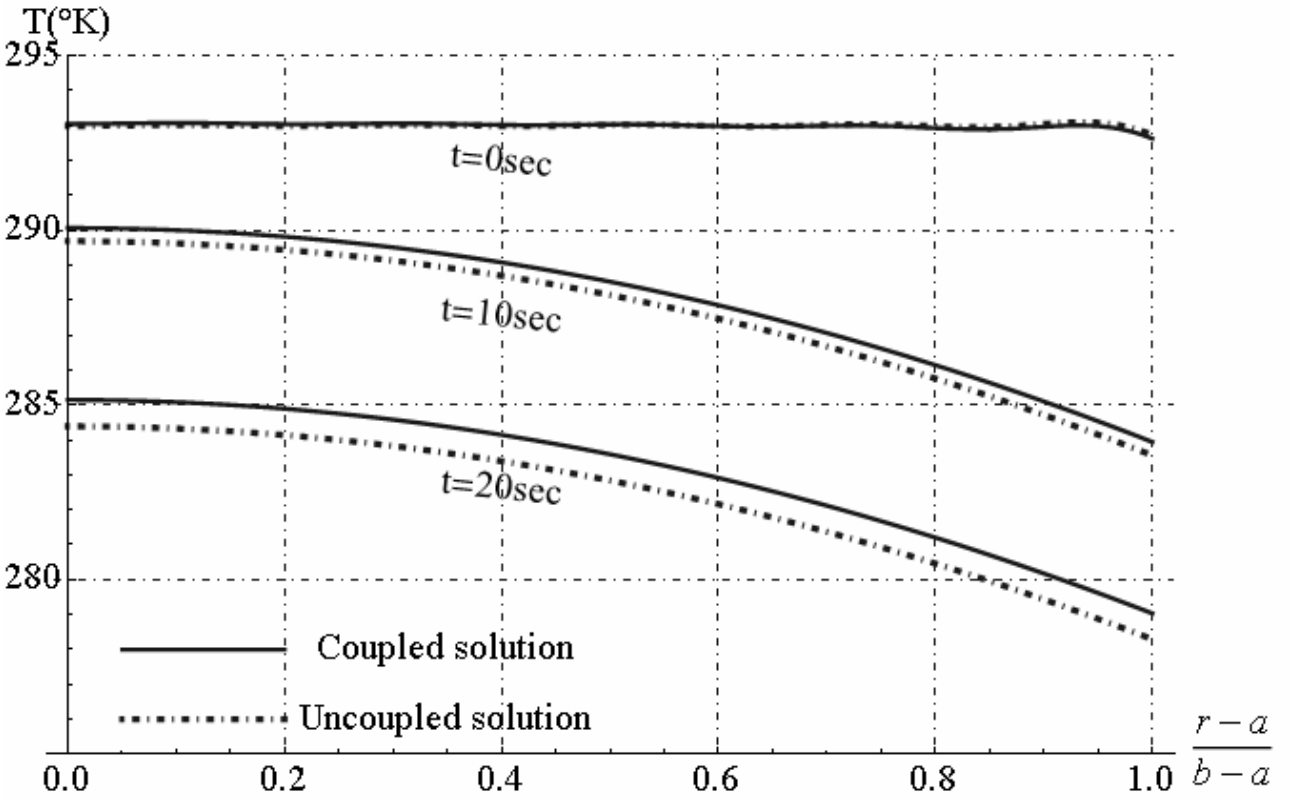

Fig. 15.29 - *Temperature function along radial direction*

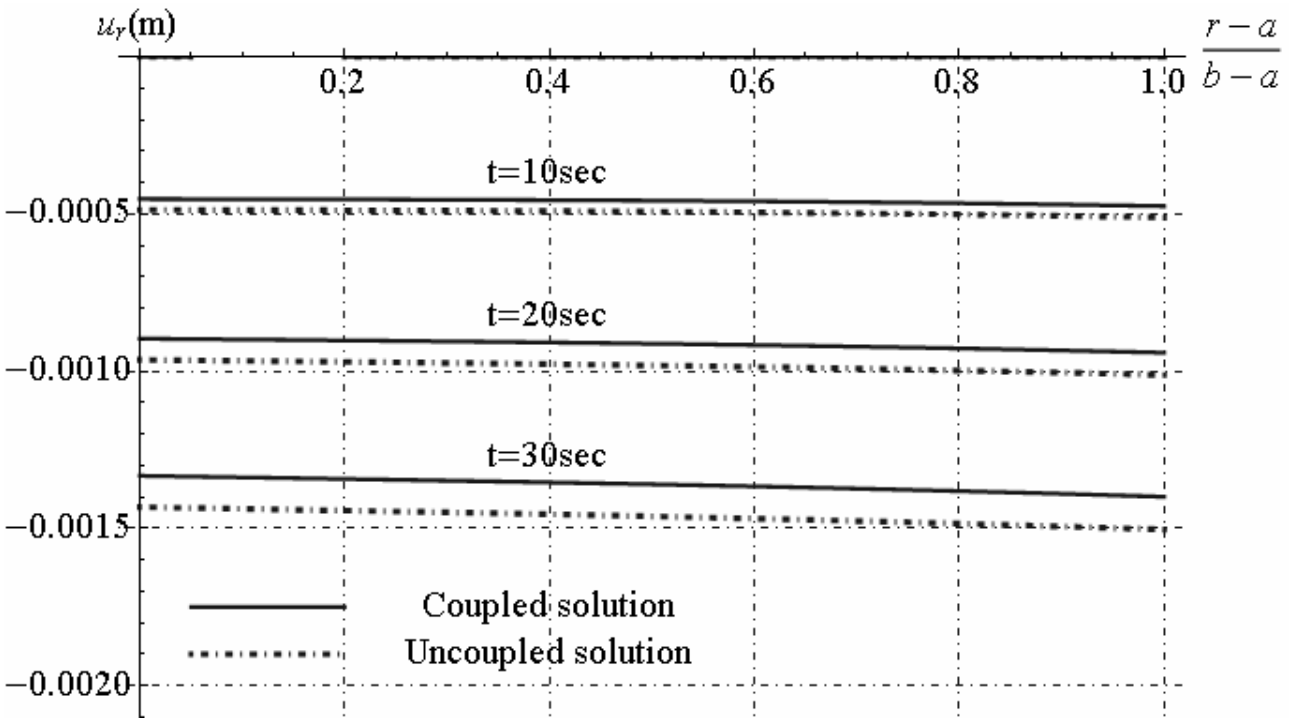

Fig. 15.30 - *Radial displacement distribution along radial direction*

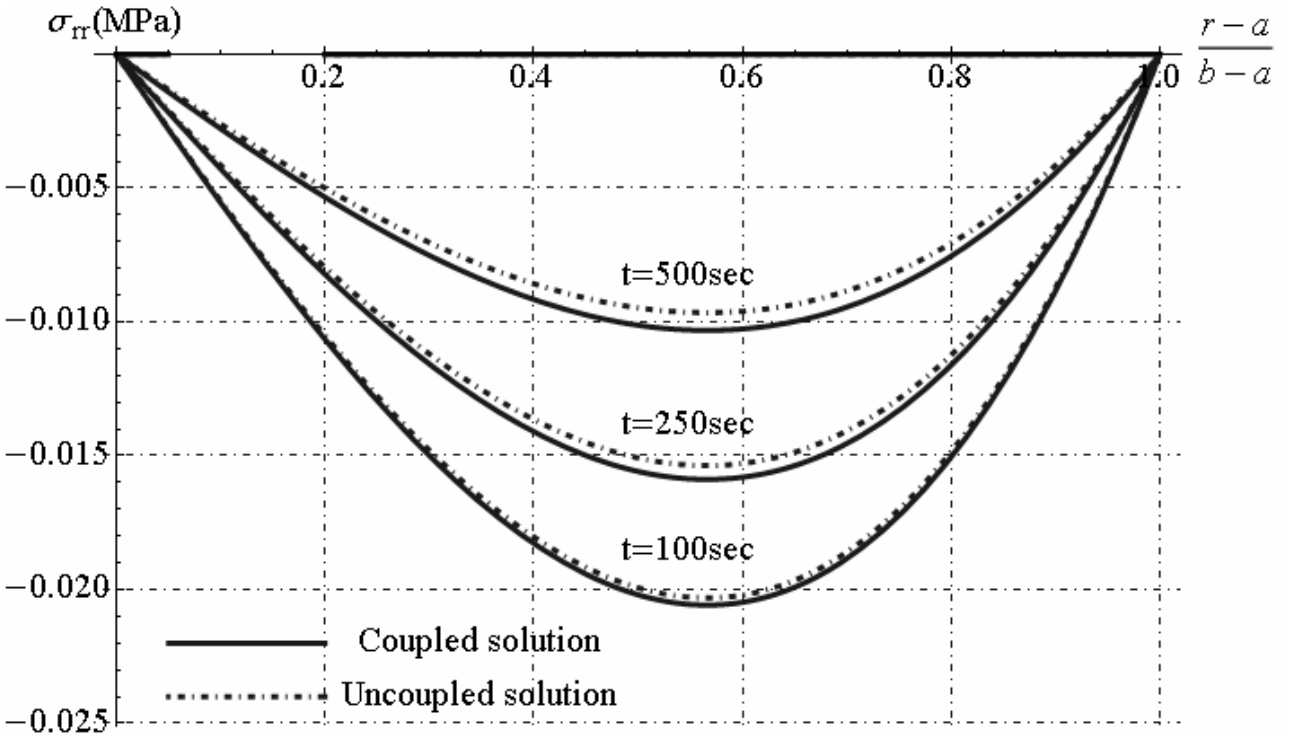

Fig. 15.31 - *Radial stress distribution along radial direction*

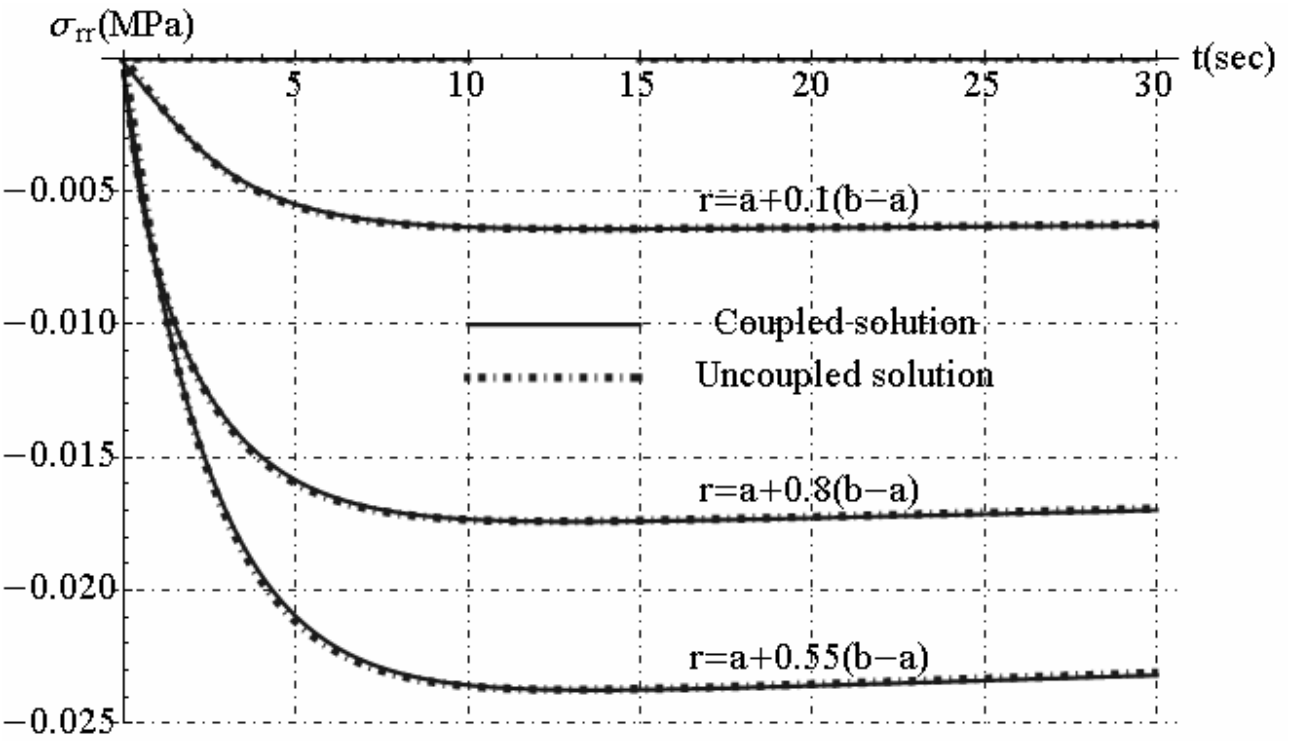

Fig. 15.32 - *Radial stress distribution in time*

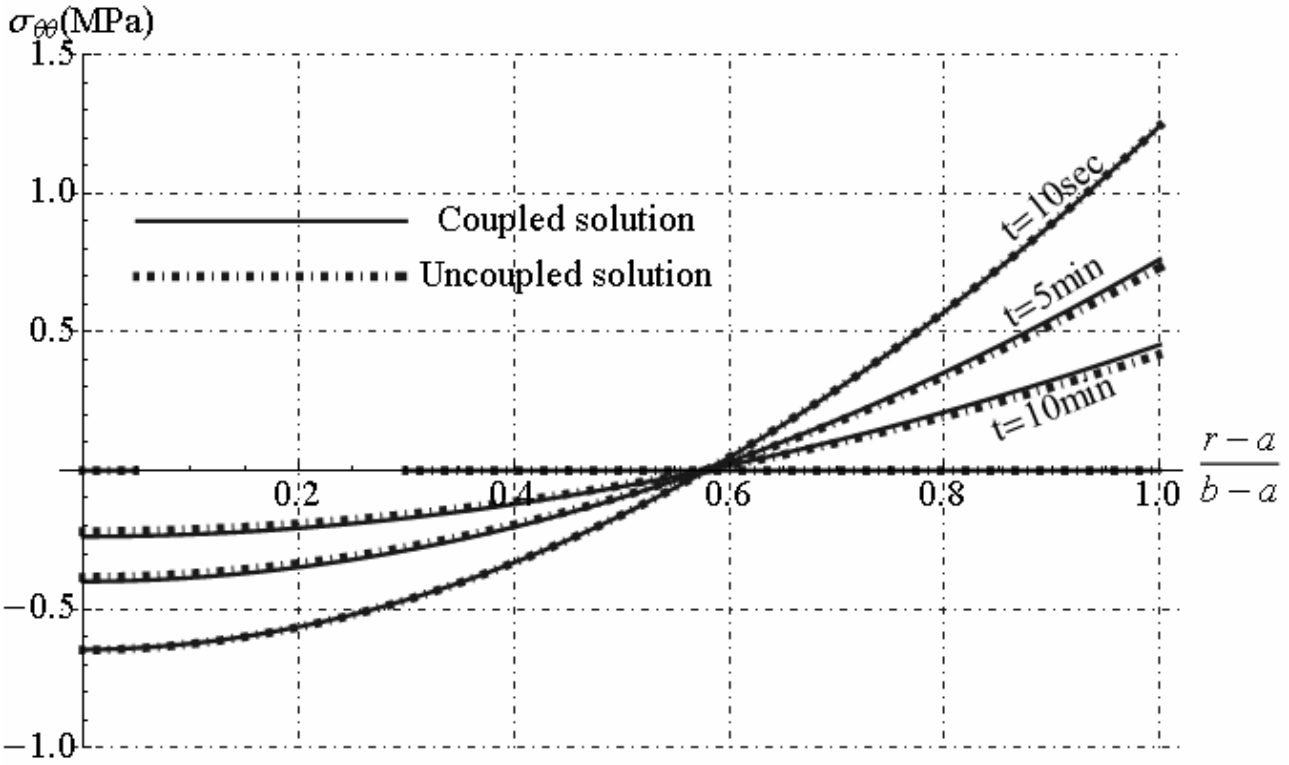

Fig. 15.33 - *Circumferential stress distribution along radial direction*

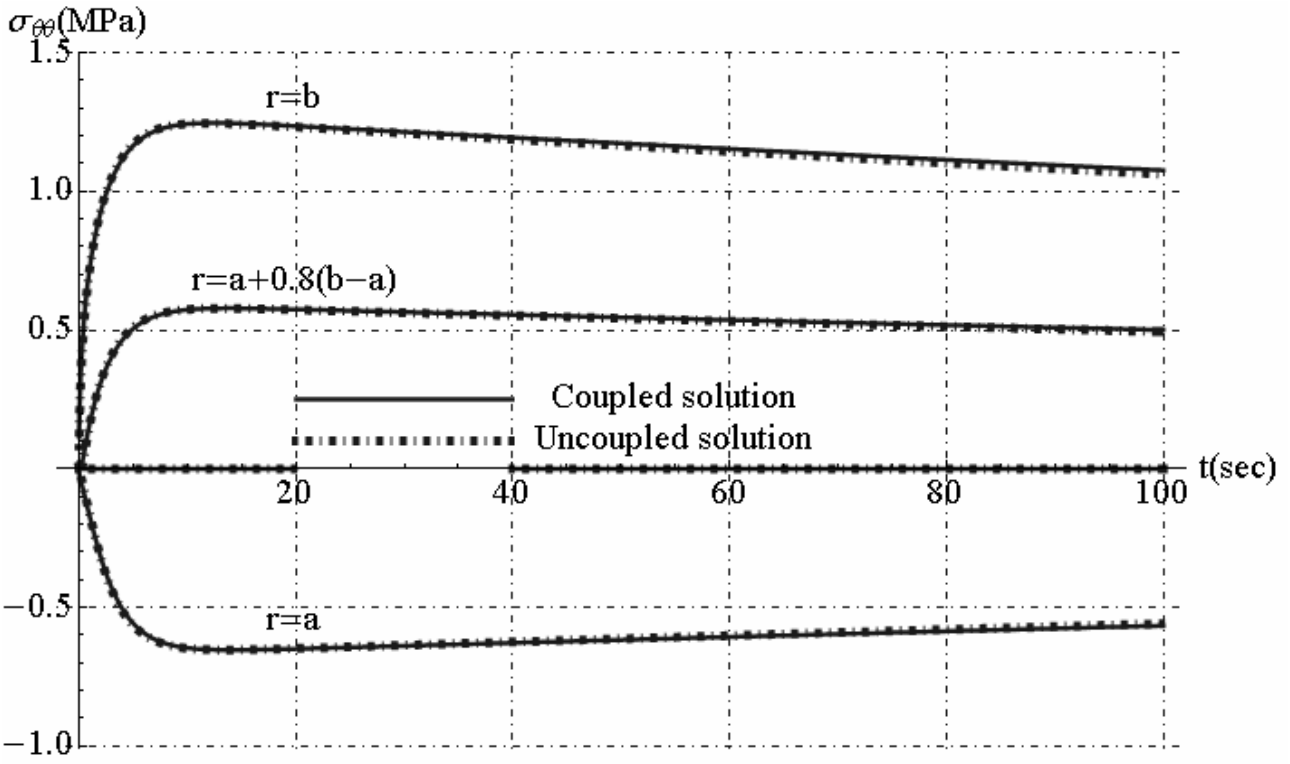

Fig. 15.34 - *Circumferential stress distribution in time*

15.10. Coupled thermo-elastic analysis in hollow sphere exposed to uniform heat flux

Let us consider a hollow sphere with inner radius "a" and outer radius "b" , subjected to radial temperature variation. The surface r = a is kept perfectly insulated while the surface r = b is exposed, for t >0, to a constant , uniform heat input q_0 . The initial temperature of the hollow sphere is zero. In this section, we determine the heat conduction, displacement and stress function in hollow sphere subjected to uniform heat input q_0 applied on external surface, starting to initial temperature in solid equal to $T_0 = T_R = const$. In this paragraph, by applying the equation of section 15.2, the coupled thermo-elastic analyses is conducted. The differential equation related to heat conduction and the corresponding boundary conditions are reported below:

$$\frac{\partial^3 T}{\partial r^3}+\frac{2}{r}\frac{\partial^2 T}{\partial r^2}-\frac{2}{r^2}\frac{\partial T}{\partial r}=\frac{(1+\delta)}{\kappa}\frac{\partial^2 T}{\partial r\,\partial t};\quad a<r<b,\quad t>0 \tag{15.149}$$

$$-k\frac{\partial T}{\partial r}=0,\quad r=a,\ t>0, \tag{15.150}$$

$$-k\frac{\partial T}{\partial r}=q_0,\quad r=b,\ t>0, \tag{15.151}$$

$$T=T_0;\quad a<r<b,\quad t=0, \tag{15.152}$$

This is an case of a problem involving a non-homogeneous boundary condition and, in particular, with the heat input specified over the entire boundary surface. It is necessary writing the solution in the follows form (see Chapter VII) :

$$T(r,t)=T_0+\zeta\, t+T_S(r)+T_C(r,t) \tag{15.153}$$

where T_S satisfies the equations:

$$\frac{d^3 T_S}{d\,r^3}+\frac{2}{r}\frac{d^2 T_S}{d\,r^2}-\frac{2}{r}\frac{d\,T_S}{d\,r}=0;\quad a<r<b, \tag{15.154}$$

$$-k\frac{dT_S}{dr}=0;\quad r=a, \tag{15.155}$$

$$-k\frac{dT_S}{dr}=q_0;\quad r=b, \tag{15.156}$$

$$\int_V T_S(r)\,dV=\int_0^{2\pi}\int_0^{\pi}\int_a^b\left(T_S(r)r^2\sin\theta\right)drd\theta d\phi=0 \tag{15.157}$$

where ζ may be determined either from the boundary conditions (15.155)-(15.157). T_C satisfies equations:

$$\frac{\partial^3 T_C}{\partial r^3}+\frac{2}{r}\frac{\partial^2 T_C}{\partial r^2}-\frac{2}{r}\frac{\partial T_C}{\partial r}=\frac{1}{\kappa}\frac{\partial T_C}{\partial t};\quad a<r<b,\quad t>0 \tag{15.158}$$

$$-k\frac{\partial T_C}{\partial r}=0;\quad r=a,\quad t>0, \tag{15.159}$$

$$-k\frac{\partial T_C}{\partial r}=0;\quad r=b,\quad t>0, \tag{15.160}$$

$$T_C=-T_S;\quad a<r<b,\quad t=0, \tag{15.161}$$

By applying the similar procedure showed in section 15.7, we obtain the temperature function and radial displacement components, as reported below:

$$T(r,t)=T_0+\left(P_1+\xi\right)t+\frac{A_1}{r}+A_2+\frac{\xi r^2}{6\kappa}+\sum_{m=1}^{\infty}\left(C_{1m}r^{-1}e^{i\omega_m r}+C_{2m}r^{-1}e^{-i\omega_m r}+C_{3m}\right)e^{-\left(\kappa\omega_m^2 t\right)/(1+\delta)} \tag{15.162}$$

$$\begin{aligned}u_r=&N_1 r+\frac{N_2}{r^2}+\frac{\alpha(3\lambda+2\mu)}{(\lambda+2\mu)}\left[\frac{A_1}{2}+\frac{A_2 r}{3}+\frac{\xi r^3}{30\kappa}-\frac{t}{3\delta}\left(P_1 r+\frac{P_2}{r^2}\right)\right]+\sum_{m=1}^{\infty}\frac{C_{4m}}{r^2}e^{-\left(\kappa\omega_m^2 t\right)/(1+\delta)}+\\&+\sum_{m=1}^{\infty}\frac{\alpha(3\lambda+2\mu)}{(\lambda+2\mu)\omega_m^2 r^2}\left[C_{1m}(1-i\omega_m r)e^{i\omega_m r}+C_{2m}(1+i\omega_m r)e^{-i\omega_m r}-\frac{C_{3m}\omega_m^2 r^3}{3\delta}\right]e^{-\left(\kappa\omega_m^2 t\right)/(1+\delta)}\end{aligned} \tag{15.163}$$

where $\zeta=P_1+\xi, A_1, A_2, N_1, N_2, P_1, P_2, \xi$ and $C_{1m}, C_{2m}, C_{3m}, C_{4m}$ are integration constants. By applying the boundary conditions reported in equations (15.155) to (15.157), and (15.159),(15.160) and (15.5), it is possible to determine the integration constants reported above as function of parameters C_{1m} and ω_m:

$$\begin{aligned}&C_{2m}=\frac{e^{2ib\omega_n}(b\omega_m+i)^2}{1+b^2\omega_m^2}C_{1m},\quad N_1=(T_0-T_R)\alpha,\ P_2=0,\\&C_{3m}=\frac{12e^{-ia\omega_m}\mu\delta\left[e^{2ia\omega_m}(i+a\omega_m)(b\omega_m-i)-e^{2\imath b\omega_m}(a\omega_m-i)(i+b\omega_m)\right]}{\omega_m^2(b^3-a^3)(1+ib\omega_m)\left[3(1+\delta)\lambda+2(1+3\delta)\mu\right]}C_{1m},\\&C_{4m}=\frac{\alpha(3\lambda+2\mu)b^3e^{-ia\omega_m}\left[e^{2ia\omega_m}(i+a\omega_m)(b\omega_m-i)-e^{2\imath b\omega_m}(a\omega_m-i)(i+b\omega_m)\right]}{\omega_m^2(a^3-b^3)(1+ib\omega_m)(\lambda+2\mu)}C_{1m},\\&\xi=\frac{3b^2q_0}{(a^3-b^3)c_v\rho},A_1=\frac{a^3b^2q_0}{(a^3-b^3)k},A_2=\frac{3b^2(6a^4+6a^3b+a^2b^2+ab^3+b^4)q_0}{10(b-a)(a^2+ab+b^2)^2k},\\&N_2=-\frac{\alpha(3\lambda+2\mu)a^3b^4(5a^2-ab-b^2)q_0}{10(a-b)(a^2+ab+b^2)^2k(\lambda+2\mu)},P_1=-\frac{9b^2q_0\delta(\lambda+2\mu)}{(a^3-b^3)\left[3(1+\delta)\lambda+2(1+3\delta)\mu\right]c_v\rho},\end{aligned} \tag{15.164}$$

he parameters ω_m can to be determined by imposing conditions reported in equation (15.143) and fixed h = 0. The roots of this transcendental equation (15.143) are an infinite number such, denoted here by $\omega_m, m=1,2,....\infty$ leading to eigenvalues or characteristic values $\lambda_m=-\omega_m^2$. The

corresponding eigenfunctions or characteristic functions $\bar{\varphi}_m(r)$ are determined by applying the equation (15.144) . Finally the parameters C_{1m} are determined by applying the relations (15.146). In this case the graphics function $g(\omega)$ given by equation (15.143) is reported below:

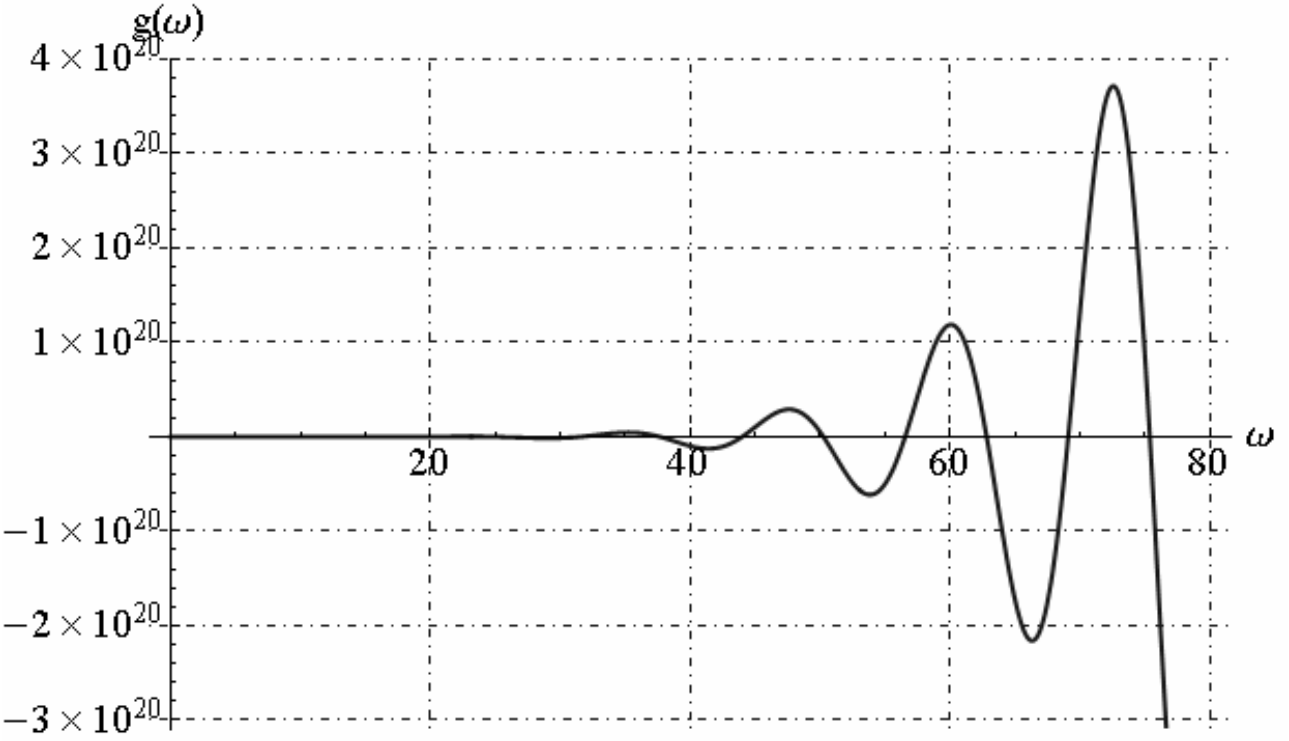

By fixed m= 20, the eigenvalues ω_m and corresponding values of constants integration A_m are reported in table 15.4:

ω_m	6.285	12.567	18.850	25.133	31.416
A_m	0.913 - 0.028 i	-0.228 + 0.004 i	0.102 - 0.001 i	$-0.057 + 0.\times 10^{-4}$ i	$0.037 + 0.\times 10^{-4}$ i
ω_m	37.699	43.983	50.266	56.549	62.832
A_m	-0.0254 + 0.0001 i	$0.0187 - 0.\times 10^{-5}$ i	$-0.0143 + 0.\times 10^{-5}$ i	$0.0113 + 0.\times 10^{-5}$ i	$-0.0091 + 0.\times 10^{-5}$ i
ω_m	69.115	75.398	81.682	87.965	94.248
A_m	$0.0076 + 0.\times 10^{-5}$ i	$-0.0063 + 0.\times 10^{-5}$ i	$0.0054 + 0.\times 10^{-5}$ i	$-0.0047 + 0.\times 10^{-5}$ i	$0.0041 + 0.\times 10^{-6}$ i
ω_m	100.531	106.814	113.097	119.381	125.664
A_m	$-0.0036 + 0.\times 10^{-6}$ i	$0.0032 + 0.\times 10^{-6}$ i	$-0.0028 + 0.\times 10^{-6}$ i	$0.0025 + 0.\times 10^{-6}$ i	$-0.0023 + 0.\times 10^{-6}$ i

Table 15.4 – *Eigenvalues ω_m and corresponding values of constants integration A_m*

We reported the comparison between uncoupled and coupled solution obtained for temperature, radial displacement and stress components along the radial direction and in time:

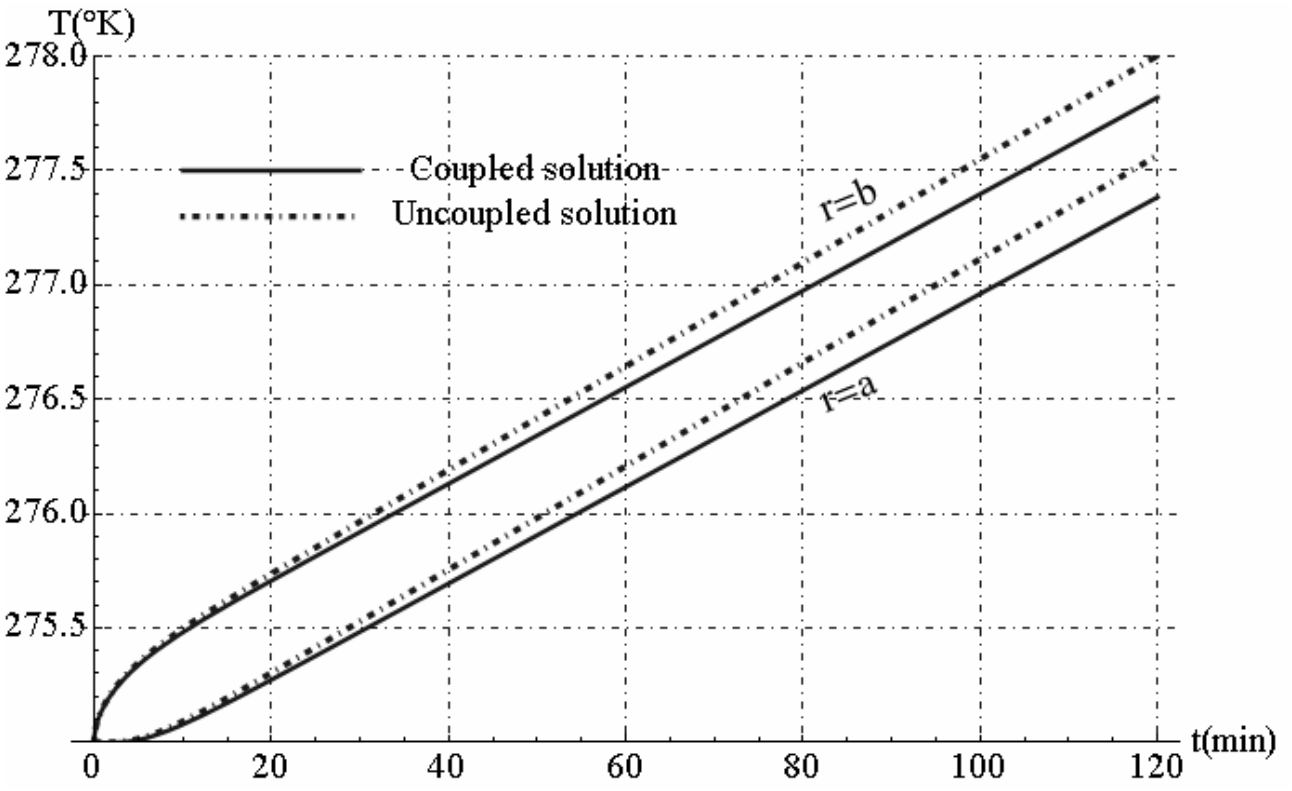

Fig. 15.35 - *Temperature function versus the time*

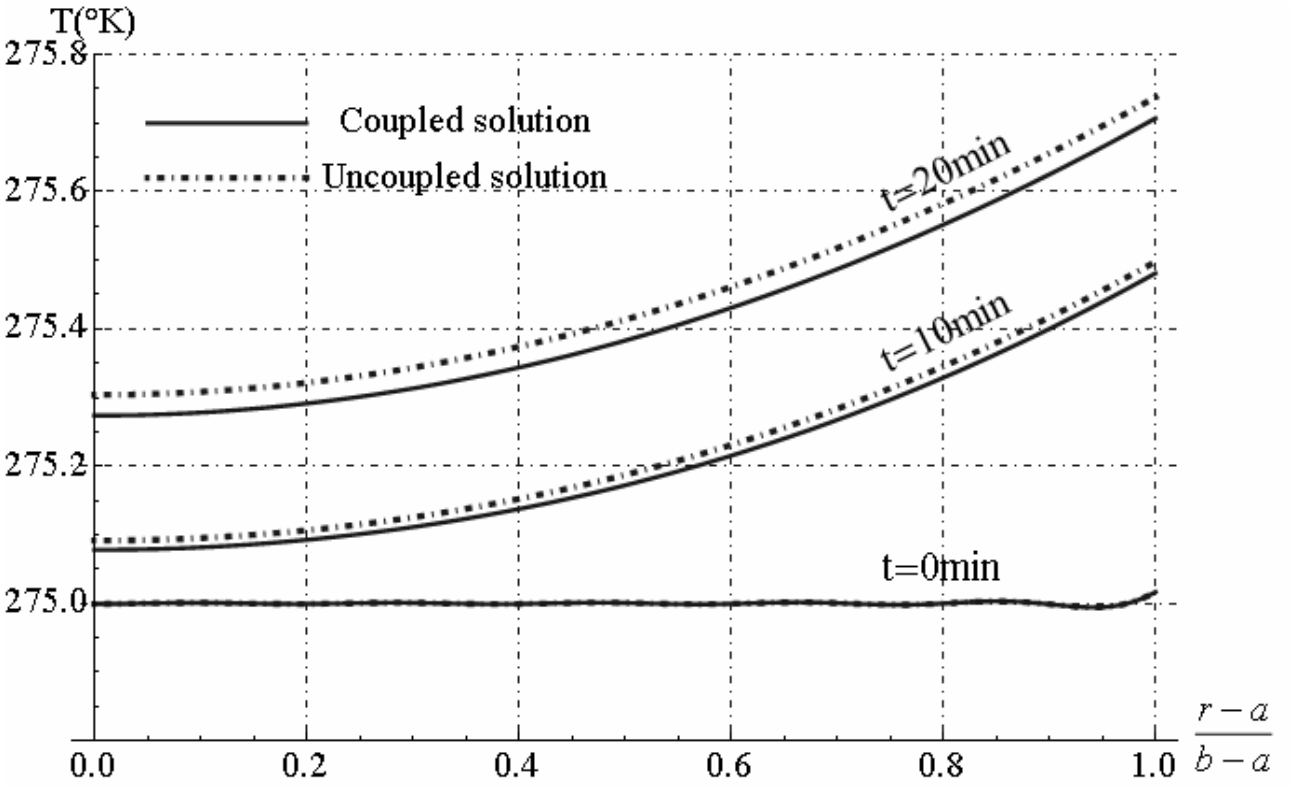

Fig. 15.36 - *Temperature function along radial direction*

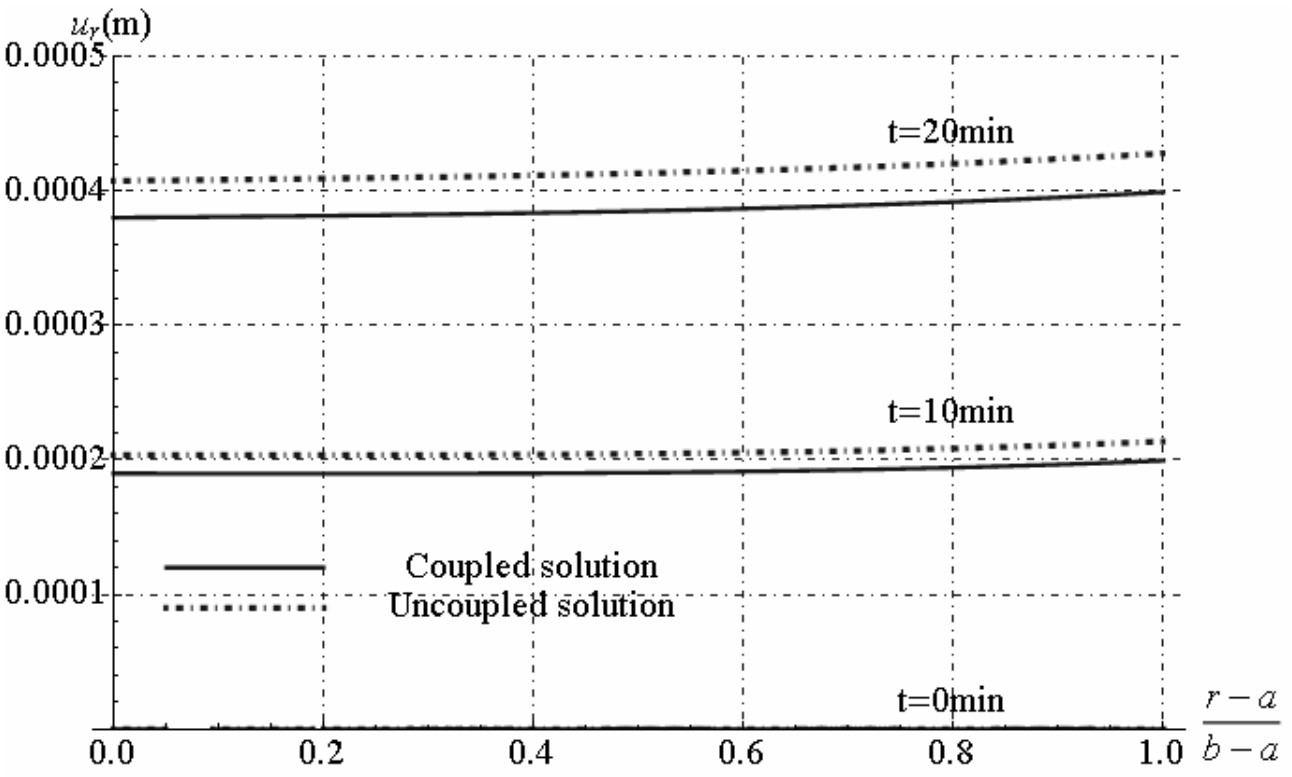

Fig. 15.37 - *Radial displacement distribution along radial direction*

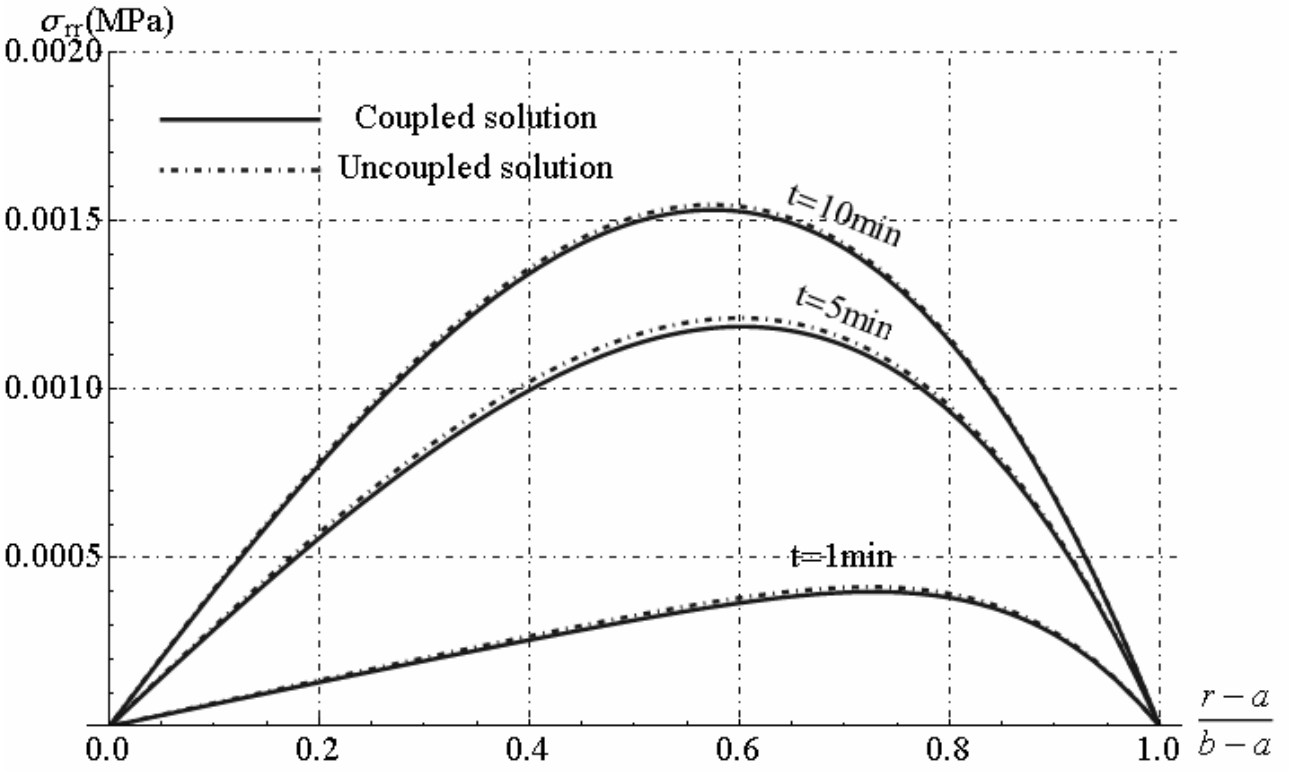

Fig. 15.38 - *Radial stress distribution along radial direction*

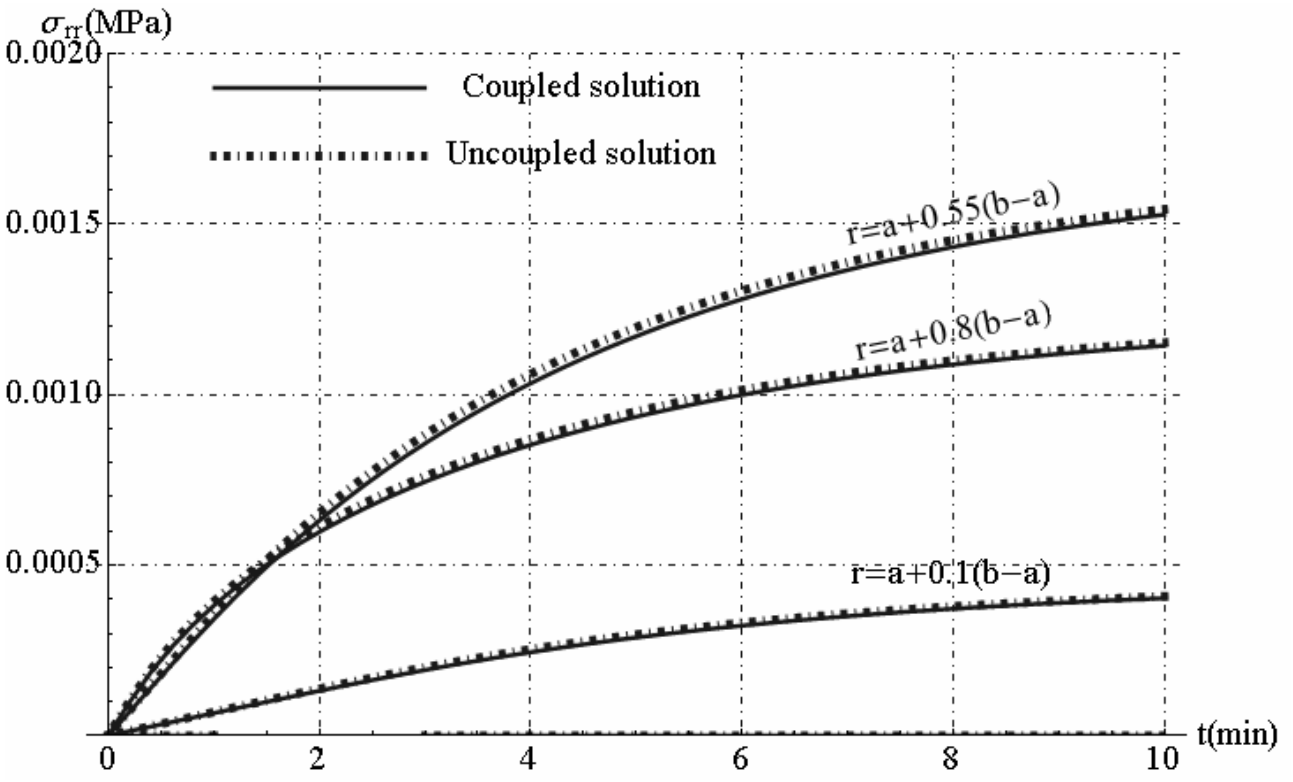

Fig. 15.39 - *Radial stress distribution in time*

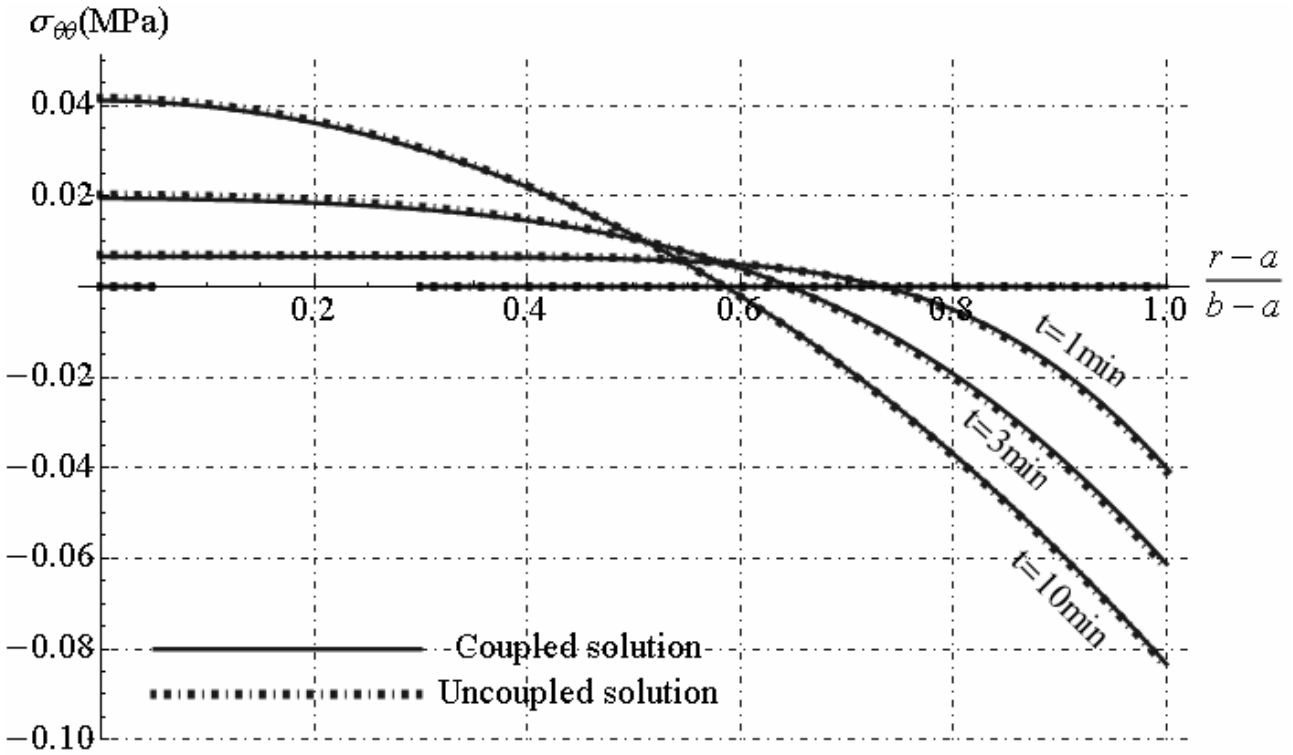

Fig. 15.40 - *Circumferential stress distribution along radial direction*

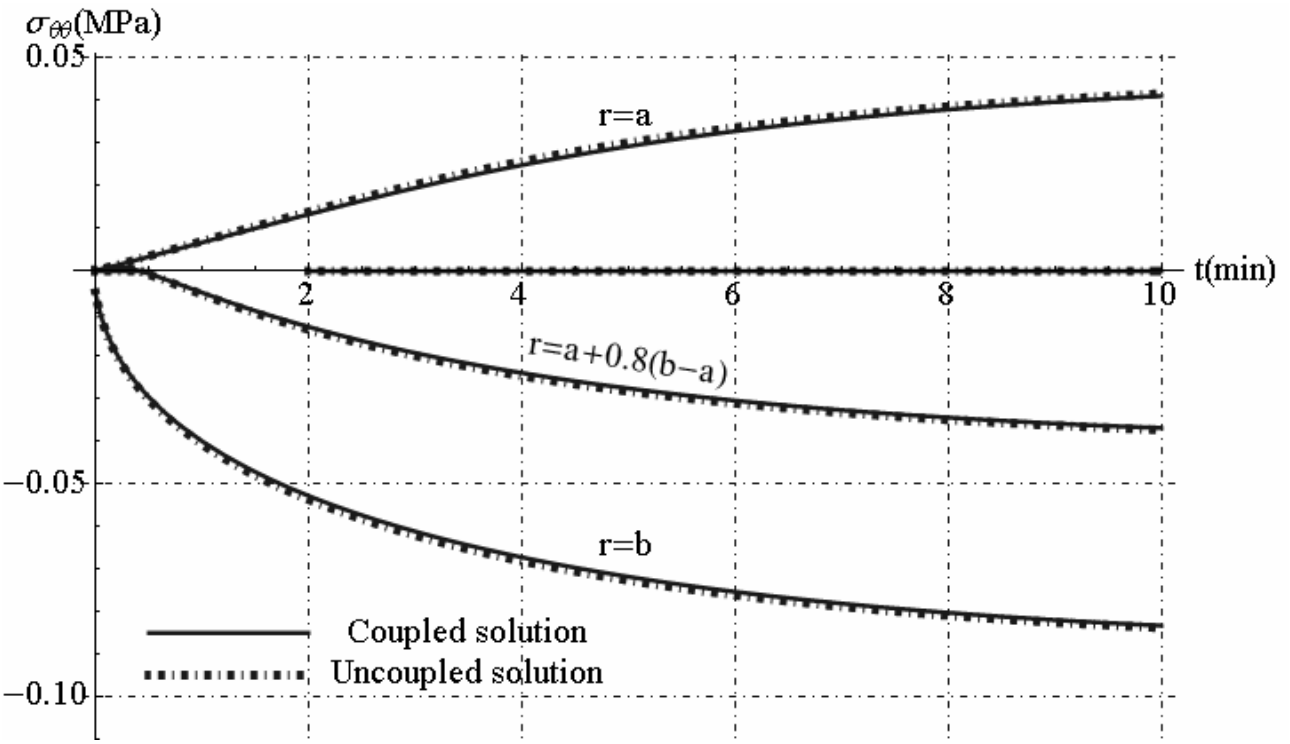

Fig. 15.41 - *Circumferential stress distribution in time*

15.11. References

[1] Boley, B.A.,Weiner, J.H., *Theory of thermal stresses*, Dover publications, inc. Mineola, New York

[2] Ciarlet, Philiphe G., *Mathematical Elasticity*, *Volume I.: Three dimensional elasticity*, Elsevier Science Publishers B.V.

[3] Fraldi, M., Nunziante, L., Carannante, F. (2007), *Axis-symmetrical Solutions for n-plies Functionally Graded Material Cylinders under Strain no-Decaying Conditions*, J. Mech. of Adv. Mat. and Struct. Vol. 14 (3), pp. 151-174 - DOI: 10.1080/15376490600719220

[4] M. Fraldi, L. Nunziante, F. Carannante, A. Prota, G. Manfredi, E. Cosenza (2008), *On the Prediction of the Collapse Load of Circular Concrete Columns Confined by FRP*, Journal Engineering structures, Vol. 30, Issue 11, November 2008, Pages 3247-3264 - DOI: 10.1016/j.engstruct.2008.04.036

[5] Fraldi, M., Nunziante, L., Chandrasekaran, S., Carannante, F., Pernice, MC. (2009), *Mechanics of distributed fibre optic sensors for strain measurements on rods*, Journal of Structural Engineering, 35, pp. 323-333, Dec. 2008- Gen. 2009

[6] M. Fraldi, F. Carannante, L. Nunziante (2012), *Analytical solutions for n-phase Functionally Graded Material Cylinders under de Saint Venant load conditions: Homogenization and effects of Poisson ratios on the overall stiffness*, Composites Part B: Engineering, Volume 45, Issue 1, February 2013, Pages 1310–1324

[7] Gurtin, M. E., *The Linear Theory of Elasticity, Handbbuch der Physik*, Springer, Berlin, 1972.

[8] Lekhnitskii, S. G., *Theory of Elasticity of an Anisotropic Body*, Mir, Moscow, 1981.

[9] Love, A. E. H., *A Treatise on the Mathematical Theory of Elasticity*, Dover Publications, Inc, New York, 1944

[10] Nunziante, L., Gambarotta, L., Tralli, A., *Scienza delle Costruzioni*, 3° Edizione, McGraw-Hill, 2011, ISBN: 9788838666971

[11] Ting TCT. *Anisotropic elasticity - Theory and applications*. Oxford University Press; 1996.

[12] Wolfram, S., *Mathematica, version 8*, Wolfram Research, Inc., Champaign, IL, 1998–2005.

CHAPTER XVI
THERMAL STRESSES IN PLATES

16.1. Introduction

Thin plates are initially flat structural members bounded by two parallel planes, called faces, and a cylindrical surface, called an edge or boundary. The generators of the cylindrical surface are perpendicular to the plane faces. The distance between the plane faces is called the thickness "s" of the plate. It will be assumed that the plate thickness is small compared with other characteristic dimensions of the faces (length, width, diameter, etc.). Geometrically, plates are bounded either by straight or curved boundaries (figure 16.1). The static or dynamic loads carried by plates are predominantly perpendicular to the plate faces. The load-carrying action of a plate is similar, to a certain extent, to that of beams or cables; thus, plates can be approximated by a gridwork of an infinite number of beams or by a network of an infinite number of cables, depending on the flexural rigidity of the structures. This two-dimensional structural action of plates results in lighter structures, and therefore offers numerous economic advantages. The plate, being originally flat, develops shear forces, bending and twisting moments to resist transverse loads. Because the loads are generally carried in both directions and because the twisting rigidity in isotropic plates is quite significant, a plate is considerably stiffer than a beam of comparable span and thickness. So, thin plates combine light weight and a form efficiency with high load-carrying capacity, economy, and technological effectiveness. Because of the distinct advantages discussed above, thin plates are extensively used in all fields of engineering. Plates are used in architectural structures, bridges, hydraulic structures, pavements, containers, airplanes, missiles, ships, instruments, machine parts, etc. We consider a plate, for which it is common to divide the thickness "s" into equal halves by a plane parallel to its faces. This plane is called the middle plane (or simply, the mid-plane) of the plate. Being subjected to transverse loads, an initially flat plate deforms and the mid-plane passes into some curvilinear surface, which is referred to as the middle surface. We will consider only plates of constant thickness. For such plates, the shape of a plate is adequately defined by describing the geometry of its middle plane. Depending on the shape of this mid-plane, we will distinguish between rectangular, circular, elliptic, etc., plates. A plate resists transverse loads by means of bending, exclusively. The flexural properties of a plate depend greatly upon its thickness in comparison with other dimensions. Plates may be classified into three groups according to the ratio a/s, where "a" is a typical dimension of plate in plane and "s" is a plate thickness. These groups are:

1. The first group is presented by thick plates having ratios $\frac{a}{s} \le 8-10$. The analysis of such bodies includes all the components of stresses, strains, and displacements as for solid bodies using the general equations of three-dimensional elasticity.
2. The second group refers to plates with ratios $\frac{a}{s} \ge 80-100$. These plates are referred to as membranes and they are devoid of flexural rigidity. Membranes carry the lateral loads by axial tensile forces N (and shear forces) acting in the plate middle surface. These forces are called membrane forces; they produce projection on a vertical axis and thus balance a lateral load applied to the plate-membrane.
3. The most extensive group represents an intermediate type of plate, so called thin plate with $80-100 \le \frac{a}{s} \le 8-10$. Depending on the value of the ratio w/s, the ratio of the maximum deflection of the plate to its thickness, the part of flexural and membrane forces here may be different.

Therefore, this group, in turn, may also be subdivided into two different classes.

a. Stiff plates. A plate can be classified as a stiff plate if $\frac{w}{s} \leq 0.2$. Stiff plates are flexurally rigid thin plates. They carry loads two dimensionally, mostly by internal bending and twisting moments and by transverse shear forces. The middle plane deformations and the membrane forces are negligible. In engineering practice, the term plate is understood to mean a stiff plate, unless otherwise specified. The concept of stiff plates introduces serious simplifications that are discussed later. A fundamental feature of stiff plates is that the equations of static equilibrium for a plate element may be set up for an original (undeformed) configuration of the plate.

b. Flexible plates. If the plate deflections are beyond a certain level, $\frac{w}{s} \geq 0.3$, then, the lateral deflections will be accompanied by stretching of the middle surface. Such plates are referred to as flexible plates. These plates represent a combination of stiff plates and membranes and carry external loads by the combined action of internal moments, shear forces, and membrane (axial) forces. Such plates, because of their favorable weight-to-load ratio, are widely used by the aerospace industry. When the magnitude of the maximum deflection is considerably greater than the plate thickness, the membrane action predominates. So, if $\frac{w}{s} > 5$, the flexural stress can be neglected compared with the membrane stress. Consequently, the load-carrying mechanism of such plates becomes of the membrane type, i.e., the stress is uniformly distributed over the plate thickness.

The above classification is, of course, conditional because the reference of the plate to one or another group depends on the accuracy of analysis, type of loading, boundary conditions, etc. We consider only small deflections of thin plates, a simplification consistent with the magnitude of deformation commonly found in plate structures.

The calculations of thermo-elastic stresses and deflections in thin plates discussed in this chapter bear a close resemblance to the corresponding ones of isothermal plate theory, and in fact frequent reference will be made to isothermal derivations and results. In particular, the reader will be referred to the book by S. Timoshenko on Theory of Plates and Shells. No attempt will be made to reproduce at length results readily accessible elsewhere, although some repetition is of course unavoidable. The derivations of this chapter are restricted to those of small-deflection theory and the effect on the deflections of loads in the plane of the plate is neglected.

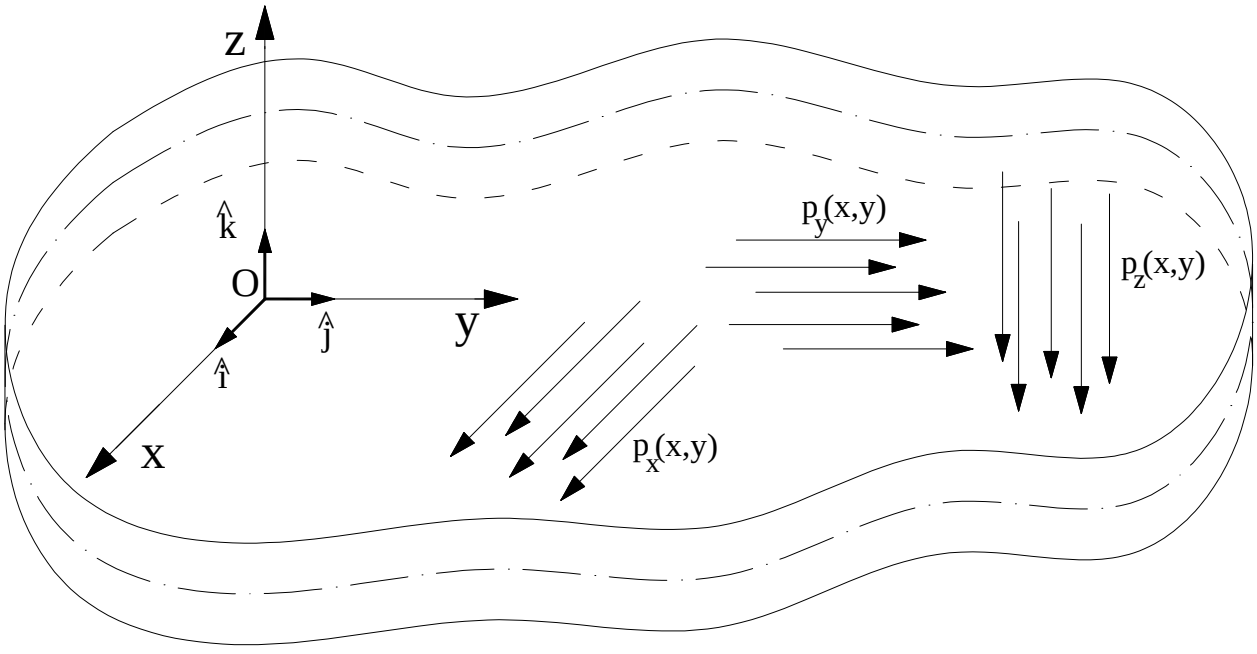

Fig. 16.1 – *Thin plate*

16.2. Basic plate field equations

16.2.1. Strain-displacement equations

Historically the first model of thin plate bending was developed by Lagrange, Poisson and Kirchhoff. It is known as the Kirchhoff plate model, of simply *Kirchhoff plate*, in honor of the German scientist who "closed" the mathematical formulation through the variational treatment of boundary conditions. Let us consider a load-free plate, shown in Figure.16.2, in which the x-y plane coincides with the plate's mid-plane and the z coordinate is perpendicular to it and is directed downwards. The fundamental assumptions of the linear, elastic, small-deflection theory of bending for thin plates may be stated as follows:

1. The material of the plate is elastic, homogeneous, and isotropic.
2. The plate is initially flat.
3. The deflection (the normal component of the displacement vector) of the mid-plane is small compared with the thickness of the plate. The slope of the deflected surface is therefore very small and the square of the slope is a negligible quantity in comparison with unity.
4. The straight lines, initially normal to the middle plane before bending, remain straight and normal to the middle surface during the deformation, and the length of such elements is not altered. This means that the vertical shear strains γ_{xz} and γ_{yz} are negligible and the normal strain ε_z may also be omitted. This assumption is referred to as the ''hypothesis of straight normals.''
5. The stress normal to the middle plane, σ_z, is small compared with the other stress components and may be neglected in the stress–strain relations.

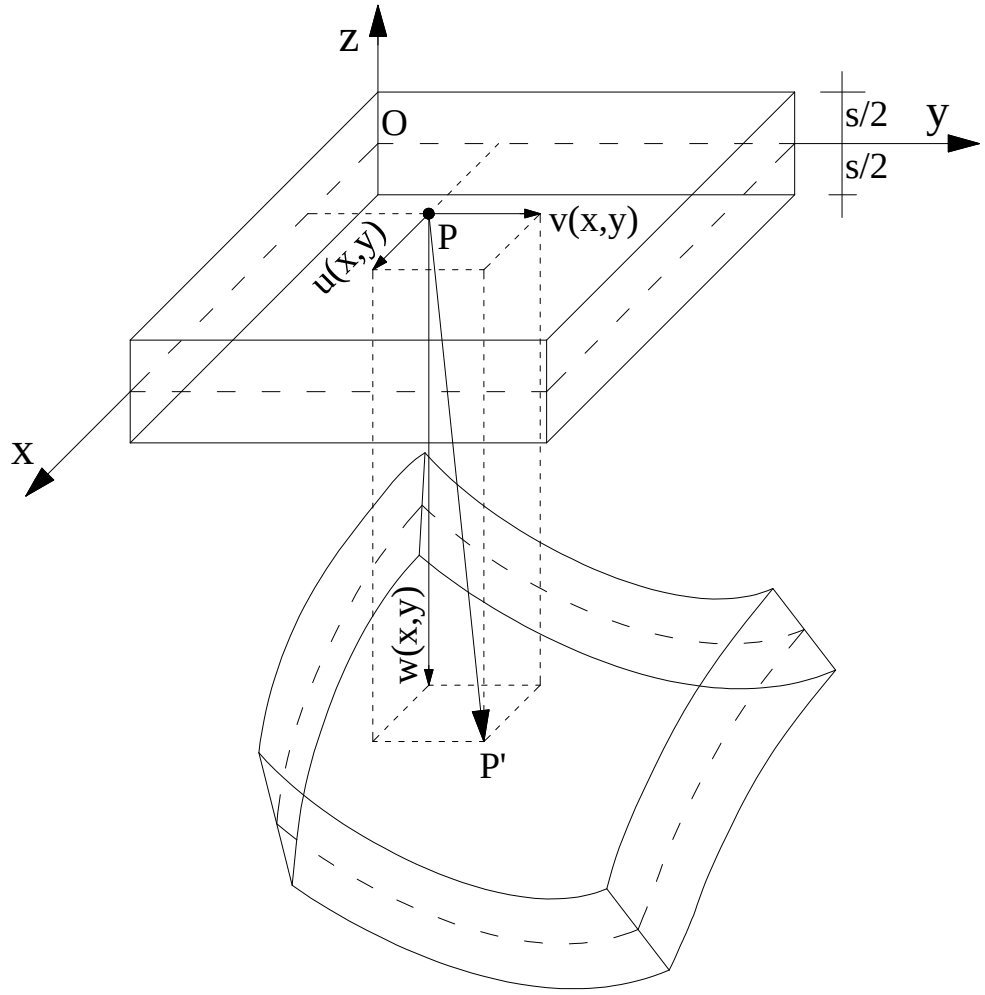

Fig. 16.2 – *Displacement components u,v and w in thin plate*

Many of these assumptions, known as Kirchhoff's hypotheses, are analogous to those associated with the simple bending theory of beams. These assumptions result in the reduction of a three-dimensional plate problem to a two-dimensional one. Consequently, the governing plate equation can be derived in a concise and straightforward manner. The plate bending theory based on the above assumptions is referred to as the classical or Kirchhoff's plate theory.

It was assumed in the foregoing discussions that the temperature of an elastic plate remains constant and has the same value at all points of the plate; hence, temperature effects were not taken into consideration. If the temperature of the plate is raised or lowered it expands or contracts, respectively. Within a certain temperature change, such expansion or contraction, for most structural materials, is directly proportional to the change in temperature. When a free plate made of homogeneous isotropic material is heated uniformly, there appear normal strains but no thermal stresses. The thermal stresses will occur in the following cases: first, if the plate experiences a non-uniform temperature field; secondly, if the displacements are prevented from occurring freely because of the restrictions placed on the boundary even with a uniform temperature; and thirdly, if the material displays anisotropy even with uniform heating – for example, if a heated plate consists of several layers of different materials (e.g., bimetallic plates).

Let us assume that the temperature of an infinitesimal plate element is increased from T_R to T. The initial temperature, T_R, is defined as a reference state of uniform temperature distribution which does not produce stress or strain in the plate. The thermal field, $T(x,y,z)$, is assumed to be known from a solution of the heat conduction problem. A thin plate of thickness "s" is considered, whose median plate lies in the x-y plane, with z denoting the distance from this plane. The displacements, in the x,y and z directions, of points on the median plate are denoted by u,v, and w respectively. The normal component of the displacement vector, w (called the deflection), and the lateral distributed load p are positive in the downward direction (Figure 16.2). As it follows from the assumption (4):

$$\varepsilon_z = 0,\ \gamma_{yz} = 0,\ \gamma_{xz} = 0, \tag{16.1}$$

The displacement-strain relationships are given by:

$$\begin{aligned} &\varepsilon_x = \frac{\partial u}{\partial x},\ \ \varepsilon_y = \frac{\partial v}{\partial y},\ \ \varepsilon_z = \frac{\partial w}{\partial z}, \\ &\gamma_{yz} = \frac{\partial w}{\partial y} + \frac{\partial v}{\partial z},\ \ \gamma_{xz} = \frac{\partial w}{\partial x} + \frac{\partial u}{\partial z},\ \ \gamma_{xy} = \frac{\partial u}{\partial y} + \frac{\partial v}{\partial x}, \end{aligned} \tag{16.2}$$

Integrating the expressions (16.2) and taking into account equation (16.1), we obtain:

$$\begin{cases} u = u_0(x,y) - z\dfrac{\partial w}{\partial x}, \\ v = v_0(x,y) - z\dfrac{\partial w}{\partial y}, \\ w = w(x,y), \end{cases} \tag{16.3}$$

We can also represent the displacement components u,v in the form:

$$u = u_0(x,y) - \vartheta_x z,\ \ v = v_0(x,y) - \vartheta_y z \tag{16.4}$$

where :

$$\vartheta_x = \frac{\partial w}{\partial x},\quad \vartheta_y = \frac{\partial w}{\partial y}, \tag{16.5}$$

are the angles of rotation of the normal to the middle surface in the Ox-z and Oy-z plane, respectively. Owing to the assumption (4), ϑ_x and ϑ_y are also slopes of the tangents to the traces of the middle surface in the abovementioned planes. The strain components are calculated on the basis of the assumptions of plane stress and that sections which are plane and perpendicular to the middle

surface remain so after heating. By substituting the displacement components (16.3) in equation (16.2), we obtain the non-zero strain components:

$$\varepsilon_x = \frac{\partial u_0}{\partial x} - z\frac{\partial^2 w}{\partial x^2}, \quad \varepsilon_y = \frac{\partial v_0}{\partial y} - z\frac{\partial^2 w}{\partial y^2}, \quad \gamma_{xy} = \frac{\partial u_0}{\partial y} + \frac{\partial v_0}{\partial x} - 2z\frac{\partial^2 w}{\partial x \partial y}, \tag{16.6}$$

where ν is the Poisson's ratio, α is the linear thermal expansion coefficient and T_R is the reference temperature. Over a moderate temperature change, α remains reasonably constant and represents an experimentally determined material property. For the sake of simplicity, we assume that the material properties of the plate are not affected by temperature changes: i.e., the modulus of elasticity, E, and Poisson's ratio, ν, are assumed to be constant. In general, a temperature increase or decrease produces changes in a plate's curvature and in the dimensions of the plate's middle surface. The second derivatives of the deflection on the right-hand side of equation (16.6) have a certain geometrical meaning.

The second derivative of the deflection $\partial^2 w/\partial x^2$, will define approximately the curvature of the section along the x axis, χ_x. Similarly $\partial^2 w/\partial y^2$ defines the curvature of the middle surface χ_y along the y axis. The curvatures χ_x and χ_y characterize the phenomenon of bending of the middle surface in planes parallel to the Ox-z and Oy-z coordinate planes, respectively. They are referred to as bending curvature and are defined by

$$\chi_x = -\frac{\partial^2 w}{\partial x^2}, \quad \chi_y = -\frac{\partial^2 w}{\partial y^2}, \tag{16.7}$$

We consider a bending curvature positive if it is convex downward, i.e., in the positive direction of the z axis. The curvature $\partial^2 w/\partial x^2$ can be also defined as the rate of change of the angle $\vartheta_x = \partial w/\partial x$ with respect to distance x along this curve. However, the above angle can vary in the y direction also. By analogy with the torsion theory of rods, the derivative $\partial^2 w/\partial x \partial y$ defines the warping of the middle surface at a point with coordinates x and y is called the twisting curvature with respect to the x and y axes and is denotes by χ_{xy}. Thus

$$\chi_{xy} = \frac{\partial^2 w}{\partial x \partial y} \tag{16.8}$$

u_0 and v_0 represent the displacement components of point of the middle surface along x and y axis, respectively (z = 0). Then, the deformation components of point of the middle surface are given by:

$$\varepsilon_x^0 = \frac{\partial u_0}{\partial x}, \quad \varepsilon_y^0 = \frac{\partial v_0}{\partial y}, \quad \gamma_{xy}^0 = \frac{\partial u_0}{\partial y} + \frac{\partial v_0}{\partial x}, \tag{16.9}$$

Taking into account equations (16.7), (16.8) and (16.9) we can rewrite equation (16.6) as follows:

$$\varepsilon_x = \varepsilon_x^0 - z\chi_x, \quad \varepsilon_y = \varepsilon_y^0 - z\chi_y, \quad \gamma_{xy} = \gamma_{xy}^0 - z\chi_{xy}, \tag{16.10}$$

16.2.2. Stresses and stress resultants

In the case of a three-dimensional state of stress, stress and strain are related by the of the generalized Hooke's law. As was mentioned earlier, Kirchhoff's assumptions (4) brought us to equation (16.1) . From a mathematical standpoint, this means that the three new equations (16.1) are added to the system of governing equations of the theory of elasticity. So, the latter becomes overdetermined and, therefore, it is necessary to also drop three equations. As a result, the three relations out of six of Hookes' law for strains (16.1) are discarded. Moreover, the normal stress component $\sigma_z = 0$. Solving Hookes' law for stress components σ_x, σ_y and τ_{xy} yields:

$$\sigma_x = \frac{E}{1-\nu^2}\left[\varepsilon_x + \nu\varepsilon_y - \alpha(1+\nu)(T-T_R)\right], \quad \sigma_y = \frac{E}{1-\nu^2}\left[\varepsilon_y + \nu\varepsilon_x - \alpha(1+\nu)(T-T_R)\right],$$
$$\tau_{xy} = \frac{E}{2(1+\nu)}\gamma_{xy}, \tag{16.11}$$

where E is the Young's modulus,. Introducing the plate curvatures, equation (16.7),(16.8),(16.9) and using equation (16.10), the above equations appear as follows:

$$\sigma_x = \frac{E}{1-\nu^2}\left[\frac{\partial u_0}{\partial x}+\nu\frac{\partial v_0}{\partial y}-z\left(\frac{\partial^2 w}{\partial x^2}+\nu\frac{\partial^2 w}{\partial y^2}\right)-\alpha(1+\nu)(T-T_R)\right],$$

$$\sigma_y = \frac{E}{1-\nu^2}\left[\frac{\partial v_0}{\partial y}+\nu\frac{\partial u_0}{\partial x}-z\left(\frac{\partial^2 w}{\partial y^2}+\nu\frac{\partial^2 w}{\partial x^2}\right)-\alpha(1+\nu)(T-T_R)\right], \qquad (16.12)$$

$$\tau_{xy} = \frac{E}{2(1+\nu)}\left[\frac{\partial u_0}{\partial y}+\frac{\partial v_0}{\partial x}-2z\frac{\partial^2 w}{\partial x\partial y}\right],$$

It is seen from equation (16.12) that Kirchhoff's assumptions have led to a completely defined law of variation of the stresses through the thickness of the plate. Therefore, as in the theory of beams, it is convenient to introduce, instead of the stress components at a point problem, the total statically equivalent forces and moments applied to the middle surface, which are known as the stress resultants and stress couples. The stress resultants and stress couples are referred to as the axial forces N_x, N_y and N_{xy}, as the shear forces, Q_x, Q_y, as well as the bending and twisting moments M_x, M_y, M_{xy}, respectively. Thus, Kirchhoff's assumptions have reduced the three-dimensional plate straining problem to the two-dimensional problem of straining the middle surface of the plate. We can express the bending and twisting moments, axial forces, as well as the shear forces, in terms of the stress components, i.e.,

$$N_x = \int_{-s/2}^{s/2}\sigma_x dz,\quad N_y = \int_{-s/2}^{s/2}\sigma_y dz,\quad N_{xy} = \int_{-s/2}^{s/2}\tau_{xy} dz,\quad Q_x = \int_{-s/2}^{s/2}\tau_{xz} dz,\quad Q_y = \int_{-s/2}^{s/2}\tau_{yz} dz,$$
$$M_x = \int_{-s/2}^{s/2}\sigma_x z dz,\quad M_y = \int_{-s/2}^{s/2}\sigma_y z dz,\quad M_{xy} = \int_{-s/2}^{s/2}\tau_{xy} z dz, \qquad (16.13)$$

Because of the reciprocity law of shear stresses ($\tau_{xy} = \tau_{yx}$), the twisting moments on perpendicular faces of an infinitesimal plate element are identical, i.e., $M_{xy} = M_{yx}$. The sign convention for the shear forces and the twisting moments is the same as that for the shear stresses. A positive bending moment is one which results in positive (tensile) stresses in the bottom half of the plate. Accordingly, all the moments and the shear forces acting on the element in figure 16.2 are positive.
Note that the relations (16.13) determine the intensities of axial forces, moments and shear forces, i.e., moments and forces per unit length of the plate mid-plane. Therefore, they have dimensional units as [force*length/length] or simply [force] for moments and [force/length] for shear and axial forces, respectively. It is important to mention that while the theory of thin plates omits the effect of the strain components $\gamma_{xz} = \tau_{xz}/G$ and $\gamma_{yz} = \tau_{yz}/G$ on bending, the vertical shear forces Q_x, Q_y are not negligible. In fact, they are necessary for equilibrium of the plate element. Substituting equation (16.12) into equation (16.13) and integrating over the plate thickness, we derive the following formulas for the stress resultants and couples in terms of the curvatures and the deflection:

$$N_x = \frac{E\,s}{1-\nu^2}\left(\frac{\partial u_0}{\partial x}+\nu\frac{\partial v_0}{\partial y}\right)-\frac{N_T}{1-\nu},\quad N_y = \frac{E\,s}{1-\nu^2}\left(\frac{\partial v_0}{\partial y}+\nu\frac{\partial u_0}{\partial x}\right)-\frac{N_T}{1-\nu},$$

$$N_{xy} = \frac{E\,s}{2(1+\nu)}\left(\frac{\partial u_0}{\partial y}+\frac{\partial v_0}{\partial x}\right),\quad M_{xy} = (1-\nu)D\frac{\partial^2 w}{\partial x\partial y}, \qquad (16.14)$$

$$M_x = -D\left(\frac{\partial^2 w}{\partial x^2}+\nu\frac{\partial^2 w}{\partial y^2}\right)-\frac{M_T}{1-\nu},\quad M_y = -D\left(\frac{\partial^2 w}{\partial y^2}+\nu\frac{\partial^2 w}{\partial x^2}\right)-\frac{M_T}{1-\nu},$$

where

$$D = \frac{E\,s^3}{12\left(1-\nu^2\right)} \tag{16.15}$$

is the flexural rigidity of the plate. It plays the same role as the flexural rigidity EI in beam bending. Note that D > EI; hence, a plate is always stiffer than a beam of the same span and thickness. The symbols N_T and M_T denote the quantities :

$$N_T = \alpha E \int_{-s/2}^{s/2} \left(T - T_R\right) dz, \qquad M_T = \alpha E \int_{-s/2}^{s/2} \left(T - T_R\right) z\, dz \tag{16.16}$$

are termed the thermal stress resultants, i.e., the *thermal equivalent normal force and bending moment*, respectively. It is often convenient to express the stresses directly in terms of the forces and moments; this is done by means of the formulas:

$$\begin{aligned}
\sigma_x &= \frac{1}{s}\left[N_x + \frac{N_T}{\left(1-\nu\right)}\right] + \frac{12z}{s^3}\left[M_x + \frac{M_T}{\left(1-\nu\right)}\right] - \frac{\alpha E}{1-\nu}\left(T - T_R\right), \\
\sigma_y &= \frac{1}{s}\left[N_y + \frac{N_T}{\left(1-\nu\right)}\right] + \frac{12z}{s^3}\left[M_y + \frac{M_T}{\left(1-\nu\right)}\right] - \frac{\alpha E}{1-\nu}\left(T - T_R\right), \\
\tau_{xy} &= \frac{N_{xy}}{s} - \frac{12\,z}{s^3} M_{xy},
\end{aligned} \tag{16.17}$$

which are derived by substituting (16.6) into (16.11), and eliminating the displacement derivates by means of (16.14). Determination of the remaining three stress components τ_{xz}, τ_{yz} and σ_z, through the use of Hooke's law is not possible due to the fourth and fifth assumptions, since these stresses are not related to strains. The differential equations of equilibrium for a plate element under a general state of stress (assuming that the body forces are zero) serve well for this purpose, however. If the faces of the plate are free of any tangent external loads, then τ_{xz}, τ_{yz} are zero for $z = \pm s/2$. In case of $u_0 = v_0 = 0$, from the first two equilibrium equations and equations (16.11) and (16.12), the shear stresses τ_{xz}, τ_{yz} are:

$$\begin{cases}
\tau_{xz} = -\int\left(\dfrac{\partial \sigma_x}{\partial x} + \dfrac{\partial \tau_{xy}}{\partial y}\right) dz = \dfrac{E}{1-\nu}\dfrac{\partial}{\partial x}\left[\dfrac{\nabla^2 w}{2\left(1+\nu\right)}\left(z^2 - \dfrac{s^2}{4}\right)\right] + \dfrac{\alpha E}{1-\nu}\dfrac{\partial}{\partial x}\displaystyle\int_{-s/2}^{s/2} T dz \\
\tau_{yz} = -\int\left(\dfrac{\partial \tau_{xy}}{\partial x} + \dfrac{\partial \sigma_y}{\partial y}\right) dz = \dfrac{E}{1-\nu}\dfrac{\partial}{\partial y}\left[\dfrac{\nabla^2 w}{2\left(1+\nu\right)}\left(z^2 - \dfrac{s^2}{4}\right)\right] + \dfrac{\alpha E}{1-\nu}\dfrac{\partial}{\partial y}\displaystyle\int_{-s/2}^{s/2} T dz
\end{cases} \tag{16.18}$$

where ∇^2 is the Laplace operator, given by:

$$\nabla^2 w = \frac{\partial^2 w}{\partial x^2} + \frac{\partial^2 w}{\partial y^2} \tag{16.19}$$

It is observed from equations (16.17) and (16.18) that the stress components σ_x, σ_y and τ_{xy} (in-plane stresses) vary linearly over the plate thickness, whereas the shear stresses τ_{xz}, τ_{yz} vary according to a parabolic law. The component σ_z is determined by using the third of equilibrium equation, upon substitution of τ_{xz}, τ_{yz} from equations (16.18) and integration. As a result, we obtain:

$$\sigma_z = \frac{E}{2\left(1-\nu^2\right)}\left(\frac{s^3}{12} + \frac{s^2 z}{4} - \frac{z^3}{3}\right)\nabla^2\left(\nabla^2 w\right) + \frac{\alpha E}{1-\nu}\int_{-s/2}^{s/2}\left(\int_{-s/2}^{s/2} \nabla^2 T dz\right) dz \tag{16.20}$$

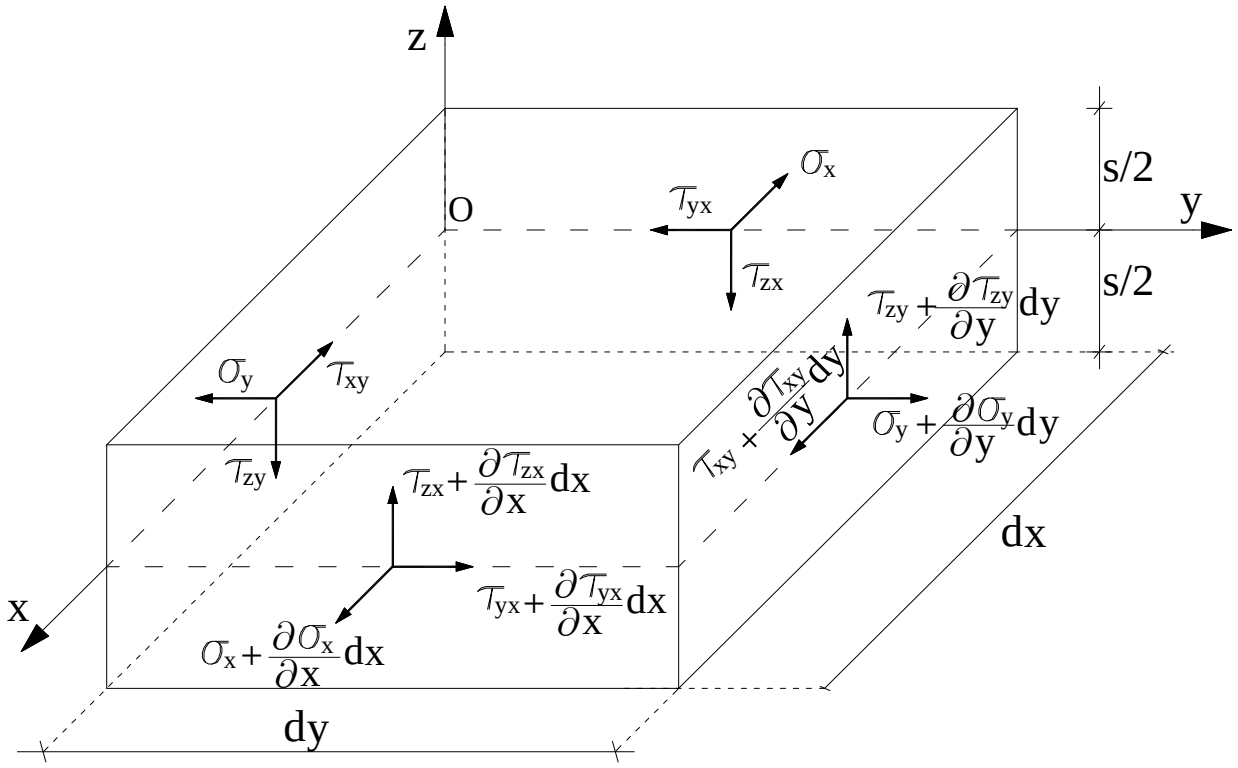

Fig. 16.3 – *Stress components in thin plate*

16.2.3. Equilibrium equations

The components of stress (and, thus, the stress resultants and stress couples) generally vary from point to point in a loaded plate. These variations are governed by the static conditions of equilibrium. Let us consider equilibrium of an element $s \cdot dx \cdot dy$ of the plate subject to a vertical distributed load of intensity $p_z(x,y)$ and distributed load $p_x(x,y)$ and $p_y(x,y)$ applied to an upper surface of the plate, as shown in figures 16.3 and 16.4. Since the stress resultants and stress couples are assumed to be applied to the middle plane of this element, a distributed loads are transferred to the mid-plane. Note that as the element is very small, the force and moment components may be considered to be distributed uniformly over the mid-plane of the plate element: in figures 16.3 and 16.4 they are shown, for the sake of simplicity, by a single vector. As shown in figures 16.3 and 16.4, in passing from the section x to the section x + dx an intensity of stress resultants changes by a value of partial differential. The same is true for the sections y and y+dy . For the system of forces and moments shown in figures 16.3 and 16.4, the following three independent conditions of equilibrium may be set up. The determination of six quantities $N_x, N_y, N_{xy}, M_x, M_y, M_{xy}$ defined in equation (16.13) is most conveniently carried out in two steps: in first of these the two-dimensional equilibrium and compatibility equations in the x-y plane are used to determine forces N_x, N_y, N_{xy}, and in the second, the equilibrium equation of forces in the z direction and of bending and twisting moments M_x, M_y, M_{xy} are written in terms of displacements so as to determine the deflection w and hence, from equations (16.14), the moments M. An outline of these derivations will now be given. The equations of equilibrium in the plane of the plate are:

$$\frac{\partial N_x}{\partial x}+\frac{\partial N_{xy}}{\partial y}+p_x(x,y)=0, \quad \frac{\partial N_{xy}}{\partial x}+\frac{\partial N_y}{\partial y}+p_y(x,y)=0, \tag{16.21}$$

In the case $p_x = p_y = 0$, it is possible to solve equations (16.21) by introducing the existence of a stress-function $F(x,y)$ defined by:

$$N_x = \frac{\partial^2 F}{\partial y^2}, \quad N_y = \frac{\partial^2 F}{\partial x^2}, \quad N_{xy} = -\frac{\partial^2 F}{\partial x \partial y}, \tag{16.22}$$

The determination of the solution F requires the solution of a two-dimensional thermo-elastic problem of plane stress. In particular, F must correspond to displacement $u_0(x,y)$ and $v_0(x,y)$, satisfying the first three equations of (16.14) . Alternative formulations of this type of problem is reported below. For a simply connected plate, F must satisfy the equation of compatibility , namely

$$\frac{\partial^2}{\partial y^2}\left[\frac{N_x - \nu N_y + N_T}{s}\right] - 2(1+\nu)\frac{\partial^2}{\partial x \partial y}\left[\frac{N_{xy}}{t}\right] + \frac{\partial^2}{\partial x^2}\left[\frac{N_y - \nu N_x + N_T}{s}\right] = 0 \tag{16.23}$$

Which is easily put in terms of F by introducing equations (16.22). For plates of constant thickness, equation (16.23) reduces to:

$$\nabla^4 F = -\nabla^2 N_T \tag{16.24}$$

The equation (16.24) is the governing differential equation for the two-dimensional thermo-elastic problem of plane stress for thin plates. The second part of the solution, namely the determination of the transverse displacement w, is the more direct concern of plate theory. The basic equations for this part of the calculations will now be outlined. The equilibrium equations of forces in the z direction and of moments about the x and y axes acting on an element of volume $s \cdot dx \cdot dy$ fo the plates as shown figure 16.4 are, respectively, as follows:

$$\begin{cases} \dfrac{\partial Q_x}{\partial x} + \dfrac{\partial Q_y}{\partial y} + p_z(x,y) = 0 \\ \dfrac{\partial M_{xy}}{\partial x} - \dfrac{\partial M_y}{\partial y} + Q_y = 0 \\ \dfrac{\partial M_{xy}}{\partial y} - \dfrac{\partial M_x}{\partial x} + Q_x = 0 \end{cases} \tag{16.25}$$

Where Q_x and Q_y are shear forces per unit of length acting on a surface whose normal is indicated by the subscript, and $p_z(x,y)$ is the distributed transverse loading for unit of area. With the substitution of Q_x and Q_y from second and third of (16.25) into the first of these, the equilibrium equation of forces in the z direction assumes the form:

$$\frac{\partial^2 M_x}{\partial x^2} - 2\frac{\partial^2 M_{xy}}{\partial x \partial y} + \frac{\partial^2 M_y}{\partial y^2} = -p_z(x,y) \tag{16.26}$$

The governing equation for the deflection w is now obtained by substituting into this result the expressions for the moments of equations (16.14). The results is:

$$\frac{\partial^2}{\partial x^2}\left[D\left(\frac{\partial^2 w}{\partial x^2} + \nu\frac{\partial^2 w}{\partial y^2}\right)\right] + 2(1-\nu)\frac{\partial^2}{\partial y \partial x}\left[D\frac{\partial^2 w}{\partial y \partial x}\right] + \frac{\partial^2}{\partial y^2}\left[D\left(\frac{\partial^2 w}{\partial y^2} + \nu\frac{\partial^2 w}{\partial x^2}\right)\right] = p_z - \frac{\nabla^2 M_T}{(1-\nu)} \tag{16.27}$$

For plates of uniform thickness , this equation reduces to:

$$D\nabla^4 w = p_z(x,y) - \frac{\nabla^2 M_T}{1-\nu} \tag{16.28}$$

where

$$\nabla^4(\ ) = \frac{\partial^4}{\partial x^4}(\ ) + 2\frac{\partial^4}{\partial x^2 \partial y^2}(\ ) + \frac{\partial^4}{\partial y^4}(\ ) \tag{16.29}$$

is commonly called the bi-harmonic operator. The (16.28) governing differential equation for the deflections for thin plate bending analysis based on Kirchhoff's assumptions. This equation was obtained by Lagrange in 1811. Mathematically, the differential equation (16.28) can be classified as a linear partial differential equation of the fourth order having constant coefficients. If only the

effect of non-uniform heating on a free plate is desired, the loading $p_z(x,y)$ may be set equal to zero and then (16.28) takes the form:

$$\nabla^4 w = -\frac{\nabla^2 M_T}{D(1-\nu)} = -\frac{12(1+\nu)}{E s^3}\nabla^2 M_T = -\frac{6\mu}{s^3}\nabla^2 M_T \tag{16.30}$$

These equations show that the superposition of deflections due to temperature alone and those due to transverse loads alone is possible. Once a deflection function $w(x,y)$ has been determined from equation (16.30), the stress resultants and the stresses can be evaluated by using equations (16.14) and (16.17). Since we have assumed the validity of Kirchhoff's small-deflection theory, the governing equations of thermal bending, Equation (16.28), and thermal stretching or contracting, equation (16.24), are independent of each other.

In order to determine the deflection function, it is required to integrate equation (16.30) with the constants of integration dependent upon the appropriate boundary conditions. We will discuss this procedure later. Expressions for the vertical forces Q_x and Q_y, may now be written in terms of the deflection $w(x,y)$ from equation (16.25) together with equation (16.14), as follows:

$$\begin{cases} Q_x = -D\dfrac{\partial}{\partial x}\left(\dfrac{\partial^2 w}{\partial x^2}+\dfrac{\partial^2 w}{\partial y^2}\right) - \dfrac{1}{1-\nu}\dfrac{\partial M_T}{\partial x} = -D\dfrac{\partial}{\partial x}\left(\nabla^2 w\right) - \dfrac{1}{1-\nu}\dfrac{\partial M_T}{\partial x} \\ Q_y = -D\dfrac{\partial}{\partial y}\left(\dfrac{\partial^2 w}{\partial x^2}+\dfrac{\partial^2 w}{\partial y^2}\right) - \dfrac{1}{1-\nu}\dfrac{\partial M_T}{\partial y} = -D\dfrac{\partial}{\partial y}\left(\nabla^2 w\right) - \dfrac{1}{1-\nu}\dfrac{\partial M_T}{\partial y} \end{cases} \tag{16.31}$$

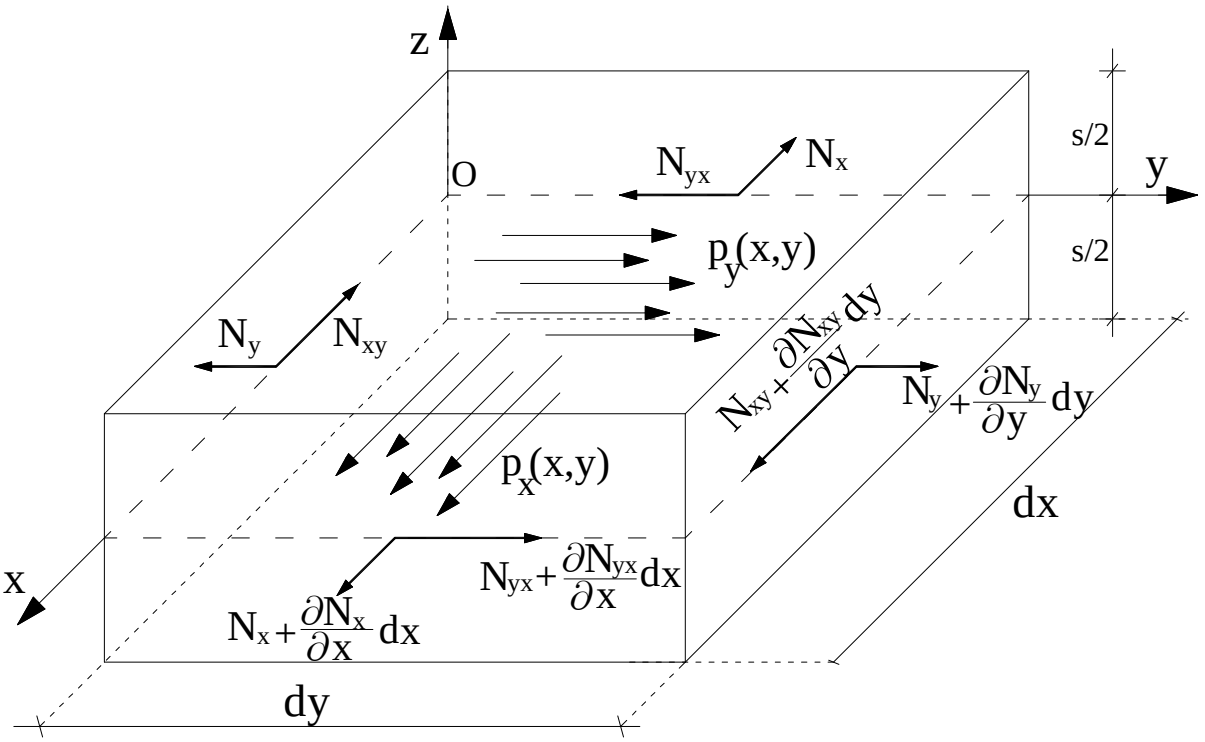

Fig 16.4 - *Axial forces N_x, N_y and N_{xy} in thin plate*

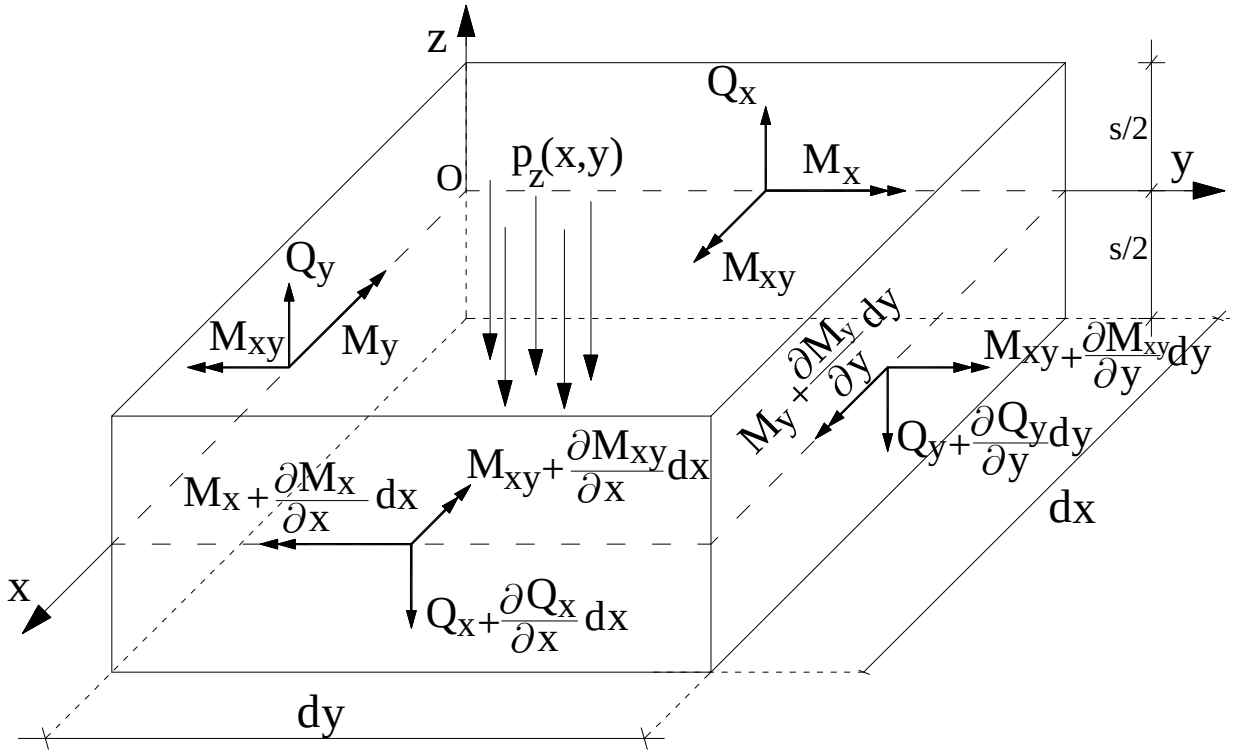

Fig 16.5 - *Shear forces Q_x, Q_y, bending moments M_x, M_y and twisting moment M_{xy} in thin plate*

16.2.4. Plate boundary conditions

Equation (16.30) represents the governing equation of plate bending and must be solved under suitable boundary conditions at the edgs of the plate. The most frequently used of these conditions are listed below; in this discussion the coordinates (s,n) are, respectively, parallel to and normal to the edge of the plate.

First case : For a built-in edge the deflection and its derivative along a normal to the edge must be zero:

$$w = 0; \quad \frac{\partial w}{\partial n} = 0 \tag{16.32}$$

The normal derivative is related to the derivatives in the x and y directions by the formula:

$$\frac{\partial w}{\partial n} = \frac{\partial w}{\partial x}\cos\beta + \frac{\partial w}{\partial y}\sin\beta \tag{16.33}$$

with the notation and sign convention of figure 16.6.

Second case: At a simply supported edge the deflection and the tangential component of the bending moment are zero, that is:

$$w = 0; \quad M_n = 0 \tag{16.34}$$

In order to be used in conjunction with equation (16.30), the second of these conditions must now be expressed in terms of w; this may be done in two ways, both of which will be outlined. The same results are, of course by either derivation. The moments M_n, M_s and M_{ns} are related to the moments M_x, M_y and M_{xy} by means of the relations:

$$\begin{cases} M_n = M_x \cos^2\beta + M_y \sin^2\beta - 2M_{xy}\sin\beta\cos\beta \\ M_s = M_x \sin^2\beta + M_y \cos^2\beta + 2M_{xy}\sin\beta\cos\beta \\ M_{ns} = \left(M_x - M_y\right)\sin\beta\cos\beta + M_{xy}\left(\cos^2\beta - \sin^2\beta\right) \end{cases} \tag{16.35}$$

Which follow directly from equations (16.13) and transform law's of tensor stress. Introducing now (16.14) one obtains:

$$\begin{cases} M_n = -D\left[\left(\dfrac{\partial^2 w}{\partial x^2} + \nu\dfrac{\partial^2 w}{\partial y^2}\right)\cos^2\beta + \left(\dfrac{\partial^2 w}{\partial y^2} + \nu\dfrac{\partial^2 w}{\partial x^2}\right)\sin^2\beta + 2(1-\nu)\dfrac{\partial^2 w}{\partial x\partial y}\sin\beta\cos\beta\right] - \dfrac{M_T}{1-\nu} \\ M_s = -D\left[\left(\dfrac{\partial^2 w}{\partial y^2} + \nu\dfrac{\partial^2 w}{\partial x^2}\right)\cos^2\beta + \left(\dfrac{\partial^2 w}{\partial x^2} + \nu\dfrac{\partial^2 w}{\partial y^2}\right)\sin^2\beta - 2(1-\nu)\dfrac{\partial^2 w}{\partial x\partial y}\sin\beta\cos\beta\right] - \dfrac{M_T}{1-\nu} \\ M_{ns} = (1-\nu)D\left[\left(\dfrac{\partial^2 w}{\partial y^2} - \dfrac{\partial^2 w}{\partial x^2}\right)\sin\beta\cos\beta + \dfrac{\partial^2 w}{\partial x\partial y}\left(\cos^2\beta - \sin^2\beta\right)\right] \end{cases} \tag{16.36}$$

The boundary conditions (16.34) are easily expressed in terms of w by the first of these equations. As an alternative derivation of equations (16.36), note first that the relations between the moments M_n, M_s and M_{ns}, the curvature χ_n, χ_s and the twist χ_{ns} are of the same form as equation (16.14), namely :

$$M_n = D\left(\chi_n + \nu\chi_s\right) - \frac{M_T}{1-\nu},\quad M_s = D\left(\chi_s + \nu\chi_n\right) - \frac{M_T}{1-\nu},\quad M_{ns} = (1-\nu)\chi_{ns} \tag{16.37}$$

The relations between $\chi_n, \chi_s, \chi_{ns}$ and the quantities $\chi_x, \chi_y, \chi_{xy}$ are shown in Timoshenko to be of the form:

$$\begin{cases} \chi_n = \chi_x \cos^2\beta + \chi_y \sin^2\beta - 2\chi_{xy}\sin\beta\cos\beta \\ \chi_s = \chi_x \sin^2\beta + \chi_y \cos^2\beta + 2\chi_{xy}\sin\beta\cos\beta \\ \chi_{ns} = \left(\chi_x - \chi_y\right)\sin\beta\cos\beta + \chi_{xy}\left(\cos^2\beta - \sin^2\beta\right) \end{cases} \tag{16.38}$$

Substituting of these relations into (16.37) yields one again equations (16.36), provided that expressions (16.7) and (16.8) are used for $\chi_x, \chi_y, \chi_{xy}$. Equations (16.36) may be simplified in rectangular plate, they reduce the last three of (16.14). In conclusion, one may remark that while the isothermal boundary conditions for a simply supported edge are homogeneous, in the thermal case they are not because of the presence of the term $M_T/(1-\nu)$ in all bending moments.

Third case: At a free edge of plate one must satisfy the requirements that the bending moment M_n, the shear force Q_n, and the twisting moments M_{ns} be zero. The latter moment is, however, statically equivalent to a distributed force of intensity $-\dfrac{\partial M_{ns}}{\partial s}(n=0)$ and, in addition , to concentrated forces R at the corners (if any) of the plate of magnitude:

$$R = \left[M_{ns}(n=0)\right]_1 - \left[M_{ns}(n=0)\right]_2 \tag{16.39}$$

Where the subscripts 1 and 2 indicate the values of M_{ns} on opposite sides of the corner. A joint boundary condition is thus arrived at for the shear forces and twisting moments at a free edge, namely,

$$Q_n - \frac{\partial M_{ns}}{\partial s} = 0 \tag{16.40}$$

This boundary condition must be supplemented by the requirement that R=0 at any unsupported corner, with R defined as above. It is now again necessary, as in second case, to express explicitly

in terms of w the edge conditions just stated. It will first be noted that the condition of moment equilibrium contained in either the second or third of (16.25) may be written, in the orthogonal (s,n) coordinate system previously introduced, as

$$Q_n = \frac{\partial M_n}{\partial n} - \frac{\partial M_{ns}}{\partial s} \tag{16.41}$$

The boundary conditions at a free edge are then

$$M_n = 0; \quad \frac{\partial M_n}{\partial n} - 2\frac{\partial M_{ns}}{\partial s} = 0 \tag{16.42}$$

These equations may be put in terms of w by the introduced of the expressions (16.36). The form then assumed by the first of them has already been discussed; the second, for the case of uniform thickness, may be written in terms of w by means of the relation:

$$\frac{\partial M_n}{\partial n} - 2\frac{\partial M_{ns}}{\partial s} = -D\left\{\frac{\partial}{\partial n}\left(\nabla^2 w\right) + \left(1-\nu\right)\frac{\partial}{\partial s}\left[\begin{array}{l}\left(\dfrac{\partial^2 w}{\partial y^2} - \dfrac{\partial^2 w}{\partial x^2}\right)\sin\beta\cos\beta + \\ + \dfrac{\partial^2 w}{\partial x \partial y}\left(\cos^2\beta - \sin^2\beta\right)\end{array}\right]\right\} - \frac{1}{1-\nu}\frac{\partial M_T}{\partial n} \tag{16.43}$$

where

$$\frac{\partial}{\partial n} = \cos\beta\frac{\partial}{\partial x} + \sin\beta\frac{\partial}{\partial y}, \quad \frac{\partial}{\partial s} = \cos\beta\frac{\partial}{\partial y} - \sin\beta\frac{\partial}{\partial x} \tag{16.44}$$

In the special case of the rectangular plate, equation (16.43) gives (with $\beta = 0, n = x, s = y$)

$$D\left[\frac{\partial^3 w}{\partial x^3} + \left(2-\nu\right)\frac{\partial^3 w}{\partial x \partial y^2}\right] + \frac{1}{1-\nu}\frac{\partial M_T}{\partial x} = 0 \tag{16.45}$$

As the boundary condition on an edge for which x is constant. The reaction R of (16.39) is expressed directly in terms of w by the third of (16.36) for an arbitrary coordinate system, by the last of (16.14) for a rectangular system. It my be noted at a free edge, as at a simply supported one, the thermal-boundary conditions are not homogeneous, in contrast to the isothermal case.

Four case: For edges elastic support the boundary conditions are readily derived with aid of the formulas just given and will not be discussed here in detail. The reader may also find helpful in such cases Timoshenko's analysis of the corresponding isothermal case.

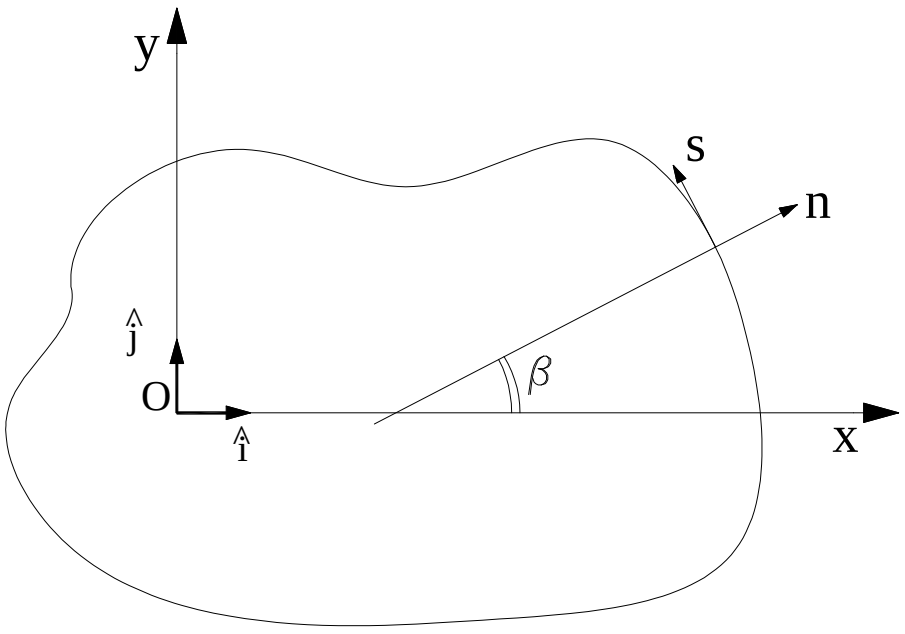

Figure 16.6 – *Plate with arbitrary planform*

16.3. Rectangular plates

We begin the application of the developed plate bending theory with thin rectangular plates. These plates represent an excellent model for development and as a check of various methods for solving the governing differential equation of plate. In this section we consider some mathematically ‘‘exact’’ solutions in the form of double and single trigonometric series applied to rectangular plates with various types of supports and transverse loads, plates on an elastic foundation, continuous plates, etc.

16.3.1. Pure bending of plates

Consider a rectangular plate with a free boundary and assume that this plate is subjected to distributed bending moments over its edges $M_x = m_1,\ M_y = m_2$ (figure 16.7). In this particular case, the governing differential equation (16.28) becomes

$$\frac{\partial^4 w}{\partial x^4} + 2\frac{\partial^4 w}{\partial x^2 \partial y^2} + \frac{\partial^4 w}{\partial y^4} = 0 \tag{16.46}$$

This equation will be satisfied if we make

$$w(x,y) = \frac{1}{2}\left(C_1 x^2 + C_2 y^2\right) \tag{16.47}$$

The constants of integration C_1, C_2 may be evaluated from the following boundary conditions:

$$M_x = m_1, \quad M_y = m_2 \tag{16.48}$$

Using equations (16.14), (16.47), and (16.48), we obtain

$$C_1 = \frac{\nu m_2 - m_1}{D\left(1-\nu^2\right)}, \quad C_2 = \frac{\nu m_1 - m_2}{D\left(1-\nu^2\right)} \tag{16.49}$$

Substituting the above into Equation(16.47) yields the deflection surface, as shown below:

$$w(x,y) = \frac{1}{2D\left(1-\nu^2\right)}\left[\left(\nu m_2 - m_1\right)x^2 + \left(\nu m_1 - m_2\right)y^2\right] \tag{16.50}$$

Hence, in all sections of the plate parallel to the x and y axes, only the constant bending moments $M_x = m_1,\ M_y = m_2$ will act. Other stress resultants and stress couples are zero, i.e.,

$$M_{xy} = Q_x = Q_y = 0 \tag{16.51}$$

This case of bending of plates may be referred to as a pure bending. Let us consider some particular cases of pure bending of plates:

a) $m_1 = m_2 = m$, then

$$w(x,y) = -\frac{m}{2D(1+\nu)}\left(x^2 + y^2\right) \tag{16.52}$$

This is an equation of the elliptic paraboloid of revolution. The curved plate in this case represents a part of a sphere because the radii of curvature are the same at all the planes and all the points of the plate.

b) $m_1 = m,\ m_2 = 0,$ then

$$w(x,y) = \frac{m}{2D\left(1+\nu^2\right)}\left(-x^2 + \nu y^2\right) \tag{16.53}$$

A surface described by this equation has a saddle shape and is called the hyperbolic paraboloid of revolution. Horizontals of this surface are hyperbolas, asymptotes of which are given by the straight lines $x/y = \pm\sqrt{\nu}$. As is seen, due to the Poisson effect the plate bends not only in the plane of the applied bending moment $M_x = m_1 = m$ but it also has an opposite bending in the perpendicular plane.

c) $m_1 = m,\ m_2 = -m,$ then

$$w(x,y)=\frac{m}{2D(1-\nu)}\left(-x^2+y^2\right) \tag{16.54}$$

This is an equation of an hyperbolic paraboloid with asymptotes inclined at 45 to the x and y axes. Let us determine the moments M_n and M_{nt} from equations (16.35) in skew sections hat are parallel to the asymptotes. Letting $\alpha=45°$, we obtain

$$M_n=0,\ M_{nt}=-m \tag{16.55}$$

Thus, a part of the plate isolated from the whole plate and equally inclined to the x and y axes will be loaded along its boundary by uniform twisting moments of intensity m. Hence, this part of the plate is subjected to pure twisting. Let us replace the twisting moments by the effective shear forces V_α, rotating these moments through 90. Along the whole sides of the isolated part we obtain $V_\alpha=0$, but at the corner points the concentrated forces S=2m are applied. Thus, for the model of Kirchhoff's plate, an application of self-balanced concentrated forces at corners of a rectangular plate produces a deformation of pure torsion because over the whole surface of the plate $M_{nm}=m=\text{const}$.

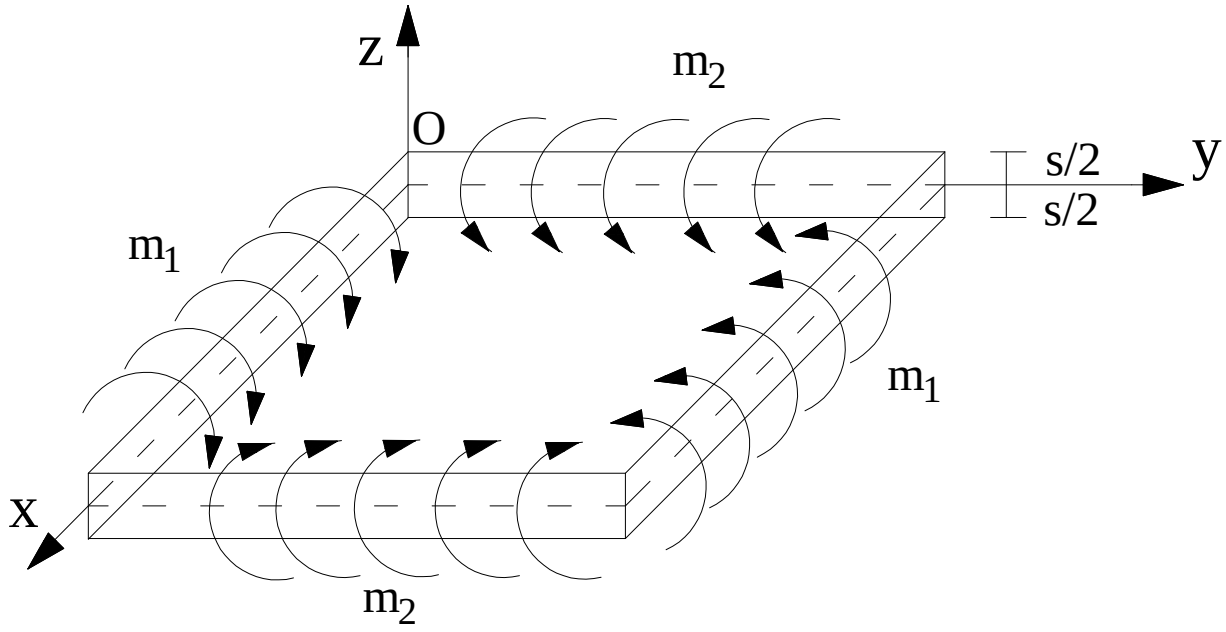

Fig. 16.7 – *Plate subjected to distributed bending moments over its edges* $M_x=m_1,\ M_y=m_2$

16.3.2. Navier's method (Double series solution)

Plate subjected to a uniform load

In 1820, Navier presented a paper to the French Academy of Sciences on the solution of bending of simply supported plates by double trigonometric series. Consider a rectangular plate of sides a and b, simply supported on all edges and subjected to a uniform load $p(x,y)$. The origin of the coordinates is placed at the upper left corner as shown in figure 16.8 . The boundary conditions for a simply supported plate are the following :

$$\begin{aligned} &w(0,y)=w(a,y)=w(x,0)=w(x,b)=0\\ &\frac{\partial^2 w}{\partial x^2}=0 \ \text{ at } \ x=0,\ x=a,\\ &\frac{\partial^2 w}{\partial y^2}=0 \ \text{ at } \ y=0,\ x=b, \end{aligned} \tag{16.56}$$

In this case, the solution of the governing differential equation (16.28) with $M_T = 0$ i.e., the expressions of the deflection surface $w(x,y)$, and the distributed surface load $p(x,y)$, have to be sought in the form of an infinite Fourier series, as follows:

$$\begin{cases} w(x,y) = \sum_{m=1}^{\infty}\sum_{n=1}^{\infty} w_{nm} \sin\left(\frac{m\pi x}{a}\right)\sin\left(\frac{n\pi y}{b}\right) \\ p(x,y) = \sum_{m=1}^{\infty}\sum_{n=1}^{\infty} p_{nm} \sin\left(\frac{m\pi x}{a}\right)\sin\left(\frac{n\pi y}{b}\right) \end{cases} \tag{16.57}$$

where w_{nm} and p_{nm} represent coefficients to be determined. It can be easily verified that the expression for deflections (16.57) automatically satisfies the prescribed boundary conditions (16.56) . Let us consider a general load configuration. To determine the Fourier coefficients p_{nm}, each side of equation (16.57) is multiplied by $\sin\left(\frac{l\pi x}{a}\right)\sin\left(\frac{k\pi y}{b}\right)$, and integrated twice between the limits 0;a and 0;b, as follows:

$$\begin{aligned} &\int_0^b\int_0^a p(x,y)\sin\left(\frac{m\pi x}{a}\right)\sin\left(\frac{n\pi y}{b}\right)dxdy = \\ &= \sum_{m=1}^{\infty}\sum_{n=1}^{\infty} p_{nm}\int_0^b\int_0^a \sin\left(\frac{m\pi x}{a}\right)\sin\left(\frac{n\pi y}{b}\right)\sin\left(\frac{l\pi x}{a}\right)\sin\left(\frac{k\pi y}{b}\right)dxdy \end{aligned} \tag{16.58}$$

It can be shown by direct integration that:

$$\int_0^a \sin\left(\frac{m\pi x}{a}\right)\sin\left(\frac{l\pi x}{a}\right)dx = \begin{cases} 0 & \text{if } m \neq l \\ a/2 & \text{if } m = l \end{cases} \tag{16.59}$$

$$\int_0^b \sin\left(\frac{n\pi y}{b}\right)\sin\left(\frac{k\pi y}{b}\right)dy = \begin{cases} 0 & \text{if } n \neq k \\ b/2 & \text{if } n = k \end{cases} \tag{16.60}$$

The coefficients of the double Fourier expansion are therefore the following:

$$p_{nm} = \frac{4}{ab}\int_0^b\int_0^a p(x,y)\sin\left(\frac{m\pi x}{a}\right)\sin\left(\frac{n\pi y}{b}\right)dxdy \tag{16.61}$$

Since the representation of the deflection (16.57) satisfies the boundary conditions (16.56), then the coefficients w_{nm} must satisfy first equation of (16.28). Substitution of first equation of (16.57) into equation (16.28) results in the following equation:

$$\sum_{m=1}^{\infty}\sum_{n=1}^{\infty}\left\{w_{nm}\left[\left(\frac{m\pi}{a}\right)^4 + 2\left(\frac{m\pi}{a}\right)^2\left(\frac{n\pi}{b}\right)^2 + \left(\frac{n\pi}{b}\right)^4\right] - \frac{p_{nm}}{D}\right\}\sin\left(\frac{m\pi x}{a}\right)\sin\left(\frac{n\pi y}{b}\right) \tag{16.62}$$

This equation must apply for all values of x and y. We conclude therefore that

$$w_{nm}\pi^4\left(\frac{m^2}{a^2} + \frac{n^2}{b^2}\right)^2 - \frac{p_{nm}}{D} = 0 \tag{16.63}$$

from which

$$w_{nm} = \frac{1}{\pi^4 D}\frac{p_{nm}}{\left[(m/a)^2 + (n/b)^2\right]^2} \tag{16.64}$$

Substituting the above into first equation of(16.57), one obtains the equation of the deflected surface, as follows:

$$w(x,y) = \frac{1}{\pi^4 D}\sum_{m=1}^{\infty}\sum_{n=1}^{\infty}\frac{p_{nm}}{\left[(m/a)^2 + (n/b)^2\right]^2}\sin\left(\frac{m\pi x}{a}\right)\sin\left(\frac{n\pi y}{b}\right) \tag{16.65}$$

where p_{nm} is given by equation (16.61) . It can be shown, by noting that :

$$\left|\sin\left(\frac{m\pi x}{a}\right)\right| \le 1, \ \left|\sin\left(\frac{n\pi y}{b}\right)\right| \le 1, \quad \forall x, y \quad \forall n, m \in N \tag{16.66}$$

Then, the series (16.65) is convergent. Substituting w(x,y) into the equations (16.14) and (16.31), we can find the bending moments and the shear forces in the plate, and then using the expressions (16.17), determine the stress components. For the moments in the plate, for instance, we obtain the following:

$$\begin{aligned}
M_x &= \frac{1}{\pi^2}\sum_{m=1}^{\infty}\sum_{n=1}^{\infty} p_{nm} \frac{\left[(m/a)^2 + \nu(n/b)^2\right]^2}{\left[(m/a)^2 + (n/b)^2\right]^2} \sin\left(\frac{m\pi x}{a}\right)\sin\left(\frac{n\pi y}{b}\right) \\
M_y &= \frac{1}{\pi^2}\sum_{m=1}^{\infty}\sum_{n=1}^{\infty} p_{nm} \frac{\left[(n/b)^2 + \nu(m/a)^2\right]^2}{\left[(m/a)^2 + (n/b)^2\right]^2} \sin\left(\frac{m\pi x}{a}\right)\sin\left(\frac{n\pi y}{b}\right) \\
M_{xy} &= -\frac{\nu}{\pi^2}\sum_{m=1}^{\infty}\sum_{n=1}^{\infty} \frac{p_{nm} mn}{ab\left[(m/a)^2 + (n/b)^2\right]^2} \cos\left(\frac{m\pi x}{a}\right)\cos\left(\frac{n\pi y}{b}\right)
\end{aligned} \tag{16.67}$$

The infinite series solution for the deflection (16.65) generally converges quickly; thus, satisfactory accuracy can be obtained by considering only a few terms. Since the stress resultants and couples are obtained from the second and third derivatives of the deflection w(x,y), the convergence of the infinite series expressions of the internal forces and moments is less rapid, especially in the vicinity of the plate edges. This slow convergence is also accompanied by some loss of accuracy in the process of calculation. The accuracy of solutions and the convergence of series expressions of stress resultants and couples can be improved by considering more terms in the expansions and by using a special technique for an improvement of the convergence of Fourier's series.

Plate under an arbitrary temperature distribution

Consider a rectangular plate of sides a and b, simply supported on all edges under an arbitrary temperature distribution with $p(x,y) = 0$. The origin of the coordinates is placed at the upper left corner as shown in figure 16.8. The boundary conditions for a simply supported plate are the following :

$$\begin{aligned}
&w(0,y) = w(a,y) = w(x,0) = w(x,b) = 0 \\
&\frac{\partial^2 w}{\partial x^2} + \frac{M_T}{(1-\nu)D} = 0 \ \text{ at } \ x = 0, \ x = a, \\
&\frac{\partial^2 w}{\partial y^2} + \frac{M_T}{(1-\nu)D} = 0 \ \text{ at } \ y = 0, \ x = b,
\end{aligned} \tag{16.68}$$

where in general M_T is a function of x and y. In this case, the solution of the governing differential equation (16.28) is clearly equivalent to the set:

$$\begin{cases} D\nabla^2 w + \dfrac{M_T}{1-\nu} = f(x,y) \\ \nabla^2 f(x,y) = 0 \end{cases} \tag{16.69}$$

On the boundary w = 0, and therefore also $\left(\partial^2 w/\partial s^2\right) = 0$; hence

$$D\nabla^2 w = -\frac{M_T}{1-\nu} \quad \text{on the boundary} \tag{16.70}$$

The boundary condition on the function *f* is then, from the first of equation (16.69), *f = 0* ; hence the appropriate solution of the second of these equation is *f = 0* . The problem is reduced to the solution of :

$$D\nabla^2 w = -\frac{M_T}{1-\nu} \tag{16.71}$$

Under the condition that :

$$w = 0 \quad \text{on the boundary} \tag{16.72}$$

This reduced problem can be solved in terms of a double trigonometric series, each term of which satisfies the boundary condition just stated, namely by setting:

$$w(x,y) = \sum_{m=1}^{\infty}\sum_{n=1}^{\infty} w_{nm} \sin\left(\frac{m\pi x}{a}\right)\sin\left(\frac{n\pi y}{a}\right) \tag{16.73}$$

The right-hand side of (16.71) is expressed in a similar form, that is

$$M_T(x,y) = \sum_{m=1}^{\infty}\sum_{n=1}^{\infty} a_{nm} \sin\left(\frac{m\pi x}{a}\right)\sin\left(\frac{n\pi y}{a}\right) \tag{16.74}$$

where the Fourier coefficients a_{nm} are

$$a_{nm} = \frac{4}{ab}\int_0^a\int_0^b M_T(x,y)\sin\left(\frac{m\pi x}{a}\right)\sin\left(\frac{n\pi y}{a}\right)dydx \tag{16.75}$$

Substituting these two series into (16.71), and equating coefficients of like terms one obtains

$$w_{nm} = \frac{a_{nm}}{(1-\nu)\pi^2 D}\left[\frac{1}{\left(\frac{m}{a}\right)^2 + \left(\frac{n}{b}\right)^2}\right] \tag{16.76}$$

An explicit solution has thus been obtained. Note, however, that equation (16.73), although quite useful for the calculation of the deflections themselves, may, in the case of certain temperature distributions, be unsatisfactory for the calculation of the bending moments near the edges of the plate; a solution of equation (16.71) in a different form must then be derived.

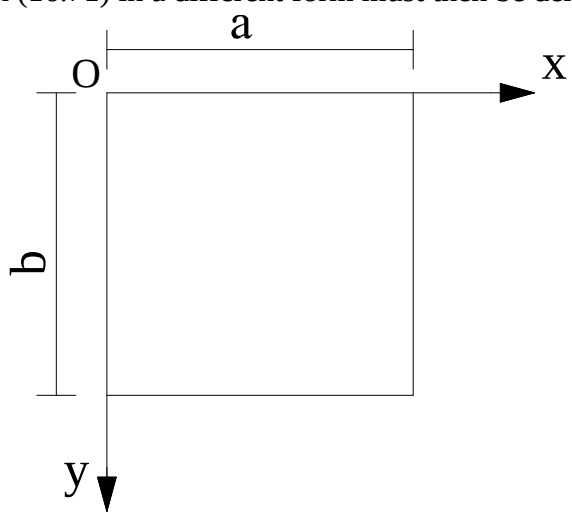

Fig. 16.8 – *Cartesian Coordinate system of plate*

16.4. Circular plates

Circular plates are common in many structures such as nozzle covers, end closures in pressure vessels, pump diaphragms, turbine disks, and bulkheads in submarines and airplanes, etc. When circular plates are analyzed, it is convenient to express the governing differential equation of plates in polar coordinates. This can be readily accomplished by a coordinate transformation. An

alternative approach based on the procedure presented in section 16.2 for rectangular plates to derive the basic relationships for the lateral deflections of circular plates may be used also.

16.4.1 Basic relations in polar coordinates

As mentioned earlier, we use the polar coordinates r and θ in solving the bending problems for circular plates. If the coordinate transformation technique is used, the following geometrical relations between the Cartesian and polar coordinates are applicable (Figure 16.9):

$$x = r\cos\theta, \quad y = r\sin\theta, \quad r = \sqrt{x^2 + y^2}, \ \theta = Arc\tan\left(\frac{y}{x}\right) \tag{16.77}$$

Referring to the above

$$\begin{aligned} &\frac{\partial r}{\partial x} = \frac{x}{\sqrt{x^2+y^2}} = \frac{x}{r} = \cos\theta, \ \ \frac{\partial r}{\partial y} = \frac{y}{\sqrt{x^2+y^2}} = \frac{y}{r} = \sin\theta, \\ &\frac{\partial \theta}{\partial x} = -\frac{y}{r^2} = -\frac{\sin\theta}{r}, \quad \frac{\partial \theta}{\partial y} = \frac{x}{r^2} = \frac{\cos\theta}{r}, \end{aligned} \tag{16.78}$$

Inasmuch as the deflection is a function of r and θ, the chain rule together with the relations (16.78) lead to the following

$$\begin{cases} \dfrac{\partial w}{\partial x} = \dfrac{\partial w}{\partial r}\dfrac{\partial r}{\partial x} + \dfrac{\partial w}{\partial \theta}\dfrac{\partial \theta}{\partial x} = \dfrac{\partial w}{\partial r}\cos\theta - \dfrac{1}{r}\dfrac{\partial w}{\partial \theta}\sin\theta \\ \dfrac{\partial w}{\partial y} = \dfrac{\partial w}{\partial r}\dfrac{\partial r}{\partial y} + \dfrac{\partial w}{\partial \theta}\dfrac{\partial \theta}{\partial y} = \dfrac{\partial w}{\partial r}\sin\theta + \dfrac{1}{r}\dfrac{\partial w}{\partial \theta}\cos\theta \end{cases} \tag{16.79}$$

By applying the relations (16.79), we determine the Laplacian operator in polar coordinate:

$$\nabla^2 w = \frac{\partial^2 w}{\partial x^2} + \frac{\partial^2 w}{\partial y^2} = \frac{\partial^2 w}{\partial r^2} + \frac{1}{r}\frac{\partial w}{\partial r} + \frac{1}{r^2}\frac{\partial^2 w}{\partial \theta^2} \tag{16.80}$$

After repeating twice the operation ∇^2, we obtain the operator $\nabla^2\left(\nabla^2 w\right) = \nabla^4 w$:

$$\nabla^4 w = \frac{\partial^4 w}{\partial r^4} + \frac{2}{r}\frac{\partial^3 w}{\partial r^3} - \frac{1}{r^2}\frac{\partial^2 w}{\partial r^2} + \frac{1}{r^3}\frac{\partial w}{\partial r} + \frac{2}{r^2}\frac{\partial^4 w}{\partial r^2 \partial \theta^2} - \frac{2}{r^3}\frac{\partial^3 w}{\partial \theta^2 \partial r} + \frac{4}{r^4}\frac{\partial^2 w}{\partial \theta^2} + \frac{1}{r^4}\frac{\partial^4 w}{\partial \theta^4} \tag{16.81}$$

The governing differential equation for the plate deflection in polar coordinates becomes:

$$D\nabla^4 w = p(x,y) - \frac{1}{1-\nu}\left[\frac{\partial^2 M_T}{\partial r^2} + \frac{1}{r}\frac{\partial M_T}{\partial r} + \frac{1}{r^2}\frac{\partial^2 M_T}{\partial \theta^2}\right] \tag{16.82}$$

Let us set up the relationships between moments and curvatures. Consider now the state of moment and shear force on an infinitesimal element of thickness s, described in polar coordinates, as shown in figure 16.7. Note that, to simplify the derivations, the x axis is taken in the direction of the radius r, at $\theta = 0$. Then, the radial M_r, tangential M_θ, twisting $M_{r\theta}$ moments, and the vertical shear forces Q_r, Q_θ will have the same values as the moments M_x, M_y, M_{xy}, and shears Q_x, Q_y at the same point in the plate. Thus, transforming the expressions for moments (16.14) and shear forces (16.31) into polar coordinates, we can write the following:

$$\begin{aligned} &M_r = -D\left[\frac{\partial^2 w}{\partial r^2} + \frac{\nu}{r}\left(\frac{\partial w}{\partial r} + \frac{1}{r}\frac{\partial^2 w}{\partial \theta^2}\right)\right] - \frac{M_T}{1-\nu}, \\ &M_\theta = -D\left[\nu\frac{\partial^2 w}{\partial r^2} + \frac{1}{r}\left(\frac{\partial w}{\partial r} + \frac{1}{r}\frac{\partial^2 w}{\partial \theta^2}\right)\right] - \frac{M_T}{1-\nu}, \ M_{r\theta} = -\frac{D(1-\nu)}{r}\frac{\partial}{\partial \theta}\left(\frac{\partial w}{\partial r} - \frac{1}{r}\frac{\partial w}{\partial \theta}\right), \\ &Q_r = -D\frac{\partial}{\partial r}\left(\nabla^2 w - \frac{M_T}{1-\nu}\right), \ \ Q_\theta = -\frac{D}{r}\frac{\partial}{\partial \theta}\left(\nabla^2 w - \frac{M_T}{1-\nu}\right) \end{aligned} \tag{16.83}$$

Similarly, the formulas for the plane stress components, from Equation (16.17), are written in the following form:

$$\sigma_r = +\frac{12z}{s^3}\left[M_r + \frac{M_T}{(1-\nu)}\right] - \frac{\alpha E}{1-\nu}(T - T_R),$$
$$\sigma_\theta = +\frac{12z}{s^3}\left[M_\theta + \frac{M_T}{(1-\nu)}\right] - \frac{\alpha E}{1-\nu}(T - T_R),\ \tau_{r\theta} = -\frac{12\,z}{s^3}M_{r\theta}, \tag{16.84}$$

where M_r, M_θ and $M_{r\theta}$ are determined by Equations (16.83). Clearly the maximum stresses take place on the surfaces $s = \pm s/2$ of the plate. Into polar coordinates gives the effective transverse shear forces. They may be written for an edge with outward normal in the r and θ directions, as follows:

$$V_r = Q_r + \frac{1}{r}\frac{\partial M_{r\theta}}{\partial \theta} = -D\left[\frac{\partial}{\partial r}\left(\nabla^2 w - \frac{M_T}{1-\nu}\right) + \frac{(1-\nu)}{r^2}\frac{\partial^2}{\partial \theta^2}\left(\frac{\partial w}{\partial r} - \frac{1}{r}\frac{\partial w}{\partial \theta}\right)\right],$$
$$V_\theta = Q_\theta + \frac{\partial M_{r\theta}}{\partial r} = -D\frac{\partial}{\partial \theta}\left[\frac{1}{r}\left(\nabla^2 w - \frac{M_T}{1-\nu}\right) + (1-\nu)\frac{\partial}{\partial r}\left(\frac{1}{r}\frac{\partial w}{\partial r} - \frac{1}{r^2}\frac{\partial w}{\partial \theta}\right)\right] \tag{16.85}$$

The boundary conditions at the edges of a circular plate of radius "a" may readily be written as follows:

a) Clamped edge r = a

$$w(r=a) = 0, \quad \frac{\partial w}{\partial r}(r=a) = 0, \tag{16.86}$$

b) Simply supported edge r = a

$$w(r=a) = 0, \quad M_r(r=a) = 0, \tag{16.87}$$

c) Free edge r = a

$$M_r(r=a) = 0,\ V_r(r=a) = 0, \tag{16.88}$$

16.4.2. Axisymmetrically heated circular plates

When an applied loading and end restraints of the circular plate are independent of the angle θ, then the deflection of the plate and the stress resultants and stress couples will depend upon the radial position r only. Such a bending of the circular plate is referred to as axially symmetrical and the following simplifications can be made:

$$\frac{\partial^k ()}{\partial \theta^k} = M_{r\theta} = M_\theta = 0; \quad k = 1,2,3,4 \tag{16.89}$$

The previous equations for the bending of a circular plate can therefore be simplified to:

$$M_r = -D\left(\frac{d^2 w}{dr^2} + \frac{\nu}{r}\frac{dw}{dr}\right) - \frac{M_T}{1-\nu},\ \ M_\theta = -D\left(\nu\frac{d^2 w}{dr^2} + \frac{1}{r}\frac{dw}{dr}\right) - \frac{M_T}{1-\nu},$$
$$Q_r = -D\frac{d}{dr}\left(\frac{d^2 w}{dr^2} + \frac{1}{r}\frac{dw}{dr} - \frac{M_T}{1-\nu}\right) = -D\frac{d}{dr}\left[\frac{1}{r}\frac{d}{dr}\left(r\frac{dw}{dr}\right) - \frac{M_T}{1-\nu}\right], \tag{16.90}$$

The differential equation of the deflected surface of the circular plate, Equation (16.82), reduces now to:

$$D\left(\frac{d^4 w}{dr^4} + \frac{2}{r}\frac{d^3 w}{dr^3} - \frac{1}{r^2}\frac{d^2 w}{dr^2} + \frac{1}{r^3}\frac{dw}{dr}\right) = p(r) - \frac{1}{1-\nu}\left(\frac{d^2 M_T}{dr^2} + \frac{1}{r}\frac{dM_T}{dr}\right) \tag{16.91}$$

The Equation (16.91) appears in the form:

$$\frac{D}{r}\frac{d}{dr}\left\{r\frac{d}{dr}\left[\frac{1}{r}\frac{d}{dr}\left(r\frac{dw}{dr}\right)\right]\right\} = p(r) - \frac{1}{(1-\nu)r}\frac{d}{dr}\left(r\frac{dM_T}{dr}\right) \tag{16.92}$$

The rigorous solution of equation (16.92) is obtained as the sum of the complementary solution of the homogeneous differential equation, w_h, and the particular solution, w_p, i.e.,

$$w = w_h + w_p \tag{16.93}$$

The complementary solution w_h of (16.92) is given by:

$$w_h = C_1 \log r + C_2 r^2 \log r + C_3 r^2 + C_4 \tag{16.94}$$

where C_1, C_2, C_3, C_4 are constants that can be evaluated from the boundary conditions. The particular solution, w_p, is obtained by successive integration of equation (16.92):

$$w_p = \int \frac{1}{r} \int r \int \frac{1}{r} \int \frac{r p(r)}{D} dr dr dr dr - \int \frac{1}{r} \int \frac{r M_T}{(1-\nu) D} dr dr \tag{16.95}$$

Case 1) If the plate is under a uniform loading $p = p_0$, and $M_T = 0$ the particular solution is

$$w_p = \frac{p_0 r^4}{64 D} \tag{16.96}$$

For purposes of calculation, the following quantities are given explicitly:

$$w = C_1 \log r + C_2 r^2 \log r + C_3 r^2 + C_4 + \frac{p_0 r^4}{64 D} \tag{16.97}$$

$$\frac{dw}{dr} = \frac{C_1}{r} + C_2 r (2 + \log r) + 2 C_3 r + \frac{p_0 r^4}{16 D} \tag{16.98}$$

$$M_r = -D \left[C_1 \frac{\nu - 1}{r^2} + 2 C_2 (1+\nu) \log r + 2 C_3 (1+\nu) + \left(\frac{p_0 r^2}{16 D} + C_2 \right) (3+\nu) \right]$$

$$M_\theta = -D \left[C_1 \frac{\nu - 1}{r^2} + 2 C_2 (1+\nu) \log r + 2 C_3 (1+\nu) + \left(\frac{p_0 r^2}{16 D} + C_2 \right) (1+3\nu) \right] \tag{16.99}$$

$$Q_r = -4D \left(\frac{C_2}{r} + \frac{p_0 r}{8 D} \right)$$

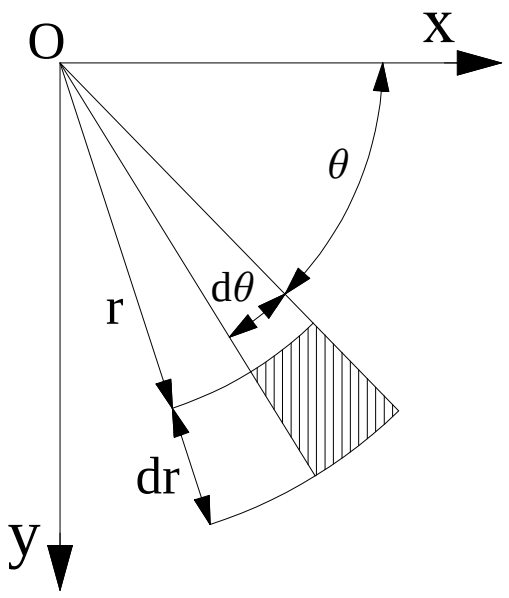

Fig. 16.9 – *Polar coordinates system of plate*

16.5 References

[1] Bruno A. Boley and Jerome H. Weiner, *Theory of thermal stresses*, Dover publications, inc. Mineola, New York

[2] Eduard Ventsel, Theodor Krauthammer, *Thin Plates and Shells: Theory, Analysis and Applications*, The Pennsylvania State University Park, Pennsylvania

CHAPTER XVII
STEADY-STATE PROBLEM FOR MULTILAYERED CYLINDERS

17.0. Introduction

By using a multi-layered approach based on the theory of laminated composites, the solutions of temperature, displacements, and thermal/mechanical stresses in a functionally graded circular hollow cylinder are presented in this chapter. The cylinder has finite length and is subjected to axisymmetric thermal and mechanical loads. The material properties are assumed to be temperature-independent and radially dependent, but are assumed to be homogeneous in each layer.
Functionally graded materials (FGM) and laminated composites are important non-homogeneous materials designed to work in a high-temperature environment. A number of research works have been carried out for thermo-elastic problems of functionally graded structures. Obata and Noda studied the one-dimensional steady thermal stresses in a functionally graded circular hollow cylinder and hollow sphere by use of a perturbation method. By introducing the theory of laminated composites, Ootao and Tanigawa treated the three-dimensional transient thermal stresses of functionally graded rectangular plates due to partial heat supply, and analyzed the piezo-thermo-elastic problem of a functionally graded rectangular plate bonded to a piezoelectric plate.
Kim and Noda researched the two-dimensional unsteady thermo-elastic problems of functionally graded infinite hollow cylinders by using a Green's function approach. Jabbari et al. derived analytical solutions for one-dimensional steady-state thermo-elastic problems of functionally graded circular hollow cylinders in the case of material models expressed as power functions of r, and treated the two-dimensional thermo-elastic problems of the functionally graded cylinder by using the Fourier transform. Erashlan obtained analytical solutions for thermally induced axisymmetric and elastic–plastic deformations in non uniform heat-generating composite tubes. Liew et al. obtained analytical solutions of a functionally graded circular hollow cylinder by a novel limiting process that employs the solutions of homogeneous circular hollow cylinders. Shao and Wang derived analytical solutions of mechanical stresses of a functionally graded circular hollow cylinder with finite length. Ma and Wang investigated the nonlinear bending and post-buckling behaviour of a functionally graded circular plate subjected to thermal/mechanical loadings based on classical plate theory. In their studies, the material properties were considered as both temperature dependent and temperature independent.
In this chapter, we consider a steady-state thermo-elastic problem of multilayered cylinder with finite length. The thermal and mechanical loads applied on the cylinder are axisymmetric in the hoop direction and vary in the axial direction. In order to obtain analytical solutions of temperature, displacements, and stresses for the two-dimensional thermo-elastic problem, the cylinder is assumed to be composed of n fictitious layers in the radial direction. The material properties of each layer are assumed to be homogeneous.

17.1. Basic equations for steady-state problem

Let us consider an multilayered cylinder composed by *n* fictitious hollow cylindrical phases, with finite length L (Figure n.1). The external radius and internal radius of the multilayer cylinders are denoted by $R^{(n)}$ and $R^{(0)}$, respectively. The radius at interface between the generic phase *i-th* and the phase *(i+1)-th* are denoted with $R^{(i)}$. The mechanical and thermal properties of each layer are assumed to be homogeneous and isotropic and are denoted with apex (i). Cylindrical coordinates r, θ and z are used in the analysis. The multilayered cylinder is subjected to gradient temperature, between the inner and the outer surface, that are T_e and T_i, respectively. The multilayered cylinder is subjected to an external constant pressure p_e and an internal constant pressure p_i applied on the inner and the outer surface $r = R^{(n)}$ and $r = R^{(0)}$, respectively. Moreover, it is subjected to axial force N on the two bases. In follows, details of multilayered cylinder are shown in figure 17.1. The basic thermo-elastic equations for the *i*-th layer can be expressed as reported below:

Strain-Displacement relations:

In isotropic-thermal elasticity case, the strains are related to the displacements by purely geometrical considerations. Let us assume that multilayered cylinder subjected to axial-symmetric mechanical and thermal loads. Then, in cylindrical coordinate the displacement components are given by:

$$u_r^{(i)} = u_r^{(i)}(r,z),\ \ u_\theta^{(i)} = 0,\ u_z^{(i)} = u_z^{(i)}(r,z),\quad \forall i \in \{1,2,...n\} \tag{17.1}$$

where with apex 1,2,…n denote the hollow phases of multilayered cylinder . The functions $u_r^{(i)}, u_z^{(i)}$ are the radial and axial displacements in the *i*-th layer, respectively. The superscript *"i"* represents the *i*-th layer. Then, the strain-displacement relations take the form:

$$\varepsilon_{rr}^{(i)} = u_{r,r}^{(i)},\quad \varepsilon_{\theta\theta}^{(i)} = r^{-1}u_r^{(i)},\quad \varepsilon_{zz}^{(i)} = u_{z,z}^{(i)},\ \varepsilon_{rz} = (1/2)\left(u_{r,z}^{(i)} + u_{z,r}^{(i)}\right),\quad \varepsilon_{r\theta} = \varepsilon_{\theta z} = 0,\ \ \forall i \in \{1,2,...n\} \tag{17.2}$$

Thermo-elastic stress-strain relations:

$$\begin{aligned}
\sigma_{rr}^{(i)} &= \lambda^{(i)}\left(r^{-1}u_r^{(i)} + u_{z,z}^{(i)}\right) + \left(2\mu^{(i)} + \lambda^{(i)}\right)u_{r,r}^{(i)} - \left(3\lambda^{(i)} + 2\mu^{(i)}\right)\alpha^{(i)}\left(T^{(i)} - T_R\right)\\
\sigma_{\theta\theta}^{(i)} &= \lambda^{(i)}\left(u_{r,r}^{(i)} + u_{z,z}^{(i)}\right) + \left(2\mu^{(i)} + \lambda^{(i)}\right)r^{-1}u_r^{(i)} - \left(3\lambda^{(i)} + 2\mu^{(i)}\right)\alpha^{(i)}\left(T^{(i)} - T_R\right)\\
\sigma_{zz}^{(i)} &= \lambda^{(i)}\left(u_{r,r}^{(i)} + r^{-1}u_r^{(i)}\right) + \left(2\mu^{(i)} + \lambda^{(i)}\right)u_{z,z}^{(i)} - \left(3\lambda^{(i)} + 2\mu^{(i)}\right)\alpha^{(i)}\left(T^{(i)} - T_R\right)\\
\tau_{rz}^{(i)} &= \left(u_{r,z}^{(i)} + u_{z,r}^{(i)}\right)\mu^{(i)};\ \ \tau_{\theta z}^{(i)} = \tau_{r\theta}^{(i)} = 0; \qquad \forall i \in \{1,2,...n\}
\end{aligned} \tag{17.3}$$

where $\mu^{(i)}, \lambda^{(i)}, \alpha^{(i)}, T^{(i)}$ are the Lamè elastic constants, thermo-elastic coefficients and temperature in the *i*-th layer, respectively. Moreover let us assume that the function of temperature in each phase is given by:

$$T^{(i)} = T^{(i)}(r,z) \quad \forall i \in \{1,2,....,n\} \tag{17.4}$$

Equilibrium equations:

The equations of equilibrium are the same as those of isothermal elasticity since they are based on purely mechanical considerations. By applying the hypothesis of the axial-symmetric steady-state temperature loads and in absence of the body force, the equilibrium equations become:

$$\begin{cases} \sigma_{rr,r}^{(i)} + \tau_{rz,z}^{(i)} + r^{-1}\left(\sigma_{rr}^{(i)} - \sigma_{\theta\theta}^{(i)}\right) = 0 \\ \tau_{rz,r}^{(i)} + \sigma_{zz,z}^{(i)} + r^{-1}\tau_{rz}^{(i)} = 0 \end{cases} \quad \forall i \in \{1,2,...n\} \tag{17.5}$$

Equilibrium and compatibility boundary conditions

The results obtained until now satisfy the equilibrium and compatibility equations inside each generic *i*-th phase of multilayered cylinder, subjected to axis-symmetrical strains or steady-state temperature loads. Under both the hypothesis of linear isotropic elastic behaviour of the homogeneous materials and the assumption of perfect bond at the cylindrical interfacial boundaries (no de-lamination or friction phenomena), we have now to establish the satisfaction of both the equilibrium and the compatibility equations at the boundary surfaces between two generic adjacent phases. To obtain this, we will make reference to the generic case, in which a multilayered cylinder is constituted by a central *core* and *n* arbitrary hollow phases (figure 17.1). In this framework the following boundary conditions be established. In particular, we begin writing the compatibility equations at the generic interface, that is:

$$\begin{cases} u_r^{(i)}(r = R^{(i)}) = u_r^{(i+1)}(r = R^{(i+1)}) \\ u_z^{(i)}(r = R^{(i)}) = u_z^{(i+1)}(r = R^{(i+1)}) \end{cases} \quad \forall i \in \{1,2,...n-1\} \tag{17.6}$$

The equilibrium equations at the generic interface are given by:

$$\begin{cases} \sigma_{rr}^{(i)}(r = R^{(i)}) = \sigma_{rr}^{(i+1)}(r = R^{(i+1)}) \\ \tau_{rz}^{(i)}(r = R^{(i)}) = \tau_{rz}^{(i+1)}(r = R^{(i+1)}) \end{cases} \quad \forall i \in \{1,2,...n-1\} \tag{17.7}$$

The equilibrium equations for the tractions on the inner and the outer spherical boundary surface, give:

$$\begin{cases} \sigma_{rr}^{(1)}(r=R^{(0)})=p_i\ , \quad \tau_{rz}^{(1)}(r=R^{(0)})=0\ , \\ \sigma_{rr}^{(n)}(r=R^{(n)})=p_e\ , \quad \tau_{rz}^{(n)}(r=R^{(n)})=0\ , \end{cases} \tag{17.8}$$

where p_e, p_i are the pressure applied on the inner and the outer surface of multilayered cylinder, respectively. Finally, it remains to consider the last equilibrium equation in z-direction on one of the basis of multilayered cylinder, being the other end condition automatically satisfied. Therefore, without loss of generality, for z = 0 we can write:

$$\sum_{i=1}^{n}\int_0^{2\pi}\int_{R^{(i-1)}}^{R^{(i)}}\sigma_{zz}^{(i)}(z=0)\,r\,dr\,d\theta=N_z \tag{17.9}$$

where N_z is the axial force applied on the bases of multilayered cylinder

Heat conduction equation

The conduction equation is wrote in hypothesis of steady-state problem and of the axial-symmetric load conditions for each phases of multilayered cylinder:

$$T_{,rr}^{(i)}+r^{-1}T_{,r}^{(i)}+T_{,zz}^{(i)}=0 \qquad \forall i\in\{1,2,...n\} \tag{17.10}$$

Temperature boundary and continuity conditions

At the interfaces between the phases, the temperature and heat flux is the same. Then we can write the following conditions:

$$\begin{cases} T^{(i)}(r=R^{(i)})=T^{(i+1)}(r=R^{(i)}) \\ k^{(i)}T_{,r}^{(i)}(r=R^{(i)})=k^{(i+1)}T_{,r}^{(i+1)}(r=R^{(i)}) \end{cases} \quad \forall i\in\{0,1,...n-1\} \tag{17.11}$$

on the inner and the outer surface the temperature is equal to T_e and T_i, respectively:

$$T^{(n)}(r=R^{(n)})=T_e, \quad T^{(1)}(r=R^{(0)})=T_i \tag{17.12}$$

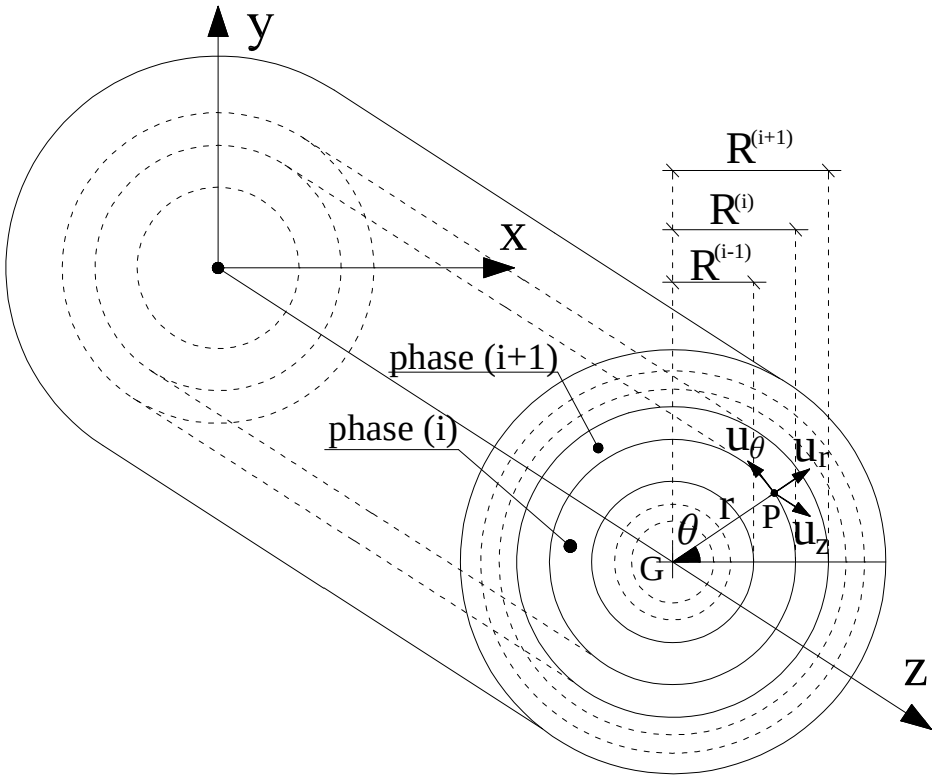

Fig. 17.1 - *Multilayered cylinder composed by n-hollow cylinders*

17.2. Multilayered cylinder under radial temperature variation and uniform pressure in plane strain

Let us consider an multilayered cylinder constituted by n-hollow cylinder phases as decrypted in section 17.1. The equations field in each phase are composed by equilibrium and heat conduction equations. By substituting the strain-displacement relations (17.2) in stress-strain relations (17.3) and these in equilibrium equations (17.5), we obtain the displacement formulation of the equilibrium equations. The elastic moduli $E^{(i)}$ and $\nu^{(i)}$ can be to express as functions of the Lamé coefficients, by invoking the well-known following relations:

$$E^{(i)}=\left[\mu^{(i)}(2\mu^{(i)}+3\lambda^{(i)})\right]\Big/(\mu^{(i)}+\lambda^{(i)}),\quad \nu^{(i)}=\lambda^{(i)}\Big/\left[2(\mu^{(i)}+\lambda^{(i)})\right], \tag{17.13}$$

Then, the equations field to satisfy in thermo-elastic axial-symmetric steady-state problem, in cylindrical coordinate, are given by:

$$\begin{cases}\left[r^{-1}\left(r\,u_r^{(i)}\right)_{,r}\right]_{,r}+(1/2)\left[\left(1-2\nu^{(i)}\right)u_{r,z}^{(i)}+u_{z,r}^{(i)}\right]_{,z}\Big/\left(1-\nu^{(i)}\right)=2\zeta^{(i)}T_{,r}^{(i)}\\ (1/2)r^{-1}\left[\left(r\,u_{r,z}^{(i)}\right)_{,r}+\left(1-2\nu^{(i)}\right)\left(r\,u_{z,r}^{(i)}\right)_{,r}\right]\Big/\left(1-\nu^{(i)}\right)+u_{z,zz}^{(i)}=2\zeta^{(i)}T_{,z}^{(i)}\\ T_{,rr}^{(i)}+r^{-1}T_{,r}^{(i)}+T_{,zz}^{(i)}=0\end{cases} \tag{17.14}$$

where the constant $\zeta^{(i)}=\left[\alpha^{(i)}\left(1+\nu^{(i)}\right)\right]\Big/\left[2\left(1-\nu^{(i)}\right)\right]$. For the case of plane strain, the displacement component $u_z^{(i)}$ vanishes. If the hollow cylinder is subjected to radial temperature variation and radial uniform pressure, the displacement components reduce to sole $u_r^{(i)}=u_r^{(i)}(r)$ and the temperature is a function of sole variable r : $T^{(i)}=T^{(i)}\left(r\right)$. In this case the equilibrium equations reduce to one ordinary differential equation. The equations field (17.14) become:

$$\left[r^{-1}\left(r\,u_r^{(i)}\right)_{,r}\right]_{,r}=2\zeta^{(i)}T_{,r}^{(i)},\qquad T_{,rr}^{(i)}+r^{-1}T_{,r}^{(i)}=0,\qquad \forall i\in\{1,2,...,n\} \tag{17.15}$$

By applying the formulas in Chapter XIV, we determine the displacement solution in each phases of multilayered cylinder, as reported below:

$$u_r^{(i)}=2\zeta^{(i)}r^{-1}\int rT^{(i)}\left(r\right)dr+C_1^{(i)}r+C_2^{(i)}r^{-1}\quad \forall i\in\{1,2,....,n\} \tag{17.16}$$

where $C_1^{(i)},C_2^{(i)}$ are constants integration to determine. By integrating the Fourier's equation reported in (17.15), we determine the well know temperature function for steady-state problem in each phases:

$$T^{(i)}\left(r\right)=A_1^{(i)}\log r+A_2^{(i)}\quad \forall i\in\{1,2,....,n\} \tag{17.17}$$

where $A_1^{(i)},A_2^{(i)}$ are constants integration to determine. Then, the heat flux in each phases is given by:

$$q^{(i)}=-k^{(i)}T_{,r}^{(i)}=-k^{(i)}A_1^{(i)}r^{-1}\quad \forall i\in\{1,2,...,n\} \tag{17.18}$$

By substituting the temperature function (17.17) in equation (17.16), we obtain the explicit expression of displacement function:

$$u_r^{(i)}=C_1^{(i)}r+C_2^{(i)}r^{-1}+\zeta^{(i)}r\left[A_1^{(i)}\left(\log r-1/2\right)+A_2^{(i)}\right]\quad \forall i\in\{1,2,...n\} \tag{17.19}$$

By applying the strain-displacement relationship, we determine the no-vanishing strain components:

$$\begin{cases}\varepsilon_{rr}^{(i)}=C_1^{(i)}-C_2^{(i)}r^{-2}+\zeta^{(i)}\left[A_1^{(i)}\left(\log r+1/2\right)+A_2^{(i)}\right]\\ \varepsilon_{\theta\theta}^{(i)}=C_1^{(i)}+C_2^{(i)}r^{-2}+\zeta^{(i)}\left[A_1^{(i)}\left(\log r-1/2\right)+A_2^{(i)}\right]\end{cases}\quad \forall i\in\{1,2,...n\} \tag{17.20}$$

By applying the stress-strain relationship, we obtain the non-zero stress components:

$$\begin{cases} \sigma_{rr}^{(i)} = \dfrac{E^{(i)}}{1+\nu^{(i)}}\left\{\dfrac{C_1^{(i)}}{1-2\nu^{(i)}} - C_2^{(i)} r^{-2} - \zeta^{(i)}\left[A_1^{(i)}\left(\log r - 1/2\right) + A_2^{(i)}\right]\right\} + \Omega^{(i)} T_R, \\ \sigma_{\theta\theta}^{(i)} = \dfrac{E^{(i)}}{1+\nu^{(i)}}\left\{\dfrac{C_1^{(i)}}{1-2\nu^{(i)}} + C_2^{(i)} r^{-2} - \zeta^{(i)}\left[A_1^{(i)}\left(\log r + 1/2\right) + A_2^{(i)}\right]\right\} + \Omega^{(i)} T_R, \quad \forall i \in \{1,2,...n\} \\ \sigma_{zz}^{(i)} = \dfrac{E^{(i)}}{1+\nu^{(i)}}\left\{\dfrac{2C_1^{(i)}\nu^{(i)}}{1-2\nu^{(i)}} - 2\zeta^{(i)}\left(A_1^{(i)} \log r + A_2^{(i)}\right)\right\} + \Omega^{(i)} T_R \end{cases} \tag{17.21}$$

where $\Omega^{(i)} = \alpha^{(i)} E^{(i)} \big/ \left(1-2\nu^{(i)}\right)$. The equivalent stress determines whether yielding occurs. For planar isotropy and non-homogeneity in radial direction, the equivalent stress based on the Henchy-von Mises criteria is given by follows equation:

$$\sigma_{eq}^{(i)} = 2^{-1/2}\left[\left(\sigma_{rr}^{(i)} - \sigma_{\theta\theta}^{(i)}\right)^2 + \left(\sigma_{rr}^{(i)} - \sigma_{zz}^{(i)}\right)^2 + \left(\sigma_{\theta\theta}^{(i)} - \sigma_{zz}^{(i)}\right)^2\right]^{1/2} \tag{17.22}$$

By substituting the equation (17.21) in (17.22), the equivalent stress is given by:

$$\sigma_{eq}^{(i)} = \frac{E^{(i)}}{1+\nu^{(i)}}\sqrt{\begin{array}{l} C_1^{(i)2} + 3C_2^{(i)2} r^{-4} + \zeta^{(i)}\left[2C_1^{(i)}\left(A_1^{(i)} \log r + A_2^{(i)}\right) - 3A_1^{(i)} C_2^{(i)} r^{-2}\right] + \\ \zeta^{(i)2}\left[2A_2^{(i)2} + 2A_1^{(i)} A_2^{(i)} \log r + A_1^{(i)2}\left(3/4 + \log^2 r\right)\right] \end{array}} \tag{17.23}$$

Finally, by utilizing the expressions of the temperature, heat flux, radial displacement and radial stress in each phases, we can write in explicit the boundary conditions for multilayered cylinder. Then, the compatibility boundary conditions (17.6), become one equation :

$$\begin{array}{l} C_1^{(i)} - C_1^{(i+1)} + \left(C_2^{(i)} - C_2^{(i+1)}\right) R^{(i)-2} = \zeta^{(i+1)}\left[A_1^{(i+1)}\left(\log R^{(i)} - 1/2\right) + A_2^{(i+1)}\right] + \\ \qquad - \zeta^{(i)}\left[A_1^{(i)}\left(\log R^{(i)} - 1/2\right) + A_2^{(i)}\right] \quad \forall i \in \{1,2,...,(n-1)\} \end{array} \tag{17.24}$$

The equilibrium conditions (17.7) at interfaces between the phases, are given by:

$$\begin{array}{l} \dfrac{E^{(i)}}{\left(1+\nu^{(i)}\right)}\left[\dfrac{C_1^{(i)}}{1-2\nu^{(i)}} - \dfrac{C_2^{(i)}}{R^{(i)2}}\right] - \dfrac{E^{(i+1)}}{\left(1+\nu^{(i+1)}\right)}\left[\dfrac{C_1^{(i+1)}}{1-2\nu^{(i+1)}} - \dfrac{C_2^{(i+1)}}{R^{(i)2}}\right] = T_R\left(\Omega^{(i+1)} - \Omega^{(i)}\right) + \\ \qquad + \psi^{(i)}\left[A_2^{(i)} + A_1^{(i)}\left(\log R^{(i)} - 1/2\right)\right] - \psi^{(i+1)}\left[A_2^{(i+1)} + A_1^{(i+1)}\left(\log R^{(i)} - 1/2\right)\right] \\ \qquad\qquad \forall i \in \{1,2,...,(n-1)\} \end{array} \tag{17.25}$$

where $\psi^{(i)} = (1/2)\left[\left(\alpha^{(i)} E^{(i)}\right)\big/\left(1-\nu^{(i)}\right)\right]$.

The equilibrium equations on the external and internal surface of the solid (17.8) become:

$$\begin{cases} \dfrac{E^{(1)}}{1+\nu^{(1)}}\left(\dfrac{C_1^{(1)}}{1-2\nu^{(1)}} - \dfrac{C_2^{(1)}}{R^{(0)2}}\right) = -\Omega^{(1)} T_R + \psi^{(1)}\left[A_1^{(1)}\left(\log R^{(0)} - 1/2\right) + A_2^{(1)}\right] + p_i \\ \dfrac{E^{(n)}}{1+\nu^{(n)}}\left(\dfrac{C_1^{(n)}}{1-2\nu^{(n)}} - \dfrac{C_2^{(n)}}{R^{(n)2}}\right) = -\Omega^{(n)} T_R + \psi^{(n)}\left[A_1^{(n)}\left(\log R^{(n)} - 1/2\right) + A_2^{(n)}\right] + p_e \end{cases} \tag{17.26}$$

The temperature and continuity boundary conditions at interfaces between the adjacent phases (17.11) become:

$$\begin{cases} \left[A_1^{(i+1)} - A_1^{(i)}\right]\log R^{(i)} + A_2^{(i+1)} - A_2^{(i)} = 0 \\ k^{(i+1)} A_2^{(i+1)} - k^{(i)} A_2^{(i)} = 0 \end{cases} \qquad \forall i \in \{1,2,...,(n-1)\} \tag{17.27}$$

Finally, it is remains to consider the boundary conditions on the external and internal surface related to temperature (17.12):

$$\begin{cases} A_1^{(1)} \log R^{(0)} + A_2^{(1)} = T_i \\ A_1^{(n)} \log R^{(n)} + A_2^{(n)} = T_e \end{cases} \tag{17.28}$$

The equations (17.24) to (17.28) represents an algebraic system constituted by $4\times n$ equations, where the unknown parameters are $4\times n$, as reported below:

$$A_1^{(i)}, A_2^{(i)}, C_1^{(i)}, C_2^{(i)} \quad \forall i \in \{1,2,...,n\} \tag{17.29}$$

The algebraic system mentioned above, can be subdivided in two uncoupled algebraic systems:

(i) the first composed by equations (17.24), (17.25) and (17.26) ; It is characterized by $2\times n$ equations in $2\times n$ unknown parameters $C_1^{(i)}, C_2^{(i)} \quad \forall i \in \{1,2,...,n\}$

(ii) the second composed by equations (17.27) and (17.28); It is characterized by $2\times n$ equations in $2\times n$ unknown parameters $A_1^{(i)}, A_2^{(i)} \quad \forall i \in \{1,2,...,n\}$

In order to solve the first algebraic system (i), it is easy to determine the constants $A_1^{(i)}, A_2^{(i)} \quad \forall i \in \{2,3...,n\}$ as function of the constants $A_1^{(1)}, A_2^{(1)}$. By solving the algebraic system (17.27), we obtain the following relations:

$$A_1^{(i)} = A_1^{(1)} \left(k^{(1)} / k^{(i)} \right); \quad A_2^{(i)} = A_2^{(1)} + A_1^{(1)} k^{(1)} \sum_{j=1}^{i-1} \log R^{(j)} \left(\frac{1}{k^{(j)}} - \frac{1}{k^{(j+1)}} \right); \quad \forall i \in \{2,3,...,n\} \tag{17.30}$$

By substituting the equations (17.30) in algebraic system (17.28), fixed i = n, we determine the constants $A_1^{(1)}, A_2^{(1)}$ as reported below:

$$A_1^{(1)} = \frac{T_e - T_i}{\omega \log R^{(0)}}; \quad A_2^{(1)} = T_i - \frac{T_e - T_i}{\omega}; \tag{17.31}$$

where $\omega = \left(k^{(1)} / \log R^{(0)} \right) \left[\sum_{j=1}^{n} \log \left(\sqrt[k^{(j)}]{R^{(j)} / R^{(j-1)}} \right) \right]$ is non-dimensional constant parameter for fixed number of the phases. Finally, we write the solution in closed form of the algebraic system (i) as follows:

$$\begin{cases} A_1^{(i)} = \dfrac{\left(T_e - T_i\right)}{k^{(i)}} \left[1 \Big/ \log \left(\prod_{j=1}^{n} \sqrt[k^{(j)}]{R^{(j)} / R^{(j-1)}} \right) \right] \\ A_2^{(i)} = T_i + \left(T_e - T_i\right) \left\{ \dfrac{\log \left[\left(\prod_{j=1}^{i} \sqrt[k^{(j)}]{R^{(j)} / R^{(j-1)}} \right) \Big/ \sqrt[k^{(i)}]{R^{(i)}} \right]}{\log \left(\prod_{j=1}^{n} \sqrt[k^{(j)}]{R^{(j)} / R^{(j-1)}} \right)} \right\} \end{cases} \quad \forall i \in \{1,2,...,n\} \tag{17.32}$$

Then, the temperature function in each phases is given by:

$$T^{(i)}(r) = T_i + \left(T_e - T_i\right) \left\{ \frac{\log \left[\left(\sqrt[k^{(i)}]{r / R^{(i)}} \right) \prod_{j=1}^{i} \sqrt[k^{(j)}]{R^{(j)} / R^{(j-1)}} \right]}{\log \left(\prod_{j=1}^{n} \sqrt[k^{(j)}]{R^{(j)} / R^{(j-1)}} \right)} \right\} \quad \forall i \in \{1,2,...,n\} \tag{17.33}$$

In order to solve the second algebraic system (ii), let us consider the algebraic system composed by equilibrium and compatibility conditions (17.24)- (17.25), which can be written as:

$$\mathbf{Q} \cdot \mathbf{X} = \mathbf{L} \tag{17.34}$$

where the vectors $\mathbf{L} = \left[\left(\mathbf{L}_1^{(2)} - \mathbf{L}_1^{(1)} \right), \left(\mathbf{L}_2^{(3)} - \mathbf{L}_2^{(2)} \right), ..., \left(\mathbf{L}_i^{(i+1)} - \mathbf{L}_i^{(i)} \right), ..., \left(\mathbf{L}_{n-1}^{(n-1)} - \mathbf{L}_{n-1}^{(n-1)} \right) \right]^T$ is characterized by following sub-vectors:

$$\begin{aligned}
\mathbf{L}_i^{(i)} &= \begin{bmatrix} \zeta^{(i)}\left(\log R^{(i)} - 1/2\right) & \zeta^{(i)} \\ -\psi^{(i)}\left(\log R^{(i)} - 1/2\right) & -\psi^{(i)} \end{bmatrix} \begin{bmatrix} A_1^{(i)} \\ A_2^{(i)} \end{bmatrix} + \begin{bmatrix} 0 \\ \Omega^{(i)} \end{bmatrix} T_R, \qquad \forall i \in \{1,2,...,n\} \\
\mathbf{L}_i^{(i+1)} &= \begin{bmatrix} \zeta^{(i+1)}\left(\log R^{(i)} - 1/2\right) & \zeta^{(i+1)} \\ -\psi^{(i+1)}\left(\log R^{(i)} - 1/2\right) & -\psi^{(i+1)} \end{bmatrix} \begin{bmatrix} A_1^{(i+1)} \\ A_2^{(i+1)} \end{bmatrix} + \begin{bmatrix} 0 \\ \Omega^{(i+1)} \end{bmatrix} T_R, \quad \forall i \in \{1,2,...,n-1\}
\end{aligned} \tag{17.35}$$

and $\mathbf{X} = [\mathbf{X}^{(1)}, \mathbf{X}^{(2)}, ..., \mathbf{X}^{(n)}]^T$ collect the unknowns sub-vectors $\mathbf{X}^{(i)}$, as reported below:

$$\mathbf{X}^{(i)} = \begin{bmatrix} C_1^{(i)}, & C_2^{(i)} \end{bmatrix}^T, \quad \forall i \in \{1,2,....,n\} \tag{17.36}$$

The matrix $\mathbf{Q}$ is composed by following sub-matrices:

$$\mathbf{Q} = \begin{bmatrix} \mathbf{B}_1^{(1)} & -\mathbf{B}_1^{(2)} & \mathbf{0} & \mathbf{0} & \cdots & \mathbf{0} & \mathbf{0} & \mathbf{0} \\ \mathbf{0} & \mathbf{B}_2^{(2)} & -\mathbf{B}_2^{(3)} & \mathbf{0} & \cdots & \mathbf{0} & \mathbf{0} & \mathbf{0} \\ \mathbf{0} & \mathbf{0} & \mathbf{B}_3^{(3)} & -\mathbf{B}_3^{(4)} & \cdots & \mathbf{0} & \mathbf{0} & \mathbf{0} \\ \vdots & \vdots & \vdots & \vdots & \vdots & \vdots & \vdots & \vdots \\ \mathbf{0} & \mathbf{0} & \mathbf{0} & \mathbf{0} & \cdots & \mathbf{B}_{n-2}^{(n-2)} & -\mathbf{B}_{n-2}^{(n-1)} & \mathbf{0} \\ \mathbf{0} & \mathbf{0} & \mathbf{0} & \mathbf{0} & \cdots & \mathbf{0} & \mathbf{B}_{n-1}^{(n-1)} & -\mathbf{B}_{n-1}^{(n)} \end{bmatrix} \tag{17.37}$$

where the generic matrices $\mathbf{B}_i^{(i)}, \mathbf{B}_i^{(i+1)}$ are given by:

$$\mathbf{B}_i^{(i)} = \begin{bmatrix} 1 & R^{(i)-2} \\ \dfrac{E^{(i)}}{\left(1+\nu^{(i)}\right)\left(1-2\nu^{(i)}\right)} & -\dfrac{E^{(i)}R^{(i)-2}}{\left(1+\nu^{(i)}\right)} \end{bmatrix}, \quad \mathbf{B}_i^{(i+1)} = \begin{bmatrix} 1 & R^{(i)-2} \\ \dfrac{E^{(i+1)}}{\left(1+\nu^{(i+1)}\right)\left(1-2\nu^{(i+1)}\right)} & -\dfrac{E^{(i+1)}R^{(i)-2}}{\left(1+\nu^{(i+1)}\right)} \end{bmatrix}, \tag{17.38}$$

are (2×2) matrices with nonzero determinant, whose components were already gave above.
The determinant of the matrices (17.38) is given by:

$$\det[\mathbf{B}_i^{(i)}] = \frac{2E^{(i)}\left(\nu^{(i)}-1\right)}{R^{(i)}\left(1+\nu^{(i)}\right)\left(1-2\nu^{(i)}\right)} \neq 0, \quad \det[\mathbf{B}_i^{(i+1)}] = \frac{E^{(i+1)}\left(\nu^{(i+1)}-1\right)}{R^{(i)}\left(1+\nu^{(i+1)}\right)\left(1-2\nu^{(i+1)}\right)} \neq 0, \tag{17.39}$$

However, in force of the special form of **Q** derived above, one can rewrite the reduced algebraic problem in order to have the solution without recall any numerical strategy. To make this, let us we can write the algebraic system (17.34) in follows manner:

$$\begin{cases} \mathbf{B}_1^{(2)}\mathbf{X}^{(2)} = \mathbf{B}_1^{(1)}\mathbf{X}^{(1)} + \mathbf{L}_1^{(2)} - \mathbf{L}_1^{(1)} \\ \mathbf{B}_2^{(3)}\mathbf{X}^{(3)} = \mathbf{B}_2^{(2)}\mathbf{X}^{(2)} + \mathbf{L}_2^{(3)} - \mathbf{L}_2^{(2)} \\ \vdots \\ \mathbf{B}_i^{(i+1)}\mathbf{X}^{(i+1)} = \mathbf{B}_i^{(i)}\mathbf{X}^{(i)} + \mathbf{L}_i^{(i+1)} - \mathbf{L}_i^{(i)} \\ \vdots \\ \mathbf{B}_{n-2}^{(n-1)}\mathbf{X}^{(n-1)} = \mathbf{B}_{n-2}^{(n-2)}\mathbf{X}^{(n-2)} + \mathbf{L}_{n-2}^{(n-1)} - \mathbf{L}_{n-2}^{(n-2)} \\ \mathbf{B}_{n-1}^{(n)}\mathbf{X}^{(n)} = \mathbf{B}_{n-1}^{(n-1)}\mathbf{X}^{(n-1)} + \mathbf{L}_{n-1}^{(n)} - \mathbf{L}_{n-1}^{(n-1)} \end{cases} \tag{17.40}$$

By applying an *in-cascade* procedure, we finally obtain

$$\mathbf{X}^{(i)} = \mathbf{\Phi}^{(i)} \cdot \mathbf{X}^{(1)} + \mathbf{\Psi}^{(i)} \quad \forall i \in \{2,3,...,n\} \tag{17.41}$$

where $\mathbf{\Phi}^{(i)}, \mathbf{\Psi}^{(i)}$ are matrix and vector, respectively. The expressions of $\mathbf{\Phi}^{(i)}, \mathbf{\Psi}^{(i)}$ are given by:

$$\begin{cases} \mathbf{\Phi}^{(i)} = \prod_{j=1}^{i-1}\left(\left[\mathbf{B}_{i-j}^{(i-j+1)} \right]^{-1} \cdot \mathbf{B}_{i-j}^{(i-j)} \right) \\ \mathbf{\Psi}^{(i)} = \left[\mathbf{B}_{i-1}^{(i)} \right]^{-1} \cdot \left\{ \mathbf{L}_{i-1}^{(i-1)} - \mathbf{L}_{i-1}^{(i)} + \sum_{j=1}^{i-2} \left[\prod_{k=1}^{j} \left(\mathbf{B}_{i-k}^{(i-k)} \cdot \left[\mathbf{B}_{i-k-1}^{(i-k)} \right]^{-1} \right) \right] \cdot \left(\mathbf{L}_{i-j-1}^{(i-j-1)} - \mathbf{L}_{i-j-1}^{(i-j)} \right) \right\} \end{cases} \quad \forall i \in \{2,3,...,n\} \tag{17.42}$$

where *dot* stands for scalar product. The equations (17.41)-(17.42) permit to write the generic unknowns sub-vector $\mathbf{X}^{(i)}$ as function of a transferring matrix $\mathbf{\Phi}^{(i)}$ and vector $\mathbf{\Psi}^{(i)}$, and the unknowns sub-vector $\mathbf{X}^{(1)}$. The problem is hence reduced to an algebraic one in which only the two coefficients – collected in $\mathbf{X}^{(1)}$ – related to the first phase have to be determined, by imposing two boundary conditions described by the equations obtained above. Therefore, in order to find the two unknowns collected in $\mathbf{X}^{(1)}$, it remains to rewrite the boundary conditions (17.26) in matrix form. In particular, by applying the equation (17.41) for $i = n$, we obtain the follows relationship:

$$\mathbf{X}^{(n)} = \mathbf{\Phi}^{(n)} \cdot \mathbf{X}^{(1)} + \mathbf{\Psi}^{(n)} \tag{17.43}$$

Then, the boundary conditions (17.26), become:

$$\mathbf{P} \cdot \mathbf{X}^{(1)} = \Upsilon \tag{17.44}$$

where the matrix $\mathbf{P}$ and vector Υ are given by**:**

$$\mathbf{P} = \left[\mathbf{P}_1 \quad \left(\mathbf{\Phi}^{(n)} \right)^T \cdot \mathbf{P}_2 \right]^T, \quad \Upsilon = \left[\Upsilon_1 \quad \Upsilon_2 \right]^T, \tag{17.45}$$

where $\mathbf{P}_1, \mathbf{P}_2$ are two vectors and Υ_1, Υ_2 are two scalars, as reported below:

$$\begin{aligned} &\mathbf{P}_1 = \frac{E^{(1)}}{\left(1+\nu^{(1)}\right)} \left[\frac{1}{\left(1-2\nu^{(1)}\right)}, -R^{(0)-2} \right]^T, \ \mathbf{P}_2 = \frac{E^{(n)}}{\left(1+\nu^{(n)}\right)} \left[\frac{1}{\left(1-2\nu^{(n)}\right)}, -R^{(n)-2} \right]^T \\ &\Upsilon_1 = -\Omega^{(1)} T_R + \psi^{(1)} \left[A_1^{(1)} \left(\log R^{(0)} - 1/2 \right) + A_2^{(1)} \right] + p_i; \\ &\Upsilon_2 = -\Omega^{(n)} T_R + \psi^{(n)} \left[A_1^{(n)} \left(\log R^{(n)} - 1/2 \right) + A_2^{(n)} \right] + p_e - \mathbf{P}_2 \cdot \mathbf{\Psi}^{(n)} \end{aligned} \tag{17.46}$$

Then, by inverting, all the $2 \times n$ unknown coefficients , we obtain the unknown parameters:

$$\begin{cases} \mathbf{X}^{(1)} = \mathbf{P}^{-1} \cdot \Upsilon, \\ \mathbf{X}^{(i)} = \mathbf{\Phi}^{(i)} \cdot \mathbf{P}^{-1} \cdot \Upsilon + \mathbf{\Psi}^{(i)} \quad \forall i \in \{2,3,...,n\} \end{cases} \tag{17.47}$$

By substituting the relationships (17.47) and (17.32) in equation (17.19), we obtain the explicit analytical expression of displacement solution in each phases of multilayered cylinder.

17.3. Parametric analysis for multilayered cylinder composed by two phases

Let us consider a multilayered cylinder composed by two hollow cylinders. The inner radius of multilayered cylinder is assumed to be $R^{(0)}$ and the thickness of any phases is equal to δ. Then, we can write the following relationships:

$$R^{(1)} = \left(1+\xi\right) R^{(0)}, \ R^{(2)} = \left(1+2\xi\right) R^{(0)}, \quad \xi = \delta / R^{(0)}, \tag{17.48}$$

The multilayered cylinder is subjected only the gradient of temperature between the internal and external surfaces $\Delta T = T_e - T_i$, but the internal and external pressure are assumed vanishing.

We consider four cases :

(i) variation of Poisson's ratio in two phases, with fixed values of the Young's moduli, thermal conductivity coefficients and linear thermal expansion coefficients;

(ii) variation of Young's moduli in two phases, with fixed values of the Poisson's ratio, thermal conductivity coefficients and linear thermal expansion coefficients;

(iii) variation of linear thermal expansion coefficients in two phases, with fixed values of the Young's moduli, Poisson's ratio and thermal conductivity coefficients;

(iv) variation of thermal conductivity coefficients in two phases, with fixed values of the Young's moduli, Poisson's ratio and linear thermal expansion coefficients;

Let us assume the following non-dimensional parameter for graphics of the displacement, strain and stress functions:

$$\begin{aligned}&\bar{r}=\frac{r-R^{(0)}}{R^{(n)}-R^{(0)}};\ \bar{T}=\frac{T^{(i)}-T_i}{T_e-T_i};\ \bar{u}_r^{(i)}=\frac{2u_r^{(i)}}{\alpha^{(1)}\left(T_e-T_i\right)R^{(0)}};\\&\bar{\varepsilon}_{rr}^{(i)}=\frac{2\varepsilon_{rr}^{(i)}}{\alpha^{(1)}\left(T_e-T_i\right)};\ \bar{\varepsilon}_{\theta\theta}^{(i)}=\frac{2\varepsilon_{\theta\theta}^{(i)}}{\alpha^{(1)}\left(T_e-T_i\right)};\ \bar{\sigma}_{rr}^{(i)}=\frac{\sigma_{rr}^{(i)}}{\beta^{(1)}};\ \bar{\sigma}_{\theta\theta}^{(i)}=\frac{\sigma_{\theta\theta}^{(i)}}{\beta^{(1)}};\ \bar{\sigma}_{eq}^{(i)}=\frac{\sigma_{eq}^{(i)}}{\beta^{(1)}};\end{aligned}\tag{17.49}$$

where $\beta^{(1)}$ is given by follows relationship:

$$\beta^{(1)}=(1/2)\left[\alpha^{(1)}E^{(1)}\left(T_e-T_i\right)\right]/\left(1-\nu^{(1)}\right);\tag{17.50}$$

In the first case (i) let us assume $E^{(1)}=E^{(2)}$, $k^{(1)}=k^{(2)}$, $\alpha^{(1)}=\alpha^{(2)}$, then the only free parameters are Poisson's ratio in two phases. Let us consider six cases in which is fixed Poisson's ratio of the phase (1) $\nu^{(1)}=0.3$, but in phase (2) the Poisson's ratio assume the following values: 0, 0.1, 0.2, 0.3, 0.4, 0.49. The Fig. 17.2 shows the radial displacement along radial direction. Fig. 17.3 and 17.4 show the radial and circumferential strain along radial direction, respectively. In particular, if the ratio $\nu^{(2)}/\nu^{(1)}$ increase, then the radial and circumferential strain increase along radial direction. If the ratio $\nu^{(2)}/\nu^{(1)}$ increase, then the radial, circumferential and axial stress increase in phase (1) and decrease in phase (2), as shown the figures 17.5, 17.6 and 17.7. The equivalent stress determines whether yielding occurs. For planar isotropy and non-homogeneity in radial direction, the equivalent stress based on the Henchy- von Mises criteria is given by follows equation:

$$\sigma_{eq}^{(i)}=2^{-1/2}\left[\left(\sigma_{rr}^{(i)}-\sigma_{\theta\theta}^{(i)}\right)^2+\left(\sigma_{rr}^{(i)}-\sigma_{zz}^{(i)}\right)^2+\left(\sigma_{\theta\theta}^{(i)}-\sigma_{zz}^{(i)}\right)^2\right]^{1/2}\tag{17.51}$$

The equivalent stress increase with ratio $\nu^{(2)}/\nu^{(1)}$ as showed in figure 17.8. The non-dimensional graphics of the radial displacement, strain and stress as reported below:

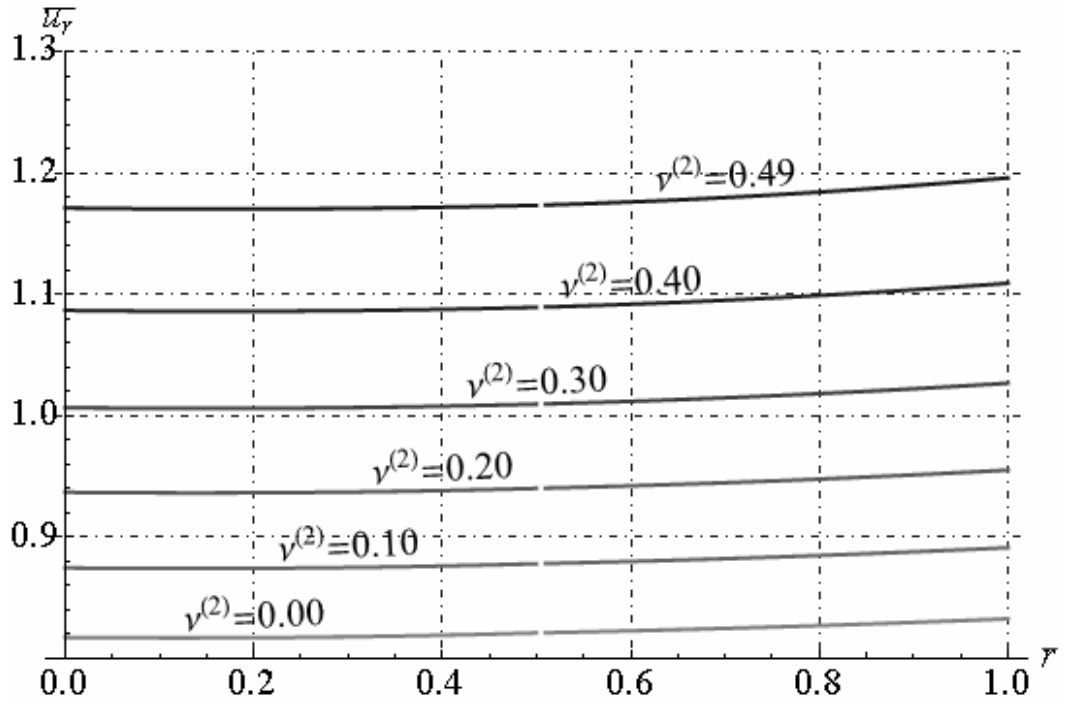

Fig. 17.2 - *Non-dimensional radial displacement along radial direction* $(\nu^{(1)}=0.3)$

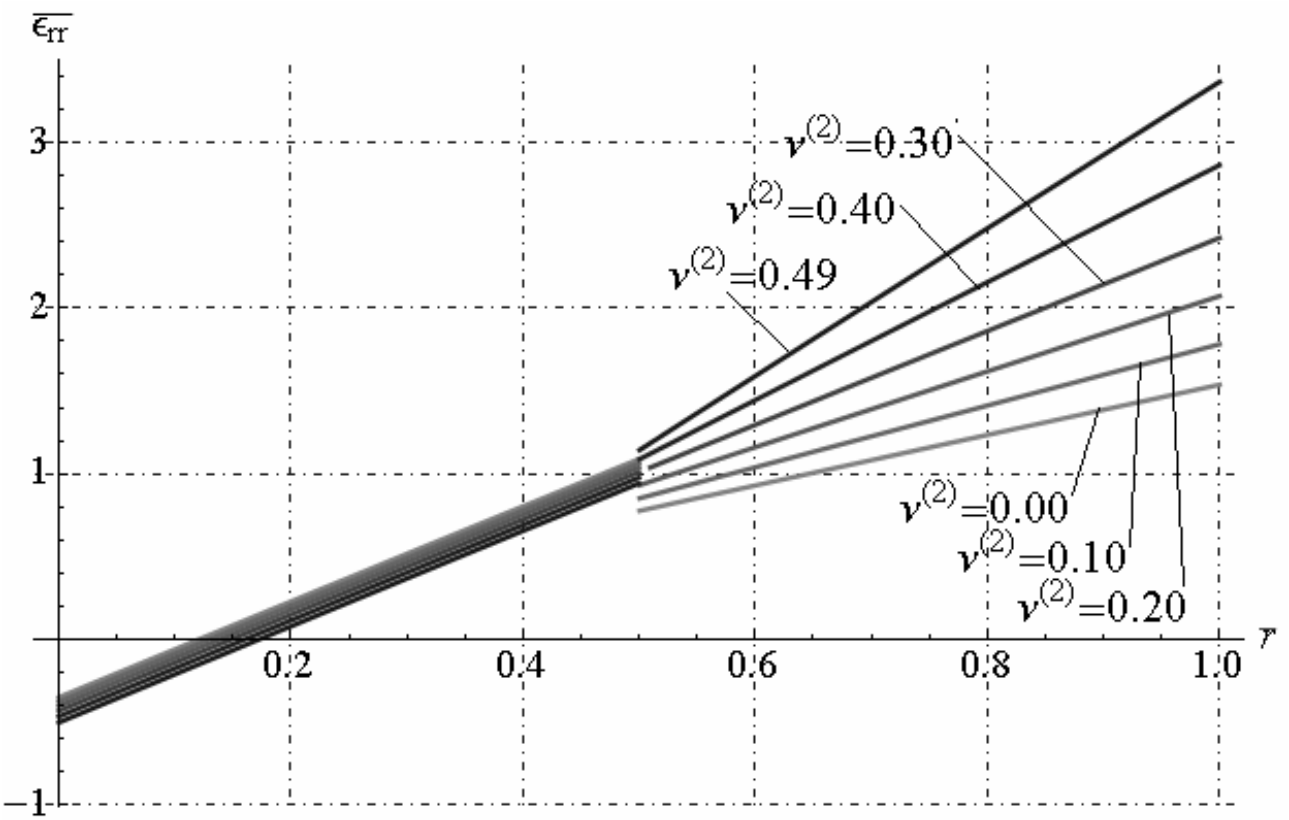

Fig. 17.3 - *Non-dimensional radial strain distribution along radial direction* ($\nu^{(1)} = 0.3$)

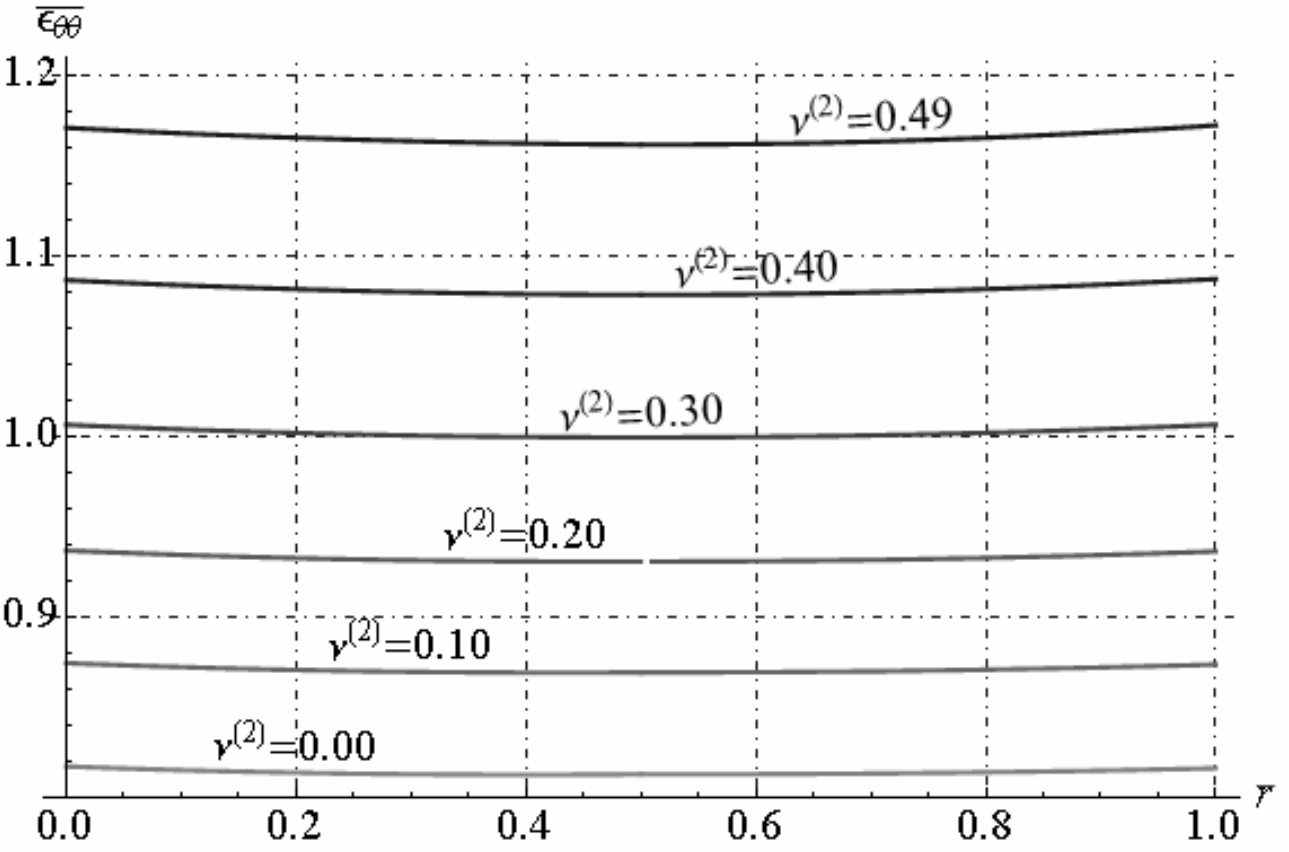

Fig. 17.4 - *Non-dimensional circumferential strain along radial direction* ($\nu^{(1)} = 0.3$)

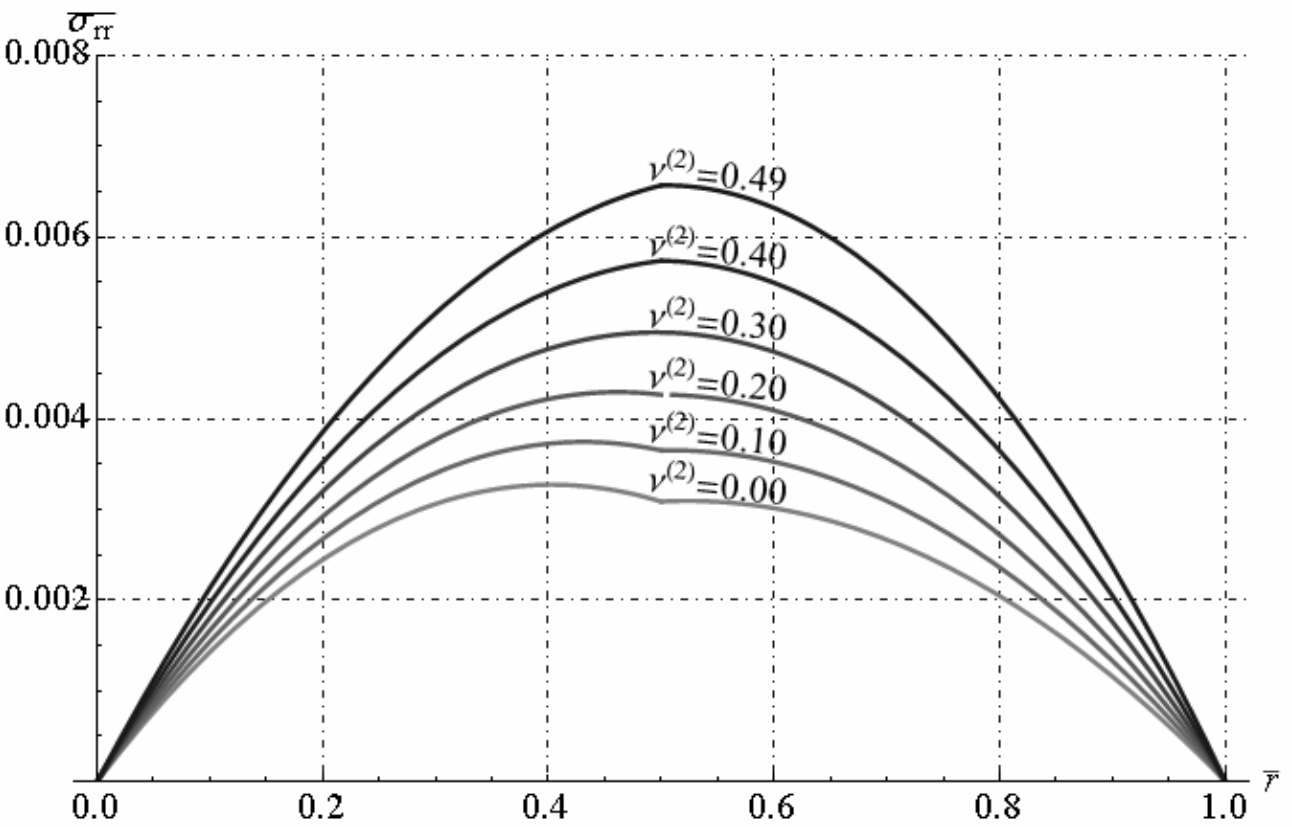

Fig. 17.5 - *Non-dimensional radial stress distribution along radial direction* ($\nu^{(1)} = 0.3$)

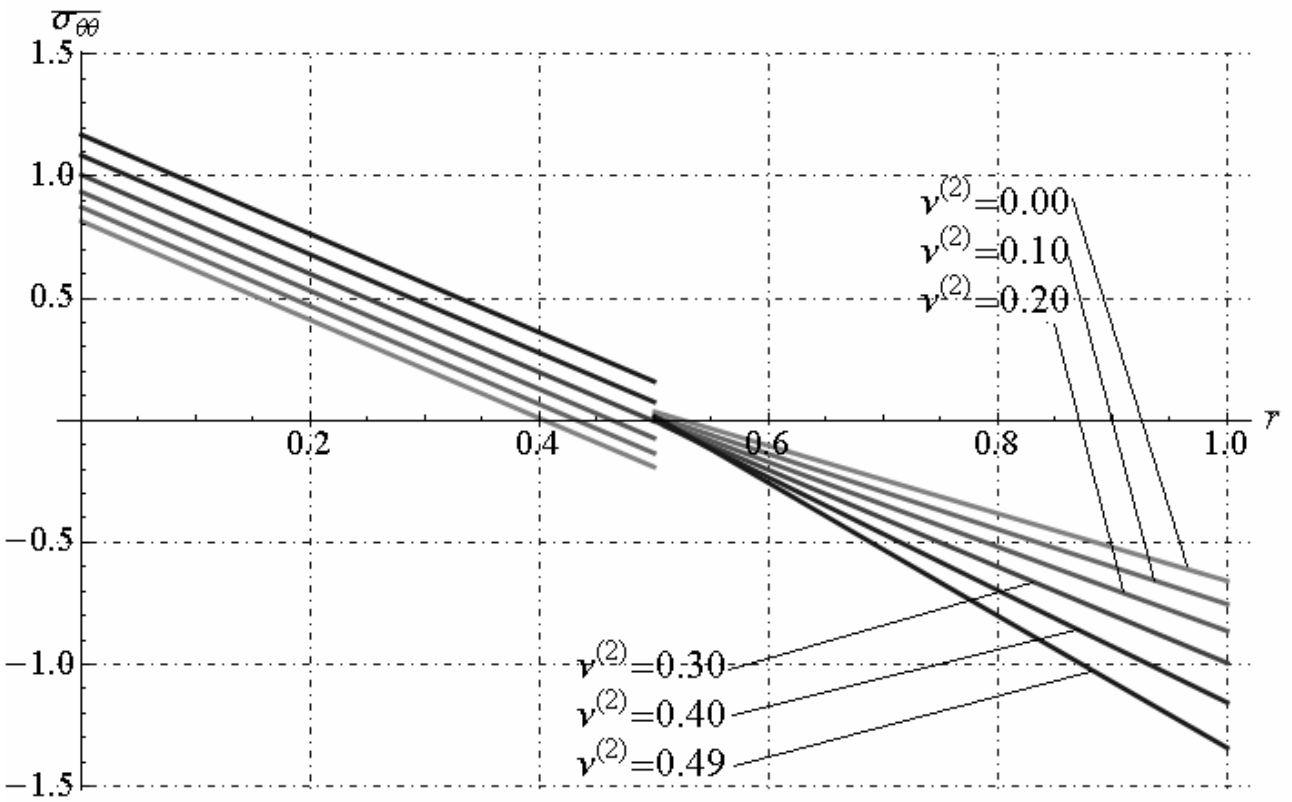

Fig. 17.6 - *Non-dimensional circumferential stress along radial direction* ($\nu^{(1)} = 0.3$)

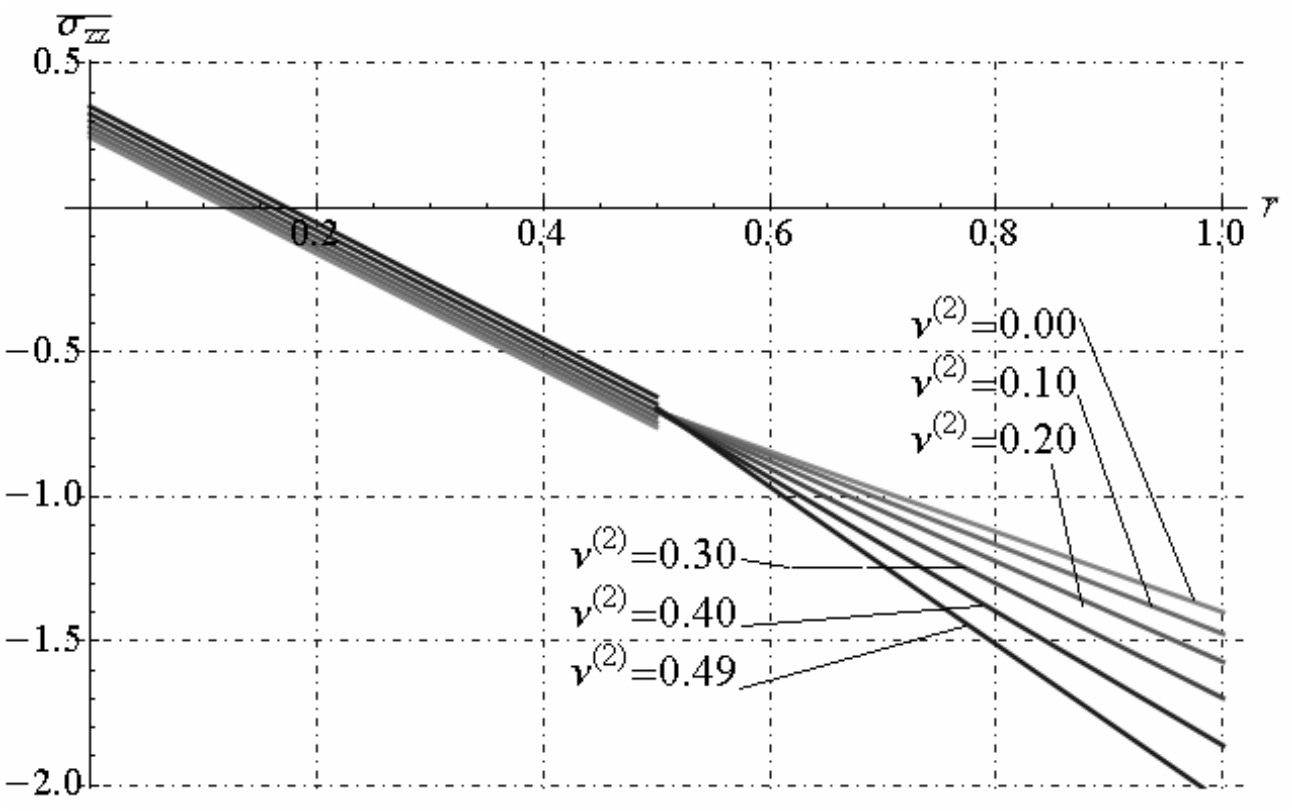

Fig. 17.7 - *Non-dimensional axial stress along radial direction* $(\nu^{(1)} = 0.3)$

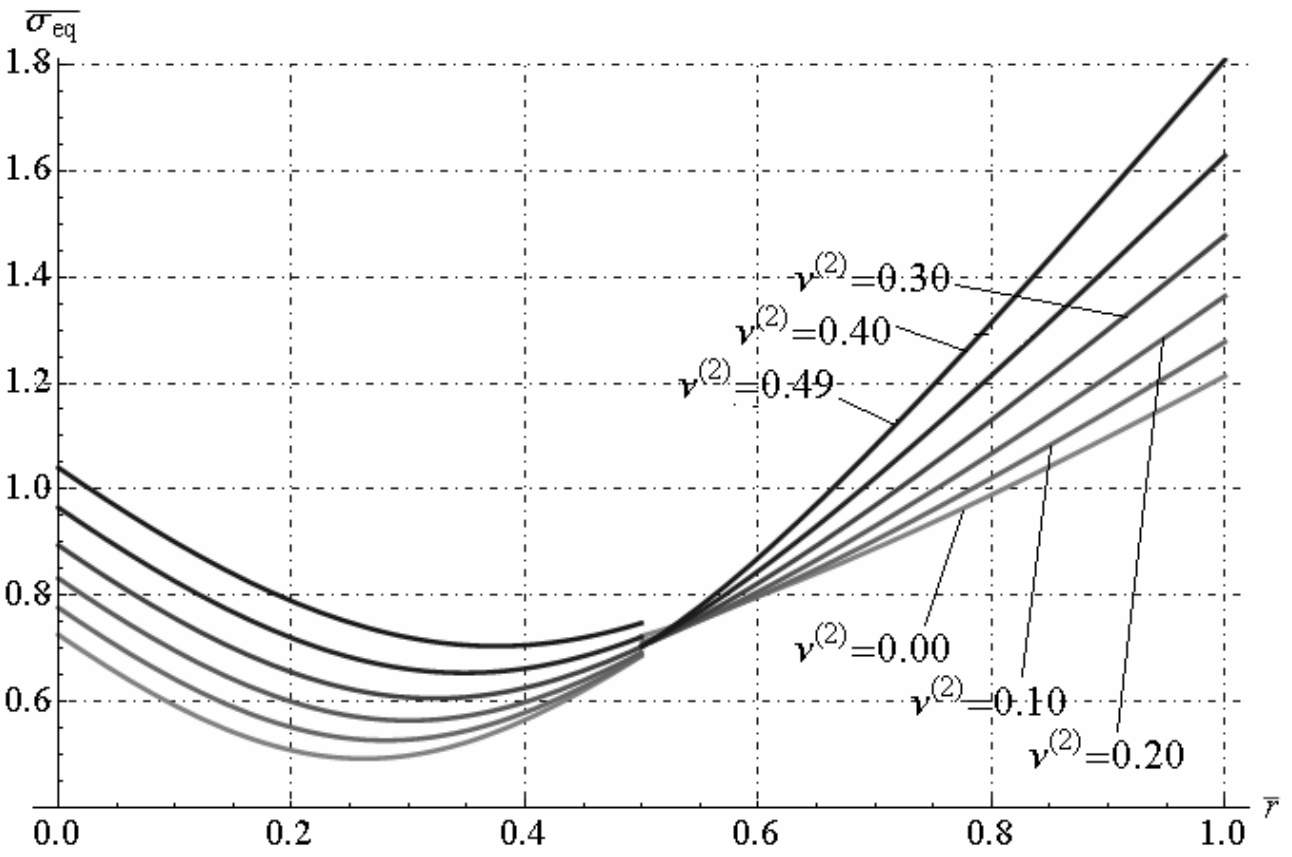

Fig. 17.8 - *Non-dimensional equivalent stress along radial direction* $(\nu^{(1)} = 0.3)$

In the second case (ii) let us assume $\nu^{(1)} = \nu^{(2)}$, $k^{(1)} = k^{(2)}$, $\alpha^{(1)} = \alpha^{(2)}$, then the only free parameters are Young's moduli in two phases. Let us consider six cases in which are selected the different ratio of the Young's moduli $E^{(2)}/E^{(1)}$ as follows : 0.1, 0.5, 1.0, 2.0, 5.0, 10.0. Figure 17.10 shows that if the ratio $E^{(2)}/E^{(1)}$ increase the radial strain decrease in both phases. Conversely, figure 17.11 shows that if the ratio $E^{(2)}/E^{(1)}$ increase the circumferential strain increase in both phases. Fig. 17.12, 17.13 and 17.14 show the radial, circumferential and axial stresses along radial direction, respectively. As expected, the circumferential and axial stresses distribution exhibits significant jumps at all interfaces as shown in Fig. 17.13. These discontinuities are due to the differences between Young's modulus. The circumferential and axial stresses varies characteristically in each layer in view of the occurrence of discontinuities at all interfaces shown in the Fig. 17.13. In particular, if the ratio $E^{(2)}/E^{(1)}$ increase, the radial, circumferential, axial and equivalent stresses increase along radial direction as shown the figures 17.12, 17.13, 17.14 and 17.15.

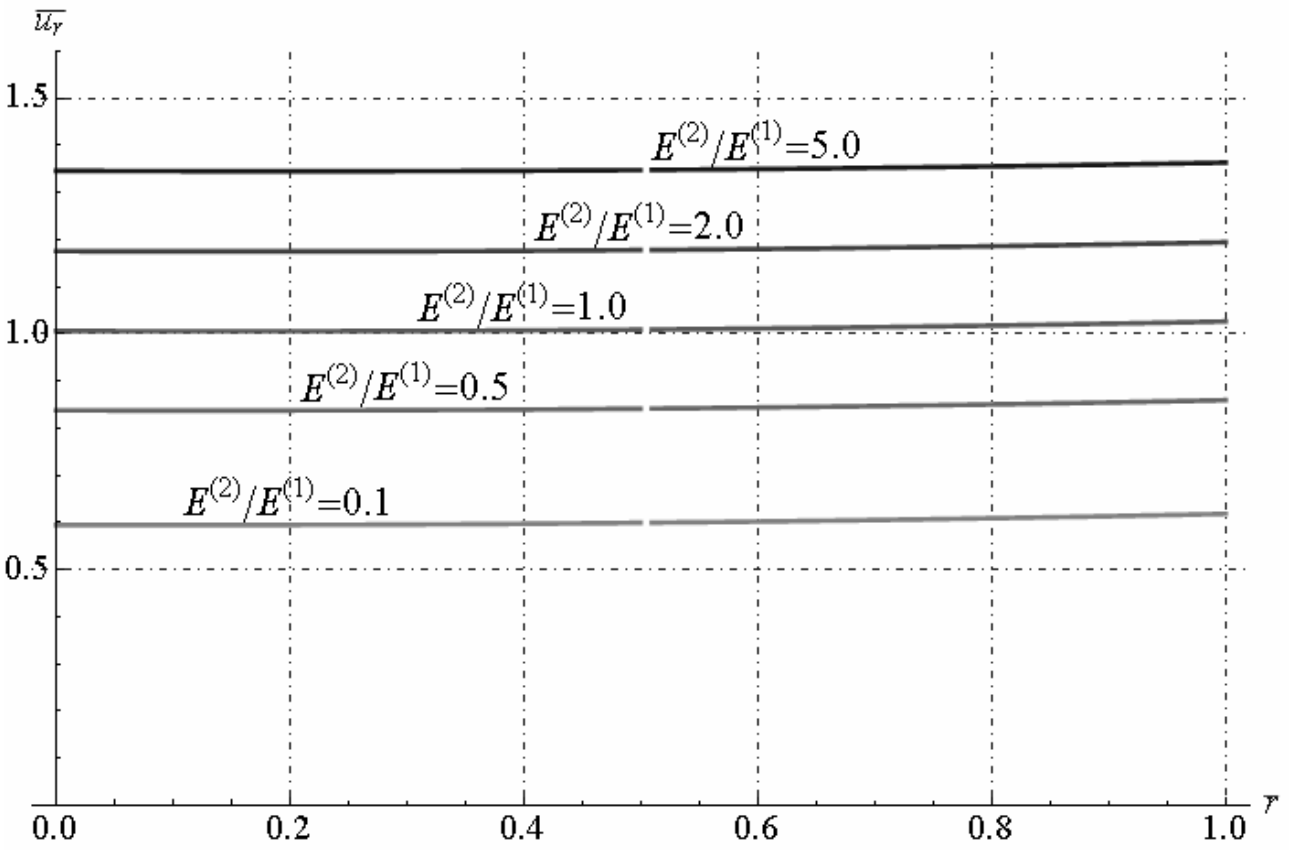

Fig. 17.9 -*Non-dimensional radial displacement along radial direction (Young's moduli variation)*

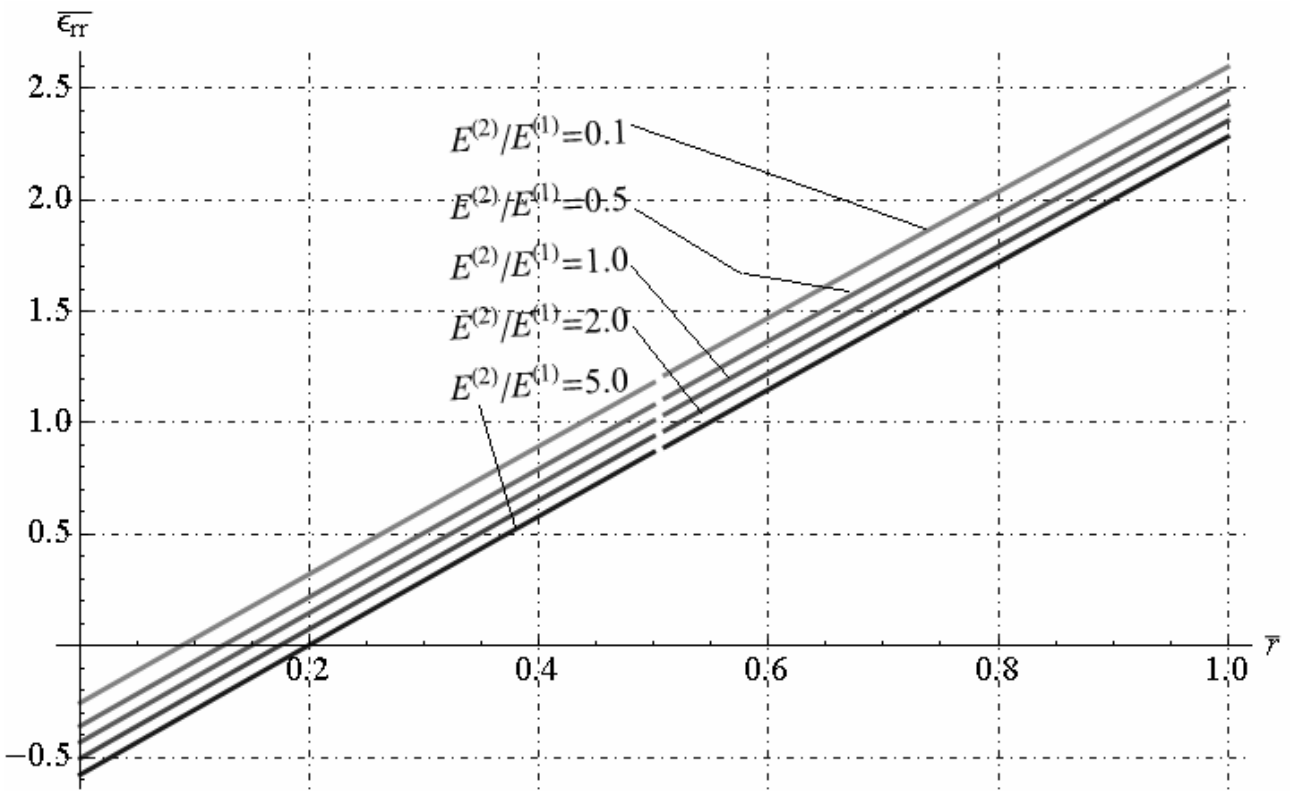

Fig. 17.10 - *Non-dimensional radial strain along radial direction (Young's moduli variation)*

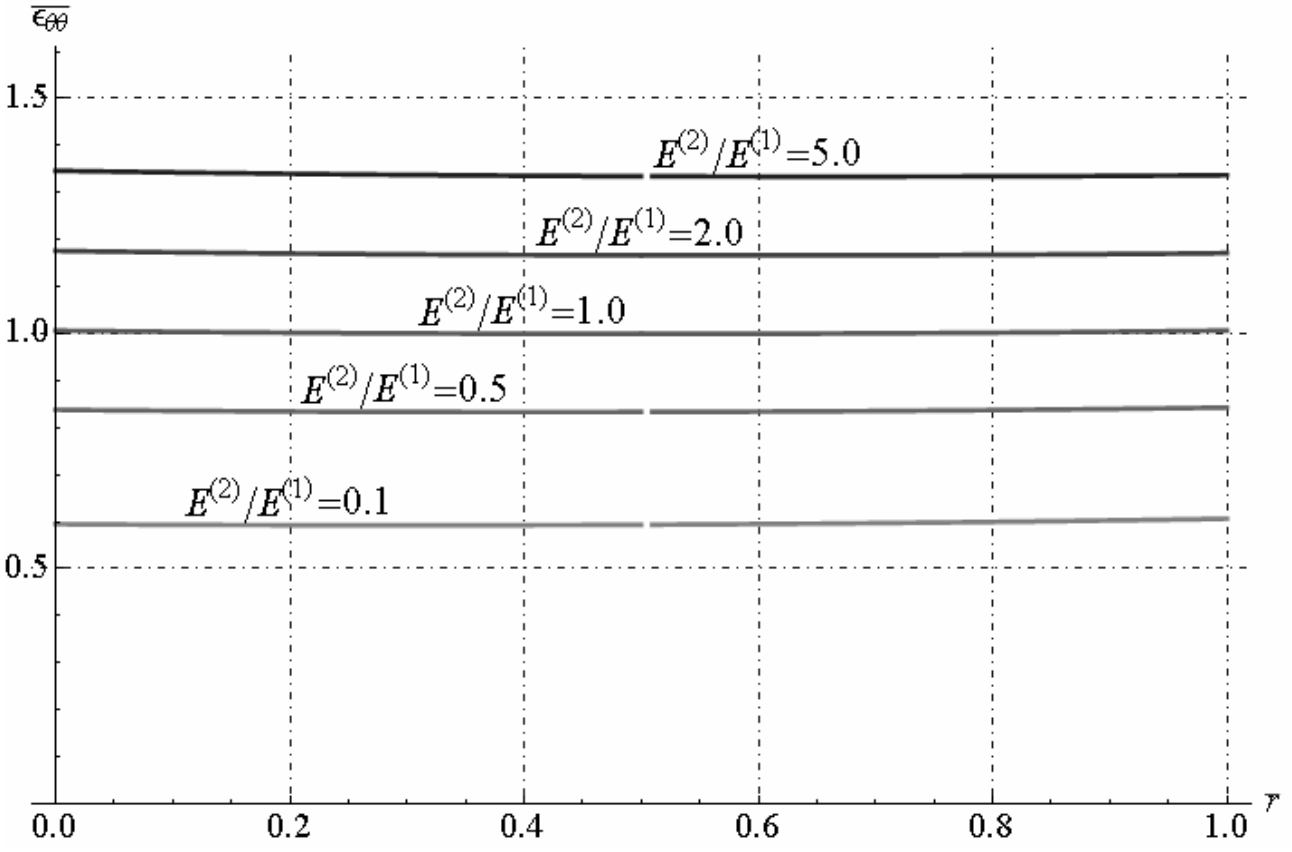

Fig. 17.11 - *Non-dimensional circumferential strain along radial direction (Young's moduli variation)*

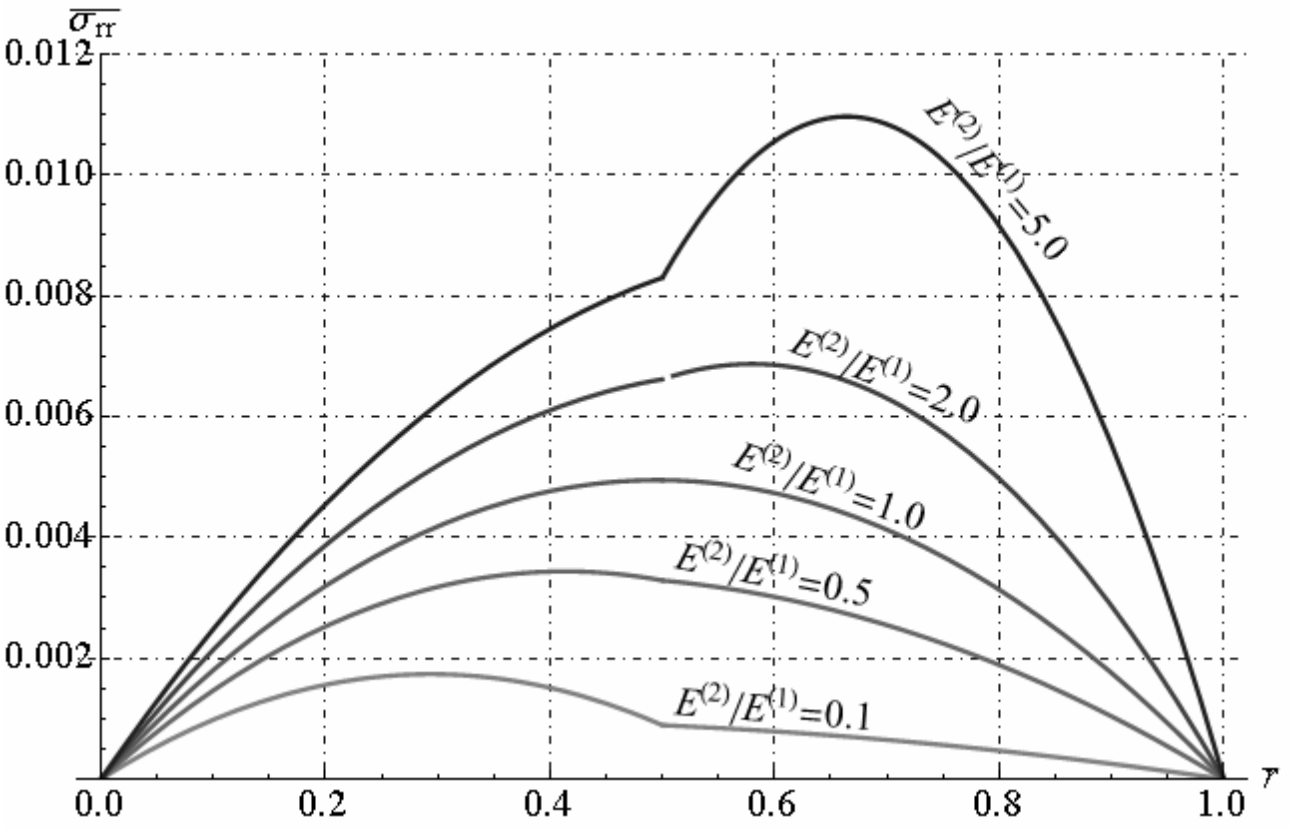

Fig. 17.12 - *Non-dimensional radial stress along radial direction (Young's moduli variation)*

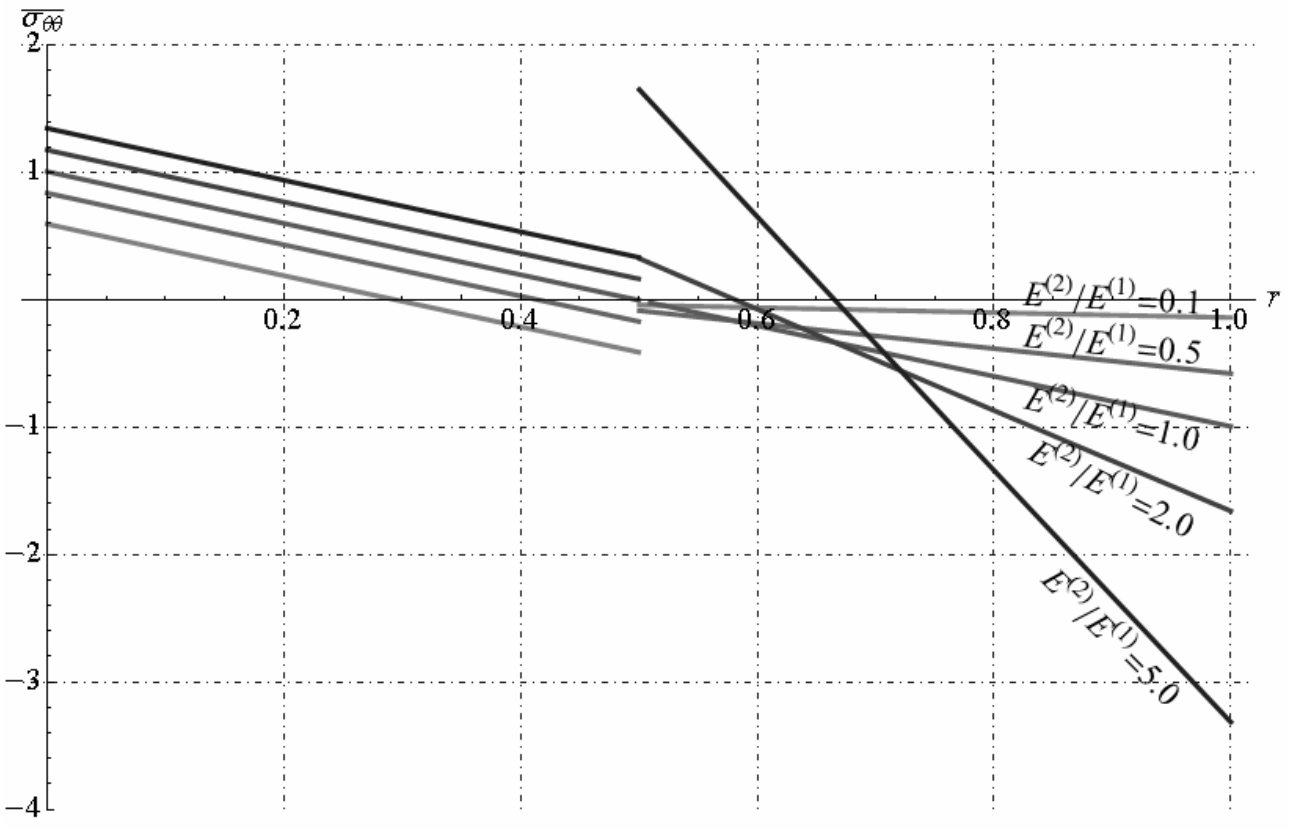

Fig. 17.13 - *Non-dimensional circumferential stress along radial direction (Young's moduli variation)*

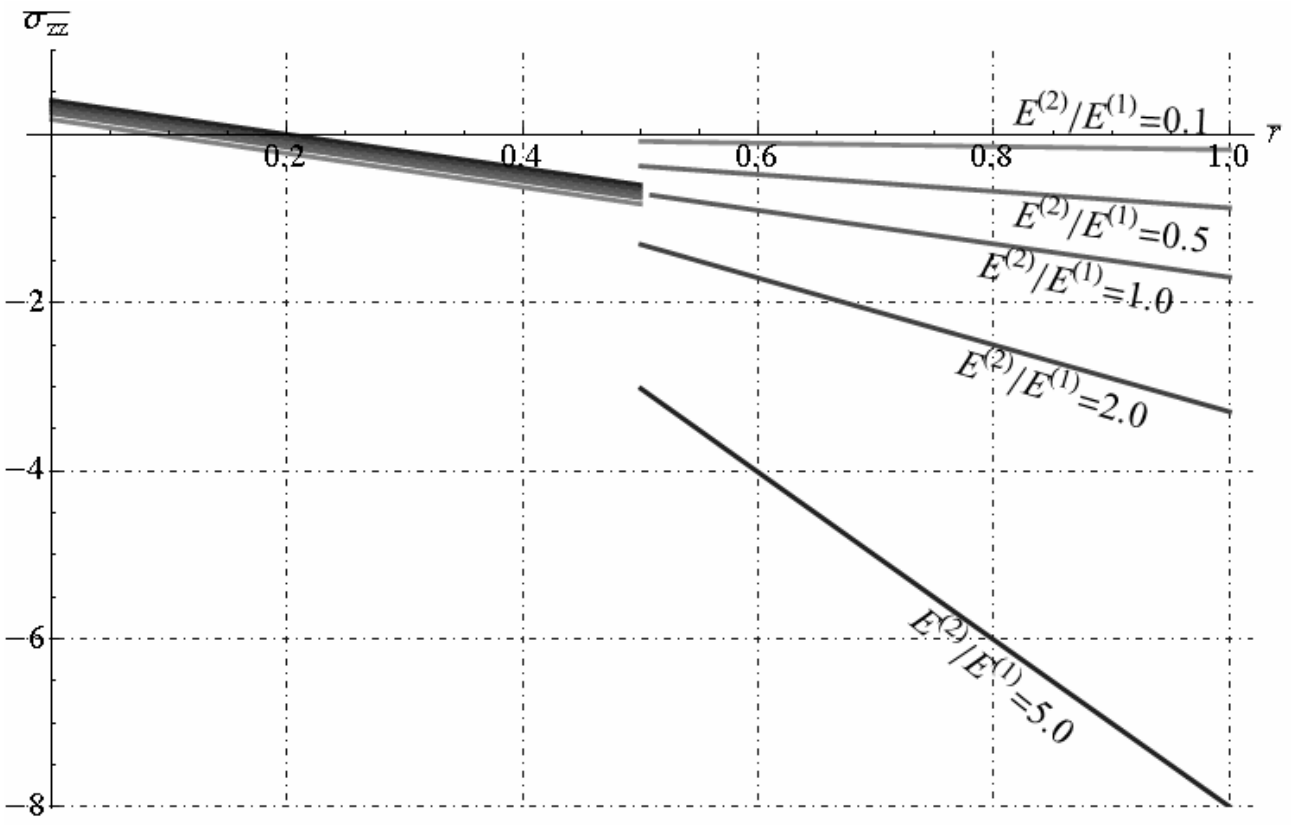

Fig. 17.14 - *Non-dimensional axial stress along radial direction (Young's moduli variation)*

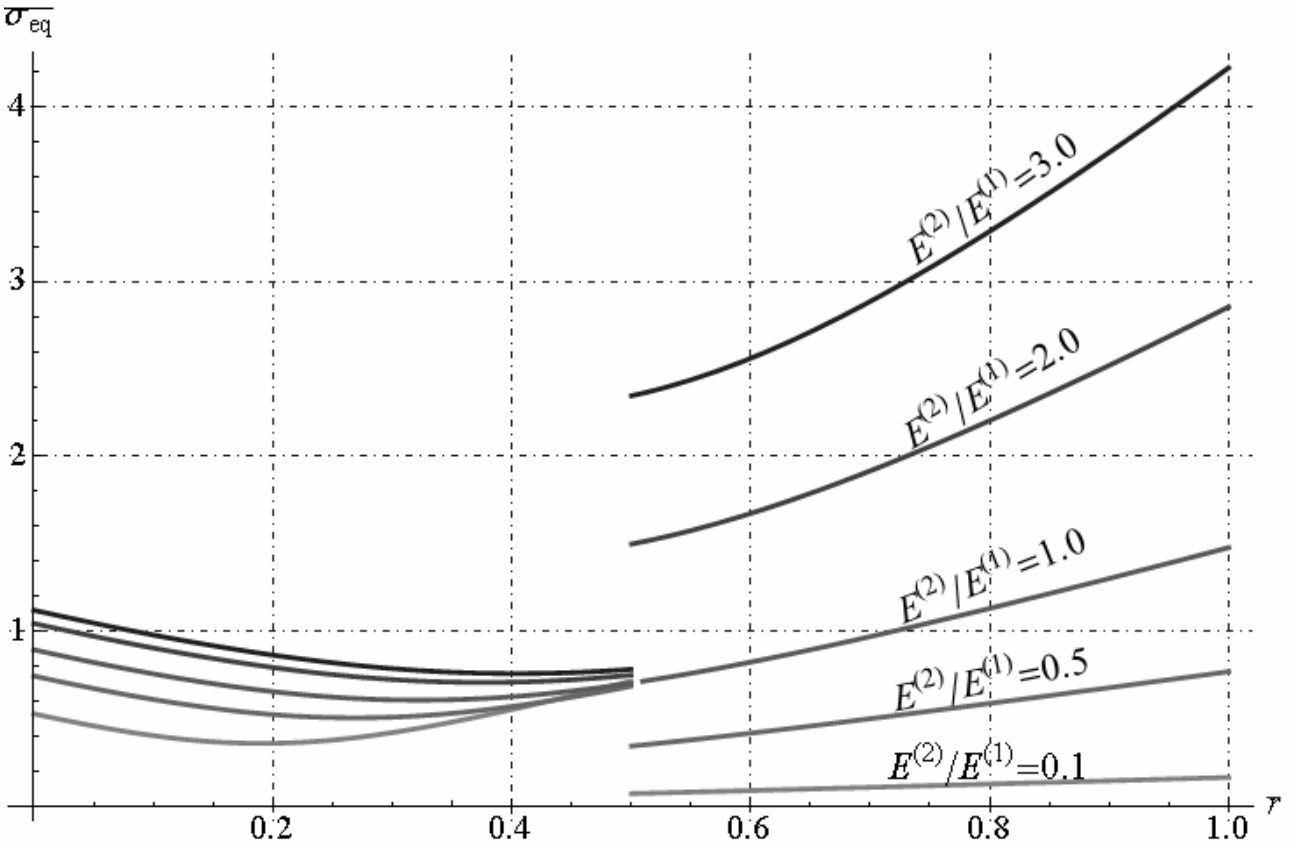

Fig. 17.15 - *Non-dimensional equivalent stress along radial direction (Young's moduli variation)*

In the third case (iii) let us assume $E^{(1)} = E^{(2)}$, $\nu^{(1)} = \nu^{(2)} = 0.3$, $k^{(1)} = k^{(2)}$, then the only free parameters are linear thermal expansion coefficients in two phases. Let us consider six cases in which are selected the different ratios of linear thermal expansion coefficients $\alpha^{(2)}/\alpha^{(1)}$ as follows : 0.1, 0.5, 0.8, 1.0, 1.5, 2.0. Figure 17.16 and 17.18 shows that if the ratio $\alpha^{(2)}/\alpha^{(1)}$ increase, then the radial displacement and circumferential strain increase. Moreover, if the ratio $\alpha^{(2)}/\alpha^{(1)}$ increase, then the radial strain increase in phase (2) and decrease in phase (1). The radial stress increase with ratio $\alpha^{(2)}/\alpha^{(1)}$ as showed in figure 17.19. The circumferential and axial stresses increase in absolute value with ratio $\alpha^{(2)}/\alpha^{(1)}$, as reported in figure 17.20 and 17.21. Finally, if the ratio $\alpha^{(2)}/\alpha^{(1)}$ increase the equivalent stress increase in both phases (1) and (2) (figure 17.22).

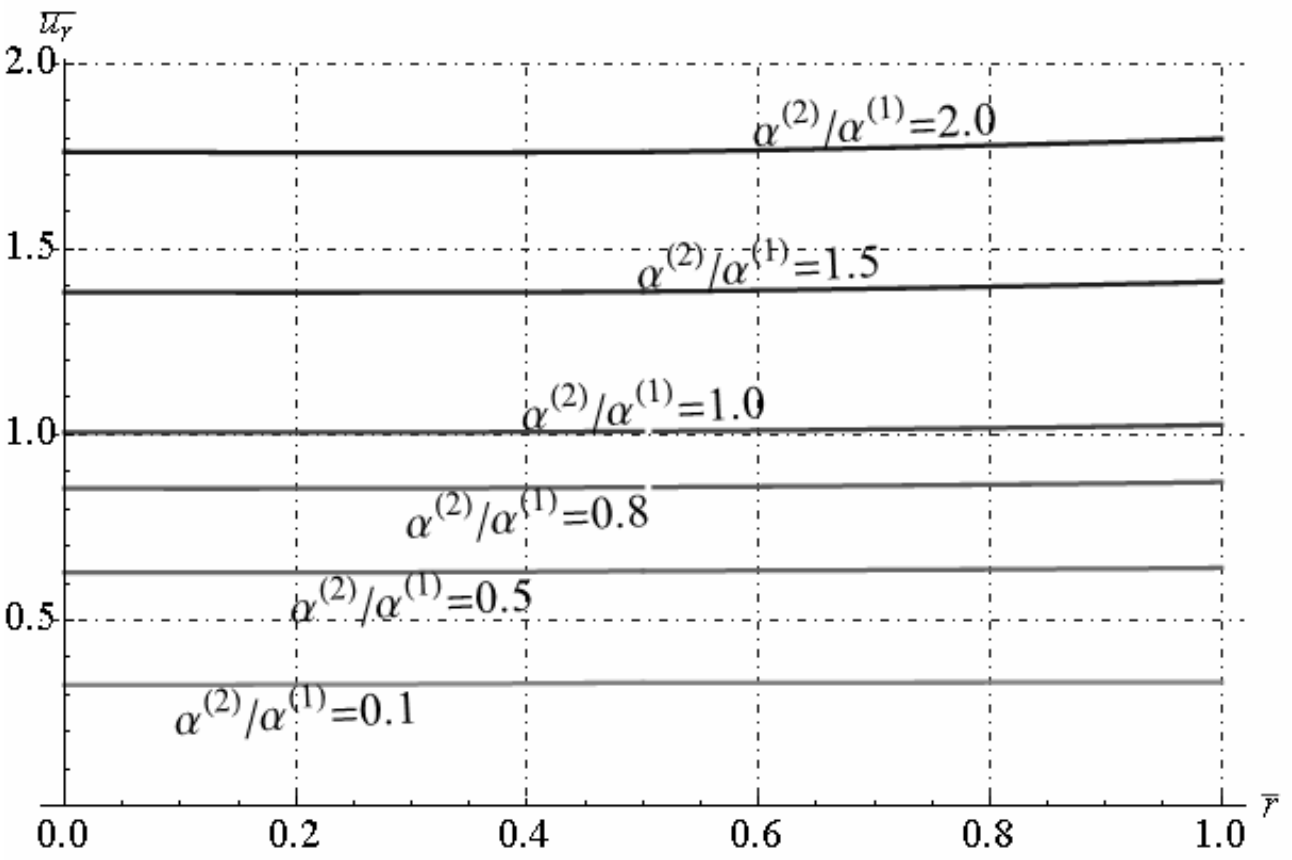

Fig. 17.17 - *Non-dimensional radial displacement along radial direction (Linear thermal expansion coefficient variation)*

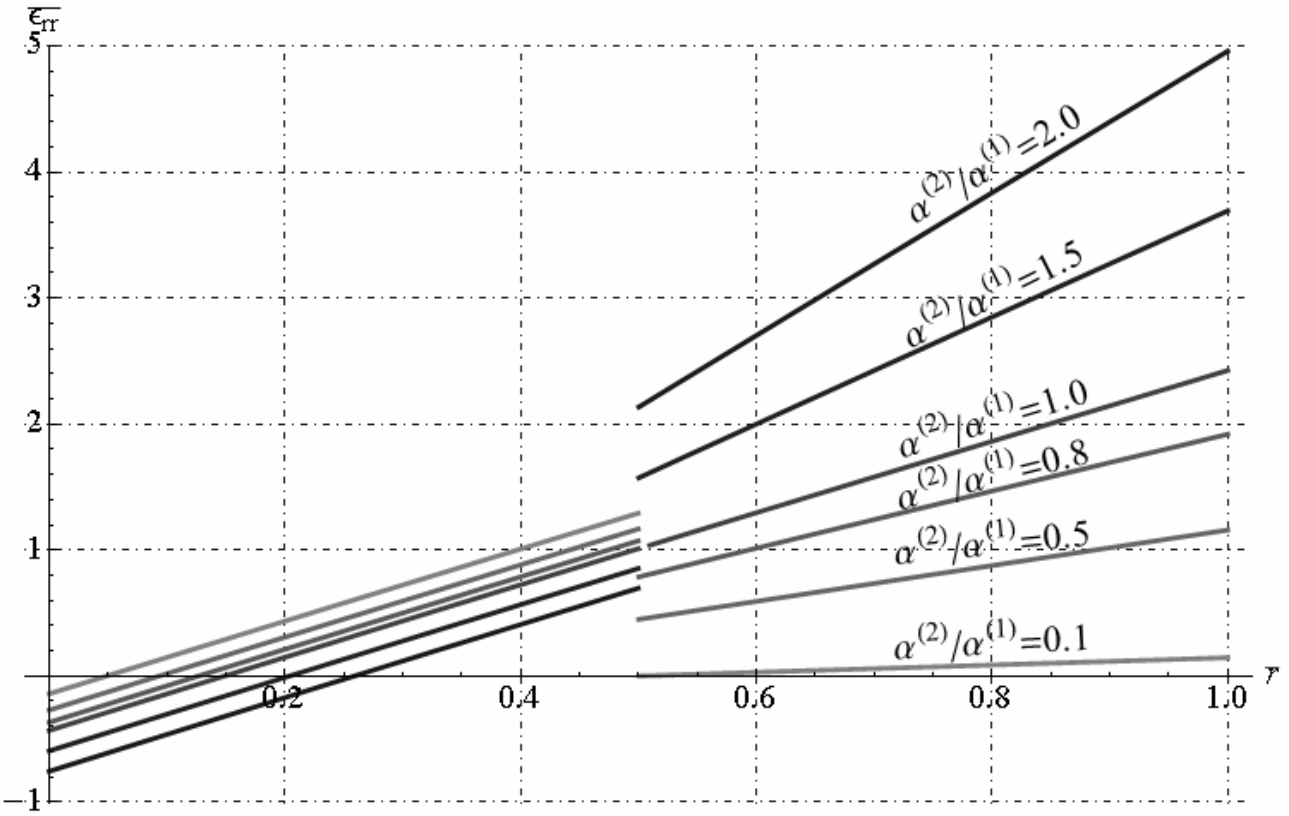

Fig. 17.17 - *Non-dimensional radial strain along radial direction (Linear thermal expansion coefficient variation)*

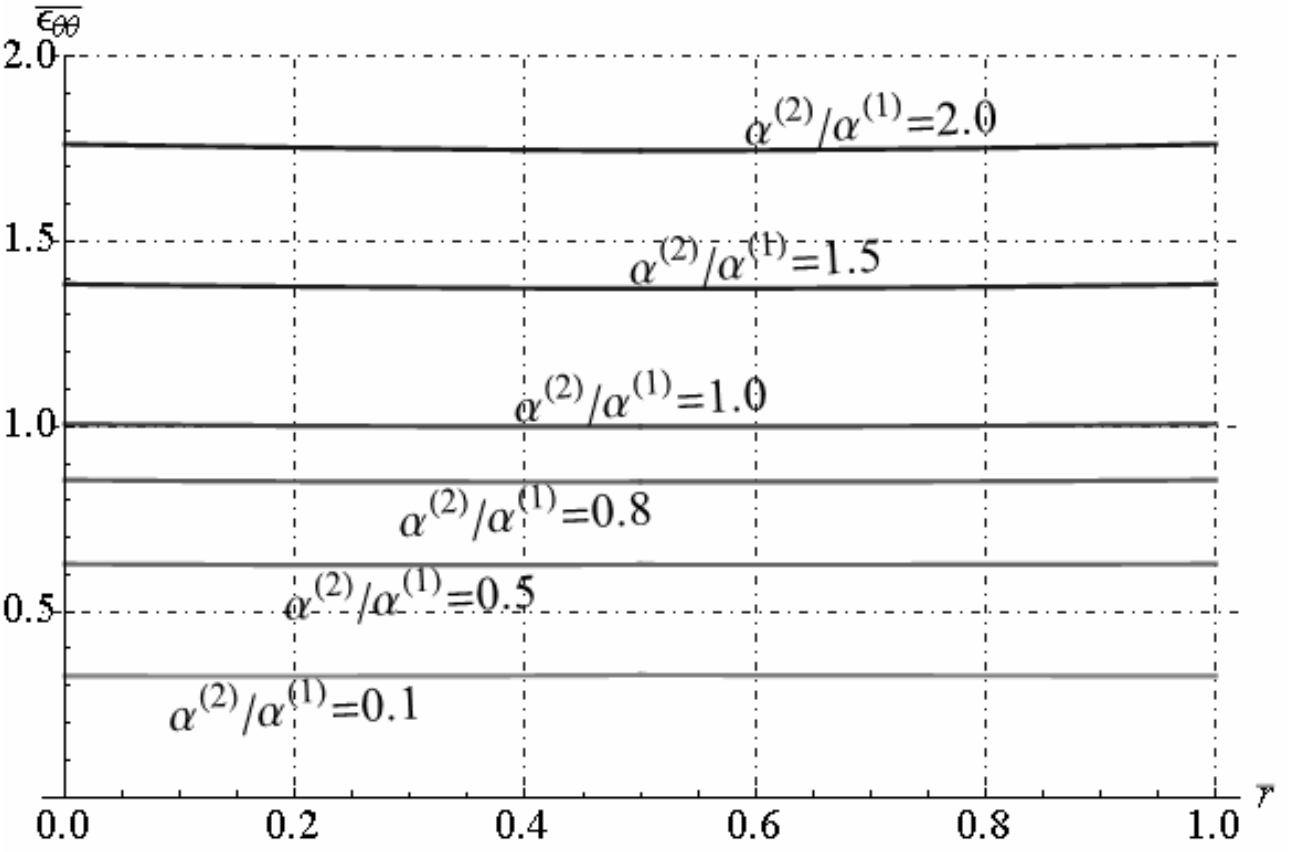

Fig. 17.18 - *Non-dimensional circumferential strain along radial direction (Linear thermal expansion coefficient variation)*

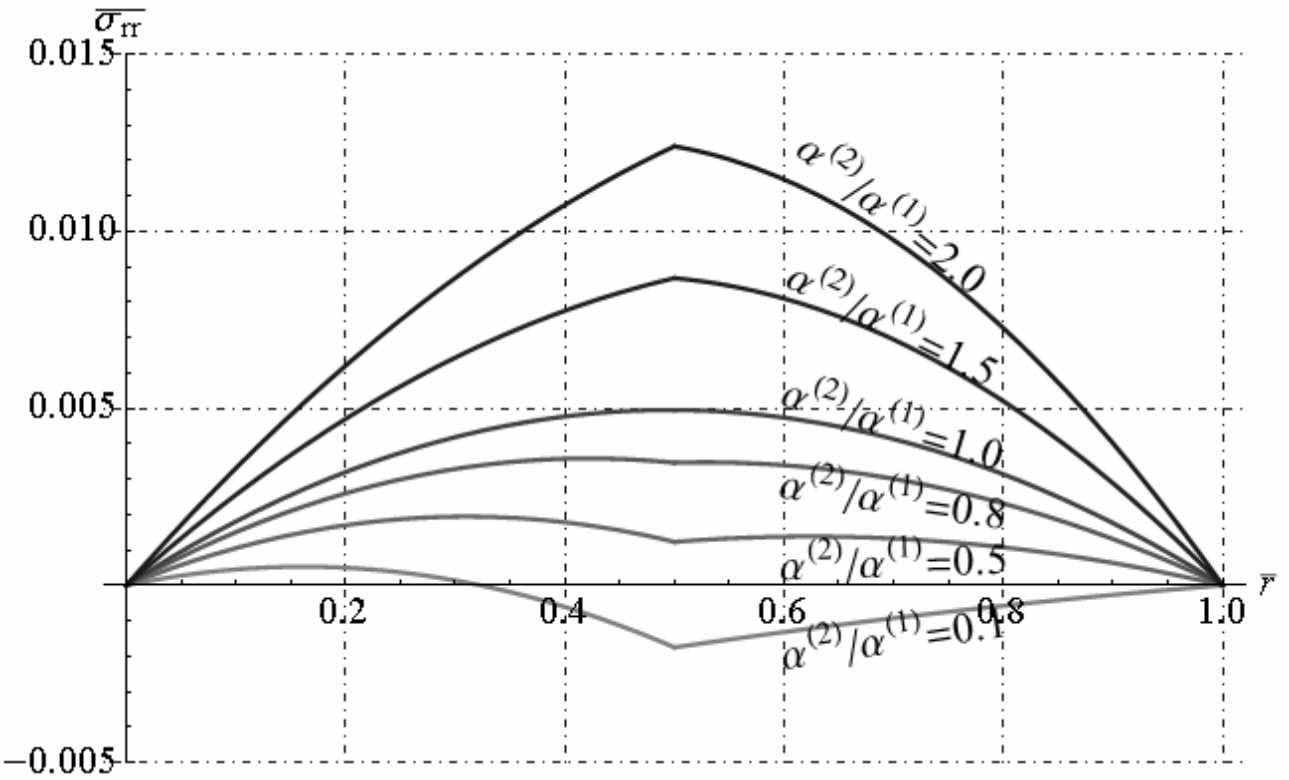

Fig. 17.19 - *Non-dimensional radial stress along radial direction (Linear thermal expansion coefficient variation)*

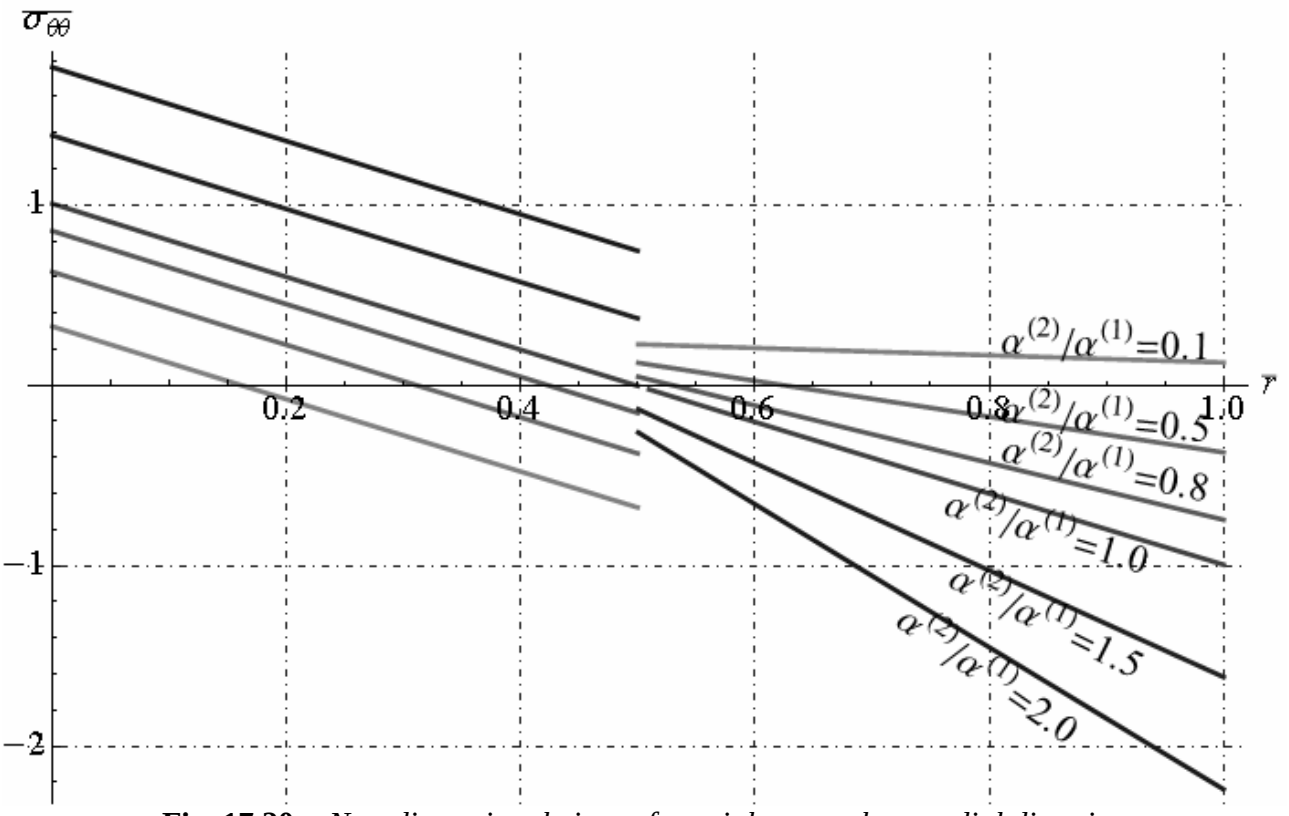

Fig. 17.20 - *Non-dimensional circumferential stress along radial direction (Linear thermal expansion coefficient variation)*

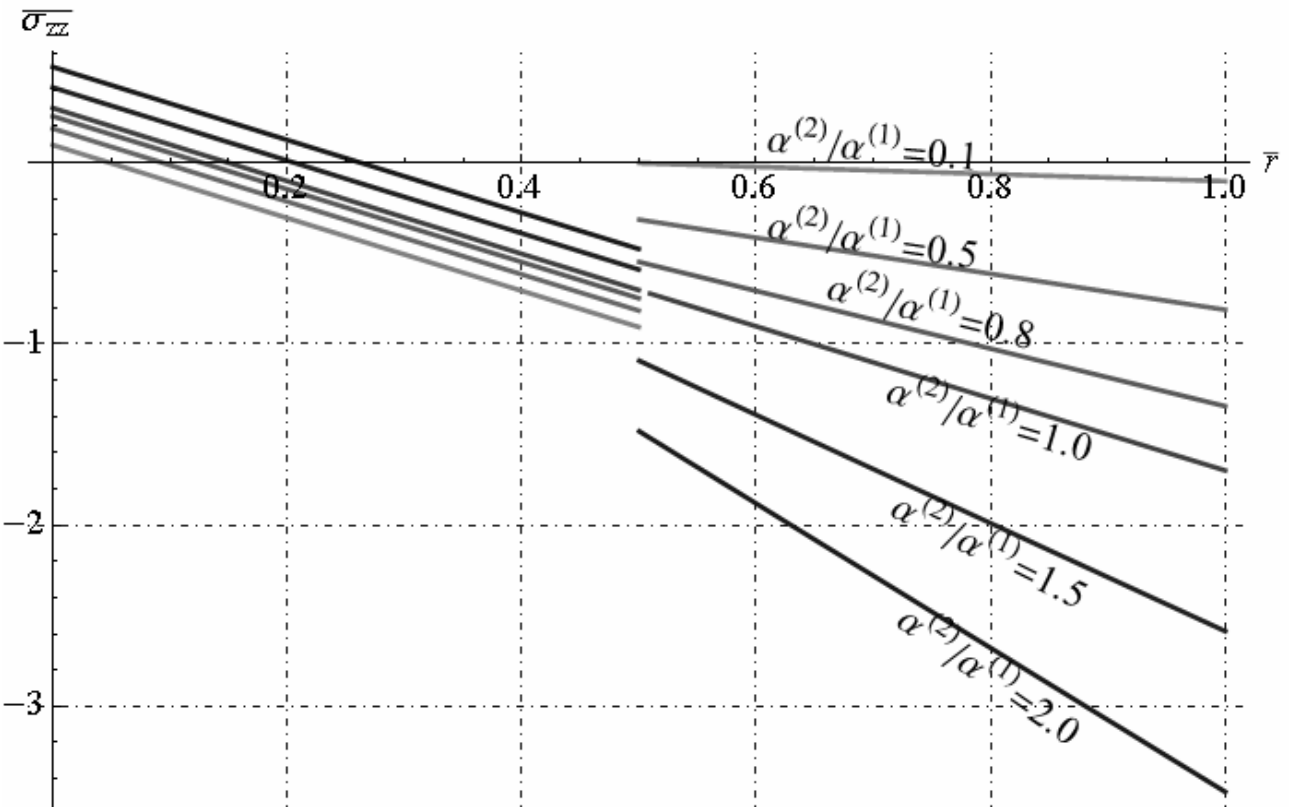

Fig. 17.21 - *Non-dimensional axial stress along radial direction (Linear thermal expansion coefficient variation)*

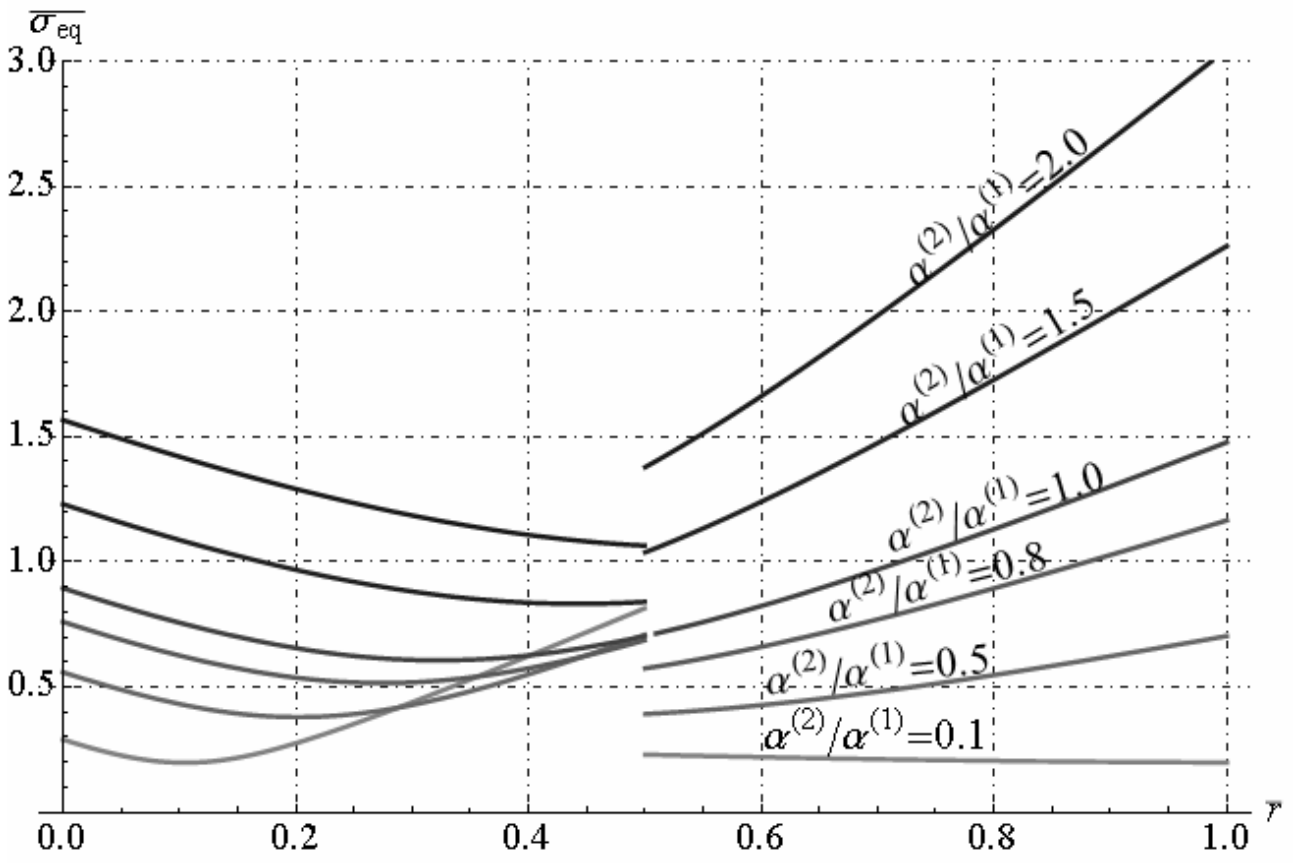

Fig. 17.22. *Non-dimensional equivalent stress along radial direction (Linear thermal expansion coefficient variation)*

In the four case (iv) let us assume $E^{(1)} = E^{(2)}$, $\nu^{(1)} = \nu^{(2)} = 0.3$, $\alpha^{(1)} = \alpha^{(2)}$, then the only free parameters are thermal conductivity coefficient in two phases. Let us consider six cases in which are selected the different ratio of thermal conductivity coefficient $k^{(2)}/k^{(1)}$ as follows : 0.1, 0.5, 1.0, 2.0, 5.0, 10.0. In particular, if the ratio $k^{(2)}/k^{(1)}$ increase, then the radial displacement and circumferential strain increase along radial direction as showed in figures 17.23 and 17.25. In phase (1) the radial strain assumes maximum value if $k^{(2)} > k^{(1)}$ and in phase (2) the radial strain assume maximum value if $k^{(2)} < k^{(1)}$.

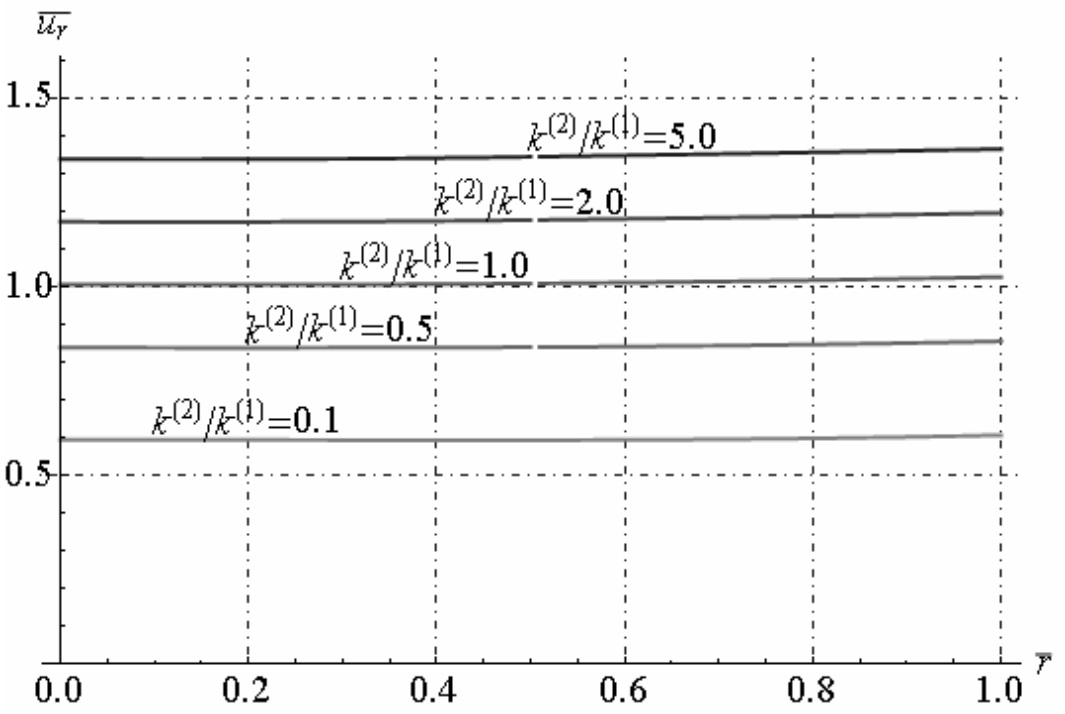

Fig. 17.23 - *Non-dimensional radial displacement along radial direction (Thermal conductivity coefficient variation)*

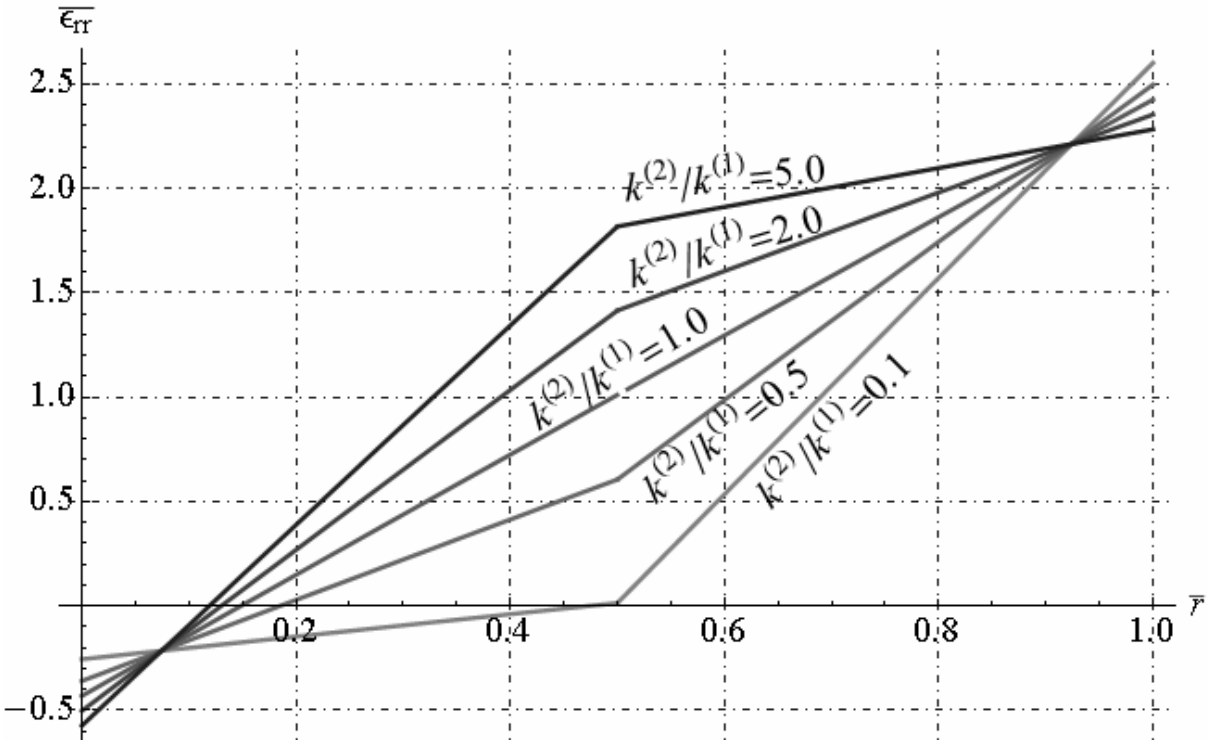

Fig. 17.24 - *Non-dimensional radial strain along radial direction (Thermal conductivity coefficient variation)*

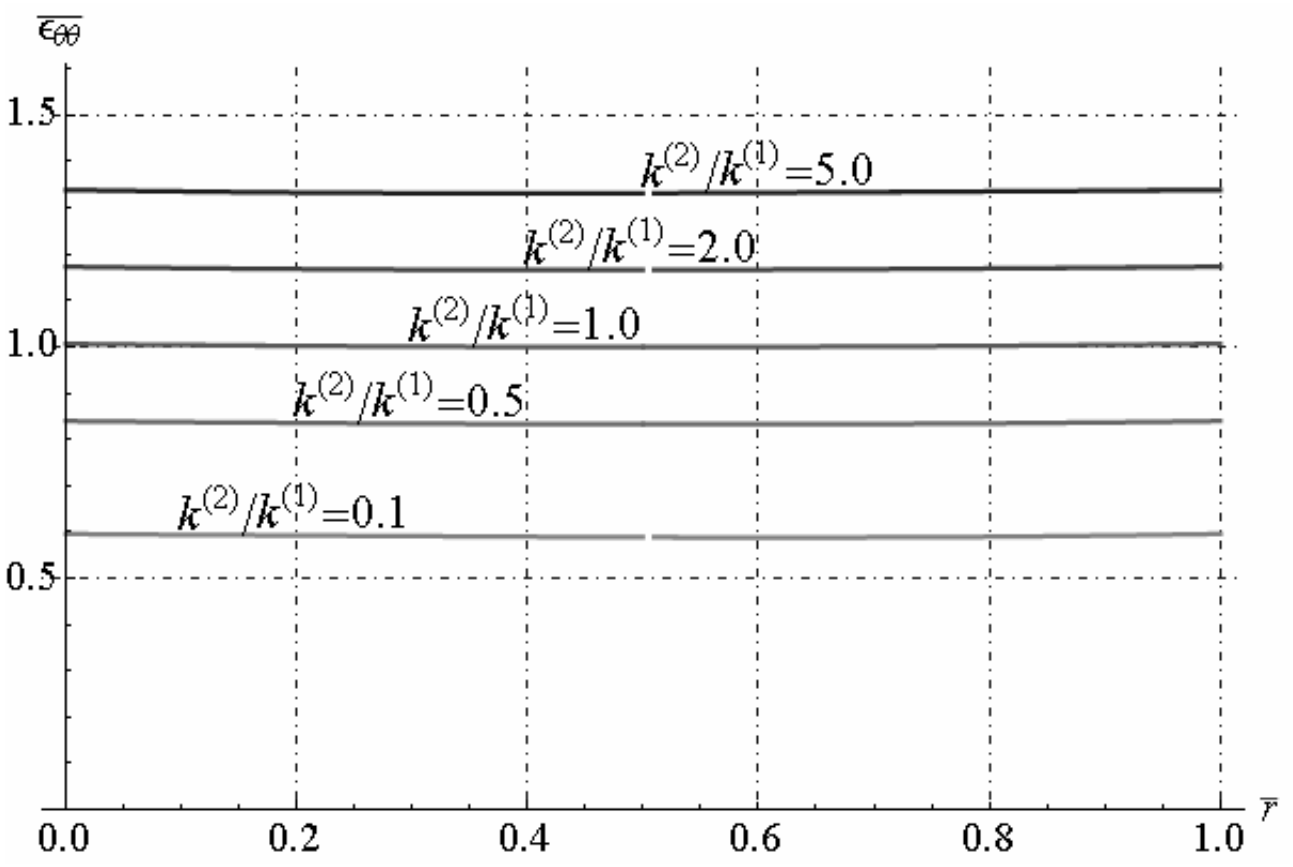

Fig. 17.25 - *Non-dimensional circumferential strain along radial direction (Thermal conductivity coefficient variation)*

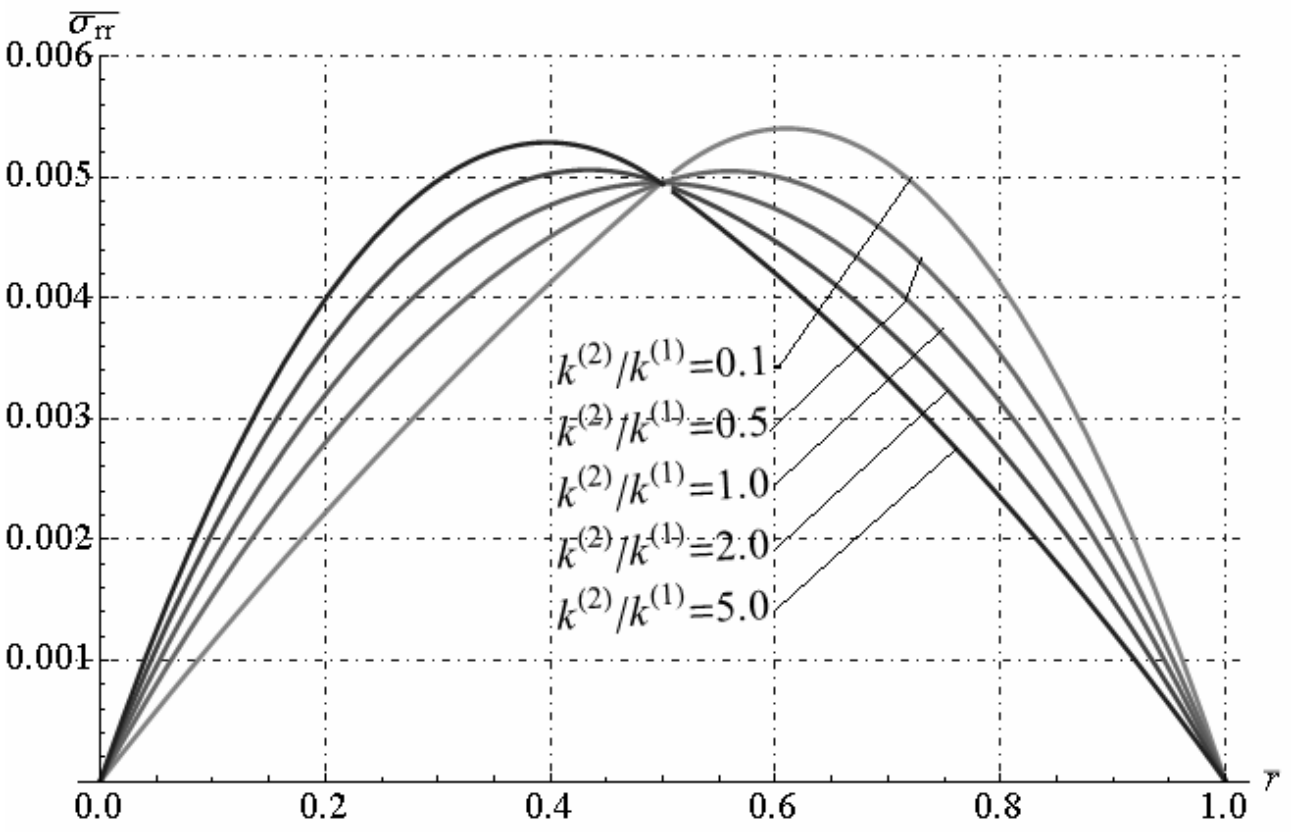

Fig. 17.26 - *Non-dimensional radial stress along radial direction (Thermal conductivity coefficient variation)*

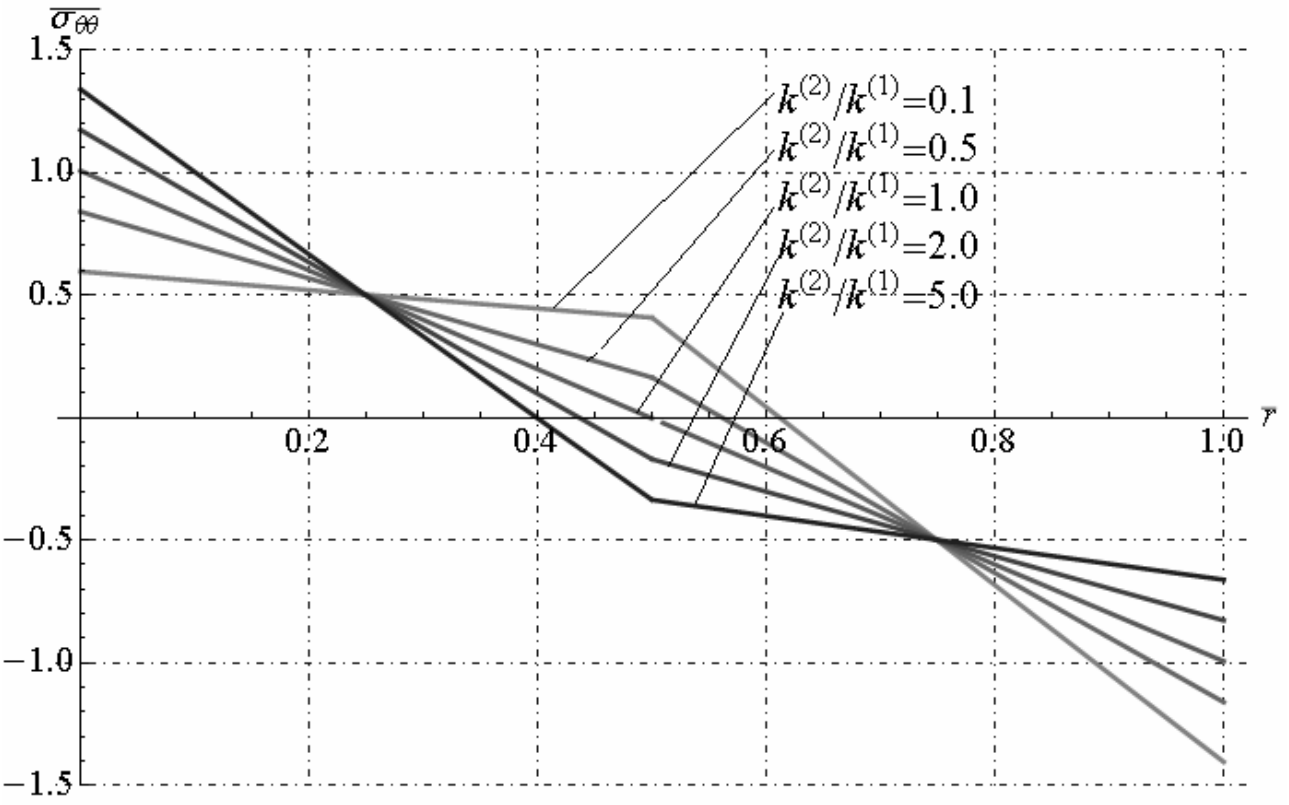

Fig. 17.27 - *Non-dimensional circumferential stress along radial direction (Thermal conductivity coefficient variation)*

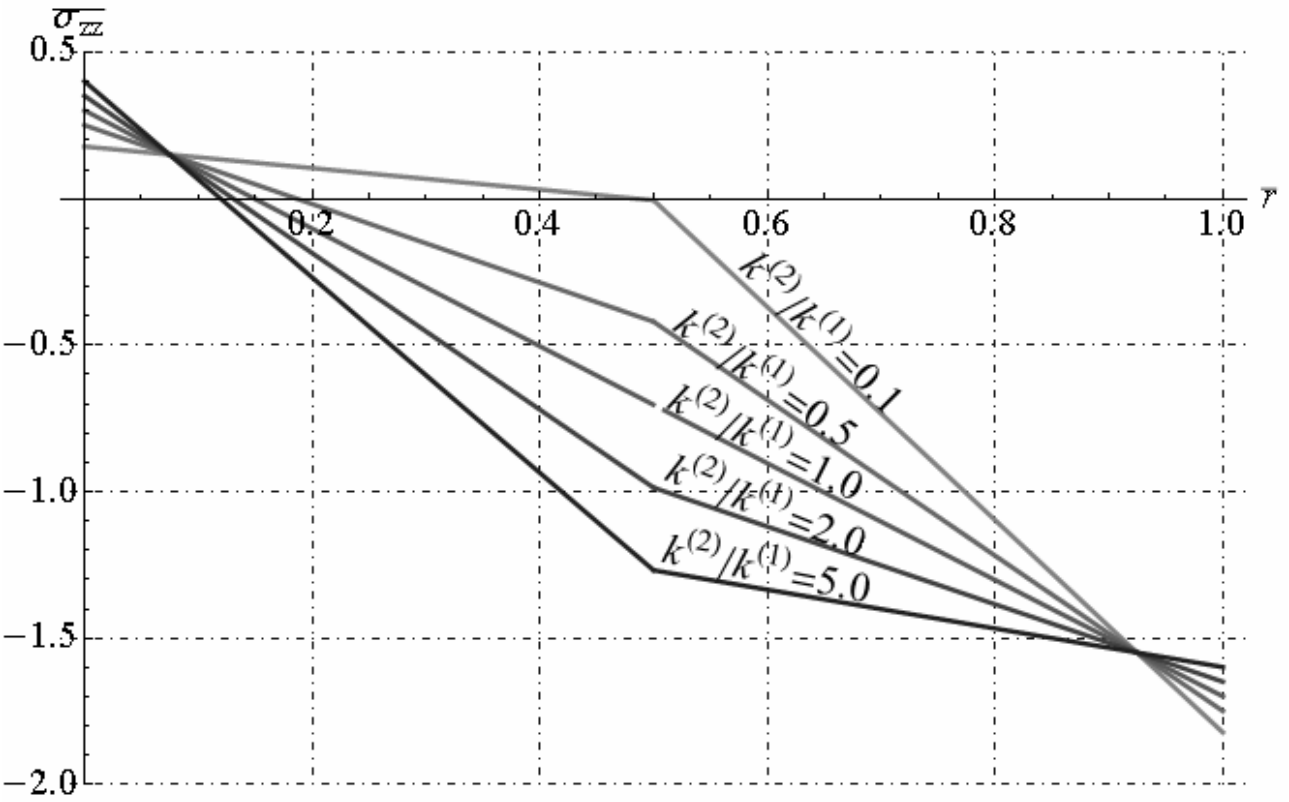

Fig. 17.28 - *Non-dimensional axial stress along radial direction (Thermal conductivity coefficient variation)*

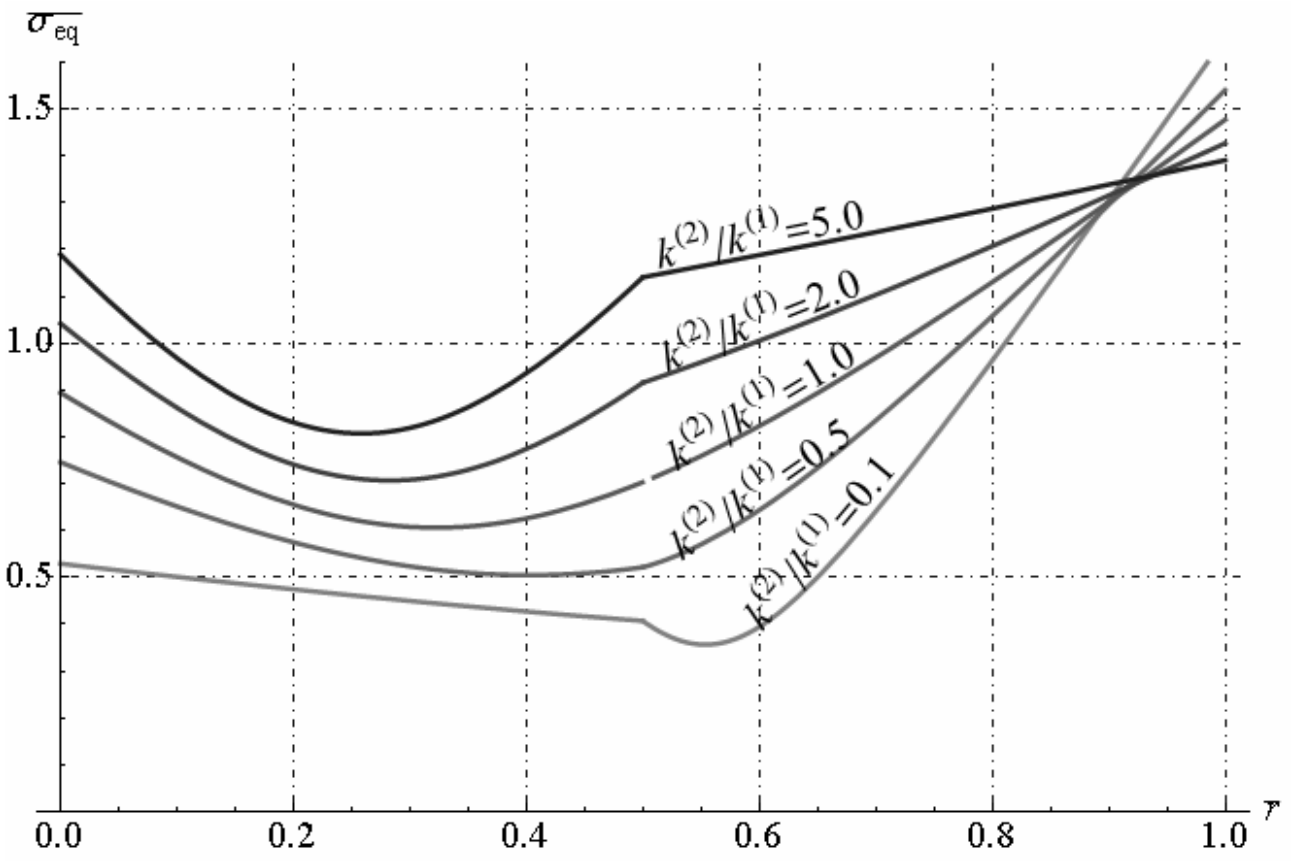

Fig. 17.29 - *Non-dimensional equivalent stress along radial direction (Thermal conductivity coefficient variation)*

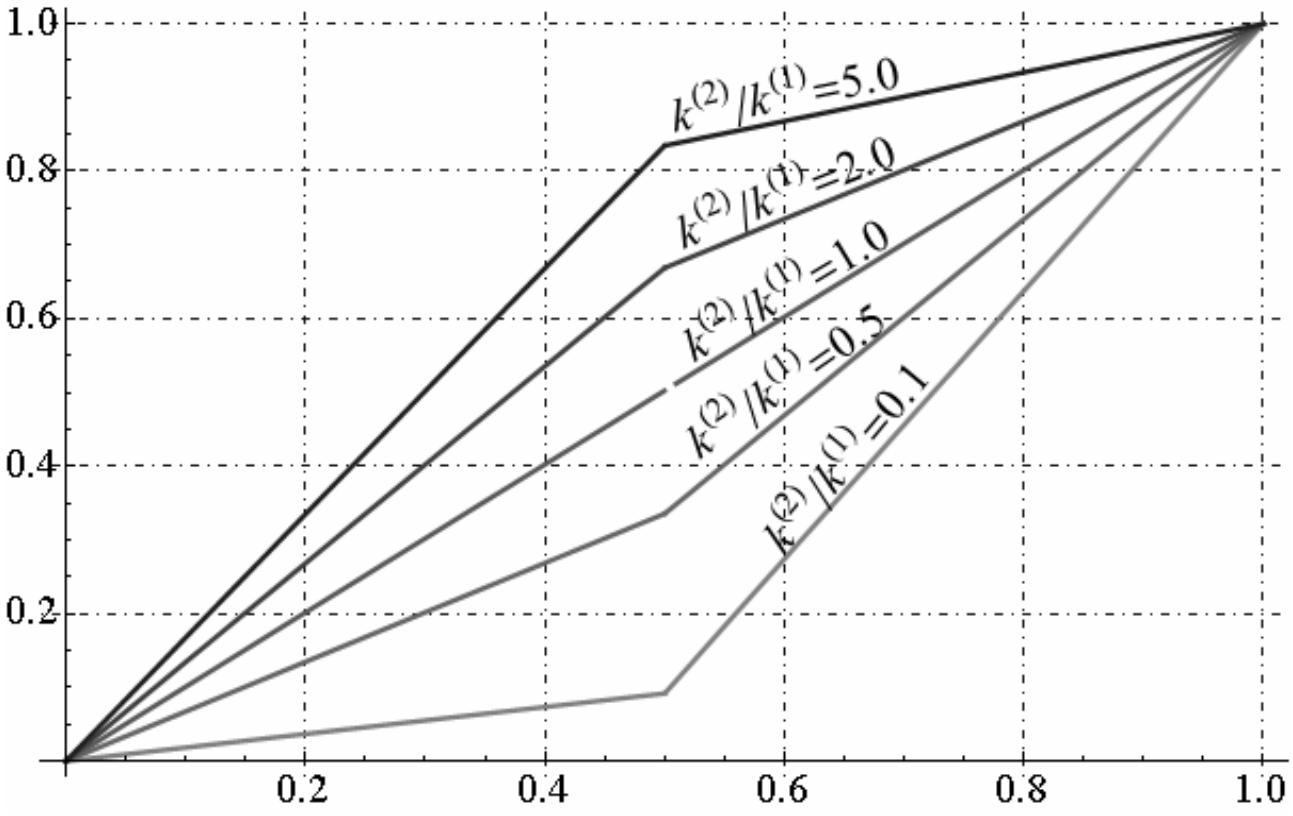

Fig. 17.30 - *Non-dimensional temperature along radial direction (Thermal conductivity coefficient variation)*

Finally, we reported the maximum absolute value of non-dimensional equivalent stress in phase (1) and in phase (2) for four case, as reported below:

(i) Poisson's ratio variation in both phases;
(ii) Young's moduli and linear thermal expansion coefficient variation;
(iii) Young's moduli and thermal conductivity coefficient variation;
(iv) Thermal conductivity coefficient and linear thermal expansion coefficient variation;

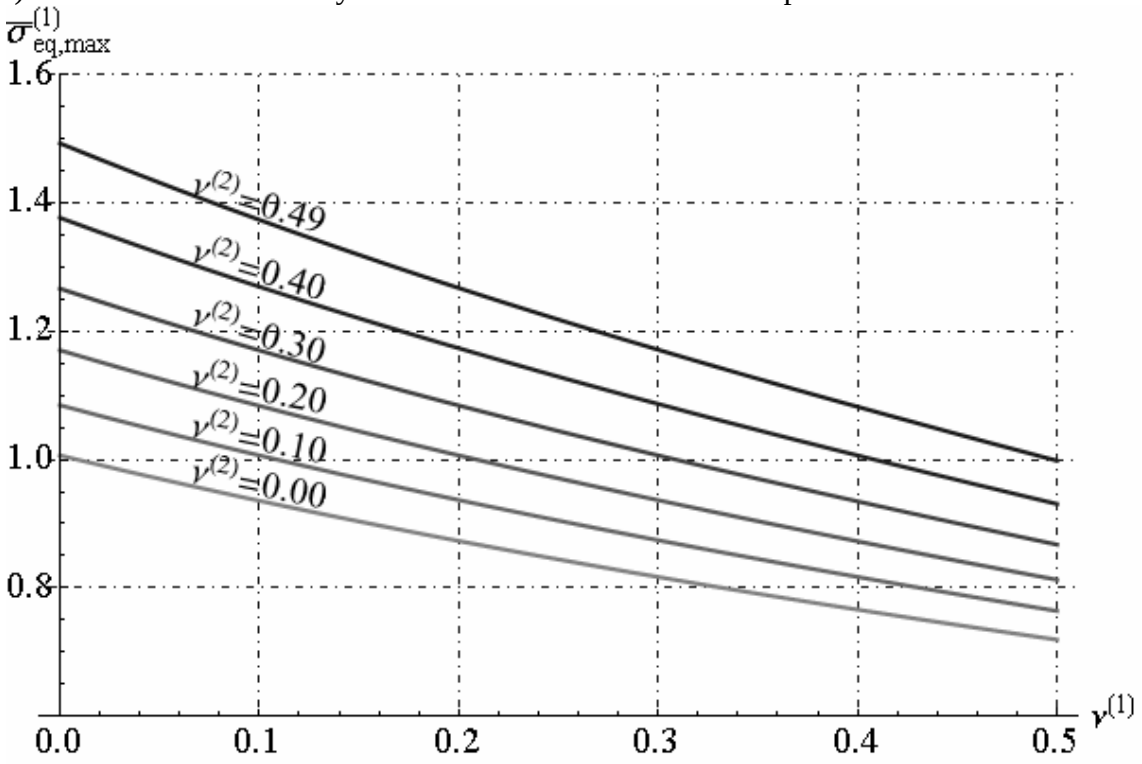

Fig. 17.31 - *Maximum absolute value of non-dimensional equivalent stress in phase (1) - Poisson's ratio variation –*

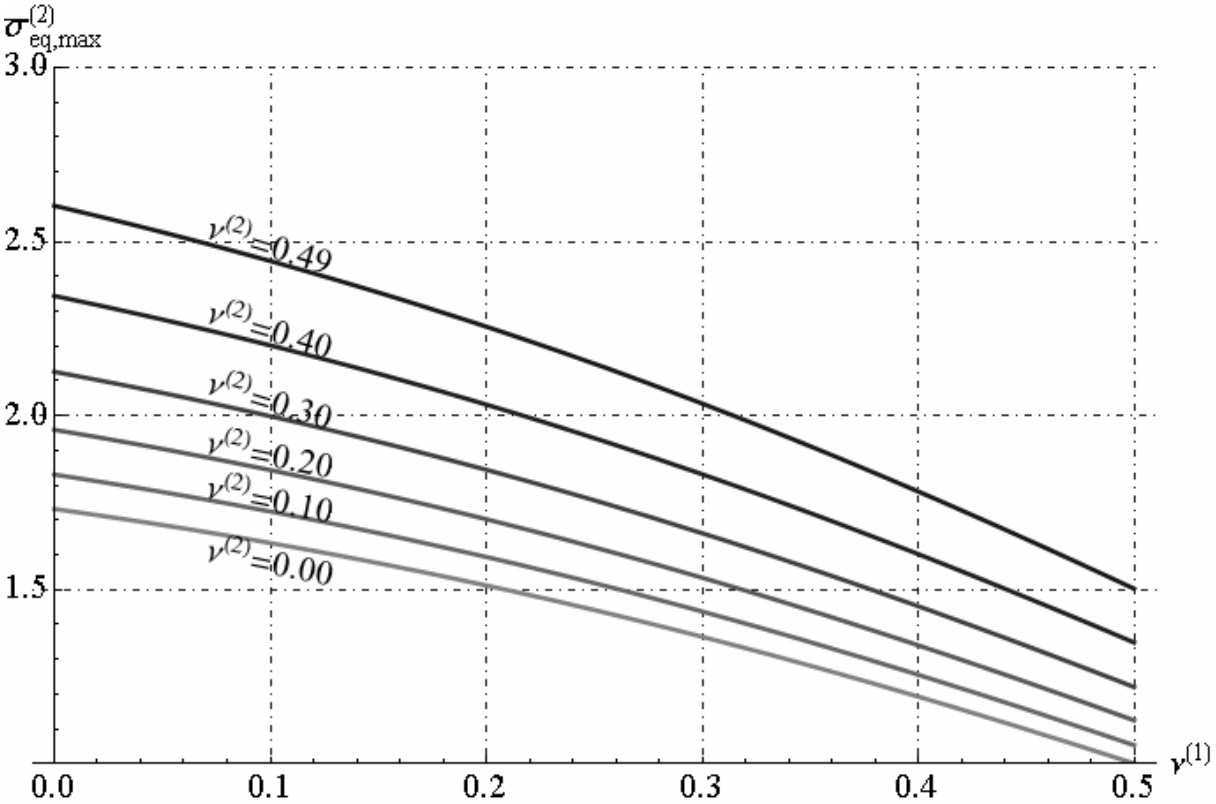

Fig. 17.32 - *Maximum absolute value of non-dimensional equivalent stress in phase (2) - Poisson's ratio variation -*

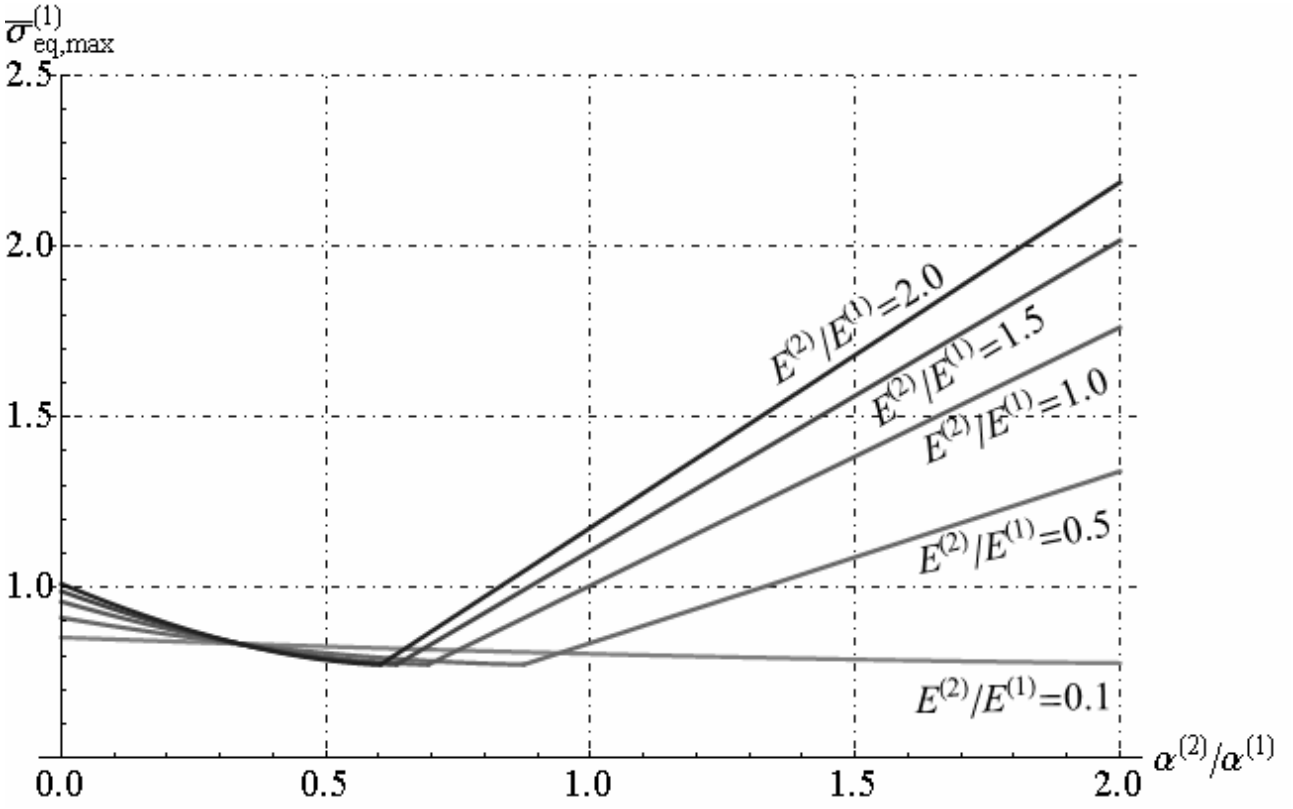

Fig. 17.33 - *Maximum absolute value of non-dimensional equivalent stress in phase (1) - Young's moduli and linear thermal expansion coefficient variation -*

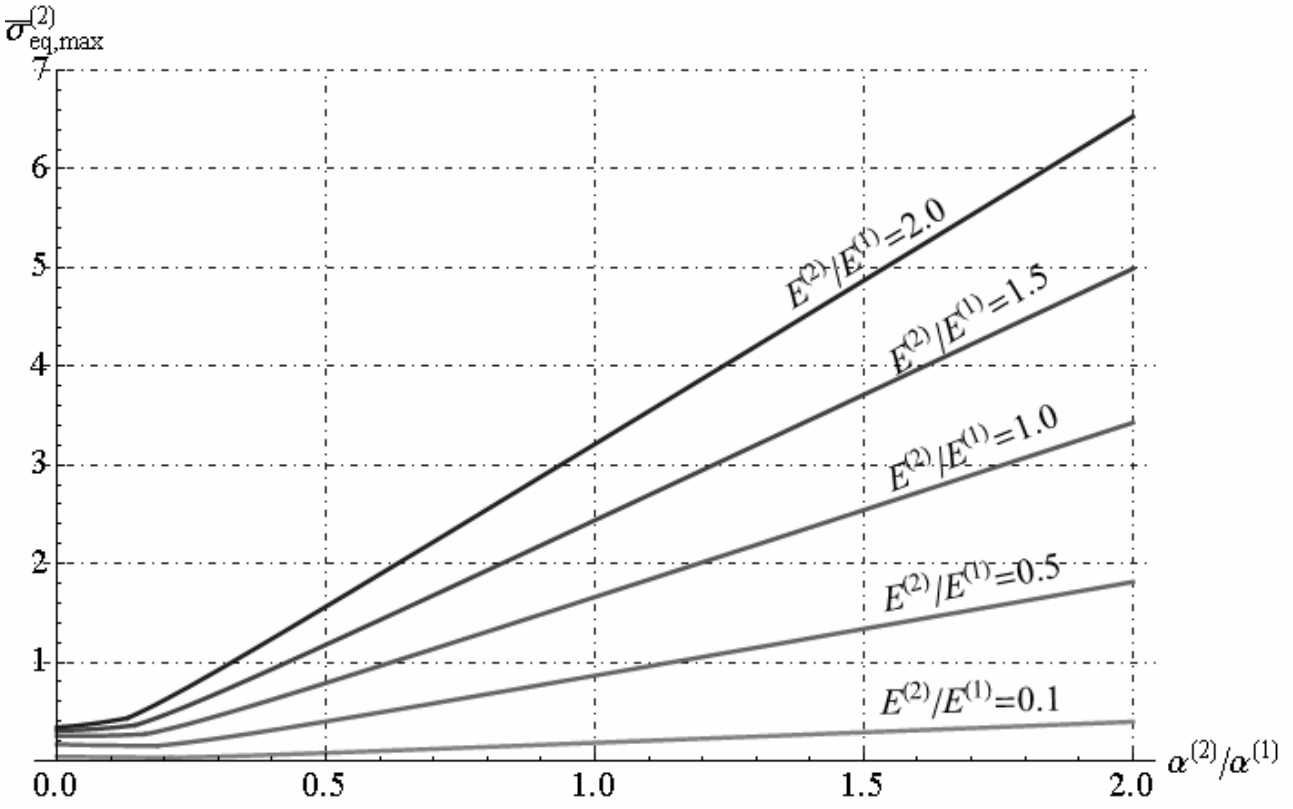

Fig. 17.34 - *Maximum absolute value of non-dimensional equivalent stress in phase (2) - Young's moduli and linear thermal expansion coefficient variation -*

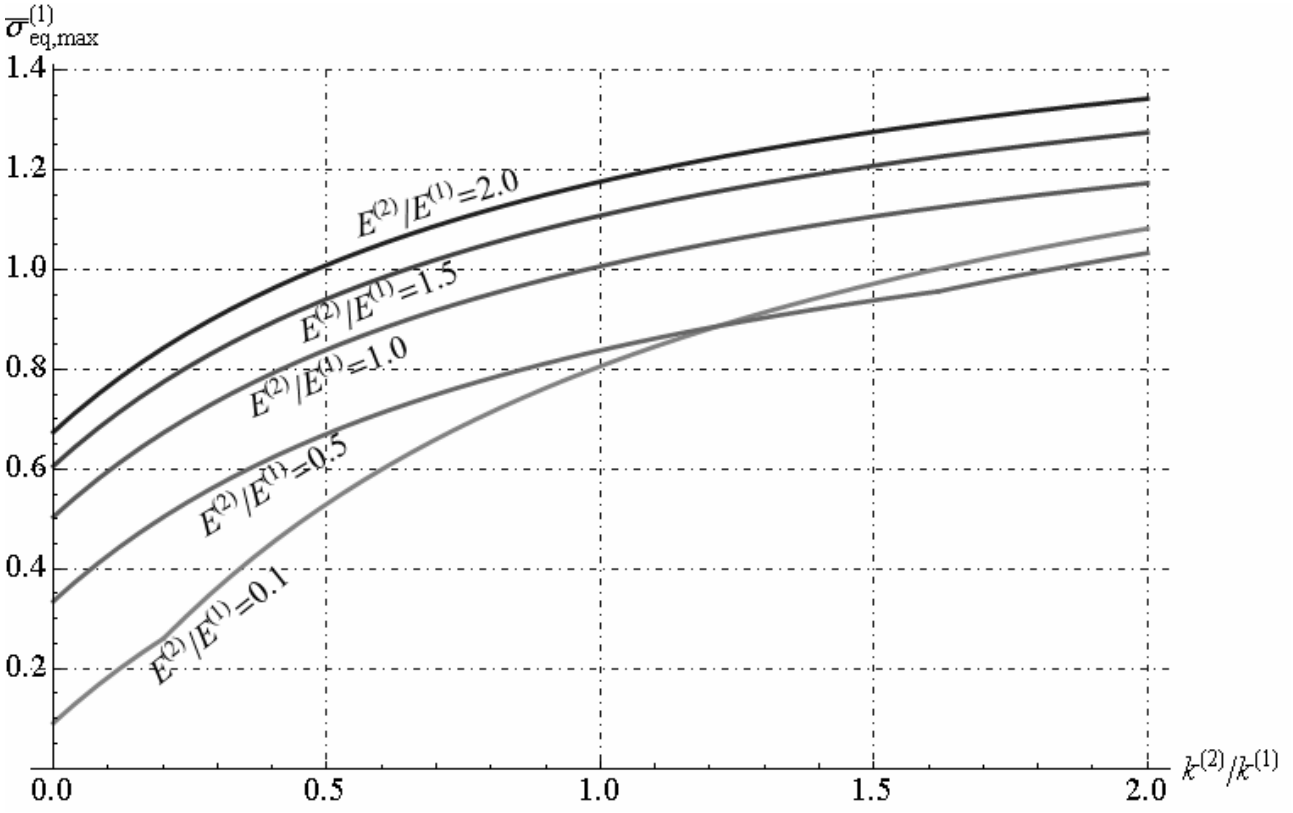

Fig. 17.35 - *Maximum absolute value of non-dimensional equivalent stress in phase (1) - Young's moduli and thermal conductivity coefficient variation -*

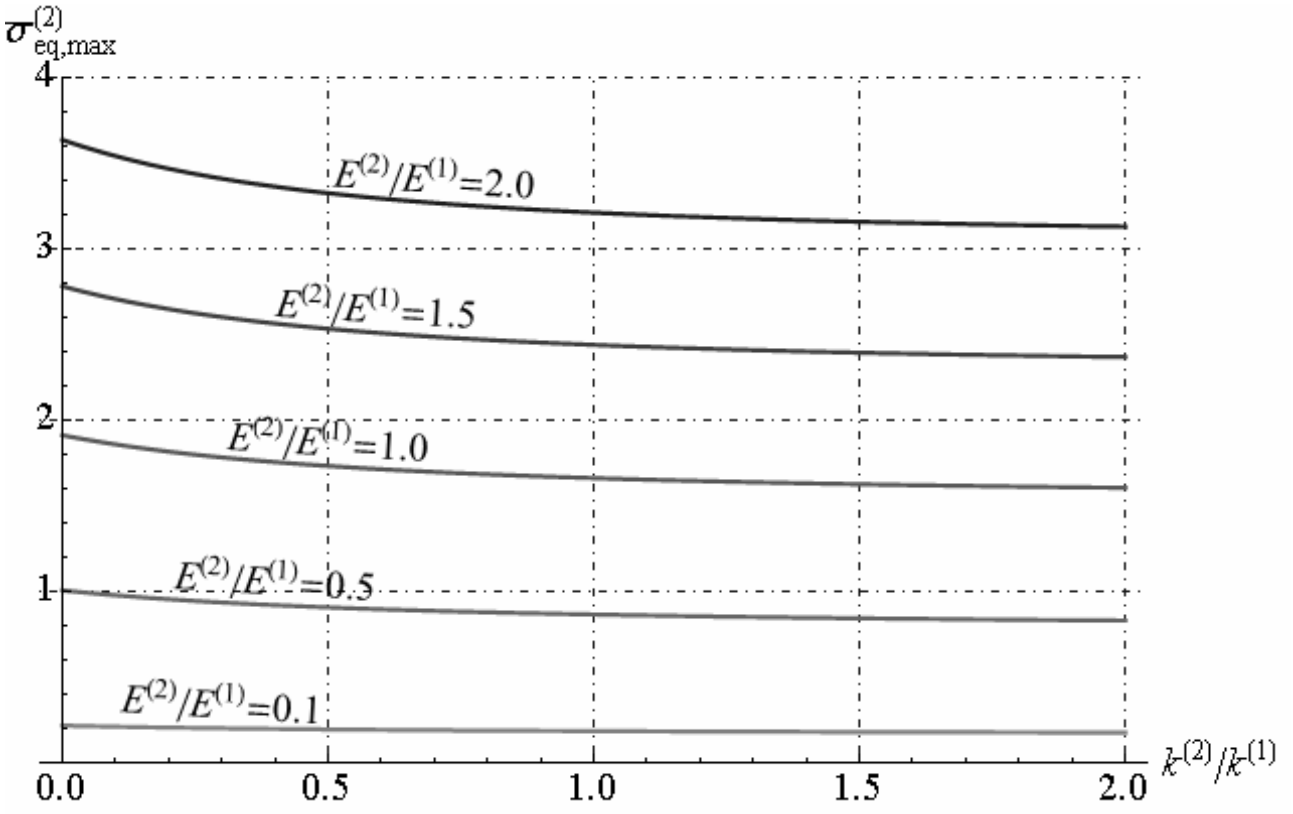

Fig. 17.36 - *Maximum absolute value of non-dimensional equivalent stress in phase (2) - Young's moduli and thermal conductivity coefficient variation –*

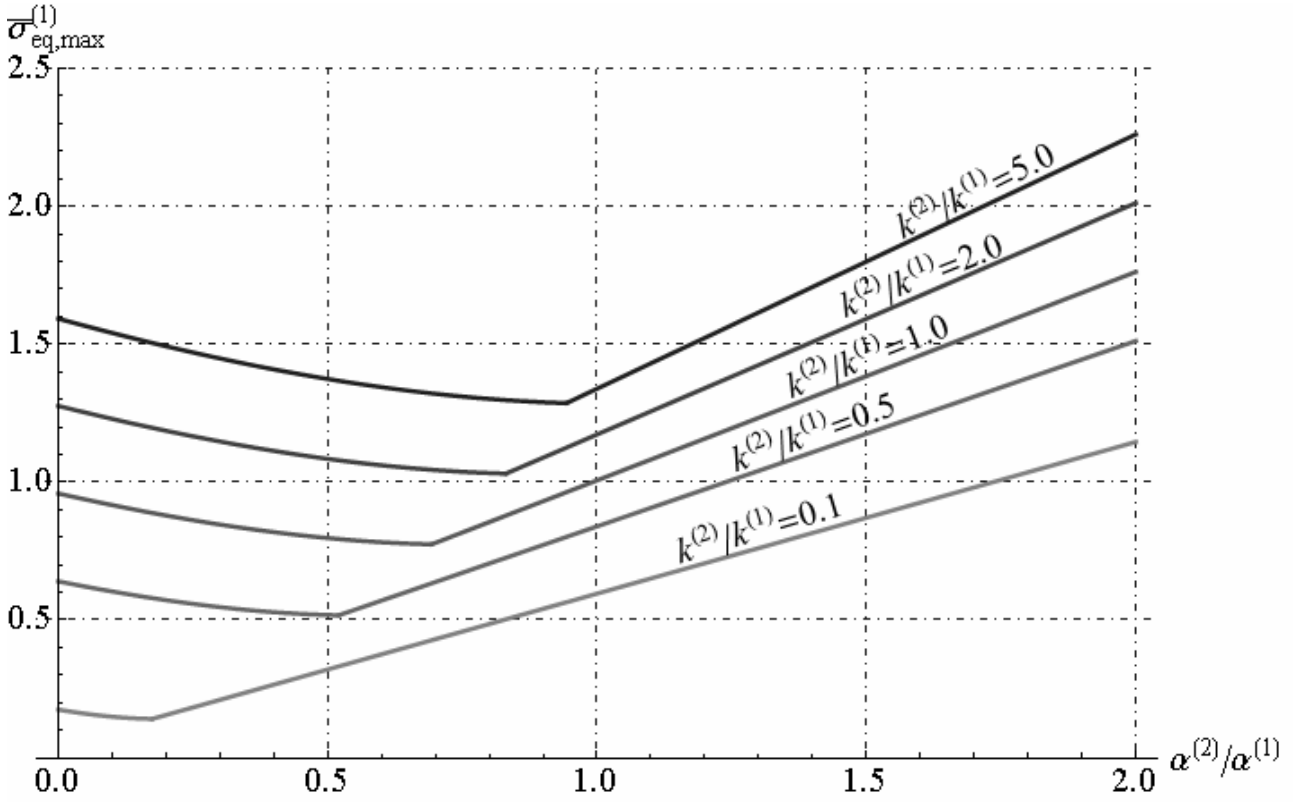

Fig. 17.37 - *Maximum absolute value of non-dimensional equivalent stress in phase (1) - thermal conductivity coefficient and linear thermal expansion coefficient variation* –

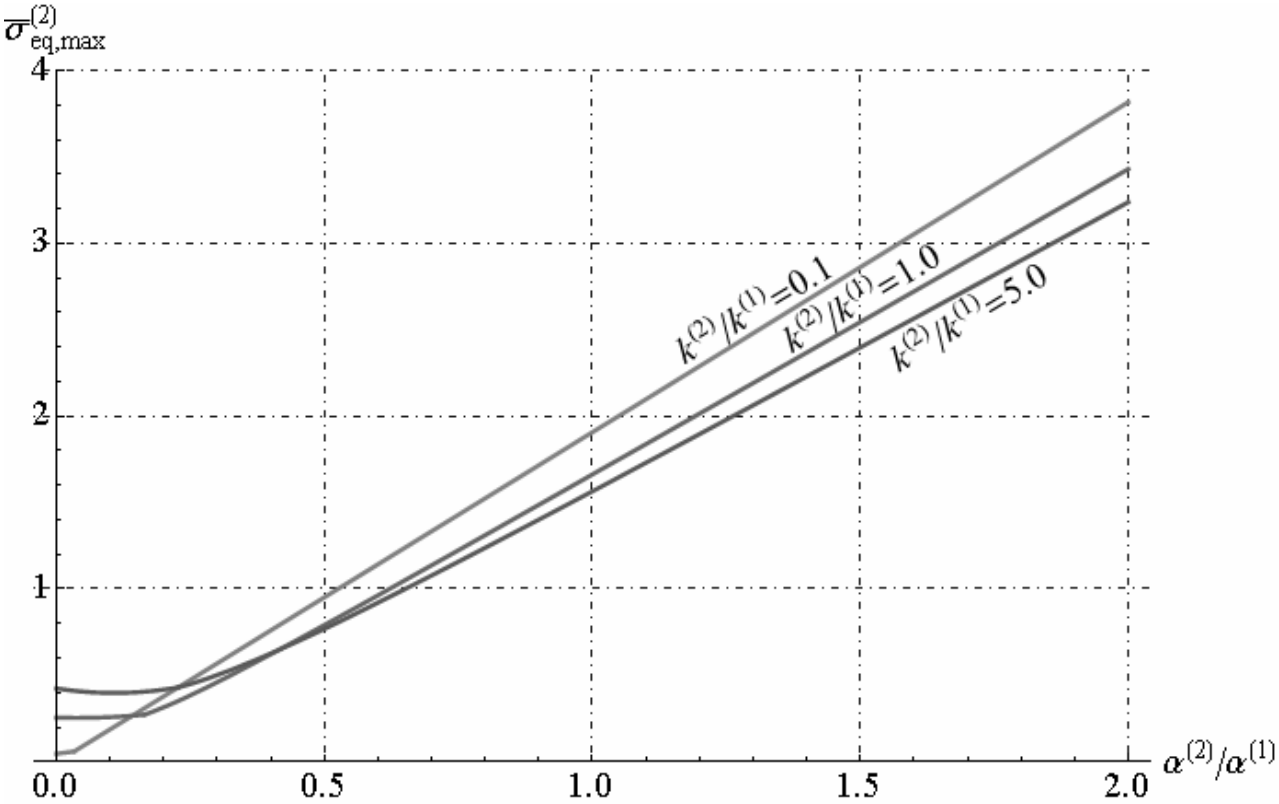

Fig. 17.38 - *Maximum absolute value of non-dimensional equivalent stress in phase (2) - thermal conductivity coefficient and linear thermal expansion coefficient variation -*

17.4. Numerical example for multilayered cylinder composed by three phases

In this study, we present some numerical results for the temperature distributions in multilayered cylinder constituted by three phases, subjected to the considered boundary conditions and the resulting displacement and thermal stresses. For the multilayered cylinder the geometry and material quantities are shown in Table 1. The inner radius of multilayered cylinder is assumed to be $R^{(0)}$ and the thickness of any phases is equal to δ. Then, we can write the following relationships:

$$R^{(1)} = (1+\xi)R^{(0)},\ R^{(2)} = (1+2\xi)R^{(0)},\ R^{(3)} = (1+3\xi)R^{(0)},\ \xi = \delta/R^{(0)}, \tag{17.52}$$

where $\xi = \delta/R^{(0)}$ represent the ratio between the thickness of any hollow cylinder and inner radius. Let us consider two case, in which the boundary conditions at the inner and the outer surfaces are assumed to be :

$$\begin{aligned} &(i)\ \begin{cases} T^{(1)}(r=R^{(0)}) = T_i = T_R = 298°K \\ T^{(3)}(r=R^{(3)}) = T_e = 308°K \end{cases} \quad \begin{cases} \sigma_{rr}^{(1)}(r=R^{(0)}) = p_i = 0 \\ \sigma_{rr}^{(3)}(r=R^{(3)}) = p_e = 0 \end{cases} \\ &(ii)\ \begin{cases} T^{(1)}(r=R^{(0)}) = T_i = T_R = 298°K \\ T^{(3)}(r=R^{(3)}) = T_e = 298°K \end{cases} \quad \begin{cases} \sigma_{rr}^{(1)}(r=R^{(0)}) = p_i = 10MPa \\ \sigma_{rr}^{(3)}(r=R^{(3)}) = p_e = 20MPa \end{cases} \end{aligned} \tag{17.53}$$

In each cases, let us consider three sub-cases, in which are chance the position of materials, as reported below:

(a) phase 1: Stainless steel, phase 2 : Zinc, phase 3 : Aluminium;
(b) phase 1: Aluminium, phase 2 : Stainless steel, phase 3 : Zinc
(c) phase 1: Aluminium, phase 2 : Zinc, phase 3 : Stainless steel;

In case (i) the multilayered cylinder are subjected to an gradient of temperature between inner and outer surfaces, but the external load vanishing. In second case (ii) the multilayered cylinder is subjected to gradient of pressure between inner and outer surfaces, but the temperature is uniform and equal to T_R. In total, we studied six cases, in which the ratio ξ is assumed equal to 0.01.

The Fig. 17.47, shows the temperature distributions along the radial direction in the first case considered. The temperature gradient varies in each layer because of the difference in the thermal conductivity coefficients. Fig. 17.40 and 17.48 shows the radial displacement distributions along the radial direction in the two cases considered.

In particular in the first case (i), the assembling give by sub-case (c) the radial displacement assume the minimum value, but in case (ii) the minimum values of radial displacement are given by sub-case (a). The figures 17.41 and 17.21 show the thermal radial and circumferential strain distribution along the radial direction in the case (i), respectively.

The figures 17.49 and 17.50 show the thermal radial, circumferential and equivalent stress distribution along the radial direction in case (ii), respectively. As expected, the circumferential stress distribution exhibits significant jumps at all interfaces as shown in figures 17.44 and 17.52. These discontinuities are due to the differences in material properties such as the coefficient of linear thermal expansion and Young's modulus. The circumferential stress varies characteristically in each layer in view of the occurrence of discontinuities at all interfaces. In other figures we reported the dimensional parameters distribution along the non-dimensional radial direction.

	Aluminium	**Zinc**	**Stainless steel**
$E\left[N\,m^{-2}\right]$	$70\cdot10^{9}$	$108\cdot10^{9}$	$215\cdot10^{9}$
$k\left[W\,m^{-1}K^{-1}\right]$	237	116	30
ν	0.35	0.25	0.30
$\alpha\left[m\cdot m^{-1}K^{1}\right]$	$23.1\cdot10^{-6}$	$30.2\cdot10^{-6}$	$12\cdot10^{-6}$
$\rho\left[kg\,m^{-3}\right]$	2700	7140	7800
$c_{v}\left[kJ\cdot kg^{-1}K^{-1}\right]$	0.90	0.39	0.46

Table 17.1 - *The geometry and material constants of multilayered cylinder*

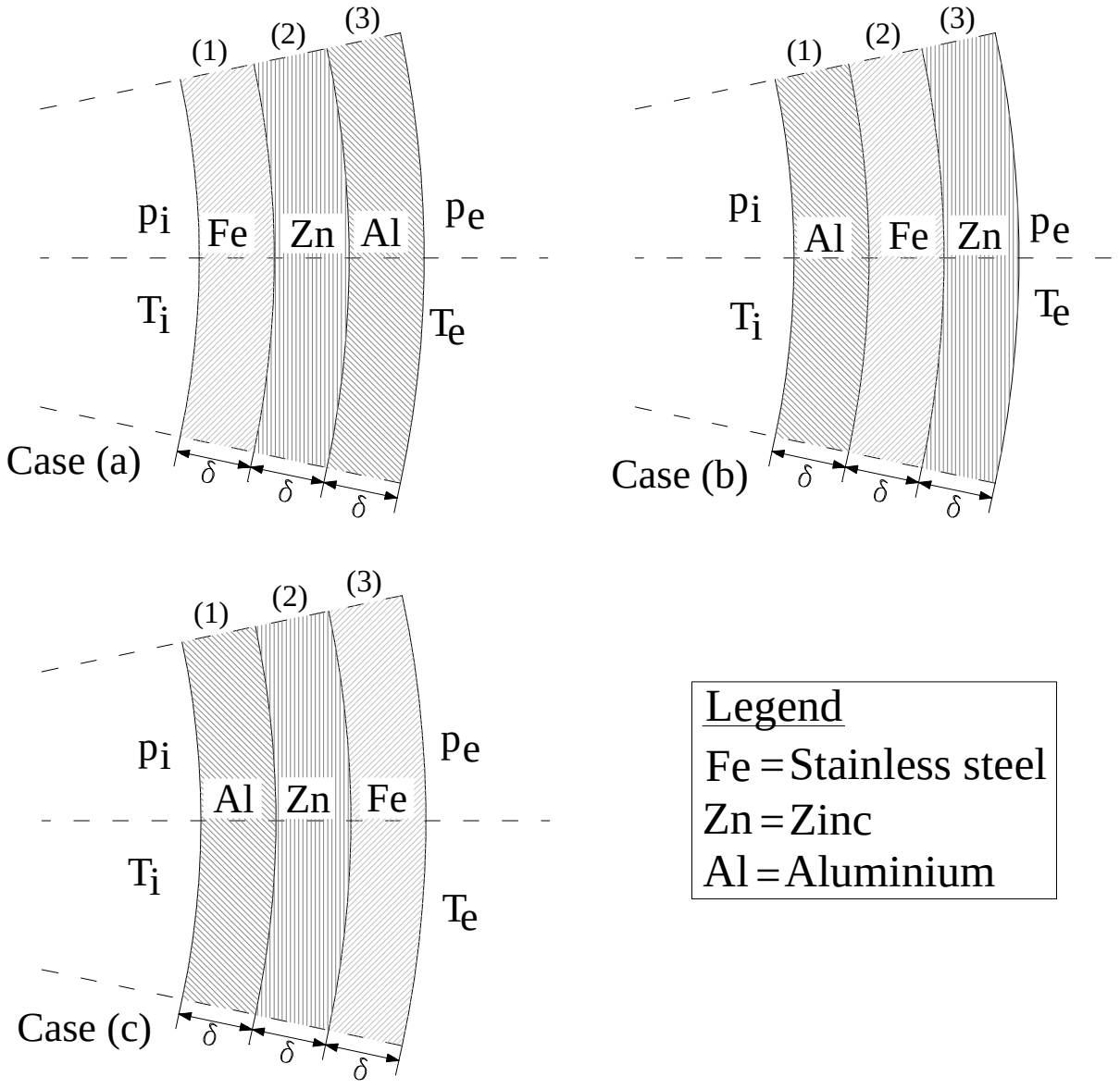

Fig. 17.39 - *Multilayered cylinder composed by three hollow cylinders*

We reported the numerical results for case (i) as follows :

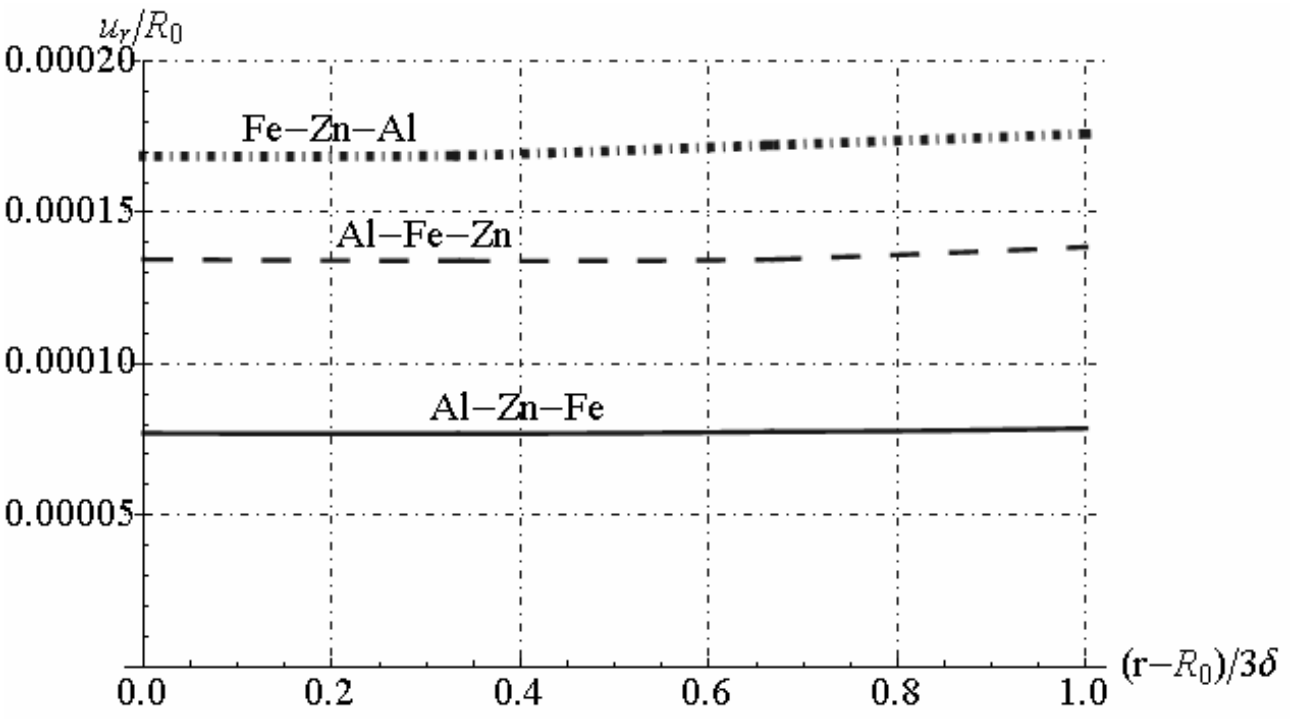

Fig. 17.40 - *Radial displacement distribution along radial direction*

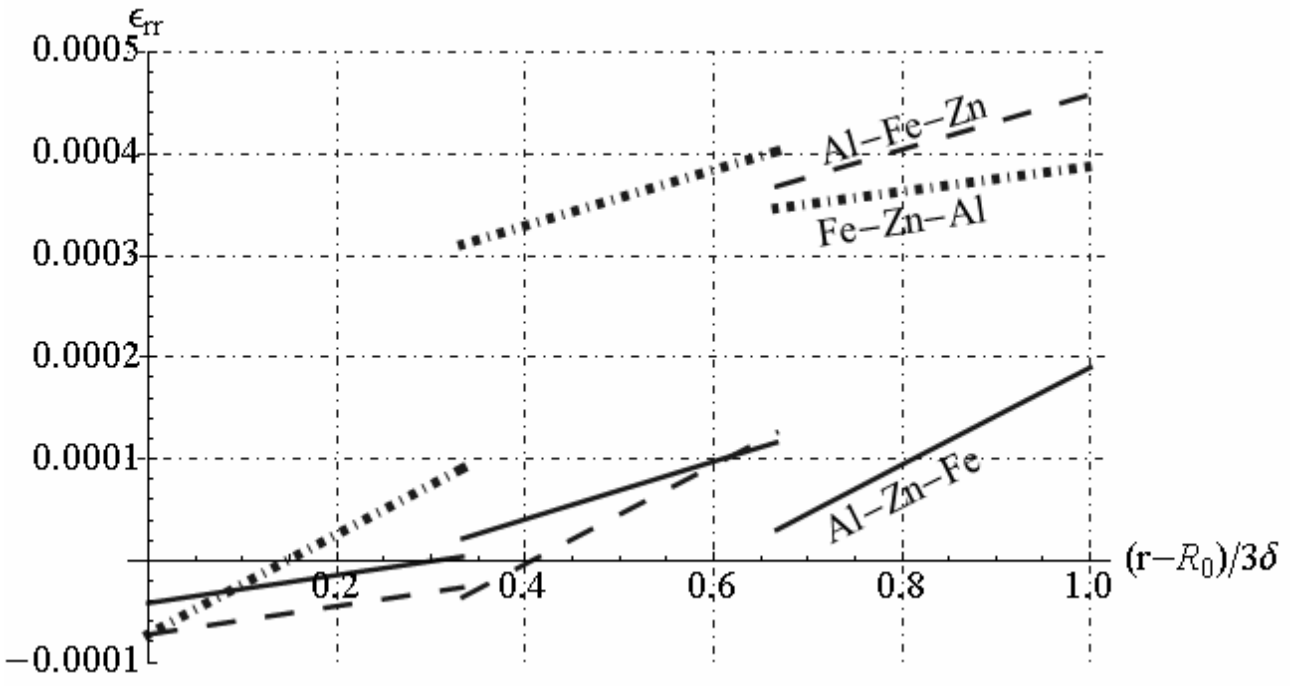

Fig. 17.41 - *Radial strain distribution along radial direction*

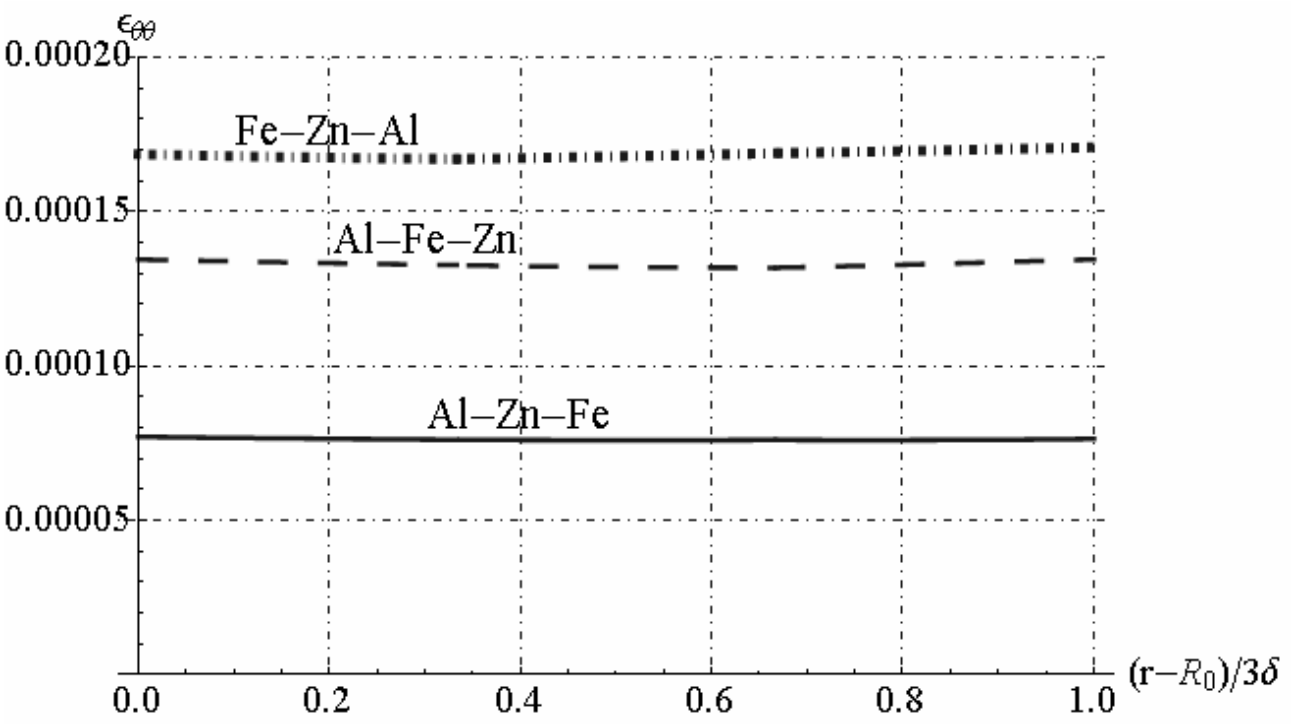

Fig. 17.42 - *Circumferential strain along radial direction*

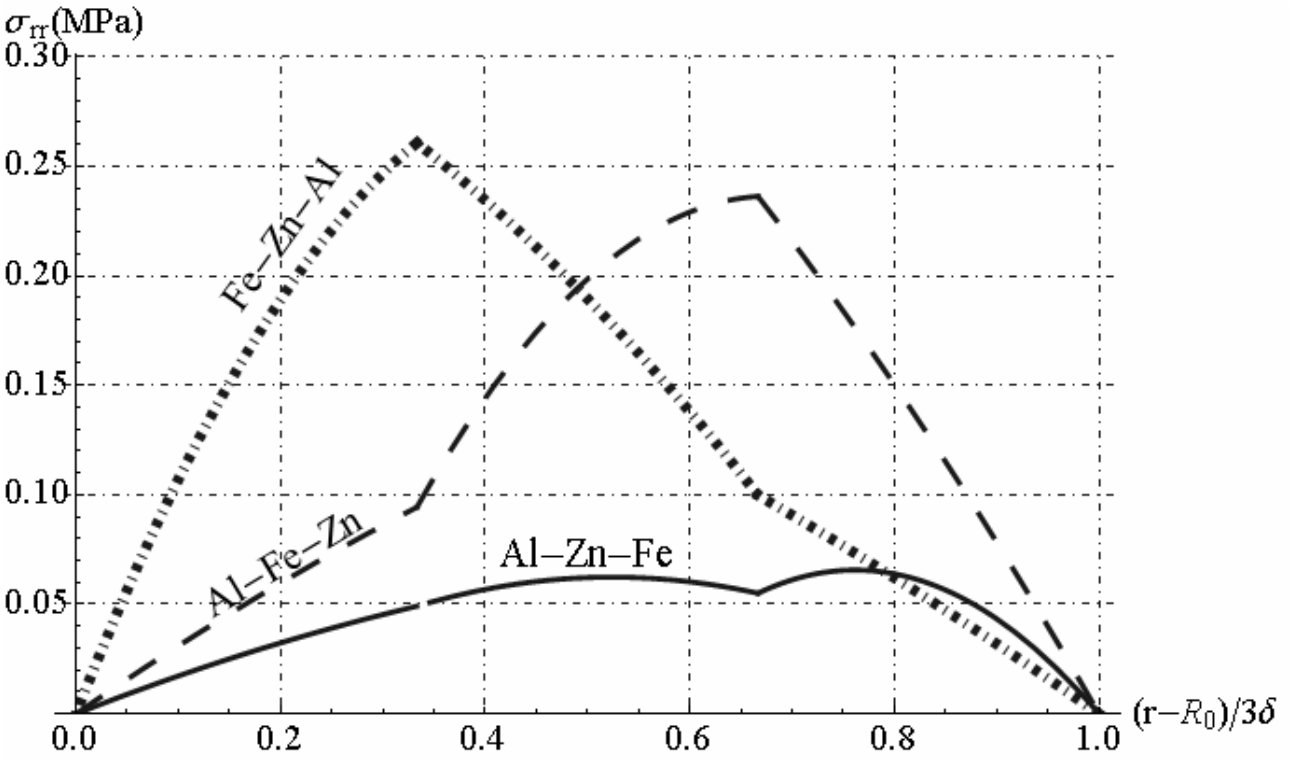

Fig. 17.43 - *Radial stress distribution along radial direction*

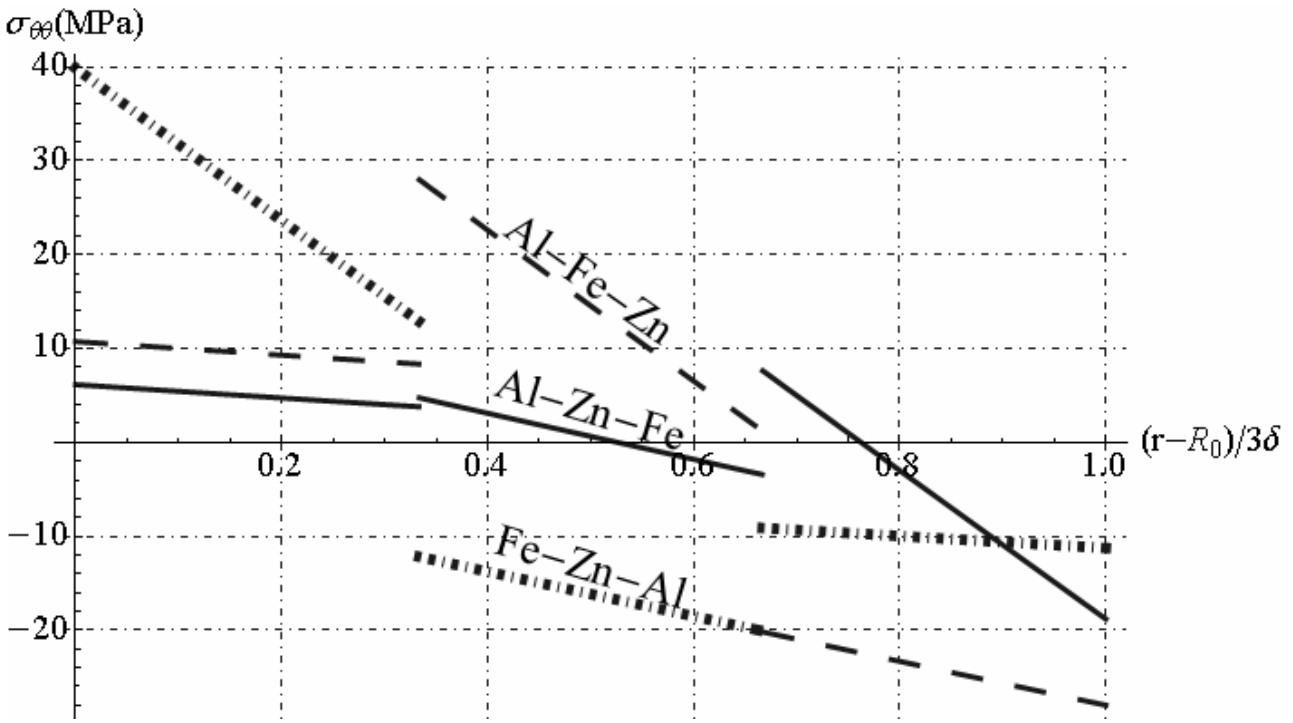

Fig. 17.44 - *Circumferential stress along radial direction*

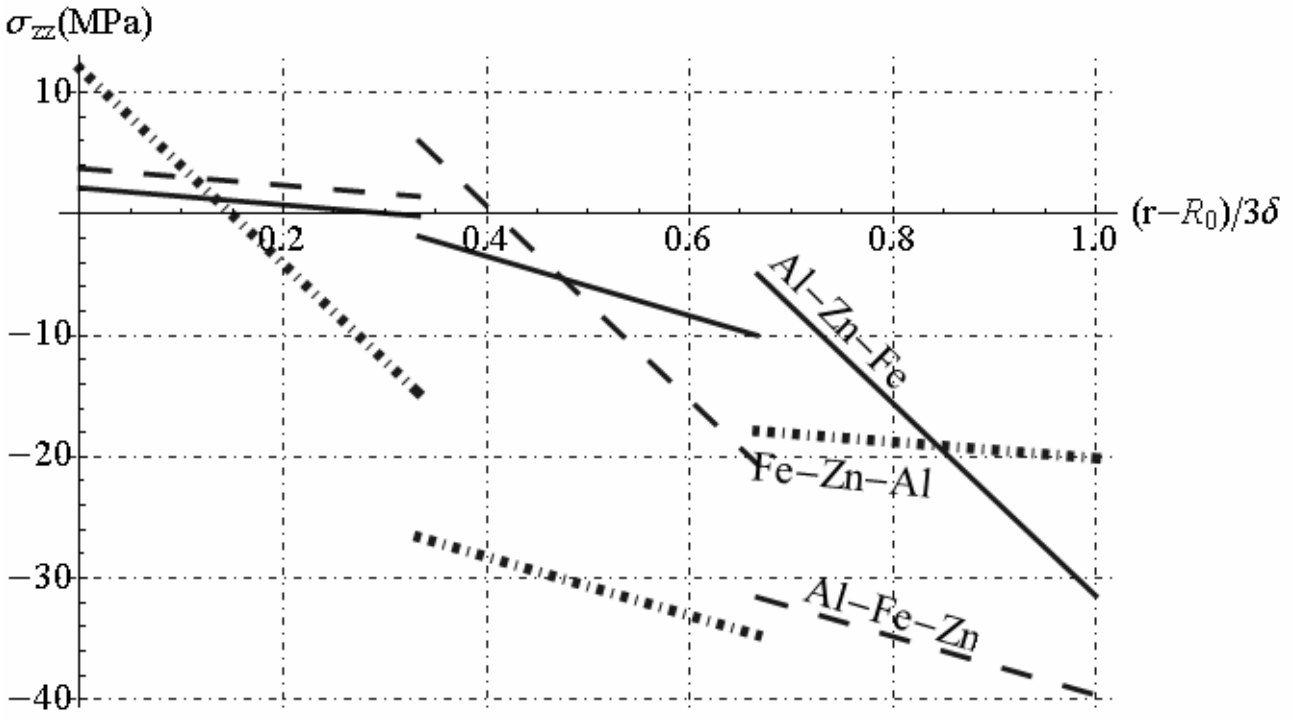

Fig. 17.45 - *Axial stress along radial direction*

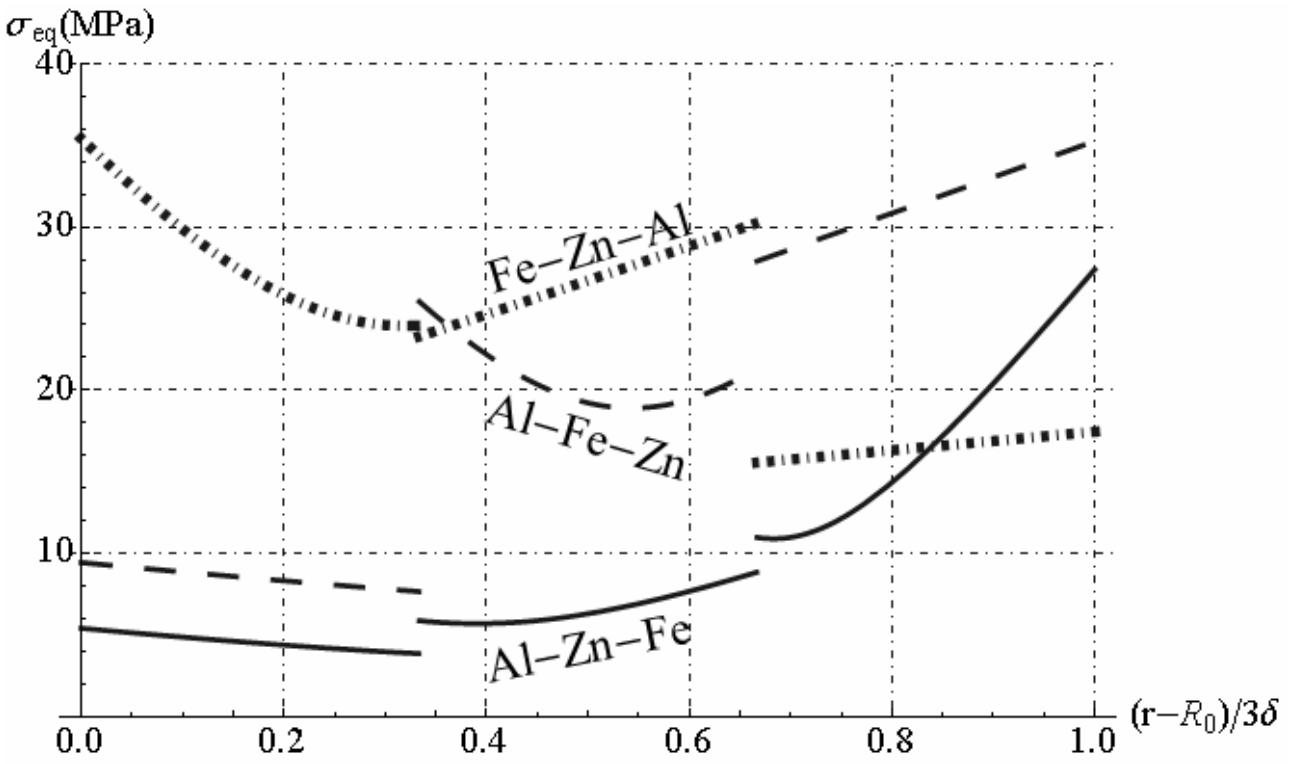

Fig. 17.46 - *Hencky von Mises's equivalent stress along radial direction*

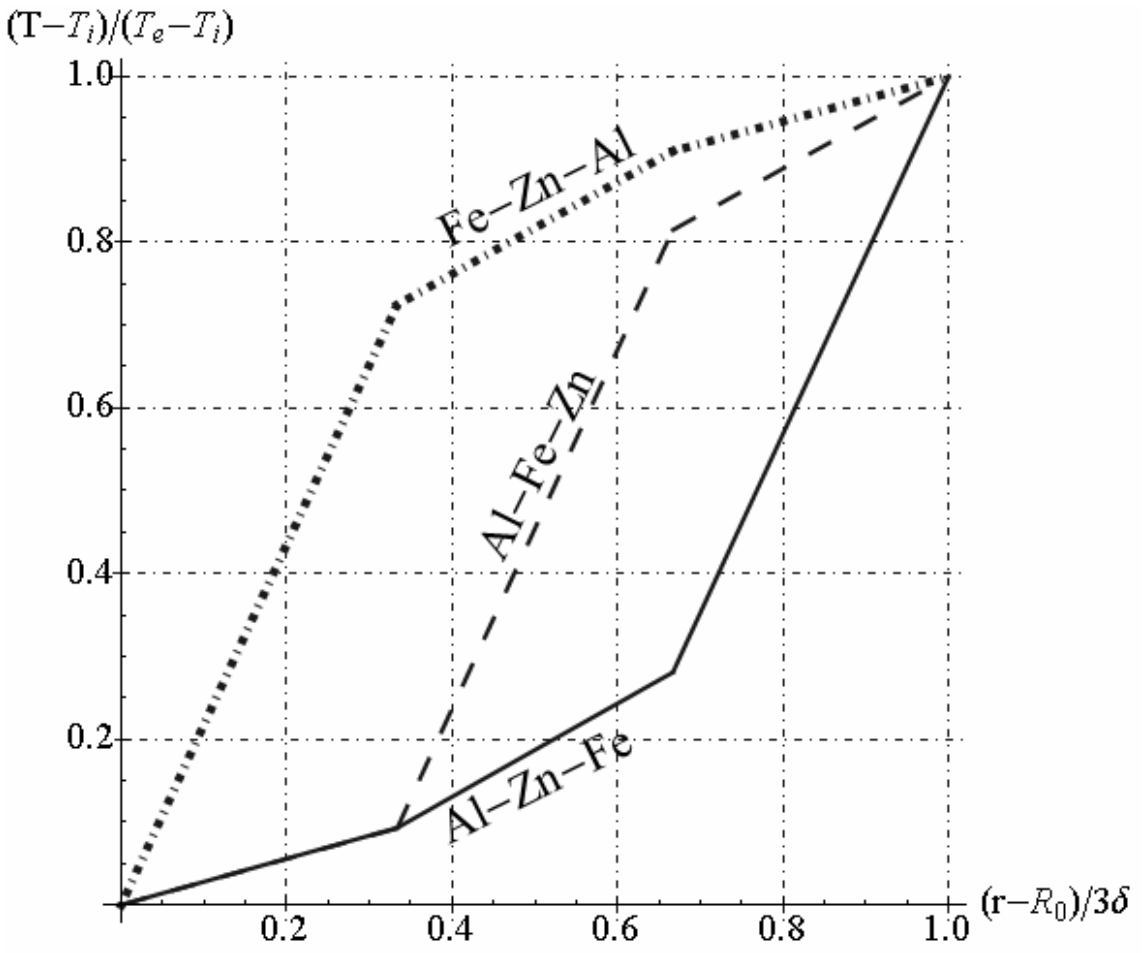

Fig. 17.47 - *Non-dimensional temperature distribution along radial direction*

We reported the numerical results for case (ii) as follows :

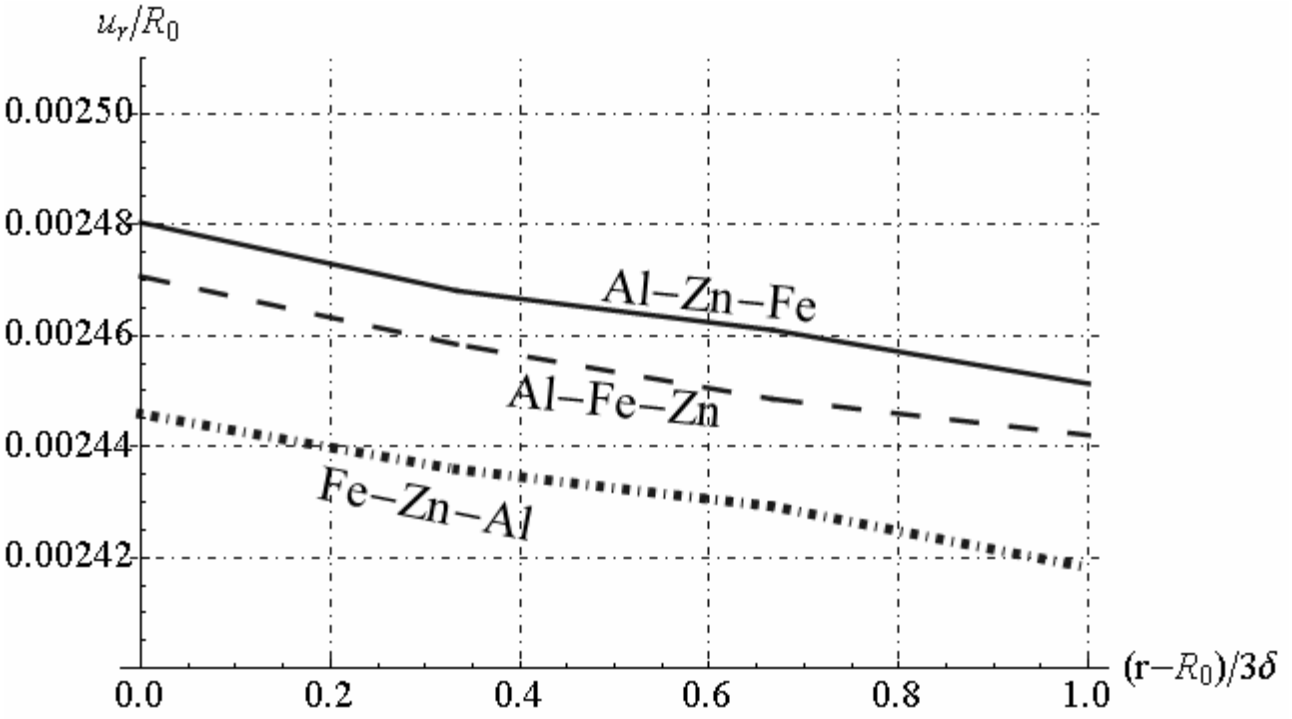

Fig. 17.48 - *Non dimensional radial displacement distribution along radial direction*

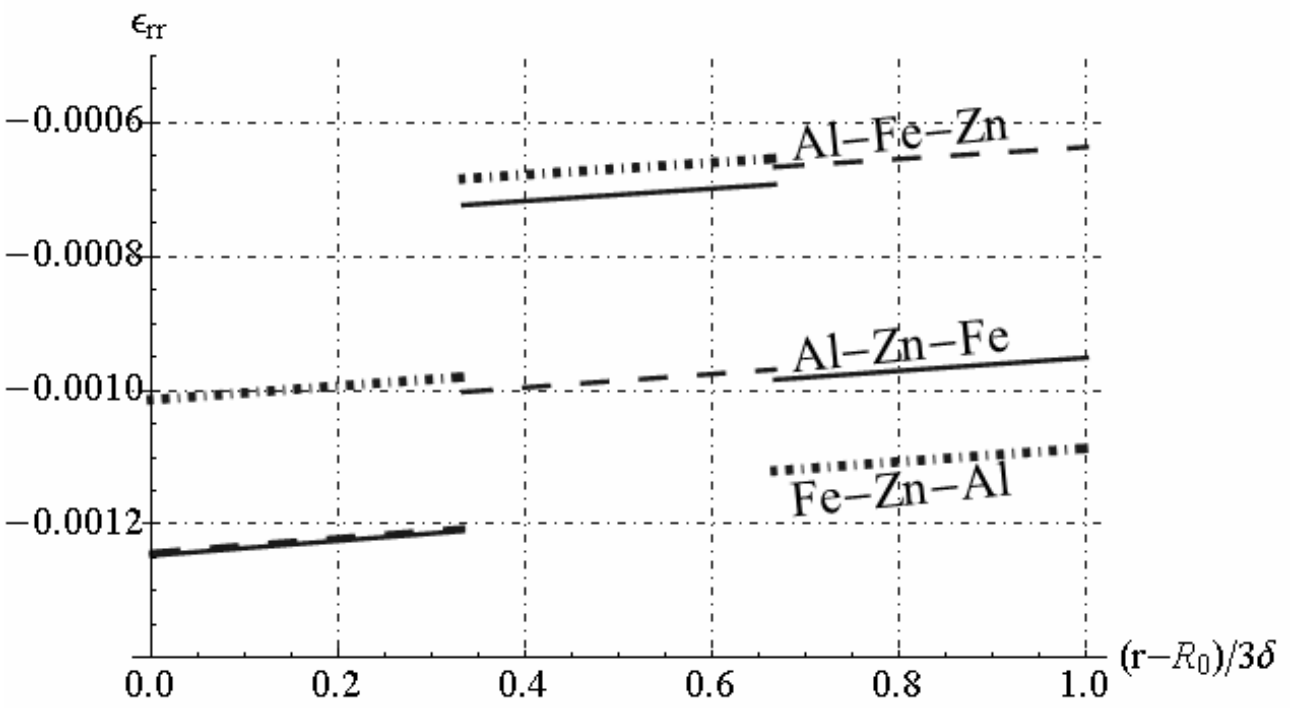

Fig. 17.49 - *Radial strain distribution along radial direction*

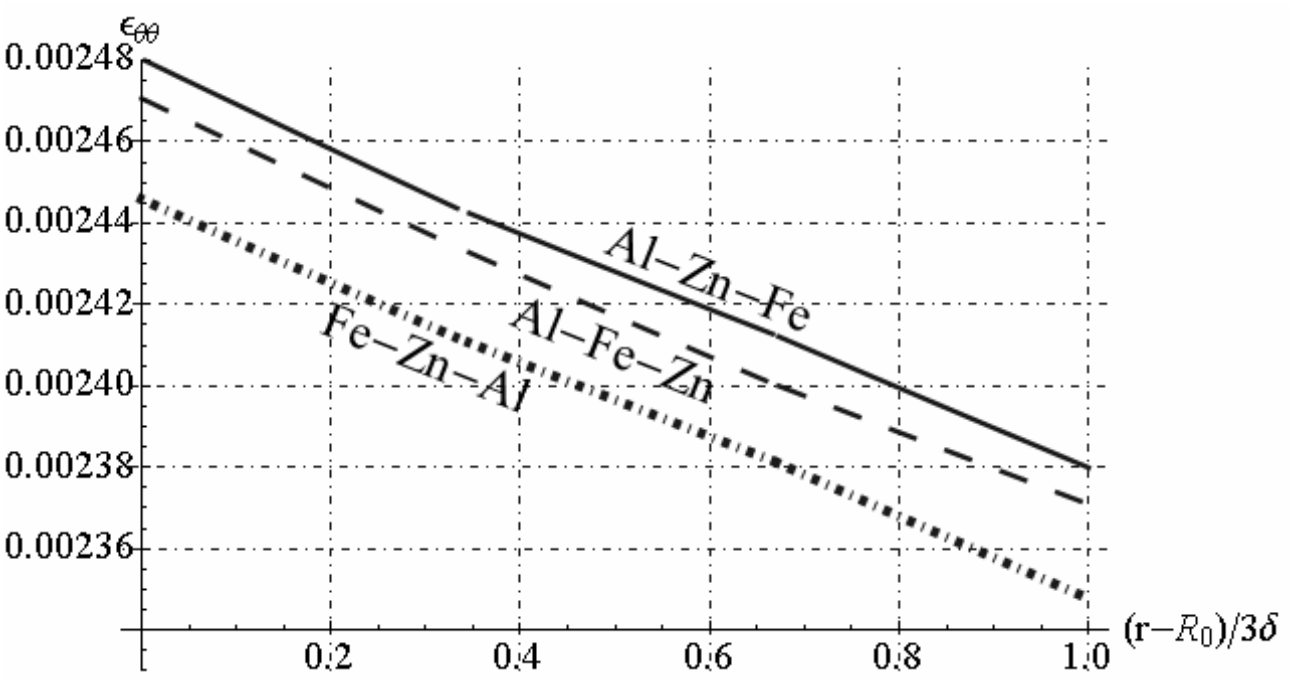

Fig. 17.50 - *Circumferential strain along radial direction*

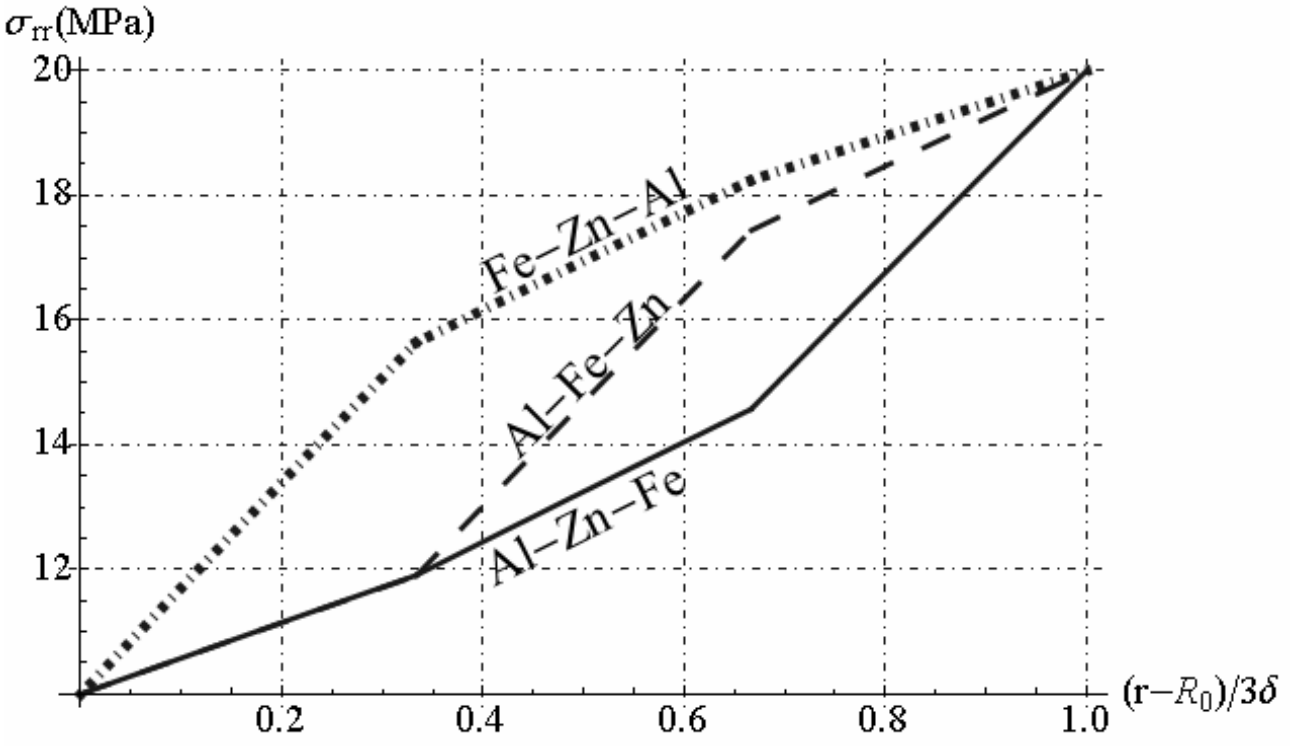

Fig. 17.51 - *Radial stress distribution along radial direction*

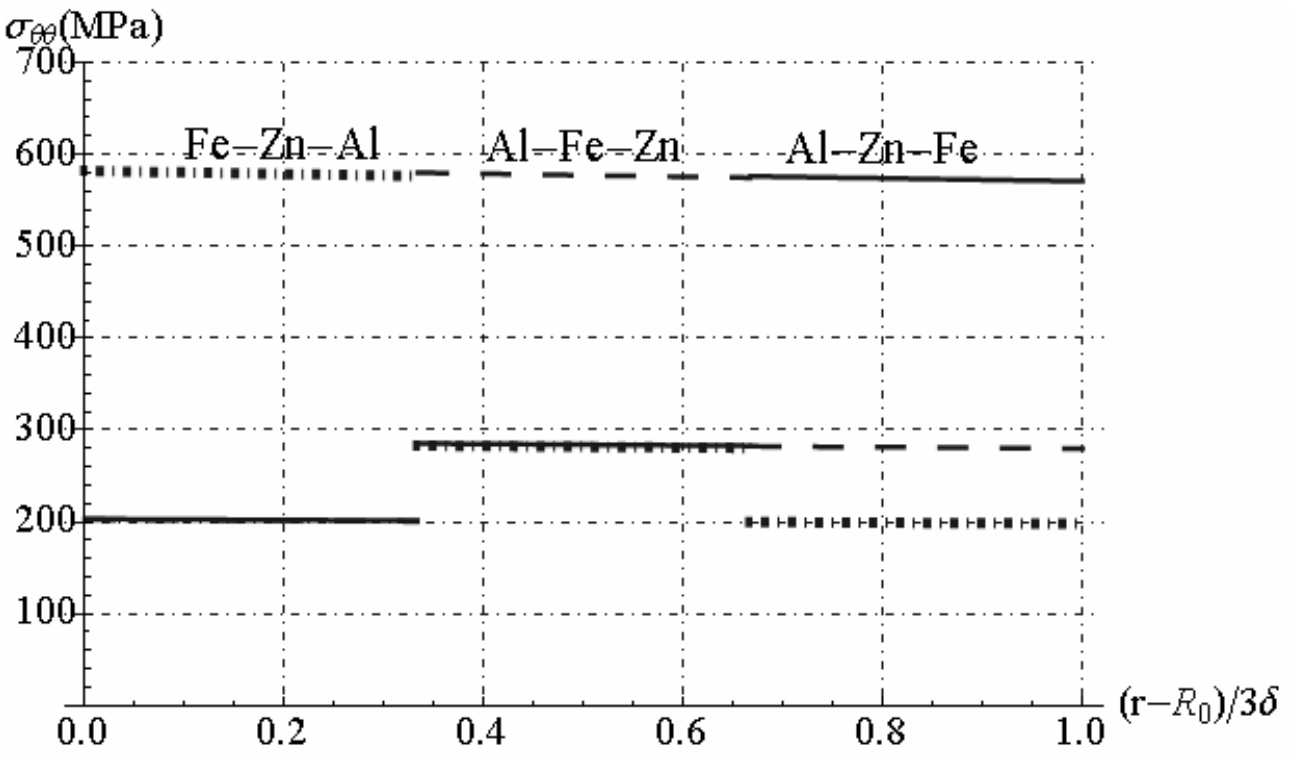

Fig. 17.52 - *Circumferential stress along radial direction*

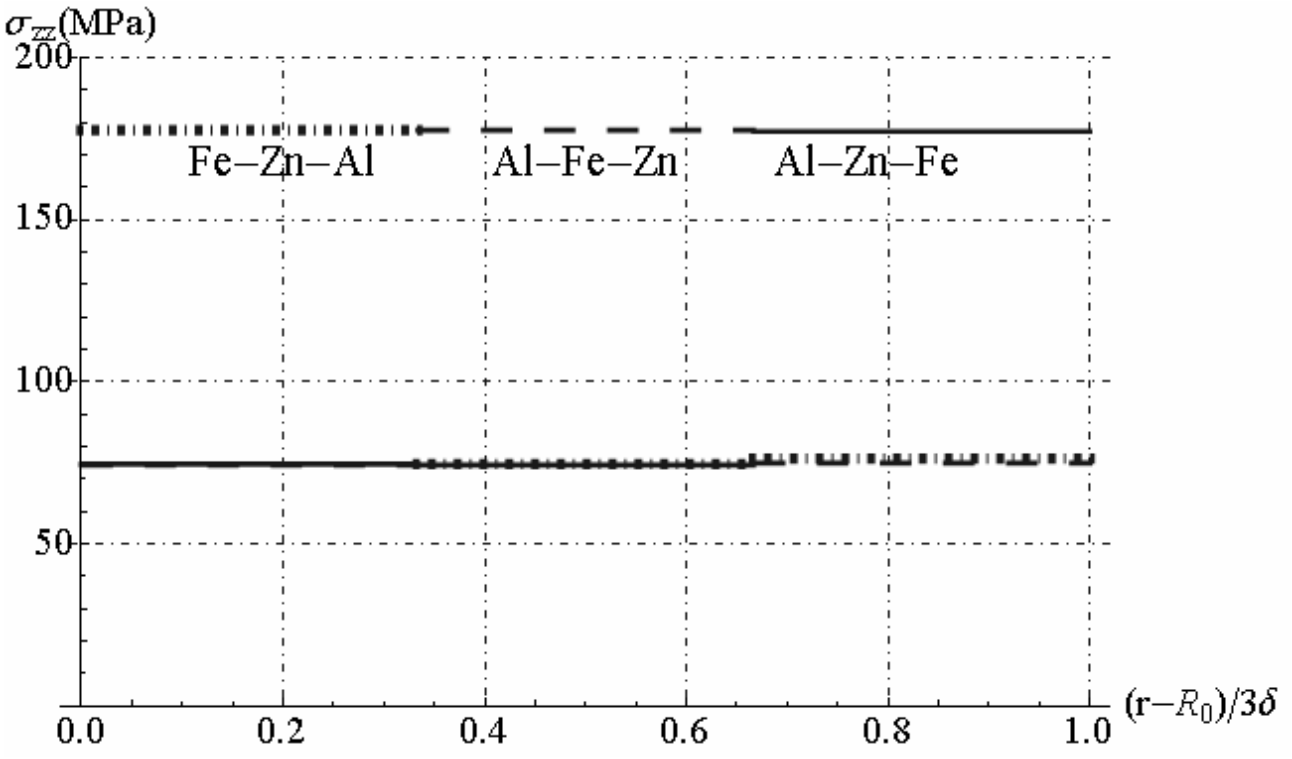

Fig. 17.53 - *Axial stress along radial direction*

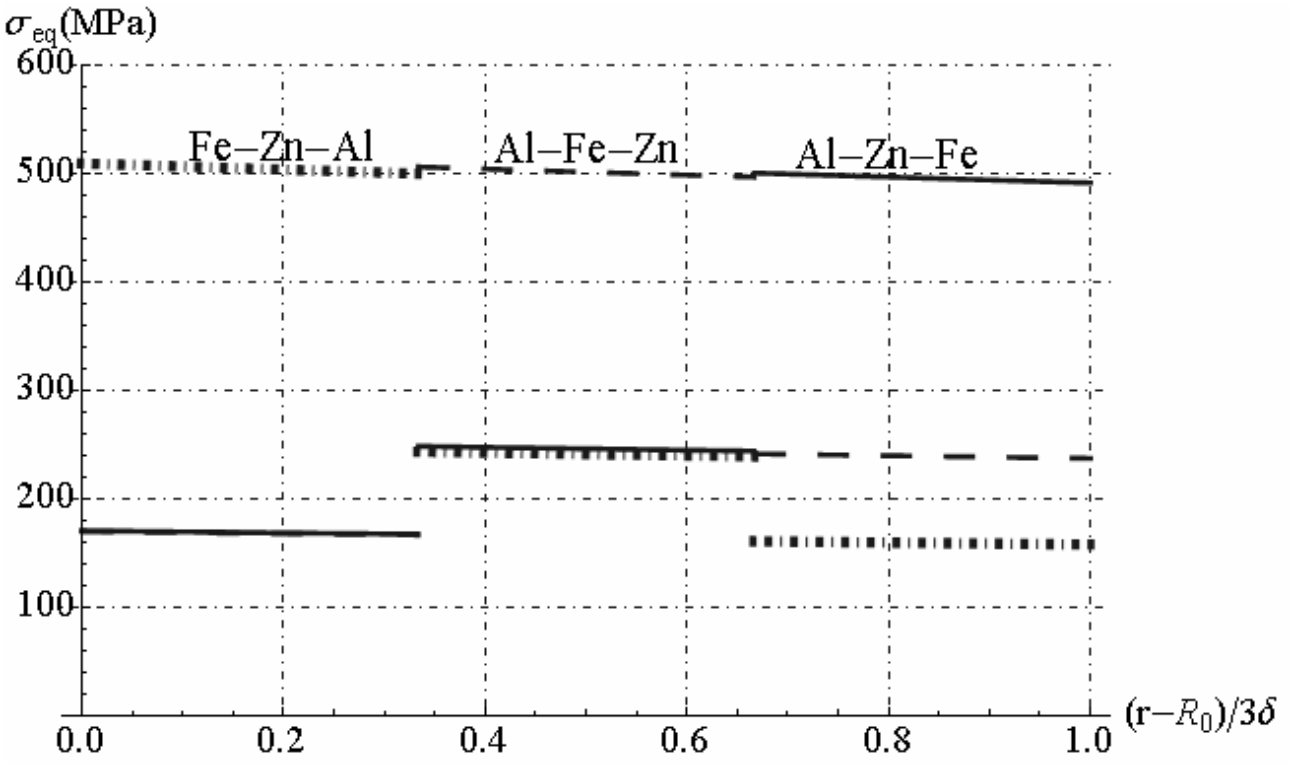

Fig. 17.54 - *Equivalent stress along radial direction*

17.5. Conclusions

In this study, analytical and numerical results for a multilayered cylinder were obtained. The analytical thermo-elastic solution in closed form is employed to obtain the parametric analyses for bi-layer hollow cylinders and the numerical results for cylindrical tank composed by three phases. The temperature, displacement and thermal stress distributions were obtained which can be applied to mechanical parts in precision measurement or design useful structural applications. The proposed method may be readily extended to solve a wide range of physical engineering problems. In particular, the parametric analyses presented in this paper can be to utilized for to optimize the designer of the composite cylindrical tank subjected to mechanical and thermal loads. By summarized the results obtained by parametric analyses, it is possible reduce the maximum equivalent stress in cylindrical tank by utilizing hollow cylinders constituted by materials with selected mechanical and thermal property.

17.6. Nomenclature

k thermal conductivity coefficient,
α linear thermal expansion coefficient
E Young's modulus,
ν Poisson's ratio
T_i temperature on the inner surface,
T_e temperature on the outer surface
p_i pressure on the inner surface,
p_e pressure on the outer surface
$T, \overline{T}$ dimensional and non-dimensional temperature
$r, \overline{r}$ dimensional and non-dimensional radial coordinate
$\varepsilon_{jk}^{(i)}, \overline{\varepsilon}_{jk}^{(i)}$ dimensional and non-dimensional strain components in generic *i*-th phase
$\sigma_{jk}^{(i)}, \overline{\sigma}_{jk}^{(i)}$ dimensional and non-dimensional stress components in generic *i*-th phase

$u_r^{(i)}, \overline{u}_r^{(i)}$ dimensional and non-dimensional radial component of displacement in generic *i*-th phase

17.7. References

[1] Horgan CO, Chan AM. The pressurized hollow cylinder or disk problem for functionally graded isotropic linearly elastic materials. J. Elasticity 1999;55:43e59.
[2] Horgan CO, Chan AM. The stress response of functionally graded isotropic linearly elastic rotating disks. J. Elasticity 1999;55:219e30.
[3] Tutuncu N, Ozturk M. Exact solutions for stress in functionally grade pressure vessels. Composites: Part B 2001;32:683e6.
[4] Tutuncu N. Stresses in thick-walled FGM cylinders with exponentially-varying properties. Eng. Struct 2007;29:2032e5.
[5] Dryden J, Jayaraman K. Effect of inhomogeneity on the stress pipes. J. Elasticity 2006;83:179e89.
[6] Eraslan AN, Akis T. Plain strain analytical solutions for a functionally graded Elastic-plastic pressurized tube. Int. J. Pressure Vessels Piping 2006;83: 635e44.
[7] Shi ZF, Zhang TT, Xiang HJ. Exact solutions of heterogeneous elastic hollow cylinders. Compos. Struct 2007;79:140e7.
[8] Noda N. Thermal stresses in materials with temperature-dependent properties. Appl. Mech. Rev. 1991;44:383e7.
[9] Zimmerman RW, Lutz MP. Thermal stress and thermal expansion in a uniformly heated functionally graded cylinder. J. Therm. Stress 1999;22: 177e88.
[10] Lutz MP, Zimmerman RW. Thermal stress and effective thermal expansion coefficient of a functionally gradient sphere. J. Therm. Stress 1996;19:39e54.
[11] Jabbari M, Sohrabpour S, Elsami MR. Mechanical and thermal stresses in a functionally graded hollow cylinder due to radially symmetric loads. Int. J. Press. Vessels Piping 2002;79:493e7.
[12] Elsami MR, Babaei MH, Poultangari R. Thermal and mechanical stresses in a functionally graded thick sphere. Int. J. Press. Vessels Piping 2005;82:522e7.
[13] Fraldi, M., Nunziante, L., Carannante, F. (2007), *Axis-symmetrical Solutions for n-plies Functionally Graded Material Cylinders under Strain no-Decaying Conditions*, J. Mech. of Adv. Mat. and Struct. Vol. 14 (3), pp. 151-174 - DOI: 10.1080/15376490600719220
[14] M. Fraldi, L. Nunziante, F. Carannante, A. Prota, G. Manfredi, E. Cosenza (2008), *On the Prediction of the Collapse Load of Circular Concrete Columns Confined by FRP*, Journal Engineering structures, Vol. 30, Issue 11, November 2008, Pages 3247-3264 - DOI: 10.1016/j.engstruct.2008.04.036
[15] Fraldi, M., Nunziante, L., Chandrasekaran, S., Carannante, F., Pernice, MC. (2009), *Mechanics of distributed fibre optic sensors for strain measurements on rods*, Journal of Structural Engineering, 35, pp. 323-333, Dec. 2008- Gen. 2009
[16] M. Fraldi, F. Carannante, L. Nunziante (2012), *Analytical solutions for n-phase Functionally Graded Material Cylinders under de Saint Venant load conditions: Homogenization and effects of Poisson ratios on the overall stiffness*, Composites Part B: Engineering, Volume 45, Issue 1, February 2013, Pages 1310–1324
[17] Nunziante, L., Gambarotta, L., Tralli, A., *Scienza delle Costruzioni*, 3° Edizione, McGraw-Hill, 2011, ISBN: 9788838666971
[18] Obata Y, Noda N. Steady thermal stresses in a hollow circular cylinder and a hollow sphere of a functionally gradient material. J. Therm. Stresses 1994;17:471e87.
[19] Tokovyy YuV, Ma C-C. Analysis of 2D non-axisymmetric elasticity and thermoelasticity problems for radially inhomogenenous hollow cylinders. J. Eng. Math. 2008;61:171e84.
[20] You LH, Ou H, Li J. Stress analysis of functionally graded thick-walled cylindrical vessels. AIAA J 2007;45:2790e8.
[21] Li X-F, Peng X-L. A pressurized functionally graded hollow cylinder with arbitrarily varying material properties. J. Elasticity 2009;96:81e95.

[22] Li X-F, Peng X-L, Kang Y-A. Pressurized hollow spherical vessels with arbitrary radial nonhomogeneity. AIAA J 2009;47:2262e5.
[23] Atkinson KE, Shampine LF. Algorithm 876: solving Fredholm integral equations of the second kind in MATLAB. ACM Trans. Math. Soft 2008;34:21.
[24] Zhao J, Ai X, Li Y, Zhou Y. Thermal shock resistance of functionally gradient solid cylinders. Mater. Sci. Eng., A 2006;418:99e110.
[25] Zhang X-H, Han J-C, Du S-Y, Wood JV. Microstructure and mechanical properties of TiCeNi functionally graded materials by simultaneous combustion synthesis and compaction. J. Mater. Sci. 2000;35:1925e30.
[26] Shackelford James F, Alexander W. Materials science and engineering handbook. Boca Raton: CRC Press LLC; 2001.
[27] Bruno A. Boley and Jerome H. Weiner, *Theory of thermal stresses*, Dover publications, inc. Mineola, New York

CHAPTER XVIII
STEADY-STATE PROBLEM FOR MULTILAYERED SPHERES

18.0. Introduction

The Functionally Graded Materials, afterwards denoted by FGMs, are often found in many engineering applications. In the framework of Theory of Elasticity, FGMs are mostly treated as non-homogeneous materials whose mechanical and thermal material properties continuously or in a piece-wise continuous manner (*laminated composites*) vary along a spatial direction. FGMs are a new branch in the Mechanic of Materials which can be used in various conditions such as thermal and mechanical load applications. The mechanical benefits obtained by a FGMs might be significant, as it can be seen by the excellent structure performance of some of these materials. Hence, there has been a considerable interest in the application of these materials in recent years, in areas such as high temperature applications and industrial fields (electronics, biomaterials and so on). The increment of the using of composite materials in engineering application, as FGMs, has developed a considerable researching activity in this area. An understanding of thermal stresses in isotropic bodies is essential for a comprehensive study of their response due to an exposure to a temperature field, which may in turn occurs in service or during manufacturing stages. In literature, the FGMs are microscopic inhomogeneous composites characterized by continuously varying of mechanical and thermal property, according to a certain power law, along a fixed direction, in contrast with classical composite materials whose properties abruptly vary from one lamina to the other (Ibrahim et al. [12]). FGMs were firstly developed by a group of Japanese scientists, used in aggressive environments and have been widely explored in various engineering applications including electron, chemistry, optics, biomedicine, etc. [13]. The exact solutions for the stresses in functionally graded cylindrical and spherical vessels, subjected to internal pressure alone, are given by Tutuncu and Ozturk [25]. These authors consider radially varying inhomogeneous material properties with material stiffness obeying to a simple power law and stress distributions depending on an inhomogeneity constant. This can be adapted for specific applications in order to control the stress distribution; including continuously varying volume fraction of the constituents. The analytical solution for stresses in spheres and cylinders made of FGMs are given by Lutz and Zimmerman [16]. These authors consider thick spheres and cylinders under radial thermal loads, composed by radially graded materials, with linear composition of the constituent materials. Obata and Noda [20] studied one-dimensional steady-state thermal stresses in a functionally graded circular hollow cylinder and a hollow sphere by using a perturbation approaching. The object of this study is to achieve the effect of composites on stresses and to design the optimum FGM hollow circular cylinder and hollow sphere under different assumptions of temperature distributions. Liew et al. [15] present an analysis that determines the thermo-mechanical behaviour of FGMs composed by hollow circular cylinders. These solutions are obtained by an original limiting process that employs the solutions of homogeneous hollow circular cylinders. These solutions are not determined by the recourse to basic theory or equations of non-homogeneous thermo-elasticity, but by the thermal stresses results that occur in the FGM cylinder, except in trivial case of zero temperature and heat resistance that may be improved by a proper variation of material composition. Thermal stresses in FGM cylinder are governed by more factors than that of homogeneous. Shao [24] presents the solution of a functionally graded circular hollow cylinder of finite length by using a multi-layered approaching of the theory of laminated composites which is subjected to axisymmetric thermal and mechanical loads. The properties of material are independent of temperature with radially varying and are homogeneous in each layer. The results are also presented for a mullite/molybdenum functionally graded circular hollow cylinder. Zong -Yi Lee [28] studied a quasi-static coupled thermo-elastic problem for multilayered spheres. By using Laplace transform with respect to time, the general solutions of the governing equations are obtained in transform domain. The solution is obtained by using the matrix similarity transformation and inverse Laplace transform. The solutions are obtained in temperature and thermal deformation distributions caused by transient state. It is demonstrated that computational

procedures established are capable of solving the generalized thermo-elasticity problem of multilayered spheres. You et al. [26] present an accurate method to carry out elastic analysis of thick-walled spherical pressure vessels subjected to internal pressure. Two kinds of pressure vessel are considered: The first one consists in two homogeneous layers near to the inner and the outer surface of the vessel and a functionally graded layer in the middle; the second one consists in the FGM only. The effects of Young's modulus of the outer layer, and Young's modulus and geometric size of the middle layer, on deformations and stresses in vessels consisting in the three different layers, are examined. A method to obtain an almost constant circumferential stress in vessels, composed by FGM, is investigated. Ahmet and Tolga [2] present plane strain analytical solutions of functionally graded elastic and elastic–plastic pressurized tube. These solutions are obtained by small deformation theory. The modulus of elasticity and the uniaxial yield limit of the tube material are assumed to radially vary according to parabolic forms. The plastic model is based on Tresca yield criterion, and on its flow rule and ideally plastic material behaviour. Elastic, partially plastic and fully plastic stresses are shown and significantly affected by material in-homogeneity. With a suitable selection of material parameters, the in-homogeneous elastic-plastic solution reduces to a homogeneous one. Chen and Lin [5] carried out the elastic analysis for a thick cylinder as well as spherical pressure vessel made of FGMs with an exponentially varying property which has a significant role in stress distribution along radial direction. Shao and Ma [24] carried out thermo-mechanical analysis of functionally graded hollow circular cylinders subjected to mechanical loads and linearly increasing boundary temperature. Thermo-mechanical properties of FGM are not dependent by temperature, but they continuously vary in radial direction of cylinder. By employing Laplace transform techniques and series solving method for ordinary differential equation, it is possible to determine solutions for time-dependent temperature and thermo-mechanical stresses. Moreover, in Shao and Ma's work [20] is reported an example of a molybdenum/mullite FGM, where material properties exponentially vary. F. Alavi et. al. [1] studied thermo-elastic behaviour of thick functionally graded hollow sphere under combined thermal and mechanical loads. Mechanical and thermal properties of FGM sphere are assumed to be functions of radial position. Y.Z. Chen, X.Y. Lin [5] propose elastic analysis for a thick cylinder made of FGMs by assuming exponential function form for mechanical property. Peng and Li [22] present a method to analyze steady-state thermal stresses in a functionally graded hollow cylinder with thermo-elastic parameters that varies in radial direction, and the boundary value of a thermo-elastic problem is changed into Fredholm integral equation. The distribution of thermal stresses and radial displacement are presented, and the influence of gradient variation of material properties on thermal stresses is observed. Nayak, P.; Mondal, S. C. [17] carried out a general analytical solution in order to obtain the thermo-mechanical radial, tangential, and effective stresses of a thick spherical vessel made of FGMs. Finally, P. Nayak, S.C. Mondal, A. Nandi [18] present an analysis of a functionally graded thick cylindrical vessel with radially varying properties in the form of displacement, strain and stress for thermal, mechanical and thermo-mechanical loads. Further more, these authors validate the method of solution and the results by means of reducing it to those of thick cylindrical pressure vessels of isotropic-homogeneous materials. The properties of material of the vessel are assumed to be graded in radial direction based on power-law index function of radius. This Chapter aims to determine the displacements, strains, and stresses from the general analytical solution of multilayered sphere composed by an arbitrary number of layers constituted by materials with generic modulus of elasticity, thermal expansion coefficient and thermal conductivity. Material properties are assumed to be temperature-independent and homogeneous in each layer. The multilayered sphere is considered as an classical composite material whose properties abruptly vary from one hollow sphere to the other.

18.1. Basic equations for steady-state problem

Let us consider an multilayered sphere composed by *n* fictitious hollow spherical phases (Figure n.1). The external radius and internal radius of multilayered sphere are denoted by $R^{(n)}$ and $R^{(0)}$, respectively. The radius at interface between the generic phase *i-th* and the phase *(i+1)-th* are

denoted with $R^{(i)}$. The mechanical and thermal properties of each layer are assumed to be homogeneous and isotropic and are denoted with apex (i). Spherical coordinates r, θ and ϕ are used in this analysis. The multilayered sphere is subjected to gradient temperature, between the inner and the outer surface, that are T_e and T_i, respectively. Moreover, the multilayered sphere is subjected to an external constant pressure p_e and an internal constant pressure p_i applied on the inner and the outer surface $r = R^{(n)}$ and $r = R^{(0)}$, respectively. Details of multilayered sphere are shown in Figure n.1. Afterwards, it is presented a method to solve a mono-dimensional thermo-elastic problem. The basic thermo-elastic equations for the *i*-th layer can be expressed as reported below:

Strain-Displacement relations:

In isotropic-thermal elasticity case, the strains are related to the displacements by purely geometrical considerations. The multilayered sphere is subjected to spherical symmetric steady-state temperature loads. Then, in spherical coordinate, the displacement components for generic phase are given by:

$$u_r^{(i)} = u_r^{(i)}(r), \quad u_\theta^{(i)} = 0, \; u_\phi^{(i)} = 0, \quad \forall i \in \{1,2,...n\} \tag{18.1}$$

where we denote with apex 1,2,…n the hollow phases of multilayered sphere. Then, the strain-displacement relations take the form:

$$\varepsilon_{rr}^{(i)} = \frac{\partial u_r^{(i)}}{\partial r}, \quad \varepsilon_{\theta\theta}^{(i)} = \varepsilon_{\phi\phi}^{(i)} = \frac{u_r^{(i)}}{r}, \quad \varepsilon_{\theta\phi}^{(i)} = \varepsilon_{r\theta}^{(i)} = \varepsilon_{r\phi}^{(i)} = 0 \quad \forall i \in \{1,2,...n\} \tag{18.2}$$

where $u_r^{(i)}, u_\theta^{(i)}, u_\phi^{(i)}$, are the radial and circumferential displacements in the *i*-th layer ($R^{(i)} < r < R^{(i+1)}$). The superscript *"i"* represents the *i*-th layer.

Thermo-elastic stress-strain relations:

$$\begin{aligned}
\sigma_{rr}^{(i)} &= \left(2\mu^{(i)} + \lambda^{(i)}\right)\frac{\partial u_r^{(i)}}{\partial r} + \lambda^{(i)}\frac{2u_r^{(i)}}{r} - \left(3\lambda^{(i)} + 2\mu^{(i)}\right)\alpha^{(i)}\left(T^{(i)} - T_R\right) \\
\sigma_{\theta\theta}^{(i)} &= \sigma_{\phi\phi}^{(i)} = \left(\mu^{(i)} + \lambda^{(i)}\right)\frac{2u_r^{(i)}}{r} + \lambda^{(i)}\frac{\partial u_r^{(i)}}{\partial r} - \left(3\lambda^{(i)} + 2\mu^{(i)}\right)\alpha^{(i)}\left(T^{(i)} - T_R\right) \\
\tau_{r\phi}^{(i)} &= \tau_{\theta\phi}^{(i)} = \tau_{r\theta}^{(i)} = 0; \qquad \forall i \in \{1,2,...n\}
\end{aligned} \tag{18.3}$$

where $\mu^{(i)}, \lambda^{(i)}, \alpha^{(i)}, T^{(i)}$ are the Lamè elastic constants, thermo-elastic coefficients and temperature in the *i*-th layer, respectively; T_R is the reference temperature . Moreover, let us assume that the function of the temperature in each phase is given by:

$$T^{(i)} = T^{(i)}(r) \quad \forall i \in \{1,2,....,n\} \tag{18.4}$$

Equilibrium equations:

The equations of equilibrium are the same as those of isothermal elasticity since they are based on purely mechanical considerations. By applying the hypothesis of the axial-symmetric steady-state temperature loads and in absence of the body force, the equilibrium equations become one equation:

$$\frac{\partial \sigma_{rr}^{(i)}}{\partial r} + \frac{2\left(\sigma_{rr}^{(i)} - \sigma_{\theta\theta}^{(i)}\right)}{r} = 0 \quad \forall i \in \{1,2,...n\} \tag{18.5}$$

Equilibrium and compatibility boundary conditions

The results obtained until now satisfy the equilibrium and compatibility equations inside each generic *i*-th phase of a composite spherical solid subjected to axis-symmetrical strains or steady-state temperature loads. Under both the hypothesis of linear isotropic elastic behaviour of the homogeneous materials and the assumption of perfect bond at the spherical interfacial boundaries

(no de-lamination or friction phenomena), we have now to establish the satisfaction of both the equilibrium and the compatibility equations at the boundary surfaces between two generic adjacent phases. To obtain this, we will make reference to the generic case, in which multilayered sphere constituted by *n* arbitrary hollow phases (Fig. 12.1). In this framework the following boundary conditions be established. In particular, we begin writing the compatibility equations at the generic interface, that is:

$$u_r^{(i)}(r = R^{(i)}) = u_r^{(i+1)}(r = R^{(i)}) \quad \forall i \in \{1, 2, ...n-1\} \tag{18.6}$$

The equilibrium equations at the generic interface are given by:

$$\sigma_{rr}^{(i)}(r = R^{(i)}) = \sigma_{rr}^{(i+1)}(r = R^{(i)}) \quad \forall i \in \{1, 2, ...n-1\} \tag{18.7}$$

The equilibrium equations for the tractions on the inner and the outer spherical boundary surface, give:

$$\begin{cases} \sigma_{rr}^{(n)}(r = R^{(n)}) = p_e \\ \sigma_{rr}^{(1)}(r = R^{(0)}) = p_i \end{cases} \tag{18.8}$$

where p_e, p_i are the pressure applied on the inner and the outer surface of multilayered sphere, respectively.

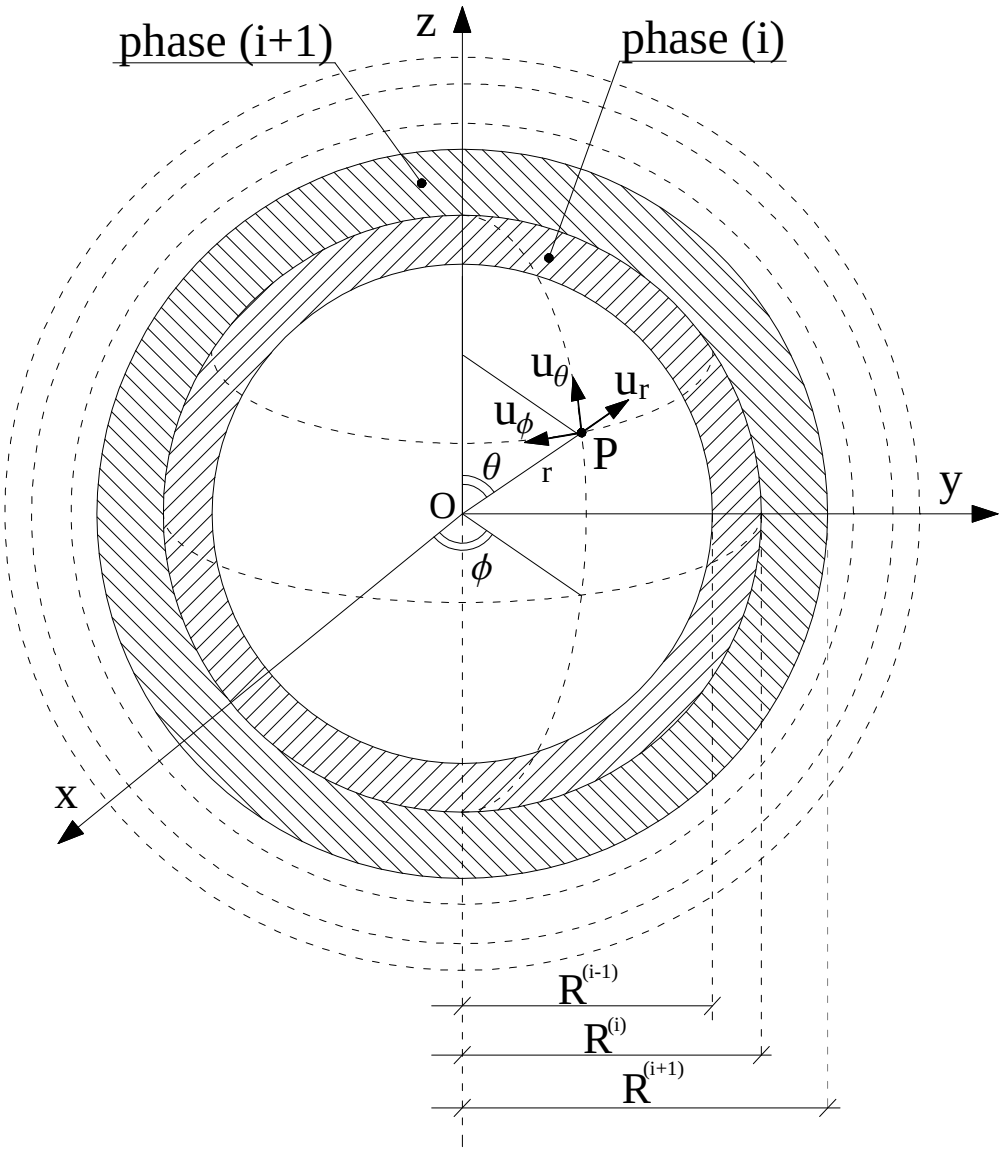

Fig. 18.1 - *Multilayered sphere composed by n-hollow spheres*

Heat conduction equation

The conduction equation is wrote in hypothesis of the steady-state problem and of the spherical symmetric load conditions for each phases of multilayered sphere:

$$\frac{\partial^2 T^{(i)}}{\partial r^2}+\frac{2}{r}\frac{\partial T^{(i)}}{\partial r}=0 \qquad \forall i\in\{1,2,...n\} \tag{18.9}$$

Temperature boundary and continuity conditions

At the interfaces between the phases, the temperature and heat flux is the same. Then, we can write the following conditions:

$$\begin{cases} T^{(i)}(r=R^{(i)})=T^{(i+1)}(r=R^{(i)}) \\ k^{(i)}\dfrac{\partial T^{(i)}(r=R^{(i)})}{\partial r}=k^{(i+1)}\dfrac{\partial T^{(i+1)}(r=R^{(i)})}{\partial r} \end{cases} \quad \forall i\in\{1,2,...n-1\} \tag{18.10}$$

on the inner and the outer surface the temperature is equal to T_e and T_i, respectively:

$$\begin{cases} T^{(n)}(r=R^{(n)})=T_e \\ T^{(1)}(r=R^{(0)})=T_i \end{cases} \tag{18.11}$$

18.2. Multilayered sphere under radial temperature variation and uniform pressure

Let us consider an multilayered sphere constituted by n-hollow spherical phase as decrypted in section 17.1. The equations field in each phase are composed by equilibrium and heat conduction equations. By substituting the strain-displacement relations (18.2) in stress-strain relations (18.3) and these in equilibrium equations (18.5), we obtain the displacement formulation of the equilibrium equations. Then, the equations field to satisfy in thermo-elastic steady-state problem with spherical symmetry are given by:

$$\begin{cases} \dfrac{d}{dr}\left[\dfrac{1}{r^2}\dfrac{d\left(r^2u_r^{(i)}\right)}{dr}\right]=\left(\dfrac{3\lambda^{(i)}+2\mu^{(i)}}{2\mu^{(i)}+\lambda^{(i)}}\right)\alpha^{(i)}\dfrac{dT^{(i)}}{dr}=\alpha^{(i)}\left(\dfrac{1+\nu^{(i)}}{1-\nu^{(i)}}\right)\dfrac{dT^{(i)}}{dr} \\ \dfrac{d^2T^{(i)}}{dr^2}+\dfrac{2}{r}\dfrac{dT^{(i)}}{dr}=0 \qquad\qquad \forall i\in\{1,2,...,n\} \end{cases} \tag{18.12}$$

By applying the formulas in chapter 15, we determine the displacement solution in each phases of multilayered sphere, as reported below:

$$u_r^{(i)}=\frac{\alpha^{(i)}}{r^2}\left(\frac{3\lambda^{(i)}+2\mu^{(i)}}{\lambda^{(i)}+2\mu^{(i)}}\right)\int r^2T^{(i)}\left(r\right)dr+C_1^{(i)}r+\frac{C_2^{(i)}}{r^2} \quad \forall i\in\{1,2,....,n\} \tag{18.13}$$

where $C_1^{(i)},C_2^{(i)}$ are constants integration to determine. By integrating the Fourier's equation reported in (18.12), we determine the well know temperature function for steady-state problem in each phases:

$$T^{(i)}\left(r\right)=A_1^{(i)}+\frac{A_2^{(i)}}{r} \quad \forall i\in\{1,2,....,n\} \tag{18.14}$$

where $A_1^{(i)},A_2^{(i)}$ are constants integration to determine. Then, the heat flux in each phases is given by:

$$q^{(i)}=-k^{(i)}\frac{dT^{(i)}}{dr}=\frac{k^{(i)}A_2^{(i)}}{r^2} \quad \forall i\in\{1,2,...,n\} \tag{18.15}$$

By substituting the temperature function (18.14) in equation (18.13), we obtain the explicit expression of displacement function:

$$u_r^{(i)} = C_1^{(i)} r + \frac{C_2^{(i)}}{r^2} + \alpha^{(i)} \left(\frac{3\lambda^{(i)} + 2\mu^{(i)}}{\lambda^{(i)} + 2\mu^{(i)}} \right) \left(\frac{A_1^{(i)} r}{3} + \frac{A_2^{(i)}}{2} \right) \qquad \forall i \in \{1, 2, ...n\} \tag{18.16}$$

By applying the strain-displacement relationship, we determine the non-zero strain components:

$$\begin{cases} \varepsilon_{rr}^{(i)} = C_1^{(i)} - \dfrac{6C_2^{(i)}}{3r^3} + \dfrac{A_1^{(i)} \alpha^{(i)}}{3} \left(1 + \dfrac{2\lambda^{(i)}}{2\mu^{(i)} + \lambda^{(i)}} \right); \\ \varepsilon_{\theta\theta}^{(i)} = \varepsilon_{\phi\phi}^{(i)} = C_1^{(i)} + \dfrac{C_2^{(i)}}{r^3} + \dfrac{\alpha^{(i)} \left(3\lambda^{(i)} + 2\mu^{(i)} \right) \left(3A_2^{(i)} + 2A_1^{(i)} r \right)}{6\left(2\mu^{(i)} + \lambda^{(i)} \right)}; \end{cases} \quad \forall i \in \{1, 2, ...n\} \tag{18.17}$$

By applying the stress-strain relationship, we obtain the non-zero stress components:

$$\begin{cases} \sigma_{rr}^{(i)} = -\dfrac{4\mu^{(i)} C_2^{(i)}}{r^3} + \left(3\lambda^{(i)} + 2\mu^{(i)} \right) \left[C_1^{(i)} - \dfrac{2\alpha^{(i)} \mu^{(i)}}{\lambda^{(i)} + 2\mu^{(i)}} \left(\dfrac{2A_1^{(i)}}{3} + \dfrac{A_2^{(i)}}{r} \right) + \alpha^{(i)} T_R \right] \\ \sigma_{\theta\theta}^{(i)} = \sigma_{\phi\phi}^{(i)} = \dfrac{2\mu^{(i)} C_2^{(i)}}{r^3} + \left(3\lambda^{(i)} + 2\mu^{(i)} \right) \left[C_1^{(i)} - \dfrac{\alpha^{(i)} \mu^{(i)}}{\lambda^{(i)} + 2\mu^{(i)}} \left(\dfrac{4A_1^{(i)}}{3} + \dfrac{A_2^{(i)}}{r} \right) + \alpha^{(i)} T_R \right] \end{cases} \tag{18.18}$$

$$\forall i \in \{1, 2, ...n\}$$

Finally, by utilizing the expressions of the temperature, heat flux, radial displacement and radial stress in each phases, we can write in explicit the boundary conditions for multilayered sphere. For our convenience, we use the elastic moduli $E^{(i)}$ and $\nu^{(i)}$ as functions of the Lamé coefficients, by invoking the well-known following relations:

$$E^{(i)} = \frac{\mu^{(i)} (2\mu^{(i)} + 3\lambda^{(i)})}{(\mu^{(i)} + \lambda^{(i)})}, \quad \nu^{(i)} = \frac{\lambda^{(i)}}{2(\mu^{(i)} + \lambda^{(i)})}. \tag{18.19}$$

Then, the compatibility boundary conditions (18.6), become :

$$C_1^{(i)} - C_1^{(i+1)} + \frac{C_2^{(i)} - C_2^{(i+1)}}{R^{(i)3}} = \zeta^{(i+1)} \left(\frac{A_1^{(i+1)}}{3} + \frac{A_2^{(i+1)}}{2R^{(i)}} \right) - \zeta^{(i)} \left(\frac{A_1^{(i)}}{3} + \frac{A_2^{(i)}}{2R^{(i)}} \right) \tag{18.20}$$

$$\forall i \in \{1, 2, ..., (n-1)\}$$

where the constant $\zeta^{(i)} = \alpha^{(i)} \left(\dfrac{1+\nu^{(i)}}{1-\nu^{(i)}} \right)$. The equilibrium conditions (18.7) at interfaces between the phases, are given by:

$$\begin{aligned} &\frac{C_1^{(i)} E^{(i)}}{2\left(1-2\nu^{(i)}\right)} - \frac{C_2^{(i)} E^{(i)}}{\left(1+\nu^{(i)}\right) R^{(i)3}} - \frac{C_1^{(i+1)} E^{(i+1)}}{2\left(1-2\nu^{(i+1)}\right)} + \frac{C_2^{(i+1)} E^{(i+1)}}{\left(1+\nu^{(i+1)}\right) R^{(i)3}} = \frac{T_R}{2} \left(\frac{\alpha^{(i+1)} E^{(i+1)}}{1-2\nu^{(i+1)}} - \frac{\alpha^{(i)} E^{(i)}}{1-2\nu^{(i)}} \right) + \\ &+ \psi^{(i)} \left(\frac{A_1^{(i)}}{3} + \frac{A_2^{(i)}}{2R^{(i)}} \right) - \psi^{(i+1)} \left(\frac{A_1^{(i+1)}}{3} + \frac{A_2^{(i+1)}}{2R^{(i)}} \right) \quad \forall i \in \{1, 2, ..., (n-1)\} \end{aligned} \tag{18.21}$$

where $\psi^{(i)} = \dfrac{\alpha^{(i)} E^{(i)}}{1-\nu^{(i)}}$. The equilibrium equations on the external and internal surface of the solid (18.8) become:

$$\begin{cases} \dfrac{C_1^{(1)} E^{(1)}}{2\left(1-2\nu^{(1)}\right)} - \dfrac{C_2^{(1)} E^{(1)}}{\left(1+\nu^{(1)}\right) R^{(0)3}} = -\dfrac{\alpha^{(1)} E^{(1)} T_R}{2\left(1-2\nu^{(1)}\right)} + \psi^{(1)} \left(\dfrac{A_1^{(1)}}{3} + \dfrac{A_2^{(1)}}{2R^{(0)}} \right) + \dfrac{p_i}{2} \\ \dfrac{C_1^{(n)} E^{(n)}}{2\left(1-2\nu^{(n)}\right)} - \dfrac{C_2^{(n)} E^{(n)}}{\left(1+\nu^{(n)}\right) R^{(n)3}} = -\dfrac{\alpha^{(n)} E^{(n)} T_R}{2\left(1-2\nu^{(n)}\right)} + \psi^{(n)} \left(\dfrac{A_1^{(n)}}{3} + \dfrac{A_2^{(n)}}{2R^{(n)}} \right) + \dfrac{p_e}{2} \end{cases} \tag{18.22}$$

The temperature and continuity boundary conditions at interfaces between the adjacent phases (18.10) become:

$$\begin{cases} \left[A_1^{(i+1)} - A_1^{(i)} \right] R^{(i)} + A_2^{(i+1)} - A_2^{(i)} = 0 \\ k^{(i+1)} A_2^{(i+1)} - k^{(i)} A_2^{(i)} = 0 \end{cases} \qquad \forall i \in \{1,2,...,(n-1)\} \tag{18.23}$$

Finally, it is remains to consider the boundary conditions on the external and internal surface related to temperature (18.11):

$$\begin{cases} A_1^{(1)} R^{(0)} + A_2^{(1)} = T_i R^{(0)} \\ A_1^{(n)} R^{(n)} + A_2^{(n)} = T_e R^{(n)} \end{cases} \tag{18.24}$$

The equations (18.20) to (18.24) represents an algebraic system constituted by $4 \times n$ equations, where the unknown parameters are $4 \times n$, as reported below:

$$A_1^{(i)}, A_2^{(i)}, C_1^{(i)}, C_2^{(i)} \quad \forall i \in \{1,2,...,n\} \tag{18.25}$$

The algebraic system mentioned above, can be subdivided in two uncoupled algebraic systems:

(i) the first composed by equations (18.20), (18.21) and (18.22) ; It is characterized by $2 \times n$ equations in $2 \times n$ unknown parameters $C_1^{(i)}, C_2^{(i)} \quad \forall i \in \{1,2,...,n\}$

(ii) the second composed by equations (18.23) and (18.24); It is characterized by $2 \times n$ equations in $2 \times n$ unknown parameters $A_1^{(i)}, A_2^{(i)} \quad \forall i \in \{1,2,...,n\}$

In order to solve the first algebraic system (i), it is easy to determine the constants $A_1^{(i)}, A_2^{(i)} \quad \forall i \in \{2,3...,n\}$ as function of the constants $A_1^{(1)}, A_2^{(1)}$. By solving the algebraic system (18.23), we obtain the following relations:

$$A_1^{(i)} = A_1^{(1)} + A_2^{(1)} k^{(1)} \sum_{j=1}^{i-1} \frac{1}{R^{(j)}} \left(\frac{1}{k^{(j)}} - \frac{1}{k^{(j+1)}} \right); \quad A_2^{(i)} = A_2^{(1)} \frac{k^{(1)}}{k^{(i)}}; \quad \forall i \in \{2,3,...,n\} \tag{18.26}$$

By substituting the equations (18.26) in algebraic system (18.24), fixed i = n, we determine the constants $A_1^{(1)}, A_2^{(1)}$ as reported below:

$$A_1^{(1)} = T_i - \frac{T_e - T_i}{\omega}; \quad A_2^{(1)} = \frac{T_e - T_i}{\omega} R^{(0)}; \tag{18.27}$$

where $\omega = k^{(1)} R^{(0)} \left[\sum_{j=1}^{n} \frac{1}{k^{(j)}} \left(\frac{1}{R^{(j)}} - \frac{1}{R^{(j-1)}} \right) \right]$ is non-dimensional constant parameter for fixed number of the phases. Finally, we write the solution in closed form of the algebraic system (i) as follows:

$$\begin{cases} A_1^{(i)} = T_i + \left(T_e - T_i \right) \left[\dfrac{-\dfrac{1}{k^{(i)} R^{(i)}} + \sum_{j=1}^{i} \dfrac{1}{k^{(j)}} \left(\dfrac{1}{R^{(j)}} - \dfrac{1}{R^{(j-1)}} \right)}{\sum_{j=1}^{n} \dfrac{1}{k^{(j)}} \left(\dfrac{1}{R^{(j)}} - \dfrac{1}{R^{(j-1)}} \right)} \right] \\ A_2^{(i)} = \dfrac{\left(T_e - T_i \right)}{k^{(i)}} \left[1 \Big/ \sum_{j=1}^{n} \dfrac{1}{k^{(j)}} \left(\dfrac{1}{R^{(j)}} - \dfrac{1}{R^{(j-1)}} \right) \right] \end{cases} \quad \forall i \in \{1,2,...,n\} \tag{18.28}$$

Then, the temperature function in each phases is given by:

$$T^{(i)}(r) = T_i + \left(T_e - T_i \right) \left[\frac{\dfrac{1}{k^{(i)}} \left(\dfrac{1}{r} - \dfrac{1}{R^{(i)}} \right) + \sum_{j=1}^{i} \dfrac{1}{k^{(j)}} \left(\dfrac{1}{R^{(j)}} - \dfrac{1}{R^{(j-1)}} \right)}{\sum_{j=1}^{n} \dfrac{1}{k^{(j)}} \left(\dfrac{1}{R^{(j)}} - \dfrac{1}{R^{(j-1)}} \right)} \right] \quad \forall i \in \{1,2,...,n\} \tag{18.29}$$

In order to solve the second algebraic system (ii), let us consider the algebraic system composed by equilibrium and compatibility conditions (18.20)- (18.21), which can be written as:

$$\mathbf{Q} \cdot \mathbf{X} = \mathbf{L} \tag{18.30}$$

where the vectors $\mathbf{L}=\left[\left(\mathbf{L}_1^{(2)}-\mathbf{L}_1^{(1)}\right),\left(\mathbf{L}_2^{(3)}-\mathbf{L}_2^{(2)}\right),...,\left(\mathbf{L}_i^{(i+1)}-\mathbf{L}_i^{(i)}\right),...,\left(\mathbf{L}_{n-1}^{(n-1)}-\mathbf{L}_{n-1}^{(n-1)}\right)\right]^T$ is characterized by following sub-vectors:

$$\mathbf{L}_i^{(i)}=\begin{bmatrix}\dfrac{\zeta^{(i)}}{3} & \dfrac{\zeta^{(i)}}{2R^{(i)}}\\ -\dfrac{\psi^{(i)}}{3} & -\dfrac{\psi^{(i)}}{2R^{(i)}}\end{bmatrix}\begin{bmatrix}A_1^{(i)}\\ A_2^{(i)}\end{bmatrix}+\begin{bmatrix}0\\ \dfrac{\alpha^{(i)}E^{(i)}}{1-2\nu^{(i)}}\end{bmatrix}T_R,\quad \forall i\in\{1,2,...,n\} \tag{18.31}$$

$$\mathbf{L}_i^{(i+1)}=\begin{bmatrix}\dfrac{\zeta^{(i+1)}}{3} & \dfrac{\zeta^{(i+1)}}{2R^{(i)}}\\ -\dfrac{\psi^{(i+1)}}{3} & -\dfrac{\psi^{(i+1)}}{2R^{(i)}}\end{bmatrix}\begin{bmatrix}A_1^{(i+1)}\\ A_2^{(i+1)}\end{bmatrix}+\begin{bmatrix}0\\ \dfrac{\alpha^{(i+1)}E^{(i+1)}}{1-2\nu^{(i+1)}}\end{bmatrix}T_R,\quad \forall i\in\{1,2,...,n\} \tag{18.32}$$

and $\mathbf{X}=[\mathbf{X}^{(1)},\mathbf{X}^{(2)},...,\mathbf{X}^{(n)}]^T$ collect the unknowns sub-vectors, as reported below:

$$\mathbf{X}^{(i)}=\begin{bmatrix}C_1^{(i)} & C_2^{(i)}\end{bmatrix}^T,\quad \forall i\in\{1,2,....,n\} \tag{18.33}$$

The matrix $\mathbf{Q}$ is composed by following sub-matrices:

$$\mathbf{Q}=\begin{bmatrix}\mathbf{B}_1^{(1)} & -\mathbf{B}_1^{(2)} & \mathbf{0} & \mathbf{0} & \cdots & \mathbf{0} & \mathbf{0} & \mathbf{0}\\ \mathbf{0} & \mathbf{B}_2^{(2)} & -\mathbf{B}_2^{(3)} & \mathbf{0} & \cdots & \mathbf{0} & \mathbf{0} & \mathbf{0}\\ \mathbf{0} & \mathbf{0} & \mathbf{B}_3^{(3)} & -\mathbf{B}_3^{(4)} & \cdots & \mathbf{0} & \mathbf{0} & \mathbf{0}\\ \vdots & \vdots & \vdots & \vdots & \vdots & \vdots & \vdots & \vdots\\ \mathbf{0} & \mathbf{0} & \mathbf{0} & \mathbf{0} & \cdots & \mathbf{B}_{n-2}^{(n-2)} & -\mathbf{B}_{n-2}^{(n-1)} & \mathbf{0}\\ \mathbf{0} & \mathbf{0} & \mathbf{0} & \mathbf{0} & \cdots & \mathbf{0} & \mathbf{B}_{n-1}^{(n-1)} & -\mathbf{B}_{n-1}^{(n)}\end{bmatrix} \tag{18.34}$$

where the generic matrices $\mathbf{B}_i^{(i)},\mathbf{B}_i^{(i+1)}$ are given by:

$$\mathbf{B}_i^{(i)}=\begin{bmatrix}1 & \dfrac{1}{R^{(i)3}}\\ \dfrac{E^{(i)}}{2\left(1-2\nu^{(i)}\right)} & -\dfrac{E^{(i)}}{\left(1+\nu^{(i)}\right)R^{(i)3}}\end{bmatrix},\quad \mathbf{B}_i^{(i+1)}=\begin{bmatrix}1 & \dfrac{1}{R^{(i)3}}\\ \dfrac{E^{(i+1)}}{2\left(1-2\nu^{(i+1)}\right)} & -\dfrac{E^{(i+1)}}{\left(1+\nu^{(i+1)}\right)R^{(i)3}}\end{bmatrix}, \tag{18.35}$$

are (2×2) matrices with nonzero determinant, whose components were already gave above.
The determinant of the matrices (18.35) is given by:

$$\det[\mathbf{B}_i^{(i)}]=\frac{3E^{(i)}\left(1-\nu^{(i)}\right)}{2R^{(i)3}\left(\nu^{(i)}+2\nu^{(i)2}-1\right)}\neq 0,\quad \det[\mathbf{B}_i^{(i+1)}]=\frac{3E^{(i+1)}\left(1-\nu^{(i+1)}\right)}{2R^{(i)3}\left(\nu^{(i+1)}+2\nu^{(i+1)2}-1\right)}\neq 0, \tag{18.36}$$

However, in force of the special form of $\mathbf{Q}$ derived above, one can rewrite the reduced algebraic problem in order to have the solution without recall any numerical strategy. To make this, let us we can write the algebraic system (18.30) in follows manner:

$$\begin{cases}\mathbf{B}_1^{(2)}\mathbf{X}^{(2)}=\mathbf{B}_1^{(1)}\mathbf{X}^{(1)}+\mathbf{L}_1^{(2)}-\mathbf{L}_1^{(1)}\\ \mathbf{B}_2^{(3)}\mathbf{X}^{(3)}=\mathbf{B}_2^{(2)}\mathbf{X}^{(2)}+\mathbf{L}_2^{(3)}-\mathbf{L}_2^{(2)}\\ \vdots\\ \mathbf{B}_i^{(i+1)}\mathbf{X}^{(i+1)}=\mathbf{B}_i^{(i)}\mathbf{X}^{(i)}+\mathbf{L}_i^{(i+1)}-\mathbf{L}_i^{(i)}\\ \vdots\\ \mathbf{B}_{n-2}^{(n-1)}\mathbf{X}^{(n-1)}=\mathbf{B}_{n-2}^{(n-2)}\mathbf{X}^{(n-2)}+\mathbf{L}_{n-2}^{(n-1)}-\mathbf{L}_{n-2}^{(n-2)}\\ \mathbf{B}_{n-1}^{(n)}\mathbf{X}^{(n)}=\mathbf{B}_{n-1}^{(n-1)}\mathbf{X}^{(n-1)}+\mathbf{L}_{n-1}^{(n)}-\mathbf{L}_{n-1}^{(n-1)}\end{cases} \tag{18.37}$$

By applying an *in-cascade* procedure, we finally obtain

$$\mathbf{X}^{(i)} = \mathbf{\Phi}^{(i)} \cdot \mathbf{X}^{(1)} + \mathbf{\Psi}^{(i)} \quad \forall i \in \{2,3,...,n\} \tag{18.38}$$

where $\mathbf{\Phi}^{(i)}, \mathbf{\Psi}^{(i)}$ are matrix and vector, respectively. The expressions of $\mathbf{\Phi}^{(i)}, \mathbf{\Psi}^{(i)}$ are given by:

$$\begin{cases} \mathbf{\Phi}^{(i)} = \prod_{j=1}^{i-1} \left(\left[\mathbf{B}_{i-j}^{(i-j+1)} \right]^{-1} \cdot \mathbf{B}_{i-j}^{(i-j)} \right) \\ \mathbf{\Psi}^{(i)} = \left[\mathbf{B}_{i-1}^{(i)} \right]^{-1} \cdot \left\{ \mathbf{L}_{i-1}^{(i-1)} - \mathbf{L}_{i-1}^{(i)} + \sum_{j=1}^{i-2} \left[\prod_{k=1}^{j} \left(\mathbf{B}_{i-k}^{(i-k)} \cdot \left[\mathbf{B}_{i-k-1}^{(i-k)} \right]^{-1} \right) \right] \cdot \left(\mathbf{L}_{i-j-1}^{(i-j-1)} - \mathbf{L}_{i-j-1}^{(i-j)} \right) \right\} \end{cases} \tag{18.39}$$

$$\forall i \in \{2,3,...,n\}$$

where *dot* stands for scalar product. The equations (18.38)-(18.39) permit to write the generic unknowns sub-vector $\mathbf{X}^{(i)}$ as function of a transferring matrix $\mathbf{\Phi}^{(i)}$ and vector $\mathbf{\Psi}^{(i)}$, and the unknowns sub-vector $\mathbf{X}^{(1)}$. The problem is hence reduced to an algebraic one in which only the two coefficients – collected in $\mathbf{X}^{(1)}$ – related to the first phase have to be determined, by imposing two boundary conditions described by the equations obtained above. Therefore, in order to find the two unknowns collected in $\mathbf{X}^{(1)}$, it remains to rewrite the boundary conditions (18.22) in matrix form. In particular, by applying the equation (18.38) for $i = n$, we obtain the follows relationship:

$$\mathbf{X}^{(n)} = \mathbf{\Phi}^{(n)} \cdot \mathbf{X}^{(1)} + \mathbf{\Psi}^{(n)} \tag{18.40}$$

Then, the boundary conditions (18.22), become:

$$\mathbf{P} \cdot \mathbf{X}^{(1)} = \Upsilon \tag{18.41}$$

where the matrix $\mathbf{P}$ and vector Υ are given by**:**

$$\mathbf{P} = \left[\mathbf{P}_1 \quad \left(\mathbf{\Phi}^{(n)} \right)^T \cdot \mathbf{P}_2 \right]^T, \quad \Upsilon = \left[\Upsilon_1 \quad \Upsilon_2 \right]^T, \tag{18.42}$$

where $\mathbf{P}_1, \mathbf{P}_2$ are two vectors and Υ_1, Υ_2 are two scalars, as reported below:

$$\begin{aligned} \mathbf{P}_1 &= \left[\frac{E^{(1)}}{2\left(1-2\nu^{(1)}\right)}, -\frac{E^{(1)}}{\left(1+\nu^{(1)}\right)R^{(0)3}} \right]^T, \ \mathbf{P}_2 = \left[\frac{E^{(n)}}{2\left(1-2\nu^{(n)}\right)}, -\frac{E^{(n)}}{\left(1+\nu^{(n)}\right)R^{(n)3}} \right]^T \\ \Upsilon_1 &= -\frac{\alpha^{(1)}E^{(1)}T_R}{2\left(1-2\nu^{(1)}\right)} + \psi^{(1)}\left(\frac{A_1^{(1)}}{3} + \frac{A_2^{(1)}}{2R^{(0)}} \right) + \frac{p_i}{2}; \\ \Upsilon_2 &= -\frac{\alpha^{(n)}E^{(n)}T_R}{2\left(1-2\nu^{(n)}\right)} + \psi^{(n)}\left(\frac{A_1^{(n)}}{3} + \frac{A_2^{(n)}}{2R^{(n)}} \right) + \frac{p_e}{2} - \mathbf{P}_2 \cdot \mathbf{\Psi}^{(n)} \end{aligned} \tag{18.43}$$

Then, by inverting, all the $2 \times n$ unknown coefficients , we obtain the unknown parameters:

$$\begin{cases} \mathbf{X}^{(1)} = \mathbf{P}^{-1} \cdot \Upsilon, \\ \mathbf{X}^{(i)} = \mathbf{\Phi}^{(i)} \cdot \mathbf{P}^{-1} \cdot \Upsilon + \mathbf{\Psi}^{(i)} \quad \forall i \in \{2,3,...,n\} \end{cases} \tag{18.44}$$

By substituting the relationships (18.44) and (18.28) in equation (18.16), we obtain the explicit analytical expression of displacement solution in each phases of multilayered sphere.

18.3. Parametric analysis for multilayered sphere composed by two phases

Let us consider a multilayer sphere composed by two hollow spheres. The inner radius of the sphere is assumed to be $R^{(0)}$ and the thickness of any phases is equal to δ. Then, we can write the following relationships:

$$R^{(1)} = \left(1+\xi\right)R^{(0)}, \ R^{(2)} = \left(1+2\xi\right)R^{(0)}, \quad \xi = \delta / R^{(0)}, \tag{18.45}$$

The multilayered sphere is subjected only the gradient of temperature between the internal and external surfaces $\Delta T = T_e - T_i$, but the internal and external pressure are assumed vanishing.

We consider four cases :

(i) variation of Poisson's ratio in two phases, with fixed values of the Young's moduli, thermal conductivity coefficient and linear thermal expansion coefficient;

(ii) variation of Young's moduli in two phases, with fixed values of the Poisson's ratio, thermal conductivity coefficient and linear thermal expansion coefficient;

(iii) variation of linear thermal expansion coefficient in two phases, with fixed values of the Young's moduli, Poisson's ratio and thermal conductivity coefficient;

(iv) variation of thermal conductivity coefficient in two phases, with fixed values of the Young's moduli, Poisson's ratio and linear thermal expansion coefficient;

Let us assume the following non-dimensional parameter for graphics of the displacement, strain and stress functions:

$$\begin{aligned} &\overline{r} = \frac{r - R^{(0)}}{R^{(n)} - R^{(0)}};\ \overline{T} = \frac{T^{(i)} - T_i}{T_e - T_i};\ \overline{u}_r^{(i)} = \frac{u_r^{(i)}}{\alpha^{(1)}\left(T_e - T_i\right)R^{(0)}/2};\ \overline{\varepsilon}_{rr}^{(i)} = \frac{\varepsilon_{rr}^{(i)}}{\alpha^{(1)}\left(T_e - T_i\right)/2}; \\ &\overline{\varepsilon}_{\theta\theta}^{(i)} = \frac{\varepsilon_{\theta\theta}^{(i)}}{\alpha^{(1)}\left(T_e - T_i\right)/2};\ \overline{\sigma}_{rr}^{(i)} = \frac{\sigma_{rr}^{(i)}}{\beta^{(1)}};\ \overline{\sigma}_{\theta\theta}^{(i)} = \frac{\sigma_{\theta\theta}^{(i)}}{\beta^{(1)}};\ \overline{\sigma}_{eq}^{(i)} = \frac{\sigma_{eq}^{(i)}}{\beta^{(1)}};\quad \sigma_{eq}^{(i)} = \sqrt{\left(\sigma_{\theta\theta}^{(i)} - \sigma_{rr}^{(i)}\right)^2}; \end{aligned} \tag{18.46}$$

where $\beta^{(1)}$ is given by follows relationship:

$$\beta^{(1)} = \left[\alpha^{(1)} E^{(1)}\left(T_e - T_i\right)\right] \Big/ \left[2\left(1 - \nu^{(1)}\right)\right]; \tag{18.47}$$

In the first case (i) let us assume $E^{(1)} = E^{(2)},\ k^{(1)} = k^{(2)},\ \alpha^{(1)} = \alpha^{(2)}$, then the only free parameters are Poisson's ratio in two phases. Let us consider six cases in which is fixed Poisson's ratio of the phase (1) $\nu^{(1)} = 0.3$, but in phase (2) the Poisson's ratio assume the following values: 0, 0.1, 0.2, 0.3, 0.4, 0.49. The Fig. 18.2 shows the radial displacement along radial direction. Fig. 18.3 and 18.4 show the radial and circumferential strain along radial direction, respectively. In particular, if the ratio $\nu^{(2)}/\nu^{(1)}$ increase, then the radial and circumferential strain increase along radial direction as shown the figures 18.3 and 18.4. If the ratio $\nu^{(2)}/\nu^{(1)}$ increase, then the radial and circumferential stress increase, as shown the figures 18.5 and 18.6. The equivalent stress determines whether yielding occurs. For planar isotropy and non-homogeneity in radial direction, the equivalent stress based on the Henchy- von Mises criteria is given by follows equation:

$$\sigma_{eq} = \sigma_{\theta\theta}^{(i)} - \sigma_{rr}^{(i)} \tag{18.48}$$

The non-dimensional graphics of the radial displacement, strain and stress as reported below:

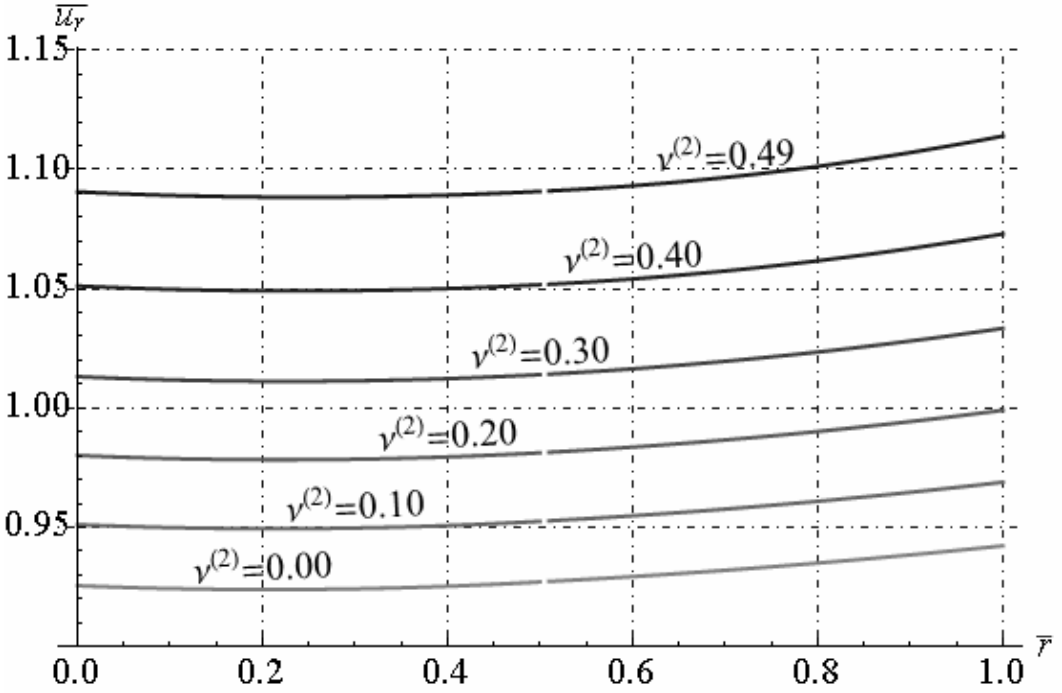

Fig. 18.2 - *Non-dimensional radial displacement along radial direction* $(\nu^{(1)} = 0.3)$

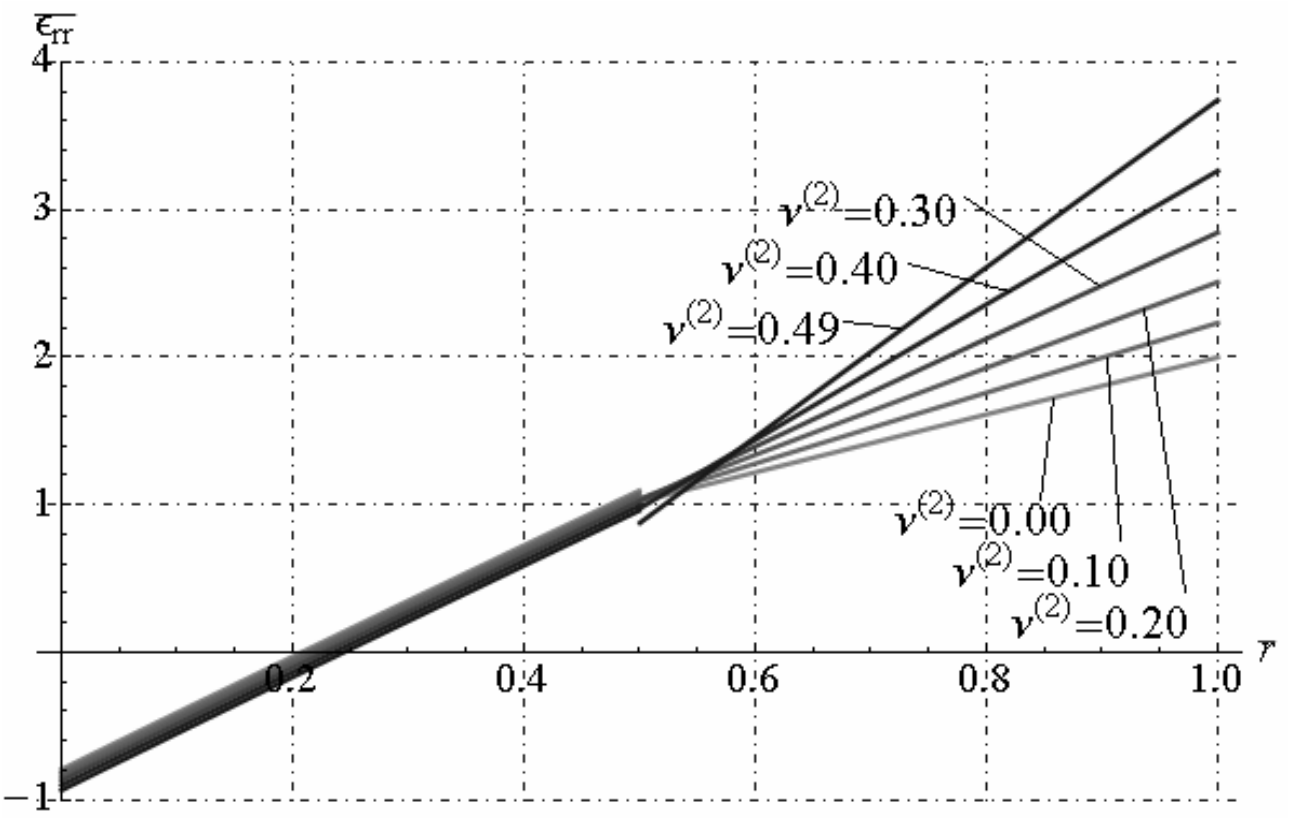

Fig. 18.3 - *Non-dimensional radial strain distribution along radial direction* $(\nu^{(1)} = 0.3)$

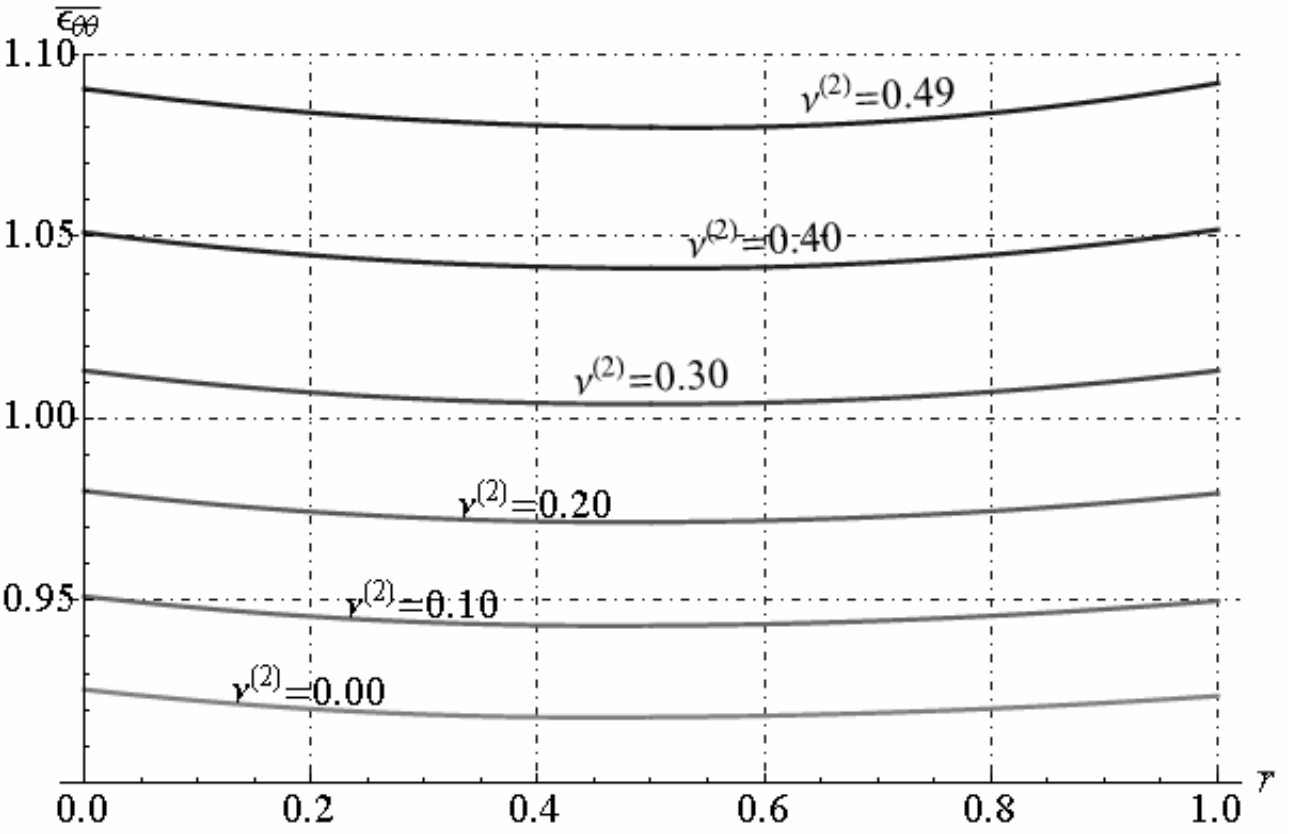

Fig. 18.4 - *Non-dimensional circumferential strain along radial direction* $(\nu^{(1)} = 0.3)$

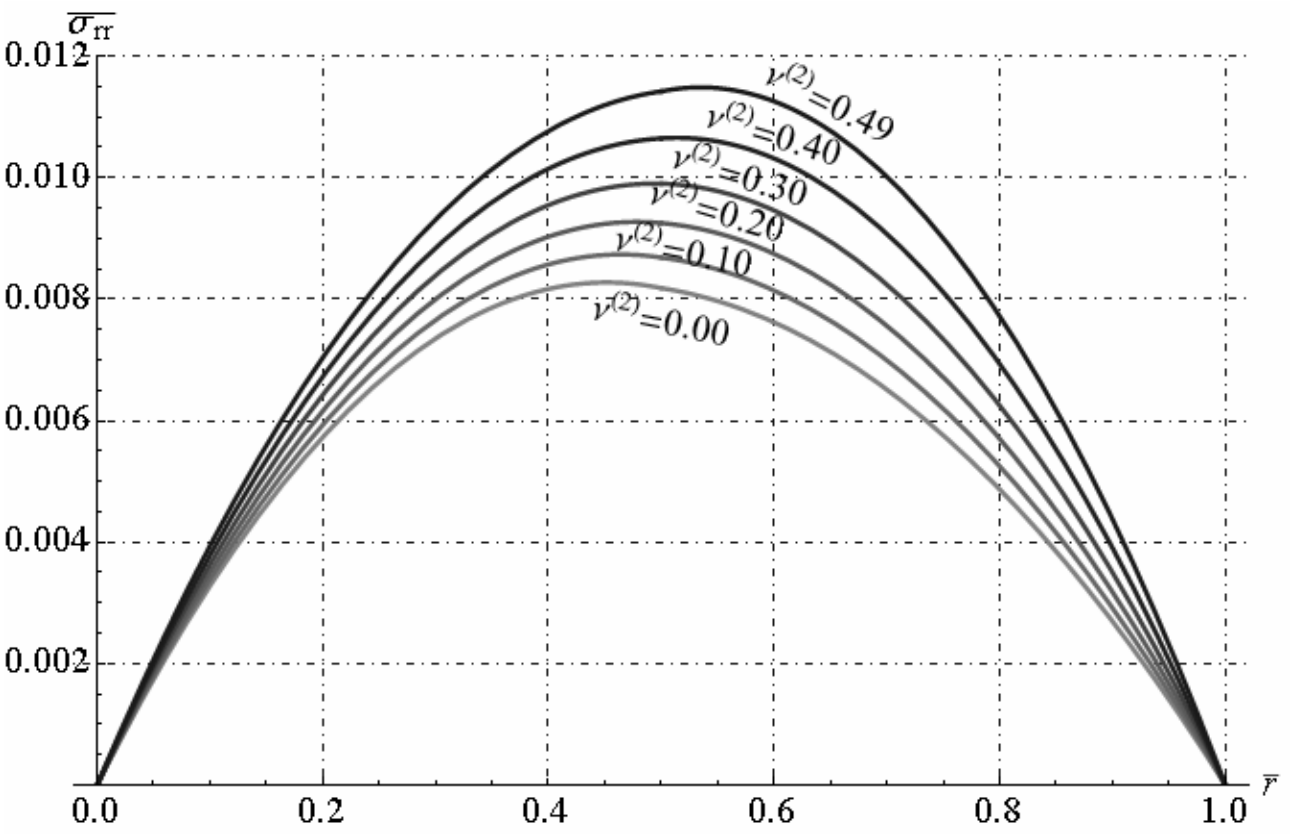

Fig. 18.5 - *Non-dimensional radial stress distribution along radial direction* $(\nu^{(1)} = 0.3)$

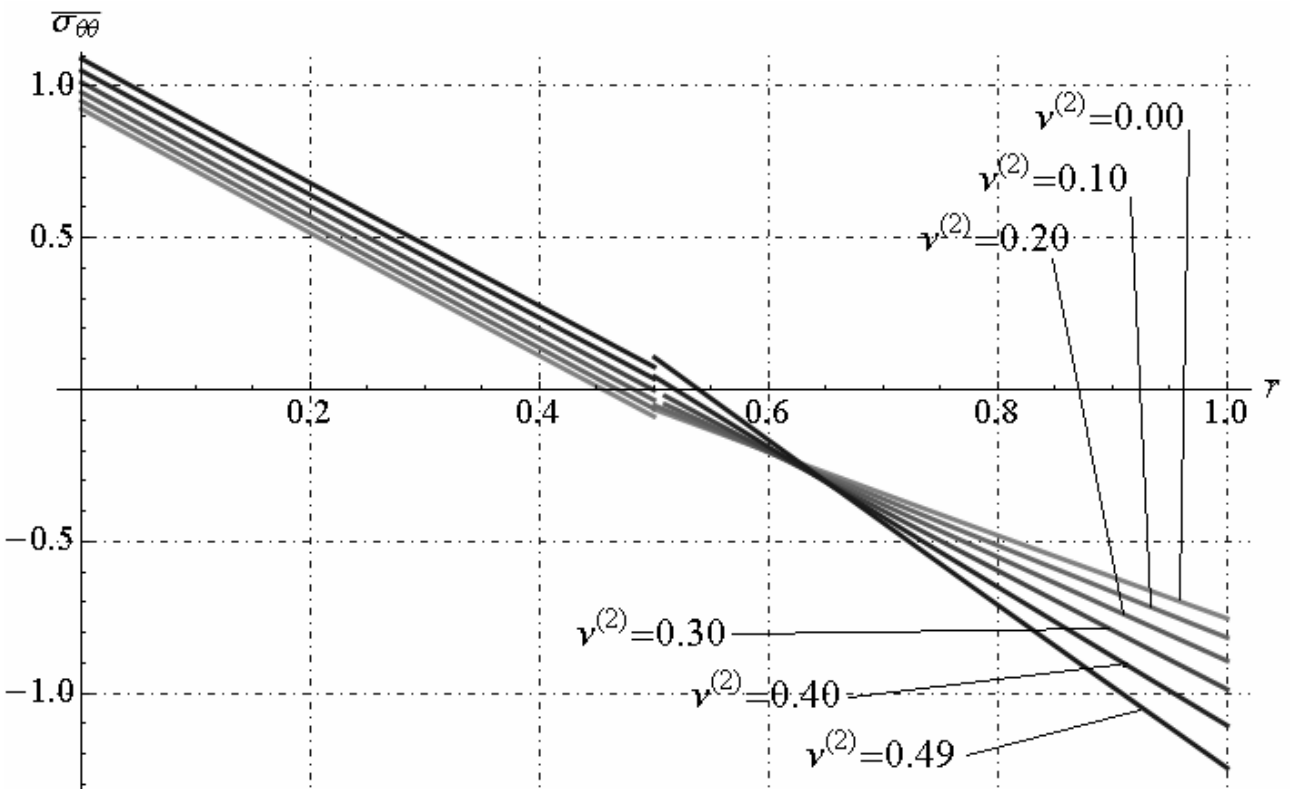

Fig. 18.6 - *Non-dimensional circumferential stress along radial direction* $(\nu^{(1)} = 0.3)$

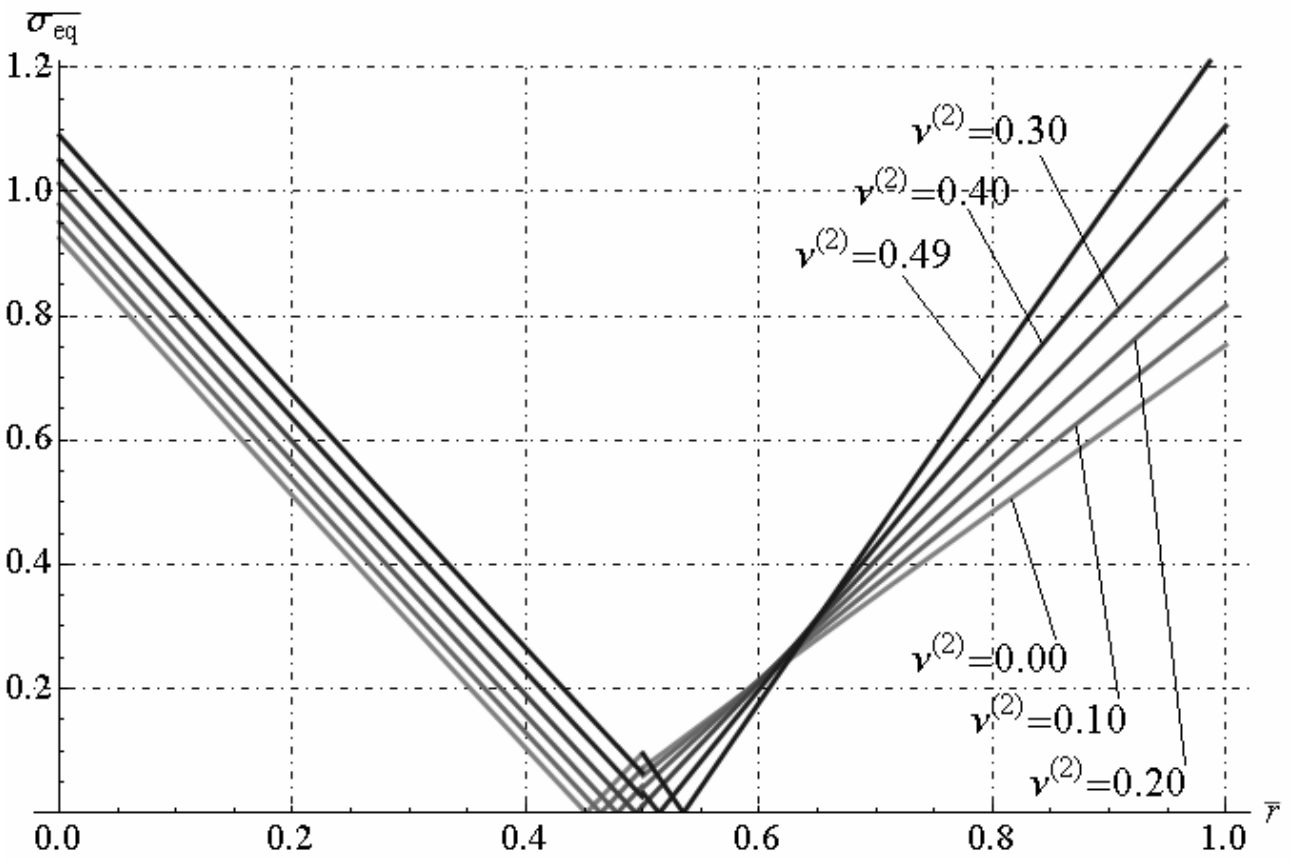

Fig. 18.7 - *Non-dimensional equivalent stress along radial direction* $(\nu^{(1)} = 0.3)$

In the second case (ii) let us assume $\nu^{(1)} = \nu^{(2)}$, $k^{(1)} = k^{(2)}$, $\alpha^{(1)} = \alpha^{(2)}$, then the only free parameters are Young's moduli in two phases. Let us consider six cases in which are selected the different ratio of the Young's moduli $E^{(2)}/E^{(1)}$ as follows : 0.1, 0.5, 1.0, 2.0, 5.0. Figure 18.9 shows that if the ratio $E^{(2)}/E^{(1)}$ increase the radial strain decrease in both phases.

Conversely, Figure 18.10 shows that if the ratio $E^{(2)}/E^{(1)}$ increase the circumferential strain increase in both phases. Fig. 18.11 and 18.12 show the radial and circumferential stress along radial direction, respectively. As expected, the circumferential stress distribution exhibits significant jumps at all interfaces as shown in Fig. 18.12. These discontinuities are due to the differences between Young's modulus. The circumferential stress varies characteristically in each layer in view of the occurrence of discontinuities at all interfaces shown in the Fig. 18.12. In particular, if the ratio $E^{(2)}/E^{(1)}$ increase, the radial, circumferential and equivalent stress increase along radial direction as shown the figures 18.11, 18.12 and 18.13.

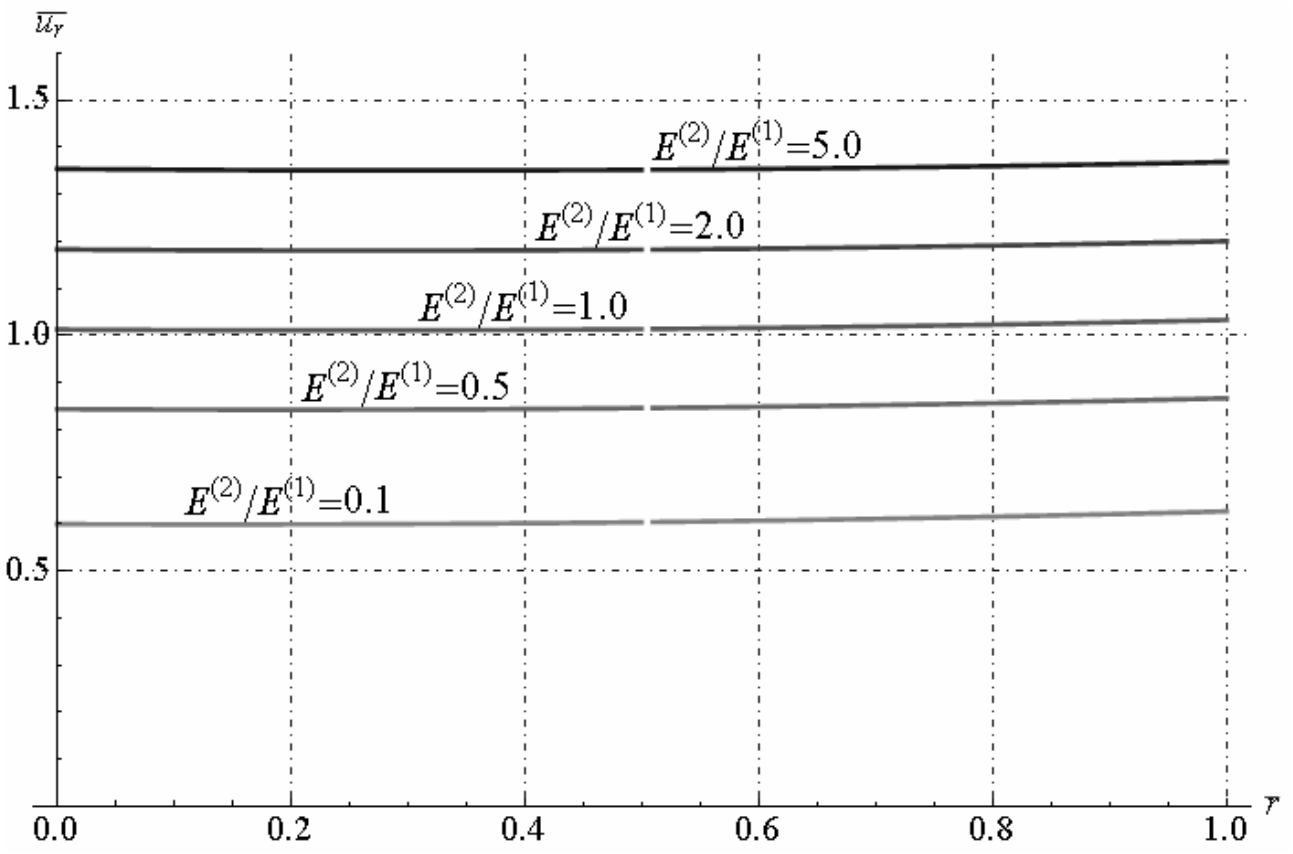

Fig. 18.8 - *Non-dimensional radial displacement along radial direction (Young's moduli variation)*

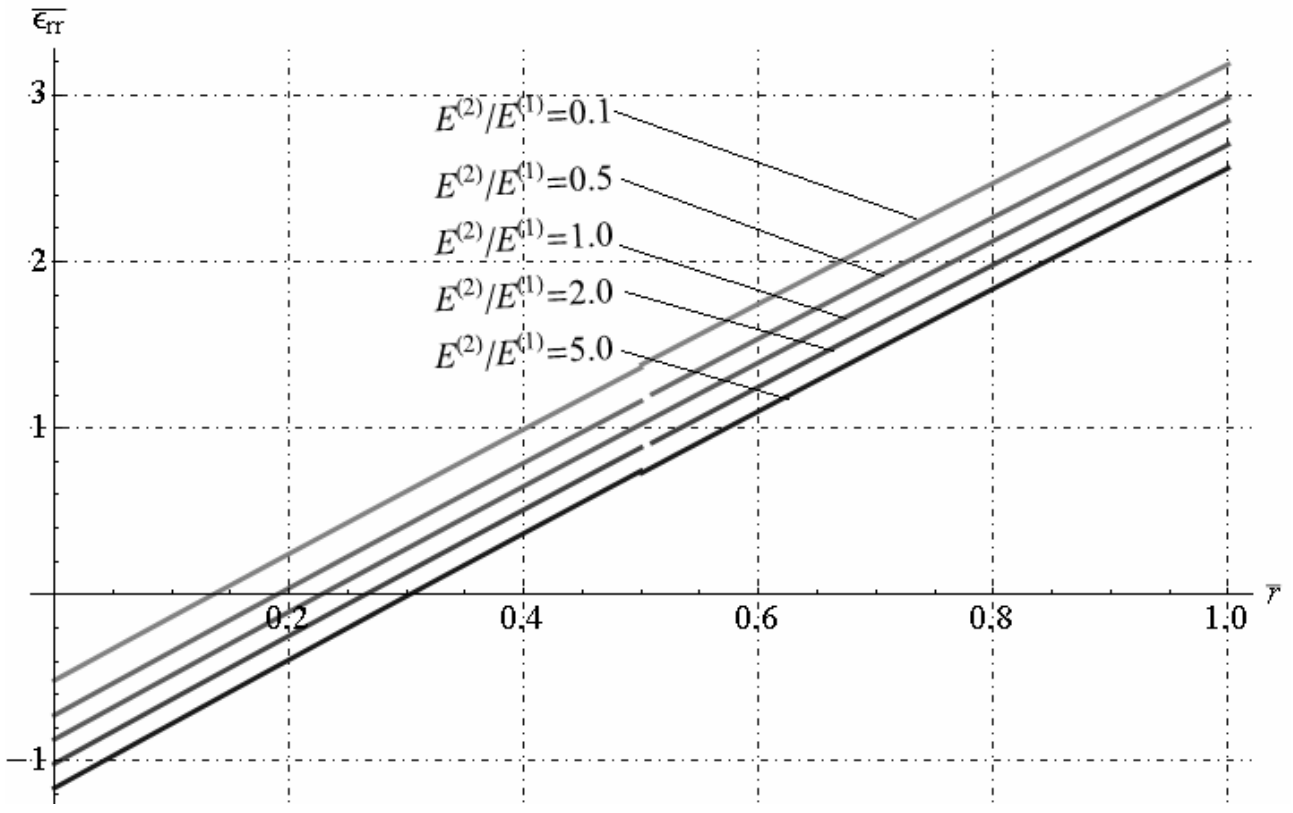

Fig. 18.9 - *Non-dimensional radial strain along radial direction (Young's moduli variation)*

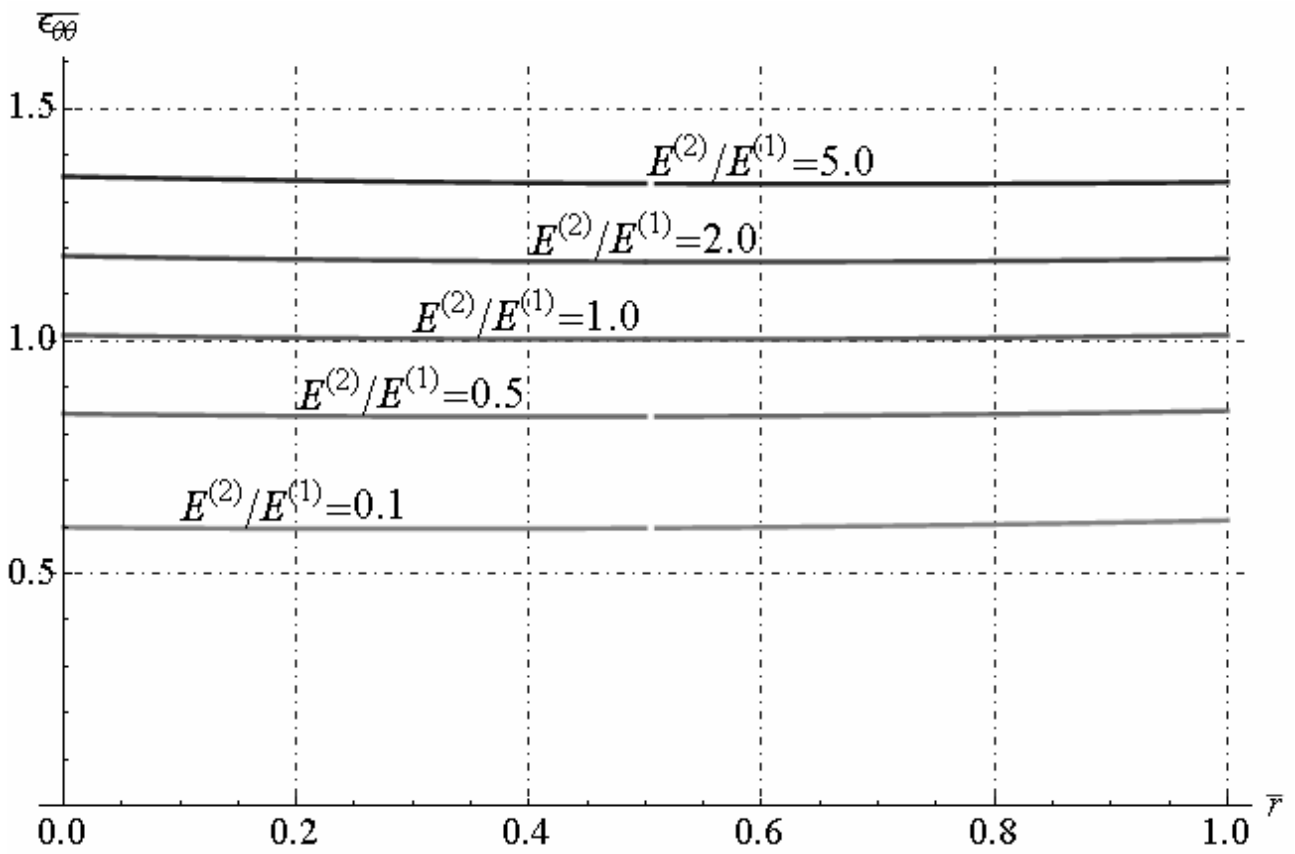

Fig. 18.10 - *Non-dimensional circumferential strain along radial direction (Young's moduli variation)*

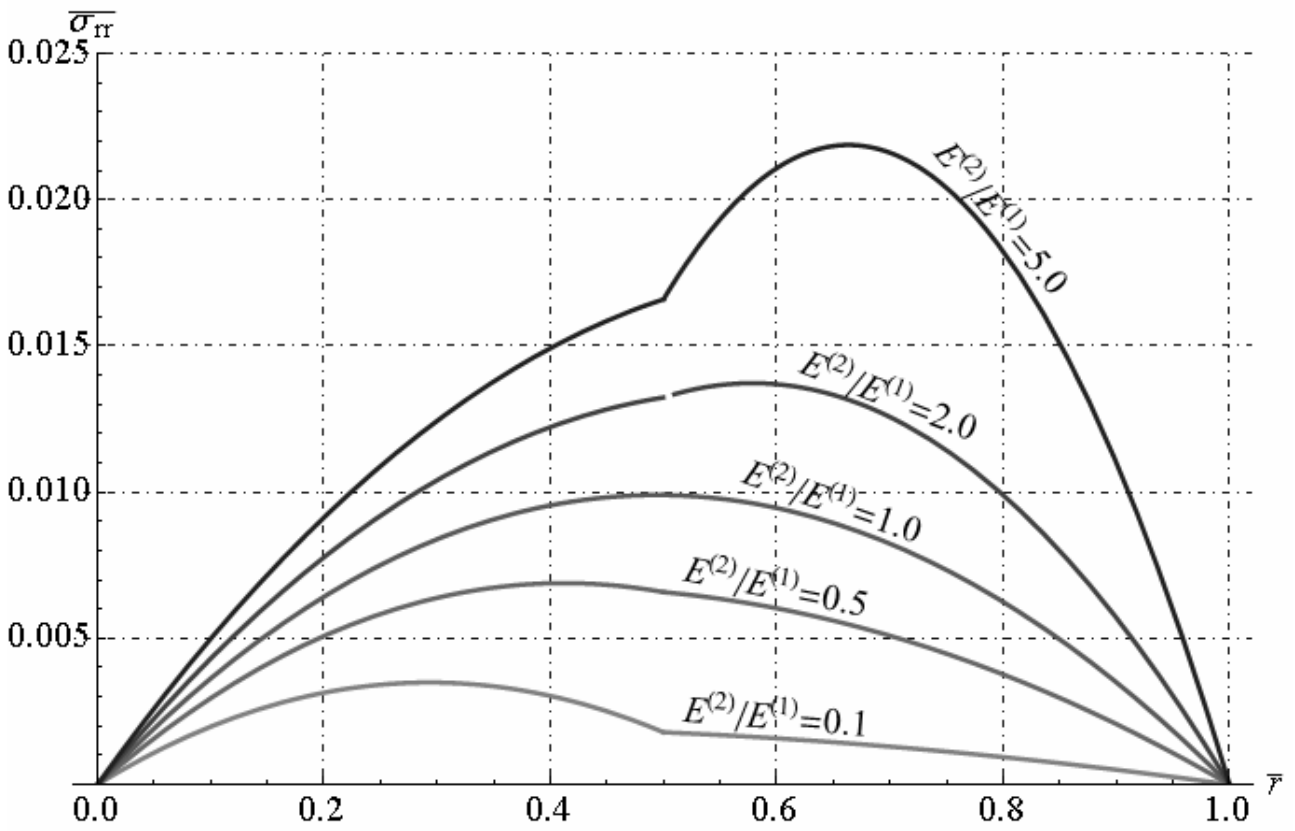

Fig. 18.11 - *Non-dimensional radial stress along radial direction (Young's moduli variation)*

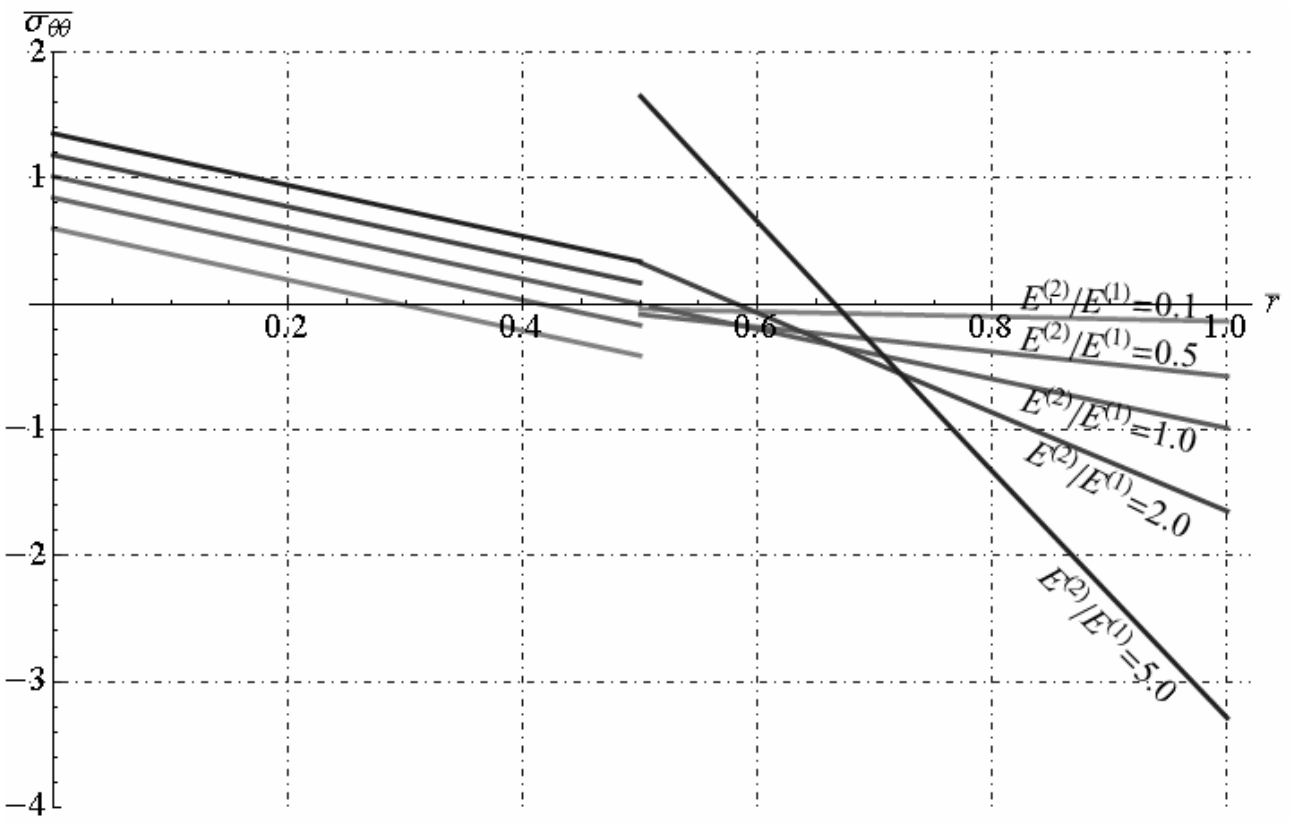

Fig. 18.12 - *Non-dimensional circumferential stress along radial direction (Young's moduli variation)*

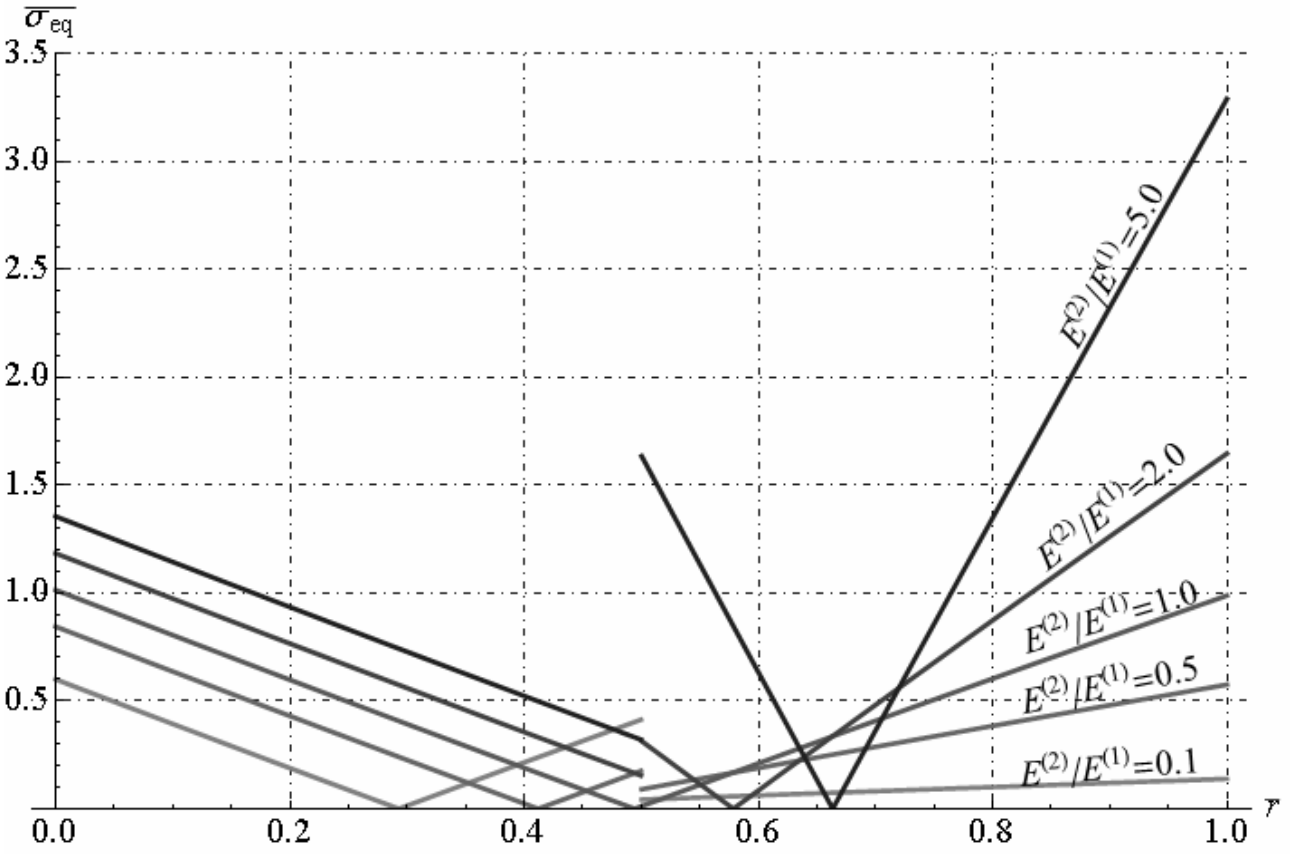

Fig. 18.13 - *Non-dimensional equivalent stress along radial direction (Young's moduli variation)*

In the third case (iii) let us assume $E^{(1)} = E^{(2)}$, $\nu^{(1)} = \nu^{(2)} = 0.3$, $k^{(1)} = k^{(2)}$, then the only free parameters are linear thermal expansion coefficient in two phases. Let us consider six cases in which are selected the different ratio of linear thermal expansion coefficient $\alpha^{(2)}/\alpha^{(1)}$ as follows : 0.1, 0.5, 0.8, 1.0, 1.5, 2.0. Figure 18.14 shows that if the ratio $\alpha^{(2)}/\alpha^{(1)}$ increase, then the radial displacement and circumferential strain increase. Moreover, if the ratio $\alpha^{(2)}/\alpha^{(1)}$ increase, then the radial strain increase in phase (2) and decrease in phase (1). The radial and circumferential stress increase with ratio $\alpha^{(2)}/\alpha^{(1)}$ in both phases.

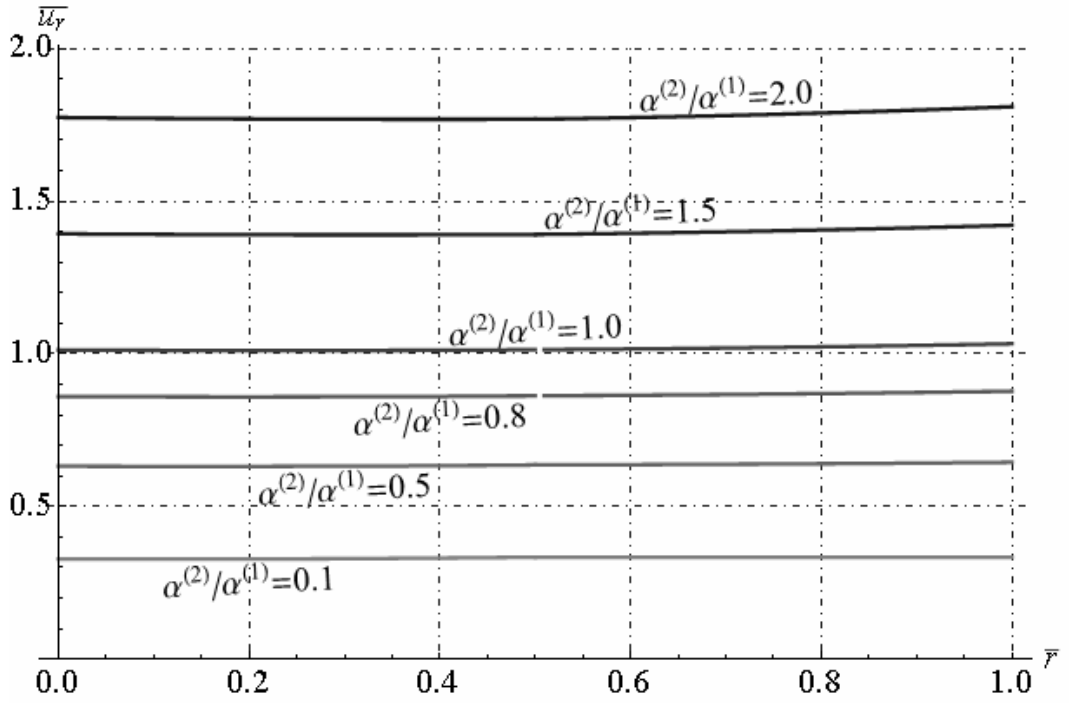

Fig. 18.14. *Non-dimensional radial displacement along radial direction (Linear thermal expansion coefficient variation)*

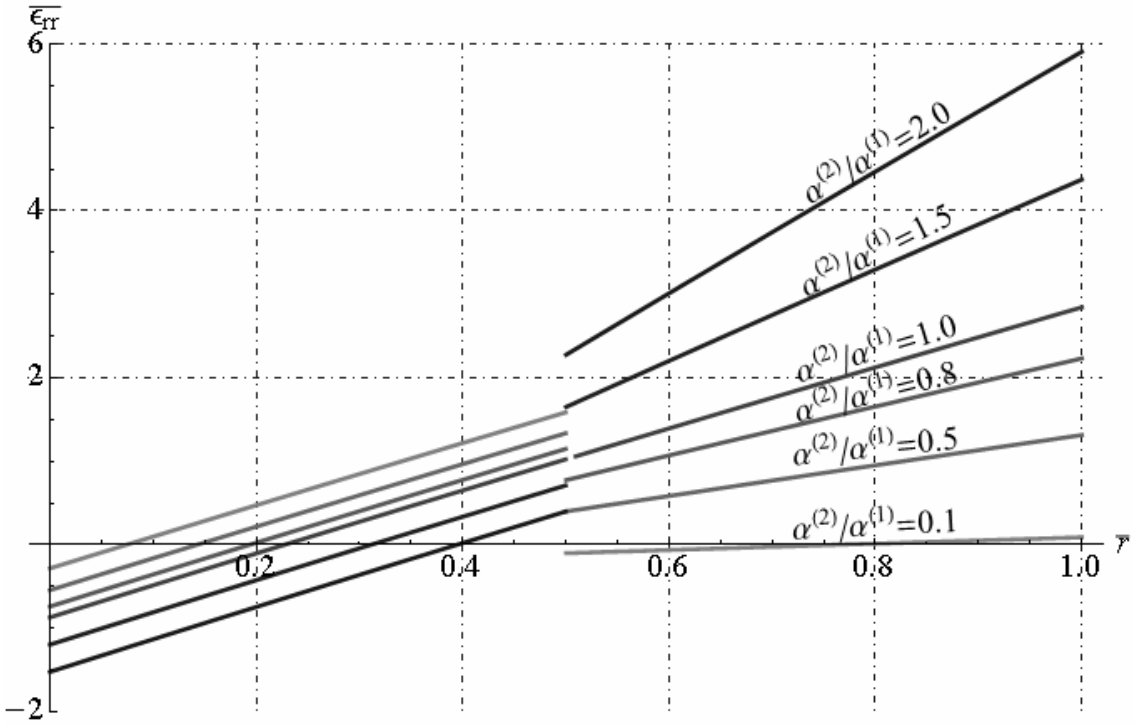

Fig. 18.15 - *Non-dimensional radial strain along radial direction (Linear thermal expansion coefficient variation)*

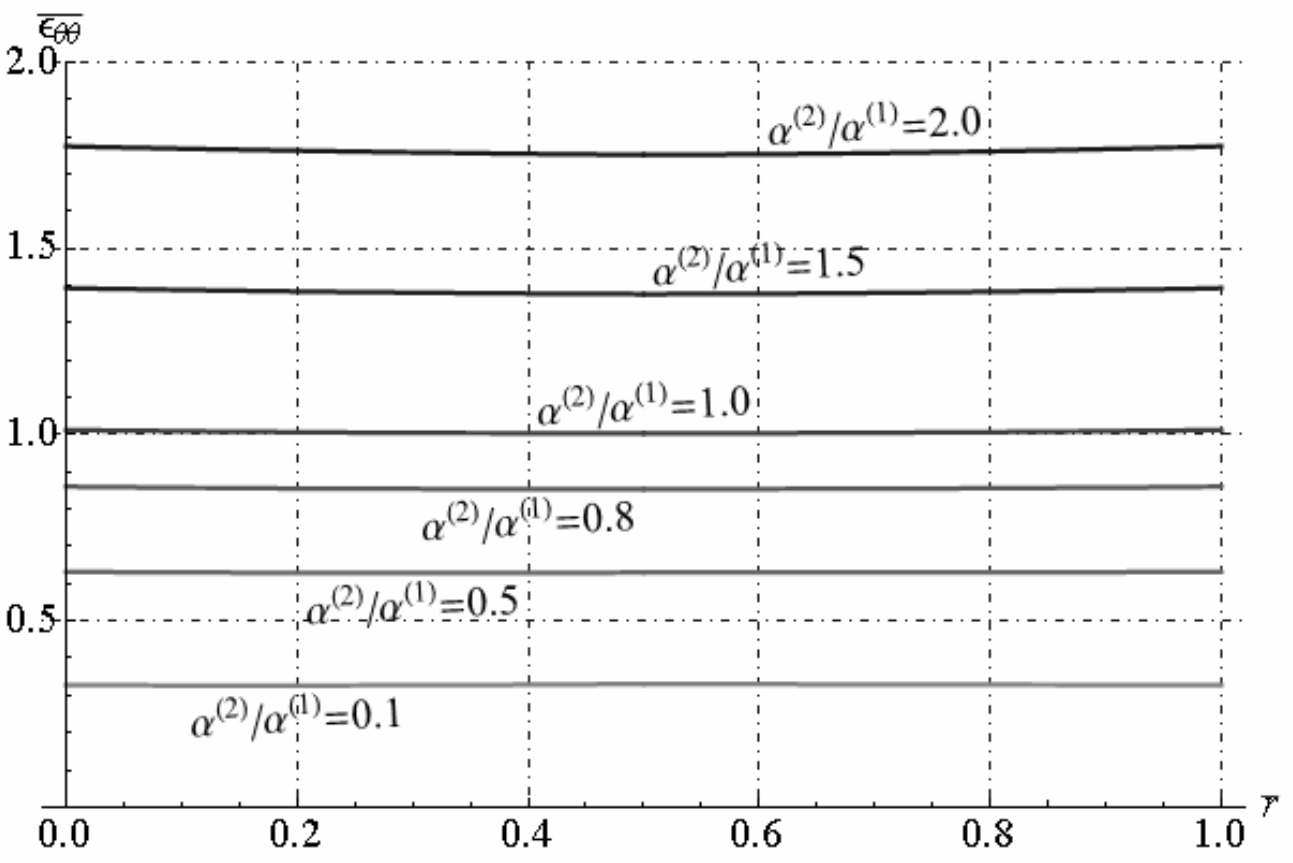

Fig. 18.16 - *Non-dimensional circumferential strain along radial direction (Linear thermal expansion coefficient variation)*

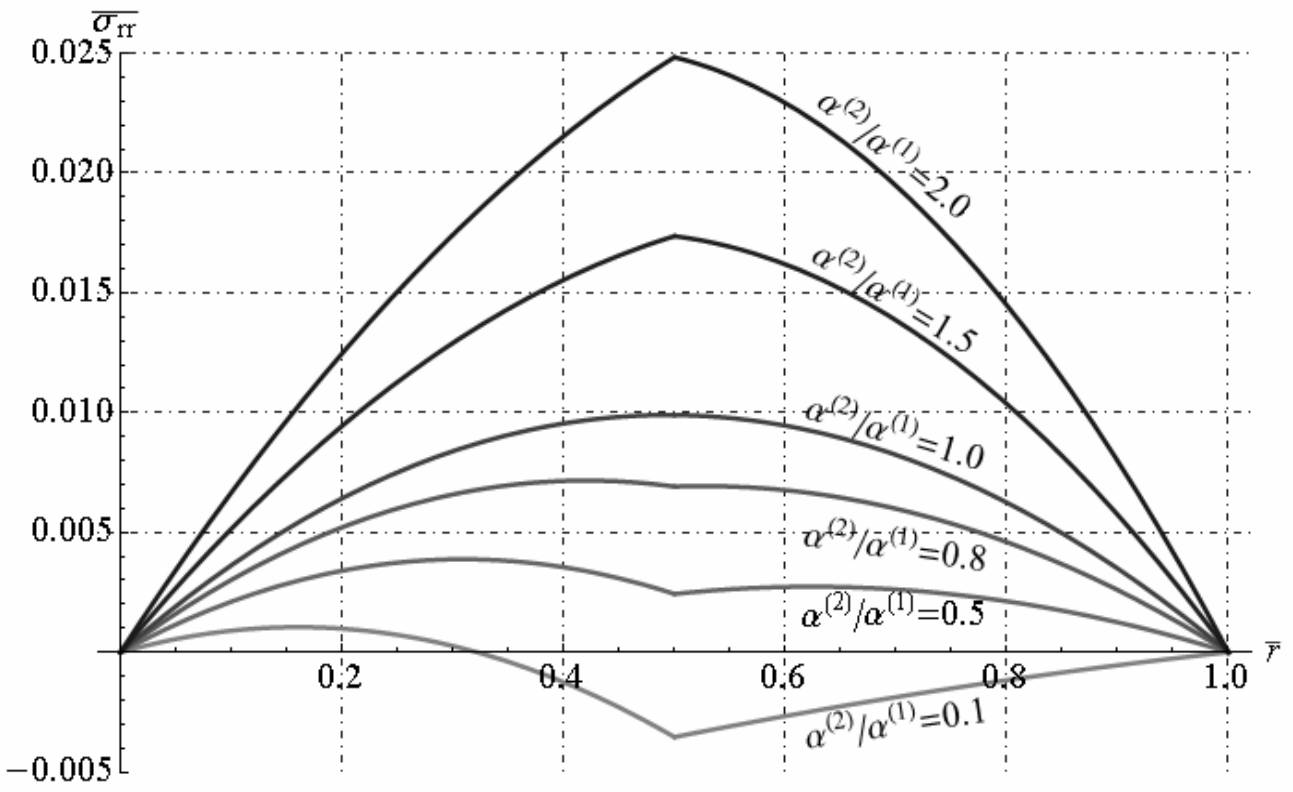

Fig. 18.17 - *Non-dimensional radial stress along radial direction (Linear thermal expansion coefficient variation)*

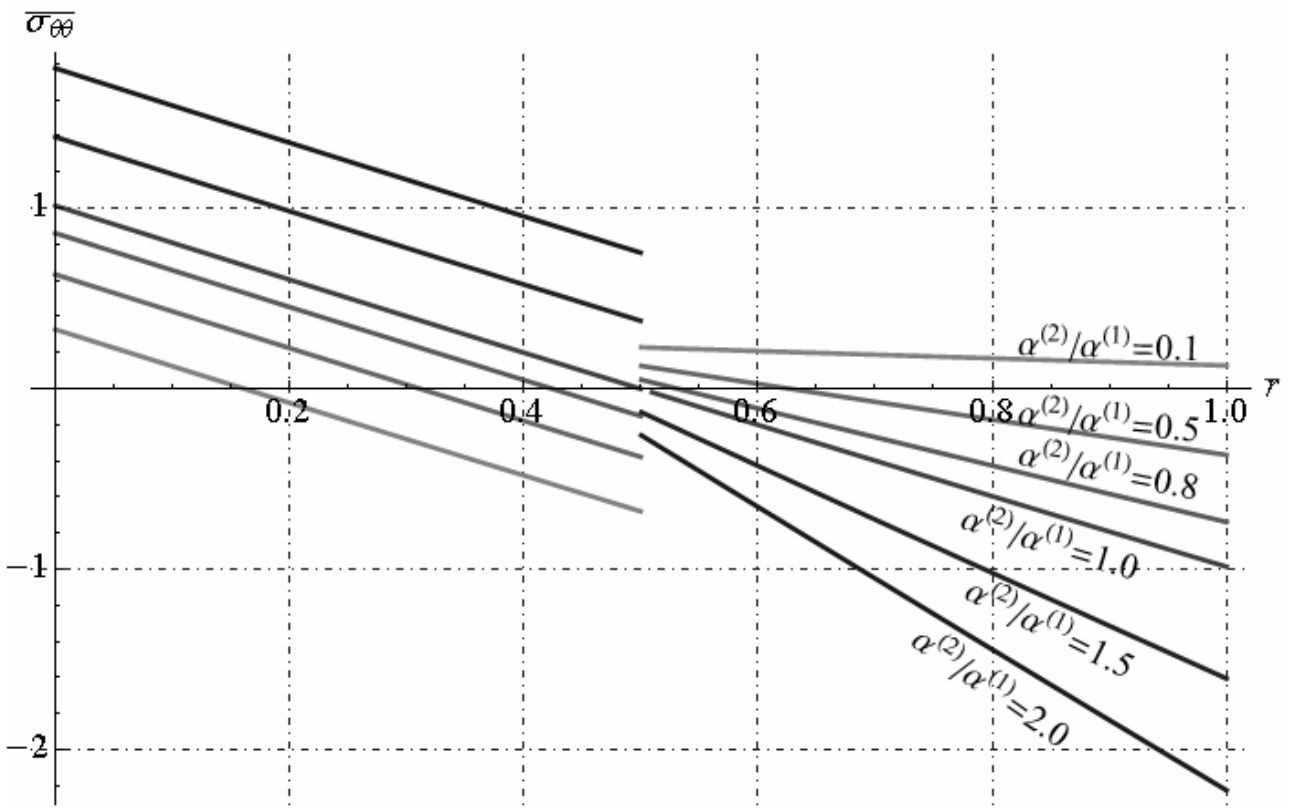

Fig. 18.18. *Non-dimensional circumferential stress along radial direction (Linear thermal expansion coefficient variation*)

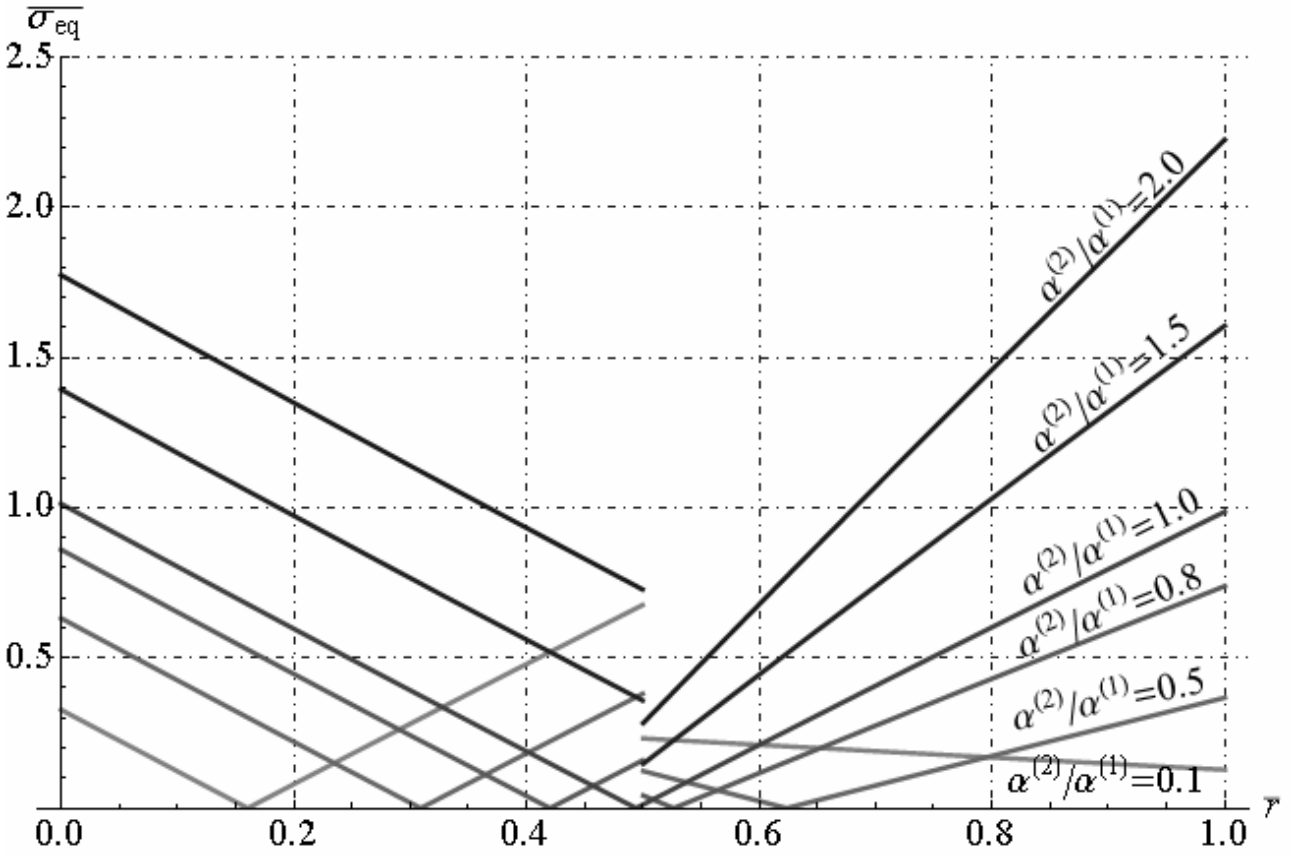

Fig. 18.19 - *Non-dimensional equivalent stress along radial direction (Linear thermal expansion coefficient variation)*

In the four case (iv) let us assume $E^{(1)} = E^{(2)}$, $\nu^{(1)} = \nu^{(2)} = 0.3$, $\alpha^{(1)} = \alpha^{(2)}$, then the only free parameters are thermal conductivity coefficient in two phases. Let us consider six cases in which are selected the different ratio of thermal conductivity coefficient $k^{(2)}/k^{(1)}$ as follows : 0.1, 0.5, 1.0, 2.0, 5.0. In particular if the ratio $k^{(2)}/k^{(1)}$ increase, then the radial displacement and circumferential strain increase along radial direction. The maximum value of radial stress is reached in phase (2) if $k^{(2)} < k^{(1)}$.

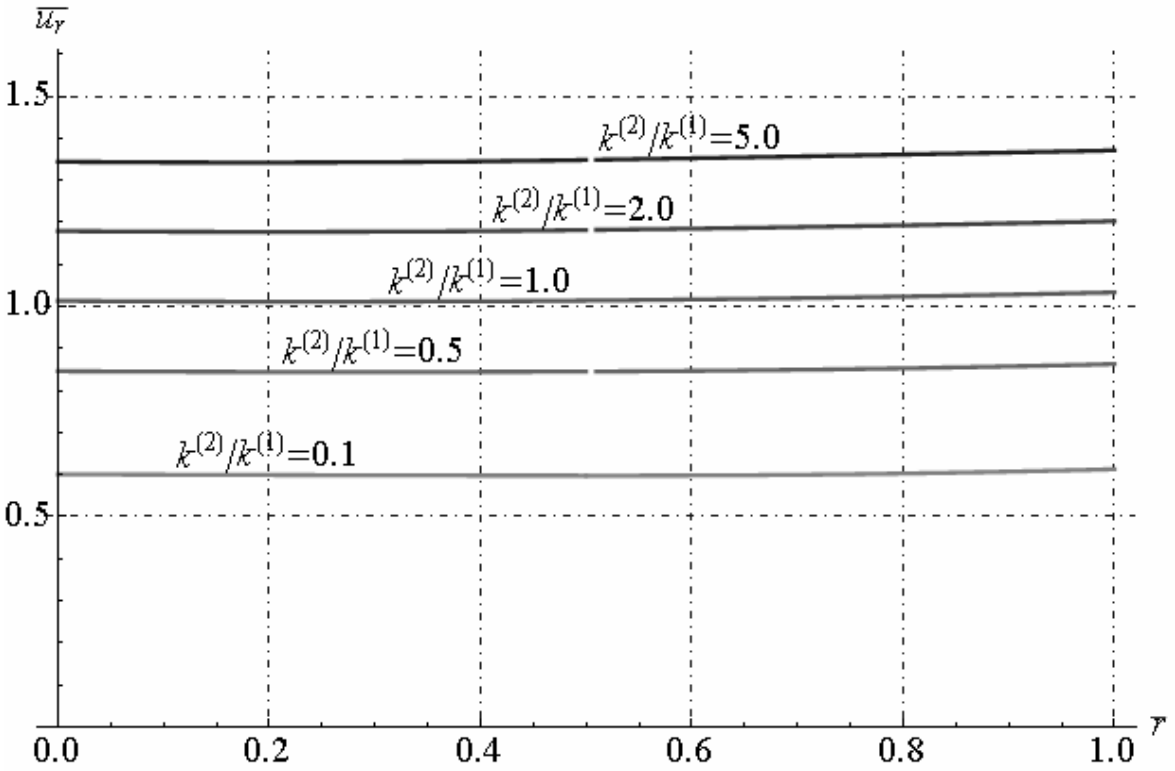

Fig. 18.20. *Non-dimensional radial displacement along radial direction (Thermal conductivity coefficient variation)*

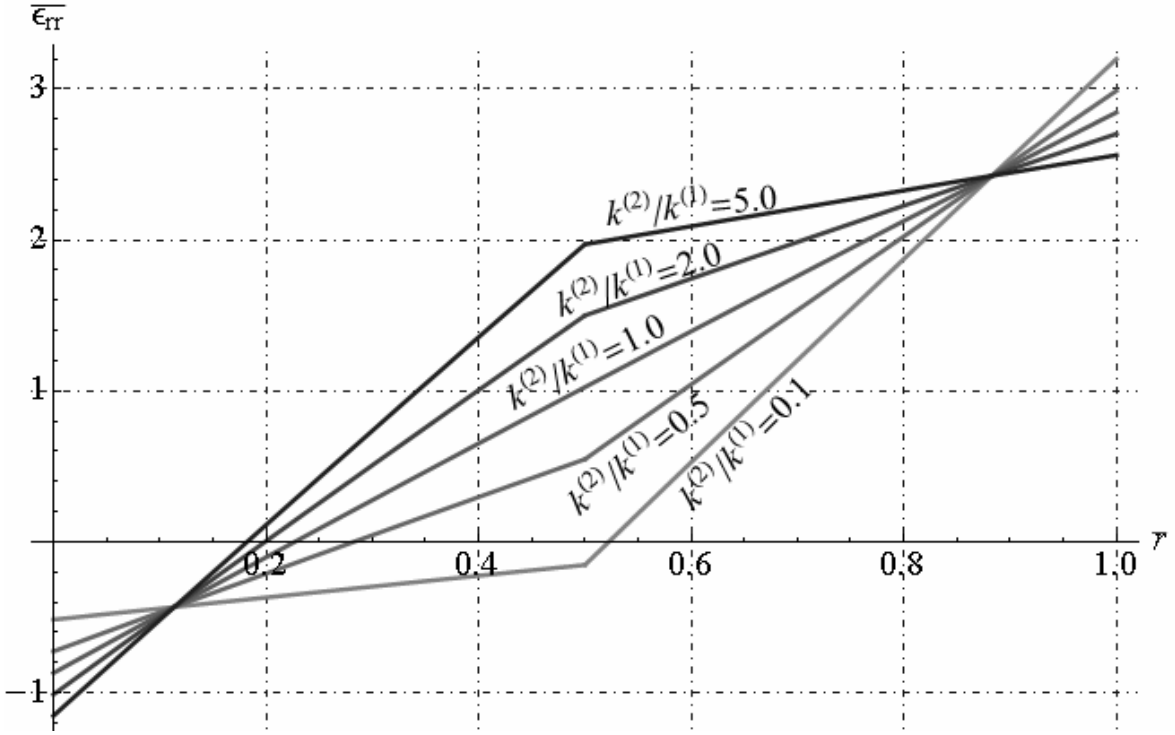

Fig. 18.21 - *Non-dimensional radial strain along radial direction (Thermal conductivity coefficient variation)*

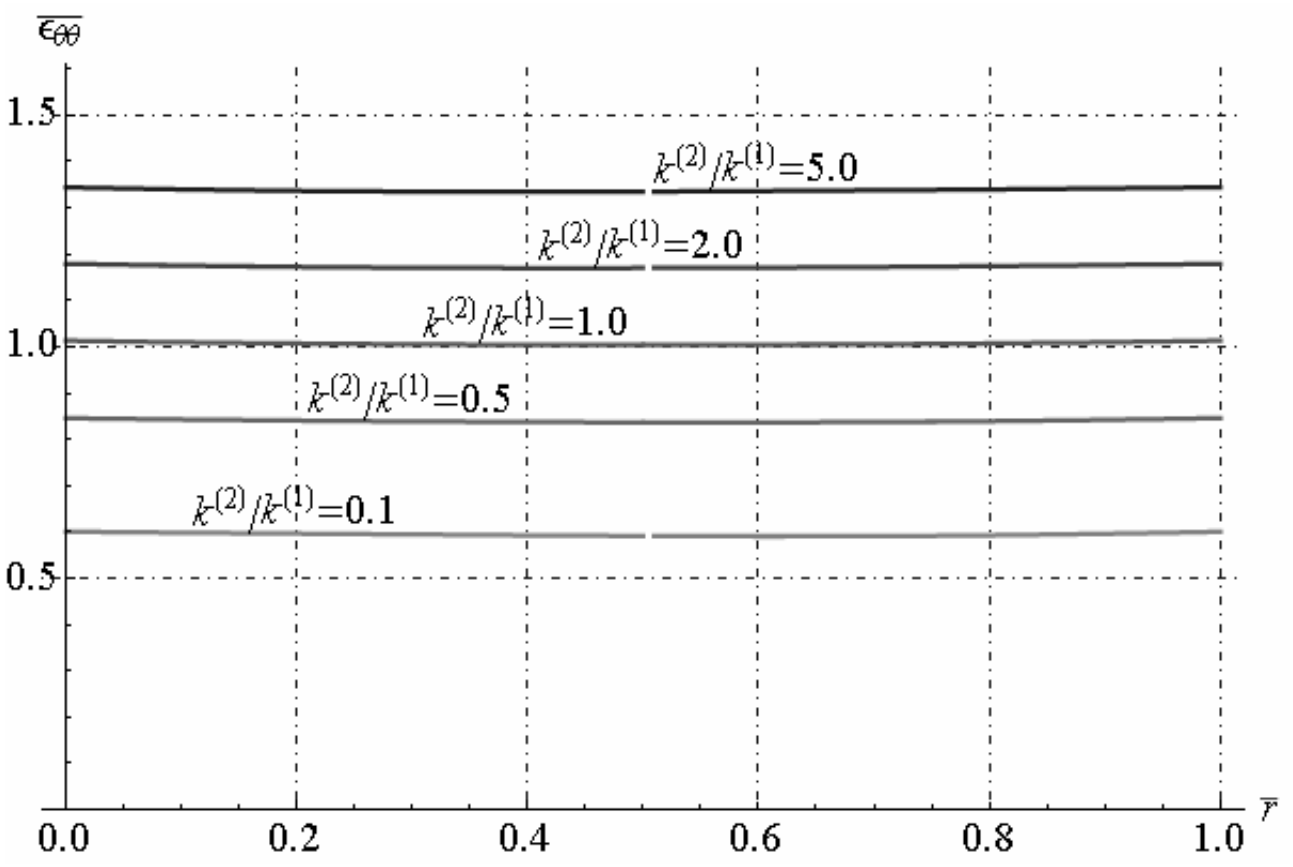

Fig. 18.22 - *Non-dimensional circumferential strain along radial direction (Thermal conductivity coefficient variation)*

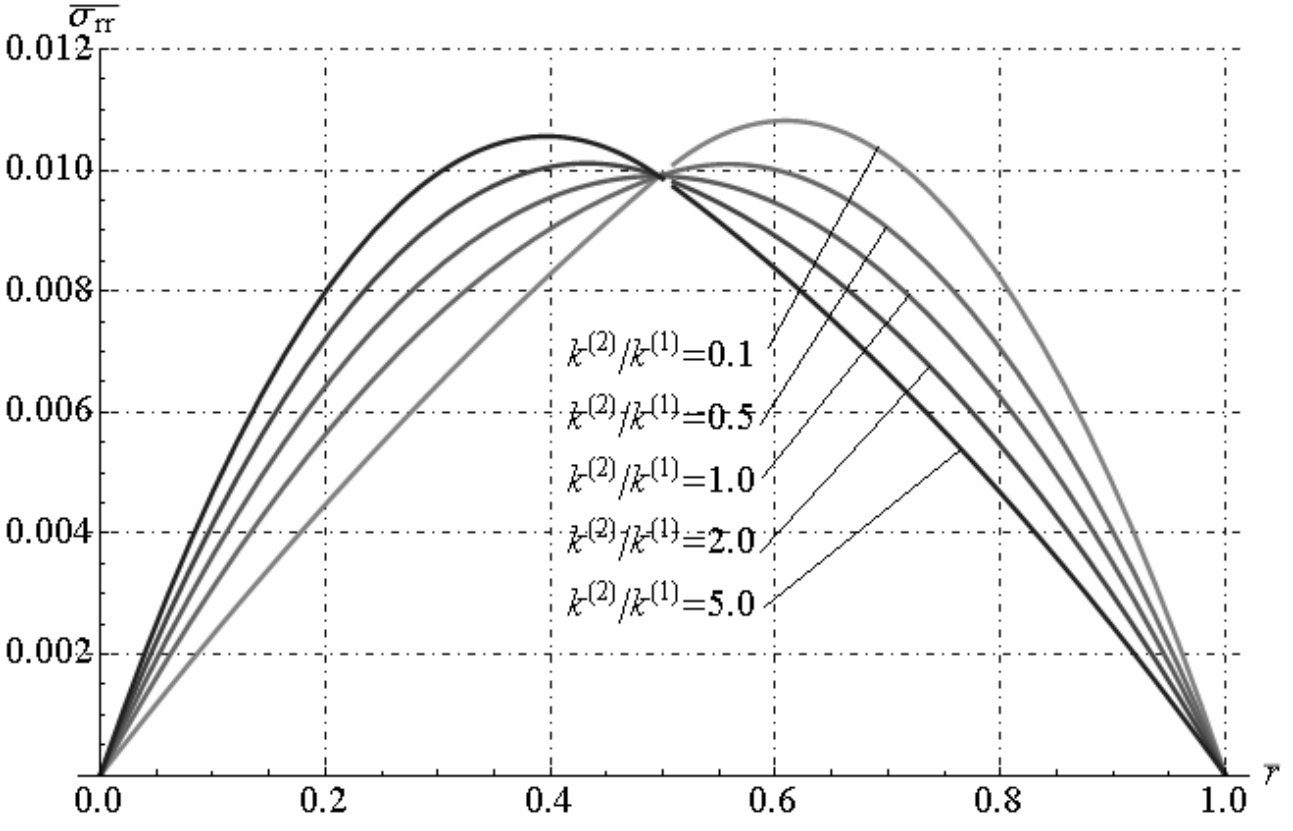

Fig. 18.23 - *Non-dimensional radial stress along radial direction (Thermal conductivity coefficient variation)*

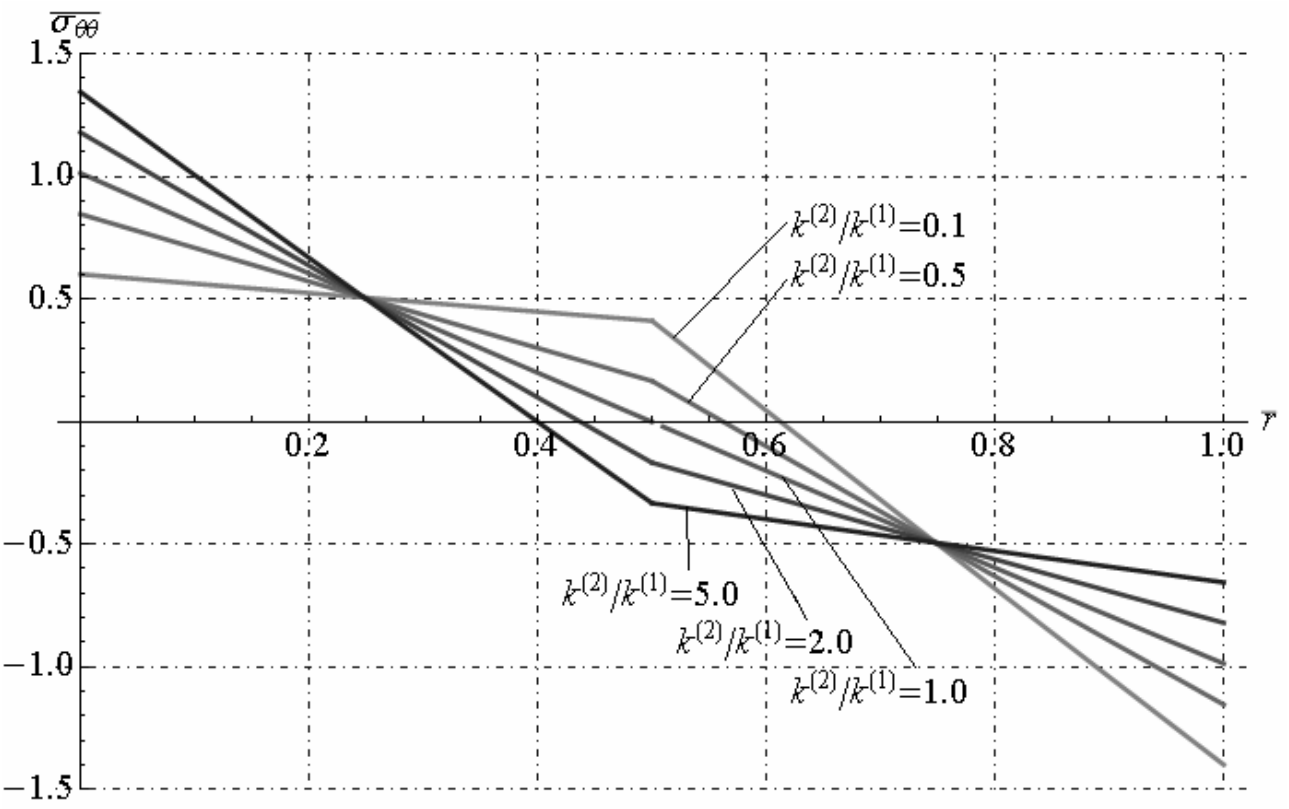

Fig. 18.24 - *Non-dimensional circumferential stress along radial direction (Thermal conductivity coefficient variation*)

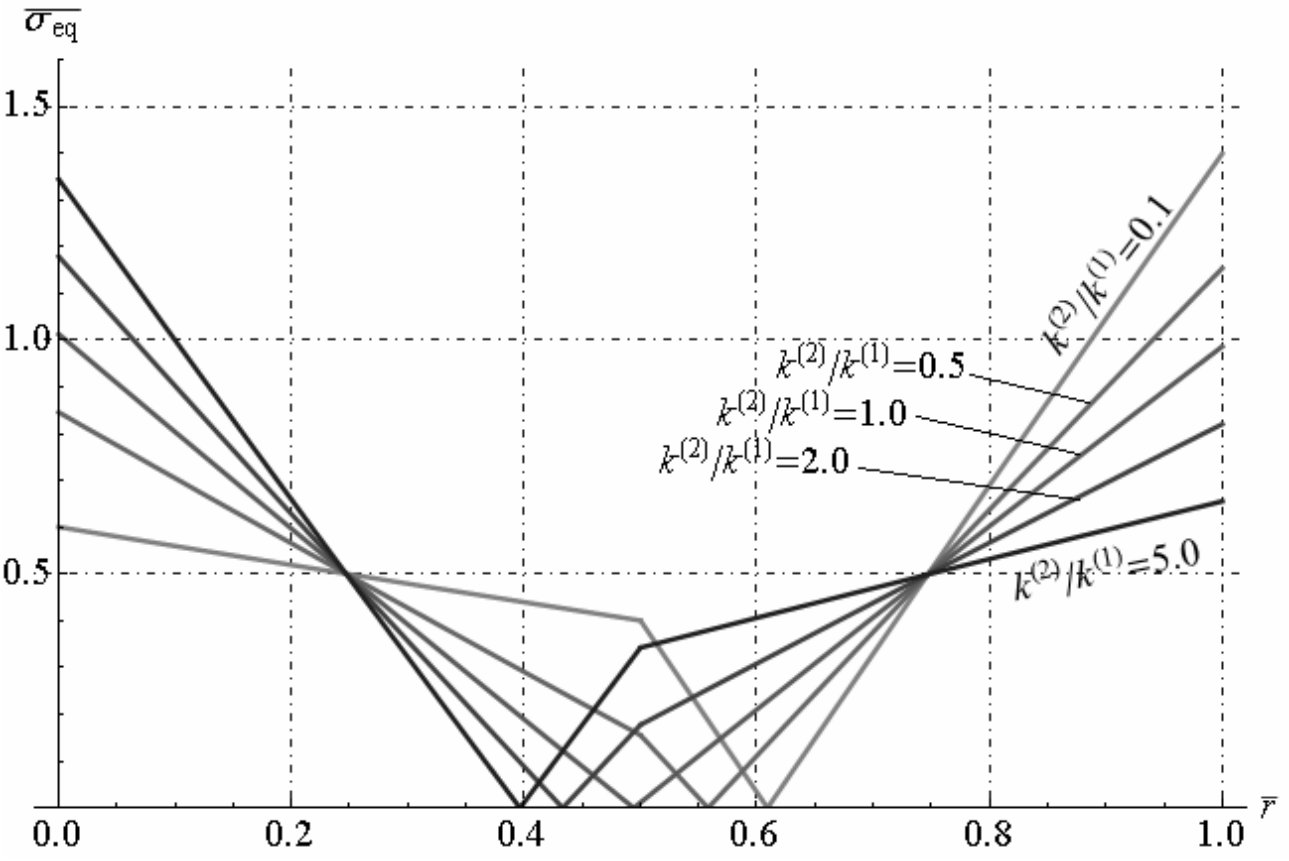

Fig. 18.25 - *Non-dimensional equivalent stress along radial direction (Thermal conductivity coefficient variation)*

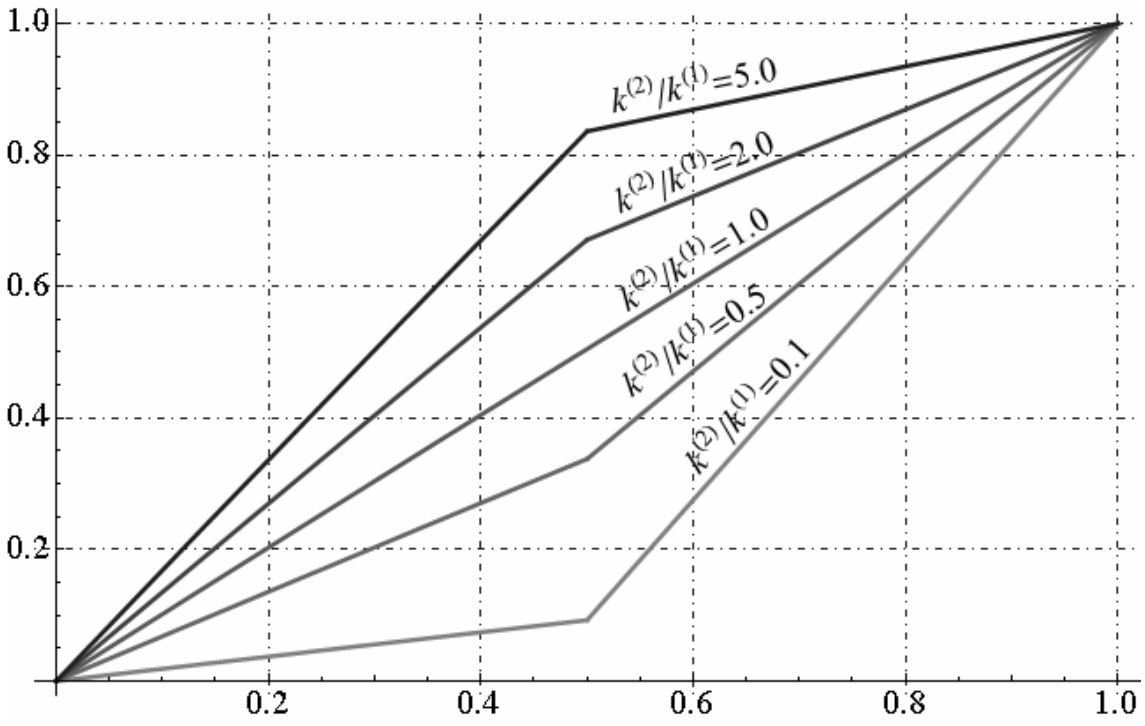

Fig. 18.26 - *Non-dimensional temperature along radial direction (Thermal conductivity coefficient variation)*

Finally, we reported the maximum absolute value of non-dimensional equivalent stress in phase (1) and in phase (2) for four case, as reported below:

(i) Poisson's variation moduli in both phases;
(ii) Young's moduli and linear thermal expansion coefficient variation;
(iii) Young's moduli and thermal conductivity coefficient variation;
(iv) Thermal conductivity coefficient and linear thermal expansion coefficient variation;

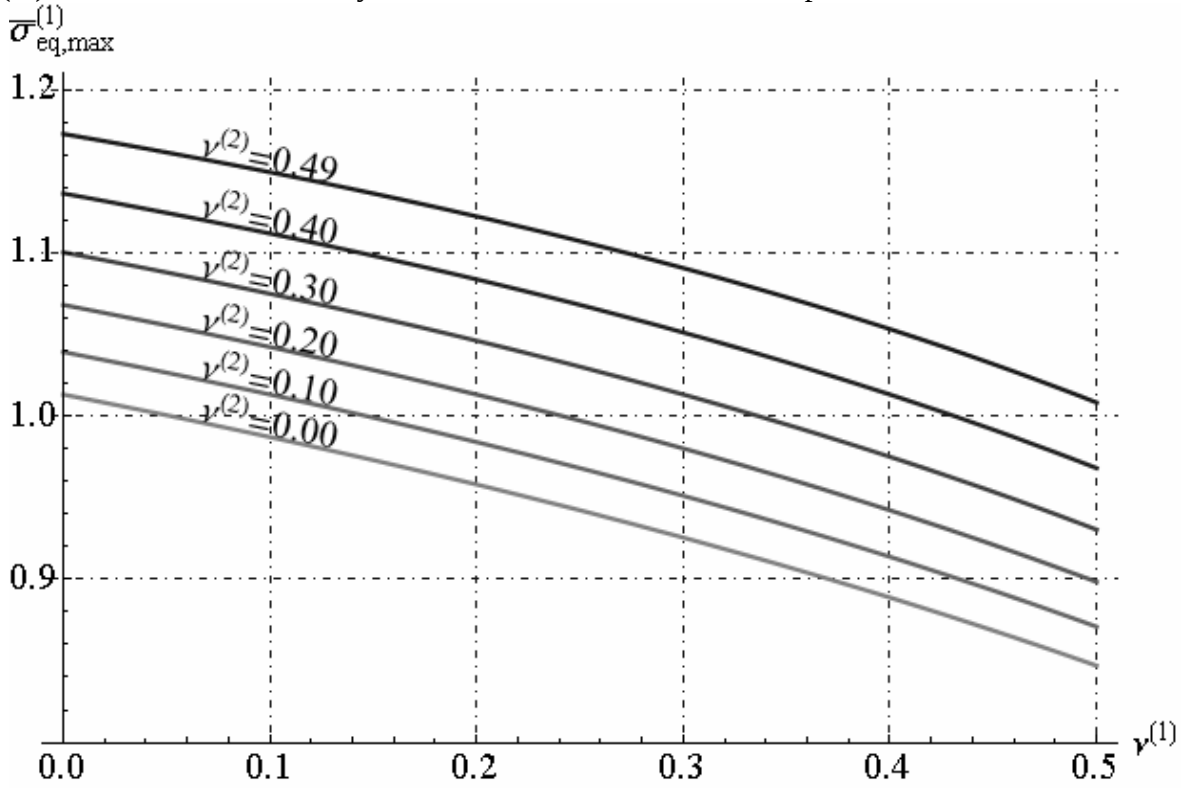

Fig. 18.27 - *Maximum absolute value of non-dimensional equivalent stress in phase (1) - Poisson's moduli variation -*

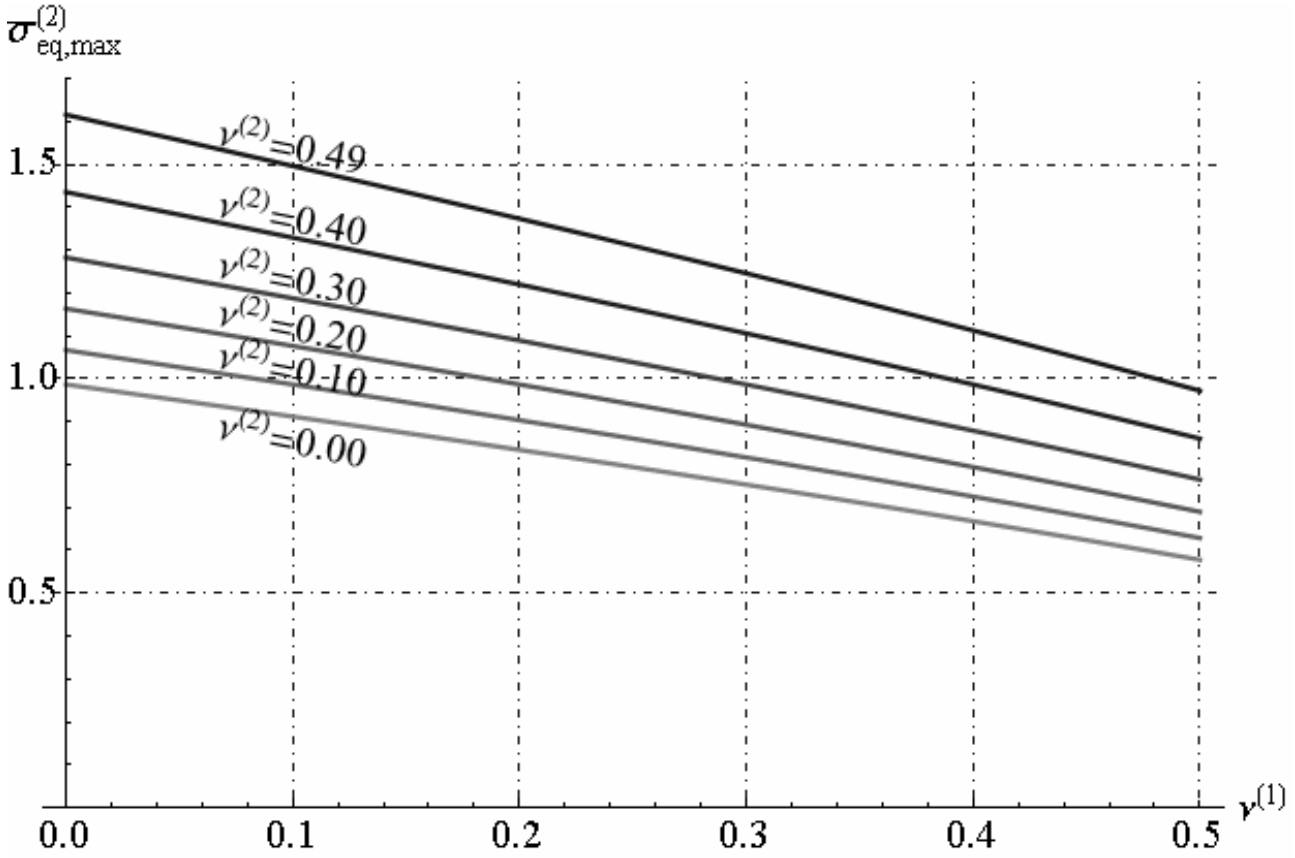

Fig. 18.28 - *Maximum absolute value of non-dimensional equivalent stress in phase (2) - Poisson's moduli variation -*

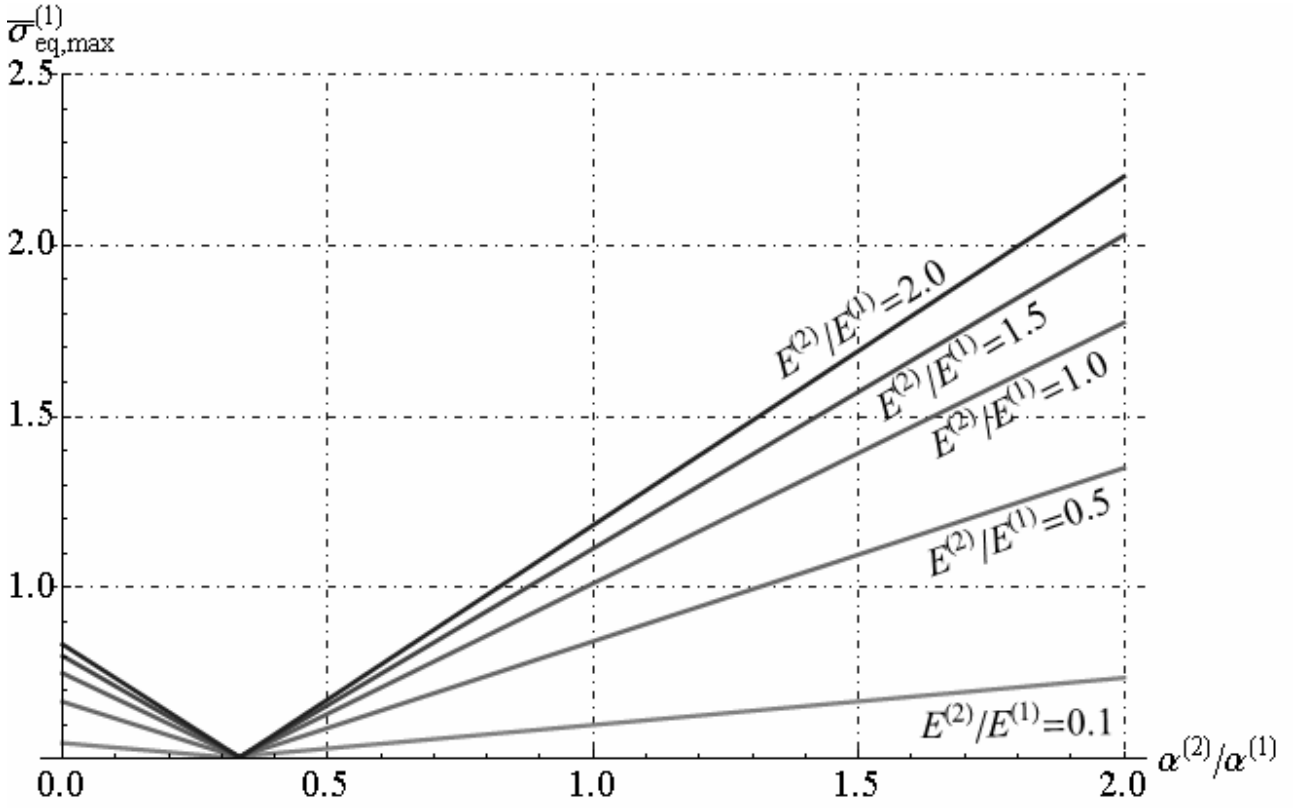

Fig. 18.29 - *Maximum absolute value of non-dimensional equivalent stress in phase (1) - Young's moduli and linear thermal expansion coefficient variation -*

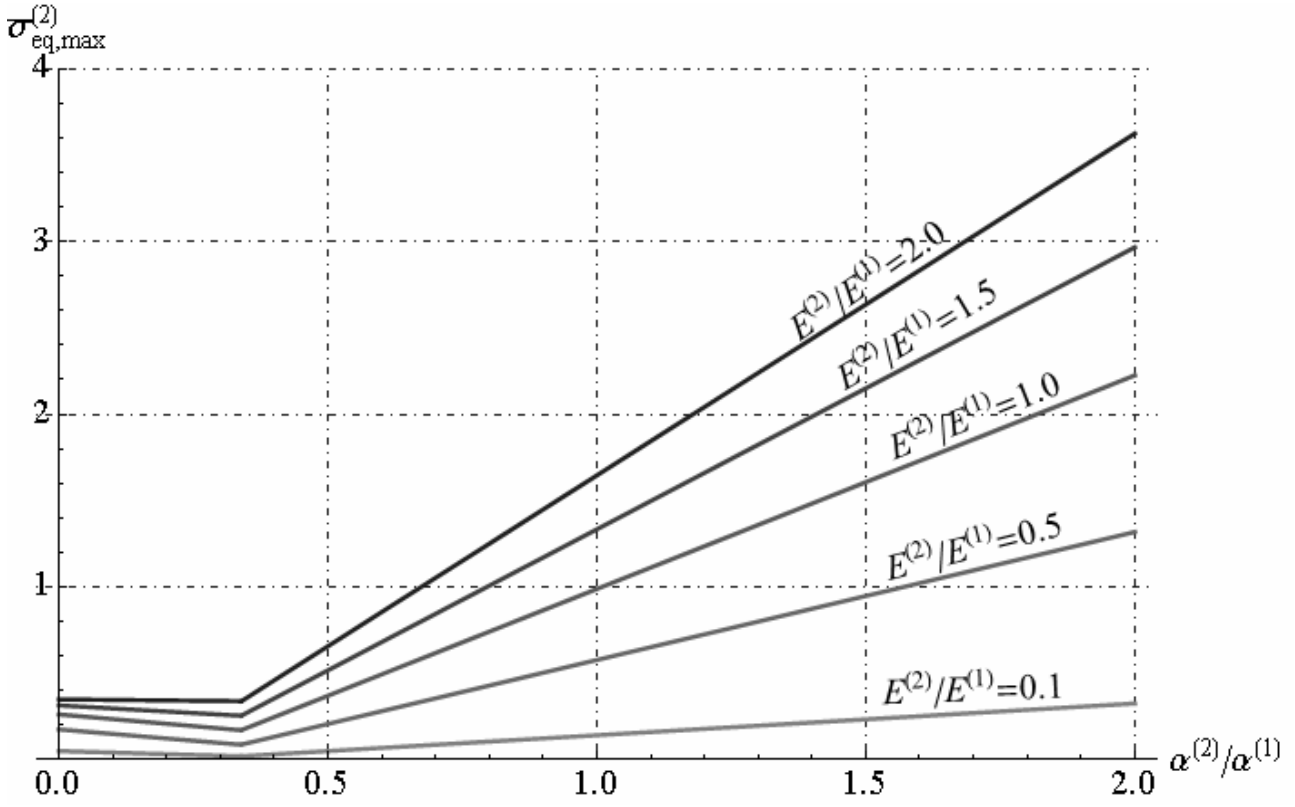

Fig. 18.30 - *Maximum absolute value of non-dimensional equivalent stress in phase (2) - Young's moduli and linear thermal expansion coefficient variation -*

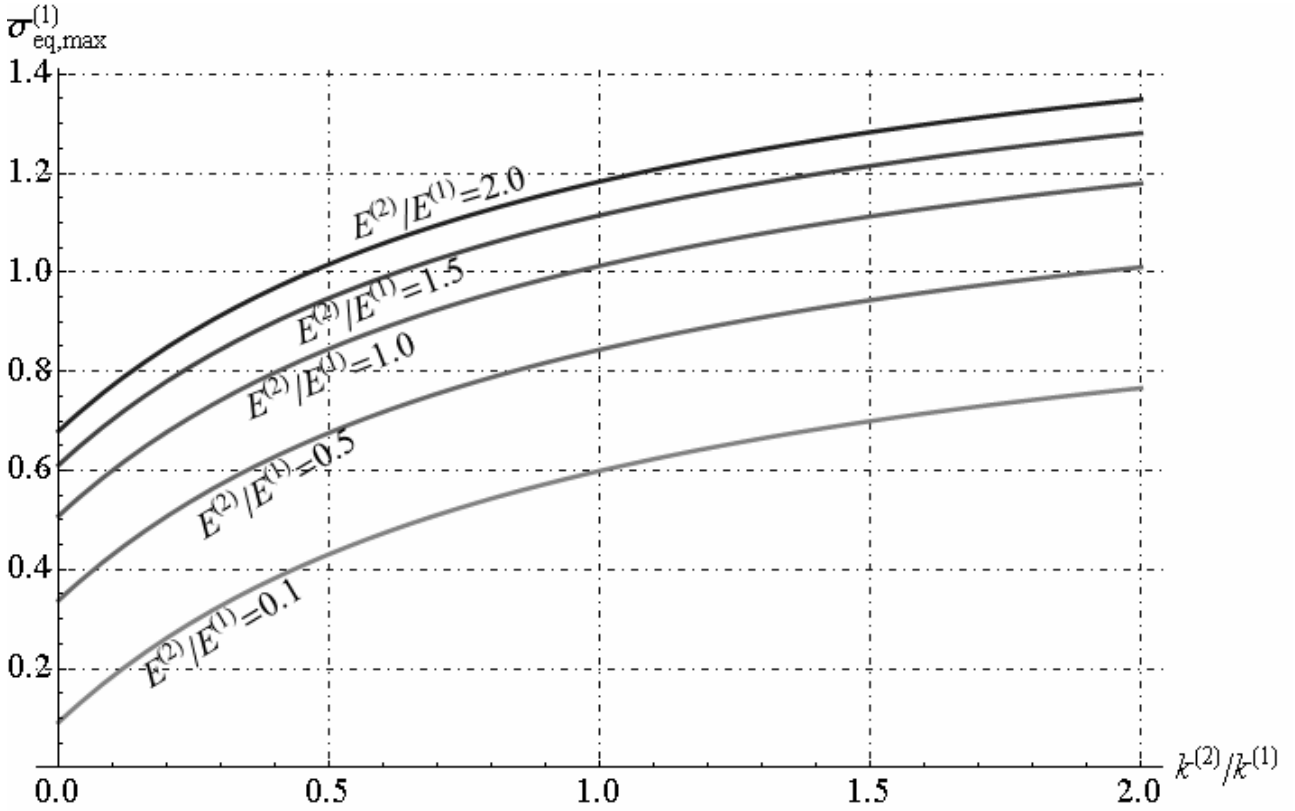

Fig. 18.31 - *Maximum absolute value of non-dimensional equivalent stress in phase (1) - Young's moduli and thermal conductivity coefficient variation -*

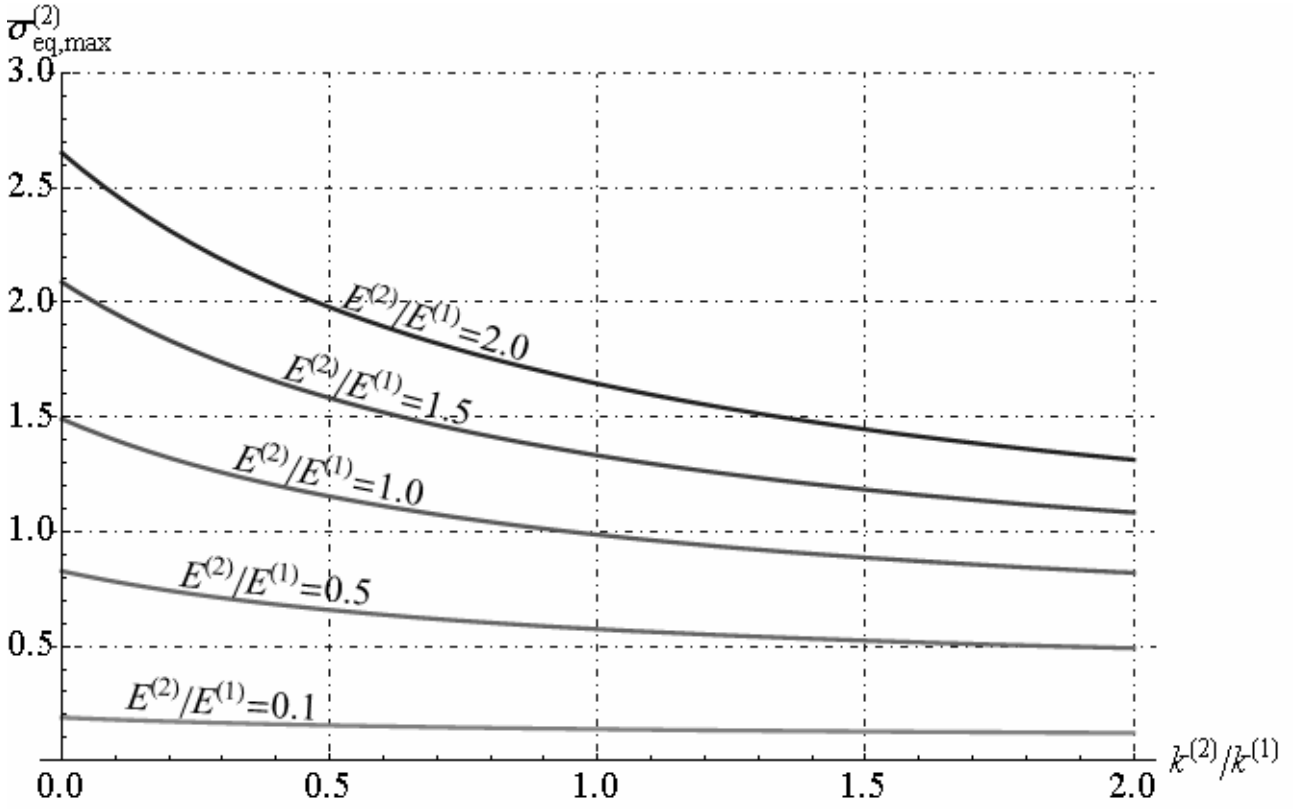

Fig. 18.32 - *Maximum absolute value of non-dimensional equivalent stress in phase (2) - Young's moduli and thermal conductivity coefficient variation –*

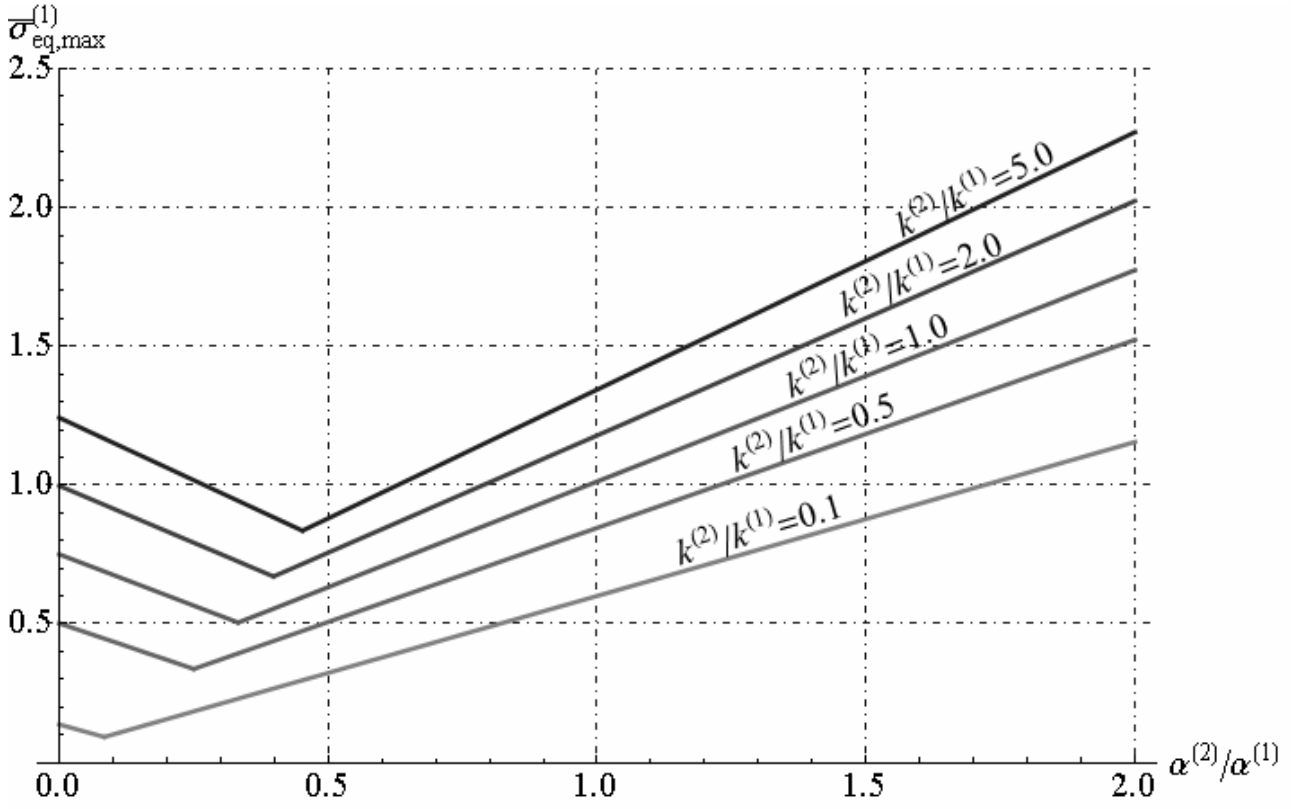

Fig. 18.33 - *Maximum absolute value of non-dimensional equivalent stress in phase (1) - thermal conductivity coefficient and linear thermal expansion coefficient variation –*

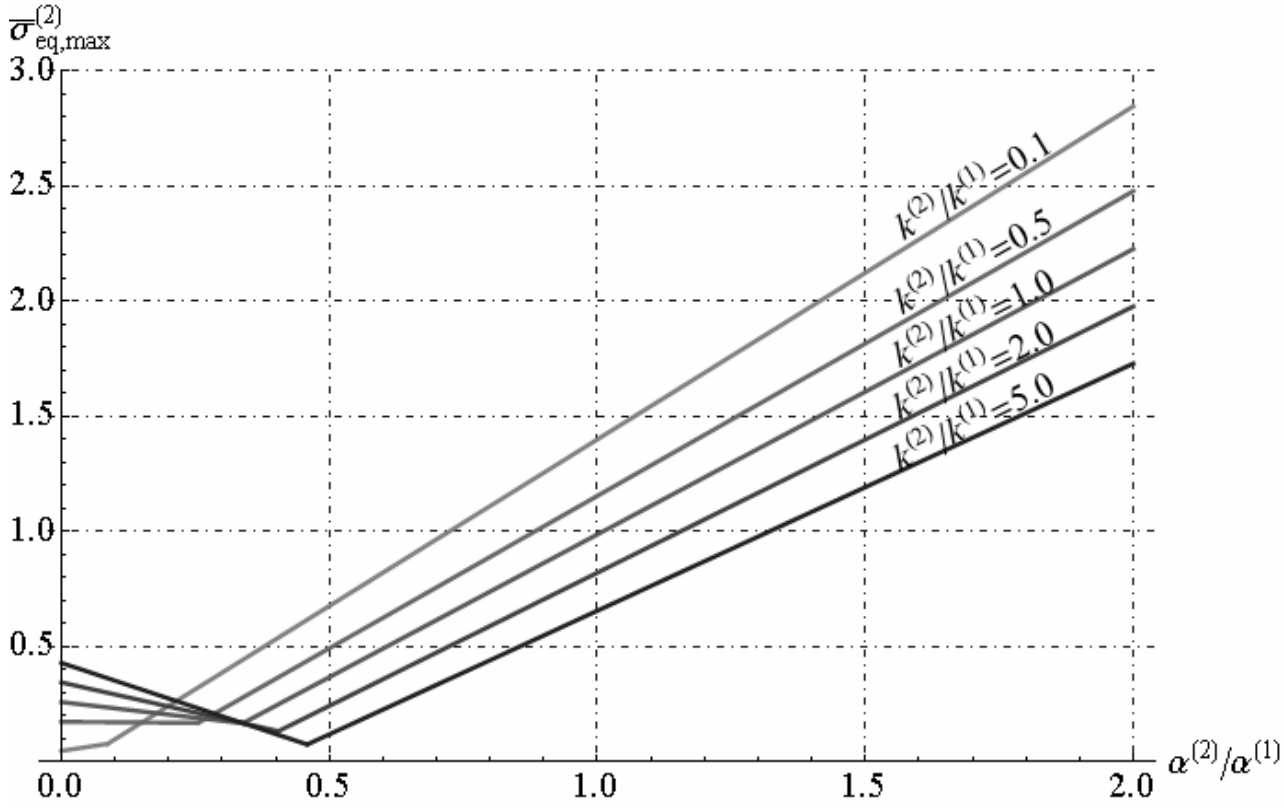

Fig. 18.34 - *Maximum absolute value of non-dimensional equivalent stress in phase (2) - thermal conductivity coefficient and linear thermal expansion coefficient variation -*

18.4. Example for multilayered sphere composed by three phases

In this study, we present some numerical results for the temperature distributions in multilayered sphere constituted by three phases, subjected to the considered boundary conditions and the resulting displacement and thermal stresses. For the multilayered sphere, the geometry and material quantities of the sphere are shown in Table 18.1. The inner radius of the sphere is assumed to be $R^{(0)}$ and the thickness of any phases is equal to δ. Then, we can write the following relationships:

$$R^{(1)} = (1+\xi)R^{(0)},\ R^{(2)} = (1+2\xi)R^{(0)},\ R^{(3)} = (1+3\xi)R^{(0)},\ \xi = \delta/R^{(0)}, \tag{18.49}$$

where $\xi = \delta/R^{(0)}$ represent the ratio between the thickness of any hollow sphere and inner radius.

Let us consider two cases, in which the boundary conditions at inner and outer surfaces are assumed to be :

$$(i)\begin{cases} T^{(1)}(r=R^{(0)}) = T_i = T_R = 298°K & \begin{cases} \sigma_{rr}^{(1)}(r=R^{(0)}) = p_i = 0 \\ \sigma_{rr}^{(3)}(r=R^{(3)}) = p_e = 0 \end{cases} \\ T^{(3)}(r=R^{(3)}) = T_e = 308°K \end{cases}$$

$$(ii)\begin{cases} T^{(1)}(r=R^{(0)}) = T_i = T_R = 298°K & \begin{cases} \sigma_{rr}^{(1)}(r=R^{(0)}) = p_i = -10MPa \\ \sigma_{rr}^{(3)}(r=R^{(3)}) = p_e = 0MPa \end{cases} \\ T^{(3)}(r=R^{(3)}) = T_e = T_R = 298°K \end{cases} \tag{18.50}$$

In each cases, let us consider three sub-cases, in which are chance the position of materials, as reported below:

(a) phase 1: Stainless steel, phase 2 : Zinc, phase 3 : Aluminium;
(b) phase 1: Aluminium, phase 2 : Stainless steel, phase 3 : Zinc
(c) phase 1: Aluminium, phase 2 : Zinc, phase 3 : Stainless steel;

In case (i) the multilayered sphere is subjected to an gradient of temperature between inner and outer surfaces, but the external load vanishing. In third case (ii) the multilayered sphere is subjected to gradient of pressure between inner and outer surfaces, but the temperature is uniform and equal to T_R. In total, we studied six cases, in which the ratio ξ is assumed equal to 0.01.

The Fig. 18.36 shows the temperature distributions along the radial direction in the case (i). The temperature gradient varies in each layer because of the difference in the thermal conductivity coefficients. Fig. 18.37 shows the radial displacement distributions along the radial direction in the case (i). In particular in the sub-case (c) the radial displacement assume the minimum value. The figures 18.38 and 18.39 show the thermal radial and circumferential strain distribution along the radial direction, respectively. The figures 18.40, 18.41 and 18.42 show the thermal radial, circumferential and equivalent stress distribution along the radial direction , respectively. As expected, the circumferential stress distribution exhibits significant jumps at all interfaces as shown in Fig. 18.41. These discontinuities are due to the differences in material properties such as the coefficient of linear thermal expansion and Young's modulus. The circumferential stress varies characteristically in each layer in view of the occurrence of discontinuities at all interfaces shown in the Fig. 18.41. The equivalent stress assume the minimum values along radius in sub-case (c) respet to sub-cases (a) and (b). In other figures we reported the dimensional parameters distribution along the non-dimensional radial direction.

	Aluminium	**Zinc**	**Stainless steel**
$E\left[N\,m^{-2}\right]$	$70\cdot10^{9}$	$108\cdot10^{9}$	$215\cdot10^{9}$
$k\left[W\,m^{-1}K^{-1}\right]$	237	116	30
ν	0.35	0.25	0.30
$\alpha\left[m\cdot m^{-1}K^{1}\right]$	$23.1\cdot10^{-6}$	$30.2\cdot10^{-6}$	$12\cdot10^{-6}$
$\rho\left[kg\,m^{-3}\right]$	2700	7140	7800
$c_v\left[kJ\cdot kg^{-1}K^{-1}\right]$	0.90	0.39	0.46

Table 18.1. *The geometry and material constants of multilayered sphere*

Phase	(1)	(2)	(3)
Case (a)	Fe	Zn	Al
Case (b)	Al	Fe	Zn
Case (c)	Al	Zn	Fe

Legend
Fe = Stainless steel
Zn = Zinc
Al = Aluminium

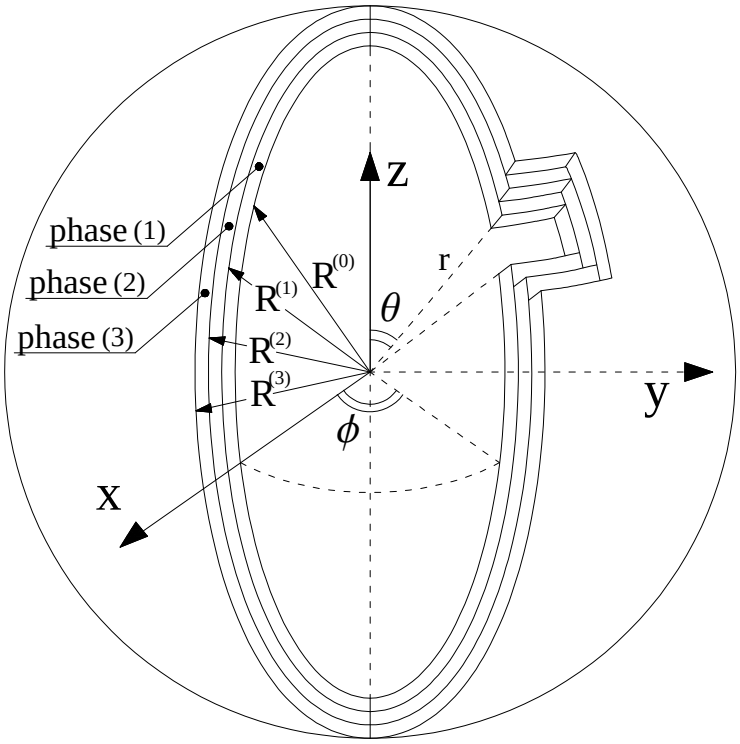

Fig. 18.35. *Multilayered sphere composed by three phases*

We reported the numerical results for case (i) as follows :

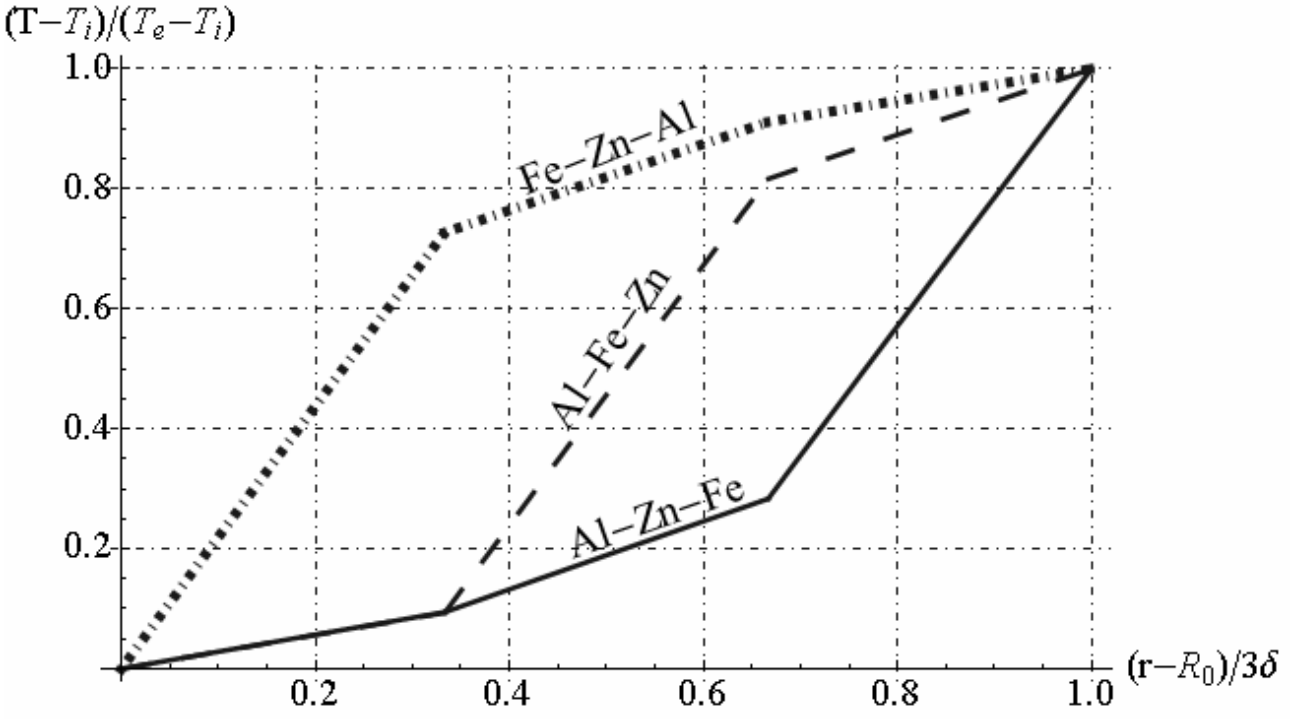

Fig. 18.36 - *Non-dimensional temperature distribution along radial direction*

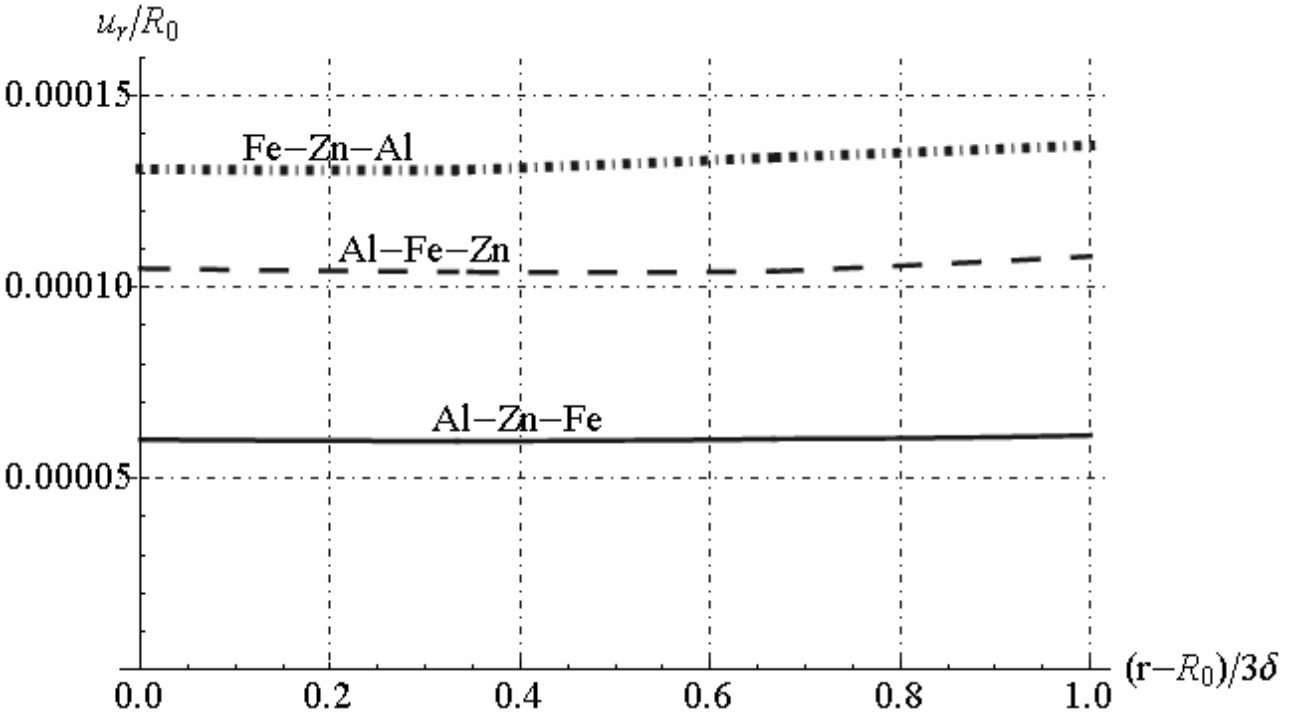

Fig. 18.37 - *Radial displacement distribution along radial direction*

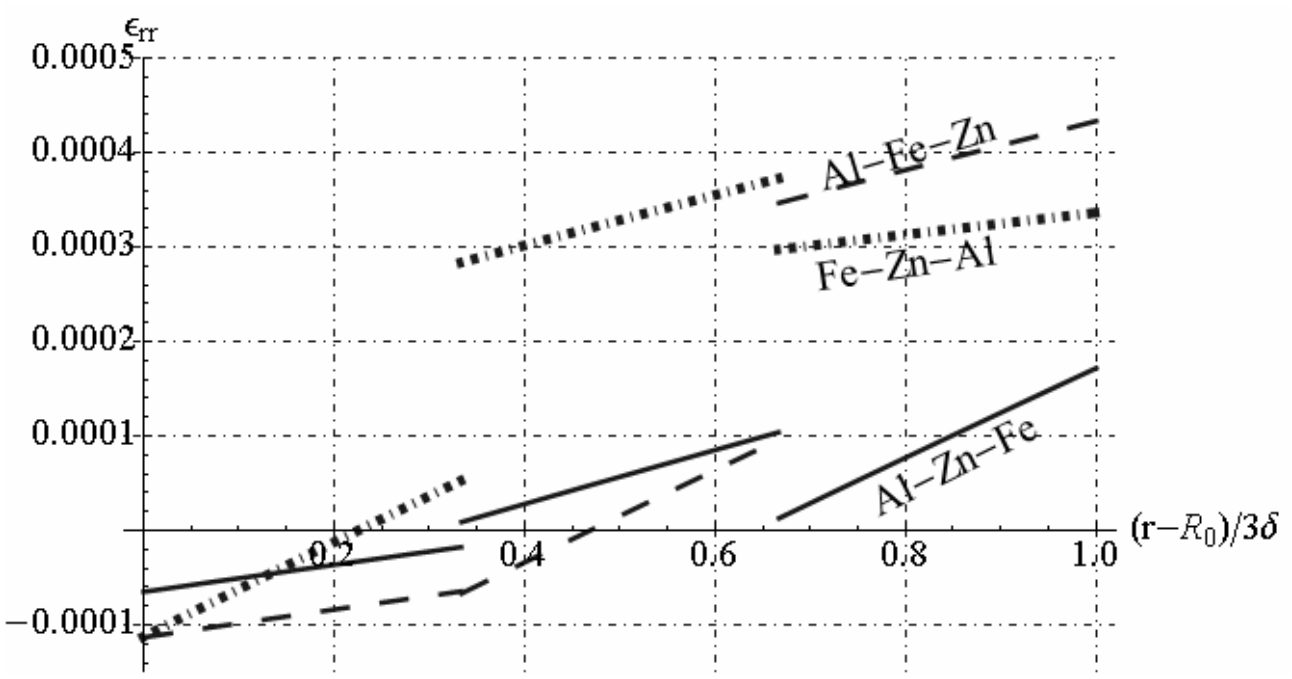

Fig. 18.38 - *Radial strain distribution along radial direction*

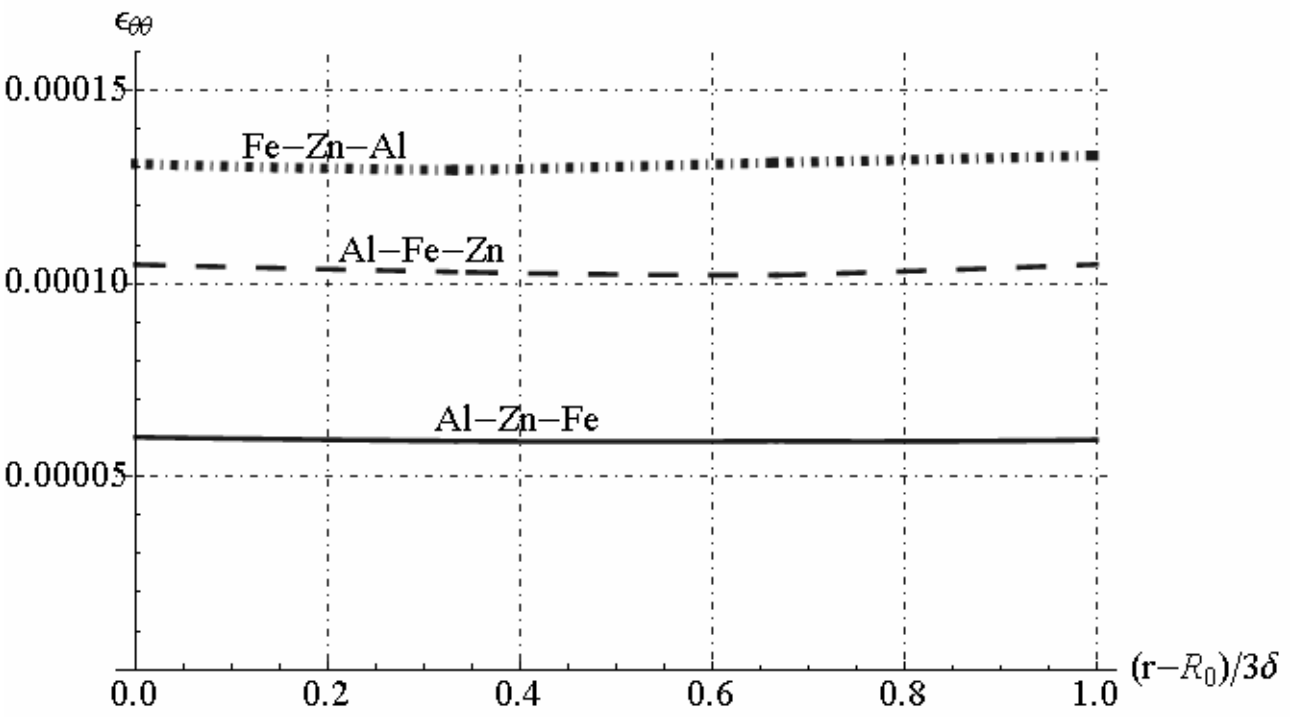

Fig. 18.39 - *Circumferential strain along radial direction*

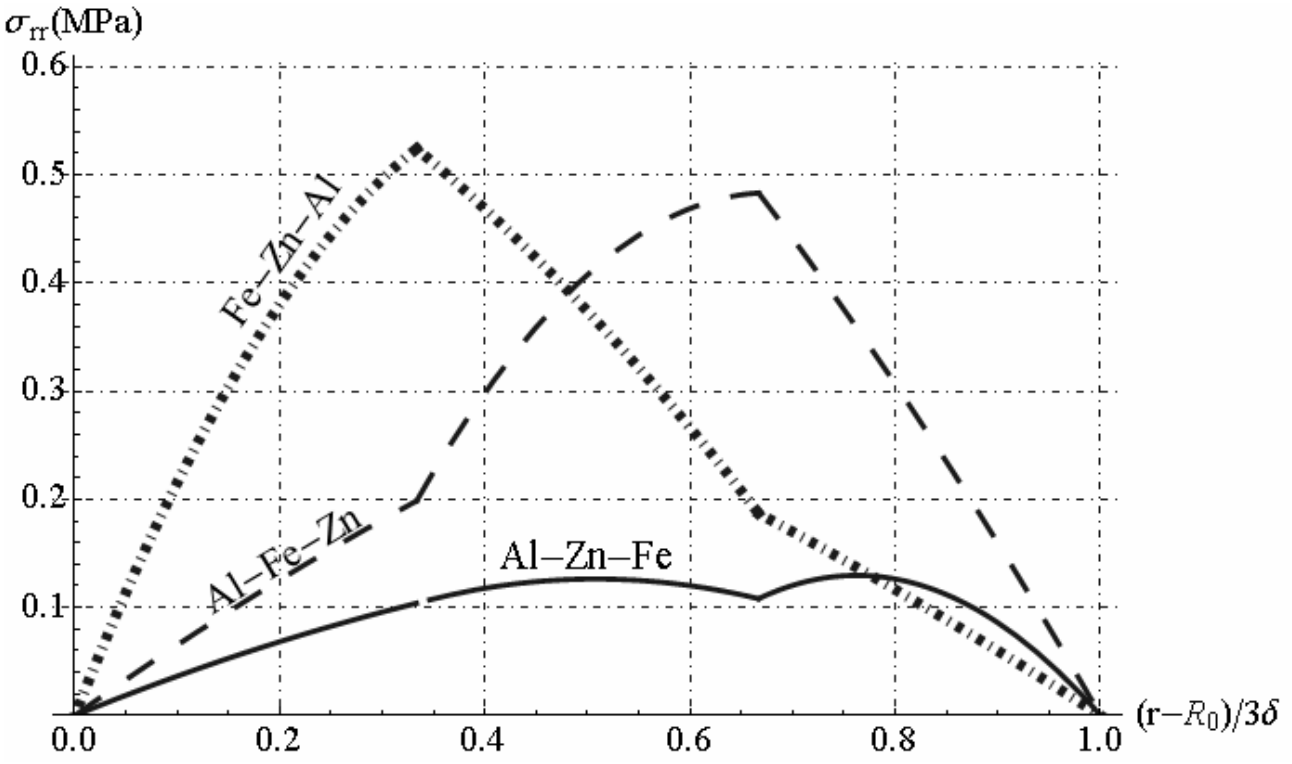

Fig. 18.40 - *Radial stress distribution along radial direction*

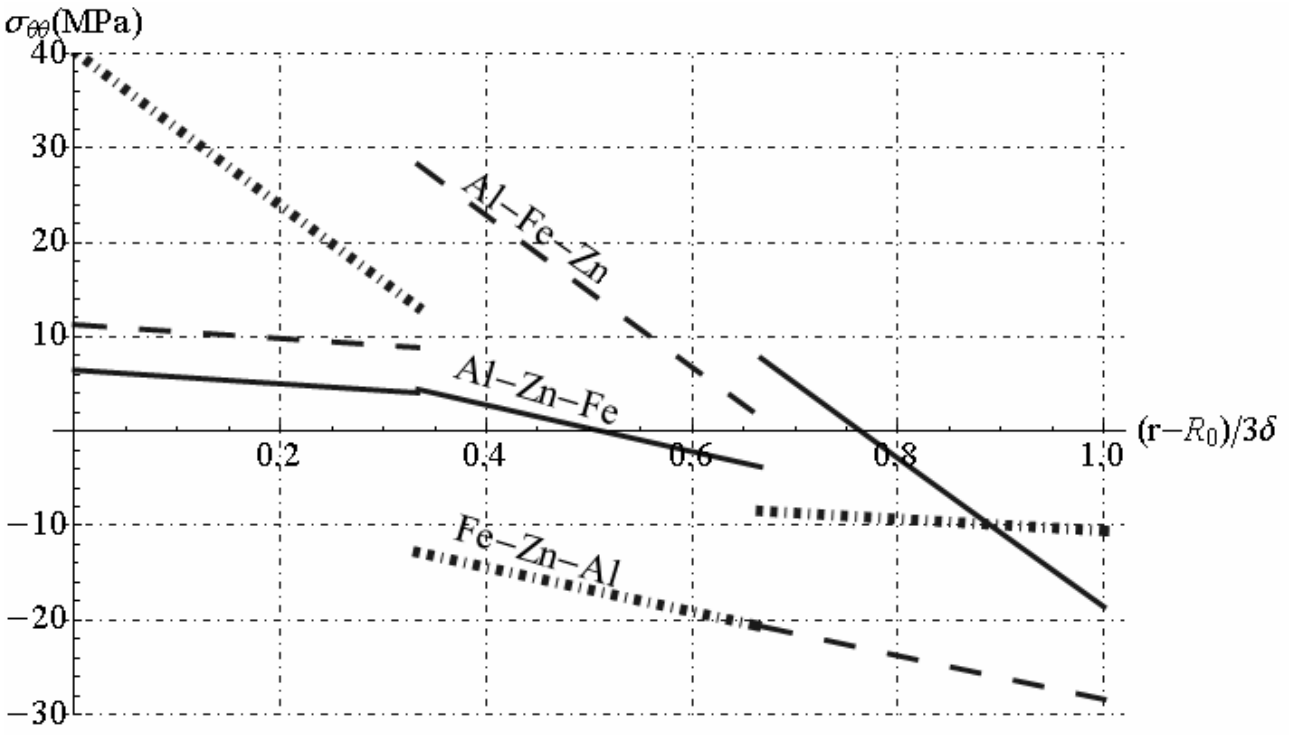

Fig. 18.41 - *Circumferential stress along radial direction*

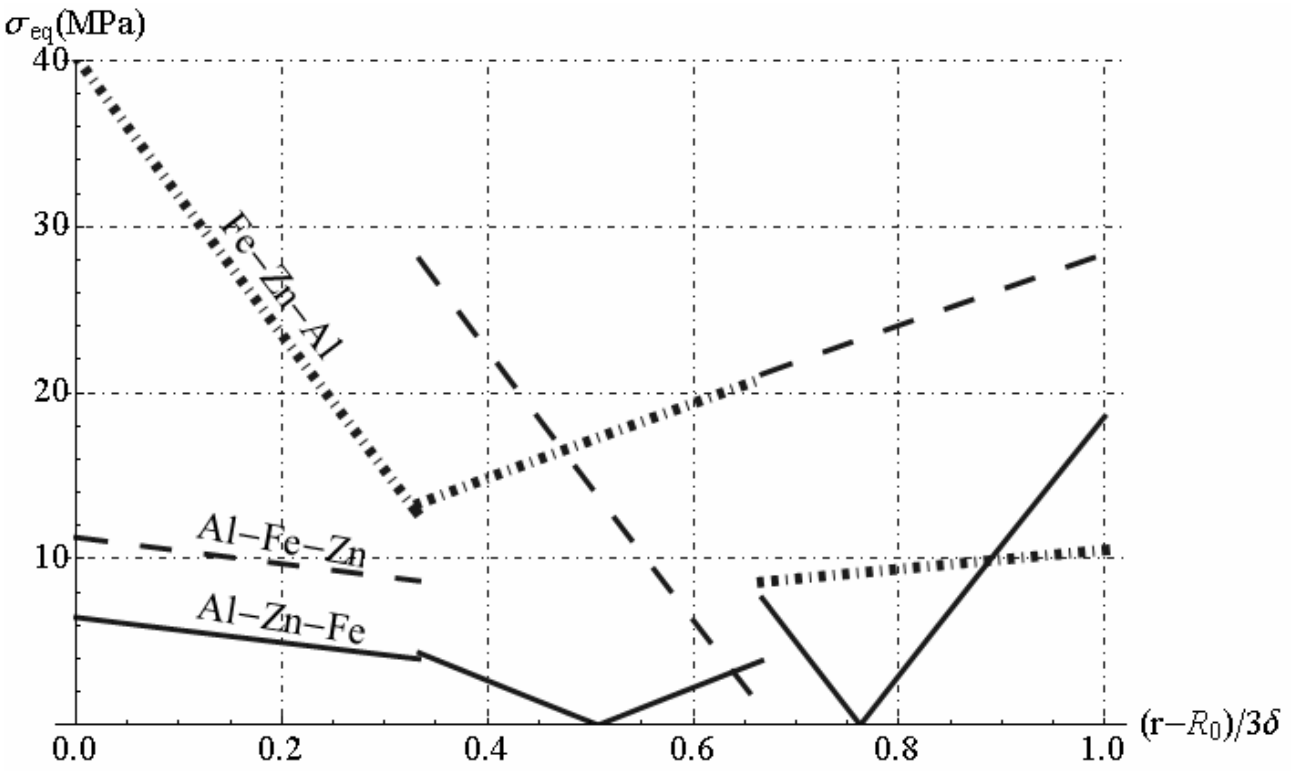

Fig. 18.42 - *Equivalent stress along radial direction*

We reported the numerical results for case (ii) as follows :

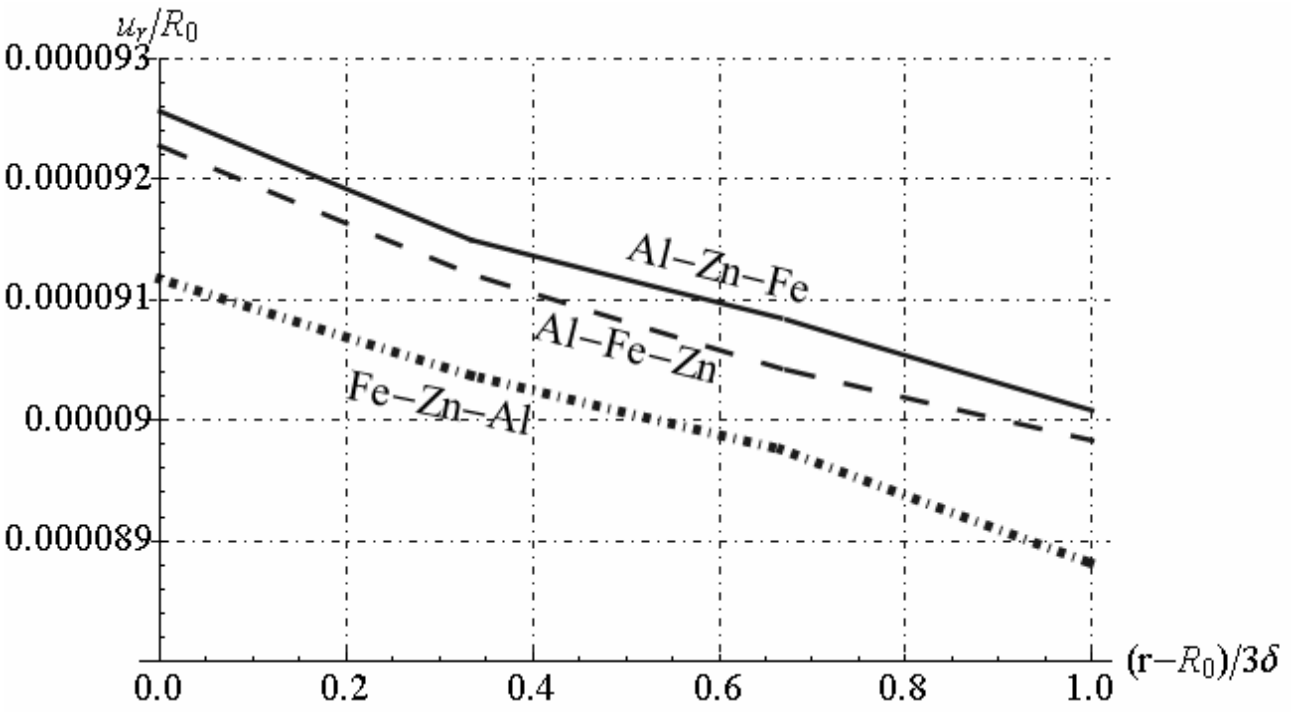

Fig. 18.43 - *Non dimensional radial displacement distribution along radial direction*

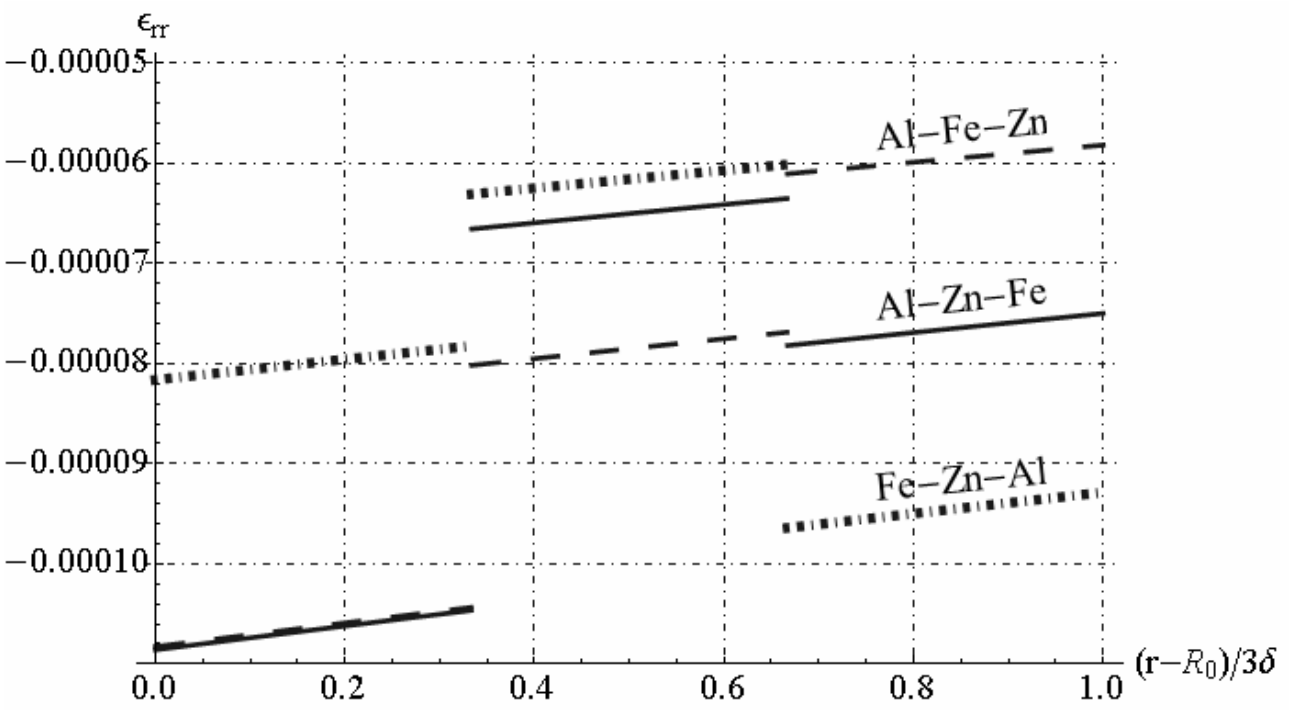

Fig. 18.44 - *Radial strain distribution along radial direction*

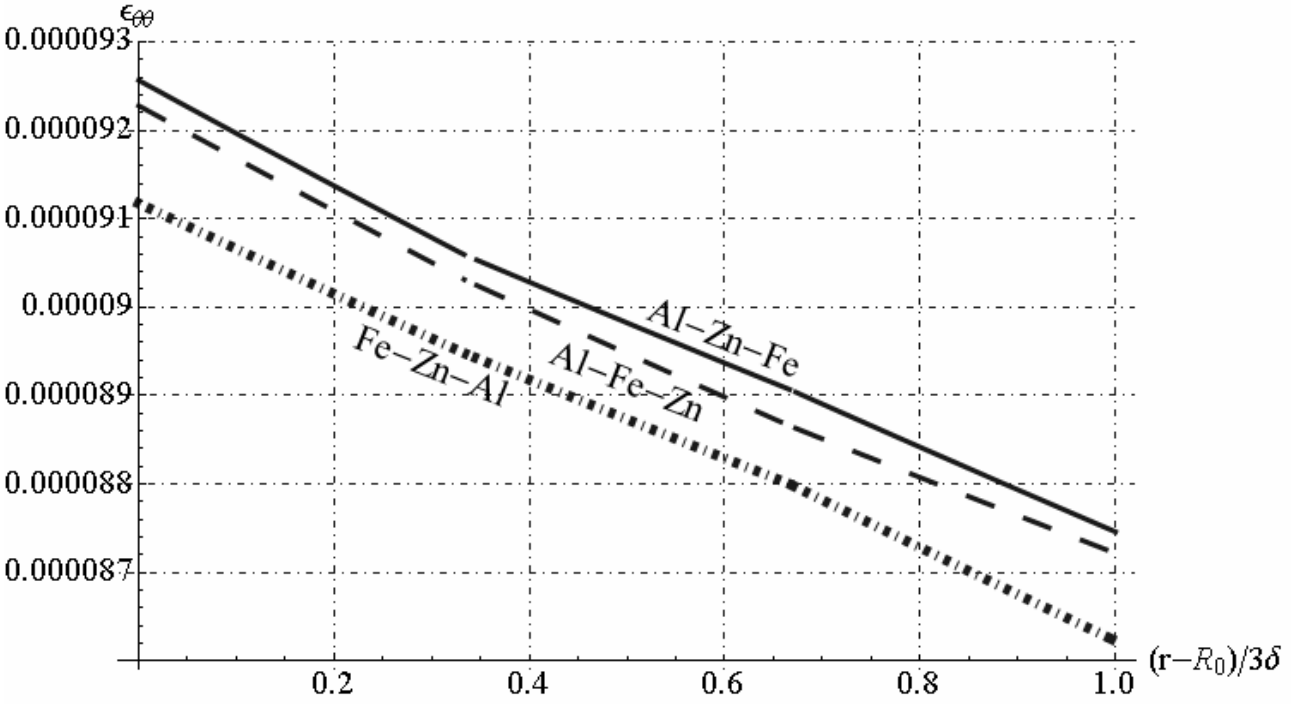

Fig. 18.45 - *Circumferential strain along radial direction*

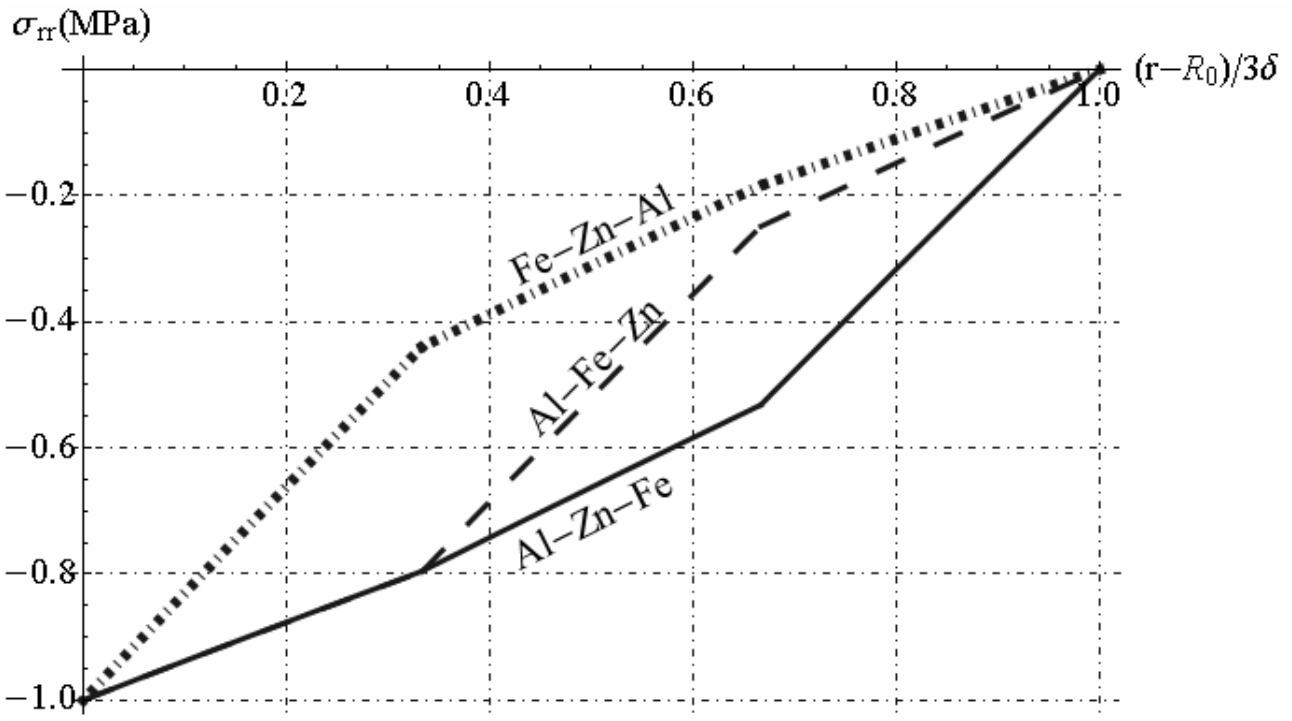

Fig. 18.46 - *Radial stress distribution along radial direction*

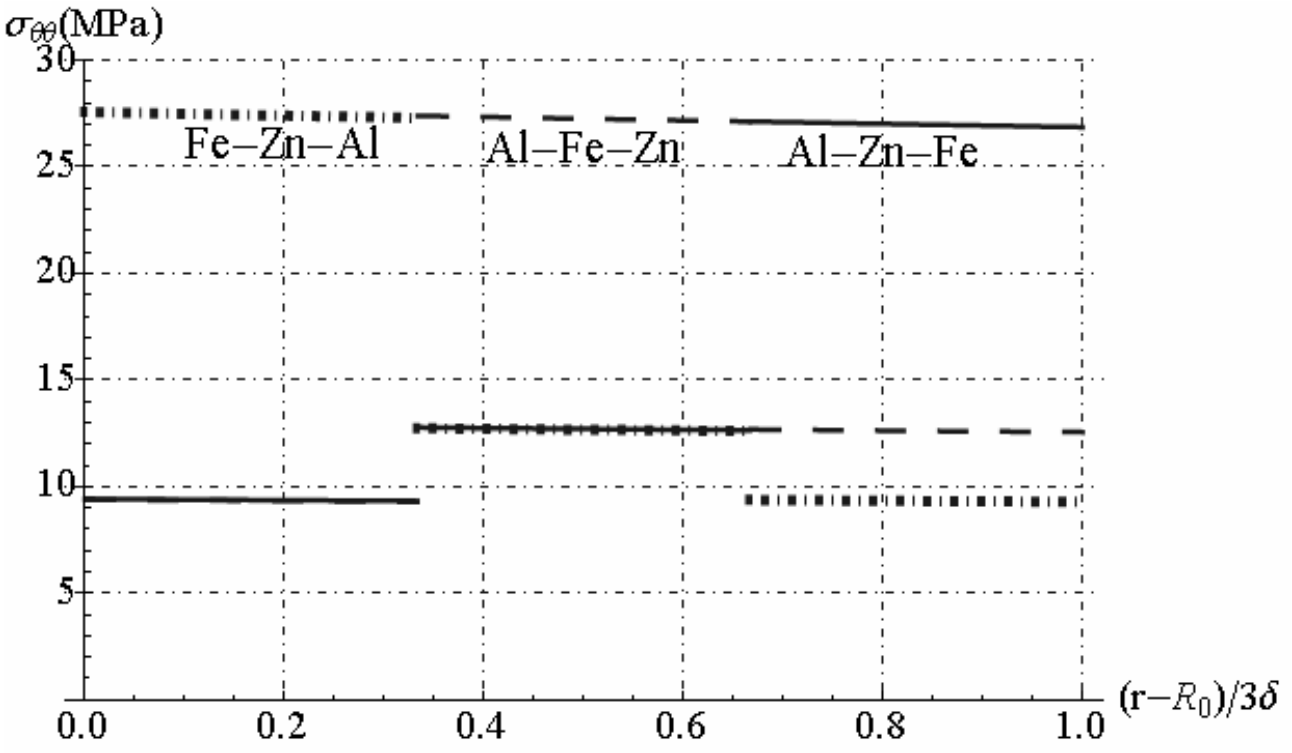

Fig. 18.47 - *Circumferential stress along radial direction*

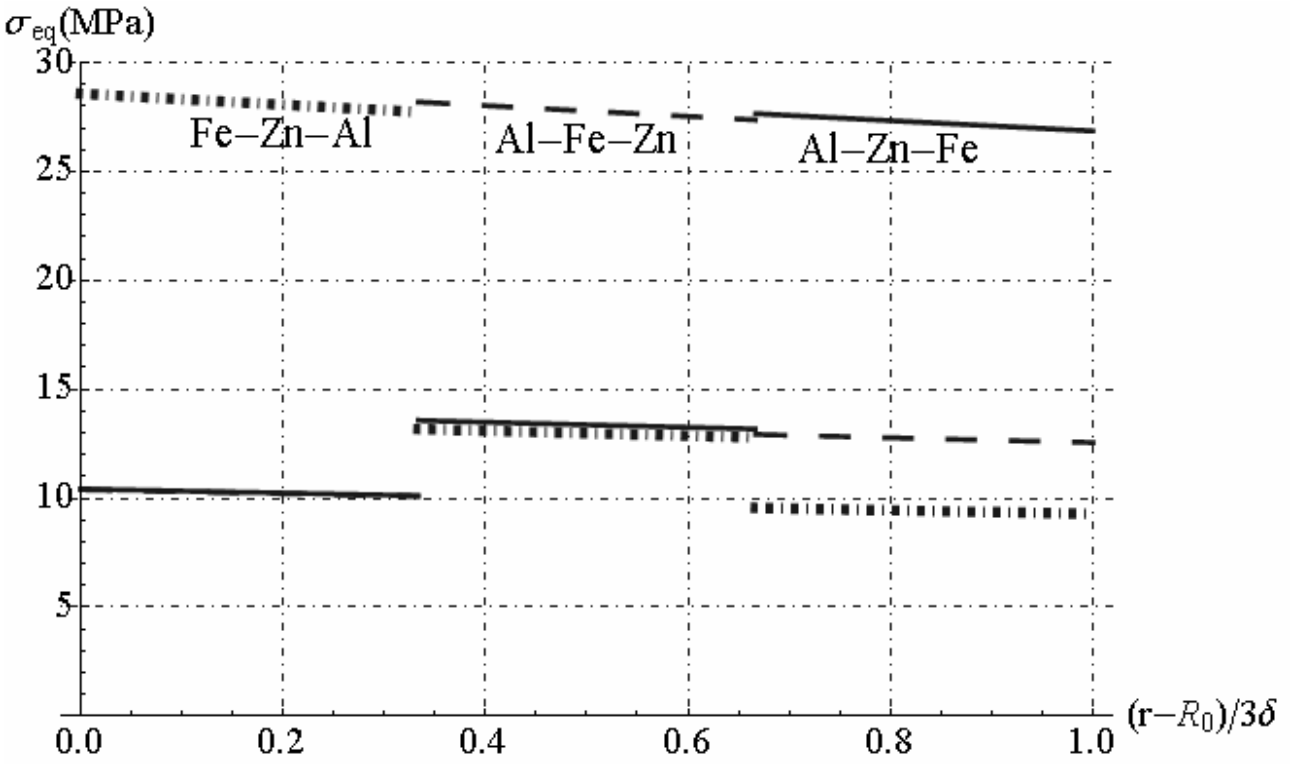

Fig. 18.48 - *Equivalent stress along radial direction*

18.5. Conclusions

In this work, analytical and numerical results for multilayered sphere are obtained. The analytical thermo-elastic solution, in closed form, is employed in order to obtain the parametric analyses for bi-layer hollow spheres and the numerical results for a spherical tank composed by three phases. The temperature, displacement and thermal stress distributions are obtained. This results can be applied to mechanical parts, in precision measurement or design of structures. The proposed method may be extended to solve a wide range of physical engineering problems. In particular, the parametric analyses presented in this paper can be utilized to optimize the designer of a composite spherical tank subjected to mechanical and thermal loads. By summarized the results obtained by parametric analyses, it is possible to reduce the maximum equivalent stress in a spherical tank by utilizing hollow spheres constituted by materials with mechanical and thermal selected properties

18.6. Nomenclature

k thermal conductivity coefficient,
α linear thermal expansion coefficient
E Young's modulus
ν Poisson's ratio
T_i temperature on the inner surface
T_e temperature on the outer surface
p_i pressure on the inner surface
p_e pressure on the outer surface
$T, \overline{T}$ dimensional and non-dimensional temperature
$r, \overline{r}$ dimensional and non-dimensional radial coordinate
$\varepsilon_{jk}^{(i)}, \overline{\varepsilon}_{jk}^{(i)}$ dimensional and non-dimensional strain components in generic *i*-th phase
$\sigma_{jk}^{(i)}, \overline{\sigma}_{jk}^{(i)}$ dimensional and non-dimensional stress components in generic *i*-th phase

$u_r^{(i)}, \bar{u}_r^{(i)}$ dimensional and non-dimensional radial component of displacement in generic *i*-th phase

18.7. References

[1] Alavi,F., Karimi, D., Bagri, A., (2008). *An investigation on thermo-elastic behaviour of functionally graded thick spherical vessels under combined thermal and mechanical loads*. Journal of Achievements in Materials and Manufacturing Engineering, vol. 31, Issue 2., pp. 422-428

[2] Ahmet, N. E.; Tolga, A. (2006): *Plane strain analytical solutions for a functionally graded elastic plastic pressurized tube*. Pressure vessels and piping, 83, pp. 635–644.

[3] Boley, B.A.,Weiner, J.H., *Theory of thermal stresses*, Dover publications, inc. Mineola, New York

[4] Chakrabarty, J. (1998): *Theory of Plasticity*. McGraw Hill, New York.

[5] Chen, Y. Z,; Lin, X. Y. (2008): *Elastic analysis for thick cylinders and spherical pressure vessels made of functionally graded materials*. Computational Materials Science, 44, pp.581–587.

[6] Delfosse, D.; Cherradi, N.; Ilschner, B. (1997): *Numerical and experimental determination of residual stresses in graded materials*. Composites, part B, 28B, pp. 127-141.

[7] Fraldi, M., Nunziante, L., Carannante, F. (2007), *Axis-symmetrical Solutions for n-plies Functionally Graded Material Cylinders under Strain no-Decaying Conditions*, J. Mech. of Adv. Mat. and Struct. Vol. 14 (3), pp. 151-174 - DOI: 10.1080/15376490600719220

[8] M. Fraldi, L. Nunziante, F. Carannante, A. Prota, G. Manfredi, E. Cosenza (2008), *On the Prediction of the Collapse Load of Circular Concrete Columns Confined by FRP*, Journal Engineering structures, Vol. 30, Issue 11, November 2008, Pages 3247-3264 - DOI: 10.1016/j.engstruct.2008.04.036

[9] Fraldi, M., Nunziante, L., Chandrasekaran, S., Carannante, F., Pernice, MC. (2009), *Mechanics of distributed fibre optic sensors for strain measurements on rods*, Journal of Structural Engineering, 35, pp. 323-333, Dec. 2008- Gen. 2009

[10] M. Fraldi, F. Carannante, L. Nunziante (2012), *Analytical solutions for n-phase Functionally Graded Material Cylinders under de Saint Venant load conditions: Homogenization and effects of Poisson ratios on the overall stiffness*, Composites Part B: Engineering, Volume 45, Issue 1, February 2013, Pages 1310–1324

[11] Nunziante, L., Gambarotta, L., Tralli, A., *Scienza delle Costruzioni*, 3° Edizione, McGraw-Hill, 2011**,** ISBN**:** 9788838666971

[12] Ibrahim, H.; Tawfik, M.; Al-Ajmi, M. (2006): *Aero-thermo-mechanical characteristic of functionally graded material panels with temperature dependant material properties*. ICFDP 8, ASME conference, Sharm El-Sheikh, Egypt.

[13] Koizumi, M. (1997): *FGM activities in Japan. Composites*, part B, 28B, pp. 1-4.

[14] Lekhnitskii, S. G., (1981), *Theory of Elasticity of an Anisotropic Body*, Mir, Moscow.

[15] Liew, K. M.; Kitipornchai, S.; Zhang, X. Z.; Lim, C. W. (2003): *Analysis of the thermal stress behaviour of functionally graded hollow circular cylinders*. Solids and Structures, 40, pp. 2355–80.

[16] Lutz, M. P.; Zimmerman, R. W. (1996): *Thermal stresses and effective thermal expansion coefficient of a functionally graded sphere*. Thermal stress,19, pp. 39-54.

[17] Nayak, P.; Mondal, S. C. (2011): *Analysis of a functionally graded thick cylindrical vessel with radially varying properties*. Engineering science and technology, 3, pp.1551-1562.

[18] Nayak, P.; Mondal, S. C., Nandi, A.,(2011), *Stress, strain and displacement of a functionally graded thick spherical vessel*, International Journal of Engineering Science and Technology (IJEST), Vol. 3 No. 4

[19] Noda, N.; Hetnarski, R. B.; Tanigawa, Y. (2003): *Thermal Stresses*. Taylor and Francis, New York.

[20] Obata, Y.; Noda, N. (1994): *Steady thermal stress in a hollow circular cylinder and a hollow sphere of a functionally gradient materials*. Thermal stress, 17, pp. 471-487.

[21] Ozisik, M. N. (1985): *Heat Transfer*. McGraw Hill, New York.

[22] Peng, X. L.; Li, X. F. (2010): *Thermo-elastic analysis of a cylindrical vessel of functionally graded materials*. Pressure vessels and piping, 87, pp. 203-210.

[23] Shao, Z. S. (2005): *Mechanical and thermal stresses of a functionally graded hollow circular cylinder with finite length*. Pressure vessel and piping, 82, pp.155-163.
[24] Shao, Z. S.; Ma, G. W. (2008): *Thermo-mechanical stresses in functionally graded circular hollow cylinder with linearly increasing boundary temperature*. Composite Structures, 83, pp.259–265.
[25] Tutuncu N, Ozturk M. (2001): *Exact solutions for stresses in functionally graded pressure vessels*. Composites, part B, 32, pp. 683- 686.
[26] You, L. H.; Zhang, J. J.; You, X. Y. (2005): *Elastic analysis of internally pressurized thick-walled spherical pressure vessels of functionally graded materials*. Pressure vessel and piping, 82, pp.347-354.
[27] Zimmerman, R. W.; Lutz, M. P. (1999): *Thermal stresses and thermal expansion in a uniformly heated functionally graded cylinder*. Thermal stress, 22, pp. 177-188.
[28] Zong -Yi Lee (2004): *Coupled problem of thermo-elasticity for multilayered spheres with time-dependent boundary conditions*. Journal of Marine Science and Technology, Vol. 12, No. 2, pp. 93-101.

CHAPTER XIX
FIRE CURVES AND MATERIAL PROPERTIES AT ELEVATED TEMPERATURE

19.1. Introduction

Most countries around the world rely on fire resistance tests to determine the performance of building materials and structural elements. The time-temperature curve used for a test is called a fire curve. There are different types of fire curves that have been established by researchers, viz. ASTM E-119 , and Eurocode. In USA, the temperature profile and duration of a standard fire for designing and testing purposes is based on the provisions of ASTM E-119.

ASTM E-119 is the widely recognized standard for fire testing in the United States. The first edition was published in 1918, with the most recent published in 2000. Technical committees help in setting up a standard, and this standard is revised as technology and understanding changes. There has been significant debate on the validity of ASTM E-119 data and methodology due to the recent events of 9/11. One has to understand that ASTM E-119 is a guideline for fire safe design of buildings and not a predictor of behaviour in an actual fire. Real fires are a function of many variables, such as fuel load, thermal radiation, heat flux, ventilation factor, and area of openings which are related to the type of construction, building occupancy, and design. The main purpose of using the ASTM E-119 protocol is to establish and document the fire rating of different elements of a building. The test does not cover flame spread, fuel contribution, or smoke density. ASTM E-119 describes different strategies for conducting fire tests on the following structural assemblies and elements:

- Bearing walls and partitions
- Non-bearing walls and partitions
- Floors and roofs
- Loaded restrained beams
- Columns

Lab testing is a very common method for determining the performance of a structural member from the view point of fire resistance. The main reason for conducting lab tests is essentially to test a structural element in a furnace from the viewpoint of critical temperature and fire endurance time or collapse mechanism. The element is then heated according to a standard time-temperature profile such as the ASTM E-119 curve. The heating process is continued until failure of the element occurs so that specific data can be taken regarding the deflections, stresses, strains, etc. This data however is not available to public, and only the critical values are published in the codes. Figure 18.1 presents a traditional setup of a lab conducted fire test.

Currently, there are studies being done and revisions are being made for the standard fire test procedure . It is suggested by British Steel and the Building research development, 1998, on the basis of full scale fire test results at Cardington, UK that the actual temperature of an element when tested separately in a furnace is quite different from the temperature of the same element when exposed to a fire within a building. This is observed due to the various connections and differences in boundary conditions that occur when the beam or an element acts as a part of a frame. However, research is ongoing and it will take some time to arrive at a clear conclusion.

19.2. Standard Fire Curves and Furnace Testing

ASTM E119, Standard Test Methods for Fire Tests of Building Construction and Materials, was one of the first tests to be published which looked to establish a fire resistance rating for steel members through a prescribed method. This test also served as a basis for the determination of fire resistance ratings in other tests such as ISO 834 and various European codes. The basic principle behind standard fire resistance testing as it exists today is to expose a single structural member or assembly to a standard fire with designated fuel load and intensity. Pass/fail criteria are based upon the peak temperature attained at the unexposed surfaced of the test article and/or whether or not the test article collapses or distorts in a fashion that allows hot gases to escape (and in the case of E119,

whether a wall can withstand the pressure of a hose stream). For most standard tests, specimens are tested unloaded and have no maximum deflection that can occur before failure. The most common structural elements that are tested are columns, beams, and floor and ceiling assemblies. Elements such as joints or connections are rarely tested. A fire resistance rating is then assigned to the specimen based on the time it took to fail. It is clear that there are many weaknesses and deficiencies in the standard fire test and fire ratings that result from these tests. Several weaknesses of the standard fire test are discussed by Bukowski. These include fuel load and the physical characteristics of the furnace. Standard fire tests provided the prescriptive ratings that were needed when prescriptive design was primarily used but with the shift towards performance-based design, other methods must be evaluated.

The standard exposure was based on fuels that were commonly found in buildings at the time when the test was first published in the early 1900s. Modern fuels can result in fires with significantly faster growth rates and higher radiative fractions that affect fire spread rate. Another consideration is the addition of automatic sprinkler systems which can limit the growth phase of the fire, something that is not part of the standard fire exposure today. Bukowski also quotes the Federal Emergency Management Agency that "The ASTM El19 Standard Fire Test was developed as a comparative test, not a predictive one. In effect, the Standard Fire Test is used to evaluate the relative performance (fire endurance) of different construction assemblies under controlled laboratory conditions. The physical limitations of the standard furnace is another major weakness of this test. A typical furnace only allows for specimens to be tested individually and cannot accommodate and include the interaction of structural systems. End restraints and loading conditions may not be reproduced effectively in the furnace, thus only the very basic structural elements can be tested. Eurocode 1 Part 2 provides data for the design fires used in calculation with the Eurocode methods. It contains information for both standard (nominal) and parametric fire curves. The main document contains defining equations for three distinct fire curves: standard, external and hydrocarbon. In all of the three fire curves described, Θ_g designates gas temperature in the fire compartment in degrees Celsius and t is the time in minutes. If each of the curves is plotted from 0 to 6000 sec on the same axis, Figure 19.1 is created. One can see from this plot that the external and hydrocarbon fires are similar in shape but the hydrocarbon fire curve has temperatures 75% higher temperature. The standard fire curve is similar in shape and values to other standard curves used by ISO and ASTM. The standard fire curve described is almost identical in behaviour to the ASTM E119 and ISO 834 standard fire curves. This curve is used as a model for representing a fully developed fire in a compartment and is represented by the equation. It is reported below the equations for three distinct fire curves : standard, external and hydrocarbon.

Standard temperature-time curve

$$\begin{aligned} \Theta_g &= 20 + 345\log_{10}(8t+1) \quad [^\circ C, \min] \\ \Theta_g &= 293.15 + 345\log_{10}\left[\frac{8t}{60}+1\right] \quad [^\circ K, \sec] \end{aligned} \tag{19.1}$$

where Θ_g is the gas temperature, t is the time. The external curve is intended for the outside of separating external walls which exposed to the external plume of a fire coming either from the inside of respective fire compartment, from a compartment situated below or adjacent to the respective external wall. Because the scope of this research is limited to internal compartment fires, this fire will not be used in analysis. The equation producing the external fire curve is given by:

External fire curve

$$\begin{aligned} \Theta_g &= 20 + 660\left(1 - 0.687e^{-0.32t} - 0.313e^{-3.8t}\right) \quad [^\circ C, \min] \\ \Theta_g &= 293.15 + 660\left(1 - 0.687e^{-\frac{0.32}{60}t} - 0.313e^{-\frac{3.8}{60}t}\right) \quad [^\circ K, \sec] \end{aligned} \tag{19.2}$$

The hydrocarbon curve, is used for representing the effects of a hydrocarbon fire and is represented from the equation below:

Hydrocarbon curve

$$\Theta_g = 20 + 1080\left(1 - 0.325e^{-0.167t} - 0.675e^{-2.5t}\right) \quad [°C, \text{min}]$$
$$\Theta_g = 293.15 + 1080\left(1 - 0.325e^{-\frac{0.167}{60}t} - 0.675e^{-\frac{2.5}{60}t}\right) \quad [°K, \text{sec}] \tag{19.3}$$

ASTM E119 test is produced from the following equation and is displayed in Figure 19.3:

$$\Theta_g = 20 + 750\left(1 - e^{-3.79553\sqrt{\frac{t}{60}}}\right) + 170.41\sqrt{\frac{t}{60}} \quad [°C, \text{min}]$$
$$\Theta_g = 293.15 + 750\left(1 - e^{-3.79553\sqrt{\frac{t}{3600}}}\right) + 170.41\sqrt{\frac{t}{3600}} \quad [°K, \text{sec}] \tag{19.4}$$

Equation proposed by Williams – Leir (1973) is given by:

$$\Theta_g = \theta_0 + a_1\left(1 - e^{-a_4 t}\right) + a_2\left(1 - e^{-a_5 t}\right) + a_3\left(1 - e^{-a_6 t}\right) \quad [K°, \text{sec}] \tag{19.5}$$

Where $a_1 = 532$, $a_2 - 186$, $a_3 = 820$, $a_4 = 0.01$, $a_5 = 0.05$, $a_6 = 0.20$, and θ_0 is the temperature ambient. The equation proposed by Fackler (1959) is reported below:

$$\Theta_g = \theta_0 + 774\left(1 - e^{-0.49\sqrt{t}}\right) + 22.2\sqrt{t} \tag{19.6}$$

In these equations above, the base temperature or ambient temperature θ_0 is not considered to be 20°C which usually is the current practice.

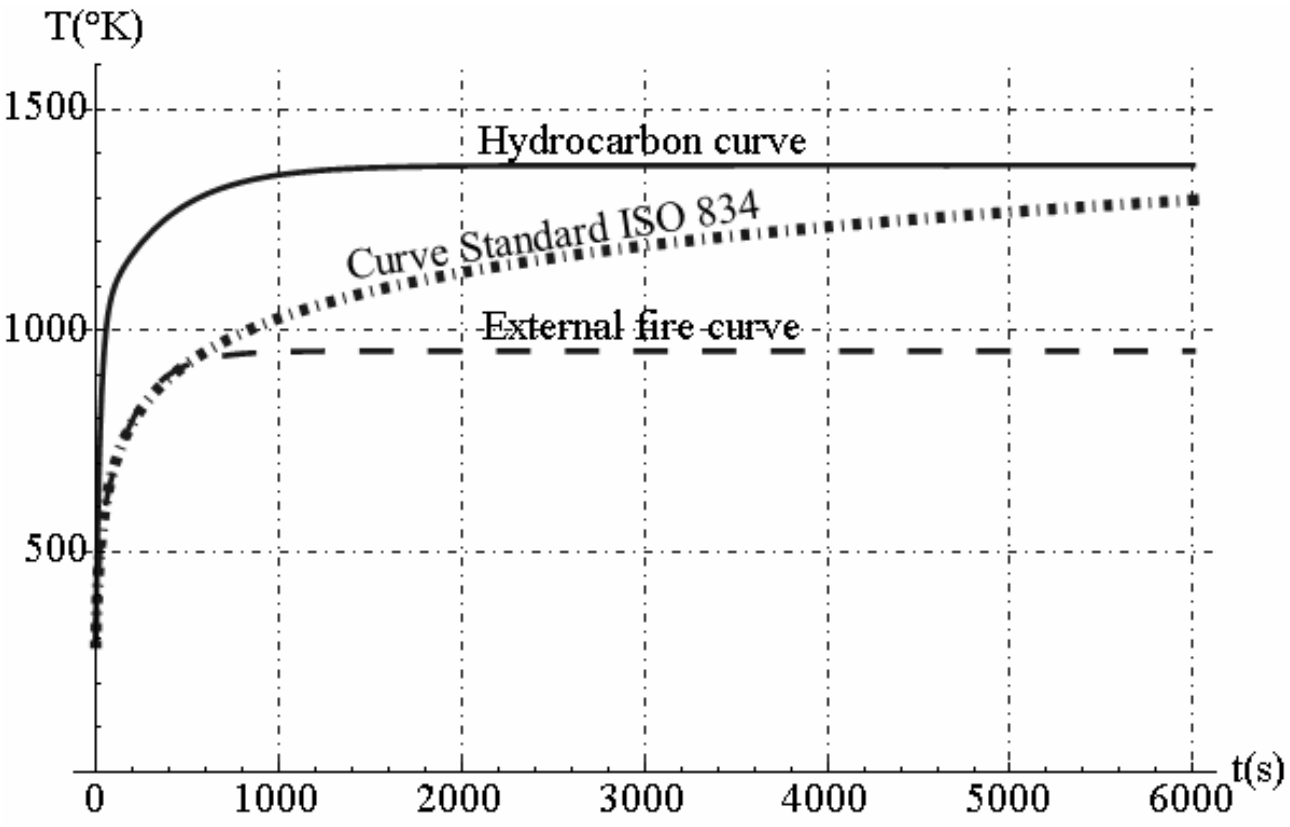

Fig. 19.1 - *Time-temperature fire curves: Standard, external and hydrocarbon [°K, sec]*

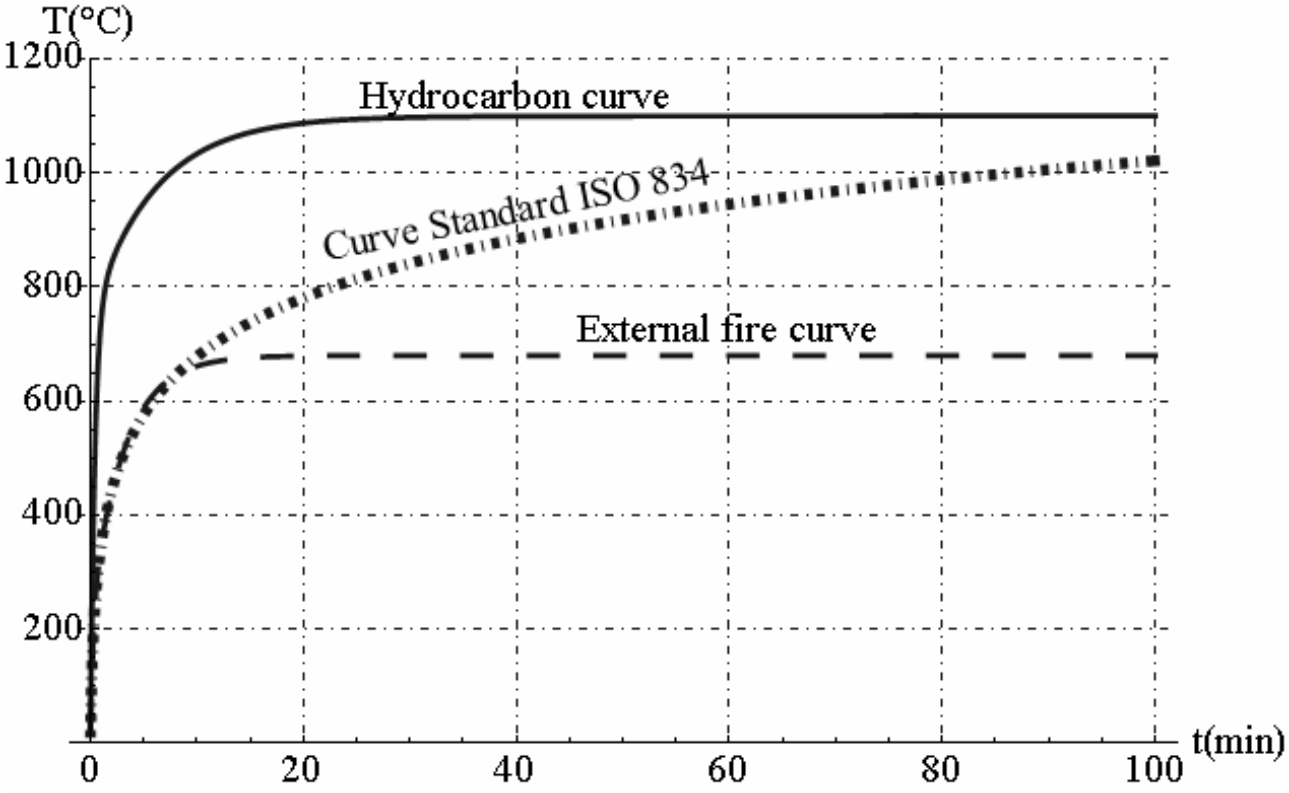

Fig. 19.2 - *Time-temperature fire curves: Standard, external and hydrocarbon [°C, min]*

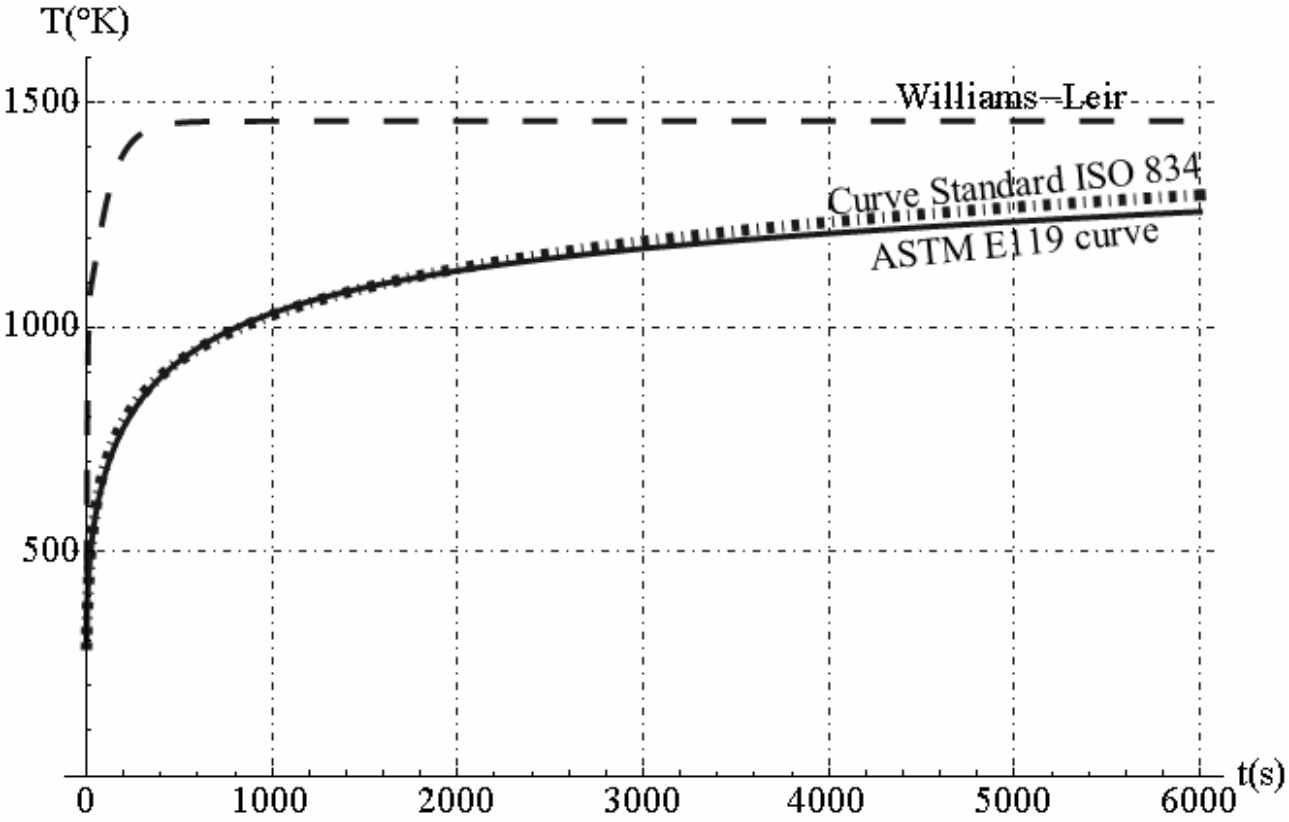

Fig. 19.3 - *Time-temperature fire curves: Standard, ASTM E119 and Williams – Leir [°K, sec]*

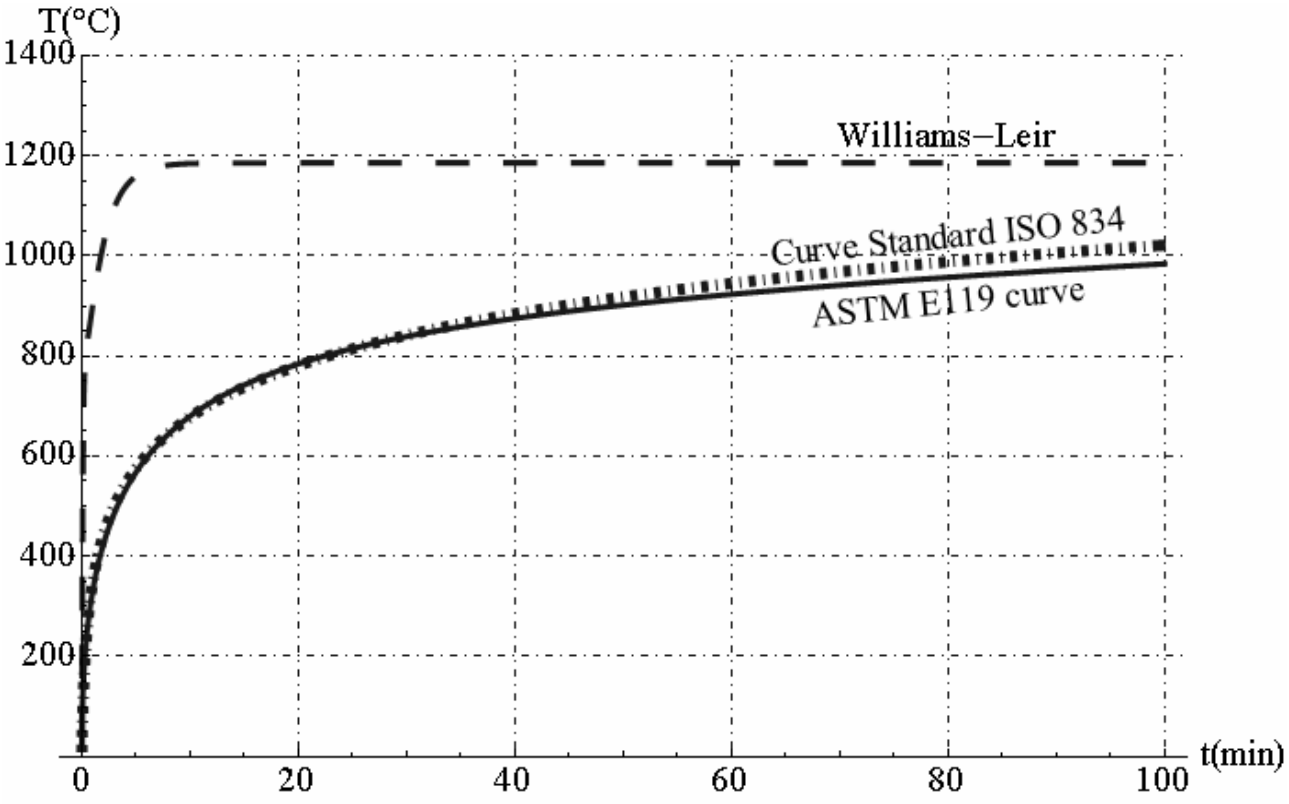

Fig. 19.4 - *Time-temperature fire curves: Standard, ASTM E119 and Williams – Leir [°C, min]*

19.3. Parametric Fire Curves

Compartment condition in an actual fire is an important study in the field of fire protection. Numerous curves have been suggested to explain the relation between temperature and time once a fire event takes place. It is important to note that factors such as thermal inertia, heat release rate, the presence of combustible materials, and the ventilation factor play a critical role in the development of these fire curves. The behaviour of compartment fire is described by three main phases, namely,

1. Growth
2. Fully developed fire
3. Decay period

Figure 19.5 represents the different phases that develop in the case of a compartment fire.

Growth: Growth is the initial phase of fire development. During this stage, combustion is restricted to certain areas of the compartment that may however result in significant localized rises in temperature. It may happen that many fires may not surpass this initial stage of fire development, due to insufficient fuel loads, limited availability of air supply, or human intervention.

Fully developed fire: The rate of increase in temperature is directly proportional to the heat release rate. Therefore, during this stage there is a large increase in the temperature of the compartment with temperatures reaching to about 1000°C. The duration of this phase depends on the volatile matter that is present in a compartment. As the rate of generation of volatile material decreases, or when there is insufficient heat available to generate such volatiles, the phase begins to cease gradually.

Decay phase: The word “decay” means decrease. As the name clearly suggests, there is a decrease in the fire intensity during this phase due to the decrease in the available fuel and the rate of fuel combustion. This phase occurs when the quantity of volatile matter continues to decrease and is consumed, after the initial stages of fire.

In addition to the standard fire curves many codes and standards are now including parametric fire curves. The concept of parametric fires provides a design method to approximate post-flashover compartment fire. A parametric fire curve takes into account the compartment size, fuel load,

ventilation conditions and the thermal properties of compartment walls and ceilings. In comparison to the standard fire curves, parametric fires provide a more realistic estimate of the compartment temperature to be used in the structural fire design of steel members.

Analyses typically assume that the temperature is uniform within the fire compartment One of the most unique characteristics of both the Eurocodes and the Swedish Design Manual is the multiple authors who contributed their work to the structural design methods of the codes. The background theory of the parametric fire model of BSEN1991-1-2 (The British Standard of Eurocode 1) was developed by Wickström inform 1980-1981. Based on the heat balance for a fire compartment, he suggested that the compartment fire depended entirely on the ratio of the opening factor to the thermal inertia of the compartment boundary. He used the test data of the 'Swedish' fire curves to validate his theoretical assumptions. Wickström expressed the compartment fire in a single power formula for the heating phase, in which the standard fire curve could be attained by assigning a ventilation factor of 0.04i m½ and a thermal inertia of 1165 $J / m^2 s^{1/2} K°$. The research conducted by Wickström has provided a solid foundation for the future use of parametric curves.

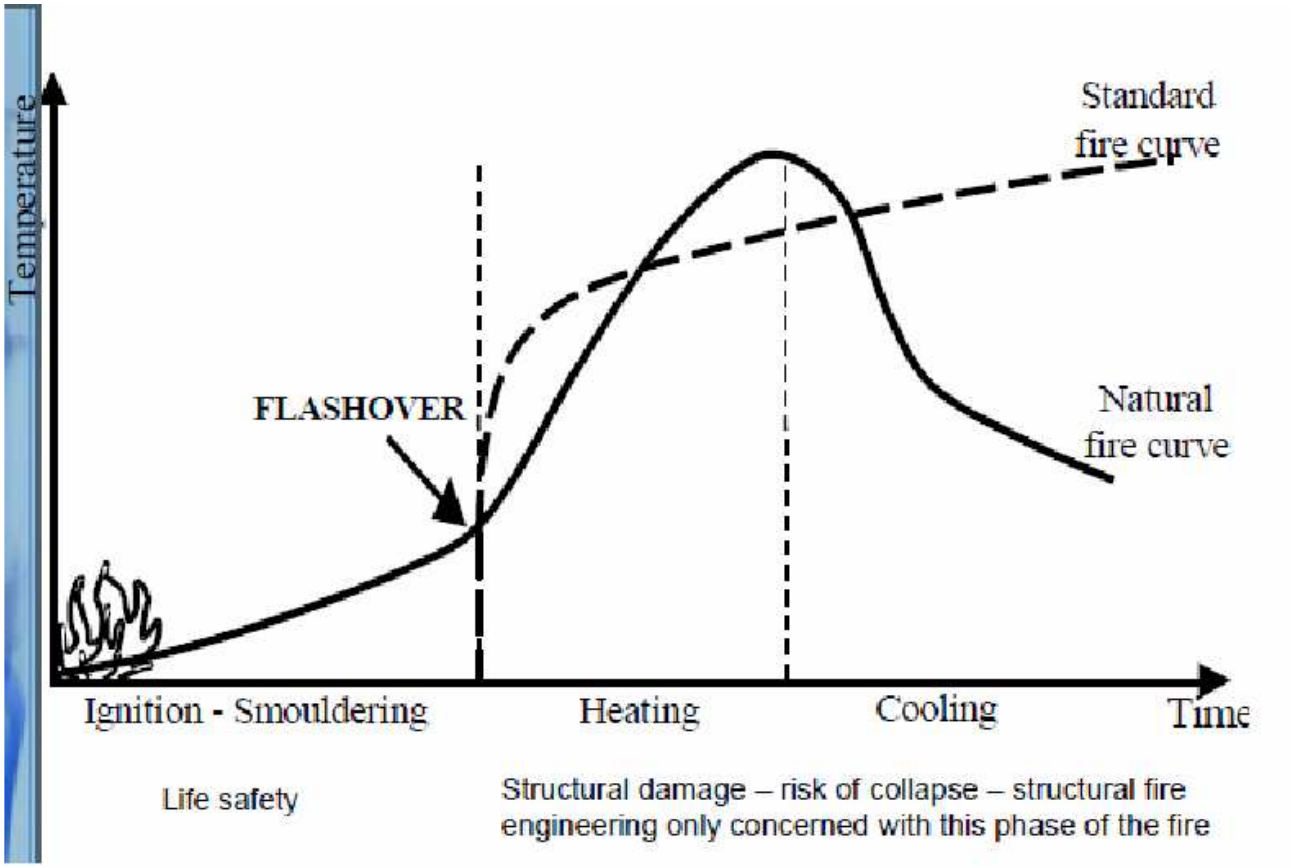

Fig. 19.5. *The behaviour of compartment fire*

19.3.1. European Parametric

Annex A in EN1991-1-2 contains the guidelines for the use of parametric fires. There are two restrictions on the parametric curves provided by this document:

(1) The temperature-time curves are valid for fire compartments up to 500 mq of floor area, without openings in the roof and for a maximum compartment height of 4 m. It is assumed that the fire load of the compartment is completely burnt out;

(2) If fire load densities are specified without specific consideration to the combustion behaviour (see annex E), then this approach should be limited to fire compartments with mainly cellulosic type fire loads;

The parametric fire curves in the heating phase can be represented by the equation:

$$\Theta_g = 20 + 1325\left(1 - 0.325e^{-0.2\,t^*} - 0.204e^{-1.7\,t^*} - 0.472e^{-19\,t^*}\right) \tag{19.7}$$

where Θg is the gas temperature in the fire compartment [°C]; t^* it the parametric time for determining compartment temperature-time response and it is given by:

$$t^* = t \cdot \Gamma\ [h] \tag{19.8}$$

Γ is the parameter to calculate parametric compartment temperature-time response. Γ is defined as

$$\Gamma = \frac{\left(\frac{F}{\sqrt{\rho c_v \lambda}}\right)^2}{(0.04/1160)^2} \tag{19.9}$$

where, F is opening factor, and $\sqrt{\rho c_v \lambda}$ is thermal inertia of the compartment boundary.

The cooling phase of this parametric curve is represented by

$$\Theta_g = \begin{cases} \Theta_{\max} - 625\left(t^* - t^*_{\max} x\right) & for\ \ t^*_{\max} \le 0.5h \\ \Theta_{\max} - 250\left(3 - t^*_{\max}\right)\left(t^* - t^*_{\max} x\right) & for\ \ 0.5h \le t^*_{\max} \le 2h \\ \Theta_{\max} - 250\left(t^* - t^*_{\max} x\right) & for\ \ t^*_{\max} \ge 2h \end{cases} \tag{19.10}$$

where $\Theta_{\max}$ is the maximum temperature that is reached during the heating phase.

$$x = \begin{cases} 1.0 & for\ \ t^*_{\max} > t_{\lim} \\ t_{\lim}\,\Gamma / t^*_{\max} & for\ \ t^*_{\max} = t_{\lim} \end{cases} \tag{19.11}$$

And $t^*_{\max}$ is given by:

$$t^*_{\max} = \frac{0.13 \cdot 10^{-3} q_{t,d}}{F\ \Gamma} \tag{19.12}$$

where $q_{t,d}$ is design fire load per unit area of compartment boundary.

The most influential variable in the parametric fire curve is the opening factor, F. It governs the behaviour of the fire and is included in almost all parametric fire equations. The opening factor represents the amount of ventilation, and it depends on the area of openings in the compartment walls, on the height of these openings and on the total area of the enclosure surfaces. The value of b is introduced into the parametric fire equation to account for multiple layers of materials that may be present in the enclosure surface. In calculation, $b = \sqrt{\rho c_v \lambda}$ and if there are not multiple layers, b can be taken as 1.

With its many variables and multiple equations needed to create both the heating phase of the fire as well as the cooling phase. The parametric curve described by EN1991 is a challenging fire curve to replicate for use in design and engineering practice. The decay curve of the parametric fire has been found not to represent the exponential time-temperature cooling characteristics of the fire tests. This can be modified with additional equations, which further add to the complexity of the EN1991 parametric fire curve.

19.3.2. Swedish Fire Curves

The design fires presented in *The Swedish Design Manual,* discussed earlier in this chapter vary greatly from those presented in EN1991. To begin, the *Manual* lists the essential requirements that must be taken into consideration in a fire model. These are:

- The quality and type of combustible material in the fire compartment
- The form and method of storage of the combustible material
- The distribution of the combustible material in the fire compartment
- The quantity of air supplied per unit time
- The geometry of the fire compartment, i.e. the areas of the floors, walls, ceiling and the openings

- The thermal properties of the structural components which enclose the fire compartment

When describing fires scenarios, Section 4 of the *Manual* refers to two classifications of fully developed fires. The focus on these fully developed fires is the ventilation in the compartment, which leads back to the opening factor and the geometry of the compartment. In the first type of fire, the rate of combustion during the flame phase is determined by the ventilation in the fire compartment and can be referred to as a ventilation-controlled fire. For second type of fire process, all of the inflowing air is not used up for combustion. Because of this, the ventilation of the fire compartment is not the limiting factor as in the first fire process. The primary factors in this fire are the properties of the combustible material, primarily the quantity and the particle shape and method of storage. This fire can be referred to as a fire-load controlled fire.
These two types of fires are important background to understand and use the design fires in the *Manual*. For a fire load of a given size, particle shape and storage density, the opening factor plays a crucial role in its behaviour. Only when the opening factor is less than a limiting value is the fire ventilation-controlled. If the opening factor is greater than the corresponding limiting value, the rate of combustion does not increase in proportion to the opening factor. This, once again, changes the fire from ventilation-controlled to load-controlled. The design fires used in the *Manual* are focused primarily on the load factor and the opening factor. The temperature curves that are presented in a later portion of section 4 are a focus of the rational fire engineering design method. They have been calculated on the assumption that the fire is controlled by ventilation during the flame phase. The most widely referenced time–temperature curves for real fire exposure are those of Magnusson and Thelandersson. When calibrating their model, Magnusson and Thelandersson manipulated the heat release rate to produce temperatures similar to those observed in short duration test fires. Magnusson and Thelandersson extrapolated their results to much higher fuel loads and a wider range of opening factors than the available test data on which the computer model was calibrated.
Results produced from Magnusson and Thelandersson on the rational fire engineering design method for steel construction can be considered conservative because the fires produce higher temperatures than may be existent in the compartment. For steel, the calculated maximum temperature for a member exposed to fire is higher if the calculation is based on the assumption that the fire is ventilation-controlled than if it is based on a load- controlled fire. The assumption of ventilation controlled fires is extremely important to recognize when comparing the design fires used in EN 1991- 1-2 to the design fires provided in this manual.
Section 4.3.3 of the *Manual* provides the calculated gas temperature-time curves for a fire compartment with different fire loads, q and different opening factors $A\sqrt{h/At}$. In this section, there are seven charts, each containing eight temperature curves. Figure 20.6 are examples of a chart and its coordinating data for an opening factor of 0.06 m^(1/2). Each chart represents a different opening factor and the individual curves on each chart represent a different fire load for that opening factor. The charts are followed by the temperature data for each time temperature curve. One can see that the larger the opening factor, the greater the maximum temperature achieved in the compartment. Within each set of curves for the various opening factors, the greater the fire load, the greater the temperatures as well. Of all of the time-temperature curves provided by the *Manual*, the curve with an opening factor of 0.3 and a fire load of 900 [Mcal/mq]/3768 [MJ/mq] achieves the highest maximum temperature of 1267 C in the compartment. As previously written significant contributions to the development of parametric curves were made by Wickström. Based on the heat balance for a fire compartment shown in Figure 19.6, Wickström suggested that the compartment fire depended entirely on the ratio of the opening factor to the thermal inertia of the compartment boundary.
He used test data of the Swedish fire curves to validate his theoretical assumptions. By curve-fitting, Wickström expressed the compartment fire in a single power formula for the heating phase, in which the standard fire curve could be attained by assigning a ventilation factor of 0.04 m½ and a thermal inertia of 1165 J/mq s½ . Due to the experimental characteristics of the Swedish fire curves,

the original application of Wickström's parametric fire curves had limitations such as maximum compartment area or thermal inertia of the material.

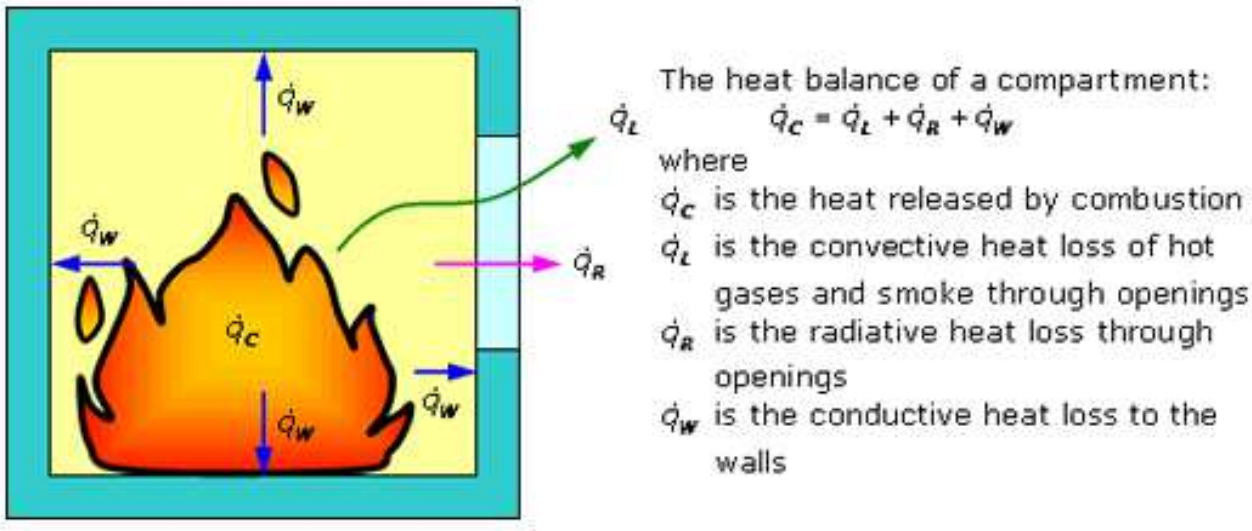

Fig. 19.6 - *Compartment Heat Balance*

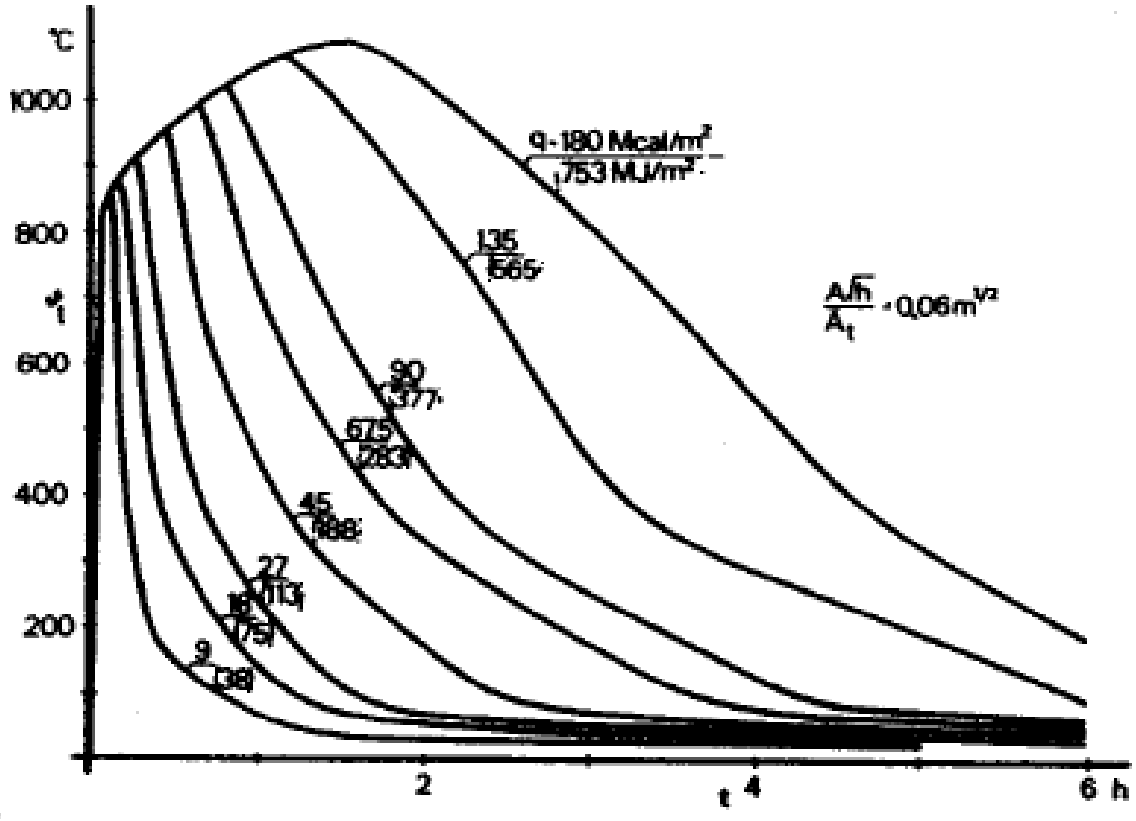

Fig. 19.7 - *Swedish Curves, Opening Factor 0.06*

19.3.3. BFD Curves

With the found complexities and inefficiencies of the European parametric curve previously described, a simple fire curve was developed by researchers with data obtained from over 142 natural fire tests. This new curve, known as the 'BFD curve' is described extensively by Barnett and Clifton in their works. While the European parametric curve consists of at least three equations for both the heating and cooling phases of the fire, there are two basic equations that describe the BFD

curve. These are:

$$T_g = T_a + T_m e^{-z}, \quad where\ z = \frac{(\log t - \log t_m)^2}{S_c} \tag{19.13}$$

where: T_g is the gas temperature at any time t (C°); T_a is the ambient temperature (C°); T_m is the maximum gas temperature generated above T_a (C°); t is the time from start of fire (min); tm is the time at which T_m occurs (min); *Sc* is the shape constant for the time-temperature curve (–).

With this fire curve, the input parameters are T_m, t_m, S_c. Changing any of these parameters changes the shape of the fire curve. Figures 19.8 through 19.10 below show the effects of each input parameter. Figure 19.8 displays the effect of changing maximum temperature, while keeping the shape factor and time to maximum temperature constant. This produces curves with higher intensities as the maximum temperature increases. Figure 19.9 displays the effects of varying the time to maximum temperature while the shape factor and maximum temperature remain constant. Finally, Figure 19.10 displays the effects of varying the shape factor while keeping the maximum temperature and the time to maximum temperature constant. These graphs show that the shape factor, or shape constant determines how long it takes before a fire begins to heat up. The larger the shape factor, the shorter the delay time. The input parameters needed for the BFD equation can be found in published fire data, design codes or by calculation. The shape constant is a relationship between the thermal insulation and the pyrolosis coefficient. For a more accurate prediction of the behavior of a fire, the shape constant can be different for both the heating and cooling phases.

Works of Barnett and Clifton discuss that the development of the BFD curves has proven to fit the results of a variety of natural fire test curves more accurately than the European parametric curves. This statement will also be shown throughout the results section of this project. Preliminary research found that studies had been done to fit the BFD curves to a few samples of the Cardington data and 87% of the curves were given one of the highest three ratings for its proximity to the BFD curve. This will also be shown in the results of this project.

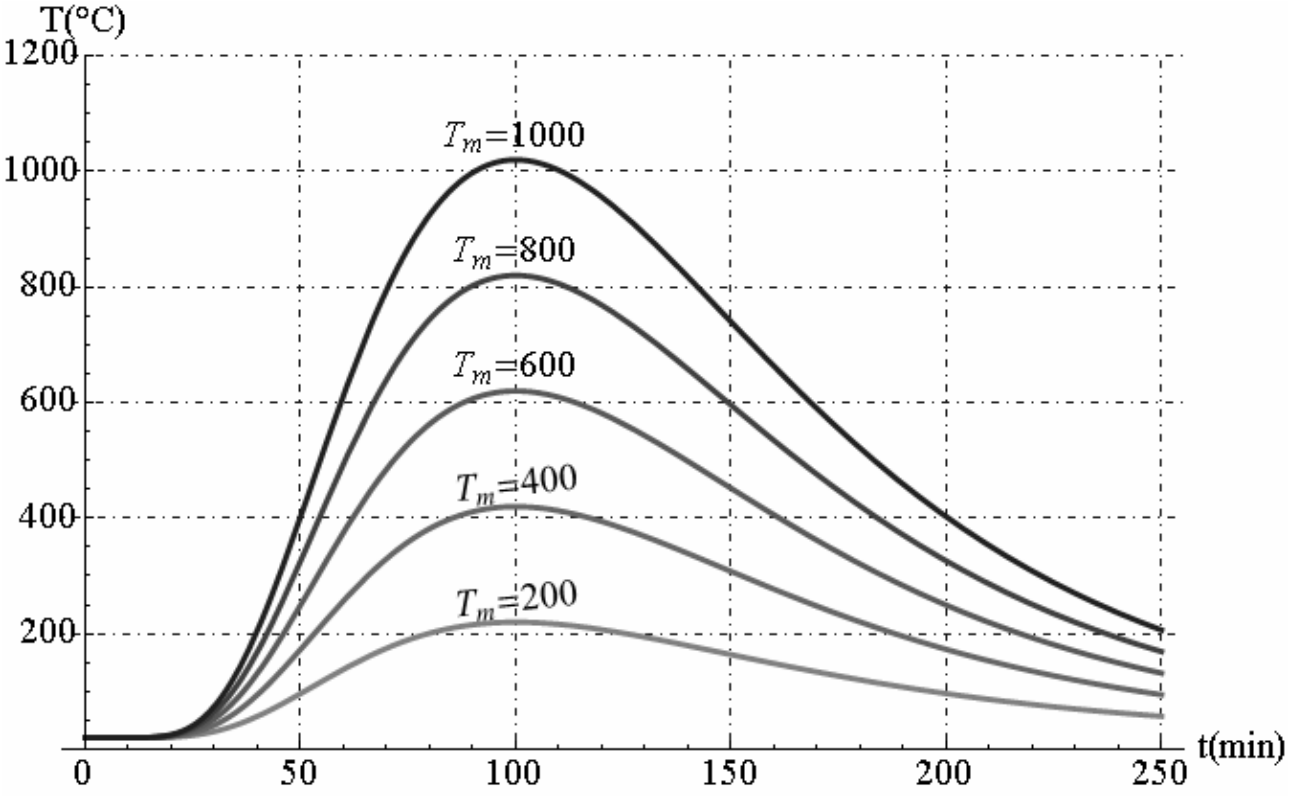

Fig. 19.8 - *BFD curves with different values for* T_m, *with fixed values of* $t_m = 100, S_c = 0.5$

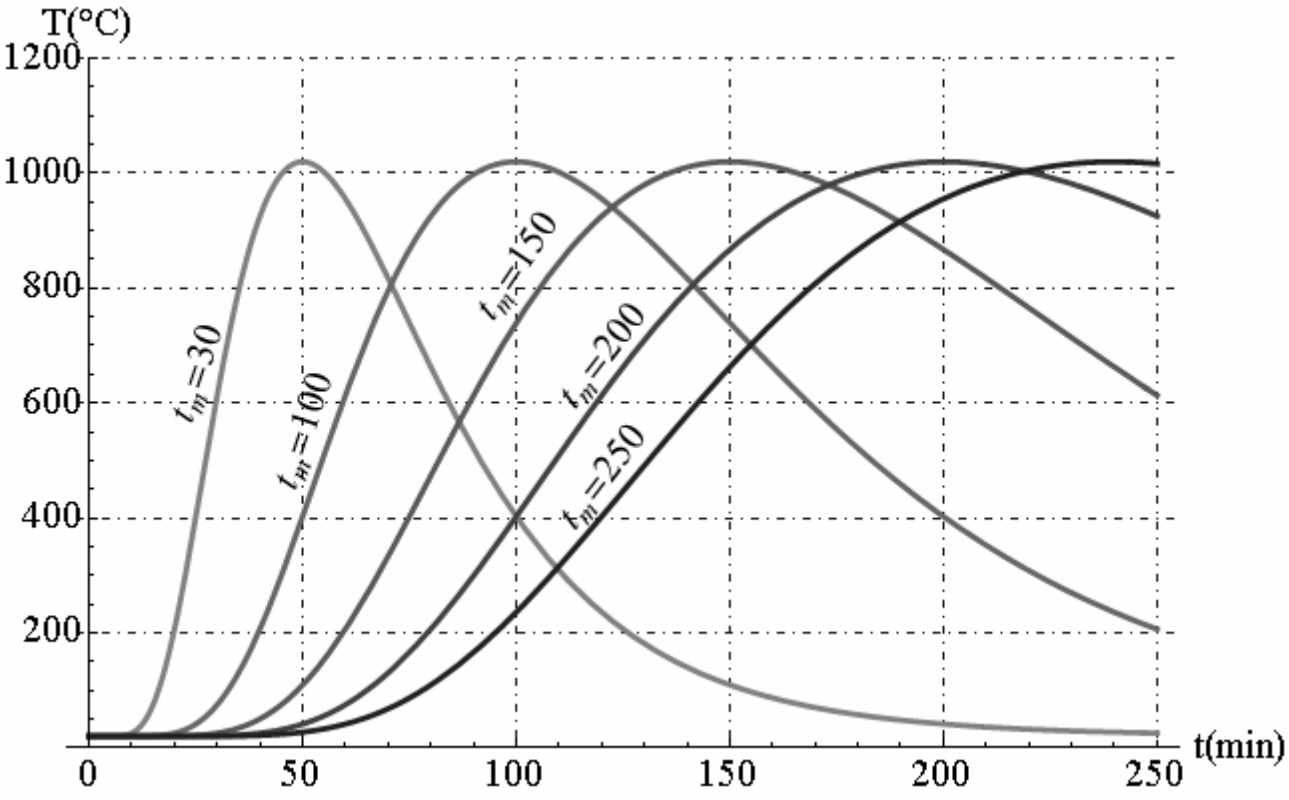

Fig. 19.9 - *BFD curves with different values for* t_m *, with fixed values of* $T_m = 1000, S_c = 0.5$

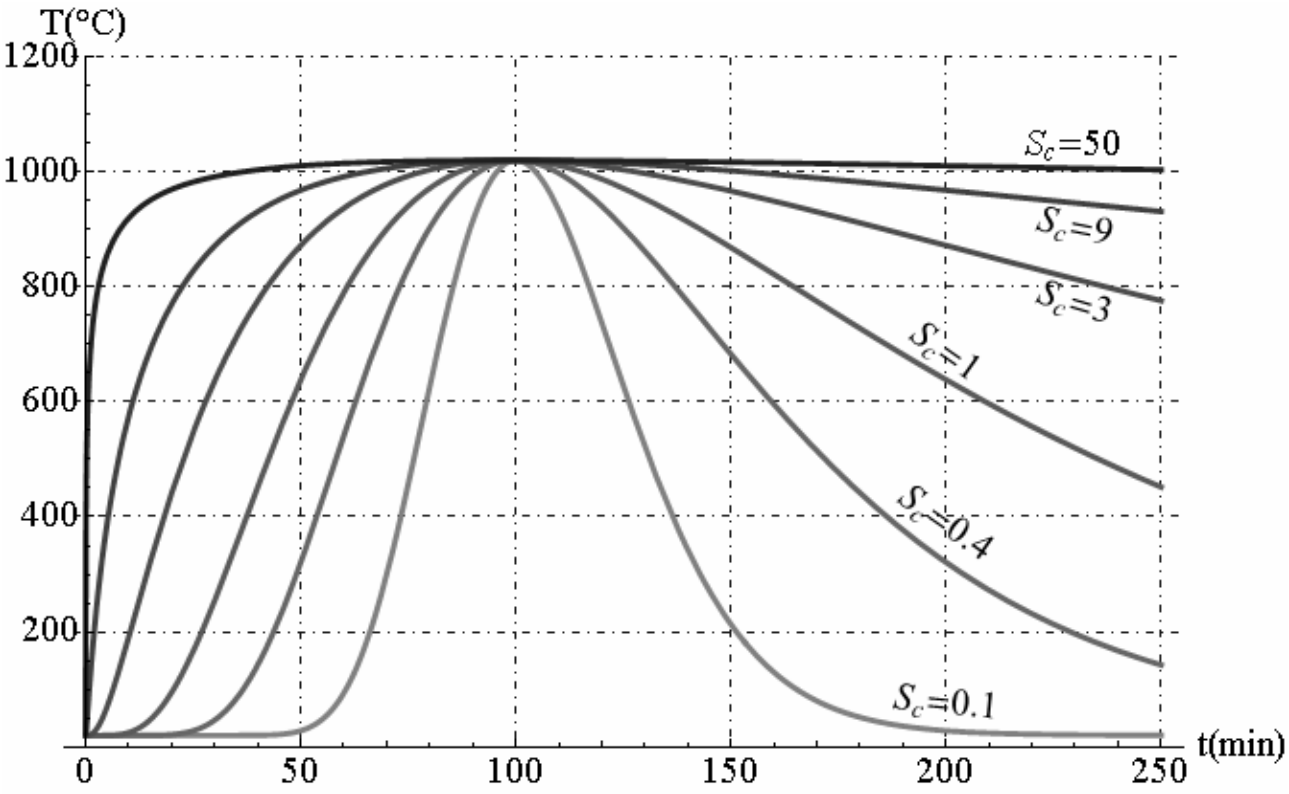

Fig. 19.10 - *BFD curves with different values for* S_c *, with fixed values of* $T_m = 1000$, $t_m = 100$,

19.3.4. CE 534 curve

Additional parametric fires that must be addressed are the 'short duration, high intensity" fire and the "long duration, low intensity" fire that were provided through previous coursework in structural fire protection and defined in the *SFPE Handbook for Fire Protection Engineering*.

Section Four, Chapter 8 of the *SFPE Handbook* presents the various fire temperature-time relations. The chapter divides the temperature course of a fire in an enclosure into three parts: the growth period, the fully developed period and the decay period. The decay period ideally represents a linear decay in the gas temperature of the enclosure and eventually a decrease in temperature of the structural members if no failure occurred. The same chapter of the *SFPE Handbook* outlines an analytical expression for determining characteristic temperature curves:

$$T = 250e^{-F^{2}t}\left[3\left(1-e^{-0.6t}\right)-\left(1-e^{-3t}\right)+4\left(1-e^{-12t}\right)\right]\left(10F\right)^{0.1/F^{0.3}}+C\left(\frac{600}{F}\right)^{0.5} \qquad (19.14)$$

where T is the fire temperature in °C; t is the time in hours; F is the opening factor in $m^{1/2}$; C is the constant to account properties of boundary material on the temperature. Using this analytical method as well as properties predefined for a short duration, high intensity as well as a longer duration, lower intensity fire, time temperature curves can be developed and used in the analysis of the steel members. The given descriptions for the behaviours of the two fires are written below. The descriptions reflect the three stages of fires previously explained.

Let us consider two example : Short duration, high intensity fire and Long duration, lower intensity fire. In first case F = 0.12 $m^{1/2}$ and the constant C = 1.0. Calculate and plot the fire temperature as a continuous function of time until the time t = 0.50 hours is reached. At time t = 0.50 hours, assume that the fire temperature decays at the rate of 20°C per minute, returning to the ambient temperature of 20°C. In the second case F = 0.04 $m^{1/2}$ and the constant C = 1.0. Calculate and plot the fire temperature as a continuous function of time until the time t = 1.5 hours is reached. At time t = 1.5 hours, assume that the fire temperature decays at the rate of 20°C per minute, returning to the ambient temperature of 20°C.

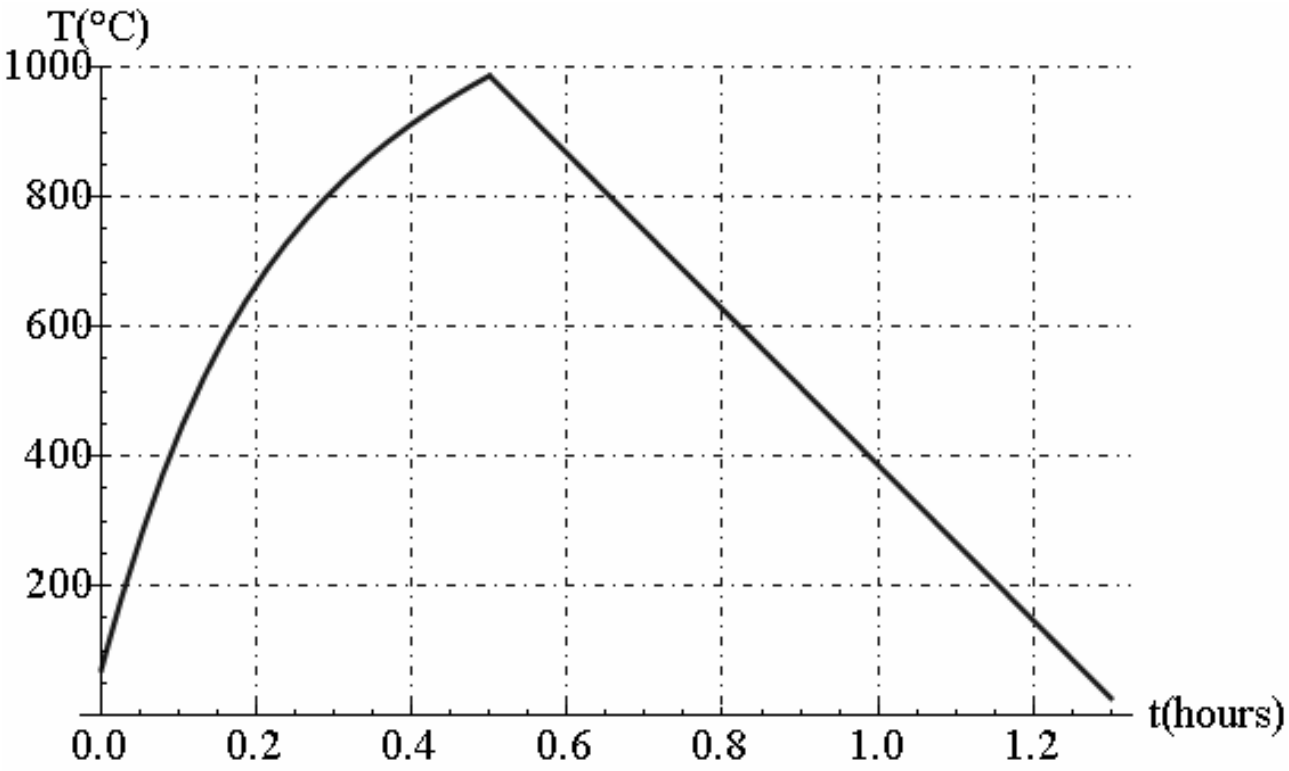

Fig. 19.11 - *Time Temperature of Short Duration, High Intensity*

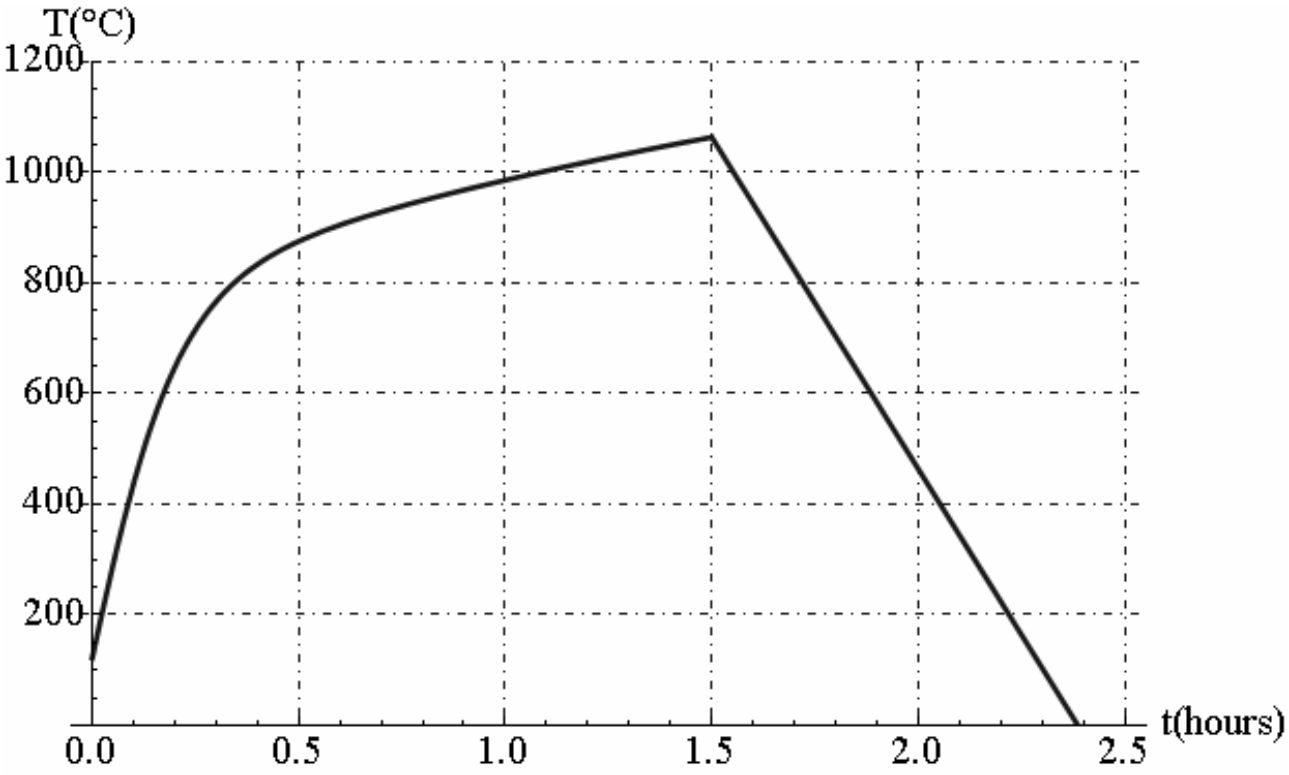

Fig. 19.12 - *Time Temperature of Long Duration, Low Intensity*

19.4. Material properties at elevated temperature

This section provides an overview of the thermal properties of steel. These properties were studied to facilitate the process of understanding and developing the models. In follows it is reported the definitions of mechanical and thermal properties of materials:

- Density (ρ): Density is a physical property of matter. In a qualitative manner density is defined as the heaviness of objects with a constant volume. It is denoted ρ . Common unit of density is kg / m^3;
- Thermal Conductivity (k): Thermal conductivity is defined as the amount of heat flux that would pass through a certain material depending on the temperature gradient over that material. Thermal conductivity plays an important role in many heat and mass transport phenomena as it is a function of Prandtl number. It is denoted as k. Commonly used units are W/mK and cal/sec - cm - °C;
- Specific Heat (c_v): Specific heat is an intensive property which means that it is independent of the mass of a substance Specific heat is defined as the amount of heat required to raise the temperature of one gram of a substance by one degree celcius. It is denoted as c_v. Common units for specific heat are J/kgK and J/kg°C;
- Coefficient of Thermal Expansion (α):The coefficient of thermal expansion is defined as the increase or elongation in length occurring in a member per unit increase in temperature. It is denoted as α. Commonly used units are in/in/°C, cm/cm/°C;
- Thermal Diffusivity: Thermal diffusivity is defined as the ratio of thermal conductivity to heat capacity. Its values are obtained on the basis of density, thermal conductivity and specific heat data for a particular material. It is denoted as ″a ″. Common units are mq/sec, cmq/sec, mmq/sec. $\kappa = k/\rho c_v$, where k = thermal conductivity in W/mK; ρc_v = volumetric heat capacity measured in $J / m^3 K°$. Substances with high thermal diffusivity rapidly adjust their temperature to that of their surroundings, because they conduct heat quickly in comparison to their thermal 'bulk';

- Emissivity: Emissivity of a material is defined as the ratio of energy radiated to energy radiated by a black body at the same temperature. It is a dimensionless quantity. It is denoted as ″e″.

19.4.1. Thermal Properties of Steel

Steel is a metal alloy whose major component is iron, with carbon being the primary alloying material. Different quality/grades of steel can be manufactured by varying the amount of carbon and its distribution in the alloy **.** Fire resistant steel is manufactured by adding molybdenum **(Mo)** and other alloying materials . The behaviour of steel when exposed to high temperatures is of critical importance for the safety and stability of the building. The temperature rise for a steel member is a function of the materials, thermal conductivity and specific heat. Thermal conductivity tends to decrease with the increase in temperature while specific heat tends to increase with the increase in temperature. The properties are discussed in the following sections with the help of graphs from different sources.

Density: The standard value for the density of structural steel proposed by Eurocode 3, Part 1.2 is $7850\,kg/m^3$**.** For most calculations and research work density is assumed to be constant with the increase in temperature. Hence, a constant value was adopted for the modelling of the beam.

Coefficient of Thermal Expansion: The coefficient of thermal expansion for steel is denoted as α_s. The thermal elongation is temperature dependent and can be evaluated based on the equations proposed in Eurocode 3, Part 1.2**.** Figure 19.13 presents the plot for thermal expansion versus temperature from Bletzacker's data:

$$\varepsilon^T = \frac{\Delta L}{L} = \begin{cases} -2.416\cdot 10^{-4} + 1.2\cdot 10^{-5} T + 0.4\cdot 10^{-8} T^2 & \forall T \in [20°C, 750°C] \\ 1.1\cdot 10^{-2} & \forall T \in [750°C, 860°C] \\ 2\cdot 10^{-5} T - 6.2\cdot 10^{-3} & \forall T > 860°C \end{cases} \tag{19.15}$$

In simple calculation models the relationship between thermal elongation and steel temperature may be consider to be constant. In this case the elongation may be determined from:

$$\varepsilon^T = \Delta L / L = 1.4\cdot 10^{-6}\left(T - 20\right) \tag{19.16}$$

In the figure 19.13 is reported the thermal elongation calculated by equation (19.16), also.

Thermal Conductivity: Units for thermal conductivity are W/mK and W/cm°C. The standard value for thermal conductivity of steel as suggested by Eurocode 3, Part 1.2 is 54 W/mK at 20°C. However, thermal conductivity k_s of steel varies with the change in temperature based on the relations established by Eurocode 3, Part 1.2 **.**

$$k_s\left(T\right) = \begin{cases} 54 - 0.0333T & \forall T \in \left[20°C, 800°C\right] \\ 27.3 & \forall T > 800°C \end{cases} \tag{19.17}$$

Figure 19.14 represents thermal conductivity values based on Equations (19.17) and approximate function of thermal conductivity given by:

$$k_s\left(T\right) = 46.710 - 0.019T \quad \forall T \in [0, 1200°C] \tag{19.18}$$

The function (19.18) gives the absolute maximum error respect to function (19.17) equal to 14%.

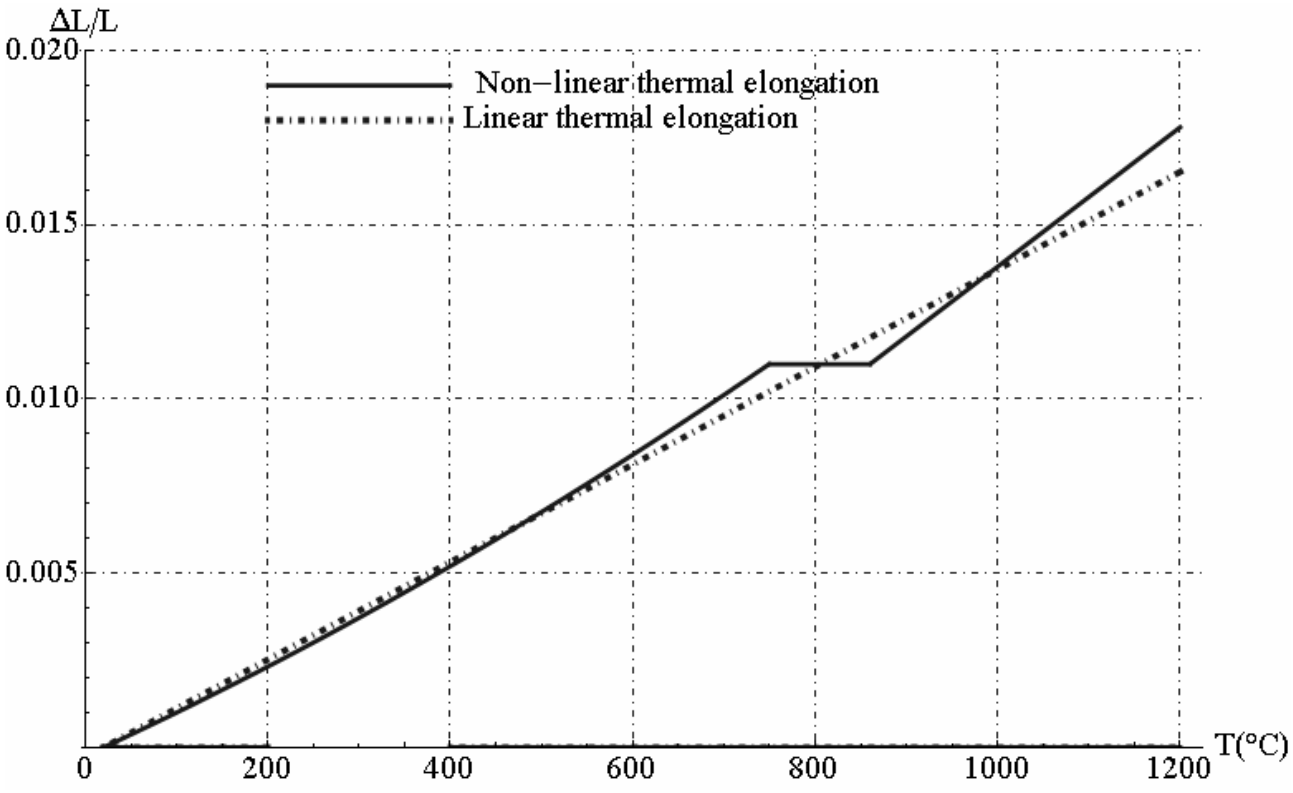

Fig. 19.13 - *Thermal elongation of steel as function of temperature*

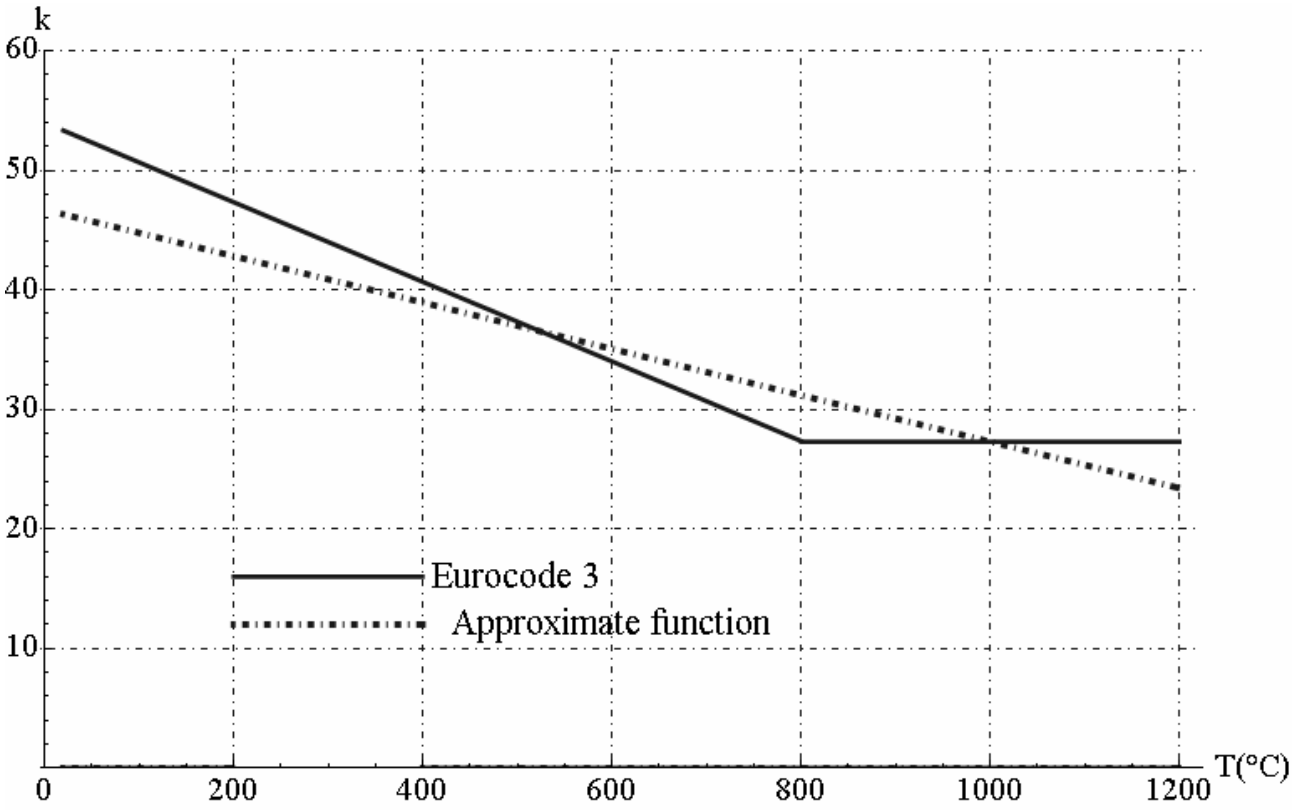

Fig. 19.14 - *Thermal conductivity of steel as function of temperature*

Specific Heat **:** Specific heat for steel is denoted as c_v. Units for specific heat are J/kg K. The equations suggested by Eurocode 3, Part 1.2 for change of specific heat of steel with temperature are presented below:

$$c_v = \begin{cases} 425 + 7.73\cdot 10^{-1} T - 1.69\cdot 10^{-3} T^2 + 2.22\cdot 10^{-6} T^3 & \forall T \in [20°C, 600°C] \\ 666 + \dfrac{13002}{738 - T} & \forall T \in [600°C, 735°C] \\ 545 + \dfrac{17820}{T - 731} & \forall T \in [735°C, 900°C] \\ 650 & \forall T \in [900°C, 1200°C] \end{cases} \tag{19.19}$$

The results of these equations are graphically represented in Figure 19.15.

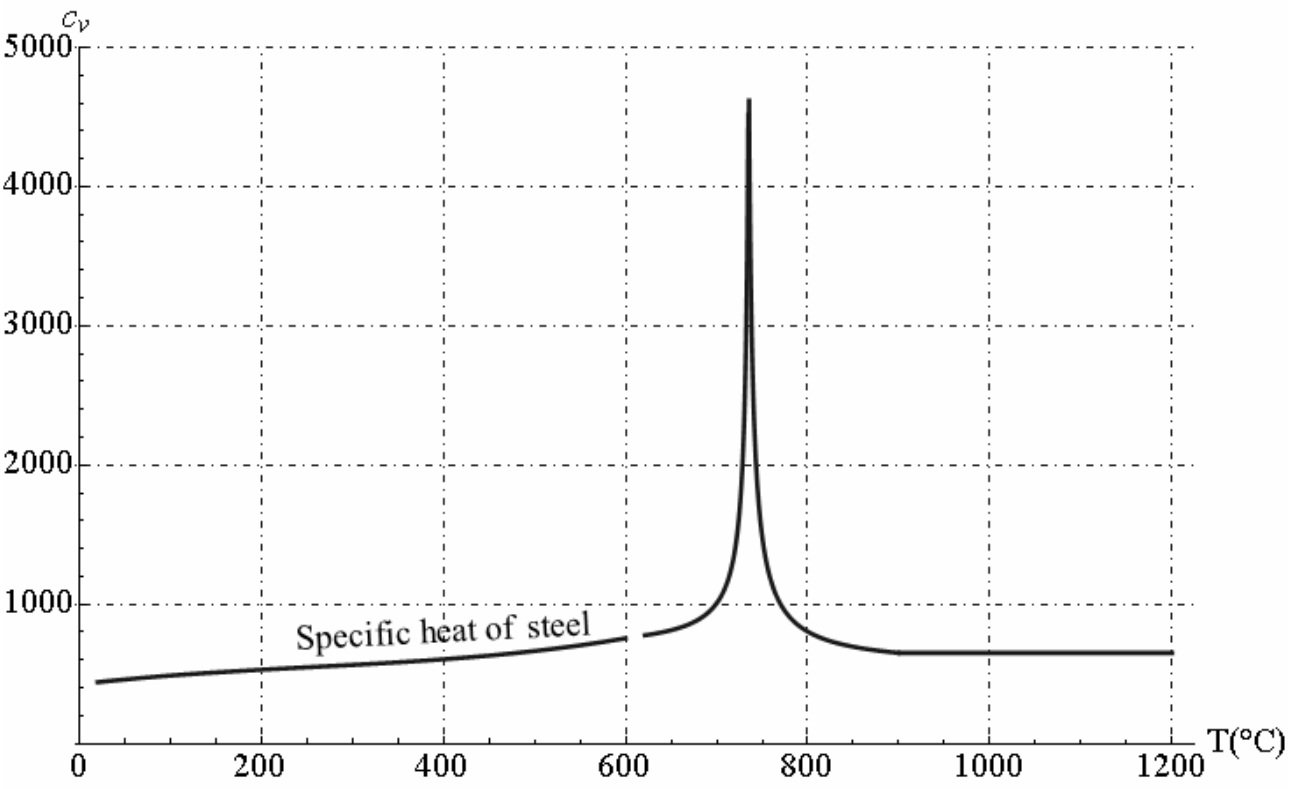

Fig. 19.15 - *Specific heat of steel as function of temperature*

Stress-strain relationship: Eurocode 3, part 1.2 , defines the variation of steel mechanical properties at high temperature for a heating rate situated between 20°C/min and 50°C/min, and has been determine for the temperature between 20°C and 1200°C. The graphical representation of the stress-strain relation proposed by EuroCode 3, part 1.2, has a linear –elliptic shape and is described by the relations reported below.

In **elastic zone** the stress-strain relation is given by linear function and the tangent modulus is equal to Young's modulus:

$$\begin{cases} \sigma(\varepsilon, T) = E(T)\,\varepsilon, \\ E_t(T) = E(T), \end{cases} \qquad \forall \varepsilon \in \left[0, \varepsilon_p(T)\right] \tag{19.20}$$

where $\varepsilon_p(T) = \dfrac{\sigma_p(T)}{E(T)}$ is the proportional strain and $\sigma_p(T)$ is the proportional stress. In **elliptic zone** the stress-strain relation is given by non-linear function:

$$\begin{cases} \sigma(\varepsilon,T)=\sigma_p(T)-c+\dfrac{b}{a}\sqrt{a^2-\left[\varepsilon_y(T)-\varepsilon\right]^2} \\ E_t(\varepsilon,T)=\dfrac{b\left[\varepsilon_y(T)-\varepsilon\right]}{a\sqrt{a^2-\left[\varepsilon_y(T)-\varepsilon\right]^2}} \end{cases} \qquad \forall\varepsilon\in\left[\varepsilon_p(T),\varepsilon_y(T)\right] \tag{19.21}$$

where $\varepsilon_y(T)=0.02$ is elastic limit strain, $\sigma_y(T)$ is elastic limit stress, and the constants a,b,c are given by following relationships:

$$\begin{aligned} a&=\sqrt{\left[\varepsilon_y(T)-\varepsilon_p(T)\right]\left[\varepsilon_y(T)-\varepsilon_p(T)+\frac{c}{E(T)}\right]}, \\ b&=\sqrt{E(T)\left[\varepsilon_y(T)-\varepsilon_p(T)\right]c+c^2}, \\ c&=\frac{\left[\sigma_y(T)-\sigma_p(T)\right]^2}{\left[\varepsilon_y(T)-\varepsilon_p(T)\right]E(T)-2\left[\sigma_y(T)-\sigma_p(T)\right]}, \end{aligned} \tag{19.22}$$

In **plastic zone** the stress-strain relation is given by:

$$\begin{cases} \sigma(\varepsilon,T)=\sigma_y(T) \\ E_t(\varepsilon,T)=0 \end{cases} \quad \forall\varepsilon\in\left[\varepsilon_y(T),\varepsilon_t(T)\right] \tag{19.23}$$

where $\varepsilon_t(T)=0.15$. In the **softening zone** the stress-strain relation is given by:

$$\sigma(\varepsilon,T)=\sigma_y\left[1-\left(\frac{\varepsilon-\varepsilon_t}{\varepsilon_u-\varepsilon_t}\right)\right] \quad \forall\varepsilon\in\left[\varepsilon_t(T),\varepsilon_u(T)\right] \tag{19.24}$$

where $\varepsilon_u(T)=0.20$ is the ultimate strain of steel. The elastic limit stress $\sigma_e(T)$, the proportional limit, $\sigma_p(T)$, and the shape of the elastic range, have been determined for temperatures situated between 20°C and 1200 °C. The following dimensionless parameters are defined:

$$K_y(T)=\frac{\sigma_e(T)}{\sigma_e(20)}, \quad K_p(T)=\frac{\sigma_p(T)}{\sigma_p(20)}, \quad K_E(T)=\frac{E(T)}{E(20)}, \tag{19.25}$$

In table 19.1 there are presented the variations of parameters $K_y(T),K_p(T),K_E(T)$ caused by temperature increasing, in steps of 100°C. For other temperatures, a linear interpolation is admitted.

$K_y(T)$	1.000	1.000	1.000	1.000	1.000	0.780	0.470	0.230	0.110	0.060	0.040	0.02	0.000
$K_p(T)$	1.000	1.000	0.807	0.613	0.420	0.360	0.180	0.075	0.050	0.0375	0.025	0.0125	0.000
$K_E(T)$	1.000	1.000	0.900	0.800	0.700	0.600	0.310	0.130	0.090	0.068	0.045	0.0225	0.000
T(°C)	20	100	200	300	400	500	600	700	800	900	1000	1100	1200

Table 19.1 - *Effect of temperature on parameters* $K_y(T),K_p(T),K_E(T)$

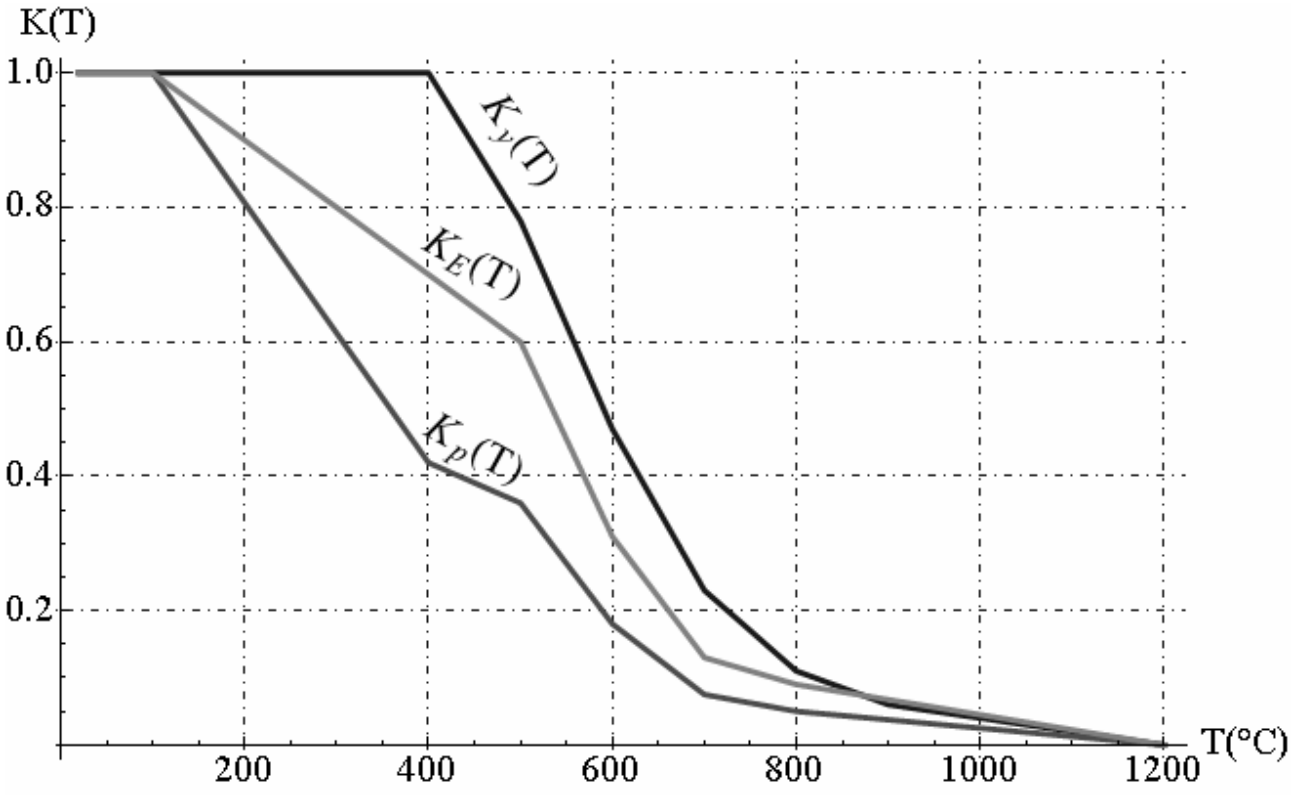

Fig. 19.16 - *Dependence of parameters* $K_y(T), K_p(T), K_E(T)$ *versus temperature, proposed by Eurocode 3, part 1.2*

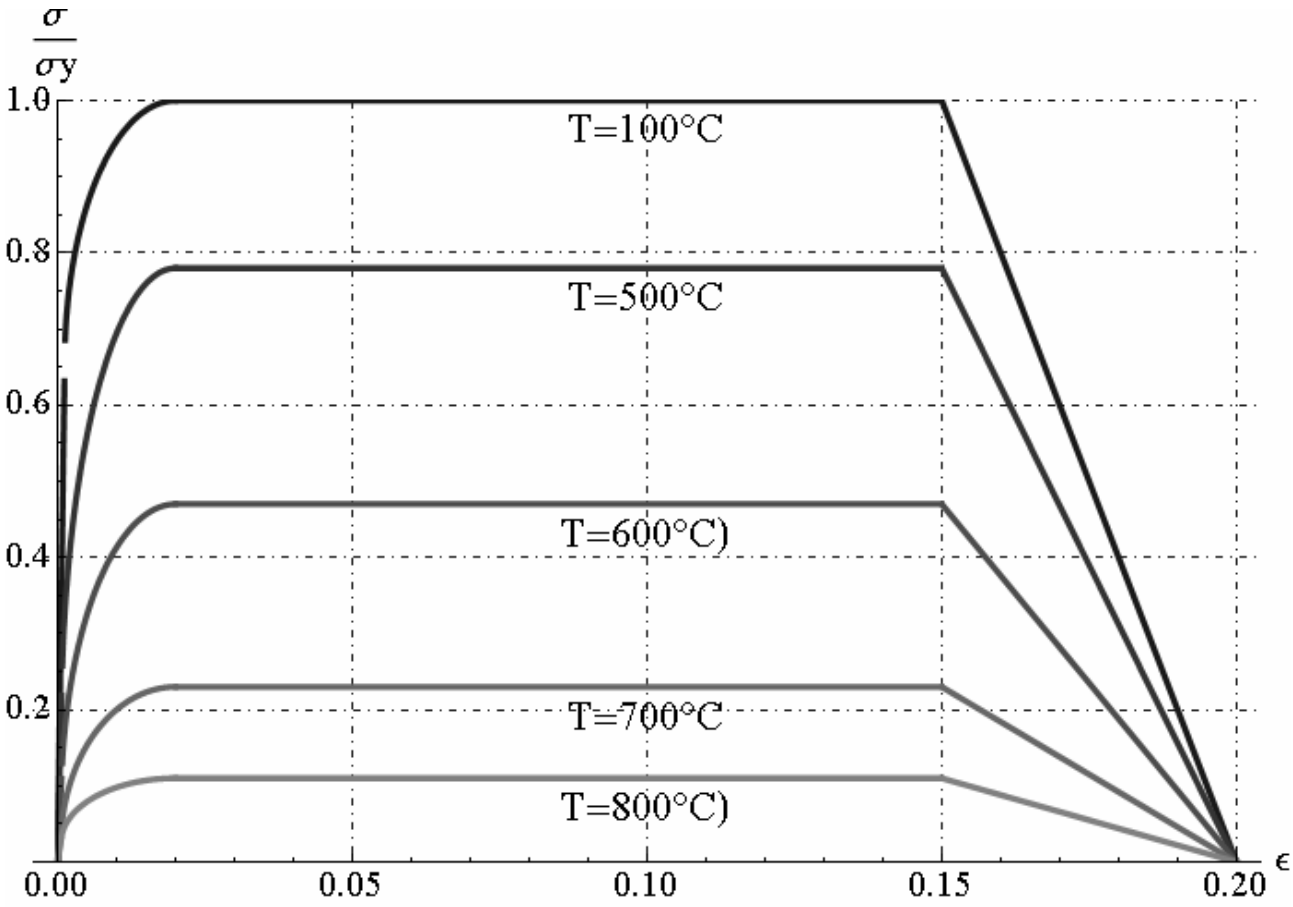

Fig. 19.17 - *Stress-strain curves as function of temperature, proposed by Eurocode 3, part 1.2*

Young's modulus: When the steel elements and structures are subjected to high temperature (fire) they progressively lose their stiffness and carrying capacity because Young's modulus E and the elastic limit σ_e are decreasing. D.T.U. proposes a set of relations referring to steel behaviour in the elastic range at high temperatures. According to D.T.U., the variation of Young's modulus must be considered only up to 1000°C, because for grater temperatures, the stele has no mechanical resistance. Young' modulus variation is defined by the relations :

$$K_E(T)=\frac{E(T)}{E(20)}=\begin{cases}1+\dfrac{T}{2000\log(T/1100)} & \forall T\in[20°C,600°C]\\ \dfrac{690-0.69T}{T-53.5} & \forall T\in[600°C,1000°C]\end{cases} \tag{19.26}$$

where $E(T)$ and $E(20)$ are Young' modulus at temperature T and 20°C, respectively.

Moreover, we proposed an analytical function characterized by polynomial law of temperature of six grade reported below:

$$\frac{E(T)}{E(20°C)}=E_0+E_1T+E_2T^2+E_3T^3+E_4T^4+E_5T^5+E_6T^6 \quad \forall T\in[20°C,1200°C] \tag{19.27}$$

where

$$\begin{aligned}&E_0=0.999,\ E_1=1.43\cdot10^{-4},\ E_2=-3.84\cdot10^{-6},\ E_3=9.28\cdot10^{-9},\\ &E_4=-1.618\cdot10^{-11},\ E_5=1.38\cdot10^{-14},\ E_6=-4.15\cdot10^{-18},\end{aligned} \tag{19.28}$$

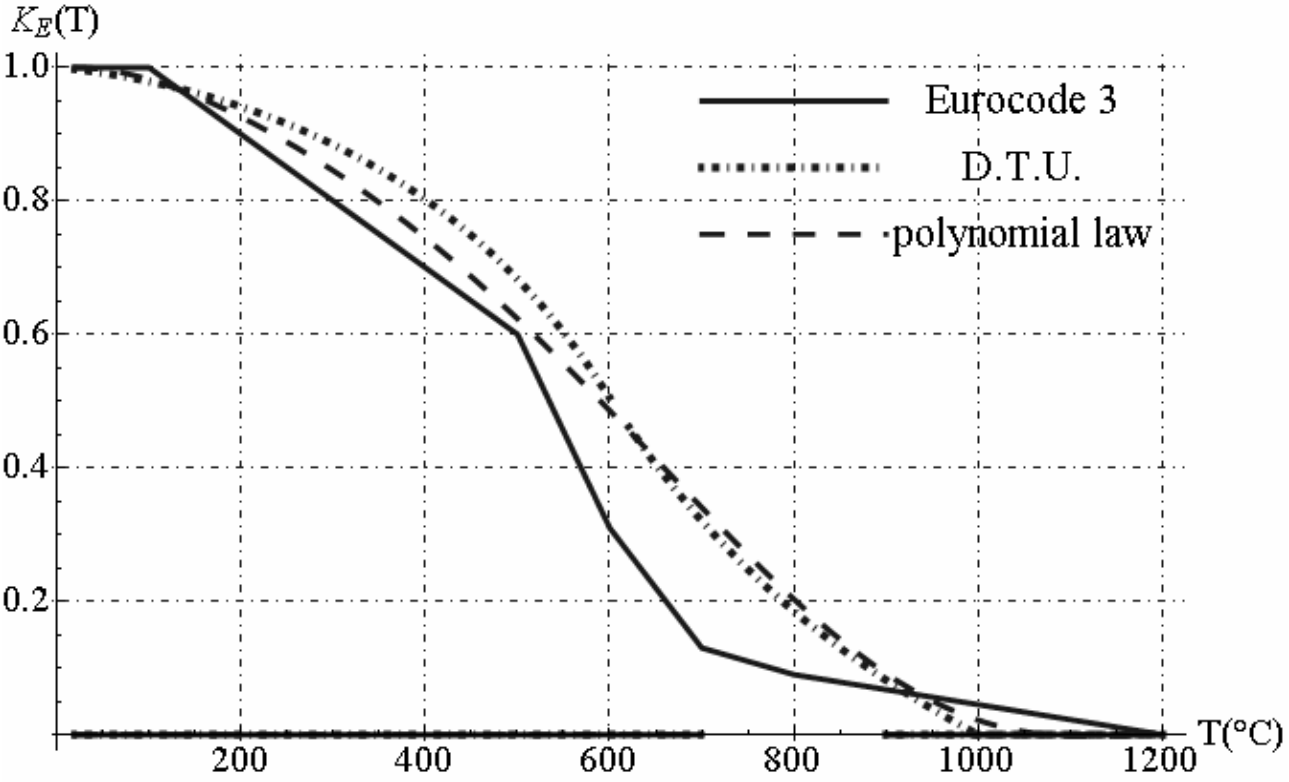

Fig. 19. 18 - *Young's modulus of steel as function of temperature. Comparison curves determined by Eurocode 3, D.T.U. and polynomial law*

Proportional stress:

We proposed an analytical function characterized by polynomial law of proportional stress reported below:

$$K_p(T)=\frac{\sigma_p(T)}{\sigma_p(20)}=B_0+B_1T+B_2T^2+B_3T^3+B_4T^4+B_5T^5+B_6T^6 \quad \forall T\in[20°C,1200°C] \tag{19.29}$$

where

$$B_0 = 0.9981,\ B_1 = 1.90\cdot 10^{-4},\ B_2 = -4.72\cdot 10^{-6},\quad B_3 = -1.056\cdot 10^{-9},$$
$$B_4 = 1.511\cdot 10^{-11},\quad B_5 = -1.491\cdot 10^{-14},\quad B_6 = 4.414\cdot 10^{-18}, \tag{19.30}$$

Elastic limit of steel (yielding stress):

The variation of elastic limit of steel is described by the following relations, according to D.T.U.:

$$K_y(T) = \frac{\sigma_y(T)}{\sigma_y(20)} = \begin{cases} 1 + \dfrac{T}{900\log(T/1750)} & \forall T \in [20°C, 600°C] \\ \dfrac{340 - 0.34T}{T - 240} & \forall T \in [600°C, 1000°C] \end{cases} \tag{19.31}$$

where $\sigma_y(T)$ and $\sigma_y(20)$ are elastic limit of steel at temperature T and 20°C, respectively. Moreover, we proposed an analytical function characterized by polynomial law of elastic limit of steel reported below:

$$K_y(T) = \frac{\sigma_y(T)}{\sigma_y(20)} = A_0 + A_1T + A_2T^2 + A_3T^3 + A_4T^4 + A_5T^5 + A_6T^6 \quad \forall T \in [20°C, 1200°C] \tag{19.32}$$

where

$$A_0 = 0.9997,\ A_1 = 2.87\cdot 10^{-5},\ A_2 = -4.852\cdot 10^{-7},\quad A_3 = -8.137\cdot 10^{-9},$$
$$A_4 = 1.478\cdot 10^{-11},\quad A_5 = -9.039\cdot 10^{-15},\quad A_6 = 1.865\cdot 10^{-18}, \tag{19.33}$$

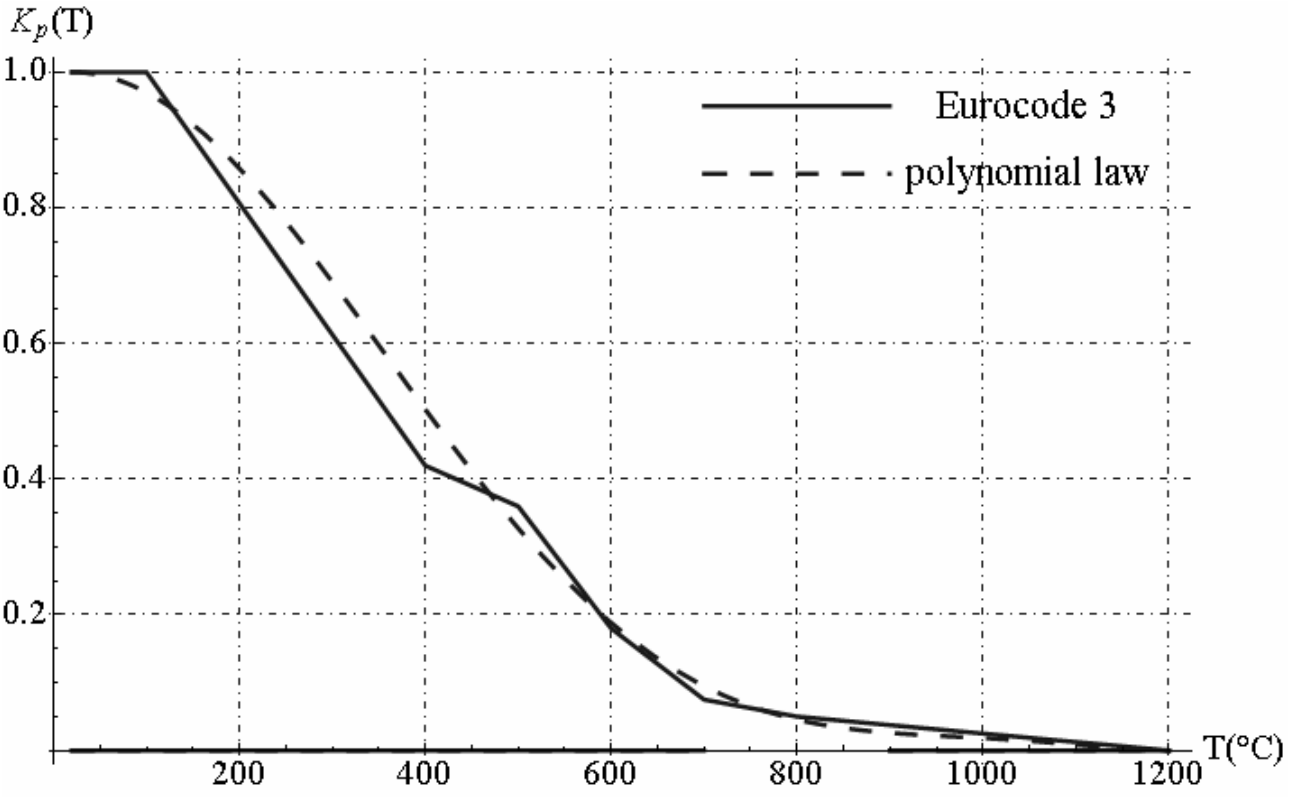

Fig. 19.19a - *Elastic limit of steel as function of temperature-*
Comparison curves determined by Eurocode 3 , D.T.U. and polynomial law

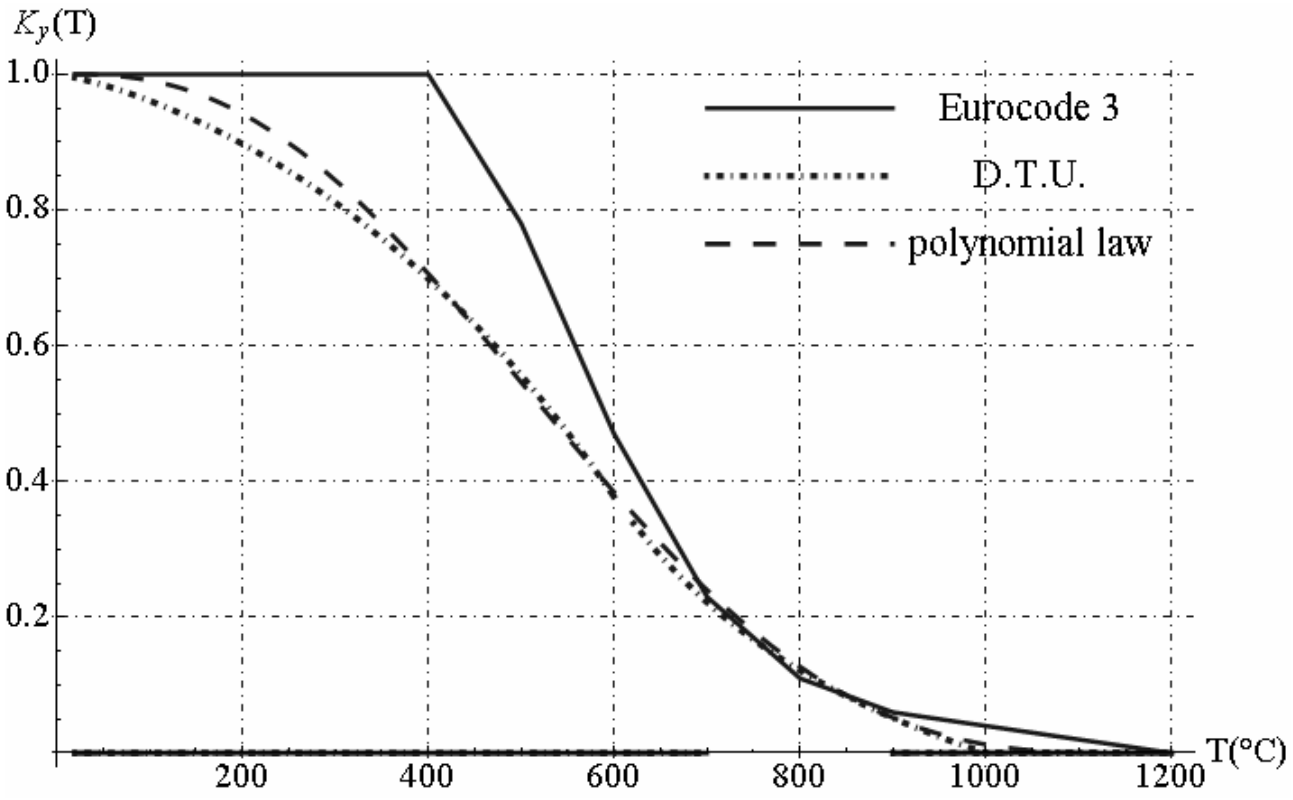

Fig. 19.19b - *Elastic limit of steel (yielding stress) as function of temperature-Comparison curves determined by Eurocode 3 and polynomial law*

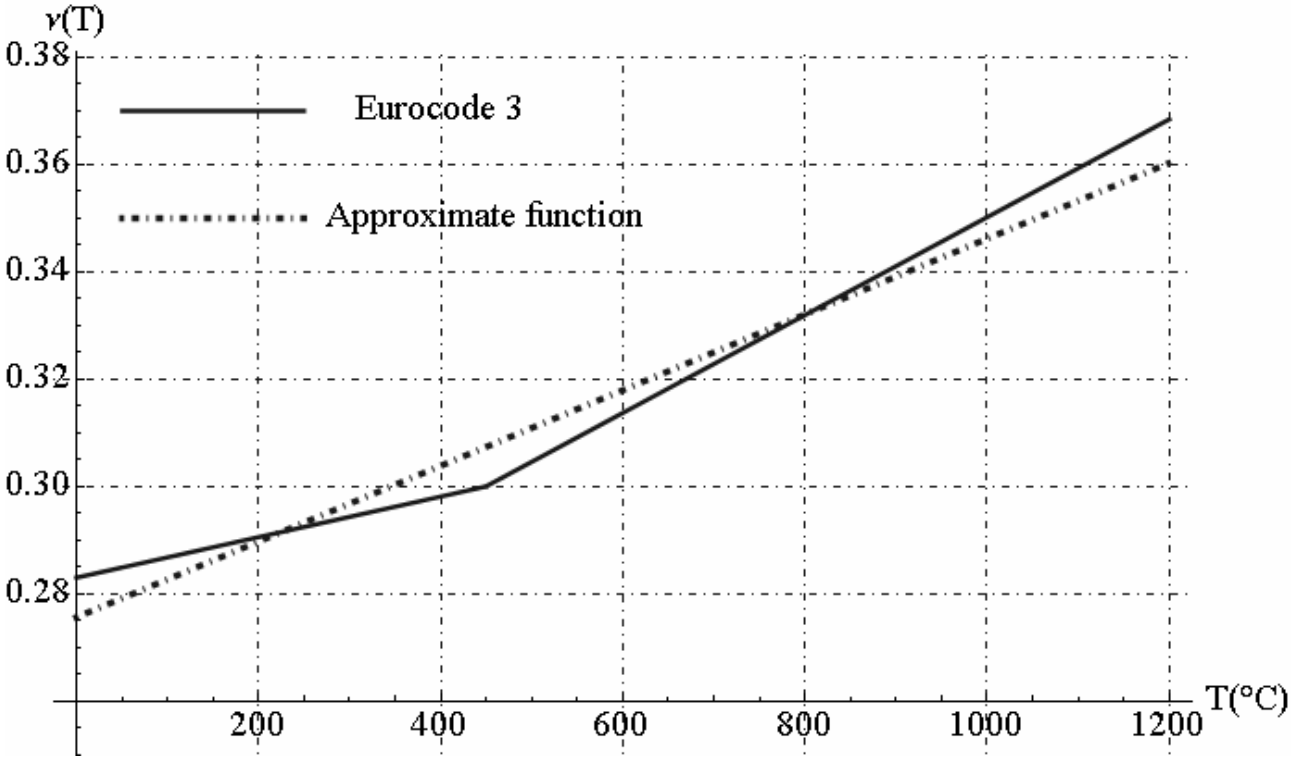

Fig. 19.20 - *The dependence between the Poisson's ratio vs temperature*

Poisson's ratio: The variation of Poisson's ratio with temperature is given by :

$$\nu_s(T)=\begin{cases}0.283+3.78\cdot10^{-5}T & \forall T\in[0,450°C]\\ 9.12\cdot10^{-5}T+0.259 & \forall T>450°C\end{cases} \tag{19.34}$$

In follows, let us consider the approximate function of Poisson's ratio versus temperature given by:

$$\nu_s(T)=0.276+7.057\cdot10^{-5}T \quad \forall T\in[0,1200°C] \tag{19.35}$$

By utilizing the relation (19.35) for Poisson's ratio, the maximum percentage error obtained reaches the value 1.5.

Tangent Modulus: The tangent modulus, $E_t(T)$, represents the shape of the characteristic diagram (relation stress-strain), where it has a non-linear shape, at temperature T. Is variation, produced by the temperature increasing, is expressed by the following relations that are graphically represented in figure 19.21.

$$E_t(T)=\begin{cases}\left(5\cdot10^{-5}T+10^{-2}\right)E(20) & \forall T\in[0,300°C]\\ \left[-7\cdot10^{-5}(T-300)+2.5\cdot10^{-2}\right]E(20) & \forall T\in[300,600°C]\\ 4\cdot10^{-2}E(20) & \forall T\in[600,1000°C]\end{cases} \tag{19.36}$$

where $E_t(T)$ and $E(20)$ are Tangent modulus and Young's modulus at temperature T and 20°C, respectively

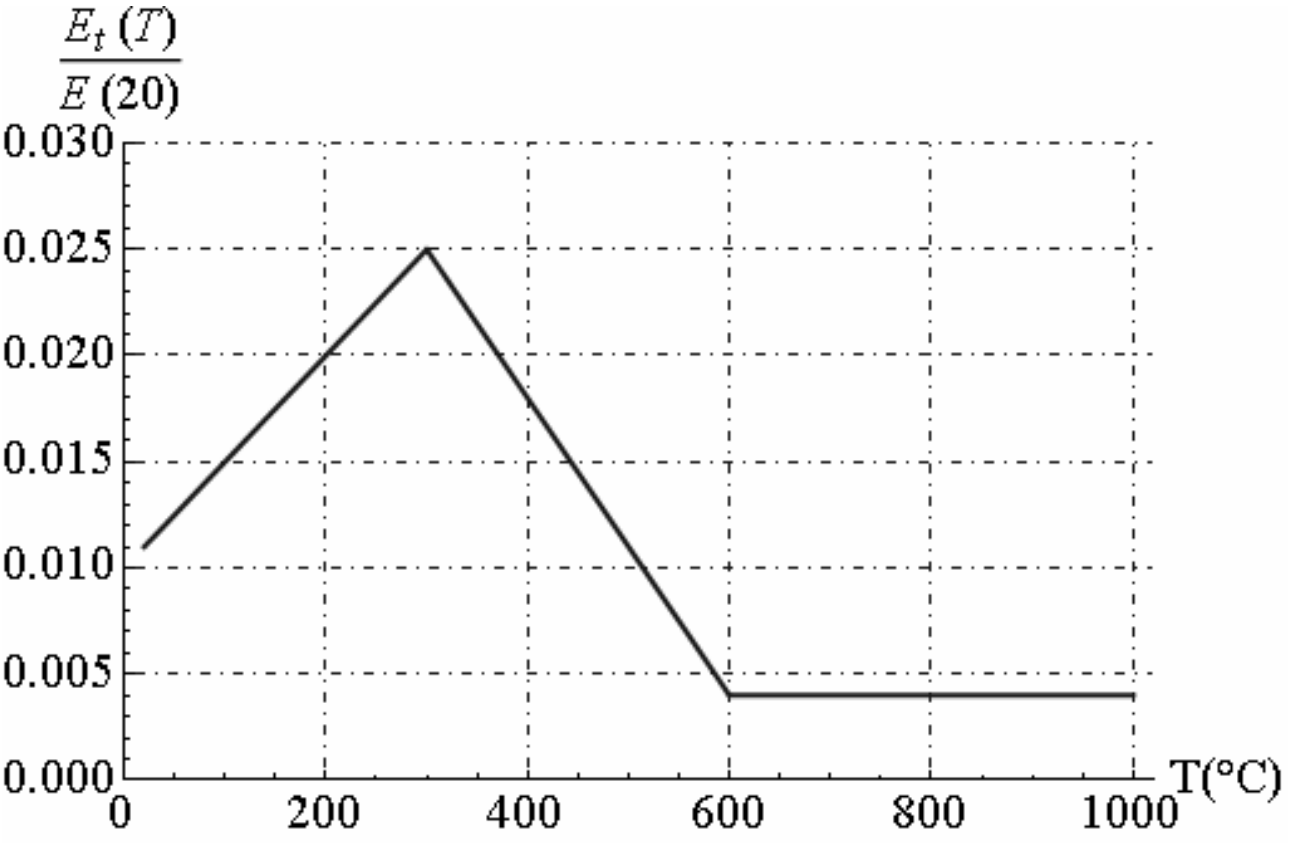

Fig. 19.21 - *The dependence between the tangent modulus versus temperature*

19.4.2. Thermal Properties of Concrete

The numerical values of resistance and properties of the deformation provided in the present section are based on both experimental evidence of type stationary (steady state) that transient (transient state) and sometimes a combination of the two. In Eurocode 1991-1-2 [1] don't

are explicitly taken into account the effects of viscosity, the models of materials are applicable to heating rate between 2°K/min and 50°K/min. For speeds outside of this interval, the validity of the values the properties of strength and deformation properties must be explicitly demonstrated.

Density: The variation in density with temperature is influenced by the water flow and is defined as follows:

$$\rho(T)=\begin{cases}\rho(20°C) & 20°C\le T\le 115°C\\ \rho(20°C)\left[1-0.02\left(\dfrac{T-115}{85}\right)\right] & 115°C\le T\le 200°C\\ \rho(20°C)\left[0.98-0.03\left(\dfrac{T-200}{200}\right)\right] & 200°C\le T\le 400°C\\ \rho(20°C)\left[0.95-0.07\left(\dfrac{T-400}{800}\right)\right] & 400°C\le T\le 1200°C\end{cases} \tag{19.37}$$

The density of concrete versus temperature is showed in figure 19.24 and density of concrete at 20°C is fixed by 2300kg/mc. The change in the volumetric specific heat $\rho(T)c_p(T)$ is illustrated in Figure 19.25 for concrete with moisture content equal to 3.0% in weight and density 2300 kg/mc.

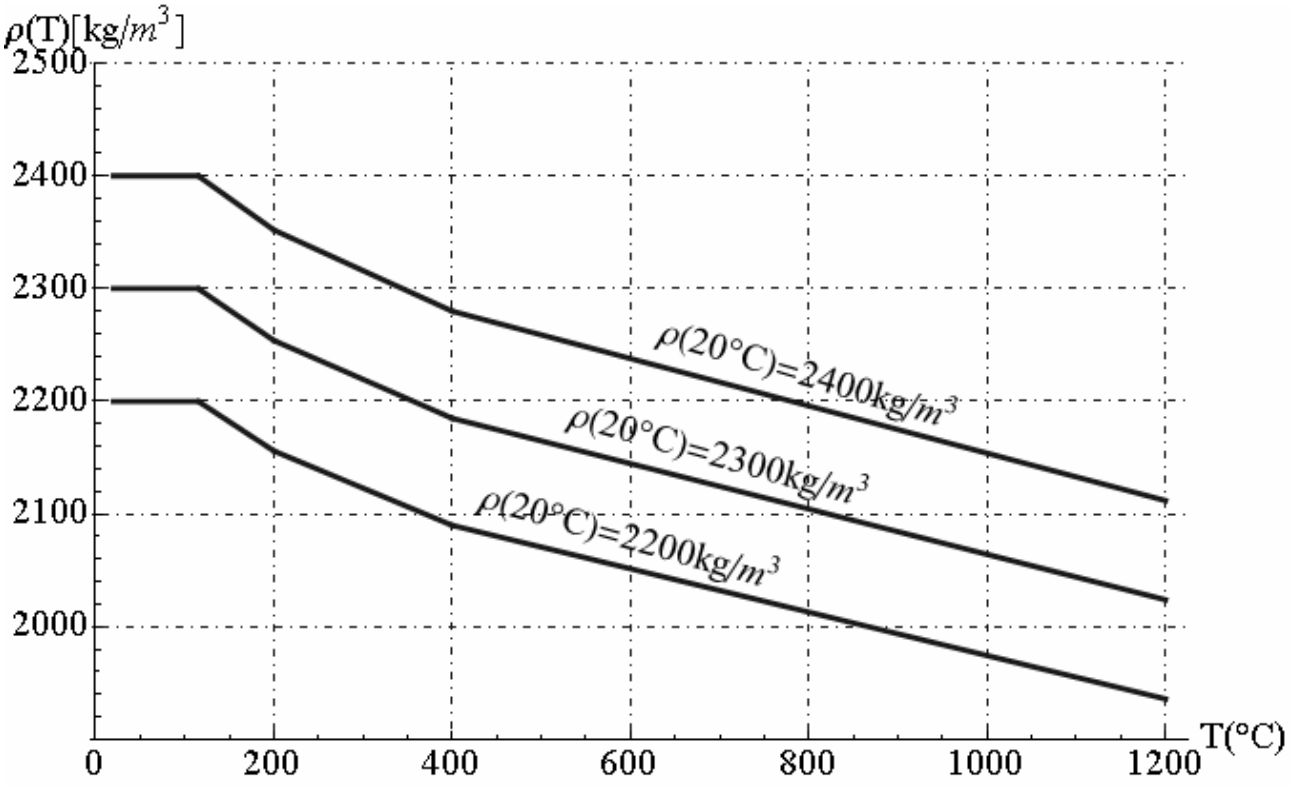

Fig. 19.22 – *Density of concrete versus temperature*

Coefficient of Thermal Expansion: The thermal deformation of the concrete $\varepsilon_c(T)$ can be determined with reference the length at 20 ° C as follows:
Siliceous aggregates:

$$\begin{cases}\varepsilon_c(T)=-1.8\cdot10^{-4}+9\cdot10^{-6}T+2.3\cdot10^{-11}T^3 & 20°C\le T\le 700°C\\ \varepsilon_c(T)=14\cdot10^{-3} & 700°C\le T\le 1200°C\end{cases} \tag{19.38}$$

Calcareous aggregates:

$$\begin{cases} \varepsilon_c(T) = -1.2\cdot 10^{-4} + 6\cdot 10^{-6} T + 1.4\cdot 10^{-11} T^3 & 20°C \le T \le 805°C \\ \varepsilon_c(T) = 12\cdot 10^{-3} & 805°C \le T \le 1200°C \end{cases} \tag{19.39}$$

T is the temperature of the concrete in degrees centigrade.

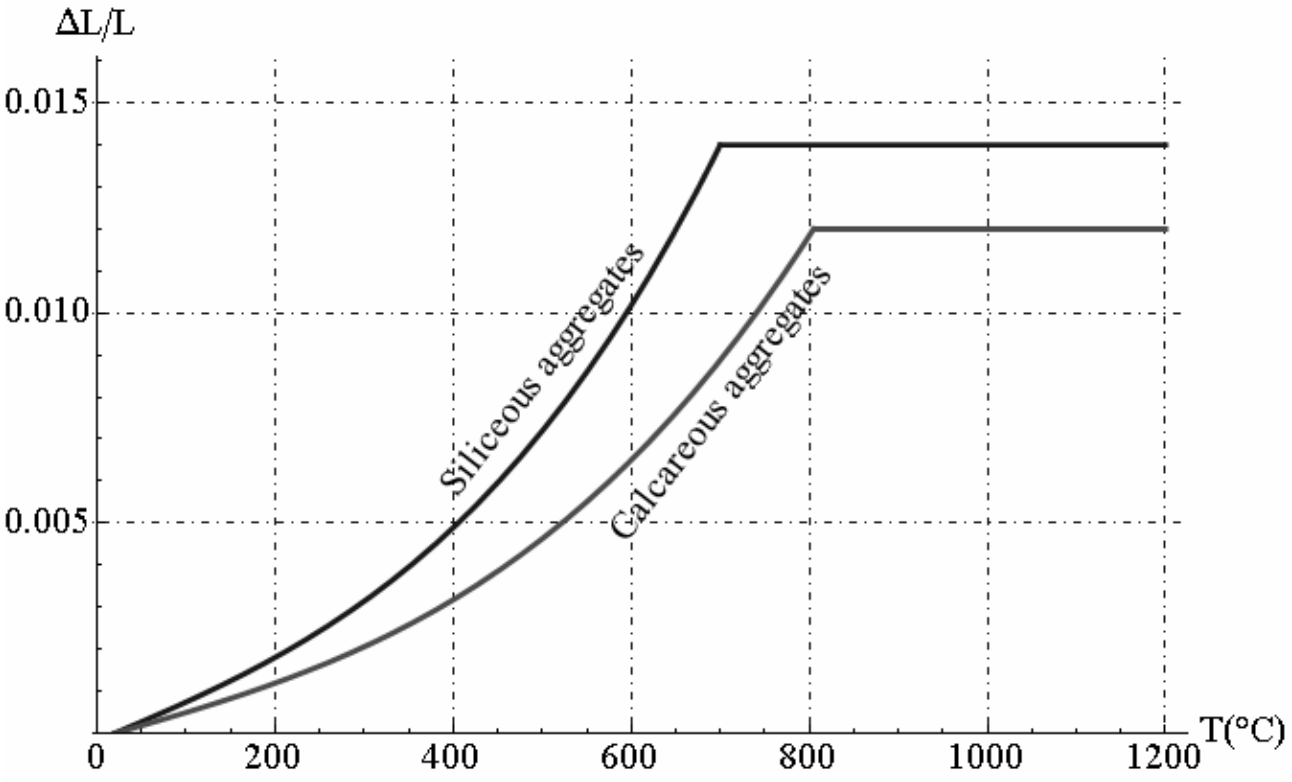

Fig. 19.23 - *Total thermal expansion of concrete*

Thermal Conductivity: The thermal conductivity k(T) of the concrete can be determined between a value lower limit and an upper limit value, as reported below. The value of thermal conductivity can be set within the range defined by Appendix national from the lower limit value and the upper limit value. Appendix A is compatible with the lower limit. The remaining sections of this Part 1-2 are independent by the choice of the thermal conductivity. The upper limit of the thermal conductivity k of the ordinary concrete can be obtained from:

$$k(T) = 2 - 0.2451\left(\frac{T}{100}\right) + 0.0107\left(\frac{T}{100}\right)^2 \quad 20°C \le T \le 1200°C \tag{19.40}$$

where T is the temperature of the concrete in centigrade grade and k(T) is thermal conductivity measured in $[W/m°K]$. The lower limit of the thermal conductivity k of the ordinary concrete can be obtained from:

$$k(T) = 1.36 - 0.136\left(\frac{T}{100}\right) + 0.0057\left(\frac{T}{100}\right)^2 \quad 20°C \le T \le 1200°C \tag{19.41}$$

The variation with temperature of the lower and upper limits of the thermal conductivity of concrete is illustrated in Figure 19.24. The average value of thermal conductivity is given:

$$k_m(T) = 1.68 - 0.19055\left(\frac{T}{100}\right) + 0.0082\left(\frac{T}{100}\right)^2 \quad 20°C \le T \le 1200°C \tag{19.42}$$

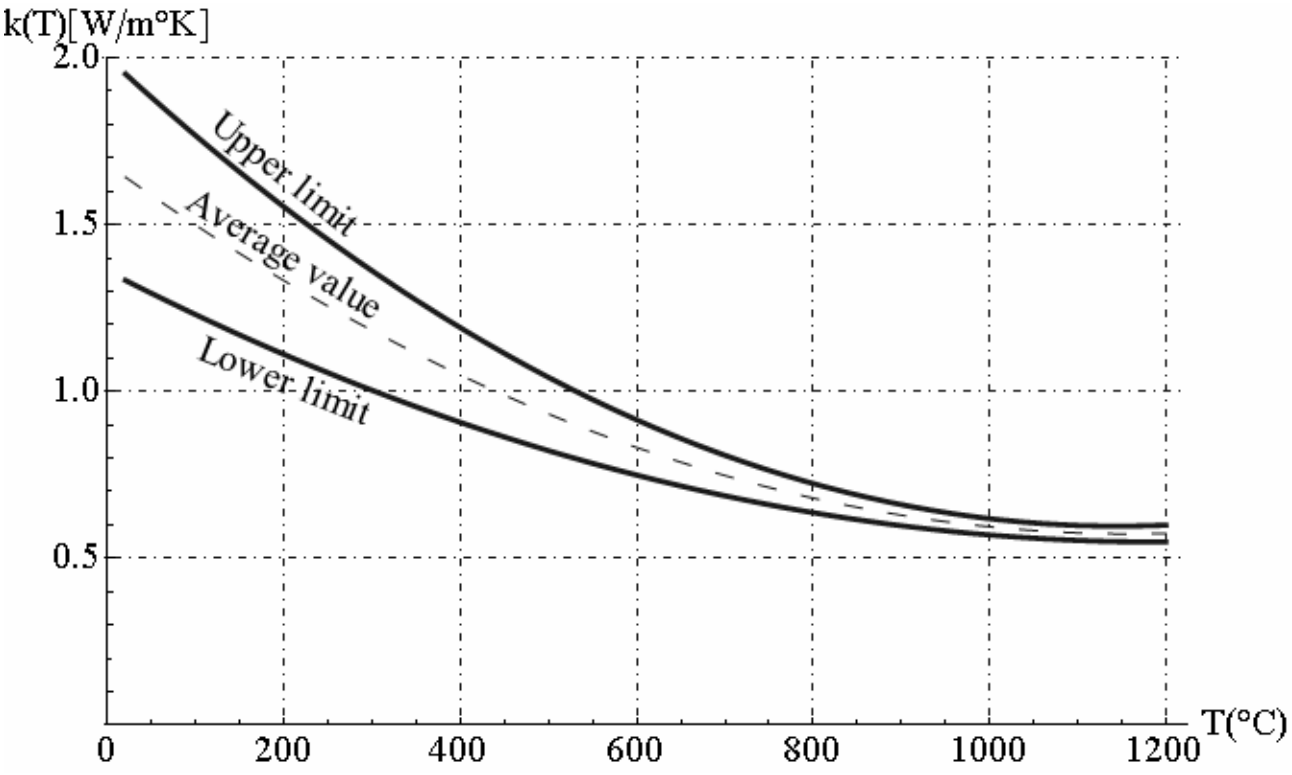

Fig. 19.24 – *Thermal conductivity versus temperature*

Specific Heat **:** The specific heat $c_p(T)$ of dry concrete (u = 0%) can be determined for Siliceous and calcareous aggregates as follows:

$$c_p(T) = \begin{cases} 900 & 20°C \le T \le 100°C \\ 900 + (T - 100) & 100°C \le T \le 200°C \\ 1000 + \dfrac{(T - 200)}{2} & 200°C \le T \le 400°C \\ 1100 & 400°C \le T \le 1200°C \end{cases} \tag{19.43}$$

where T is the temperature of the concrete in degrees centigrade and $c_p(T)$ is specific heat valuated in $\left[J/(kg \cdot °K)\right]$. In cases where it is not considered explicitly in the method of calculating the content of humidity, the date function for the specific heat of the concrete with aggregates siliceous or calcareous can be modelled through a constant value, peak ($c_{p,peak}$), placed between 100°C and 115°C decreasing linearly between 115°C and 200°C.

$c_{p,peak} = 900\, J/(kg \cdot °K)$ for moisture content of 0.00% by weight of concrete,

$c_{p,peak} = 1470\, J/(kg \cdot °K)$ for moisture content of 1.50% by weight of concrete,

$c_{p,peak} = 2020\, J/(kg \cdot °K)$ for moisture content of 3.00% by weight of concrete,

and a linear relationship between (115 ° C, $c_{p,peak}$) and (200 ° C, 1 000 J / kg K). For other moisture content is acceptable linear interpolation. The function specific heat versus temperature and the peaks of heat specific are illustrated in figure 19.25

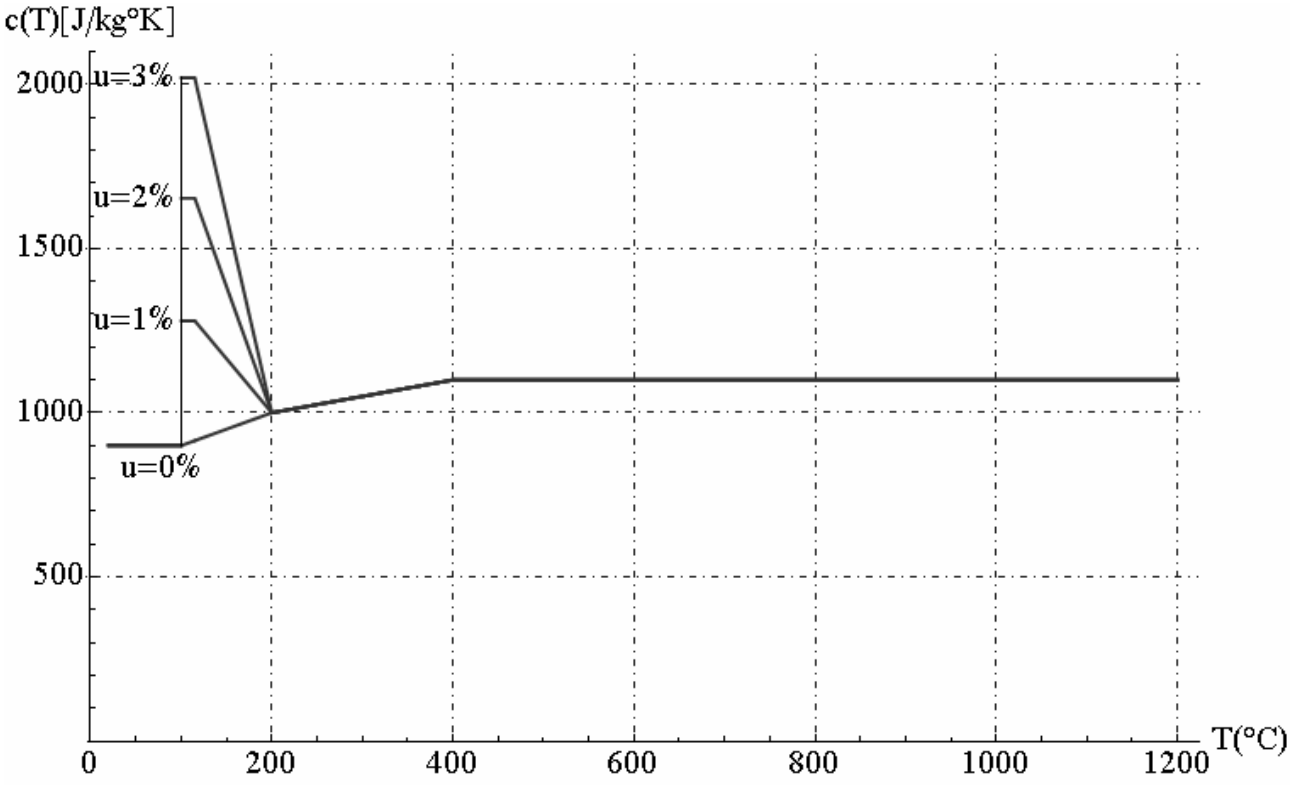

Fig. 19.25 - *Specific heat $c_p(T)$ versus temperature for 3 different moisture contents u, equal at 0, 1.5 and 3.0% by weight for concrete siliceous*

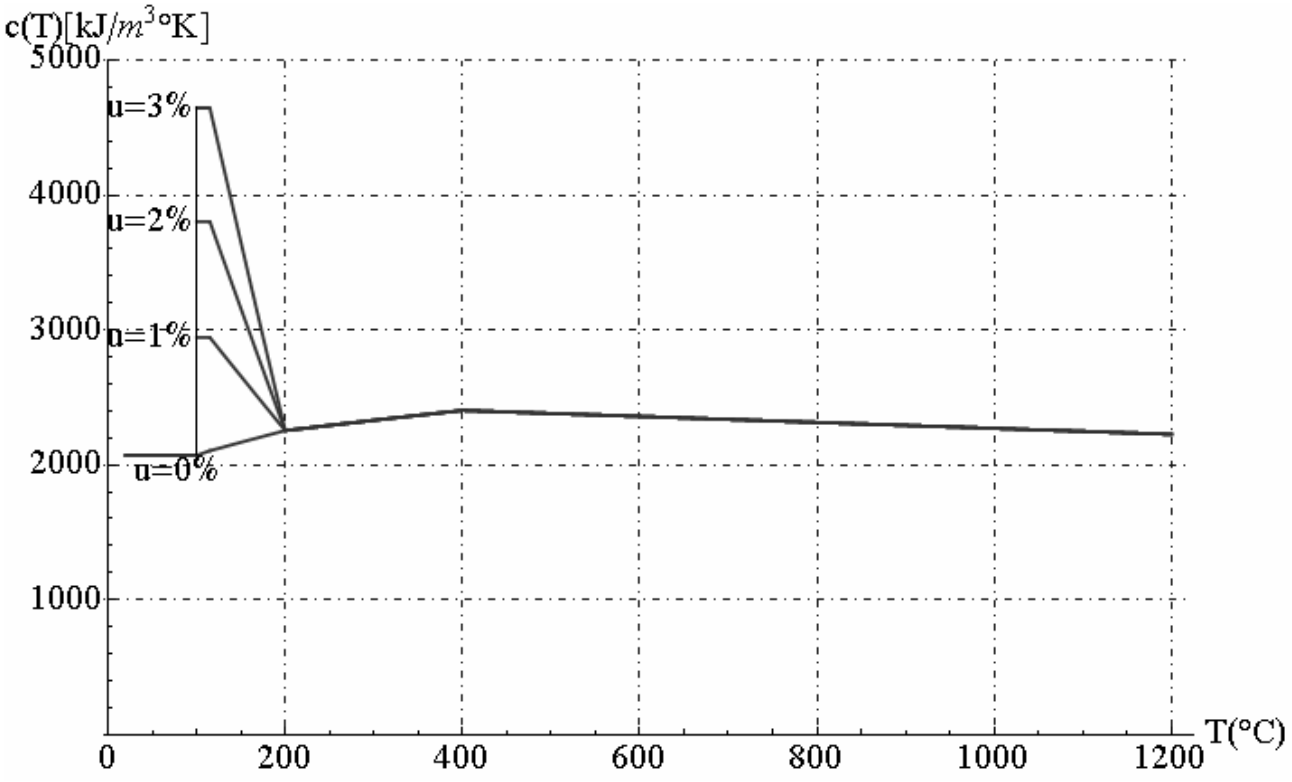

Fig. 19.26 - *Volumetric specific heat, $\rho(T)c_p(T)$ versus temperature for the moisture content u= 0.0% by weight concrete with density 2300 kg/mc*

Stress strain law for concrete in compression: The properties of resistance and deformation in uni-axial compression of concrete at high temperatures must be extrapolated from the reports stress-strain presented in Figure 19.20.

The stress-strain relations given in figure 19.20 are defined by two parameters: the compressive strength $\sigma_{c0}(T)$ and the deformation $\varepsilon_{c0}(T)$ corresponding to $\sigma_{c0}(T)$.

The values of each of the parameters are given in table 19.2 as a function of temperatures of the concrete. For intermediate values of temperature may be used linear interpolation. The parameters specified in table 19.2 can be used for concrete ordinary with siliceous or calcareous aggregates (containing at least 80% by weight of calcareous aggregates).

The values of $\sigma_{c0}(T)$, that defines the interval of the descending branch can be taken from column 4 of table 19.2 for ordinary concrete with siliceous aggregates and column 7 of table 19.2 for ordinary concrete with limestone aggregates. For thermal actions in accordance with Section 3 of EN 1991-1-2 (simulation of real fire), especially when you take into account the branch descending, it is recommended that the mathematical model for relations stress-strain of concrete specified in Figure 19.20 is modified. It is recommended that a possible increase in concrete strength during the step of extinction is not taken into consideration. Mathematical model for the stress-strain relationship of concrete in compression at high temperatures are given by:

$$\sigma_c = \begin{cases} \dfrac{3\sigma_{c0}(T)\,\varepsilon_c}{\varepsilon_{c0}(T)\left[2+\left(\dfrac{\varepsilon}{\varepsilon_{c0}(T)}\right)^3\right]} & 0 \le \varepsilon_c \le \varepsilon_{c0}(T) \\ \sigma_{c0}(T)\left[\dfrac{\varepsilon_{cu}(T)-\varepsilon_c}{\varepsilon_{cu}(T)-\varepsilon_{c0}(T)}\right] & \varepsilon_{c0}(T) \le \varepsilon_c \le \varepsilon_{cu}(T) \end{cases} \tag{19.44}$$

The values of $\dfrac{\sigma_{c0}(T)}{\sigma_{c0}(20°C)}$, $\varepsilon_{c0}(T), \varepsilon_{cu}(T)$ are reported in follows table:

	Siliceous aggregates			Calcareous aggregates		
T(℃)	$\dfrac{\sigma_{c0}(T)}{\sigma_{c0}(20°C)}$	$\varepsilon_{c0}(T)$	$\varepsilon_{cu}(T)$	$\dfrac{\sigma_{c0}(T)}{\sigma_{c0}(20°C)}$	$\varepsilon_{c0}(T)$	$\varepsilon_{cu}(T)$
20	1.00	0.0025	0.02	1.00	0.0025	0.02
100	1.00	0.004	0.0225	1.00	0.004	0.0225
200	0.95	0.0055	0.025	0.97	0.0055	0.025
300	0.85	0.007	0.0275	0.91	0.007	0.0275
400	0.75	0.01	0.03	0.85	0.01	0.03
500	0.60	0.015	0.0325	0.74	0.015	0.0325
600	0.45	0.025	0.035	0.60	0.025	0.035
700	0.30	0.025	0.0375	0.43	0.025	0.0375
800	0.15	0.025	0.04	0.27	0.025	0.04
900	0.08	0.025	0.0425	0.15	0.025	0.0425
1000	0.04	0.025	0.045	0.06	0.025	0.045
1100	0.01	0.025	0.0475	0.02	0.025	0.0475
1200	0.00	0.025	0.0475	0.00	0.025	0.0475

Table 19.2 -*Values of the main parameters of the stress-strain relationship of concrete with ordinary siliceous or calcareous aggregates at high temperatures*

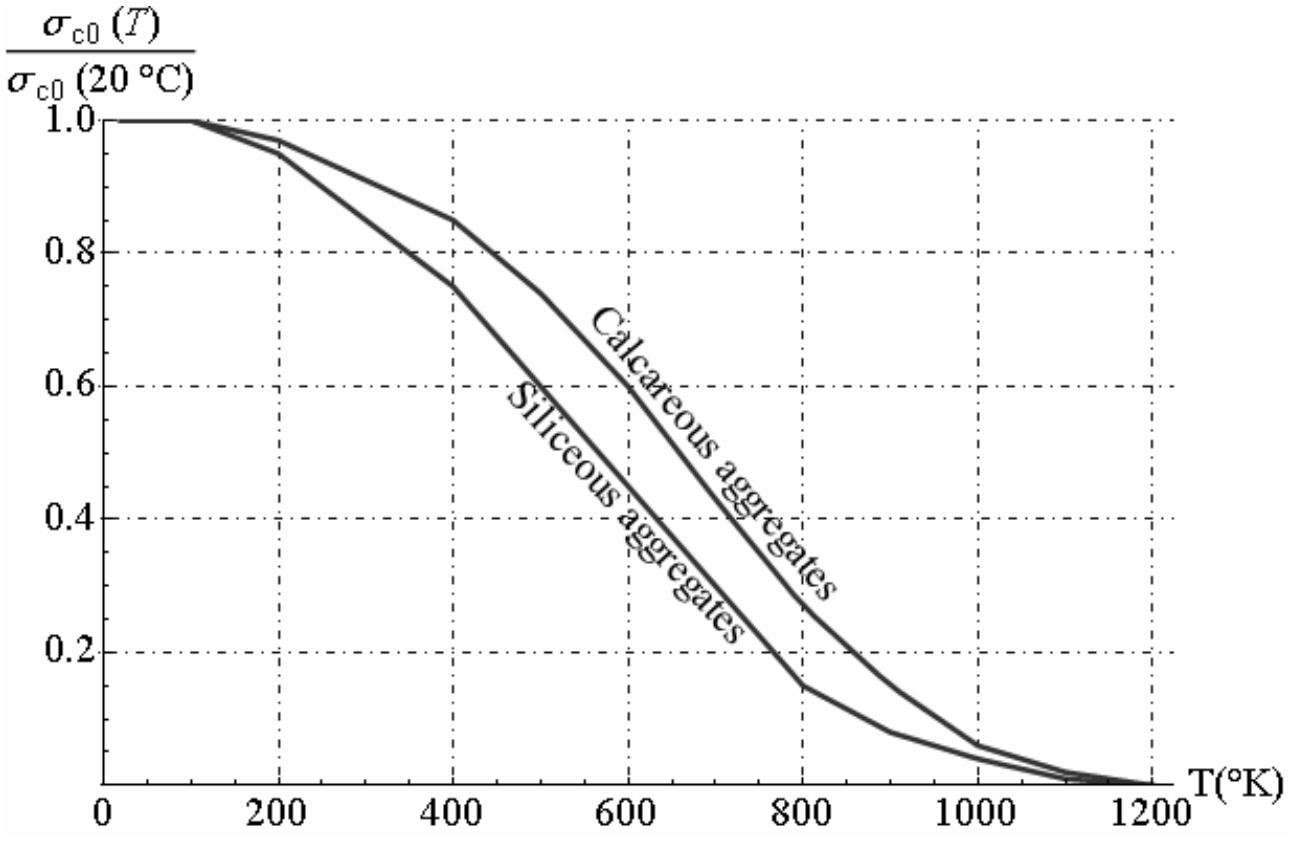

Fig. 19.27 - $\frac{\sigma_{c0}(T)}{\sigma_{c0}(20°C)}$ *versus temperature for siliceous and calcareous aggregates*

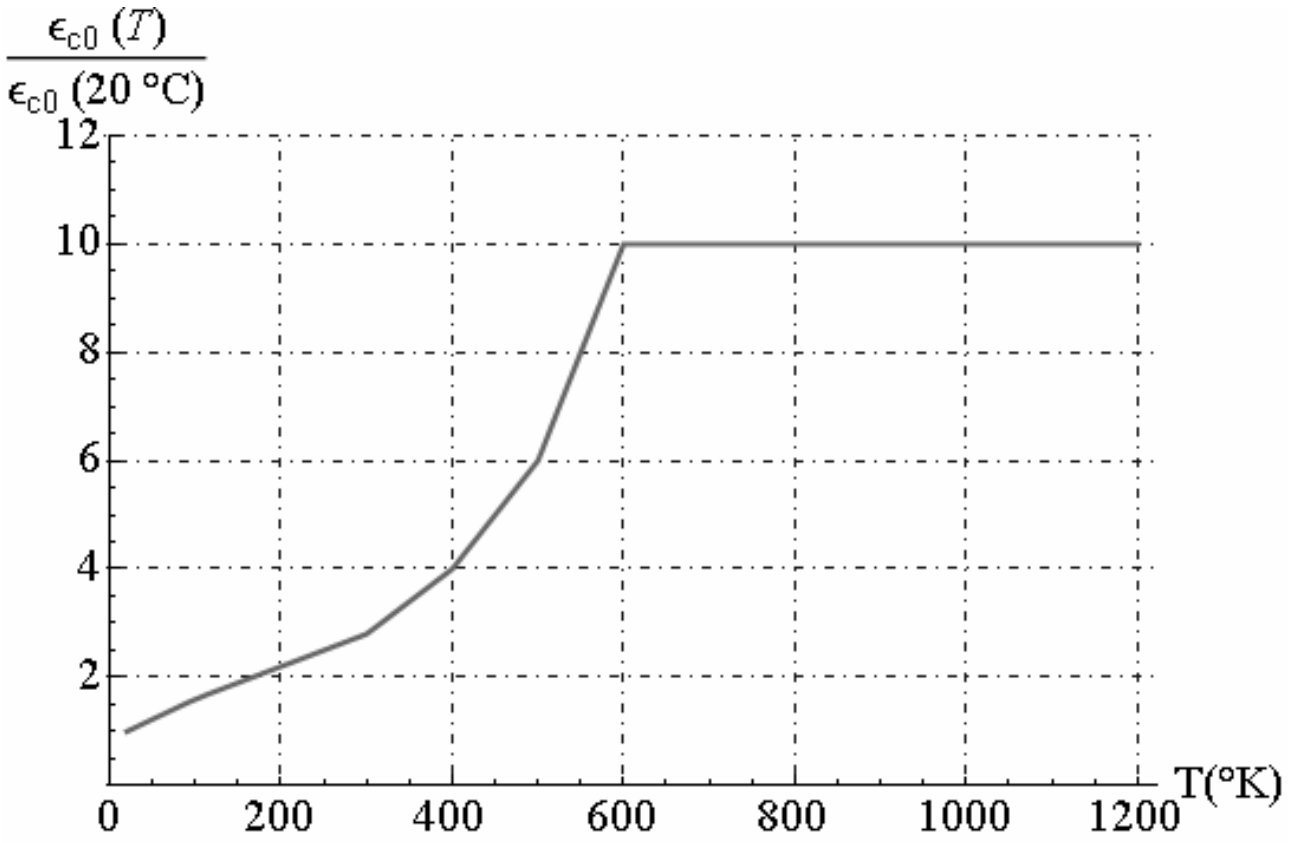

Fig. 19.28 - $\frac{\varepsilon_{c0}(T)}{\varepsilon_{c0}(20°C)}$ *versus temperature for siliceous and calcareous aggregates*

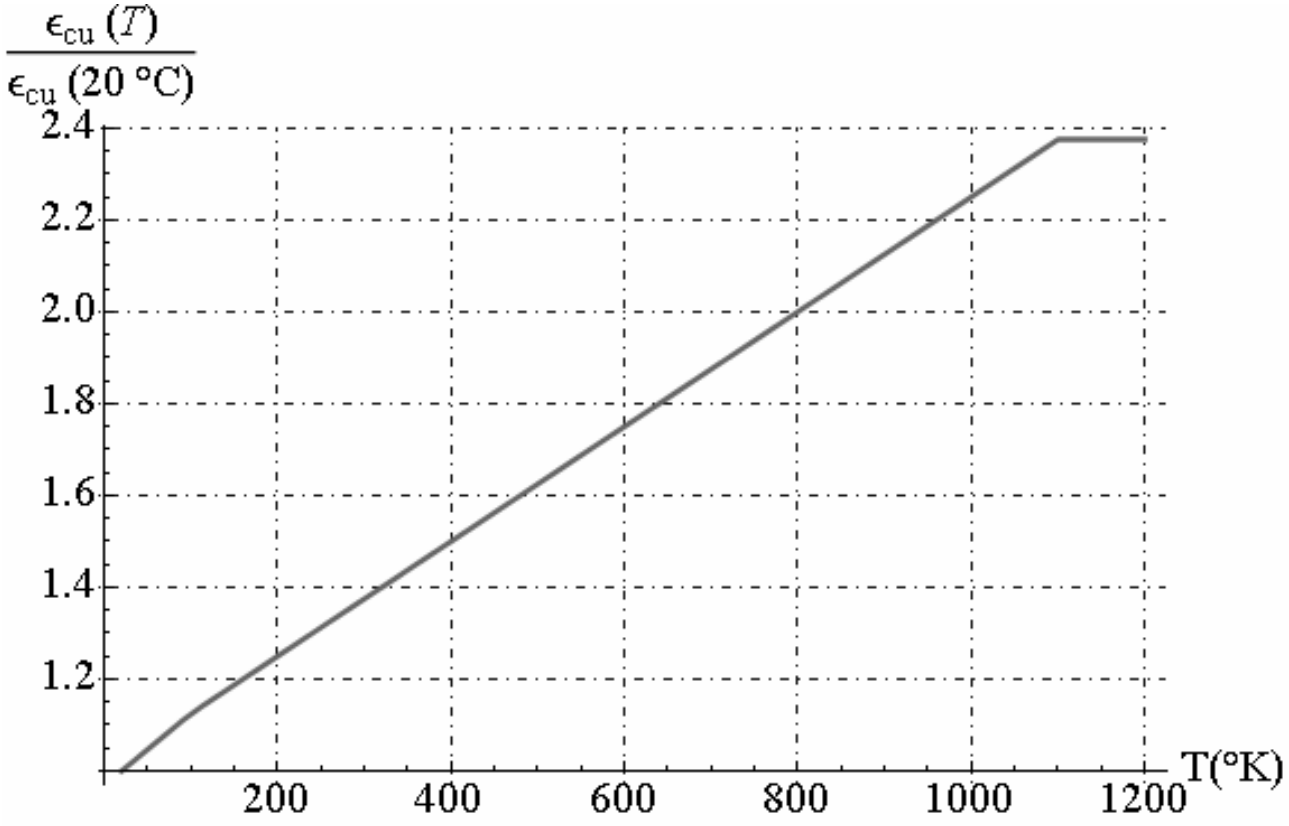

Fig. 19.29 - $\frac{\varepsilon_{cu}(T)}{\varepsilon_{cu}(20°C)}$ *versus temperature for siliceous and calcareous aggregates*

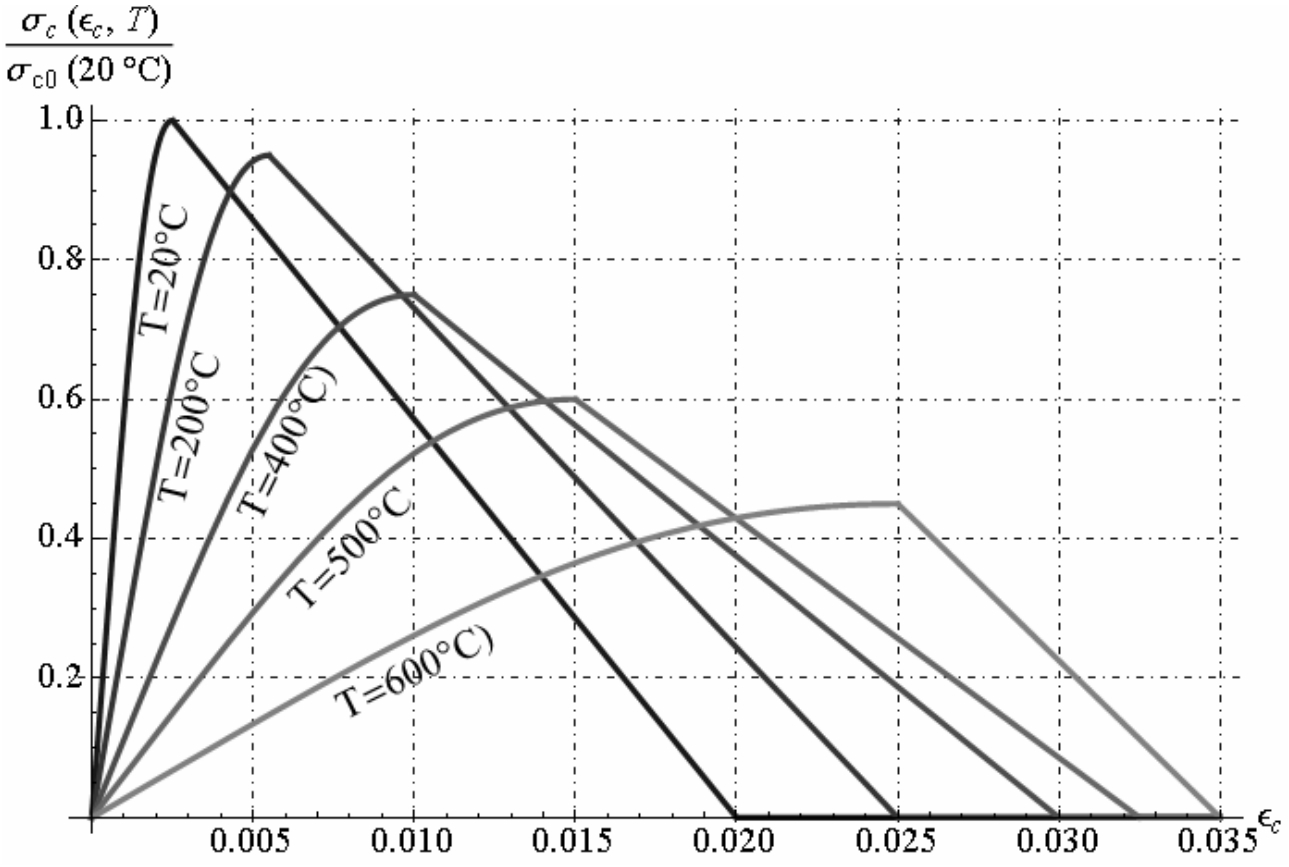

Fig. 19.30 - *Mathematical model for the stress-strain relationship of concrete with siliceous aggregates in compression at high temperatures*

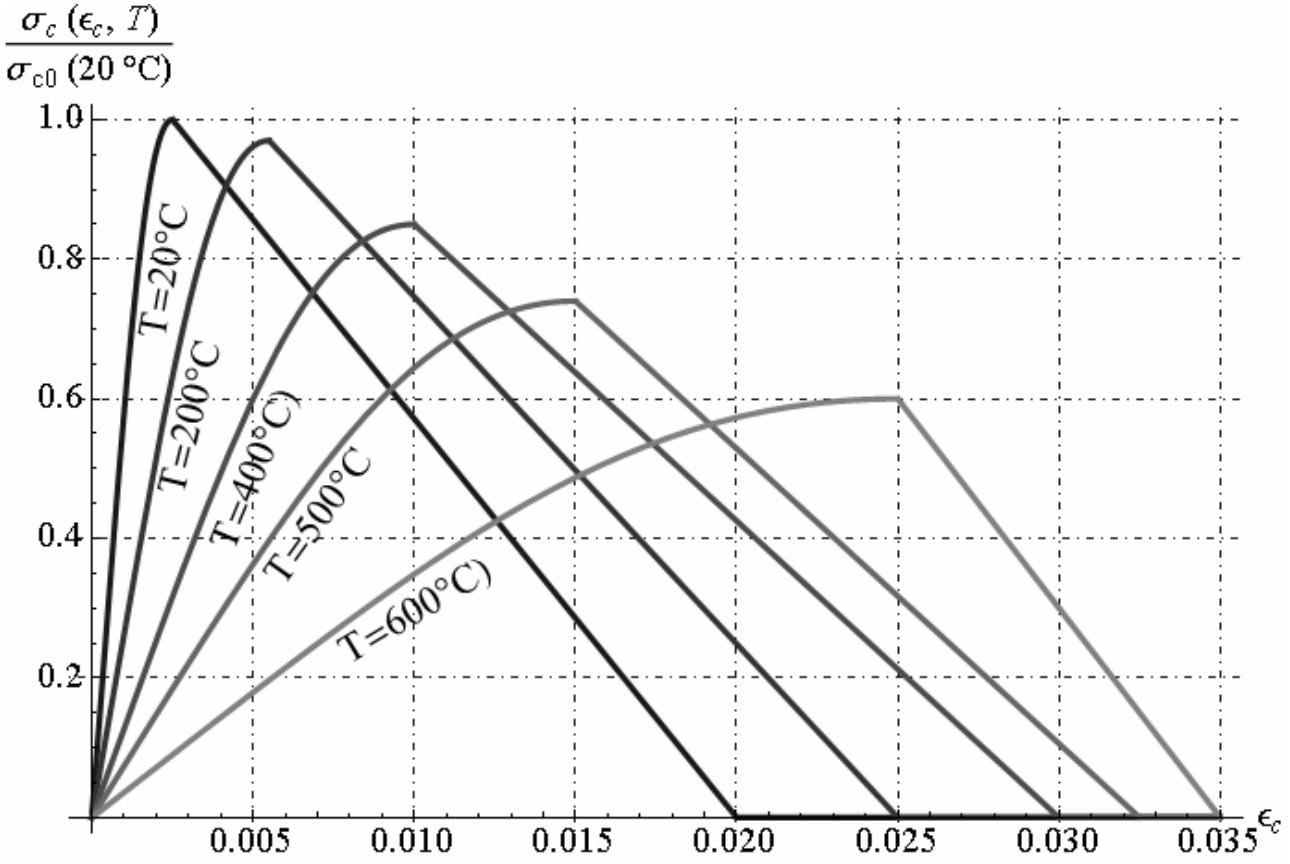

Fig. 19.31 - *Mathematical model for the stress-strain relationship of concrete with calcareous aggregates in compression at high temperatures*

Tensile strength of concrete : It is recommended that the tensile strength of the concrete is generally neglected (conservative assumption). If it is necessary to take it into account, using the simplified calculation method or advanced, can be used this point. The reduction of the tensile strength characteristic of the concrete is allowed as the coefficient $k_{c,t}(T)$ specified in the expression reported below:

$$\sigma_{ck,t}(T) = \sigma_{ck,t} k_{c,t}(T) \tag{19.45}$$

It is recommended that in the absence of more accurate information to be used the following values of $k_{c,t}(T)$ (see Figure 19.21):

$$\begin{cases} k_{c,t}(T) = 1.00 & 20°C \le T \le 100°C \\ k_{c,t}(T) = 1.00 - \left(\dfrac{T-100}{500}\right) & 100°C \le T \le 600°C \end{cases} \tag{19.46}$$

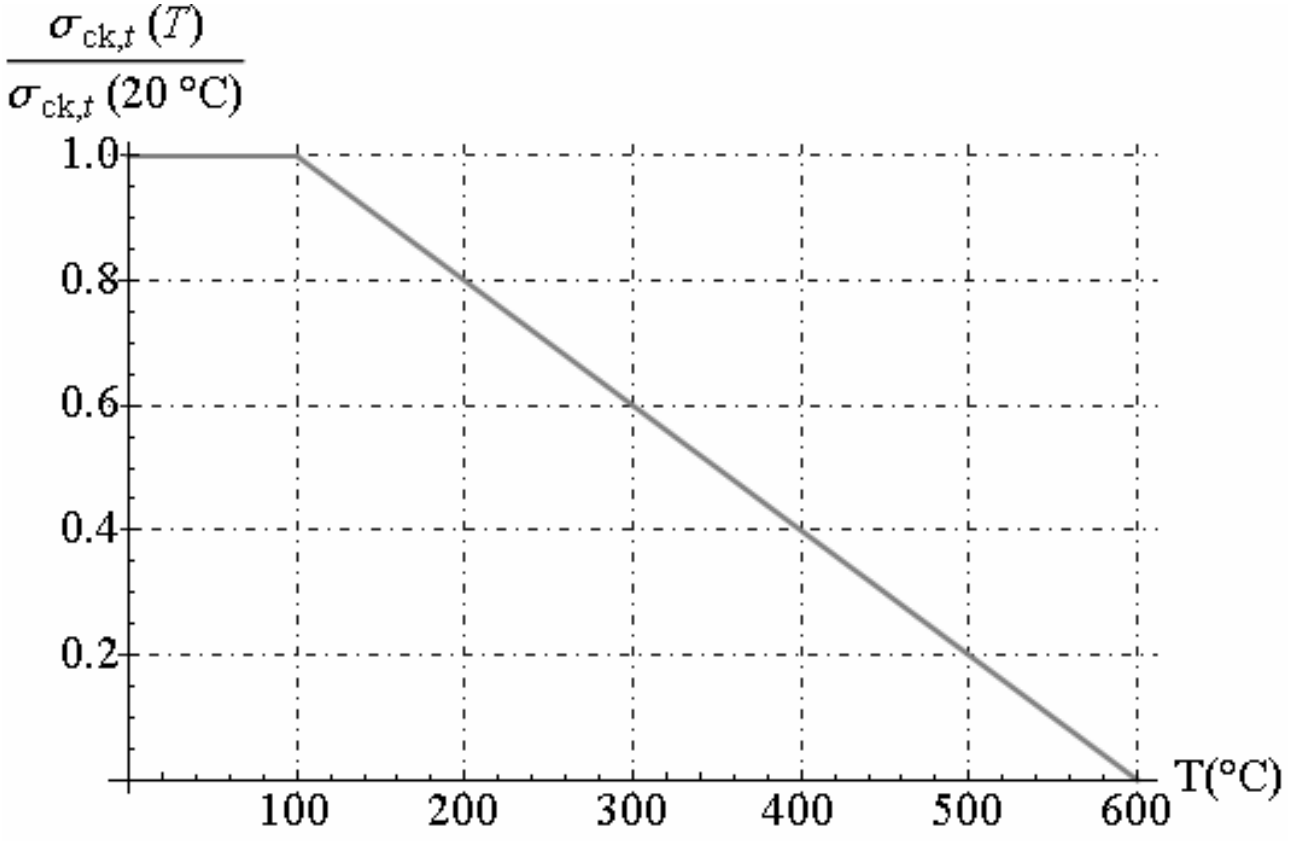

Fig. 19.32 - *Coefficient $k_{c,t}(T)$ for the decrease of the tensile strength of the concrete $\sigma_{ck,t}(T)$ to high temperatures*

19.5. References

[1] Kristin A. Collette, Comparisons of Structural Designs in Fire, Thesis Degree of Master of Science Fire Protection Engineering,

[2] Ana,-Diana Ancas and D. Gorbanescu (2006), *Theoretical models in the study of temperature effect on steel mechanical properties,* Buletinul institutului politehnic Din Iasi, Tomul LII (LVI), Fasc. 1-2, 2006, Construct II. Arhitectura.

[3] Boley, B.A.,Weiner, J.H., *Theory of thermal stresses,* Dover publications, inc. Mineola, New York

[4] Nunziante, L., Gambarotta, L., Tralli, A., *Scienza delle Costruzioni,* 3° Edizione, McGraw-Hill, 2011, ISBN: 9788838666971

[5] UNI EN 1992-1-2:2005

[6] UNI EN 1992-1-3:2005

[7] UNI 9502, seconda edizione maggio 2001

CHAPTER XX
TRANSIENT PROBLEMS FOR MULTILAYERED SPHERES

20.0. Introduction

The increasing use of composite materials in engineering application has resulted in considerable research activity in this area in recent years. An understanding of thermally induced stresses in isotropic bodies is essential for a comprehensive study of their response due to an exposure to a temperature field, which may in turn occur in service or during the manufacturing stages. Chen and Yang [1] discussed the transient response of one-dimensional quasi-static coupled thermoelasticity problems of an infinitely long cylinder composed of two different materials. They applied the Laplace transform with respect to time and used the Fourier series and matrix operations to obtain the solution. Chen and Chen [2] presented a new numerical technique hybrid numerical method for the problem of a transient linear heat conduction system. They applied the Laplace transform to remove the time-dependence from the governing equations and boundary conditions, and solved the transformed equations with the finite element and finite difference method. Ghosn and Sabbaghian [3] investigated a one-dimensional axisymmetric quasi-static coupled thermoelasticity problem. The solution technique uses Laplace transform. The inversion to real domain is obtained by means of Cauchy's theorem of residues and the convolution theorem. Jane and Lee [9] considered the same problem by using the Laplace transform and the finite difference method. The cylinder was composed of multilayers of different materials. There is no limit to the number of annular layers of the cylinder in the computational procedures. Laplace transform and finite difference methods were used to analyze problems. They obtained solutions for the temperature and thermal stress distributions in a transient state. Kandil [10] has studied the effect of steady-state temperature and pressure gradient on compound cylinders fitted together by shrink fit. Sherief and Anwar [11] discussed the problem of an infinitely long elastic circular cylinder whose inner and outer surfaces are subjected to known temperature and are traction free. They have neglected both the inertia terms and the relaxation effects. Takeuti and Furukawa [12] discussed the thermal shock problem in a plate; they included the inertia and thermoelastic coupling terms in the governing equation and obtained the exact solution for the thermal shock problem of a plate. Vollbrecht [14] has analysed the stresses in both cylindrical and spherical walls subjected to internal pressure and stationary heat flow. Zong-Yi Lee [15] presents an quasi-static coupled thermoelastic problems for multilayered spheres. Using the Laplace transform with respect to time, the general solutions of the governing equations are obtained in transform domain. The solution is obtained by using the matrix similarity transformation and inverse Laplace transform. The authors [15] obtain the solutions for the temperature and thermal deformation distributions for a transient state. F. de Monte [16] presents the transverse eigenvalue problem of non-conventional Sturm–Liouville type associated to the steady-state heat conduction in 3-D two-component slabs with imperfect thermal contact. In particular, the author [16] describes how the physical insight deriving from the transverse direction of six suitable "homogeneous parallelepipeds" inherent to the considered two-layered parallelepiped is capable of providing useful and reasonably accurate information about the best bracketing bounds (lower and upper) for the roots (eigenvalues) of the transverse eigencondition. Suneet Singh, et al.[17] present a new closed form analytical double-series solution for the multi-dimensional unsteady heat conduction problem in polar coordinates (2-D cylindrical) with multiple layers in the radial direction. Spatially non-uniform, but time-independent, volumetric heat sources are assumed in each layer. Separation of variables method is used to obtain transient temperature distribution. Prashant K. Jain, et al. [18] present an analytical double-series solution for the time-dependent asymmetric heat conduction in a multilayer annulus. Finally, M.kayhani et al. [19] present an exact general solution for steady-state conductive heat transfer in cylindrical composite laminates. Appropriate Fourier transformation has been obtained using Sturm-Liouville theorem. Series coefficients are achieved by solving a set of equations that related to thermal boundary conditions at inner and outer of the cylinder, also related to temperature continuity and heat flux continuity between each layer. The solution of this set of equations are obtained using Thomas algorithm.

In this chapter, the one-dimensional quasi-static uncoupled thermo-elastic problem of a multilayered sphere with time-dependent boundary conditions is considered. The medium is without body forces and heat generation. The analytical solution is obtained by applying the method of separation of variables.

20.1. Basic equations for time-dependent problem

Let us consider an multilayered sphere composed of *n* fictitious layers constituted by *n* hollow spherical phases (Figure n. 18.1). The external radius and internal radius of multilayered sphere are denoted by $R^{(n)}$ and $R^{(0)}$, respectively. The radius at interface between the generic phase *i-th* and the phase *(i+1)-th* are denoted with $R^{(i)}$. The mechanical and thermal properties of each layer are assumed to be homogeneous and isotropic and are denoted with apex (i). Spherical coordinates r, θ and ϕ are used in this analysis. The multilayered sphere is subjected to external heat flux that varying in the time, characterized by two functions $q_e(t), q_i(t)$ related to internal and external surfaces of solid, respectively. Moreover, the multilayered sphere is subjected to an external pressure $p_e(t)$ and an internal pressure $p_i(t)$ applied on the inner and the outer surface $r = R^{(n)}$ and $r = R^{(0)}$, respectively. These pressure are function of variable time. Details of multilayered sphere are shown Chapter XVIII (see figure 18.1). Afterwards, it is presented a method to solve a mono-dimensional thermo-elastic problem. The basic thermo-elastic equations for the *i*-th layer can be expressed as reported below. In isotropic-thermal elasticity case the strains are related to the displacements by purely geometrical considerations. If the composite material is subjected to spherical symmetric thermal loads in the time, in spherical coordinate, the displacement components for generic phase are given by:

$$u_r^{(i)} = u_r^{(i)}(r,t), \quad u_\theta^{(i)} = 0, \quad u_\phi^{(i)} = 0, \quad \forall i \in \{1,2,...n\} \tag{20.1}$$

where we denote with apex 1,2,…n the hollow phases of multilayered sphere. Then, the strain-displacement relations take the form:

$$\varepsilon_{rr}^{(i)} = u_{r,r}^{(i)}, \quad \varepsilon_{\theta\theta}^{(i)} = \varepsilon_{\phi\phi}^{(i)} = r^{-1}u_r^{(i)}, \quad \varepsilon_{\theta\phi}^{(i)} = \varepsilon_{r\theta}^{(i)} = \varepsilon_{r\phi}^{(i)} = 0 \quad \forall i \in \{1,2,...n\} \tag{20.2}$$

where $u_r^{(i)}, u_\theta^{(i)}, u_\phi^{(i)}$, are the radial and circumferential displacements in the *i*-th layer ($R^{(i)} < r < R^{(i+1)}$). The superscript *"i"* represents the *i*-th layer and the comma represents the partial derivate. Thermo-elastic stress-strain relations are given by:

$$\begin{aligned}
\sigma_{rr}^{(i)} &= \left(2\mu^{(i)} + \lambda^{(i)}\right)u_{r,r}^{(i)} + 2\lambda^{(i)}r^{-1}u_r^{(i)} - \left(3\lambda^{(i)} + 2\mu^{(i)}\right)\alpha^{(i)}\left(T^{(i)} - T_R\right) \\
\sigma_{\theta\theta}^{(i)} &= \sigma_{\phi\phi}^{(i)} = 2\left(2\mu^{(i)} + \lambda^{(i)}\right)r^{-1}u_r^{(i)} + \lambda^{(i)}u_{r,r}^{(i)} - \left(3\lambda^{(i)} + 2\mu^{(i)}\right)\alpha^{(i)}\left(T^{(i)} - T_R\right) \\
\tau_{r\phi}^{(i)} &= \tau_{\theta\phi}^{(i)} = \tau_{r\theta}^{(i)} = 0; \qquad \forall i \in \{1,2,...n\}
\end{aligned} \tag{20.3}$$

where $\mu^{(i)}, \lambda^{(i)}, \alpha^{(i)}, T^{(i)}$ are the Lamè elastic constants, linear thermal expansion coefficient and temperature in the *i*-th layer, respectively; T_R is the reference temperature . Moreover, let us assume that the function of the temperature in each phase is a function of radius and time as reported below:

$$T^{(i)} = T^{(i)}(r,t) \quad \forall i \in \{1,2,....,n\} \tag{20.4}$$

The equations of equilibrium are the same as those of isothermal elasticity since they are based on purely mechanical considerations. By applying the hypothesis of the spherical symmetric temperature loads and in absence of the body force, and neglecting the effect of the inertia, the equilibrium equations become one equation:

$$\sigma_{rr,r}^{(i)} + 2\left(\sigma_{rr}^{(i)} - \sigma_{\theta\theta}^{(i)}\right)r^{-1} = 0 \quad \forall i \in \{1,2,...n\} \tag{20.5}$$

The results obtained until now satisfy the equilibrium and compatibility equations inside each generic *i*-th phase of a composite spherical solid subjected to spherical symmetric strains or temperature loads time-dependent. Under both the hypothesis of linear isotropic elastic behaviour of

the homogeneous materials and the assumption of perfect bond at the spherical interfacial boundaries (no de-lamination or friction phenomena), we have now to establish the satisfaction of both the equilibrium and the compatibility equations at the boundary surfaces between two generic adjacent phases. To obtain this, we will make reference to the generic case, in which an multilayered sphere is constituted by *n* arbitrary hollow phase (see Chapter XVIII). In this framework the following boundary conditions be established. In particular, we begin writing the compatibility equations at the generic interface, that is:

$$u_r^{(i)}(r=R^{(i)},t)=u_r^{(i+1)}(r=R^{(i)},t) \quad \forall t\geq 0,\ \forall i\in\{1,2,...n-1\} \tag{20.6}$$

The equilibrium equations at the generic interface are given by:

$$\sigma_{rr}^{(i)}(r=R^{(i)},t)=\sigma_{rr}^{(i+1)}(r=R^{(i)},t) \quad \forall i\in\{1,2,...n-1\} \tag{20.7}$$

The equilibrium equations for tractions on the inner and the outer spherical boundary surface, give:

$$\sigma_{rr}^{(n)}(r=R^{(n)},t)=p_e(t), \quad \sigma_{rr}^{(1)}(r=R^{(0)},t)=p_i(t) \quad \forall t\geq 0 \tag{20.8}$$

where $p_e(t), p_i(t)$ are prescribed function pressure applied on the inner and the outer surface of multilayered sphere, respectively. The equation field for coupled heat conduction problem is written in hypothesis of spherical symmetric load conditions for each phases of prescribed function.

$$k^{(i)}\left(T_{,rr}^{(i)}+2r^{-1}T_{,r}^{(i)}\right)=\rho^{(i)}c^{(i)}T_{,t}^{(i)}+\alpha^{(i)}\left(3\lambda^{(i)}+2\mu^{(i)}\right)T_R\left(u_{,r}^{(i)}+2r^{-1}u_r^{(i)}\right)_{,t} \quad \forall i\in\{1,2,...n\} \tag{20.9}$$

where $\rho^{(i)}, c^{(i)}, k^{(i)}, T_R$ are density, specific heat, thermal conductivity coefficient, temperature reference for each phases, respectively. Temperature boundary and continuity conditions are written at the interfaces between the phases, and on internal and external surfaces of multilayered sphere. Then, at interfaces between the phases the following conditions can be write:

$$\begin{cases} T^{(i)}(r=R^{(i)},t)=T^{(i+1)}(r=R^{(i)},t) \\ k^{(i)}T_{,r}^{(i)}(r=R^{(i)},t)=k^{(i+1)}T_{,r}^{(i+1)}(r=R^{(i)},t) \end{cases} \quad \forall t\geq 0,\ \forall i\in\{1,2,...n-1\} \tag{20.10}$$

The boundary conditions on the inner and the outer surface impose that heat flux is equal to $q_i(t)$ and $q_e(t)$, respectively:

$$-k^{(n)}T_{,r}^{(n)}(r=R^{(n)},t)=q_e(t), \quad -k^{(1)}T_{,r}^{(1)}(r=R^{(0)},t)=q_i(t), \quad \forall t\geq 0 \tag{20.11}$$

The initial condition for temperature function is given by:

$$T=T_R; \quad R^{(i-1)}<r<R^{(i)}, \ \forall i\in\{1,2,....,n\}, \ t=0, \tag{20.12}$$

where $T_0=T_R$ is a suitable chosen reference temperature in initial condition (for t = 0).

20.2. Multilayered sphere exposed to an ambient at zero temperature through a uniform boundary conductance

Let us consider an multilayered sphere constituted by n-hollow spherical phase as decrypted in section 20.1. The surface $r=R^{(0)}$ is kept perfectly insulated while the surface $r=R^{(n)}$ is exposed, for t >0, to an ambient at zero temperature through a uniform boundary conductance h_c. The initial temperature (for t = 0) of the hollow sphere is $T_0=T_R=const$ where $T_R>0$. In this section, we determine the heat conduction, displacement and stress function in hollow sphere under decreasing of temperature from $T_R>0$ until to zero. The equations field in each phase are composed by equilibrium and heat conduction equations. By substituting the strain-displacement relations (20.2) in stress-strain relations (20.3) and these in equilibrium equations (20.5), we obtain the displacement formulation of the equilibrium equations. Then, the equations field to satisfy in uncoupled thermo-elastic problem with spherical symmetry are given by:

$$\begin{cases} \left[r^{-2}\left(r^2 u_r^{(i)}\right)_{,r} \right]_{,r} = \alpha^{(i)}\left(\dfrac{3\lambda^{(i)}+2\mu^{(i)}}{2\mu^{(i)}+\lambda^{(i)}}\right) = \alpha^{(i)}\left(\dfrac{1+\nu^{(i)}}{1-\nu^{(i)}}\right) T_{,r}^{(i)} & R^{(i-1)} \le r \le R^{(i)}, \quad \forall t \ge 0, \\ T_{,rr}^{(i)} + 2r^{-1}T_{,r}^{(i)} = \dfrac{\rho^{(i)}c^{(i)}}{k^{(i)}} T_{,t}^{(i)} = \dfrac{T_{,t}^{(i)}}{\kappa^{(i)}} & \forall i \in \{1,2,...,n\} \end{cases} \tag{20.13}$$

where $\kappa^{(i)}$ is the thermal diffusivity for generic i-th phase. By solving the Fourier's equation reported in second equation of (20.13) with method separation of variables, and by substituting the function of temperature $T^{(i)}(r,t)$ in first equation of (20.13), and by integration in two time this equation respect to variable r , the explicit displacement solution is obtained:

$$u_r^{(i)}(r,t) = \frac{\alpha^{(i)}}{r^2}\left(\frac{3\lambda^{(i)}+2\mu^{(i)}}{\lambda^{(i)}+2\mu^{(i)}}\right)\int r^2 T^{(i)}(r,t)\,dr + r\, f_1^{(i)}(t) + \frac{f_2^{(i)}(t)}{r^2}, \quad \forall i \in \{1,2,....,n\} \tag{20.14}$$

where $f_1^{(i)}(t)$, $f_2^{(i)}(t)$ are unknown functions of the time to determine. The heat conduct problem is characterized by homogeneous differential equation reported in second equation of (20.13) and boundary conditions reported in equations (20.10)-(20.11) and may be treated by the method separation of variables. A particular solution of the Fourier's differential equation is given by:

$$T^{(i)}(r,t) = \varphi^{(i)}(r)\,\psi^{(i)}(t) \qquad \forall i \in \{1,2,....,n\} \tag{20.15}$$

By substituting the function (20.15) in Fourier's heat equation we obtain two ordinary differential equations in variable radius and time, separately. The first equation for function $\varphi^{(i)}(r)$

$$\varphi_{,rr}^{(i)} + 2r^{-1}\varphi_{,r}^{(i)} + \omega^2 \beta^{(i)2}\varphi^{(i)} = 0; \tag{20.16}$$

where the coefficient $\beta^{(i)} = \sqrt{\kappa^{(1)}/\kappa^{(i)}}$ and to the following equation for $\psi^{(i)}(t)$:

$$\psi_{,t}^{(i)} + \omega^2 \beta^{(i)2}\kappa_C^{(i)}\psi^{(i)} = 0 \tag{20.17}$$

The general solution of (20.17) is:

$$\psi^{(i)}(t) = e^{-\omega^2\beta^{(i)2}\kappa_C^{(i)}t} \tag{20.18}$$

The general solution of (20.16) is:

$$\varphi^{(i)}(r) = r^{-1}\left(A^{(i)}e^{\imath\,\omega\beta^{(i)}r} + B^{(i)}e^{-\imath\,\omega\beta^{(i)}r}\right) \tag{20.19}$$

where $A^{(i)}, B^{(i)}$ are constants integration and $\imath$ is unit imaginary. The boundary conditions for heat problem (20.10) in this case become:

$$\begin{cases} A^{(i)}e^{\imath\,\omega\beta^{(i)}R^{(i)}} + B^{(i)}e^{-\imath\,\omega\beta^{(i)}R^{(i)}} - \left(A^{(i+1)}e^{\imath\,\omega\beta^{(i+1)}R^{(i)}} + B^{(i+1)}e^{-\imath\,\omega\beta^{(i+1)}R^{(i)}}\right) = 0 \\ A^{(i)}k^{(i)}\left(1-\imath\,\omega\beta^{(i)}R^{(i)}\right)e^{\imath\,\omega\beta^{(i)}R^{(i)}} - A^{(i+1)}k^{(i+1)}\left(1-\imath\,\omega\beta^{(i+1)}R^{(i+1)}\right)e^{\imath\,\omega\beta^{(i+1)}R^{(i+1)}} + \\ + B^{(i)}k^{(i)}\left(1+\imath\,\omega\beta^{(i)}R^{(i)}\right)e^{-\imath\,\omega\beta^{(i)}R^{(i)}} - B^{(i+1)}k^{(i+1)}\left(1+\imath\,\omega\beta^{(i+1)}R^{(i+1)}\right)e^{-\imath\,\omega\beta^{(i+1)}R^{(i+1)}} = 0 \\ \forall i \in \{1,2,...,n-1\} \end{cases} \tag{20.20}$$

The boundary conditions on the inner and the outer surface (20.11) become:

$$-k^{(1)}T_{,r}^{(1)}(r=R^{(0)}) = 0, \quad -k^{(n)}T_{,r}^{(n)}(r=R^{(n)}) = h_c T^{(n)}(r=R^{(n)}), \quad \forall t \ge 0 \tag{20.21}$$

where and h_c is convection coefficient on surface $r = R^{(n)}$. In explicit the equations (20.21) become:

$$\begin{cases} A^{(1)}\left(1-\imath\,\omega\beta^{(1)}R^{(0)}\right)e^{\imath\,\omega\beta^{(1)}R^{(0)}} + B^{(1)}\left(1+\imath\,\omega\beta^{(1)}R^{(0)}\right)e^{-\imath\,\omega\beta^{(1)}R^{(0)}} = 0 \\ A^{(n)}\left[k^{(n)}\left(1-\imath\,\omega\beta^{(n)}R^{(n)}\right) - h_c R^{(n)}\right]e^{\imath\,\omega\beta^{(n)}R^{(n)}} + \\ + B^{(n)}\left[k^{(n)}\left(1+\imath\,\omega\beta^{(n)}R^{(n)}\right) - h_c R^{(n)}\right]e^{-\imath\,\omega\beta^{(n)}R^{(n)}} = 0 \end{cases} \tag{20.22}$$

By first equation of (20.22), we determine $B^{(1)}$ as function of $A^{(1)}$ as follows:

$$B^{(1)} = \left[\left(i + \omega R^{(0)} \beta^{(1)} \right)^2 \Big/ \left(1 + \omega^2 \beta^{(1)2} R^{(0)2} \right) \right] A^{(1)} e^{2i\omega\beta^{(1)}R^{(0)}} \tag{20.23}$$

The equations (20.20) constituted an homogeneous algebraic system, composed by 2(n-1) equations, in unknown parameters $A^{(i)}, B^{(i)}$ with $i \in \{1, 2, ..., n\}$, which can be written as:

$$\mathbf{\Phi} \cdot \mathbf{X} = \mathbf{0} \tag{20.24}$$

where $\mathbf{X} = [\mathbf{X}^{(1)}, \mathbf{X}^{(2)}, ..., \mathbf{X}^{(n)}]^T$ collect the unknowns sub-vectors, as reported below:

$$\mathbf{X}^{(i)} = \begin{bmatrix} A^{(i)} & B^{(i)} \end{bmatrix}^T, \quad \forall i \in \{1, 2, ..., n\} \tag{20.25}$$

and $\mathbf{\Phi}$ is an $2(n-1)x2n$ rectangular matrix, composed by following sub-matrices:

$$\mathbf{\Phi} = \begin{bmatrix} \mathbf{\Phi}_1^{(1)} & -\mathbf{\Phi}_1^{(2)} & \mathbf{0} & \mathbf{0} & \cdots & \mathbf{0} & \mathbf{0} & \mathbf{0} \\ \mathbf{0} & \mathbf{\Phi}_2^{(2)} & -\mathbf{\Phi}_2^{(3)} & \mathbf{0} & \cdots & \mathbf{0} & \mathbf{0} & \mathbf{0} \\ \mathbf{0} & \mathbf{0} & \mathbf{\Phi}_3^{(3)} & -\mathbf{\Phi}_3^{(4)} & \cdots & \mathbf{0} & \mathbf{0} & \mathbf{0} \\ \vdots & \vdots & \vdots & \vdots & \vdots & \vdots & \vdots & \vdots \\ \mathbf{0} & \mathbf{0} & \mathbf{0} & \mathbf{0} & \cdots & \mathbf{\Phi}_{n-2}^{(n-2)} & -\mathbf{\Phi}_{n-2}^{(n-1)} & \mathbf{0} \\ \mathbf{0} & \mathbf{0} & \mathbf{0} & \mathbf{0} & \cdots & \mathbf{0} & \mathbf{\Phi}_{n-1}^{(n-1)} & -\mathbf{\Phi}_{n-1}^{(n)} \end{bmatrix} \tag{20.26}$$

where $\mathbf{\Phi}_i^{(i)}, \mathbf{\Phi}_i^{(i+1)}$ are $(2x2)$ generic square sub-matrices given by:

$$\begin{aligned} \mathbf{\Phi}_i^{(i)} &= \begin{bmatrix} 1 & 1 \\ k^{(i)} \left(1 - i\omega\beta^{(i)} R^{(i)} \right) & k^{(i)} \left(1 + i\omega\beta^{(i)} R^{(i)} \right) \end{bmatrix} \cdot \begin{bmatrix} e^{i\omega\beta^{(i)}R^{(i)}} & 0 \\ 0 & e^{-i\omega\beta^{(i)}R^{(i)}} \end{bmatrix}, \\ \mathbf{\Phi}_i^{(i+1)} &= \begin{bmatrix} 1 & 1 \\ k^{(i+1)} \left(1 - i\omega\beta^{(i+1)} R^{(i)} \right) & k^{(i+1)} \left(1 + i\omega\beta^{(i+1)} R^{(i)} \right) \end{bmatrix} \cdot \begin{bmatrix} e^{i\omega\beta^{(i+1)}R^{(i)}} & 0 \\ 0 & e^{-i\omega\beta^{(i+1)}R^{(i)}} \end{bmatrix}, \end{aligned} \tag{20.27}$$

The determinant of the matrices (20.27) is given by:

$$\det[\mathbf{\Phi}_i^{(i)}] = 2i\omega k^{(i)} \beta^{(i)} R^{(i)} \neq 0, \quad \det[\mathbf{\Phi}_i^{(i+1)}] = 2i\omega k^{(i+1)} \beta^{(i+1)} R^{(i)} \neq 0, \tag{20.28}$$

Then, the matrices (20.27) are invertible and by applying an *in-cascade* procedure, we obtain the generic vector $\mathbf{X}^{(i)}$ as function of vector $\mathbf{X}^{(1)}$:

$$\mathbf{X}^{(i)} = \mathbf{\Gamma}^{(i)} \cdot \mathbf{X}^{(1)} \quad \forall i \in \{2, 3, ..., n\} \tag{20.29}$$

where $\mathbf{\Gamma}^{(i)}$ is an $2x2$ square matrix given by :

$$\mathbf{\Gamma}^{(i)} = \prod_{j=1}^{i-1} \left(\left[\mathbf{\Phi}_{i-j}^{(i-j+1)} \right]^{-1} \cdot \mathbf{\Phi}_{i-j}^{(i-j)} \right) \quad \forall i \in \{2, 3, ..., n\} \tag{20.30}$$

By substituting the solutions (20.29) in boundary conditions (20.22), we obtain vector equations in unknown vector $\mathbf{X}^{(1)}$, as reported below:

$$\mathbf{\Lambda} \cdot \mathbf{X}^{(1)} = \mathbf{0} \tag{20.31}$$

where $\mathbf{\Lambda}$ is an 2x2 square matrix given by :

$$\mathbf{\Lambda} = \begin{bmatrix} \Lambda_{11} & \Lambda_{12} \\ \Lambda_{21} & \Lambda_{22} \end{bmatrix} \tag{20.32}$$

where the components $\Lambda_{11}, \Lambda_{12}, \Lambda_{21}, \Lambda_{22}$ are reported below:

$$\Lambda_{11}=\left(1-i\omega\beta^{(1)}R^{(0)}\right)e^{i\omega\beta^{(1)}R^{(0)}},\ \Lambda_{12}=\left(1+i\omega\beta^{(1)}R^{(0)}\right)e^{-i\omega\beta^{(1)}R^{(0)}},$$
$$\left[\Lambda_{21},\Lambda_{22}\right]= \tag{20.33}$$
$$=\left[\left(1-i\omega\beta^{(n)}R^{(n)}-\frac{h_cR^{(n)}}{k^{(n)}}\right)e^{i\omega\beta^{(n)}R^{(n)}},\left(1+i\omega\beta^{(n)}R^{(n)}-\frac{h_cR^{(n)}}{k^{(n)}}\right)e^{-i\omega\beta^{(n)}R^{(n)}}\right]\cdot\mathbf{\Gamma}^{(n)},$$

The algebraic system (20.31) admit not trivial solution if the determinant of matrix $\left[\mathbf{\Lambda}\right]$ is equal to zero. By imposing this condition, we obtain the transcendental equation in unknown parameter ω:

$$\det\left[\mathbf{\Lambda}\right]=0\ \Rightarrow\ g\left(\omega\right)=0 \tag{20.34}$$

The roots of this transcendental equation (20.34) are an infinite number such, denoted here by $\omega_m,\ m=1,2,....N$ leading to eigenvalues or characteristic values $\lambda_m=-\omega_m^2$. The corresponding eigenfunctions or characteristic functions $\bar{\varphi}_m^{(i)}\left(r\right)$ are, as calculated above,

$$\begin{aligned}&\bar{\varphi}_m^{(1)}\left(r\right)=\frac{\varphi_m^{(1)}\left(r\right)}{A_m^{(1)}}=\frac{1}{A_m^{(1)}r}\left[e^{i\omega_m r},e^{-i\omega_m r}\right]\cdot\mathbf{X}_m^{(1)} && \left(\beta^{(1)}=1\right)\\&\bar{\varphi}_m^{(i)}\left(r\right)=\frac{\varphi_m^{(i)}\left(r\right)}{A_m^{(1)}}=\frac{1}{A_m^{(1)}r}\left[e^{i\omega_m\beta^{(i)}r},e^{-i\omega_m\beta^{(i)}r}\right]\cdot\left(\Gamma^{(i)}\cdot\mathbf{X}_m^{(1)}\right) && \forall i\in\{2,3,...,n\}\end{aligned} \tag{20.35}$$

The temperature function in any phase can to be written in the follows form:

$$\begin{aligned}&T^{(1)}\left(r,t\right)=\sum_{m=1}^{\infty}\left\{r^{-1}\left[e^{i\omega_m r},e^{-i\omega_m r}\right]\cdot\mathbf{X}_m^{(1)}\right\}e^{-\kappa^{(1)}\omega_m^2t} && \left(\beta^{(1)}=1\right)\\&T^{(i)}\left(r,t\right)=\sum_{m=1}^{\infty}\left\{r^{-1}\left[e^{i\omega_m\beta^{(i)}r},e^{-i\omega_m\beta^{(i)}r}\right]\cdot\left(\Gamma^{(i)}\cdot\mathbf{X}_m^{(1)}\right)\right\}e^{-\kappa^{(i)}\omega_m^2\beta^{(i)2}t} && \forall i\in\{2,3,...,n\}\end{aligned} \tag{20.36}$$

where the vector $\mathbf{X}_m^{(1)}=\left[A_m^{(1)},B_m^{(1)}\right]^T$ and the unknown constant $B_m^{(i)}$ depends by $A_m^{(1)}$ as showed equations (20.23). The coefficients $A_m^{(1)}$ are determined by applying the initial condition (20.12) that yields the following relationship:

$$A_m^{(1)}=\frac{\sum_{i=1}^{n}\left[\rho^{(i)}c_v^{(i)}\int_0^{2\pi}\int_0^{\pi}\int_{R^{(i-1)}}^{R^{(i)}}\bar{\varphi}_m^{(i)}T_R\,r^2\sin\theta dr d\theta d\phi\right]}{\sum_{i=1}^{n}\left[\rho^{(i)}c_v^{(i)}\int_0^{2\pi}\int_0^{\pi}\int_{R^{(i-1)}}^{R^{(i)}}\left(\bar{\varphi}_m^{(i)}\right)^2r^2\sin\theta dr d\theta d\phi\right]} \tag{20.37}$$

By substituting the function (20.36), in equation (20.14), we obtain in explicit the displacement function in any hollow spherical phase:

$$\begin{aligned}u_r^{(i)}=&G^{(i)}r+H^{(i)}r^{-2}+\sum_{m=1}^{\infty}\left[P_m^{(i)}r+Q_m^{(i)}r^{-2}\right]e^{-\kappa^{(i)}\omega_m^2\beta^{(i)2}t}+\\&+\sum_{m=1}^{\infty}\left\{\frac{\alpha^{(i)}\left(3\lambda^{(i)}+2\mu^{(i)}\right)}{\omega_m^2\beta^{(i)2}\left(\lambda^{(i)}+2\mu^{(i)}\right)r^2}\left[\begin{array}{l}A_m^{(i)}\left(1-i\,\beta^{(i)}\omega_m r\right)e^{i\beta^{(i)}\omega_m r}+\\\quad+B_m^{(i)}\left(1+i\,\beta^{(i)}\omega_m r\right)e^{-i\beta^{(i)}\omega_m r}\end{array}\right]\right\}e^{-\kappa^{(i)}\omega_m^2\beta^{(i)2}t}\end{aligned} \tag{20.38}$$

where the integration constants $G^{(i)},H^{(i)},P_m^{(i)},Q_m^{(i)}$ are determined by applying the boundary conditions give by equations (20.6),(20.7) and (20.8). In this case the functions $f_1^{(i)}\left(t\right),\ f_2^{(i)}\left(t\right)$, reported in equation (20.14) are given by:

$$f_1^{(i)}\left(t\right)=G^{(i)}+\sum_{m=1}^{\infty}P_m^{(i)}e^{-\kappa^{(i)}\omega_m^2\beta^{(i)2}t},\quad f_2^{(i)}\left(t\right)=H^{(i)}+\sum_{m=1}^{\infty}Q_m^{(i)}e^{-\kappa^{(i)}\omega_m^2\beta^{(i)2}t}, \tag{20.39}$$

In explicit the radial and circumferential stress components are given by:

$$\sigma_{rr}^{(i)} = \left(G^{(i)} + \alpha^{(i)} T_R\right)\left(3\lambda^{(i)} + 2\mu^{(i)}\right) - 4\mu^{(i)} H^{(i)} r^{-3} +$$
$$+ \sum_{m=1}^{\infty}\left[P_m^{(i)}\left(3\lambda^{(i)} + 2\mu^{(i)}\right) - 4Q_m^{(i)}\mu^{(i)} r^{-3}\right] e^{-\omega_m^2 \beta^{(i)2} \kappa^{(i)} t} + \tag{20.40}$$
$$+ \frac{4\imath\alpha^{(i)}\mu^{(i)}\left(3\lambda^{(i)} + 2\mu^{(i)}\right)}{\beta^{(i)2}\left(\lambda^{(i)} + 2\mu^{(i)}\right)} \sum_{m=1}^{\infty}\left\{ \omega_m^{-2} r^{-3}\left[\begin{array}{l} A_m^{(i)}\left(\imath + \omega_m \beta^{(i)} r\right) e^{\imath\omega_m \beta^{(i)} r} + \\ + B_m^{(i)}\left(\imath - \omega_m \beta^{(i)} r\right) e^{-\imath\omega_m \beta^{(i)} r} \end{array}\right]\right\} e^{-\omega_m^2 \beta^{(i)2} \kappa^{(i)} t}$$

$$\sigma_{\theta\theta}^{(i)} = \left(G^{(i)} + \alpha^{(i)} T_R\right)\left(3\lambda^{(i)} + 2\mu^{(i)}\right) + 2\mu^{(i)} H^{(i)} r^{-3} +$$
$$+ \sum_{m=1}^{\infty}\left[P_m^{(i)}\left(3\lambda^{(i)} + 2\mu^{(i)}\right) + 2\mu^{(i)} Q_m^{(i)} r^{-3}\right] e^{-\omega_m^2 \beta^{(i)2} \kappa^{(i)} t} + \tag{20.41}$$
$$+ \frac{2\alpha^{(i)}\mu^{(i)}\left(3\lambda^{(i)} + 2\mu^{(i)}\right)}{\beta^{(i)2}\left(\lambda^{(i)} + 2\mu^{(i)}\right)} \sum_{m=1}^{\infty}\left\{ \begin{array}{l} \frac{A_m^{(i)}}{\omega_m^2 r^3}\left[1 - r\omega_m \beta^{(i)}\left(\imath + \omega_m \beta^{(i)} r\right)\right] e^{\imath\omega_m \beta^{(i)} r} + \\ + \frac{B_m^{(i)}}{\omega_m^2 r^3}\left[1 - r\omega_m \beta^{(i)}\left(\omega_m \beta^{(i)} r - \imath\right)\right] e^{-\imath\omega_m \beta^{(i)} r} \end{array}\right\} e^{-\omega_m^2 \beta^{(i)2} \kappa^{(i)} t}$$

It is important to note that displacement function and stress components in any phases can to be subdivided in two parts: firstly constant in time and the second depend of the time. Moreover, the tractions on the inner and the outer spherical boundary surface are vanishing and then condition (20.8) becomes:

$$\sigma_{rr}^{(1)}(r = R^{(0)}) = 0, \;\; \sigma_{rr}^{(n)}(r = R^{(n)}) = 0, \quad \forall t \geq 0 \tag{20.42}$$

The integration constants $G^{(i)}, H^{(i)}, P_m^{(i)}, Q_m^{(i)}$ are function of geometrical, mechanical and thermal parameters of spherical layers . Moreover $P_m^{(i)}, Q_m^{(i)}$ are function of constants $A_m^{(i)}, B_m^{(i)}, \omega_m$ also.
We can write the boundary conditions (20.6) and (20.7) in two uncoupled algebraic system as reported below:

$$\boldsymbol{\Omega} \cdot \mathbf{Y}_0 = \mathbf{L}_0, \qquad \boldsymbol{\Omega} \cdot \mathbf{Y}_m = \mathbf{L}_m, \quad \forall m = 1, 2, ...N \tag{20.43}$$

where the vectors $\mathbf{L}_0, \mathbf{L}_m$ are given by:

$$\mathbf{L}_j = \left[\left(\mathbf{L}_{1,j}^{(2)} - \mathbf{L}_{1,j}^{(1)}\right), \left(\mathbf{L}_{2,j}^{(3)} - \mathbf{L}_{2,j}^{(2)}\right), ..., \left(\mathbf{L}_{i,j}^{(i+1)} - \mathbf{L}_{i,j}^{(i)}\right), .., \left(\mathbf{L}_{n-1,j}^{(n)} - \mathbf{L}_{n-1,j}^{(n-1)}\right)\right]^T \quad \text{with } j \in \{0, m\} \tag{20.44}$$

These vector are characterized by following sub-vectors:

$$\mathbf{L}_{i,0}^{(i)} = \begin{bmatrix} 0 \\ \alpha^{(i)}\left(3\lambda^{(i)} + 2\mu^{(i)}\right) \end{bmatrix} T_R, \;\; \mathbf{L}_{i,0}^{(i+1)} = \begin{bmatrix} 0 \\ \alpha^{(i+1)}\left(3\lambda^{(i+1)} + 2\mu^{(i+1)}\right) \end{bmatrix} T_R,$$

$$\mathbf{L}_{i,m}^{(i)} = \frac{\zeta^{(i)} e^{-\imath\omega_m R^{(i)} \beta^{(i)}}}{\omega_m^2 R^{(i)3}} \begin{bmatrix} R^{(i)}\left(1 - \imath\omega_m R^{(i)} \beta^{(i)}\right) e^{2\imath\omega_m R^{(i)} \beta^{(i)}} & R^{(i)}\left(1 + \imath\omega_m R^{(i)} \beta^{(i)}\right) \\ 4\imath\left(1 + \imath\omega_m R^{(i)} \beta^{(i)}\right) e^{2\imath\omega_m R^{(i)} \beta^{(i)}} & 4\imath\left(1 - \imath\omega_m R^{(i)} \beta^{(i)}\right) \end{bmatrix} \cdot \begin{bmatrix} A_m^{(i)} \\ B_m^{(i)} \end{bmatrix} \tag{20.45}$$

$$\mathbf{L}_{i,m}^{(i+1)} = \frac{\zeta^{(i+1)} e^{-\imath\omega_m R^{(i)} \beta^{(i+1)}}}{\omega_m^2 R^{(i)3}} \begin{bmatrix} R^{(i)}\left(1 - \imath\omega_m R^{(i)} \beta^{(i+1)}\right) e^{2\imath\omega_m R^{(i)} \beta^{(i+1)}} & R^{(i)}\left(1 + \imath\omega_m R^{(i)} \beta^{(i+1)}\right) \\ 4\imath\left(1 + \imath\omega_m R^{(i)} \beta^{(i+1)}\right) e^{2\imath\omega_m R^{(i)} \beta^{(i+1)}} & 4\imath\left(1 - \imath\omega_m R^{(i)} \beta^{(i+1)}\right) \end{bmatrix} \cdot \begin{bmatrix} A_m^{(i+1)} \\ B_m^{(i+1)} \end{bmatrix}$$

where the constant $\zeta^{(i)} = \dfrac{\alpha^{(i)}\left(3\lambda^{(i)} + 2\mu^{(i)}\right)}{\beta^{(i)2}\left(\lambda^{(i)} + 2\mu^{(i)}\right)}$. The unknowns vectors $\mathbf{Y}_0 = [\mathbf{Y}_0^{(1)}, \mathbf{Y}_0^{(2)}, ..., \mathbf{Y}_0^{(n)}]^T$ and $\mathbf{Y}_m = [\mathbf{Y}_m^{(1)}, \mathbf{Y}_m^{(2)}, ..., \mathbf{Y}_m^{(n)}]^T$ are composed by sub-vectors reported below:

$$\mathbf{Y}_0^{(i)} = \begin{bmatrix} G^{(i)} & H^{(i)} \end{bmatrix}^T, \quad \mathbf{Y}_m^{(i)} = \begin{bmatrix} P_m^{(i)} & Q_m^{(i)} \end{bmatrix}^T, \quad \forall i \in \{1, 2, ..., n\}, \; \forall m \in \{1, 2, ..., N\} \tag{20.46}$$

and $\boldsymbol{\Omega}$ is an $2(n-1)x2n$ rectangular matrix composed by following sub-matrices:

$$\left[\boldsymbol{\Omega}\right]=\begin{bmatrix} \boldsymbol{\Omega}_1^{(1)} & -\boldsymbol{\Omega}_1^{(2)} & \mathbf{0} & \mathbf{0} & \cdots & \mathbf{0} & \mathbf{0} & \mathbf{0} \\ \mathbf{0} & \boldsymbol{\Omega}_{2,j}^{(2)} & -\boldsymbol{\Omega}_2^{(3)} & \mathbf{0} & \cdots & \mathbf{0} & \mathbf{0} & \mathbf{0} \\ \mathbf{0} & \mathbf{0} & \boldsymbol{\Omega}_3^{(3)} & -\boldsymbol{\Omega}_3^{(4)} & \cdots & \mathbf{0} & \mathbf{0} & \mathbf{0} \\ \vdots & \vdots & \vdots & \vdots & \vdots & \vdots & \vdots & \vdots \\ \mathbf{0} & \mathbf{0} & \mathbf{0} & \mathbf{0} & \cdots & \boldsymbol{\Omega}_{n-2}^{(n-2)} & -\boldsymbol{\Omega}_{n-2}^{(n-1)} & \mathbf{0} \\ \mathbf{0} & \mathbf{0} & \mathbf{0} & \mathbf{0} & \cdots & \mathbf{0} & \boldsymbol{\Omega}_{n-1}^{(n-1)} & -\boldsymbol{\Omega}_{n-1}^{(n)} \end{bmatrix}, \tag{20.47}$$

where the generic matrices $\boldsymbol{\Omega}_i^{(i)}, \boldsymbol{\Omega}_i^{(i+1)}$ are given by:

$$\boldsymbol{\Omega}_i^{(i)}=\begin{bmatrix} R^{(i)} & R^{(i)-2} \\ 3\lambda^{(i)}+2\mu^{(i)} & -4\mu^{(i)}R^{(i)-3} \end{bmatrix}, \quad \boldsymbol{\Omega}_i^{(i+1)}=\begin{bmatrix} R^{(i)} & R^{(i)-2} \\ 3\lambda^{(i+1)}+2\mu^{(i+1)} & -4\mu^{(i+1)}R^{(i)-3} \end{bmatrix}, \tag{20.48}$$

are (2×2) matrices with nonzero determinant, whose components were already gave above. The determinant of the matrices (20.48) is given by:

$$\det[\boldsymbol{\Omega}_i^{(i)}]=-\frac{3\left(2\mu^{(i)}+\lambda^{(i)}\right)}{R^{(i)2}}\neq 0, \quad \det[\boldsymbol{\Omega}_i^{(i+1)}]=-\frac{3\left(2\mu^{(i+1)}+\lambda^{(i+1)}\right)}{R^{(i)2}}\neq 0, \tag{20.49}$$

However, in force of the special form of $\boldsymbol{\Omega}$ derived above, one can rewrite the reduced algebraic problem in order to have the solution without recall any numerical strategy. To make this, let us we can rewrite two algebraic system (20.43) in follows manner:

$$\begin{cases} \boldsymbol{\Omega}_1^{(2)}\mathbf{Y}_j^{(2)}=\boldsymbol{\Omega}_1^{(1)}\mathbf{Y}_j^{(1)}+\mathbf{L}_{1,j}^{(2)}-\mathbf{L}_{1,j}^{(1)} \\ \boldsymbol{\Omega}_2^{(3)}\mathbf{Y}_j^{(3)}=\boldsymbol{\Omega}_2^{(2)}\mathbf{Y}_j^{(2)}+\mathbf{L}_{2,j}^{(3)}-\mathbf{L}_{2,j}^{(2)} \\ \vdots \\ \boldsymbol{\Omega}_i^{(i+1)}\mathbf{Y}_j^{(i+1)}=\boldsymbol{\Omega}_i^{(i)}\mathbf{Y}_j^{(i)}+\mathbf{L}_{i,j}^{(i+1)}-\mathbf{L}_{i,j}^{(i)} \qquad \forall j\in\{0,m\}, \quad \forall m\in\{1,2,....,N\} \\ \vdots \\ \boldsymbol{\Omega}_{n-2}^{(n-1)}\mathbf{Y}_j^{(n-1)}=\boldsymbol{\Omega}_{n-2}^{(n-2)}\mathbf{Y}_j^{(n-2)}+\mathbf{L}_{n-2,j}^{(n-1)}-\mathbf{L}_{n-2,j}^{(n-2)} \\ \boldsymbol{\Omega}_{n-1}^{(n)}\mathbf{Y}_j^{(n)}=\boldsymbol{\Omega}_{n-1}^{(n-1)}\mathbf{Y}_j^{(n-1)}+\mathbf{L}_{n-1,j}^{(n)}-\mathbf{L}_{n-1,j}^{(n-1)} \end{cases} \tag{20.50}$$

By applying an *in-cascade* procedure, we finally obtain

$$\begin{cases} \mathbf{Y}_0^{(i)}=\boldsymbol{\Sigma}^{(i)}\cdot\mathbf{Y}_0^{(1)}+\boldsymbol{\Psi}_0^{(i)} \\ \mathbf{Y}_m^{(i)}=\boldsymbol{\Sigma}^{(i)}\cdot\mathbf{Y}_m^{(1)}+\boldsymbol{\Psi}_m^{(i)} \end{cases} \quad \forall i\in\{2,3,...,n\}, \quad \forall m\in\{1,2,....,N\} \tag{20.51}$$

where $\boldsymbol{\Sigma}^{(i)}$ is an matrix given by following expression:

$$\boldsymbol{\Sigma}^{(i)}=\prod_{j=1}^{i-1}\left(\left[\boldsymbol{\Omega}_{i-j}^{(i-j+1)}\right]^{-1}\cdot\boldsymbol{\Omega}_{i-j}^{(i-j)}\right) \qquad \forall i\in\{2,3,...,n\} \tag{20.52}$$

and the vectors $\boldsymbol{\Psi}_0^{(i)}, \boldsymbol{\Psi}_m^{(i)}$, are reported below:

$$\begin{cases} \boldsymbol{\Psi}_0^{(i)}=\left[\boldsymbol{\Omega}_{i-1}^{(i)}\right]^{-1}\cdot\left\{\mathbf{L}_{i-1,0}^{(i-1)}-\mathbf{L}_{i-1,0}^{(i)}+\sum_{j=1}^{i-2}\left[\prod_{k=1}^{j}\left(\boldsymbol{\Omega}_{i-k}^{(i-k)}\cdot\left[\boldsymbol{\Omega}_{i-k-1}^{(i-k)}\right]^{-1}\right)\right]\cdot\left(\mathbf{L}_{i-j-1,0}^{(i-j-1)}-\mathbf{L}_{i-j-1,0}^{(i-j)}\right)\right\} \\ \boldsymbol{\Psi}_m^{(i)}=\left[\boldsymbol{\Omega}_{i-1}^{(i)}\right]^{-1}\cdot\left\{\mathbf{L}_{i-1,m}^{(i-1)}-\mathbf{L}_{i-1,m}^{(i)}+\sum_{j=1}^{i-2}\left[\prod_{k=1}^{j}\left(\boldsymbol{\Omega}_{i-k}^{(i-k)}\cdot\left[\boldsymbol{\Omega}_{i-k-1}^{(i-k)}\right]^{-1}\right)\right]\cdot\left(\mathbf{L}_{i-j-1,m}^{(i-j-1)}-\mathbf{L}_{i-j-1,m}^{(i-j)}\right)\right\} \end{cases} \tag{20.53}$$

$$\forall i\in\{2,3,...,n\}, \quad \forall m\in\{1,2,....,N\}$$

where *dot* stands for scalar product. The equations (20.52)-(20.53) permit to write two generic unknowns sub-vectors $\mathbf{Y}_0^{(i)}, \mathbf{Y}_m^{(i)}$ as function of a transferring matrix $\boldsymbol{\Sigma}^{(i)}$ and vectors $\boldsymbol{\Psi}_0^{(i)}, \boldsymbol{\Psi}_m^{(i)}$, and the unknowns sub-vectors $\mathbf{Y}_0^{(1)}, \mathbf{Y}_m^{(1)}$. The problem is hence reduced to an algebraic one in which

only the four coefficients – collected in $\mathbf{Y}_0^{(1)}, \mathbf{Y}_m^{(1)}$ – related to the first phase have to be determined, by imposing two boundary conditions described by the equations obtained above. Therefore, in order to find the four unknowns collected in $\mathbf{Y}_0^{(1)}, \mathbf{Y}_m^{(1)}$, it remains to rewrite the boundary conditions (20.42) in matrix form. In particular, by applying the equations (20.51) for $i = n$, we obtain the follows relationship:

$$\mathbf{Y}_0^{(n)} = \mathbf{\Sigma}^{(n)} \cdot \mathbf{Y}_0^{(1)} + \mathbf{\Psi}_0^{(n)}, \quad \mathbf{Y}_m^{(n)} = \mathbf{\Sigma}^{(n)} \cdot \mathbf{Y}_m^{(1)} + \mathbf{\Psi}_m^{(n)} \quad \forall m \in \{1, 2, ..., N\}, \tag{20.54}$$

Then, the boundary conditions(20.42), become two uncoupled algebraic system:

$$\mathbf{\Pi} \cdot \mathbf{Y}_0^{(1)} = \Upsilon_0, \quad \mathbf{\Pi} \cdot \mathbf{Y}_m^{(1)} = \Upsilon_m \quad \forall m \in \{1, 2, ..., N\}, \tag{20.55}$$

where the matrix $\mathbf{\Pi}$, and vectors Υ_0, Υ_m are given by**:**

$$\mathbf{\Pi} = \left[\mathbf{\Pi}_1 \quad \left(\mathbf{\Sigma}^{(n)} \right)^T \cdot \mathbf{\Pi}_2 \right]^T, \quad \Upsilon_0 = \left[\Upsilon_{1,0} \quad \Upsilon_{2,0} \right]^T, \quad \Upsilon_m = \left[\Upsilon_{1,m} \quad \Upsilon_{2,m} \right]^T \quad \forall m \in \{1, 2, ..., N\}, \tag{20.56}$$

where $\mathbf{\Pi}_1, \mathbf{\Pi}_2$ are two vectors and $\Upsilon_{1,0}, \Upsilon_{2,0}, \Upsilon_{1,m}, \Upsilon_{2,m}$ are four scalars, as reported below:

$$\begin{aligned}
&\mathbf{\Pi}_1 = \left[\left(3\lambda^{(1)} + 2\mu^{(1)} \right), -4\mu^{(1)} R^{(0)-3} \right]^T, \ \mathbf{\Pi}_2 = \left[\left(3\lambda^{(n)} + 2\mu^{(n)} \right), -4\mu^{(n)} R^{(n)-3} \right]^T \\
&\Upsilon_{1,0} = -\alpha^{(1)} \left(3\lambda^{(1)} + 2\mu^{(1)} \right) T_R; \ \ \Upsilon_{2,0} = -\alpha^{(n)} \left(3\lambda^{(n)} + 2\mu^{(n)} \right) T_R - \mathbf{\Pi}_2 \cdot \mathbf{\Psi}_0^{(n)}, \\
&\Upsilon_{1,m} = \frac{4i\zeta^{(1)}}{\omega_m^2 R^{(0)3}} \left[A_m^{(1)} \left(1 + i\omega_m R^{(0)} \beta^{(1)} \right) e^{i\omega_m R^{(0)} \beta^{(1)}} + B_m^{(1)} \left(1 - i\omega_m R^{(0)} \beta^{(1)} \right) e^{-i\omega_m R^{(0)} \beta^{(1)}} \right], \\
&\Upsilon_{1,m} = \frac{4i\zeta^{(n)}}{\omega_m^2 R^{(n)3}} \left[A_m^{(n)} \left(1 + i\omega_m R^{(n)} \beta^{(n)} \right) e^{i\omega_m R^{(n)} \beta^{(n)}} + B_m^{(n)} \left(1 - i\omega_m R^{(n)} \beta^{(n)} \right) e^{-i\omega_m R^{(n)} \beta^{(n)}} \right] - \mathbf{\Pi}_2 \cdot \mathbf{\Psi}_m^{(n)}, \\
&\qquad\qquad\qquad\qquad\qquad\qquad\qquad\qquad\qquad\qquad\qquad\qquad \forall m \in \{1, 2, ..., N\},
\end{aligned} \tag{20.57}$$

Then, by inverting, all the $2 \times n$ unknown coefficients , we obtain the unknown parameters:

$$\begin{cases}
\mathbf{Y}_0^{(1)} = \mathbf{\Pi}^{-1} \cdot \Upsilon_0, \\
\mathbf{Y}_0^{(i)} = \mathbf{\Sigma}^{(i)} \cdot \mathbf{\Pi}^{-1} \cdot \Upsilon_0 + \mathbf{\Psi}_0^{(i)} \quad \forall i \in \{2, 3, ..., n\}
\end{cases}$$
$$\begin{cases}
\mathbf{Y}_m^{(1)} = \mathbf{\Pi}^{-1} \cdot \Upsilon_m, \\
\mathbf{Y}_m^{(i)} = \mathbf{\Sigma}^{(i)} \cdot \mathbf{\Pi}^{-1} \cdot \Upsilon_m + \mathbf{\Psi}_m^{(i)} \quad \forall i \in \{2, 3, ..., n\}
\end{cases} \quad \forall m \in \{1, 2, ..., N\}, \tag{20.58}$$

By substituting the solutions (20.58) in (20.38), we obtain in explicit displacement function.

For example, let us consider, a spherical tank constituted by two phases under decreasing temperature. The phase (1) is constituted by steel and phase (2) by aluminium. It is denoted with pedix “s” the parameters of steel and pedix “a” the parameters of aluminium. The mechanical and thermal parameters considered for both phases are reported in table 20.1:

	Steel (phase 1)	**Aluminium** (phase 2)
$E\left[N\, m^{-2} \right]$	$210 \cdot 10^9$	$70 \cdot 10^9$
$k\left[W\, m^{-1} K^{-1} \right]$	45	237
ν	0.30	0.35
$\alpha\left[m \cdot m^{-1} K^1 \right]$	$12 \cdot 10^{-6}$	$23.1 \cdot 10^{-6}$
$\rho\left[kg\, m^{-3} \right]$	7800	2700
$c_v\left[J \cdot kg^{-1} K^{-1} \right]$	440	930

Table 20.1 – *Mechanical and thermal parameters of Steel and Aluminium*

The geometrical parameters of spherical tank are $R^{(0)}=1.00m$, $R^{(1)}=1.03m$, $R^{(2)}=1.08m$, $h_c=50W/m^2\cdot°K$, $T_0=T_R=300°K$. In this case the graphics function $g(\omega)$ given by equation (20.34) is reported below:

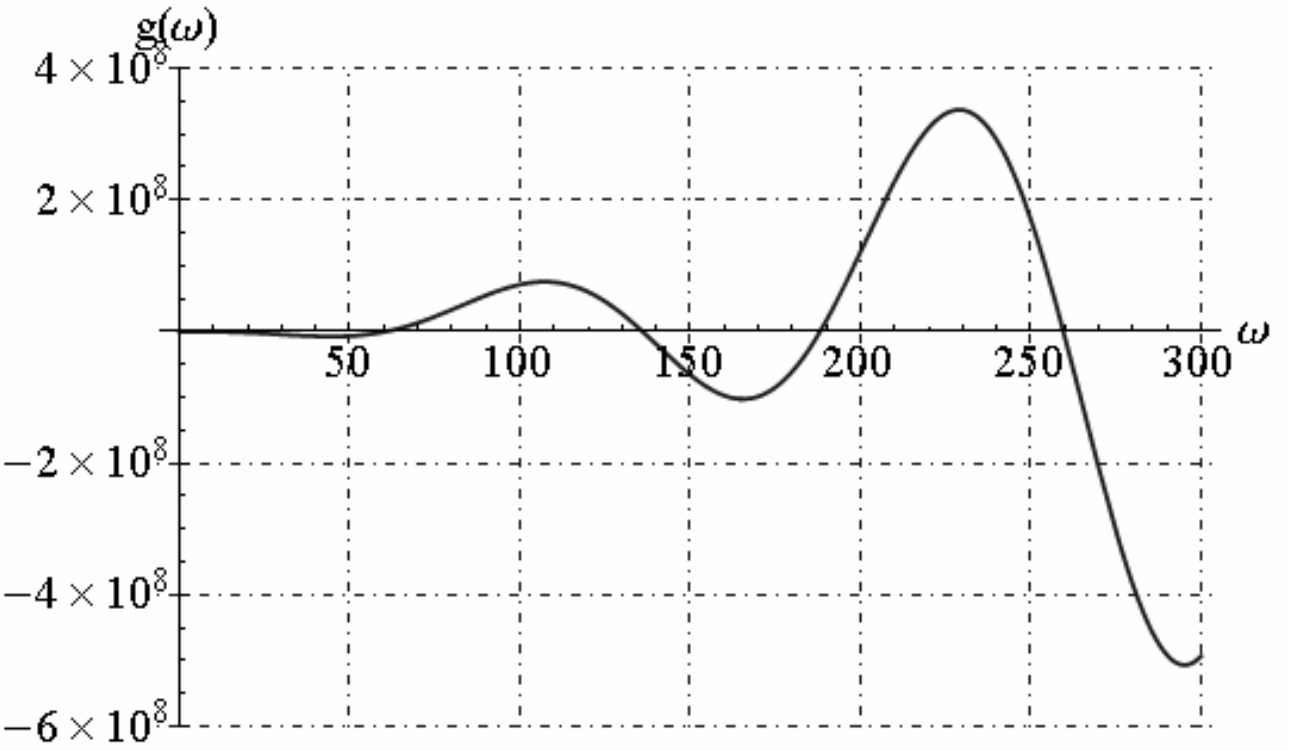

Fig. 20.1 - *Function* $g(\omega)$

By fixed m= 20, the eigenvalues ω_m of transcendental equation (20.34) and corresponding values of constants integration A_m are reported in table 20.2:

ω_m	4.235	60.356	136.051	188.112	259.623
A_m	-37.700 + 150.659 i	1.027 - 0.834 i	-0.161 + 0.236 i	-0.142 - 0.057 i	-0.030 - 0.062 i
ω_m	326.584	381.220	458.082	513.798	579.305
A_m	-0.0504 - 0.0070 i	-0.0162 + 0.0310 i	-0.0199 - 0.0133 i	0.0031 + 0.0203 i	-0.0043 + 0.0132 i
ω_m	651.969	703.695	778.701	840.407	899.389
A_m	0.00114 + 0.01267 i	-0.01077 - 0.00022 i	0.00720 + 0.00316 i	-0.00025 - 0.00765 i	0.00376 - 0.00469 i
ω_m	975.551	1028.100	1098.533	1166.777	1220.556
A_m	0.00048 + 0.00549 i	-0.00358 + 0.00369 i	-0.00200 - 0.00329 i	-0.00127 + 0.00378 i	0.00017 + 0.00345 i

Table 20.2 – *Eigenvalues* ω_m *and corresponding values of constants integration* A_m

We reported the graphics of temperature function along the radial direction and in time:

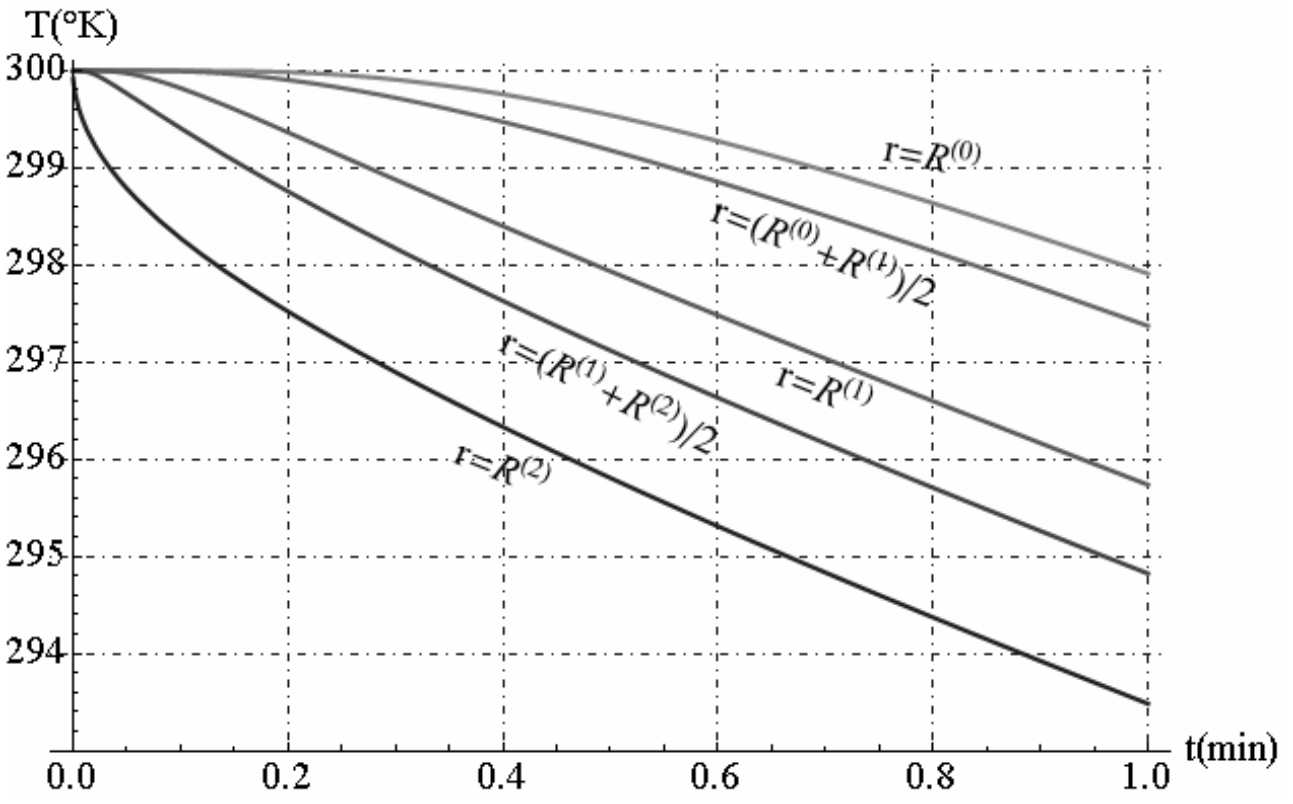

Fig. 20.2 - *Temperature function versus the time*

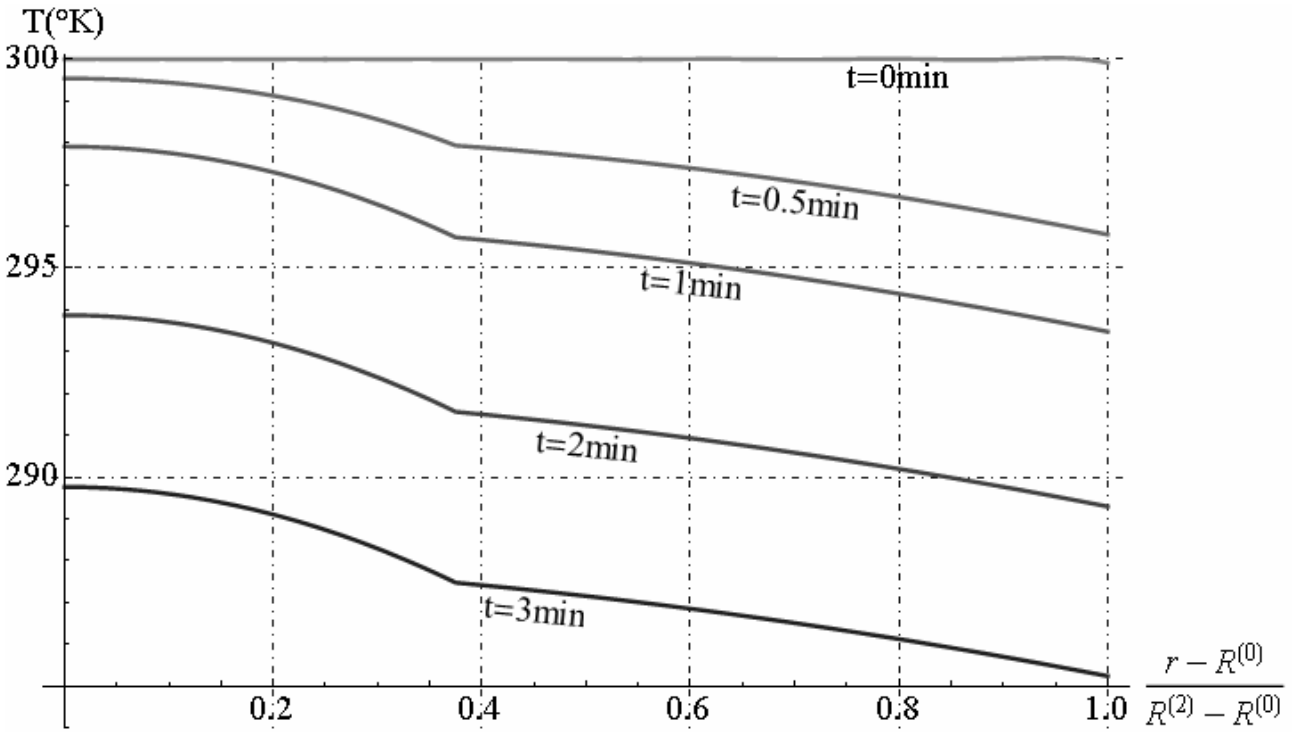

Fig. 20.3 - *Temperature distribution along radial direction*

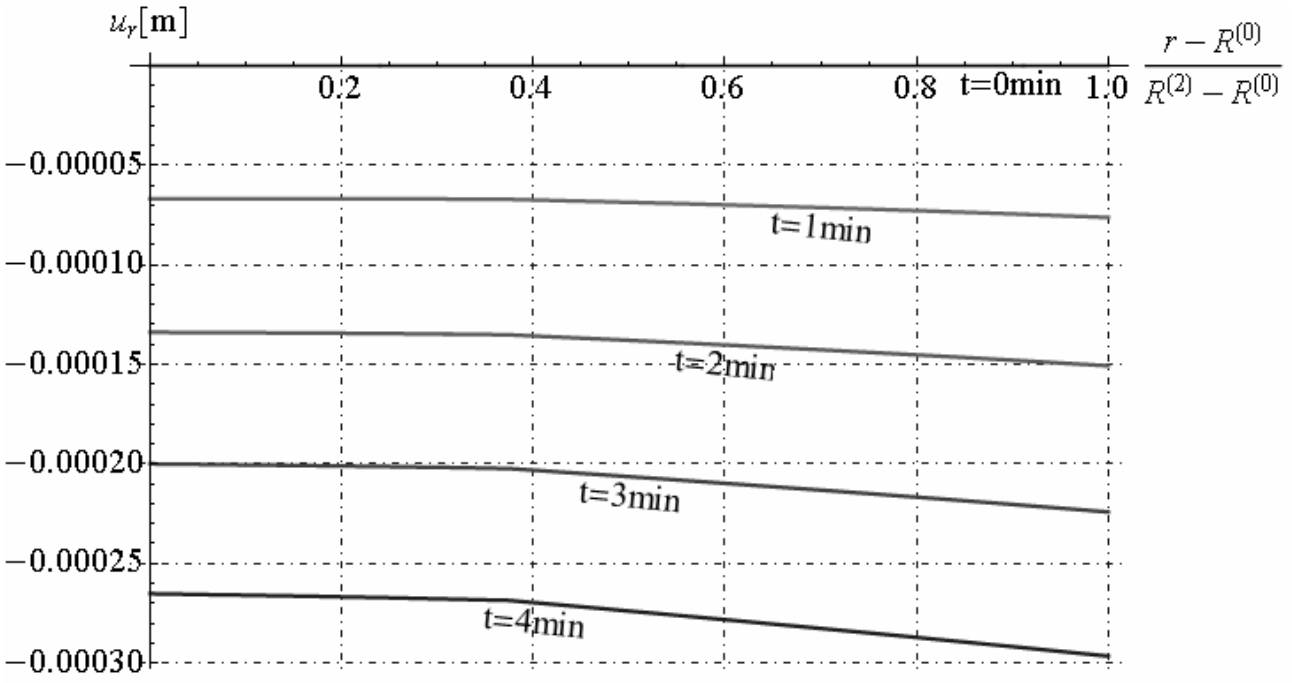

Fig. 20.4 - *Radial displacement distribution along radial direction*

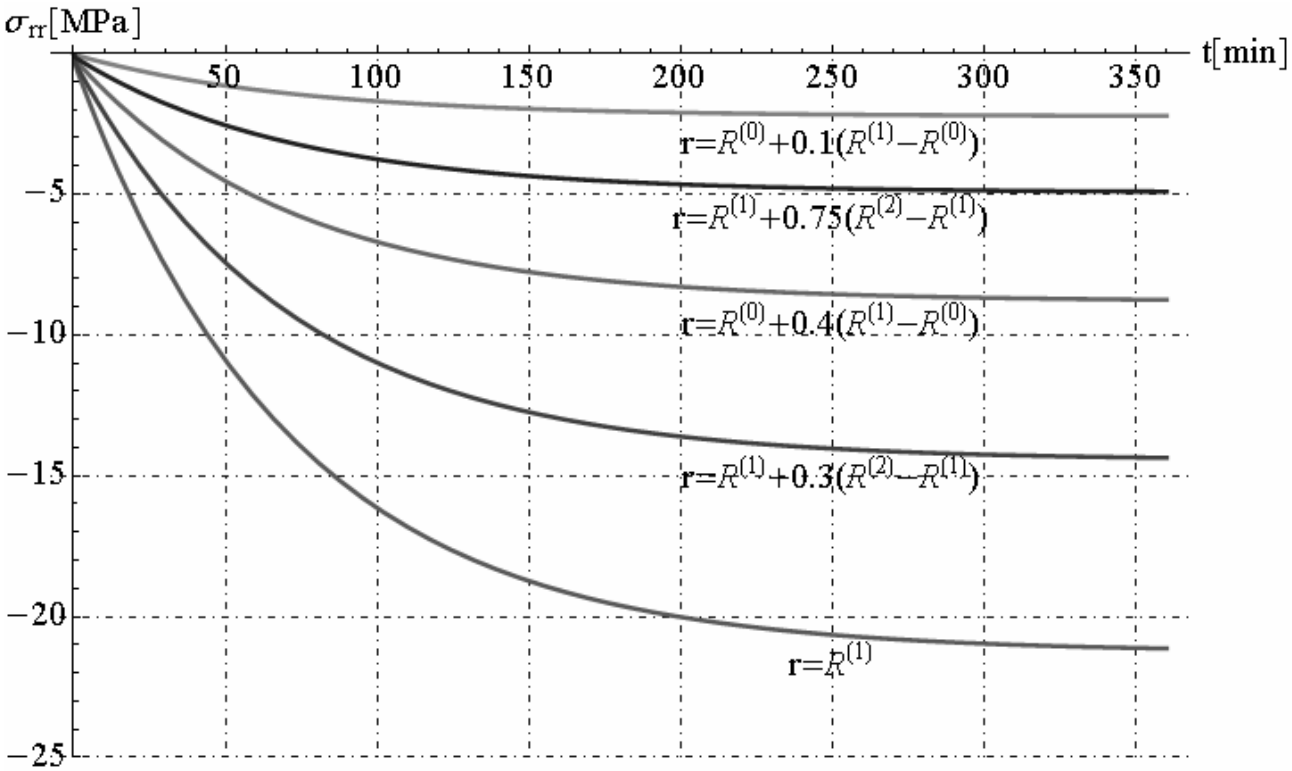

Fig. 20.5 - *Radial stress distribution in time*

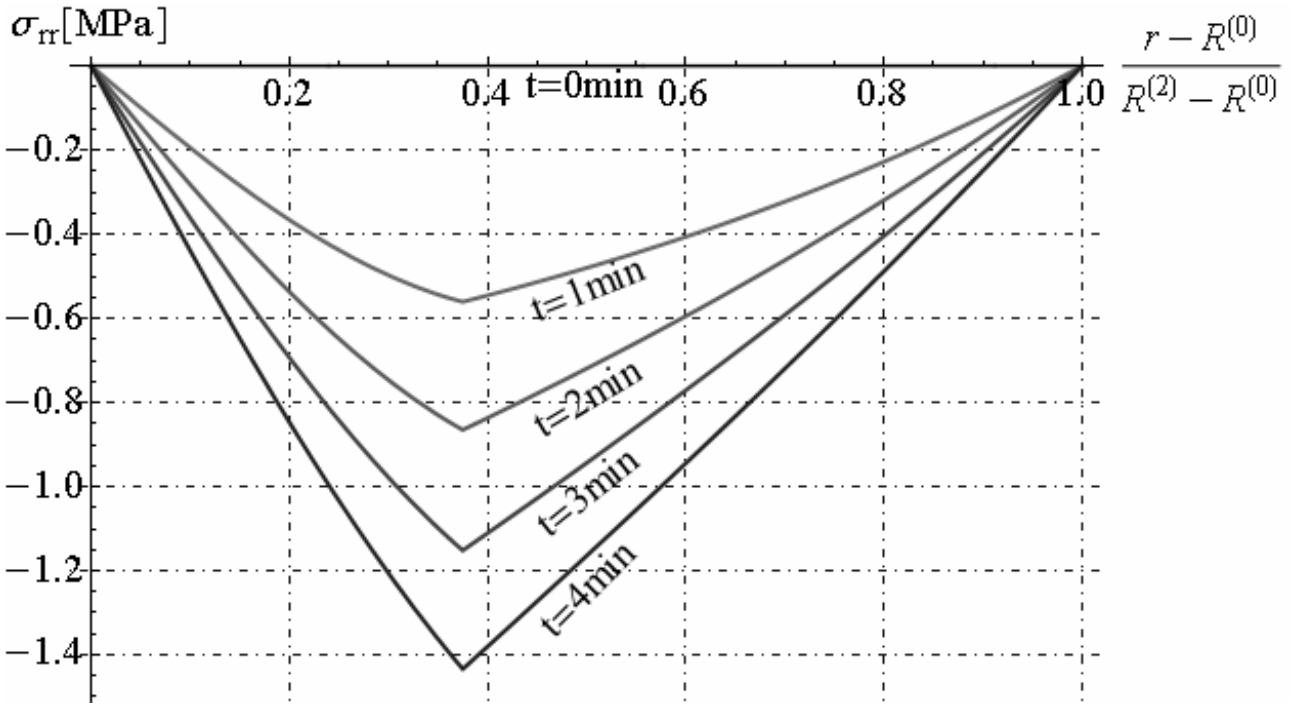

Fig. 20.6 - *Radial stress distribution along radial direction*

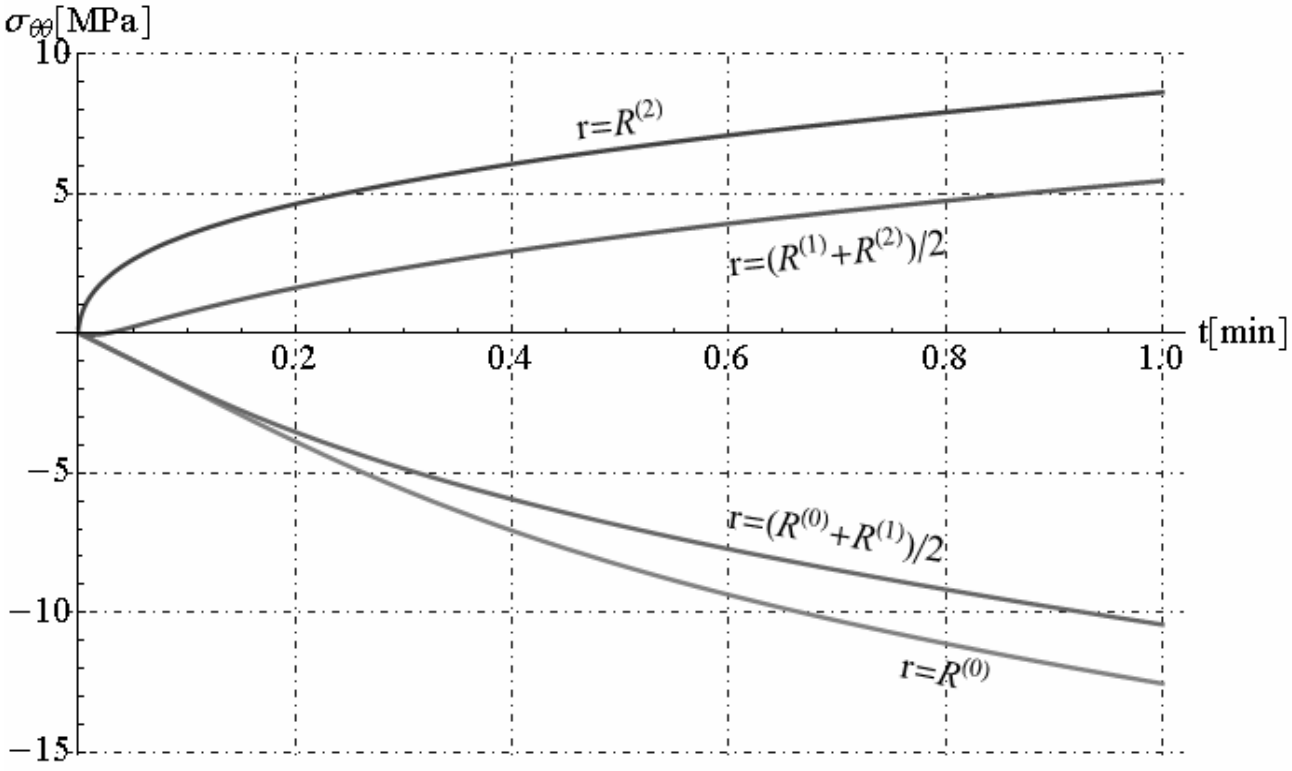

Fig. 20.7 - *Circumferential stress distribution in time*

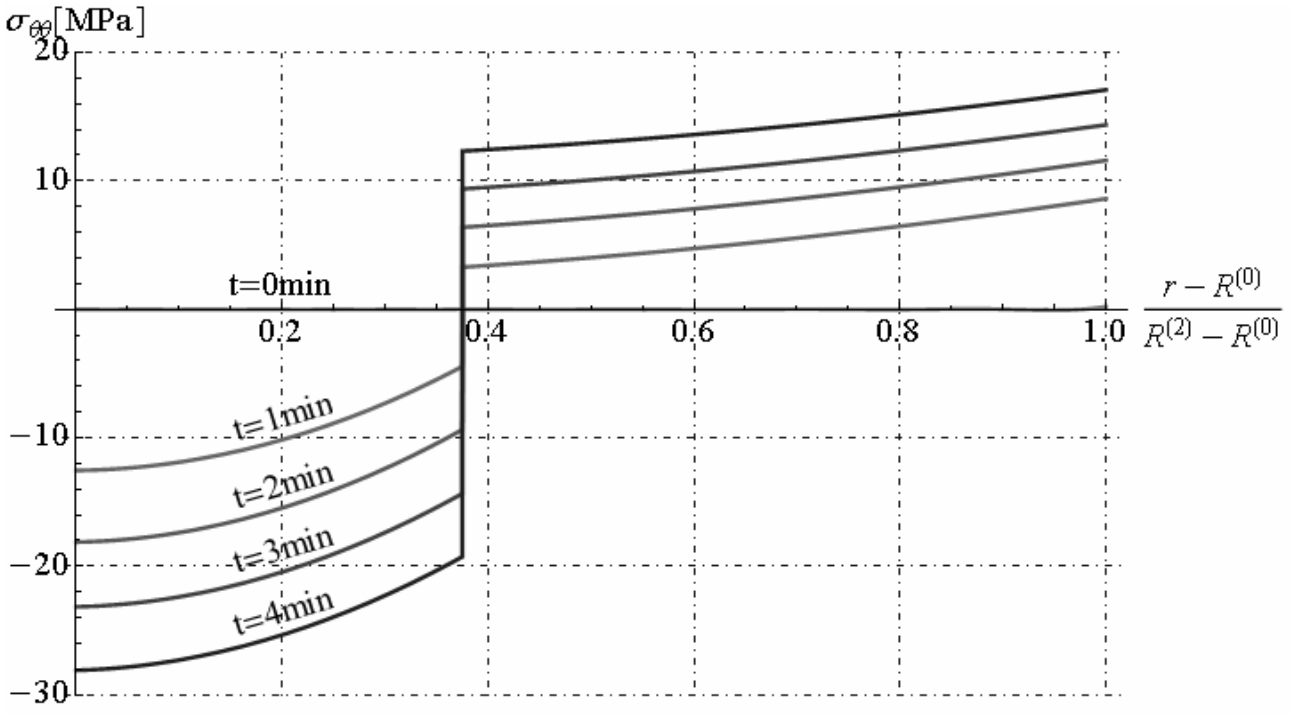

Fig. 20.8 - *Circumferential stress distribution along radial direction*

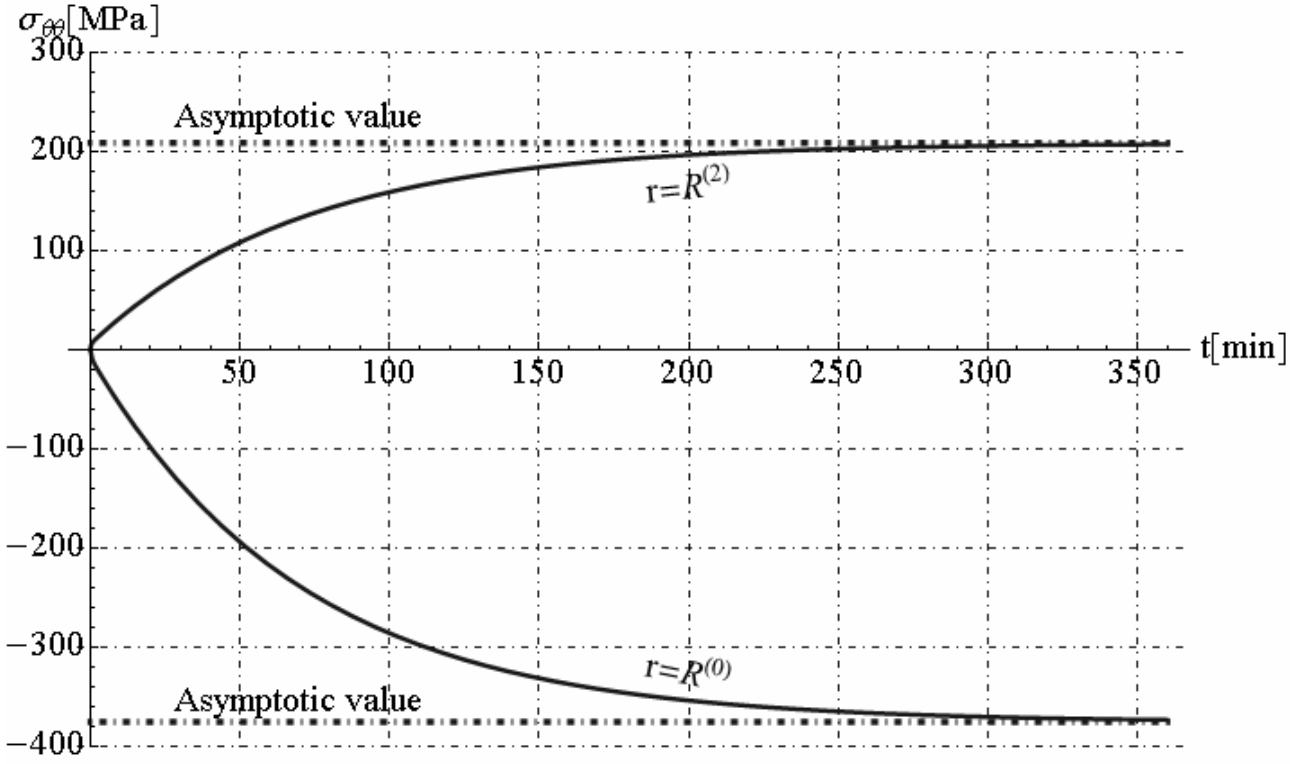

Fig. 20.9 - *Circumferential stress distribution in time with asymptotic values*

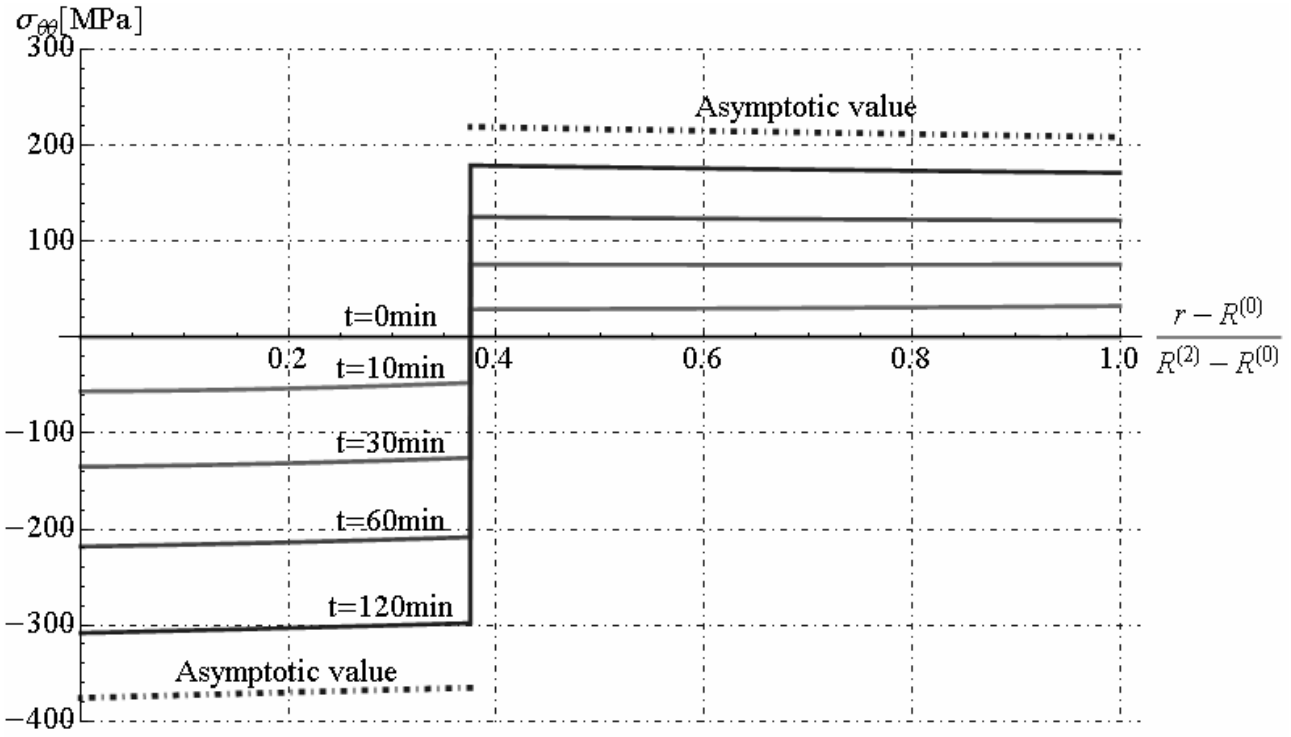

Fig. 20.10 - *Circumferential stress distribution along radial direction with asymptotic values*

Finally, we reported an other example related to spherical tank constituted by three phases under decreasing temperature. The phase (1) is constituted by titanium, phase (2) by aluminium and phase three(3) by steel. The mechanical and thermal parameters considered for three phases are reported in table 20.2.

	Titanium (phase 1)	**Aluminium** (phase 2)	**Steel** (phase 2)
$E\left[N\,m^{-2}\right]$	$108\cdot10^{9}$	$70\cdot10^{9}$	$210\cdot10^{9}$
$k\left[W\,m^{-1}K^{-1}\right]$	20	237	45
ν	0.3	0.35	0.30
$\alpha\left[m\cdot m^{-1}K^{1}\right]$	$11\cdot10^{-6}$	$23.1\cdot10^{-6}$	$12\cdot10^{-6}$
$\rho\left[kg\,m^{-3}\right]$	4000	2700	7800
$c_v\left[J\cdot kg^{-1}K^{-1}\right]$	400	930	440

Table 20.3 – *Mechanical and thermal parameters of Titanium, Aluminium and Steel*

The geometrical parameters of spherical tank are: $R^{(0)}=1.00m$, $R^{(1)}=1.03m$, $R^{(2)}=1.06m$, $R^{(3)}=1.09m$, $h_c=80W/m^2\cdot°K$, $T_0=T_R=300°K$. By fixed m= 10, the eigenvalues ω_m of transcendental equation (20.34) and corresponding values of constants integration A_m are reported in table 20.4:

ω_m	5.410	50.388	76.859	147.514	167.699
A_m	120.215 + 99.351 i	−5.000 + 0.716 i	0.184 − 1.884 i	0.599 + 0.081 i	−0.172 + 0.444 i
ω_m	235.599	265.302	309.104	364.528	389.939
A_m	0.1970 + 0.0032 i	0.0298 − 0.1855 i	−0.0325 + 0.0921 i	0.0926 − 0.0099 i	−0.0682 + 0.0276 i

Table 20.4 – *Eigenvalues ω_m and corresponding values of constants integration A_m*

In this case the graphics function $g(\omega)$ given by equation (20.34) is reported below:

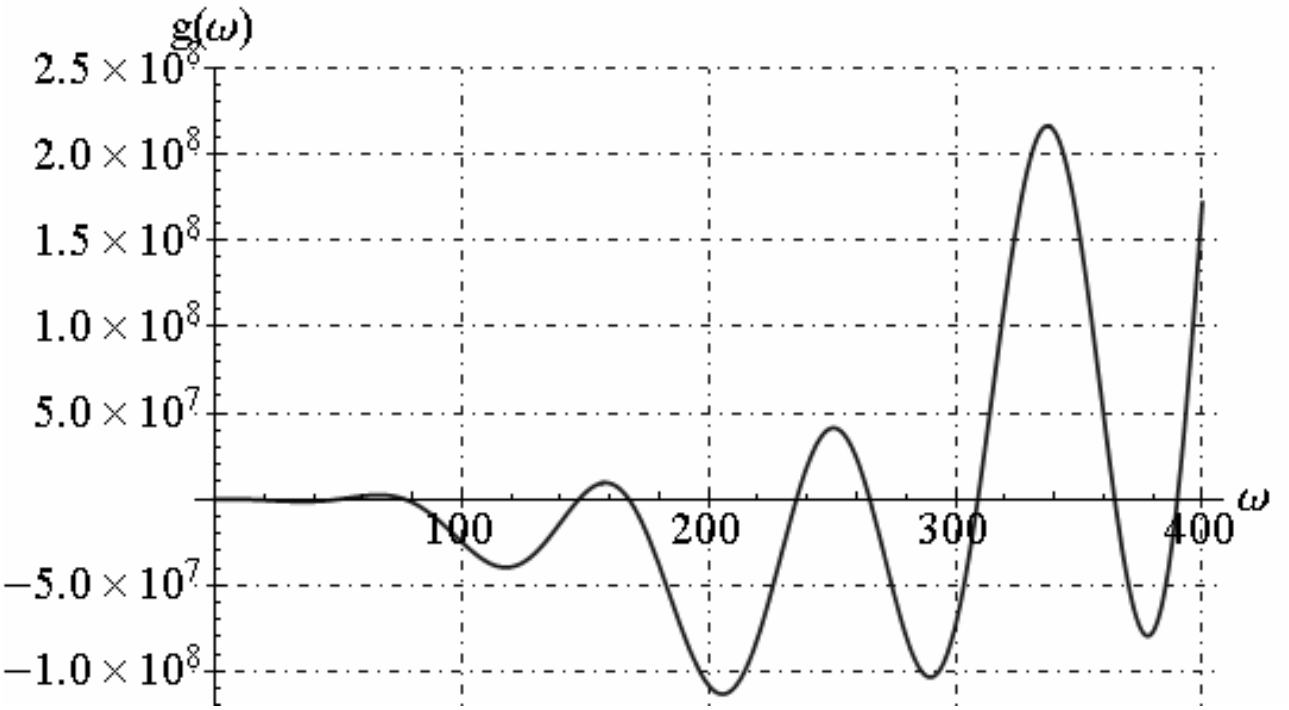

Fig. 20.11 - *Function* $g(\omega)$

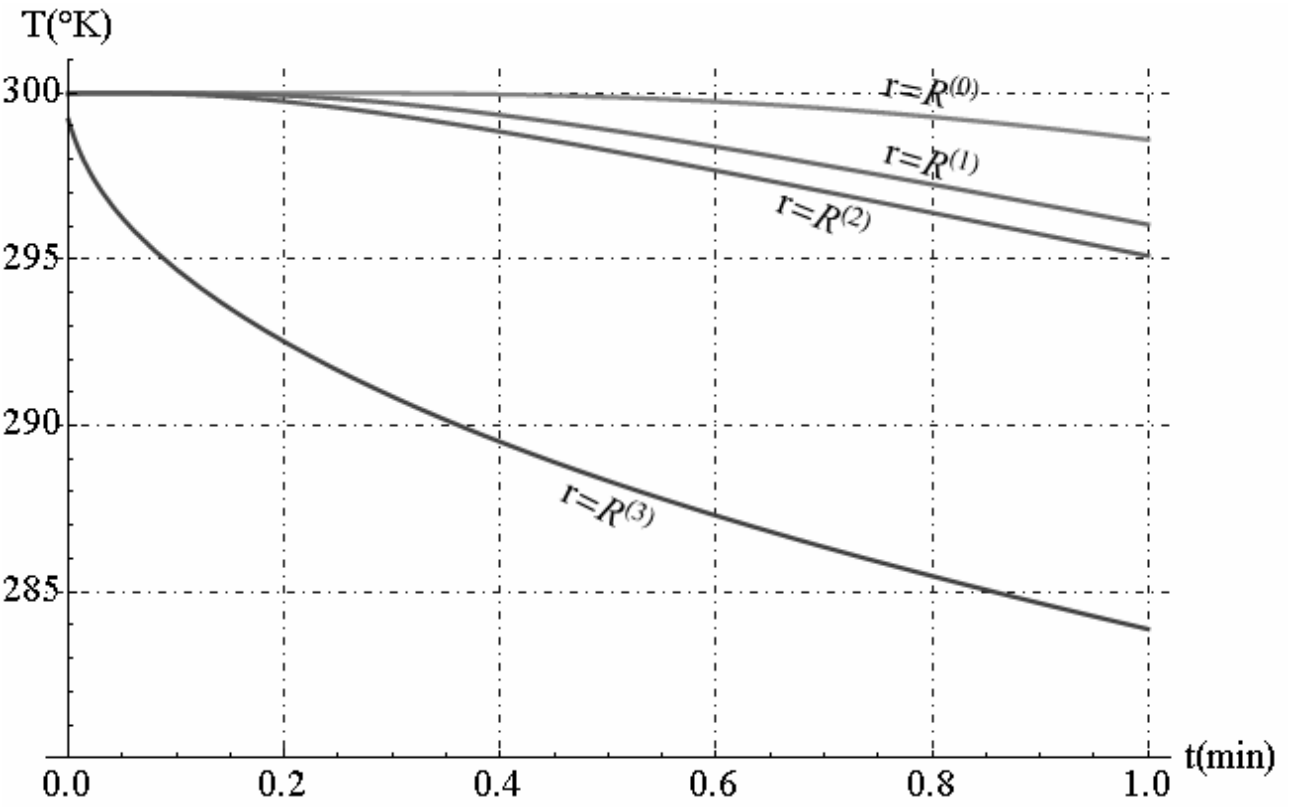

Fig. 20.12 - *Temperature function versus the time*

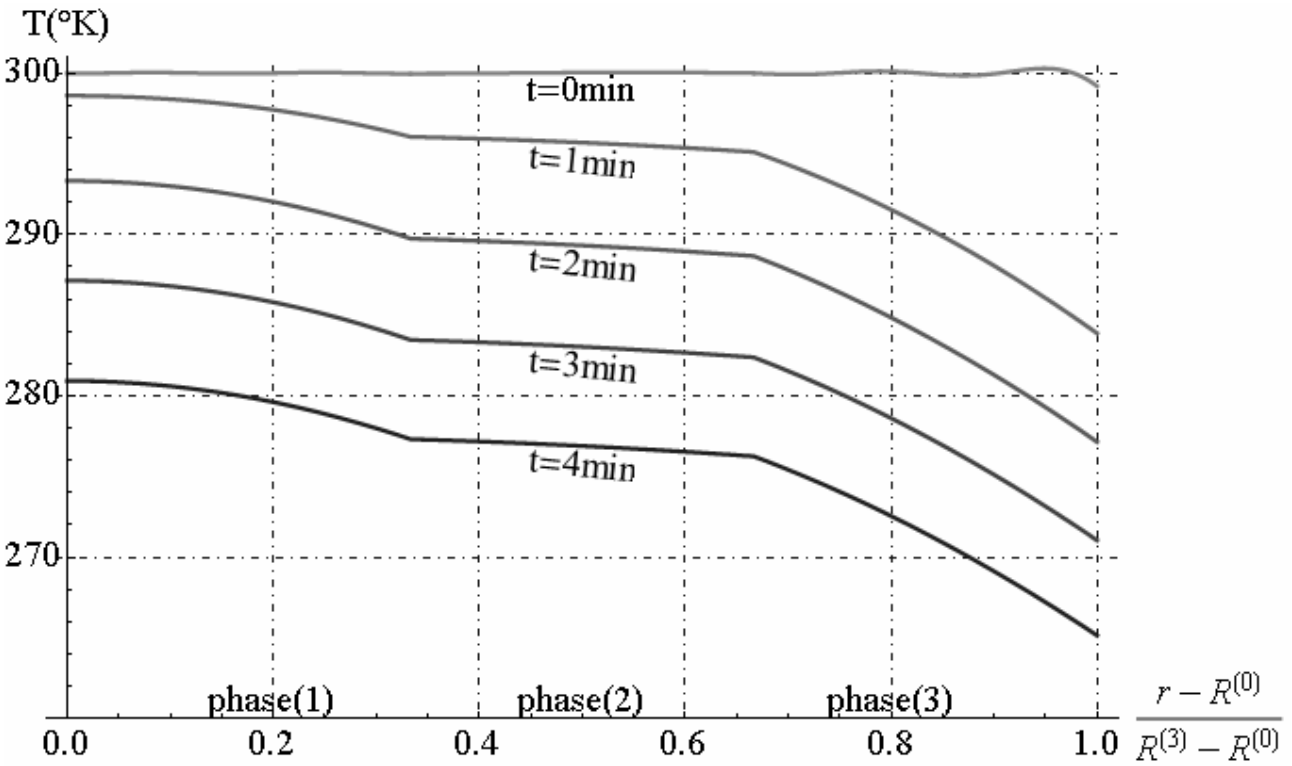

Fig. 20.13 - *Temperature distribution along radial direction*

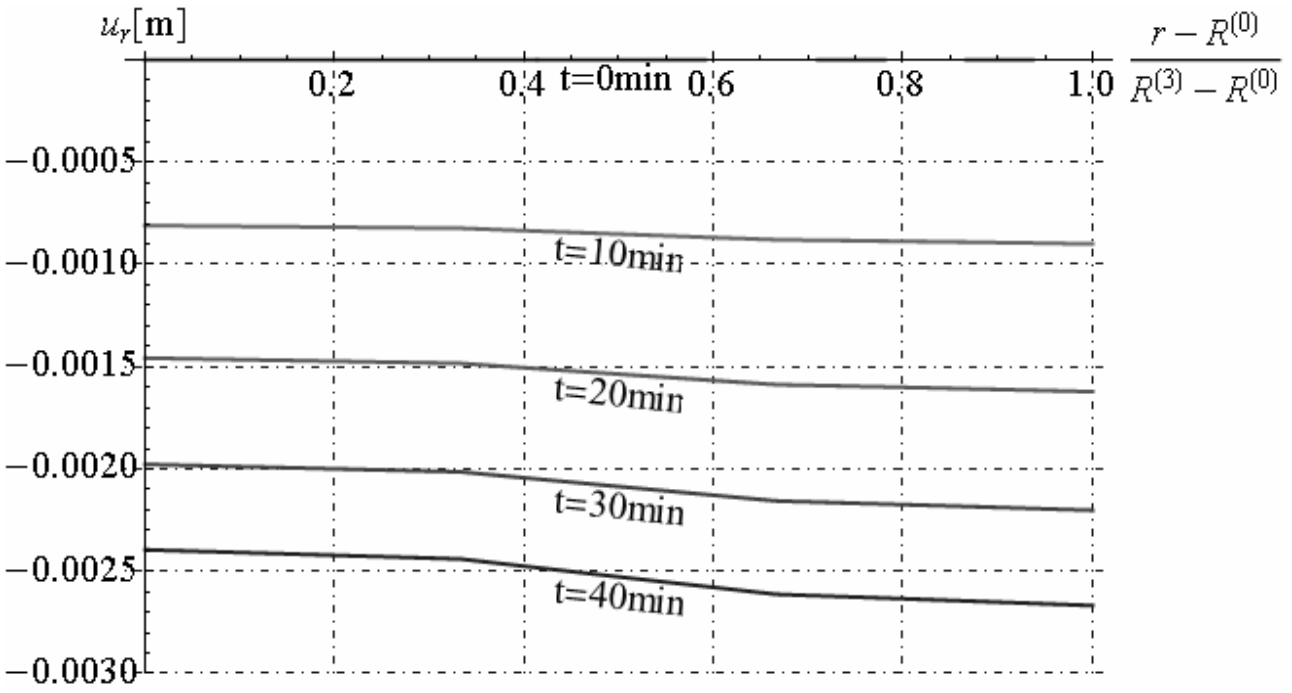

Fig. 20.14 - *Radial displacement distribution along radial direction*

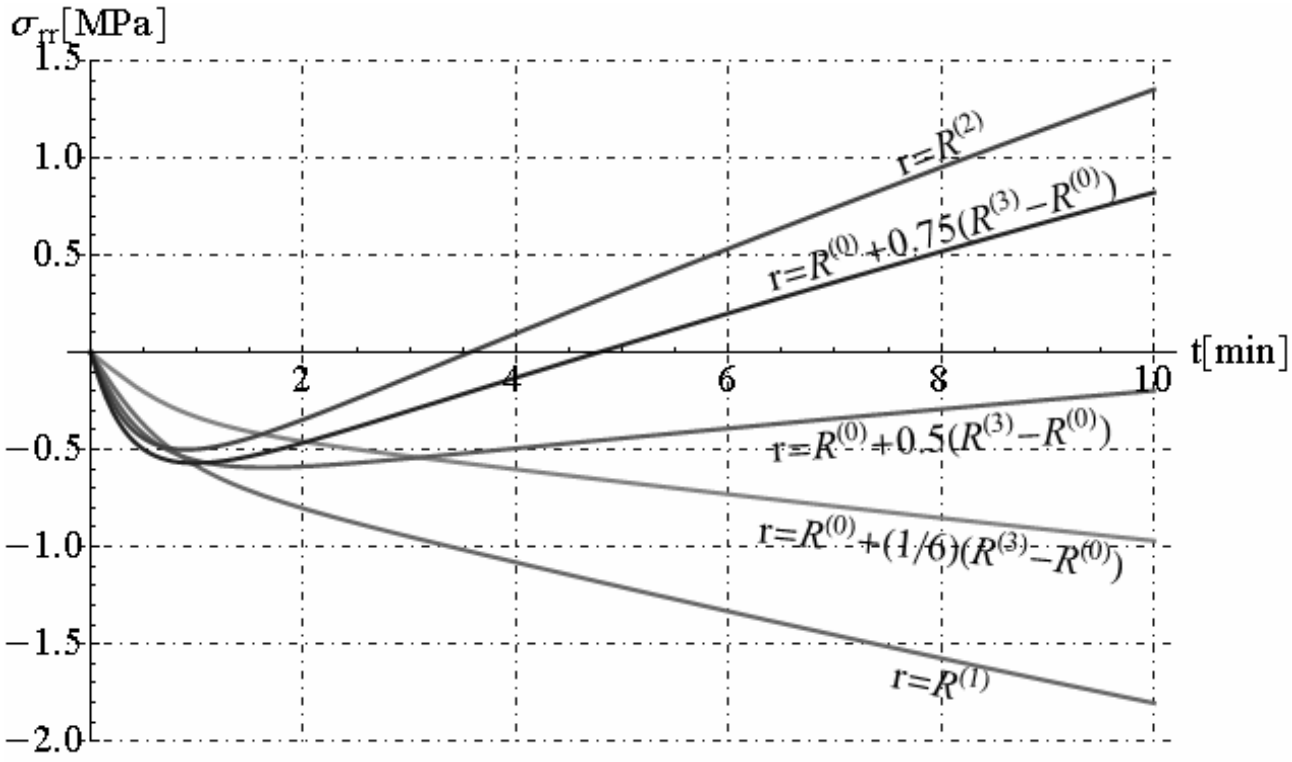

Fig. 20.15 - *Radial stress distribution in time*

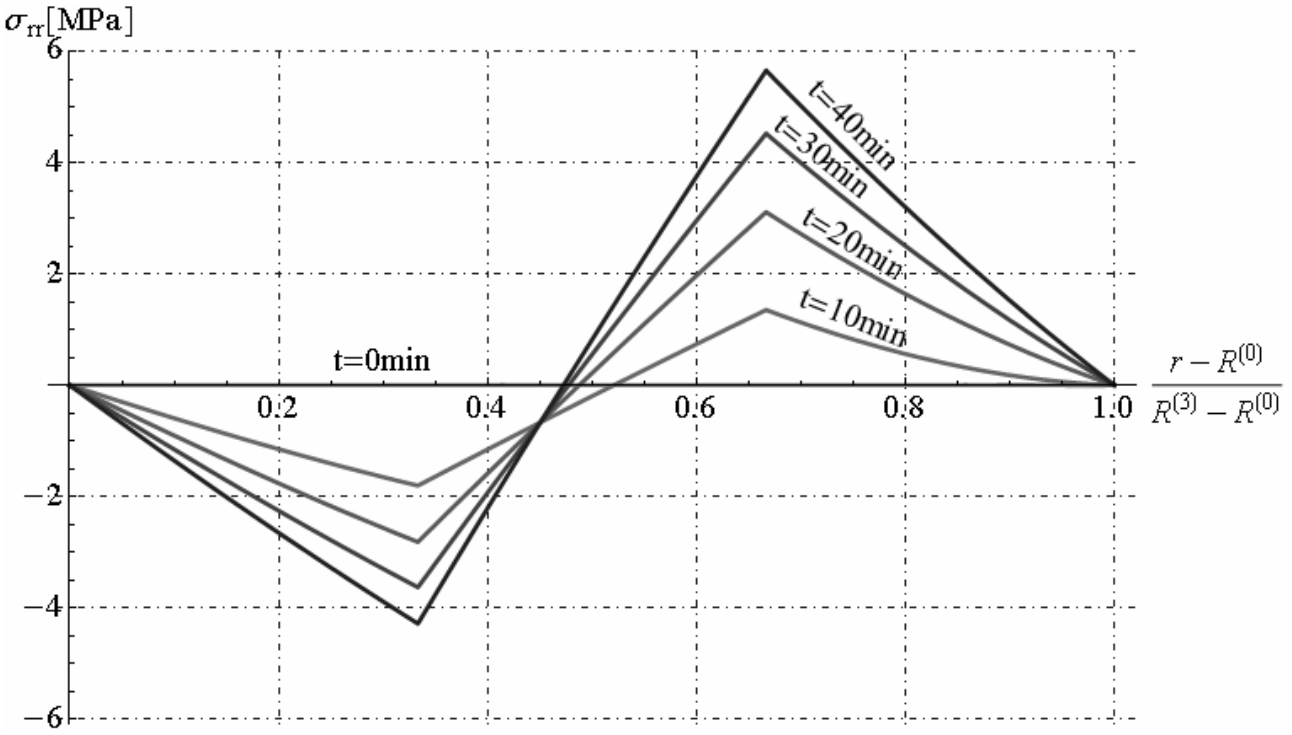

Fig. 20.16 - *Radial stress distribution along radial direction*

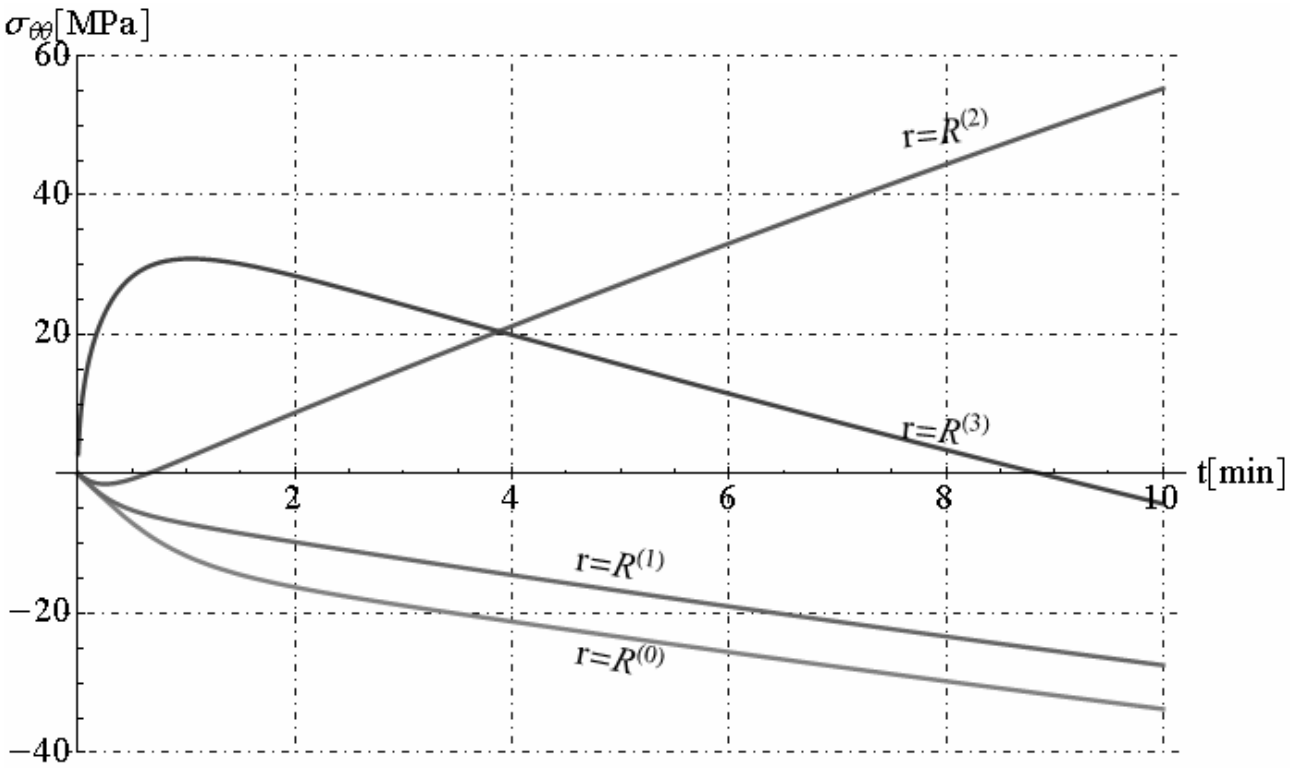

Fig. 20.17 - *Circumferential stress distribution in time*

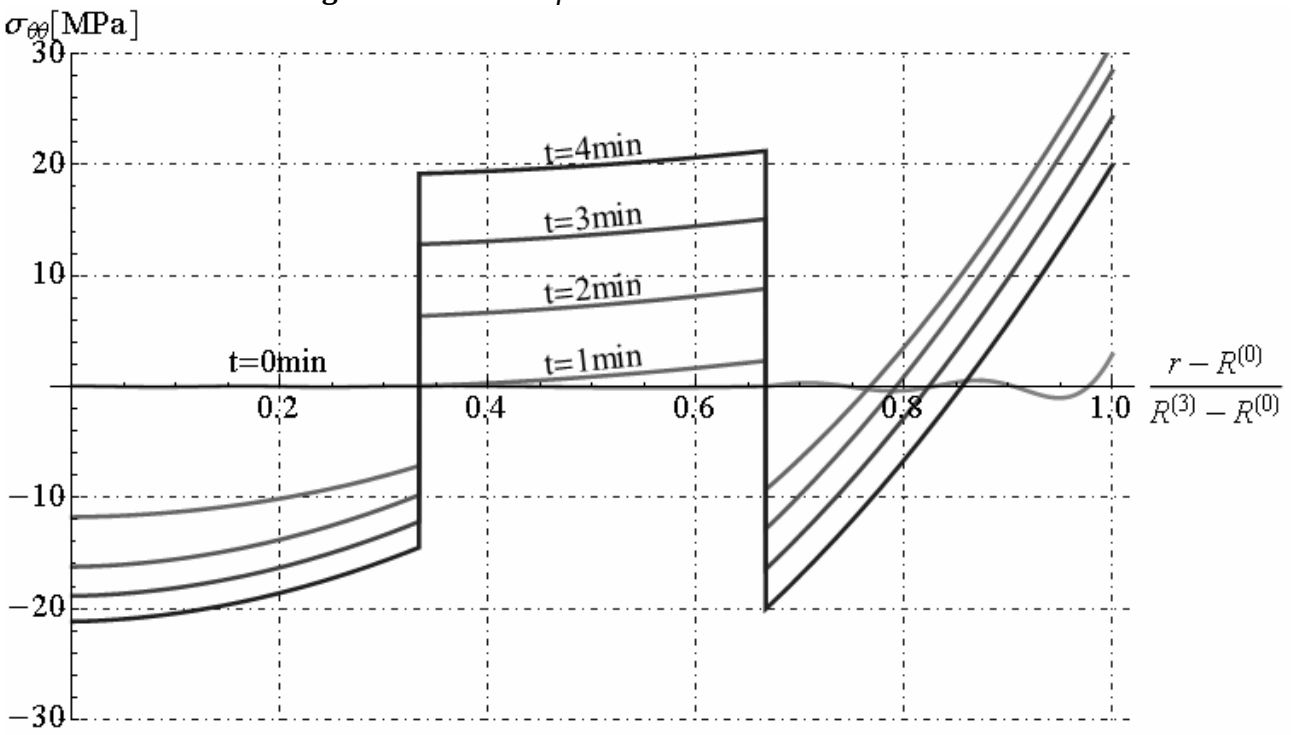

Fig. 20.18 - *Circumferential stress distribution along radial direction*

20.3. Multilayered sphere under uniform heat flux

Let us consider an multilayered sphere constituted by n-hollow spherical phase as decrypted in section 20.1. The inner surface $r = R^{(0)}$ is kept perfectly insulated while the outer surface $r = R^{(n)}$ is exposed, for t >0, to a constant, uniform heat input q_0. In this section, we determine the heat conduction, displacement and stress function in any hollow spherical phases subjected to uniform heat input q_0 applied on external surface, starting to initial temperature in solid equal to $T_0 = T_R = const$. The equations field to satisfy in uncoupled thermo-elastic problem with spherical

symmetry are reported in equations (20.13), but in this case the boundary conditions (20.11) become:

$$-k^{(1)}T_{,r}^{(1)}(r=R^{(0)})=0,\quad -k^{(n)}T_{,r}^{(n)}(r=R^{(n)})=q_0=const,\quad \forall t\geq 0 \tag{20.59}$$

and the boundary conditions (20.8) become:

$$\sigma_{rr}^{(n)}(r=R^{(n)})=0,\quad \sigma_{rr}^{(1)}(r=R^{(0)})=0,\quad \forall t\geq 0 \tag{20.60}$$

The other boundary conditions reported in section 20.1 not change. By solving the Fourier's equation reported in second equation of (20.13) with method separation of variables, and by substituting the function of temperature $T^{(i)}(r,t)$ in first equation of (20.13), and by integration in two time this equation respect to variable r, the explicit displacement solution is reported in equation (20.14). In this case, the heat conduct problem involving a non-homogeneous boundary condition and, in particular, with the heat input specified over the entire boundary surface. It is necessary writing the temperature solution, in any phases of multilayered sphere, in the follows form (see Chapter VII and Chapter XV) :

$$T^{(i)}(r,t)=T_0+\xi\, t+T_S^{(i)}(r)+T_C^{(i)}(r,t),\quad \forall i\in\{1,2,....,n\} \tag{20.61}$$

where ξ is same unknown parameter for any phases of multilayered sphere and the function $T_S^{(i)}(r)$ in generic i-th phase satisfies the field equations:

$$\frac{d^2T_S^{(i)}}{dr^2}+\frac{2}{r}\frac{dT_S^{(i)}}{dr}=\frac{\xi}{\kappa^{(i)}};\qquad \begin{matrix} R^{(i-1)}\leq r\leq R^{(i)} \\ \forall i\in\{1,2,...,n\}\end{matrix} \tag{20.62}$$

Moreover the function $T_S^{(i)}(r)$ must be satisfy the following boundary conditions :

$$-k^{(1)}\frac{dT_S^{(1)}(r)}{dr}=0,\quad r=R^{(0)}, \tag{20.63}$$

$$-k^{(n)}\frac{dT_S^{(n)}(r)}{dr}=q_0,\quad r=R^{(n)}, \tag{20.64}$$

$$-k^{(i)}\frac{dT_S^{(i)}(r)}{dr}=-k^{(i+1)}\frac{dT_S^{(i+1)}(r)}{dr},\quad r=R^{(i)},\ \forall i\in\{1,2,...,n-1\} \tag{20.65}$$

$$T_S^{(i)}(r)=T_S^{(i+1)}(r),\quad r=R^{(i)},\ \forall i\in\{1,2,...,n-1\} \tag{20.66}$$

$$\sum_{i=1}^{n}\left[\rho^{(i)}c_v^{(i)}\int_0^{2\pi}\int_0^{\pi}\int_{R^{(i-1)}}^{R^{(i)}}r^2\sin\theta\, T_S^{(i)}(r)\,dr d\theta d\phi\right]=0 \tag{20.67}$$

where ξ may be determined either from the boundary conditions (20.63)-(20.67). The function $T_C^{(i)}(r,t)$ in generic i-th phase satisfies the field equations:

$$\frac{\partial^2T_C^{(i)}(r,t)}{\partial r^2}+\frac{2}{r}\frac{\partial T_C^{(i)}(r,t)}{\partial r}=\frac{1}{\kappa^{(i)}}\frac{\partial T_C^{(i)}(r,t)}{\partial t};\qquad \begin{matrix} R^{(i-1)}\leq r\leq R^{(i)},\forall t\geq 0 \\ \forall i\in\{1,2,...,n\}\end{matrix} \tag{20.68}$$

Moreover the function $T_C^{(i)}(r,t)$ must be satisfy the following boundary conditions :

$$-k^{(1)}\frac{\partial T_C^{(1)}(r,t)}{\partial r}=0,\quad r=R^{(0)},\ \forall t\geq 0, \tag{20.69}$$

$$-k^{(n)}\frac{\partial T_C^{(n)}(r,t)}{\partial r}=0,\quad r=R^{(n)},\ \forall t\geq 0, \tag{20.70}$$

$$\begin{cases}-k^{(i)}\dfrac{\partial T_C^{(i)}(r,t)}{\partial r}=-k^{(i+1)}\dfrac{\partial T_C^{(i+1)}(r,t)}{\partial r}, \\ T_C^{(i)}(r,t)=T_C^{(i+1)}(r,t),\end{cases}\quad r=R^{(i)},\ \forall t\geq 0,\ \forall i\in\{1,2,...,n-1\} \tag{20.71}$$

$$T_C^{(i)}(r,t) = -T_S^{(i)}(r), \quad R^{(i-1)} \le r \le R^{(i)}, \ t = 0, \ \forall i \in \{1,2,...,n\} \tag{20.72}$$

The solutions of differential equation (20.62) is given by:

$$T_S^{(i)}(r) = C^{(i)} r^{-1} + D^{(i)} + \left[\xi / \left(6\kappa^{(i)}\right)\right] r^2, \quad \forall i \in \{1,2,...,n\} \tag{20.73}$$

where $C^{(i)}, D^{(i)}, \xi$ are 2n+1 unknown parameter to determine. By solving algebraic system composed by equations (20.63), (20.64),(20.65) and (20.67), we obtain integration constants $\xi, C^{(i)}$:

$$\xi = -\frac{3q_0 R^{(n)2}}{\sum_{i=1}^{n} \rho^{(i)} c_v^{(i)} \left(R^{(i)3} - R^{(i-1)3}\right)} = -\frac{q_0 S^{(n)}}{\sum_{i=1}^{n} \rho^{(i)} c_v^{(i)} V^{(i)}}, \ V^{(i)} = \frac{4}{3}\pi\left(R^{(i)3} - R^{(i-1)3}\right), \ \ S^{(n)} = 4\pi R^{(n)2}, \tag{20.74}$$

where $V^{(i)}$ and $S^{(n)}$ are volume of generic i-th phase and external surface of multilayered sphere, respectively.

$$C^{(i)} = \frac{q_0 R^{(n)2}}{k^{(i)}} \frac{\left[-\rho^{(i)} c_v^{(i)} R^{(i-1)3} + \left(1-\delta_{i1}\right) \sum_{j=1}^{i-1} \rho^{(j)} c_v^{(j)} \left(R^{(j)3} - R^{(j-1)3}\right)\right]}{\sum_{j=1}^{n} \rho^{(j)} c_v^{(j)} \left(R^{(j)3} - R^{(j-1)3}\right)} \tag{20.75}$$

where δ_{i1} is the Kronecker's delta. By solving the equations (20.66), we obtain integration constants $D^{(i)}$ as function of constants $\xi, C^{(i)}$. For brevity, we don't reported in explicit the expressions of constants $D^{(i)}$. The solution to the problem for T_C is found in much the same says way as was followed in section 20.2. The problem is therefore on with homogeneous differential equation and boundary conditions and may be treated by the method separation of variables as showed in section 20.2. The solutions of differential equation (20.68) is given by:

$$T_C^{(i)}(r,t) = r^{-1}\left[A^{(i)} e^{i\omega\beta^{(i)} r} + B^{(i)} e^{-i\omega\beta^{(i)} r}\right] e^{-\kappa^{(i)}\beta^{(i)2}\omega^2 t} \quad \forall i \in \{1,2,...,n\} \tag{20.76}$$

where $A^{(i)}, B^{(i)}, \omega$ are constants parameter to determine, the coefficient $\beta^{(i)} = \sqrt{\kappa^{(1)} / \kappa^{(i)}}$ and i is unit imaginary. The boundary conditions (20.71) for temperature function $T_C^{(i)}(r,t)$ are reported below:

$$\begin{cases} A^{(i)} e^{i\omega\beta^{(i)}R^{(i)}} + B^{(i)} e^{-i\omega\beta^{(i)}R^{(i)}} - \left(A^{(i+1)} e^{i\omega\beta^{(i+1)}R^{(i)}} + B^{(i+1)} e^{-i\omega\beta^{(i+1)}R^{(i)}}\right) = 0 \\ A^{(i)} k^{(i)} \left(1 - i\omega\beta^{(i)}R^{(i)}\right) e^{i\omega\beta^{(i)}R^{(i)}} - A^{(i+1)} k^{(i+1)} \left(1 - i\omega\beta^{(i+1)}R^{(i+1)}\right) e^{i\omega\beta^{(i+1)}R^{(i+1)}} + \\ + B^{(i)} k^{(i)} \left(1 + i\omega\beta^{(i)}R^{(i)}\right) e^{-i\omega\beta^{(i)}R^{(i)}} - B^{(i+1)} k^{(i+1)} \left(1 + i\omega\beta^{(i+1)}R^{(i+1)}\right) e^{-i\omega\beta^{(i+1)}R^{(i+1)}} = 0 \\ \forall i \in \{1,2,...,n-1\} \end{cases} \tag{20.77}$$

The boundary conditions on the inner and the outer surface (20.69) and (20.70) become:

$$\begin{cases} A^{(1)} \left(1 - i\omega\beta^{(1)}R^{(0)}\right) e^{i\omega\beta^{(1)}R^{(0)}} + B^{(1)} \left(1 + i\omega\beta^{(1)}R^{(0)}\right) e^{-i\omega\beta^{(1)}R^{(0)}} = 0 \\ A^{(n)} \left(1 - i\omega\beta^{(n)}R^{(n)}\right) e^{i\omega\beta^{(n)}R^{(n)}} + B^{(n)} \left(1 + i\omega\beta^{(n)}R^{(n)}\right) e^{-i\omega\beta^{(n)}R^{(n)}} = 0 \end{cases} \tag{20.78}$$

By first equation of (20.78), we determine $B^{(1)}$ as function of $A^{(1)}$ as follows:

$$B^{(1)} = \left[\left(i + \omega R^{(0)} \beta^{(1)}\right)^2 / \left(1 + \omega^2 \beta^{(1)2} R^{(0)2}\right)\right] A^{(1)} e^{2i\omega\beta^{(1)}R^{(0)}} \tag{20.79}$$

The equations (20.77) constituted an homogeneous algebraic system, composed by 2(n-1) equations, in unknown parameters $A^{(i)}, B^{(i)}$ with $i \in \{1,2,...,n\}$, which can be written as:

$$\mathbf{\Phi} \cdot \mathbf{X} = \mathbf{0} \tag{20.80}$$

where $\mathbf{X} = [\mathbf{X}^{(1)}, \mathbf{X}^{(2)}, ..., \mathbf{X}^{(n)}]^T$ collect the unknowns sub-vectors, as reported below:

$$\mathbf{X}^{(i)} = \begin{bmatrix} A^{(i)} & B^{(i)} \end{bmatrix}^T, \quad \forall i \in \{1,2,....,n\} \tag{20.81}$$

and $\mathbf{\Phi}$ is the matrix reported in equation (20.26). As showed in section 20.2, matrix $\mathbf{\Phi}$ is constituted by components: $\mathbf{\Phi}_i^{(i)}, \mathbf{\Phi}_i^{(i+1)}, \forall i \in \{1,2,...,n-1\}$ and vector $\mathbf{X}^{(i)}$ is obtained as function of vector $\mathbf{X}^{(1)}$ (see equation (20.29)). By substituting the solutions (20.29) in boundary conditions (20.78), we obtain vector equations in unknown vector $\mathbf{X}^{(1)}$, as reported below:

$$\mathbf{\Lambda} \cdot \mathbf{X}^{(1)} = \mathbf{0} \tag{20.82}$$

where $\mathbf{\Lambda}$ is an 2x2 square matrix given by :

$$\mathbf{\Lambda} = \begin{bmatrix} \Lambda_{11} & \Lambda_{12} \\ \Lambda_{21} & \Lambda_{22} \end{bmatrix} \tag{20.83}$$

where the components $\Lambda_{11}, \Lambda_{12}, \Lambda_{21}, \Lambda_{22}$ are reported below:

$$\begin{aligned} &\Lambda_{11} = \left(1 - i\omega\beta^{(1)}R^{(0)}\right)e^{i\omega\beta^{(1)}R^{(0)}}, \quad \Lambda_{12} = \left(1 + i\omega\beta^{(1)}R^{(0)}\right)e^{-i\omega\beta^{(1)}R^{(0)}}, \\ &\left[\Lambda_{21}, \Lambda_{22}\right] = \left[\left(1 - i\omega\beta^{(n)}R^{(n)}\right)e^{i\omega\beta^{(n)}R^{(n)}}, \left(1 + i\omega\beta^{(n)}R^{(n)}\right)e^{-i\omega\beta^{(n)}R^{(n)}}\right] \cdot \mathbf{\Gamma}^{(n)}, \end{aligned} \tag{20.84}$$

The algebraic system (20.82) admit not trivial solution if the determinant of matrix $[\mathbf{\Lambda}]$ is equal to zero. By imposing this condition, we obtain the transcendental equation in unknown parameter ω:

$$\det[\mathbf{\Lambda}] = 0 \;\Rightarrow\; g(\omega) = 0 \tag{20.85}$$

The roots of this transcendental equation (20.85) are an infinite number such, denoted here by ω_m, $m = 1,2,....N$ leading to eigenvalues or characteristic values $\lambda_m = -\omega_m^2$. The corresponding eigenfunctions or characteristic functions $\overline{\varphi}_m^{(i)}(r)$ are reported in equation (20.35). The coefficients $A_m^{(1)}$ are determined by applying the initial condition (20.72) that yields the following relationship:

$$A_m^{(1)} = -\frac{\sum_{i=1}^{n}\left[\rho^{(i)}c_v^{(i)}\int_0^{2\pi}\int_0^{\pi}\int_{R^{(i-1)}}^{R^{(i)}} r^2\overline{\varphi}_m^{(i)}T_s^{(i)}(r)\sin\theta\, dr d\theta d\phi\right]}{\sum_{i=1}^{n}\left[\rho^{(i)}c_v^{(i)}\int_0^{2\pi}\int_0^{\pi}\int_{R^{(i-1)}}^{R^{(i)}} \left(\overline{\varphi}_m^{(i)}\right)^2 r^2\sin\theta dr d\theta d\phi\right]} \tag{20.86}$$

Finally the temperature function in i-th generic phase ($\forall i \in \{1,2,....,n\}$)is given by:

$$T^{(i)}(r,t) = T_0 + \xi t + C^{(i)}r^{-1} + D^{(i)} + \frac{\xi r^2}{6\kappa^{(i)}} + \sum_{m=1}^{\infty} r^{-1}\left(A_m^{(i)}e^{i\omega_m\beta^{(i)}r} + B_m^{(i)}e^{-i\omega_m\beta^{(i)}r}\right)e^{-\kappa^{(i)}\beta^{(i)2}\omega_m^2 t} \tag{20.87}$$

By substituting the function (20.87) in equation (20.14), we obtain in explicit the displacement function in any hollow spherical phase ($\forall i \in \{1,2,....,n\}$) :

$$\begin{aligned} u_r^{(i)} &= G^{(i)}r + H^{(i)}r^{-2} + \left(N^{(i)}r + M^{(i)}r^{-2}\right)t + \frac{\alpha^{(i)}\left(3\lambda^{(i)} + 2\mu^{(i)}\right)}{6\left(\lambda^{(i)} + 2\mu^{(i)}\right)}\left(3C^{(i)} + 2D^{(i)}r + \frac{\xi r^3}{5\kappa^{(i)}}\right) + \\ &+ \sum_{m=1}^{\infty}\left\{P_m^{(i)}r + Q_m^{(i)}r^{-2} + \frac{\alpha^{(i)}\left(3\lambda^{(i)} + 2\mu^{(i)}\right)}{\omega_m^2\beta^{(i)2}\left(\lambda^{(i)} + 2\mu^{(i)}\right)r^2}\left[\begin{array}{l} A_m^{(i)}\left(1 - i\beta^{(i)}\omega_m r\right)e^{i\beta^{(i)}\omega_m r} + \\ \quad + B_m^{(i)}\left(1 + i\beta^{(i)}\omega_m r\right)e^{-i\beta^{(i)}\omega_m r} \end{array}\right]\right\}e^{-\kappa^{(i)}\omega_m^2\beta^{(i)2}t} \end{aligned} \tag{20.88}$$

where the integration constants $G^{(i)}, H^{(i)}, N^{(i)}, M^{(i)}, P_m^{(i)}, Q_m^{(i)}$ are determined by applying the boundary conditions given by equations (20.60). In this case the functions $f_1^{(i)}(t)$, $f_2^{(i)}(t)$, reported in equation (20.14) are given by:

$$f_1^{(i)}(t) = G^{(i)} + N^{(i)}t + \sum_{m=1}^{\infty}P_m^{(i)}e^{-\kappa^{(i)}\omega_m^2\beta^{(i)2}t}, \quad f_2^{(i)}(t) = H^{(i)} + M^{(i)}t + \sum_{m=1}^{\infty}Q_m^{(i)}e^{-\kappa^{(i)}\omega_m^2\beta^{(i)2}t}, \tag{20.89}$$

In explicit the radial and circumferential stress components are given by:

$$\sigma_{rr}^{(i)} = \left(3\lambda^{(i)} + 2\mu^{(i)}\right)\left(G^{(i)} + N^{(i)}t\right) - 4\mu^{(i)} r^{-3}\left(H^{(i)} + M^{(i)}t\right) +$$
$$-\frac{2\alpha^{(i)}\mu^{(i)}\left(3\lambda^{(i)} + 2\mu^{(i)}\right)}{\left(\lambda^{(i)} + 2\mu^{(i)}\right)}\left[\frac{2}{3}D^{(i)} + \frac{C^{(i)}}{r} + \frac{\xi r^2}{15\kappa^{(i)}} + \frac{\lambda^{(i)} + 2\mu^{(i)}}{2\mu^{(i)}}\left(T_0 - T_R + \xi t\right)\right] +$$
$$+\sum_{m=1}^{\infty}\left[P_m^{(i)}\left(3\lambda^{(i)} + 2\mu^{(i)}\right) - 4Q_m^{(i)}\mu^{(i)} r^{-3}\right] e^{-\omega_m^2 \beta^{(i)2}\kappa^{(i)} t} + \tag{20.90}$$
$$+\frac{4i\alpha^{(i)}\mu^{(i)}\left(3\lambda^{(i)} + 2\mu^{(i)}\right)}{\beta^{(i)2}\left(\lambda^{(i)} + 2\mu^{(i)}\right)}\sum_{m=1}^{\infty}\left\{\omega_m^{-2} r^{-3}\begin{bmatrix} A_m^{(i)}\left(i + \omega_m\beta^{(i)} r\right)e^{i\omega_m\beta^{(i)} r} + \\ +B_m^{(i)}\left(i - \omega_m\beta^{(i)} r\right)e^{-i\omega_m\beta^{(i)} r}\end{bmatrix}\right\} e^{-\omega_m^2\beta^{(i)2}\kappa^{(i)} t}$$

$$\sigma_{\theta\theta}^{(i)} = \sigma_{\phi\phi}^{(i)} = \left(3\lambda^{(i)} + 2\mu^{(i)}\right)\left(G^{(i)} + N^{(i)}t\right) + 2\mu^{(i)} r^{-3}\left(H^{(i)} + M^{(i)}t\right) +$$
$$-\frac{2\alpha^{(i)}\mu^{(i)}\left(3\lambda^{(i)} + 2\mu^{(i)}\right)}{\left(\lambda^{(i)} + 2\mu^{(i)}\right)}\left[\frac{2}{3}D^{(i)} + \frac{C^{(i)}}{2r} + \frac{2\xi r^2}{15\kappa^{(i)}} + \frac{\lambda^{(i)} + 2\mu^{(i)}}{2\mu^{(i)}}\left(T_0 - T_R + \xi t\right)\right] +$$
$$+\sum_{m=1}^{\infty}\left[P_m^{(i)}\left(3\lambda^{(i)} + 2\mu^{(i)}\right) + 2\mu^{(i)} Q_m^{(i)} r^{-3}\right] e^{-\omega_m^2 \beta^{(i)2}\kappa^{(i)} t} + \tag{20.91}$$
$$+\frac{2\alpha^{(i)}\mu^{(i)}\left(3\lambda^{(i)} + 2\mu^{(i)}\right)}{\beta^{(i)2}\left(\lambda^{(i)} + 2\mu^{(i)}\right)}\sum_{m=1}^{\infty}\left\{\begin{matrix}\frac{A_m^{(i)}}{\omega_m^2 r^3}\left[1 - r\omega_m\beta^{(i)}\left(i + \omega_m\beta^{(i)} r\right)\right]e^{i\omega_m\beta^{(i)} r} + \\ +\frac{B_m^{(i)}}{\omega_m^2 r^3}\left[1 - r\omega_m\beta^{(i)}\left(\omega_m\beta^{(i)} r - i\right)\right]e^{-i\omega_m\beta^{(i)} r}\end{matrix}\right\} e^{-\omega_m^2\beta^{(i)2}\kappa^{(i)} t}$$

Moreover, the tractions on the inner and the outer spherical boundary surface are vanishing and then condition (20.8) becomes:

$$\sigma_{rr}^{(1)}(r = R^{(0)}) = 0,\ \sigma_{rr}^{(n)}(r = R^{(n)}) = 0, \quad \forall t \geq 0 \tag{20.92}$$

The integration constants $G^{(i)}, H^{(i)}, P_m^{(i)}, Q_m^{(i)}$ are function of geometrical, mechanical and thermal parameters of spherical layers . Moreover $P_m^{(i)}, Q_m^{(i)}$ are function of constants $A_m^{(i)}, B_m^{(i)}, \omega_m$ also. For example, let us consider, a spherical tank constituted by two phases under uniform heat flux . The phase (1) is constituted by steel and phase (2) by aluminum. The mechanical and thermal parameters considered for both phases are reported in table 20.1. The geometrical parameters of spherical tank are: $R^{(0)} = 10m,\ R^{(1)} = 10.25m,\ R^{(2)} = 10.50m,\ T_0 = T_R = 300°K$. By fixed m= 20, the eigenvalues ω_m of transcendental equation (20.85) and corresponding values of constants integration A_m are reported in table 20.5:

ω_m	8.341	18.628	28.656	36.627	45.462
A_m	-0.572 - 3.421 i	0.359 - 0.481 i	-0.241 + 0.194 i	0.056 + 0.198 i	-0.068 - 0.087 i
ω_m	55.892	65.543	73.316	82.653	93.119
A_m	-0.0653 - 0.0188 i	-0.0248 - 0.0567 i	0.0199 - 0.0465 i	-0.0305 + 0.0090 i	-0.0072 + 0.0244 i
ω_m	102.305	110.114	119.892	130.288	138.968
A_m	0.0116 + 0.0234 i	0.0004 + 0.0217 i	0.0058 + 0.0135 i	0.0087 + 0.0105 i	0.0065 - 0.0128 i
ω_m	147.040	157.158	167.371	175.587	184.085
A_m	-0.0115 + 0.0016 i	0.0060 - 0.0059 i	0.0064 + 0.0060 i	-0.0087 - 0.0025 i	-0.0069 - 0.0009 i

Table 20.5 – *Eigenvalues ω_m and corresponding values of constants integration A_m*

In this case the graphics function $g(\omega)$ given by equation (20.85) is reported below:

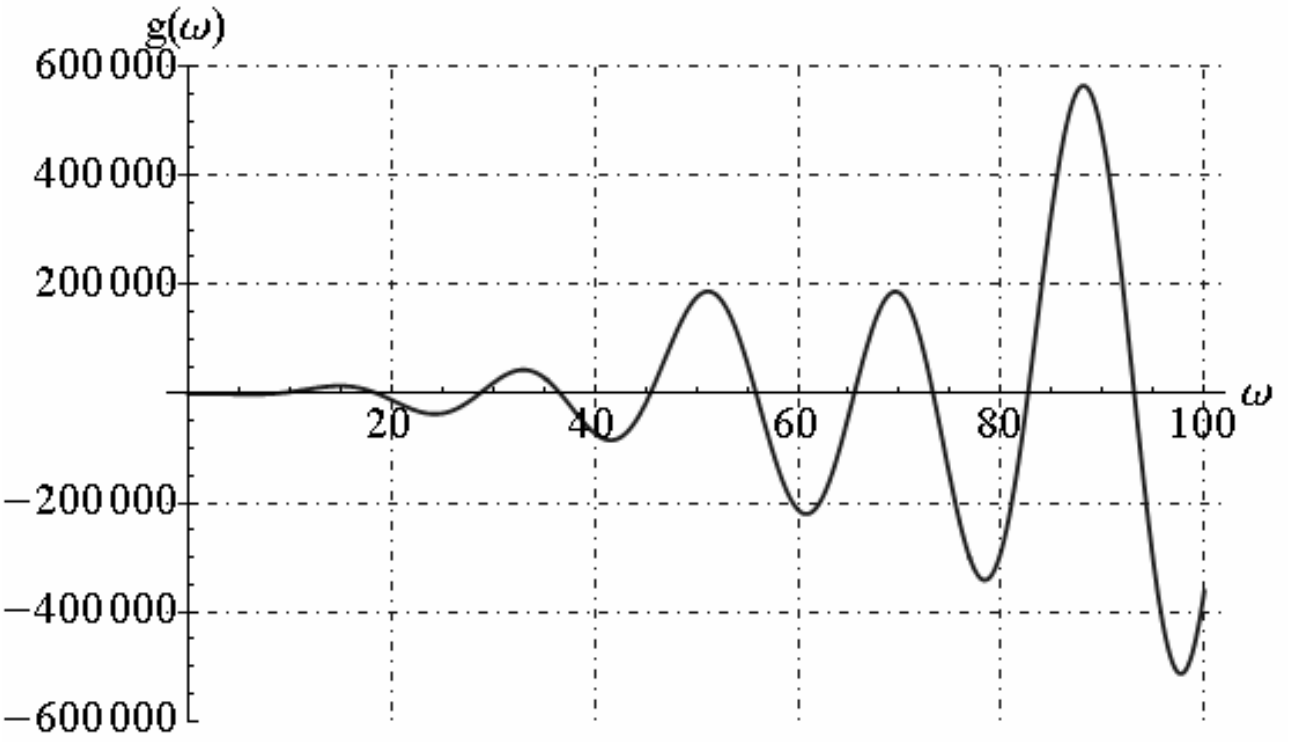

Fig. 20.19 - *Function* $g(\omega)$

We reported the graphics of temperature function along the radial direction and in time:

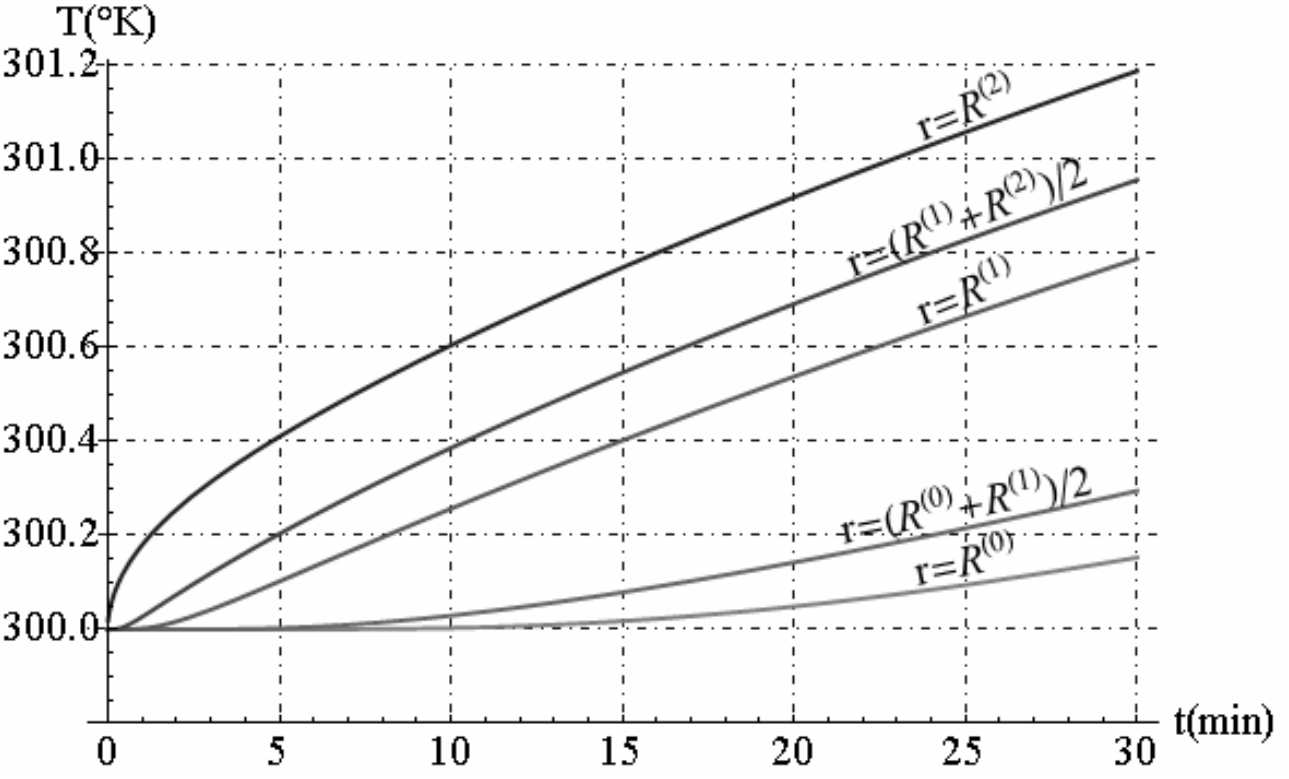

Fig. 20.20 - *Temperature function versus time*

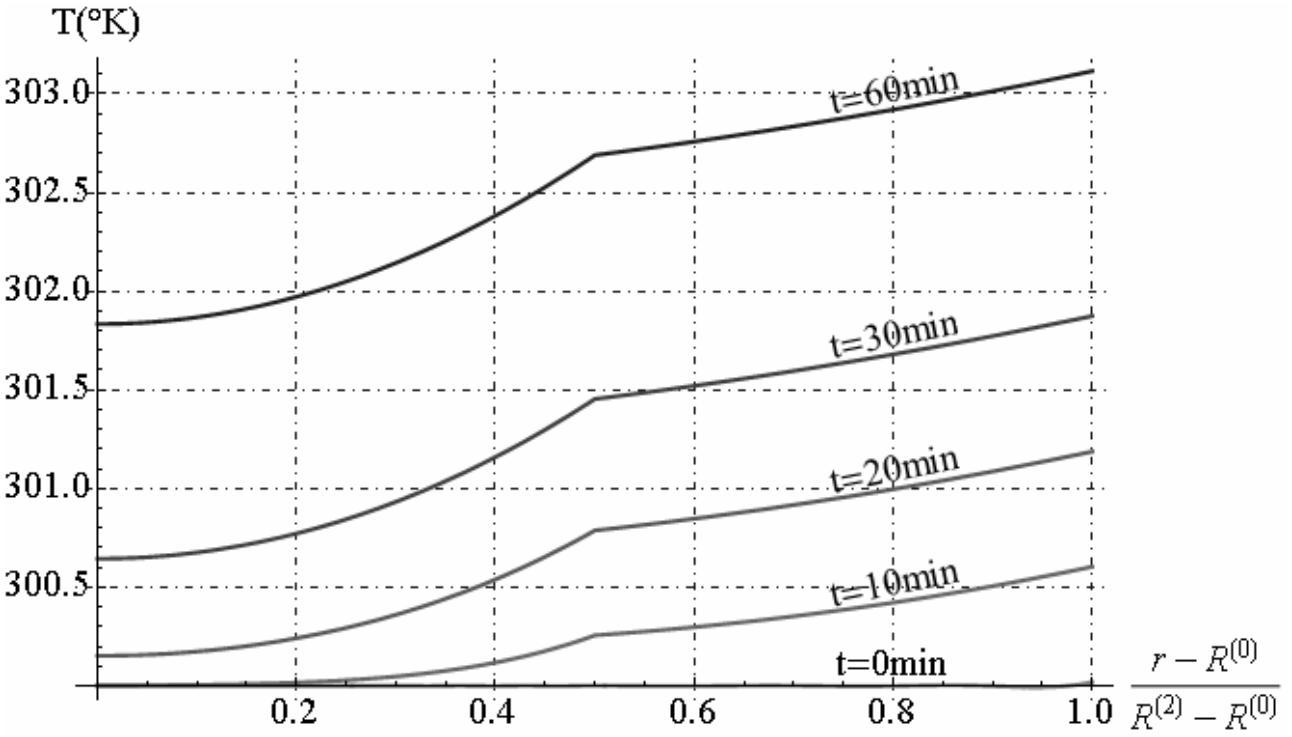

Fig. 20.21 - *Temperature function along radial direction*

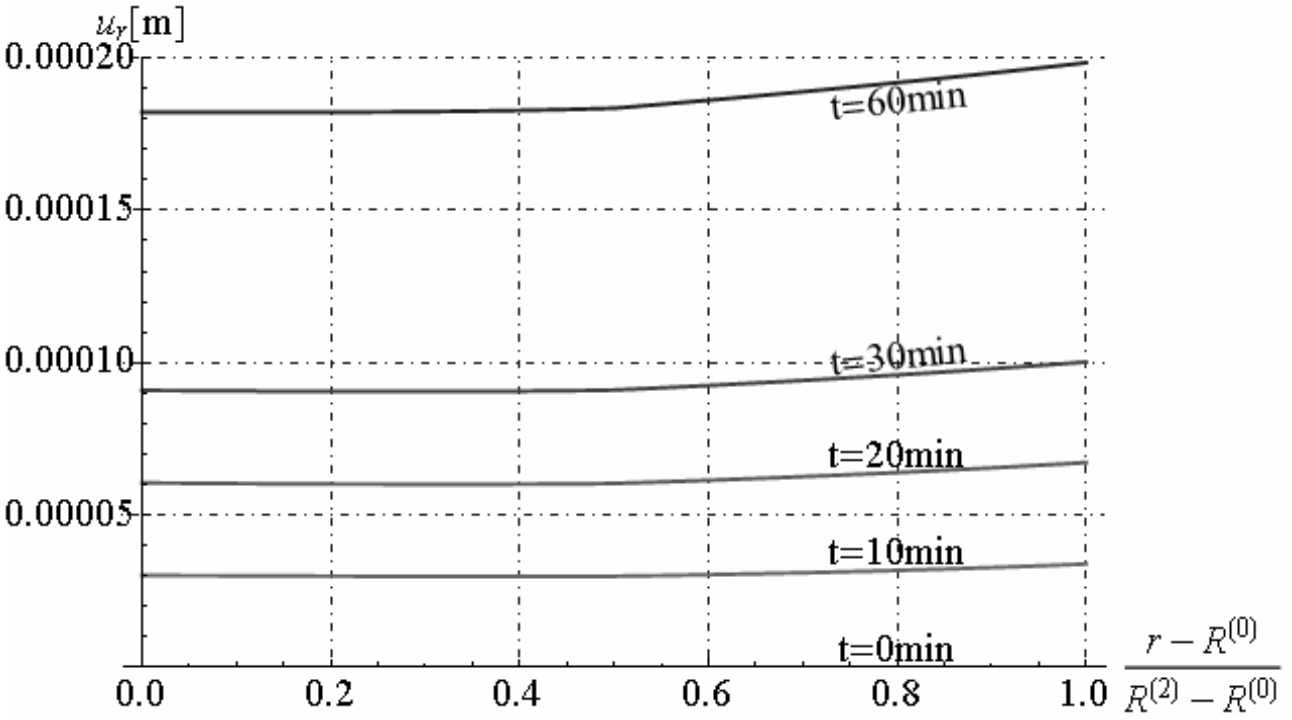

Fig. 20.22. Radial displacement along radial direction

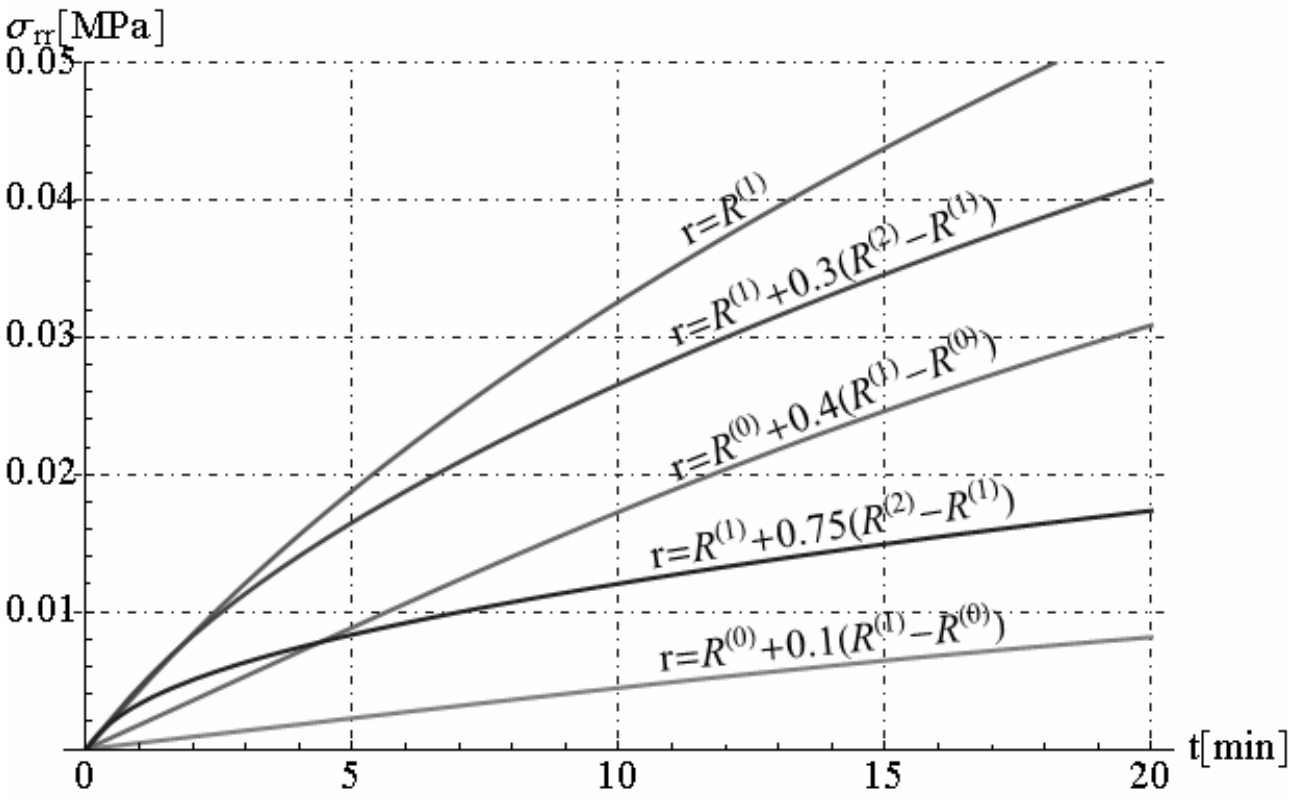

Fig. 20.23 - *Radial stress versus time*

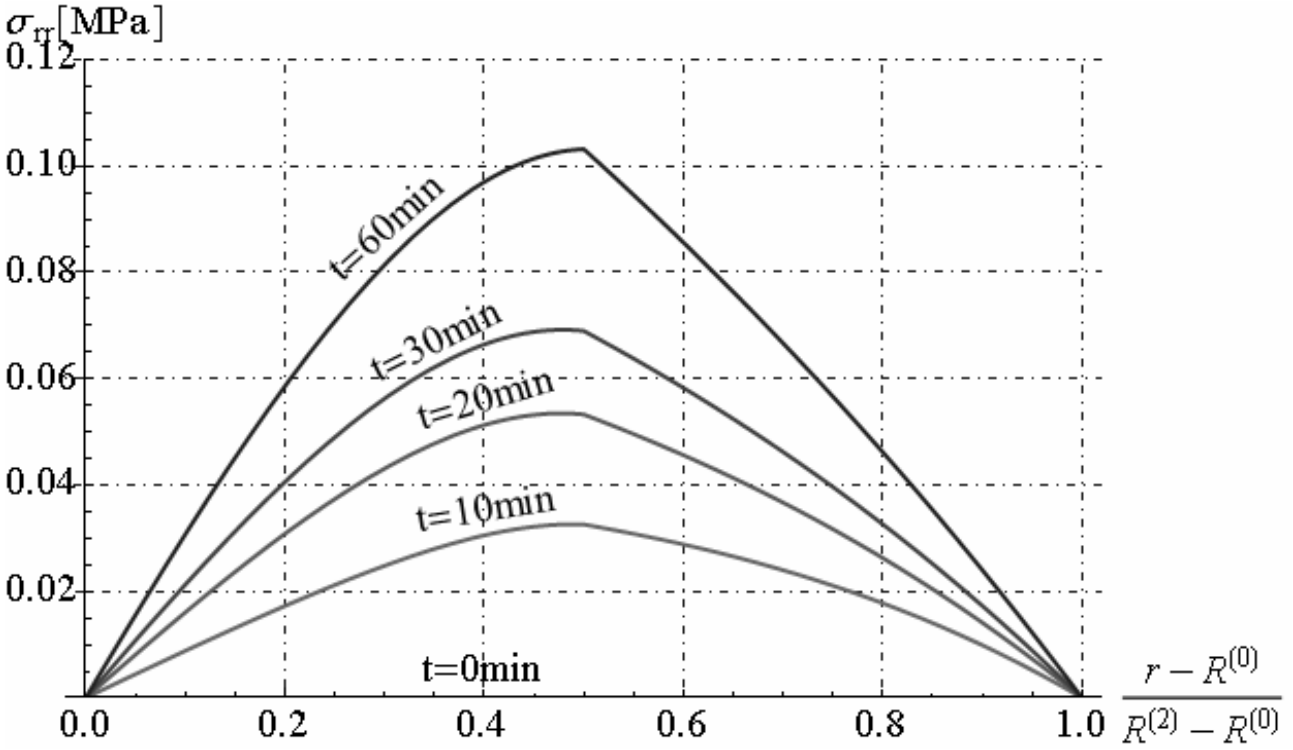

Fig. 20.24 - *Radial stress along radial direction*

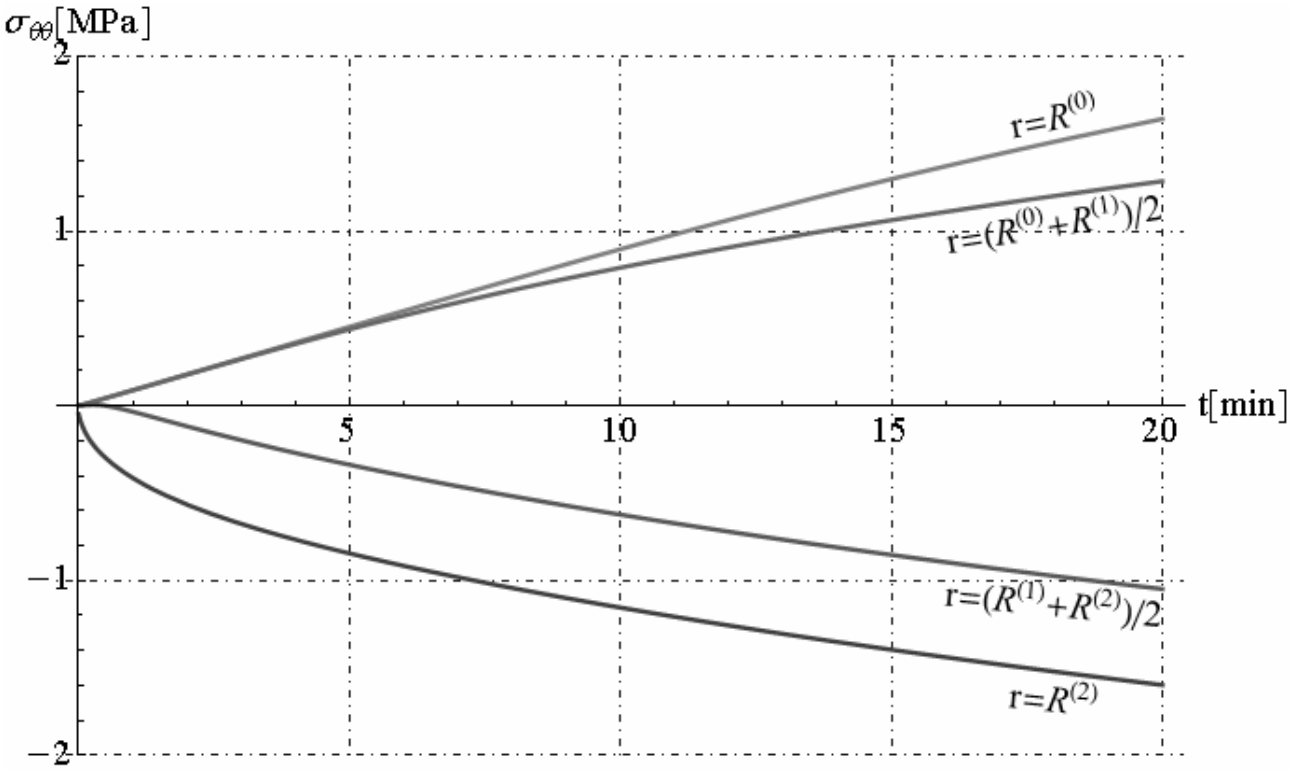

Fig. 20.25 - *Circumferential stress versus time*

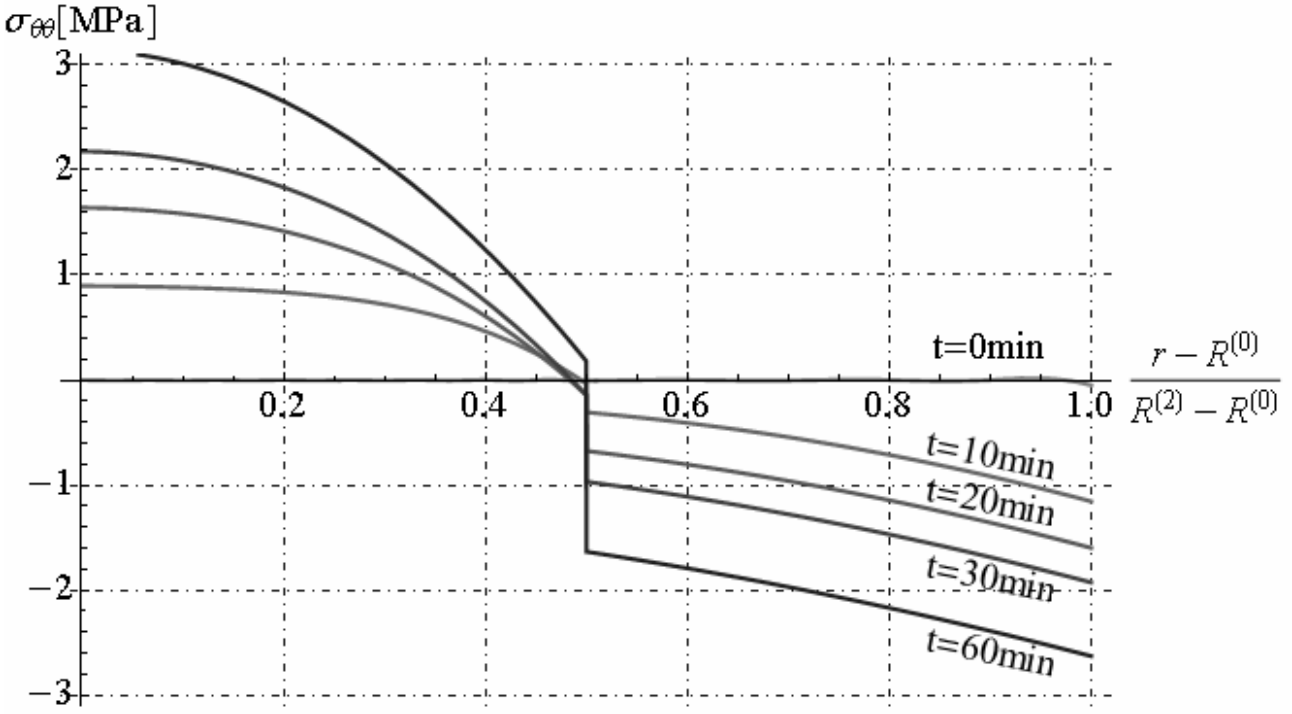

Fig. 20.26 - *Circumferential stress along radial direction*

Finally, let us consider a spherical tank composed by three phases under uniform heat flux. The phase (1) is constituted by Titanium, phase (2) by aluminium and phase (3) by steel. The mechanical and thermal parameters considered for three phases are reported in table 20.2. The geometrical parameters of spherical tank are: $R^{(0)} = 1.00m$, $R^{(2)} = 1.10m$, $R^{(3)} = 1.15m$, $T_0 = T_R = 300°K$, $q_0 = -1000W/m^2 \cdot °K$. In this case the graphics function $g(\omega)$ given by equation (20.85) is reported below:

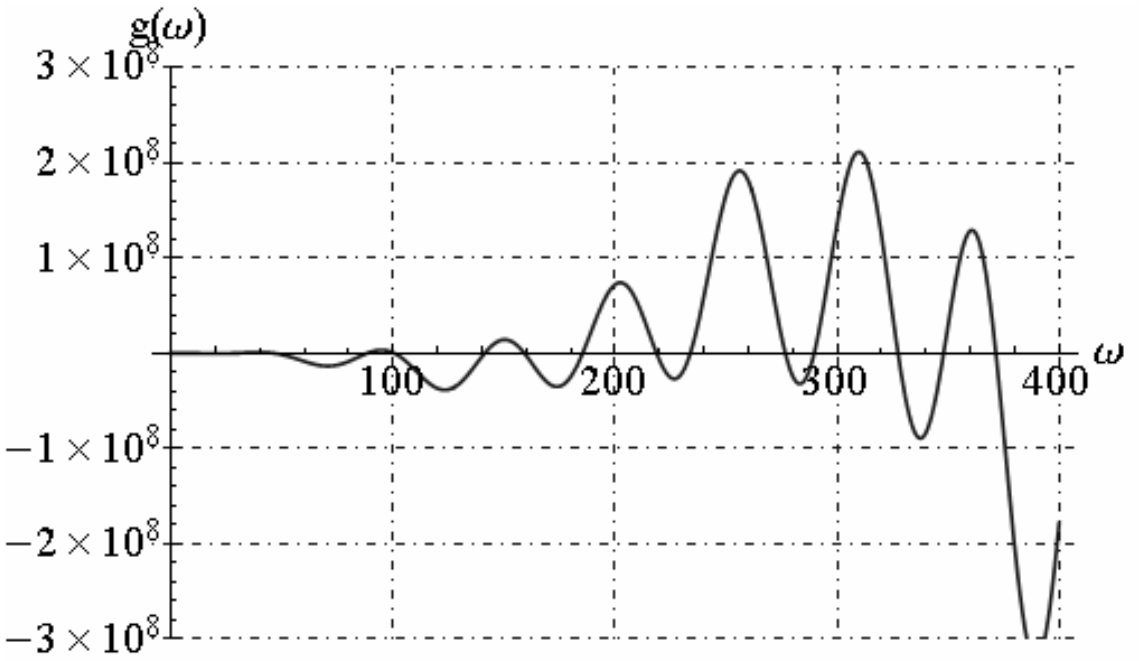

Fig. 20.27 - *Function* $g(\omega)$

By fixed m= 10, the eigenvalues ω_m of transcendental equation (20.85) and corresponding values of constants integration A_m are reported in table 20.6:

ω_m	30.128	45.905	88.448	100.545	141.305
A_m	0.1169 + 0.3579 i	0.0516 + 0.1317 i	0.0391 - 0.0211 i	-0.0350 + 0.0008 i	-0.0144 - 0.0009 i
ω_m	159.157	218.706	233.918	276.698	289.705
A_m	0.0067 + 0.0120 i	-0.0025 - 0.0064 i	0.0007 - 0.0054 i	-0.0042 + 0.0010 i	0.0032 - 0.0026 i

Table 20.6 – *Eigenvalues* ω_m *and corresponding values of constants integration* A_m

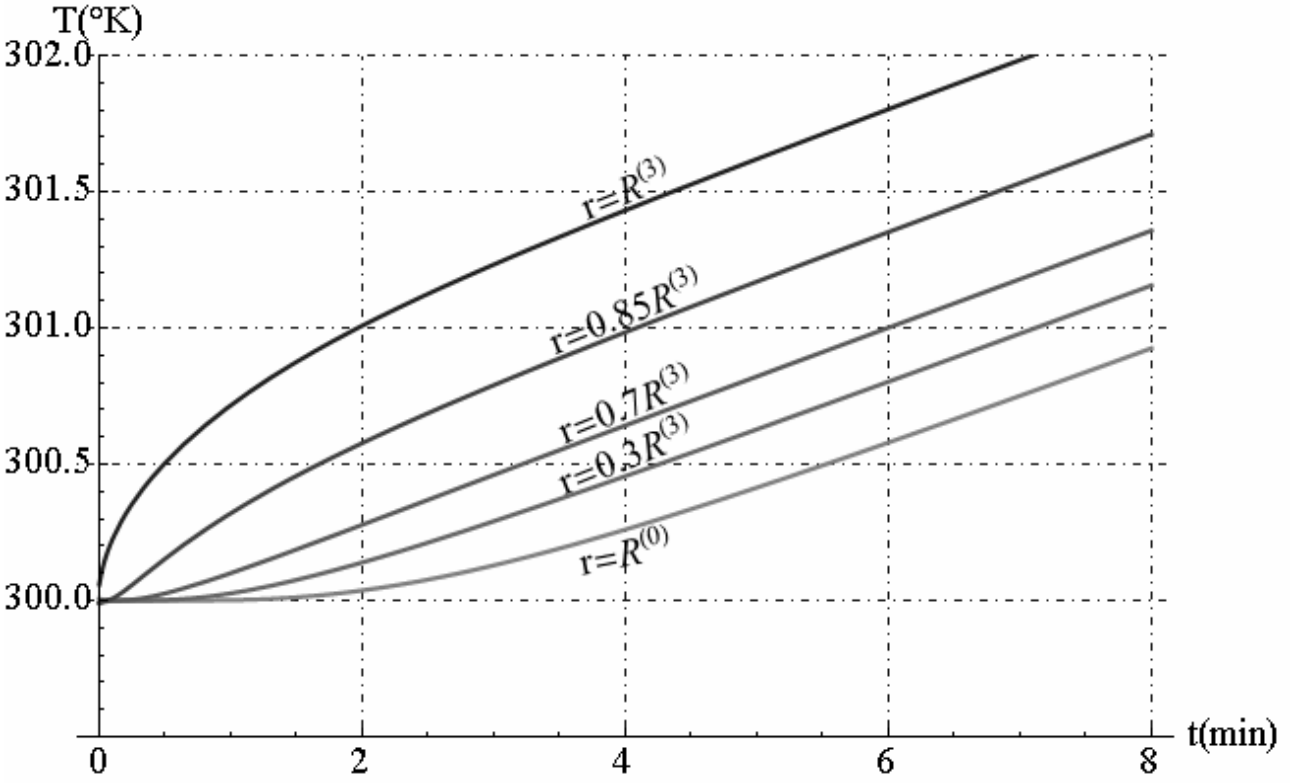

Fig. 20.28 - *Temperature function versus time*

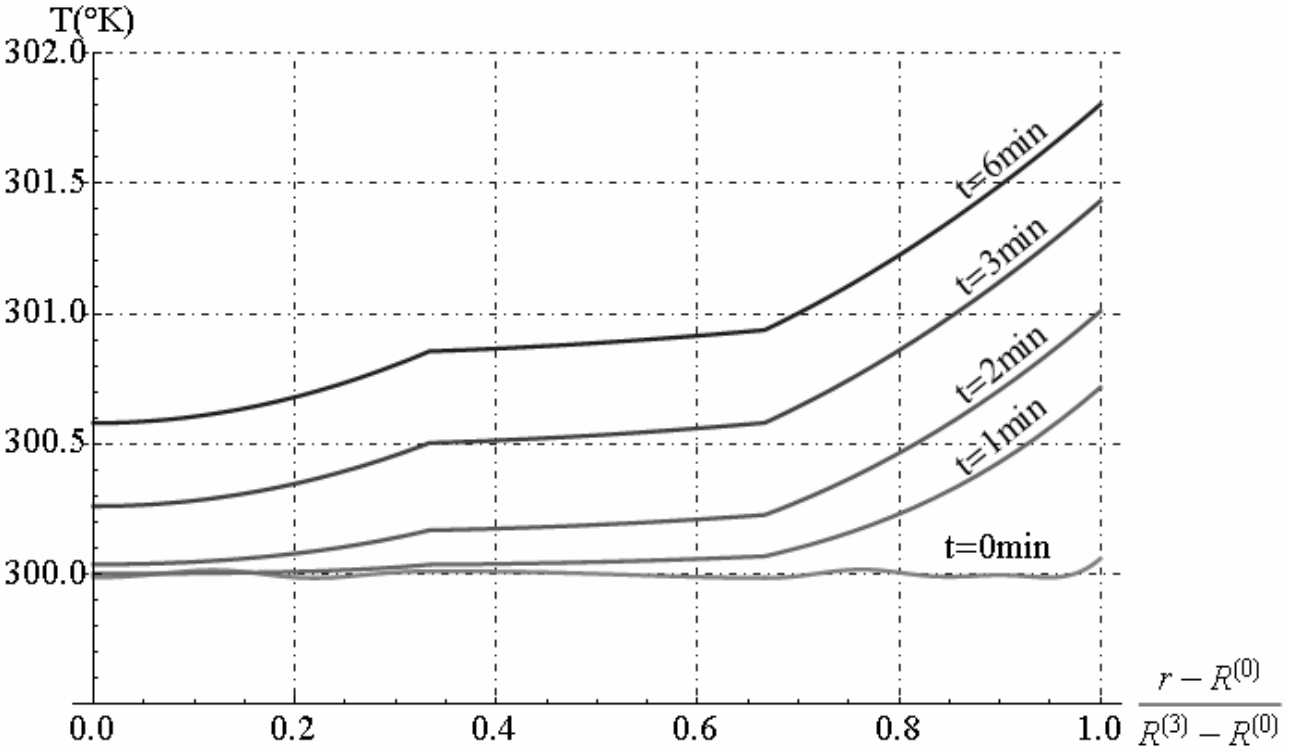

Fig. 20.29 - *Temperature function along radial direct*ion

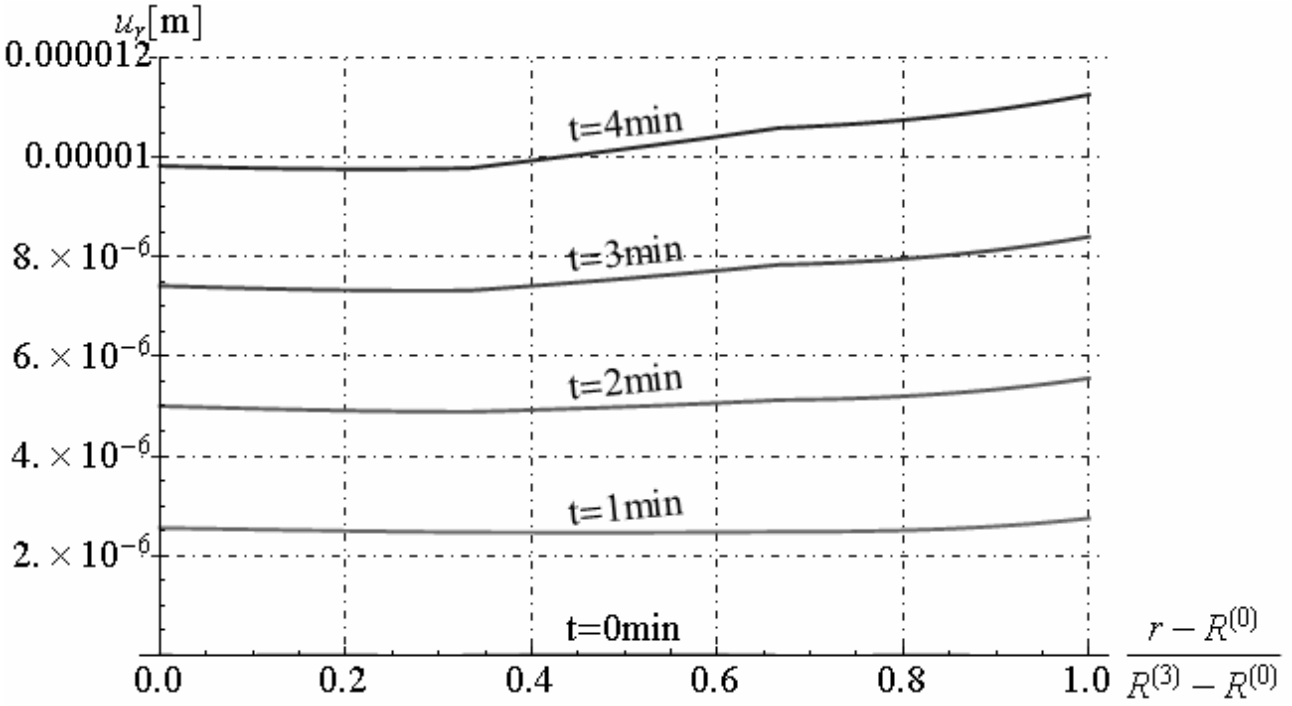

Fig. 20.30 - *Radial displacement along radial direction*

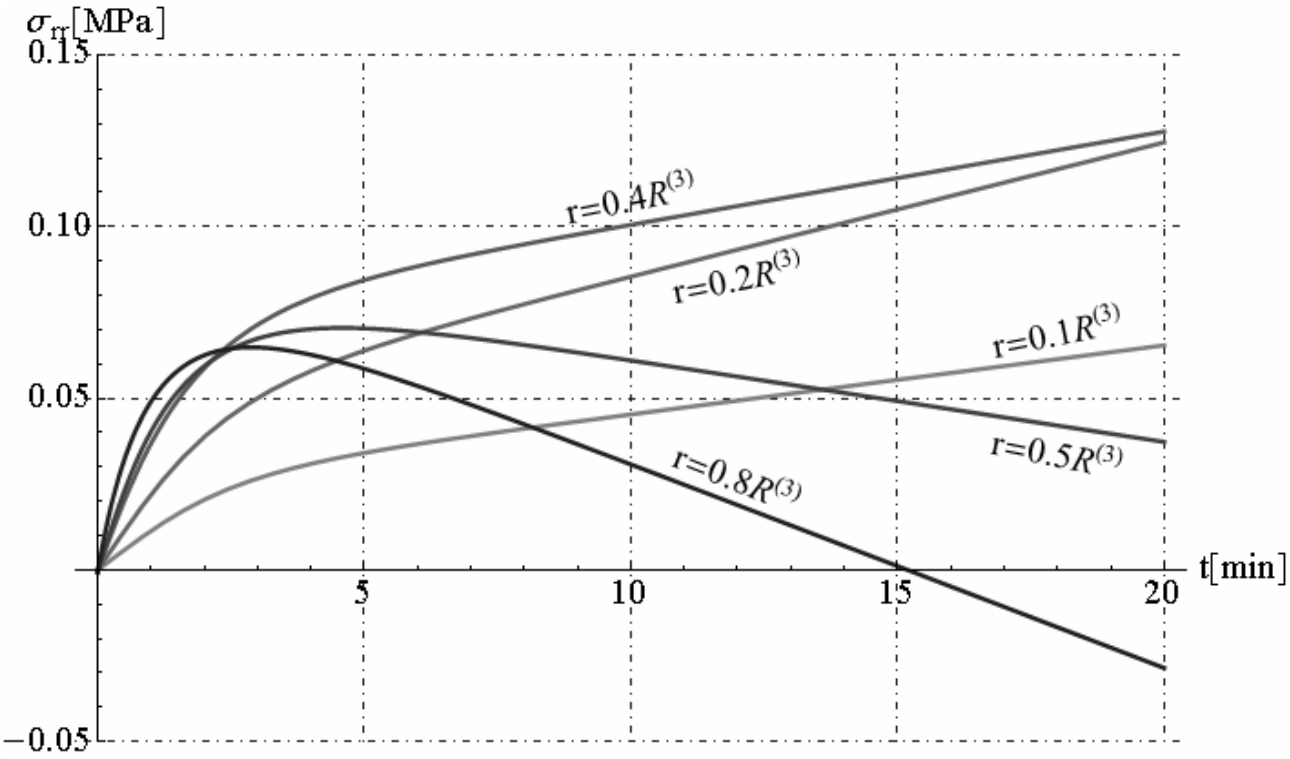

Fig. 20.31 - *Radial stress along radial direction*

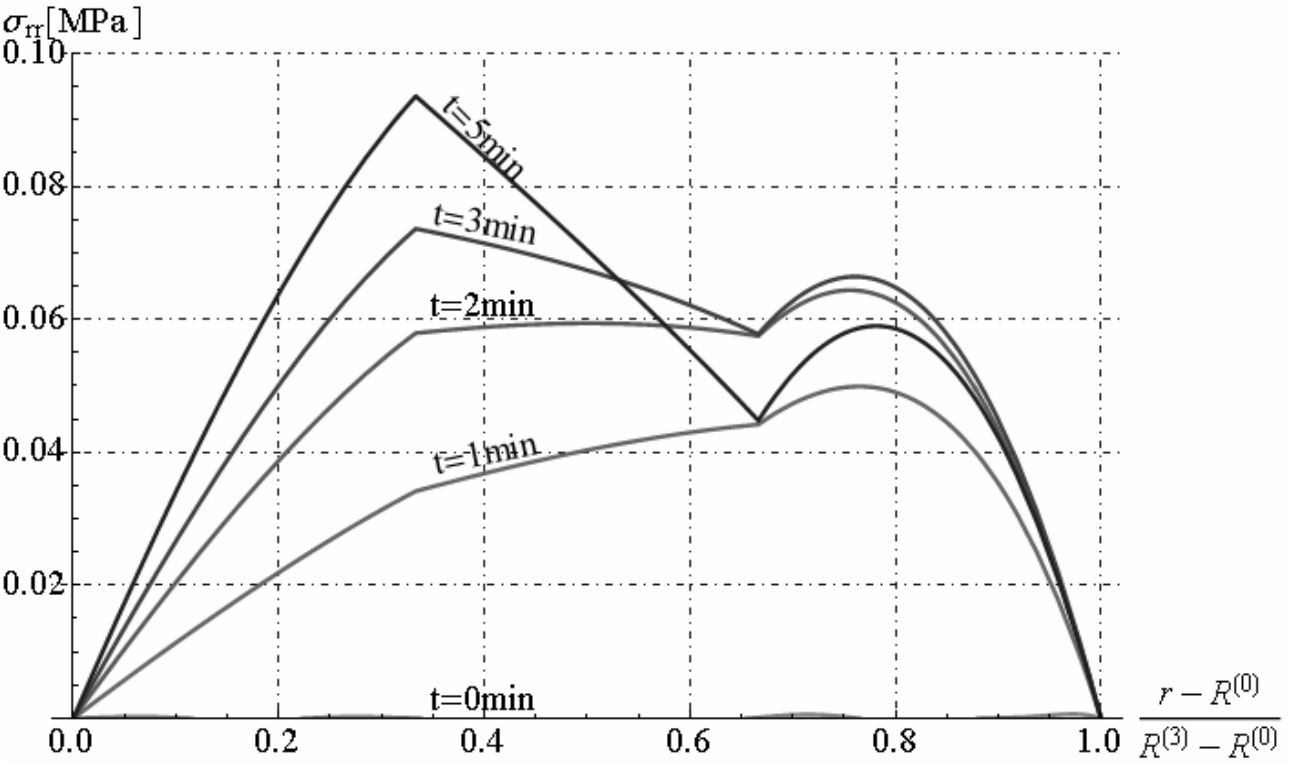

Fig. 20.32 - *Radial stress versus time*

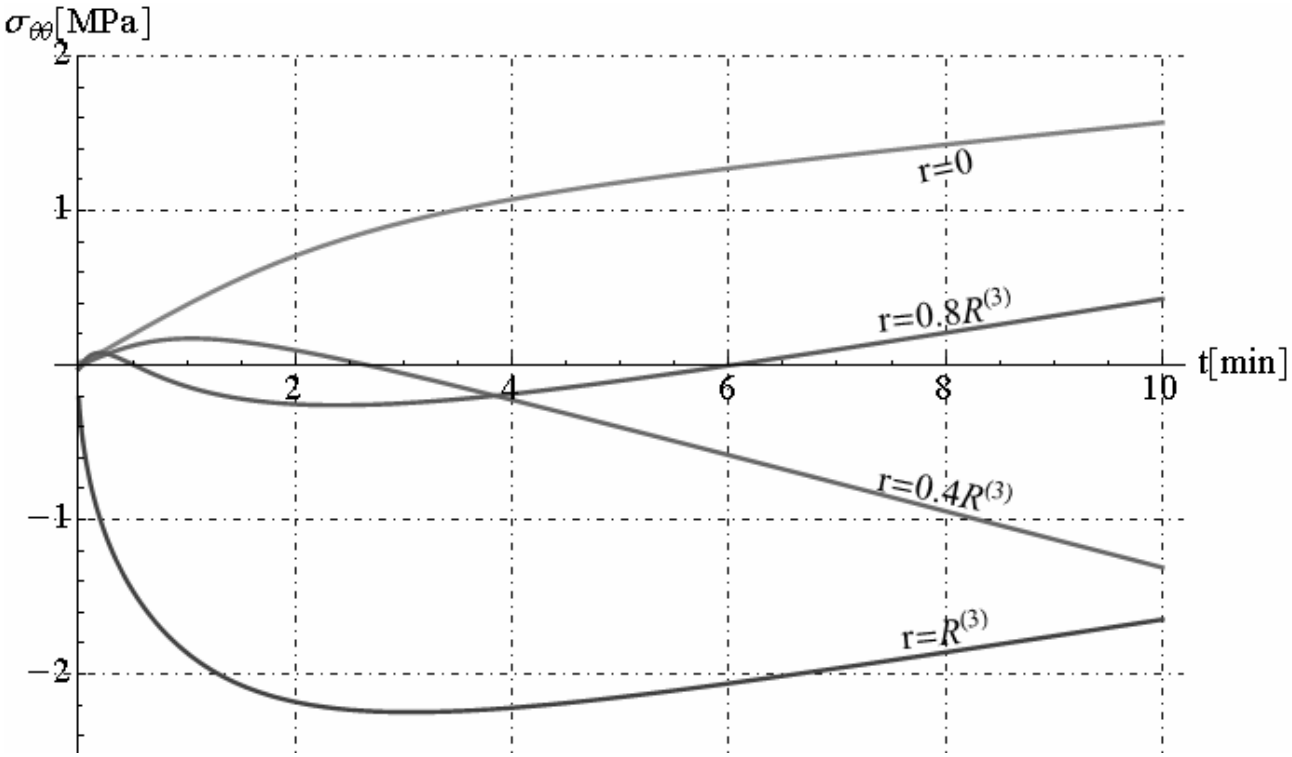

Fig. 20.33 - *Circumferential stress along radial direction*

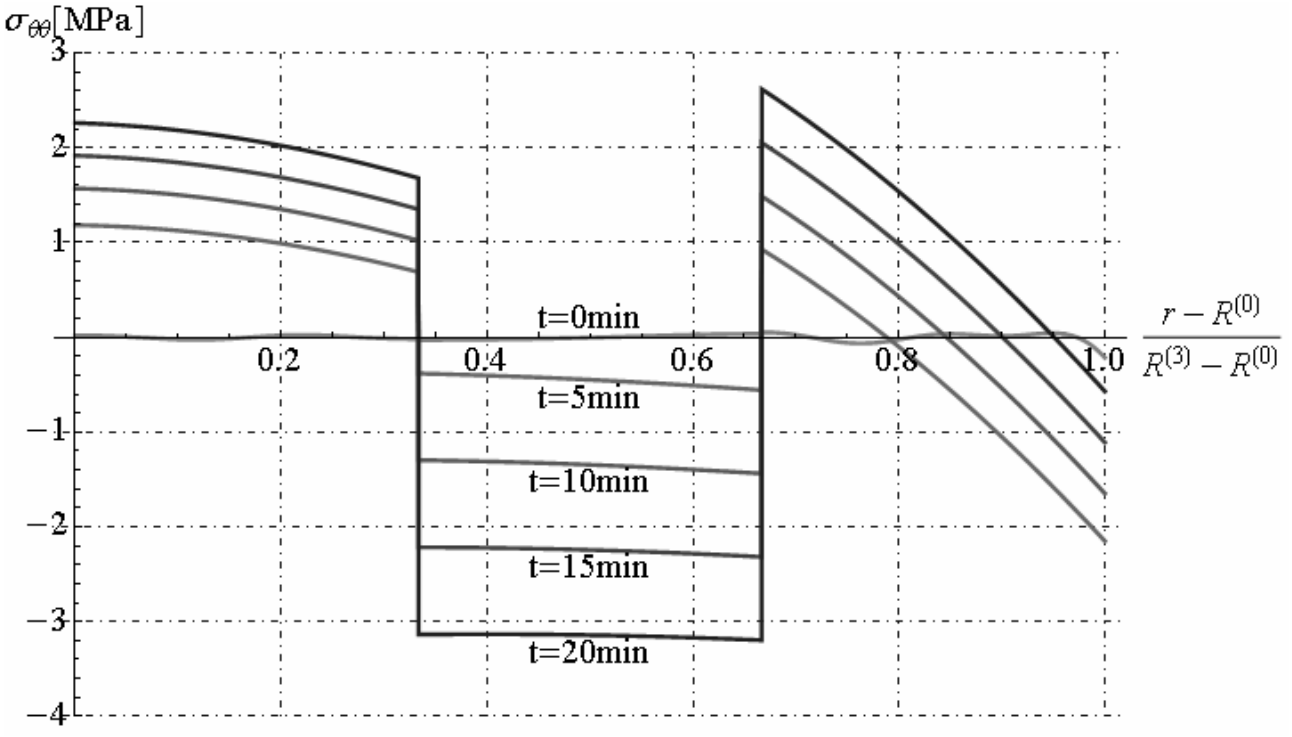

Fig. 20.34- *Circumferential stress versus time*

20.4. Multilayered sphere exposed to hydrocarbon fire

Let us consider an multilayered sphere constituted by n-hollow spherical phase as decrypted in section 20.1. The inner surface $r = R^{(0)}$ is kept perfectly insulated while the outer surface $r = R^{(n)}$ is exposed to conventional fire, for t >0. In this section, we determine the temperature, displacement and stress function in multilayered sphere by starting to initial temperature equal to $T_0 = T_R = const$.

The equations field to satisfy in uncoupled thermo-elastic problem with spherical symmetry are reported in equations (20.13), but in this case the boundary conditions (20.11) become:

$$\begin{cases} -k^{(1)}T^{(1)}_{,r}(r=R^{(0)})=0, \\ -k^{(n)}T^{(n)}_{,r}(r=R^{(n)})=h_c\left[T^{(n)}(r=R^{(n)})-\Theta_F\right], \end{cases} \quad \forall t\geq 0 \tag{20.93}$$

where Θ_F is the conventional fire curve and h_c is convection coefficient on surface $r=R^{(n)}$. In this case, we considered Hydrocarbon fire curve given by follows equation (see Chapter XIX):

$$\begin{aligned} &\Theta_F = H_0 + H_1 e^{-\xi_1 t} + H_2 e^{-\xi_2 t} \quad [^\circ K, \sec] \\ &H_0 = 1373.15^\circ K,\ H_1 = -729^\circ K,\ H_2 = -351^\circ K, \\ &\xi_1 = -2.783\cdot 10^{-3}\sec^{-1},\ \ \xi_2 = -4.416\cdot 10^{-2}\sec^{-1}, \end{aligned} \tag{20.94}$$

and the boundary conditions (20.8) become:

$$\sigma^{(n)}_{rr}(r=R^{(n)})=0, \quad \sigma^{(1)}_{rr}(r=R^{(0)})=0, \quad \forall t\geq 0 \tag{20.95}$$

The other boundary conditions reported in section 20.1 not change. By solving the Fourier's equation reported in second equation of (20.13) with method separation of variables, and by substituting the function of temperature $T^{(i)}(r,t)$ in first equation of (20.13), and by integration in two time this equation respect to variable r , the displacement solution is reported in equation (20.14). In this case, the heat conduct problem involving a non-homogeneous boundary condition and, in particular, with the heat input specified over the entire boundary surface. It is necessary writing the temperature solution, in any phases of multilayered sphere, in the follows form :

$$T^{(i)}(r,t)=H_0+e^{\xi_1 t}T^{(i)}_1(r)+e^{\xi_2 t}T^{(i)}_2(r)+T^{(i)}_C(r,t), \quad \forall i\in\{1,2,....,n\} \tag{20.96}$$

The functions $T^{(i)}_1(r)$ and $T^{(i)}_2(r)$ in generic i-th phase satisfy the field equations:

$$\frac{d^2T^{(i)}_j}{dr^2}+\frac{2}{r}\frac{dT^{(i)}_j}{dr}-\frac{\xi_j T^{(i)}_j}{\kappa^{(i)}}=0; \qquad \begin{matrix} R^{(i-1)}\leq r\leq R^{(i)} \\ \forall i\in\{1,2,...,n\},\ \ \forall j\in\{1,2\} \end{matrix} \tag{20.97}$$

Moreover the functions $T^{(i)}_1(r)$ and $T^{(i)}_2(r)$ must be satisfy the following boundary conditions :

$$-k^{(1)}\frac{dT^{(1)}_j(r)}{dr}=0, \quad r=R^{(0)}, \forall j\in\{1,2\} \tag{20.98}$$

$$-k^{(n)}\frac{dT^{(n)}_j(r)}{dr}=h_c\left[T^{(n)}_j(r)-H_j\right], \quad r=R^{(n)}, \forall j\in\{1,2\} \tag{20.99}$$

$$-k^{(i)}\frac{dT^{(i)}_j(r)}{dr}=-k^{(i+1)}\frac{dT^{(i+1)}_j(r)}{dr}, \quad r=R^{(i)},\ \forall i\in\{1,2,...,n-1\}, \forall j\in\{1,2\} \tag{20.100}$$

$$T^{(i)}_j(r)=T^{(i+1)}_j(r), \quad r=R^{(i)},\ \forall i\in\{1,2,...,n-1\}, \forall j\in\{1,2\} \tag{20.101}$$

The function $T^{(i)}_C(r,t)$ in generic i-th phase satisfies the field equations:

$$\frac{\partial^2 T^{(i)}_C(r,t)}{\partial r^2}+\frac{2}{r}\frac{\partial T^{(i)}_C(r,t)}{\partial r}=\frac{1}{\kappa^{(i)}}\frac{\partial T^{(i)}_C(r,t)}{\partial t}; \qquad \begin{matrix} R^{(i-1)}\leq r\leq R^{(i)}, \forall t\geq 0 \\ \forall i\in\{1,2,...,n\} \end{matrix} \tag{20.102}$$

Moreover the function $T^{(i)}_C(r,t)$ must be satisfy the following boundary conditions :

$$-k^{(1)}\frac{\partial T^{(1)}_C(r,t)}{\partial r}=0, \quad r=R^{(0)},\ \forall t\geq 0, \tag{20.103}$$

$$-k^{(n)}\frac{\partial T^{(n)}_C(r,t)}{\partial r}=h_c T^{(n)}_C(r,t), \quad r=R^{(n)},\ \forall t\geq 0, \tag{20.104}$$

$$\begin{cases} -k^{(i)}\dfrac{\partial T_C^{(i)}(r,t)}{\partial r} = -k^{(i+1)}\dfrac{\partial T_C^{(i+1)}(r,t)}{\partial r}, \\ T_C^{(i)}(r,t) = T_C^{(i+1)}(r,t), \end{cases} \quad r = R^{(i)},\ \forall t \geq 0,\ \forall i \in \{1,2,...,n-1\} \tag{20.105}$$

$$T_C^{(i)}(r,t) = -T_S^{(i)}(r), \quad R^{(i-1)} \leq r \leq R^{(i)},\ t = 0,\ \forall i \in \{1,2,...,n\} \tag{20.106}$$

$$T_C^{(i)}(r,t) = -\left[H_0 - T_0 + e^{\xi_1 t}T_1^{(i)}(r) + e^{\xi_2 t}T_2^{(i)}(r)\right], \quad R^{(i-1)} \leq r \leq R^{(i)},\ t = 0,\ \forall i \in \{1,2,...,n\} \tag{20.107}$$

The solutions of differential equations (20.97) are given by:

$$\begin{cases} T_1^{(i)}(r) = r^{-1}\left(C^{(i)}e^{-\eta_1^{(i)}r} + D^{(i)}e^{\eta_1^{(i)}r}\right) \\ T_2^{(i)}(r) = r^{-1}\left(G^{(i)}e^{-\eta_2^{(i)}r} + L^{(i)}e^{\eta_2^{(i)}r}\right) \end{cases} \quad \forall i \in \{1,2,...,n\} \tag{20.108}$$

where $C^{(i)}, D^{(i)}, G^{(i)}, L^{(i)}$ are 4n unknown parameters to determine and parameters $\eta_1^{(i)}, \eta_2^{(i)}$ are given by:

$$\eta_1^{(i)} = \sqrt{\frac{\xi_1}{\kappa^{(i)}}}, \quad \eta_2^{(i)} = \sqrt{\frac{\xi_2}{\kappa^{(i)}}}, \tag{20.109}$$

By solving algebraic system composed by 4n equations (20.98) to (20.101), we obtain integration constants $C^{(i)}, D^{(i)}, G^{(i)}, L^{(i)}$. For brevity, we don't reported in explicit the expressions of these constants. The solution to the problem for T_C is found in much the same says way as was followed in section 20.2. The problem is therefore on with homogeneous differential equation and boundary conditions and may be treated by the method separation of variables as showed in section 20.2. The solutions of differential equation (20.102) is given by:

$$T_C^{(i)}(r,t) = r^{-1}\left[A^{(i)}e^{\imath\,\omega\beta^{(i)}r} + B^{(i)}e^{-\imath\,\omega\beta^{(i)}r}\right]e^{-\kappa^{(i)}\beta^{(i)2}\omega^2 t} \quad \forall i \in \{1,2,...,n\} \tag{20.110}$$

where $A^{(i)}, B^{(i)}, \omega$ are constants parameter to determine, the coefficient $\beta^{(i)} = \sqrt{\kappa^{(1)}/\kappa^{(i)}}$ and $\imath$ is unit imaginary. In explicit the boundary conditions (20.105) for temperature function $T_C^{(i)}(r,t)$ are reported in equations (20.77). Moreover the boundary conditions on the inner and the outer surface (20.103) and (20.104) can be to rewrite as reported in equations (20.22). By first equation of (20.22) , we determine $B^{(1)}$ as function of $A^{(1)}$ as follows:

$$B^{(1)} = \left[\frac{\left(\imath + \omega R^{(0)}\beta^{(1)}\right)^2}{1 + \omega^2\,\beta^{(1)2}R^{(0)2}}\right]A^{(1)}e^{2\imath\,\omega\beta^{(1)}R^{(0)}} \tag{20.111}$$

The equations (20.77) constituted an homogeneous algebraic system, composed by 2(n-1) equations, in unknown parameters $A^{(i)}, B^{(i)}$ with $i \in \{1,2,...,n\}$, which can be written as:

$$\mathbf{\Phi}\cdot\mathbf{X} = \mathbf{0} \tag{20.112}$$

where $\mathbf{X} = [\mathbf{X}^{(1)}, \mathbf{X}^{(2)}, ..., \mathbf{X}^{(n)}]^T$ collect the unknowns sub-vectors, as reported below:

$$\mathbf{X}^{(i)} = \begin{bmatrix} A^{(i)} & B^{(i)} \end{bmatrix}^T, \quad \forall i \in \{1,2,....,n\} \tag{20.113}$$

and $\mathbf{\Phi}$ is the matrix reported in equation (20.26). As showed in section 20.2, matrix $\mathbf{\Phi}$ is constituted by components: $\mathbf{\Phi}_i^{(i)}, \mathbf{\Phi}_i^{(i+1)}, \forall i \in \{1,2,...,n-1\}$ and vector $\mathbf{X}^{(i)}$ is obtained as function of vector $\mathbf{X}^{(1)}$ (see equation (20.29)). By substituting the solutions (20.29) in boundary conditions (20.22), we obtain vector equations in unknown vector $\mathbf{X}^{(1)}$, as reported below:

$$\mathbf{\Lambda}\cdot\mathbf{X}^{(1)} = \mathbf{0} \tag{20.114}$$

where $\mathbf{\Lambda}$ is an 2x2 square matrix given by :

$$\mathbf{\Lambda} = \begin{bmatrix} \Lambda_{11} & \Lambda_{12} \\ \Lambda_{21} & \Lambda_{22} \end{bmatrix} \tag{20.115}$$

where the components $\Lambda_{11},\Lambda_{12},\Lambda_{21},\Lambda_{22}$ are reported in equation (20.33)

$$\begin{aligned}&\Lambda_{11}=\left(1-i\omega\beta^{(1)}R^{(0)}\right)e^{i\omega\beta^{(1)}R^{(0)}},\quad \Lambda_{12}=\left(1+i\omega\beta^{(1)}R^{(0)}\right)e^{-i\omega\beta^{(1)}R^{(0)}},\\&\left[\Lambda_{21},\Lambda_{22}\right]=\left[\left(1-i\omega\beta^{(n)}R^{(n)}\right)e^{i\omega\beta^{(n)}R^{(n)}},\left(1+i\omega\beta^{(n)}R^{(n)}\right)e^{-i\omega\beta^{(n)}R^{(n)}}\right]\cdot\mathbf{\Gamma}^{(n)},\end{aligned}\tag{20.116}$$

The algebraic system (20.114) admit not trivial solution if the determinant of the matrix $[\mathbf{\Lambda}]$ is equal to zero. By imposing this condition, we obtain the transcendental equation in unknown parameter ω:

$$\det[\mathbf{\Lambda}]=0\ \Rightarrow\ g(\omega)=0\tag{20.117}$$

The roots of this transcendental equation (20.117) are an infinite number such, denoted here by $\omega_m,\ m=1,2,....N$ leading to characteristic values $\lambda_m=-\omega_m^2$. The corresponding characteristic functions $\bar{\varphi}_m^{(i)}(r)$ are reported in equation (20.110). The coefficients $A_m^{(1)}$ are determined by applying the initial condition (20.107) that yields the following relationship:

$$A_m^{(1)}=-\frac{\sum_{i=1}^{n}\left\{\rho^{(i)}c_v^{(i)}\int_0^{2\pi}\int_0^{\pi}\int_{R^{(i-1)}}^{R^{(i)}}r^2\bar{\varphi}_m^{(i)}\left[H_0-T_0+T_1^{(i)}(r)+T_2^{(i)}(r)\right]\sin\theta\,dr d\theta d\phi\right\}}{\sum_{i=1}^{n}\left[\rho^{(i)}c_v^{(i)}\int_0^{2\pi}\int_0^{\pi}\int_{R^{(i-1)}}^{R^{(i)}}\left(\bar{\varphi}_m^{(i)}\right)^2r^2\sin\theta dr d\theta d\phi\right]}\tag{20.118}$$

Finally the temperature function in i-th generic phase is given by:

$$\begin{aligned}T^{(i)}(r,t)=H_0+r^{-1}\left(C^{(i)}e^{-\eta_1^{(i)}r}+D^{(i)}e^{-\eta_1^{(i)}r}\right)e^{\xi_1 t}+r^{-1}\left(G^{(i)}e^{-\eta_2^{(i)}r}+L^{(i)}e^{-\eta_2^{(i)}r}\right)e^{\xi_2 t}+\\+\sum_{m=1}^{\infty}r^{-1}\left(A_m^{(i)}e^{i\omega_m\beta^{(i)}r}+B_m^{(i)}e^{-i\omega_m\beta^{(i)}r}\right)e^{-\kappa^{(i)}\beta^{(i)2}\omega_m^2 t}\quad\forall i\in\{1,2,....,n\}\end{aligned}\tag{20.119}$$

By substituting the function (20.119) in equation (20.14), we obtain in explicit the displacement function in any hollow spherical phase:

$$\begin{aligned}u_r^{(i)}=&P^{(i)}r+Q^{(i)}r^{-2}+\left(U^{(i)}r+V^{(i)}r^{-2}\right)e^{\xi_1 t}+\left(W^{(i)}r+Z^{(i)}r^{-2}\right)e^{\xi_2 t}\\&+\frac{\alpha^{(i)}\left(3\lambda^{(i)}+2\mu^{(i)}\right)}{\left(\lambda^{(i)}+2\mu^{(i)}\right)}\left\{\frac{H_0 r}{3}-\left[\frac{C^{(i)}\left(1+\eta_1^{(i)}r\right)e^{-\eta_1^{(i)}r}+D^{(i)}\left(1-\eta_1^{(i)}r\right)e^{\eta_1^{(i)}r}}{\left(\eta_1^{(i)}r\right)^2}\right]e^{\xi_1 t}\right\}+\\&+\frac{\alpha^{(i)}\left(3\lambda^{(i)}+2\mu^{(i)}\right)}{\left(\lambda^{(i)}+2\mu^{(i)}\right)}\left[\frac{G^{(i)}\left(1+\eta_2^{(i)}r\right)e^{-\eta_2^{(i)}r}+L^{(i)}\left(1-\eta_2^{(i)}r\right)e^{\eta_2^{(i)}r}}{\left(\eta_2^{(i)}r\right)^2}\right]e^{\xi_2 t}+\\&+\sum_{m=1}^{\infty}\left\{N_m^{(i)}r+M_m^{(i)}r^{-2}+\frac{\alpha^{(i)}\left(3\lambda^{(i)}+2\mu^{(i)}\right)}{\omega_m^2\beta^{(i)2}\left(\lambda^{(i)}+2\mu^{(i)}\right)r^2}\left[\begin{array}{l}A_m^{(i)}\left(1-i\beta^{(i)}\omega_m r\right)e^{i\beta^{(i)}\omega_m r}+\\+B_m^{(i)}\left(1+i\beta^{(i)}\omega_m r\right)e^{-i\beta^{(i)}\omega_m r}\end{array}\right]\right\}e^{-\kappa^{(i)}\omega_m^2\beta^{(i)2}t}\\&\forall i\in\{1,2,....,n\}\end{aligned}\tag{20.120}$$

where the integration constants $P^{(i)},Q^{(i)},U^{(i)},V^{(i)},W^{(i)},Z^{(i)},N_m^{(i)},M_m^{(i)}$ are determined by applying the boundary conditions given by equations (20.6), (20.7) and (20.95). In this case the functions $f_1^{(i)}(t),\ f_2^{(i)}(t),$ reported in equation (20.14) are given by:

$$\begin{aligned}f_1^{(i)}(t)&=P^{(i)}+U^{(i)}e^{\xi_1 t}+W^{(i)}e^{\xi_2 t}+\sum_{m=1}^{\infty}N_m^{(i)}e^{-\kappa^{(i)}\omega_m^2\beta^{(i)2}t},\\f_2^{(i)}(t)&=Q^{(i)}+V^{(i)}e^{\xi_1 t}+Z^{(i)}e^{\xi_2 t}+\sum_{m=1}^{\infty}M_m^{(i)}e^{-\kappa^{(i)}\omega_m^2\beta^{(i)2}t},\end{aligned}\tag{20.121}$$

In explicit the radial and circumferential stress components are given by:

$$\sigma_{rr}^{(i)} = \left(3\lambda^{(i)} + 2\mu^{(i)}\right)\left[\alpha^{(i)}\left(T_R - H_0\right) + P^{(i)} + U^{(i)}e^{\xi_1 t} + W^{(i)}e^{\xi_2 t}\right] - 4\mu^{(i)}r^{-3}\left(Q^{(i)} + V^{(i)}e^{\xi_1 t} + Z^{(i)}e^{\xi_2 t}\right) +$$
$$+ \frac{4\mu^{(i)}\alpha^{(i)}\left(3\lambda^{(i)} + 2\mu^{(i)}\right)}{\left(\lambda^{(i)} + 2\mu^{(i)}\right)r^3\eta_1^{(i)2}}\left[C^{(i)}\left(1+\eta_1^{(i)}r\right)e^{-\eta_1^{(i)}r} + D^{(i)}\left(1-\eta_1^{(i)}r\right)e^{\eta_1^{(i)}r}\right]e^{\xi_1 t} +$$
$$+ \frac{4\mu^{(i)}\alpha^{(i)}\left(3\lambda^{(i)} + 2\mu^{(i)}\right)}{\left(\lambda^{(i)} + 2\mu^{(i)}\right)r^3\eta_2^{(i)2}}\left[G^{(i)}\left(1+\eta_2^{(i)}r\right)e^{-\eta_2^{(i)}r} + L^{(i)}\left(1-\eta_2^{(i)}r\right)e^{\eta_2^{(i)}r}\right]e^{\xi_2 t} +$$
$$+ \frac{\alpha^{(i)}\left(3\lambda^{(i)} + 2\mu^{(i)}\right)^2 H_0}{3\left(\lambda^{(i)} + 2\mu^{(i)}\right)} + \sum_{m=1}^{\infty}\left[P_m^{(i)}\left(3\lambda^{(i)} + 2\mu^{(i)}\right) - 4Q_m^{(i)}\mu^{(i)}r^{-3}\right]e^{-\omega_m^2\beta^{(i)2}\kappa^{(i)}t} +$$
$$+ \frac{4i\alpha^{(i)}\mu^{(i)}\left(3\lambda^{(i)} + 2\mu^{(i)}\right)}{\beta^{(i)2}\left(\lambda^{(i)} + 2\mu^{(i)}\right)}\sum_{m=1}^{\infty}\left\{\omega_m^{-2}r^{-3}\left[\begin{array}{l} A_m^{(i)}\left(i + \omega_m\beta^{(i)}r\right)e^{i\omega_m\beta^{(i)}r} + \\ +B_m^{(i)}\left(i - \omega_m\beta^{(i)}r\right)e^{-i\omega_m\beta^{(i)}r}\end{array}\right]\right\}e^{-\omega_m^2\beta^{(i)2}\kappa^{(i)}t} \tag{20.122}$$

$$\sigma_{\theta\theta}^{(i)} = \left(3\lambda^{(i)} + 2\mu^{(i)}\right)\left[\alpha^{(i)}\left(T_R - H_0\right) + P^{(i)} + U^{(i)}e^{\xi_1 t} + W^{(i)}e^{\xi_2 t}\right] + 2\mu^{(i)}r^{-3}\left(Q^{(i)} + V^{(i)}e^{\xi_1 t} + Z^{(i)}e^{\xi_2 t}\right) +$$
$$+ \frac{2\mu^{(i)}\alpha^{(i)}\left(3\lambda^{(i)} + 2\mu^{(i)}\right)}{\left(\lambda^{(i)} + 2\mu^{(i)}\right)r^3\eta_1^{(i)2}}\left\{C^{(i)}\left[1+\eta_1^{(i)}r\left(1+\eta_1^{(i)}r\right)\right]e^{-\eta_1^{(i)}r} + D^{(i)}\left[1-\eta_1^{(i)}r\left(1-\eta_1^{(i)}r\right)\right]e^{\eta_1^{(i)}r}\right\}e^{\xi_1 t} +$$
$$+ \frac{4\mu^{(i)}\alpha^{(i)}\left(3\lambda^{(i)} + 2\mu^{(i)}\right)}{\left(\lambda^{(i)} + 2\mu^{(i)}\right)r^3\eta_2^{(i)2}}\left\{G^{(i)}\left[1+\eta_2^{(i)}r\left(1+\eta_2^{(i)}r\right)\right]e^{-\eta_2^{(i)}r} + L^{(i)}\left[1-\eta_2^{(i)}r\left(1-\eta_2^{(i)}r\right)\right]e^{\eta_2^{(i)}r}\right\}e^{\xi_2 t} +$$
$$+ \frac{\alpha^{(i)}\left(3\lambda^{(i)} + 2\mu^{(i)}\right)^2 H_0}{3\left(\lambda^{(i)} + 2\mu^{(i)}\right)} + \sum_{m=1}^{\infty}\left[P_m^{(i)}\left(3\lambda^{(i)} + 2\mu^{(i)}\right) + 2\mu^{(i)}Q_m^{(i)}r^{-3}\right]e^{-\omega_m^2\beta^{(i)2}\kappa^{(i)}t} +$$
$$+ \frac{2\alpha^{(i)}\mu^{(i)}\left(3\lambda^{(i)} + 2\mu^{(i)}\right)}{\beta^{(i)2}\left(\lambda^{(i)} + 2\mu^{(i)}\right)}\sum_{m=1}^{\infty}\left\{\begin{array}{l}\dfrac{A_m^{(i)}}{\omega_m^2 r^3}\left[1 - r\omega_m\beta^{(i)}\left(i + \omega_m\beta^{(i)}r\right)\right]e^{i\omega_m\beta^{(i)}r} + \\ +\dfrac{B_m^{(i)}}{\omega_m^2 r^3}\left[1 - r\omega_m\beta^{(i)}\left(\omega_m\beta^{(i)}r - i\right)\right]e^{-i\omega_m\beta^{(i)}r}\end{array}\right\}e^{-\omega_m^2\beta^{(i)2}\kappa^{(i)}t} \tag{20.123}$$

Moreover, the tractions on the inner and the outer spherical boundary surface are vanishing and then condition (20.8) becomes:

$$\sigma_{rr}^{(1)}(r = R^{(0)}) = 0,\ \sigma_{rr}^{(n)}(r = R^{(n)}) = 0, \quad \forall t \geq 0 \tag{20.124}$$

The integration constants $P^{(i)}, Q^{(i)}, U^{(i)}, V^{(i)}, W^{(i)}, Z^{(i)}, N_m^{(i)}, M_m^{(i)}$ are function of geometrical, mechanical and thermal parameters of spherical layers . Moreover $P_m^{(i)}, Q_m^{(i)}$ are function of constants $A_m^{(i)}, B_m^{(i)}, \omega_m$ also. For example, let us consider, a spherical tank constituted by two phases under uniform heat flux . The phase (1) is constituted by steel and phase (2) by aluminium. The mechanical and thermal parameters considered for both phases are reported in table 20.1. The geometrical parameters of spherical tank are: $R^{(0)} = 10m$, $R^{(1)} = 10.05m$, $R^{(2)} = 10.10m$, $T_0 = T_R = 293.15°K = 20°C$. By fixed m= 20, the eigenvalues ω_m of transcendental equation (20.85) and corresponding values of constants integration A_m are reported in table 20.7:

ω_m	3.578	41.301	92.692	142.020
A_m	1810.560 - 5413.180 i	-4.404 + 42.440 i	-2.496 + 0.368 i	-0.432 + 0.086 i
ω_m	180.320	225.474	277.752	323.549
A_m	0.1681 + 0.0124 i	-0.0320 - 0.0426 i	0.0211 - 0.0077 i	-0.0142 - 0.0053 i
ω_m	361.625	410.487	462.194	503.892
A_m	-0.0089 + 0.0026 i	0.0017 + 0.0041 i	-0.0024 + 0.0019 i	-0.0025 - 0.0005 i
ω_m	544.494	595.770	645.491	684.062
A_m	-0.0013977 + 0.0008686 i	-0.0003220 + 0.0009247 i	-0.0004276 - 0.0007718 i	0.0001440 - 0.0007359 i
ω_m	728.657	780.912	827.267	865.198
A_m	-0.0001609 + 0.0004401 i	-0.0002189 - 0.0002658 i	-0.0002259 + 0.0002615 i	$-0.0002807 + 8.7 \times 10^{-6}$ i

Table 20.7 – *Eigenvalues* ω_m *and corresponding values of constants integration* A_m

In this case the graphics function $g(\omega)$ given by equation (20.85) is reported below:

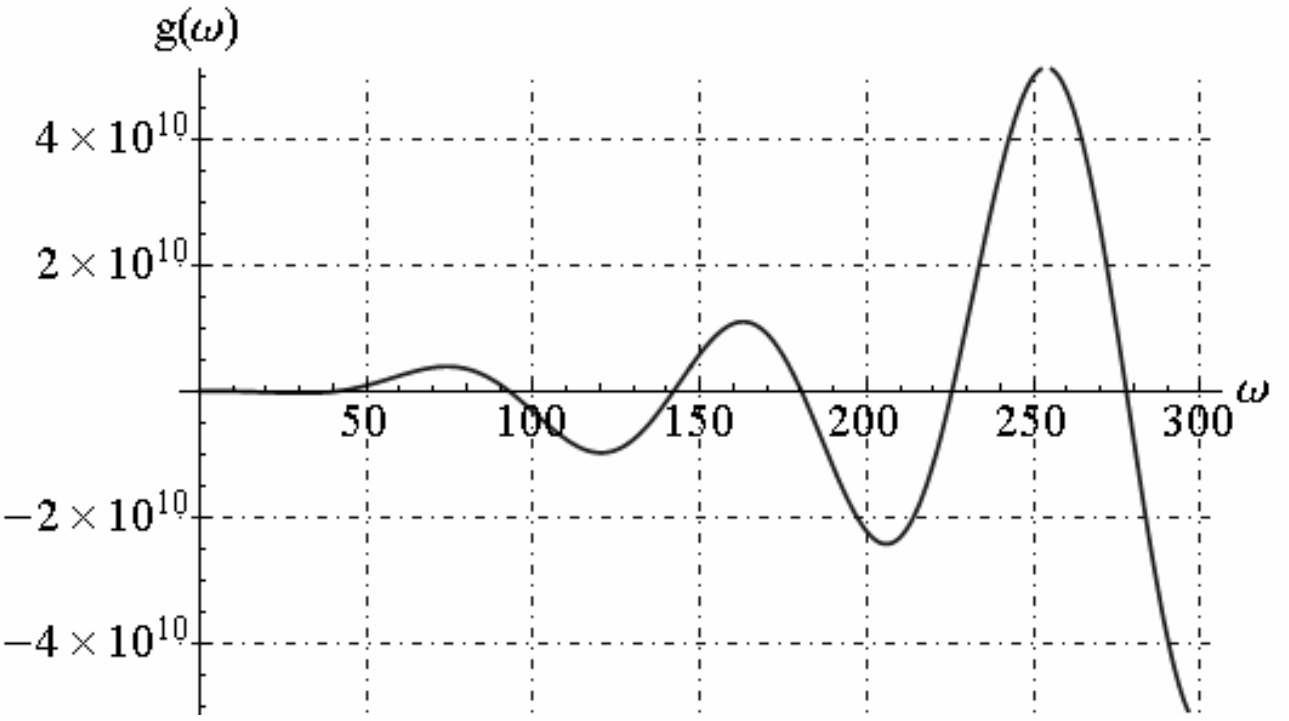

Fig. 20.35 - *Function* $g(\omega)$

We reported the graphics of temperature function along the radial direction and in time:

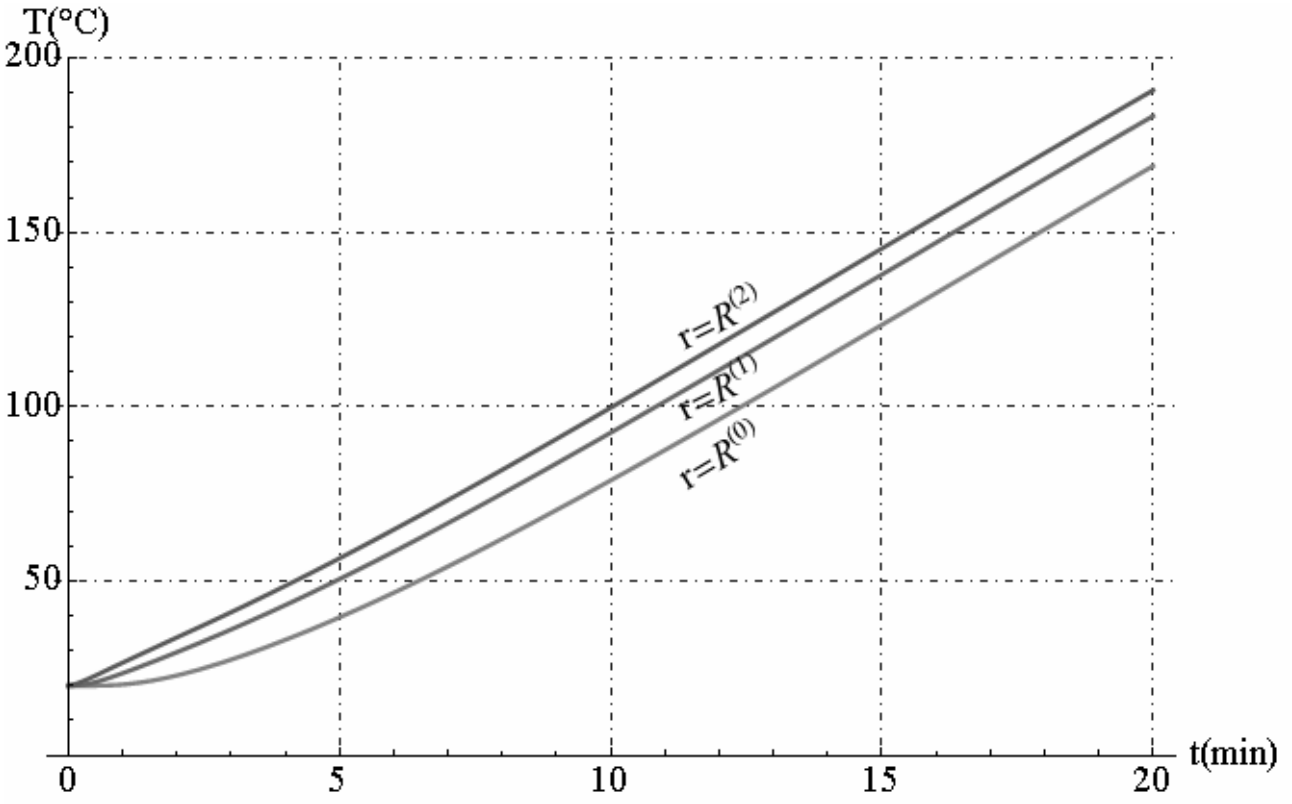

Fig. 20.36 - *Temperature function versus time*

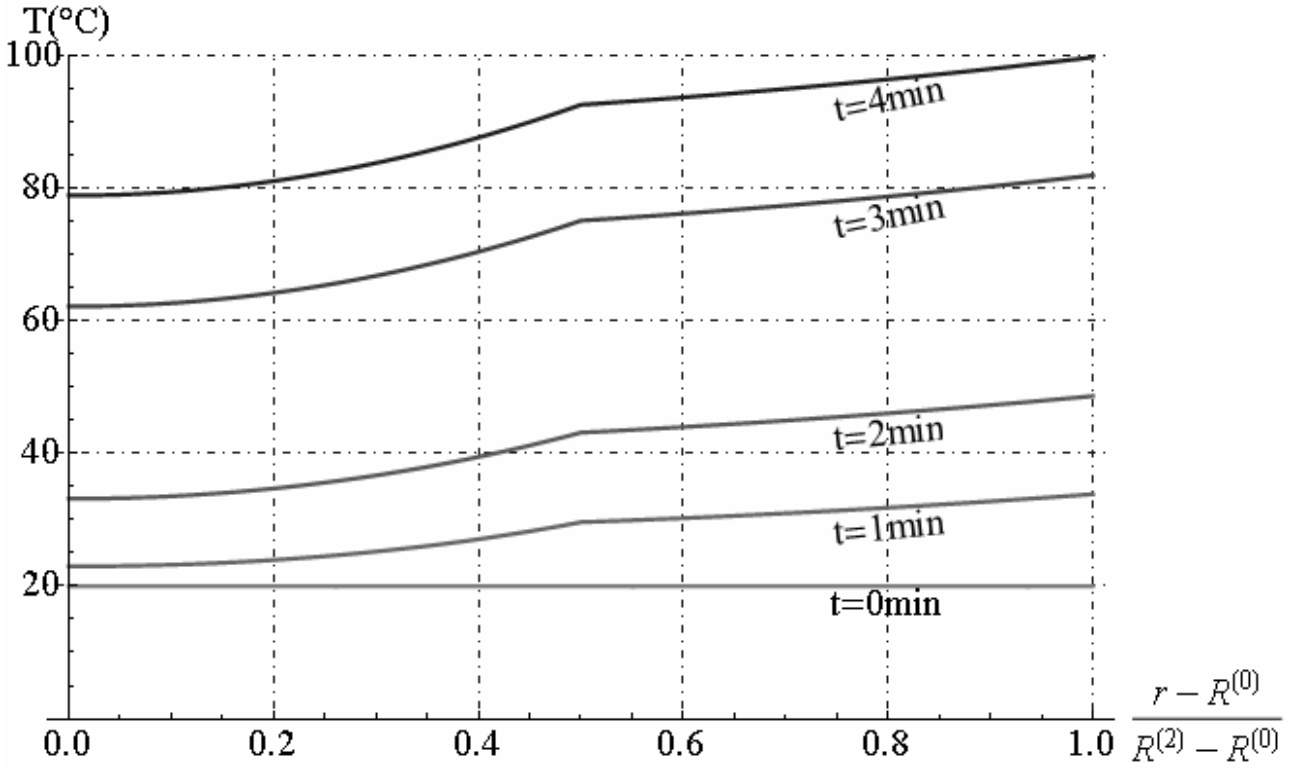

Fig. 20.37 - *Temperature function along radial direction*

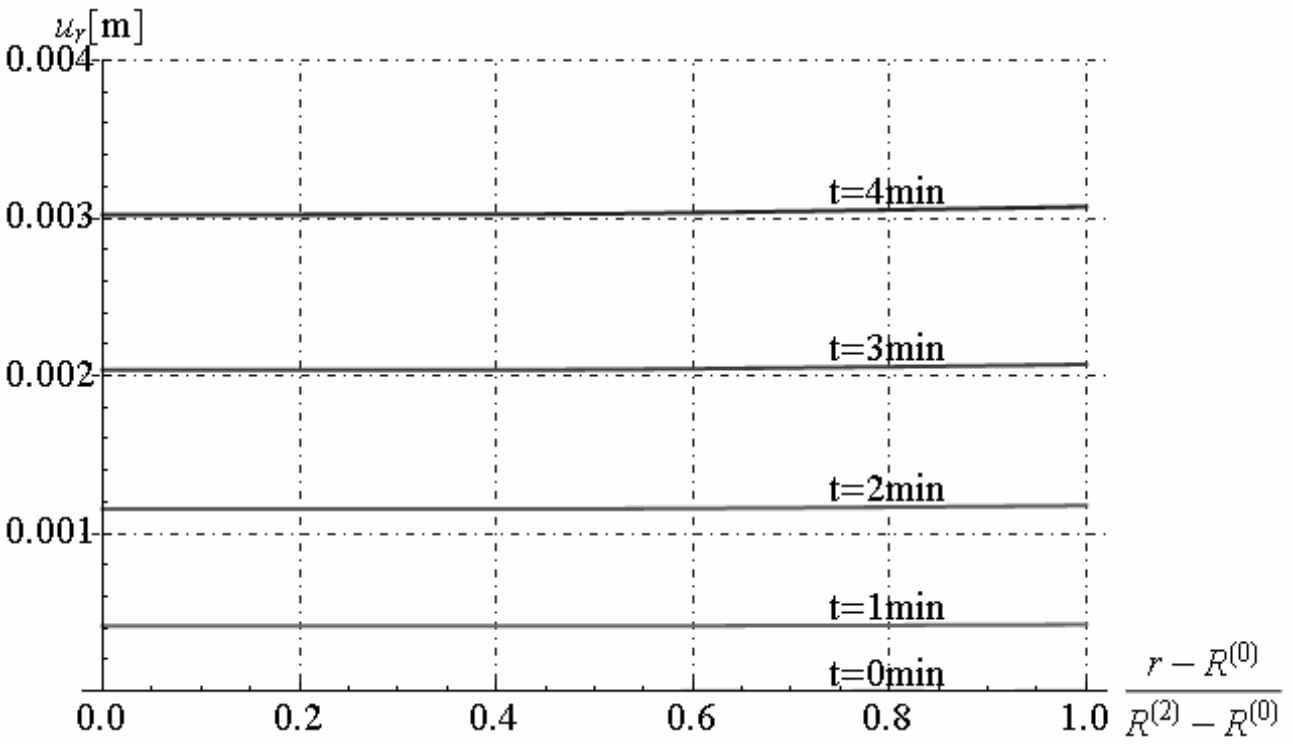

Fig. 20.38 - *Radial displacement along radial direction*

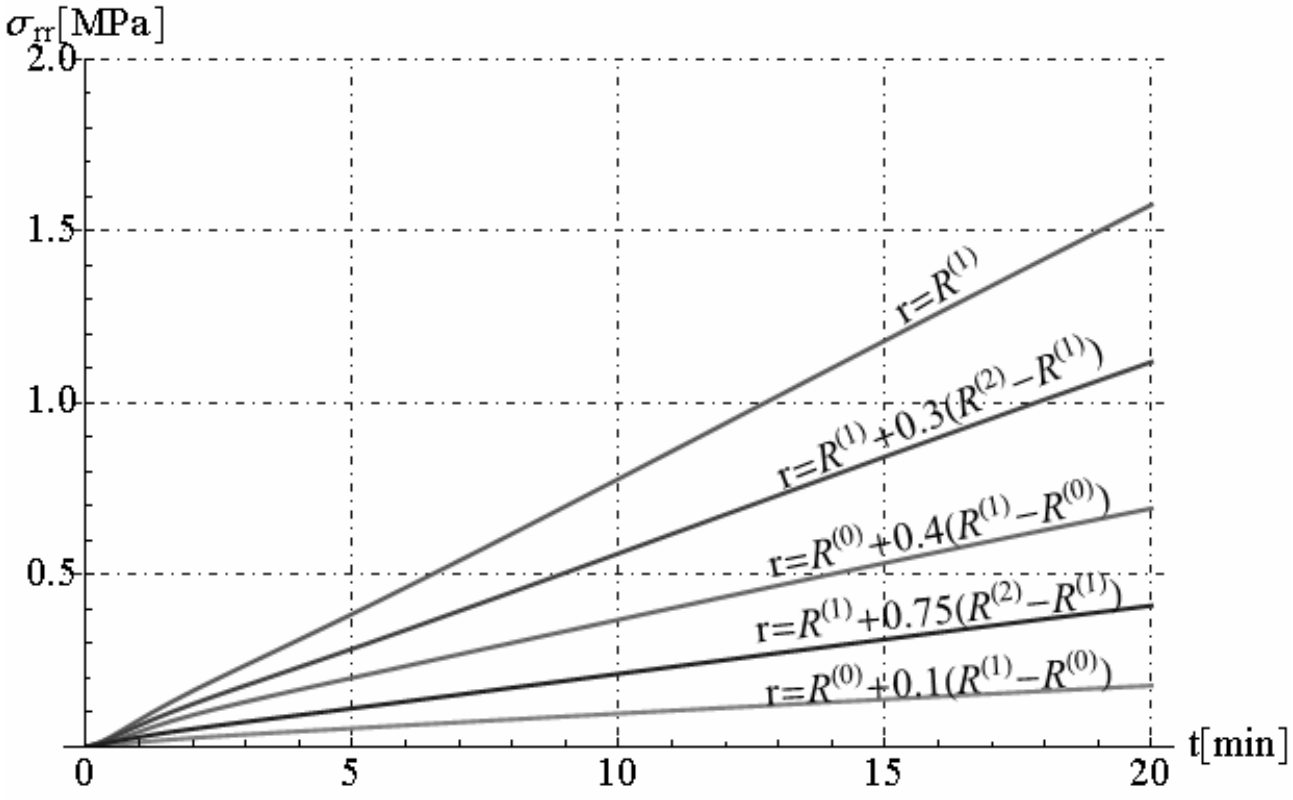

Fig. 20.39 - *Radial stress versus time*

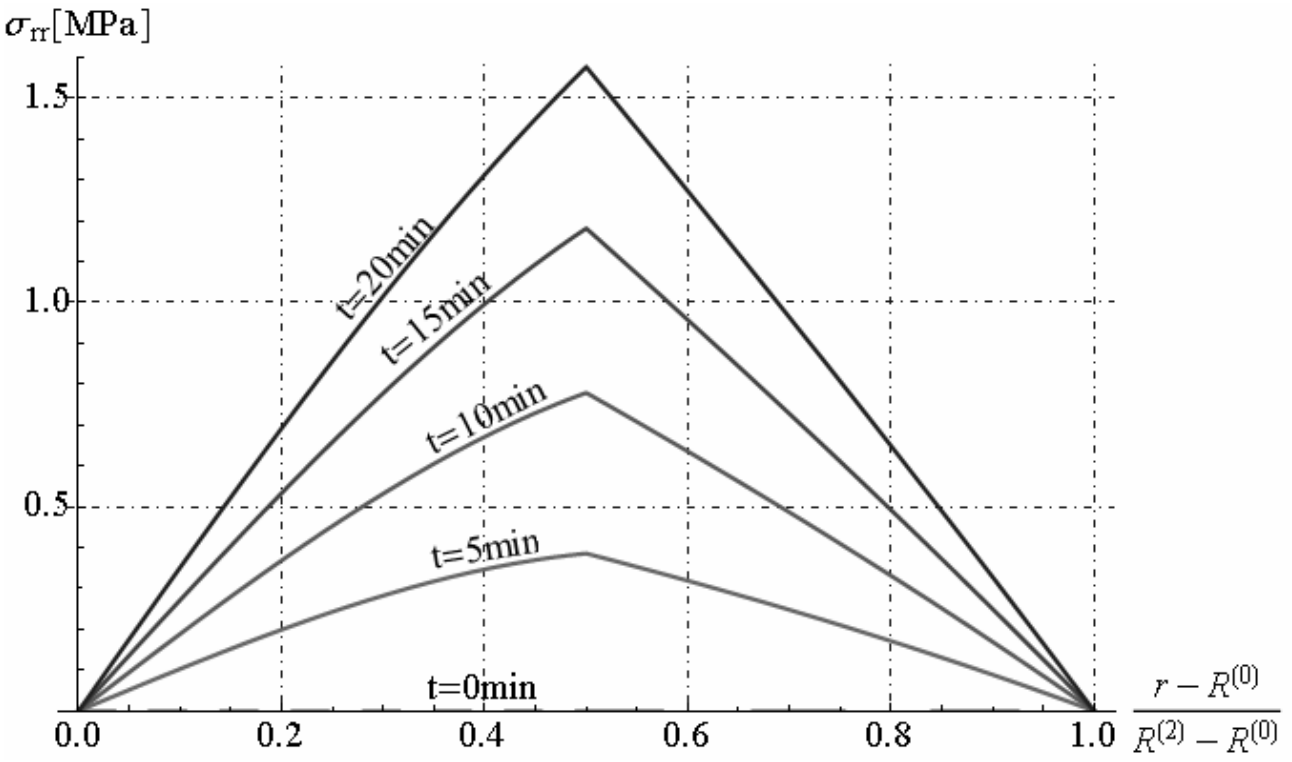

Fig. 20.40 - *Radial stress along radial direction*

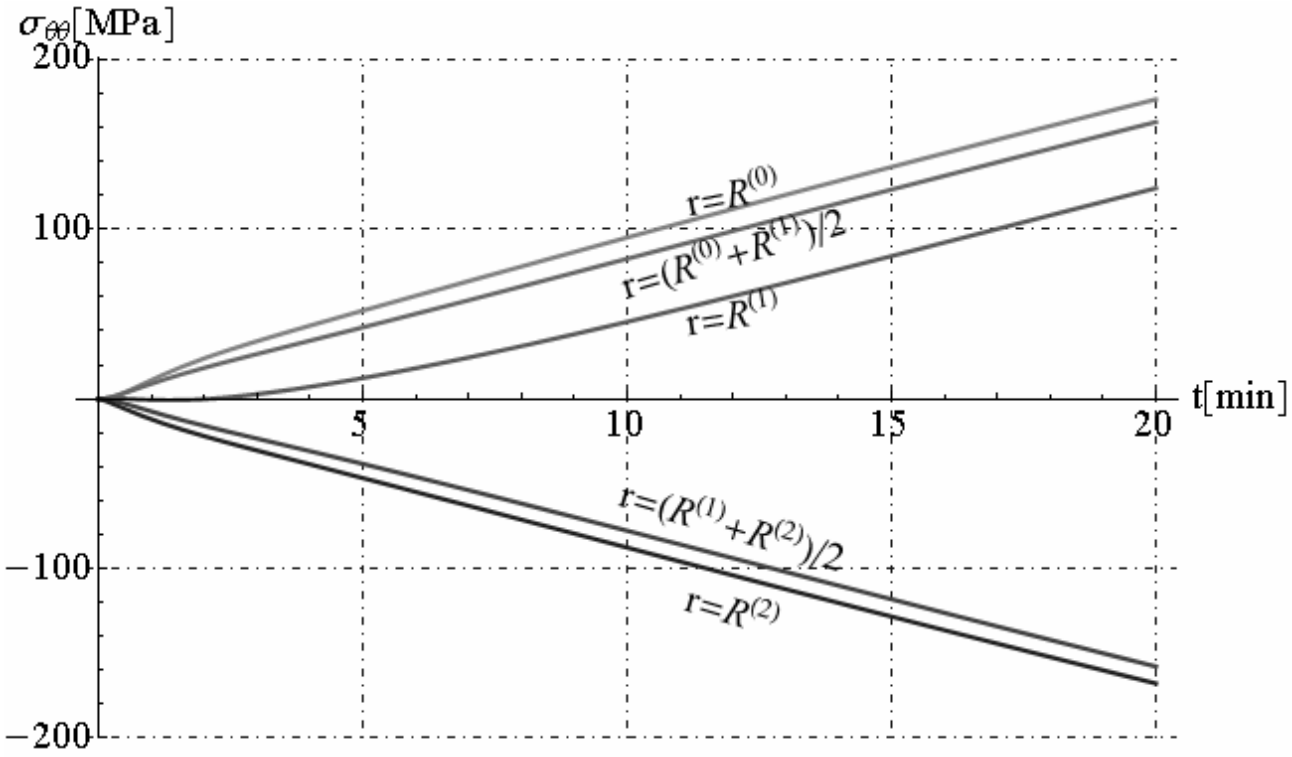

Fig. 20.41 - *Circumferential stress versus time*

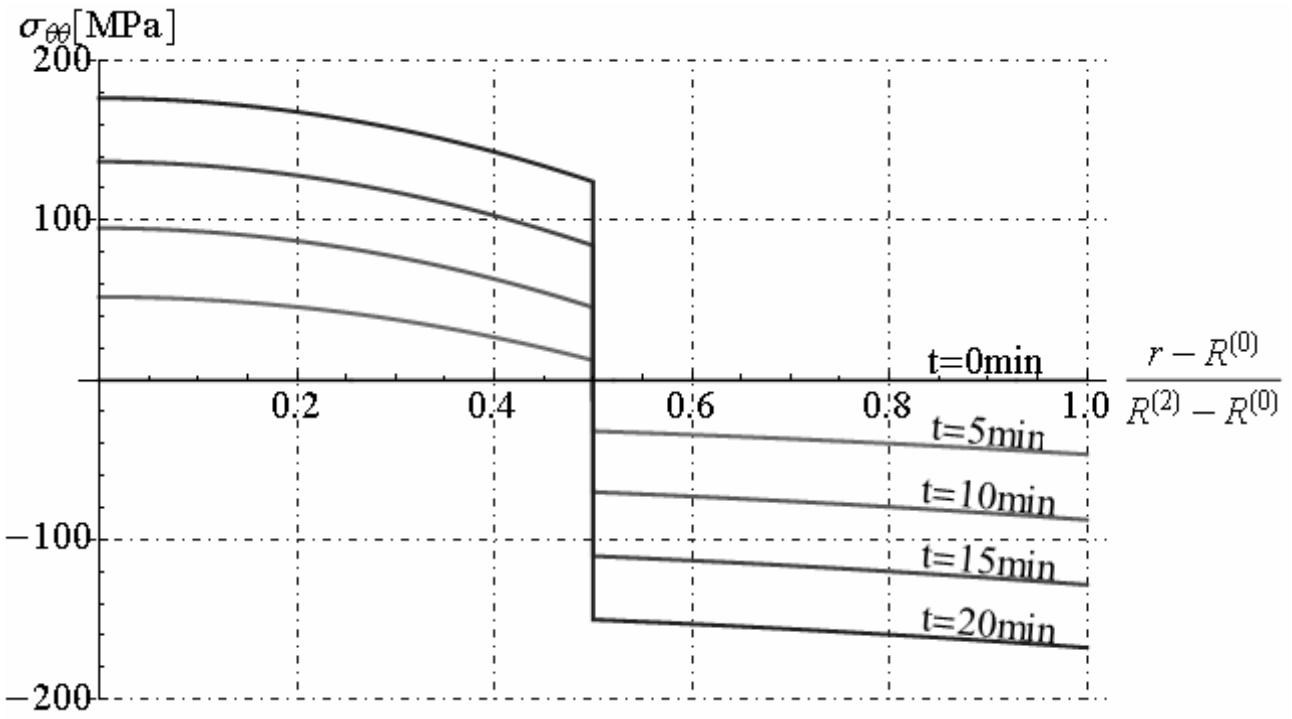

Fig. 20.42 - *Circumferential stress along radial direction*

20.5. Conclusions

In this chapter, an analytical thermo-elastic solution for spherical solid composed by multiple layers subjected to time-dependent boundary conditions, is presented. By applying the hypothesis of spherical symmetry are determined the temperature and radial displacement functions in each layer of spherical solid. Let us consider three kind of boundary conditions on inner and outer surfaces of multilayered sphere. In particular the cases analysed are: i) Multilayered sphere exposed to an ambient at zero temperature through a uniform boundary conductance, ii) Multilayered sphere exposed to uniform heat flux, iii) Multilayered sphere exposed to hydrocarbon fire. In the case iii) multilayered sphere is exposed to heat flux that varies in the time until to zero for $t \to \infty$. In three case studied the circumferential stress present the jumps in interface surface between adjacent phases, but the radial stress is continue function, as showed in figures reported in this chapter. Numerical evaluation of the series solution shows that a reasonable number of terms are sufficient to obtain results with acceptable errors for engineering applications. The technique of solutions utilised in case iii) can be developed for determine the transient stress in multilayered tank exposed to standard fire. Then, the analytical study presented can be utilized to optimize the designer of a composite spherical tank exposed to heat flux that varies in time.

20.6. References

[1] Chen, C.K. and Yang, Y.C., "Thermoelastic Transient Response of an Infinitely Long Annular Cylinder Composed of Two Different Materials," *J. Eng. Sci.*, Vol. 24, pp. 569-581 (1986).

[2] Chen, C.K. and Chen, T.M., "New Hybrid Laplace Transform/Finite Element Method for Three-Dimensional Transient Heat Conduction Problem," *Int. J. Numerical Methods Engin.*, Vol. 32, No. 1, pp. 45-61 (1991).

[3] Ghosn, A.H. and Sabbaghian, M., "Quasi-Static Coupled Problems of Thermoelasticity for Cylindrical Regions," *J. Thermal Stresses*, Vol. 5, pp. 299-313 (1982).

[4] Fraldi, M., Nunziante, L., Carannante, F. (2007), *Axis-symmetrical Solutions for n-plies Functionally Graded Material Cylinders under Strain no-Decaying Conditions*, J. Mech. of Adv. Mat. and Struct. Vol. 14 (3), pp. 151-174 - DOI: 10.1080/15376490600719220

[5] M. Fraldi, L. Nunziante, F. Carannante, A. Prota, G. Manfredi, E. Cosenza (2008), *On the Prediction of the Collapse Load of Circular Concrete Columns Confined by FRP*, Journal Engineering structures, Vol. 30, Issue 11, November 2008, Pages 3247-3264 - DOI: 10.1016/j.engstruct.2008.04.036
[6] Fraldi, M., Nunziante, L., Chandrasekaran, S., Carannante, F., Pernice, MC. (2009), *Mechanics of distributed fibre optic sensors for strain measurements on rods*, Journal of Structural Engineering, 35, pp. 323-333, Dec. 2008- Gen. 2009
[7] M. Fraldi, F. Carannante, L. Nunziante (2012), *Analytical solutions for n-phase Functionally Graded Material Cylinders under de Saint Venant load conditions: Homogenization and effects of Poisson ratios on the overall stiffness*, Composites Part B: Engineering, Volume 45, Issue 1, February 2013, Pages 1310–1324
[8] Nunziante, L., Gambarotta, L., Tralli, A., *Scienza delle Costruzioni*, 3° Edizione, McGraw-Hill, 2011, ISBN: 9788838666971
[9] Jane, K.C. and Lee, Z.Y., "Thermoelastic Transient Response of an Infinitely Long Multilayered Cylinder," *Mech. Res. Comm.*, Vol. 26, No. 6, pp. 709-718 (1999).
[10] Kandil, A., "Investigation of Stress Analysis in Compound Cylinders Under High Pressure and Temperature," M. Sc. Thesis, CIT Helwan Univ., Egypt (1975).
[11] Sherief, H.H. and Anwar, M.N., "A Problem in Generalized Thermoelasticity for an Infinitely Long Annular Cylinder," *Int. J. Eng. Sci.*, Vol. 26, pp. 301-306 (1988).
[12] Takeuti, Y. and Furukawa, T., "Some Consideration on Thermal Shock Problem in a Plate," *J. Appl. Mech.*, Vol. 48, pp. 113-118 (1981).
[13] van Wylen, G.V., Sonntag, R., and Borgnakke, C., *Fundamentals of Classical Thermodynamics*, Fourth Edition, Wiley, New York (1994).
[14] Vollbrecht, H., "Stress in Cylindrical and Spherical Walls Subjected to Internal Pressure and Stationary Heat Flow," *Verfahrenstechnik*, Vol. 8, pp. 109-112 (1974).
[15] Zong-Yi Lee, "Coupled problem of thermoelasticity for multilayered spheres with time-dependent boundary conditions ", *Journal of Marine Science and Technology*, Vol. 12, No. 2, pp. 93-101 (2004)
[16] F. de Monte, *Transverse eigenproblem of steady-state heat conduction for multi-dimensional two-layered slabs with automatic computation of eigenvalues*, International Journal of Heat and Mass Transfer 47 (2004) 191–201
[17] Suneet Singh, Prashant K. Jain, Rizwan-uddin, *Analytical solution to transient heat conduction in polar coordinates with multiple layers in radial direction*, International Journal of Thermal Sciences 47 (2008) 261–273
[18] Prashant K. Jain, Suneet Singh, Rizwan-uddin, *Analytical Solution to Transient Asymmetric Heat Conduction in a Multilayer Annulus*, Journal of Heat Transfer - January 2009, Vol. 131
[19] M.kayhani, M.,Nourouzi, and A. Amiri Delooei, *An Exact Solution of Axi-symmetric Conductive Heat Transfer in Cylindrical Composite Laminate under the General Boundary Condition*, World Academy of Science, Engineering and Technology 69 2010

CHAPTER XXI
TRANSIENT PROBLEMS FOR MULTILAYERED CYLINDERS

21.1. Basic equations for time-dependent problem in plane strain

In this chapter, the one-dimensional quasi-static uncoupled thermo-elastic problem of a multilayered cylinder with time-dependent boundary conditions is considered. The medium is without body forces and heat generation. The analytical solution is obtained by applying the method of separation of variables. It is considered a multilayered cylinder composed of *n* fictitious layers constituted by *n* hollow cylinder phases (see Chapter XVII). The external radius and internal radius of the multilayered cylinder are denoted by $R^{(n)}$ and $R^{(0)}$, respectively. The radius at interface between the generic phase *i-th* and the phase *(i+1)-th* are denoted with $R^{(i)}$. The mechanical and thermal properties of each layer are assumed to be homogeneous and isotropic and are denoted with apex (i). Cylindrical coordinates r, θ and z are used in this analysis. The multilayered cylinder is subjected to external heat flux that varying in the time, characterized by two functions $q_e(t), q_i(t)$ related to internal and external surfaces, respectively. Moreover, the multilayered cylinder is subjected to an external pressure $p_e(t)$ and an internal pressure $p_i(t)$ applied on the inner and the outer surface $r = R^{(n)}$ and $r = R^{(0)}$, respectively. These pressure are function of variable time. Details of multilayered cylinder are shown in Chapter XVII. Afterwards, it is presented a method to solve a mono-dimensional thermo-elastic problem. The basic thermo-elastic equations for the *i*-th layer can be expressed as reported below.

In isotropic-thermal elasticity case the strains are related to the displacements by purely geometrical considerations. By applying the hypothesis of *plane strain* and if the composite material is subjected to axial-symmetric thermal loads in the time, in cylindrical coordinate, the displacement components for generic phase are given by:

$$u_r^{(i)} = u_r^{(i)}(r,t), \quad u_\theta^{(i)} = 0, \quad u_z^{(i)} = 0, \quad \forall i \in \{1,2,...n\} \tag{21.1}$$

where we denote with apex 1,2,…n the hollow phases of multilayered cylinder. Then, the strain-displacement relations take the form:

$$\varepsilon_{rr}^{(i)} = u_{r,r}^{(i)}, \quad \varepsilon_{\theta\theta}^{(i)} = r^{-1}u_r^{(i)}, \quad \varepsilon_{zz}^{(i)} = \varepsilon_{\theta z}^{(i)} = \varepsilon_{r\theta}^{(i)} = \varepsilon_{rz}^{(i)} = 0 \quad \forall i \in \{1,2,...n\} \tag{21.2}$$

where $u_r^{(i)}, u_\theta^{(i)}, u_z^{(i)}$, are the radial, circumferential and axial displacement components in the *i*-th layer ($R^{(i)} < r < R^{(i+1)}$). The superscript *"i"* represents the *i*-th layer and the comma represents the partial derivate. Thermo-elastic stress-strain relations for i-th phase ($\forall i \in \{1,2,...n\}$) are given by:

$$\begin{aligned}
\sigma_{rr}^{(i)} &= \left(2\mu^{(i)} + \lambda^{(i)}\right)u_{r,r}^{(i)} + \lambda^{(i)}r^{-1}u_r^{(i)} - \alpha^{(i)}\left(3\lambda^{(i)} + 2\mu^{(i)}\right)\left(T^{(i)} - T_R\right) \\
\sigma_{\theta\theta}^{(i)} &= \lambda^{(i)}u_{r,r}^{(i)} + \left(2\mu^{(i)} + \lambda^{(i)}\right)r^{-1}u_r^{(i)} - \alpha^{(i)}\left(3\lambda^{(i)} + 2\mu^{(i)}\right)\left(T^{(i)} - T_R\right) \\
\sigma_{zz}^{(i)} &= \lambda^{(i)}\left(u_{r,r}^{(i)} + r^{-1}u_r^{(i)}\right) - \alpha^{(i)}\left(3\lambda^{(i)} + 2\mu^{(i)}\right)\left(T^{(i)} - T_R\right), \quad \tau_{rz}^{(i)} = \tau_{\theta z}^{(i)} = \tau_{r\theta}^{(i)} = 0,
\end{aligned} \tag{21.3}$$

where $\mu^{(i)}, \lambda^{(i)}, \alpha^{(i)}, T^{(i)}$ are the Lamè elastic constants, linear thermal expansion coefficient and temperature in the *i*-th layer, respectively; T_R is the reference temperature. Moreover, let us assume that the function of the temperature in each phase is a function of radius and time as reported below:

$$T^{(i)} = T^{(i)}(r,t) \quad \forall i \in \{1,2,....,n\} \tag{21.4}$$

The equations of equilibrium are the same as those of isothermal elasticity since they are based on purely mechanical considerations. By applying the hypothesis of the axial-symmetric temperature loads and in absence of the body force, and neglecting the effect of the inertia, the equilibrium equations become one equation:

$$\sigma_{rr,r}^{(i)} + \left(\sigma_{rr}^{(i)} - \sigma_{\theta\theta}^{(i)}\right)r^{-1} = 0 \quad \forall i \in \{1,2,...n\} \tag{21.5}$$

The results obtained until now satisfy the equilibrium and compatibility equations inside each generic *i*-th phase of a composite spherical solid subjected to axis-symmetrical strains or temperature loads time-dependent. Under both the hypothesis of linear isotropic elastic behaviour of the homogeneous materials and the assumption of perfect bond at the spherical interfacial boundaries (no de-lamination or friction phenomena), we have now to establish the satisfaction of both the equilibrium and the compatibility equations at the boundary surfaces between two generic adjacent phases. To obtain this, we will make reference to the generic case, in which an multilayered cylinder is constituted by *n* arbitrary hollow phases (Chapter XVII). In this framework the following boundary conditions be established. In particular, we begin writing the compatibility equations at the generic interface, that is:

$$u_r^{(i)}(r=R^{(i)},t)=u_r^{(i+1)}(r=R^{(i)},t) \quad \forall t\geq 0,\ \forall i\in\{1,2,...n-1\} \tag{21.6}$$

The equilibrium equations at the generic interface are given by:

$$\sigma_{rr}^{(i)}(r=R^{(i)},t)=\sigma_{rr}^{(i+1)}(r=R^{(i)},t) \quad \forall i\in\{1,2,...n-1\} \tag{21.7}$$

The equilibrium equations for tractions on the inner and the outer cylindrical boundary surface give:

$$\sigma_{rr}^{(n)}(r=R^{(n)},t)=p_e(t),\quad \sigma_{rr}^{(1)}(r=R^{(0)},t)=p_i(t) \quad \forall t\geq 0 \tag{21.8}$$

where $p_e(t), p_i(t)$ are the pressure applied on the inner and the outer surface of multilayered cylinder that are prescribed function only variable time, respectively. The equation field for coupled heat conduction problem is written in hypothesis of axial symmetric load conditions for each phases of multilayered cylinder.

$$k^{(i)}\left(T_{,rr}^{(i)}+r^{-1}T_{,r}^{(i)}\right)=\rho^{(i)}c^{(i)}T_{,t}^{(i)}+\alpha^{(i)}\left(3\lambda^{(i)}+2\mu^{(i)}\right)T_R\left(u_{,r}^{(i)}+r^{-1}u_r^{(i)}\right)_{,t} \quad \forall i\in\{1,2,...n\} \tag{21.9}$$

where $\rho^{(i)}, c^{(i)}, k^{(i)}, T_R$ are density, specific heat, thermal conductivity coefficient, temperature reference for each phases, respectively. Temperature boundary and continuity conditions are written at the interfaces between the phases, and on internal and external surfaces of multilayered cylinder. Then, at interfaces between the phases the following conditions can be write:

$$\begin{cases} T^{(i)}(r=R^{(i)},t)=T^{(i+1)}(r=R^{(i)},t) \\ k^{(i)}T_{,r}^{(i)}(r=R^{(i)},t)=k^{(i+1)}T_{,r}^{(i+1)}(r=R^{(i)},t) \end{cases} \quad \forall t\geq 0,\ \forall i\in\{1,2,...n-1\} \tag{21.10}$$

The boundary conditions on the inner and the outer surface impose that heat flux is equal to $q_i(t)$ and $q_e(t)$, respectively:

$$-k^{(n)}T_{,r}^{(n)}(r=R^{(n)},t)=q_e(t),\quad -k^{(1)}T_{,r}^{(1)}(r=R^{(0)},t)=q_i(t),\quad \forall t\geq 0 \tag{21.11}$$

The initial condition for temperature function is given by:

$$T=T_R;\quad R^{(i-1)}<r<R^{(i)},\ \forall i\in\{1,2,....,n\},\ t=0, \tag{21.12}$$

where $T_0=T_R$ is a suitable chosen reference temperature in initial condition (for t = 0).

21.2. Multilayered cylinder exposed to an ambient at zero temperature through a uniform boundary conductance

Let us consider an multilayered cylinder constituted by n-hollow cylindrical phases as decrypted in section 21.1. The surface $r=R^{(0)}$ is kept perfectly insulated while the surface $r=R^{(n)}$ is exposed, for t >0, to an ambient at zero temperature through a uniform boundary conductance h_c. The initial temperature (for t = 0) of the hollow cylinder is $T_0=T_R=const$ where $T_R>0$. In this section, we determine the heat conduction, displacement and stress function in hollow cylinder under decreasing of temperature from $T_R>0$ until to zero. The equations field in each phase are composed by equilibrium and heat conduction equations. By substituting the strain-displacement relations (21.2) in stress-strain relations (21.3) and these in equilibrium equations (21.5), we obtain the displacement formulation of the equilibrium equations. Then, the equations field to satisfy in uncoupled thermo-elastic problem in plane strain are given by:

$$\begin{cases} \left[r^{-1}\left(r\, u_r^{(i)} \right)_{,r} \right]_{,r} = \alpha^{(i)} \left(\dfrac{3\lambda^{(i)} + 2\mu^{(i)}}{2\mu^{(i)} + \lambda^{(i)}} \right) = \alpha^{(i)} \left(\dfrac{1+\nu^{(i)}}{1-\nu^{(i)}} \right) T_{,r}^{(i)} & R^{(i-1)} \le r \le R^{(i)}, \quad \forall t \ge 0, \\ T_{,rr}^{(i)} + r^{-1} T_{,r}^{(i)} = \dfrac{\rho^{(i)} c^{(i)}}{k^{(i)}} T_{,t}^{(i)} = \dfrac{T_{,t}^{(i)}}{\kappa^{(i)}} & \forall i \in \{1,2,...,n\} \end{cases} \tag{21.13}$$

where $\kappa^{(i)}$ is the thermal diffusivity for generic i-th phase. By solving the Fourier's equation reported in second equation of (21.13) with method separation of variables, and by substituting the function of temperature $T^{(i)}(r,t)$ in first equation of (21.13), and by integration in two time this equation respect to variable r , the explicit displacement solution is obtained:

$$u_r^{(i)}(r,t) = \frac{\alpha^{(i)}}{r} \left(\frac{3\lambda^{(i)} + 2\mu^{(i)}}{\lambda^{(i)} + 2\mu^{(i)}} \right) \int r\, T^{(i)}(r,t)\, dr + r\, f_1^{(i)}(t) + \frac{f_2^{(i)}(t)}{r}, \quad \forall i \in \{1,2,....,n\} \tag{21.14}$$

where $f_1^{(i)}(t)$, $f_2^{(i)}(t)$ are unknown functions of the time to determine.

The heat conduct problem is characterized by homogeneous differential equation reported in second equation of (21.13) and boundary conditions reported in equations (21.10)-(21.11) and may be treated by the method separation of variables. A particular solution of the Fourier's differential equation is given by:

$$T^{(i)}(r,t) = \varphi^{(i)}(r)\, \psi^{(i)}(t) \qquad \forall i \in \{1,2,....,n\} \tag{21.15}$$

By substituting the function (21.15) in Fourier's heat equation we obtain two ordinary differential equations in variable radius and time, separately. The first equation for function $\varphi^{(i)}(r)$

$$\varphi_{,rr}^{(i)} + r^{-1}\varphi_{,r}^{(i)} + \omega^2 \beta^{(i)2} \varphi^{(i)} = 0; \tag{21.16}$$

where the coefficient $\beta^{(i)} = \sqrt{\kappa^{(1)} / \kappa^{(i)}}$ and to the following equation for $\psi^{(i)}(t)$:

$$\psi_{,t}^{(i)} + \omega^2 \beta^{(i)2} \kappa^{(i)} \psi^{(i)} = 0 \tag{21.17}$$

The general solution of (21.17) is:

$$\psi^{(i)}(t) = e^{-\omega^2 \beta^{(i)2} \kappa^{(i)} t} \tag{21.18}$$

The equation (21.16) is an Bessel differential equation and the solution is given by:

$$\varphi^{(i)}(r) = A^{(i)}\, J_0\left(\beta^{(i)} \omega r \right) + B^{(i)}\, Y_0\left(\beta^{(i)} \omega r \right) \tag{21.19}$$

where $J_0\left(\beta^{(i)} \omega r \right), Y_0\left(\beta^{(i)} \omega r \right)$ are *Bessel function*, and $A^{(i)}, B^{(i)}$ are constants integration. The boundary conditions for heat problem (21.10) in this case become:

$$\begin{cases} A^{(i)}\, J_0\left(\beta^{(i)} \omega R^{(i)} \right) + B^{(i)}\, Y_0\left(\beta^{(i)} \omega R^{(i)} \right) - A^{(i+1)}\, J_0\left(\beta^{(i+1)} \omega R^{(i)} \right) - B^{(i+1)}\, Y_0\left(\beta^{(i+1)} \omega R^{(i)} \right) = 0 \\ \left[A^{(i)}\, J_1\left(\beta^{(i)} \omega R^{(i)} \right) + B^{(i)}\, Y_1\left(\beta^{(i)} \omega R^{(i)} \right) \right] k^{(i)} \beta^{(i)} + \\ \qquad - \left[A^{(i+1)}\, J_1\left(\beta^{(i+1)} \omega R^{(i)} \right) + B^{(i+1)}\, Y_1\left(\beta^{(i+1)} \omega R^{(i)} \right) \right] k^{(i+1)} \beta^{(i+1)} = 0 \\ \qquad\qquad \forall i \in \{1,2,...,n-1\} \end{cases} \tag{21.20}$$

The boundary conditions on the inner and the outer surface (21.11) become:

$$-k^{(1)} T_{,r}^{(1)}(r = R^{(0)}) = 0, \quad -k^{(n)} T_{,r}^{(n)}(r = R^{(n)}) = h_c T^{(n)}(r = R^{(n)}), \quad \forall t \ge 0 \tag{21.21}$$

In explicit the equations (21.21) become:

$$\begin{cases} A^{(1)}\, J_1\left(\beta^{(1)} \omega R^{(0)} \right) + B^{(1)}\, Y_1\left(\beta^{(1)} \omega R^{(0)} \right) = 0 \\ \omega \beta^{(n)} k^{(n)} \left[A^{(n)}\, J_1\left(\beta^{(n)} \omega R^{(n)} \right) + B^{(n)}\, Y_1\left(\beta^{(n)} \omega R^{(n)} \right) \right] + \\ \qquad - h_c \left[A^{(n)}\, J_0\left(\beta^{(n)} \omega R^{(n)} \right) + B^{(n)}\, Y_0\left(\beta^{(n)} \omega R^{(n)} \right) \right] = 0 \end{cases} \tag{21.22}$$

By first equation of (21.22), we determine $B^{(1)}$ as function of $A^{(1)}$ as follows:

$$B^{(1)} = -\left[J_1\left(\beta^{(1)}\omega R^{(0)}\right) \Big/ Y_1\left(\beta^{(1)}\omega R^{(0)}\right)\right] A^{(1)} \tag{21.23}$$

The equations (21.20) constituted an homogeneous algebraic system, composed by 2(n-1) equations, in unknown parameters $A^{(i)}, B^{(i)}$ with $i \in \{1,2,...,n\}$, which can be written as:

$$\boldsymbol{\Phi} \cdot \mathbf{X} = \mathbf{0} \tag{21.24}$$

where $\mathbf{X} = [\mathbf{X}^{(1)}, \mathbf{X}^{(2)}, ..., \mathbf{X}^{(n)}]^T$ collect the unknowns sub-vectors, as reported below:

$$\mathbf{X}^{(i)} = \left[A^{(i)} \quad B^{(i)} \right]^T, \quad \forall i \in \{1,2,....,n\} \tag{21.25}$$

and $\boldsymbol{\Phi}$ is an $2(n-1)x2n$ rectangular matrix, composed by following sub-matrices:

$$\boldsymbol{\Phi} = \begin{bmatrix} \boldsymbol{\Phi}_1^{(1)} & -\boldsymbol{\Phi}_1^{(2)} & \mathbf{0} & \mathbf{0} & \cdots & \mathbf{0} & \mathbf{0} & \mathbf{0} \\ \mathbf{0} & \boldsymbol{\Phi}_2^{(2)} & -\boldsymbol{\Phi}_2^{(3)} & \mathbf{0} & \cdots & \mathbf{0} & \mathbf{0} & \mathbf{0} \\ \mathbf{0} & \mathbf{0} & \boldsymbol{\Phi}_3^{(3)} & -\boldsymbol{\Phi}_3^{(4)} & \cdots & \mathbf{0} & \mathbf{0} & \mathbf{0} \\ \vdots & \vdots & \vdots & \vdots & \vdots & \vdots & \vdots & \vdots \\ \mathbf{0} & \mathbf{0} & \mathbf{0} & \mathbf{0} & \cdots & \boldsymbol{\Phi}_{n-2}^{(n-2)} & -\boldsymbol{\Phi}_{n-2}^{(n-1)} & \mathbf{0} \\ \mathbf{0} & \mathbf{0} & \mathbf{0} & \mathbf{0} & \cdots & \mathbf{0} & \boldsymbol{\Phi}_{n-1}^{(n-1)} & -\boldsymbol{\Phi}_{n-1}^{(n)} \end{bmatrix} \tag{21.26}$$

where $\boldsymbol{\Phi}_i^{(i)}, \boldsymbol{\Phi}_i^{(i+1)}$ are $(2x2)$ generic square sub-matrices given by:

$$\begin{aligned} \boldsymbol{\Phi}_i^{(i)} &= \begin{bmatrix} J_0\left(\beta^{(i)}\omega R^{(i)}\right) & Y_0\left(\beta^{(i)}\omega R^{(i)}\right) \\ k^{(i)}\beta^{(i)} J_1\left(\beta^{(i)}\omega R^{(i)}\right) & k^{(i)}\beta^{(i)} Y_1\left(\beta^{(i)}\omega R^{(i)}\right) \end{bmatrix}, \\ \boldsymbol{\Phi}_i^{(i+1)} &= \begin{bmatrix} J_0\left(\beta^{(i+1)}\omega R^{(i)}\right) & Y_0\left(\beta^{(i+1)}\omega R^{(i)}\right) \\ k^{(i+1)}\beta^{(i+1)} J_1\left(\beta^{(i+1)}\omega R^{(i)}\right) & k^{(i+1)}\beta^{(i+1)} Y_1\left(\beta^{(i+1)}\omega R^{(i)}\right) \end{bmatrix}, \end{aligned} \tag{21.27}$$

The determinant of the matrices (21.27) is given by:

$$\begin{aligned} \det[\boldsymbol{\Phi}_i^{(i)}] &= k^{(i)}\beta^{(i)}\left[J_0\left(\beta^{(i)}\omega R^{(i)}\right) Y_1\left(\beta^{(i)}\omega R^{(i)}\right) - Y_0\left(\beta^{(i)}\omega R^{(i)}\right) J_1\left(\beta^{(i)}\omega R^{(i)}\right)\right] \neq 0, \\ \det[\boldsymbol{\Phi}_i^{(i+1)}] &= k^{(i+1)}\beta^{(i+1)}\left[J_0\left(\beta^{(i+1)}\omega R^{(i)}\right) Y_1\left(\beta^{(i+1)}\omega R^{(i)}\right) - Y_0\left(\beta^{(i+1)}\omega R^{(i)}\right) J_1\left(\beta^{(i+1)}\omega R^{(i)}\right)\right] \neq 0, \end{aligned} \tag{21.28}$$

Then, the matrices (21.27) are invertible and by applying an *in-cascade* procedure, we obtain the generic vector $\mathbf{X}^{(i)}$ as function of vector $\mathbf{X}^{(1)}$:

$$\mathbf{X}^{(i)} = \boldsymbol{\Gamma}^{(i)} \cdot \mathbf{X}^{(1)} \quad \forall i \in \{2,3,...,n\} \tag{21.29}$$

where $\boldsymbol{\Gamma}^{(i)}$ is an $2x2$ square matrix given by :

$$\boldsymbol{\Gamma}^{(i)} = \prod_{j=1}^{i-1}\left(\left[\boldsymbol{\Phi}_{i-j}^{(i-j+1)} \right]^{-1} \cdot \boldsymbol{\Phi}_{i-j}^{(i-j)} \right) \quad \forall i \in \{2,3,...,n\} \tag{21.30}$$

By substituting the solutions (21.29) in boundary conditions (21.22), we obtain vector equations in unknown vector $\mathbf{X}^{(1)}$, as reported below:

$$\boldsymbol{\Lambda} \cdot \mathbf{X}^{(1)} = \mathbf{0} \tag{21.31}$$

where $\boldsymbol{\Lambda}$ is an 2x2 square matrix given by :

$$\boldsymbol{\Lambda} = \begin{bmatrix} \Lambda_{11} & \Lambda_{12} \\ \Lambda_{21} & \Lambda_{22} \end{bmatrix} \tag{21.32}$$

where the components $\Lambda_{11}, \Lambda_{12}, \Lambda_{21}, \Lambda_{22}$ are reported below:

$$\Lambda_{11}=J_1\left(\beta^{(1)}\omega R^{(0)}\right),\ \Lambda_{12}=Y_1\left(\beta^{(1)}\omega R^{(0)}\right),$$
$$\begin{bmatrix}\Lambda_{21}\\ \Lambda_{22}\end{bmatrix}=\begin{bmatrix}\beta^{(n)}R^{(n)}J_1\left(\omega\beta^{(n)}R^{(n)}\right)-h_cJ_0\left(\omega\beta^{(n)}R^{(n)}\right)\\ \beta^{(n)}R^{(n)}Y_1\left(\omega\beta^{(n)}R^{(n)}\right)-h_cY_0\left(\omega\beta^{(n)}R^{(n)}\right)\end{bmatrix}^T\cdot\boldsymbol{\Gamma}^{(n)},\tag{21.33}$$

The algebraic system (21.31) admit not trivial solution if the determinant of matrix $[\boldsymbol{\Lambda}]$ is equal to zero. By imposing this condition, we obtain the transcendental equation in unknown parameter ω:

$$\det[\boldsymbol{\Lambda}]=0\ \Rightarrow\ g(\omega)=0\tag{21.34}$$

The roots of this transcendental equation (21.34) are an infinite number such, denoted here by ω_m, $m=1,2,....N$ leading to eigenvalues or characteristic values $\lambda_m=-\omega_m^2$. The corresponding eigenfunctions or characteristic functions $\bar{\varphi}_m^{(i)}(r)=\varphi_m^{(i)}(r)/A_m^{(i)}$ are, as calculated above,

$$\begin{aligned}&\bar{\varphi}_m^{(1)}(r)=\left[A_m^{(1)}\right]^{-1}\left[J_0(\omega_m r),\ Y_0(\omega_m r)\right]\cdot\mathbf{X}_m^{(1)} && \left(\beta^{(1)}=1\right)\\ &\bar{\varphi}_m^{(i)}(r)=\left[A_m^{(i)}\right]^{-1}\left[J_0\left(\beta^{(n)}\omega_m r\right),\ Y_0\left(\beta^{(n)}\omega_m r\right)\right]\cdot\left(\boldsymbol{\Gamma}^{(i)}\cdot\mathbf{X}_m^{(1)}\right) && \forall i\in\{2,3,...,n\}\end{aligned}\tag{21.35}$$

The temperature function in any phase can to be written in the follows form:

$$\begin{aligned}&T^{(1)}(r,t)=\sum_{m=1}^{\infty}\left\{\left[J_0(\omega_m r),\ Y_0(\omega_m r)\right]\cdot\mathbf{X}_m^{(1)}\right\}e^{-\kappa^{(1)}\omega_m^2 t} && \left(\beta^{(1)}=1\right)\\ &T^{(i)}(r,t)=\sum_{m=1}^{\infty}\left\{\left[J_0\left(\beta^{(n)}\omega_m r\right),\ Y_0\left(\beta^{(n)}\omega_m r\right)\right]\cdot\left(\boldsymbol{\Gamma}^{(i)}\cdot\mathbf{X}_m^{(1)}\right)\right\}e^{-\kappa^{(i)}\omega_m^2\beta^{(i)2}t} && \forall i\in\{2,3,...,n\}\end{aligned}\tag{21.36}$$

where the vector $\mathbf{X}_m^{(1)}=\left[A_m^{(1)},B_m^{(1)}\right]^T$ and the unknown constant $B_m^{(i)}$ depends by $A_m^{(1)}$ as showed equations (21.23). The coefficients $A_m^{(1)}$ are determined by applying the initial condition (21.12) that yields the following relationship:

$$A_m^{(1)}=\frac{\sum_{i=1}^{n}\left[\rho^{(i)}c_v^{(i)}\int_0^{2\pi}\int_{R^{(i-1)}}^{R^{(i)}}\bar{\varphi}_m^{(i)}\,T_R\,r\,dr\,d\theta\right]}{\sum_{i=1}^{n}\left[\rho^{(i)}c_v^{(i)}\int_0^{2\pi}\int_{R^{(i-1)}}^{R^{(i)}}\left(\bar{\varphi}_m^{(i)}\right)^2 r\,dr\,d\theta\right]}\tag{21.37}$$

By substituting the function (21.36), in equation (21.14), we obtain in explicit the displacement function in any hollow cylindrical phase:

$$\begin{aligned}u_r^{(i)}&=G^{(i)}r+H^{(i)}r^{-1}+\sum_{m=1}^{\infty}\left[C_m^{(i)}r+D_m^{(i)}r^{-1}\right]e^{-\kappa^{(i)}\omega_m^2\beta^{(i)2}t}+\\&+\sum_{m=1}^{\infty}\left\{\frac{\alpha^{(i)}\left(3\lambda^{(i)}+2\mu^{(i)}\right)}{\omega_m\beta^{(i)}\left(\lambda^{(i)}+2\mu^{(i)}\right)r^2}\left[A_m^{(i)}J_0\left(\beta^{(i)}\omega_m r\right)+B_m^{(i)}Y_0\left(\beta^{(i)}\omega_m r\right)\right]\right\}e^{-\kappa^{(i)}\omega_m^2\beta^{(i)2}t}\end{aligned}\tag{21.38}$$

where the integration constants $G^{(i)},H^{(i)},C_m^{(i)},D_m^{(i)}$ are determined by applying the boundary conditions give by equations (21.6),(21.7) and (21.8). In this case the functions $f_1^{(i)}(t)$, $f_2^{(i)}(t)$, reported in equation (21.14) are given by:

$$f_1^{(i)}(t)=G^{(i)}+\sum_{m=1}^{\infty}C_m^{(i)}e^{-\kappa^{(i)}\omega_m^2\beta^{(i)2}t},\quad f_2^{(i)}(t)=H^{(i)}+\sum_{m=1}^{\infty}D_m^{(i)}e^{-\kappa^{(i)}\omega_m^2\beta^{(i)2}t},\tag{21.39}$$

In explicit the radial, circumferential and axial stress components are given by:

$$\sigma_{rr}^{(i)} = 2G^{(i)}\left(\lambda^{(i)}+2\mu^{(i)}\right)+\alpha^{(i)}T_R\left(3\lambda^{(i)}+2\mu^{(i)}\right)-2\mu^{(i)}H^{(i)}r^{-2}+$$
$$+2\sum_{m=1}^{\infty}\left[C_m^{(i)}\left(\lambda^{(i)}+\mu^{(i)}\right)-D_m^{(i)}\mu^{(i)}r^{-2}\right]e^{-\omega_m^2\beta^{(i)2}\kappa^{(i)}t}+ \tag{21.40}$$
$$+2\alpha^{(i)}\mu^{(i)}\frac{\left(3\lambda^{(i)}+2\mu^{(i)}\right)}{\left(\lambda^{(i)}+2\mu^{(i)}\right)}\sum_{m=1}^{\infty}\left[A^{(i)}J_1\left(\beta^{(i)}\omega r\right)+B^{(i)}Y_1\left(\beta^{(i)}\omega r\right)\right]e^{-\omega_m^2\beta^{(i)2}\kappa^{(i)}t}$$

$$\sigma_{\theta\theta}^{(i)} = 2G^{(i)}\left(\lambda^{(i)}+2\mu^{(i)}\right)+\alpha^{(i)}T_R\left(3\lambda^{(i)}+2\mu^{(i)}\right)+2\mu^{(i)}H^{(i)}r^{-2}+$$
$$+2\sum_{m=1}^{\infty}\left[C_m^{(i)}\left(\lambda^{(i)}+\mu^{(i)}\right)+D_m^{(i)}\mu^{(i)}r^{-2}\right]e^{-\omega_m^2\beta^{(i)2}\kappa^{(i)}t}+ \tag{21.41}$$
$$+\frac{2\alpha^{(i)}\mu^{(i)}\left(3\lambda^{(i)}+2\mu^{(i)}\right)}{\beta^{(i)}\omega r\left(\lambda^{(i)}+2\mu^{(i)}\right)}\sum_{m=1}^{\infty}\left\{\begin{array}{l}\left[A^{(i)}J_1\left(\beta^{(i)}\omega r\right)+B^{(i)}Y_1\left(\beta^{(i)}\omega r\right)\right]+\\ -\beta^{(i)}\omega r\left[A^{(i)}J_2\left(\beta^{(i)}\omega r\right)+B^{(i)}Y_2\left(\beta^{(i)}\omega r\right)\right]\end{array}\right\}e^{-\omega_m^2\beta^{(i)2}\kappa^{(i)}t}$$

$$\sigma_{zz}^{(i)} = 2G^{(i)}\lambda^{(i)}+\alpha^{(i)}T_R\left(3\lambda^{(i)}+2\mu^{(i)}\right)+$$
$$+2\sum_{m=1}^{\infty}\left\{C_m^{(i)}\lambda^{(i)}-\frac{\alpha^{(i)}\mu^{(i)}\left(3\lambda^{(i)}+2\mu^{(i)}\right)}{\left(\lambda^{(i)}+2\mu^{(i)}\right)}\left[A^{(i)}J_0\left(\beta^{(i)}\omega r\right)+B^{(i)}Y_0\left(\beta^{(i)}\omega r\right)\right]\right\}e^{-\omega_m^2\beta^{(i)2}\kappa^{(i)}t} \tag{21.42}$$

It is important to note that displacement function and stress components in any phases can to be subdivided in two parts: firstly constant in time and the second depend of the time. Moreover, the tractions on the inner and the outer cylindrical boundary surface are vanishing and then condition (21.8) becomes:

$$\sigma_{rr}^{(1)}(r=R^{(0)},t)=0,\ \sigma_{rr}^{(n)}(r=R^{(n)},t)=0,\quad \forall t\geq 0 \tag{21.43}$$

The integration constants $G^{(i)},H^{(i)},C_m^{(i)},D_m^{(i)}$ are function of geometrical, mechanical and thermal parameters of spherical layers . Moreover $C_m^{(i)},D_m^{(i)}$ are function of constants $A_m^{(i)},B_m^{(i)},\omega_m$ also. We can write the boundary conditions (21.6) and (21.7) in two uncoupled algebraic system as :

$$\boldsymbol{\Omega}\cdot\mathbf{W}_0=\mathbf{L}_0,\quad \boldsymbol{\Omega}\cdot\mathbf{W}_m=\mathbf{L}_m,\quad \forall m=1,2,....N \tag{21.44}$$

where the vectors $\mathbf{L}_0,\mathbf{L}_m$ are given by:

$$\mathbf{L}_j=\left[\left(\mathbf{L}_{1,j}^{(2)}-\mathbf{L}_{1,j}^{(1)}\right),\left(\mathbf{L}_{2,j}^{(3)}-\mathbf{L}_{2,j}^{(2)}\right),...,\left(\mathbf{L}_{i,j}^{(i+1)}-\mathbf{L}_{i,j}^{(i)}\right),..,\left(\mathbf{L}_{n-1,j}^{(n)}-\mathbf{L}_{n-1,j}^{(n-1)}\right)\right]^T\quad \text{with } j\in\{0,m\} \tag{21.45}$$

These vector are characterized by following sub-vectors:

$$\mathbf{L}_{i,0}^{(i)}=\begin{bmatrix}0\\ \alpha^{(i)}\left(3\lambda^{(i)}+2\mu^{(i)}\right)\end{bmatrix}T_R,\ \mathbf{L}_{i,0}^{(i+1)}=\begin{bmatrix}0\\ \alpha^{(i+1)}\left(3\lambda^{(i+1)}+2\mu^{(i+1)}\right)\end{bmatrix}T_R,$$
$$\mathbf{L}_{i,m}^{(i)}=\frac{\zeta^{(i)}R^{(i)}}{\omega_m}\begin{bmatrix}R^{(i)}J_1\left(\omega_mR^{(i)}\beta^{(i)}\right) & R^{(i)}Y_1\left(\omega_mR^{(i)}\beta^{(i)}\right)\\ -2\mu^{(i)}J_1\left(\omega_mR^{(i)}\beta^{(i)}\right) & -2\mu^{(i)}Y_1\left(\omega_mR^{(i)}\beta^{(i)}\right)\end{bmatrix}\cdot\begin{bmatrix}A_m^{(i)}\\ B_m^{(i)}\end{bmatrix} \tag{21.46}$$
$$\mathbf{L}_{i,m}^{(i+1)}=\frac{\zeta^{(i+1)}R^{(i)}}{\omega_m}\begin{bmatrix}R^{(i)}J_1\left(\omega_mR^{(i)}\beta^{(i+1)}\right) & R^{(i)}Y_1\left(\omega_mR^{(i)}\beta^{(i+1)}\right)\\ -2\mu^{(i+1)}J_1\left(\omega_mR^{(i)}\beta^{(i+1)}\right) & -2\mu^{(i+1)}Y_1\left(\omega_mR^{(i)}\beta^{(i+1)}\right)\end{bmatrix}\cdot\begin{bmatrix}A_m^{(i+1)}\\ B_m^{(i+1)}\end{bmatrix}$$

where the constant $\zeta^{(i)}=\dfrac{\alpha^{(i)}\left(3\lambda^{(i)}+2\mu^{(i)}\right)}{\beta^{(i)}\left(\lambda^{(i)}+2\mu^{(i)}\right)}$. The unknowns vectors $\mathbf{W}_0=[\mathbf{W}_0^{(1)},\mathbf{W}_0^{(2)},...,\mathbf{W}_0^{(n)}]^T$ and $\mathbf{W}_m=[\mathbf{W}_m^{(1)},\mathbf{W}_m^{(2)},...,\mathbf{W}_m^{(n)}]^T$ are composed by sub-vectors reported below:

$$\mathbf{W}_0^{(i)}=\begin{bmatrix}G^{(i)} & H^{(i)}\end{bmatrix}^T,\quad \mathbf{W}_m^{(i)}=\begin{bmatrix}C_m^{(i)} & D_m^{(i)}\end{bmatrix}^T,\quad \forall i\in\{1,2,....,n\},\ \forall m\in\{1,2,....,N\} \tag{21.47}$$

and $\boldsymbol{\Omega}$ is an $2(n-1)x2n$ rectangular matrix composed by following sub-matrices:

$$[\boldsymbol{\Omega}]=\begin{bmatrix} \boldsymbol{\Omega}_1^{(1)} & -\boldsymbol{\Omega}_1^{(2)} & \mathbf{0} & \mathbf{0} & \cdots & \mathbf{0} & \mathbf{0} & \mathbf{0} \\ \mathbf{0} & \boldsymbol{\Omega}_{2,j}^{(2)} & -\boldsymbol{\Omega}_2^{(3)} & \mathbf{0} & \cdots & \mathbf{0} & \mathbf{0} & \mathbf{0} \\ \mathbf{0} & \mathbf{0} & \boldsymbol{\Omega}_3^{(3)} & -\boldsymbol{\Omega}_3^{(4)} & \cdots & \mathbf{0} & \mathbf{0} & \mathbf{0} \\ \vdots & \vdots & \vdots & \vdots & \vdots & \vdots & \vdots & \vdots \\ \mathbf{0} & \mathbf{0} & \mathbf{0} & \mathbf{0} & \cdots & \boldsymbol{\Omega}_{n-2}^{(n-2)} & -\boldsymbol{\Omega}_{n-2}^{(n-1)} & \mathbf{0} \\ \mathbf{0} & \mathbf{0} & \mathbf{0} & \mathbf{0} & \cdots & \mathbf{0} & \boldsymbol{\Omega}_{n-1}^{(n-1)} & -\boldsymbol{\Omega}_{n-1}^{(n)} \end{bmatrix}, \tag{21.48}$$

where the generic matrices $\boldsymbol{\Omega}_i^{(i)}, \boldsymbol{\Omega}_i^{(i+1)}$ are given by:

$$\boldsymbol{\Omega}_i^{(i)}=\begin{bmatrix} R^{(i)} & R^{(i)-1} \\ 2\left(\lambda^{(i)}+\mu^{(i)}\right) & -2\mu^{(i)}R^{(i)-2} \end{bmatrix}, \quad \boldsymbol{\Omega}_i^{(i+1)}=\begin{bmatrix} R^{(i)} & R^{(i)-1} \\ 2\left(\lambda^{(i+1)}+\mu^{(i+1)}\right) & -2\mu^{(i+1)}R^{(i)-2} \end{bmatrix}, \tag{21.49}$$

are (2×2) matrices with nonzero determinant, whose components were already gave above.
The determinant of the matrices (21.49) is given by:

$$\det[\boldsymbol{\Omega}_i^{(i)}]=-2\left(2\mu^{(i)}+\lambda^{(i)}\right)R^{(i)-1}\neq 0, \quad \det[\boldsymbol{\Omega}_i^{(i+1)}]=-2\left(2\mu^{(i+1)}+\lambda^{(i+1)}\right)R^{(i)-2}\neq 0, \tag{21.50}$$

However, in force of the special form of $\boldsymbol{\Omega}$ derived above, one can rewrite the reduced algebraic problem in order to have the solution without recall any numerical strategy. To make this, let us we can rewrite two algebraic system (21.44) in follows manner:

$$\begin{cases} \boldsymbol{\Omega}_1^{(2)}\mathbf{W}_j^{(2)}=\boldsymbol{\Omega}_1^{(1)}\mathbf{W}_j^{(1)}+\mathbf{L}_{1,j}^{(2)}-\mathbf{L}_{1,j}^{(1)} \\ \boldsymbol{\Omega}_2^{(3)}\mathbf{W}_j^{(3)}=\boldsymbol{\Omega}_2^{(2)}\mathbf{W}_j^{(2)}+\mathbf{L}_{2,j}^{(3)}-\mathbf{L}_{2,j}^{(2)} \\ \vdots \\ \boldsymbol{\Omega}_i^{(i+1)}\mathbf{W}_j^{(i+1)}=\boldsymbol{\Omega}_i^{(i)}\mathbf{W}_j^{(i)}+\mathbf{L}_{i,j}^{(i+1)}-\mathbf{L}_{i,j}^{(i)} \qquad \forall j\in\{0,m\}, \quad \forall m\in\{1,2,....,N\} \\ \vdots \\ \boldsymbol{\Omega}_{n-2}^{(n-1)}\mathbf{W}_j^{(n-1)}=\boldsymbol{\Omega}_{n-2}^{(n-2)}\mathbf{W}_j^{(n-2)}+\mathbf{L}_{n-2,j}^{(n-1)}-\mathbf{L}_{n-2,j}^{(n-2)} \\ \boldsymbol{\Omega}_{n-1}^{(n)}\mathbf{W}_j^{(n)}=\boldsymbol{\Omega}_{n-1}^{(n-1)}\mathbf{W}_j^{(n-1)}+\mathbf{L}_{n-1,j}^{(n)}-\mathbf{L}_{n-1,j}^{(n-1)} \end{cases} \tag{21.51}$$

By applying an *in-cascade* procedure, we finally obtain

$$\begin{cases} \mathbf{W}_0^{(i)}=\boldsymbol{\Sigma}^{(i)}\cdot\mathbf{W}_0^{(1)}+\boldsymbol{\Psi}_0^{(i)} \\ \mathbf{W}_m^{(i)}=\boldsymbol{\Sigma}^{(i)}\cdot\mathbf{W}_m^{(1)}+\boldsymbol{\Psi}_m^{(i)} \end{cases} \quad \forall i\in\{2,3,...,n\}, \quad \forall m\in\{1,2,....,N\} \tag{21.52}$$

where $\boldsymbol{\Sigma}^{(i)}$ is an matrix given by following expression:

$$\boldsymbol{\Sigma}^{(i)}=\prod_{j=1}^{i-1}\left(\left[\boldsymbol{\Omega}_{i-j}^{(i-j+1)}\right]^{-1}\cdot\boldsymbol{\Omega}_{i-j}^{(i-j)}\right) \qquad \forall i\in\{2,3,...,n\} \tag{21.53}$$

and the vectors $\boldsymbol{\Psi}_0^{(i)}, \boldsymbol{\Psi}_m^{(i)},$ are reported below:

$$\begin{cases} \boldsymbol{\Psi}_0^{(i)}=\left[\boldsymbol{\Omega}_{i-1}^{(i)}\right]^{-1}\cdot\left\{\mathbf{L}_{i-1,0}^{(i-1)}-\mathbf{L}_{i-1,0}^{(i)}+\sum_{j=1}^{i-2}\left[\prod_{k=1}^{j}\left(\boldsymbol{\Omega}_{i-k}^{(i-k)}\cdot\left[\boldsymbol{\Omega}_{i-k-1}^{(i-k)}\right]^{-1}\right)\right]\cdot\left(\mathbf{L}_{i-j-1,0}^{(i-j-1)}-\mathbf{L}_{i-j-1,0}^{(i-j)}\right)\right\} \\ \boldsymbol{\Psi}_m^{(i)}=\left[\boldsymbol{\Omega}_{i-1}^{(i)}\right]^{-1}\cdot\left\{\mathbf{L}_{i-1,m}^{(i-1)}-\mathbf{L}_{i-1,m}^{(i)}+\sum_{j=1}^{i-2}\left[\prod_{k=1}^{j}\left(\boldsymbol{\Omega}_{i-k}^{(i-k)}\cdot\left[\boldsymbol{\Omega}_{i-k-1}^{(i-k)}\right]^{-1}\right)\right]\cdot\left(\mathbf{L}_{i-j-1,m}^{(i-j-1)}-\mathbf{L}_{i-j-1,m}^{(i-j)}\right)\right\} \end{cases} \tag{21.54}$$

$$\forall i\in\{2,3,...,n\}, \quad \forall m\in\{1,2,....,N\}$$

where *dot* stands for scalar product. The equations (21.53)-(21.54) permit to write two generic unknowns sub-vectors $\mathbf{W}_0^{(i)}, \mathbf{W}_m^{(i)}$ as function of a transferring matrix $\boldsymbol{\Sigma}^{(i)}$ and vectors $\boldsymbol{\Psi}_0^{(i)}, \boldsymbol{\Psi}_m^{(i)},$

and the unknowns sub-vectors $\mathbf{W}_0^{(1)}, \mathbf{W}_m^{(1)}$. The problem is hence reduced to an algebraic one in which only the four coefficients – collected in $\mathbf{W}_0^{(1)}, \mathbf{W}_m^{(1)}$ – related to the first phase have to be determined, by imposing two boundary conditions described by the equations obtained above. Therefore, in order to find the four unknowns collected in $\mathbf{W}_0^{(1)}, \mathbf{W}_m^{(1)}$, it remains to rewrite the boundary conditions (21.43) in matrix form. In particular, by applying the equations (21.52) for $i = n$, we obtain the follows relationship:

$$\mathbf{W}_0^{(n)} = \mathbf{\Sigma}^{(n)} \cdot \mathbf{W}_0^{(1)} + \mathbf{\Psi}_0^{(n)}, \quad \mathbf{W}_m^{(n)} = \mathbf{\Sigma}^{(n)} \cdot \mathbf{W}_m^{(1)} + \mathbf{\Psi}_m^{(n)} \quad \forall m \in \{1,2,....,N\}, \tag{21.55}$$

Then, the boundary conditions(21.43), become two uncoupled algebraic system:

$$\mathbf{\Pi} \cdot \mathbf{W}_0^{(1)} = \Upsilon_0, \quad \mathbf{\Pi} \cdot \mathbf{W}_m^{(1)} = \Upsilon_m \quad \forall m \in \{1,2,....,N\}, \tag{21.56}$$

where the matrix $\mathbf{\Pi}$, and vectors Υ_0, Υ_m are given by**:**

$$\mathbf{\Pi} = \left[\mathbf{\Pi}_1 \quad \left(\mathbf{\Sigma}^{(n)}\right)^T \cdot \mathbf{\Pi}_2 \right]^T, \quad \Upsilon_0 = \left[\Upsilon_{1,0} \quad \Upsilon_{2,0} \right]^T, \quad \Upsilon_m = \left[\Upsilon_{1,m} \quad \Upsilon_{2,m} \right]^T \quad \forall m \in \{1,2,....,N\}, \tag{21.57}$$

where $\mathbf{\Pi}_1, \mathbf{\Pi}_2$ are two vectors and $\Upsilon_{1,0}, \Upsilon_{2,0}, \Upsilon_{1,m}, \Upsilon_{2,m}$ are four scalars, as reported below:

$$\begin{cases} \mathbf{\Pi}_1 = \left[2\left(\lambda^{(1)} + \mu^{(1)}\right), -2\mu^{(1)} R^{(0)-2} \right]^T, \ \mathbf{\Pi}_2 = \left[2\left(\lambda^{(n)} + \mu^{(n)}\right), -2\mu^{(n)} R^{(n)-2} \right]^T \\ \Upsilon_{1,0} = -\alpha^{(1)} \left(3\lambda^{(1)} + 2\mu^{(1)}\right) T_R; \ \ \Upsilon_{2,0} = -\alpha^{(n)} \left(3\lambda^{(n)} + 2\mu^{(n)}\right) T_R - \mathbf{\Pi}_2 \cdot \mathbf{\Psi}_0^{(n)}, \end{cases}$$

$$\begin{cases} \Upsilon_{1,m} = \dfrac{2\mu^{(1)}\zeta^{(1)}}{\omega_m} \left[A_m^{(1)} J_1\left(\omega_m R^{(0)} \beta^{(1)}\right) + B_m^{(1)} Y_1\left(\omega_m R^{(0)} \beta^{(1)}\right) \right], \\ \Upsilon_{2,m} = \dfrac{2\mu^{(n)}\zeta^{(n)}}{\omega_m} \left[A_m^{(n)} J_1\left(\omega_m R^{(n)} \beta^{(n)}\right) + B_m^{(n)} Y_1\left(\omega_m R^{(n)} \beta^{(n)}\right) \right] - \mathbf{\Pi}_2 \cdot \mathbf{\Psi}_m^{(n)} \end{cases}, \ \forall m \in \{1,2,....,N\}, \tag{21.58}$$

Then, by inverting, all the $2 \times n$ unknown coefficients , we obtain the unknown parameters:

$$\begin{cases} \mathbf{W}_0^{(1)} = \mathbf{\Pi}^{-1} \cdot \Upsilon_0, \\ \mathbf{W}_0^{(i)} = \mathbf{\Sigma}^{(i)} \cdot \mathbf{\Pi}^{-1} \cdot \Upsilon_0 + \mathbf{\Psi}_0^{(i)} \quad \forall i \in \{2,3,...,n\} \end{cases}$$

$$\begin{cases} \mathbf{W}_m^{(1)} = \mathbf{\Pi}^{-1} \cdot \Upsilon_m, \\ \mathbf{W}_m^{(i)} = \mathbf{\Sigma}^{(i)} \cdot \mathbf{\Pi}^{-1} \cdot \Upsilon_m + \mathbf{\Psi}_m^{(i)} \quad \forall i \in \{2,3,...,n\} \end{cases} \quad \forall m \in \{1,2,....,N\}, \tag{21.59}$$

By substituting the solutions (21.59) in (21.38), we obtain in explicit displacement function. For example, let us consider, an multilayered cylinder constituted by two phases under decreasing temperature. The phase (1) is constituted by steel and phase (2) by aluminium. It is denoted with pedix “s” the parameters of steel and pedix “a” the parameters of aluminium. The mechanical and thermal parameters considered for both phases are reported in table 21.1:

	Steel (phase 1)	**Aluminium** (phase 2)
$E\left[N\,m^{-2}\right]$	$210 \cdot 10^9$	$70 \cdot 10^9$
$k\left[W\,m^{-1}K^{-1}\right]$	45	237
ν	0.30	0.35
$\alpha\left[m \cdot m^{-1}K^{1}\right]$	$12 \cdot 10^{-6}$	$23.1 \cdot 10^{-6}$
$\rho\left[kg\,m^{-3}\right]$	7800	2700
$c_v\left[J \cdot kg^{-1}K^{-1}\right]$	440	930

Table 21.1 – *Mechanical and thermal parameters of Steel and Aluminium*

The geometrical parameters of multilayered cylinder composed by two phases are: $R^{(0)}=1.00m,\ R^{(1)}=1.03m,\ R^{(2)}=1.08m,\ h_c=50W/m^2\cdot°K,\ T_0=T_R=300°K$. By fixed m= 20, the eigenvalues ω_m of transcendental equation (21.34) and corresponding values of constants integration A_m are reported in table 21.2:

ω_m	4.1512	60.4033	136.053	188.107	259.635
A_m	-741.919	24.6825	-7.90168	-1.96788	0.871828
ω_m	326.578	381.225	458.086	513.794	579.311
A_m	-1.32115	-1.57136	-0.244858	-0.670918	-0.720135
ω_m	651.967	703.695	778.704	840.404	899.392
A_m	-0.503598	-0.477107	0.193784	0.367525	0.432385
ω_m	975.552	1028.1	1098.54	1166.78	1220.56
A_m	-0.26674	-0.3972	0.0718733	-0.294447	-0.195553

Table 21.2 – *Eigenvalues ω_m and corresponding values of constants integration A_m*

In this case the graphics function $g(\omega)$ given by equation (21.34) is reported below:

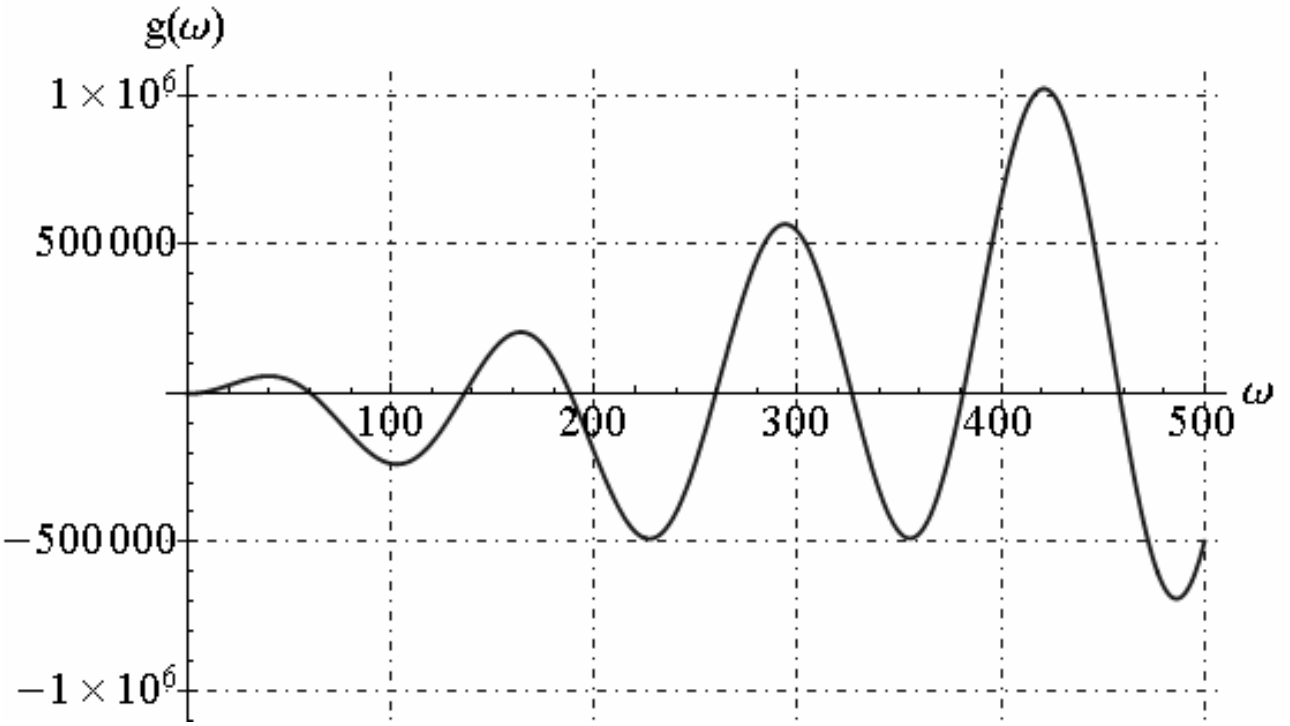

Fig. 21.1 - *Function $g(\omega)$*

We reported the graphics of temperature function along the radial direction and in time:

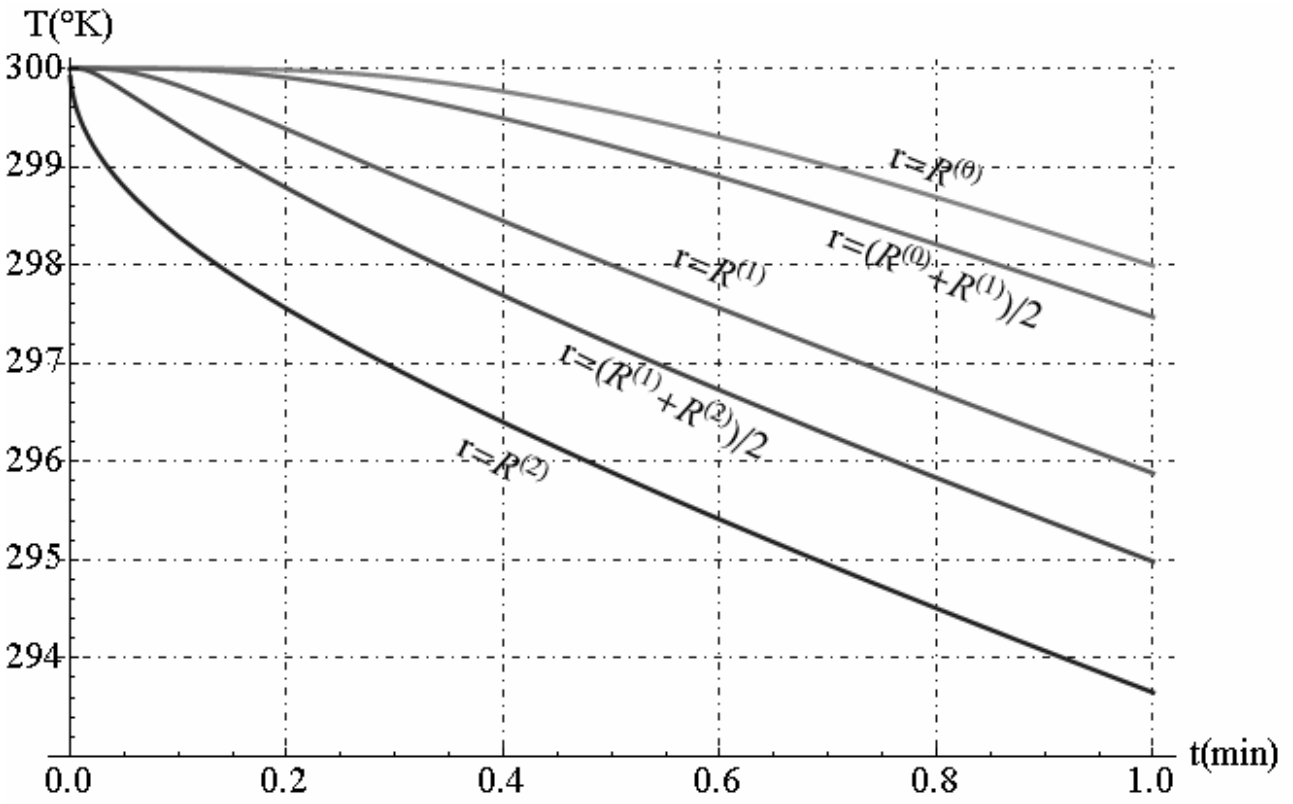

Fig. 21.2 - *Temperature function versus the time*

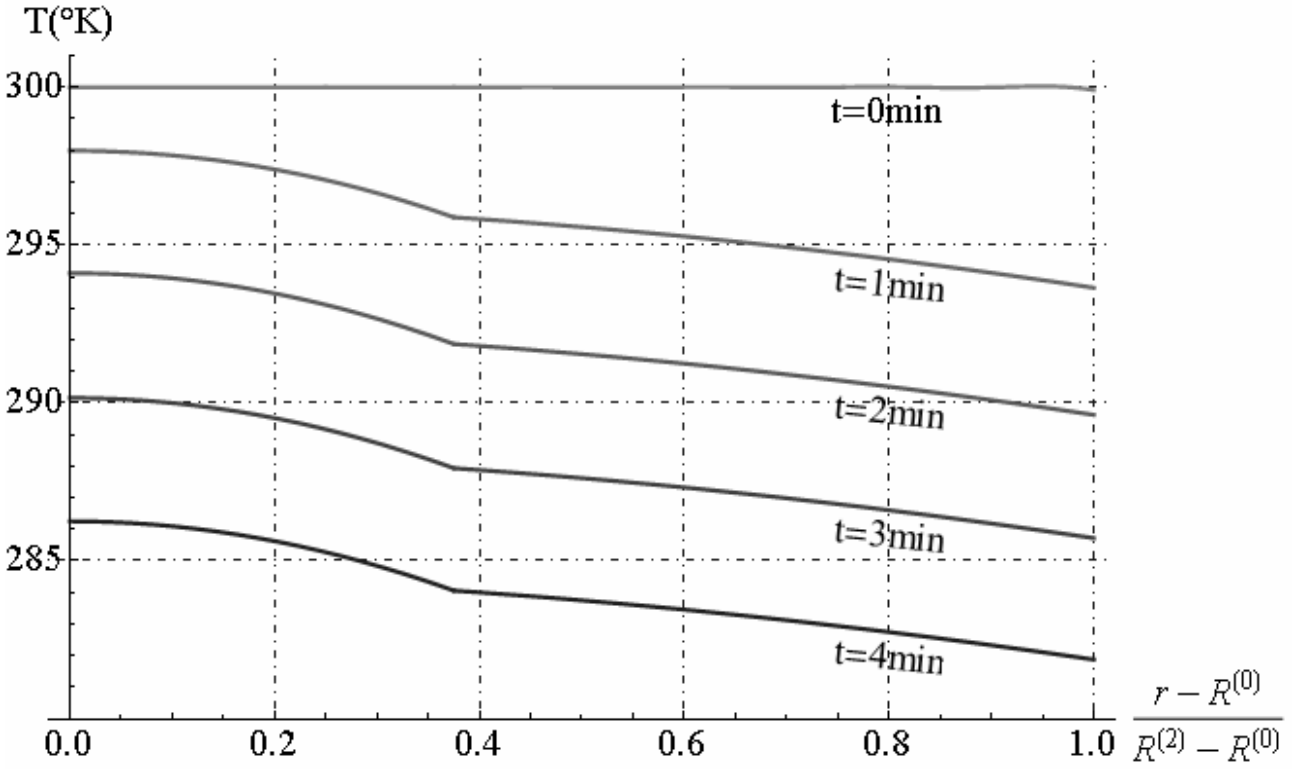

Fig. 21.3 - *Temperature distribution along radial direction*

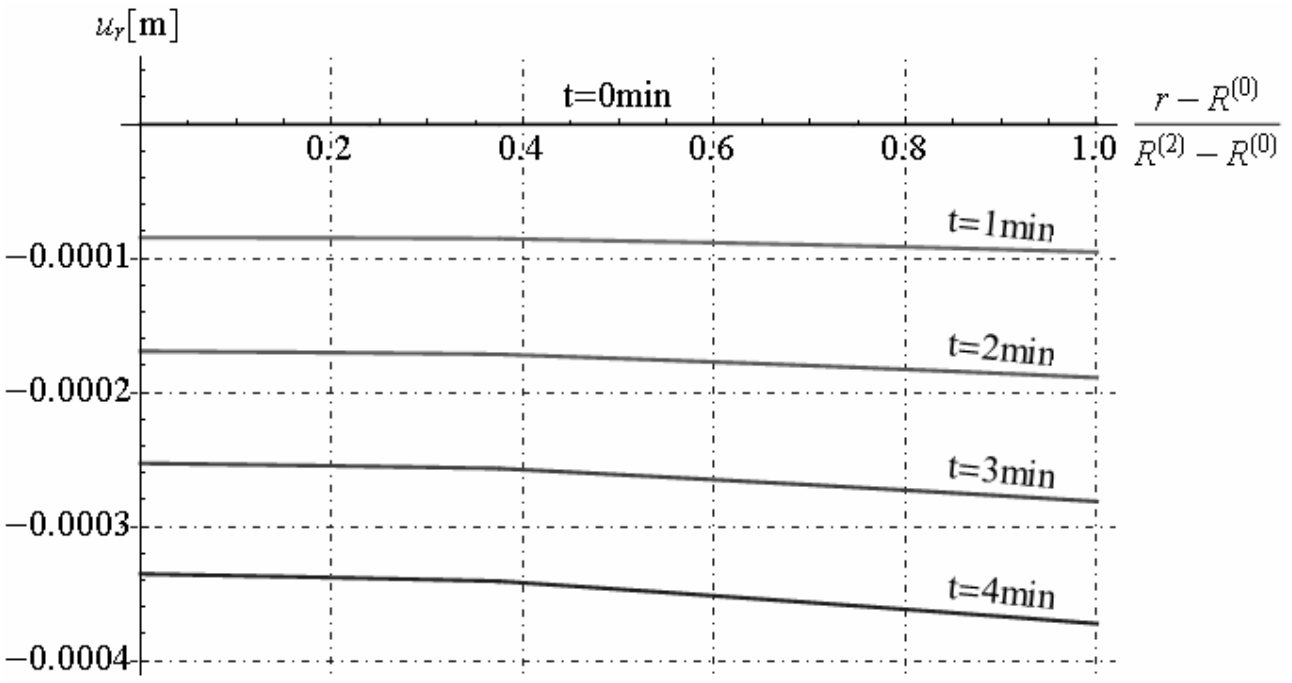

Fig. 21.4 - *Radial displacement distribution along radial direction*

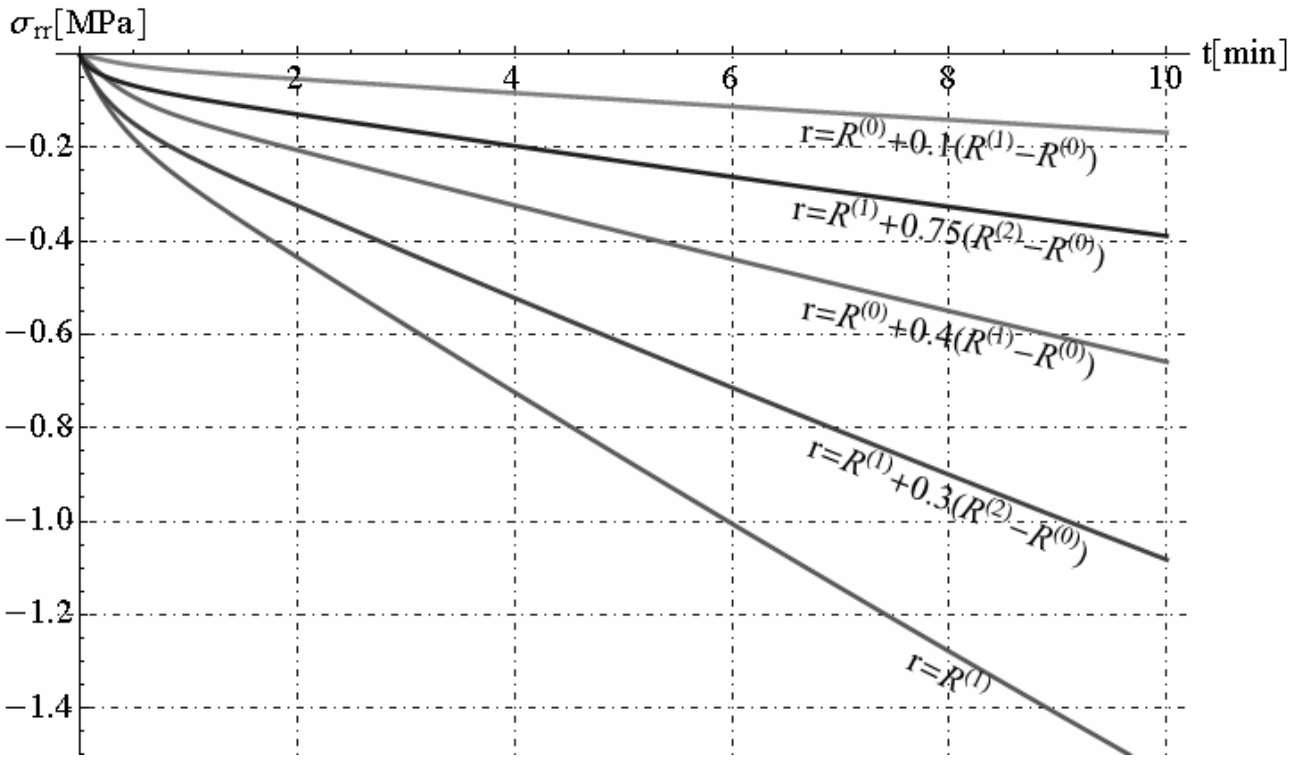

Fig. 21.5 - *Radial stress distribution in time*

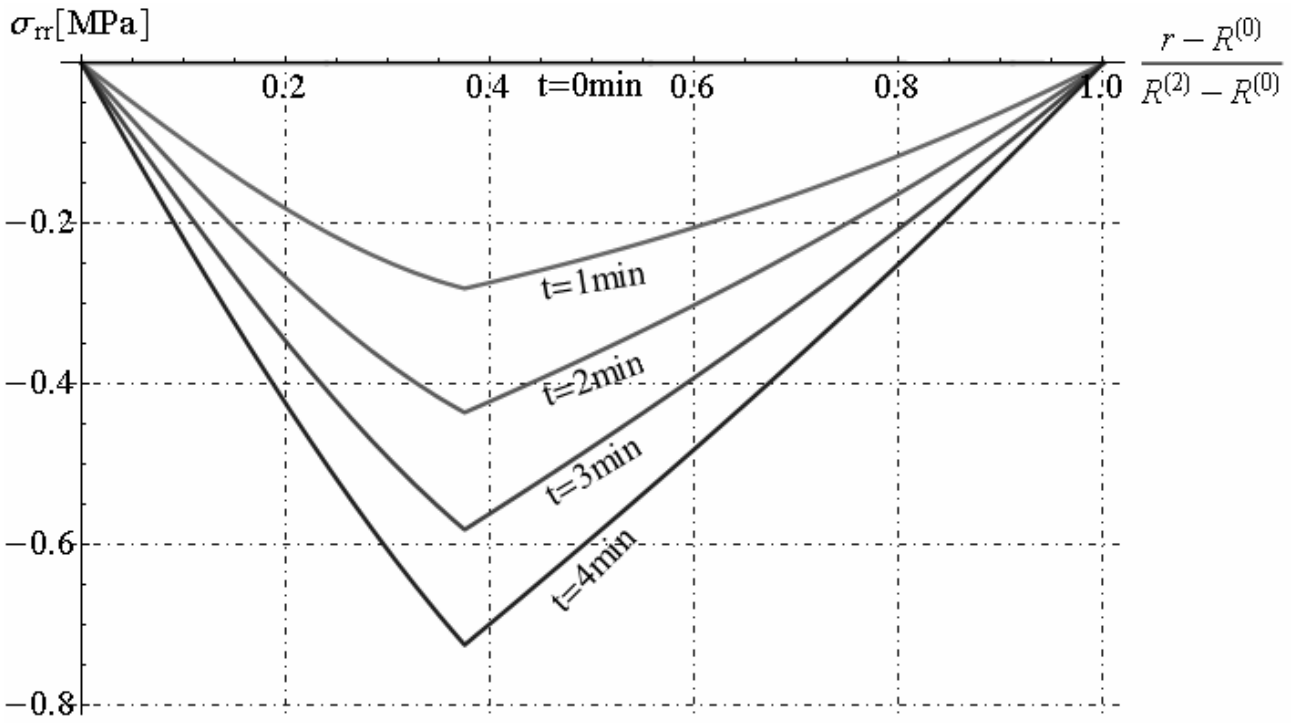

Fig. 21.6 - *Radial stress distribution along radial direction*

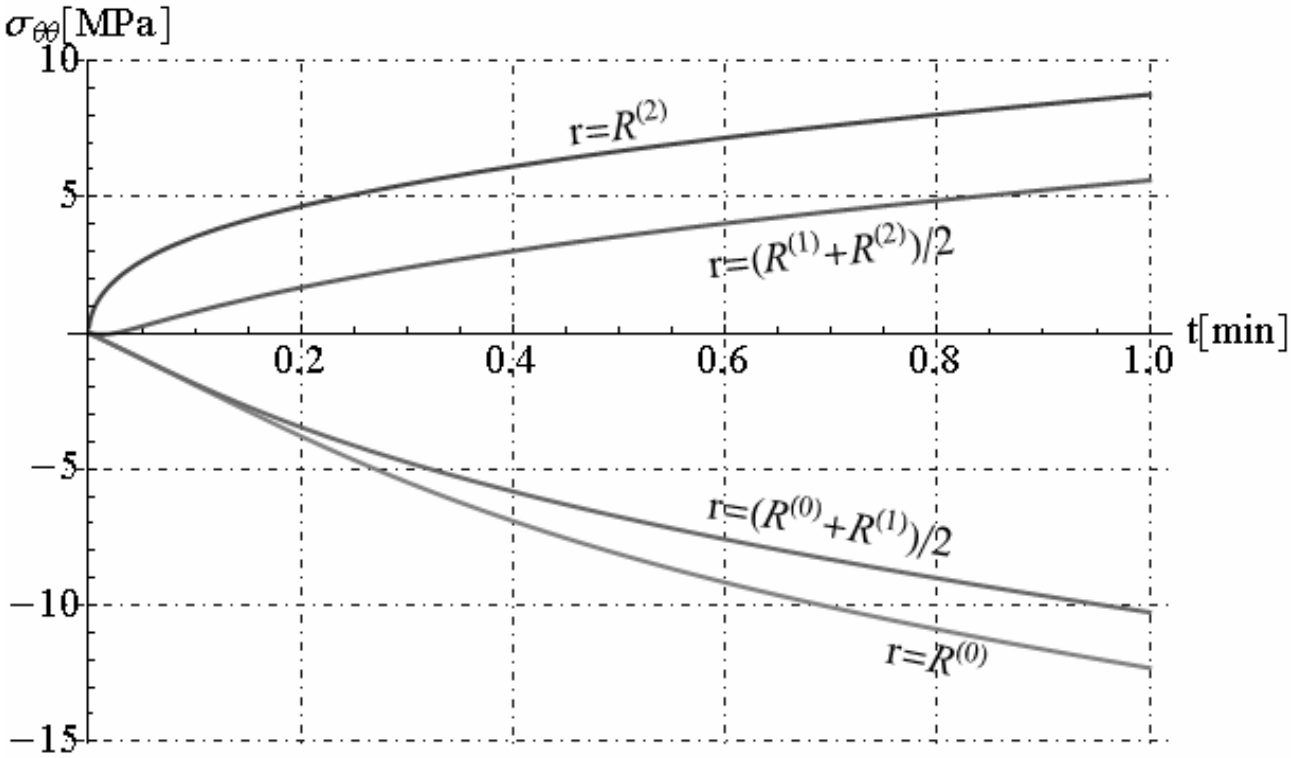

Fig. 21.7 - *Circumferential stress distribution in time*

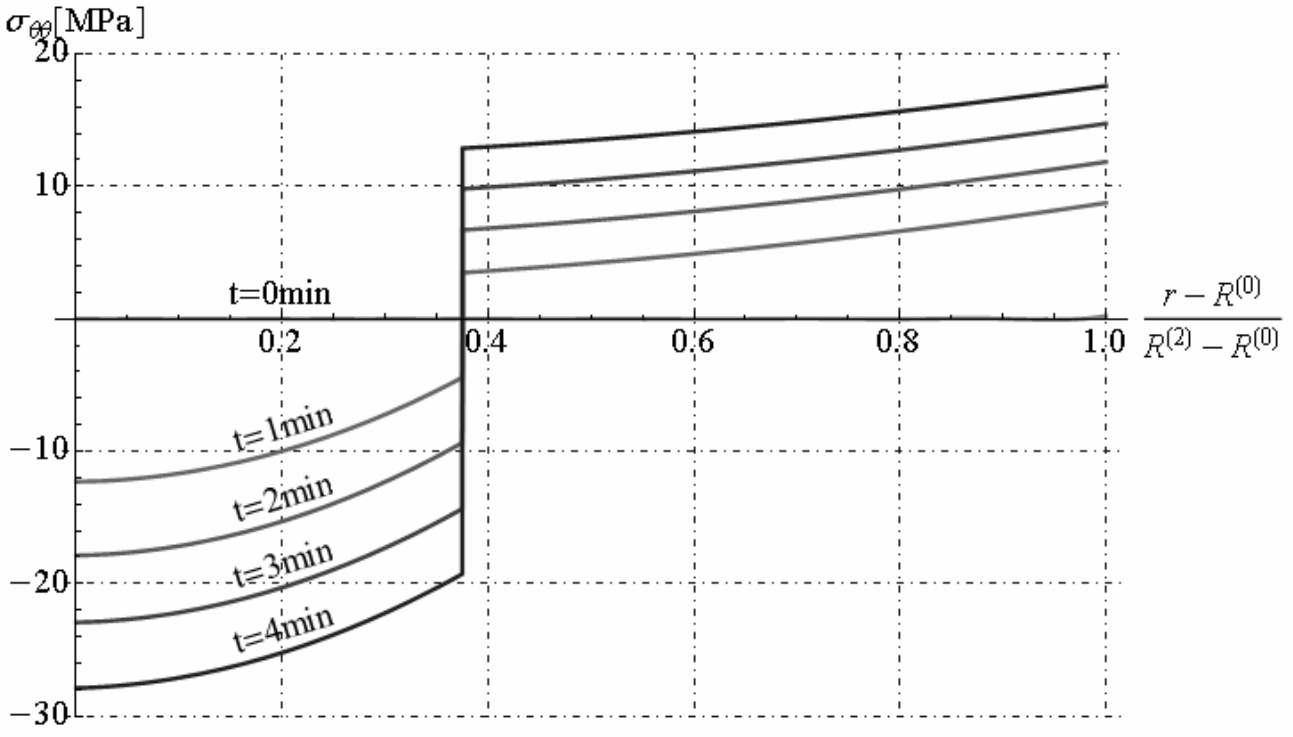

Fig. 21.8 - *Circumferential stress distribution along radial direction*

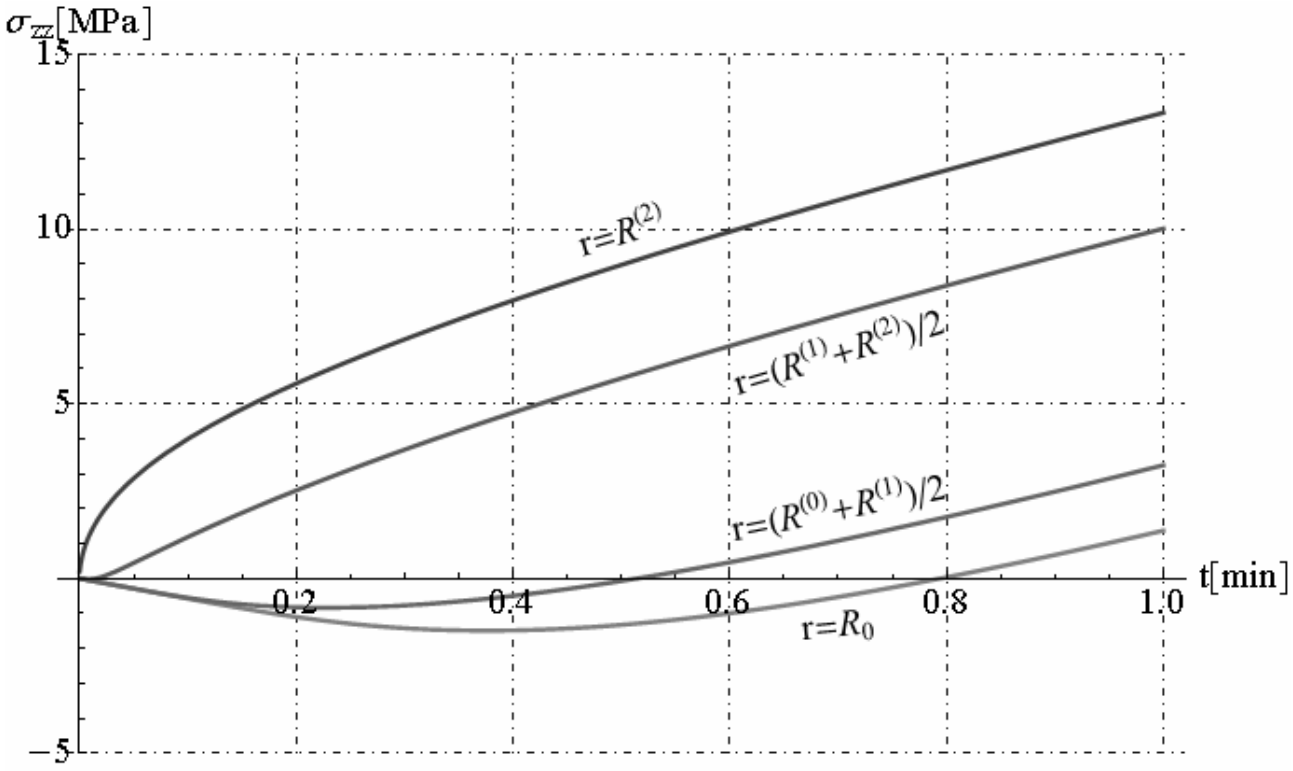

Fig. 21.9 - *Axial stress distribution in time*

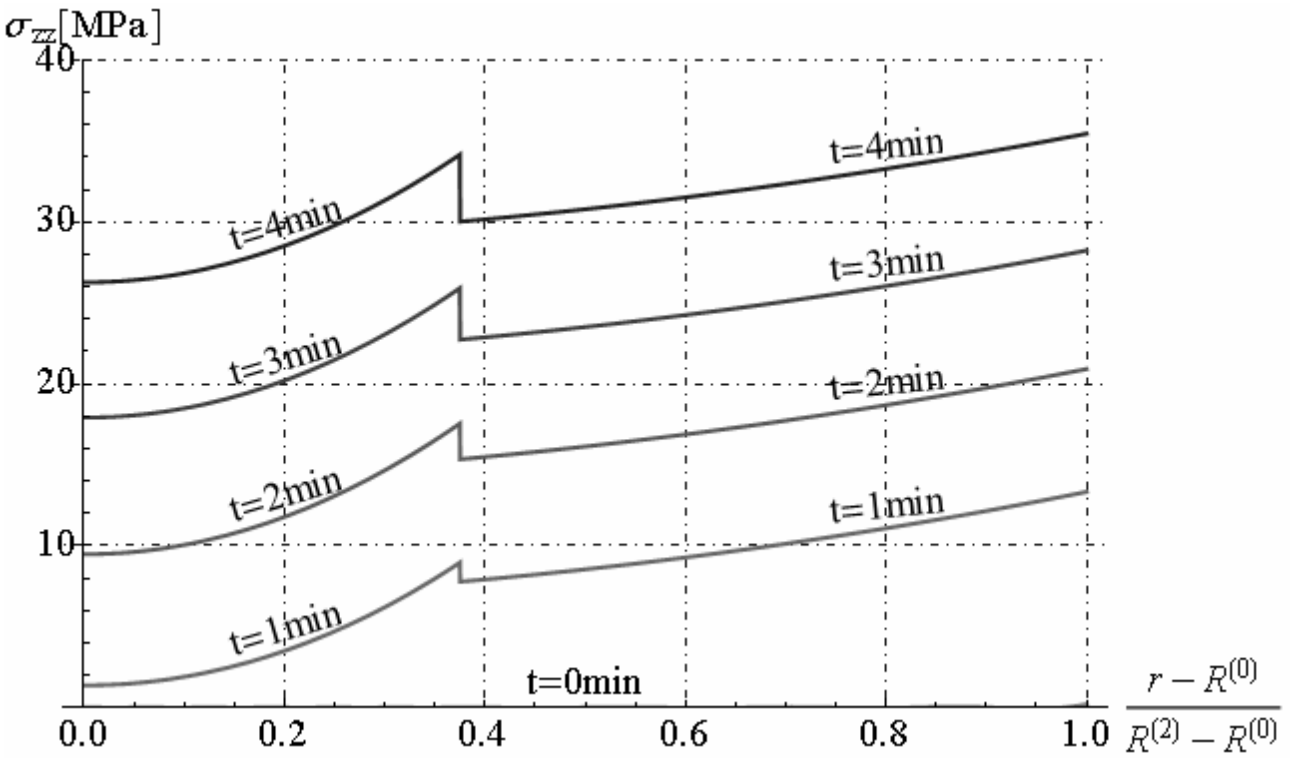

Fig. 21.10 - *Axial stress distribution along radial direction*

21.3. Multilayered cylinder exposed to uniform heat flux

Let us consider an multilayered cylinder constituted by n-hollow cylindrical phases as decrypted in section 21.1. The inner surface $r = R^{(0)}$ is kept perfectly insulated while the outer surface $r = R^{(n)}$ is exposed, for t >0, to a constant uniform heat input q_0. In this section, we determine the heat conduction, displacement and stress function in any hollow cylindrical phases subjected to uniform heat input q_0 applied on external surface, starting to initial temperature in composite solid equal to $T_0 = T_R = const$. The equations field to satisfy in uncoupled thermo-elastic problem with axis-symmetry and in plane strain are reported in equations (21.13), but in this case the boundary conditions (21.11) become:

$$-k^{(1)}T^{(1)}_{,r}(r = R^{(0)}, t) = 0, \quad -k^{(n)}T^{(n)}_{,r}(r = R^{(n)}, t) = q_0 = const, \quad \forall t \geq 0 \tag{21.60}$$

and the boundary conditions (21.8) become:

$$\sigma^{(n)}_{rr}(r = R^{(n)}, t) = 0, \quad \sigma^{(1)}_{rr}(r = R^{(0)}, t) = 0, \quad \forall t \geq 0 \tag{21.61}$$

The other boundary conditions reported in section 21.1 don't change. By solving the Fourier's equation reported in second equation of (21.13) with method separation of variables, and by substituting the function of temperature $T^{(i)}(r,t)$ in first equation of (21.13), and by integration in two time this equation respect to variable r , the explicit displacement solution is reported in equation (21.14). In this case, the heat conduct problem involving a non-homogeneous boundary condition and, in particular, with the heat input specified over the entire boundary surface. It is necessary writing the temperature solution, in any phases of multilayered cylinder, in the follows form (see Chapter VII and Chapter XVII) :

$$T^{(i)}(r,t) = T_0 + \xi\, t + T^{(i)}_S(r) + T^{(i)}_C(r,t), \quad \forall i \in \{1, 2, ..., n\} \tag{21.62}$$

where ξ is same unknown parameter for any phases of multilayered cylinder and the function $T^{(i)}_S(r)$ in generic i-th phase satisfies the field equations:

$$\frac{d^2T_S^{(i)}}{dr^2}+\frac{1}{r}\frac{dT_S^{(i)}}{dr}=\frac{\xi}{\kappa^{(i)}};\qquad \begin{matrix} R^{(i-1)}\le r\le R^{(i)} \\ \forall i\in\{1,2,...,n\}\end{matrix} \tag{21.63}$$

Moreover the function $T_S^{(i)}(r)$ must be satisfy the following boundary conditions :

$$-k^{(1)}\frac{dT_S^{(1)}(r)}{dr}=0,\quad r=R^{(0)}, \tag{21.64}$$

$$-k^{(n)}\frac{dT_S^{(n)}(r)}{dr}=q_0,\quad r=R^{(n)}, \tag{21.65}$$

$$-k^{(i)}\frac{dT_S^{(i)}(r)}{dr}=-k^{(i+1)}\frac{dT_S^{(i+1)}(r)}{dr},\quad r=R^{(i)},\ \forall i\in\{1,2,...,n-1\} \tag{21.66}$$

$$T_S^{(i)}(r)=T_S^{(i+1)}(r),\quad r=R^{(i)},\ \forall i\in\{1,2,...,n-1\} \tag{21.67}$$

$$\sum_{i=1}^{n}\left[\rho^{(i)}c_v^{(i)}\int_0^{2\pi}\int_{R^{(i-1)}}^{R^{(i)}} rT_S^{(i)}(r)\,dr\,d\theta\right]=0 \tag{21.68}$$

where ξ may be determined either from the boundary conditions (21.64) -(21.68). The function $T_C^{(i)}(r,t)$ in generic i-th phase satisfies the field equations:

$$\frac{\partial^2T_C^{(i)}(r,t)}{\partial r^2}+\frac{1}{r}\frac{\partial T_C^{(i)}(r,t)}{\partial r}=\frac{1}{\kappa^{(i)}}\frac{\partial T_C^{(i)}(r,t)}{\partial t};\qquad \begin{matrix} R^{(i-1)}\le r\le R^{(i)},\forall t\ge 0 \\ \forall i\in\{1,2,...,n\}\end{matrix} \tag{21.69}$$

Moreover the function $T_C^{(i)}(r,t)$ must be satisfy the following boundary conditions :

$$-k^{(1)}\frac{\partial T_C^{(1)}(r,t)}{\partial r}=0,\quad r=R^{(0)},\ \forall t\ge 0, \tag{21.70}$$

$$-k^{(n)}\frac{\partial T_C^{(n)}(r,t)}{\partial r}=0,\quad r=R^{(n)},\ \forall t\ge 0, \tag{21.71}$$

$$\begin{cases}-k^{(i)}\dfrac{\partial T_C^{(i)}(r,t)}{\partial r}=-k^{(i+1)}\dfrac{\partial T_C^{(i+1)}(r,t)}{\partial r}, \\ T_C^{(i)}(r,t)=T_C^{(i+1)}(r,t),\end{cases}\quad r=R^{(i)},\ \forall t\ge 0,\ \forall i\in\{1,2,...,n-1\} \tag{21.72}$$

$$T_C^{(i)}(r,t)=-T_S^{(i)}(r),\quad R^{(i-1)}\le r\le R^{(i)},\ t=0,\ \forall i\in\{1,2,...,n\} \tag{21.73}$$

The solutions of differential equation (21.63) is given by:

$$T_S^{(i)}(r)=C^{(i)}+D^{(i)}\log r+\frac{\xi}{4\kappa^{(i)}}r^2,\quad \forall i\in\{1,2,...,n\} \tag{21.74}$$

where $C^{(i)},D^{(i)},\xi$ are 2n+1 unknown parameter to determine. By solving algebraic system composed by equations (21.64), (21.65),(21.66) and (21.68), we obtain integration constants $\xi,D^{(i)}$:

$$\xi=-\frac{2q_0R^{(n)2}}{\sum_{i=1}^{n}\rho^{(i)}c_v^{(i)}\left(R^{(i)2}-R^{(i-1)2}\right)}=-\frac{q_0S^{(n)}}{\sum_{i=1}^{n}\rho^{(i)}c_v^{(i)}V^{(i)}},\ V^{(i)}=1\cdot\pi\left(R^{(i)2}-R^{(i-1)2}\right),\ \ S^{(n)}=1\cdot 2\pi R^{(n)}, \tag{21.75}$$

where $V^{(i)}$ and $S^{(n)}$ are volume of generic i-th phase and external surface of multilayer cylinder with unitary high, respectively.

$$D^{(i)}=\frac{q_0R^{(n)}}{k^{(i)}}\frac{\left[-\rho^{(i)}c_v^{(i)}R^{(i-1)2}+(1-\delta_{i1})\sum_{j=1}^{i-1}\rho^{(j)}c_v^{(j)}\left(R^{(j)2}-R^{(j-1)2}\right)\right]}{\sum_{j=1}^{n}\rho^{(j)}c_v^{(j)}\left(R^{(j)2}-R^{(j-1)2}\right)} \tag{21.76}$$

where δ_{i1} is the Kronecker's delta. By solving the equations (21.67), we obtain integration constants $C^{(i)}$ as function of constants $\xi, D^{(i)}$. For brevity, we don't reported in explicit the expressions of constants $C^{(i)}$. The solution to the problem for T_C is found in much the same says way as was followed in section 21.2. The problem is therefore on with homogeneous differential equation and boundary conditions and may be treated by the method separation of variables as showed in section 21.2. The solutions of differential equation (21.69) is given by:

$$T_C^{(i)}(r,t) = \left[A^{(i)} J_0\left(\omega \beta^{(i)} r\right) + B^{(i)} Y_0\left(\omega \beta^{(i)} r\right) \right] e^{-\kappa^{(i)} \beta^{(i)2} \omega^2 t} \quad \forall i \in \{1,2,...,n\} \tag{21.77}$$

where $A^{(i)}, B^{(i)}, \omega$ are constants parameter to determine, the coefficient $\beta^{(i)} = \sqrt{\kappa^{(1)} / \kappa^{(i)}}$. The boundary conditions (21.72) for temperature function $T_C^{(i)}(r,t)$ are reported below:

$$\begin{cases} A^{(i)} J_0\left(\omega \beta^{(i)} R^{(i)}\right) + B^{(i)} Y_0\left(\omega \beta^{(i)} R^{(i)}\right) - \left[A^{(i+1)} J_0\left(\omega \beta^{(i+1)} R^{(i)}\right) + B^{(i+1)} Y_0\left(\omega \beta^{(i+1)} R^{(i)}\right) \right] = 0 \\ k^{(i)} \beta^{(i)} \left[A^{(i)} J_1\left(\omega \beta^{(i)} R^{(i)}\right) + B^{(i)} Y_1\left(\omega \beta^{(i)} R^{(i)}\right) \right] + \\ \qquad - k^{(i+1)} \beta^{(i+1)} \left[A^{(i+1)} J_1\left(\omega \beta^{(i+1)} R^{(i)}\right) + B^{(i+1)} Y_1\left(\omega \beta^{(i+1)} R^{(i)}\right) \right] = 0 \\ \qquad\qquad \forall i \in \{1,2,...,n-1\} \end{cases} \tag{21.78}$$

The boundary conditions on the inner and the outer surface (21.70) and (21.71) become:

$$\begin{cases} A^{(1)} J_1\left(\omega \beta^{(1)} R^{(0)}\right) + B^{(1)} Y_1\left(\omega \beta^{(1)} R^{(0)}\right) = 0 \\ A^{(n)} J_1\left(\omega \beta^{(n)} R^{(n)}\right) + B^{(n)} Y_1\left(\omega \beta^{(n)} R^{(n)}\right) = 0 \end{cases} \tag{21.79}$$

By first equation of (21.79), we determine $B^{(1)}$ as function of $A^{(1)}$ as follows:

$$B^{(1)} = -\frac{J_1\left(\omega R^{(0)} \beta^{(1)}\right)}{Y_1\left(\omega R^{(0)} \beta^{(1)}\right)} A^{(1)} \tag{21.80}$$

The equations (21.78) constituted an homogeneous algebraic system, composed by 2(n-1) equations, in unknown parameters $A^{(i)}, B^{(i)}$ with $i \in \{1,2,...,n\}$, which can be written as:

$$\mathbf{\Phi} \cdot \mathbf{X} = \mathbf{0} \tag{21.81}$$

where $\mathbf{X} = [\mathbf{X}^{(1)}, \mathbf{X}^{(2)}, ..., \mathbf{X}^{(n)}]^T$ collect the unknowns sub-vectors, as reported below:

$$\mathbf{X}^{(i)} = \begin{bmatrix} A^{(i)} & B^{(i)} \end{bmatrix}^T, \quad \forall i \in \{1,2,....,n\} \tag{21.82}$$

and $\mathbf{\Phi}$ is the matrix reported in equation (21.26). As showed in section 21.2, matrix $\mathbf{\Phi}$ is constituted by components: $\mathbf{\Phi}_i^{(i)}, \mathbf{\Phi}_i^{(i+1)}, \forall i \in \{1,2,...,n-1\}$ and vector $\mathbf{X}^{(i)}$ is obtained as function of vector $\mathbf{X}^{(1)}$ (see equation (21.29)). By substituting the solutions (21.29) in boundary conditions (21.79), we obtain vector equations in unknown vector $\mathbf{X}^{(1)}$, as reported below:

$$\mathbf{\Lambda} \cdot \mathbf{X}^{(1)} = \mathbf{0} \tag{21.83}$$

where $\mathbf{\Lambda}$ is an 2x2 square matrix given by :

$$\mathbf{\Lambda} = \begin{bmatrix} \Lambda_{11} & \Lambda_{12} \\ \Lambda_{21} & \Lambda_{22} \end{bmatrix} \tag{21.84}$$

where the components $\Lambda_{11}, \Lambda_{12}, \Lambda_{21}, \Lambda_{22}$ are reported below:

$$\begin{aligned} &\Lambda_{11} = J_1\left(\omega \beta^{(1)} R^{(0)}\right), \quad \Lambda_{12} = Y_1\left(\omega \beta^{(1)} R^{(0)}\right), \\ &[\Lambda_{21}, \Lambda_{22}] = \left[J_1\left(\omega \beta^{(n)} R^{(n)}\right), Y_1\left(\omega \beta^{(n)} R^{(n)}\right) \right] \cdot \mathbf{\Gamma}^{(n)}, \end{aligned} \tag{21.85}$$

where $\mathbf{\Gamma}^{(n)}$ is given by equation (21.30) with i = n. The algebraic system (21.83) admit not trivial solution if the determinant of the matrix $[\mathbf{\Lambda}]$ is equal to zero. By imposing this condition, we obtain the transcendental equation in unknown parameter ω:

$$\det[\mathbf{\Lambda}]=0 \;\Rightarrow\; g(\omega)=0 \tag{21.86}$$

The roots of this transcendental equation (21.86) are an infinite number such, denoted here by ω_m, $m=1,2,....N$ leading to eigenvalues or characteristic values $\lambda_m=-\omega_m^2$. The corresponding eigenfunctions or characteristic functions $\overline{\varphi}_m^{(i)}(r)$ are reported in equation (21.35). The coefficients $A_m^{(1)}$ are determined by applying the initial condition (21.73) that yields the following relationship:

$$A_m^{(1)}=-\frac{\sum_{i=1}^{n}\left[\rho^{(i)}c_v^{(i)}\int_0^{2\pi}\int_{R^{(i-1)}}^{R^{(i)}} r\,\overline{\varphi}_m^{(i)}\,T_s^{(i)}(r)\,dr d\theta\right]}{\sum_{i=1}^{n}\left[\rho^{(i)}c_v^{(i)}\int_0^{2\pi}\int_{R^{(i-1)}}^{R^{(i)}}\left(\overline{\varphi}_m^{(i)}\right)^2 r dr d\theta\right]} \tag{21.87}$$

Finally the temperature function in i-th generic phase is given by:

$$\begin{aligned}T^{(i)}(r,t)&=T_0+\xi t+C^{(i)}+D^{(i)}\log r+\frac{\xi r^2}{4\kappa^{(i)}}+\\&+\sum_{m=1}^{\infty}\left[A_m^{(i)}J_0\left(\omega_m\beta^{(i)}r\right)+B_m^{(i)}Y_0\left(\omega_m\beta^{(i)}r\right)\right]e^{-\kappa^{(i)}\beta^{(i)2}\omega_m^2 t}\qquad \forall i\in\{1,2,....,n\}\end{aligned} \tag{21.88}$$

By substituting the function (21.88) in equation (21.14), we obtain in explicit the displacement function in any hollow spherical phase:

$$\begin{aligned}u_r^{(i)}&=G^{(i)}r+\frac{H^{(i)}}{r}+\left(N^{(i)}r+\frac{M^{(i)}}{r}\right)t+\frac{\beta^{(i)}\zeta^{(i)}r}{2}\left[C^{(i)}+D^{(i)}\left(\log r-\frac{1}{2}\right)+\frac{\xi r^2}{8\kappa^{(i)}}\right]+\\&+\sum_{m=1}^{\infty}\left\{P_m^{(i)}r+\frac{Q_m^{(i)}}{r}+\frac{\zeta^{(i)}}{\omega_m}\left[A_m^{(i)}J_1\left(\beta^{(i)}\omega_m r\right)+B_m^{(i)}Y_1\left(\beta^{(i)}\omega_m r\right)\right]\right\}e^{-\kappa^{(i)}\omega_m^2\beta^{(i)2}t}\\&\qquad\qquad \forall i\in\{1,2,....,n\}\end{aligned} \tag{21.89}$$

where the integration constants $G^{(i)},H^{(i)},N^{(i)},M^{(i)},P_m^{(i)},Q_m^{(i)}$ are determined by applying the boundary conditions given by equations (21.61). In this case the functions $f_1^{(i)}(t)$, $f_2^{(i)}(t)$, reported in equation (21.14) are given by:

$$f_1^{(i)}(t)=G^{(i)}+N^{(i)}t+\sum_{m=1}^{\infty}P_m^{(i)}e^{-\kappa^{(i)}\omega_m^2\beta^{(i)2}t},\quad f_2^{(i)}(t)=H^{(i)}+M^{(i)}t+\sum_{m=1}^{\infty}Q_m^{(i)}e^{-\kappa^{(i)}\omega_m^2\beta^{(i)2}t}, \tag{21.90}$$

In explicit the radial and circumferential stress components are given by:

$$\begin{aligned}\sigma_{rr}^{(i)}&=2\left(\lambda^{(i)}+2\mu^{(i)}\right)\left(G^{(i)}+N^{(i)}t\right)-2\mu^{(i)}r^{-2}\left(H^{(i)}+M^{(i)}t\right)-\frac{\mu^{(i)}\zeta^{(i)}\beta^{(i)}\xi r^2}{8\kappa^{(i)}}\\&-\zeta^{(i)}\beta^{(i)}\mu^{(i)}\left[C^{(i)}+D^{(i)}\left(\log r-\frac{1}{2}\right)\right]-\alpha^{(i)}\left(3\lambda^{(i)}+2\mu^{(i)}\right)\left(T_0-T_R+\xi t\right)\\&+2\sum_{m=1}^{\infty}\left[P_m^{(i)}\left(\lambda^{(i)}+\mu^{(i)}\right)-Q_m^{(i)}\mu^{(i)}r^{-2}\right]e^{-\omega_m^2\beta^{(i)2}\kappa^{(i)}t}+\\&+2\mu^{(i)}\zeta^{(i)}\sum_{m=1}^{\infty}\left\{\frac{1}{\omega_m r}\left[A_m^{(i)}J_1\left(\omega_m\beta^{(i)}r\right)+B_m^{(i)}Y_1\left(\omega_m\beta^{(i)}r\right)\right]\right\}e^{-\omega_m^2\beta^{(i)2}\kappa^{(i)}t}\end{aligned} \tag{21.91}$$

$$\sigma_{\theta\theta}^{(i)} = 2\left(\lambda^{(i)} + 2\mu^{(i)}\right)\left(G^{(i)} + N^{(i)}t\right) + 2\mu^{(i)} r^{-2}\left(H^{(i)} + M^{(i)}t\right) - \frac{3\mu^{(i)}\zeta^{(i)}\beta^{(i)}\xi r^2}{8\kappa^{(i)}}$$
$$- \zeta^{(i)}\beta^{(i)}\mu^{(i)}\left[C^{(i)} + D^{(i)}\left(\log r - \frac{1}{2}\right)\right] - \alpha^{(i)}\left(3\lambda^{(i)} + 2\mu^{(i)}\right)\left(T_0 - T_R + \xi t\right) +$$
$$+ 2\sum_{m=1}^{\infty}\left[P_m^{(i)}\left(\lambda^{(i)} + \mu^{(i)}\right) + \mu^{(i)} Q_m^{(i)} r^{-2}\right] e^{-\omega_m^2 \beta^{(i)2}\kappa^{(i)} t} +$$
$$+ 2\zeta^{(i)}\mu^{(i)}\sum_{m=1}^{\infty}\left\{\begin{aligned}&\frac{A_m^{(i)}}{\omega_m r}\left[J_1\left(r\omega_m\beta^{(i)}\right) - r\omega_m\beta^{(i)} J_0\left(r\omega_m\beta^{(i)}\right)\right] + \\ &+ \frac{B_m^{(i)}}{\omega_m r}\left[J_1\left(r\omega_m\beta^{(i)}\right) - r\omega_m\beta^{(i)} J_0\left(r\omega_m\beta^{(i)}\right)\right]\end{aligned}\right\} e^{-\omega_m^2\beta^{(i)2}\kappa^{(i)}t} \tag{21.92}$$

$$\sigma_{zz}^{(i)} = 2\lambda^{(i)}\left(G^{(i)} + N^{(i)}t\right) - \alpha^{(i)}\left(3\lambda^{(i)} + 2\mu^{(i)}\right)\left(T_0 - T_R + \xi t\right) +$$
$$+ 2\mu^{(i)}\beta^{(i)}\zeta^{(i)}\left(C^{(i)} + D^{(i)}\log r\right) + \frac{\mu^{(i)}\zeta^{(i)}\beta^{(i)}\xi r^2}{2\kappa^{(i)}} + \tag{21.93}$$
$$+ 2\sum_{m=1}^{\infty}\left\{P_m^{(i)}\lambda^{(i)} + \mu^{(i)}\zeta^{(i)}\beta^{(i)}\left[A_m^{(i)} J_0\left(r\omega_m\beta^{(i)}\right) + B_m^{(i)} Y_0\left(r\omega_m\beta^{(i)}\right)\right]\right\} e^{-\omega_m^2\beta^{(i)2}\kappa^{(i)}t}$$

Moreover, the tractions on the inner and the outer spherical boundary surface are vanishing and then condition (21.8) becomes:

$$\sigma_{rr}^{(1)}(r = R^{(0)}) = 0,\ \sigma_{rr}^{(n)}(r = R^{(n)}) = 0, \quad \forall t \geq 0 \tag{21.94}$$

The integration constants $G^{(i)}, H^{(i)}, P_m^{(i)}, Q_m^{(i)}$ are function of geometrical, mechanical and thermal parameters of spherical layers . Moreover $P_m^{(i)}, Q_m^{(i)}$ are function of constants $A_m^{(i)}, B_m^{(i)}, \omega_m$ also. For example, let us consider, an multilayered cylinder constituted by two phases under uniform heat flux . The phase (1) is constituted by steel and phase (2) by aluminium. The mechanical and thermal parameters considered for both phases are reported in table 21.1. The geometrical parameters of multilayered cylinder composed by two phases are: $R^{(0)} = 10m,\ R^{(1)} = 10.25m,\ R^{(2)} = 10.50m,$ $T_0 = T_R = 300°K\ q_0 = -500W/m^2 \cdot °K,$.By fixed m= 20, the eigenvalues ω_m of transcendental equation (21.86) and corresponding values of constants integration A_m are reported in table 21.3

ω_m	8.22296	18.5262	28.3906	36.051	45.0891
A_m	7.39586	1.24849	1.19622	0.0122434	-0.355103
ω_m	55.5459	64.7026	72.3196	82.0947	92.4357
A_m	0.0718165	0.236587	-0.316028	-0.205368	-0.198533
ω_m	100.773	108.896	119.152	129.095	136.809
A_m	-0.0139715	-0.0604639	-0.11885	0.0680165	-0.0977722
ω_m	145.73	156.181	165.451	173.037	182.72
A_m	-0.0353959	-0.0777249	-0.0307723	-0.012174	0.0257277

Table 21.3 – *Eigenvalues ω_m and corresponding values of constants integration A_m*

In this case the graphics function $g(\omega)$ given by equation (21.86) is reported below:

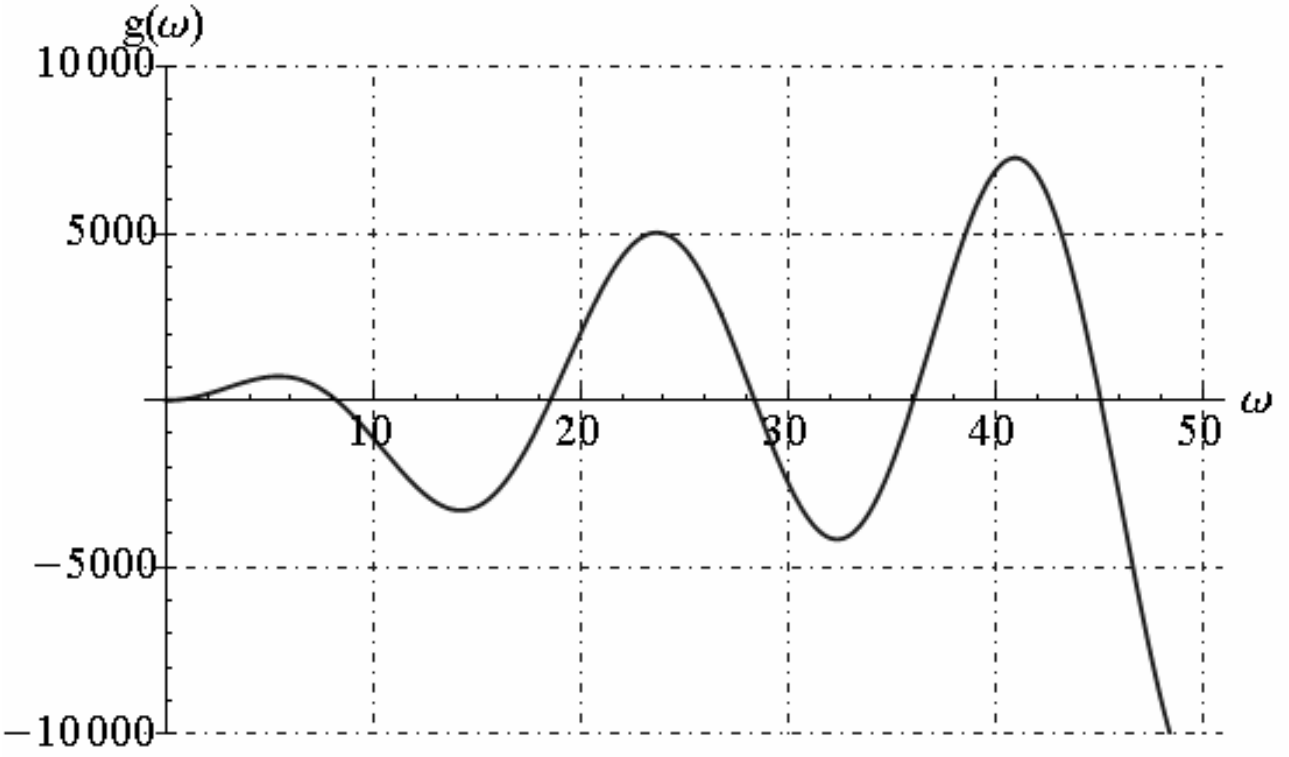

Fig. 21.11 - *Function* $g(\omega)$

We reported the graphics of temperature function along the radial direction and in time:

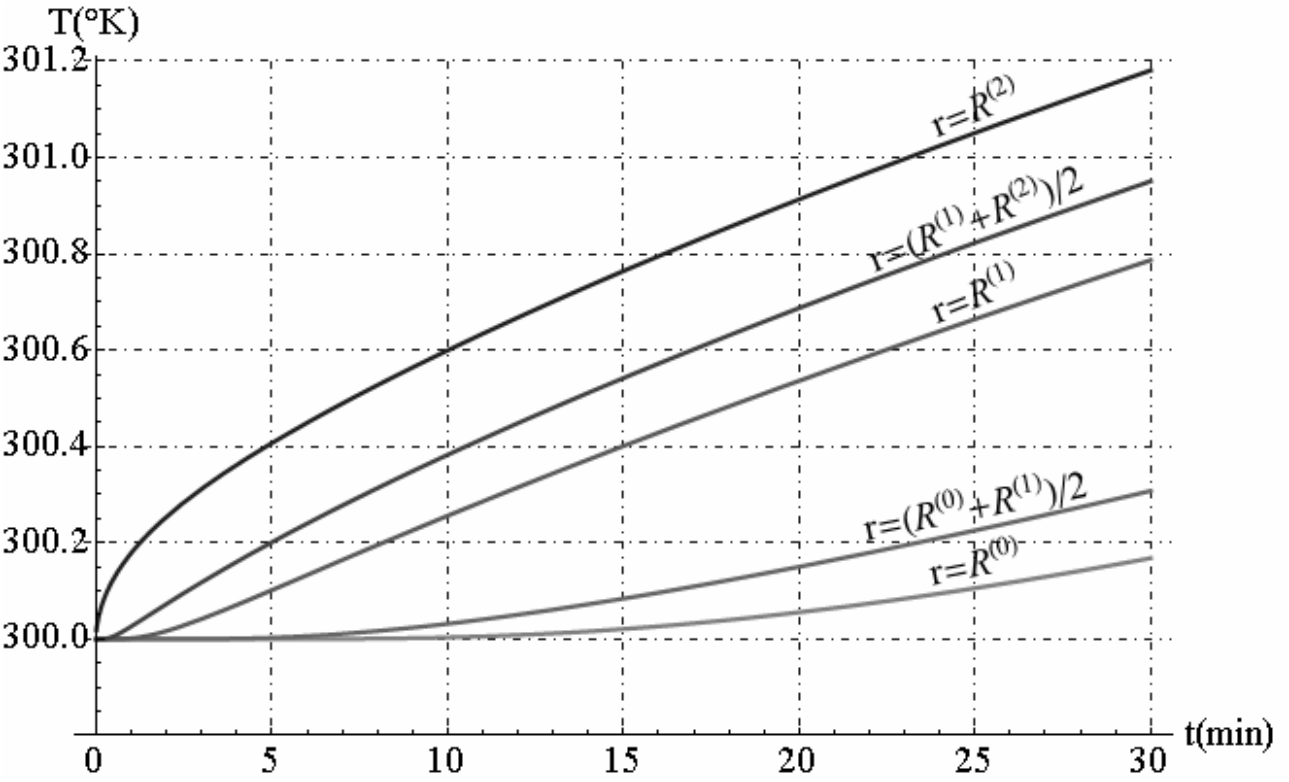

Fig. 21.12 - *Temperature function versus time*

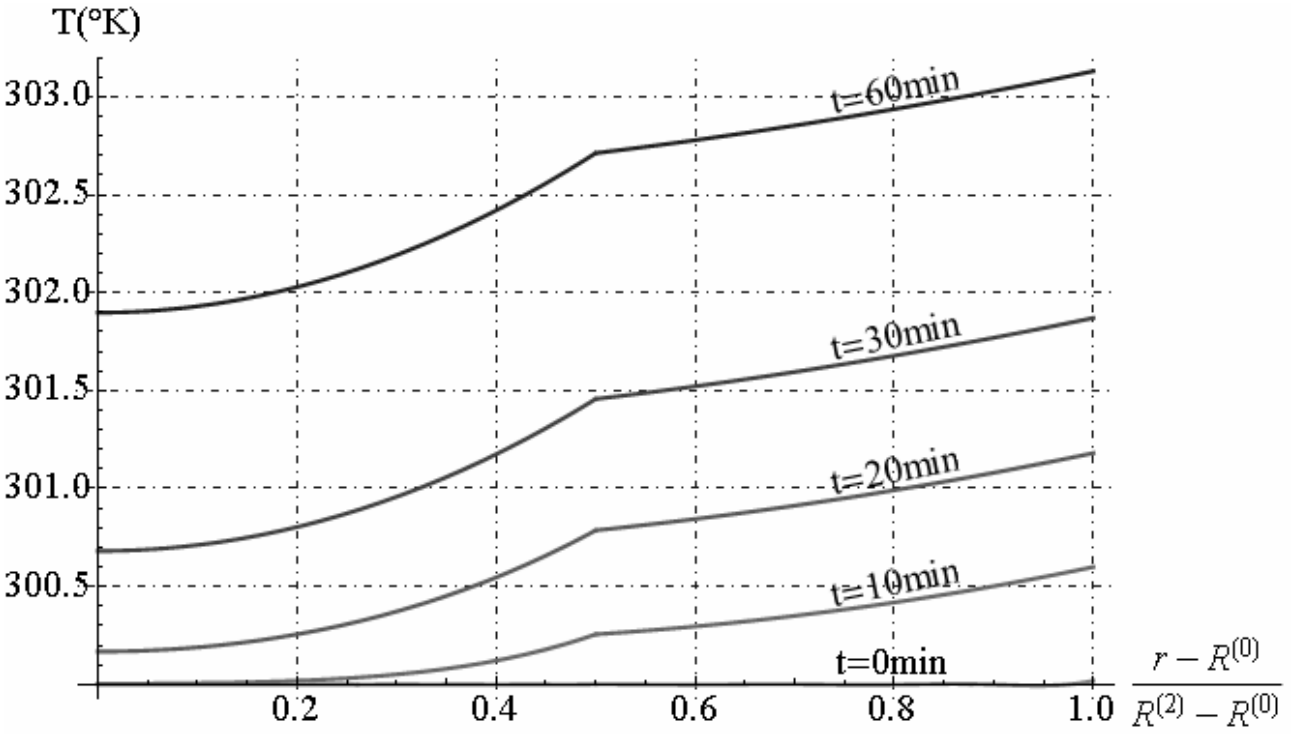

Fig. 21.13 - *Temperature function along radial direction*

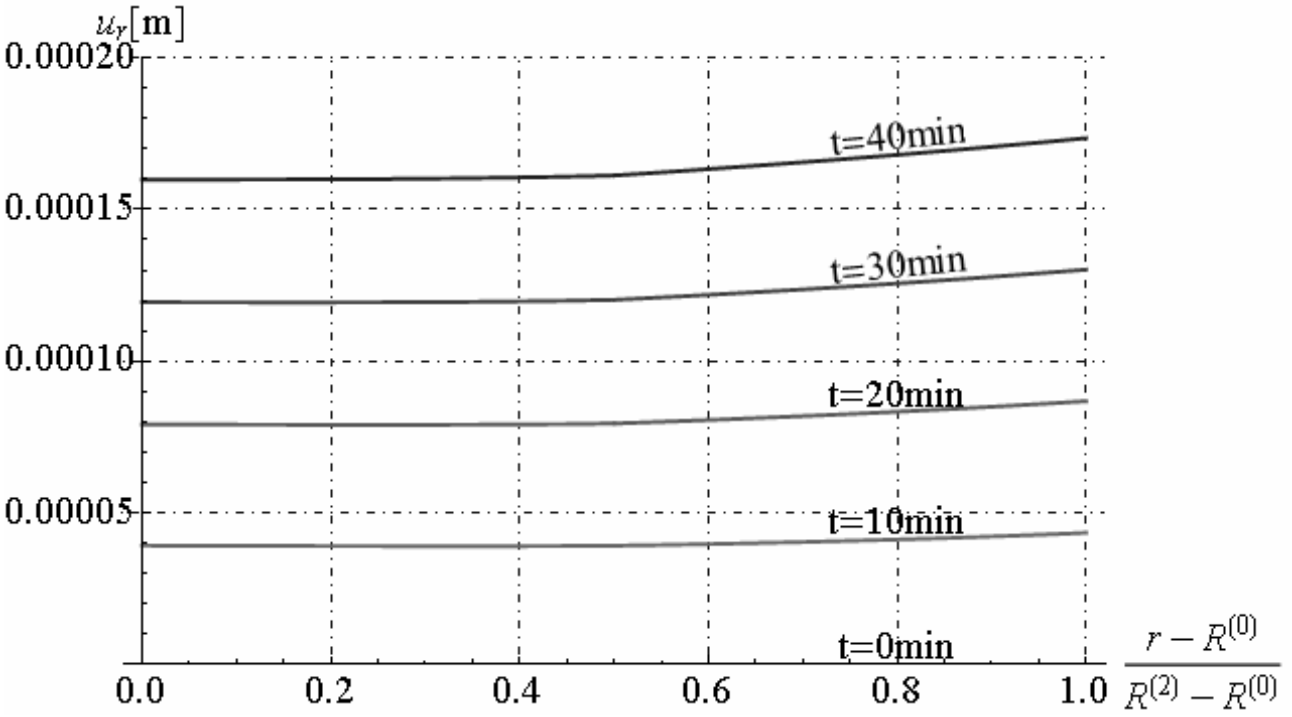

Fig. 21.14 - *Radial displacement along radial direction*

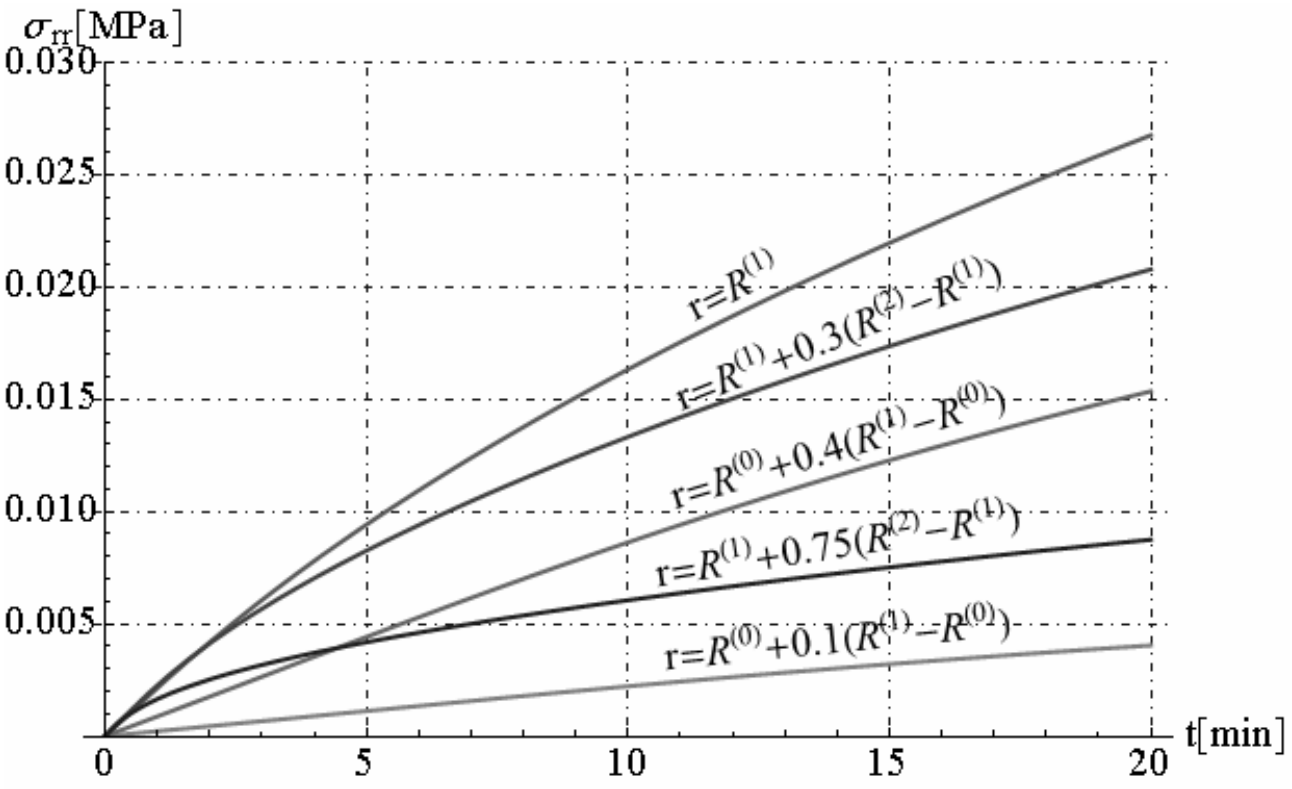

Fig. 21.15 - *Radial stress along radial direction*

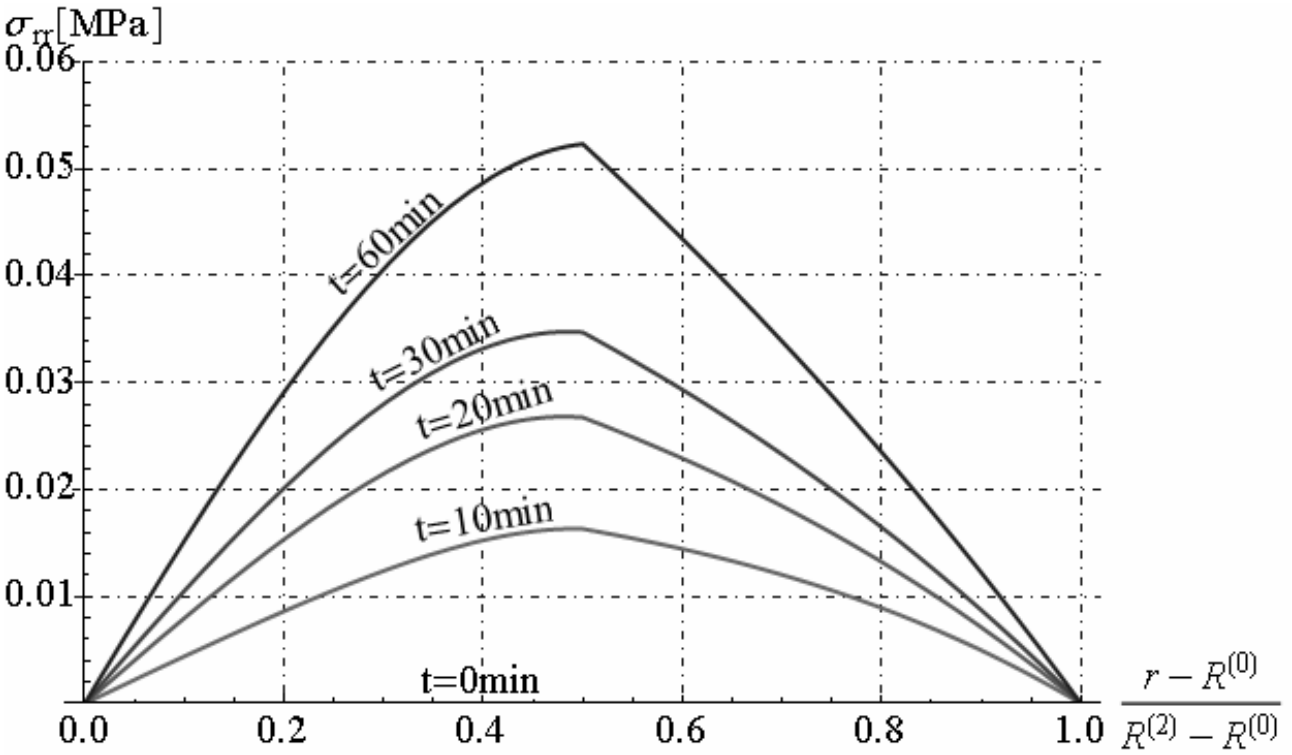

Fig. 21.16 - *Radial stress versus time*

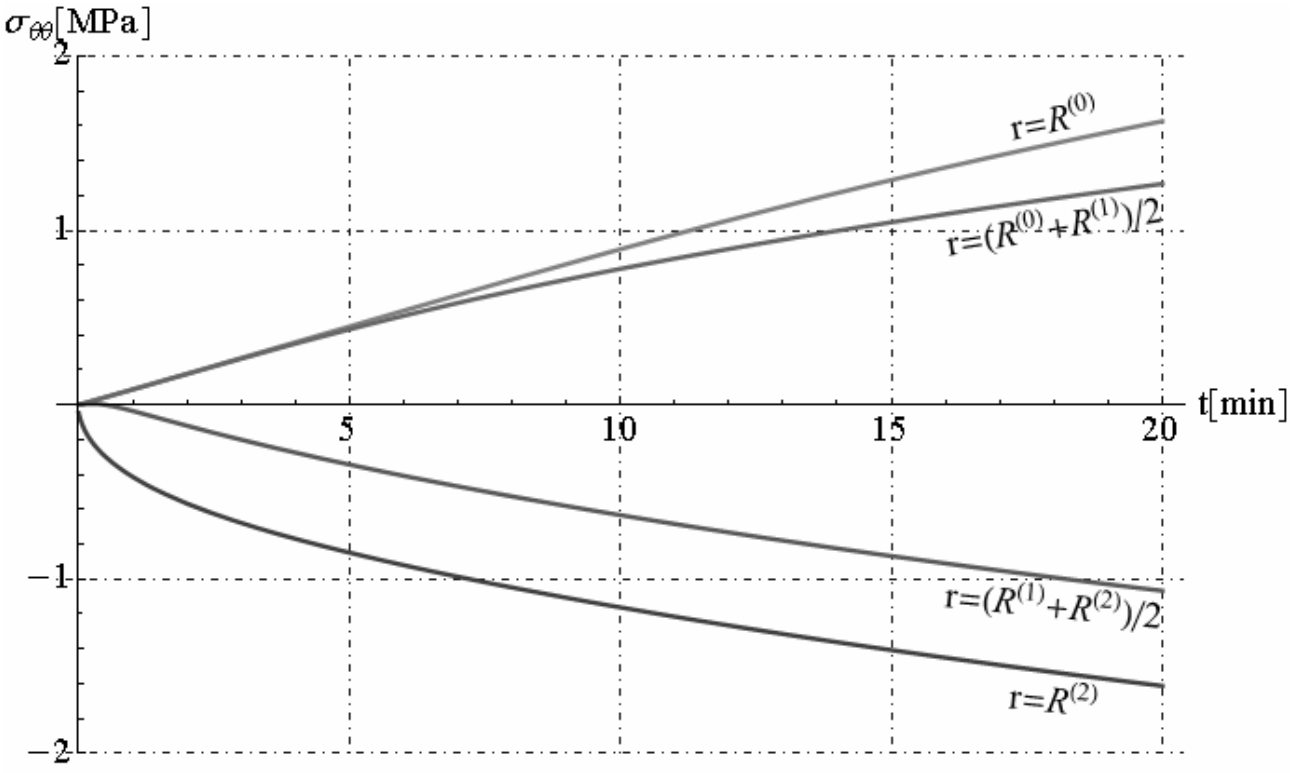

Fig. 21.17 - *Circumferential stress along radial direction*

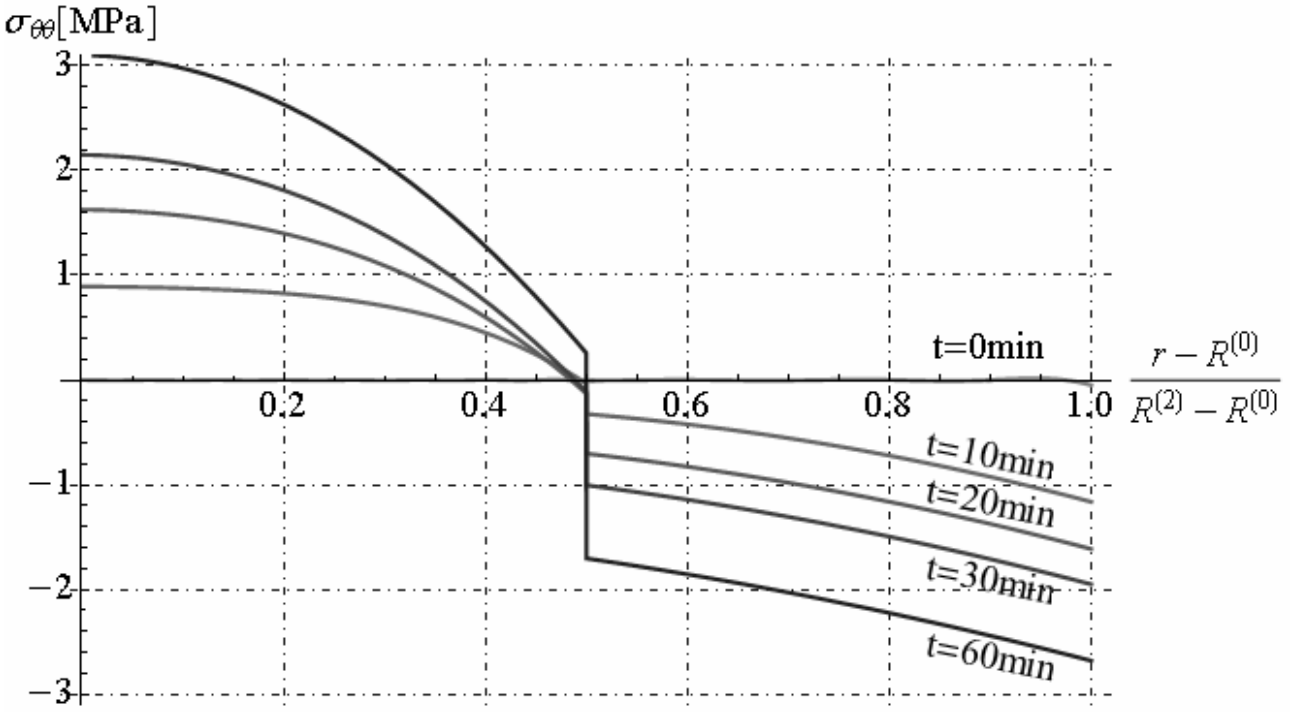

Fig. 21.18 - *Circumferential stress versus time*

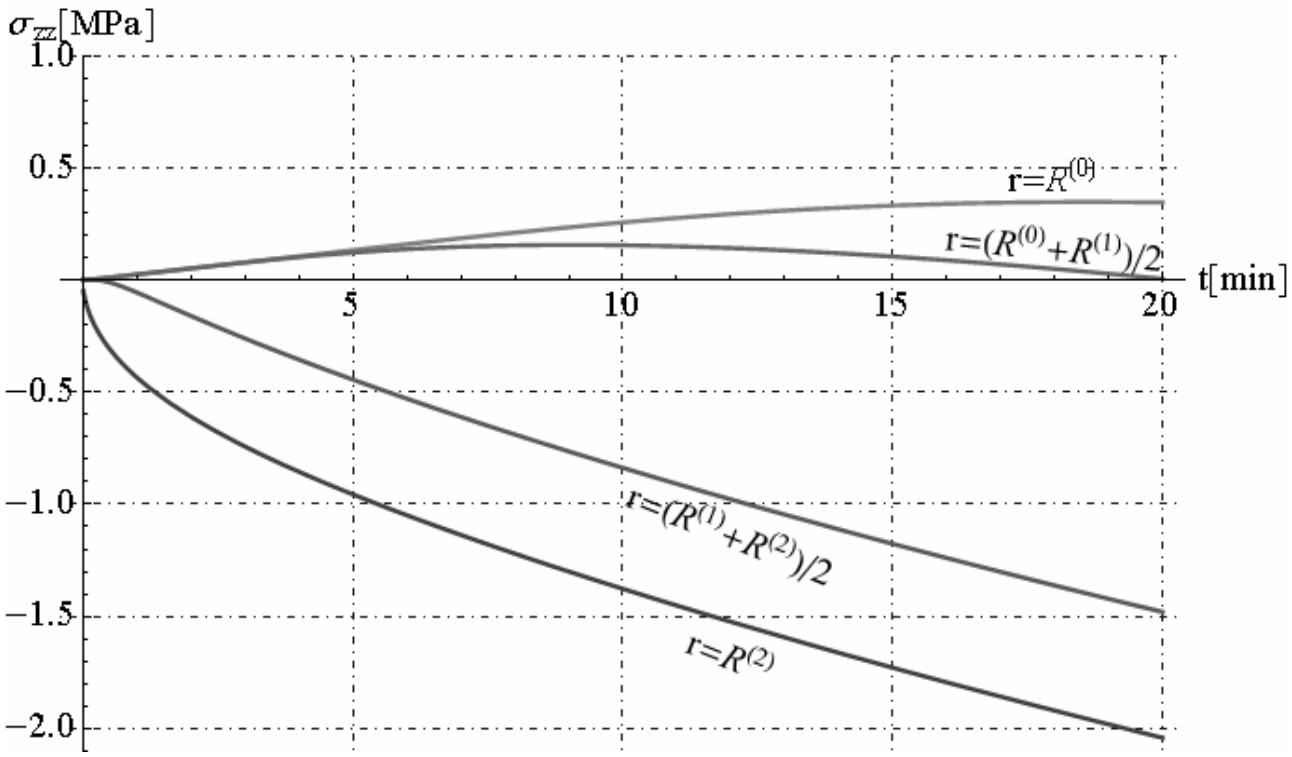

Fig. 21.19 - *Axial stress along radial direction*

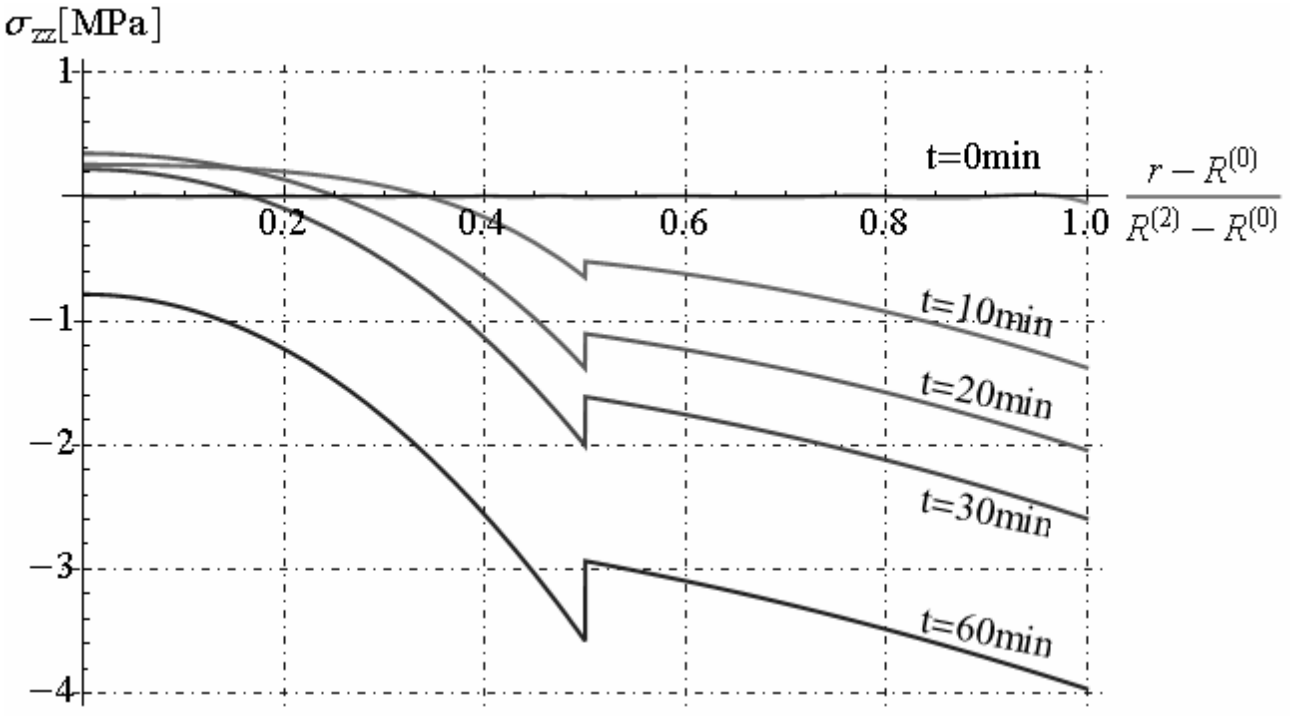

Fig. 21.20 - *Axial stress versus time*

21.4. Multilayered cylinder exposed to hydrocarbon fire

Let us consider an multilayered cylinder constituted by n-hollow cylindrical phases as decrypted in section 21.1. The inner surface $r = R^{(0)}$ is kept perfectly insulated while the outer surface $r = R^{(n)}$ is exposed to conventional fire, for t >0. In this section, we determine the temperature, displacement

and stress function in multilayered cylinder by starting to initial temperature equal to $T_0 = T_R = const$. The equations field to satisfy in uncoupled thermo-elastic problem with cylindrical symmetry and in plane strain are reported in equations (21.13), but in this case the boundary conditions (21.11) become:

$$\begin{cases} -k^{(1)} T^{(1)}_{,r}(r = R^{(0)}) = 0, \\ -k^{(n)} T^{(n)}_{,r}(r = R^{(n)}) = h_c \left[T^{(n)}(r = R^{(n)}) - \Theta_F \right], \end{cases} \quad \forall t \geq 0 \tag{21.95}$$

where Θ_F is the conventional fire curve and h_c is convection coefficient on surface $r = R^{(n)}$. In this case, we considered Hydrocarbon fire curve given by follows equation (see Chapter XIX):

$$\begin{aligned} &\Theta_F = H_0 + H_1 e^{-\xi_1 t} + H_2 e^{-\xi_2 t} \quad [^\circ K, \sec] \\ &H_0 = 1373.15^\circ K,\ H_1 = -729^\circ K,\ H_2 = -351^\circ K, \\ &\xi_1 = -2.783 \cdot 10^{-3} \sec^{-1},\ \ \xi_2 = -4.416 \cdot 10^{-2} \sec^{-1}, \end{aligned} \tag{21.96}$$

and the boundary conditions (21.8) become:

$$\sigma^{(n)}_{rr}(r = R^{(n)}, t) = 0, \quad \sigma^{(1)}_{rr}(r = R^{(0)}, t) = 0, \quad \forall t \geq 0 \tag{21.97}$$

The other boundary conditions reported in section 21.1 don't change. By solving the Fourier's equation reported in second equation of (21.13) with method separation of variables, and by substituting the function of temperature $T^{(i)}(r,t)$ in first equation of (21.13), and by integration in two time this equation respect to variable r, the displacement solution is reported in equation (21.14). In this case, the heat conduct problem involving a non-homogeneous boundary condition and, in particular, with the heat input specified over the entire boundary surface. It is necessary writing the temperature solution, in any phases of multilayered cylinder, in the follows form :

$$T^{(i)}(r,t) = H_0 + e^{\xi_1 t} T^{(i)}_1(r) + e^{\xi_2 t} T^{(i)}_2(r) + T^{(i)}_C(r,t), \quad \forall i \in \{1, 2, ..., n\} \tag{21.98}$$

The functions $T^{(i)}_1(r)$ and $T^{(i)}_2(r)$ in generic i-th phase satisfy the field equations:

$$\frac{d^2 T^{(i)}_j}{d r^2} + \frac{1}{r} \frac{d T^{(i)}_j}{d r} - \frac{\xi_j T^{(i)}_j}{\kappa^{(i)}} = 0; \qquad \begin{matrix} R^{(i-1)} \leq r \leq R^{(i)} \\ \forall i \in \{1, 2, ..., n\}, \ \ \forall j \in \{1, 2\} \end{matrix} \tag{21.99}$$

Moreover the function $T^{(i)}_S(r)$ must be satisfy the following boundary conditions :

$$-k^{(1)} \frac{d T^{(1)}_j(r)}{d r} = 0, \quad r = R^{(0)}, \forall j \in \{1, 2\} \tag{21.100}$$

$$-k^{(n)} \frac{d T^{(n)}_j(r)}{d r} = h_c \left[T^{(n)}_j(r) - H_j \right], \quad r = R^{(n)}, \forall j \in \{1, 2\} \tag{21.101}$$

$$-k^{(i)} \frac{d T^{(i)}_j(r)}{d r} = -k^{(i+1)} \frac{d T^{(i+1)}_j(r)}{d r}, \quad r = R^{(i)}, \ \forall i \in \{1, 2, ..., n-1\}, \forall j \in \{1, 2\} \tag{21.102}$$

$$T^{(i)}_j(r) = T^{(i+1)}_j(r), \quad r = R^{(i)}, \ \forall i \in \{1, 2, ..., n-1\}, \forall j \in \{1, 2\} \tag{21.103}$$

The function $T^{(i)}_C(r,t)$ in generic i-th phase satisfies the field equations:

$$\frac{\partial^2 T^{(i)}_C(r,t)}{\partial r^2} + \frac{1}{r} \frac{\partial T^{(i)}_C(r,t)}{\partial r} = \frac{1}{\kappa^{(i)}} \frac{\partial T^{(i)}_C(r,t)}{\partial t}; \qquad \begin{matrix} R^{(i-1)} \leq r \leq R^{(i)}, \forall t \geq 0 \\ \forall i \in \{1, 2, ..., n\} \end{matrix} \tag{21.104}$$

Moreover the function $T^{(i)}_C(r,t)$ must be satisfy the following boundary conditions :

$$-k^{(1)} \frac{\partial T^{(1)}_C(r,t)}{\partial r} = 0, \quad r = R^{(0)}, \ \forall t \geq 0, \tag{21.105}$$

$$-k^{(n)}\frac{\partial T_C^{(n)}(r,t)}{\partial r}=h_c T_C^{(n)}(r,t),\quad r=R^{(n)},\ \forall t\geq 0, \tag{21.106}$$

$$\begin{cases}-k^{(i)}\dfrac{\partial T_C^{(i)}(r,t)}{\partial r}=-k^{(i+1)}\dfrac{\partial T_C^{(i+1)}(r,t)}{\partial r},\\ T_C^{(i)}(r,t)=T_C^{(i+1)}(r,t),\end{cases}\quad r=R^{(i)},\ \forall t\geq 0,\ \forall i\in\{1,2,...,n-1\} \tag{21.107}$$

$$T_C^{(i)}(r,t)=-\left[H_0-T_0+e^{\xi_1 t}T_1^{(i)}(r)+e^{\xi_2 t}T_2^{(i)}(r)\right],\quad R^{(i-1)}\leq r\leq R^{(i)},\ t=0,\ \forall i\in\{1,2,...,n\} \tag{21.108}$$

The solutions of differential equation (21.99) is given by:

$$\begin{cases}T_1^{(i)}(r)=C^{(i)}J_0\left(i\eta_1^{(i)}r\right)+D^{(i)}Y_0\left(-i\eta_1^{(i)}r\right)\\ T_2^{(i)}(r)=G^{(i)}J_0\left(i\eta_2^{(i)}r\right)+L^{(i)}Y_0\left(-i\eta_2^{(i)}r\right)\end{cases}\quad \forall i\in\{1,2,...,n\} \tag{21.109}$$

where i is unit imaginary, $C^{(i)},D^{(i)},G^{(i)},L^{(i)}$ are 4n unknown parameters to determine and parameters $\eta_1^{(i)},\eta_2^{(i)}$ are given by:

$$\eta_1^{(i)}=\sqrt{\frac{\xi_1}{\kappa^{(i)}}},\quad \eta_2^{(i)}=\sqrt{\frac{\xi_2}{\kappa^{(i)}}}, \tag{21.110}$$

By solving algebraic system composed by 4n equations (21.100) to (21.103), we obtain integration constants $C^{(i)},D^{(i)},G^{(i)},L^{(i)}$. For brevity, we don't reported in explicit the expressions of these constants. The solution to the problem for T_C is found in much the same says way as was followed in section 21.2. The problem is therefore on with homogeneous differential equation and boundary conditions and may be treated by the method separation of variables as showed in section 21.2. The solutions of differential equation (21.104) is given by:

$$T_C^{(i)}(r,t)=\left[A^{(i)}J_0\left(\omega\beta^{(i)}r\right)+B^{(i)}Y_0\left(\omega\beta^{(i)}r\right)\right]e^{-\kappa^{(i)}\beta^{(i)2}\omega^2 t}\quad \forall i\in\{1,2,...,n\} \tag{21.111}$$

where $A^{(i)},B^{(i)},\omega$ are constants parameter to determine, the coefficient $\beta^{(i)}=\sqrt{\kappa^{(1)}/\kappa^{(i)}}$. In explicit the boundary conditions (21.107) for temperature function $T_C^{(i)}(r,t)$ are reported in equation (21.78). Moreover the boundary conditions on the inner and the outer surface (21.105) and (21.106) can be to rewrite as reported in equations (21.22). By first equation of (21.22), we determine $B^{(1)}$ as function of $A^{(1)}$ as follows:

$$B^{(1)}=-\frac{J_1\left(\omega R^{(0)}\beta^{(1)}\right)}{Y_1\left(\omega R^{(0)}\beta^{(1)}\right)}A^{(1)} \tag{21.112}$$

The equations (21.78) constituted an homogeneous algebraic system, composed by 2(n-1) equations, in unknown parameters $A^{(i)},B^{(i)}$ with $i\in\{1,2,...,n\}$, which can be written as:

$$\mathbf{\Phi}\cdot\mathbf{X}=\mathbf{0} \tag{21.113}$$

where $\mathbf{X}=[\mathbf{X}^{(1)},\mathbf{X}^{(2)},...,\mathbf{X}^{(n)}]^T$ collect the unknowns sub-vectors, as reported below:

$$\mathbf{X}^{(i)}=\begin{bmatrix}A^{(i)} & B^{(i)}\end{bmatrix}^T,\quad \forall i\in\{1,2,....,n\} \tag{21.114}$$

and $\mathbf{\Phi}$ is the matrix reported in equation (21.26). As showed in section 21.2, matrix $\mathbf{\Phi}$ is constituted by components: $\mathbf{\Phi}_i^{(i)},\mathbf{\Phi}_i^{(i+1)},\forall i\in\{1,2,...,n-1\}$ and vector $\mathbf{X}^{(i)}$ is obtained as function of vector $\mathbf{X}^{(1)}$ (see equation (21.29)). By substituting the solutions (21.29) in boundary conditions (21.22), we obtain vector equations in unknown vector $\mathbf{X}^{(1)}$, as reported below:

$$\mathbf{\Lambda}\cdot\mathbf{X}^{(1)}=\mathbf{0} \tag{21.115}$$

where $\mathbf{\Lambda}$ is an 2x2 square matrix given by :

$$\mathbf{\Lambda}=\begin{bmatrix}\Lambda_{11} & \Lambda_{12}\\ \Lambda_{21} & \Lambda_{22}\end{bmatrix} \tag{21.116}$$

where the components $\Lambda_{11},\Lambda_{12},\Lambda_{21},\Lambda_{22}$ are reported below:

$$\begin{aligned}&\Lambda_{11}=J_1\left(\omega\beta^{(1)}R^{(0)}\right),\quad \Lambda_{12}=Y_1\left(\omega\beta^{(1)}R^{(0)}\right),\\&\left[\Lambda_{21},\Lambda_{22}\right]=\left[J_1\left(\omega\beta^{(n)}R^{(n)}\right),Y_1\left(\omega\beta^{(n)}R^{(n)}\right)\right]\cdot\mathbf{\Gamma}^{(n)},\end{aligned}\tag{21.117}$$

Where $\mathbf{\Gamma}^{(n)}$ is given by equation (21.30) with i = n. The algebraic system (21.115) admit not trivial solution if the determinant of the matrix $[\mathbf{\Lambda}]$ is equal to zero. By imposing this condition, we obtain the transcendental equation in unknown parameter ω:

$$\det[\mathbf{\Lambda}]=0\ \Rightarrow\ g(\omega)=0\tag{21.118}$$

The roots of this transcendental equation (21.118) are an infinite number such, denoted here by $\omega_m,\ m=1,2,....N$ leading to eigenvalues or characteristic values $\lambda_m=-\omega_m^2$. The corresponding eigenfunctions or characteristic functions $\overline{\varphi}_m^{(i)}(r)$ are reported in equation (21.111). The coefficients $A_m^{(1)}$ are determined by applying the initial condition (21.108) that yields the following relationship:

$$A_m^{(1)}=-\frac{\sum_{i=1}^{n}\left\{\rho^{(i)}c_v^{(i)}\int_0^{2\pi}\int_{R^{(i-1)}}^{R^{(i)}}r\,\overline{\varphi}_m^{(i)}\left[H_0-T_0+T_1^{(i)}(r)+T_2^{(i)}(r)\right]drd\theta\right\}}{\sum_{i=1}^{n}\left[\rho^{(i)}c_v^{(i)}\int_0^{2\pi}\int_{R^{(i-1)}}^{R^{(i)}}\left(\overline{\varphi}_m^{(i)}\right)^2 rdrd\theta\right]}\tag{21.119}$$

Finally the temperature function in i-th generic phase is given by:

$$\begin{aligned}T^{(i)}(r,t)=H_0+&\left[C^{(i)}J_0\left(i\eta_1^{(i)}r\right)+D^{(i)}Y_0\left(-i\eta_1^{(i)}r\right)\right]e^{\xi_1 t}+\left[G^{(i)}J_0\left(i\eta_2^{(i)}r\right)+L^{(i)}Y_0\left(-i\eta_2^{(i)}r\right)\right]e^{\xi_2 t}+\\&+\sum_{m=1}^{\infty}\left[A_m^{(i)}J_0\left(\omega_m\beta^{(i)}r\right)+B_m^{(i)}Y_0\left(\omega_m\beta^{(i)}r\right)\right]e^{-\kappa^{(i)}\beta^{(i)2}\omega_m^2 t}\qquad\forall i\in\{1,2,....,n\}\end{aligned}\tag{21.120}$$

By substituting the function (21.120) in equation (21.14), we obtain in explicit the displacement function in any hollow cylindrical phase:

$$\begin{aligned}u_r^{(i)}=&P^{(i)}r+\frac{Q^{(i)}}{r}+\left(U^{(i)}r+\frac{V^{(i)}}{r}\right)e^{\xi_1 t}+\left(W^{(i)}r+\frac{Z^{(i)}}{r}\right)e^{\xi_2 t}+\\&+\frac{\alpha^{(i)}\left(3\lambda^{(i)}+2\mu^{(i)}\right)}{\lambda^{(i)}+2\mu^{(i)}}\left\{\begin{aligned}&(1/3)H_0r+i\eta_1^{(i)-1}\left[D^{(i)}Y_1\left(-i\eta_1^{(i)}r\right)-C^{(i)}J_1\left(i\eta_1^{(i)}r\right)\right]e^{\xi_1 t}+\\&+i\eta_2^{(i)-1}\left[L^{(i)}Y_1\left(-i\eta_2^{(i)}r\right)-G^{(i)}J_1\left(i\eta_2^{(i)}r\right)\right]e^{\xi_2 t}\end{aligned}\right\}\\&+\sum_{m=1}^{\infty}\left\{P_m^{(i)}r+\frac{Q_m^{(i)}}{r}+\frac{\zeta^{(i)}}{\omega_m}\left[A_m^{(i)}J_1\left(\beta^{(i)}\omega_m r\right)+B_m^{(i)}Y_1\left(\beta^{(i)}\omega_m r\right)\right]\right\}e^{-\kappa^{(i)}\omega_m^2\beta^{(i)2}t}\\&\qquad\qquad\forall i\in\{1,2,....,n\}\end{aligned}\tag{21.121}$$

where the integration constants $P^{(i)},Q^{(i)},U^{(i)},V^{(i)},W^{(i)},Z^{(i)},N_m^{(i)},M_m^{(i)}$ are determined by applying the boundary conditions given by equations (21.97). In this case the functions $f_1^{(i)}(t),\ f_2^{(i)}(t)$, reported in equation (21.14) are given by:

$$\begin{aligned}f_1^{(i)}(t)&=P^{(i)}+U^{(i)}e^{\xi_1 t}+W^{(i)}e^{\xi_2 t}+\sum_{m=1}^{\infty}N_m^{(i)}e^{-\kappa^{(i)}\omega_m^2\beta^{(i)2}t},\\f_2^{(i)}(t)&=Q^{(i)}+V^{(i)}e^{\xi_1 t}+Z^{(i)}e^{\xi_2 t}+\sum_{m=1}^{\infty}M_m^{(i)}e^{-\kappa^{(i)}\omega_m^2\beta^{(i)2}t},\end{aligned}\tag{21.122}$$

In explicit the radial, circumferential and axial stress components are given by:

$$\sigma_{rr}^{(i)} = 2\left(\lambda^{(i)}+\mu^{(i)}\right)\left(P^{(i)}+U^{(i)}e^{\xi_1 t}+W^{(i)}e^{\xi_2 t}\right)-2\mu^{(i)}r^{-2}\left(Q^{(i)}+V^{(i)}e^{\xi_1 t}+Z^{(i)}e^{\xi_2 t}\right)+$$
$$+\frac{2i\mu^{(i)}\zeta^{(i)}\beta^{(i)}}{\eta_1^{(i)}r}\left[C^{(i)}J_1\left(i\eta_1^{(i)}r\right)-D^{(i)}Y_1\left(-i\eta_1^{(i)}r\right)\right]e^{\xi_1 t}+(2/3)\zeta^{(i)}\beta^{(i)}\left(\lambda^{(i)}+\mu^{(i)}\right)H_0+$$
$$+\frac{2i\mu^{(i)}\zeta^{(i)}\beta^{(i)}}{\eta_2^{(i)}r}\left[G^{(i)}J_1\left(i\eta_2^{(i)}r\right)-L^{(i)}Y_1\left(-i\eta_2^{(i)}r\right)\right]e^{\xi_2 t}-\left(3\lambda^{(i)}+2\mu^{(i)}\right)\left(H_0-T_R\right)+$$
$$+2\sum_{m=1}^{\infty}\left[N_m^{(i)}\left(\lambda^{(i)}+\mu^{(i)}\right)-M_m^{(i)}\mu^{(i)}r^{-2}\right]e^{-\omega_m^2\beta^{(i)2}\kappa^{(i)}t}+$$
$$-2\mu^{(i)}\zeta^{(i)}\sum_{m=1}^{\infty}\left\{\frac{1}{\omega_m r}\left[A_m^{(i)}J_1\left(\omega_m\beta^{(i)}r\right)+B_m^{(i)}Y_1\left(\omega_m\beta^{(i)}r\right)\right]\right\}e^{-\omega_m^2\beta^{(i)2}\kappa^{(i)}t} \tag{21.123}$$

$$\sigma_{\theta\theta}^{(i)} = 2\left(\lambda^{(i)}+\mu^{(i)}\right)\left(P^{(i)}+U^{(i)}e^{\xi_1 t}+W^{(i)}e^{\xi_2 t}\right)+2\mu^{(i)}r^{-2}\left(Q^{(i)}+V^{(i)}e^{\xi_1 t}+Z^{(i)}e^{\xi_2 t}\right)+$$
$$+2\mu^{(i)}\zeta^{(i)}\beta^{(i)}\left\{\left[C^{(i)}J_2\left(i\eta_1^{(i)}r\right)-D^{(i)}Y_2\left(-i\eta_1^{(i)}r\right)\right]e^{\xi_1 t}+\left[G^{(i)}J_1\left(i\eta_2^{(i)}r\right)-L^{(i)}Y_1\left(-i\eta_2^{(i)}r\right)\right]e^{\xi_2 t}\right\}$$
$$+\frac{2i\mu^{(i)}\zeta^{(i)}\beta^{(i)}}{\eta_1^{(i)}r}\left[C^{(i)}J_1\left(i\eta_1^{(i)}r\right)-D^{(i)}Y_1\left(-i\eta_1^{(i)}r\right)\right]e^{\xi_1 t}+(2/3)\zeta^{(i)}\beta^{(i)}\left(\lambda^{(i)}+\mu^{(i)}\right)H_0+$$
$$+\frac{2i\mu^{(i)}\zeta^{(i)}\beta^{(i)}}{\eta_2^{(i)}r}\left[G^{(i)}J_1\left(i\eta_2^{(i)}r\right)-L^{(i)}Y_1\left(-i\eta_2^{(i)}r\right)\right]e^{\xi_2 t}-\left(3\lambda^{(i)}+2\mu^{(i)}\right)\left(H_0-T_R\right)+$$
$$+2\sum_{m=1}^{\infty}\left[N_m^{(i)}\left(\lambda^{(i)}+\mu^{(i)}\right)+\mu^{(i)}M_m^{(i)}r^{-2}\right]e^{-\omega_m^2\beta^{(i)2}\kappa^{(i)}t}+$$
$$+2\zeta^{(i)}\mu^{(i)}\sum_{m=1}^{\infty}\left\{\begin{array}{l}\frac{A_m^{(i)}}{\omega_m r}\left[J_1\left(r\omega_m\beta^{(i)}\right)-r\omega_m\beta^{(i)}J_0\left(r\omega_m\beta^{(i)}\right)\right]+\\ +\frac{B_m^{(i)}}{\omega_m r}\left[J_1\left(r\omega_m\beta^{(i)}\right)-r\omega_m\beta^{(i)}J_0\left(r\omega_m\beta^{(i)}\right)\right]\end{array}\right\}e^{-\omega_m^2\beta^{(i)2}\kappa^{(i)}t} \tag{21.124}$$

$$\sigma_{zz}^{(i)} = 2\lambda^{(i)}\left(P^{(i)}+U^{(i)}e^{\xi_1 t}+W^{(i)}e^{\xi_2 t}\right)-\alpha^{(i)}\left(3\lambda^{(i)}+2\mu^{(i)}\right)\left(H_0-T_R+\xi t\right)+(2/3)\lambda^{(i)}\zeta^{(i)}\beta^{(i)}H_0+$$
$$-2\mu^{(i)}\zeta^{(i)}\beta^{(i)}\left\{e^{\xi_1 t}\left[C^{(i)}J_0\left(i\eta_1^{(i)}r\right)+D^{(i)}Y_0\left(-i\eta_1^{(i)}r\right)\right]+e^{\xi_2 t}\left[G^{(i)}J_1\left(i\eta_2^{(i)}r\right)+L^{(i)}Y_1\left(-i\eta_2^{(i)}r\right)\right]\right\}$$
$$+2\sum_{m=1}^{\infty}\left\{N_m^{(i)}\lambda^{(i)}+\mu^{(i)}\zeta^{(i)}\beta^{(i)}\left[A_m^{(i)}J_0\left(r\omega_m\beta^{(i)}\right)+B_m^{(i)}Y_0\left(r\omega_m\beta^{(i)}\right)\right]\right\}e^{-\omega_m^2\beta^{(i)2}\kappa^{(i)}t} \tag{21.125}$$

where the constant $\zeta^{(i)}=\dfrac{\alpha^{(i)}\left(3\lambda^{(i)}+2\mu^{(i)}\right)}{\beta^{(i)}\left(\lambda^{(i)}+2\mu^{(i)}\right)}$. Moreover, the tractions on the inner and the outer spherical boundary surface are vanishing and then condition (21.8) becomes:

$$\sigma_{rr}^{(1)}(r=R^{(0)})=0,\ \ \sigma_{rr}^{(n)}(r=R^{(n)})=0,\quad \forall t\geq 0 \tag{21.126}$$

The integration constants $G^{(i)},H^{(i)},P_m^{(i)},Q_m^{(i)}$ are function of geometrical, mechanical and thermal parameters of spherical layers . Moreover $P_m^{(i)},Q_m^{(i)}$ are function of constants $A_m^{(i)},B_m^{(i)},\omega_m$ also.

For example, let us consider, an multilayered cylinder constituted by two phases under uniform heat flux . The phase (1) is constituted by steel and phase (2) by aluminium. The mechanical and thermal parameters considered for both phases are reported in table 19.1. The geometrical parameters of multilayered cylinder composed by two phases are:

$$R^{(0)} = 10m,\ R^{(1)} = 10.05m,\ R^{(2)} = 10.10m,\ T_0 = T_R = 293.15°K = 20°C \quad (21.127)$$

In this case the graphics function $g(\omega)$ given by equation (21.86) is reported below:

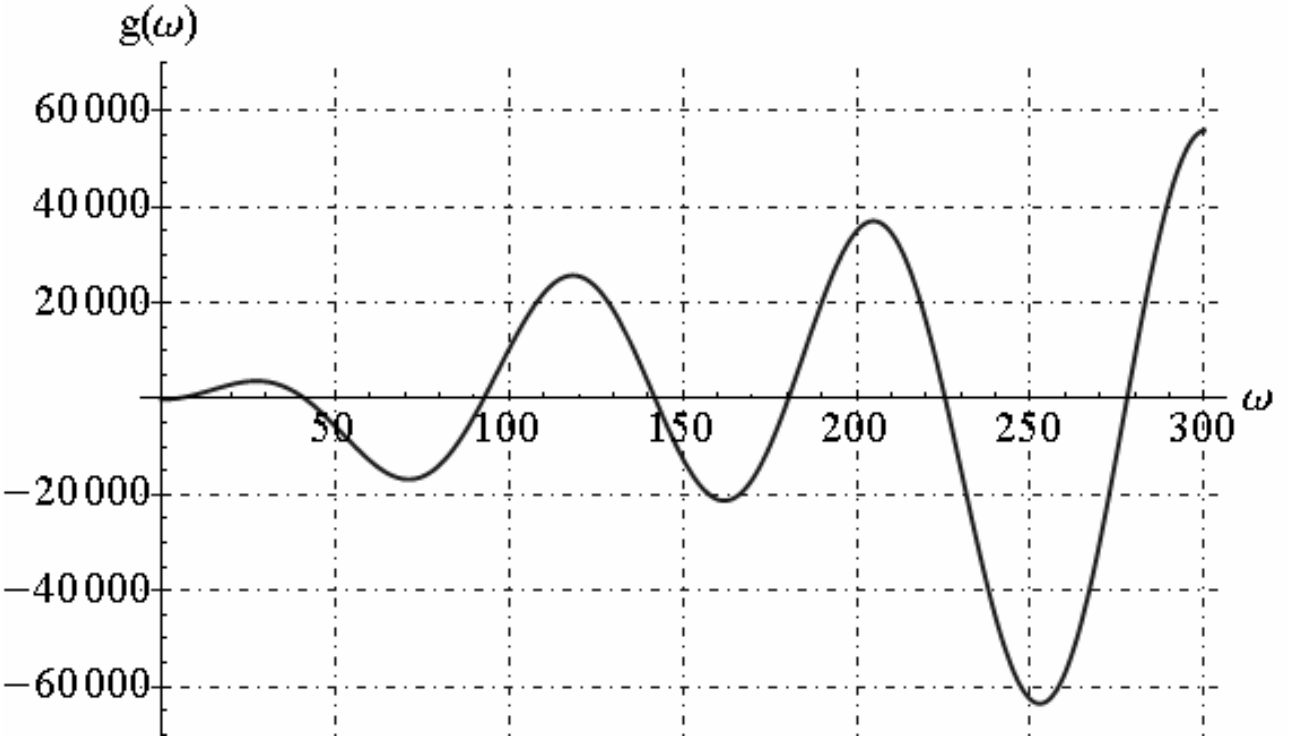

Fig. 21.21 - *Function* $g(\omega)$

By fixed m= 20, the eigenvalues ω_m of transcendental equation (21.86) and corresponding values of constants integration A_m are reported in table 21.4:

ω_m	3.568	41.306	92.695	142.020
A_m	$8024.352 + 0.\times10^{-4}\,i$	$-161.150 + 0.\times10^{-4}\,i$	$-15.719 + 0.\times10^{-4}\,i$	$-3.459 + 0.\times10^{-4}\,i$
ω_m	180.320	225.475	277.753	323.549
A_m	$1.1669 + 0.\times10^{-5}\,i$	$0.0814 + 0.\times10^{-5}\,i$	$0.2687 + 0.\times10^{-5}\,i$	$-0.0900 + 0.\times10^{-5}\,i$
ω_m	361.625	410.488	462.195	503.891
A_m	$-0.1219 + 0.\times10^{-5}\,i$	$-0.0272 + 0.\times10^{-5}\,i$	$-0.0522 + 0.\times10^{-5}\,i$	$-0.0253 + 0.\times10^{-5}\,i$
ω_m	544.494	595.770	645.491	684.062
A_m	$-0.0295153 + 0.\times10^{-8}\,i$	$-0.0169315 + 0.\times10^{-8}\,i$	$0.0048450 + 0.\times10^{-8}\,i$	$0.0128357 + 0.\times10^{-8}\,i$
ω_m	728.658	780.912	827.267	865.198
A_m	$-0.0090337 + 0.\times10^{-8}\,i$	$0.0007040 + 0.\times10^{-8}\,i$	$-0.0078184 + 0.\times10^{-8}\,i$	$-0.0047515 + 0.\times10^{-8}\,i$

Table 21.4 – *Eigenvalues* ω_m *and corresponding values of constants integration* A_m

We reported the graphics of temperature function along the radial direction and in time:

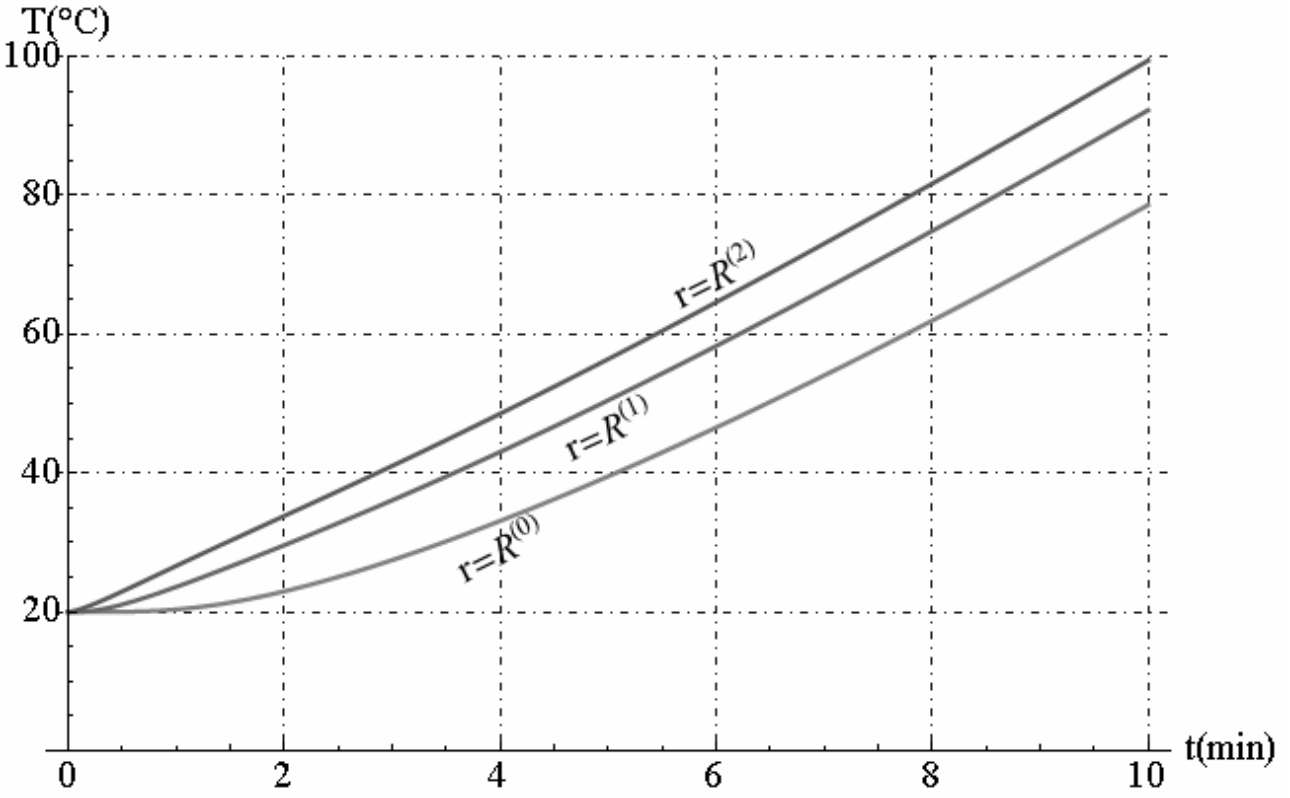

Fig. 21.22 - *Temperature function versus time*

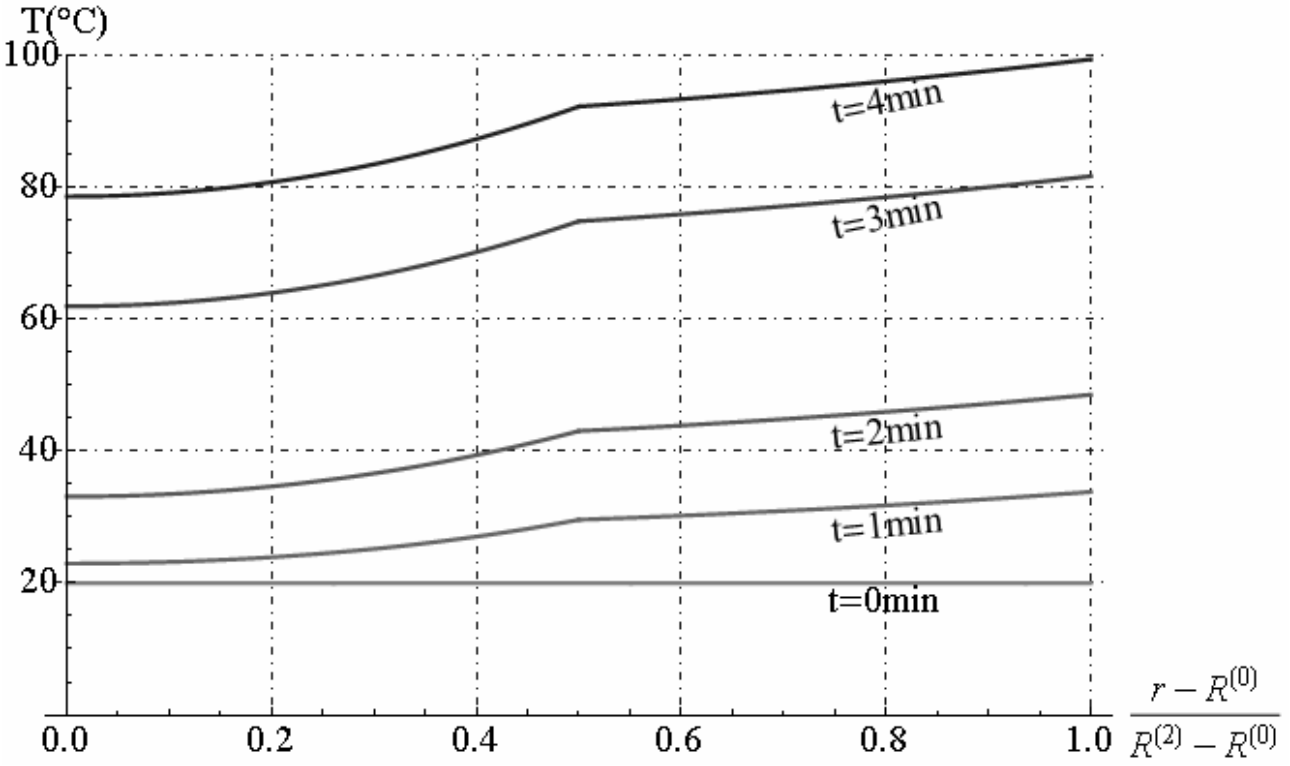

Fig. 21.23 - *Temperature function along radial direction*

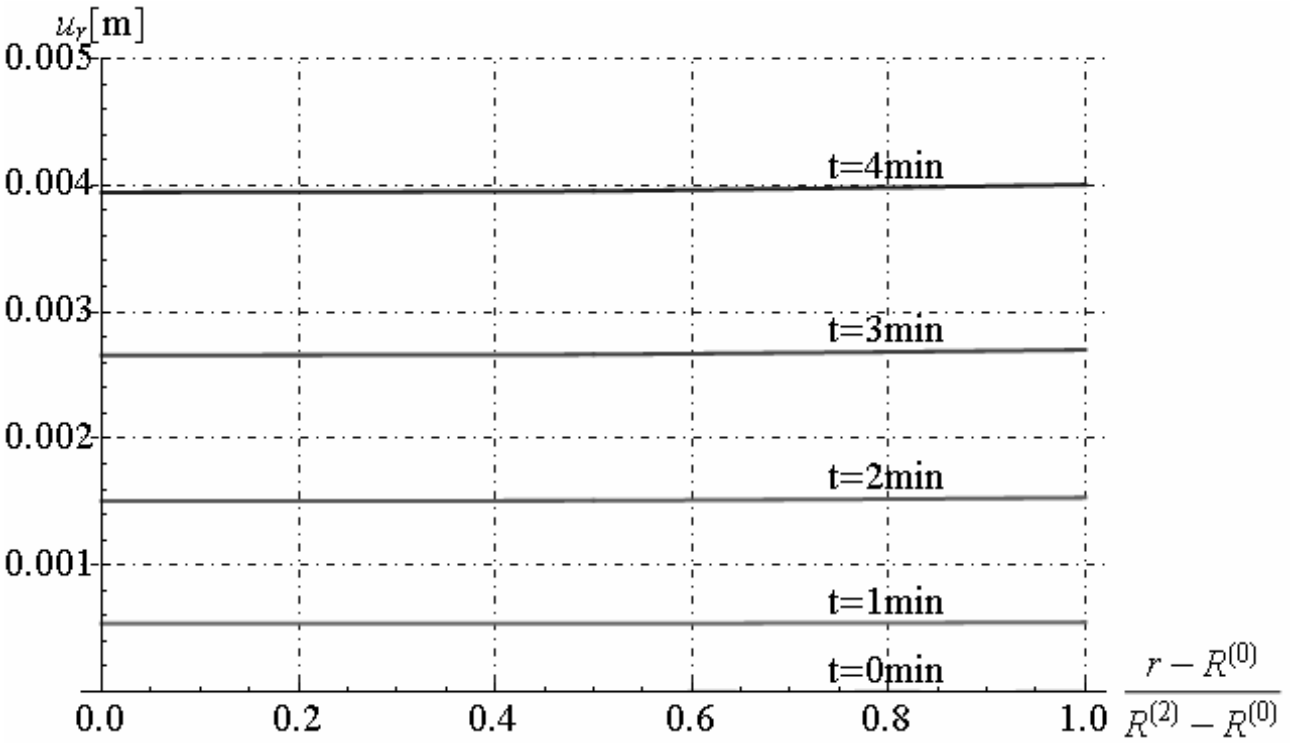

Fig. 21.24 - *Radial displacement along radial direction*

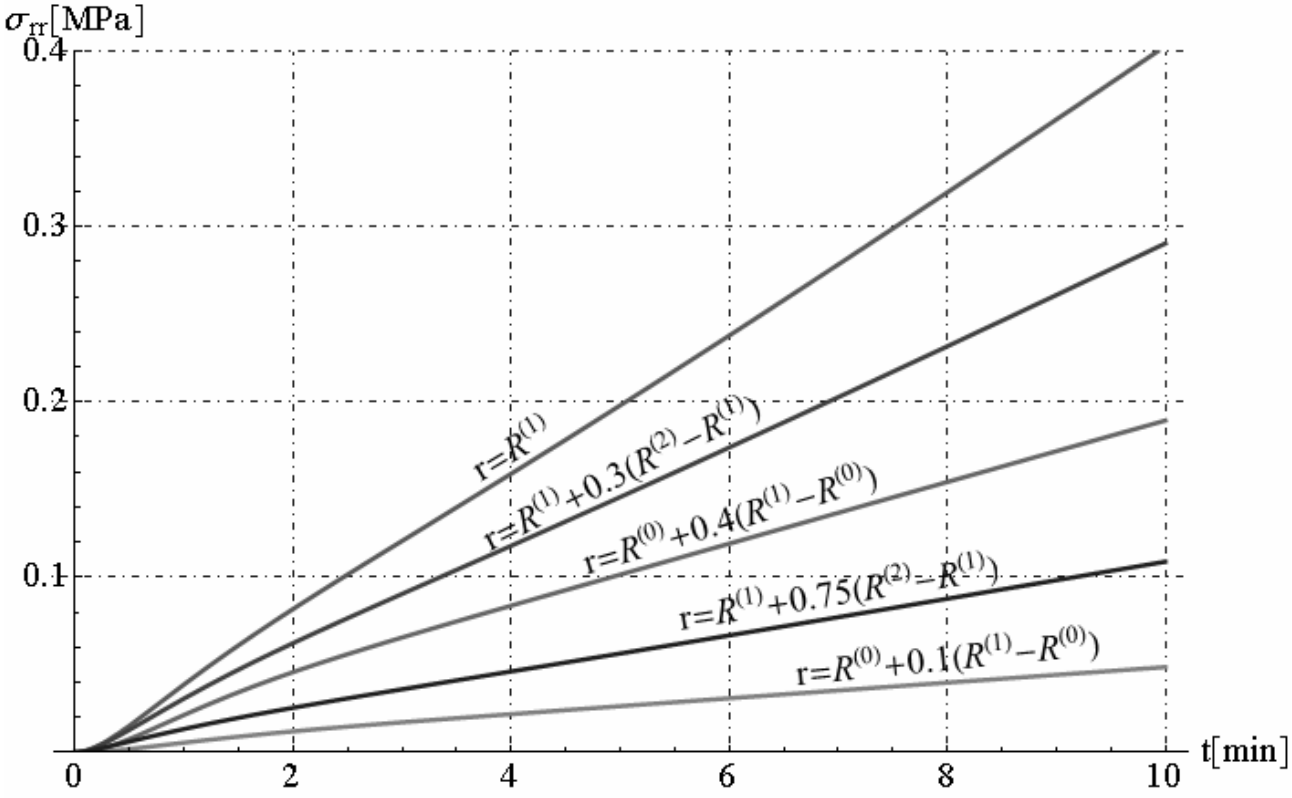

Fig. 21.25 - *Radial stress along radial direction*

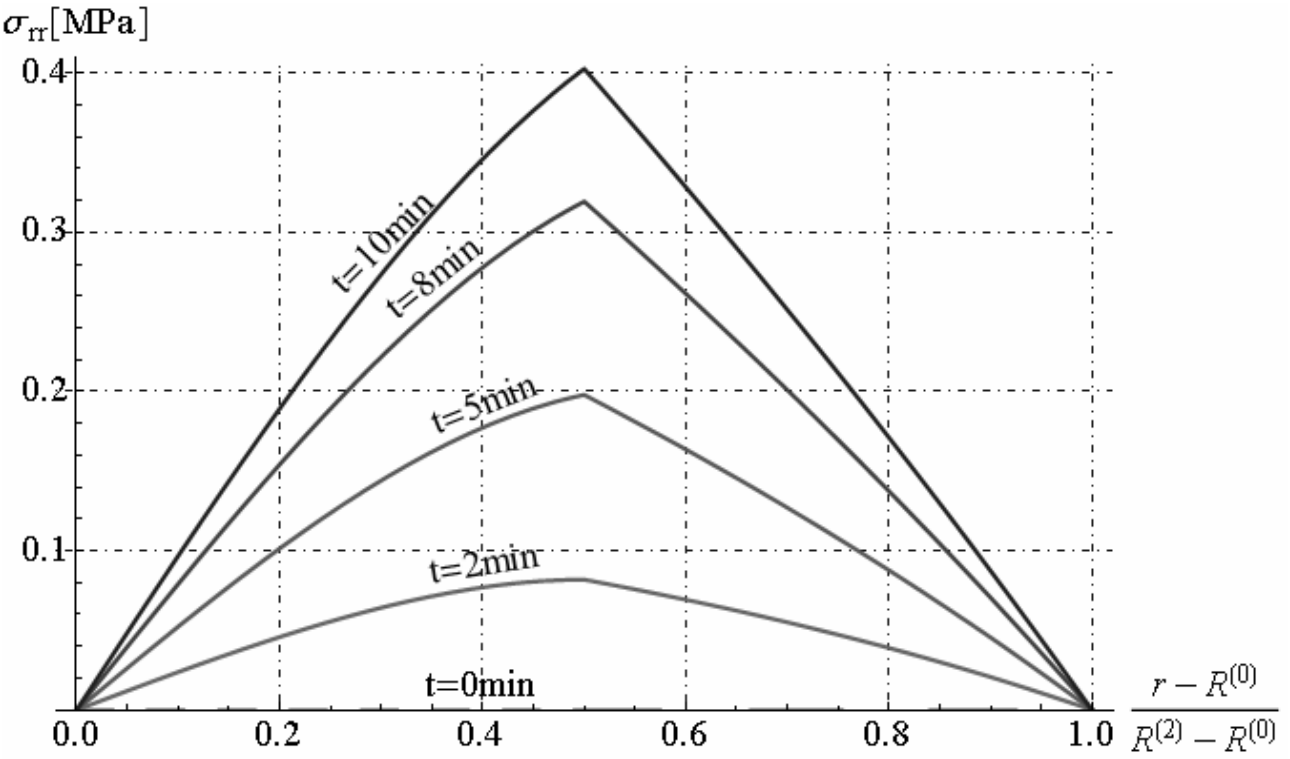

Fig. 21.26 - *Radial stress versus time*

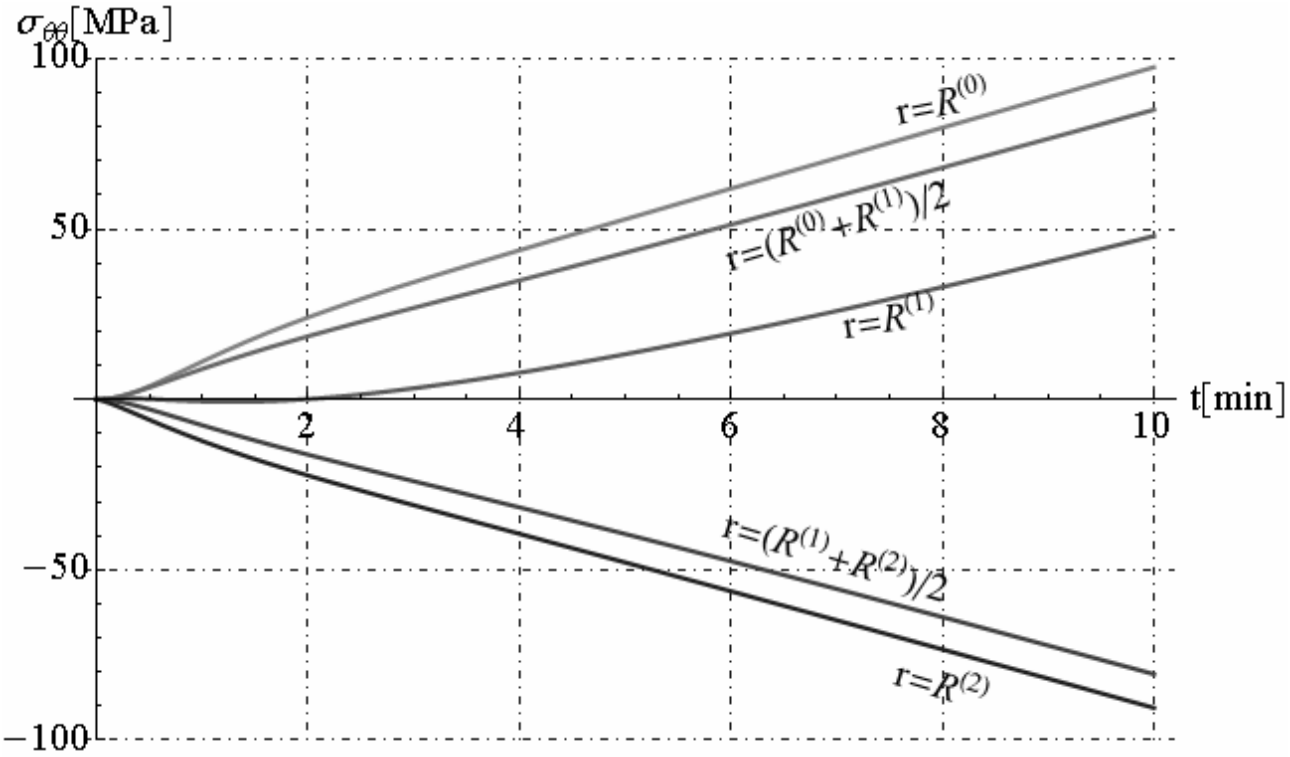

Fig. 21.27 - *Circumferential stress along radial direction*

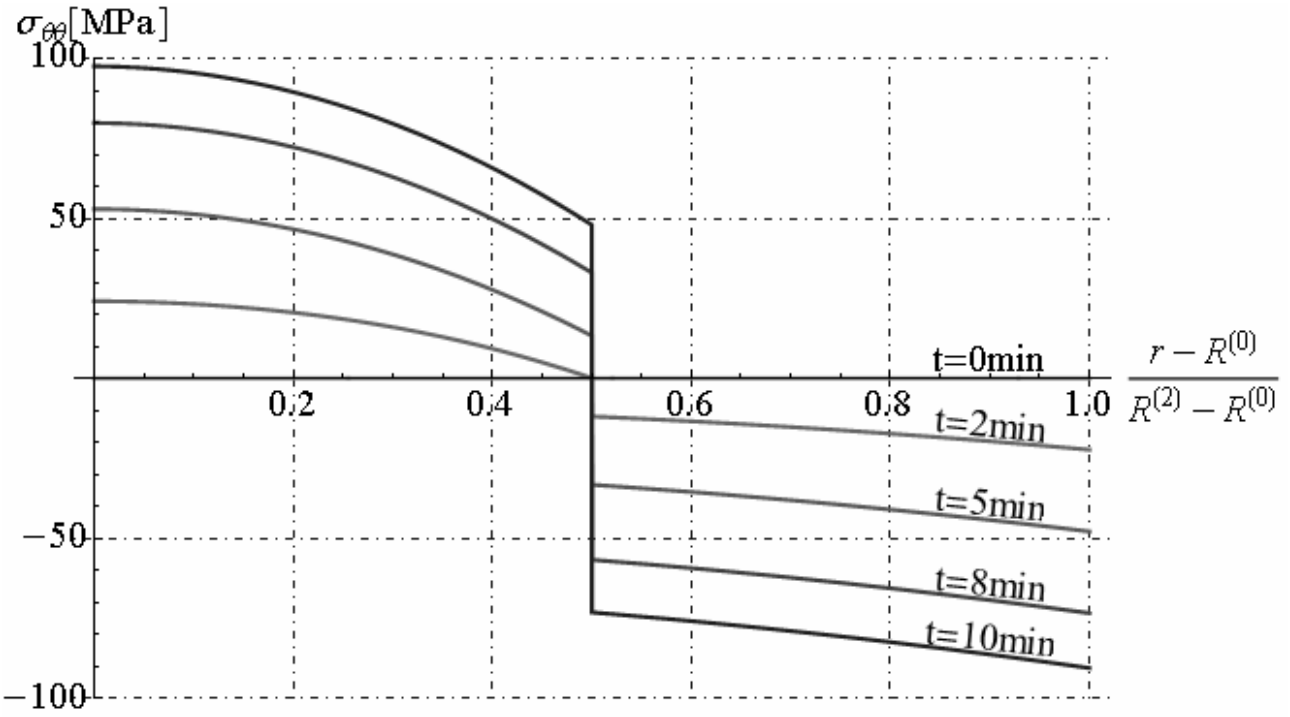

Fig. 21.28 - *Circumferential stress versus time*

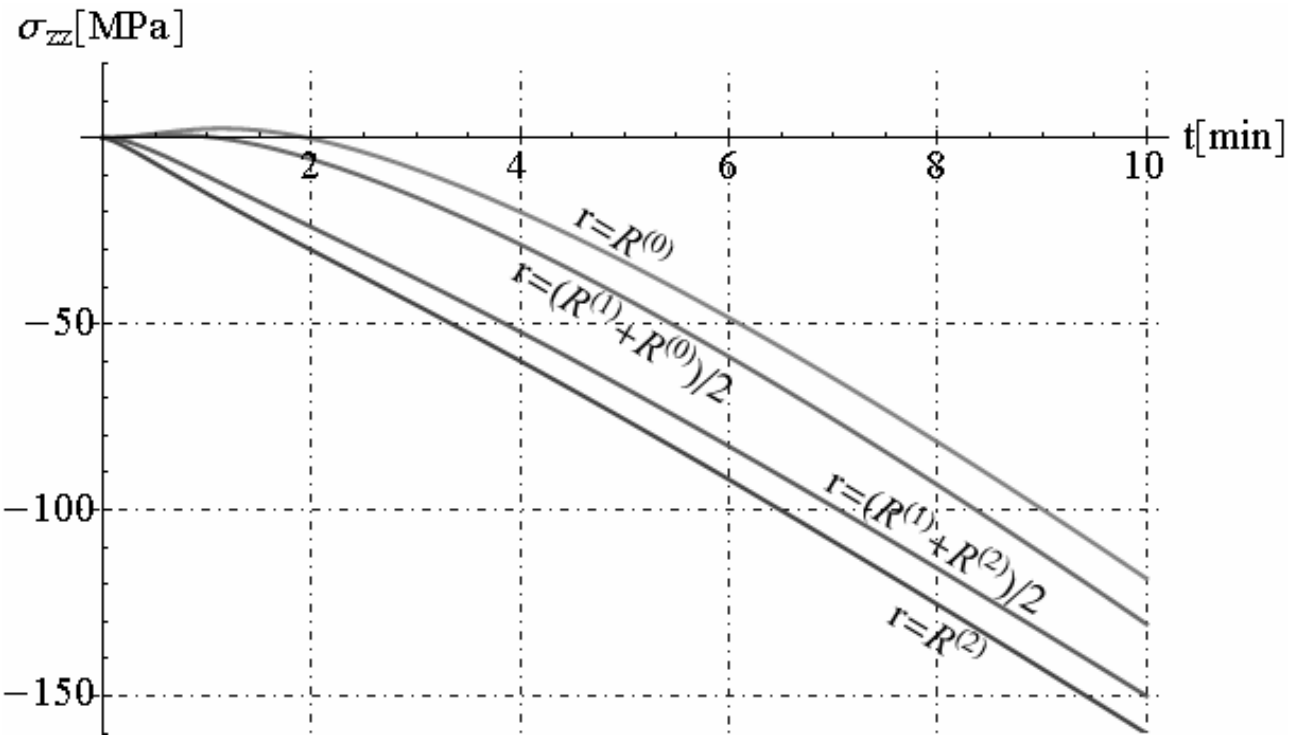

Fig. 21.29 - *Axial stress along radial direction*

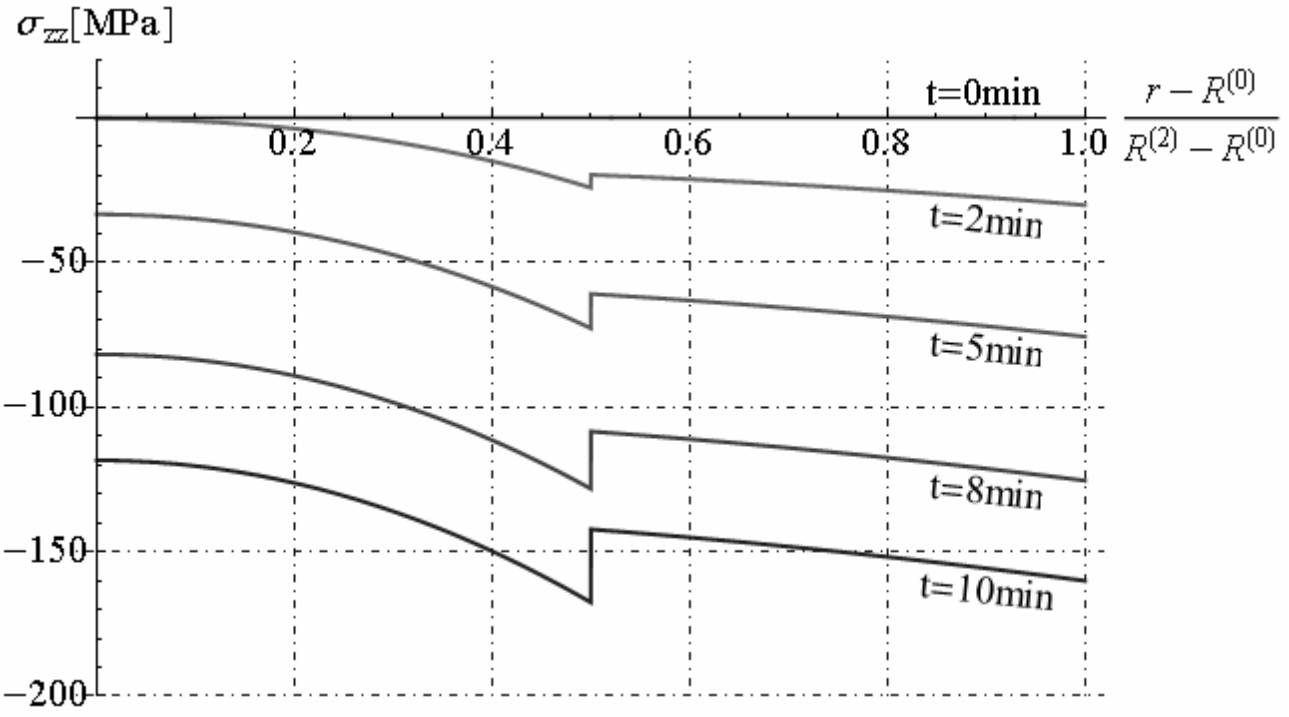

Fig. 21.30 - *Axial stress versus time*

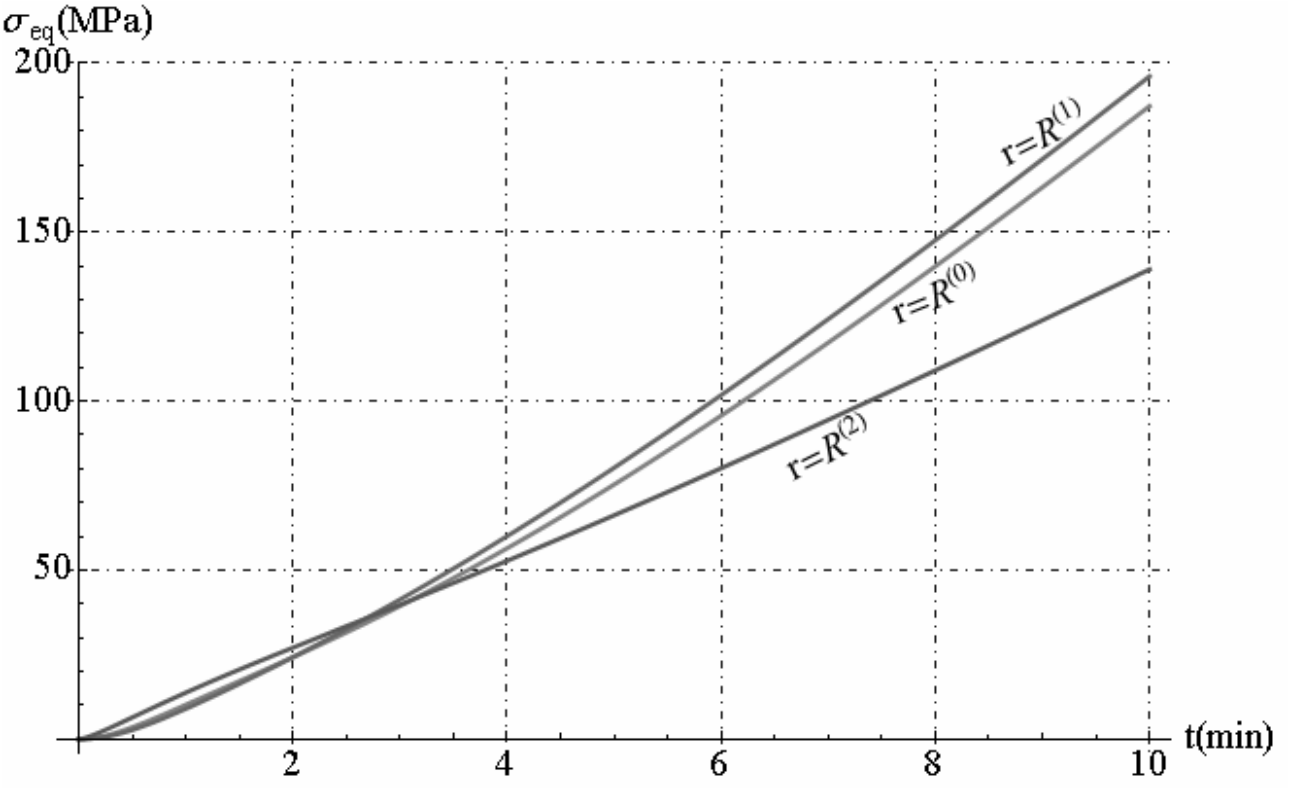

Fig. 21.31 - *Hencky von Mises's equivalent stress along radial direction*

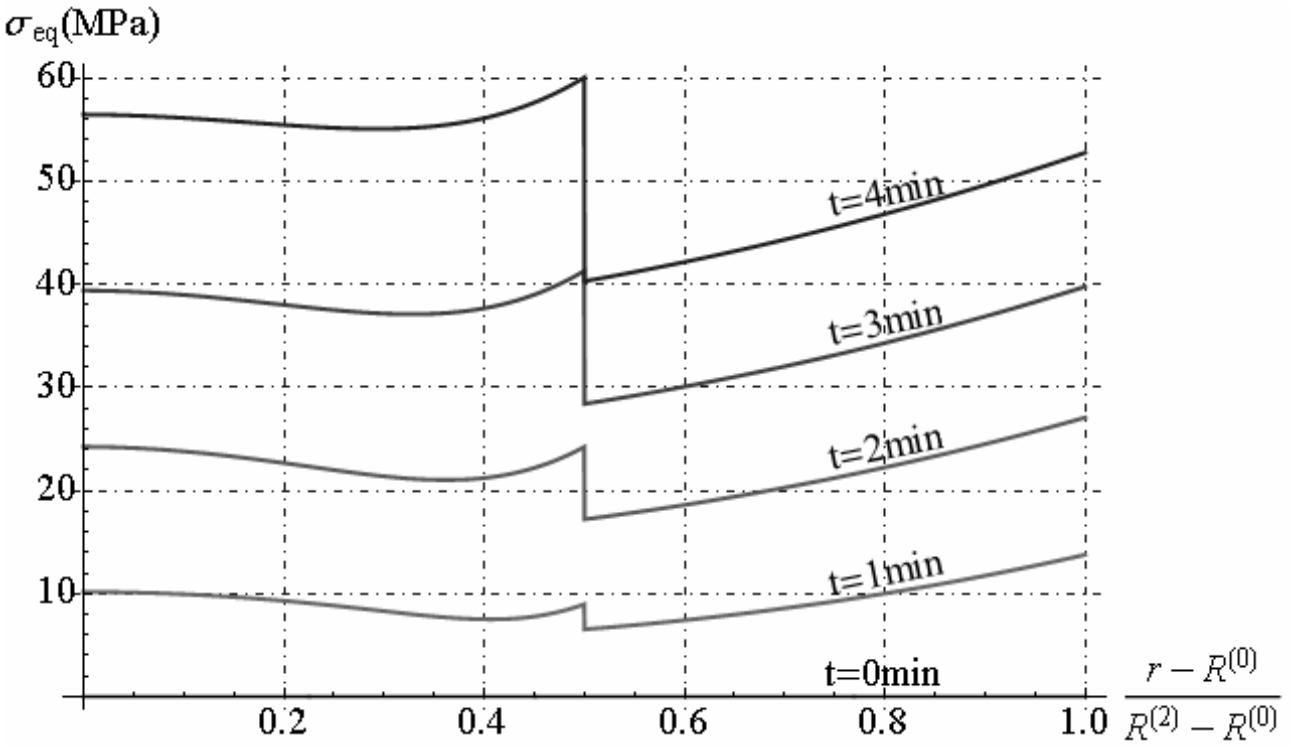

Fig. 21.32 - *Hencky von Mises's equivalent stress versus time*

21.5. Conclusions

In this chapter, an analytical thermo-elastic solution for cylindrical solid composed by multiple layers subjected to time-dependent boundary conditions, is presented. By applying the hypothesis of plane strain are determined the temperature and radial displacement functions in each layer of cylindrical solid. Let us consider three kind of boundary conditions on inner and outer surfaces of multilayered cylinder. In particular the cases analysed are: i) Multilayered cylinder exposed to an ambient at zero temperature through a uniform boundary conductance, ii) Multilayered cylinder exposed to uniform heat flux, iii) Multilayered cylinder exposed to hydrocarbon fire. In the case iii) multilayered cylinder is exposed to heat flux that varies in the time until to zero for $t \to \infty$. In three case studied the axial and circumferential stress present the jumps in interface surface between adjacent phases, but the radial stress is continue function, as showed in figures reported in this chapter. Numerical evaluation of the series solution shows that a reasonable number of terms are sufficient to obtain results with acceptable errors for engineering applications. The technique of solutions utilised in case iii) can be developed for determine the transient stress in multilayered cylinder pipeline exposed to standard fire. Then, the analytical study presented can be utilized to optimize the designer of a composite cylindrical pipeline exposed to heat flux that varies in time.

21.6. References

[1] Chen, C.K. and Yang, Y.C., "Thermoelastic Transient Response of an Infinitely Long Annular Cylinder Composed of Two Different Materials," *J. Eng. Sci.*, Vol. 24, pp. 569-581 (1986).

[2] Chen, C.K. and Chen, T.M., "New Hybrid Laplace Transform/Finite Element Method for Three-Dimensional Transient Heat Conduction Problem," *Int. J. Numerical Methods Engin.*, Vol. 32, No. 1, pp. 45-61 (1991).

[3] Ghosn, A.H. and Sabbaghian, M., "Quasi-Static Coupled Problems of Thermoelasticity for Cylindrical Regions," *J. Thermal Stresses*, Vol. 5, pp. 299-313 (1982).

[4] Fraldi, M., Nunziante, L., Carannante, F. (2007), *Axis-symmetrical Solutions for n-plies Functionally Graded Material Cylinders under Strain no-Decaying Conditions*, J. Mech. of Adv. Mat. and Struct. Vol. 14 (3), pp. 151-174 - DOI: 10.1080/15376490600719220

[5] M. Fraldi, L. Nunziante, F. Carannante, A. Prota, G. Manfredi, E. Cosenza (2008), *On the Prediction of the Collapse Load of Circular Concrete Columns Confined by FRP*, Journal Engineering structures, Vol. 30, Issue 11, November 2008, Pages 3247-3264 - DOI: 10.1016/j.engstruct.2008.04.036
[6] Fraldi, M., Nunziante, L., Chandrasekaran, S., Carannante, F., Pernice, MC. (2009), *Mechanics of distributed fibre optic sensors for strain measurements on rods*, Journal of Structural Engineering, 35, pp. 323-333, Dec. 2008- Gen. 2009
[7] M. Fraldi, F. Carannante, L. Nunziante (2012), *Analytical solutions for n-phase Functionally Graded Material Cylinders under de Saint Venant load conditions: Homogenization and effects of Poisson ratios on the overall stiffness*, Composites Part B: Engineering, Volume 45, Issue 1, February 2013, Pages 1310–1324
[8] Nunziante, L., Gambarotta, L., Tralli, A., *Scienza delle Costruzioni*, 3° Edizione, McGraw-Hill, 2011, ISBN: 9788838666971
[9] Jane, K.C. and Lee, Z.Y., "Thermoelastic Transient Response of an Infinitely Long Multilayered Cylinder," *Mech. Res. Comm.*, Vol. 26, No. 6, pp. 709-718 (1999).
[10] Kandil, A., "Investigation of Stress Analysis in Compound Cylinders Under High Pressure and Temperature," M. Sc. Thesis, CIT Helwan Univ., Egypt (1975).
[11] Sherief, H.H. and Anwar, M.N., "A Problem in Generalized Thermoelasticity for an Infinitely Long Annular Cylinder," *Int. J. Eng. Sci.*, Vol. 26, pp. 301-306 (1988).
[12] Takeuti, Y. and Furukawa, T., "Some Consideration on Thermal Shock Problem in a Plate," *J. Appl. Mech.*, Vol. 48, pp. 113-118 (1981).
[13] van Wylen, G.V., Sonntag, R., and Borgnakke, C., *Fundamentals of Classical Thermodynamics*, Fourth Edition, Wiley, New York (1994).
[14] Vollbrecht, H., "Stress in Cylindrical and Spherical Walls Subjected to Internal Pressure and Stationary Heat Flow," *Verfahrenstechnik*, Vol. 8, pp. 109-112 (1974).
[15] Zong-Yi Lee, "Coupled problem of thermoelasticity for multilayered spheres with time-dependent boundary conditions ", *Journal of Marine Science and Technology*, Vol. 12, No. 2, pp. 93-101 (2004)
[16] F. de Monte, *Transverse eigenproblem of steady-state heat conduction for multi-dimensional two-layered slabs with automatic computation of eigenvalues*, International Journal of Heat and Mass Transfer 47 (2004) 191–201
[17] Suneet Singh, Prashant K. Jain, Rizwan-uddin, *Analytical solution to transient heat conduction in polar coordinates with multiple layers in radial direction*, International Journal of Thermal Sciences 47 (2008) 261–273
[18] Prashant K. Jain, Suneet Singh, Rizwan-uddin, *Analytical Solution to Transient Asymmetric Heat Conduction in a Multilayer Annulus*, Journal of Heat Transfer - January 2009, Vol. 131
[19] M.kayhani, M.,Nourouzi, and A. Amiri Delooei, *An Exact Solution of Axi-symmetric Conductive Heat Transfer in Cylindrical Composite Laminate under the General Boundary Condition*, World Academy of Science, Engineering and Technology 69 2010

CHAPTER XXII
SPHERICAL TANK FILLED WITH GAS EXPOSED TO FIRE

22.1. Introduction

A pressure tank is a closed container designed to hold gases or liquids at a pressure substantially different from the ambient pressure. The pressure differential is dangerous and many fatal accidents have occurred in the history of pressure tank development and operation. Consequently, pressure tank design, manufacture, and operation are regulated by engineering authorities backed by legislation. For these reasons, the definition of a pressure tank varies from country to country, but involves parameters such as maximum safe operating pressure and temperature. Pressure tanks can theoretically be almost any shape, but shapes made of sections of spheres, cylinders, and cones are usually employed. A common design is a cylinder with end caps called heads. Head shapes are frequently either hemispherical or dished (torispherical). More complicated shapes have historically been much harder to analyze for safe operation and are usually far more difficult to construct. Theoretically almost any material with good tensile properties that is chemically stable in the chosen application could be employed. However, pressure vessel design codes and application standards (ASME BPVC Section II, EN 13445-2 etc.) contain long lists of approved materials with associated limitations in temperature range. Many pressure tanks are made of steel. To manufacture a cylindrical or spherical pressure vessel, rolled and possibly forged parts would have to be welded together. Some mechanical properties of steel, achieved by rolling or forging, could be adversely affected by welding, unless special precautions are taken. In addition to adequate mechanical strength, current standards dictate the use of steel with a high impact resistance, especially for vessels used in low temperatures. In applications where carbon steel would suffer corrosion, special corrosion resistant material should also be used. Some pressure tanks are made of composite materials, such as filament wound composite using carbon fibers held in place with a polymer. Due to the very high tensile strength of carbon fibers these tanks can be very light, but are much more difficult to manufacture. The composite material may be wound around a metal liner, forming a composite over wrapped pressure tank. Other very common materials include polymers such as PET in carbonated beverage containers and copper in plumbing. Pressure tanks may be lined with various metals, ceramics, or polymers to prevent leaking and protect the structure of the tank from the contained medium. This liner may also carry a significant portion of the pressure load. Pressure tanks are designed to operate safely at a specific pressure and temperature, technically referred to as the "Design Pressure" and "Design Temperature". A tank that is inadequately designed to handle a high pressure constitutes a very significant safety hazard. Because of that, the design and certification of pressure tanks is governed by design codes such as the ASME Boiler and Pressure Vessel Code in North America, the Pressure Equipment Directive of the EU (PED), Japanese Industrial Standard (JIS), CSA B51 in Canada, Australian Standards in Australia and other international standards like Lloyd's, Germanischer Lloyd, Det Norske Veritas, Société Générale de Surveillance (SGS S.A.), Stoomwezen etc.

In this chapter is studied an spherical tank methane gas-filled exposed to fire characterized by hydrocarbon fire curve. The interaction between spherical tank and gas is studied. By applying the several hypothesis, we determine approximate analytical thermo-elastic solution for spherical tank. By applying the solution, the variation of temperature methane and in spherical tank in time is determine. Finally, an example is reported in which an spherical tank with inner radius $R_0 = 10m$ and thickness s = 2.5cm is considered. Moreover the collapse temperature of spherical tank exposed to fire is determined.

Figure 22.1- *Spherical tank methane gas- filled*

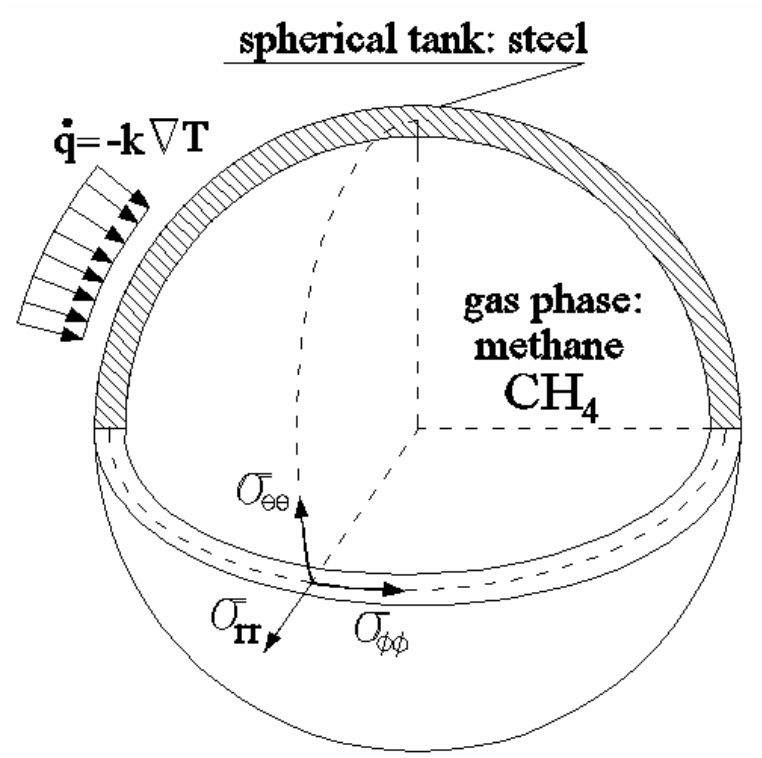

Figure 22.2 - *Spherical tank model methane gas-filled*

22.2. Real gas equations

22.2.1. Ideal gas law and van der Waals equation

Equations of state play an important role in chemical engineering design and they have assumed an expanding role in the study of the phase equilibria of fluids and fluid mixtures. Originally, equations of state were used mainly for pure components. When first applied to mixtures, they were used only for mixtures of nonpolar (Soave, 1972; Peng and Robinson, 1976) and slightly polar compounds (Huron et al., 1978; Asselineau et al., 1978; Graboski and Daubert, 1978). Since then, equations of state have developed rapidly for the calculation of phase equilibria in non-polar and polar mixtures. The advantage of the equations of state method is its applicability over wide ranges of temperature and pressure to mixtures of diverse components, from the light gases to heavy liquids. They can be used for the representation of vapour-liquid, liquid-liquid and supercritical fluid phase equilibria and they can be also applied to the gas, liquid and supercritical phases without encountering any conceptual difficulties.

Many equations of state have been proposed in the literature with either an empirical, semi-empirical or theoretical basis. Comprehensive reviews can be found in the works of Martin (1979), Gubbins (1983), Tsonopoulos and Heidman (1985), Han et al. (1988), Anderko (1990), Sandler (1994) and Donohue and Economou (1995).

The van der Waals equation of state was the first equation to predict vapour –liquid coexistence. Later, the Redlich-Kwong equation of state (Redlich and Kwong, 1949) improved the accuracy of the van der Waals equation by proposing a temperature dependence for the attractive term. Soave (1972) and Peng and Robinson (1976) proposed additional modifications for Redlich-Kwong equation to more accurately predict the vapour pressure, liquid density, and equilibria ratios. Carnahan and Starling (1969), Guggenheim (1965) and Boublik (1981) modified the repulsive term of van der Waals equation of state and obtained their accurate expressions for hard sphere fluid. Christoforakos and Franck (1986) modified both the attractive and repulsive terms of van der Waals equation of state. In addition to modelling small molecules, considerable emphasis has been placet recently on modelling long molecules. Based on Prigogine's (1957) and Flory's (1965) theory, Beret and Prausnitz (1975) and Donohue and Prausnitz (1978) constructed an equation for molecules treated as chains of segments, Perturbed-Hard-Chain-Theory (PHCT). To overcome the mathematical complexity of PHCT, Kim et al. (1986) developed a simplified version of PHCT (SPHCT) by replacing the complex attractive part of PHCT by a simplex expression. To take into account the increase in attractions due to dipolar and quadrupolar forces, Vimalchand and Donohue (1985) obtained fairly accurate multipolar misture calculations by using the Perturbed Anisotropic Chain Theory (PACT). Ikonomou and Donohue (1986) extended the PACT to obtain an equation of state which takes into account the existence of hydrogen bonding, that is the Associated Perturbed Anisotropic Chain Theory (APACT).

Advances in statistical mechanics and increase of computer power allowed the development of equation of state based on molecular principles that are accurate for real fluids and mixtures. Using Wertheim's theory, Chapman et al. (1990) and Huang and Radosz (1990) developed the Statistical-Associating-Fluid -Theory (SAFT) which is accurate for pure fluids and mixtures containing associating fluids. Recently, various modified versions, such as LJ-SAFT (Kraska and Gubbins, 1996a & b), SAFT-VR (Gil-Villegas et al., 1997), have been developed.

The ideal gas law is the equation of state of a hypothetical ideal gas. It is a good approximation to the behaviour of many gases under many conditions, although it has several limitations. It was first stated by **Émile Clapeyron** in 1834 as a combination of Boyle's law and Charles's law. It can also be derived from kinetic theory, as was achieved (apparently independently) by August Krönig in 1856 and Rudolf Clausius in 1857. The state of an amount of gas is determined by its pressure, volume, and temperature. The modern form of the equation relates these simply in two main forms. The temperature used in the equation of state is an absolute temperature: in the SI system of units, kelvin. The most frequently introduced form is:

$$pV = nRT \tag{22.1}$$

where “p” is the pressure of the gas, “V” is the volume of the gas, n is the amount of substance of gas (also known as number of moles), “T” is the temperature of the gas and “R” is the ideal, or universal, gas constant, equal to the product of Boltzmann's constant and Avogadro's constant. In SI units, n is measured in moles, and T in Kelvin. R has the value 8.314472 J/(mol·°K) or 0.08206 (L·atm)/(mol·°K). How much gas is present could be specified by giving the mass instead of the chemical amount of gas. Therefore, an alternative form of the ideal gas law may be useful. The chemical amount (n) (in moles) is equal to the mass (m) (in grams) divided by the molar mass (M) (in grams per mole):

$$n = \frac{m}{M} \tag{22.2}$$

By replacing n with m / M, and subsequently introducing density ρ = m/V, we get:

$$p = \frac{\rho R}{M} T = \frac{RT}{V_M} \tag{22.3}$$

where $V_M = \frac{M}{\rho} = \frac{V}{n}$ is the molar volume. Defining the specific gas constant $R_{specific}$ as the ratio R/M,

$$p = \rho R_{specific} T \tag{22.4}$$

This form of the ideal gas law is very useful because it links pressure, density, and temperature in a unique formula independent of the quantity of the considered gas. Alternatively, the law may be written in terms of the specific volume v, the reciprocal of density, as:

$$p v = R_{specific} T \tag{22.5}$$

It is common, especially in engineering applications, to represent the ideal gas constant by the symbol R. In such cases, the universal gas constant is usually given a different symbol such as R to distinguish it. In any case, the context and/or units of the gas constant should make it clear as to whether the universal or specific gas constant is being referred to.

The **van der Waals equation** of state, proposed in 1873 (Rowlinson, 1988), was the first equation capable of representing vapour-liquid coexistence:

$$p = \frac{nRT}{V - nb} - \frac{n^2 a}{V^2} \tag{22.6}$$

where *p* represents pressure, T is temperature, V is volume , n the amount of substance (in moles) and R is the gas constant. By applying the relationships (22.2), we can rewrite the equation (22.6) in follows manner:

$$p = \frac{R\,T}{(M/\rho) - b} - \frac{a}{(M/\rho)^2} \tag{22.7}$$

The van der Waals constants a and b are characteristic of the substance and are independent of temperature. They are related to the critical temperature and pressure, T_c and p_c by :

$$a = \frac{27 R^2 T_c^2}{64 p_c}, \quad b = \frac{R T_c}{8 p_c}, \tag{22.8}$$

The parameter *a* is a measure of the attractive forces between the molecules and the parameter *b* is a measure of the size of the molecules (hard body term). Both adjustable parameters *a* and *b* can be obtained from the critical properties of the fluid. The van der Waals equation can be regarded as a “hard-sphere (repulsive) + attractive” term equation of state composed from the contribution of repulsive and attractive intermolecular interactions, respectively. It gives a qualitative description of the vapour and liquid phases and phase transitions (Van Konynenburg and Scott, 1980), but it is

rarely sufficiently accurate for critical properties and phase equilibria calculations. A simple example is that for all fluids, the critical compressibility predicted by Equation (22.6) is 0.375, whereas the real value for different hydrocarbons varies from 0.24 to 0.29. The van der Waals equation has been superseded by a large number of other, more accurate equations of state.

22.2.2. Modification of the Attractive Term

Many modifications of the attractive term have been proposed. Some of these are listed and compared in Table 21.2. Benedict et al. (1940) suggested a multi-parameter equation of state, known as the **Benedict-Webb-Rubin (BWR) equation**:

$$p = \frac{n\,RT}{V} + n^2\left(\frac{B_0 RT - A_0 - C_0 / T^2}{V^2}\right) + n^3\left(\frac{bRT - a}{V^3}\right) + \frac{n^6 \alpha a}{V^6} + \frac{n^3 c}{V^3 T^2}\left(1 + \frac{n^2\gamma}{V^2}\right) e^{-\frac{n^2\gamma}{V^2}} \qquad (22.9)$$

where $A_0, B_0, C_0, a, b, c, \alpha, \gamma$ are eight adjustable parameters. The BWR equation could treat supercritical components and was able to work in the critical area. However, the BWR equation suffers from three major disadvantages. First, the parameters for each compound must be determined separately by reduction of plentiful, accurate pressure-volume-temperature (PVT) and vapour-liquid-equilibrium (VLE) data. Second, the large number of adjustable parameters makes it difficult to extend to mixtures. Third, its analytical complexity results in a relatively long computing time.

Perhaps, the most important model for the modification of the van der Waals equation of state is the **Redlich-Kwong (RK) equation** (Redlich and Kwong, 1949). It retains the van der Waals hard-sphere term but a temperature dependence was introduced in the attractive term:

$$p = \frac{n\,RT}{V - nb} - \frac{n^2 a}{V\left(V + nb\right)\sqrt{T}} \qquad (22.10)$$

By applying the relationships (22.2), we can rewrite the equation (22.10) in follows manner:

$$p = \frac{RT}{\left(M/\rho\right) - b} - \frac{a}{\left(M/\rho\right)\left[\left(M/\rho\right) + b\right]\sqrt{T}} \qquad (22.11)$$

For pure substances the equation parameters *a* and *b* are usually expressed as:

$$a = \frac{0.4278\,R^2 T_c^{2.5}}{p_c}, \quad b = \frac{0.0867\,RT_c}{p_c}, \qquad (22.12)$$

where T_c, p_c are critical temperature and pressure of gas, respectively.

Carnahan and Starling (1972) used the Redlich-Kwong equation of state to compute the gas phase enthalpies for a variety of substances, many of which are polar and/or not spherically symmetric. Their results showed that the Redlich-Kwong equation is a significant improvement over the van der Waals equation. Abbott (1979) also concluded that the Redlich-Kwong equation performed relatively well for the simple fluids Ar, Kr, and Xe (for which the acentric factor is equal to zero), but it did not perform well for complex fluids with Non-zero acentric factors.

The Redlich-Kwong equation of state can be used for mixtures by applying mixing rules to the equation of state parameters. It offered remarkable success in improving the van der Waals equation with a better description of the attractive term. Joffe and Zudkevitch (1966) showed that substantial improvement in the representation of fugacity of gas mixtures could be obtained by treating interaction parameters as empirical parameters. The results of the critical properties calculations for binary mixtures indicated that adjusting the value of binary interaction parameters in the mixing rules of the parameter a of the Redlich-Kwong equation of state could reduce the average error levels in the predicted critical properties for most binary mixtures. Spear et al. (1969) demonstrated that the Redlich-Kwong equation of state could be used to calculate the gas-liquid critical properties of binary mixtures. Chueh and Prausnitz (1967a & b) also showed that the Redlich-Kwong equation can be adapted to predict both vapour and liquid properties. Several other workers (Deiters and Schneider, 1976; Baker and Luks, 1980) applied the Redlich-Kwong equation to the critical properties and the high pressure phase equilibria of binary mixtures. For ternary mixtures, Spear et

al. (1971) gave seven examples of systems for which the gas-liquid critical properties of hydrocarbon mixtures could be calculated by using the Redlich-Kwong equation of state. The results showed that the accuracy of the Redlich-Kwong equation of state calculations for ternary systems was only slightly less than that for the constituent binaries. The success of the Redlich-Kwong equation has been the impetus for many further empirical improvements.

Soave (1972) suggested replacing the term $a/\sqrt{T}$ with a more general temperature-dependent term a(T), that is:

$$p = \frac{nRT}{V - nb} - \frac{n^2 a(T)}{V(V + nb)} \tag{22.13}$$

where

$$a(T) = 0.4274 \frac{R^2 T_c^2}{p_c} \left\{ 1 + m \left[1 - \sqrt{\frac{T}{T_c}} \right] \right\}^2, \quad m = 0.480 + 1.57\omega - 0.176\omega^2, \; b = 0.08664 \frac{RT_c}{p_c}, \tag{22.14}$$

ω is the acentric factor. To test the accuracy of Soave -Redlich-Kwong (SRK) equation, the vapour pressures of a number of hydrocarbons and several binary systems were calculated and compared with experimental data (Soave, 1972). In contrast to the original Redlich- Kwong equation, Soave's modification fitted the experimental curve well and was able to predict the phase behaviour of mixtures in the critical region. Elliott and Daubert (1985) reported an accurate representation of vapour-liquid equilibria with the Soave equation for 95 binary systems containing hydrocarbon, hydrogen, nitrogen, hydrogen sulfide, carbon monoxide, and carbon dioxide. Elliott and Daubert (1987) also showed that the Soave equation improved the accuracy of the calculated critical properties of these mixtures. Accurate results (Han et al., 1988) were also obtained for calculations of the vapour –liquid equilibrium of symmetric mixtures and methane-containing mixtures.

In 1976, **Peng and Robinson** (1976) redefined a(T) as:

$$a(T) = 0.45724 \frac{R^2 T_c^2}{p_c} \left\{ 1 + k \left[1 - \sqrt{\frac{T}{T_c}} \right] \right\}^2, \; b = 0.0778 \frac{RT_c}{p_c}, \tag{22.15}$$

$$k = 0.37464 + 1.5422\omega - 0.26922\omega^2,$$

Recognising that the critical compressibility factor of the Redlich-Kwong equation (Zc = 0.333) is overestimated, they proposed a different volume dependence:

$$p = \frac{nRT}{V - nb} - \frac{n^2 a(T)}{V(V + nb) + nb(V - nb)} \tag{22.16}$$

The Peng-Robinson (PR) equation slightly improves the prediction of liquid volumes and predicts a critical compressibility of $Zc = 0.307$. Peng and Robinson (1976) gave examples of the use of the Peng-Robinson equation for predicting the vapour pressure and volumetric behaviour of single - component systems, and the phase behaviour and volumetric behaviour of binary, ternary and multicomponent system, and concluded that Eq.(3.10) can be used to accurately predict the vapour pressures of pure substances and equilibrium ratios of mixtures. The Peng-Robinson equation performed as well as or better than the Soave -Redlich-Kwong equation. Han et al. (1988) reported that the Peng-Robinson equation was superior for predicting vapour-liquid equilibrium in hydrogen and nitrogen containing mixtures. The Peng-Robinson and Soave-Redlich-Kwong equations are widely used in industry. The advantages of these equations are that they can accurately and easily represent the relation among temperature, pressure, and phase compositions in binary and multicomponent systems. They only require the critical properties and acentric factor for the generalised parameters, little computer time and lead to good phase equilibrium prediction. However, the success of these modifications is restricted to the estimation of vapour pressure. The calculated saturated liquid volumes are not improved and are invariably higher than the measured data. **Fuller** (1976) proposed a three parameter equation of state which has the form:

$$p = \frac{nRT}{V - nb} - \frac{n^2 a(T)}{V(V + ncb)} \tag{22.17}$$

with the additional parameter added is denoted as *c*. At the critical point

$$a(T) = \Omega_a(\beta)\frac{R^2 T_c}{p_c}\alpha(T), \quad b = \Omega_b(\beta)\frac{RT_c}{p_c}, \quad c(\beta) = \frac{1}{\beta}\left(\sqrt{\frac{1}{\beta} - \frac{3}{4}} - \frac{3}{2}\right),$$

$$\beta_c = \frac{b}{V_c}(T = T_c), \quad \Omega_b(\beta) = \beta\frac{(1-\beta)(2+c\beta) - (1+c\beta)}{(2+c\beta)(1-\beta)^2}, \quad \Omega_a(\beta) = \frac{(1+c\beta)^2\,\Omega_b(\beta)}{\beta(2+c\beta)(1-\beta)^2}, \tag{22.18}$$

$$\alpha(T) = \left[1 + q(\beta)\left(1 - T\sqrt{R}\right)\right]^2, \; q(\beta) = m(\beta/0.26)^{1/4}, \; m = 0.480 + 1.5740\omega - 0.176\omega^2,$$

$$Z_c(\beta) = \frac{p_c V_c}{RT_c} = -\frac{(1-c\beta)(2+c_c\beta_c) - (1+c_c\beta_c)}{(2+c_c\beta_c)(1-\beta_c)^2},$$

Fuller's modification contain two features. First, the equation of state leads to a variable critical compressibility factor, and second, a new universal temperature function is incorporated in the equation making both the *a* and *b* parameters functions of temperature. Fuller's equation can be reduced to the Soave-Redlich-Kwong and van der Waals equations. If β_c = 0.259921, then we have *c* = 1, Ω_a = 0.4274802 , Ω_b = 0.0866404 , Z_c = 0.333, and the Soave- Redlich-Kwong equation is obtained. If β_c has a value of 1/3, then *c* = 0 , Ω_a = 0.421875, Ω_b = 0.125, Z_c = 0.375, and van der Waals equation is obtained. Fuller (1976) reported that the proposed modification produced a root-mean-square error in saturated liquid volumes of less than 5%. In the majority of cases it also improved the vapour pressure deviations of the original Soave-Redlich-Kwong equation. The results of calculations indicated that this equation is capable of describing even polar molecules with reasonable accuracy. Similar to Fuller's equation, Table 21.1 also shows that a feature of many of the empirical improvements is the addition of adjustable parameters. A disadvantage of three parameters (or more parameters) equation of state is that the additional parameters must be obtained from additional pure component data. They almost invariably require one (or more) additional mixing rules when the equation is extended to mixtures. The Peng-Robinson and Soave-Redlich-Kwong equations fulfil the requirements of both simplicity and accuracy since they require little input information, except for the critical properties and acentric factor for the generalised parameters *a* and *b*. Consequently, although many equations of state have been developed, the Peng-Robinson and Soave- Redlich-Kwong equations are widely used in industry, and often yield a more accurate representation (Palenchar et al. 1986) than other alternatives.

22.2.3. Modification of the Repulsive Term

The other way to modify the van der Waals equation is to examine the repulsive term of a hard sphere fluid. Many accurate representations have been developed for the repulsive interactions of hard spheres and incorporated into the equation of state. Several proposals have been reported; some of them are summarised in Table 21.1. Among them, the most widely used equation is the **Carnahan-Starling equation**. Carnahan and Starling (1969) obtained an accurate expression for the compressibility factor of hard spere fluids which compared well with molecular-dynamics data (Reed and Gubbins, 1973). The form is:

$$Z_c = \frac{1 + y + y^2 - y^3}{(1-y)^3} \tag{22.19}$$

with $y = b / 4V$ and *b* is the volume occupied by 1 mol of molecules. To improve the accuracy of the van der Waals equation, Carnahan and Starling (1972) substituted equation (22.19) for the traditional term $RT / (V - b)$ resulting in the following equation of state:

$$p = \frac{nRT\left(1+y+y^2-y^3\right)}{V\left(1-y\right)^3} - \frac{n^2 a}{V^2}, \tag{22.20}$$

Both *a* and *b* can be obtained by using critical properties ($a = 0.4964R^2T_c^2 p_c^{-1}, b = 0.18727RT_c p_c^{-1}$). Sadus (1993) has demonstrated that Carnahan-Starling equation can be used to predict the Type III equilibria of non-polar mixtures with considerable accuracy.

The **Guggenheim equation** (Guggenheim, 1965) is a simple alternative to the Carnarhan-Starling. It also incorporates an improved hard-sphere repulsion term in conjunction with the simple van der Waals description of attractive interactions.

$$p = \frac{nRT}{V\left(1-y\right)^4} - \frac{n^2 a}{V^2} \tag{22.21}$$

The covolume ($b = 0.18284RT_c p_c^{-1}$) and attractive ($a = 0.49002R^2T_c^2 p_c^{-1}$) equation of state parameters are related to the critical properties. The Guggenheim equation has been used to predict the critical properties of diverse range of binary mixtures (Hicks and Young, 1976; Hurle et al., 1977a & b; Hicks et al., 1977 & 1978; Semmens et al., 1980; Sadus and Young, 1985a & b; Waterson and Young, 1978; Toczylkin and Young, 1977, 1980a & b &c; and Sadus, 1992a &1994). Despite the diversity of the systems studied, good results were consistently reported for the gas-liquid critical locus. The critical liquid-liquid equilibria of Type II mixtures was also represented adequately. In contrast, calculations involving Type III equilibria are typically only semiquantitative (Christou et al., 1986) because of the added difficulty of predicting the transition between gas-liquid and liquid-liquid behaviour. The Guggenheim equation has also been proved valuable in calculating both the gas-liquid critical properties (Sadus and Young, 1988) and general critical transitions of ternary mixtures (Sadus, 1992a).

Boublik (1981) has generalised the Carnahan-Starling hard sphere potential for molecules of arbitrary geometry via the introduction for a nonsphericity parameter (α). Svenda and Kohler (1983) employed the Boublik expression in conjunction with Kihara's (1963) concept of a hard convex body (HCB) to obtain a generalised van der Waals equation of state:

$$p = \frac{nRT\left[1+\left(3\alpha-2\right)y+\left(3\alpha^2-3\alpha+1\right)y^2-\alpha^2 y^3\right]}{V\left(1-y\right)^3} - \frac{n^2 a}{V^2} \tag{22.22}$$

Sadus et al. (1988) and Christou et al. (1991) have used equation (22.22) for the calculation of the gas-liquid critical properties of binary mixtures containing nonspherical molecules. The results obtained were slightly better than could be obtained from similar calculations using the Guggenheim equation of state. Sadus (1993) proposed an alternative procedure for obtaining the equatio n of state parameters. Equation (22.22) in conjunction with this modified procedure can be used to predict Type III critical equilibria of nonpolar binary mixtures with a good degree of accuracy. Sadus (1994) compared the compressibility factors predicted by the van der Waals, Guggenheim and Carnahan-Starling hard-sphere contributions with molecular simulation data (Alder and Wainwright, 1960, Barker and Henderson, 1971) for one -component hard-sphere fluid The results demonstrated that the hard-sphere term of Guggenheim equation is as accurate as Carnahan-Starling term at low to moderately high densities.

22.2.4. Modification of both Attractive and Repulsive Terms

Other equations of state have been formed by modifying both attractive and repulsive terms, or by combining an accurate hard sphere model with an empirical temperature dependent attractive contribution. **Carnahan and Starling (1972)** combined the Redlich-Kwong attractive term with their repulsive term:

$$p = \frac{nRT\left(1+y+y^2-y^3\right)}{V\left(1-y\right)^3} - \frac{n^2 a}{V\left(V+nb\right)\sqrt{T}}, \tag{22.23}$$

Their results (Carnahan and Starling, 1972) demonstrated that this combination improved the predication of hydrocarbon densities and supercritical phase equilibria. De Santis et al. (1976) also tested equation (22.23) and concluded that equation (22.23) yielded good results for the case of pure components in the range spanning ideal gas to saturated liquids. When applied to mixtures for predicting vapour-liquid equilibria, good accuracy in wide ranges of temperature and pressare can be obtained.

McElroy (1983) has combined the Guggenheim hard sphere model with the attractive term of the Redlich-Kwong equation:

$$p = \frac{nRT}{V(1-y)^4} - \frac{n^2 a}{V(V+nb)\sqrt{T}} \tag{22.24}$$

The accuracy of this equation has not been widely tested.

Christoforakos and Franck (1986) proposed an equation of state which used the Carnahan-Starling (1969) expression for the construction of repulsive term and a square well intermolecular potential to obtain the contribution of attractive intermolecular interaction to address deficiencies in the representation of both attractive and repulsive interactions:

$$p = \frac{nRT}{V}\left[\frac{V^3 + n\beta V^2 + n^2\beta^2 V - n^3\beta^3}{(V-n\beta)^3}\right] - \frac{4\beta n^2 RT}{V^2}\left(\lambda^3 - 1\right)\left(e^{\frac{\varepsilon}{RT}} - 1\right) \tag{22.25}$$

where $\beta = b\left(T_c/T\right)^{3/m}$, m is typically assigned a value of 10, and V denotes volume. The other equation of state parameters can be derived from the critical properties:

$$b = 0.04682\frac{RT_c}{p_c}, \quad \frac{\varepsilon}{R} = T_c \log\left[1 + \frac{2.65025}{\lambda^3 - 1}\right], \tag{22.26}$$

The ε parameter reflects the depth of the square well intermolecular potential and λ is the relative width of the well. This equation was successfully applied to the high temperature and high pressure phase behaviour of some binary aqueous mixtures (Christoforakos and Franck ,1986).

Heilig and Franck (1989 & 1990) modified the Christoforakos-Franck equation of state and they also employ a temperature-dependent Carnahan-Starling (1969) representation of repulsive forces between hard-spheres and a square-well representation for attractive forces,

$$p = \frac{nRT}{V}\left[\frac{V^3 + n\beta V^2 + n^2\beta^2 V - n^3\beta^3}{(V-n\beta)^3}\right] - \frac{n^2 BRT}{V^2 + n(C/B)V} \tag{22.27}$$

where $b = b_c\left(T_c/T\right)^Z$, b_c is the critical molecular volume and $z = 0$. The B and C terms in Equation (22.27) represent the contributions from the second and third virial coefficients, respectively, of a hard-sphere fluid interacting via a square-well potential. This potential is characterised by three parameters reflecting intermolecular separation (σ), intermolecular attraction (ε/RT) and the relative width of the well (λ). The following universal values (Mather et al., 1993) were obtained by solving the critical conditions of a one-component fluid, for example, λ = 1.26684, $N_A\sigma^3/V_c = 0.24912$ (where N_A denotes Avogadro's constant) and $\varepsilon/RT_c = 1.51147$. Accurate calculations of the critical properties of both binary and ternary mixtures (Heilig and Franck, 1989 & 1990) have been reported. Shmonov et al. (1993) used Equation (22.27) to predict high-pressure phase equilibria for the water + methane mixture and reported that the Heilig-Franck equation of state was likely to be more accurate than other "hard sphere + attractive term" equations of state for the calculation of phase equilibria involving a polar molecule.

Shah et al. (1994) developed a new equation of state. They used Z_{hs} and Z_{att} as the repulsive and the attractive contribution to the compressibility, respectively,

$$Z_{hs} = \frac{V}{(V-nk_0\alpha)} + \frac{\alpha V k_1}{(V-nk_0\alpha)^2}, \quad Z_{att} = -\frac{a\,nV^2 + n^2 k_0\alpha c V}{V(V+ne)(V-nk_0\alpha)RT}, \tag{22.28}$$

where

$$\alpha = 0.165 V_c \left\{ e^{\left[-0.03125 \log\left(\frac{T}{T_c}\right) - 0.0054 \left(\log\left(\frac{T}{T_c}\right)\right)^2 \right]} \right\}^3 \tag{22.29}$$

represents the molar hard-sphere volume of the fluid, $k_0 = 1.2864$, $k_1 = 2.8225$, and e is a constant, and a and c are temperature-dependent parameters. A new equation, called the quartic equation of state, was formed as :

$$p = \frac{nRT}{V - nk_0\alpha} + \frac{n^2 \alpha k_1 RT}{(V - nk_0\alpha)^2} - \frac{a n^2 V + n^3 k_0 \alpha c}{V(V + ne)(V - nk_0\alpha)} \tag{22.30}$$

It only needs three properties of a fluid, critical temperature, critical volume, and acentric factor, to be specified to reproduce pressure-volume-temperature and thermodynamic properties accurately. Although it is a quartic equation and yields four roots, one root is always negative and hence physically meaningless, and three roots behave like three roots of an equation. Shah et al. (1994) compared their quartic equation with the Peng- Robinson (1976) and Kubic (1982) equations of state and concluded that it was more accurate than either the Peng-Robinson or the Kubic equation of state. Lin et al. (1996) extended the generalised quartic equation of state, Eq.(3.37) to polar fluids. When applied to polar fluids, the equation requires four characteristic properties of the pure component, critical temperature, critical volume, acentric factor and dipole moment. They calculated thermodynamic properties of 30 polar compounds, and also compared with experimental literature values and the Peng-Robinson equation for seven polar compounds. Their results showed that various thermodynamic properties predicted from the generalised quartic equation of state were in satisfactory agreement with the experimental data over a wide range of states and for a variety of thermodynamic properties. The generalised quartic equation of state made good improvement in calculating the enthalpy departure, second virial coefficients, and the pressure-volume-temperature properties.

Equation	Year	Repulsive term
Reiss et al.	1959	$\frac{RT(1+y+y^2)}{V(1-y)^3}$
Thiele	1963	$\frac{RT(1+y+y^2)}{V(1-y)^3}$
Guggenheim	1965	$\frac{RT}{V(1-y)^4}$
Carnahan-Starling	1969	$\frac{RT(1+y+y^2-y^3)}{V(1-y)^3}$
Scott	1971	$\frac{RT(V+b)}{V(V-b)}$
Boublik	1981	$\frac{RT(1+(3\alpha-2)y+(3\alpha^2-3\alpha+1)y^2-\alpha^2 y^3)}{V(1-y)^3}$

Table 22.1 Summary of Modification of Repulsive term of the van der Waals Equation

Equation	Year	Attractive term
Redlich-Kwong	1949	$\frac{a}{T^{0.5}V(V+b)}$
Soave	1972	$\frac{a(T)}{V(V+b)}$
Peng-Robinson	1976	$\frac{a(T)}{V(V+b)+b(V-b)}$
Fuller	1976	$\frac{a(T)}{V(V+cb)}$
Heyen	1980 (Sandler, 1994)	$\frac{a(T)}{V^2+(b(T)+c)V-b(T)c}$
Schmidt-Wenzel	1980	$\frac{a(T)}{V^2+ubV+wb^2}$
Harmens-Knapp	1980	$\frac{a(T)}{V^2+Vcb-(c-1)b^2}$
Kubic	1982	$\frac{a(T)}{(V+c)^2}$
Patel-Teja	1982	$\frac{a(T)}{V(V+b)+c(V-b)}$
Adachi et al.	1983	$\frac{a(T)}{(V-b_2)(V+b_3)}$
Stryjek-Vera	1986a	$\frac{a(T)}{(V^2+2bV-b^2)}$
Yu and Lu	1987	$\frac{a(T)}{V(V+c)+b(3V+c)}$
Trebble and Bishnoi	1987	$\frac{a(T)}{V^2+(b+c)V-(bc+d^2)}$
Schwartzentruber and Renon	1989	$\frac{a(T)}{(V+c)(V+2c+b)}$

Table 22.2 Summary of Modification of the attractive term of the van der Waals Equation

22.3. Spherical tank filled with methane gas exposed to fire

22.3.1. First model: Heat transfer by only thermal convection

Let us consider a spherical tank with inner radius "R_0" and outer radius "R_0+s" – where "s" is the thickness of spherical tank -, exposed to conventional fire. The spherical tank contains the methane gas with initial pressure p_0 and initial temperature T_0. In this section, we determine the temperature, displacement and stress function in hollow spherical tank by starting to initial temperature in solid and gas equal to $T_0=T_R$. Moreover, we determine the variation of pressure and temperature in gas as function of the time. Let us assume the following hypothesis:

1) Heat transfer by only thermal convection (this hypothesis is don't apply for high temperature)

2) Spherical tank is characterized by homogeneous material : steel with specific heat coefficient c_s and density ρ_s constant respect to temperature;

3) The gradient of temperature along thickness of spherical tank are negligible and then $T_s=T_s(t)$. The thickness "s" is more less to radius R_0: $s\ll R_0$;

4) Spherical tank is subjected to Hydrocarbon fire curve given by:

$$\Theta_F=293.15+1080\left(1-0.325e^{-\frac{0.167}{60}t}-0.675e^{-\frac{2.5}{60}t}\right)\ [°K,\sec] \tag{22.31}$$

5) Ideal gas law, Van der Waals and Redlich-Kwong equation of state are considered for methane gas. Let us consider the average temperature and pressure of gas as functions only variable time: $\overline{T}_g=\overline{T}_g(t),\overline{p}_g=\overline{p}_g(t)$

$$\begin{cases}\overline{T}_g(t)=\dfrac{1}{(4/3)\pi R_0^3}\displaystyle\int_0^{2\pi}\int_0^{\pi}\int_0^{R_0}T_g(r,t)r^2\sin\theta dr d\theta d\phi\\ \overline{p}_g(t)=\dfrac{1}{(4/3)\pi R_0^3}\displaystyle\int_0^{2\pi}\int_0^{\pi}\int_0^{R_0}p_g(r,t)r^2\sin\theta dr d\theta d\phi\end{cases} \tag{22.32}$$

We consider the specific heat of gas c_g constant respect to variation of temperature. Moreover, the variation of volume of spherical tank is negligible and then average density of gas ρ_g is constant respect to temperature.

6) The variation of Young's modulus respect to temperature considered (see chapter XIX) is given by follows relationship:

$$\frac{E_s(T)}{E_s(20°C)}=E_0+E_1T+E_2T^2+E_3T^3+E_4T^4+E_5T^5+E_6T^6\quad\forall T\in[20°C,1200°C] \tag{22.33}$$

where

$$\begin{aligned}&E_0=0.999,\ E_1=1.43\cdot10^{-4},\ E_2=-3.84\cdot10^{-6},\ E_3=9.28\cdot10^{-9},\\&E_4=-1.618\cdot10^{-11},\ E_5=1.38\cdot10^{-14},\ E_6=-4.15\cdot10^{-18},\end{aligned} \tag{22.34}$$

7) The variation of steel elastic limit of stress considered (see chapter XIX) is described by the following relations:

$$\frac{\sigma_y(T)}{\sigma_y(20°C)}=A_0+A_1T+A_2T^2+A_3T^3+A_4T^4+A_5T^5+A_6T^6\quad\forall T\in[20°C,1200°C] \tag{22.35}$$

where

$$\begin{aligned}&A_0=0.999,\ A_1=2.87\cdot10^{-5},\ A_2=-4.85\cdot10^{-7},\ A_3=-8.137\cdot10^{-9},\\&A_4=1.478\cdot10^{-11},\ A_5=-9.039\cdot10^{-15},\ A_6=1.865\cdot10^{-18},\end{aligned} \tag{22.36}$$

8) The approximate function of Poisson's ratio versus temperature considered (see chapter XX) is given by:

$$\nu(T) = 0.276 + 7.057 \cdot 10^{-5} T \quad \forall T \in [0, 1200°C] \tag{22.37}$$

9) The stress-strain relationship is perfectly elastic until elastic limit of stress.

The differential equation related to heat conduction and the corresponding boundary conditions are reported below. By applying divergence theorem, the Fourier's equation becomes:

$$\int_V k \nabla_2 T = -\int_V div\,\mathbf{q}\, dV = -\int_S \mathbf{q} \cdot \mathbf{n}\, ds = \int_V \rho\, c_v \frac{\partial T}{\partial t} dV \tag{22.38}$$

where $\mathbf{q} = -k\nabla T$ is heat flux, **n** in unit vector orthogonal at surface of spherical tank, V and S are volume and surface of solid, respectively. By applying the second and third hypothesis (2)-(3), we can rewrite the equation (22.38) for gas phase and spherical tank as follows:

$$\begin{cases} 4\pi R_0^2 s \rho_s c_s \dfrac{d\,T_s(t)}{dt} = -\left[4\pi (R_0 + s)^2 q_e + 4\pi R_0^2 q_i \right] & \text{(spherical tank)} \\ \dfrac{4}{3}\pi R_0^3 \rho_g c_g \dfrac{d\,\overline{T}_g(t)}{dt} = -4\pi R_0^2 q_i & \text{(gas phase)} \end{cases} \tag{22.39}$$

where q_i, q_e are heat fluxes on inner and outer surfaces of spherical tank, respectively. By applying the first hypothesis (1) reported above, heat transfer by only thermal convection is given by:

$$q_i = h_i \left[T_s(t) - \overline{T}_g(t) \right], \quad q_e = h_e \left[T_s(t) - \Theta_F(t) \right], \tag{22.40}$$

where h_e, h_i are convection coefficients for outer and inner surfaces of spherical tank, respectively These parameters assume the following values: $h_e = 50\ W/(m^2 \cdot °K)$, $h_i = 9\ W/(m^2 \cdot °K)$. $\Theta_F(t)$ represent the function of fire curve given by (22.31). We can rewrite the function $\Theta_F(t)$ in follows form:

$$\Theta_F(t) = H_0 + H_1 e^{\xi_1 t} + H_2 e^{\xi_2 t} \ [°K, \sec] \tag{22.41}$$

where the coefficients $H_0, H_1, H_2, \xi_1, \xi_2$ are reported :

$$H_0 = 1373.15,\ H_1 = -729,\ H_2 = -351,\ \xi_1 = -2.78 \cdot 10^{-3},\ \xi_2 = -4.17 \cdot 10^{-2},$$

By substituting the relationship (22.40) in to first equation (22.39) we obtain:

$$4\pi R_0^2 s \rho_s c_s \frac{d\,T_s(t)}{dt} = -\left\{ 4\pi (R_0 + s)^2 h_e \left[T_s(t) - \Theta_F(t) \right] + 4\pi R_0^2 h_i \left[T_s(t) - \overline{T}_g(t) \right] \right\} \tag{22.42}$$

By neglecting the term s^2 in equation (22.42) ($s \ll R_0$), we obtain the follows expression:

$$\frac{d\,T_s(t)}{dt} = -\frac{1}{s\,\rho_s c_s} \left\{ \left(1 + \frac{2s}{R_0} \right) h_e \left[T_s(t) - \Theta_F(t) \right] + h_i \left[T_s(t) - \overline{T}_g(t) \right] \right\} \tag{22.43}$$

The second equation (22.39) for methane gas becomes:

$$\frac{d\,\overline{T}_g(t)}{dt} = -\frac{3h_i}{\rho_g c_g R_0} \left[\overline{T}_g(t) - T_s(t) \right] \tag{22.44}$$

By solving the equation (22.44) respect to $T_s(t)$, we obtain:

$$T_s(t) = \overline{T}_g(t) + \left(\frac{\rho_g c_g R_0}{3h_i} \right) \frac{d\,\overline{T}_g(t)}{dt} \tag{22.45}$$

By substituting the equation (22.45) in to (22.42), we obtain the differential equation in only unknown function $\overline{T}_g(t)$:

$$B_2 \frac{d^2 \overline{T}_g(t)}{d\,t^2} + B_1 \frac{d\,\overline{T}_g(t)}{d\,t} + \overline{T}_g(t) = \Theta_F(t) = H_0 + H_1 e^{\xi_1 t} + H_2 e^{\xi_2 t} \tag{22.46}$$

B_1, B_2 are constants given by following relationships:

$$B_1 = R_0 \frac{\rho_g c_g \left[R_0 \left(h_i + h_e \right) + 2 h_e s \right] + 3 \rho_s c_s h_i s}{3 h_i h_e \left(R_0 + 2 s \right)}, \quad B_2 = \frac{\rho_g c_g \rho_s c_s R_0^2 s}{3 h_i h_e \left(R_0 + 2 s \right)}, \tag{22.47}$$

By solving the differential equation (22.46), we obtain the average temperature in gas $\overline{T}_g(t)$:

$$\overline{T}_g(t) = H_0 + C_1 e^{\omega_1 t} + C_2 e^{\omega_2 t} + C_3 e^{\xi_1 t} + C_4 e^{\xi_2 t} \tag{22.48}$$

where the integration constants C_1, C_2 are to determine and the constants $C_3, C_4, \omega_1, \omega_2$ are given by:

$$\begin{aligned} &C_3 = H_1 \Big/ \left[1 + \xi_1 \left(B_1 + \xi_1 B_2 \right) \right], \quad C_4 = H_2 \Big/ \left[1 + \xi_2 \left(B_1 + \xi_2 B_2 \right) \right], \\ &\omega_1 = -\left[B_1 + \sqrt{B_1^2 - 4 B_2} \right] \Big/ \left(2 B_2 \right), \quad \omega_2 = -\left[B_1 - \sqrt{B_1^2 - 4 B_2} \right] \Big/ \left(2 B_2 \right), \end{aligned} \tag{22.49}$$

By substituting the function (22.48) in equation (22.45), we obtain the temperature in spherical tank:

$$T_s(t) = H_0 + D_1 e^{\omega_1 t} + D_2 e^{\omega_2 t} + D_3 e^{\xi_1 t} + D_4 e^{\xi_2 t} \tag{22.50}$$

where the integration constants D_1, D_2, D_3, D_4 are reported below:

$$\begin{aligned} &D_1 = C_1 \left(1 + \frac{\rho_g c_g R_0}{3 h_i} \omega_1 \right), \quad D_2 = C_2 \left(1 + \frac{\rho_g c_g R_0}{3 h_i} \omega_2 \right), \\ &D_3 = C_3 \left(1 + \frac{\rho_g c_g R_0}{3 h_i} \xi_1 \right), \quad D_4 = C_4 \left(1 + \frac{\rho_g c_g R_0}{3 h_i} \xi_2 \right), \end{aligned} \tag{22.51}$$

By imposing the initial conditions for spherical tank and gas, we determine the integration constants C_1, C_2 :

$$\overline{T}_g(t=0) = T_s(t=0) = T_0 = T_R \;\rightarrow\; \begin{cases} C_1 = \dfrac{\left(C_3 + C_4 + H_0 - T_R \right) \omega_2}{\omega_1 - \omega_2} - \dfrac{\xi_1 C_3 + \xi_2 C_4}{\omega_1 - \omega_2} \\ C_2 = \dfrac{\xi_1 C_3 + \xi_2 C_4}{\omega_1 - \omega_2} - \dfrac{\left(C_3 + C_4 + H_0 - T_R \right) \omega_1}{\omega_1 - \omega_2} \end{cases} \tag{22.52}$$

Moreover, the temperature functions $\overline{T}_g(t), T_s(t)$ assume an asymptotic value for $t \to \infty$:

$$\lim_{t \to \infty} \overline{T}_g(t) = \lim_{t \to \infty} T_s(t) = \lim_{t \to \infty} \Theta_F(t) = H_0 \tag{22.53}$$

By applying the procedure examined in section 15.3, it is possible to determine displacement component $u_r(r,t)$, strain and stress components in spherical tank as reported below. The displacement function $u_r(r,t)$ is given by:

$$u_r = g_1(t) \cdot r + \frac{g_2(t)}{r^2} \tag{22.54}$$

For the spherical tank of inner radius R_0 and outer radius $R_0 + s$ the functions of time $g_1(t)$ and $g_2(t)$ must be determined from the condition that :

$$\sigma_{rr}(r = R_0) = p_g(t), \quad \sigma_{rr}(r = R_0 + s) = 0, \tag{22.55}$$

where $p_g(t)$ is pressure of methane gas exercised on inner surface of spherical tank. The pressure of gas can be to determine by applying the equations of state for real gas examined in section 21.2. In this case the volume of spherical tank remain constant with increase of temperature and then the density of gas is constant. In this paragraph, let us consider three different equation of state for methane gas: i) ideal gas law, ii) Van der Waals equation of state, iii) Redlich-Kwong equation of state. By applying ideal gas law (22.3), the pressure is given by:

$$p_g(t) = \frac{\rho_g \tilde{R}}{M} \overline{T}_g(t) \tag{22.56}$$

$\tilde{R} = 8.314472 J/(mol \cdot °K)$ is is the ideal, or universal, gas constant, and M is the molar mass of gas. We can rewrite the formula (22.56) in follows manner:

$$\tilde{p}_g(t) = \chi \cdot \tilde{T}_g(t), \quad \text{where} \quad \chi = \frac{\rho_g \tilde{R} T_c}{p_c M}, \; \tilde{T}_g(t) = \frac{\overline{T}_g(t)}{T_c}, \quad \tilde{p}_g(t) = \frac{\overline{p}_g(t)}{p_c}, \tag{22.57}$$

where T_c, p_c are critical temperature and pressure of gas, respectively. χ, $\tilde{T}_g(t)$ and $\tilde{p}_g(t)$ are no-dimensionless parameters. By applying Van der Waals equation of state (22.7) and equation (22.8), we obtain the pressure of gas as reported below:

$$\tilde{p}_g(t) = \left(\frac{8\chi}{8-\chi} \right) \tilde{T}_g(t) - \frac{27}{64} \chi^2 \tag{22.58}$$

By applying Redlich-Kwong equation of state (22.11) and equation (22.12), we obtain the pressure of gas:

$$\tilde{p}_g(t) = \left(\frac{\chi}{1-0.08662\chi} \right) \tilde{T}_g(t) - \left(\frac{0.42748\chi^2}{1+0.08662\chi} \right) \frac{1}{\sqrt{\tilde{T}_g(t)}} \tag{22.59}$$

In this case the equation (22.57),(22.58),(22.59) furnish the same values in the range of temperature considered for fire curves. From the strain-displacement relation and Hooke's law the non-zero stress components are:

$$\begin{aligned} \sigma_{rr} &= (3\lambda + 2\mu)\left\{ g_1(t) - \alpha_s \left[T_s(t) - T_R \right] \right\} - 4\mu r^{-3} g_2(t), \\ \sigma_{\theta\theta} &= \sigma_{\phi\phi} = (3\lambda + 2\mu)\left\{ g_1(t) - \alpha_s \left[T_s(t) - T_R \right] \right\} + 2\mu r^{-3} g_2(t), \end{aligned} \tag{22.60}$$

By substituting the stress functions (22.60) in boundary conditions (22.55), we determine the unknown functions $g_1(t)$ and $g_2(t)$:

$$\begin{aligned} g_1(t) &= \alpha_s \left[T_s(t) - T_R \right] + \frac{\overline{p}_g(t) R_0^3}{(3\lambda_s + 2\mu_s) s \left[s^2 + 3R_0(R_0 + s) \right]}, \\ g_2(t) &= \frac{\overline{p}_g(t) R_0^3 (R_0 + s)^3}{4\mu_s s \left[s^2 + 3R_0(R_0 + s) \right]}, \end{aligned} \tag{22.61}$$

Finally, the displacement solution for a spherical tank is :

$$u_r = \alpha_s \left[T_s(t) - T_R \right] r + \frac{\overline{p}_g(t) R_0^3}{s \left[s^2 + 3R_0(R_0 + s) \right]} \left[\frac{r}{(3\lambda_s + 2\mu_s)} + \frac{(R_0 + s)^3}{4\mu_s r^2} \right] \tag{22.62}$$

The strain components are:

$$\begin{aligned} \varepsilon_{rr} &= \alpha_s \left[T_s(t) - T_R \right] + \frac{\overline{p}_g(t) R_0^3}{s \left[s^2 + 3R_0(R_0 + s) \right]} \left[\frac{1}{(3\lambda_s + 2\mu_s)} - \frac{(R_0 + s)^3}{2\mu_s r^3} \right], \\ \varepsilon_{\theta\theta} &= \varepsilon_{\phi\phi} = \alpha_s \left[T_s(t) - T_R \right] + \frac{\overline{p}_g(t) R_0^3}{s \left[s^2 + 3R_0(R_0 + s) \right]} \left[\frac{1}{(3\lambda_s + 2\mu_s)} + \frac{(R_0 + s)^3}{4\mu_s r^3} \right], \end{aligned} \tag{22.63}$$

The stress components are:

$$\begin{aligned} \sigma_{rr} &= \frac{\overline{p}_g(t) R_0^3}{s \left[s^2 + 3R_0(R_0 + s) \right]} \left[1 - \left(\frac{R_0 + s}{r} \right)^3 \right], \\ \sigma_{\theta\theta} &= \sigma_{\phi\phi} = \frac{\overline{p}_g(t) R_0^3}{s \left[s^2 + 3R_0(R_0 + s) \right]} \left[1 + \frac{1}{2} \left(\frac{R_0 + s}{r} \right)^3 \right], \end{aligned} \tag{22.64}$$

The equivalent stress of Hencky von-Mises is given by:

$$\sigma_{eq}=\sqrt{\frac{\left(\sigma_{rr}-\sigma_{\theta\theta}\right)^2+\left(\sigma_{rr}-\sigma_{\phi\phi}\right)^2+\left(\sigma_{\theta\theta}-\sigma_{\phi\phi}\right)^2}{2}}=\frac{3\overline{p}_g(t)\left(R_0+s\right)^3R_0^3}{2s\left[s^2+3R_0\left(R_0+s\right)\right]r^3}, \tag{22.65}$$

The maximum and minimum values of equivalent stress are given by:

$$\max[\sigma_{eq}]=\frac{3\left(R_0+s\right)^3\overline{p}_g(t)}{2s\left[s^2+3R_0\left(R_0+s\right)\right]},\ \min[\sigma_{eq}]=\frac{3R_0^3\overline{p}_g(t)}{2s\left[s^2+3R_0\left(R_0+s\right)\right]}, \tag{22.66}$$

By equating the relations (22.66) and (22.35), it is possible to determine the collapse point of spherical tank (figure 21.16). Moreover, it is possible determine temperature collapse in spherical tank (figure 21.17) and collapse temperature in gas methane (figure 21.18).

For example, let us consider a spherical tank with inner radius $R_0=10m$ and thickness s = 2.5 cm. The thermal property of steel and methane gas are reported below:

$$c_s=475J/kg\cdot°K,\ k_s=45W/m\cdot°K,\ \rho_s=7.8\cdot10^3kg/m^3,\ \alpha_s=1.2\cdot10^{-5},\ T_0=T_R=293.15°K,$$

$$c_g=1735J/kg\cdot°K,\ \rho_g=0.656kg/m^3,\ R=8.134472J/mol\cdot°K,\quad m=0.016kg/mol,$$

In this case collapse of spherical tank is characterized by following parameters :

$$t_C=43\,\text{min},\ \max[\sigma_{eq}]=65.85MPa,\ T_s=777.13°C,\ \overline{T}_g=689.27°C, \tag{22.67}$$

By applying the procedure reported above we determine temperature distributions versus time in spherical tank and in methane gas (figure 21.3)

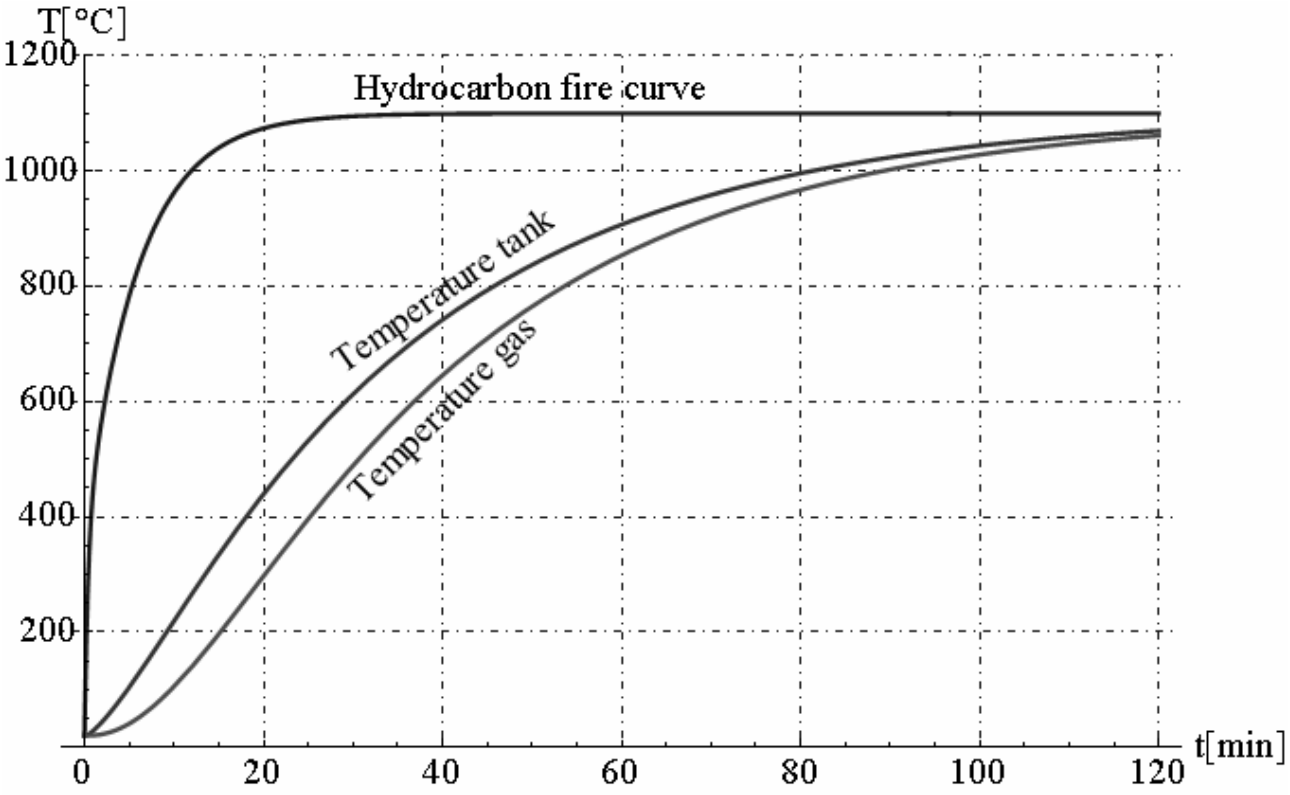

Figure 22.3 - *Temperature profiles versus time: Hydrocarbon fire curve, spherical tank and gas methane*

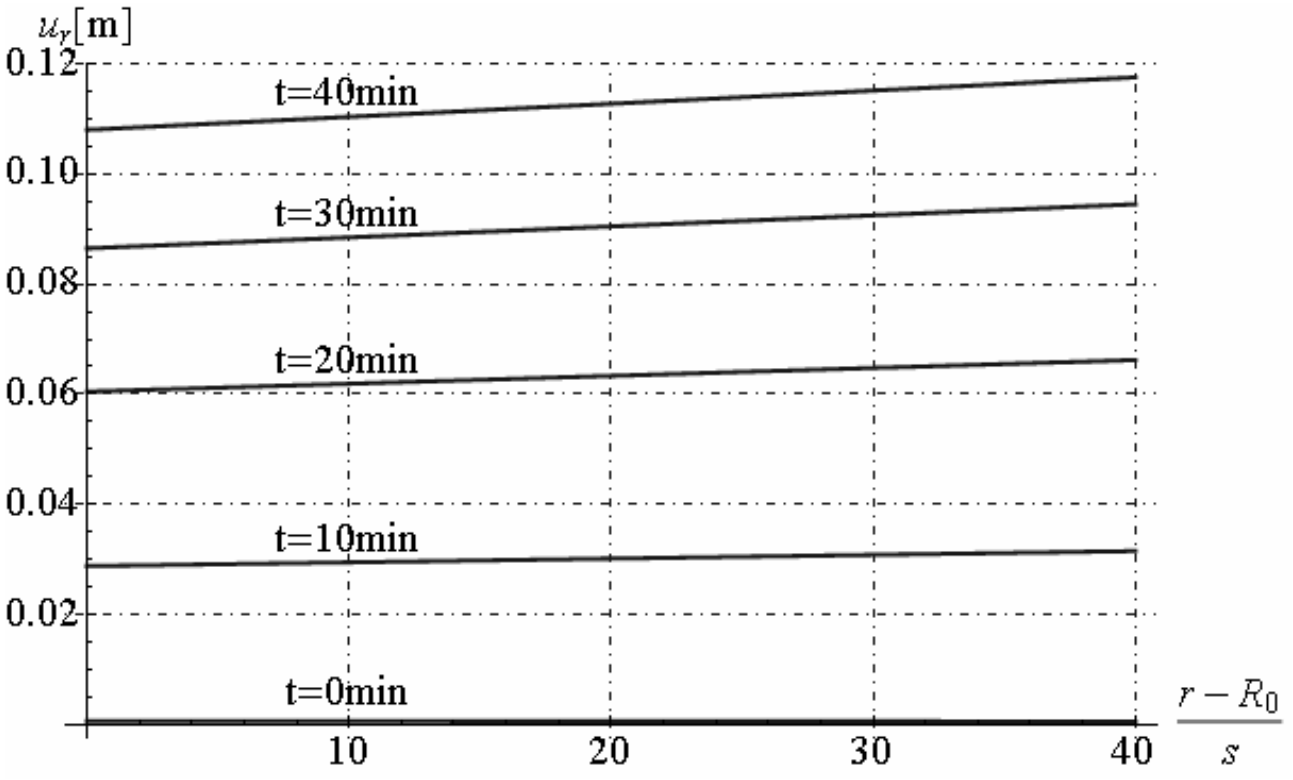

Figure 22.4 - *Radial displacement along radius direction*

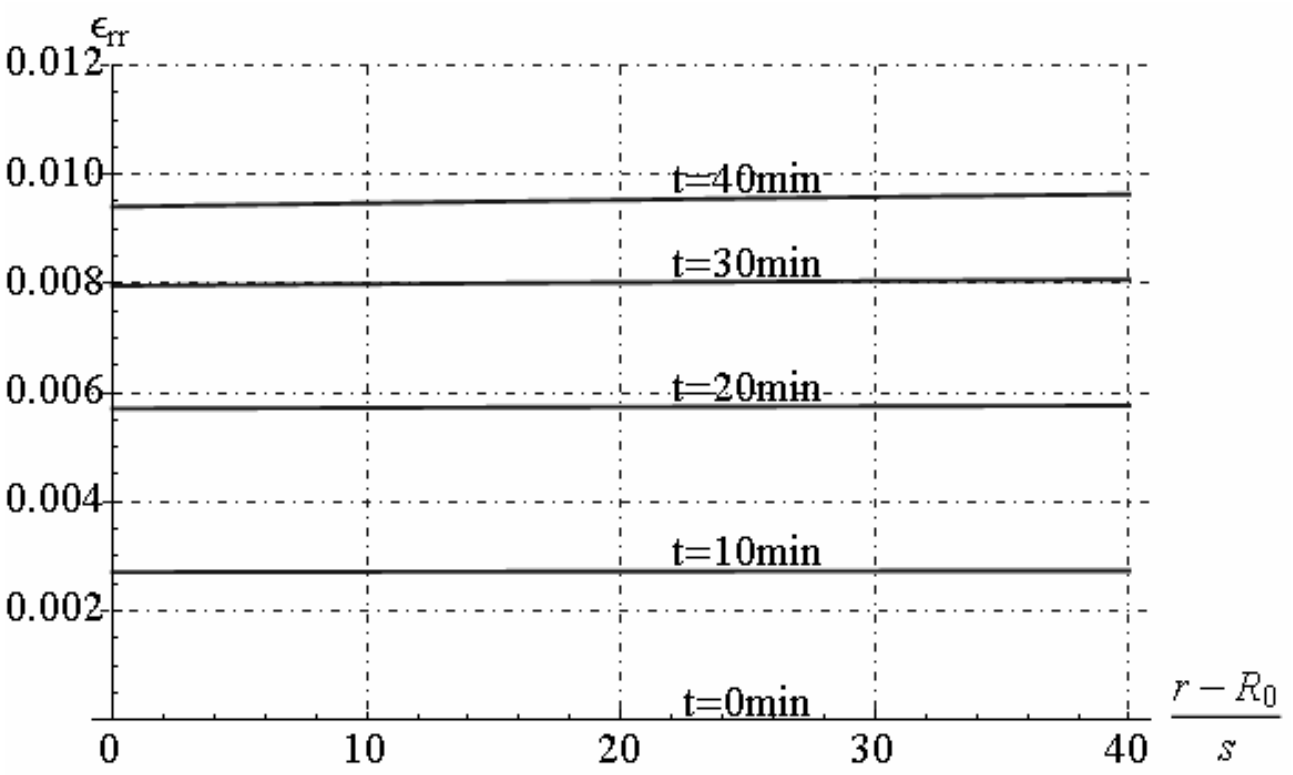

Figure 22.5 - *Radial strain along radius direction*

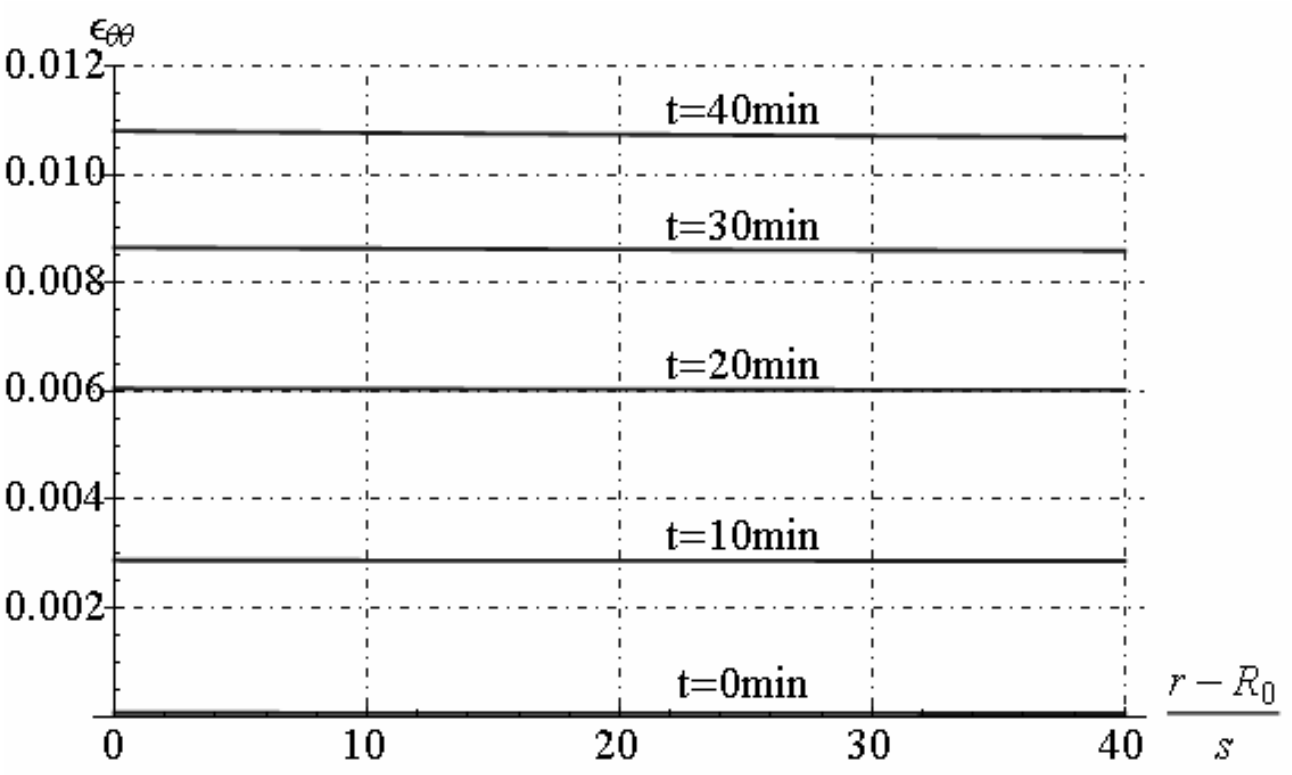

Figure 22.6 - *Circumferential strain along radius direction*

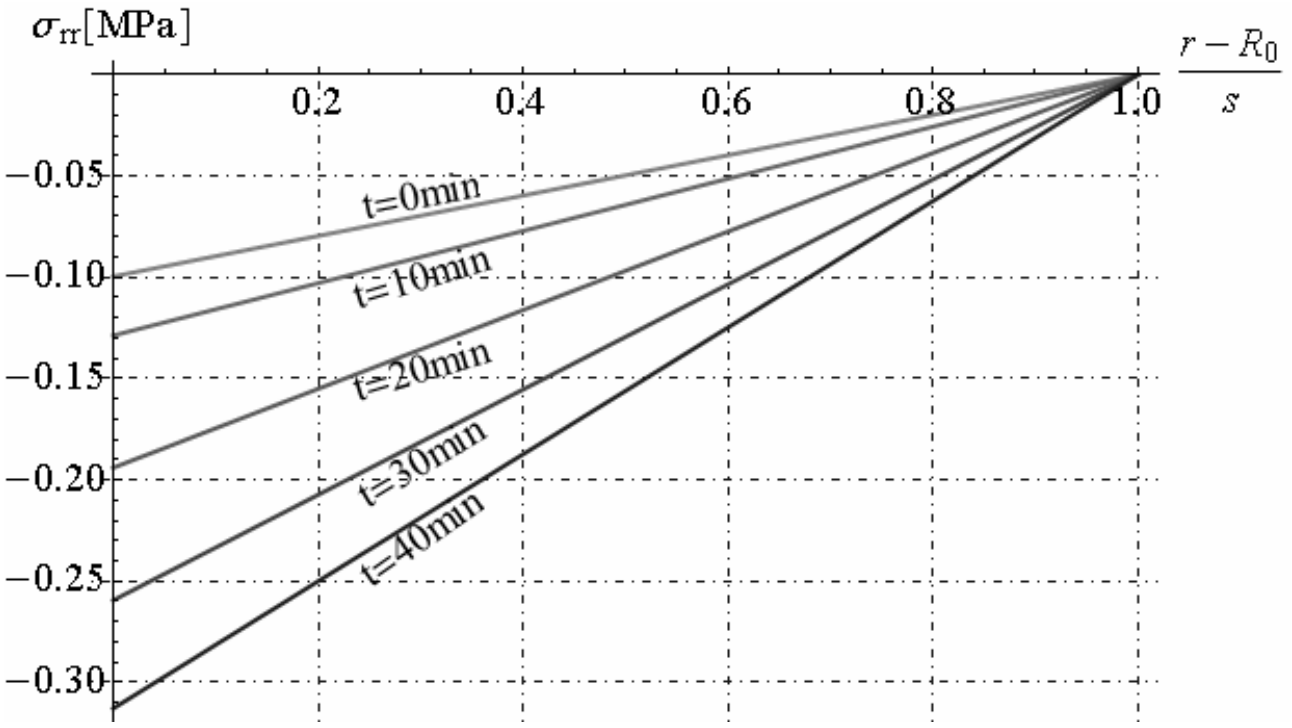

Figure 22.7 - *Radial stress along radius direction*

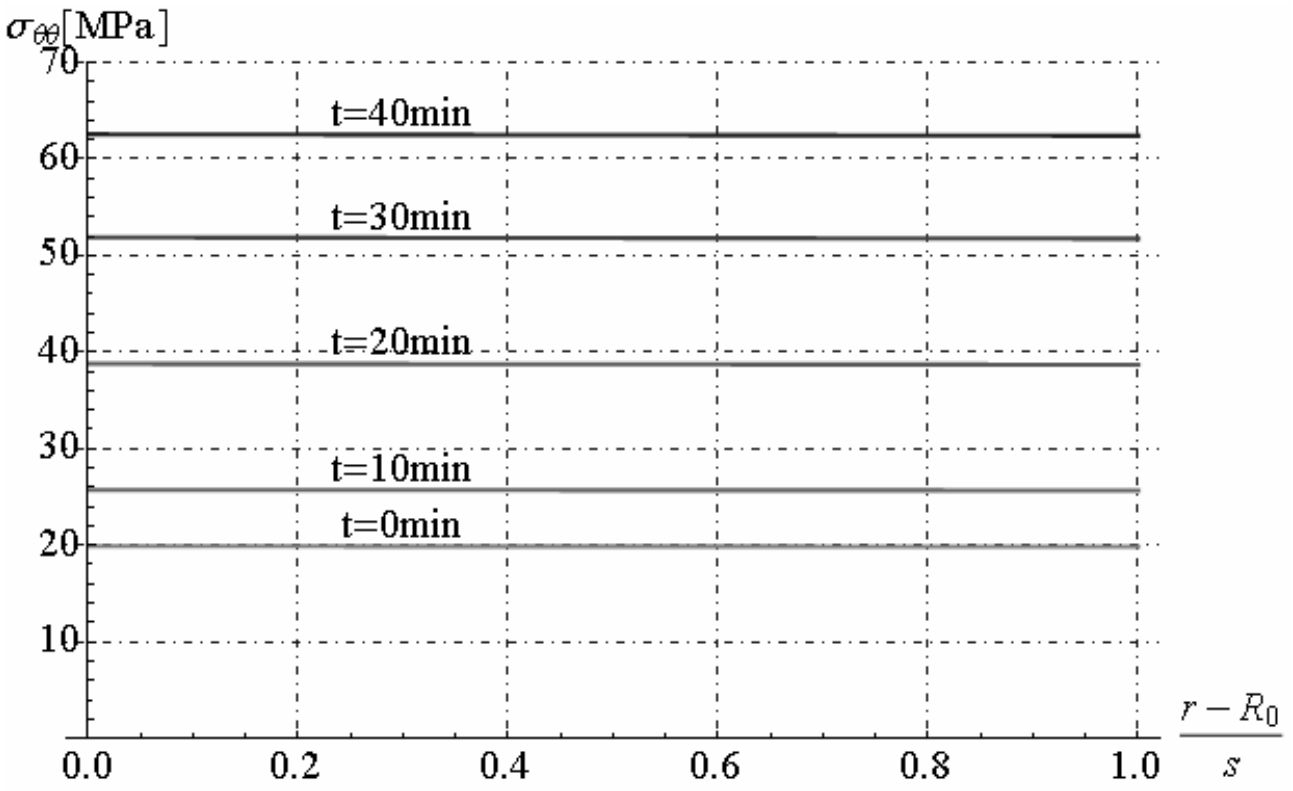

Figure 22.8 - *Circumferential stress along radius direction*

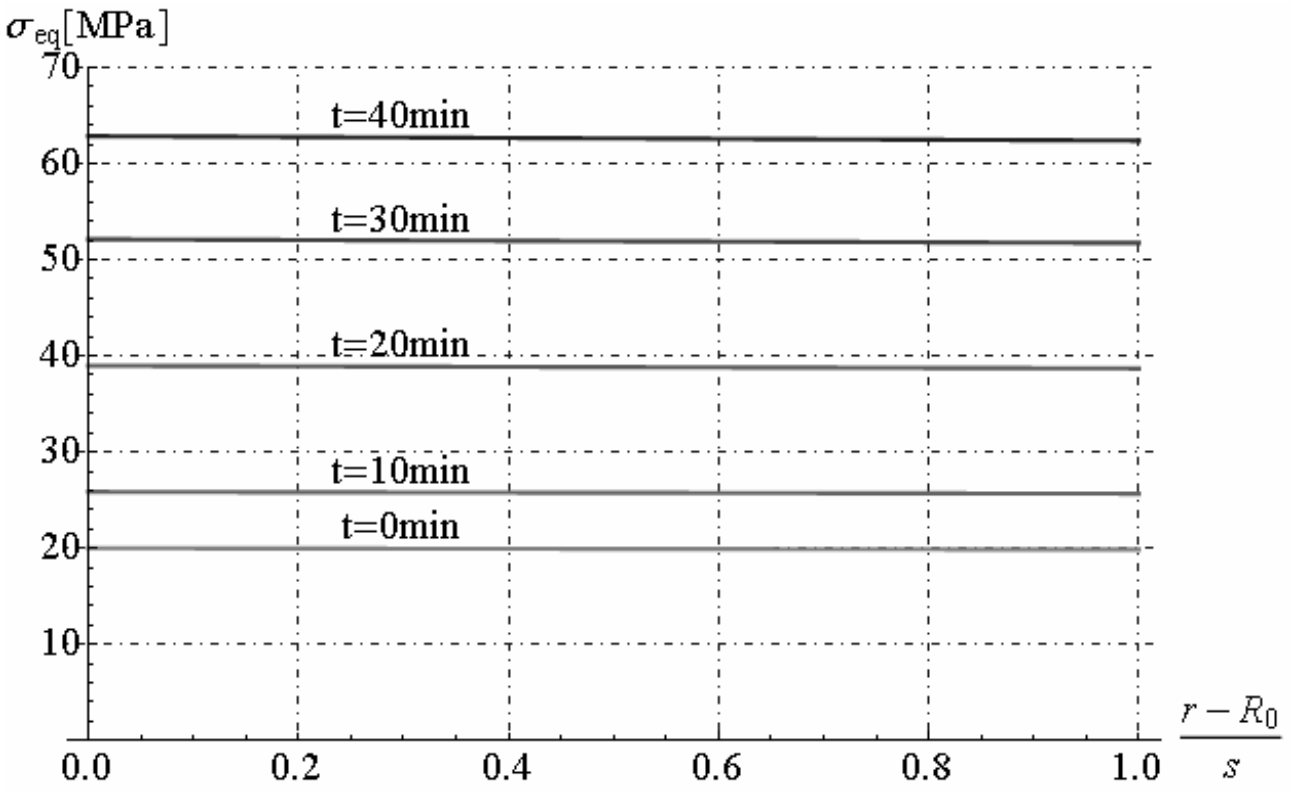

Figure 22.9 - *Hencky von-Mises's equivalent stress along radius direction*

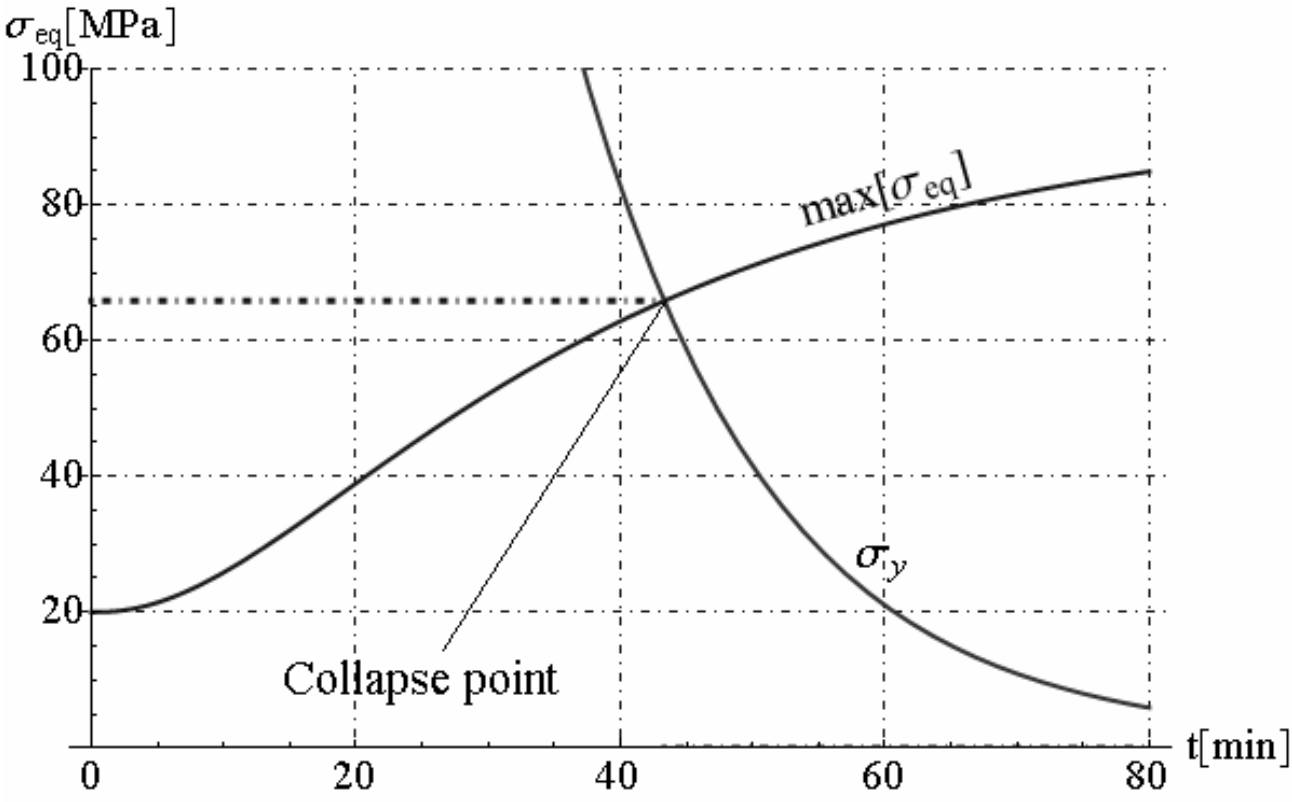

Figure 22.10 - *Collapse point of spherical tank*

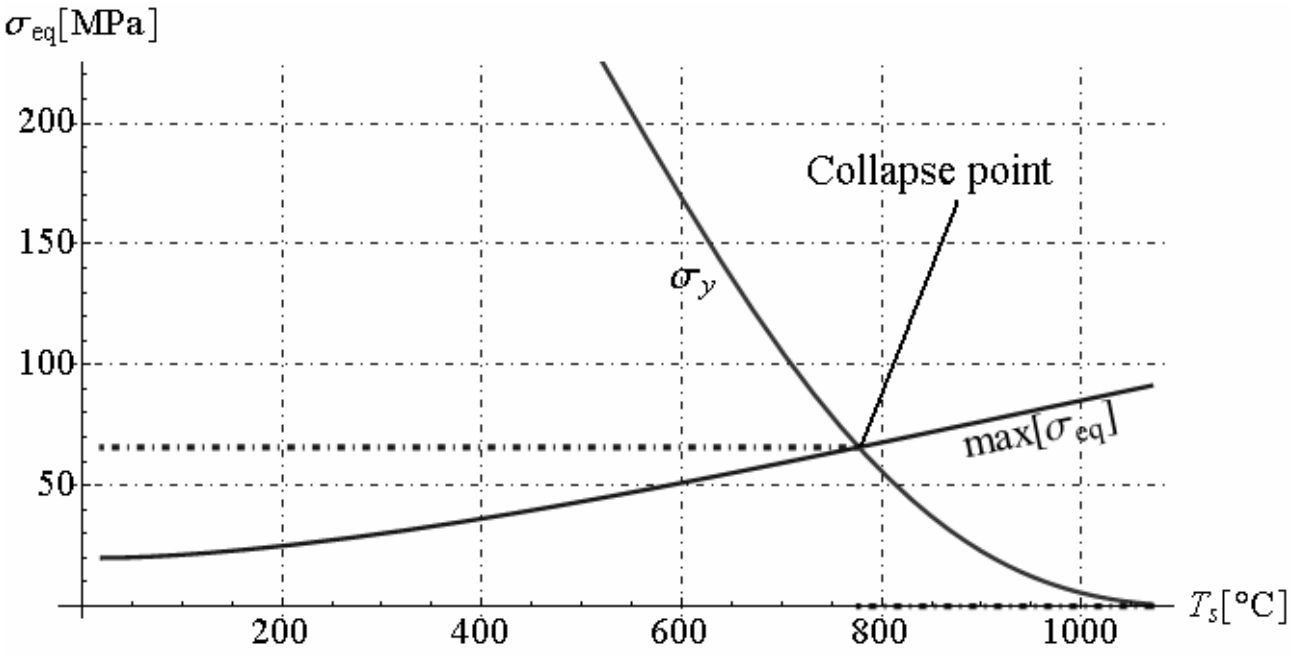

Figure 22.11 - *Collapse Temperature of spherical tank*

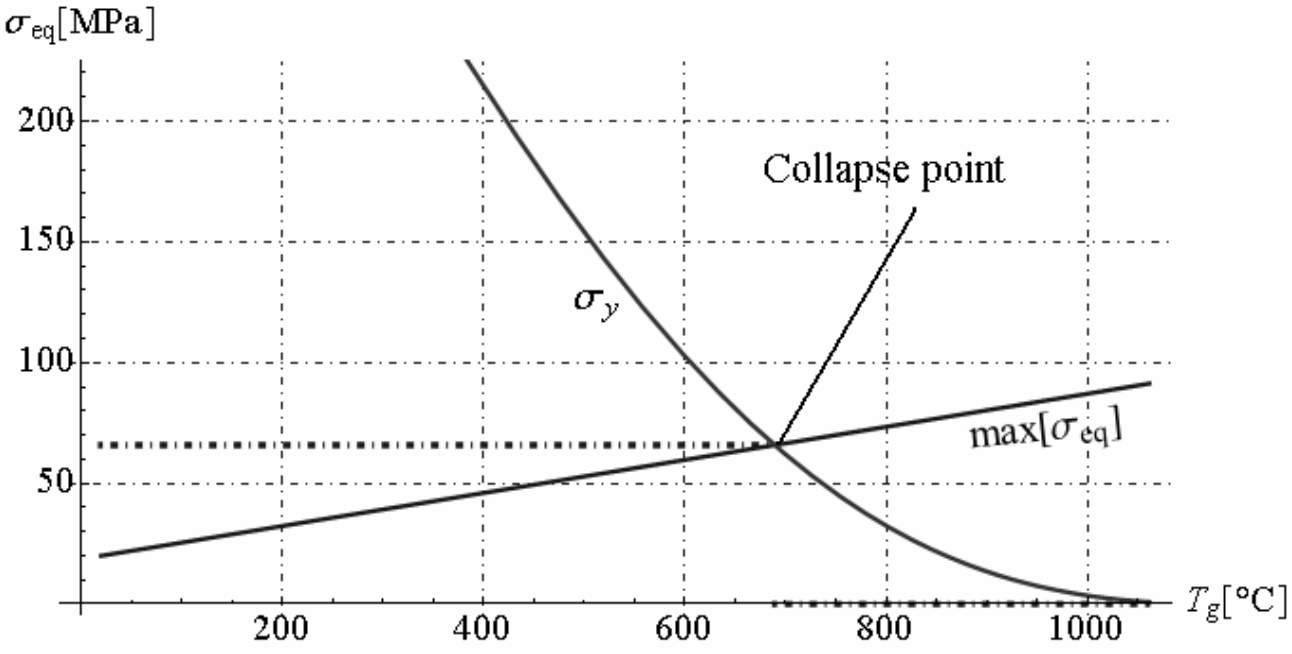

Figure 22.12 - *Collapse temperature in gas methane*

22.3.2. Parametric analyses for spherical tank exposed to fire

In this section, a parametric analyses is conducted for determine the temperature, average gas pressure and Hencky-von Mises's equivalent stress at collapse of spherical tank. The parameters considered are thickness and radius of spherical tank, but the properties of tank not change. Moreover, we make a comparison between parameters at collapse (temperature, maximum equivalent stress and time) for three different gases: Methane, Hydrogen and Oxygen. The physical parameters of these gases are reported in table 22.3. By applying the procedure showed in section 22.3, it is possible to note that the collapse occurs before if the tank is filled with oxygen compared to hydrogen and methane (figure 22.13). The average gas pressure at collapse increases with increasing thickness of spherical tank (figure 22.16). The Hencky-von Mises's equivalent stress at collapse decrease with increasing thickness. The average pressure in the gas to collapse is greater if the gas contained in the tank is oxygen. Finally, we note that in figure 22.13 to figure 22.17, Methane and Hydrogen assume values almost equal although two different gases, while the oxygen assumes completely different values.

	ρ	c_v	M	T_c	p_c
	kg/m^3	$J/(kg\cdot°K)$	kg/mol	°K	MPa
Methane (CH_4)	0.656	1735.4	$16\cdot10^{-3}$	191.1	4.64
Hydrogen (H_2)	0.08988	10183	$2\cdot10^{-3}$	33.3	1.30
Oxygen (O_2)	1.429	658	$16\cdot10^{-3}$	154.8	5.08

Table 22.3 - *Physical parameters of Methane, Hydrogen and Oxygen*

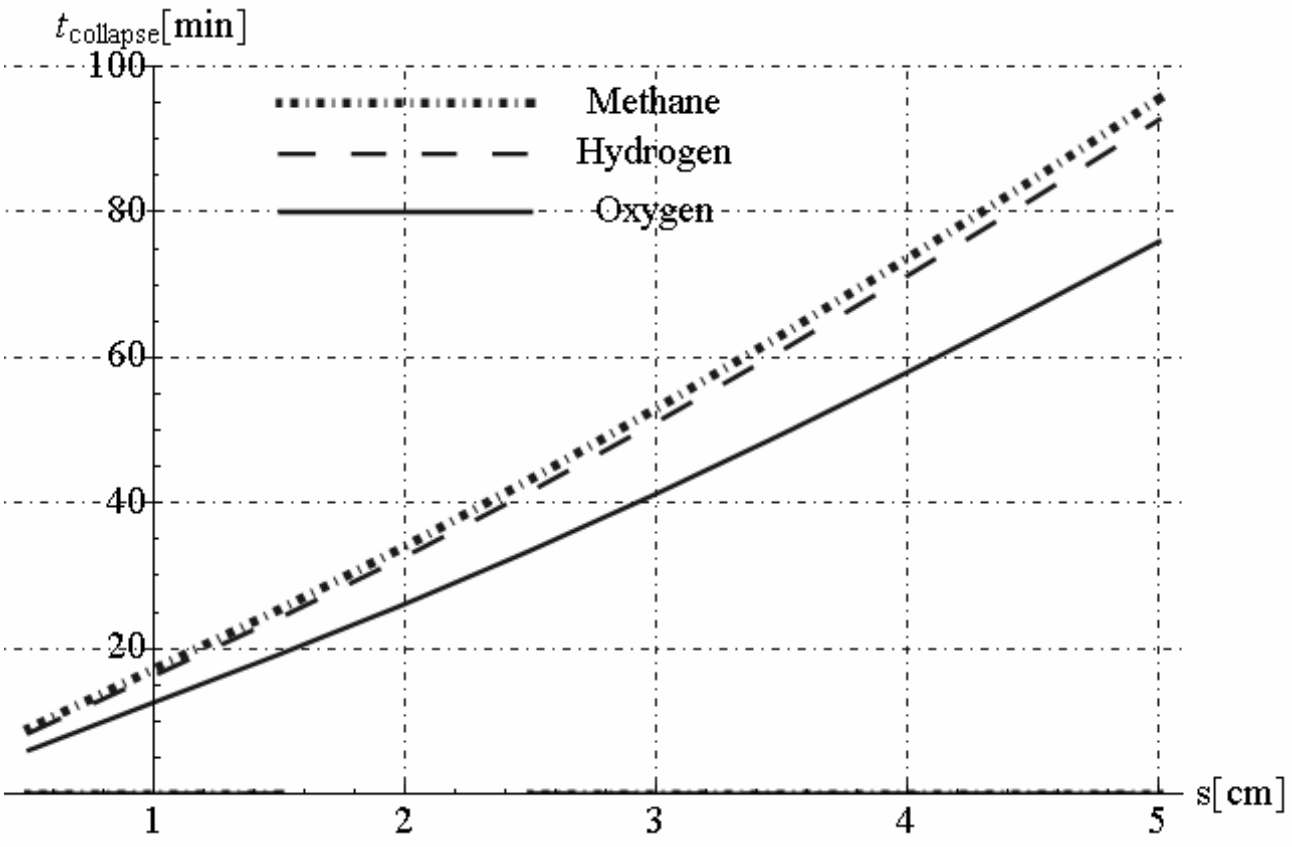

Figure 22.13 - *Collapse instant versus thickness of spherical tank*

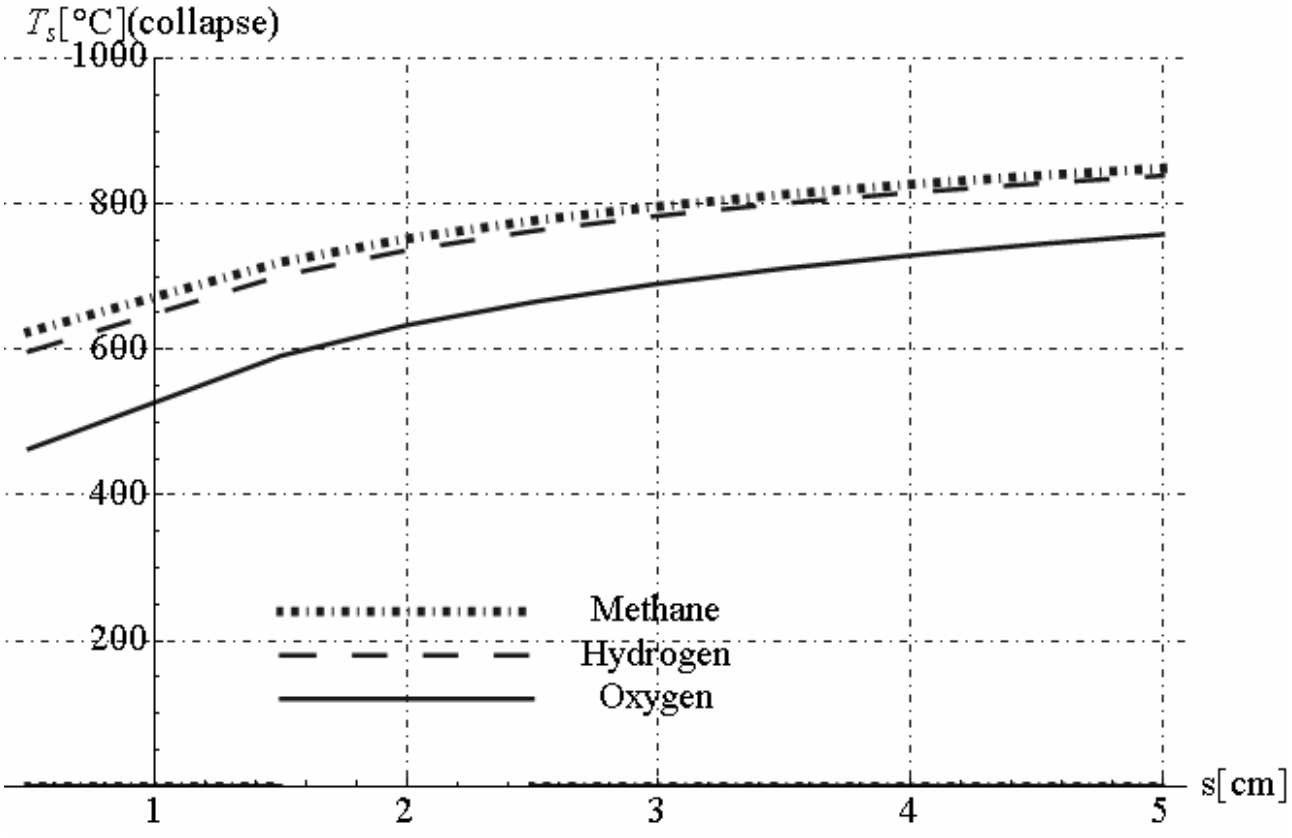

Figure 22.14 - *Tank temperature at collapse versus thickness of spherical tank*

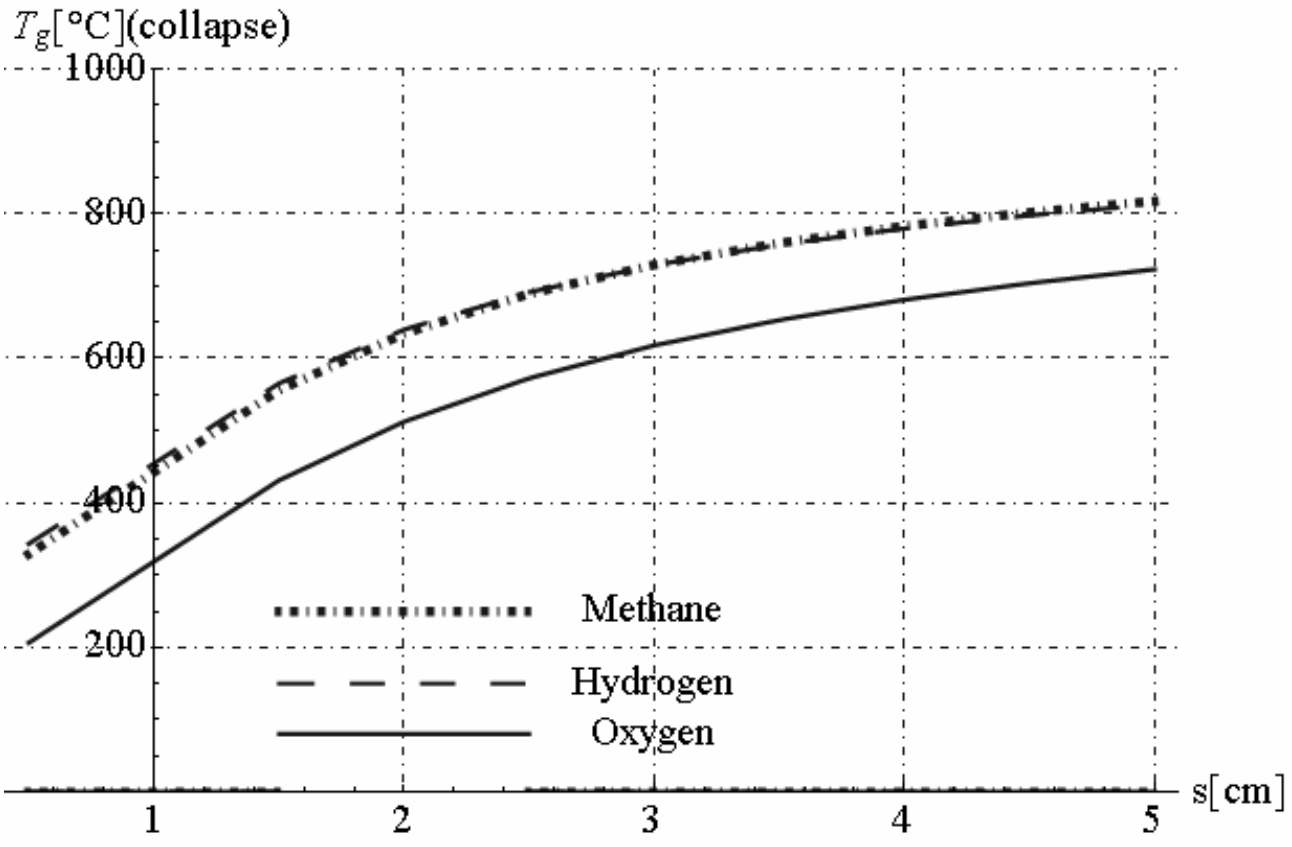

Figure 22.15 - *Average gas temperature at collapse versus thickness of spherical tank*

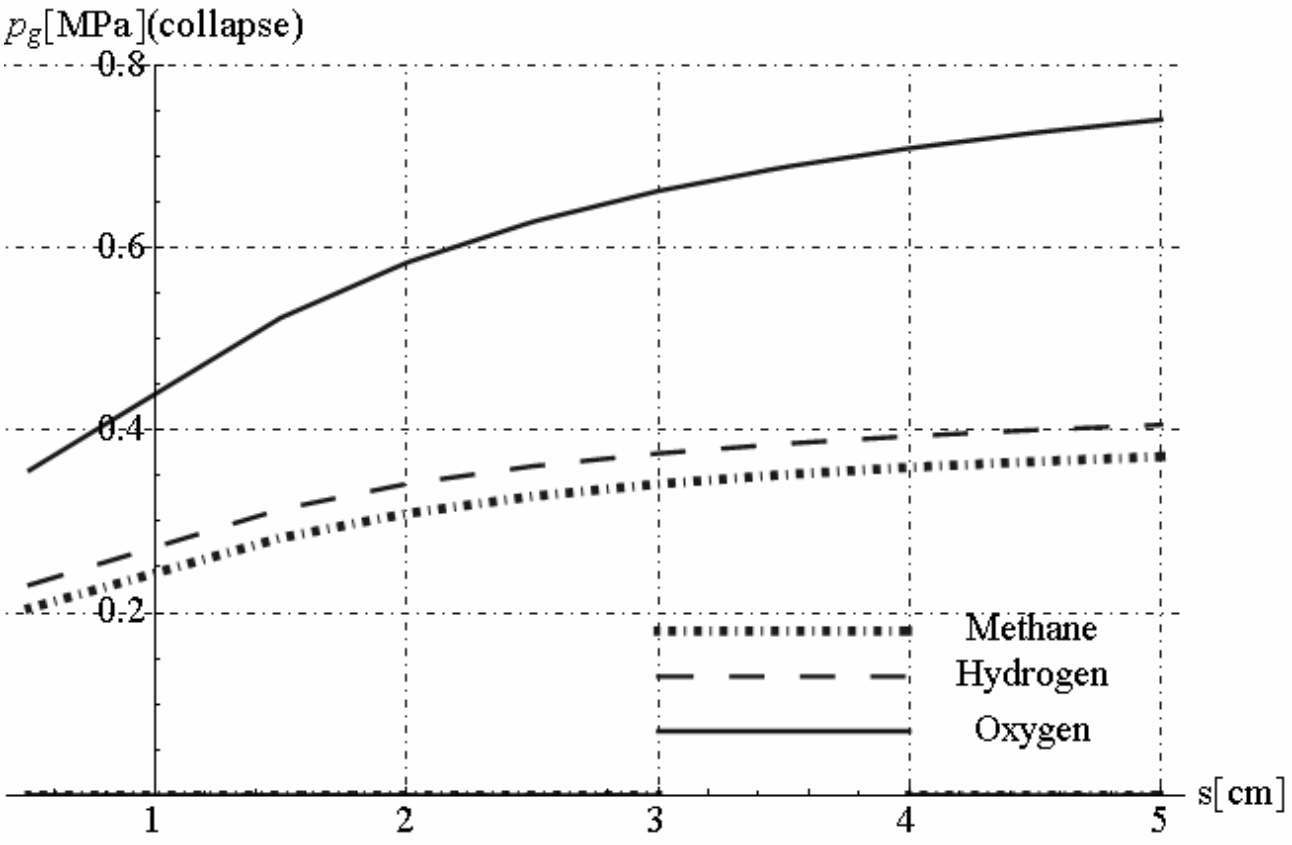

Figure 22.16 - *Average gas pressure at collapse versus thickness of spherical tank*

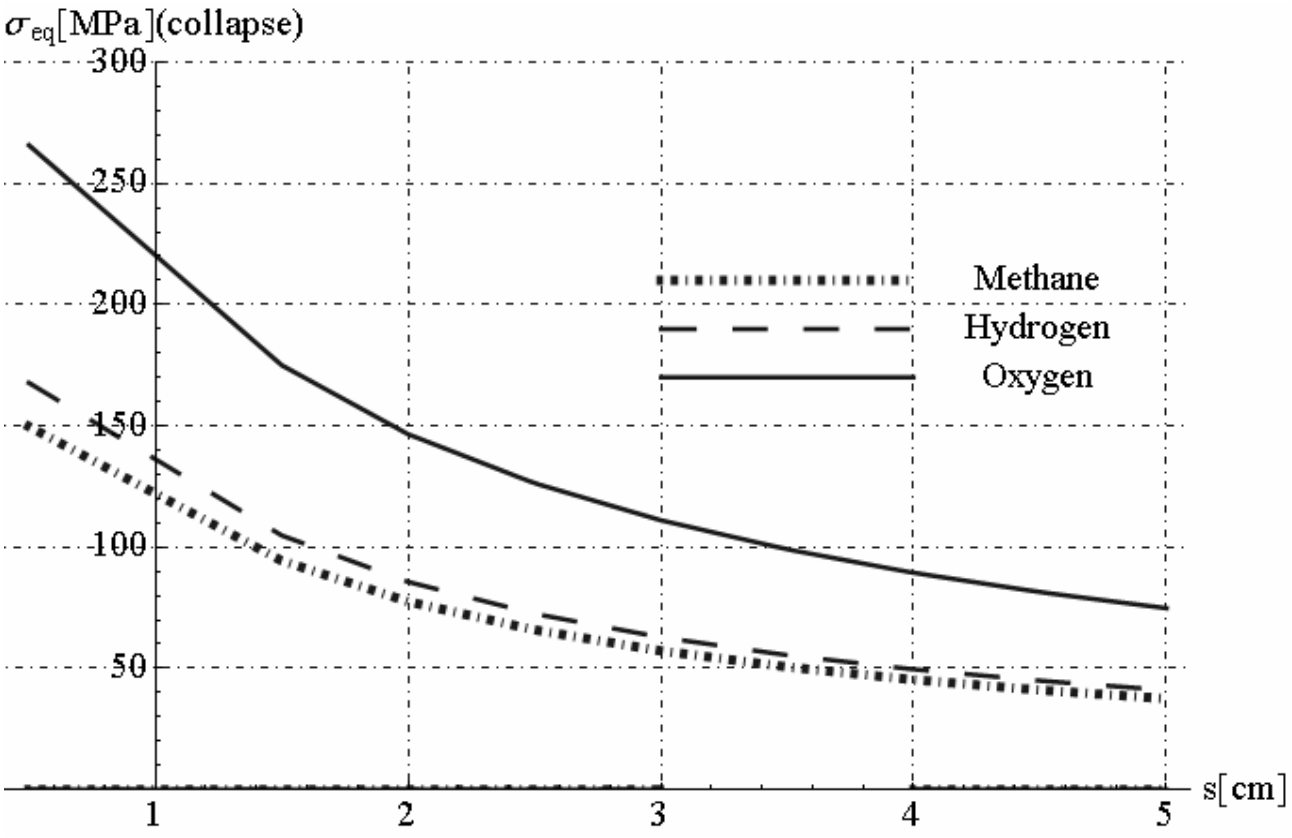

Figure 22.17 - *Maximum Hencky-von Mises's equivalent stress at collapse versus thickness of spherical tank*

22.3.3. Second model: Heat transfer by thermal convection and thermal radiation

Let us consider a spherical tank with inner radius " R_0 " and outer radius " $R_0 + s$ " – where "s" is the thickness of spherical tank -, exposed to conventional fire, as described in section 22.3.1. The spherical tank contains the methane gas with initial pressure p_0 and initial temperature T_0. In this section, we determine the temperature, displacement and stress function in hollow spherical tank by considering thermal convection and thermal radiation. Thermal radiation is energy emitted by matter as electromagnetic waves due to the pool of thermal energy that all matter possesses that has a temperature above absolute zero. Thermal radiation propagates without the presence of matter through the vacuum of space. Thermal radiation is a direct result of the random movements of atoms and molecules in matter. Since these atoms and molecules are composed of charged particles (protons and electrons), their movement results in the emission of electromagnetic radiation, which carries energy away from the surface. In this case, it is don't possible to neglect thermal radiation because spherical tank is subjected to high temperature. The relations (22.40) become:

$$\begin{aligned} q_i &= h_i\left[T_s(t) - \overline{T}_g(t)\right] + \sigma\varepsilon_{res}\left[T_s^4(t) - \overline{T}_g^4(t)\right], \\ q_e &= h_e\left[T_s(t) - \Theta_F(t)\right] + \sigma\varepsilon_{res}\left[T_s^4(t) - \Theta_F^4(t)\right], \end{aligned} \tag{22.68}$$

where $\sigma, \varepsilon_{res}$ are Stefan-Boltzmann costant = $5.67 \cdot 10^{-8} W/\left(m^2 \cdot °K^4\right)$ and emissivities of inner and outer surfaces. By substituting the relations (22.68) in equation (22.39) and neglecting terms s^2, we obtain for spherical tank :

$$s\,\rho_s c_s \frac{d\,T_s(t)}{dt} = -\left(1+\frac{2s}{R_0}\right)\left\{h_e\left[T_s(t)-\Theta_F(t)\right]+\sigma\,\varepsilon_{res}\left[T_s^4(t)-\Theta_F^4(t)\right]\right\}+ \\ -\left\{h_i\left[T_s(t)-\overline{T}_g(t)\right]+\sigma\,\varepsilon_{res}\left[T_s^4(t)-\overline{T}_g^4(t)\right]\right\} \tag{22.69}$$

and for methane gas:

$$\frac{d\,\overline{T}_g(t)}{dt} = -\left\{\frac{3h_i}{\rho_g c_g R_0}\left[\overline{T}_g(t)-T_s(t)\right]+\frac{3\sigma\,\varepsilon_{res}}{\rho_g c_g R_0}\left[\overline{T}_g^4(t)-T_s^4(t)\right]\right\} \tag{22.70}$$

The numerical solution of differential equations (22.69) and (22.70) in unknown functions $T_s(t), \overline{T}_g(t)$, furnishes the collapse temperature of spherical tank. For example, let us consider a spherical tank with inner radius $R_0 = 10m$ and thickness s = 2.5 cm. The thermal property of steel and methane gas are reported in section 21.3.1. In this case collapse of spherical tank is characterized by following parameters :

$$t_C = 17\,\text{min},\ \max[\sigma_{eq}] = 69.71MPa,\ T_s = 768.86°C,\ \overline{T}_g = 745.58°C, \tag{22.71}$$

By comparison the first and second model, we note that collapse temperature in tank and in gas assume values almost equal, but instant of collapse is different. In particular, if we consider heat transfer by thermal radiation and thermal convection, instant of collapse occurs before respect to case in which thermal radiation is neglected. We reported the graphics of functions $T_s(t), \overline{T}_g(t)$ and comparison with solution reported in section 21.3.1. Moreover, we reported the comparison between first and second model of elastic solution obtained .

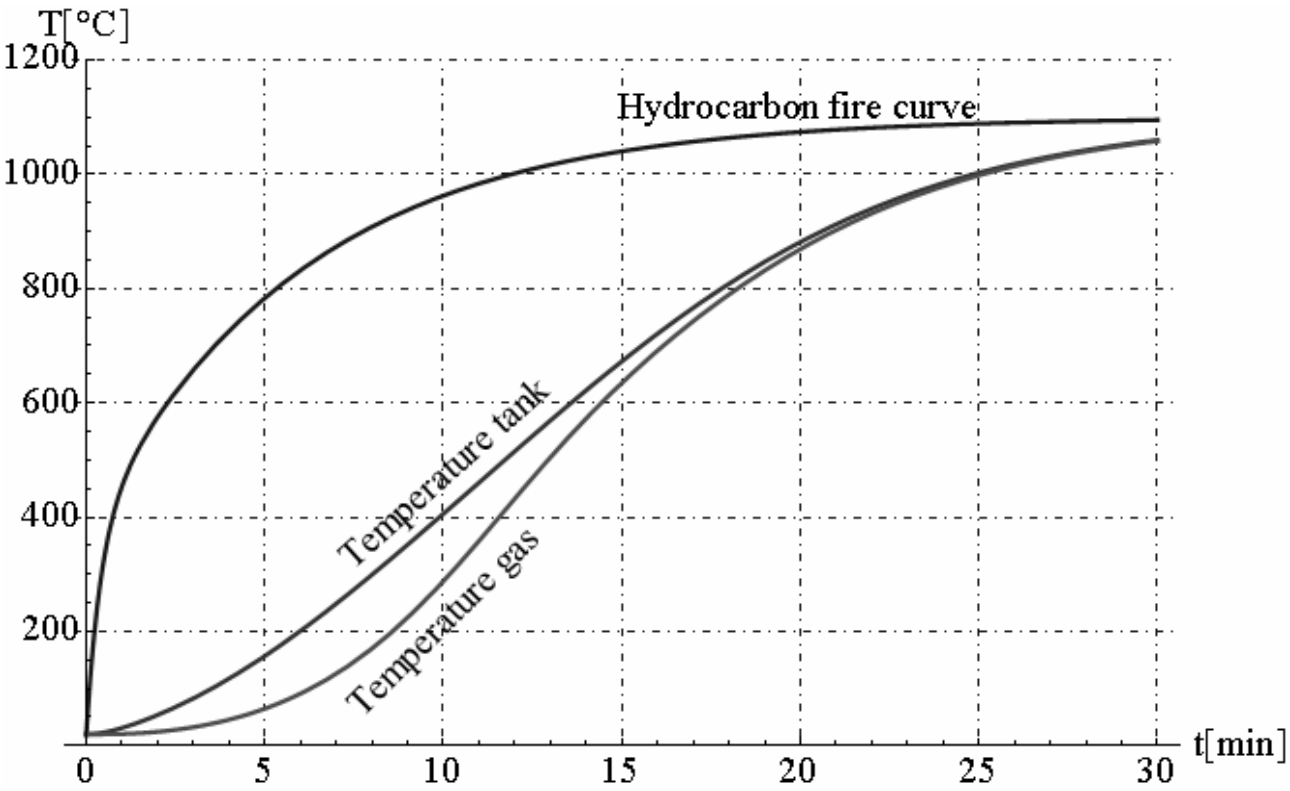

Figure 22.18 - *Temperature profiles versus time: Hydrocarbon fire curve, spherical tank and gas methane (heat transfer by thermal radiation and thermal convection)*

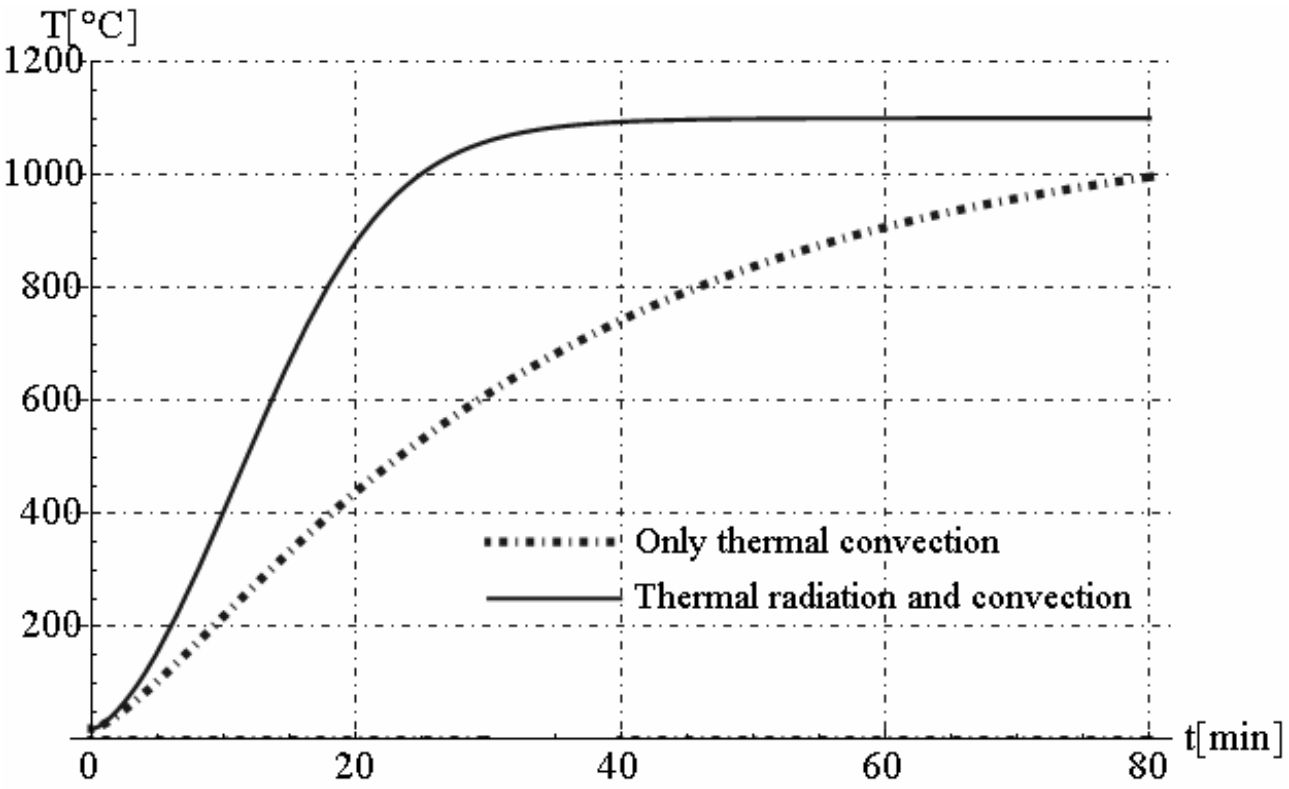

Figure 22.19 - *Temperature in steel versus time (Comparison between first and second model)*

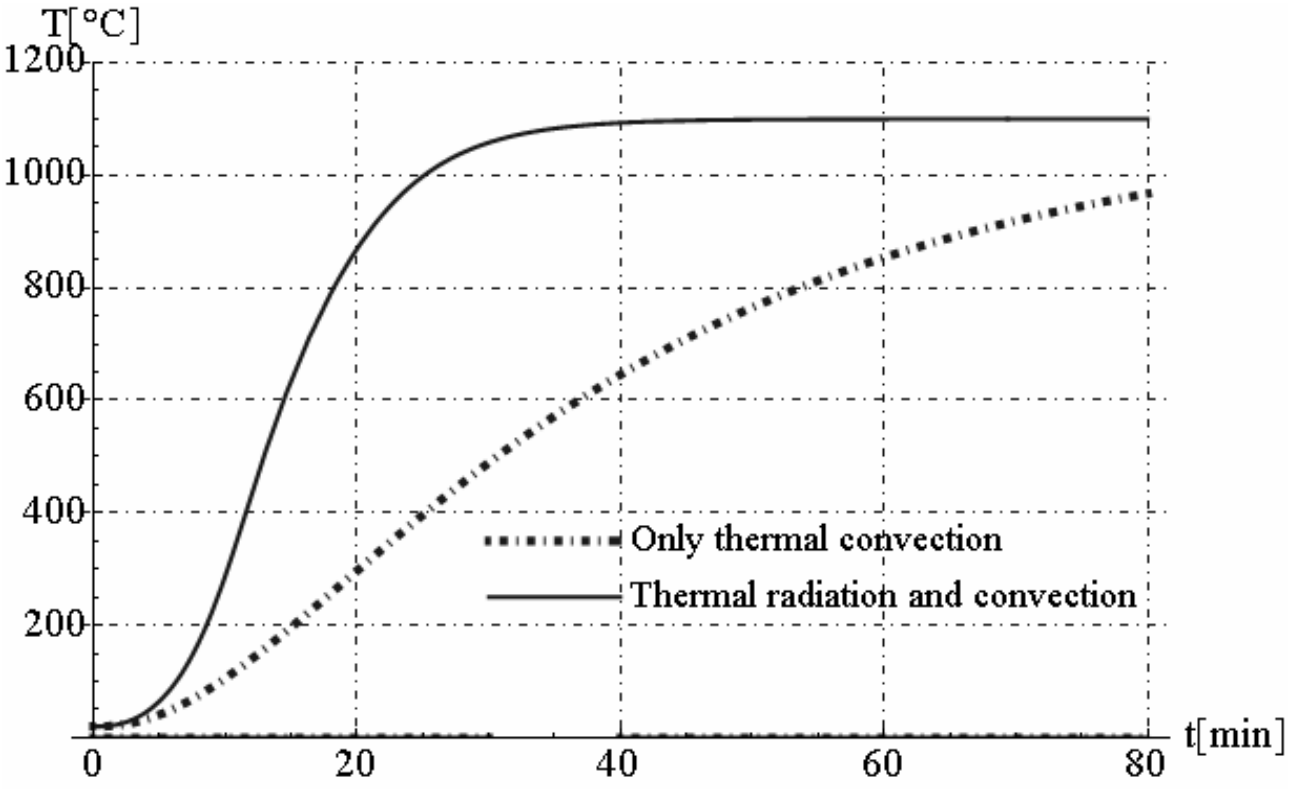

Figure 22.20 - *Average gas temperature versus time (Comparison between first and second model)*

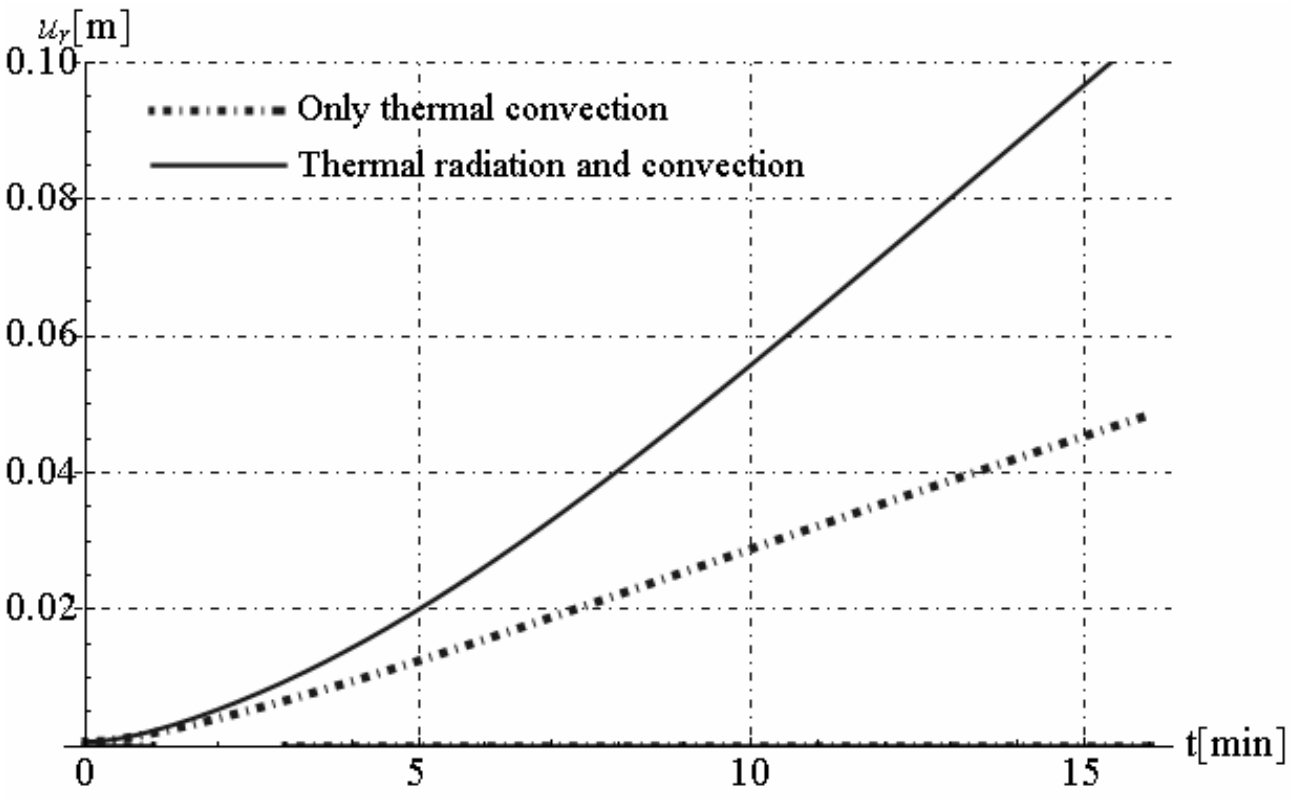

Figure 22.21 - *Maximum radial displacement versus time*
(Comparison between first and second model)

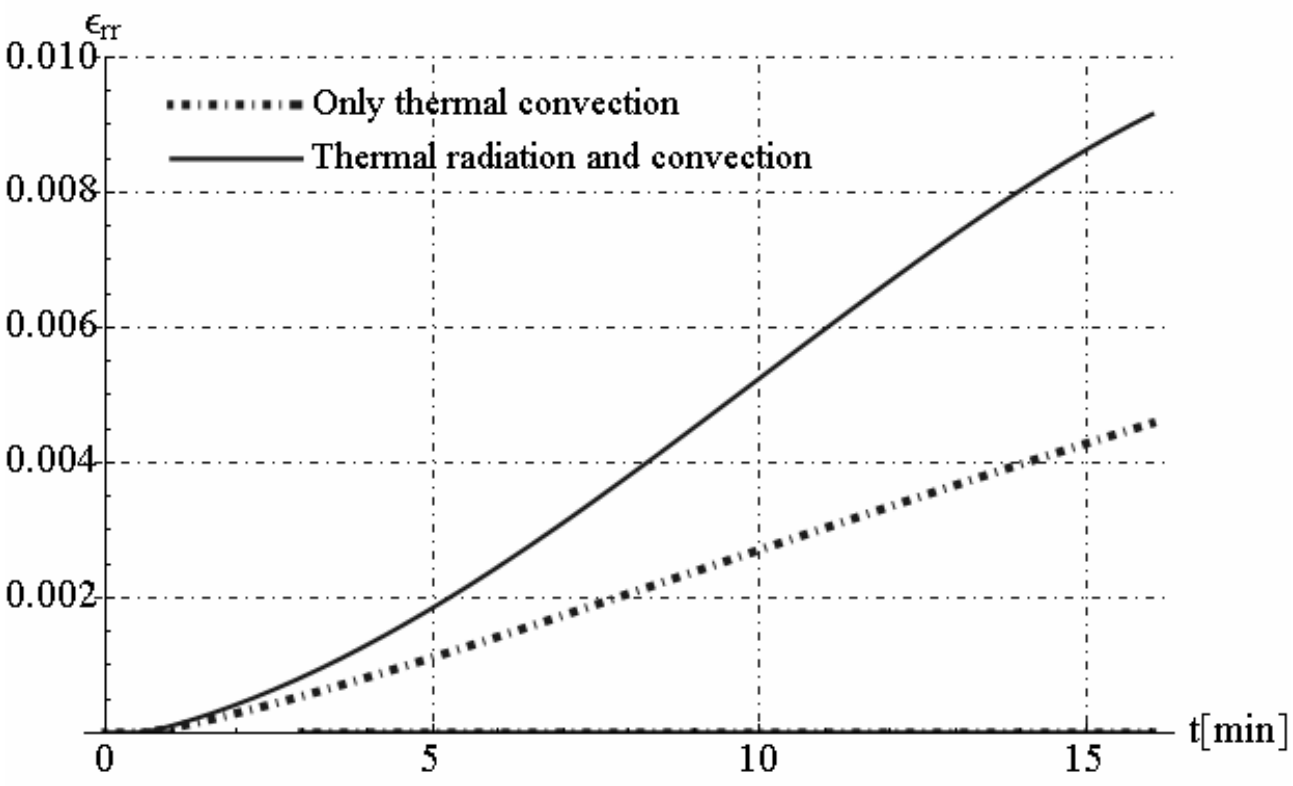

Figure 22.22 - *Maximum radial strain versus time*
(Comparison between first and second model)

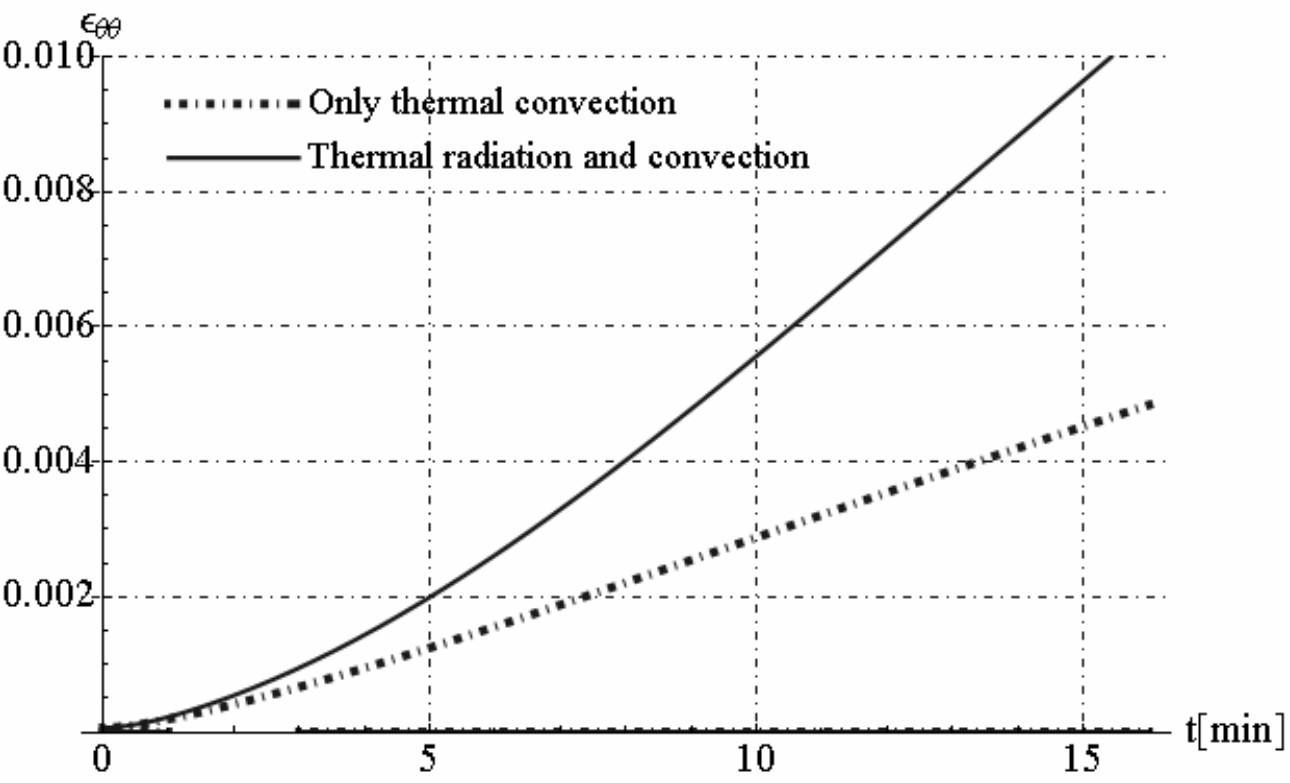

Figure 22.23 - *Maximum circumferential strain versus time*
(Comparison between first and second model)

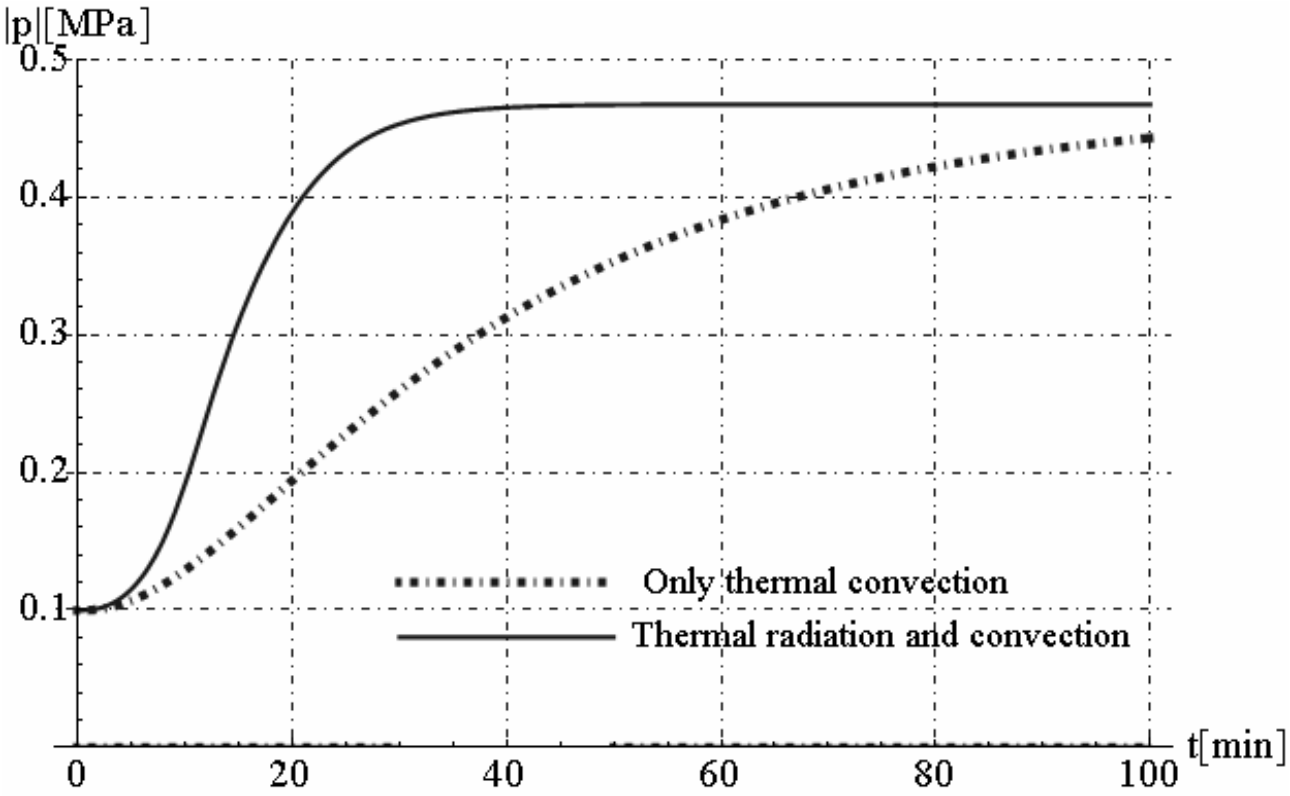

Figure 22.24 - *Average gas pressure versus time*
(Comparison between first and second model)

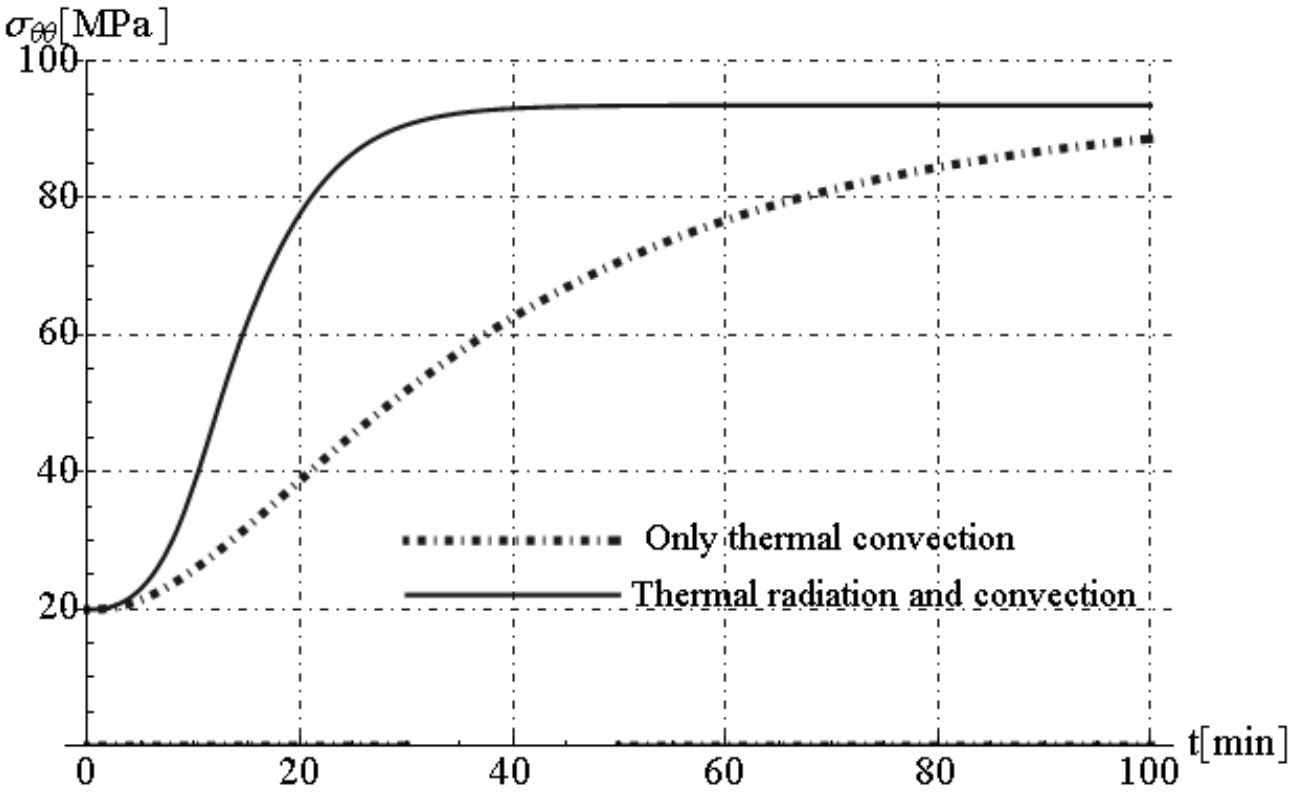

Figure 22.25 - *Maximum circumferential stress versus time*
(Comparison between first and second model)

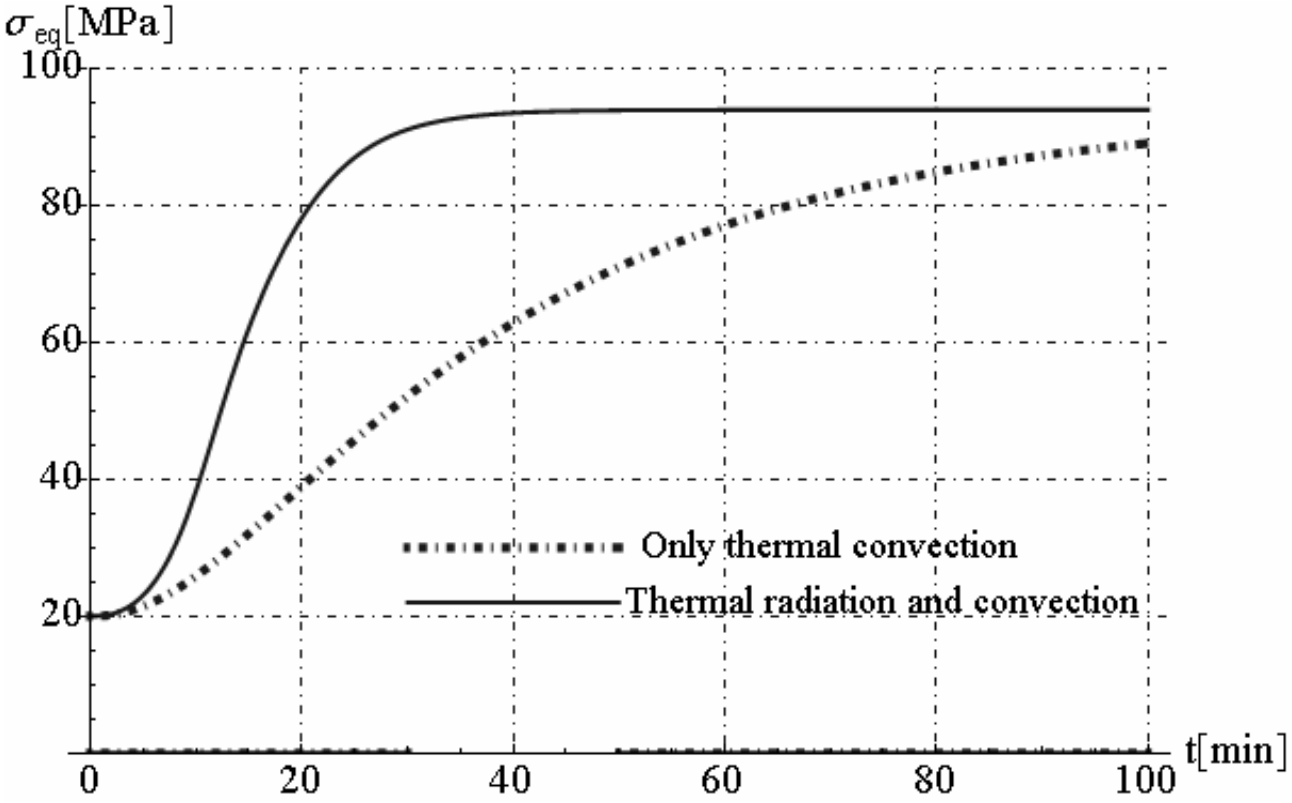

Figure 22.26 - *Maximum equivalent stress versus time*
(Comparison between first and second model)

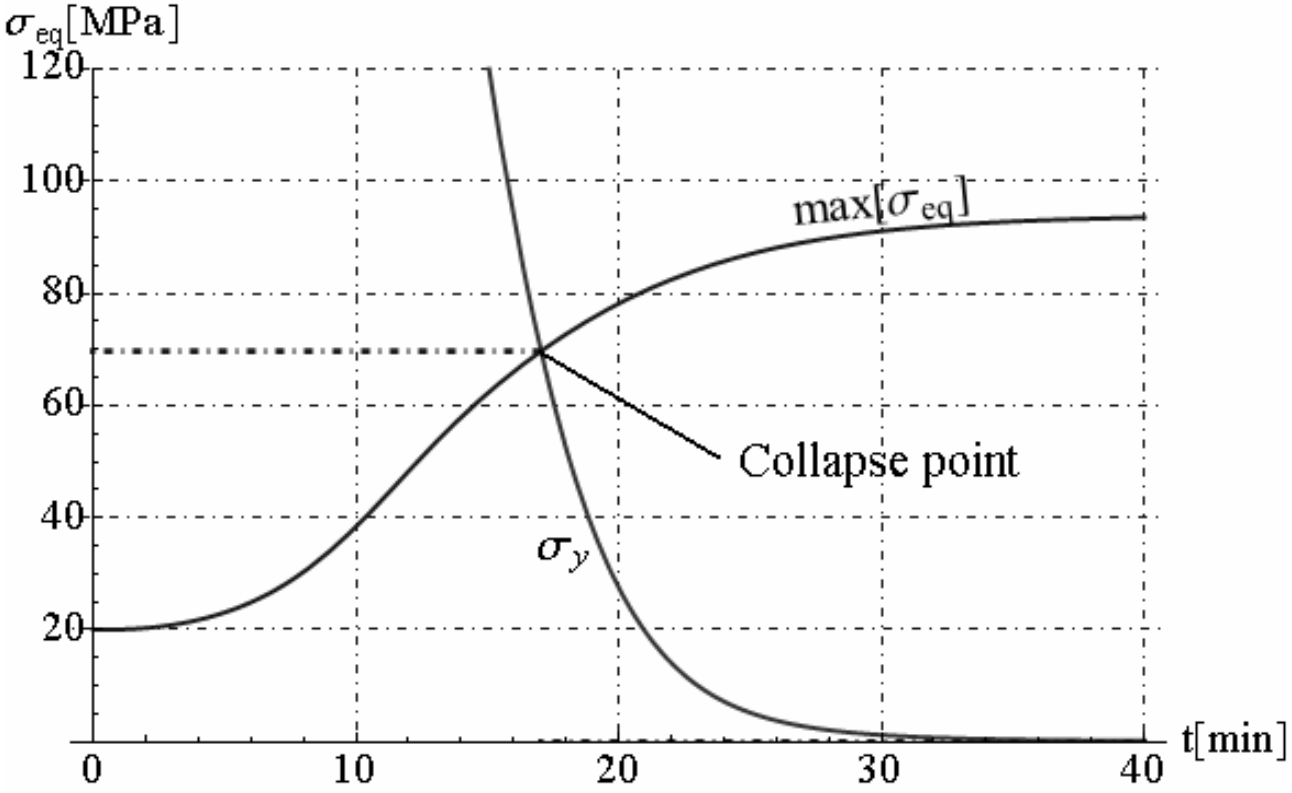

Figure 22.27 - *Collapse point of spherical tank*
(heat transfer by thermal radiation and thermal convection)

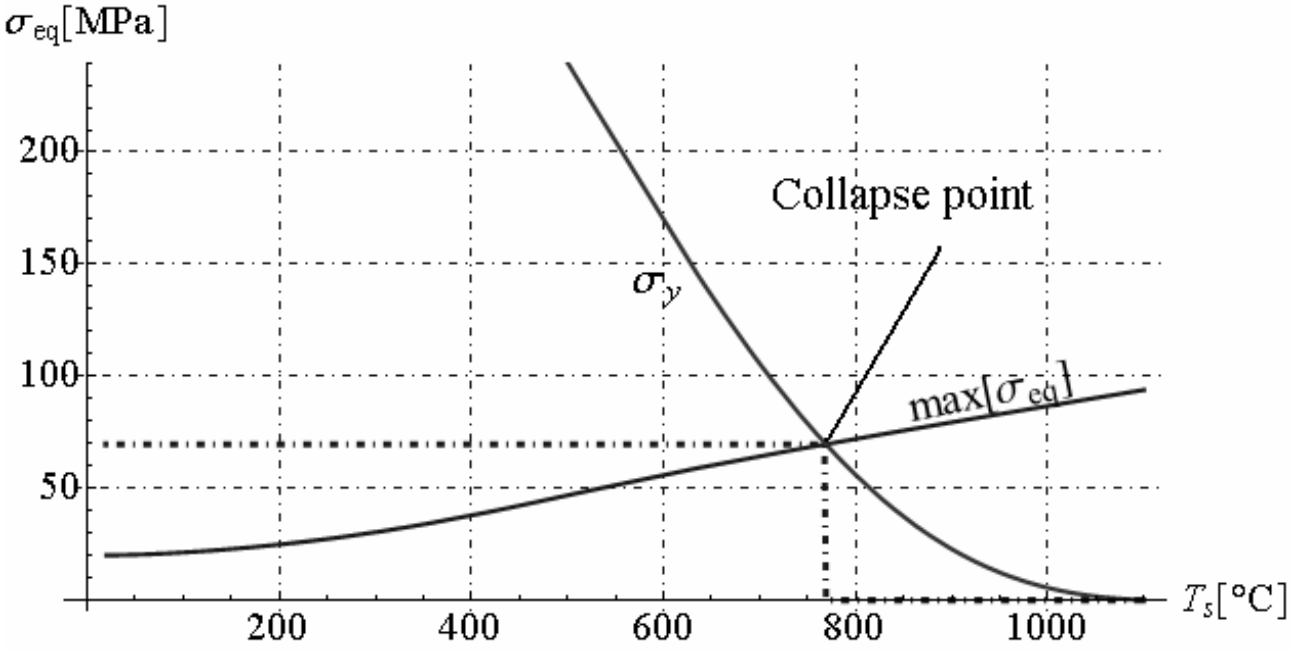

Figure 22.28 - *Collapse Temperature of spherical tank*
(heat transfer by thermal radiation and thermal convection)

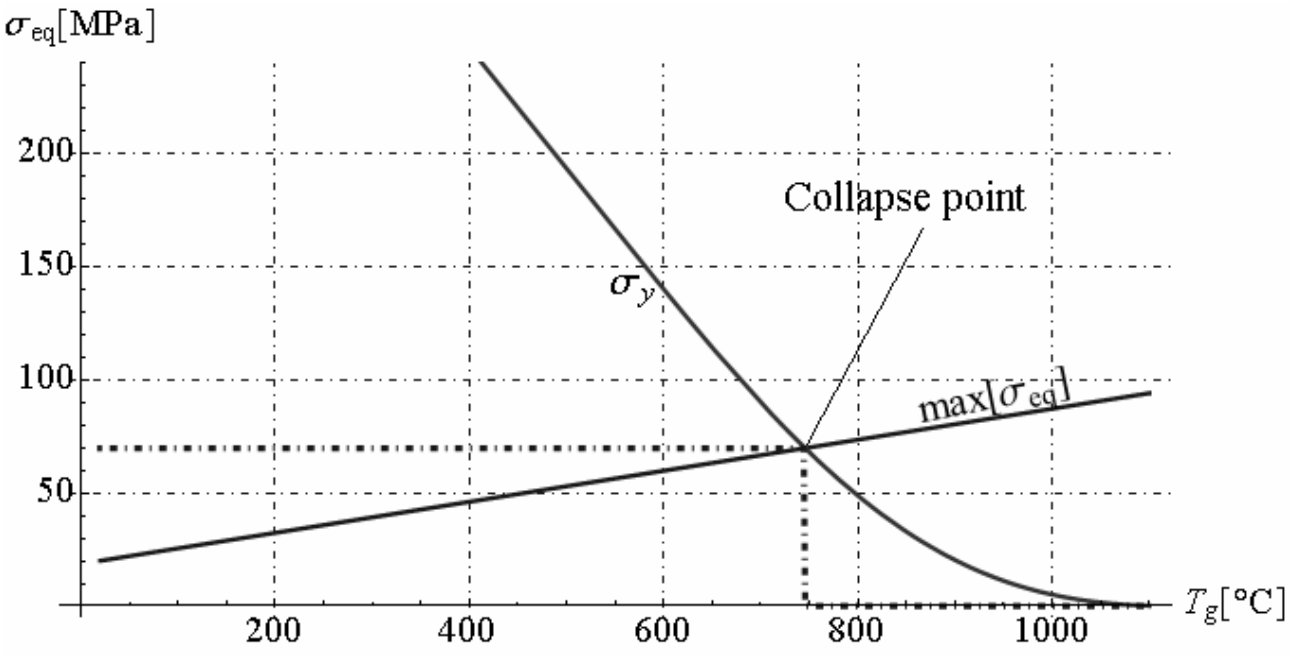

Figure 22.29 - *Collapse temperature in gas methane (heat transfer by thermal radiation and thermal convection)*

22.4. Conclusions

In this chapter is reported an approximate analytical thermo-elastic solution for spherical tank methane gas-filled exposed to hydrocarbon fire. The interaction between spherical tank and internal gas is studied. By applying a suitable simplified hypothesis on the mechanics of problem, we determine the analytical thermo-elastic solution for spherical tank. In this study we reported two analytical model that simulate the interaction between spherical tank and methane gas. In the first model, let us consider that heat transfer occurs by only thermal convection, but in second model the heat transfer occurs by thermal convection and thermal radiation. In this chapter, we determine the temperature, displacement and stress function in hollow spherical tank exposed to hydrocarbon fire. Moreover, we determine the average temperature and average pressure in methane gas, as function of time. The stresses in spherical tank increases over time because the fire increases the average temperature and pressure in the methane gas. By applying the Henchy von Mises's criterion for steel tank, we determine the temperature of the collapse itself, taking into account the reduced strength of steel with temperature. The maximum Hencky-von Mises's equivalent stress in spherical tank, at collapse, assume almost same value in both analytical models. Conversely, the collapse temperature calculated in the first model is less than that calculated in accordance with the second model. Finally, instant collapse of the tank calculated with the first model takes place much later than estimated with the second model. In conclusions, it is very important to consider heat transfer by thermal convection and thermal radiation, for determine the instant of collapse of tank exposed to fire. Conversely, the maximum Hencky-von Mises's equivalent stress in spherical tank, can be to determine by neglecting the heat transfer by thermal radiation.

22.5. References

[1] Ana,-Diana Ancas and D. Gorbanescu (2006), *Theoretical models in the study of temperature effect on steel mechanical properties,* Buletinul institutului politehnic Din Iasi, Tomul LII (LVI), Fasc. 1-2, 2006, Construct II. Arhitectura.

[2] Alavi,F., Karimi, D., Bagri, A., (2008). *An investigation on thermo-elastic behaviour of functionally graded thick spherical vessels under combined thermal and mechanical loads*. Journal of Achievements in Materials and Manufacturing Engineering, vol. 31, Issue 2., pp. 422-428

[3] Ahmet, N. E.; Tolga, A. (2006): *Plane strain analytical solutions for a functionally graded elastic plastic pressurized tube*. Pressure vessels and piping, 83, pp. 635–644.

[4] Benedict, M., Webb, G. R. and Rubin, L. C. (1940). *An Empirical Equation for thermodynamic Properties of Light Hydrocarbons and Their Mixtures. I. Methane, Ethane, Propane and Butane*. J. Chem. Phys. 8, 334-345.
[5] Boley, B.A.,Weiner, J.H., *Theory of thermal stresses*, Dover publications, inc. Mineola, New York
[6] Boublik, T. (1970). *Hard-Sphere Equation of State*. J. Chem. Phys., 53, 471-473.
[7] Boublik, T. (1981). *Statistical Thermodynamics of Nonspherical Molecule Fluids*. Ber. Bunsenges. Phys. Chem. 85, 1038-1041.
[8] Carnahan, N. F. and Starling, K. E. (1969). *Equation of State for Nonattracting Rigid Spheres*. J. Chem. Phys., 51, 635-636.
[9] Carnahan, N. F. and Starling, K. E. (1972). *Intermolecular Repulsions and the Equation of State for Fluids*. AIChE J., 18, 1184-1189.
[10] Chakrabarty, J. (1998): *Theory of Plasticity*. McGraw Hill, New York.
[11] Chen, Y. Z,; Lin, X. Y. (2008): *Elastic analysis for thick cylinders and spherical pressure vessels made of functionally graded materials*. Computational Materials Science, 44, pp.581–587.
[12] Christoforakos, M. and Franck, E. U. (1986). *An Equation of State for Binary Fluid Mixtures to High Temperatures and High Pressures*. Ber. Bunsenges. Phys. Chem., 90, 780-789.
[13] Delfosse, D.; Cherradi, N.; Ilschner, B. (1997): *Numerical and experimental determination of residual stresses in graded materials*. Composites, part B, 28B, pp. 127-141.
[14] Fraldi, M., Nunziante, L., Carannante, F. (2007), *Axis-symmetrical Solutions for n-plies Functionally Graded Material Cylinders under Strain no-Decaying Conditions*, J. Mech. of Adv. Mat. and Struct. Vol. 14 (3), pp. 151-174 - DOI: 10.1080/15376490600719220
[15] M. Fraldi, L. Nunziante, F. Carannante, A. Prota, G. Manfredi, E. Cosenza (2008), *On the Prediction of the Collapse Load of Circular Concrete Columns Confined by FRP*, Journal Engineering structures, Vol. 30, Issue 11, November 2008, Pages 3247-3264 - DOI: 10.1016/j.engstruct.2008.04.036
[16] Fraldi, M., Nunziante, L., Chandrasekaran, S., Carannante, F., Pernice, MC. (2009), *Mechanics of distributed fibre optic sensors for strain measurements on rods*, Journal of Structural Engineering, 35, pp. 323-333, Dec. 2008- Gen. 2009
[17] M. Fraldi, F. Carannante, L. Nunziante (2012), *Analytical solutions for n-phase Functionally Graded Material Cylinders under de Saint Venant load conditions: Homogenization and effects of Poisson ratios on the overall stiffness*, Composites Part B: Engineering, Volume 45, Issue 1, February 2013, Pages 1310–1324
[18] Fuller, G. G. (1976). *A Modified Redlich-Kwong-Soave Equation of State Capable of Representing the Liquid State*. Ind. Eng. Chem. Fundam., 15, 254-257.
[19] Guggenheim, E. A. (1965). *Variations on van der Waals' Equation of State for High Densities*. Mol. Phys., 9, 199-200.
[20] Heilig, M. and Franck, E. U. (1989). *Calculation of Thermodynamic Properties of Binary Fluid Mixtures to High Temperatures and High Pressures*. Ber. Bunsenges. Phys. Chem. 93, 898-905.
[21] Heilig, M. and Franck, E. U. (1990). *Phase Equilibria of Multicomponent Fluid Systems to High Pressures and Temperatures*. Ber. Bunsenges. Phys. Chem., 94, 27-35.
[22] Ibrahim, H.; Tawfik, M.; Al-Ajmi, M. (2006): *Aero-thermo-mechanical characteristic of functionally graded material panels with temperature dependant material properties*. ICFDP 8, ASME conference, Sharm El-Sheikh, Egypt.
[23] Koizumi, M. (1997): *FGM activities in Japan. Composites*, part B, 28B, pp. 1-4.
[24] Lekhnitskii, S. G., (1981), *Theory of Elasticity of an Anisotropic Body*, Mir, Moscow.
[25] Liew, K. M.; Kitipornchai, S.; Zhang, X. Z.; Lim, C. W. (2003): *Analysis of the thermal stress behaviour of functionally graded hollow circular cylinders*. Solids and Structures, 40, pp. 2355–80.
[26] Lutz, M. P.; Zimmerman, R. W. (1996): *Thermal stresses and effective thermal expansion coefficient of a functionally graded sphere*. Thermal stress,19, pp. 39-54.

[27] McElroy, P. J. (1983). *Association Parameters for Fluid Mixture Property Estimation*. CHEMECA 83: Aust. Chem. Eng. Conf., 11th, 449-454.
[28] Mèthode de prèvision pour le calcul du comportement an fen des structures en acier. D.T.U., Rev. Constr. Methal., 3 (1982)
[39] Nayak, P.; Mondal, S. C. (2011): *Analysis of a functionally graded thick cylindrical vessel with radially varying properties*. Engineering science and technology, 3, pp.1551-1562.
[30] Nayak, P.; Mondal, S. C., Nandi, A.,(2011), *Stress, strain and displacement of a functionally graded thick spherical vessel*, International Journal of Engineering Science and Technology (IJEST), Vol. 3 No. 4;
[31] Noda, N.; Hetnarski, R. B.; Tanigawa, Y. (2003): *Thermal Stresses*. Taylor and Francis, New York.
[32] Nunziante, L., Gambarotta, L., Tralli, A., *Scienza delle Costruzioni*, 3° Edizione, McGraw-Hill, 2011, ISBN: 9788838666971
[33] Obata, Y.; Noda, N. (1994): *Steady thermal stress in a hollow circular cylinder and a hollow sphere of a functionally gradient materials*. Thermal stress, 17, pp. 471-487.
[34] Ozisik, M. N. (1985): *Heat Transfer*. McGraw Hill, New York.
[35] Peng, X. L.; Li, X. F. (2010): *Thermo-elastic analysis of a cylindrical vessel of functionally graded materials*. Pressure vessels and piping, 87, pp. 203-210.
[36] Peng, D. Y. and Robinson, D. B., (1976). *A New Two-Constant Equation of Sta*te. Ind. Eng. Chem. Fundam., 15, 59-64.
[37] Redlich, O. and Kwong, J. N. S. (1949). *On the Thermodynamics of Solutions. V: An Equation of State. Fugacities of Gaseous Solutions*. Chem. Rev., 44, 233-244.
[38] Shah, V. M., Bienkowski, P. R. and Cochran, H. D. (1994). *Generalized Quartic Equation of State for Pure Nonpolar Fluids*. AIChE J., 40, 152-159.
[39] Shah, V. M., Lin, Y. L., Bienkowski, P. R. and Cochran, H. D. (1996). *A Generalized Quartic Equation of State*. Fluid Phase Equilib ., 116, 87-93.
[40] Shao, Z. S. (2005): *Mechanical and thermal stresses of a functionally graded hollow circular cylinder with finite length*. Pressure vessel and piping, 82, pp.155-163.
[41] Shao, Z. S.; Ma, G. W. (2008): *Thermo-mechanical stresses in functionally graded circular hollow cylinder with linearly increasing boundary temperature*. Composite Structures, 83, pp.259–265.
[42] Soave, G. (1972). *Equilibrium Constants from a Modified Redlich-Kwong Equation of State*. Chem. Eng. Sci., 27 , 1197-1203.
[43] Soave, G. (1984). *Improvement of the van der Waals Equation of State*. Chem. Eng. Sci., 39, 357-369.
[44] Soave, G. (1992). *A New Expression of q(α) for the Modified Huron-Vidal Method*. Fluid Phase Equilib., 72, 325-327.
[45] Soave, G., Bertucco, A. and Vecchiato, L. (1994). *Equation of State Group Contributions from Infinite-Dilution Activity Coefficients*. Ind. Eng. Chem. Res., 33, 975-980.
[46] Structural Fire Design, Draft Modified Clauses, Eurocode 3, part 1.2, CEN/TC 250/SC3/N11 (1993)
[47] Tutuncu N, Ozturk M. (2001): *Exact solutions for stresses in functionally graded pressure vessels*. Composites, part B, 32, pp. 683- 686.
[48] You, L. H.; Zhang, J. J.; You, X. Y. (2005): *Elastic analysis of internally pressurized thick-walled spherical pressure vessels of functionally graded materials*. Pressure vessel and piping, 82, pp.347-354.
[49] Zimmerman, R. W.; Lutz, M. P. (1999): *Thermal stresses and thermal expansion in a uniformly heated functionally graded cylinder.* Thermal stress, 22, pp. 177-188.
[50] Zong -Yi Lee (2004): *Coupled problem of thermo-elasticity for multilayered spheres with time-dependent boundary conditions*. Journal of Marine Science and Technology, Vol. 12, No. 2, pp. 93-101

CHAPTER XXIII
THERMAL STRESS IN INSULATED PIPELINES

23.1. Introduction

In recent years, new demands for insulated pipes operating at higher temperatures of up to approximately 150°C have indicated that there is a need to qualify the insulation material to withstand thermal degradation as well as the physical stresses incurred on buried pipeline systems at these temperatures. One of the few standards for evaluating pipe insulated with polyurethane foam operating at high temperatures is the European Standard EN 253. However, this standard was based on the requirements of the district heating industry and does not reflect some of the potential differences in materials of construction or service environments being proposed for pipelines.

Selection of piping system is an important aspect of system design in any energy consuming system. The selection issues such as material of pipe, configuration, diameter, insulation etc have their own impact on the overall energy consumption of the system. Piping is one of those few systems when you oversize, you will generally save energy; unlike for a motor or a pump. Piping system design in large industrial complexes like Refineries, Petrochemicals, Fertilizer Plants etc are done now a day with the help of design software, which permits us to try out numerous possibilities. It is the relatively small and medium users who generally do not have access to design tools use various rules of thumbs for selecting size of pipes in industrial plants. These methods of piping design are based on either " worked before" or "educated estimates". Since everything we do is based on sound economic principles to reduce cost, some of the piping design thumb rules are also subject to modification to suit the present day cost of piping hardware cost and energy cost.

There are many reasons for insulating a pipeline, most important being the energy cost of not insulating the pipe. Adequate thermal insulation is essential for preventing both heat loss from hot surfaces of ovens/furnaces/piping and heat gain in refrigeration systems. Inadequate thickness of insulation or deterioration of existing insulation can have a significant impact on the energy consumption. The material of insulation is also important to achieve low thermal conductivity and also low thermal inertia. Development of superior insulating materials and their availability at reasonable prices have made retrofitting or re-insulation a very attractive energy saving options.

The insulated pipelines constituted by composed material can be consider as multilayered cylinder. Multilayered cylinder are important non-homogeneous materials designed to work in a high-temperature environment. A number of research works have been carried out for thermo-elastic problems of multilayered structures. Obata and Noda studied the one-dimensional steady thermal stresses in a functionally graded circular hollow cylinder and hollow sphere by use of a perturbation method. By introducing the theory of laminated composites, Ootao and Tanigawa treated the three-dimensional transient thermal stresses of functionally graded rectangular plates due to partial heat supply, and analyzed the piezo-thermo-elastic problem of a functionally graded rectangular plate bonded to a piezoelectric plate. Kim and Noda researched the two-dimensional unsteady thermo-elastic problems of functionally graded infinite hollow cylinders by using a Green's function approach. Jabbari et al. derived analytical solutions for one-dimensional steady-state thermo-elastic problems of functionally graded circular hollow cylinders in the case of material models expressed as power functions of r, and treated the two-dimensional thermo-elastic problems of the functionally graded cylinder by using the Fourier transform. Erashlan obtained analytical solutions for thermally induced axisymmetric and elastic–plastic deformations in non uniform heat-generating composite tubes. Liew et al. obtained analytical solutions of a functionally graded circular hollow cylinder by a novel limiting process that employs the solutions of homogeneous circular hollow cylinders. Shao and Wang derived analytical solutions of mechanical stresses of a functionally graded circular hollow cylinder with finite length. Ma and Wang investigated the nonlinear bending and postbuckling behaviour of a functionally graded circular plate subjected to thermal/mechanical loadings based on classical plate theory. In their studies, the material properties were considered as both temperature dependent and temperature independent.

Besides, most studies are conducted on thermal insulation systems in order to evaluate material performance under representative conditions of pressure, temperature and ageing media, as studied by Choqueuse et al. and Gimenez et al. Up to now, just few experimental recent studies deal with thermal performance evaluation on large-scale multilayered insulated pipelines submitted to severe conditions. Such upscale structure tests were performed by Haldane et al., in the Heriot–Watt and TNO Institute of Applied Physics work, who developed a direct measurement system to determine in-situ the thermal characteristics of insulated pipes submitted to hydrostatic pressures up to 145 bar, internally heated with circulating oil (up to 140 °C) and with external cooling at 8 °C. Finally, Bouchonneau et al. present the numerical and experimental characterizations of an industrial multilayered insulated pipeline tested in service conditions.
In this chapter, the industrial insulated pipeline is modelled as multilayered cylinder, subjected to mechanical and thermal loads. By using a multi-layered approach based on the theory of laminated composites, the solutions of temperature, displacements, and thermal/mechanical stresses in multilayered cylinder are presented. The material properties are assumed to be temperature-independent and radially dependent, but are assumed to be homogeneous in each layer. Steady-state thermo-elastic problem of multilayered cylinder subjected to axis-symmetric thermal and mechanical loads is considered. In order to obtain analytical solutions of temperature, displacements, and stresses for the two-dimensional thermo-elastic problem, the cylinder is assumed to be composed of n fictitious layers in the radial direction. The material properties of each layer are assumed to be homogeneous.
By applying the analytical thermo-elastic solution reported in Chapter XVII, a parametric analysis is conducted for study the mechanical behaviour of a industrial insulated pipeline composed by three phases: steel, insulate coating, and outer layer made of polyethylene to protect the insulation (see figure 23.1). Finally, it is presented numerical example by considering three types of materials for insulate coating: (1) Expanded Polyurethane; (2) Laminate glass; (3) Syntatic foam.
In this model, the insulate coating is not selected, but a parametric analyses is conducted varying the Young's modulus, Poisson's ratio, thermal conductivity and linear expansion coefficient. In this analyses the maximum equivalent stress of Hencky- von Mises is determined in steel phase and in insulate coating. Finally, is reported a numerical example in which the insulate coating is composed by polyurethane rigid foam.

23.2. Design of radius and thickness for insulated pipelines according to EN 253

Insulation materials are classified into organic and inorganic types. Organic insulations are based on hydrocarbon polymers, which can be expanded to obtain high void structures. Examples are thermocol (Expanded Polystyrene) and Poly Urethane Form(PUF). Inorganic insulation is based on Siliceous/Aluminous/Calcium materials in fibrous, granular or powder forms. Examples are Mineral wool, Calcium silicate etc. Properties of common insulating materials are reported below:

- Calcium Silicate: Used in industrial process plant piping where high service temperature and compressive strength are needed. Temperature ranges varies from 40 C to 950 C;
- Glass mineral wool: These are available in flexible forms, rigid slabs and preformed pipe work sections. Good for thermal and acoustic insulation for heating and chilling system pipelines. Temperature range of application is –10 to 500 C;
- Thermocol: These are mainly used as cold insulation for piping and cold storage construction;
- Expanded nitrile rubber: This is a flexible material that forms a closed cell integral vapour barrier. Originally developed for condensation control in refrigeration pipe work and chilled water lines; now-a-days also used for ducting insulation for air conditioning;
- Rock mineral wool: This is available in a range of forms from light weight rolled products to heavy rigid slabs including preformed pipe sections. In addition to good thermal insulation properties, it can also provide acoustic insulation and is fire retardant.

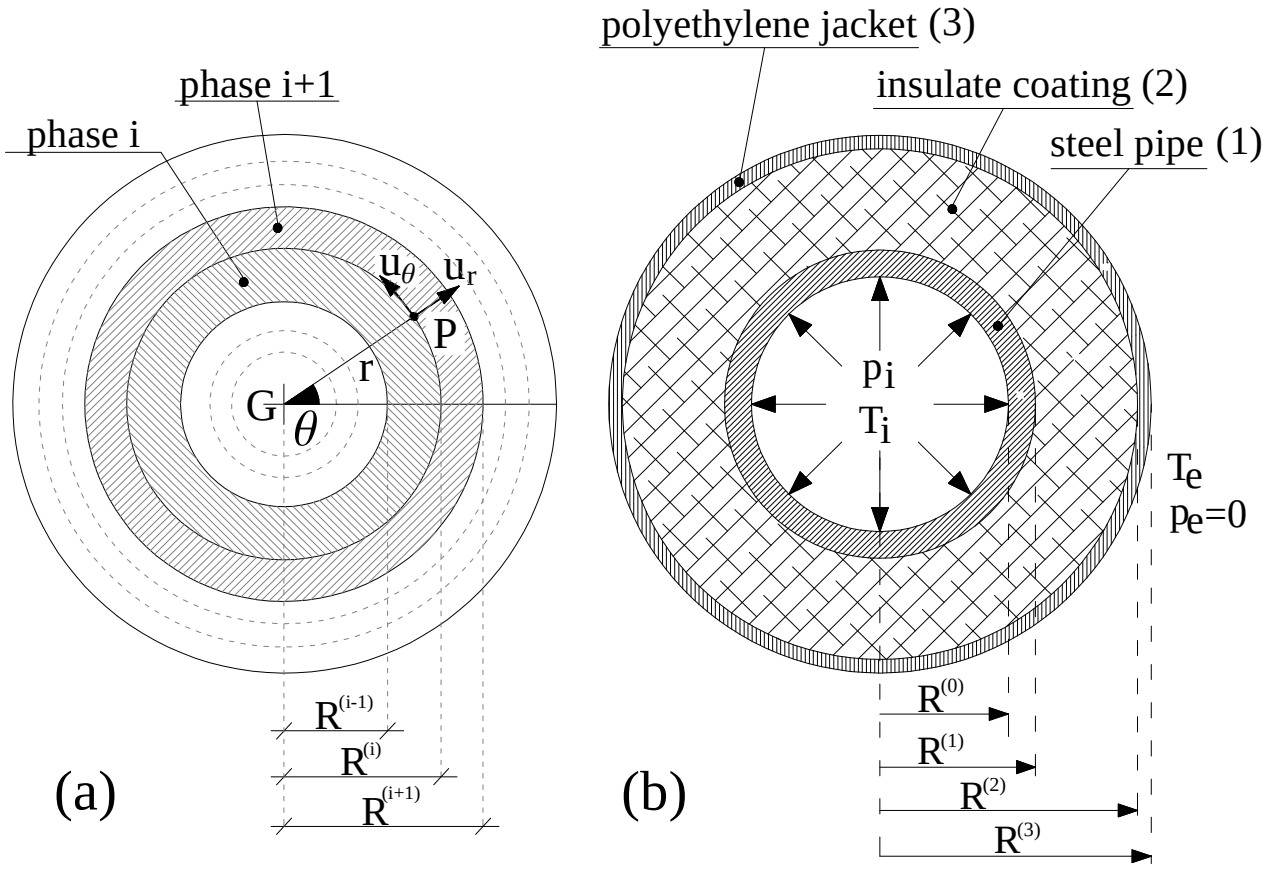

Fig. 23.1 – *a)* *Multilayered cylinder composed by n-hollow cylinders* ***; b)*** *Cross section of insulated pipeline composed by three phases*

The thermal conductivity of a material is the heat loss per unit area per unit insulation thickness per unit temperature difference. The thermal conductivity of materials increases with temperature. So thermal conductivity is always specified at the mean temperature (mean of hot and cold face temperatures) of the insulation material. Generally, the industrial insulate pipeline is composed by three phase: (1) steel pipe, (2) insulate coating, and (3) external casing. The minimum dimensions of thickness of the steel pipe and casing are prescribed in European Standards EN 253, as function of nominal outside diameter. In particular the diameter of steel pipe shall be in accordance with Table 2 of EN 253 which is derived from EN 10220. The nominal wall thicknesses of steel pipe shall be in accordance with EN 10220 with a minimum as indicated in Table 2 of EN 253. It is possible to determine an analytical curve that furnished the minimum values of thickness as function of inner radius of steel pipe. This curve fitting the values given by EN 253 as reported below (the parameters are valuated in m):

$$\delta^{(1)} = 7 \cdot 10^{-2} \sqrt{R^{(0)} / 10} \ \ [m] \tag{23.1}$$

where $\delta^{(1)}$ and $R^{(0)}$ are thickness and inner radius of phase (1) that correspond to steel pipe, respectively. Analogous it is possible to determine the analytical curve that furnished the minimum values of thickness as function of maximum radius of casing . This curve fitting the values given by EN 253 as reported below:

$$\delta^{(3)} = 5 \cdot 10^{-2} \sqrt{R^{(2)} / 10} \ \ [m] \tag{23.2}$$

where $\delta^{(3)}$ and $R^{(2)}$ are thickness and inner radius of phase (3) that correspond to casing, respectively. By applying the relationship (23.1) and (23.2), the expressions of radius of single phases are given by:

$$R^{(1)} = \sqrt{R^{(0)}}\left(\sqrt{R^{(0)}} + 7\cdot 10^{-5/2}\right), \quad R^{(2)} = R^{(1)} + \delta^{(2)},$$
$$R^{(3)} = R^{(2)} + 5\sqrt{7\cdot 10^{-11/2}\sqrt{R^{(0)}} + \left(R^{(0)} + \delta^{(2)}\right)\cdot 10^{-3}}, \tag{23.3}$$

By applying the expressions (23.3), the geometrical parameters of insulate pipeline depends only two parameters $R^{(0)}$ and $\delta^{(2)}$. The maximum radius of casing and minimum radius of pipe steel are 708.5mm and 8.65mm, respectively, as reported in EN 253. The inner radius $R^{(0)}$ of steel pipe and thickness of insulate coating $\delta^{(2)}$ can to vary in following ranges:.

$$R^{(0)} \in [8.65\cdot 10^{-3} m, 0.69m], \quad \delta^{(2)} \in [0, 0.7m], \tag{23.4}$$

If the inner radius $R^{(0)}$ is fixed , the thickness $\delta^{(2)}$ must be satisfy the follows inequality:

$$0 \le \delta^{(2)} \le 0.708 - \sqrt{R^{(0)}}\left(\sqrt{R^{(0)}} + 7\cdot 10^{-5/2}\right) \tag{23.5}$$

If the thickness $\delta^{(2)}$ is fixed , the inner radius $R^{(0)}$ must be satisfy the follows inequality:

$$8.65\cdot 10^{-3} m \le R^{(0)} \le 0.7 - \delta^{(2)} - 3.5\cdot 10^{-5}\left[-7 + \sqrt{49 + 4\cdot 10^{5}\left(R^{(0)} - \delta^{(2)}\right)}\right] \tag{23.6}$$

23.3. Parametric analysis of insulated pipeline composed by three phases

In this section a industrial insulated pipeline is modelled by multilayer cylinder composed by three hollow cylinders (Figure n.1). The materials that characterised the insulated pipeline are steel (phase 1) the insulated coating (phase 2), and polyethylene to protect the insulation (phase 3), respectively. In according to European Standards EN 253, the inner radius and thickness of pipeline and polyethylene jacket are fixed by applying the limitation reported in table 2 of European Standards EN 253. The mechanical and thermal property of steel and polyethylene jacket are reported in table n.1, but varying the properties of insulated coating. The inner radius of steel pipe and thickness of insulate coating are fixed: $R_0 = 0.20m$, $\delta^{(2)} = 0.20m$. Two load conditions are considered: (a) pipeline subjected to gradient of temperature between the internal and external surfaces $\Delta T = T_{\text{int}} - T_{ext}$; (b) pipeline subjected to only internal pressure. These load conditions are analysed separately. In particular, for first load condition (a), two sub-cases are considered in which are varying only two parameters and other are fixed : (i) variation of Poisson's ratio and Young's modulus, with fixed values of the thermal conductivity coefficients and linear thermal expansion coefficients; (ii) variation of Young's moduli and linear thermal expansion coefficient, with fixed values of the Poisson's ratio and thermal conductivity coefficients. In second load condition (b) is studied one case where the parameters vary are Poisson's ratio and Young's modulus.

The equivalent stress determines whether yielding occurs. For planar isotropy and non-homogeneity in radial direction, the equivalent stress based on the Henchy- von Mises criteria is given by follows equation:

$$\sigma_{eq}^{(i)} = 2^{-1/2}\left[\left(\sigma_{rr}^{(i)} - \sigma_{\theta\theta}^{(i)}\right)^2 + \left(\sigma_{rr}^{(i)} - \sigma_{zz}^{(i)}\right)^2 + \left(\sigma_{\theta\theta}^{(i)} - \sigma_{zz}^{(i)}\right)^2\right]^{1/2} \tag{23.7}$$

The following non-dimensional parameters for the maximum absolute value of non-dimensional equivalent stress are assumed:

$$\bar{\sigma}_{eq}^{(i)} = \frac{\sigma_{eq}^{(i)}}{\alpha^{(i)} E^{(i)}(T_i - T_e)}, \quad for \quad p_{\text{int}} = 0 \;\; and \;\; T_i > T_e = T_R, \tag{23.8}$$

$$\bar{\sigma}_{eq}^{(i)} = \sigma_{eq}^{(i)} \big/ p_{\text{int}}, \quad for \quad p_{\text{int}} \neq 0 \;\; and \;\; T_e = T_i = T_R, \tag{23.9}$$

In figures 23.2, 23.3, 23.4, 23.5, 23.6, 23.7, 23.8, 23.9, 23.10 are reported the maximum values of the non- dimensional equivalent stress calculated by formulas (23.8) and (23.9) in steel pipe, insulate coating and polyethylene jacket, respectively. Figures 23.2, 23.3, 23.4, 23.5, 23.6, 23.7 are related to load condition (a) characterized by gradient of temperature between inner surface of steel pipe and external surface of polyethylene jacket. Figures 23.2, 23.3, 23.4 are determined by varying

only Poisson's ratio and Young's modulus. These figures show that by increasing Young's modulus of insulate coating, the maximum values of the equivalent stress increase in steel pipe, but remaining practically constant in polyethylene jacket and insulate coating. Moreover, by increasing the Poisson's ratio of insulate coating, the maximum values of the equivalent stress increase in all three phases. If insulated coating is composed by auxetic material with negative Poisson's ratio, the maximum equivalent stress in steel pipe, insulted coating and polyethylene jacket reduces sensibility. Figures 23.5, 23.6, 23.7 are determined by varying only Young's modulus and linear thermal expansion coefficient. These figures show that by increasing Young's modulus of insulate coating, the maximum values of the equivalent stress increase in steel pipe, but remaining practically constant in polyethylene jacket and insulate coating. Moreover, by increasing linear thermal expansion coefficient of insulate coating, the maximum values of the equivalent stress increase in all three phases. Figures 23.8, 23.9, 23.10 are related to load condition (b) characterized by internal radial pressure in insulated pipeline. These figures are determined by varying only Poisson's ratio and Young's modulus. By increasing Young's modulus in insulate coating, the maximum equivalent stress decrease in steel pipe and polyethylene jacket, but increase in insulate coating. By decreasing the Poisson's ratio in insulate coating, maximum values of equivalent stress increase in polyethylene jacket and insulate coating, but decrease in steel pipe. For negative values of Poisson's ratio in insulate coating, the maximum equivalent stress reduce sensibility in steel pipe, but increase polyethylene jacket and insulate coating. The mechanical behaviour of insulated pipeline is different for two load conditions (a) and (b) considered.

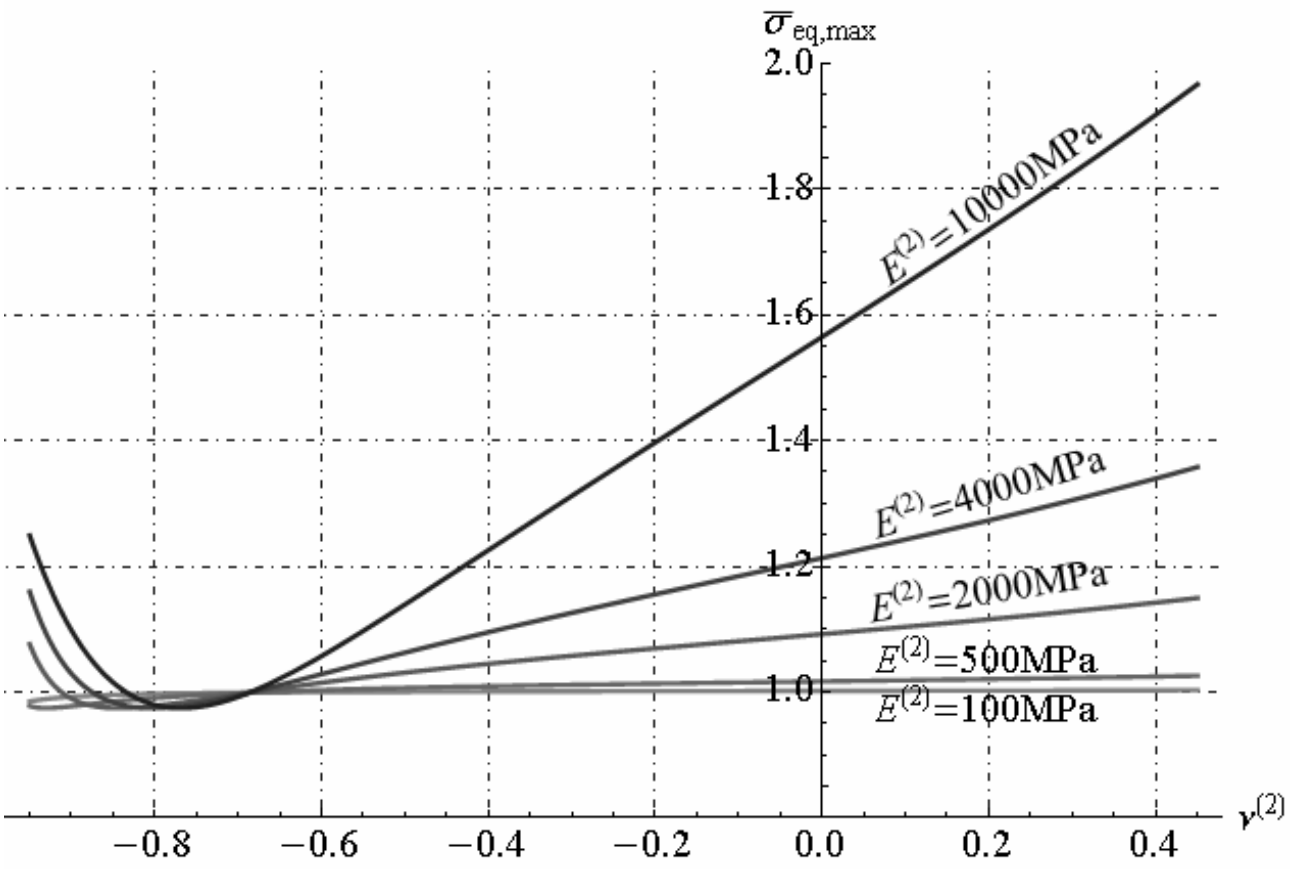

Fig. 23.2 - *Maximum value of non-dimensional equivalent stress in steel pipe (phase n.1). Insulate pipeline subjected to gradient temperature - Poisson's ratio and Young's modulus variation*

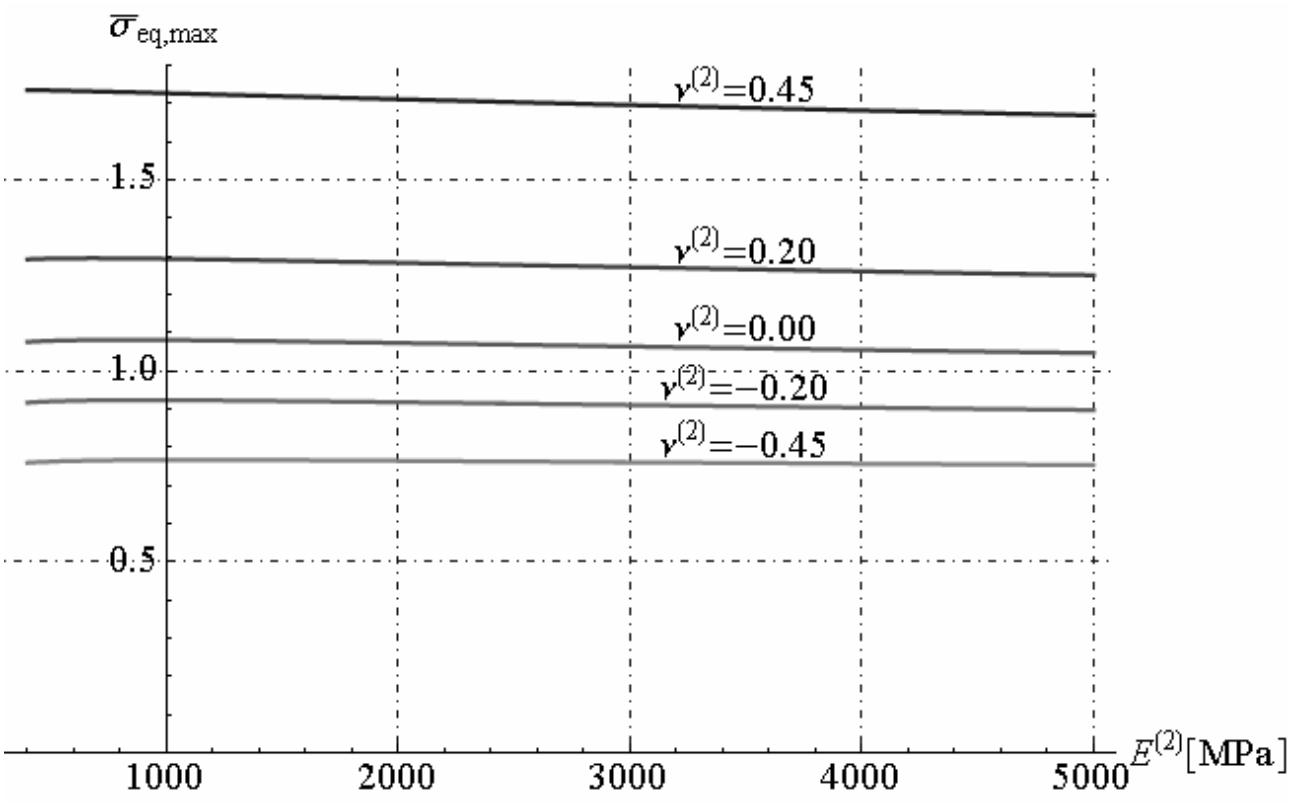

Fig. 23.3 - *Maximum value of non-dimensional equivalent stress in insulated coating (phase 2). Insulate pipeline subjected to gradient temperature - Poisson's ratio and Young's modulus variation*

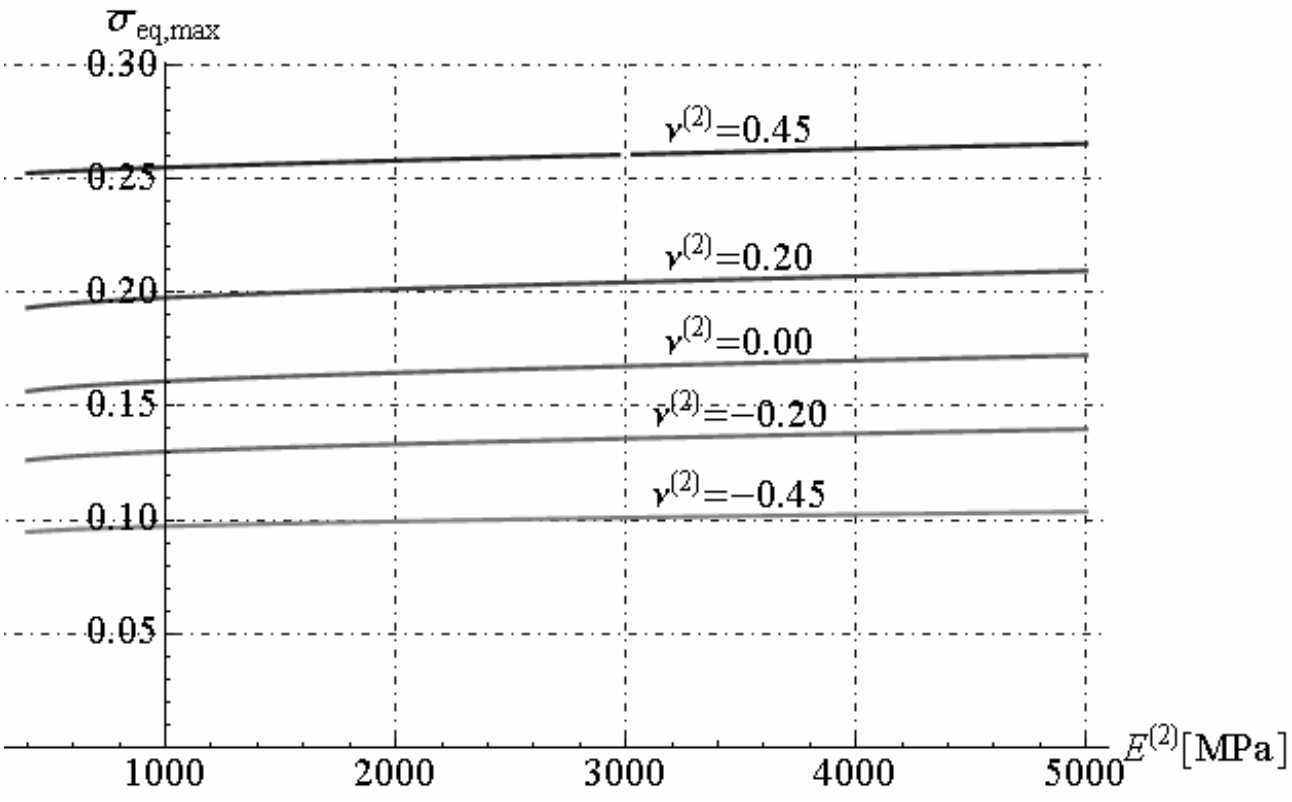

Fig. 23.4 - *Maximum value of non-dimensional equivalent stress in polyethylene jacket (phase 3). Insulate pipeline subjected to gradient temperature - Poisson's ratio and Young's modulus variation*

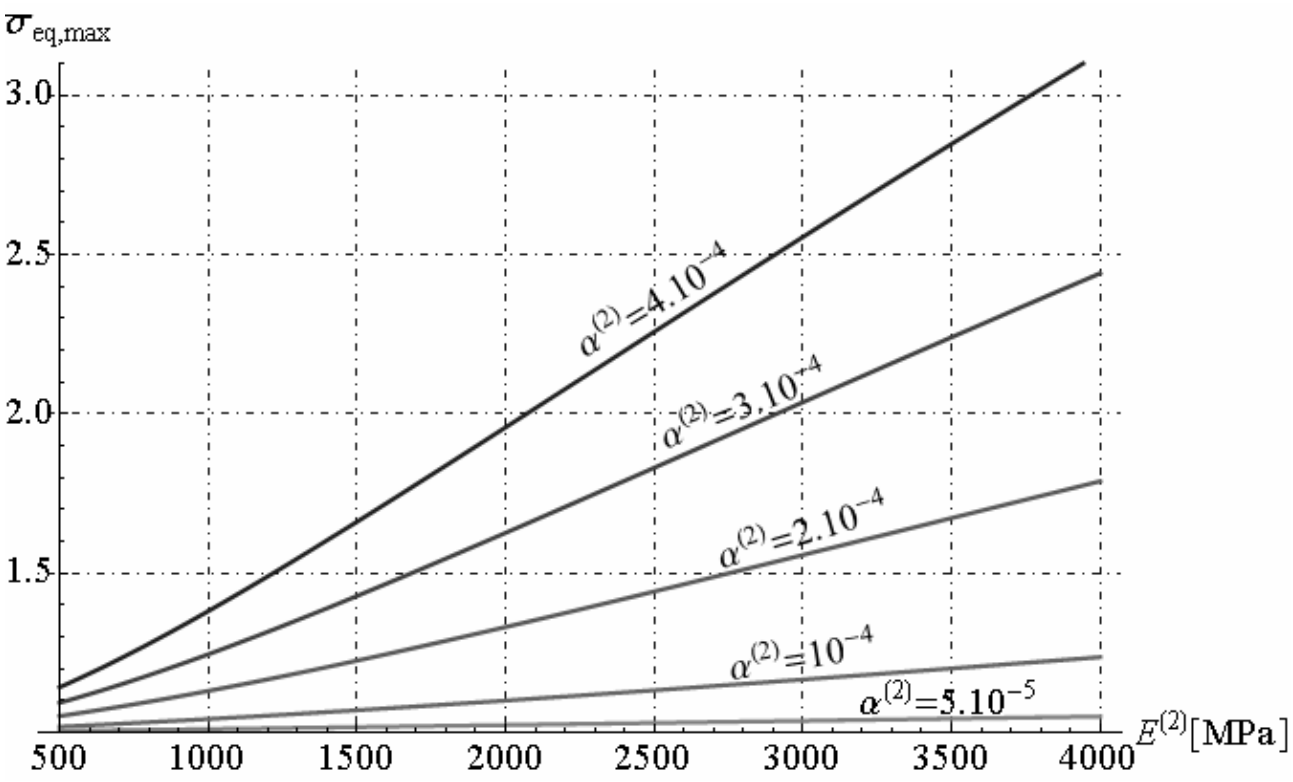

Fig. 23.5 - *Maximum value of non-dimensional equivalent stress in steel pipe (phase n.1). Insulate pipeline subjected to gradient temperature - Young's modulus and linear thermal expansion coefficient variation –*

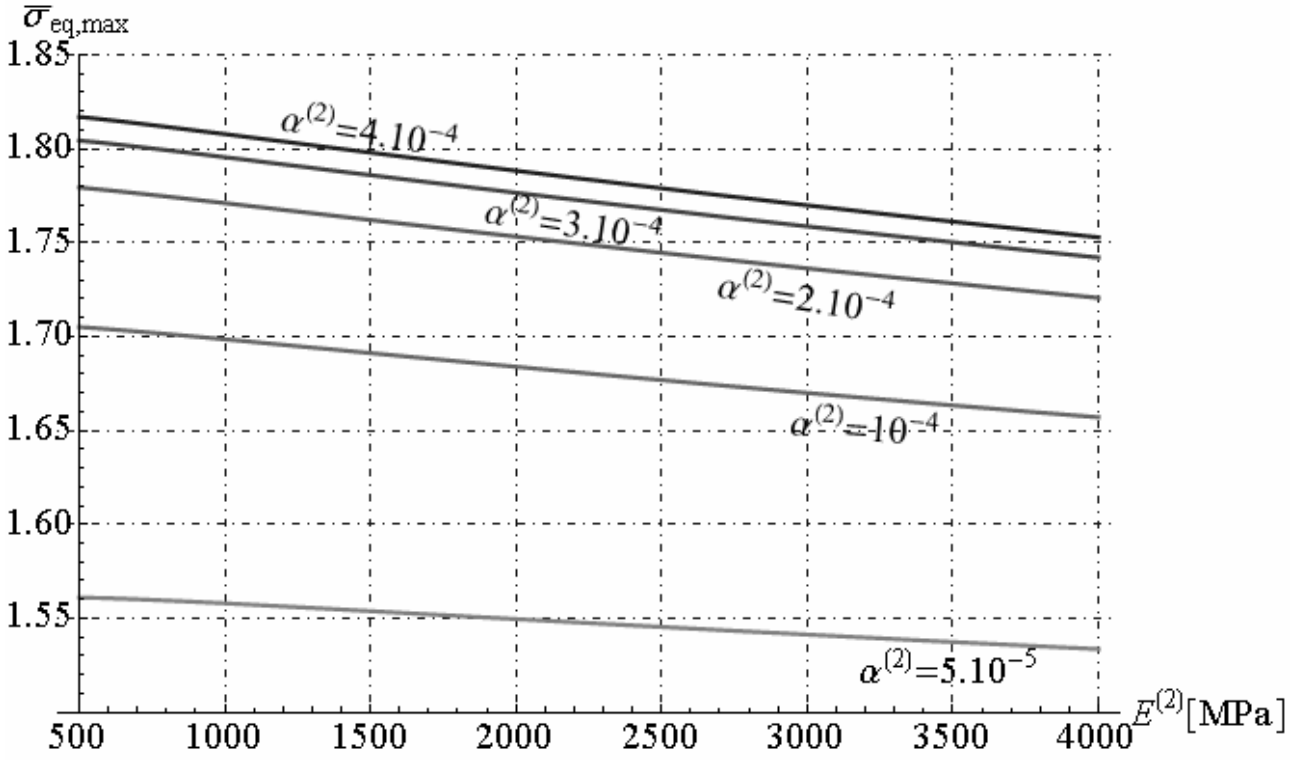

Fig. 23.6 - *Maximum value of non-dimensional equivalent stress in insulated coating (phase 2). Insulate pipeline subjected to gradient temperature - Young's modulus and linear thermal expansion coefficient variation –*

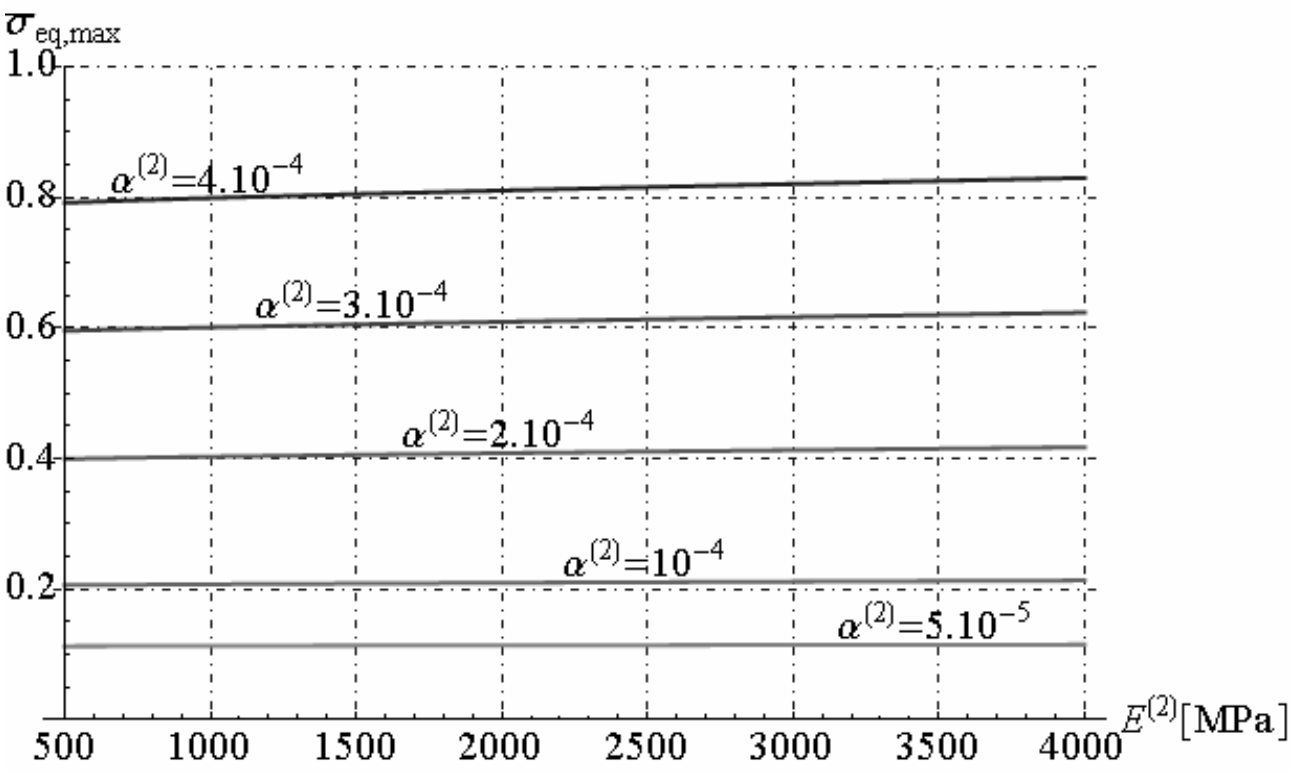

Fig. 23.7 - *Maximum value of non-dimensional equivalent stress in polyethylene jacket (phase 3). Insulate pipeline subjected to gradient temperature - Young's modulus and linear thermal expansion coefficient variation –*

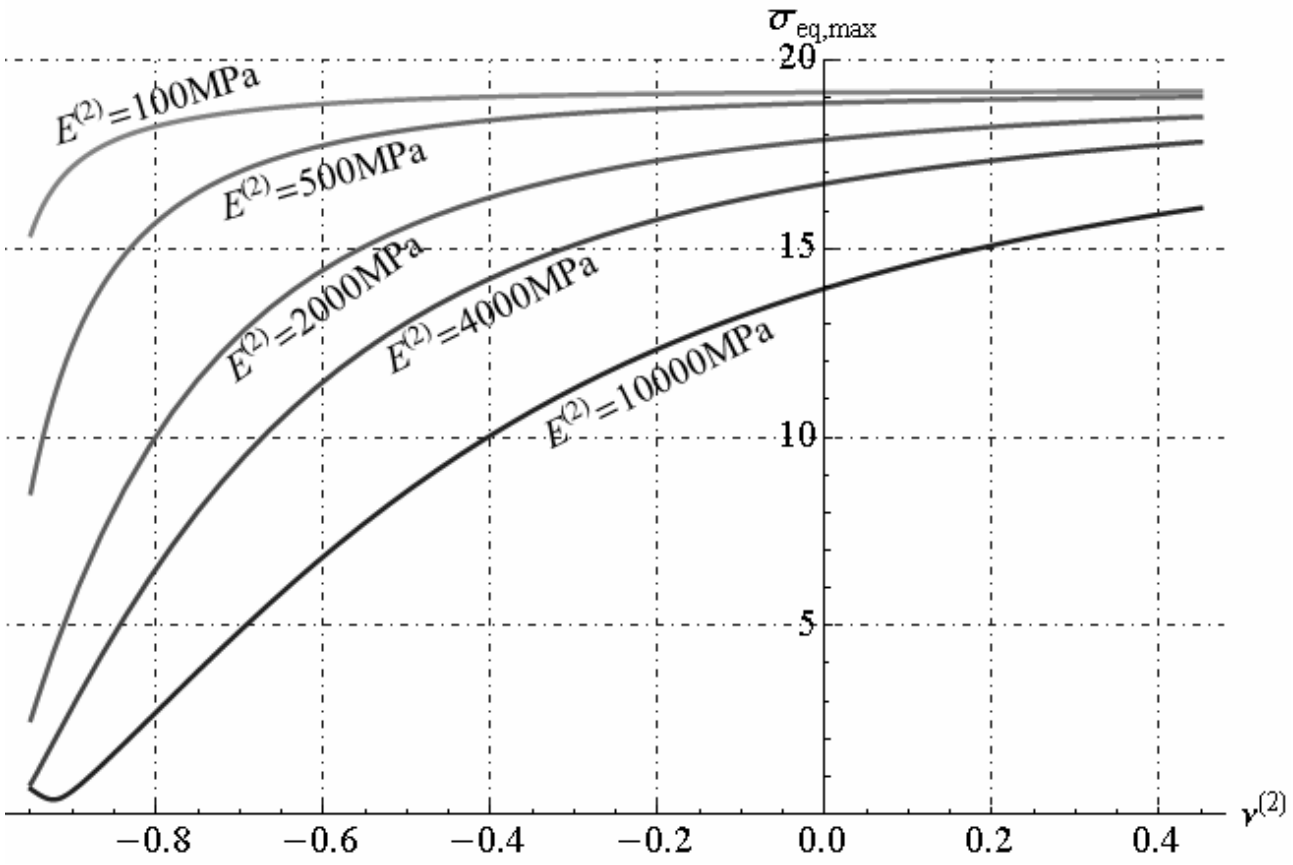

Fig. 23.8 *Maximum value of non-dimensional equivalent stress in steel pipe (phase n.1). Insulate pipeline subjected to internal radial pressure - Poisson's ratio and Young's modulus variation*

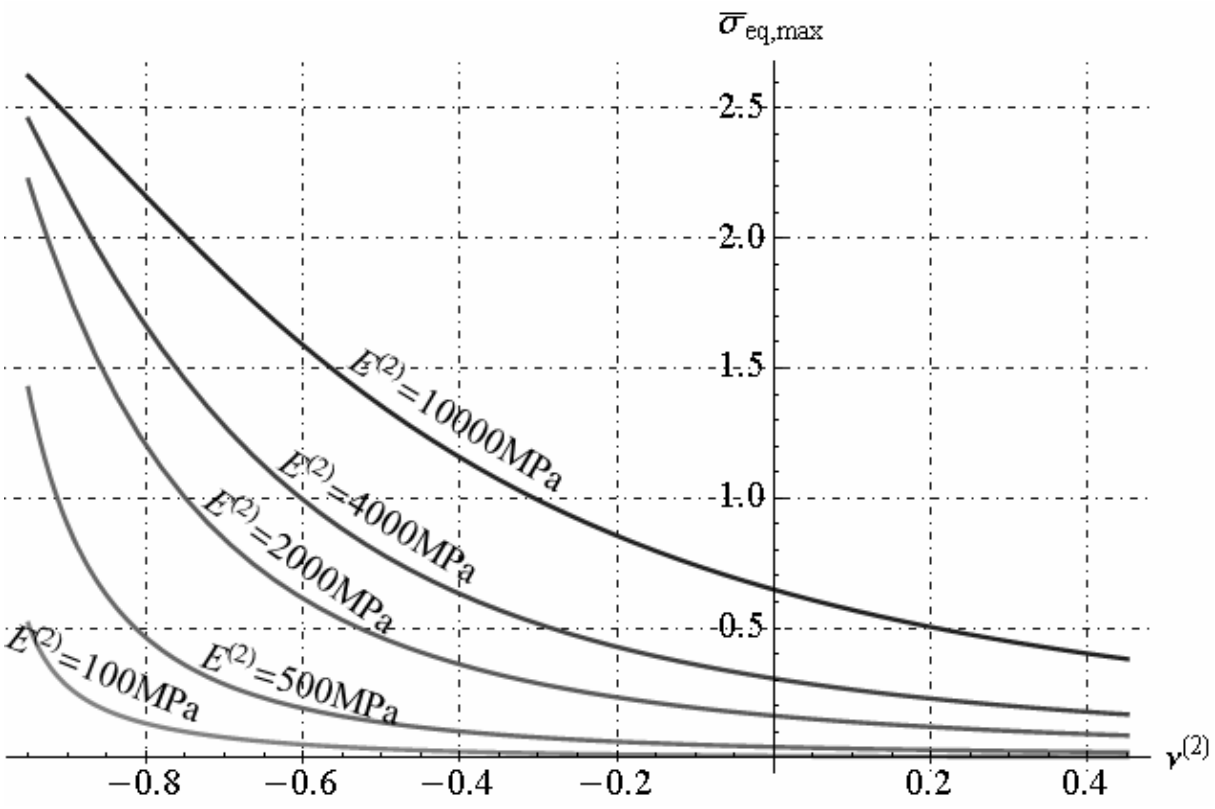

Fig. 23.9 *Maximum value of non-dimensional equivalent stress in insulated coating (phase 2). Insulate pipeline subjected to internal radial pressure - Poisson's ratio and Young's modulus variation -*

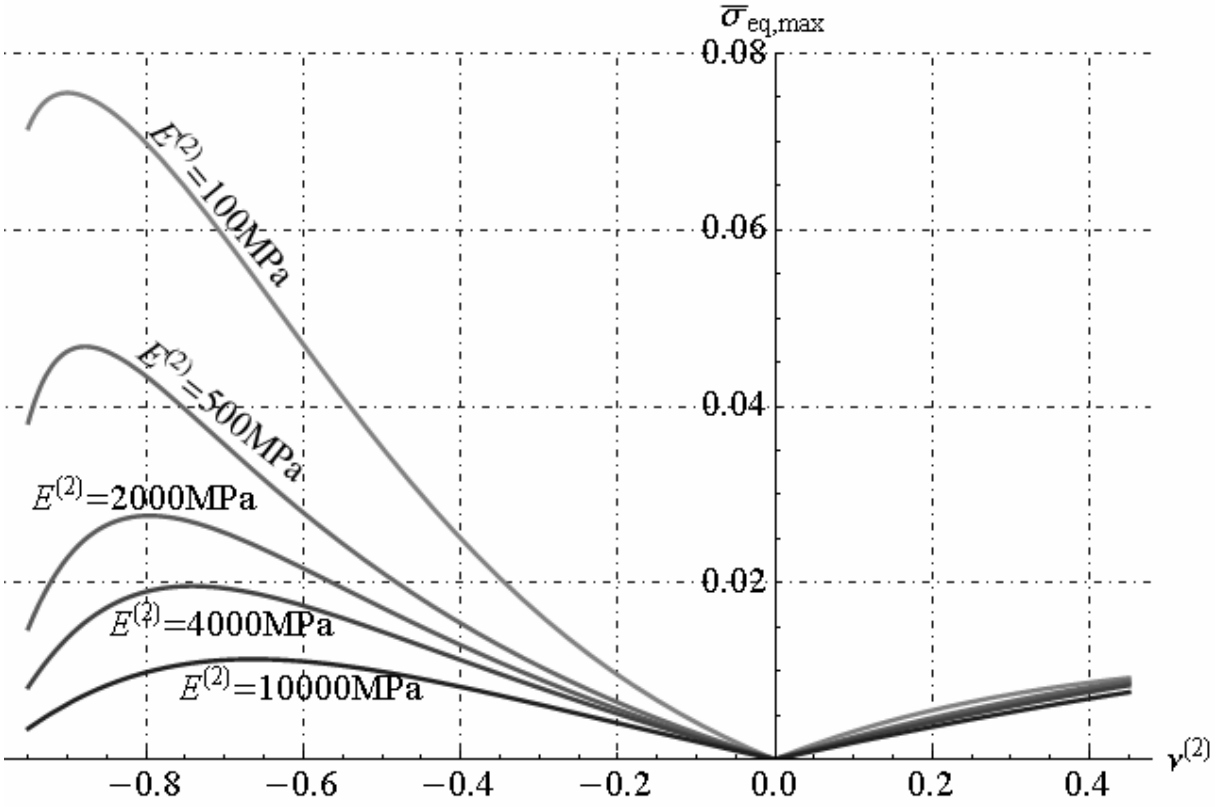

Fig. 23.10 *Maximum value of non-dimensional equivalent stress in polyethylene jacket. Insulate pipeline subjected to internal radial pressure - Poisson's ratio and Young's modulus variation –*

23.4. Numerical example for insulated pipeline structure

In this section is reported a numerical examples for insulated pipeline constituted by three phases: steel pipe, insulate coating and polyethylene jacket. Numerical example are development by fixing thermal and mechanical properties of insulate coating for different materials. The mechanical and thermal property of steel and polyethylene jacket are reported in table n.1. The non-dimensional equivalent stress, calculated by applying formulas (23.8) and (23.9), is evaluated for three types of materials that characterized the insulate coating: (1) Expanded Polyurethane; (2) Laminate glass; (3) Syntatic foam. The mechanical and thermal properties of these materials are reported in table n.2. In three cases studied the inner radius of steel pipe and thickness of insulate coating are fixed: $R_0 = 0.10m$, $\delta^{(2)} = 0.30m$. Figure 23.11 shows the equivalent stress versus the radius in steel pipe. If insulate coating is constituted by laminate glass - case (2) - the non-dimensional equivalent stress of Hencky von-Mises assume values more less respect to other cases (1) and (3) studied, because liner thermal expansion coefficient of laminate glass is more less of expanded polyurethane and syntatic foam. Figure 23.12 shows non-dimensional equivalent stress versus the radius in insulate coating. If insulate coating is constituted by expanded polyurethane – case (1) - the non-dimensional equivalent stress assume values more than respect to other cases (2) and (3) studied. Finally, figure 23.13 shows non-dimensional equivalent stress versus the radius in polyethylene jacket. If insulate coating is constituted by laminate glass - case (2) - the non-dimensional equivalent stress of Hencky von-Mises assume values more less respect to other cases (1) and (3). Then, if laminate glass is utilized as insulate coating, the equivalent stress in steel pipe and in polyethylene jacket are reduced respect to other two cases examined.

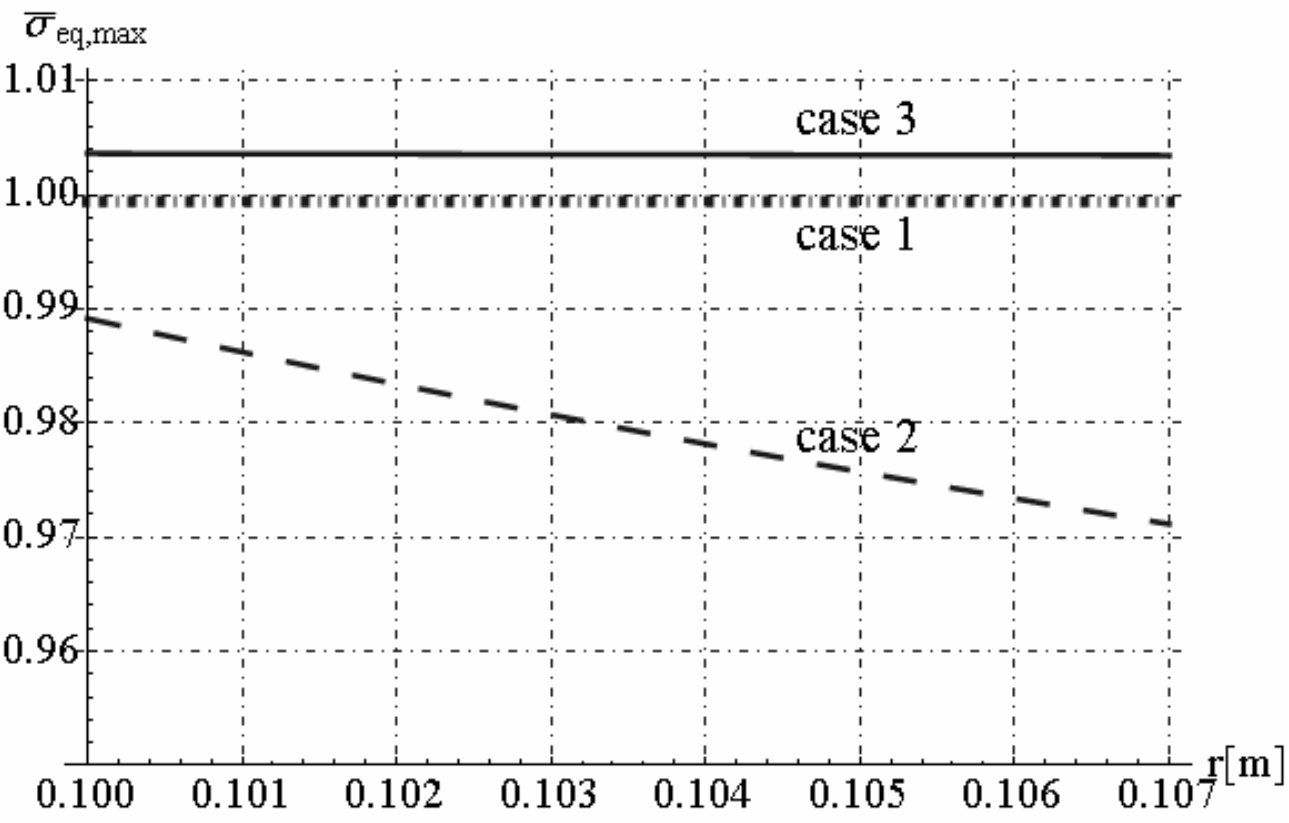

Fig. 23.11 - *Non-dimensional equivalent stress in steel pipe vs radius. Insulate pipeline subjected to gradient temperature - case (1): Expanded Polyurethane; case (2): Laminate glass; case (3): Syntatic foam;*

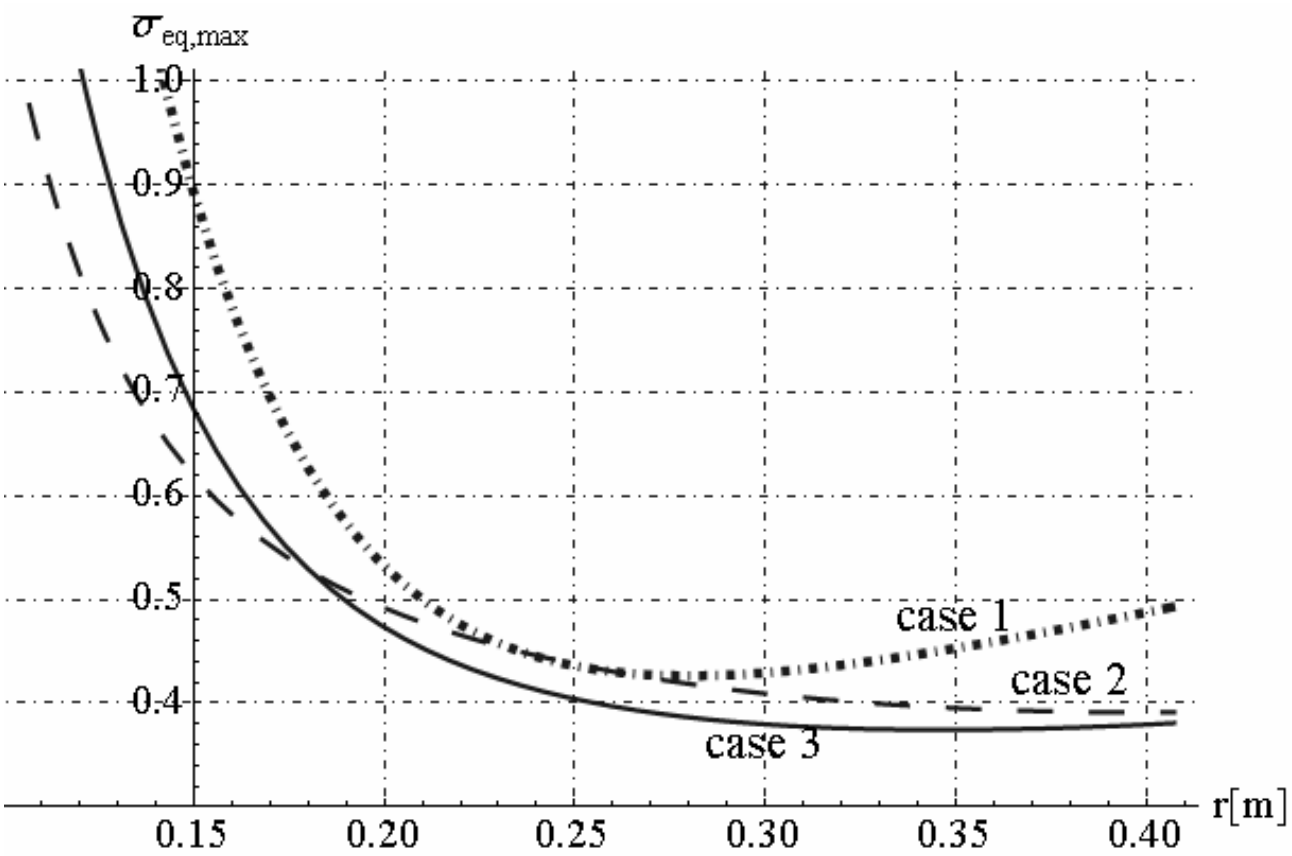

Fig. 23.12 - *Non-dimensional equivalent stress in insulate coating vs radius. Insulate pipeline subjected to gradient temperature - case (1): Expanded Polyurethane; case (2): Laminate glass; case (3): Syntatic foam;*

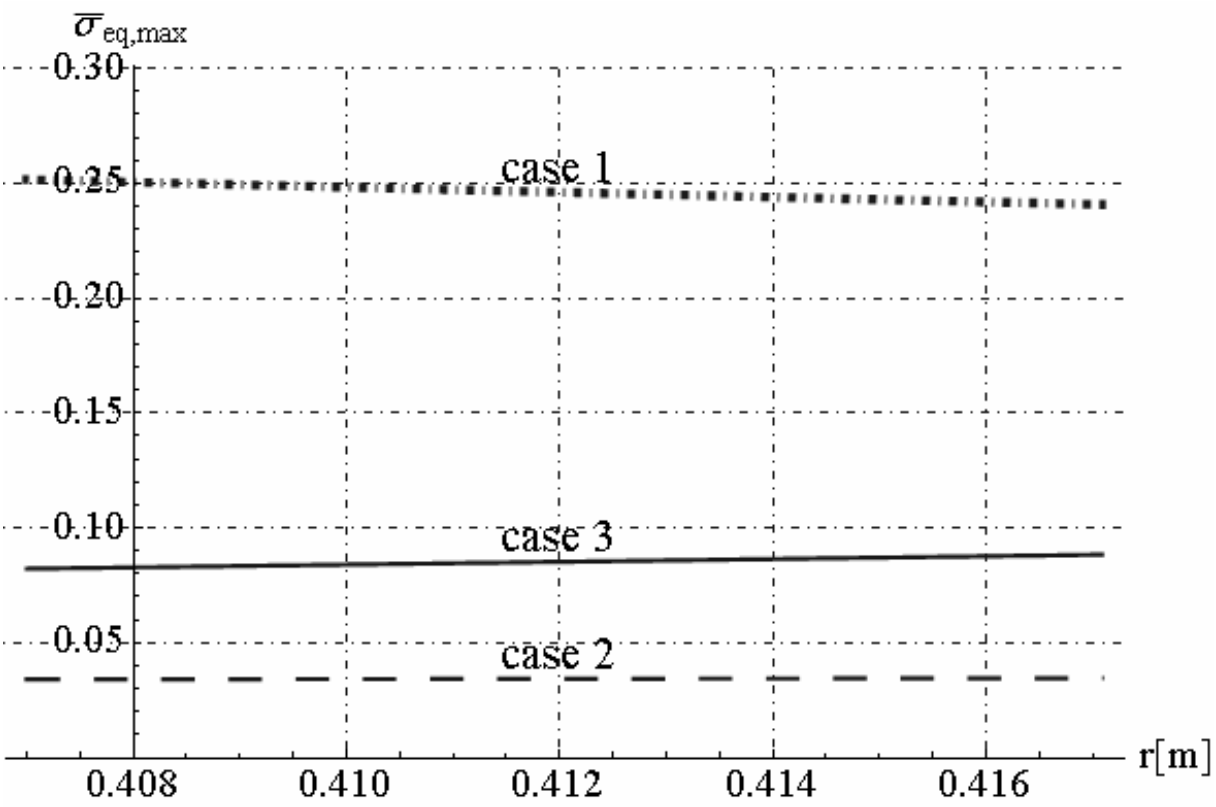

Fig. 23.13 - *Non-dimensional equivalent stress in polyethylene jacket vs radius. Insulate pipeline subjected to gradient temperature - case (1): Expanded Polyurethane; case (2): Laminate glass; case (3): Syntatic foam;*

	Steel pipe	Polyethylene jacket
$E\left[N\,m^{-2}\right]$	$210\cdot10^{9}$	$0.7\cdot10^{9}$
$k\left[W\,m^{-1}K^{-1}\right]$	45	0.40
ν	0.30	0.42
$\alpha\left[m\cdot m^{-1}K^{1}\right]$	$1.2\cdot10^{-5}$	$2.25\cdot10^{-4}$

Table 23.1 - *Mechanical and thermal parameters of steel and polyethylene*

	$E\left[N\,m^{-2}\right]$	ν	$k\left[W\,m^{-1}K^{-1}\right]$	$\alpha\left[m\cdot m^{-1}K^{1}\right]$
Expanded Polyurethane	$0.025\cdot10^{9}$	0.49	0.017	$1.25\cdot10^{-4}$
Laminate glass	$26\cdot10^{9}$	0.28	0.036	$1.9\cdot10^{-5}$
Syntatic foam	$1.10\cdot10^{9}$	0.32	0.165	$5.0\cdot10^{-5}$

Table 23.2 - *Mechanical and thermal parameters of following materials: (1) Expanded Polyurethane; (2) Laminate glass; (3) Syntatic foam;*

23.5. Conclusions

In this study, analytical and numerical results for a multilayered cylinders were obtained. The analytical thermo-elastic solution in closed form is employed to obtain the parametric analyses for insulated pipeline. In particular, the parametric analyses presented in this paper can be to utilized for to optimize the designer of the industrial insulate pipeline subjected to mechanical and thermal loads. By summarized the results obtained, it is possible reduce the maximum equivalent stress in insulate pipeline by utilizing the multilayer hollow cylinders constituted by insulated coating with selected mechanical and thermal property. When the insulate pipeline is subjected to only gradient temperature with insulated coating composed by auxetic material (negative Poisson's ratio), the maximum equivalent stress in steel pipe, insulated coating and polyethylene jacket reduces significantly. Moreover, maximum equivalent stress reduces in steel pipe, coating and jacket if linear thermal expansion coefficient of insulate coating assume values close to that of steel. In the case of insulate pipeline subjected to only radial pressure, insulated coating with negative Poisson's ratio reduces maximum equivalent stress only in steel phase, but increases the value in other two phases. The temperature, displacement and thermal stress distributions obtained in this model, can be applied to mechanical parts in precision measurement or design useful structural applications. Finally, the proposed method may be readily extended to solve a wide range of physical engineering problems.

23.6. References

[1] Alavi,F., Karimi, D., Bagri, A., (2008). *An investigation on thermo-elastic behaviour of functionally graded thick spherical vessels under combined thermal and mechanical loads*. Journal of Achievements in Materials and Manufacturing Engineering, vol. 31, Issue 2., pp. 422-428

[2] Ahmet, N. E.; Tolga, A. (2006): *Plane strain analytical solutions for a functionally graded elastic plastic pressurized tube*. Pressure vessels and piping, 83, pp. 635–644.

[3] Boley, B.A.,Weiner, J.H., *Theory of thermal stresses*, Dover publications, inc. Mineola, New York.

[4] Chakrabarty, J. (1998): *Theory of Plasticity*. McGraw Hill, New York.

[5] Chen, Y. Z,; Lin, X. Y. (2008): *Elastic analysis for thick cylinders and spherical pressure vessels made of functionally graded materials*. Computational Materials Science, 44, pp.581–587.

[6] Delfosse, D.; Cherradi, N.; Ilschner, B. (1997): *Numerical and experimental determination of residual stresses in graded materials*. Composites, part B, 28B, pp. 127-141.
[7] Fraldi, M., Nunziante, L., Carannante, F. (2007), *Axis-symmetrical Solutions for n-plies Functionally Graded Material Cylinders under Strain no-Decaying Conditions*, J. Mech. of Adv. Mat. and Struct. Vol. 14 (3), pp. 151-174 - DOI: 10.1080/15376490600719220
[8] M. Fraldi, L. Nunziante, F. Carannante, A. Prota, G. Manfredi, E. Cosenza (2008), *On the Prediction of the Collapse Load of Circular Concrete Columns Confined by FRP*, Journal Engineering structures, Vol. 30, Issue 11, November 2008, Pages 3247-3264 - DOI: 10.1016/j.engstruct.2008.04.036
[9] Fraldi, M., Nunziante, L., Chandrasekaran, S., Carannante, F., Pernice, MC. (2009), *Mechanics of distributed fibre optic sensors for strain measurements on rods*, Journal of Structural Engineering, 35, pp. 323-333, Dec. 2008- Gen. 2009
[10] M. Fraldi, F. Carannante, L. Nunziante (2012), *Analytical solutions for n-phase Functionally Graded Material Cylinders under de Saint Venant load conditions: Homogenization and effects of Poisson ratios on the overall stiffness*, Composites Part B: Engineering, Volume 45, Issue 1, February 2013, Pages 1310–1324
[11] Nunziante, L., Gambarotta, L., Tralli, A., *Scienza delle Costruzioni*, 3° Edizione, McGraw-Hill, 2011, ISBN: 9788838666971
[12] Ibrahim, H.; Tawfik, M.; Al-Ajmi, M. (2006): *Aero-thermo-mechanical characteristic of functionally graded material panels with temperature dependant material properties*. ICFDP 8, ASME conference, Sharm El-Sheikh, Egypt.
[13] Koizumi, M. (1997): *FGM activities in Japan. Composites*, part B, 28B, pp. 1-4.
[14] Lekhnitskii, S. G., (1981), *Theory of Elasticity of an Anisotropic Body*, Mir, Moscow.
[15] Liew, K. M.; Kitipornchai, S.; Zhang, X. Z.; Lim, C. W. (2003): *Analysis of the thermal stress behaviour of functionally graded hollow circular cylinders*. Solids and Structures, 40, pp. 2355–80.
[16] Lutz, M. P.; Zimmerman, R. W. (1996): *Thermal stresses and effective thermal expansion coefficient of a functionally graded sphere*. Thermal stress,19, pp. 39-54.
[17] Nayak, P.; Mondal, S. C. (2011): *Analysis of a functionally graded thick cylindrical vessel with radially varying properties*. Engineering science and technology, 3, pp.1551-1562.
[18] Nayak, P.; Mondal, S. C., Nandi, A.,(2011), *Stress, strain and displacement of a functionally graded thick spherical vessel*, International Journal of Engineering Science and Technology (IJEST), Vol. 3 No. 4
[19] Noda, N.; Hetnarski, R. B.; Tanigawa, Y. (2003), *Thermal Stresses*. Taylor and Francis, New York.
[20] Obata, Y.; Noda, N. (1994), *Steady thermal stress in a hollow circular cylinder and a hollow sphere of a functionally gradient materials*. Thermal stress, 17, pp. 471-487.
[21] Ozisik, M. N. (1985), *Heat Transfer*. McGraw Hill, New York.
[22] Peng, X. L.; Li, X. F. (2010), *Thermo-elastic analysis of a cylindrical vessel of functionally graded materials*. Pressure vessels and piping, 87, pp. 203-210.
[23] Shao, Z. S. (2005): *Mechanical and thermal stresses of a functionally graded hollow circular cylinder with finite length*. Pressure vessel and piping, 82, pp.155-163.
[24] Shao, Z. S.; Ma, G. W. (2008), *Thermo-mechanical stresses in functionally graded circular hollow cylinder with linearly increasing boundary temperature*. Composite Structures, 83, pp.259–265.
[25] Tutuncu N, Ozturk M. (2001), *Exact solutions for stresses in functionally graded pressure vessels*. Composites, part B, 32, pp. 683- 686.
[26] You, L. H.; Zhang, J. J.; You, X. Y. (2005): *Elastic analysis of internally pressurized thick-walled spherical pressure vessels of functionally graded materials*. Pressure vessel and piping, 82, pp.347-354.
[27] Zimmerman, R. W.; Lutz, M. P. (1999): *Thermal stresses and thermal expansion in a uniformly heated functionally graded cylinder.* Thermal stress, 22, pp. 177-188.

[28] Zong -Yi Lee (2004): *Coupled problem of thermo-elasticity for multilayered spheres with time-dependent boundary conditions*. Journal of Marine Science and Technology, Vol. 12, No. 2, pp. 93-101

[29] Bouchonneau, N., Sauvant-Moynot, V., Choqueuse, D., Grosjean, F., Poncet, E., Perreux, D., (2010) *Experimental testing and modelling of an industrial insulated pipeline for deep sea application*, Journal of Petroleum Science and Engineering, Vol. 73 pp. 1–12

[30] Berti, E., (2004). *Syntactic polypropylene coating solution provides thermal insulation for Bonga risers*, Offshore Magazine, 64, 2.

[31] Bouchonneau, N., Sauvant-Moynot, V., Grosjean, F., Choqueuse, D., Poncet, E., Perreux,D., (2007). *Thermal insulation material for subsea pipelines: benefits of instrumented full scale testing to predict the long term thermo-mechanical behaviour*. Proceedings of the Offshore Technology Conference — OTC 18679, Houston, Texas, USA.

[32] Choqueuse, D., Chomard, A., Bucherie, C., (2002). *Insulation materials for ultra deep seaflow assurance: evaluation of the material properties*. Proceedings of the Offshore Technology Conference — OTC 14115, Houston, Texas, USA.

[33] Choqueuse, D., Chomard, A., Chauchot, P., (2004). *How to provide relevant data for the prediction of long term behavior of insulation materials under hot/wet conditions*. Proceedings of the Offshore Technology Conference — OTC 16503, Houston, Texas, USA.

[34] Choqueuse, D., Chauchot, P., Sauvant-Moynot, V., Lefebvre, X., (2005). Recent progress min analysis and testing of insulation and buoyancy materials. Proceedings of the Fourth International Conference on Composite Materials for Offshore Operations — CMOO-4, Houston, Texas USA.

[35] Gimenez, N., Sauvant-Moynot, V., Sautereau, H., (2005), *Wet ageing of syntactic foams under high pressure/high temperature in deionized and artificial sea water*. Proceedings of the Twenty-Fourth International Conference on Offshore Mechanics and Artic Engineering, Halkidiki, Greece.

[36] Haldane, D., Scrimshaw, K.H., (2001), *Development of an alternative approach to the testing of thermal insulation materials for subsea applications*. Proceedings of the Fourteenth International Conference on Pipeline Protection, Barcelona, Spain, pp. 29–39.

[37] Haldane, D., Graff, F.V.D., Lankhorst, A.M., (1999), *A direct measurement system to obtain the thermal conductivity of pipeline insulation coating systems under simulated service conditions*. Proceedings of the Offshore Technology Conference — OTC 11040, Houston, Texas, USA, pp. 1–16.

CHAPTHER XXIV
ANALYTICAL PREDICTION OF THE ULTIMATE COMPRESSIVE STRENGHT IN CYLINDRICAL CONCRETE SPECIMENS CONFINED BY F.R.P.

24.1. Introduction

The present chapter establishes a constructive method for obtaining closed-form elastic and post-elastic solutions for multilayered cylinder, constituted by an isotropic central core and *n* arbitrary cylindrically orthotropic hollow phases. To this purpose, in Chapter IX. it is developed a mathematical procedure aimed to construct exact elastic solutions for multilayered cylinder, constituted by *n* cylindrical hollow phases and a central core, each of them modelled as linearly elastic, homogeneous and isotropic (Figure 24.1). Under the hypotheses of axis-symmetrical boundary conditions and perfectly bonded phases, analytical solutions for self-equilibrated axial forces applied at the extremities of the object are derived, in a completely general way, that is for arbitrary elastic moduli and number of phases. The approach is based on a specific choice of Love's bi-harmonic scalar functions $\chi^{(i)}(r, z)$, [13], where (*i*) stands for the generic *i*-th phase. As already proved by some of the Authors in a previous work [14] with reference to a more general case, the field differential equations involving partial derivatives reduce to a set of Euler-like ordinary one-dimensional uncoupled differential equations, that can be analytically solved by means of an *in cascade* technique. As a consequence, the continuity conditions for displacements and stresses at the interfaces become algebraic: the whole set of boundary conditions can be then written in a matrix form and solved straightforwardly [14].

In the Chapter XII. the above described strategy is generalized to multilayered cylinder constituted by cylindrically orthotropic hollow phases, by invoking the classical Complex Potential Theory for anisotropic materials [10] and using a suitable rearrangement of the equations suggested by Ting [12]. In this way, due to the permanency of the axis-symmetry of the problem, an strategy analogous to that constructed for isotropic multilayered cylinder is obtained and the Boundary Value Problem (BVP) is hence reduced again to an algebraic one, governed by a matrix whose order is depending upon the number of hollow phases and whose coefficients are explicitly related to the geometrical and mechanical parameters of the object. Afterwards, in the Chapter XII, this last procedure is specialized to an multilayered cylinder composed by two-phase, constituted by an isotropic core and a surrounding hollow cylindrically orthotropic phase, by explicitly furnishing the elastic solutions in terms of stress, strain and displacement fields for the case of axial forces applied at the ends of the solid. With the aim of studying cylindrical concrete specimens reinforced by means of Fibre Reinforced Polymeric sheets in compression, the elastic solutions found in the case analysed in Chapter XII are extended to the post-elastic range, by investigating the evolution of the stress field when the core phase is characterized by an Intrinsic Curve or Schleicher-like elastic-plastic response with associate flow rule and the cylindrically orthotropic hollow phase obeys to an elastic-brittle Tsai-Hill anisotropic yield criterion. The choice of these post-elastic behaviours is suggested by experimental evidences reported in literature for these materials, as well as the cylindrical orthotropy of the hollow phase intrinsically yields to consider several perfectly bonded FRP layers as an equivalent one, interpreting their overall mechanical response by invoking the theory of homogenization and the mechanics of composites [15]. At the end, a numerical example application to cylindrical concrete specimens reinforced with Carbon FRP is presented, by furnishing a predictive formula – derived from the previously obtained analytical solutions - for estimating the overall collapse mechanism, the concrete ultimate compressive strength and the confining pressure effect. The results are finally compared with several experimental literature data, highlighting the very good agreement between the theoretical predictions and the laboratory measurements.

24.2. Closed-form solutions for multilayered cylinder composed by isotropic phases

In this section is reported exact closed-form elastic solutions for isotropic multilayered cylinder under special axis-symmetrical boundary conditions, that is axial forces applied at the extremities of

the solid. In Chapter IX it is investigated about a class of axis-symmetrical solutions for multilayered cylinder, called there *non-decaying solutions*, characterised by the following form of the Love's function:

$$\chi^{(i)}(r,z)=\sum_{k=0}^{4} z^k f_k^{(i)}(r), \quad \forall i\in\{0,1,2,...,n\} \tag{24.1}$$

where $f_k^{(i)}(r)$ are unknowns to be determined. By conditioning (24.1) to satisfy field and boundary equations at the interfaces between adjacent phases, it is possible to prove (see Chapter XI) that the Love's function (24.1) represents the complete set of elastic solutions producing ε_{zz} not depending on the radial coordinate r: as a consequence, this set of solutions was called ε_{zz} *-non-decaying* , in the sense that - passing from a phase to another phase in the radial direction of multilayered cylinder - the axial strain results always uniform. In Chapter IX it is also shown that the loads able to generate this special situation are reducible to any possible combination of the following cases: self-equilibrated axial forces N_z applied at the ends of multilayered cylinder; anti-plane uniform shear tractions τ_0 prescribed on the cylindrical external surface of the solid; linearly varying with z pressures, $p(z)=p_0+p_1 z$, applied on the cylindrical boundary. In the subsequent section, it will be then developed the elastic solution associated to the same loads, in the framework of anisotropic materials, for multilayered cylinder composed by cylindrically orthotropic *hollow phases*. The *core* of these orthotropic cylinders will remain isotropic: this assumption explains the presentation of the isotropic elastic solutions before to extend the results to the orthotropic case and is motivated by a mechanical consistency requirement. For seek of brevity, remanding to the reader to the Chapter IX for the mathematical passages, the elastic solution for the isotropic core phase is only reported in explicit. In particular, it is possible to prove that – in the case of axial load applied at the object ends - by excluding the terms affected by r^{-1} and $\log r$ appearing for the generic *i*-th hollow phase, for the cylindrical core phase we find the displacement in the following general form:

$$\begin{cases} u_r^{(0)}=-\dfrac{r}{\mu^{(0)}}\left(C_{2/1}^{(0)}+2zC_{2/2}^{(0)}\right), \\ u_z^{(0)}=\varepsilon_0 z+\dfrac{\varepsilon_1 z^2}{2}+\left[\dfrac{4C_{2/2}^{(0)}(\mu^{(0)}+\lambda^{(0)})-\varepsilon_1\mu^{(0)}(2\mu^{(0)}+\lambda^{(0)})}{4\mu^{(0)2}}\right]r^2 \end{cases} \tag{24.2}$$

where the superscript "(0)" stands for the *core*-phase and $C_{n/k}^{(0)}$ are algebraic coefficients to determine by means of the equilibrium and compatibility conditions at the interfaces. By applying the strain-displacement and stress-strain relationship for isotropic material, we obtain the stresses in the core phase:

$$\begin{aligned} &\sigma_{rr}^{(0)}=\sigma_{\theta\theta}^{(0)}=\varepsilon_0\lambda^{(0)}-2\frac{\left(\mu^{(0)}+\lambda^{(0)}\right)}{\mu^{(0)}}\left(C_{2/1}^{(0)}+2C_{2/2}^{(0)}z\right),\ \ \tau_{\theta z}^{(0)}=\tau_{r\theta}^{(0)}=0, \\ &\sigma_{zz}^{(0)}=\varepsilon_0\left(2\mu^{(0)}+\lambda^{(0)}\right)-\frac{2\lambda^{(i)}}{\mu^{(i)}}\left(C_{2/1}^{(0)}+2C_{2/2}^{(0)}z\right),\ \ \tau_{rz}^{(0)}=r\left(\frac{2\lambda^{(0)}}{\mu^{(0)}}C_{2/2}^{(0)}\right). \end{aligned} \tag{24.3}$$

The results obtained above satisfy the equilibrium and compatibility in terms of field equations, that is inside each generic *i*-th phase of multilayered cylinder. Under the assumption of elastic response and perfect bond at the cylindrical interfacial boundaries (no de-lamination or friction phenomena), we have now to establish the equilibrium and the compatibility at the interfaces between two generic adjacent phases, as well as the equilibrium with the prescribed loads on the external boundary. In particular, due to the axis-symmetry of the problem, these conditions reduce to equating radial and axial displacement components at each interface, as well as the radial and anti-plane shear stresses. These last stress components have to be also vanishing on the external cylindrical surface of the object, while the stress $\sigma_{zz}^{(i)}$ emerging at the multilayered cylinder

extremities must be equal to the overall force N_z. As analytically shown in the subsequent section, the whole set of boundary conditions generates a linear algebraic problem.

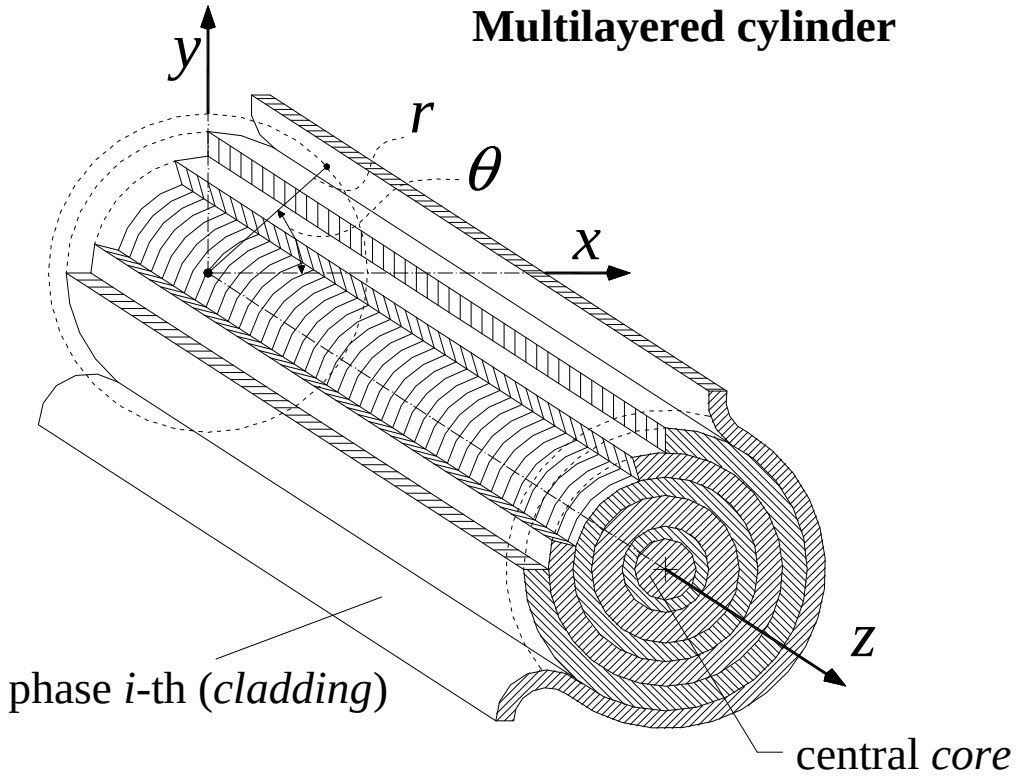

Figure 24.1 - *Sketch of multilayered cylinder*

24.3. Elastic solutions for multilayered cylinder composed by cylindrically orthotropic phases

Let us consider an multilayered cylinder composed by an isotropic core and *n orthotropic* surrounding cylindrical hollow phases, also called *jackets* in what follows: $\{r,\theta,z\}$ are the principal directions of the material cylindrical orthotropy and the load is the same of the previous isotropic case. It is worth to highlight that the axis-symmetry of the problem is therefore still present, but the core is the sole phase for which we can recall the obtained solutions in terms of displacements and stresses, being the Love's function not representative of a possible solution for cylindrically orthotropic BVPs. In the case that the material of hollow phases possesses cylindrically orthotropy, then the linearly elastic constitutive relation of the ith phase, in the Voigt notation, is:

$$\sigma_k = C_{kj}^{(i)} \varepsilon_j \tag{24.4}$$

where stress and strain vectors and the Elasticity matrix are respectively:

$$\left[\sigma_k\right] = \begin{bmatrix} \sigma_{rr} \\ \sigma_{\theta\theta} \\ \sigma_{zz} \\ \tau_{\theta z} \\ \tau_{rz} \\ \tau_{r\theta} \end{bmatrix}, \quad \left[\varepsilon_j\right] = \begin{bmatrix} \varepsilon_{rr} \\ \varepsilon_{\theta\theta} \\ \varepsilon_{zz} \\ \gamma_{\vartheta z} \\ \gamma_{rz} \\ \gamma_{r\theta} \end{bmatrix}, \quad \mathbb{C}^{(i)} = \begin{bmatrix} c_{11}^{(i)} & c_{12}^{(i)} & c_{13}^{(i)} & 0 & 0 & 0 \\ c_{12}^{(i)} & c_{22}^{(i)} & c_{23}^{(i)} & 0 & 0 & 0 \\ c_{13}^{(i)} & c_{23}^{(i)} & c_{33}^{(i)} & 0 & 0 & 0 \\ 0 & 0 & 0 & c_{44}^{(i)} & 0 & 0 \\ 0 & 0 & 0 & 0 & c_{55}^{(i)} & 0 \\ 0 & 0 & 0 & 0 & 0 & c_{66}^{(i)} \end{bmatrix} \tag{24.5}$$

By applying the procedure illustrated in Chapter XII for multilayered cylinder composed by cylindrically orthotropic phases, we obtain for i-th generic hollow phase that circumferential displacement component vanishes ($u_\theta^{(i)} = 0$), but other displacement components are given by:

$$\begin{cases} u_r^{(i)} = \dfrac{\varepsilon_0^{(i)}(c_{23}^{(i)} - c_{13}^{(i)})}{(c_{11}^{(i)} - c_{22}^{(i)})} r + C_1^{(i)} \cosh\left(\sqrt{\dfrac{c_{22}^{(i)}}{c_{11}^{(i)}}} \log r \right) + i\, C_2^{(i)} \sinh\left(\sqrt{\dfrac{c_{22}^{(i)}}{c_{11}^{(i)}}} \log r \right) \\ u_z^{(i)} = \varepsilon_0^{(i)} z \end{cases} \tag{24.6}$$

By using the compatibility equations, the displacement (24.6) furnishes the strains:

$$\begin{aligned} \varepsilon_{rr}^{(i)} &= \frac{\varepsilon_0^{(i)}\left(c_{23}^{(i)} - c_{13}^{(i)}\right)}{\left(c_{11}^{(i)} - c_{22}^{(i)}\right)} + \frac{C_1^{(i)}}{r}\sqrt{\frac{c_{22}^{(i)}}{c_{11}^{(i)}}} \sinh\left(\sqrt{\frac{c_{22}^{(i)}}{c_{11}^{(i)}}} \log r \right) + i \frac{C_2^{(i)}}{r}\sqrt{\frac{c_{22}^{(i)}}{c_{11}^{(i)}}} \cosh\left(\sqrt{\frac{c_{22}^{(i)}}{c_{11}^{(i)}}} \log r \right), \\ \varepsilon_{\theta\theta}^{(i)} &= \frac{\varepsilon_0^{(i)}\left(c_{23}^{(i)} - c_{13}^{(i)}\right)}{\left(c_{11}^{(i)} - c_{22}^{(i)}\right)} + \frac{C_1^{(i)}}{r} \cosh\left(\sqrt{\frac{c_{22}^{(i)}}{c_{11}^{(i)}}} \log r \right) + i \frac{C_2^{(i)}}{r} \sinh\left(\sqrt{\frac{c_{22}^{(i)}}{c_{11}^{(i)}}} \log r \right), \\ \varepsilon_{zz}^{(i)} &= \varepsilon_0^{(i)}, \quad \gamma_{r\theta}^{(i)} = \gamma_{rz}^{(i)} = \gamma_{\theta z}^{(i)} = 0, \end{aligned} \tag{24.7}$$

Moreover, from the constitutive law (24.5), the non-zero stress components assume the following form:

$$\begin{aligned} \sigma_{rr}^{(i)} &= \frac{\varepsilon_0^{(i)}\left[c_{23}^{(i)}\left(c_{11}^{(i)} + c_{22}^{(i)}\right) - c_{13}^{(i)}\left(c_{22}^{(i)} + c_{12}^{(i)}\right)\right]}{c_{11}^{(i)} - c_{22}^{(i)}} + \left(\frac{C_1^{(i)} c_{12}^{(i)} + i\, C_2^{(i)} \sqrt{c_{11}^{(i)} c_{22}^{(i)}}}{r} \right) \cosh\left(\sqrt{\frac{c_{22}^{(i)}}{c_{11}^{(i)}}} \log r \right) + \\ &\left(\frac{C_1^{(i)} \sqrt{c_{11}^{(i)} c_{22}^{(i)}} + i\, C_2^{(i)} c_{12}^{(i)}}{r} \right) \sinh\left(\sqrt{\frac{c_{22}^{(i)}}{c_{11}^{(i)}}} \log r \right) \end{aligned} \tag{24.8}$$

$$\begin{aligned} \sigma_{\theta\theta}^{(i)} &= \frac{\varepsilon_0^{(i)}\left[c_{23}^{(i)}\left(c_{11}^{(i)} + c_{12}^{(i)}\right) - c_{13}^{(i)}\left(c_{22}^{(i)} + c_{12}^{(i)}\right)\right]}{c_{11}^{(i)} - c_{22}^{(i)}} + \left(\frac{C_1^{(i)} c_{12}^{(i)} + i\, C_2^{(i)} \sqrt{c_{11}^{(i)} c_{22}^{(i)}}}{r} \right) \sqrt{\frac{c_{22}^{(i)}}{c_{11}^{(i)}}} \sinh\left(\sqrt{\frac{c_{22}^{(i)}}{c_{11}^{(i)}}} \log r \right) + \\ &\left(\frac{C_1^{(i)} \sqrt{c_{11}^{(i)} c_{22}^{(i)}} + i\, C_2^{(i)} c_{12}^{(i)}}{r} \right) \sqrt{\frac{c_{22}^{(i)}}{c_{11}^{(i)}}} \cosh\left(\sqrt{\frac{c_{22}^{(i)}}{c_{11}^{(i)}}} \log r \right), \end{aligned} \tag{24.9}$$

$$\begin{aligned} \sigma_{zz}^{(i)} &= \frac{\varepsilon_0^{(i)}\left[c_{23}^{(i)2} - c_{13}^{(i)2} + c_{33}^{(i)}\left(c_{11}^{(i)} - c_{22}^{(i)}\right)\right]}{c_{11}^{(i)} - c_{22}^{(i)}} + \frac{1}{r}\left(C_1^{(i)} c_{23}^{(i)} + i\, C_2^{(i)} c_{13}^{(i)} \sqrt{\frac{c_{22}^{(i)}}{c_{11}^{(i)}}} \right) \cosh\left(\sqrt{\frac{c_{22}^{(i)}}{c_{11}^{(i)}}} \log r \right) + \\ &\left(C_1^{(i)} c_{13}^{(i)} \sqrt{\frac{c_{22}^{(i)}}{c_{11}^{(i)}}} + i\, C_2^{(i)} c_{23}^{(i)} \right) \sinh\left(\sqrt{\frac{c_{22}^{(i)}}{c_{11}^{(i)}}} \log r \right), \end{aligned} \tag{24.10}$$

It is worth to note that the found solution results able to also represent, as particular cases, the situations where isotropy or different types of transverse isotropy occur, as showed in Chapter XII.

24.4. Boundary conditions at the interfaces and on the external surface

By making reference to an multilayered cylinder made of a central isotropic *core* and to $n \in \mathbb{N}$ arbitrary surrounding hollow cylindrically orthotropic phases, subjected to axial load N_z, the displacement field for the core is obtained by equation (24.2):

$$u_r^{(0)} = \varepsilon_r^{(0)} r, \quad u_\theta^{(0)} = 0, \quad u_z^{(0)} = \varepsilon_0^{(0)} z \tag{24.11}$$

where $\varepsilon_r^{(0)} = C_{2/1}^{(0)} / \mu^{(0)}$, $\varepsilon_0^{(0)} = \varepsilon_0$, $C_{2/2}^{(0)} = \varepsilon_1 = 0$. By applying the equations (24.3), we obtain non-zero stress components for core phase:

$$\sigma_{rr}^{(0)} = \sigma_{\theta\theta}^{(0)} = \varepsilon_0^{(0)} \lambda^{(0)} + 2\varepsilon_r^{(0)}\left(\mu^{(0)} + \lambda^{(0)}\right), \quad \sigma_{zz}^{(0)} = \varepsilon_0^{(0)}\left(2\mu^{(0)} + \lambda^{(0)}\right) + 2\lambda^{(i)}\varepsilon_r^{(0)}, \tag{24.12}$$

The displacement components for the *i*-th generic phase are given by equations (24.6). The displacements and the stress above obtained satisfy the field equations in each phase of the object. Then, it remains to consider the boundary conditions at the interfaces, where perfect bond is assumed, and the equilibrium on the lateral cylindrical surface (zero tractions) and at the ends, where axial forces are applied.

The unknown algebraic parameters to determine are below summarized:

$$\varepsilon_r^{(0)}, \varepsilon_0^{(0)}, \varepsilon_0^{(i)}, C_1^{(i)}, C_2^{(i)}. \tag{24.13}$$

In particular, the first two coefficients in (24.13) represent the unknowns related to the *core*, while the other ones, whose number is $3\times n$, represent the unknown parameters corresponding to the hollow phases. Hence, the total number of unknowns is $(2+3\times n)$, which equals the number of algebraic equations to solve, as described in Chapter XII. Indeed, as we will show in the following, the boundary equations at the interfaces are three, while the boundary conditions on the external cylindrical surface and on the end basis are two. With references to Chapter XII the algebraic system to solve is characterized by boundary conditions at the interfaces and on the external surface, as reported below:

$$\begin{cases} u_z^{(i)}(r=R^{(i)}) = u_z^{(i+1)}(r=R^{(i)}) \\ u_r^{(i)}(r=R^{(i)}) = u_r^{(i+1)}(r=R^{(i)}) \qquad \forall i \in \{0,1,2,...,n-1\} \\ \sigma_{rr}^{(i)}(r=R^{(i)}) = \sigma_{rr}^{(i+1)}(r=R^{(i)}) \end{cases} \tag{24.14}$$

$$\sigma_{rr}^{(n)}(r=R^{(n)}) = 0, \qquad \sum_{i=0}^{n} \int_0^{2\pi} \int_0^{R^{(i)}} \sigma_{zz}^{(i)} r dr d\theta = N_z$$

where $R^{(i)}$ is the outer radius of the generic *i*-th phase and $\mp N_z$ are the axial forces applied on the bases $z=0, z=L$, respectively. The explicit expressions of equations (24.14) is reported in Chapter XII.

24.5. Closed-form elastic solutions for multilayered cylinder composed by two cylindrically orthotropic phases

Let us now consider an multilayered cylinder constituted by an isotropic central core, Figure 24.2, and a sole cylindrically orthotropic surrounding phase or jacket, under axis-symmetrical boundary conditions characterized by axial forces acting at the extremities of the object. As a matter of fact this one is a particular case of great utility for many applications, as will be shown later.

In this case, the displacements for the two phase are represented by the equations (24.11) and (24.6) respectively, while (24.12) furnishes the stress within the core and (24.8),(24.9),(24.10) give the stresses inside the hollow phase. In the following, we will denote with the apices “0” and “1” the quantities related to the core and to the jacket phase, respectively.

In order to obtain the analytical solution of the problem in explicit form, we should solve the algebraic system corresponding to the boundary conditions (24.14), for determining the five unknown coefficients $\{\varepsilon_0^{(0)}, \varepsilon_0^{(1)}, \varepsilon_r^{(0)}, C_1^{(1)}, C_2^{(1)}\}$. The solution of algebraic system (24.14) particularized for multilayered cylinder composed by isotropic central core and cylindrically orthotropic jacket phase is reported in paragraph 12.3 (Chapter XII).

24.6. Closed-form non-linear solutions for multilayered cylinder composed by two cylindrically orthotropic phases

The interest in the elastic and post-elastic analysis of multilayered cylinder covers many engineering fields. The pipelines for transport of liquids are layered shells in the form of hollow cylinders, where the local buckling, large displacements and elastic-plastic phenomena are the main responsible of the failure mechanism occurring in the sub-marine applications. In biological tissues, hierarchical structures of muscles and arterial walls, as well as the osteons – base unit of the cortical bone – exhibit multilayered cylinder like architectures at the micro-scale level and often analytical solutions are required for deriving their overall linear and non-linear homogenized constitutive behaviour, useful for studying mechanical interactions with prosthesis devices or for predicting growth phenomena.

Moreover, in the last years, due to the increasing interest in the restoration of concrete civil structures, many experimental and theoretical applications have been carried out on the modelling

of the elastic and post-elastic mechanical response of structural concrete elements reinforced by means of Aramidic, Glass or Carbon-Fiber Reinforced Polymeric sheets (AFRP, GFRP, CFRP): in this context, to estimate the confining effects of these kind of reinforcements and quantitatively predict the increasing strength of concrete beams and columns constitutes the most important goal. In this framework, many efforts have been made: Wu, Lu and Wu [23] studied strength and ductility phenomena in concrete cylindrical specimens reinforced by FRP tissues, by obtaining some interpolating curves able to fit a number of experimental results; Wu, Wu and Lu [24] also presented a design-oriented stress-strain law for concrete prisms confined with FRP composites; Xiao and Wu [25], in one of the pioneer works, analyzed compressive behaviour of FRP concrete specimens, and several other papers have been presented in literature on this topic, for example by Green et al [26], Karabinis and Rousakis [27], Li [28], Prota et al [29]. In this framework, the present section is aimed to determine the post-elastic response of multilayered cylinder composed by two phases, analytically, in order to use the results for predicting ultimate strength and confining pressures at the interface between the isotropic *core* and the hollow anisotropic *jacket* phase, when the object is stressed by compressive axial forces. The approach is developed in a completely general way: however, the above described constituent phases can be identified with concrete and FRP sheets, these ones being homogenized over the total number of layers (see Figure 24.2). In particular, with reference to the literature data, the concrete material is modelled as elastic-plastic, with associated flow rule, and both the cases of Schleicher and Intrinsic Curve Yield Criteria are considered. On the other hand, the FRP phase is assumed to be elastic-brittle, with Tsai-Hill (modified Tsai-Wu-Hill) Limit Domain. These selected failure domains allow to consider the different compressive and tensile strength in the concrete and the anisotropy of the failure modes in the FRP ([15], [26] and [27]).

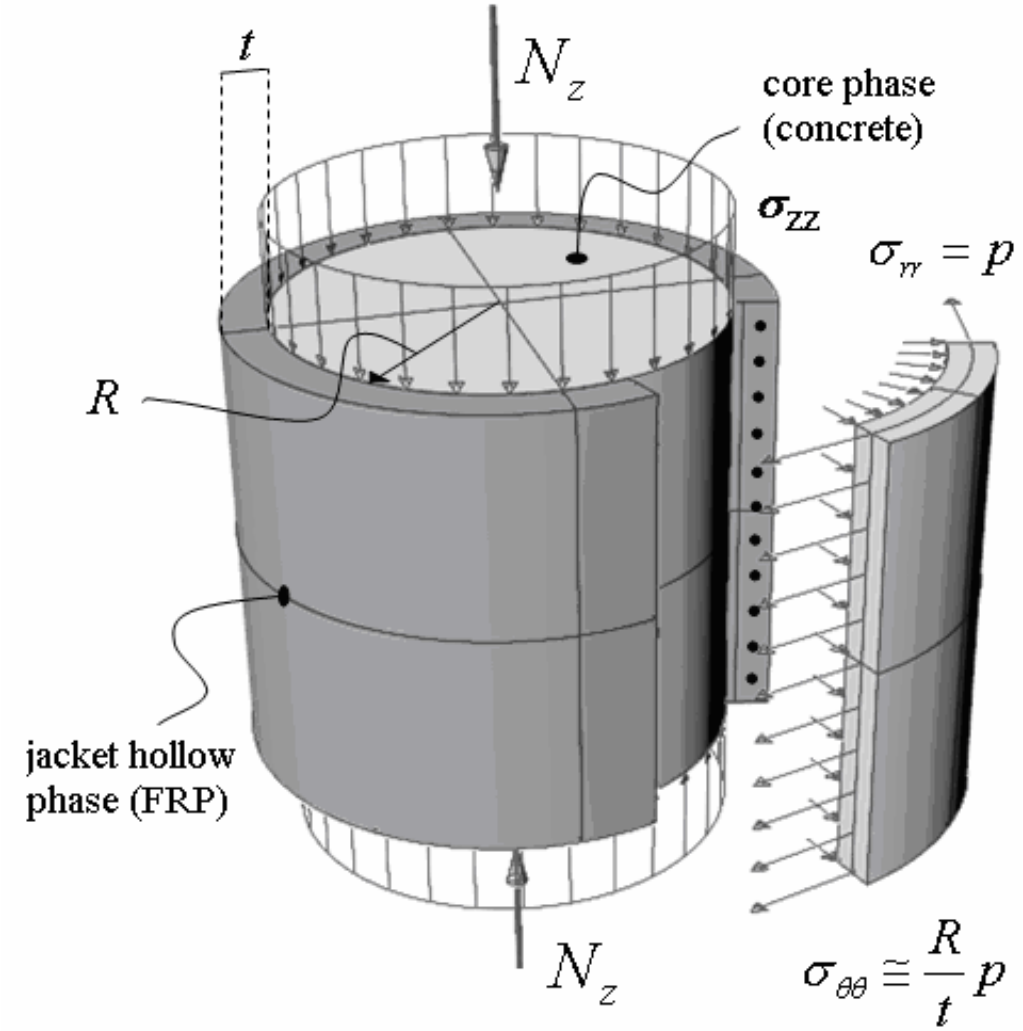

Figure 24.2 - *Multilayered cylinder composed by two phases under axial load* N_z

24.6.1. Preliminary remarks: qualitative results for bi-layer cylinder elastic response

Due to the closed-form elastic solutions obtained in the previous section, it is possible to establish the statements summarized in what follows, on the base of which the non linear solutions will be constructed.

1. When bi-layer cylinder is loaded by compressive axial forces, the stress and strain fields in the concrete – both in the linear and in the non-linear range – are everywhere uniform. In particular, the radial stress equates the hoop one, i.e. $\sigma_{rr}^{(c)} = \sigma_{\theta\theta}^{(c)} = p$, where p represents here the confining pressure at the interface between concrete and FRP.
2. Due to the axis-symmetry of both the elastic and inelastic problems, the maximum value of all the stress components is contemporary reached at the interface between concrete and FRP: this means that – independently from the chosen failure criterion – the crisis starts there (i.e., crack propagation, as well as brittle rupture).
3. The obtained analytical solution shows that the mean slope of the hoop stresses within the FRP, is weakly variable across the overall thickness t of the FRP, where – with reference to the above approach - $t = \sum_{i=1}^{n} t_i = \sum_{i=1}^{n} (R^{(i+1)} - R^{(i)})$, n being the total number of FRP layers (Figure 24.2). As a consequence, in analogy with the classical isotropic case of thin tubes under internal uniform radial pressures, thanks to the averaged equilibrium, it is consistent to assume $\sigma_{\theta\theta}^{f}(r = R^c) \simeq \sigma_{\theta\theta}^{f}(r = R^c + t) = pR^c t^{-1}$, where *f* and *c* apexes stand for FRP and concrete core, respectively. It is worth to note that this last consideration doesn't mean that the radial stresses in the FRP are neglected. More precisely, $\sigma_{rr}^{f} = p$ at the interface represents a significant stress component on the overall strength of the jacket, and not only a load as in the theory of shells. The reason of this influence can be easily understood if one considers the anisotropy of the strength, that is the compressive strength in the FRP radial direction and the tensile strength in the hoop (fibres) direction. The confining pressure is then involved in the brittle failure by the Tsai-Hill criterion, *p* playing the role of a driving parameter in the evolution of the stress path along the Plastic Surface related to the concrete phase (Figure 24.3).

By following a Limit Analysis step-by-step procedure, it will be then possible to follow the post-elastic behaviour and the increasing compressive strength of the concrete by involving the sole stress state in the object. Moreover, as we will show in what follows, the approach leads to an analytical formula able to fit with very good agreement the experimental tests reported by several authors [19] showing that the compressive ultimate strength is a function of the geometrical ratio $R^c t^{-1}$ and of the ultimate stresses in both concrete and FRP, only.

24.6.2. Aniso-strength elastic-plastic materials: the concrete core phase

Determination of the Intrinsic Curve

In order to obtain the explicit expression of the intrinsic curve in the $\sigma - \tau$ Mohr plane for a material with different tensile and compressive strengths, we have to first consider the Mohr circles corresponding to the uniaxial tests in tension and compression and then enveloping, for example with a parabola, these limit circles, by imposing then that any other possible limit circle be tangent to this curve. To make this, let us consider the uniaxial compressive stress state characterized by the maximum eigenvalues (in modulus) equal to the ultimate compressive strength σ_c; the Mohr circle equation is:

$$\left(\sigma + \frac{\sigma_c}{2}\right)^2 + \tau^2 = \frac{\sigma_c^2}{4} \tag{24.15}$$

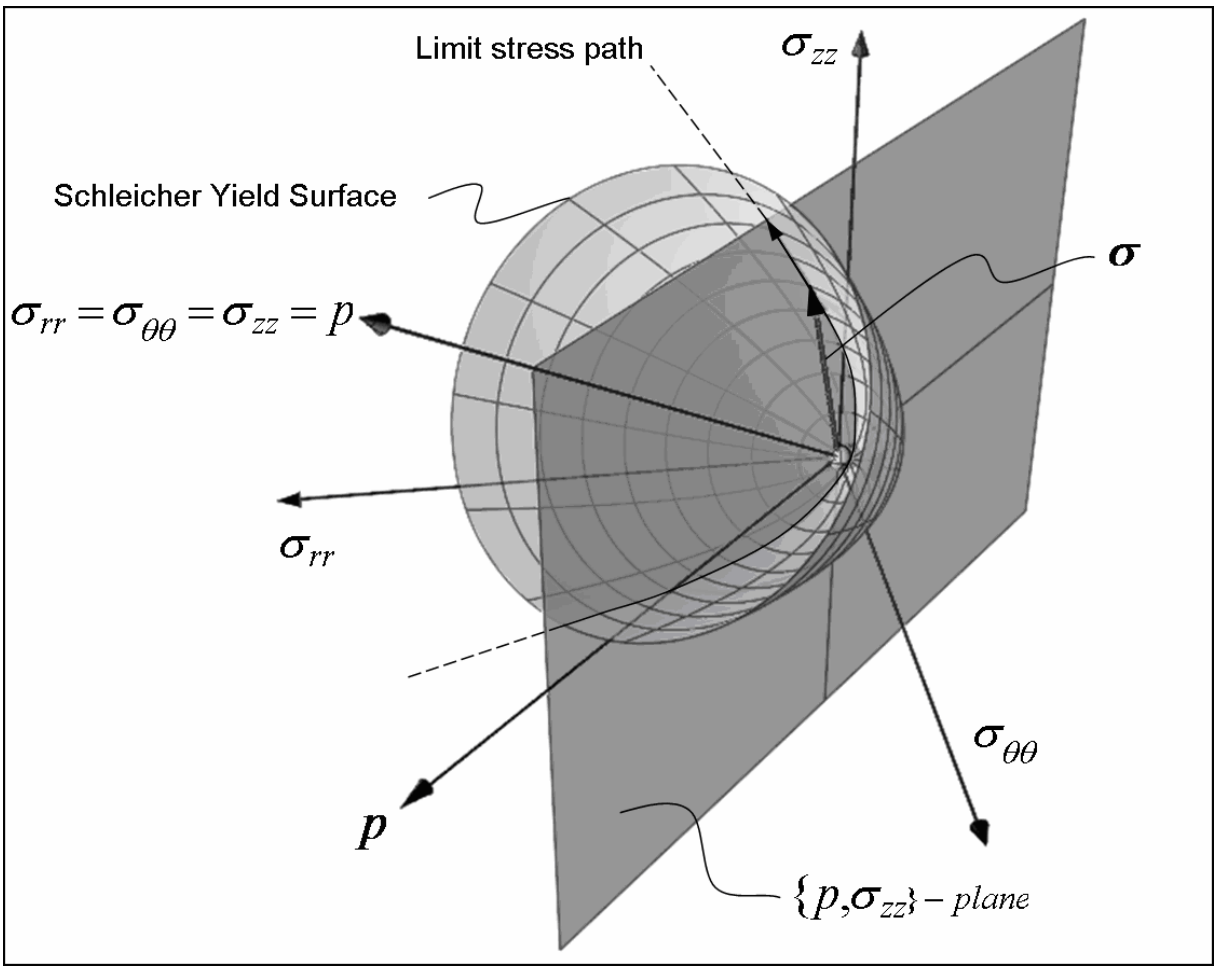

Figure 24.3 - *Illustration of the 3-D Schleicher yield surface and its projection in the* $\{p - \sigma_{zz}\}$ *plane: limit stress vector* $\boldsymbol{\sigma}$ *and related post-elastic admissible path.*

By applying the same line of reasoning, the uni-axial tensile strength σ_t gives:

$$\left(\sigma - \frac{\sigma_t}{2}\right)^2 + \tau^2 = \frac{\sigma_t^2}{4} = \frac{\alpha^2 \sigma_c^2}{4} \tag{24.16}$$

where the real parameter $\alpha \in (0,1)$ represents the ratio between tensile and compressive strengths, whose values are usually lower than the unity. As said before, by choosing as intrinsic curve a parabola in the $\sigma - \tau$ Mohr plane, this has to be tangent to the two crisis circles, with its vertex placed at $\sigma = \sigma_t$. Hence, let be

$$\sigma = a_0 \tau^2 + \sigma_t = a_0 \tau^2 + \alpha \sigma_c \tag{24.17}$$

the equation of this parabola (Figure 24.4). The intersection points with the compressive crisis circle (24.15) are obtainable by solving the following algebraic system:

$$\begin{cases} \left(\sigma + \dfrac{\sigma_c}{2}\right)^2 + \tau^2 = \dfrac{\sigma_c^2}{4} \\ \sigma = a_0 \tau^2 + \alpha \sigma_c \end{cases} \tag{24.18}$$

whose solutions are characterized by the four roots:

$$\tau = \pm \sqrt{\frac{1 + a_0 \sigma_c (1 + 2\alpha) \pm \sqrt{1 + a_0 \sigma_c (2 + 4\alpha + a_0 \sigma_c)}}{2 a_0^2}} \tag{24.19}$$

The tangency condition to the compressive crisis circle is furnished by:

$$1+a_0\sigma_c\left(2+4\alpha+a_0\sigma_c\right)=0 \quad \Rightarrow \quad a_0=-\frac{1+2\alpha\pm 2\sqrt{\alpha\left(1+\alpha\right)}}{\sigma_c} \tag{24.20}$$

The equation (24.17) becomes:

$$\sigma=-\frac{1+2\alpha+2\sqrt{\alpha\left(1+\alpha\right)}}{\sigma_c}\tau^2+\alpha\sigma_c \tag{24.21}$$

Moreover, it is necessary to establish that the parabola be tangent to the tensile crisis circle (24.16), too, so that:

$$\begin{cases}\left(\sigma-\dfrac{\alpha\sigma_c}{2}\right)^2+\tau^2=\dfrac{\alpha^2\sigma_c^2}{4}\\ \sigma=a_0\tau^2+\alpha\sigma_c\end{cases} \tag{24.22}$$

whose roots are:

$$\tau=0; \quad \tau=\frac{\pm\sqrt{-1-a_0\alpha\sigma_c}}{a_0}. \tag{24.23}$$

Then, by imposing that:

$$-1-a_0\alpha\sigma_c=0 \quad \Rightarrow \quad a_0=-\frac{1}{\alpha\sigma_c} \tag{24.24}$$

and by using the results (24.24) and (24.20), it remains to search the range of a_0 for obtaining the intrinsic curve satisfying the following inequality:

$$\frac{1}{\alpha\sigma_c}-\frac{1+2\alpha+\sqrt{\alpha\left(1+\alpha\right)}}{\sigma_c}\geq 0 \tag{24.25}$$

which means that the parabola describing the intrinsic curve never intersects in more than one point the compressive and tensile crisis circles. In other words, the inequality (24.25) means the root (24.20) be greater than that (24.24). Numerical computation yields to obtain the interval of admissible values of α, that is $\alpha\in(0,\,0.3949)$. This is consistent with the major part of real materials exhibiting different compressive and tensile strengths.

It is now useful to explicitly obtain the equation of the generic Mohr crisis circles tangent to the intrinsic curve corresponding to stress states where $\{\sigma_{rr}=\sigma_{\theta\theta}=p,\sigma_{zz}\}$, with $\sigma_{zz}<p<0$, being this the case under analysis. Hence, by writing the generic Mohr circle defined by negative eigenvalues $\{\sigma_{rr}=\sigma_I=p<0,\sigma_{\theta\theta}=\sigma_{II}=p<0,\sigma_{zz}=\sigma_{III}<p\}$ as follows

$$\left(\sigma-\frac{\sigma_{zz}+p}{2}\right)^2+\tau^2=\frac{\left(\sigma_{zz}-p\right)^2}{4} \tag{24.26}$$

and then by solving the algebraic system:

$$\begin{cases}\left(\sigma-\dfrac{\sigma_{zz}+p}{2}\right)^2+\tau^2=\dfrac{\left(\sigma_{zz}-p\right)^2}{4}\\ \sigma=a_0\tau^2+\alpha\sigma_c\end{cases} \tag{24.27}$$

the four real roots of (24.27) are given by:

$$\tau=\pm\sqrt{\frac{1-a_0\left(p-2\alpha\sigma_c+\sigma_{zz}\right)\pm\sqrt{1+a_0^2\left(p-\sigma_{zz}\right)^2-2a_0\left(p-2\alpha\sigma_c+\sigma_{zz}\right)}}{2a_0^2}} \tag{24.28}$$

The tangency condition requires that:

$$1+a_0^2\left(p-\sigma_{zz}\right)^2-2a_0\left(p-2\alpha\sigma_c+\sigma_{zz}\right)=0 \tag{24.29}$$

from which we obtain:

$$\sigma_{zz} = \frac{1 + a_0 p \pm 2\sqrt{a_0 \left(p - \alpha \sigma_c \right)}}{a_0} \tag{24.30}$$

By selecting the second root σ_{zz} into (24.30) and substituting the above obtained expression of a_0 we have:

$$\sigma_{zz} = p + \sigma_c \, \Phi(\alpha) - 2\sqrt{\sigma_c \, \Phi(\alpha) \left(p - \alpha \sigma_c \right)} \tag{24.31}$$

which constitutes the closed-form relationship between the compressive crisis value σ_{zz} and $\sigma_{rr} = \sigma_{\theta\theta} = p < 0$, being $\Phi(\alpha) = 2\sqrt{\alpha(1+\alpha)} - (1+2\alpha) < 0, \ \forall \alpha \in (0,1)$. The equation (24.31) can be then regarded as the constitutive non-linear evolution law of a stress state characterized by $\{\sigma_{rr} = \sigma_{\theta\theta} = p, \sigma_{zz}\}$, with $\sigma_{zz} < p < 0$.

Alternative Schleicher Criterion

The Schleicher criterion assumes as plasticity surface, in the eigenvalues stress space, a paraboloid surface whose axis is coincident with the hydrostatic axis, obtained by modifying the classical Huber-Hencky-Von Mises yield surface by means of the introduction of the first invariant of the stress tensor $\boldsymbol{\sigma}$, $J_1(\boldsymbol{\sigma}) = \mathrm{tr}\,\boldsymbol{\sigma}$. Then, two uniaxial strength parameters are introduced, $0 \le \sigma_t < \sigma_c$, representing the tensile and compressive strength, respectively. The yield surface f is then described by the following equation:

$$f\left[J_1(\boldsymbol{\sigma}), J_2(\boldsymbol{\sigma}), \sigma_t, \sigma_c \right] = 0 \tag{24.32}$$

where the well-known second invariant of the stress is $J_2(\boldsymbol{\sigma}) = \sigma_I \sigma_{II} + \sigma_{II} \sigma_{III} + \sigma_{III} \sigma_I$ and $\{\sigma_I, \sigma_{II}, \sigma_{III}\}$ represent the eigenvalues of the stress tensor $\boldsymbol{\sigma}$. The explicit form of f is:

$$(\sigma_I - \sigma_{II})^2 + (\sigma_{II} - \sigma_{III})^2 + (\sigma_{III} - \sigma_I)^2 - 2(\sigma_t - \sigma_c)(\sigma_I + \sigma_{II} + \sigma_{III}) = 2\sigma_t \sigma_c \tag{24.33}$$

that reduce to the Huber-Hencky-Von Mises criterion when $\sigma_t = \sigma_c$. Due to the specific form of the stress within the concrete core phase, it is useful to write the Schleicher criterion in the plane $p - \sigma_{III}$, (Figures 24.3, 24.4c and 24.4d), where $\{\sigma_I = \sigma_{rr} = \sigma_{II} = \sigma_{\theta\theta} = p, \sigma_{III} = \sigma_{zz}\}$ and – as considered for the intrinsic curve case - $\sigma_t = \alpha \sigma_c$. The equation of the parabola in the plane $p - \sigma_{III}$ reads:

$$(p - \sigma_{zz})^2 + \sigma_c (1 - \alpha)(2p + \sigma_{zz}) - \alpha \sigma_c^2 = 0 \tag{24.34}$$

Hence, from this equation, we can easily derive the expression of the stress σ_{zz} as function of p, that gives the relation between these stress components when the stress vector, represented in the $p - \sigma_{III}$ plane, belongs to the yield surface (see Figures 24.3, 24.4c and 24.4d):

$$\sigma_{zz} = p + \left(\frac{\alpha - 1}{2} \right) \sigma_c - \sqrt{\sigma_c \left[3p(\alpha - 1) + \sigma_c \left(\frac{1 + \alpha}{2} \right)^2 \right]} \tag{24.35}$$

Analytical form of the Intrinsic curve criterion:

$$\sigma_{zz} = p + \sigma_c \Phi(\alpha) \pm 2\sqrt{\sigma_c (p - \alpha \sigma_c)\Phi(\alpha)}$$

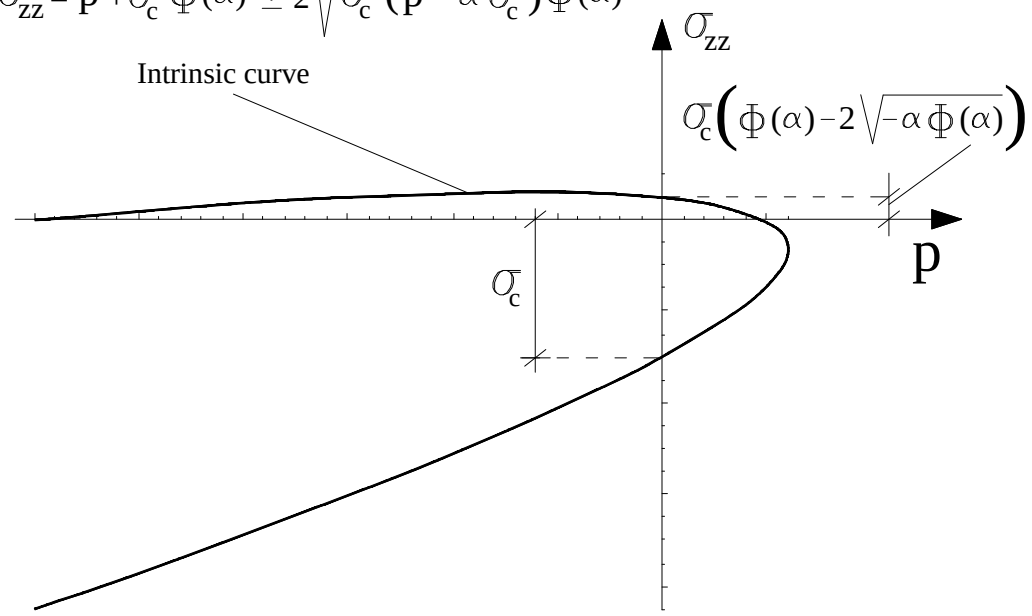

Figure 24.4a - Intrinsic curve in the $\{p - \sigma_{zz}\}$ plane

Analytical form of the Intrinsic curve criterion: $\longrightarrow$ $\tau = \pm\sqrt{\dfrac{(\alpha\sigma_c - \sigma)\sigma_c}{1 + 2\alpha + 2\sqrt{\alpha(1+\alpha)}}}$

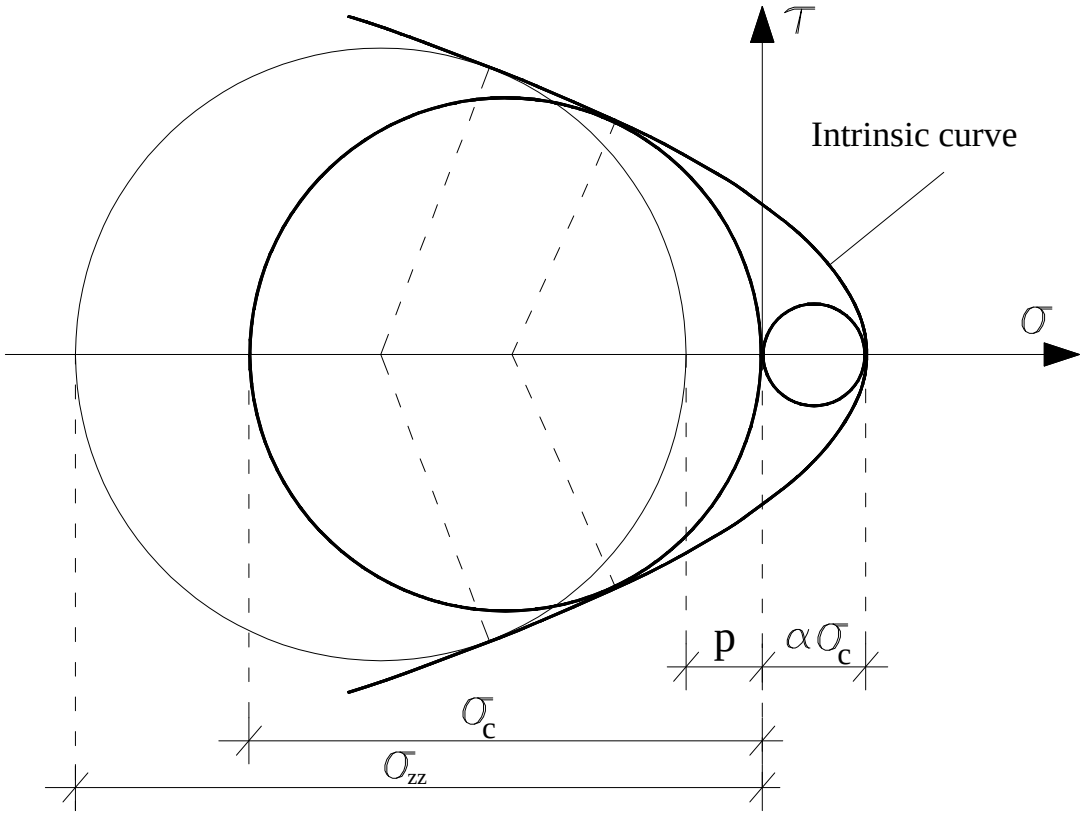

Figure 24.4b - *Intrinsic curve showing the two crisis tensile and compressive circles in the Mohr plane, with the generic enveloped crisis circle*

Analytical form of the Schleicher criterion:

$$\sigma_{zz} = p - \frac{\sigma_c(1-\alpha)}{2} \pm \frac{1}{2}\sqrt{\sigma_c\,[12\,p\,(\alpha-1) + \sigma_c\,(1+\alpha)^2]}$$

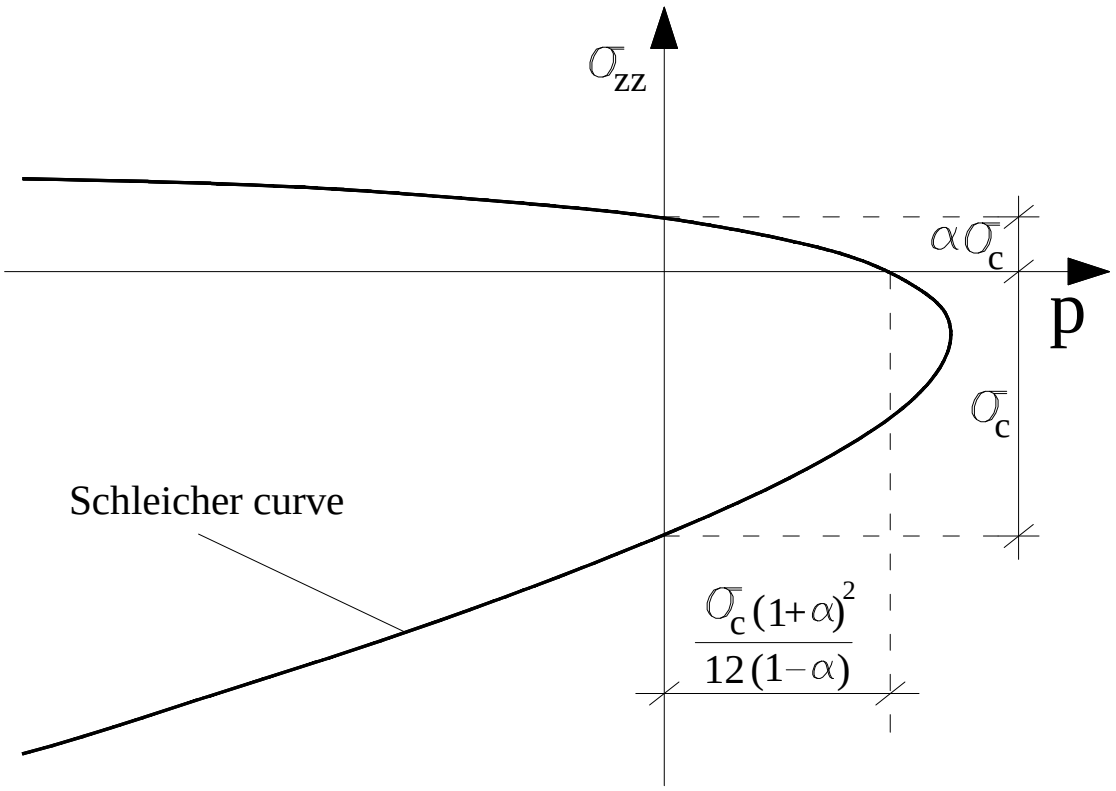

Figure 24.4c - *Schleicher criterion in the* $\{p-\sigma_{zz}\}$ *plane*

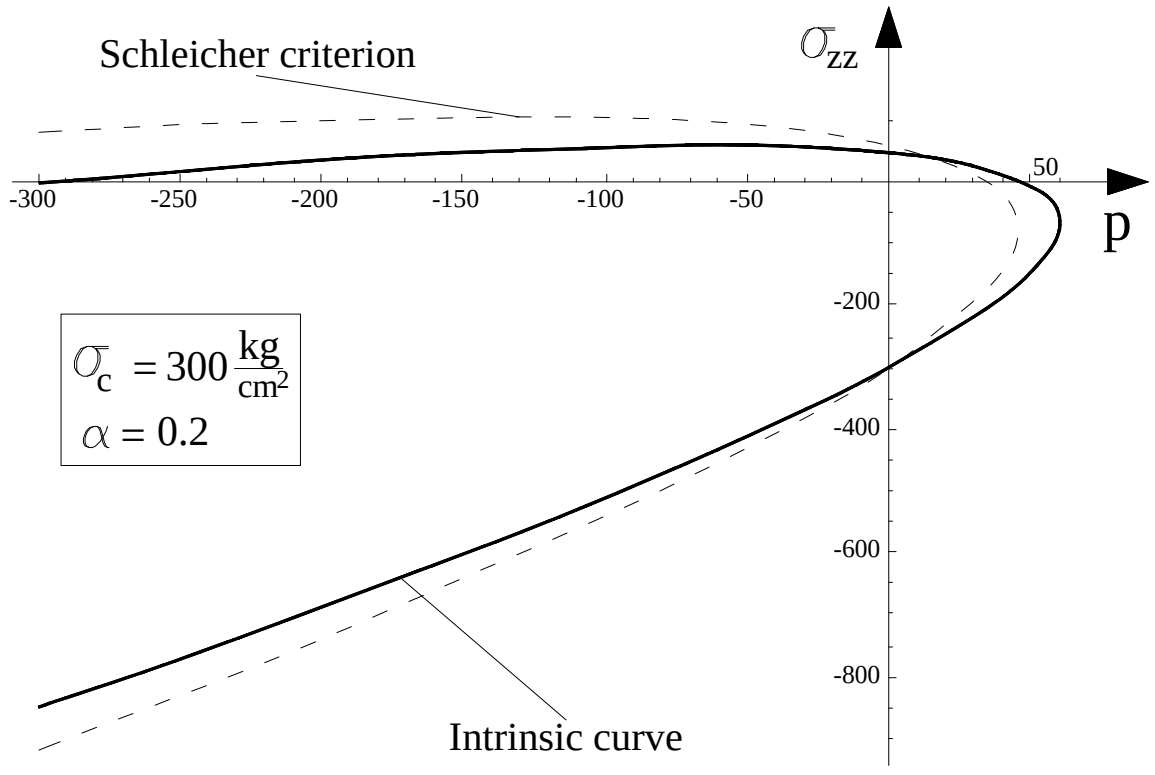

Figure 24.4d - *Comparison between Schleicher criterion and Intrinsic curve in the* $\{p-\sigma_{zz}\}$ *plane*

24.6.3. Tsai-Hill anisotropic criterion: elastic-brittle composite materials (FRP jacket phase)

In order to characterize the yield surface for inelastic composite materials, several proposals are presented in literature, based on both experimental tests and theoretical approaches invoking the non-linear theory of the homogenization, see Christensen [19], Debotton [30], Voyiadjis and Thiagarajan [31]. The difficulty of representing the limit condition for such of materials is related to the fact that their *elastic anisotropy*, due to the presence of planes of material symmetry observed at the micro-scale level (fiber direction in a matrix, arrangement of the solid phases in the representative volume element, etc.) reflects *strength anisotropy* in the plastic, damage or brittle post-elastic behaviour, too. This kind of *induced* inelastic anisotropy is generally highlighted by means of the exhibition of both different compressive and tensile strengths in a given direction and directional-depending strengths. Obviously, all possible combinations of these inelastic anisotropies could appear in the non-linear response of the material, as well as only aniso-strength or directional-depending strengths can be exhibited.

For the present study case, that is the cylindrical two-phase FGM with fiber-reinforced hollow jacket phase, as suggested in literature by Christensen [19] and Nanni [32], it results sufficiently accurate to assume for the elastic-brittle behaviour of the FRP jacket the Tsai-Hill criterion, here specialized for plane stress states $\{\sigma_{rr} = p < 0, \sigma_{\theta\theta} > 0\}$ which take place in the case of increasing axial compressive force acting on the central core ends of the object. Rigorously speaking, as obtained above from the elastic solution, the stress in the jacket phase is three-dimensional, due to the presence of σ_{zz}. Parametric evaluation of the ratio between this stress component and the other two ones in radial and circumferential directions, say σ_{rr} and $\sigma_{\theta\theta}$, shows that the weight of σ_{zz} in the jacket can be neglected if compared with the other two ones. This authorizes us to consider substantially plane the stress state in the FRP. The Tsai-Hill domain can be written as follows:

$$\left(\frac{\sigma_{xx}}{\sigma_{xxu}}\right)^2 + \left(\frac{\sigma_{yy}}{\sigma_{yyu}}\right)^2 - \frac{\sigma_{xx}\sigma_{yy}}{\sigma_{xxu}^2} + \left(\frac{\tau_{xy}}{\tau_{xyu}}\right)^2 \leq 1 \tag{24.36}$$

where $\{\sigma_{xxu}, \sigma_{yyu}\}$ represent the compressive radial strength and the ultimate tensile strength, respectively, while τ_{xyu} is the ultimate shear stress.

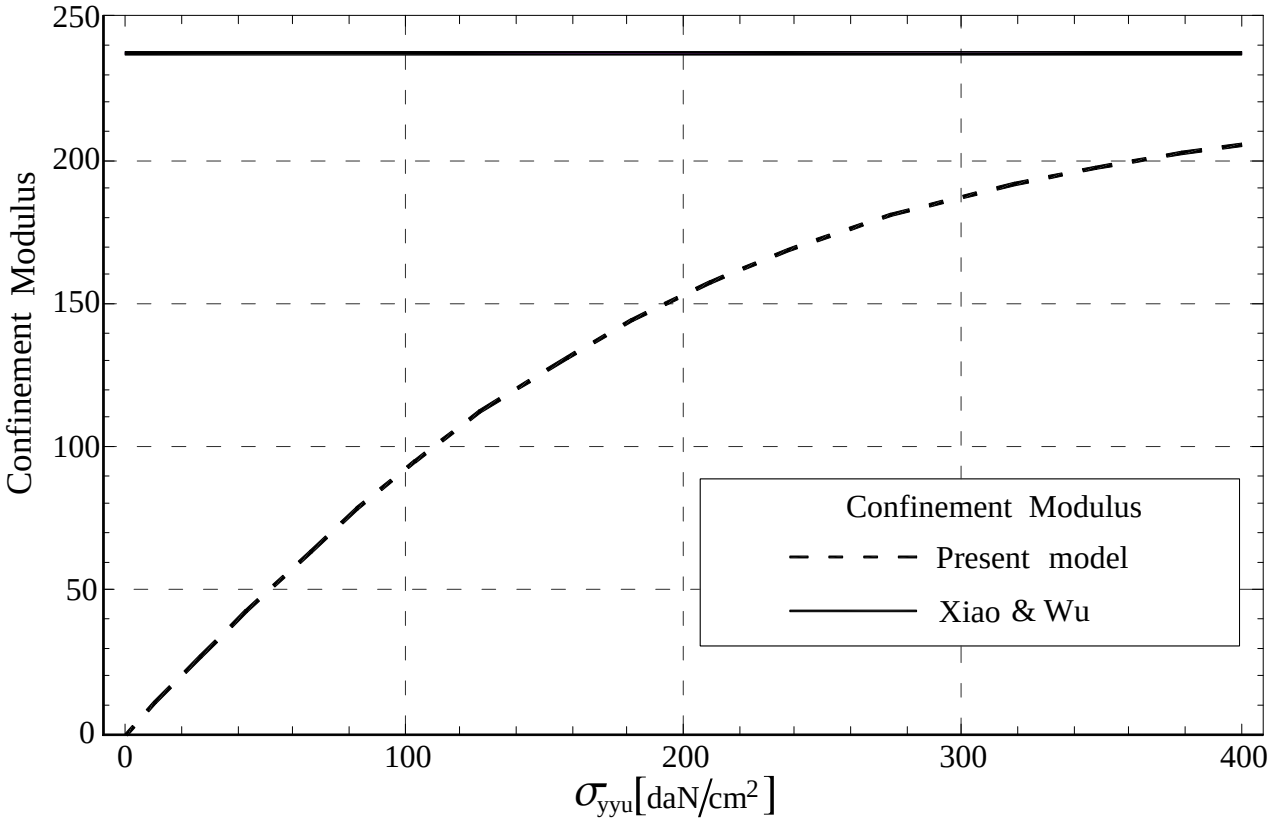

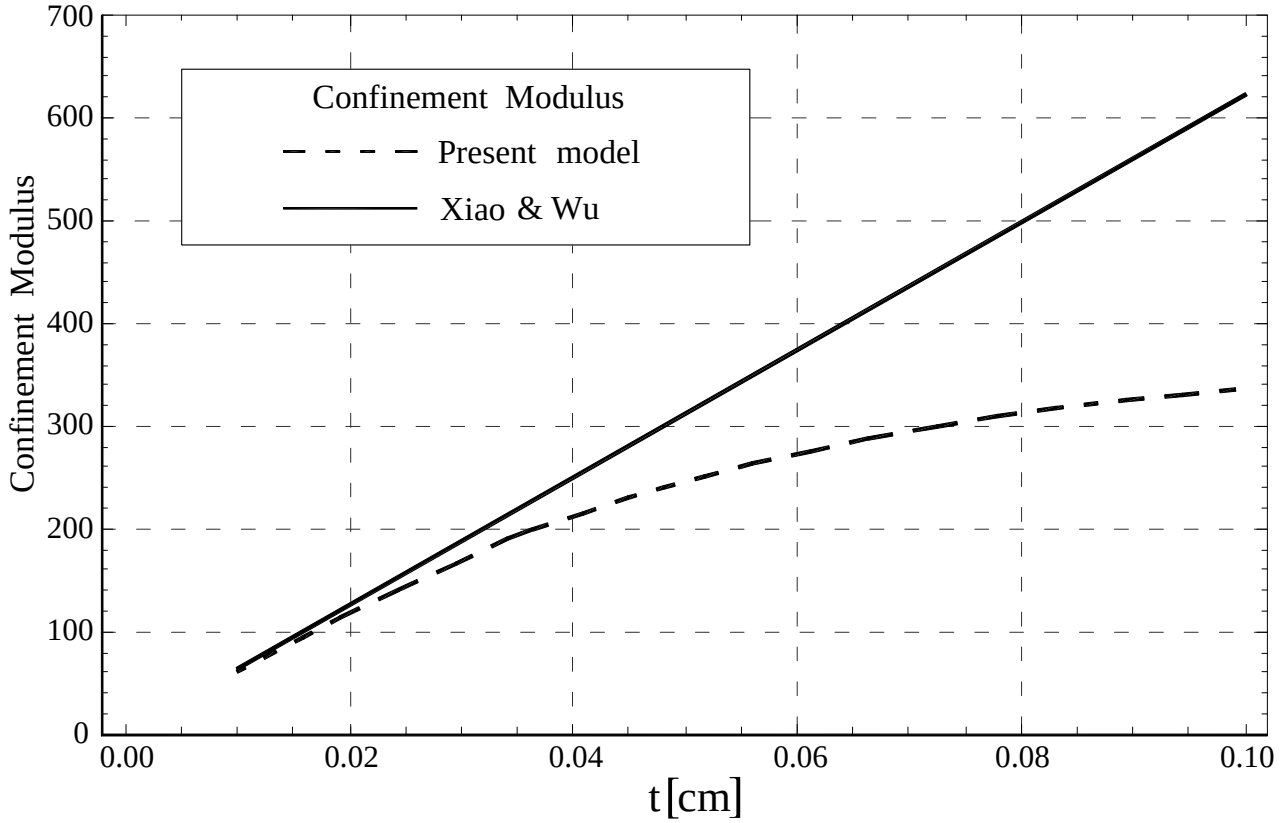

Figure 24.5 - *The two graphics illustrated in the present figure are intended to highlight the difference in the estimating the confining pressure for heavily FRP confined concrete specimens, by using the proposed model and the empirical one by Xiao and Wu [25]. In particular, the first graphic (top) shows the deviation between the pressure obtained by means of the present model (dashed curve) and the pressure calculated by Xiao and Wu (continuous curve), when the overall FRP thickness for a fixed radius of the concrete specimen varies (abscissa). The second graphic (bottom) shows the same comparison of above, with reference to the variation of the FRP radial ultimate stress, for a selected tensile strength of the FRP.*

Moreover, we here assume $\sigma_{xx} = \sigma_{II} = \sigma_{\theta\theta}$, $\sigma_{yy} = \sigma_{I} = \sigma_{rr}$, $\tau_{xy} = 0$, so that the equation (24.36) takes the form:

$$\left(\frac{\sigma_{\theta\theta}}{\sigma_{\theta u}}\right)^2 + \left(\frac{\sigma_{rr}}{\sigma_{ru}}\right)^2 - \frac{\sigma_{\theta\theta}\sigma_{rr}}{\sigma_{\theta u}^2} \leq 1 \tag{24.37}$$

where $\{\sigma_{yyu} = \sigma_{ru}, \sigma_{xxu} = \sigma_{\theta u}\}$. Also, let set $\sigma_{ru} = \beta\sigma_{\theta u}$, where, for fiber-composite materials, $\beta \in (0,1)$. By recalling the conditions derived from the sensitivity analysis of the elastic solutions and from the overall equilibrium equation written on a generic element of the jacket phase of multilayered cylinder (see the statements 1., 2. and 3. highlighted in the preliminary remarks), it is possible to write:

$$\sigma_{\theta\theta}(r = R) = \frac{R}{t}\sigma_{rr}(r = R) \equiv p\frac{R}{t} = \frac{p}{\omega} \tag{24.38}$$

By recalling that, as said before, the maximum values of the stresses in the hollow phase is reached at the interface between core and jacket, by virtue of the assumption of elastic-brittle behaviour of the composite material, the crisis has to appear wherever at the interface $r = R$, being R the radius of the concrete phase. Hence, the substitution of (24.38) into (24.37) gives:

$$\left(\frac{p}{\sigma_{\theta u}}\right)^2 \left(\frac{1}{\omega^2} + \frac{1}{\beta^2} - \frac{1}{\omega}\right) \leq 1 \tag{24.39}$$

where $\omega = t / R$. From the equation (24.39) it is then possible to obtain the crisis pressure p, e.g. confining stress at the interface, as follows:

$$p = -\frac{\sigma_{\theta u}\,\beta\omega}{\sqrt{\omega^2 + \beta^2\left(1-\omega\right)}} = -\sigma_{\theta u}\,\Psi(\beta,\omega) \tag{24.40}$$

where $[\omega^2 + \beta^2\left(1-\omega\right)] > 0,\ \forall\{\omega,\beta\} \in (0,1),\ \ \Psi(\beta,\omega) = -\omega\beta\left[\omega^2 + \beta^2\left(1-\omega\right)\right]^{-1/2}$.

It is worth noting that the formula (24.40) represents the effective value of the confining pressure and it results to be an explicit function of the ratio between the overall thickness of the FRP sheet and the concrete cross section radius, $\omega = t / R$, of the ratio $\beta = \sigma_{ru} / \sigma_{\theta u}$ of the radial and circumferential FRP strength parameters characterizing the Tsai_Hill criterion, and explicitly of the FRP tensile strength $\sigma_{\theta u}$. This evidence yields to compare the proposed value for the confining pressure (24.40) with the usual empirical formula, such as that reported in the work by Xiao and Wu [25], which on the contrary, by utilizing the Mariotti's assumption, starts from a simplified hypothesis on the FRP failure (that is the absence of the influence of the compressive radial stresses) and leads to p as confining pressure. Thus, with reference to the estimation of the confining pressure, the difference between the proposed model and that above mentioned suggested in [25] is represented by the factor $\Psi(\beta,\omega)$ appearing in (24.40). From the engineering point of view, this means that the present approach highlights a non-linear sensitivity of the confining pressure to the parameters ω and β. Figure 24.5 shows the deviation between the two formulae.

24.6.4. Overall post-elastic behaviour of bi-layer cylinder: Core and Jacket phases

In order to predict the overall strength of the FGM under analysis, we can substitute (24.40) into (24.31), for the Intrinsic Curve, or into (24.35), for the Schleicher Criterion. By following this way, it is then possible to relate - in a very useful closed-form - the actual ultimate compressive strength $\sigma_{zz}^{(c)}$ in the core phase to the sole set of geometrical and mechanical parameters, that is the *geometrical ratio*, $\omega = t\,R^{-1}$, the *strength ratios*, $\{\alpha = \sigma_t \sigma_c^{-1}, \beta = \sigma_{ru}\sigma_{\theta u}^{-1}\}$, the compressive strength of the core, σ_c, and the tensile strength of the hollow phase, $\sigma_{\theta u}$, as follows:

$$\sigma_{zz}^{(c)} = -\sigma_{\theta u}\Psi(\beta,\omega) + \sigma_c\,\Phi\left(\alpha\right) - 2\sqrt{-\sigma_c\,\Phi\left(\alpha\right)[\sigma_{\theta u}\Psi(\beta,\omega) + \alpha\sigma_c]} \tag{24.41}$$

for the case in which the concrete obeys to the Intrinsic Curve, and

$$\sigma_{zz}^{(c)} = -\sigma_{\theta u}\Psi(\beta,\omega) + \left(\frac{\alpha-1}{2}\right)\sigma_c - \sqrt{\sigma_c\left[3\sigma_{\theta u}\Psi(\beta,\omega)\left(1-\alpha\right) + \sigma_c\left(\frac{1+\alpha}{2}\right)^2\right]} \tag{24.42}$$

for the case where the core phase obeys to the Schleicher Criterion.

Finally, due to the form of the equations (24.41) and (24.42), it is possible to summarize the expression of the actual ultimate compressive strength $\sigma_{zz}^{(c)}$ as written down:

$$\sigma_{zz}^{(c)} = -\sigma_{\theta u}\Psi(\beta,\omega) + \sigma_c\,\xi_1\left(\alpha\right) - 2\sqrt{-\sigma_c\,\xi_2\left(\alpha\right)[\sigma_{\theta u}\Psi(\beta,\omega) + \xi_3(\alpha)\sigma_c]} \tag{24.43}$$

where a suitable setting of "transferring" coefficients $\{\xi_1,\xi_2,\xi_3\}$ yields to reduce the equation (24.43) to both the Intrinsic Curve (24.41) and Schleicher (24.42) cases. The specific values of these coefficients are reported in Table 24.1. Equation (24.43) can be then utilized in many practical engineering applications, for example the case of circular concrete columns reinforced with FRP, for quantitatively estimating the benefits of the confining effect directly in terms of overall increasing compressive stress on the concrete specimen.

In order to show the actual capacity of the proposed formula (24.43) of fitting with very accuracy the experimental results, for example those recently obtained by Wu et al [23] for a wide range of cylindrical concrete specimens confined with several types of FRP tissues, in Figures 24.6a, 24.6b, 24.6c and 24.6d are illustrated four cases.

	Intrinsic Curve	*Schleicher Criterion*
$\xi_1(\alpha)$	$\Phi(\alpha)$	$(\alpha-1)/2$
$\xi_2(\alpha)$	$\Phi(\alpha)$	$(3/4)(\alpha-1)$
$\xi_3(\alpha)$	α	$\left[(1+\alpha)^2\right]/[12(\alpha-1)]$

Table 24.1 - *Transferring coefficients* $\xi_i(\alpha)$ *in equation (24.43)*

The graphics are all plotted in a typical two-dimensional space, where on the abscissa is reported the so-called technical dimensionless *modulus of Carbon-FRP*, defined as ratio between the ultimate radial stress at the interface concrete-FRP, $\sigma_{rr} = \sigma_{\theta u} t R^{-1}$ (extreme confining pressure) and compressive uniaxial strength in the concrete, σ_c, while the ordinate axes are referred to the values of the ratio σ_{zz}^u / σ_c. As detailed in the captions of the Figure, the graphics compare Wu et al experimental data (bold dots) and their corresponding numerical interpolations (continuous lines) with the analytical curves obtained by means of the present approach and formula (24.43)(dashed curves), for different concrete compressive strengths σ_c and selected geometrical and mechanical parameters. In both the cases of high and common CFRP moduli (Figures 24.6a, 24.6b, 24.6c and 24.6d) and by using the Schleicher and Intrinsic Curve criteria, the results show how the analytical-based predictions are very close with the experiments.

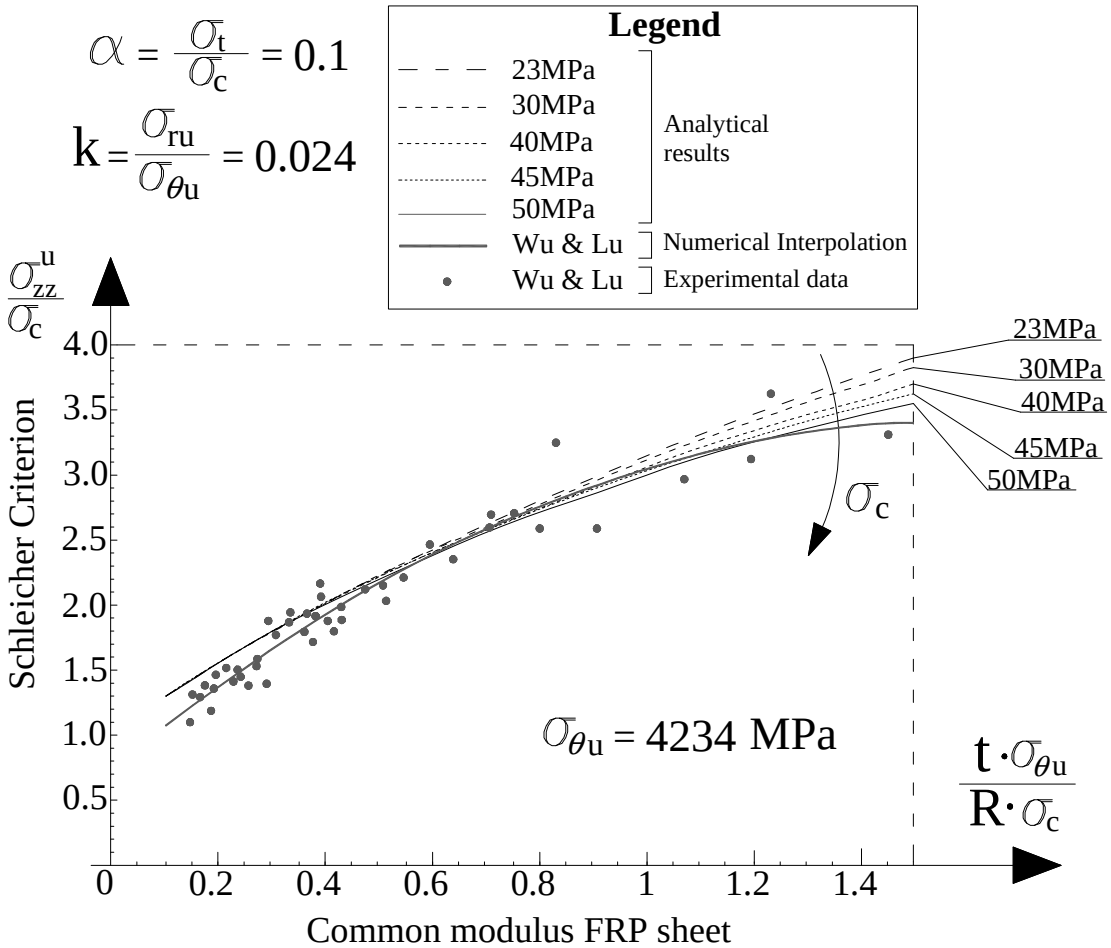

Figure 24.6a - *Comparison between experimental data (Wu & Lu), numerical interpolating (Wu & Lu) and proposed analytical curves for estimating the ultimate compressive strength in the concrete. The horizontal axes represent the so-called CFRP modulus, and the graphic is showed for common Carbon FRP sheet and for concrete modelled with Schleicher criterion*

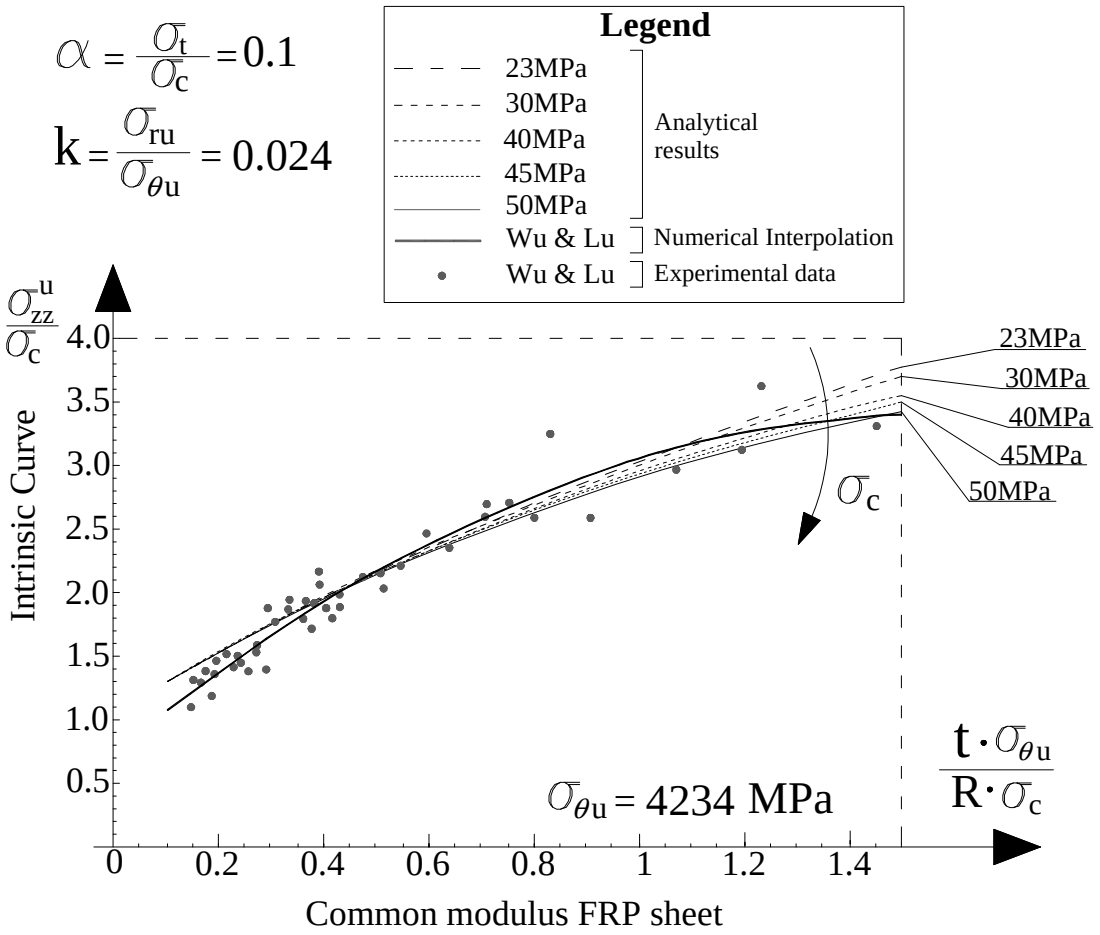

Figure 24.6b. *Comparison between experimental data (Wu & Lu), numerical interpolating (Wu & Lu) and proposed analytical curves for estimating the ultimate compressive strength in the concrete. The horizontal axes represent the so-called CFRP modulus, and the graphic is showed for common Carbon FRP sheet and for concrete modelled with Intrinsic curve*

24.6.5. On the estimation of the FRP hoop strain at failure

Another interesting result emerging from the proposed approach is constituted by the possibility of using it for explaining the variation of the effective strain at failure of FRP jackets, that is different to the strain at failure measured from tests in direct tension or split-disk tests. In fact, many works (for example, Xiao and Wu [25]) noted a discrepancy between the effective (hoop) strain at failure of FRP jackets and that measured from tests in direct tension. In some cases, depending on both the overall thickness and the modulus and strength of the FRP sheets, this difference seems to be varying from 20% up to about 50%. On the base of the present model, it is possible the forecast of the circumferential strain until brittle failure of the FRP, and therefore to explain the experimentally observed strain discrepancy. Here the key role is played by the fact that the resulting stress field in the FRP is three-dimensional, that is characterized by a very low value of the axial stress, say σ_{zz}, and the contemporary presence of (compressive) radial stresses and (tensile) hoop stresses. Moreover, by neglecting the axial stress, these main stress components vary along the overall thickness of the FRP sheets: in particular, at the interface concrete/FRP both the radial and hoop stress components are present (the radial stresses being the confining pressures), while at the external cylindrical surface, due to the absence of applied radial pressure, the sole circumferential stress does not vanish. Also, from engineering point of view, it is possible to note that a not significant hoop stress variation along the FRP thickness is revealed.

Therefore, obeying the assumed Tsai-Hill criterion, the brittle crisis - and thus the crack propagation phenomenon - starts from points placed at the concrete/FRP interface and there the actual yield stress level at failure is characterized by the contemporary presence of two main stress components,

that is a compressive radial stress and a tensile hoop stress, the last one being obviously less than the ultimate tensile stress measured from direct tension tests. As a consequence, the hoop strain at the interface shall be greater than that calculated in presence of the sole hoop stress when it equates the FRP tensile strength, because - by virtue of the constitutive anisotropic law - the hoop strain is increased by the cogent compressive radial stress. On the contrary, at the external surface, where the hoop strain can be directly measured, the absence of radial stresses and the presence of circumferential stresses lower than the ultimate FRP tensile strength determine a decrease of the hoop strain at the failure. Thus, this explains the observed strain discrepancy.
The Figure 24.7 illustrates the possible variation of the hoop strain on the FRP external cylindrical surface with the ultimate radial strength of the FRP (reported on the abscissa) and also when different Young's moduli and number of FRP layers (1, 2 and 3 sheets each one of 0.381 mm) are considered. It is evident how, making variable these parameters, possible significant reduction of the strain at failure can be registered, respect to that waited by thinking to the uniaxial test.

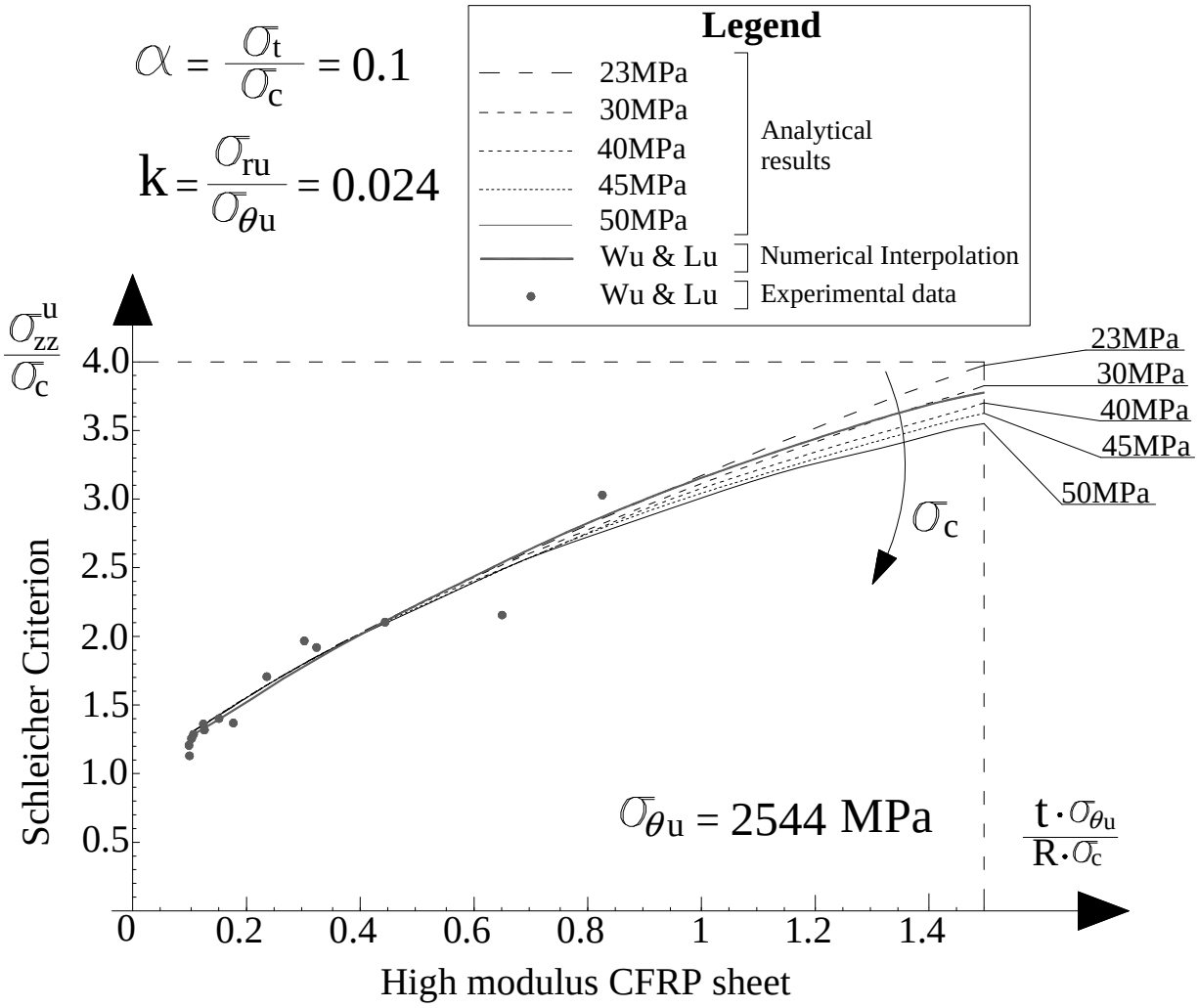

Figure 24.6c - *Comparison between experimental data (Wu & Lu), numerical interpolating (Wu & Lu) and proposed analytical curves for estimating the ultimate compressive strength in the concrete. The horizontal axes represent the so-called CFRP modulus, and the graphic is showed for high Carbon FRP sheet and for concrete modelled with Schleicher criterion*

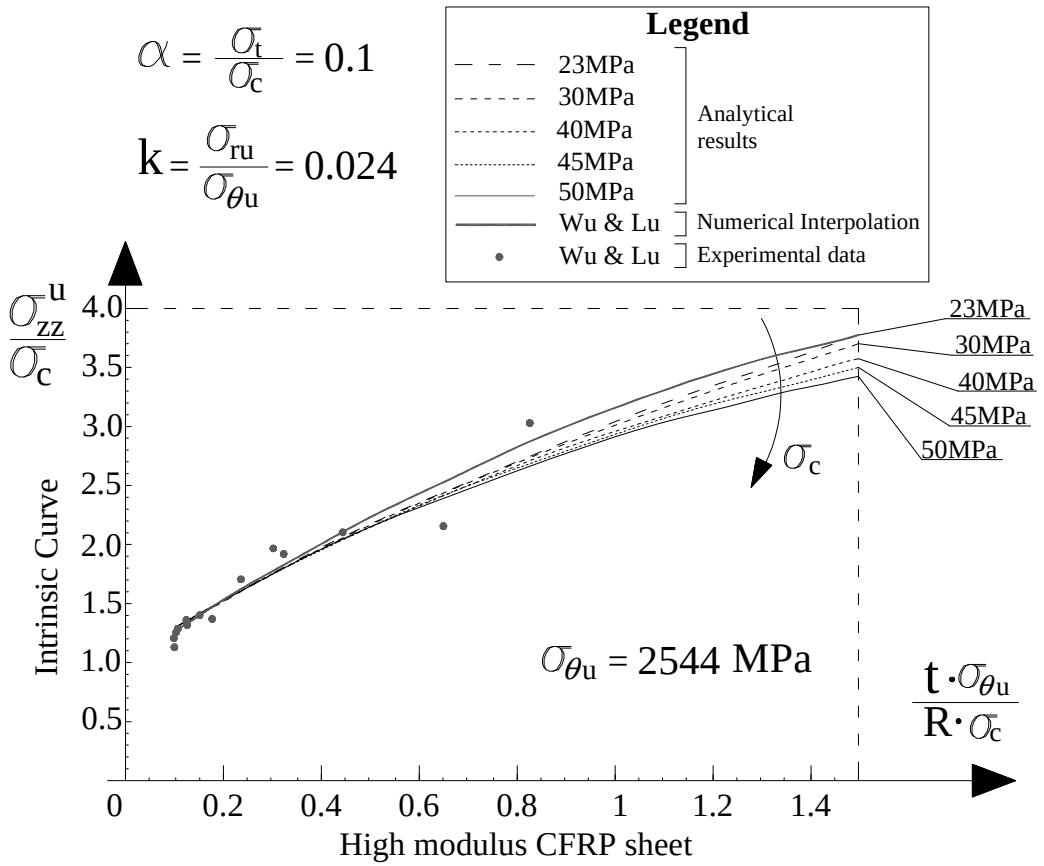

Figure 24.6d -*Comparison between experimental data (Wu & Lu), numerical interpolating (Wu & Lu) and proposed analytical curves for estimating the ultimate compressive strength in the concrete. The horizontal axes represent the so-called CFRP modulus, and the graphic is showed for high Carbon FRP sheet and for concrete modelled with Intrinsic curve.*

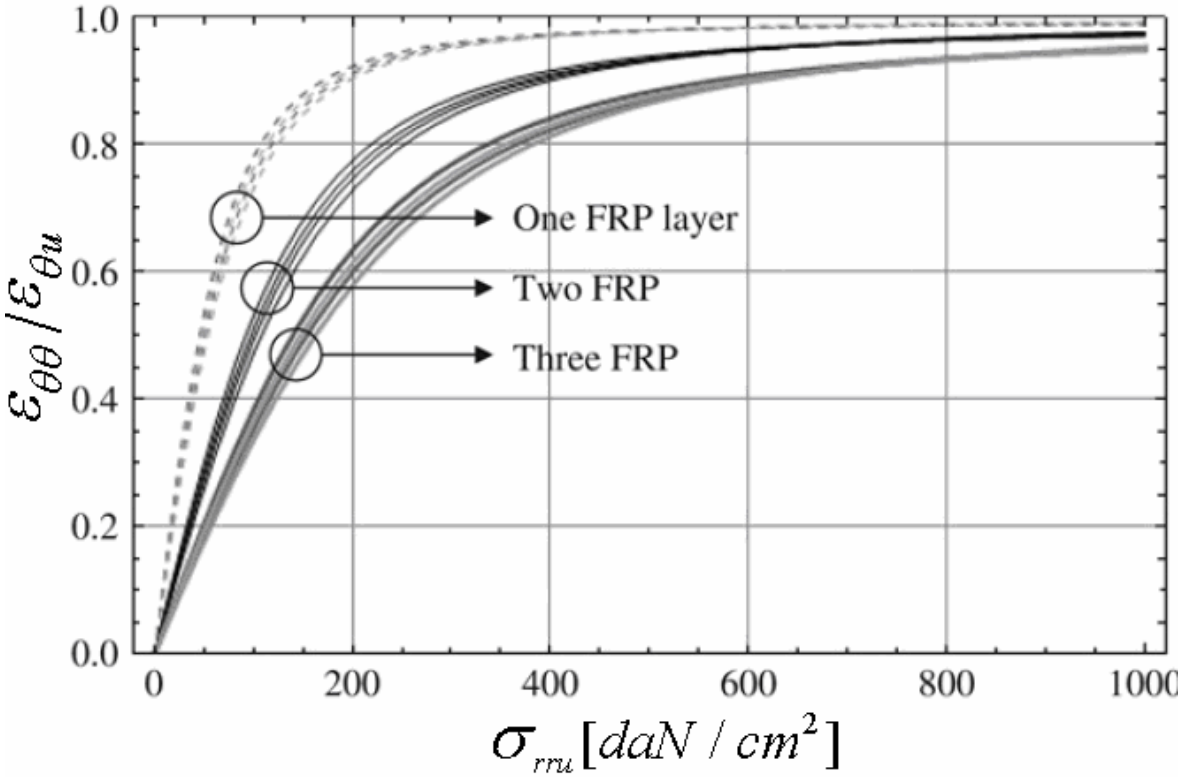

Figure 24.7 - *Analytical prediction of the ratio between actual failure hoop strain on the FRP external cylindrical surface and ultimate FRP strain with varying ultimate radial strength of the FRP (reported on the abscissa). The twelve curves illustrated in the graphics can be distinguished*

in three groups, as is shown by the figure. Each of the four curves belonging to a selected group has been obtained by considering four corresponding possible FRP Young's moduli in the fiber direction. The three groups are then carried out by setting in the model 1, 2 and 3 FRP sheets, each one of 0.381 mm. The main result is therefore related to the increase of the difference between ultimate uniaxial strain and actual strain at failure with the increasing number of FRP layers

24.6.6. Assessment and design formulae for concrete columns confined by FRP sheets

Assessment formula:
With the aim of obtaining a design formula of practical interest in civil engineering applications, we can recall the equation (24.43), making reference – for example - to the Schleicher criterion for modeling the concrete. By substituting in (24.43) the values collected in Table 24.1, we obtain:

$$\sigma_{zz}^{(c)} = -\frac{\sigma_{\theta u} t \beta}{\sqrt{t^2 + \beta^2 R(R-t)}} + \frac{\sigma_c(\alpha - 1)}{2} - \sqrt{\sigma_c \left[\frac{3\sigma_{\theta u}\, \beta t (1-\alpha)}{\sqrt{t^2 + \beta^2 R(R-t)}} + \sigma_c \left(\frac{1+\alpha}{2} \right)^2 \right]} \qquad (24.44)$$

As already said, the formula (24.44) can be regarded as an assessment formula, helpful for directly estimating the ultimate compressive strength of a cylindrical concrete specimen confined by FRP, when geometrical and mechanical parameters of both the constituent materials are prescribed. In Figure 24.8, the stress-strain relationship for heavily confined concrete specimens is also illustrated, making reference to different numbers of layers and elastic moduli of the FRP sheets.

Design formulae:
On the other hand, the closed form of (24.44) allows us to obtain two design formulae able to give in output either the minimum overall thickness of the FRP sheet or the desired increase of the load capacity. To make this, we define another parameter, say $k \equiv \sigma_{zz}^{(c)} / \sigma_c > 1$, representing the ratio between the expected compressive concrete strength (due to the confining effect of the FRP) and the unconfined (FRP-free) concrete compressive strength. By inverting (24.44) we obtain the design formula in terms of FRP overall thickness:

$$t = \frac{R\beta\xi\left(-\beta\xi + \sqrt{\beta^2\left(4+\xi^2\right) - 4\xi^2}\right)}{2\left(\beta^2 - \xi^2\right)} \qquad (24.45)$$

where

$$\xi = \frac{\sigma_c}{\sigma_{\theta u}} \left[k + 1 - \alpha - \sqrt{1 + (\alpha - 1)(\alpha - 3k)} \right] \qquad (24.46)$$

Following a complementary way, by invoking the formula (24.45), it is possible to obtain the strength-increasing coefficient k as design parameter, that is as function of FRP thickness t and varying compressive unconfined concrete strengths σ_c, writing:

$$k = \frac{1-\alpha}{2} + \frac{\sigma_{1u}}{\sigma_c}\Psi + \sqrt{\left(\frac{1+\alpha}{2}\right)^2 + 3(1-\alpha)\frac{\sigma_{1u}}{\sigma_c}\Psi} \qquad (24.47)$$

where – as already above defined - $\Psi = t\beta\left[t^2 + R(R-t)\beta^2\right]^{-1/2}$.

Figure 24.9. collects the curves giving the thickness t necessary to obtain two times the unconfined compressive concrete strength ($k = 2$), as function of the tensile FRP strength, for a selected set of geometrical and mechanical parameters, (i.e.: $R = 15cm,\ \alpha = 0.1,\ \beta = 0.02$).
Figure 24.10 shows the graphic of k versus thickness t, for some usual compressive concrete strength values.

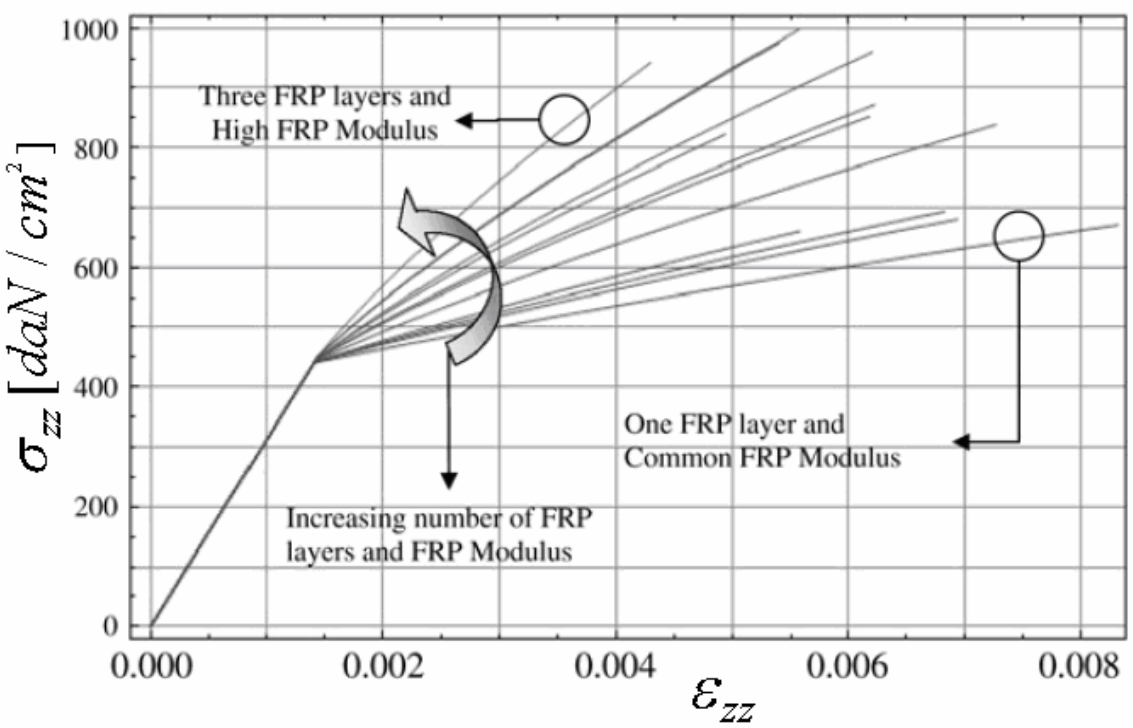

Figure 24.8 – *Stress-strain relationship for heavily confined concrete: the post-elastic branches are calculated for different possible FRP Young's moduli in the fibre direction and FRP layers. The mean slope of the quasi-linear ultra-elastic branches increases with the number of FRP sheets and with the FRP Young's modulus, determining - in some cases - ultimate compressive concrete strengths greater more than two times the compressive stress of the unconfined concrete*

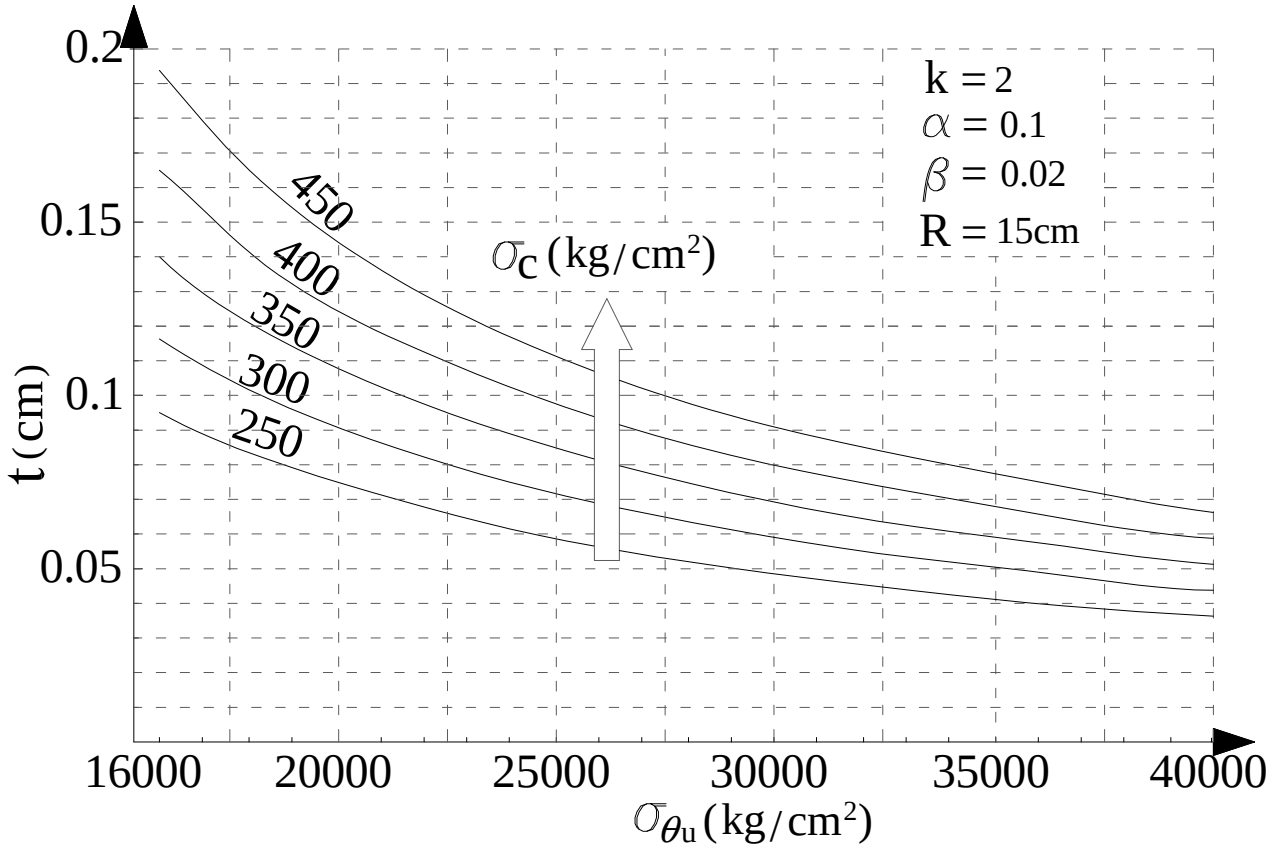

Figure 24.9 - *Graphic showing the overall thickness of the FRP sheet as function of FRP tensile strength, for different values of unconfined compressive concrete strength*

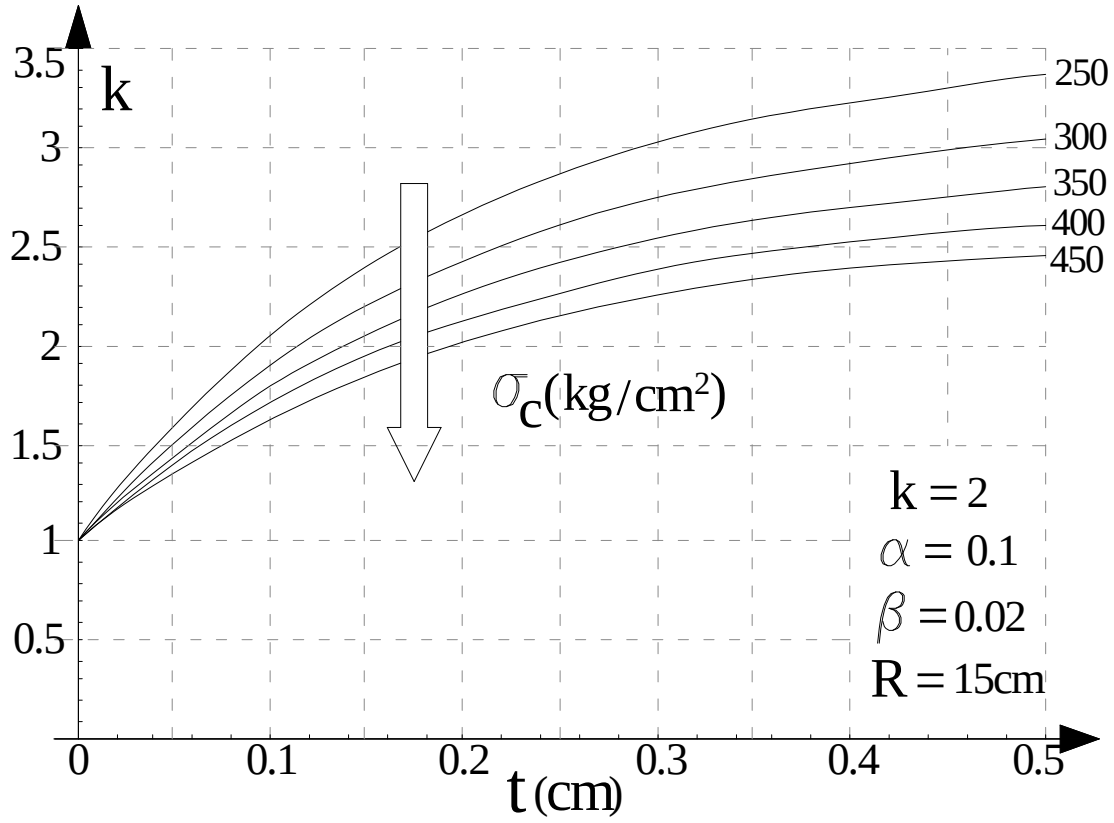

Figure 24.10 - *Graphic showing the increasing coefficient k as function of the overall FRP thickness t, for different values of unconfined compressive concrete strength.*

24.7. Numerical example: complete elastic and post-elastic solutions of Carbon-FRP cylindrical concrete specimens under compression

The following numerical example is illustrated for showing the applicability of the proposed strategy to practical problems, by determining the elastic and post-elastic solutions in explicit form for a cylindrical concrete specimen confined with FRP. The example makes reference to the experimental results obtained by Xiao and Wu [25].

Since we already showed that there are no significant differences in the quantitative response of the concrete when Schleicher or Intrinsic Curve criteria are adopted for modelling its post-elastic behaviour (Figures 24.4a and 24.4c), the application is specialized to the Schleicher-like plastic response.

24.7.1. Elastic response

In order to fix the ideas, let us consider a cylindrical concrete specimen whose core diameter is *D*, characterized by elastic constants $E^{(c)}$, $\nu^{(c)}$ and with compressive strength $\sigma_c = f_{c0}$. Let this specimen be confined by means of three layers of FRP tissue with unidirectional arrangement of the fibres, each of one with thickness $t_i = 0.0381$ cm and be $t = \sum_{i=1}^{3} t_i$ the overall thickness of the hollow phase that we here consider as one, in terms of homogenization. Due to the orientation of the carbon fibres embedded into the polymeric matrix, the FRP is considered as an orthotropic material, whose useful elastic coefficients – in the cylindrical reference system – are $E_{rr}, E_{\theta\theta}, E_{zz}, \nu_{r\theta}, \nu_{rz}, \nu_{\theta z}$.

It is important to emphasize here that the elastic moduli for the composite FRP were obtained by means of an homogenization technique, based on the knowledge of the mechanical parameters of the constitutive materials and their corresponding volume fractions. In particular, as suggested by the literature, the Young's moduli E_{rr} and $E_{\theta\theta}$ are referred to the Reuss and Voigt estimations

respectively, being E_{zz} lower than E_{rr} for taking into account the specific contact conditions between two adjacent layers of FRP sheets.

Materials	Young's modulus	Poisson's ratio	Material Strength
Concrete Core	$E^{(c)} = 313237 kg\ cm^{-2}$	$\nu^{(c)} = 0.18.$	$\sigma_c = f_{c0} = 438\ \ kg\ cm^{-2}$ $\sigma_t = f_{c0}/10 = 43.8\ \ kg\ cm^{-2}$
FRP sheet homogenized parameters	$E_{rr} = 3\times10^4 kg\ cm^{-2},$ $E_{\theta\theta} = 1.05\times10^6 kg\ cm^{-2},$ $E_{zz} = 6\times10^3 kg\ cm^{-2}$	$\nu_{r\theta} = 0.32,$ $\nu_{rz} = 0.35,$ $\nu_{\theta z} = 0.32.$	$\sigma_{xxu} = 1.577\times10^4\ kg\ cm^{-2}$ $\sigma_{yyu} = 1.3\times10^2 kg\ cm^{-2}$

Table 24.2 - *Mechanical properties of concrete and FRP (Diameter of specimen: $D = 15.2\ cm$)*

Then, by taking into account the values of the geometrical and mechanical parameters above introduced, collected in Table 24.2, and by applying the elastic solution reported in paragraph 24.3 and 24.4, the constant integrations are given by :

$$\begin{aligned} &\varepsilon_r^{(c)} = -3.124\cdot10^{-9} N_z, \quad \varepsilon_0^{(c)} = \varepsilon_0^{(j)} = 1.757\cdot10^{-8} N_z, \\ &C_1^{(j)} = -1.70\cdot10^{-3} N_z, \quad C_2^{(j)} = -1.70\cdot10^{-3} i\ N_z, \end{aligned} \tag{24.48}$$

where N_z is the axial force applied at the ends of the object. By virtue of the results above obtained, the displacement field for the concrete core phase becomes:

$$u_r^{(c)} = -3.124\cdot10^{-9} N_z\ r,\ \ u_\theta^{(c)} = 0,\ \ u_z^{(c)} = 1.757\cdot10^{-8} N_z\ z \tag{24.49}$$

from which the following strains in concrete are written down:

$$\varepsilon_{rr}^{(c)} = \varepsilon_{\theta\theta}^{(c)} = -3.124\cdot10^{-9} N_z\ , \qquad \varepsilon_{zz}^{(c)} = 1.757\cdot10^{-8} N_z, \tag{24.50}$$

It is worth to note that, in the elastic range, the axial strain in the z direction is about one order of magnitude greater than that of the corresponding radial and circumferential strain components, while two orders of magnitude characterize the ratio between the axial stress and the radial and hoop ones in the concrete core:

$$\sigma_{rr}^{(c)} = \sigma_{\theta\theta}^{(c)} = 1.62\cdot10^{-5} N_z\ , \qquad \sigma_{zz}^{(c)} = 5.51\cdot10^{-3} N_z. \tag{24.51}$$

By using these results, the displacement field for the jacket orthotropic phase is:

$$\begin{aligned} &u_r^{(j)} = \left[-8.38\cdot10^{-12} r - 1.70\cdot10^{-3}\left(r^{5.84} - r^{-5.84}\right)\right] N_z \\ &u_\theta^{(j)} = 0, \quad u_z^{(j)} = 1.757\cdot10^{-8} N_z\ z \end{aligned} \tag{24.52}$$

As a consequence, the non-zero strain components in the FRP are:

$$\begin{aligned} &\varepsilon_{rr}^{(j)} = \left[-8.38\cdot10^{-12} + 9.93\cdot10^{-3} r^{-6.84} - 4.82\cdot10^{-13} r^{4.84}\right] N_z, \\ &\varepsilon_{\theta\theta} = \left[-8.38\cdot10^{-12} - 1.70\cdot10^{-3} r^{-6.84} - 8.247\cdot10^{-14} r^{4.84}\right] N_z\ , \\ &\varepsilon_{zz}^{(j)} = 1.757\cdot10^{-8} N_z, \end{aligned} \tag{24.53}$$

and the non-zero stress components are:

$$\begin{aligned} &\sigma_{rr}^{(j)} = \left[3.79\cdot10^{-5} + 288.43\, r^{-6.84} - 1.575\cdot10^{-8} r^{4.84}\right] N_z, \\ &\sigma_{\theta\theta}^{(j)} = \left[3.79\cdot10^{-5} - 1814.64\, r^{-6.84} - 9.204\cdot10^{-8} r^{4.84}\right] N_z\ , \\ &\sigma_{zz}^{(j)} = \left[1.08\cdot10^{-4} + 17.11\, r^{-6.84} - 1.27\cdot10^{-9} r^{4.84}\right] N_z, \end{aligned} \tag{24.54}$$

As it will be highlighted in the following, differently from the concrete phase, in the FRP the hoop stress reaches an outstanding value respect to the axial one. It is worth to note that, without FRP phase, the ultimate strength of concrete would be $\sigma_{zz}^{(c)} = f_{c0}$ and then its limit load should become:

$$\sigma_{zz}^{(c)} = 5.51\cdot10^{-3} N_z = 438\ kgcm^{-2} \quad \Rightarrow \quad N_z = 79523 kg \tag{24.55}$$

where the obtained value of N_z represents the limit compressive load of the un-reinforced concrete element. On the contrary, as a consequence of the confining effect due to the presence of the FRP, we will see that both the elastic limit and the ultimate collapse axial force of the restored cylindrical concrete specimen significantly increase.

24.7.2. Post-elastic response

As already shown above, the post-elastic response of the concrete element starts in presence of the limit value of the axial force (24.55). For increasing values of N_z the concrete is in plastic condition and the stresses have to follow the path belonging to the limit domain (Figure 24.3). On the contrary, the FRP is still in the elastic range. Due to the specific form of the stress tensor within the concrete core phase

$$\boldsymbol{\sigma} = \begin{bmatrix} p & 0 & 0 \\ 0 & p & 0 \\ 0 & 0 & \sigma_{zz} \end{bmatrix} = \begin{bmatrix} \sigma_I & 0 & 0 \\ 0 & \sigma_{II} & 0 \\ 0 & 0 & \sigma_{III} \end{bmatrix} \tag{24.56}$$

it is more useful to restrict the Schleicher criterion to the plane $(\mathbf{p}, \sigma_{III})$, as represented in Figure 24.6. Here $\mathbf{p}$ is the vector bisector of the angle between axes (σ_I, σ_{II}).

By assuming for the present case $\{\sigma_t = f_{c0}/10, \sigma_c = -f_{c0}\}$, equation (24.34) finally becomes:

$$2p^2 - p\left(3.6 f_{c0} + 4\sigma_{zz}\right) + 2\sigma_{zz}^2 - 1.8 f_{c0}\sigma_{zz} - 0.2 f_{c0}^2 = 0 \tag{24.57}$$

In Figure 24.11 are also illustrated the linear and non linear stress path curves in the plane $(\mathbf{p}, \sigma_{zz})$. There, it can be noted the increase of the effective compressive strength of the concrete, due to the contemporary presence of the confining stresses $\sigma_{rr} = \sigma_{\theta\theta} = p$. The elastic limit force is then obtainable:

$$6.04 \cdot 10^{-5}\left(N_z^{el} - 80306\right)\left(N_z^{el} + 7915\right) = 0 \quad \Rightarrow \quad N_z^{el} = 80306kg \tag{24.58}$$

In particular, the intersection point of the linear path with the Schleicher curve, in this plane, is characterized by the following coordinates:

$$p = 1.30kg/cm^2, \quad \sigma_{zz} = 442.48kg/cm^2 > f_{c0} = 438kg/cm^2 \tag{24.59}$$

to which corresponds the axial limit load $N_z^{el} = 80306kg$. Behind the load $N_z^{el} = 80306kg$, the relationship between $\sigma_{zz}^{(c)}$ and p becomes non linear and the stress path is constrained to run on the Schleicher curve, as shown in Figure 24.11. By setting $\sigma_{zz}^{(c)} = N_z / A_c$, with $A_c = \pi D^2/4$, and substituting the axial stress $\sigma_{zz}^{(c)}$ into the equation (4.12), we obtain the new form (The notation adopted here for the circumferential and radial stresses $\sigma_{\theta\theta}^{(c)} = \sigma_{rr}^{(c)} = p$ is motivated by the fact that – for the equilibrium also in the non linear range, the radial stresses emerging at the interface between concrete and FRP jacket have to be equal and so, being this radial stresses technically called *confining pressures*, it results helpful to identify those stress components with the pressure p. Also, the possibility of writing p as a function of the axial force N_z leads to directly estimate the ultimate load of multilayered cylinder and then its compressive capacity) of the pressure p as a function of the force F into the elastic-plastic range, driven by the FRP confining effect:

$$p = \frac{N_z}{A_c} + \frac{3.6}{4} f_{c0} - \frac{3.82}{4}\sqrt{f_{c0}\left(f_{c0} + 2.97\frac{N_z}{A_c}\right)} \tag{24.60}$$

It is worth to note that, as the load N_z increases, after the stress vector has touched the Schleicher curve, the structural element shows an elastic-plastic response, in the sense that the stress in the core runs along the limit yield boundary domain, while the FRP is still in elastic conditions. In order to follow the evolution of the mechanical response in the FRP phase, we note that the axial stress $\sigma_{zz}^{(j)}$ remains constant, with a value practically vanishing if compared with the radial and hoop stresses

$\sigma_{rr}^{(j)}, \sigma_{\theta\theta}^{(j)}$ present in the jacket ($\sigma_{zz}^{(j)} = 4\, kg\, cm^{-2}$ for the case at hand). Into the FRP phase, the displacements, the strains and the stresses are still deducible from the equations above obtained, wherever being the stresses in the elastic range. However, it is necessary to rewrite the boundary conditions in terms of the stresses as follows:

$$\begin{cases} \sigma_{rr}^{(j)}(r = R^{(c)}) = 394.2 + \dfrac{N_z}{A_c} - 34.39\sqrt{147.62 + \dfrac{N_z}{A_c}} \\ \sigma_{rr}^{(j)}(r = R^{(j)}) = 0, \qquad \int_0^{2\pi}\int_{R^{(c)}}^{R^{(j)}} \sigma_{zz}^{(j)} r dr d\theta = 14.66 \end{cases} \tag{24.61}$$

By solving the system respect to the unknown parameters $\varepsilon_0^{(j)}, C_1^{(j)}, C_2^{(j)}$, we obtain their values as functions of the axial load N_z, that is:

$$\begin{aligned} \varepsilon_0^{(j)} &= 0.023 + 7.99\cdot 10^{-8} N_z - 1.89\cdot 10^{-3}\sqrt{147.62 + 5.51\cdot 10^{-3} N_z} \\ C_1^{(j)} &= -43584 - 0.61 N_z + 3803\sqrt{147.62 + 5.51\cdot 10^{-3} N_z} \\ C_2^{(j)} &= \left(-43584 - 0.61\, N_z + 3803\sqrt{147.62 + 5.51\cdot 10^{-3} N_z}\right) i \end{aligned} \tag{24.62}$$

Substitution of (24.62) into the expressions of the strains gives:

$$\begin{aligned} \varepsilon_{rr}^{(j)} &= r^{-6.84}\left(254741 - 22227\sqrt{147.62 + 5.51\cdot 10^{-3} N_z} + 3.56 N_z\right) + \\ &+ r^{4.84}\left(-1.10\cdot 10^{-5} + 9.49\cdot 10^{-7}\sqrt{147.62 + 5.51\cdot 10^{-3} N_z} - 1.52\cdot 10^{-10} N_z\right) + \\ &- 1.10\cdot 10^{-5} + 9.02\cdot 10^{-7}\sqrt{147.62 + 5.51\cdot 10^{-3} N_z} - 1.44\cdot 10^{-10} N_z \\ \varepsilon_{\theta\theta}^{(j)} &= r^{-6.84}\left(-43584 + 3803\sqrt{147.62 + 5.51\cdot 10^{-3} N_z} - 0.61 N_z\right) + \\ &+ r^{4.84}\left(-1.86\cdot 10^{-6} + 1.62\cdot 10^{-7}\sqrt{147.62 + 5.51\cdot 10^{-3} N_z} - 2.60\cdot 10^{-11} N_z\right) + \\ &- 1.10\cdot 10^{-5} + 9.02\cdot 10^{-7}\sqrt{147.62 + 5.51\cdot 10^{-3} N_z} - 1.45\cdot 10^{-10} N_z \\ \varepsilon_{zz}^{(j)} &= 0.023 + 3.03\cdot 10^{-7} N_z - 1.89\cdot 10^{-3}\sqrt{147.62 + 5.51\cdot 10^{-3} N_z} \end{aligned} \tag{24.63}$$

as well as the stresses become:

$$\begin{aligned} \sigma_{rr}^{(j)} &= r^{-6.84}\left(7.40\cdot 10^{9} + 103475 N_z - 6.46\cdot 10^{8}\sqrt{147.62 + 5.51\cdot 10^{-3} N_z}\right) + \\ &+ r^{4.84}\left(-0.36 - 4.97\cdot 10^{-6} N_z + 0.031\sqrt{147.62 + 5.51\cdot 10^{-3} N_z}\right) + \\ &+ 49.71 - 4.08\sqrt{147.62 + 5.51\cdot 10^{-3} N_z} + 6.55\cdot 10^{-4} N_z \\ \sigma_{\theta\theta}^{(j)} &= r^{-6.84}\left(-4.33\cdot 10^{10} - 604800 N_z - 3.77\cdot 10^{9}\sqrt{147.62 + 5.51\cdot 10^{-3} N_z}\right) + \\ &+ r^{4.84}\left(-2.07 - 2.90\cdot 10^{-5} N_z + 0.181\sqrt{147.62 + 5.51\cdot 10^{-3} N_z}\right) + \\ &+ 49.71 - 4.08\sqrt{147.62 + 5.51\cdot 10^{-3} N_z} + 6.54\cdot 10^{-4} N_z \\ \sigma_{zz}^{(j)} &= r^{-6.84}\left(4.39\cdot 10^{8} + 6137 N_z + 3.83\cdot 10^{7}\sqrt{147.62 + 5.51\cdot 10^{-3} N_z}\right) + \\ &+ r^{4.84}\left(-0.029 - 4.01\cdot 10^{-7} N_z + 2.5\cdot 10^{-3}\sqrt{147.62 + 5.51\cdot 10^{-3} N_z}\right) + \\ &141.68 - 11.64\sqrt{147.62 + 5.51\cdot 10^{-3} N_z} + 1.87\cdot 10^{-3} N_z \end{aligned} \tag{24.64}$$

The final goal is now to determine the load N_z producing the collapse of the FRP, say the limit load under which the whole concrete specimen collapses. To make this, as detailed in the previous section, we use for the FRP sheet the elastic-brittle criterion based on the Tsai-Hill yield surface, written in the plane of the significant principal stresses $\sigma_{rr}^{(j)}$ and $\sigma_{\theta\theta}^{(j)}$. The explicit form of this criterion is rewritten down:

$$\left(\frac{\sigma_I}{\sigma_{xxu}}\right)^2+\left(\frac{\sigma_{II}}{\sigma_{yyu}}\right)^2-\frac{\sigma_I\sigma_{II}}{\sigma_{xxu}^2}\le 1 \tag{24.65}$$

where $\sigma_I \equiv \sigma_{\theta\theta}, \sigma_{II} \equiv \sigma_{rr}$, and $\{\sigma_{xxu}, \sigma_{yyu}\}$ represent the uniaxial compressive strength of the fibre and the tensile strength in the radial direction of FRP, respectively. For the present case, by considering the values suggested by literature for the FRP [27], it was estimated:

$$\sigma_{xxu}=1.577\times 10^4\, kg\, cm^{-2}, \quad \sigma_{yyu}=1.3\times 10^2\, kg\, cm^{-2}, \tag{24.66}$$

where, as it will be considered later, the ultimate strength σ_{yyu} has to be assumed variable in the range $\sigma_{yyu}\in\left[1.3\cdot 10^2, 4.0\cdot 10^2\right]$, due to some variability of the experimental measures related to the dependence of this parameter on the in situ practical application and manufacturing of the FRP tissue. The assumption of brittleness of the FRP, in agreement with the experience of laboratory tests, and the axial-symmetry of the problem, lead to limit the analysis of the failure of the orthotropic jacket phase at those points where the overall stress state in the FRP reaches the Tsai-Hill yield surface, that is at the interface between concrete and first layer of FRP material. Thus, by equating there the radial stresses, and by involving the adopted anisotropic criterion, we obtain the following collapse load, $N_z^{ult}=115306\, kg$, in correspondence of which the strains and stresses in the jacket assume the values:

$$\begin{aligned}&\varepsilon_{rr}=-4.01\cdot 10^{-3}, \quad \varepsilon_{\theta\theta}=12.75\cdot 10^{-3}, \quad \varepsilon_{zz}=-5.03\cdot 10^{-3},\\ &\sigma_{rr}=-67.29 kg/cm^2, \quad \sigma_{\theta\theta}=13460 kg/cm^2, \quad \sigma_{zz}=-10.28 kg/cm^2\end{aligned} \tag{24.67}$$

As numerical example, we also report the corresponding critical values for the case in which the ultimate strength of the FRP in radial direction changes:

$$\sigma_{xxu}=15770 kg/cm^2, \quad \sigma_{yyu}=400 kg/cm^2, \tag{24.68}$$

from which, by following an analogous procedure, we calculate a collapse load determining the brittle failure of the FRP, equal to $N_z^{ult}=119895 kg$, while the strain and stress component at this state are:

$$\begin{aligned}&\varepsilon_{rr}=-4.61\cdot 10^{-3}, \quad \varepsilon_{\theta\theta}=14.62\cdot 10^{-3}, \quad \varepsilon_{zz}=-5.57\cdot 10^{-3},\\ &\sigma_{rr}=-77.13 kg/cm^2, \quad \sigma_{\theta\theta}=15435 kg/cm^2, \quad \sigma_{zz}=-10.61 kg/cm^2\end{aligned} \tag{24.69}$$

Moreover, we also report the corresponding critical values for the case in which the ultimate strength of the FRP in radial direction changes:

$$\sigma_{xxu}=15770 kg/cm^2, \quad \sigma_{yyu}=50 kg/cm^2, \tag{24.70}$$

from which, by following an analogous procedure, we calculate a collapse load determining the brittle failure of the FRP, equal to $N_z^{ult}=103056 kg$, while the strain and stress component at this state are:

$$\begin{aligned}&\varepsilon_{rr}=-2.48\cdot 10^{-3}, \quad \varepsilon_{\theta\theta}=8\cdot 10^{-3}, \quad \varepsilon_{zz}=-3.65\cdot 10^{-3},\\ &\sigma_{rr}=-42.19 kg/cm^2, \quad \sigma_{\theta\theta}=8441 kg/cm^2, \quad \sigma_{zz}=-9.42 kg/cm^2\end{aligned} \tag{24.71}$$

Finally, it is important to note that, if the concrete is confined by means of three layers of FRP tissue, exhibits an increasing of its compressive limit load of about the 70 %. This kind of effect is already well known from the qualitative point of view and quantitatively registered by several authors by means of laboratory tests. Also, the obtained solution furnishes predictions about the strain fields very closely to the experimental tests [25]. It is worth to also highlight that this

increasing compressive strength can be significantly greater, if the number of FRP sheets and the tensile strength of the tissue increase (see Figure 24.8 and [19]). It is easy to verify that the same result, in terms of ultimate compressive strength of the concrete, can be reached straightforwardly if the predicting formula (24.43) is considered, by setting the parameters as assumed in the present example.

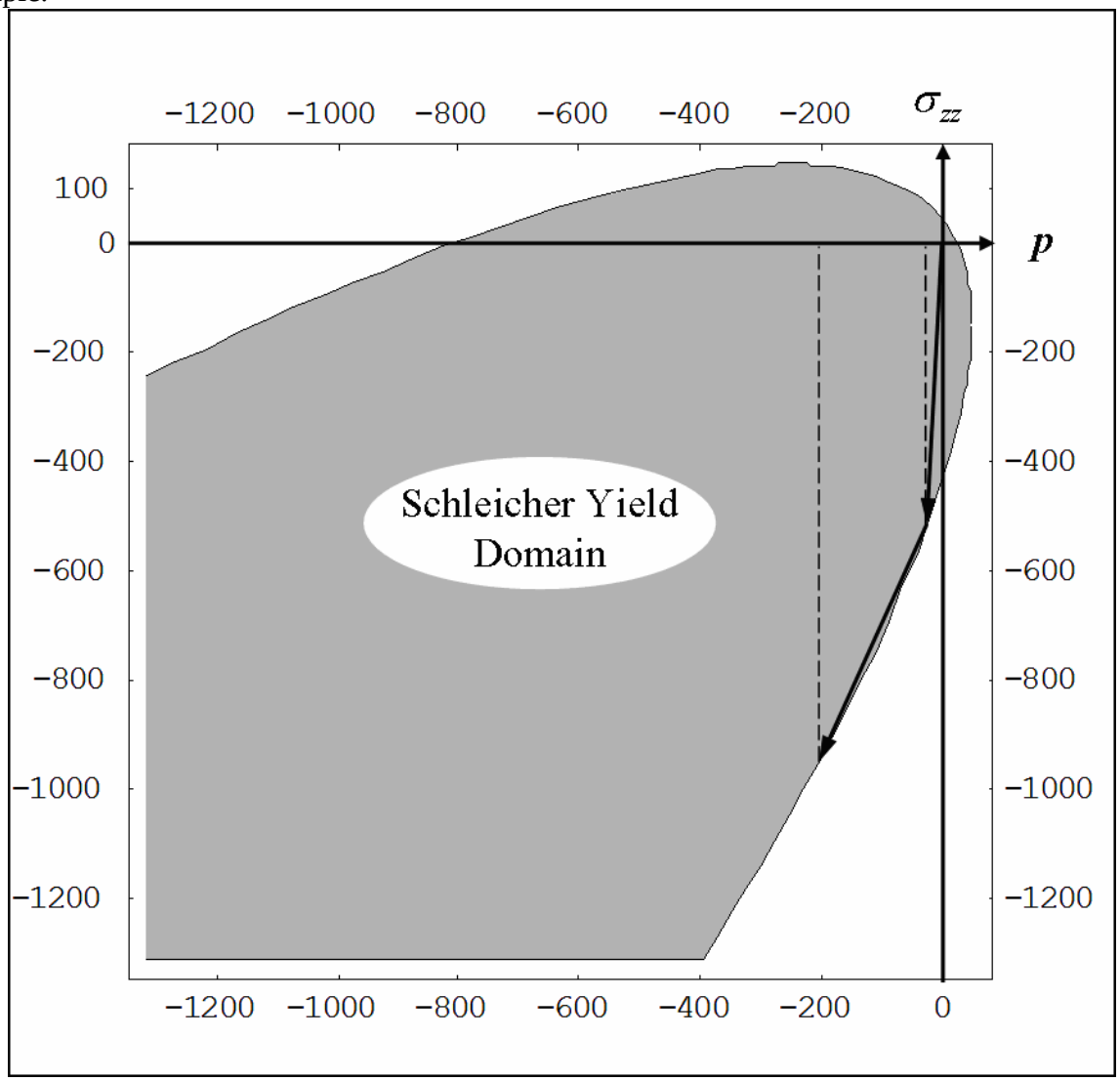

Figure 24.11 - *Schleicher yield criterion in the two-dimensional space* $\{\sigma_{33} - p\}$*: stress vector at the elastic limit and admissible stress path on the plastic boundary domain.*

24.7.3. Direct estimating of the FRP overall thickness by using the proposed design formulae

In order to complete the example application, in the following it will be shown the technical procedure for designing the thickness t of the FRP sheet confining a cylindrical concrete specimen. To make this, let us assume the following geometrical and mechanical parameters:

$R = 15\,cm, \sigma_c = 250 kg/cmq,\ k = 2,\ \alpha = \sigma_t / \sigma_c = 0.1,\ \beta = \sigma_{yyu} / \sigma_{\theta u} = 0.02,\quad \sigma_{\theta u} = 16000\,kg/cmq$

For the present case, formula (24.46) gives $\xi = \frac{\sigma_c}{\sigma_{xxu}}\left[k + 1 - \alpha - \sqrt{1 + (\alpha - 1)(\alpha - 3k)}\right] = 0.00606$, and - by substituting ξ into (24.45), it is easy to verify that the thickness $t = 0.095 cm$. Thus, one can note that the initial unconfined compressive load was $N_z^{ult} = \frac{\pi D^2}{4}\sigma_c = 176715 kg$, while – due to the obtained FRP thickness, the final ultimate compressive load is actually increased, reaching two times the initial value, that is: $\bar{N}_z^{ult} = 2\,N_z^{ult} = 353430\,kg$.

24.8. Conclusions

In the present chapter it is developed a mathematical strategy able to obtain analytical elastic and post-elastic solutions for multilayered cylinder composed by cylindrically orthotropic phases, constituted by a central isotropic core and n hollow anisotropic phases. The treatment of the problem within the elastic range is formulated by invoking the classical Complex Potential Theory for anisotropic materials and using a suitable rearrangement of the equations. In this way, due to the axis-symmetry of both the object geometry and the load condition, the Boundary Value Problem (BVP) is reduced to an algebraic one, governed by a matrix whose order is depending upon the number of hollow phases and whose coefficients are explicitly related to the geometrical and mechanical parameters of the object. Afterwards, with the aim of studying cylindrical concrete specimens reinforced by means of Fibre Reinforced Polymeric sheets in compression, the found elastic solutions are extended to the post-elastic range, by investigating the evolution of the stress field when the core is characterized by an Intrinsic Curve or Schleicher-like elastic-plastic response with associate flow rule and the cylindrically orthotropic hollow phase obeys to an elastic-brittle Tsai-Hill anisotropic yield criterion. By following a Limit Analysis step-by-step procedure, an analytical predictive formula for estimating the overall collapse mechanism, the concrete ultimate compressive strength and the confining pressure effect are derived, showing that the compressive ultimate strength is a function of the geometrical ratio $R^c t^{-1}$ and of the ultimate stresses in both concrete and FRP, only. The results are finally compared with several experimental literature data, highlighting the very good agreement between the theoretical predictions and the laboratory measurements. The opinion of the Authors is that this strategy can be usefully adopted for designing new FRP concrete elements or as assessment tool in the treatment of restored civil structures, as well as for performing sensitivity analyses in other more general contexts

24.9. References

[1] Liew, K.M., Kitipornchai, S., Zhang, X.Z., Lim, C.W., (2003), Analysis of the thermal stress behaviour of functionally graded hollow circular cylinders, International Journal of Solids and Structures, vol. 40, 2355-2380.

[2] Shao, Z. S., (2005), Mechanical and thermal stresses of a functionally graded circular hollow cylinder with finite length, International Journal of Pressure Vessels an Piping, vol. 82, 155-163.

[3] Mian, M., Abid, Spencer, A. J. M., (1998), Exact solutions for functionally graded and laminated elastic materials, J. Mech. Phys. Solids, Vol. 46, n. 12, 2283-2295.

[4] Fraldi, M, Cowin, S. C., (2004), Inhomogeneous elastostatic problem solutions constructed from stress-associated homogeneous solutions, Journal of the Mechanics and Physics of Solids, 52, 2207-2233.

[5] Alshits, V. I., Kirchner, O. K., (2001). Cylindrically anisotropic, radially inhomogeneous elastic materials. Proc. Roy. Soc. Lond. A457, 671-693.

[6] Chouchaoui, C. S., Ochoa, O. O. (1999), Similitude study for a laminated cylindrical tube under tensile, torsion, bending, internal and external pressure. Part I: governing equations, Composite Structures, 44, 221-229.

[7] Chen, T., Chung, C. T., Lin, W. L., (2000), A revisit of a cylindrically anisotropic tube subjected to pressuring, shearing, torsion, extension and a uniform temperature change, International Journal of Solids and Structures, 37, 5143-5159.

[8] Tarn, J. Q., (2001), Exact solutions for functionally graded anisotropic cylinders subjected to thermal and mechanical loads, International Journal of Solids and Structures, 38, 8189-8206.

[9] Tarn, J. Q., Wang, Y. M., (2001), Laminated composite tubes under extension, torsion, bending, shearing and pressuring: a state space approach, International Journal of Solids and Structures, 38, 9053-9075.

[10] Lekhnitskii, S. G., (1981), Theory of Elasticity of an Anisotropic Body, Mir, Moscow.

[11] Huang, C. H., Dong, S. B., (2001), Analysis of laminated circular cylinders of materials with the most general form of cylindrical anisotropy. I. Axially symmetric deformations. International Journal of Solids and Structures, 38, 6163-6182.

[12] Ting, T. C. T., (1999), Pressuring, shearing, torsion and extension of a circular tube or bar of cylindrically anisotropic material, Proc. Roy. Soc. Lond. A452, 2397-2421.
[13] Love, A. E. H., (1944), A treatise on the mathematical theory of elasticity, Dover Publications, Inc, New York.
[14] Fraldi, M., Nunziante, L., Carannante, F. (2007), *Axis-symmetrical Solutions for n-plies Functionally Graded Material Cylinders under Strain no-Decaying Conditions*, J. Mech. of Adv. Mat. and Struct. Vol. 14 (3), pp. 151-174 - DOI: 10.1080/15376490600719220
[15] M. Fraldi, L. Nunziante, F. Carannante, A. Prota, G. Manfredi, E. Cosenza (2008), *On the Prediction of the Collapse Load of Circular Concrete Columns Confined by FRP*, Journal Engineering structures, Vol. 30, Issue 11, November 2008, Pages 3247-3264 - DOI: 10.1016/j.engstruct.2008.04.036
[16] Fraldi, M., Nunziante, L., Chandrasekaran, S., Carannante, F., Pernice, MC. (2009), *Mechanics of distributed fibre optic sensors for strain measurements on rods*, Journal of Structural Engineering, 35, pp. 323-333, Dec. 2008- Gen. 2009
[17] M. Fraldi, F. Carannante, L. Nunziante (2012), *Analytical solutions for n-phase Functionally Graded Material Cylinders under de Saint Venant load conditions: Homogenization and effects of Poisson ratios on the overall stiffness*, Composites Part B: Engineering, Volume 45, Issue 1, February 2013, Pages 1310–1324
[18] Nunziante, L., Gambarotta, L., Tralli, A., *Scienza delle Costruzioni*, 3° Edizione, McGraw-Hill, 2011, ISBN: 9788838666971
[19] Christensen, R. M., (1997), Stress based Yield/Failure criteria for fiber composites, International Journal Solid and Structures, vol. 34, No. 5, pp. 529-543.
[20] Gurtin, M. E., (1972), The Linear Theory of Elasticity, Handbbuch der Physik, Springer, Berlin.
[21] Ting, T.C.T., (1996), Anisotropic Elasticity- Theory and Applications. Oxford University Press.
[22] Cowin, S. C., Fraldi, M., (2005), On singularities associated with the curvilinear anisotropic elastic symmetries, International Journal of Non-Linear Mechanics, 40, 361–371.
[23] Wu, G., Lu, Z.T., Wu, Z.S., (2006), Strength and ductility of concrete cylinders confined with FRP composites, Construction and Building Materials, vol. 20 , pp. 134–148.
[24] Wu, G., Wu, Z.S., Lu, Z.T., (2007), Design-oriented stress–strain model for concrete prisms confined with FRP composites, Construction and Building Materials vol. 21, pp. 1107–1121.
[25] Xiao, Y., Wu, H., (2000), Compressive behaviour of concrete confined by carbon fiber composite jackets, Journal of materials in Civil Engineering , pp. 139-146.
[26] Green, M. F., Bisby, L. A., Fam, A. Z., Kodur, V. K. R., (2006), FRP confined concrete columns: Behaviour under extreme conditions, Cement & Concrete Composites, vol. 28 , pp. 928–937.
[27] Karabinis, A.I., Rousakis, T.C., (2002), Concrete confined by FRP material: a plasticity approach, Engineering Structures, vol. 24, pp. 923–932.
[28] Li, G., (2006), Experimental study of FRP confined concrete cylinders, Engineering Structures, vol. 28, pp. 1001–1008.
[29] Prota, A., Manfredi, G., Cosenza, E., (2006), Ultimate behavior of axially loaded RC wall-like columns confined with GFRP, Composites: Part B, 37, pp. 670-678.
[30] Debotton, G., (1995), The effective yield strength of fiber-reinforced composites, International Journal Solids and Structures, vol. 32, No. 12, pp. 1743-1757.
[31] Voyiadjis, G.Z., Thiagarajan, G., (1995), An anisotropic yield surface model for directionally reinforced metal-matrix composites, International Journal of Plasticity , vol. 11, No.8 , pp. 867-894.
[32] Nanni, A., (2003), North American design guidelines for concrete reinforcement and strengthening using FRP: principles, applications and unresolved issues, Construction and Building Materials, vol. 17, pp. 439–446.

CHAPTER XXV
METALLIC PIPELINES INSULATED BY CERAMIC MATERIAL

25.1. Introduction

FGM components are generally constructed to sustain elevated temperatures and severe temperature gradients. Low thermal conductivity, low coefficient of thermal expansion and core ductility have enabled the FGM material to withstand higher temperature gradients for a given heat flux. Examples of structures undergo extremely high temperature gradients are plasma facing materials, propulsion system of planes, cutting tools, engine exhaust liners, aerospace skin structures, incinerator linings, thermal barrier coatings of turbine blades, thermal resistant tiles, and directional heat flux materials. Continuously varying the volume fraction of the mixture in the FGM materials eliminates the interface problems and mitigating thermal stress concentrations and causes a more smooth stress distribution. Extensive thermal stress studies made by Noda reveal that the weakness of the fiber reinforced laminated composite materials, such as delamination, huge residual stress, and locally large plastic deformations, may be avoided or reduced in FGM materials (Noda, 1991). Tanigawa presented an extensive review that covered a wide range of topics from thermo-elastic to thermo-inelastic problems. He compiled a comprehensive list of papers on the analytical models of thermo-elastic behavior of FGM (Tanigawa, 1995). The analytical solution for the stresses of FGM in the one-dimensional case for spheres and cylinders are given by Lutz and Zimmerman (Lutz & Zimmerman, 1996 & 1999). These authors consider the non-homogeneous material properties as linear functions of radius. Obata presented the solution for thermal stresses of a thick hollow cylinder, under a two-dimensional transient temperature distribution, made of FGM (Obata et al., 1999). Sutradhar presented a Laplace transform Galerkin BEM for 3-D transient heat conduction analysis by using the Green's function approach where an exponential law for the FGMs was used (Sutradhar et al., 2002). Kim and Noda studied the unsteady-state thermal stress of FGM circular hollow cylinders by using of Green's function method (Kim & Noda, 2002). Reddy and co-workers carried out theoretical as well as finite element analyses of the thermo-mechanical behaviour of FGM cylinders, plates and shells. Geometric non-linearity and effect of coupling item was considered for different thermal loading conditions (Praveen & Reddy, 1998, Reddy & Chin, 1998, Paraveen et al., 1999, Reddy, 2000, Reddy & Cheng, 2001). Shao and Wang studied the thermo-mechanical stresses of FGM hollow cylinders and cylindrical panels with the assumption that the material properties of FGM followed simple laws, e.g., exponential law, power law or mixture law in thickness direction. An approximate static solution of FGM hollow cylinders with finite length was obtained by using of multi-layered method; analytical solution of FGM cylindrical panel was carried out by using the Frobinus method; and analytical solution of transient thermo-mechanical stresses of FGM hollow cylinders were derived by using the Laplace transform technique and the power series method, in which effects of material gradient and heat transfer coefficient on time-dependent thermal mechanical stresses were discussed in detail (Shao, 2005, Shao & Wang, 2006, Shao & Wang, 2007). Similarly, Ootao and Tanigawa obtained the analytical solutions of unsteady-state thermal stress of FGM plate and cylindrical panel due to non-uniform heat supply (Ootao & Tanigawa, 1999, 2004, 2005). Using the multi-layered method and through a novel limiting process, Liew obtained the analytical solutions of steady-state thermal stress in FGM hollow circular cylinder (Liew & et al., 2003). Using finite difference method, Awaji and Sivakuman studied the transient thermal stresses of a FGM hollow circular cylinder, which is cooled by surrounding medium (Awaji & Sivakuman, 2001). Ching and Yen evaluated the transient thermoelastic deformations of 2-D functionally graded beams under non-uniformly convective heat supply (Ching & Yen, 2006). By using the Hermitian transfinite element method, Mohammad Azadi et al., nonlinear transient heat transfer and thermoelastic stress analyses are performed for thick-walled FGM cylinder which materials are temperature-dependent. Time variations of the temperature, displacements, and stresses are obtained through a numerical Laplace inversion. Finally, results obtained considering the temperature-dependency of the material properties. In this paper those results are the temperature distribution and the radial and circumferential stresses are investigated

versus time, geometrical parameters and index of power law (N) and then they are compared with those derived based on temperature independency assumption. Two main novelties of this research are incorporating the temperature-dependency of the material properties and proposing a numerical transfinite element procedure that may be used in Picard iterative algorithm to update the material properties in a highly nonlinear formulation. In contrast to before researches, second order elements are employed. Therefore, proposed transfinite element method may be adequately used in problems where time integration method is not recommended because of truncation errors (e.g. coupled thermo-elasticity problems with very small relaxation times) or where improper choice of time integration step may lead to loss of the higher frequencies in the dynamic response. Also, accumulated errors that are common in the time integration method and in many cases lead to remarkable errors, numerical oscillations, or instability, do not happen in this technique.
In this chapter it is reported a analytical thermo-elastic solution in closed form for bi-layer hollow cylinder subjected to time-dependent boundary conditions. It is assumed that each hollow cylinder is composed by a homogeneous and thermo-isotropic material, characterized by different mechanical and thermal parameters, i.e. modulus of elasticity, thermal expansion coefficient and thermal conductivity. Moreover, these material properties in each hollow cylinder are assumed to be temperature-independent. In other words, the bi-layer hollow cylinder is considered as a classical composite material whose properties abruptly vary from one hollow cylinder to the other. In particular, it is obtained a new analytical solution for a bi-layer hollow cylinder, constituted by two phases: Ceramic (Si_3N_4) and Metal ($Ti-6Al-4V$) subjected to heat flux on inner surface.

25.2. Bi-layer hollow cylinder in plane strain: Basic equations

In this paragraph, the one-dimensional quasi-static uncoupled thermo-elastic problem of a bi-layered cylinders with time-dependent boundary conditions is considered. The medium is without body forces and heat generation. The analytical solution is obtained by applying the method of separation of variables. It is considered a solid composed of 2 fictitious layers constituted by 2 hollow cylinder phases. The external radius and internal radius of the bi-layer hollow cylinder are denoted by $R^{(2)}$ and $R^{(0)}$, respectively. The radius at interface between the phase 1 and the phase 2 is denoted with $R^{(1)}$. The mechanical and thermal properties of each layer are assumed to be homogeneous and isotropic . Cylindrical coordinates r, θ and z are used in this analysis. The bi-layer hollow cylinder is subjected to constant heat flux on internal surface, but convection condition on external surface is considered. The initial temperature (for t = 0) of the hollow cylinder is $T_0 = T_R = const$ where $T_R > 0$. In isotropic-thermal elasticity case, the equations field to satisfy in uncoupled thermo-elastic problem in plane strain are given by:

$$\begin{cases} \left[r^{-1}\left(r\, u_r^{(i)} \right)_{,r} \right]_{,r} = \alpha^{(i)} \left(\dfrac{3\lambda^{(i)} + 2\mu^{(i)}}{2\mu^{(i)} + \lambda^{(i)}} \right) = \alpha^{(i)} \left(\dfrac{1+\nu^{(i)}}{1-\nu^{(i)}} \right) T_{,r}^{(i)} \\ T_{,rr}^{(i)} + r^{-1} T_{,r}^{(i)} = \dfrac{\rho^{(i)} c^{(i)}}{k^{(i)}} T_{,t}^{(i)} = \dfrac{T_{,t}^{(i)}}{\kappa^{(i)}} \end{cases} \quad \begin{matrix} R^{(i-1)} \le r \le R^{(i)}, \quad \forall t \ge 0, \\ \forall i \in \{1,2\} \end{matrix} \tag{25.1}$$

where $\kappa^{(1)}, \kappa^{(2)}$ are the thermal diffusivity for phase (1) and (2), respectively. By solving the Fourier's equation reported in second equation of (25.1) with method separation of variables, and by substituting the function of temperature $T^{(i)}(r,t)$ in first equation of (25.1), and by integration in two time this equation respect to variable r , the explicit displacement solution is obtained:

$$u_r^{(i)}(r,t) = \frac{\alpha^{(i)}}{r} \left(\frac{3\lambda^{(i)} + 2\mu^{(i)}}{\lambda^{(i)} + 2\mu^{(i)}} \right) \int r\, T^{(i)}(r,t)\, dr + r\, f_1^{(i)}(t) + \frac{f_2^{(i)}(t)}{r}, \quad \forall i \in \{1,2,....,n\} \tag{25.2}$$

where $f_1^{(i)}(t)$, $f_2^{(i)}(t)$ are unknown functions of the time to determine. The boundary conditions at interface surface ($r = R^{(1)}$) between two phases to satisfy, as showed in Chapter XXI, are given by:

$$\begin{cases} u_r^{(1)}(r=R^{(1)},t)=u_r^{(2)}(r=R^{(1)},t) \\ \sigma_{rr}^{(1)}(r=R^{(1)},t)=\sigma_{rr}^{(2)}(r=R^{(1)},t) \end{cases} \quad \forall t\geq 0 \tag{25.3}$$

The bi-layer hollow cylinder is not loaded on the inner and the outer cylindrical boundary surfaces. Then, the equilibrium equations for the tractions on boundary surface are give:

$$\sigma_{rr}^{(1)}(r=R^{(0)},t)=0, \quad \sigma_{rr}^{(2)}(r=R^{(2)},t)=0 \quad \forall t\geq 0 \tag{25.4}$$

Temperature boundary and continuity conditions are written at the interfaces between two phases of bi-layer hollow cylinder:

$$\begin{cases} T^{(1)}(r=R^{(1)},t)=T^{(2)}(r=R^{(1)},t) \\ k^{(1)}T_{,r}^{(1)}(r=R^{(1)},t)=k^{(2)}T_{,r}^{(2)}(r=R^{(1)},t) \end{cases} \quad \forall t\geq 0, \tag{25.5}$$

Moreover, the bi-layer hollow cylinder is subjected to uniform heat input q_0 applied on internal surface $r=R^{(0)}$, starting to initial temperature in composite solid equal to $T_0=T_R=const$, while the surface $r=R^{(2)}$ is exposed, for t >0, to an ambient at T_0 temperature through a uniform boundary conductance h_c :

$$\begin{cases} -k^{(1)}T_{,r}^{(1)}(r=R^{(0)},t)=q_i=q_0, \\ -k^{(2)}T_{,r}^{(2)}(r=R^{(2)},t)=q_e=h_c\left[T^{(2)}(r=R^{(2)},t)-T_R\right] \end{cases} \quad \forall t\geq 0 \tag{25.6}$$

The initial condition for temperature functions is given by:

$$T^{(i)}=T_R; \quad R^{(i-1)}<r<R^{(i)}, \quad \forall i\in\{1,2\}, \; t=0, \tag{25.7}$$

where $T_0=T_R$ is a suitable chosen reference temperature in initial condition (for t = 0).

25.3. Uncoupled thermo-elastic analysis in bi-layer hollow cylinder

In this case, the heat conduct problem involving a non-homogeneous boundary condition and, in particular, with the heat input specified over the entire boundary surface. It is necessary writing the temperature solution, in both phase of bi-layer, in the follows form (see Chapter VII and Chapter XXI) :

$$T^{(i)}(r,t)=T_0+T_S^{(i)}(r)+T_C^{(i)}(r,t), \quad \forall i\in\{1,2\} \tag{25.8}$$

where the functions $T_S^{(1)}(r), T_S^{(2)}(r)$ satisfy the field equations:

$$\frac{d^2T_S^{(i)}}{dr^2}+\frac{1}{r}\frac{dT_S^{(i)}}{dr}=0; \quad R^{(i-1)}\leq r\leq R^{(i)}, \quad \forall i\in\{1,2\} \tag{25.9}$$

and these functions must be satisfy the following boundary conditions, also :

$$\begin{cases} -k^{(1)}\dfrac{dT_S^{(1)}(r)}{dr}=-k^{(2)}\dfrac{dT_S^{(2)}(r)}{dr}, & r=R^{(1)} \\ T_S^{(1)}(r)=T_S^{(2)}(r), & r=R^{(1)} \\ -k^{(0)}\dfrac{dT_S^{(1)}(r)}{dr}=q_0, & r=R^{(0)} \\ -k^{(2)}\dfrac{dT_S^{(2)}(r)}{dr}=h_c\left[T_S^{(2)}(r)-T_0\right], & r=R^{(n)} \end{cases} \tag{25.10}$$

The functions $T_C^{(1)}(r,t), T_C^{(2)}(r,t)$ satisfy the field equations:

$$\frac{\partial^2T_C^{(i)}(r,t)}{\partial r^2}+\frac{1}{r}\frac{\partial T_C^{(i)}(r,t)}{\partial r}=\frac{1}{\kappa^{(i)}}\frac{\partial T_C^{(i)}(r,t)}{\partial t}; \quad \begin{matrix} R^{(i-1)}\leq r\leq R^{(i)}, \forall t\geq 0 \\ \forall i\in\{1,2\} \end{matrix} \tag{25.11}$$

and these functions must be satisfy the following boundary conditions, also :

$$\begin{cases} -k^{(1)}\dfrac{\partial T_C^{(1)}(r,t)}{\partial r} = -k^{(2)}\dfrac{\partial T_C^{(2)}(r,t)}{\partial r}, & r = R^{(1)} \\ T_C^{(1)}(r,t) = T_C^{(2)}(r,t), & r = R^{(1)} \end{cases} \quad \forall t \geq 0, \tag{25.12}$$

$$\begin{cases} -k^{(1)}\dfrac{\partial T_C^{(1)}(r,t)}{\partial r} = 0, & r = R^{(0)} \\ -k^{(2)}\dfrac{\partial T_C^{(2)}(r,t)}{\partial r} = h_c T_C^{(2)}(r,t), & r = R^{(2)} \end{cases} \quad \forall t \geq 0 \tag{25.13}$$

The initial condition for temperature functions becomes:

$$T_C^{(i)}(r,t) = -T_S^{(i)}(r), \quad R^{(i-1)} \leq r \leq R^{(i)}, \ t = 0, \ \ \forall i \in \{1,2\} \tag{25.14}$$

The solutions of differential equation (25.9) is given by:

$$T_S^{(i)}(r) = C^{(i)} + D^{(i)} \log r, \quad \forall i \in \{1,2\} \tag{25.15}$$

where $C^{(1)}, D^{(1)}, C^{(2)}, D^{(2)}$ are 4 unknown parameters to determine. By solving algebraic system composed by equations (25.10), we obtain integration constants $C^{(1)}, D^{(1)}, C^{(2)}, D^{(2)}$:

$$\begin{aligned} C^{(1)} &= \frac{q_0 R^{(0)}}{k^{(1)}}\left[\log R^{(1)} + \frac{k^{(1)}}{k^{(2)}}\log\frac{R^{(2)}}{R^{(1)}} + \frac{k^{(1)}}{h_c R^{(2)}}\right], \quad D^{(1)} = -\frac{q_0 R^{(0)}}{k^{(1)}}, \\ C^{(2)} &= \frac{q_0 R^{(0)}}{k^{(2)}}\left[\log R^{(2)} + \frac{k^{(2)}}{h_c R^{(2)}}\right], \quad D^{(2)} = -\frac{q_0 R^{(0)}}{k^{(2)}}, \end{aligned} \tag{25.16}$$

The solution to the problem for T_C is found in much the same says way as was followed in Chapter XXI. The problem is therefore on with homogeneous differential equation and boundary conditions and may be treated by the method separation of variables as showed in Chapter XXI. The solutions of differential equation (25.11) is given by:

$$T_C^{(i)}(r,t) = \left[A^{(i)} J_0\left(\omega\beta^{(i)} r\right) + B^{(i)} Y_0\left(\omega\beta^{(i)} r\right)\right] e^{-\kappa^{(i)}\beta^{(i)2}\omega^2 t} \quad \forall i \in \{1,2\} \tag{25.17}$$

where $A^{(i)}, B^{(i)}, \omega$ are constants parameter to determine, the coefficient $\beta^{(i)} = \sqrt{\kappa^{(1)}/\kappa^{(i)}}$. The boundary conditions (25.12) for temperature function $T_C^{(i)}(r,t)$ are reported below:

$$\begin{cases} A^{(1)} J_0\left(\omega\beta^{(1)} R^{(1)}\right) + B^{(1)} Y_0\left(\omega\beta^{(1)} R^{(1)}\right) - \left[A^{(2)} J_0\left(\omega\beta^{(2)} R^{(1)}\right) + B^{(2)} Y_0\left(\omega\beta^{(2)} R^{(1)}\right)\right] = 0 \\ k^{(1)}\beta^{(1)}\left[A^{(1)} J_1\left(\omega\beta^{(1)} R^{(1)}\right) + B^{(1)} Y_1\left(\omega\beta^{(1)} R^{(1)}\right)\right] + \\ \qquad - k^{(2)}\beta^{(2)}\left[A^{(2)} J_1\left(\omega\beta^{(2)} R^{(1)}\right) + B^{(2)} Y_1\left(\omega\beta^{(2)} R^{(1)}\right)\right] = 0 \end{cases} \tag{25.18}$$

The boundary conditions on the inner and the outer surface (25.13) become:

$$\begin{cases} A^{(1)} J_1\left(\omega\beta^{(1)} R^{(0)}\right) + B^{(1)} Y_1\left(\omega\beta^{(1)} R^{(0)}\right) = 0 \\ A^{(2)} J_1\left(\omega\beta^{(2)} R^{(2)}\right) + B^{(2)} Y_1\left(\omega\beta^{(2)} R^{(2)}\right) = 0 \end{cases} \tag{25.19}$$

By first equation of (25.19), we determine $B^{(1)}$ as function of $A^{(1)}$ as follows:

$$B^{(1)} = -\frac{J_1\left(\omega R^{(0)}\beta^{(1)}\right)}{Y_1\left(\omega R^{(0)}\beta^{(1)}\right)} A^{(1)} \tag{25.20}$$

The equations (25.18) constituted an homogeneous algebraic system, composed by 2 equations, in unknown parameters $A^{(1)}, B^{(1)}, A^{(2)}, B^{(2)}$, which can be written as:

$$\mathbf{\Phi} \cdot \mathbf{X} = \mathbf{0} \tag{25.21}$$

where $\mathbf{X} = [\mathbf{X}^{(1)}, \mathbf{X}^{(2)}]^T$ collect the unknowns sub-vectors, as reported below:

$$\mathbf{X}^{(1)} = \left[A^{(1)} \quad B^{(1)} \right]^T, \quad \mathbf{X}^{(2)} = \left[A^{(2)} \quad B^{(2)} \right]^T, \tag{25.22}$$

and $\mathbf{\Phi}$ is an $2x4$ rectangular matrix, composed by following sub-matrices:

$$\mathbf{\Phi} = \left[\mathbf{\Phi}_1^{(1)} \quad -\mathbf{\Phi}_1^{(2)} \right] \tag{25.23}$$

where $\mathbf{\Phi}_1^{(1)}, \mathbf{\Phi}_1^{(2)}$ are $(2x2)$ square sub-matrices given by:

$$\begin{aligned} \mathbf{\Phi}_1^{(1)} &= \begin{bmatrix} J_0\left(\beta^{(1)}\omega R^{(1)}\right) & Y_0\left(\beta^{(1)}\omega R^{(1)}\right) \\ k^{(1)}\beta^{(1)} J_1\left(\beta^{(1)}\omega R^{(1)}\right) & k^{(1)}\beta^{(1)} Y_1\left(\beta^{(1)}\omega R^{(1)}\right) \end{bmatrix}, \\ \mathbf{\Phi}_1^{(2)} &= \begin{bmatrix} J_0\left(\beta^{(2)}\omega R^{(1)}\right) & Y_0\left(\beta^{(2)}\omega R^{(1)}\right) \\ k^{(2)}\beta^{(2)} J_1\left(\beta^{(2)}\omega R^{(1)}\right) & k^{(2)}\beta^{(2)} Y_1\left(\beta^{(2)}\omega R^{(1)}\right) \end{bmatrix}, \end{aligned} \tag{25.24}$$

The determinant of the matrices (25.24) is given by:

$$\begin{aligned} \det[\mathbf{\Phi}_1^{(1)}] &= k^{(1)}\beta^{(1)}\left[J_0\left(\beta^{(1)}\omega R^{(1)}\right) Y_1\left(\beta^{(1)}\omega R^{(1)}\right) - Y_0\left(\beta^{(i)}\omega R^{(i)}\right) J_1\left(\beta^{(1)}\omega R^{(1)}\right)\right] \neq 0, \\ \det[\mathbf{\Phi}_1^{(2)}] &= k^{(2)}\beta^{(2)}\left[J_0\left(\beta^{(2)}\omega R^{(1)}\right) Y_1\left(\beta^{(2)}\omega R^{(1)}\right) - Y_0\left(\beta^{(2)}\omega R^{(1)}\right) J_1\left(\beta^{(2)}\omega R^{(1)}\right)\right] \neq 0, \end{aligned} \tag{25.25}$$

Then, the matrices (25.24) are invertible and we obtain the vector $\mathbf{X}^{(2)}$ as function of vector $\mathbf{X}^{(1)}$:

$$\mathbf{X}^{(2)} = \mathbf{\Gamma} \cdot \mathbf{X}^{(1)} \tag{25.26}$$

where $\mathbf{\Gamma}$ is an $2x2$ square matrix given by :

$$\mathbf{\Gamma} = \left[\mathbf{\Phi}_1^{(2)} \right]^{-1} \cdot \mathbf{\Phi}_1^{(1)} \tag{25.27}$$

By substituting the solutions (25.26) in boundary conditions (25.19), we obtain vector equations in unknown vector $\mathbf{X}^{(1)}$, as reported below:

$$\mathbf{\Lambda} \cdot \mathbf{X}^{(1)} = \mathbf{0} \tag{25.28}$$

where $\mathbf{\Lambda}$ is an 2x2 square matrix given by :

$$\mathbf{\Lambda} = \begin{bmatrix} \Lambda_{11} & \Lambda_{12} \\ \Lambda_{21} & \Lambda_{22} \end{bmatrix} \tag{25.29}$$

where the components $\Lambda_{11}, \Lambda_{12}, \Lambda_{21}, \Lambda_{22}$ are reported below:

$$\begin{aligned} &\Lambda_{11} = J_1\left(\beta^{(1)}\omega R^{(0)}\right), \ \Lambda_{12} = Y_1\left(\beta^{(1)}\omega R^{(0)}\right), \\ &\begin{bmatrix} \Lambda_{21} \\ \Lambda_{22} \end{bmatrix} = \begin{bmatrix} \beta^{(2)} R^{(2)} J_1\left(\omega\beta^{(2)} R^{(2)}\right) - h_c J_0\left(\omega\beta^{(2)} R^{(2)}\right) \\ \beta^{(2)} R^{(2)} Y_1\left(\omega\beta^{(2)} R^{(2)}\right) - h_c Y_0\left(\omega\beta^{(2)} R^{(2)}\right) \end{bmatrix}^T \cdot \mathbf{\Gamma}, \end{aligned} \tag{25.30}$$

The algebraic system (25.28) admit not trivial solution if the determinant of matrix $[\mathbf{\Lambda}]$ is equal to zero. By imposing this condition, we obtain the transcendental equation in unknown parameter ω:

$$\det[\mathbf{\Lambda}] = 0 \ \Rightarrow \ g(\omega) = 0 \tag{25.31}$$

The roots of this transcendental equation (25.31) are an infinite number such, denoted here by $\omega_m, \ m = 1, 2, ...N$ leading to characteristic values $\lambda_m = -\omega_m^2$. The corresponding characteristic functions $\bar{\varphi}_m^{(1)}(r), \bar{\varphi}_m^{(2)}(r)$ are, as calculated above,

$$\begin{cases} \bar{\varphi}_m^{(1)}(r) = \dfrac{\varphi_m^{(1)}(r)}{A_m^{(1)}} = \dfrac{1}{A_m^{(1)}}\left[J_0(\omega_m r), \ Y_0(\omega_m r)\right] \cdot \mathbf{X}_m^{(1)} \quad (\beta^{(1)} = 1) \\ \bar{\varphi}_m^{(2)}(r) = \dfrac{\varphi_m^{(2)}(r)}{A_m^{(1)}} = \dfrac{1}{A_m^{(1)}}\left[J_0\left(\beta^{(2)}\omega_m r\right), \ Y_0\left(\beta^{(2)}\omega_m r\right)\right] \cdot \left(\mathbf{\Gamma} \cdot \mathbf{X}_m^{(1)}\right) \end{cases} \tag{25.32}$$

The temperature function in two phases can to be written in the follows form:

$$\begin{cases} T^{(1)}(r,t) = \sum_{m=1}^{\infty} \left\{ \left[J_0(\omega_m r),\ Y_0(\omega_m r) \right] \cdot \mathbf{X}_m^{(1)} \right\} e^{-\kappa^{(1)} \omega_m^2 t} & \left(\beta^{(1)} = 1\right) \\ T^{(2)}(r,t) = \sum_{m=1}^{\infty} \left\{ \left[J_0\left(\beta^{(2)} \omega_m r\right),\ Y_0\left(\beta^{(2)} \omega_m r\right) \right] \cdot \left(\boldsymbol{\Gamma} \cdot \mathbf{X}_m^{(1)} \right) \right\} e^{-\kappa^{(2)} \omega_m^2 \beta^{(2)2} t} \end{cases} \tag{25.33}$$

where the vector $\mathbf{X}_m^{(1)} = \left[A_m^{(1)}, B_m^{(1)} \right]^T$ and the unknown constant $B_m^{(1)}$ depends by $A_m^{(1)}$ as showed equations (25.20). The coefficients $A_m^{(1)}$ are determined by applying the initial condition (25.7) that yields the following relationship:

$$A_m^{(1)} = -\frac{\sum_{i=1}^{n} \left[\rho^{(i)} c_v^{(i)} \int_0^{2\pi} \int_{R^{(i-1)}}^{R^{(i)}} r \, \bar{\varphi}_m^{(i)} \, T_s^{(i)}(r) \, dr d\theta \right]}{\sum_{i=1}^{n} \left[\rho^{(i)} c_v^{(i)} \int_0^{2\pi} \int_{R^{(i-1)}}^{R^{(i)}} \left(\bar{\varphi}_m^{(i)} \right)^2 r dr d\theta \right]} \tag{25.34}$$

Finally the temperature functions in two phases are given by:

$$\begin{cases} T^{(1)}(r,t) = T_0 + C^{(1)} + D^{(1)} \log r + \sum_{m=1}^{\infty} \left[A_m^{(1)} J_0(\omega_m r) + B_m^{(1)} Y_0(\omega_m r) \right] e^{-\kappa^{(1)} \omega_m^2 t}, & \left(\beta^{(1)} = 1\right) \\ T^{(2)}(r,t) = T_0 + C^{(2)} + D^{(2)} \log r + \sum_{m=1}^{\infty} \left[A_m^{(2)} J_0\left(\omega_m \beta^{(2)} r\right) + B_m^{(2)} Y_0\left(\omega_m \beta^{(2)} r\right) \right] e^{-\kappa^{(2)} \beta^{(2)2} \omega_m^2 t} \end{cases} \tag{25.35}$$

By substituting the functions (25.35), in equation (25.2), we obtain in explicit the displacement function in any hollow cylindrical phase:

$$\begin{aligned} u_r^{(i)} = {} & G^{(i)} r + \frac{H^{(i)}}{r} + \frac{\beta^{(i)} \zeta^{(i)} r}{2} \left[C^{(i)} + D^{(i)} \left(\log r - \frac{1}{2} \right) \right] + \\ & + \sum_{m=1}^{\infty} \left\{ P_m^{(i)} r + \frac{Q_m^{(i)}}{r} + \frac{\zeta^{(i)}}{\omega_m} \left[A_m^{(i)} J_1\left(\beta^{(i)} \omega_m r\right) + B_m^{(i)} Y_1\left(\beta^{(i)} \omega_m r\right) \right] \right\} e^{-\kappa^{(i)} \omega_m^2 \beta^{(i)2} t} \quad \forall i \in \{1,2\} \end{aligned} \tag{25.36}$$

where the constant $\zeta^{(i)} = \left[\alpha^{(i)} \left(3\lambda^{(i)} + 2\mu^{(i)} \right) \right] \Big/ \left[\beta^{(i)} \left(\lambda^{(i)} + 2\mu^{(i)} \right) \right]$ and the integration constants $G^{(1)}, H^{(1)}, P_m^{(1)}, Q_m^{(1)}, G^{(2)}, H^{(2)}, P_m^{(2)}, Q_m^{(2)}$ are determined by applying the boundary conditions given by equations (25.3) and (25.4). In this case the functions $f_1^{(i)}(t)$, $f_2^{(i)}(t)$, reported in equation (25.2) are given by:

$$f_1^{(i)}(t) = G^{(i)} + \sum_{m=1}^{\infty} P_m^{(i)} e^{-\kappa^{(i)} \omega_m^2 \beta^{(i)2} t}, \quad f_2^{(i)}(t) = H^{(i)} + \sum_{m=1}^{\infty} Q_m^{(i)} e^{-\kappa^{(i)} \omega_m^2 \beta^{(i)2} t}, \quad \forall i \in \{1,2\} \tag{25.37}$$

In explicit the radial, circumferential and axial stress components are given by:

$$\begin{aligned} \sigma_{rr}^{(i)} = {} & 2\left(\lambda^{(i)} + 2\mu^{(i)} \right) G^{(i)} - 2\mu^{(i)} r^{-2} H^{(i)} - \zeta^{(i)} \beta^{(i)} \mu^{(i)} \left[C^{(i)} + D^{(i)} \left(\log r - \frac{1}{2} \right) \right] + \\ & - \alpha^{(i)} \left(3\lambda^{(i)} + 2\mu^{(i)} \right) \left(T_0 - T_R \right) + 2 \sum_{m=1}^{\infty} \left[P_m^{(i)} \left(\lambda^{(i)} + \mu^{(i)} \right) - Q_m^{(i)} \mu^{(i)} r^{-2} \right] e^{-\omega_m^2 \beta^{(i)2} \kappa^{(i)} t} + \\ & + 2\mu^{(i)} \zeta^{(i)} \sum_{m=1}^{\infty} \left\{ \frac{1}{\omega_m r} \left[A_m^{(i)} J_1\left(\omega_m \beta^{(i)} r\right) + B_m^{(i)} Y_1\left(\omega_m \beta^{(i)} r\right) \right] \right\} e^{-\omega_m^2 \beta^{(i)2} \kappa^{(i)} t} \quad \forall i \in \{1,2\} \end{aligned} \tag{25.38}$$

$$\sigma_{\theta\theta}^{(i)} = 2\left(\lambda^{(i)}+2\mu^{(i)}\right)G^{(i)} + 2\mu^{(i)} r^{-2} H^{(i)} - \zeta^{(i)}\beta^{(i)}\mu^{(i)}\left[C^{(i)} + D^{(i)}\left(\log r - \frac{1}{2}\right)\right]$$

$$-\alpha^{(i)}\left(3\lambda^{(i)}+2\mu^{(i)}\right)\left(T_0 - T_R\right) + 2\sum_{m=1}^{\infty}\left[P_m^{(i)}\left(\lambda^{(i)}+\mu^{(i)}\right) + \mu^{(i)} Q_m^{(i)} r^{-2}\right] e^{-\omega_m^2 \beta^{(i)2}\kappa^{(i)} t} + \tag{25.39}$$

$$+2\zeta^{(i)}\mu^{(i)}\sum_{m=1}^{\infty}\left\{\begin{array}{l}\dfrac{A_m^{(i)}}{\omega_m r}\left[J_1\left(r\omega_m\beta^{(i)}\right) - r\omega_m\beta^{(i)} J_0\left(r\omega_m\beta^{(i)}\right)\right] + \\ + \dfrac{B_m^{(i)}}{\omega_m r}\left[J_1\left(r\omega_m\beta^{(i)}\right) - r\omega_m\beta^{(i)} J_0\left(r\omega_m\beta^{(i)}\right)\right]\end{array}\right\} e^{-\omega_m^2\beta^{(i)2}\kappa^{(i)}t} \quad \forall i \in \{1,2\}$$

$$\sigma_{zz}^{(i)} = 2\lambda^{(i)} G^{(i)} - \alpha^{(i)}\left(3\lambda^{(i)}+2\mu^{(i)}\right)\left(T_0 - T_R\right) + 2\mu^{(i)}\beta^{(i)}\zeta^{(i)}\left(C^{(i)} + D^{(i)}\log r\right) +$$

$$+2\sum_{m=1}^{\infty}\left\{P_m^{(i)}\lambda^{(i)} + \mu^{(i)}\zeta^{(i)}\beta^{(i)}\left[A_m^{(i)} J_0\left(r\omega_m\beta^{(i)}\right) + B_m^{(i)} Y_0\left(r\omega_m\beta^{(i)}\right)\right]\right\} e^{-\omega_m^2\beta^{(i)2}\kappa^{(i)}t} \tag{25.40}$$

$$\forall i \in \{1,2\}$$

It is important to note that displacement function and stress components in both phases (1) and (2) can to be subdivided in two parts: firstly constant in time and the second depend of the time.

The integration constants $G^{(i)}, H^{(i)}, C_m^{(i)}, D_m^{(i)} \quad \forall i \in \{1,2\}$ are function of geometrical, mechanical and thermal parameters of spherical layers . Moreover $C_m^{(i)}, D_m^{(i)}$ are function of constants $A_m^{(i)}, B_m^{(i)}, \omega_m$ also with apix $i \in \{1,2\}$.We can write the boundary conditions (25.3) and (25.4) in two uncoupled algebraic system as reported below:

$$\mathbf{\Omega}\cdot\mathbf{W}_0 = \mathbf{L}_0, \qquad \mathbf{\Omega}\cdot\mathbf{W}_m = \mathbf{L}_m, \quad \forall m = 1,2,....N \tag{25.41}$$

where the vectors $\mathbf{L}_0, \mathbf{L}_m$ are given by:

$$\mathbf{L}_0 = \left[\left(\mathbf{L}_{1,0}^{(2)} - \mathbf{L}_{1,0}^{(1)}\right)\right]^T, \ \mathbf{L}_m = \left[\left(\mathbf{L}_{1,m}^{(2)} - \mathbf{L}_{1,m}^{(1)}\right)\right]^T, \tag{25.42}$$

These vector are characterized by following sub-vectors:

$$\mathbf{L}_{1,0}^{(1)} = \begin{bmatrix} 0 \\ \alpha^{(1)}\left(3\lambda^{(1)}+2\mu^{(1)}\right)\end{bmatrix} T_R, \ \mathbf{L}_{1,0}^{(1)} = \begin{bmatrix} 0 \\ \alpha^{(2)}\left(3\lambda^{(2)}+2\mu^{(2)}\right)\end{bmatrix} T_R,$$

$$\mathbf{L}_{1,m}^{(1)} = \frac{\zeta^{(1)} R^{(1)}}{\omega_m}\begin{bmatrix} R^{(1)} J_1\left(\omega_m R^{(1)}\beta^{(1)}\right) & R^{(1)} Y_1\left(\omega_m R^{(1)}\beta^{(1)}\right) \\ -2\mu^{(1)} J_1\left(\omega_m R^{(1)}\beta^{(1)}\right) & -2\mu^{(1)} Y_1\left(\omega_m R^{(1)}\beta^{(1)}\right)\end{bmatrix}\cdot\begin{bmatrix} A_m^{(1)} \\ B_m^{(1)}\end{bmatrix} \tag{25.43}$$

$$\mathbf{L}_{1,m}^{(2)} = \frac{\zeta^{(2)} R^{(1)}}{\omega_m}\begin{bmatrix} R^{(1)} J_1\left(\omega_m R^{(1)}\beta^{(2)}\right) & R^{(1)} Y_1\left(\omega_m R^{(1)}\beta^{(2)}\right) \\ -2\mu^{(2)} J_1\left(\omega_m R^{(1)}\beta^{(2)}\right) & -2\mu^{(2)} Y_1\left(\omega_m R^{(1)}\beta^{(2)}\right)\end{bmatrix}\cdot\begin{bmatrix} A_m^{(2)} \\ B_m^{(2)}\end{bmatrix}$$

The unknowns vectors $\mathbf{W}_0 = [\mathbf{W}_0^{(1)}, \mathbf{W}_0^{(2)}]^T$ and $\mathbf{W}_m = [\mathbf{W}_m^{(1)}, \mathbf{W}_m^{(2)}]^T$ are composed by sub-vectors reported below:

$$\begin{cases} \mathbf{W}_0^{(1)} = \left[G^{(1)} \quad H^{(1)}\right]^T, \ \mathbf{W}_0^{(2)} = \left[G^{(2)} \quad H^{(2)}\right]^T, \\ \mathbf{W}_m^{(1)} = \left[C_m^{(1)} \quad D_m^{(1)}\right]^T, \ \mathbf{W}_m^{(2)} = \left[C_m^{(2)} \quad D_m^{(2)}\right]^T, \quad \forall m \in \{1,2,....,N\}\end{cases} \tag{25.44}$$

and $\mathbf{\Omega}$ is an $2x4$ rectangular matrix composed by following sub-matrices:

$$[\mathbf{\Omega}] = \left[\mathbf{\Omega}_1^{(1)} \quad -\mathbf{\Omega}_1^{(2)}\right], \tag{25.45}$$

where the generic matrices $\mathbf{\Omega}_1^{(1)}, \mathbf{\Omega}_1^{(2)}$ are given by:

$$\mathbf{\Omega}_1^{(1)} = \begin{bmatrix} R^{(1)} & 1/R^{(1)} \\ 2\left(\lambda^{(1)}+\mu^{(1)}\right) & -2\mu^{(1)} R^{(1)-2}\end{bmatrix}, \quad \mathbf{\Omega}_1^{(2)} = \begin{bmatrix} R^{(1)} & 1/R^{(1)} \\ 2\left(\lambda^{(2)}+\mu^{(2)}\right) & -2\mu^{(2)} R^{(i)-2}\end{bmatrix}, \tag{25.46}$$

are (2×2) matrices with nonzero determinant, whose components were already gave above. The determinant of the matrices (25.46) is given by:

$$\det[\mathbf{\Omega}_1^{(1)}] = -\frac{2\left(2\mu^{(1)}+\lambda^{(1)}\right)}{R^{(1)}} \neq 0, \quad \det[\mathbf{\Omega}_1^{(2)}] = -\frac{2\left(2\mu^{(2)}+\lambda^{(2)}\right)}{R^{(1)2}} \neq 0, \tag{25.47}$$

However, in force of the special form of $\mathbf{\Omega}$ derived above, one can rewrite the reduced algebraic problem in order to have the solution without recall any numerical strategy. To make this, let us we can rewrite two algebraic system (25.41) in follows manner:

$$\begin{aligned} &\mathbf{\Omega}_1^{(2)}\mathbf{W}_0^{(2)} = \mathbf{\Omega}_1^{(1)}\mathbf{W}_0^{(1)} + \mathbf{L}_{1,0}^{(2)} - \mathbf{L}_{1,0}^{(1)} \\ &\mathbf{\Omega}_1^{(2)}\mathbf{W}_m^{(2)} = \mathbf{\Omega}_1^{(1)}\mathbf{W}_m^{(1)} + \mathbf{L}_{1,m}^{(2)} - \mathbf{L}_{1,m}^{(1)} \quad \forall m \in \{1,2,....,N\} \end{aligned} \tag{25.48}$$

By solving the equations (25.48), we finally obtain

$$\begin{cases} \mathbf{W}_0^{(2)} = \left[\mathbf{\Omega}_1^{(2)}\right]^{-1}\left[\mathbf{\Omega}_1^{(1)}\mathbf{W}_0^{(1)} + \mathbf{L}_{1,0}^{(2)} - \mathbf{L}_{1,0}^{(1)}\right] \\ \mathbf{W}_m^{(2)} = \left[\mathbf{\Omega}_1^{(2)}\right]^{-1}\left[\mathbf{\Omega}_1^{(1)}\mathbf{W}_m^{(1)} + \mathbf{L}_{1,m}^{(2)} - \mathbf{L}_{1,m}^{(1)}\right] \end{cases} \quad \forall m \in \{1,2,....,N\} \tag{25.49}$$

The problem is hence reduced to an algebraic one in which only the four coefficients – collected in $\mathbf{W}_0^{(1)}, \mathbf{W}_m^{(1)}$ – related to the first phase have to be determined, by imposing two boundary conditions described by the equations obtained above. Therefore, in order to find the four unknowns collected in $\mathbf{W}_0^{(1)}, \mathbf{W}_m^{(1)}$, it remains to rewrite the boundary conditions (25.4) in matrix form as reported below:

$$\mathbf{\Pi}\cdot\mathbf{W}_0^{(1)} = \Upsilon_0, \quad \mathbf{\Pi}\cdot\mathbf{W}_m^{(1)} = \Upsilon_m \quad \forall m \in \{1,2,....,N\}, \tag{25.50}$$

where the matrix $\mathbf{\Pi}$, and vectors Υ_0, Υ_m are given by**:**

$$\mathbf{\Pi} = \begin{bmatrix}\mathbf{\Pi}_1 & \mathbf{\Pi}_2\end{bmatrix}^T, \quad \Upsilon_0 = \begin{bmatrix}\Upsilon_{1,0} & \Upsilon_{2,0}\end{bmatrix}^T, \quad \Upsilon_m = \begin{bmatrix}\Upsilon_{1,m} & \Upsilon_{2,m}\end{bmatrix}^T \quad \forall m \in \{1,2,....,N\}, \tag{25.51}$$

where $\mathbf{\Pi}_1, \mathbf{\Pi}_2$ are two vectors and $\Upsilon_{1,0}, \Upsilon_{2,0}, \Upsilon_{1,m}, \Upsilon_{2,m}$ are four scalars, as reported below:

$$\begin{aligned} &\mathbf{\Pi}_1 = \left[2\left(\lambda^{(1)}+\mu^{(1)}\right), -2\mu^{(1)}R^{(0)-2}\right]^T, \ \mathbf{\Pi}_2 = \left[2\left(\lambda^{(2)}+\mu^{(2)}\right), -2\mu^{(2)}R^{(2)-2}\right]^T \cdot \left[\mathbf{\Omega}_1^{(2)}\right]^{-1}\cdot\mathbf{\Omega}_1^{(1)}, \\ &\Upsilon_{1,0} = -\alpha^{(1)}\left(3\lambda^{(1)}+2\mu^{(1)}\right)T_R, \ \Upsilon_{1,m} = \frac{2\mu^{(1)}\zeta^{(1)}}{\omega_m}\left[A_m^{(1)}J_1\left(\omega_m R^{(0)}\beta^{(1)}\right) + B_m^{(1)}Y_1\left(\omega_m R^{(0)}\beta^{(1)}\right)\right], \\ &\Upsilon_{2,0} = -\alpha^{(2)}\left(3\lambda^{(2)}+2\mu^{(2)}\right)T_R + \left[2\left(\lambda^{(2)}+\mu^{(2)}\right), -2\mu^{(2)}R^{(2)-2}\right]^T \cdot \left[\mathbf{L}_{1,0}^{(1)} - \mathbf{L}_{1,0}^{(2)}\right], \\ &\Upsilon_{2,m} = \frac{2\mu^{(2)}\zeta^{(2)}}{\omega_m}\left[A_m^{(2)}J_1\left(\omega_m R^{(2)}\beta^{(2)}\right) + B_m^{(2)}Y_1\left(\omega_m R^{(2)}\beta^{(2)}\right)\right] + \\ &\qquad + \left[2\left(\lambda^{(2)}+\mu^{(2)}\right), -2\mu^{(2)}R^{(2)-2}\right]^T \cdot \left[\mathbf{L}_{1,m}^{(1)} - \mathbf{L}_{1,m}^{(2)}\right], \quad \forall m \in \{1,2,....,N\}, \end{aligned} \tag{25.52}$$

Then, by inverting the equations (25.50), we obtain the 4 unknown coefficients $G^{(1)}, H^{(1)}, C_m^{(1)}, D_m^{(1)}$ as reported below

$$\mathbf{W}_0^{(1)} = \mathbf{\Pi}^{-1}\cdot\Upsilon_0, \ \mathbf{W}_m^{(1)} = \mathbf{\Pi}^{-1}\cdot\Upsilon_m, \tag{25.53}$$

By substituting the solutions (25.53) in (25.36), we obtain in explicit displacement function.

25.4. Numerical application: Metallic pipeline internally coated with ceramic materia

Let us consider, a composite circular cylinder constituted by two phases subjected to uniform heat input q_0 applied on internal surface $r = R^{(0)}$, starting to initial temperature in composite solid equal to $T_0 = T_R = const$. The external surface $r = R^{(2)}$ is exposed, for t >0, to an ambient at T_0 temperature through a uniform boundary conductance h_c. The initial temperature (for t = 0) of the bi-layer hollow cylinder is $T_0 = T_R = const$ where $T_R > 0$. The phase (1) is constituted by Ceramic (Si_3N_4) and phase (2) by Metal ($Ti-6Al-4V$). It is denoted with apix "1" the parameters of

Ceramic and apix "2" the parameters of Metal (see figure 25.1). The mechanical and thermal parameters considered for both phases are reported in table 25.1.

	phase n.1: Ceramic (Si_3N_4)	**phase n.2: Metal** $(Ti-6Al-4V)$
$E\left[N\,m^{-2}\right]$	$348.43\cdot10^{9}$	$122.557\cdot10^{9}$
$k\left[W\,m^{-1}K^{-1}\right]$	1.209	13.723
ν	0.24	0.29
$\alpha\left[m\cdot m^{-1}K^{1}\right]$	$5.872\cdot10^{-6}$	$7.579\cdot10^{-6}$
$\rho\left[kg\,m^{-3}\right]$	4429	2370
$c_v\left[J\cdot kg^{-1}K^{-1}\right]$	555.110	625.297

Table 25.1 – *Mechanical and thermal parameters of Ceramic and Metal*

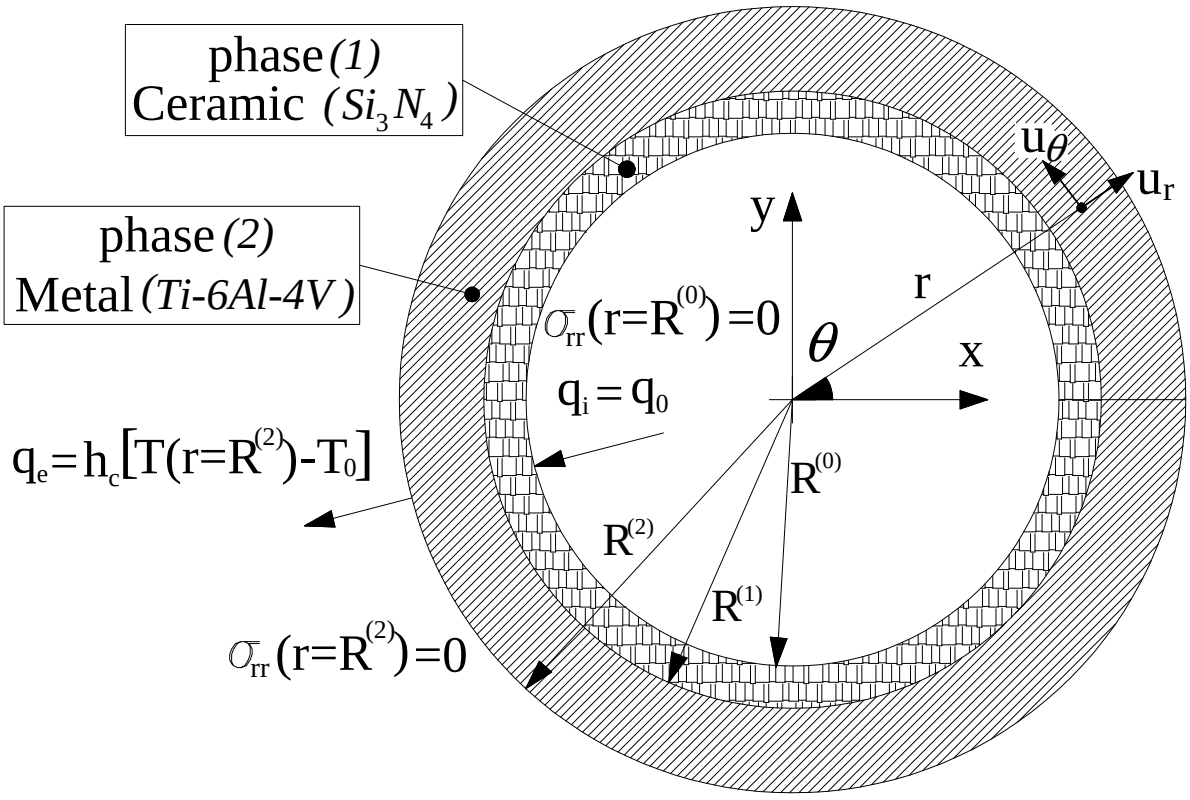

Figure 25.1 – *Metallic pipelines insulated by ceramic phase*

The geometrical parameters of bi-layer hollow cylinder are :

$$R^{(0)}=12.7mm,\ R^{(2)}=25.4mm,\ \ R^{(1)}=R^{(0)}+\frac{1}{3}\left[R^{(2)}-R^{(0)}\right]=16.93mm,$$

The uniform heat input q_0 applied on internal surface $r=R^{(0)}$, uniform boundary conductance h_c and the initial temperature are reported below:

$$h_c=8W/m^2\cdot{}^{\circ}K,\quad q_0=1000W/m^2,\ T_0=T_R=300^{\circ}K$$

In this case the graphics function $g(\omega)$ given by equation (25.31) is reported below:

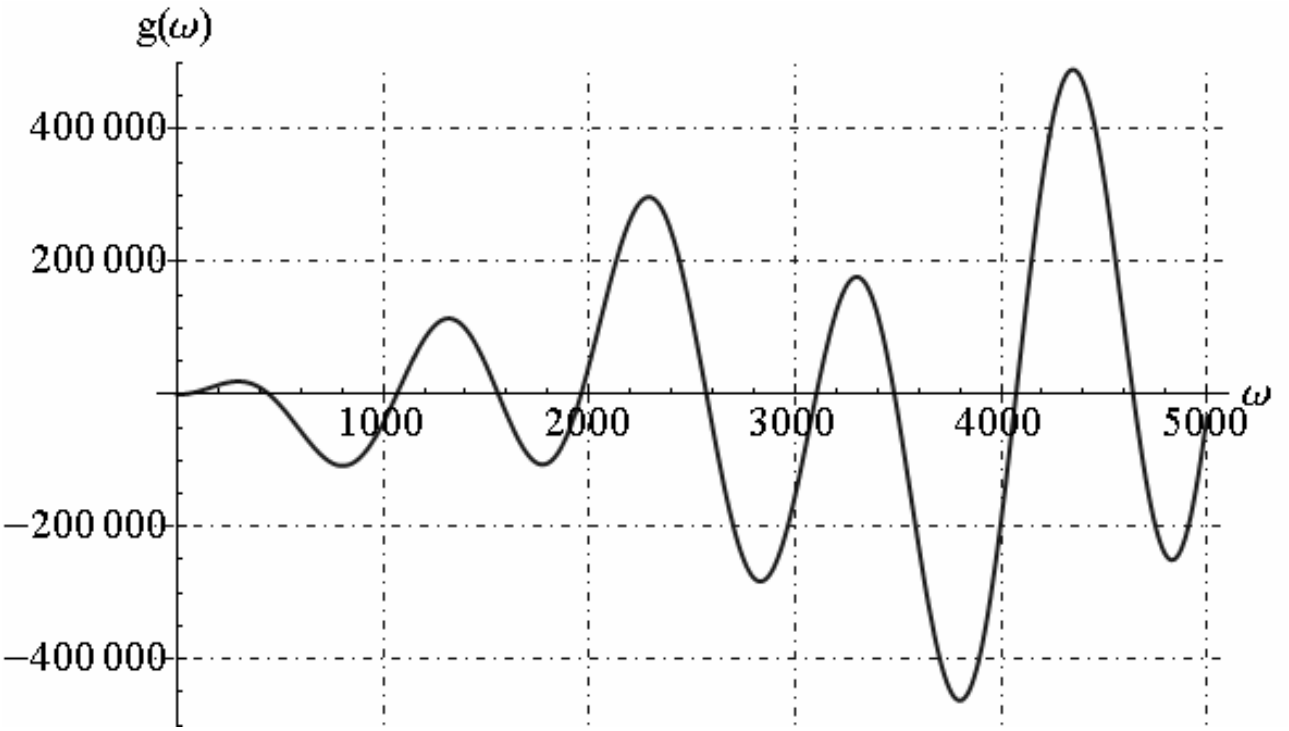

Figure 25.2 - *Function* $g(\omega)$

By fixed m= 20, the roots ω_m of transcendental equation (25.31) and corresponding values of constants integration A_m are reported in table 25.2:

ω_m	31.3029	445.496	1065.75	1558.88	1960.64
A_m	-71.2291	-1.02022	-1.27766	-0.415915	-0.2486
ω_m	2569.77	3103.18	3482.64	4073.24	4641.83
A_m	-0.32154	-0.0994751	-0.152911	-0.139505	0.00549799
ω_m	5014.06	5576.35	6171.43	6555.05	7080.19
A_m	-0.090383	-0.067738	0.045121	-0.0376525	-0.0301055
ω_m	7692.08	8103.58	8586.06	9205.52	9655.96
A_m	0.0537606	0.00112701	-0.00699962	0.049092	0.0206186

Table 25.2 – *Roots* ω_m *and corresponding values of constants integration* A_m

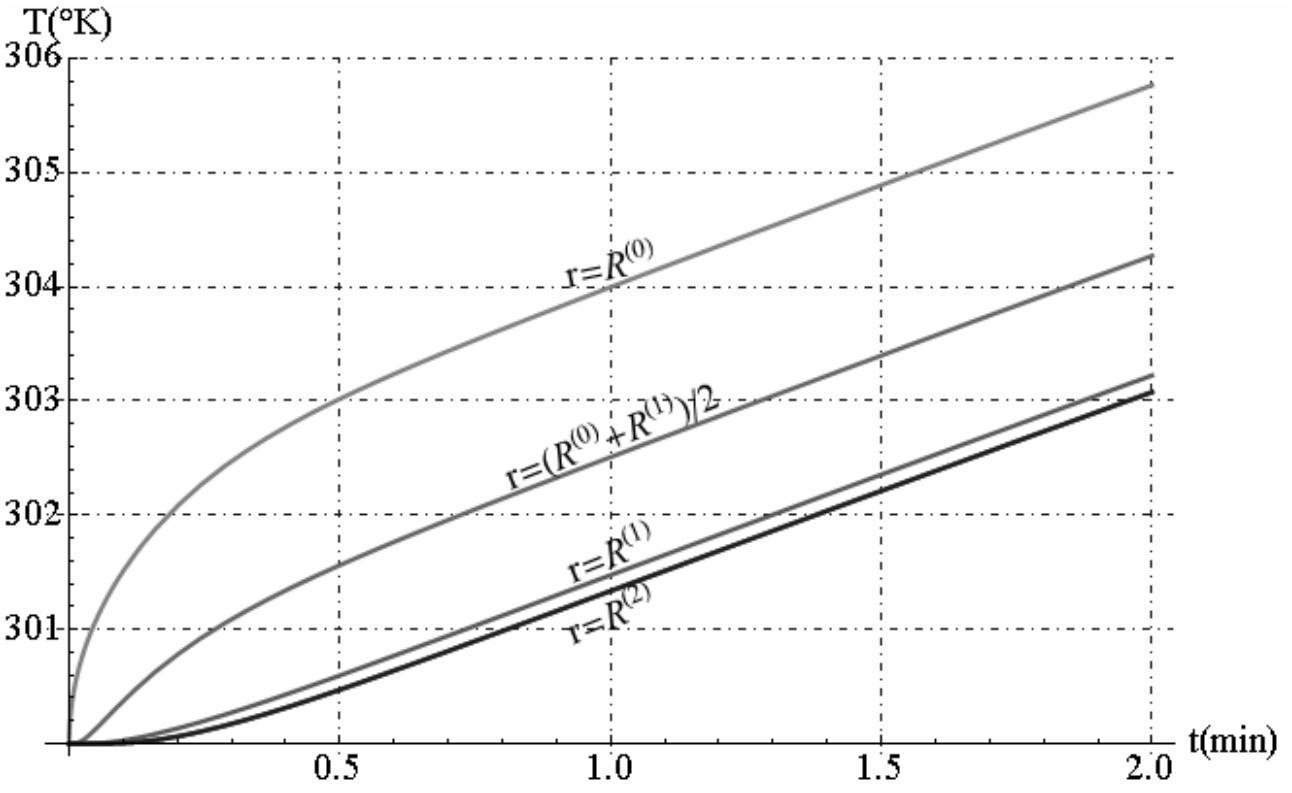

Fig. 25.3 - *Temperature function versus time*

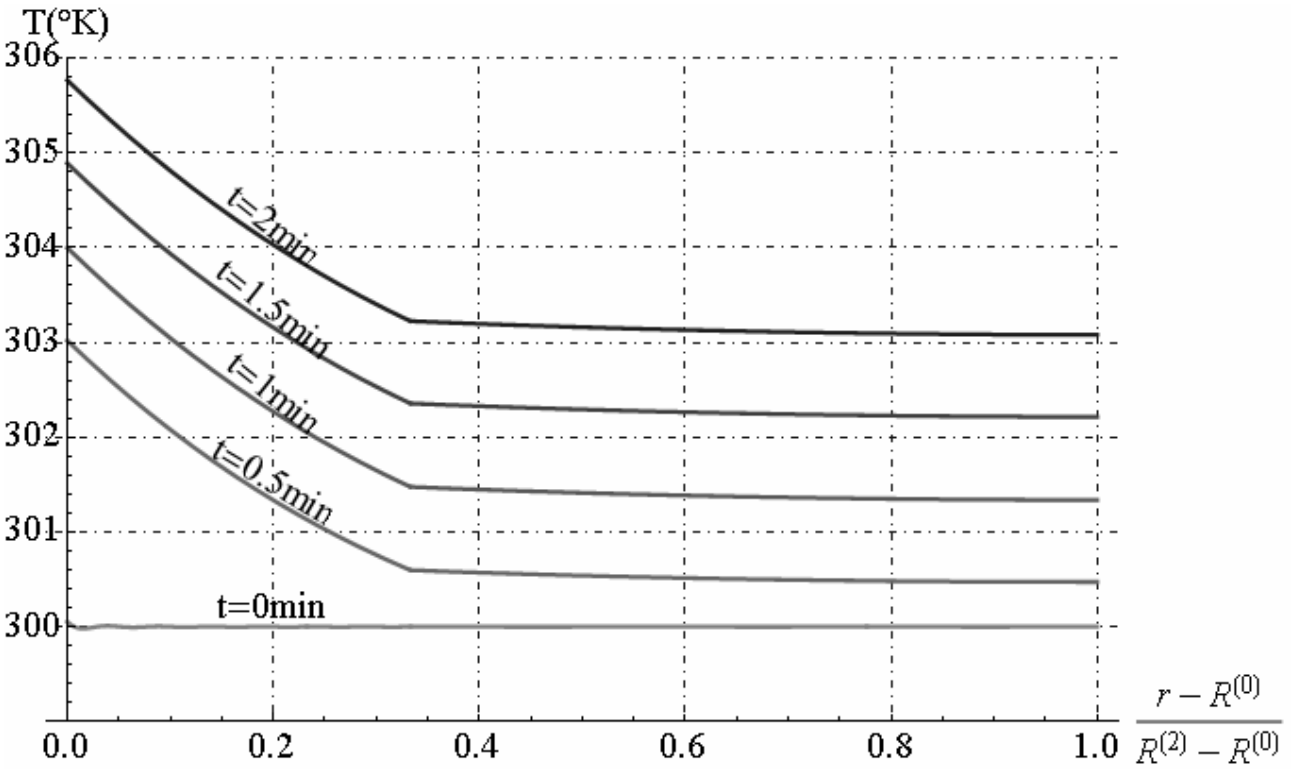

Fig. 25.4 - *Temperature function along radial direction for t = 0.0, 0.5, 1.0, 1.5, 2.0min*

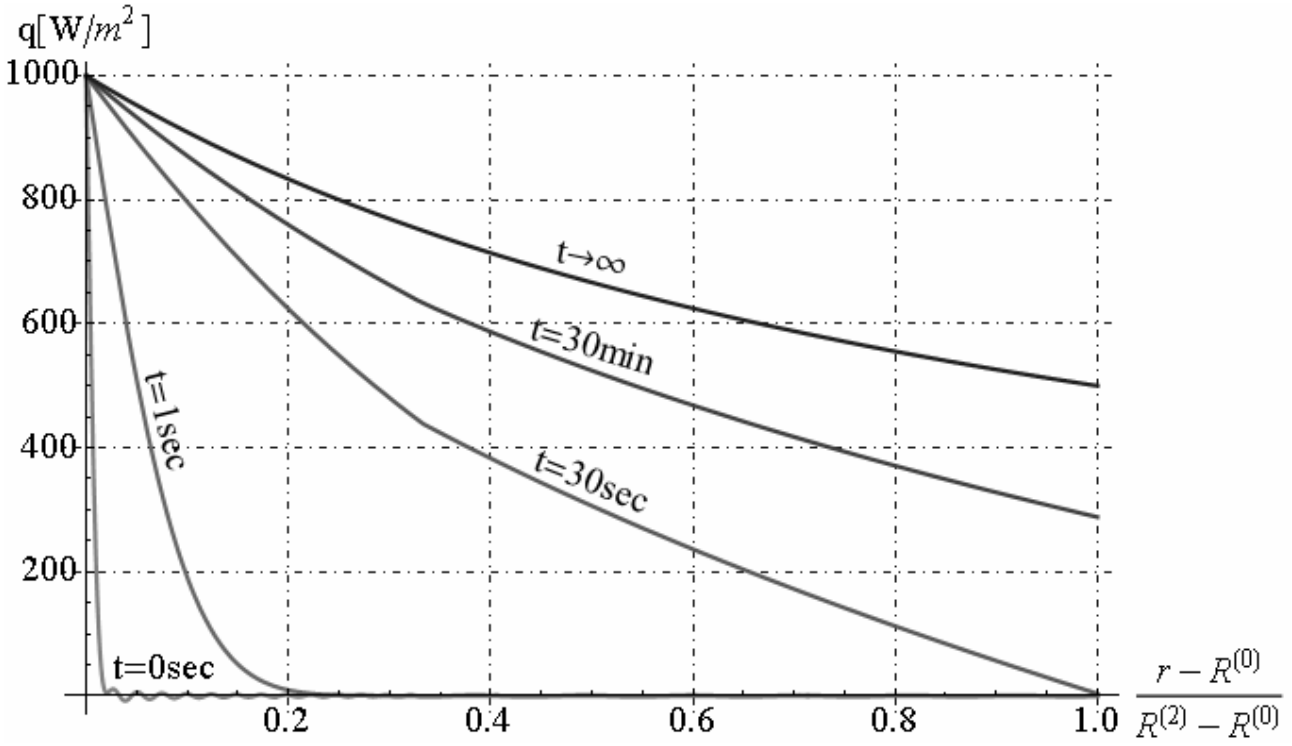

Fig. 25.5 – *Heat flux function along radial direction for t = 0.0, 30s, 30min, $t \to \infty$,*

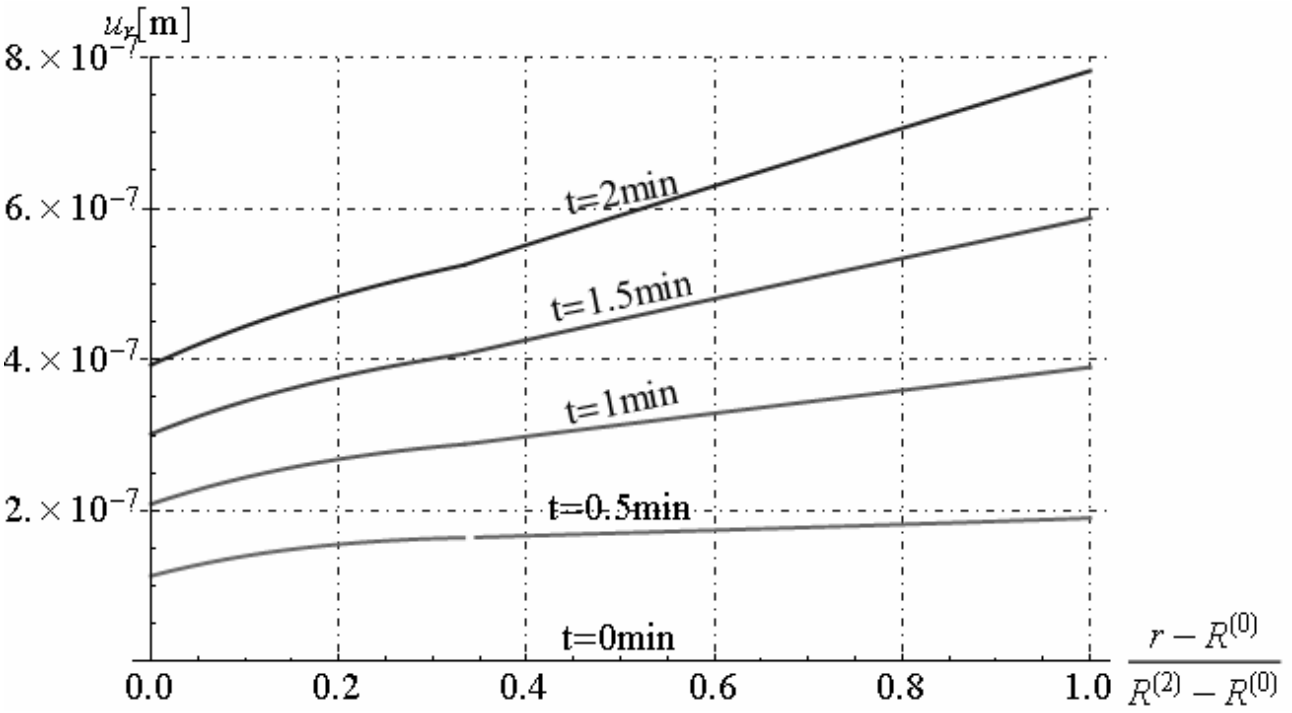

Fig. 25.6 - *Radial displacement along radial direction for t = 0.0, 0.5, 1.0, 1.5, 2.0min*

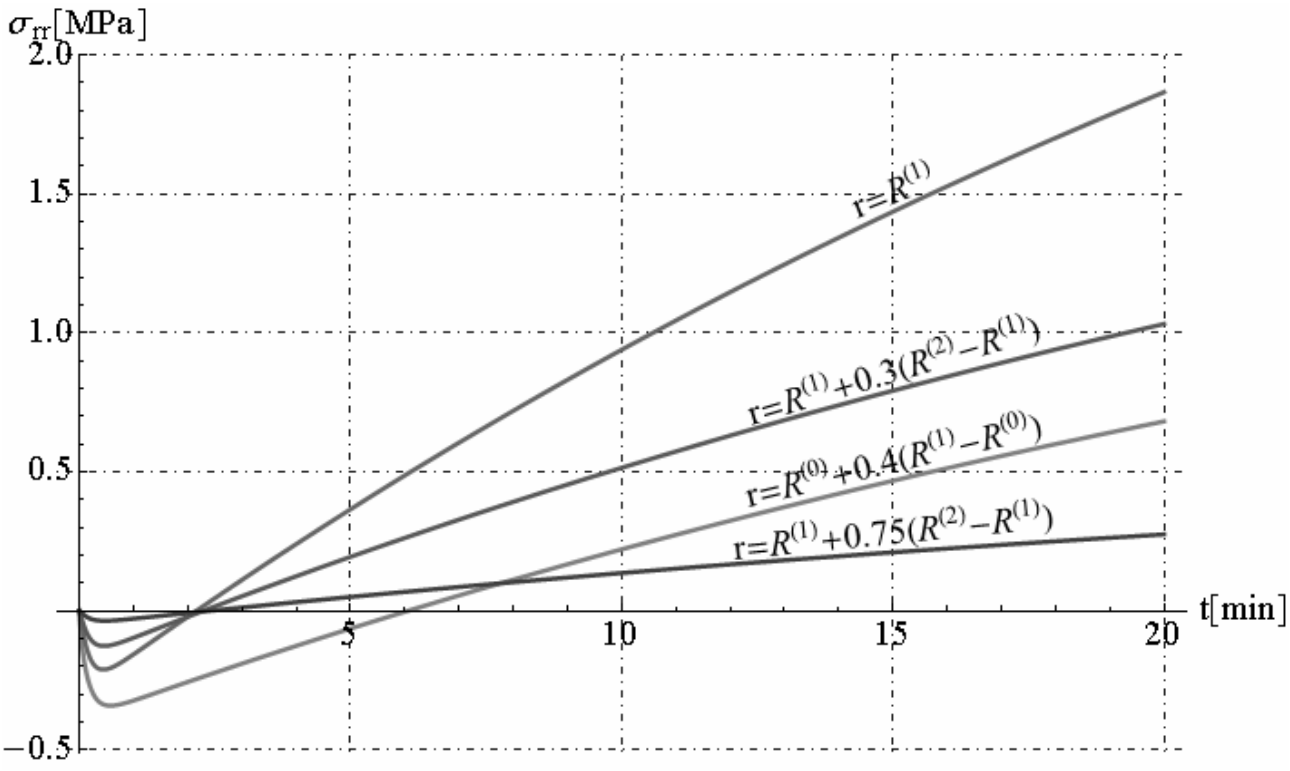

Fig. 25.7 - *Radial stress versus time*

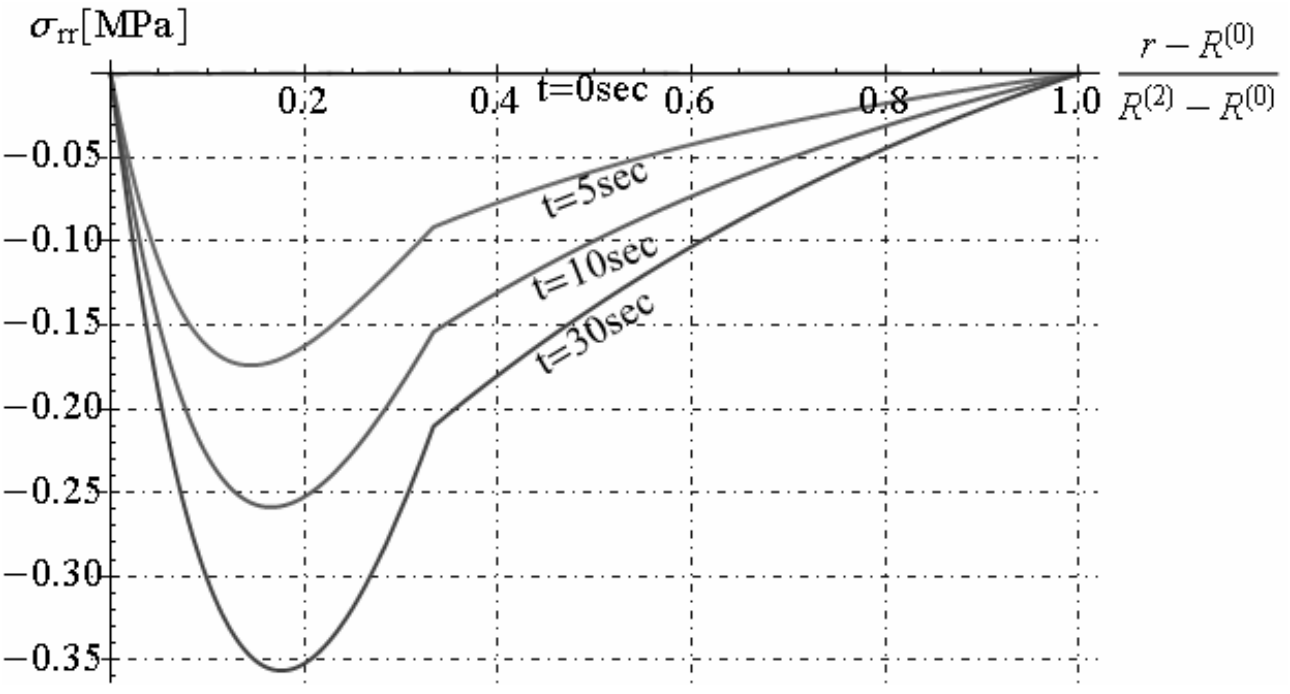

Fig. 25.8 - *Radial stress along radial direction for t = 0, 10, 20, 30sec*

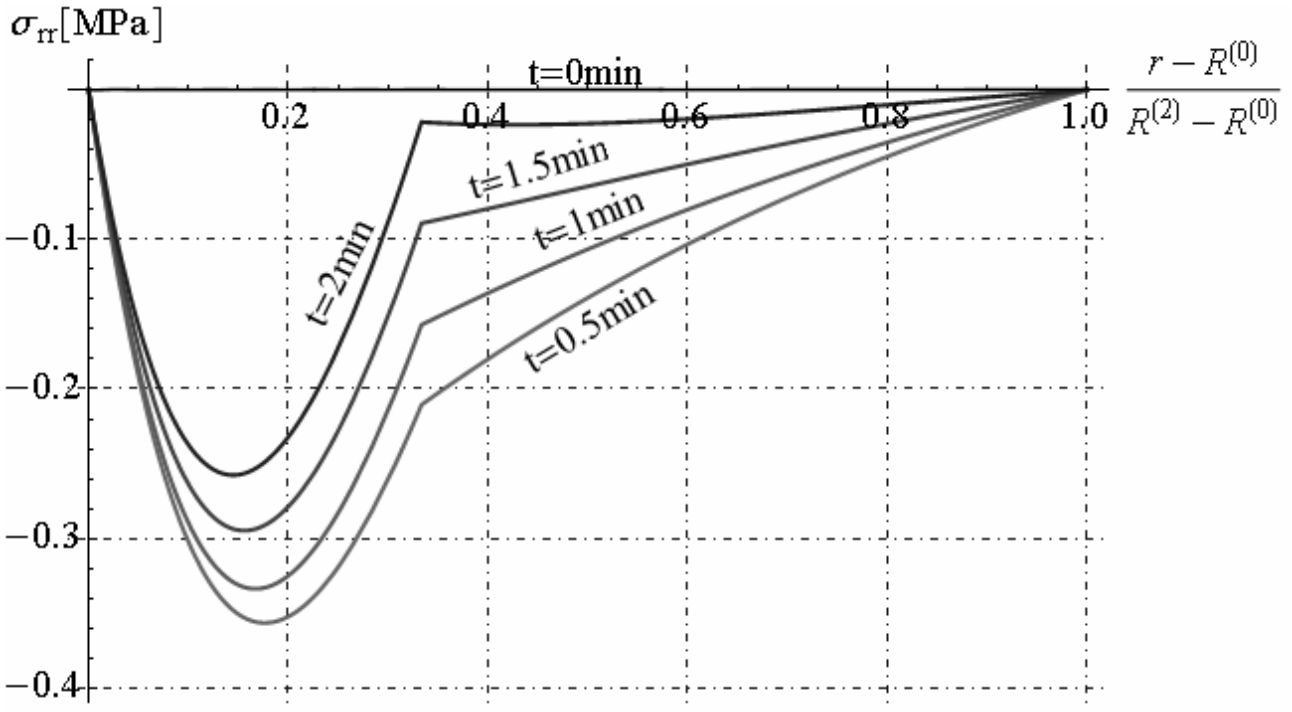

Fig. 25.9 - *Radial stress along radial direction for t = 0.0, 0.5, 1.0, 1.5, 2.0min*

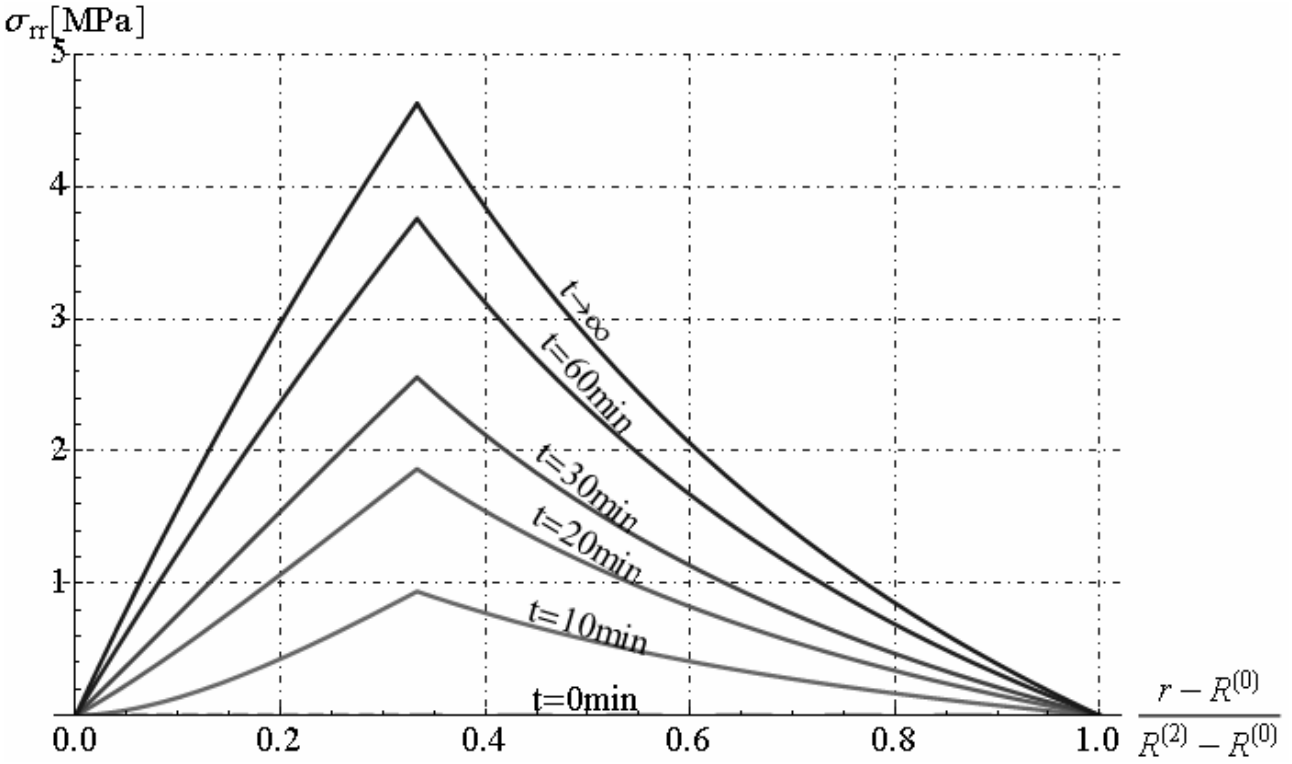

Fig. 25.10 - *Radial stress along radial direction for t = 0, 10, 20, 30, 60min, $t \to \infty$*

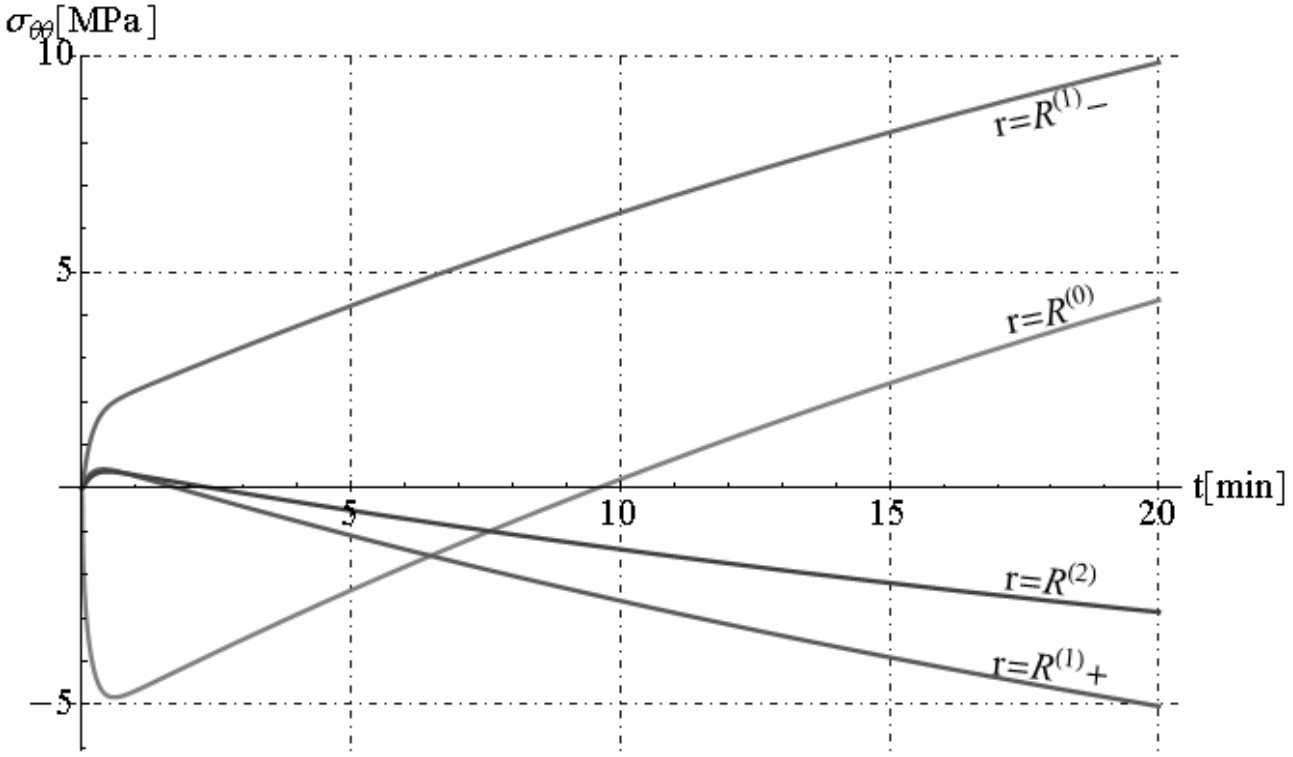

Fig. 25.11 - *Circumferential stress versus time*

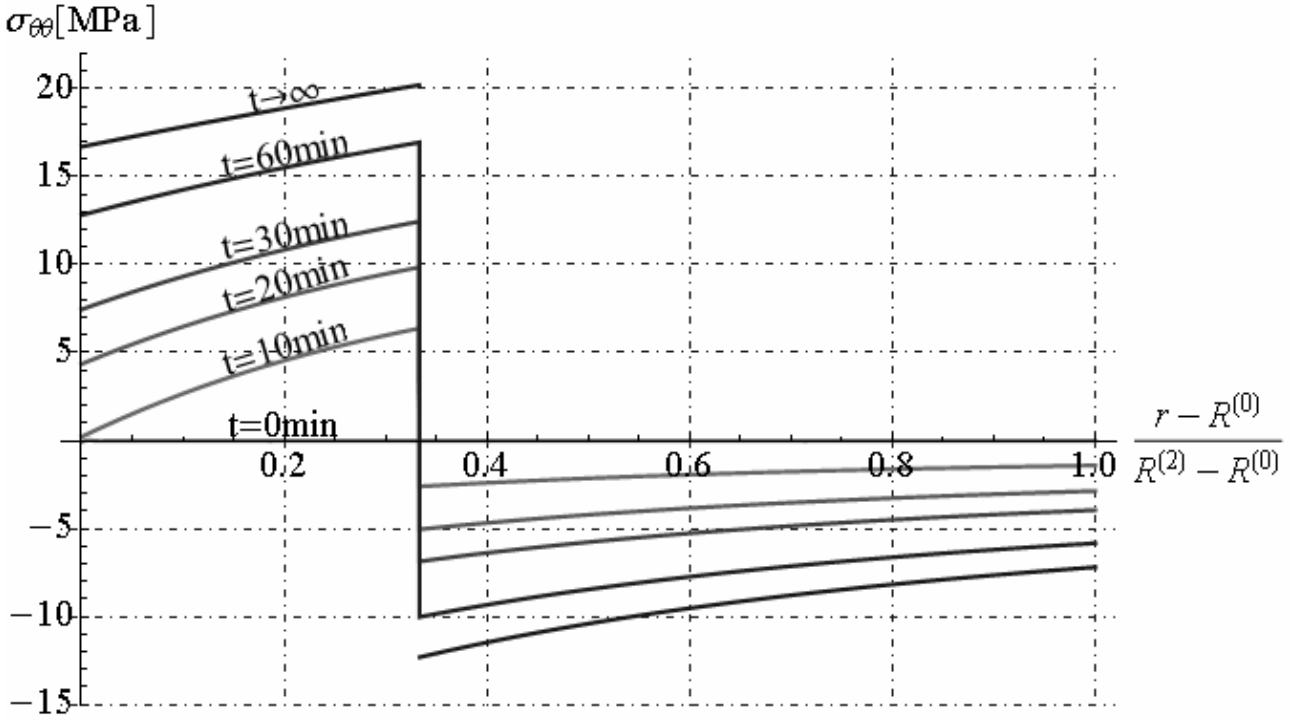

Fig. 25.12 - *Circumferential stress along radial direction for t = 0, 10, 20, 30, 60min, $t \to \infty$*

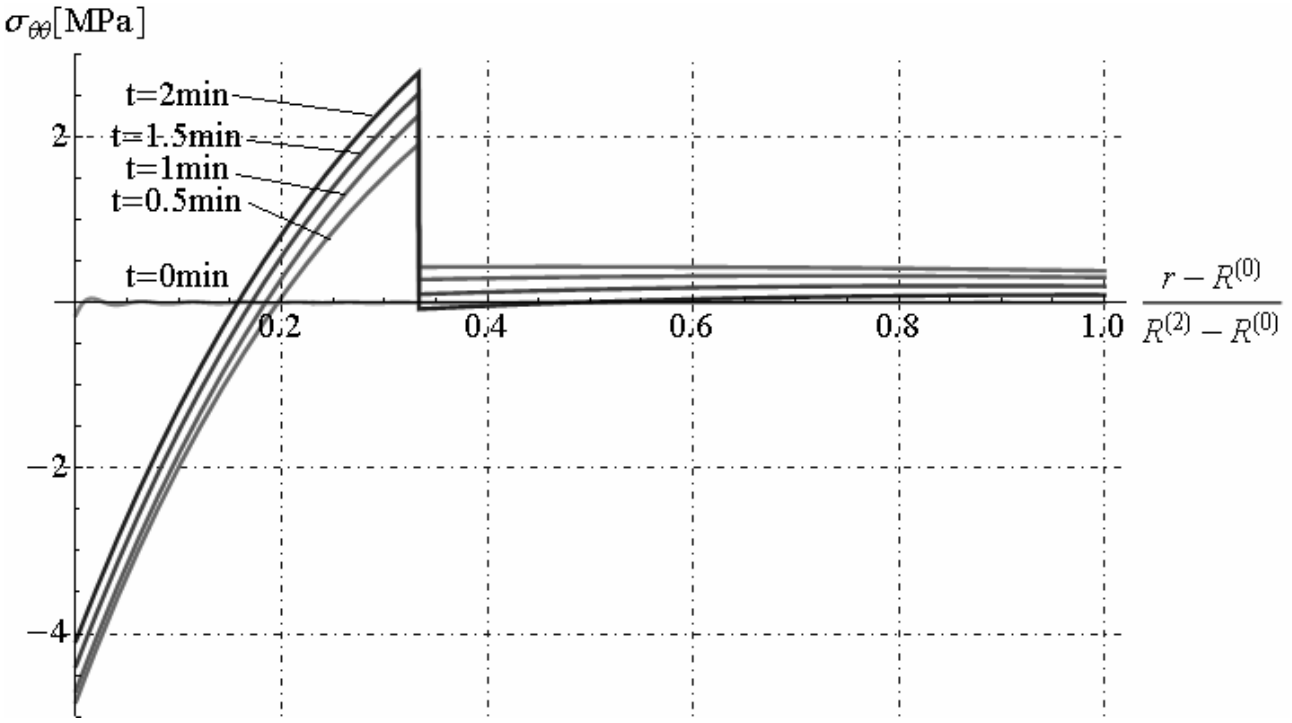

Fig. 25.13 - *Circumferential stress along radial direction for t = 0.0, 0.5, 1.0, 1.5, 2.0min*

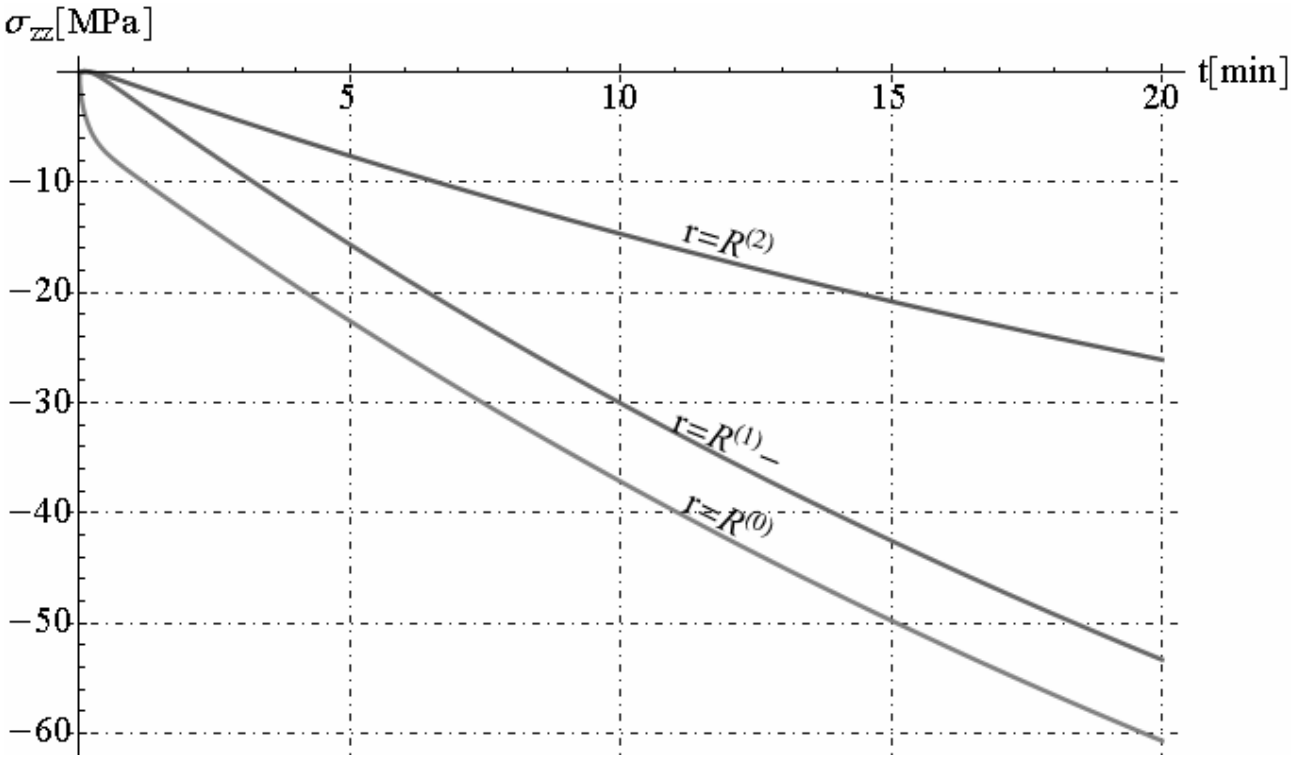

Fig. 25.14 - *Axial stress versus time*

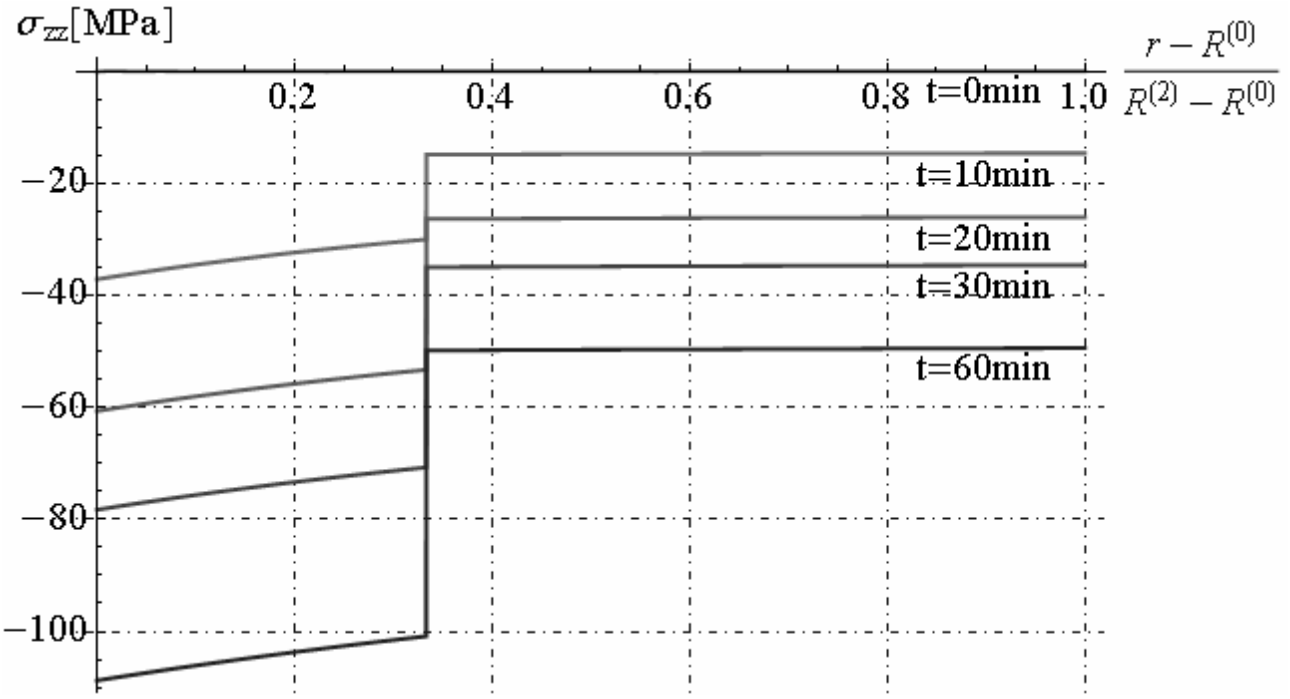

Fig. 25.15 - *Axial stress along radial direction for t = 0, 10, 20, 30, 60min*

25.5. Conclusions

In this chapter it is reported a new thermo-elastic solution in close form for bi-layer hollow cylinder under time-dependent boundary conditions. In particular, the external surface $r = R^{(2)}$ of bi-layer hollow cylinder is exposed, for t >0, to an ambient at T_0 temperature through a uniform boundary conductance h_c, while the inner surface is exposed to constant heat flux in time. By applying the analytical solution, we obtain temperature profile along radial direction for different values of time, as reported in figure 25.4. The gradient of temperature in ceramic phase (1) is greater than that metallic phase (2) because $k^{(2)} > k^{(1)}$. The sign of radial stress in ceramic and metal phases vary in the time, as showed in figures 25.6, 25.7, 25.8, 25.9. In the first 2 minutes, the radial stress component is negative (compression), in both phases. Successively, by increasing the variable time, radial stress component becomes positive (traction), in both phases. In the first 2 minutes, in metal phase, the hoop stress is positive (traction), but successively the hoop stress becomes negative in each point (compression). In ceramic phase the hoop stress component assumes a approximately bi-triangular profile, along radial direction until to 10 minutes. Then, by increasing the variable time, the hoop stress component becomes positive (traction) in any points of ceramic phase.

25.6. References

[1] Noda, N. (1991). Thermal stresses in materials with temperature-dependent properties. *Journal of Applied Mechanics*, Vol. 44 (83-97)

[2] Tanigawa, Y. (1995). Some basic thermo-elastic problems for non-homogeneous structural materials, *Journal of Applied Mechanics*, Vol. 48 (377-89)

[3] Lutz, M.P. & Zimmerman, R.W. (1996). Thermal stresses and effective thermal expansion coefficient of a functionally graded sphere. *Journal of Thermal Stresses*, Vol. 19 (39- 54)

[4] Zimmerman, R.W. & Lutz, M.P. (1999). Thermal stress and thermal expansion in a uniformly heated functionally graded cylinder, *Journal of Thermal Stresses*, Vol. 22 (177-88)

[5] Obata, Y.; Kanayama, K.; Ohji, T. & Noda, N. (1999). Two-dimensional unsteady thermal stresses in a partially heated circular cylinder made of functionally graded material, *Journal of Thermal Stresses*

[6] Sutradhar, A.; Paulino, G.H. & Gray, L.J. (2002). Transient heat conduction in homogeneous and non-homogeneous materials by the Laplace transform Galerkin boundary element method, *Eng. Anal. Boundary Element*, Vol. 26 (119-32)
[7] Kim, K.S. & Noda, N. (2002). Green's function approach to unsteady thermal stresses in an infinite hollow cylinder of functionally graded material, *Acta Mechanics*, Vol. 156 (145-61)
[8] Fraldi, M., Nunziante, L., Carannante, F. (2007), *Axis-symmetrical Solutions for n-plies Functionally Graded Material Cylinders under Strain no-Decaying Conditions*, J. Mech. of Adv. Mat. and Struct. Vol. 14 (3), pp. 151-174 - DOI: 10.1080/15376490600719220
[9] M. Fraldi, L. Nunziante, F. Carannante, A. Prota, G. Manfredi, E. Cosenza (2008), *On the Prediction of the Collapse Load of Circular Concrete Columns Confined by FRP*, Journal Engineering structures, Vol. 30, Issue 11, November 2008, Pages 3247-3264 - DOI: 10.1016/j.engstruct.2008.04.036
[10] Fraldi, M., Nunziante, L., Chandrasekaran, S., Carannante, F., Pernice, MC. (2009), *Mechanics of distributed fibre optic sensors for strain measurements on rods*, Journal of Structural Engineering, 35, pp. 323-333, Dec. 2008- Gen. 2009
[11] M. Fraldi, F. Carannante, L. Nunziante (2012), *Analytical solutions for n-phase Functionally Graded Material Cylinders under de Saint Venant load conditions: Homogenization and effects of Poisson ratios on the overall stiffness*, Composites Part B: Engineering, Volume 45, Issue 1, February 2013, Pages 1310–1324
[12] Nunziante, L., Gambarotta, L., Tralli, A., *Scienza delle Costruzioni*, 3° Edizione, McGraw-Hill, 2011**,** ISBN**:** 9788838666971
[13] Praveen, G.N. & Reddy, J.N. (1998). Nonlinear transient thermo-elastic analysis of functionally graded ceramic–metal plates, *International Journal of Solids Structures*, Vol. 35 (4457–76)
[14] Reddy, J.N. & Chin, C.D. (1998). Thermo-mechanical analysis of functionally graded cylinders and plates, *International Journal of Solids Structures*, Vol. 21 (593–626)
[15] Praveen, G.N.; Chin, C.D. & Reddy, J.N. (1999) Thermo-elastic analysis of a functionally graded ceramic–metal cylinder, *ASCE Journal of Engineering Mechanics*, Vol. 125 (1259–67)
[16] Reddy, J.N. (2000). Analysis of functionally graded plates, *International Journal of Numerical Meth. Eng.*, Vol. 47 (663–84)
[17] Reddy, J.N. & Cheng, Z.Q. (2001). Three-dimensional thermo-mechanical deformations of functionally graded rectangular plates. *European Journal of Mechanics A/Solids*, Vol. 20 (841–60)
[18] Reddy, J.N. & Cheng, Z.Q. (2003). Frequency of functionally graded plates with threedimensional asymptotic approach, *Journal of Engineering Mechanics*, Vol. 129 (896– 900)
[19] Shao, Z.S. (2005). Mechanical and thermal stresses of a functionally graded hollow circular cylinder with finite length, *International Journal of Pressure Vessel Pipe*, Vol. 82 (155– 63)
[20] Shao, Z.S. & Wang, T.J. (2006). Three-dimensional solutions for the stress fields in functionally graded cylindrical panel with finite length and subjected to thermal/mechanical loads, *International Journal of Solids Structures*, Vol. 43 (3856– 74)
[21] Shao, Z.S.; Wang, T.J. & Ang, K.K. (2007). Transient thermo-mechanical analysis of functionally graded hollow circular cylinders, *Journal of Thermal Stresses*, Vol. 30 (81–104)
[22] Ootao, Y. & Tanigawa, Y. (1999). Three-dimensional transient thermal stresses of functionally graded rectangular plate due to partial heating, *Journal of Thermal Stresses*, Vol. 22 (35–55)
[23] Ootao, Y. & Tanigawa, Y. (2004). Transient thermo-elastic problem of functionally graded thick strip due to non-uniform heat supply, *Composite Structures*, Vol. 63, No. 2 (139–46)
[24] Ootao, Y. & Tanigawa, Y. (2005). Two-dimensional thermo-elastic analysis of a functionally graded cylindrical panel due to non-uniform heat supply, *Mech. Res. Commun.*, Vol. 32 (429–43)
[25] Liew, K.M.; Kitiporncai, S.; Zhang, X.Z. & Lim, C.W. (2003). Analysis of the thermal stress behavior of functionally graded hollow circular cylinders, *International Journal of Solids Structures*, Vol. 40 (2355–80)

[26] Awaji, H. & Sivakuman, R. (2001) Temperature and stress distributions in a hollow cylinder of functionally graded material: the case of temperature-dependent material properties, *Journal of Am. Ceram. Soc.*, Vol. 84 (1059–65)
[27] Ching, H.K.& Yen, S.C. (2006). Transient thermo-elastic deformations of 2-D functionally graded beams under non-uniformly convective heat supply, *Composite Structures*, Vol. 73, No. 4 (381–93)
[28] Honig, G. & Hirdes, U. (1984) A method for the numerical inversion of Laplace transforms, *Journal of Computer Applied Mathematics*, Vol. 10 (113–132)
[29] Mohammad Azadi and Mahboobeh Azadi, *Thermoelastic Stresses in FG-Cylinders* (2011)
[30] F. de Monte, *Transverse eigenproblem of steady-state heat conduction for multi-dimensional two-layered slabs with automatic computation of eigenvalues*, International Journal of Heat and Mass Transfer 47 (2004) 191–201
[31] Suneet Singh, Prashant K. Jain, Rizwan-uddin, *Analytical solution to transient heat conduction in polar coordinates with multiple layers in radial direction*, International Journal of Thermal Sciences 47 (2008) 261–273
[32] Prashant K. Jain, Suneet Singh, Rizwan-uddin, *Analytical Solution to Transient Asymmetric Heat Conduction in a Multilayer Annulus*, Journal of Heat Transfer - January 2009, Vol. 131
[33] M.kayhani, M., Nourouzi, and A. Amiri Delooei, *An Exact Solution of Axi-symmetric Conductive Heat Transfer in Cylindrical Composite Laminate under the General Boundary Condition*, World Academy of Science, Engineering and Technology 69 2010

CONCLUSIONS

In the present thesis is furnished a general approach to construct exact termo-elastic solutions for **multilayered cylinders and spheres**, subjected to mechanical and thermal load. These solutions are utilized for several engineering applications and we report some applications in last analyze chapters of present thesis. The relevant results obtained in this thesis are reported below:

1) By applying the analytical solutions for **multilayered cylinder** subjected to DSV load conditions, reported in chapter X, were calculated **axial, bending, torsion and shear stiffness** of the solid considered. The axial stiffness k_ε , bending stiffness k_χ , shear stiffness k_γ are not equal to the sum of stiffness of single phases, as so far usually assumed in simplified procedures, but strongly dependent on values of Poisson's moduli and on geometrical parameters;
2) In chapter XVII and XVIII are reported the steady-state problem for **multilayered cylinder and sphere subjected to gradient of temperature and pressure** between the inner and the outer surface, respectively. The Henchy von-Mises's equivalent stress in bi-layered cylinder and sphere, is more influenced by ratio of linear thermal expansion coefficient of two phases, respectively.
3) In chapter XX and XXI are reported the **transient problems for multilayered sphere and cylinder** subjected to three type of time dependent boundary conditions, respectively. In particular, is reported the thermal analyses of spherical tank, composed by two hollow spherical layers, exposed to hydrocarbon fire.
4) In chapter XXII it is studied a **spherical tank methane gas-filled exposed to fire** characterized by hydrocarbon fire curve. By applying a suitable simplified hypothesis on the mechanics of problem, it is determine the analytical thermo-elastic solution for spherical tank. In particular, are reported two analytical model that simulation the interaction between spherical tank and methane gas. In the first model, let us consider that heat transfer occurs by only thermal convection, but in second model the heat transfer occurs by thermal convection and thermal radiation. The collapse temperature and maximum Henchy von-Mises's equivalent stress at collapsed are determined in both models considered.
5) In chapter XXIII, an **industrial insulated pipeline is modelled as multilayered cylinder**, subjected to internal pressure and gradient of temperature between inner and outer surfaces. By applying the analytical solutions reported in this chapter, it is showed that maximum Hencky **von Mises's equivalent stress in three phases of pipeline is more influenced by Poisson's ratio** and linear thermal expansion coefficient of insulate coating.
6) In chapter XXIV it is analyzed a **cylindrical concrete specimen under axial force within Fibre Polymeric Reinforcing sheets**. The elastic solutions found in Chapter XII are here extended to the post-elastic range. The evolution of the stress field when the core phase is characterized by an Intrinsic Curve or Schleicher-like elastic-plastic response with associate flow rule and the cylindrically orthotropic hollow phase obeys to is shown the elastic-brittle Tsai-Hill anisotropic yield criterion. This analytical model furnished a predictive formula for estimating the overall collapse mechanism, the concrete ultimate compressive strength and the confining pressure effect.
7) In chapter XXV it is reported an analytical thermo-elastic solution in closed form for bi-layer hollow cylinder subjected to time-dependent boundary conditions. In particular, it is obtained a new analytical solution for a **metallic pipelines internally coated with ceramic material**, constituted by two phases: Ceramic (Si_3N_4) and Metal ($Ti-6Al-4V$) subjected to heat flux on inner surface.